

NCHRP 24-17

**LOAD AND RESISTANCE FACTOR DESIGN  
(LRFD) FOR DEEP FOUNDATIONS**

**APPENDIX A  
SURVEYS - STATE OF PRACTICE DESIGN AND  
CONSTRUCTION**

Prepared for  
National Cooperative Highway Research Program  
Transportation Research Board  
National Research Council

Ching L. Kuo  
Geostructures Corp.  
2713 Falling Leaves Drive, Valrico, FL 33594

Bjorn Birgisson and Michael McVay  
Department of Civil Engineering  
University of Florida  
Gainesville, FL 32611-6580

Samuel G. Paikowsky  
Geotechnical Engineering Research Laboratory  
Department of Civil and Environmental Engineering  
University of Massachusetts  
Lowell, Massachusetts

July 2002

Appendix A Final Report TOC

### **ACKNOWLEDGEMENT OF SPONSORSHIP**

This work was sponsored by the American Association of State Highway and Transportation Officials, in cooperation with the Federal Highway Administration, and was conducted in the National Cooperative Highway Research Program, which is administered by the Transportation Research Board of the National Research Council.

### **DISCLAIMER**

This is an uncorrected draft as submitted by the research agency. The opinions and conclusions expressed or implied in the report are those of the research agency. They are not necessarily those of the Transportation Research Board, the National Research Council, the Federal Highway Administration, the American Association of State Highway and Transportation Officials, or the individual states participating in the National Cooperative Highway Research Program.



## TABLE OF CONTENTS

1. Survey of Current Use of AASHTO Specifications (1999)
2. Questionnaire
  - 2.1 Copy of the Questionnaire
  - 2.2 Summary Write-Up
  - 2.3 Summary Tables

## **Survey of Current use of AASHTO Specifications**

- **The attached copy of a survey and summary of responses was conducted and kindly provided by Mr. Andy Muñoz, Jr., a Geotechnical Engineer with the FHWA Southwest district.**



REGION 6

**U.S. DEPARTMENT OF TRANSPORTATION  
FEDERAL HIGHWAY ADMINISTRATION  
P.O. BOX 902003  
819 TAYLOR STREET, ROOM 8A00  
FORT WORTH, TEXAS 76102-9003**

June 30, 1999

REFER TO **HRC-SO-TX**  
5021

Mr. Samuel G. Paikowsky  
Geotechnical Research Laboratory  
Department of Civil & Environmental Engineering  
University of Massachusetts Lowell  
One University Avenue  
Lowell, MA 01854

Dear Sam:

As per our discussion last week in Boston, enclosed for your information is a copy of the three transparencies I recently used for a presentation on "*CURRENT AASHTO STANDARD SPECIFICATIONS FOR GEOTECHNICAL DESIGN*". The information was obtained from a letter survey I conducted of State DOT Geotechnical Engineers on a nation-wide basis. Responses are considered "unofficial", but provide a good understanding of the current state-of-the-practice at this time.

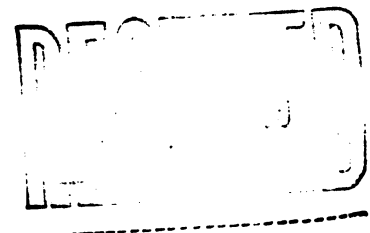
The following provides a brief explanation of each page:

1. Copy of letter sent to all State Geotechnical Engineers with four questions.
2. Crossed States are those that responded (63%).
3. Summary of responses received with key comments provided by some State DOT.

Sincerely,

Andy Muñoz, Jr., P.E.  
Geotechnical Engineer

Enclosures ( 3 pages)



**U.S. DEPARTMENT OF TRANSPORTATION  
Federal Highway Administration  
819 Taylor Street - Room 8A00  
FORT WORTH, TEXAS 76102-9003**

**(817) 978-4382  
FAX: (817) 978-4144**

May 10, 1999  
HNG-06  
5021

***Dear State Geotechnical Engineer;***

The purpose of this letter is to request your comments concerning your involvement with the AASHTO STANDARD SPECIFICATIONS that involve Geotechnical Engineering Design.

This is a topic of discussion at the 24th S.W. Geotechnical Engineers Conference, scheduled for June 16-18, 1999 in Sacramento, California and I need your quick and brief responses by June 1.

I have assembled a summary list of the AASHTO STANDARD SPECIFICATIONS from the subcommittees of "Highway Bridges" and "Materials" that involves Geotechnical Engineering and enclosed is a copy for your information. Please review the list and provide "off-the-cuff" comments on the following:

- (1) Does your Geotechnical Department have a copy of the four sources of AASHTO Specs listed in the enclosure?
- (2) Are these AASHTO Specs routinely used by the State DOT engineers for their designs and analyses?
- (3) Were you involved in the development or revision of any of the AASHTO Specs?
- (4) Is your State DOT committed to LRFD for Foundation Design and what is your time-table?

Thank you for returning your response by June 1 to:

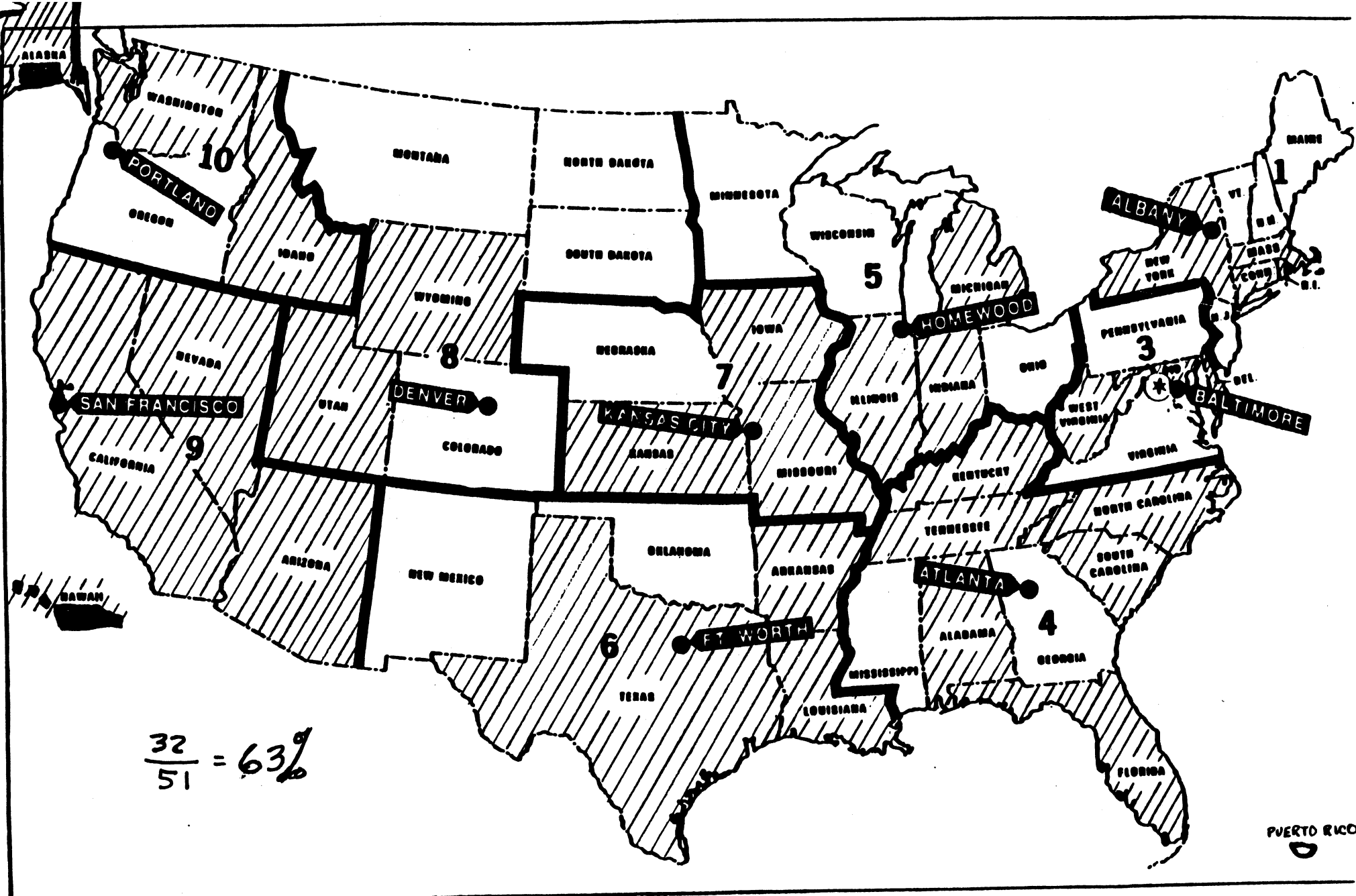
Andy Muñoz, Jr., P.E.  
Geotechnical Engineer  
Federal Highway Administration  
819 Taylor Street - Room 8A00  
Fort Worth, TX 76102  
E-mail: andy.munoz@fhwa.dot.gov

Sincerely,

A handwritten signature in black ink that reads "Andy Muñoz Jr." in a cursive style.

Andy Muñoz, Jr., P.E.  
Geotechnical Engineer

Enclosure



$$\frac{32}{51} = 63\frac{9}{51}$$

★ Washington, D.C. Headquarters

● Field Region Headquarters

NOTE: FHWA Region 1 Conforms to Standard Regions 1 and 2

June 1999

A. Mung

# CURRENT AASHTO STANDARD SPECIFICATIONS FOR GEOTECHNICAL DESIGN

1) Does your Geotechnical Department have a copy of the four sources of AASHTO Specs listed in the enclosure?

Yes !

- (1) S.S. For Hwy. Bridges --- 30
- (2) LRFD Bridge Design Specs -- 25
- (3) Materials - S & T - - - 28
- (4) Subsurface Investigation -- 29

2) Are these AASHTO Specs routinely used by the State DOT engineers for their designs and analyses?

Yes - 18

No - 3 CA-HI-SC

Some - 11

\* Used primarily as guide or reference

\* Some portions are very conservative (ARI)

\* AASHTO Specs same as FHWA Manuals & other Guidance (WA)

+ Have own Manuals & Specs plus use FHWA Manuals & NAVFAC (CA)

3) Were you involved in the development or revision of any of the AASHTO Specs?

Yes - - - 8 AK-FL-ID-MIS-NY-TX-UT-WA

No/Review - 24 CA - revising AASHTO to suit own needs

\* More Geotechnical Representation needed

\* Tony Allan (WA) only Geotech in Bridge Subcommittee

4) Is your State DOT committed to LRFD for Foundation Design and what is your timetable?

Yes -- 14 AK-DL-FL-ID-KA-MARY-MASS-MICH-NY-NC-TENN-UT-WA-W.Va.

No/Maybe - 18 AL-ARI-ARK-CA-CONN-HI-ILL-In-Io-KY-MIS-NV-RI-SC-TX-WY-LA-D.C.

1. When AASHTO sunsets Blue Specs & starts using the Red Spec.
2. Additional Research must be performed on local conditions & materials to establish design parameters.
3. Studying & Modifying AASHTO LRFD & may use on trial basis.
4. Most new projects designed by consultants will use LRFD
5. With some adjustments & calibration For soil resistance Factors For piles & drilled shafts.
6. Serious Reservations.
7. Have significantly modified the AASHTO LRFD pile spec. For use in WADOT.  
LRFD Loads & Wall Chapters to be updated with results From NCHRP project 20-07 Task 88.  
Training for State & Consultants major hurdle. U. of Wash. developing LRFD Training Course for WADOT.

## **State of Practice Questionnaire**

A questionnaire concerning the design and construction practices of deep foundations used by the Highway Departments was developed and distributed to 298 State Highway officials, TRB representatives and State and FHWA geotechnical engineers.





Geotechnical Engineering Research Laboratory  
One University Avenue  
Lowell, Massachusetts 01854  
Tel: (978) 934-2277 Fax: (978) 934-3046  
e-mail: Samuel\_Paikowsky@uml.edu  
web site: <http://www.eng.uml.edu/Dept/civ/geotechnical>  
**DEPARTMENT OF CIVIL AND  
ENVIRONMENTAL ENGINEERING**

Samuel G. Paikowsky, Sc.D  
Professor



August 9, 1999

RE: NCHRP Project 24-17  
**Deep Foundation Design and Construction Practices**

«Title» «FirstName» «LastName»  
«JobTitle»  
«Company»  
«Address1»  
«Address2»  
«City», «State» «PostalCode»

Dear «Title» «LastName»,

The Geotechnical Research Laboratory at the University of Massachusetts Lowell in cooperation with the Universities of Maryland, Florida and others is conducting project 24-17 under the AASHTO-sponsored National Cooperative Highway Research Program (NCHRP). The objective of this project is to provide recommended revisions to the driven pile and drilled shaft portions of Section 10 of the AASHTO LRFD Bridge Design Specifications to reflect current practice in geotechnical design and construction. The revisions will include resistance factors based on analyses of databases containing data from case histories.

To maximize the effectiveness of the recommendations, the research team would appreciate your help with the following:

1. Complete the attached survey, which is aimed at obtaining information about the practices of deep foundation design and construction. Your response will enable us to better address the needs of the different DOT agencies. If you find difficulty in completing the questionnaire and would like to discuss it by phone with a member of the research team please contact one of us using the information attached. When completed, please return the questionnaire to:

Dr Ching L. Kuo  
Geo Structures Corporation  
2713 Falling Leaves Drive  
Valrico, FL 33594

2. We would very much appreciate your help in obtaining information related to pile and/or drilled shaft field-testing. These data can relate to one or all of the following categories:



Geotechnical Engineering Research Laboratory  
Sc.D

One University Avenue  
Lowell, Massachusetts 01854  
Tel: (978) 934-2277 Fax: (978) 934-3046  
e-mail: Samuel\_Paikowsky@uml.edu

web site: <http://www.eng.uml.edu/Dept/civ/geotechnical>

DEPARTMENT OF CIVIL AND  
ENVIRONMENTAL ENGINEERING

Samuel G. Paikowsky,

Professor

- Dynamic measurements (PDA) during end of driving and/or restrrike with the relevant static load test to failure.
- Any testing on drilled shafts (static load test, Osterberg cell load test, Statnamic).

If the information is available in a report we will be glad to make the copies and send you back the originals. Please send the information to the undersigned, which will distribute it to the appropriate team member.

We realize how busy you are and therefore sincerely appreciate your efforts in sharing your department's experience with others that can profit from it. Your cooperation is highly appreciated and the quality of our work depends on it.

Sincerely yours,

Samuel G. Paikowsky

Cc: TRB State Representative

Team Member	Phone	Fax	e-mail
Bjorn Birgisson	(352) 846-3429	(352) 392-3394	bbirg@ce.ufl.edu
Ching L. Kuo	(813) 886-1075	(813) 888-6514	chingkuo@aol.com
Michael McVay	(352) 392-8697	(352) 392-3394	mcm@ce.ufl.edu
Samuel G. Paikowsy	(978) 934-2277	(978) 934-3046	Samuel_Paikowsky@uml.edu

Winword/Research/Ongoing Research/NCHRP LRFD/Databases/Survey/Coverletter

**NCHRP PROJECT 24-17  
LRFD DEEP FOUNDATION DESIGN**

**August 1999**

**SURVEY ON THE APPLICATION OF DEEP FOUNDATIONS**

STATE: \_\_\_\_\_ DEPARTMENT: \_\_\_\_\_

ENGINEER: \_\_\_\_\_ TITLE: \_\_\_\_\_

PHONE: \_\_\_\_\_ FAX: \_\_\_\_\_

E-MAIL: \_\_\_\_\_

**Please send back to:**

Dr. Ching L. Kuo  
Geo Structures Corporation  
2713 Falling Leaves Drive  
Valrico, FL 33594

**FOUNDATION ALTERNATIVES**

1. What is the breakdown of foundation types used in your bridge structures?

<input type="checkbox"/> Shallow Foundation	_____ %
<input type="checkbox"/> Driven Piles	_____ %
<input type="checkbox"/> Drilled Shafts	_____ %
<input type="checkbox"/> Others	_____ %

Comment:

---

---

---

2. Do you have a preferred type of deep foundation?

<input type="checkbox"/> Driven Pile	
<input type="checkbox"/> Drilled Shaft	
<input type="checkbox"/> Others	_____

3. Which type of driven piles do you use most (Please rank according to their usage; 1 for most used, 6 for least used)?
- ☐ Prestressed Concrete Pile
  - ☐ Steel H-Pile
  - ☐ Open-end Steel Pipe Pile
  - ☐ Closed-end Steel Pipe Pile
  - ☐ Timber Pile
  - ☐ Others \_\_\_\_\_

## DRIVEN PILES

### Design Considerations

1. What are the static axial geotechnical design methods and/or computer programs you use for driven pile design?
- ☐  $\alpha$  - method (Tomlinson, 1987)
  - ☐  $\beta$  - method (Esrig & Kirby, 1979)
  - ☐  $\gamma$  - method (Vijayvergiya and Focht, 1972)
  - ☐ Nordlund method (Nordlund, 1963)
  - ☐ Nottingham and Schmertmann method for CPT (1975)
  - ☐ Schmertmann method for SPT (Sharp, 1987)
  - ☐ Meyerhof method (1976) modified by Zeitlen and Paikowsky (1982)
  - ☐ Others \_\_\_\_\_

If computer programs are used in design, are they developed by:

- ☐ In-House
- ☐ FHWA
- ☐ Commercial
- ☐ Others \_\_\_\_\_

2. What are the dynamic axial geotechnical design methods, and/or computer programs you use for driven pile design?

Dynamic Formula

- ☐ Engineering News Record (ENR) F.S. = \_\_\_\_\_
- ☐ Gates, F.S. = \_\_\_\_\_
- ☐ Other, Specify \_\_\_\_\_, F.S. = \_\_\_\_\_

Computer Program

- ☐ WEAP by GRL
- ☐ Other, Specify \_\_\_\_\_

3. What are the primary parameters used in your design and/or computer program?
  - ☐ SPT-N Value
  - ☐ CPT Data
  - ☐ Pressuremeter Data
  - ☐ Dilatometer Data
  - ☐ Friction Angle ( $\phi$ ) and Cohesion (c)
  - ☐ Others \_\_\_\_\_
  
4. If friction angle ( $\phi$ ) and cohesion (c) are used in the design, how are the design parameters determined?
  - ☐ Laboratory Testing  
Type of Test: \_\_\_\_\_
  - ☐ Correlation with in-situ testing  
Type of test: \_\_\_\_\_  
Type of correlation: \_\_\_\_\_
  
5. How do you assess the side friction coefficient?
  - (a) In cohesive soil ( $C_A$  - adhesion) \_\_\_\_\_
  - (b) In cohesionless soil ( $\delta$  - interfacial friction angle) \_\_\_\_\_
  
6. Which methodology are you currently using for geotechnical and structural design?
  - ☐ Allowable Stress Design (ASD)
  - ☐ AASHTO Load Factor Design (LFD)
  - ☐ AASHTO Load and Resistance Factors Design (LRFD)
  - ☐ Others \_\_\_\_\_
  
7. Do you apply a partial safety factor for the side friction and the end bearing to determine the allowable capacity ASD methodology?
  - ☐ No. Use global F.S. = \_\_\_\_\_
  - ☐ Yes. F.S. = \_\_\_\_\_ for Side Friction, F.S. = \_\_\_\_\_ for End Bearing
  
8. Do you consider pile settlement in design?
  - ☐ No.
  - ☐ Yes. Tolerable settlement is typically \_\_\_\_\_.
  
9. What are the lateral geotechnical/structural design methods and/or computer programs you use for driven pile design?
  - ☐ Simplified methods (e.g., Broms, 1964)
  - ☐ p-y curve methods
  - ☐ Others \_\_\_\_\_

If computer programs are used in design, are they developed by:

- ☐ In-House
- ☐ FHWA
- ☐ Commercial
- ☐ Others \_\_\_\_\_

9. What are the controlling factors when designing piles subjected to lateral load?
- ☐ Lateral deflection. The tolerate deflection is \_\_\_\_\_.
  - ☐ Lateral pile capacity. The method used is \_\_\_\_\_ and the safety factor is \_\_\_\_\_.
10. Do you consider downdrag force in design?
- ☐ No.
  - ☐ Yes. Which method do you use? \_\_\_\_\_
11. Do you take into account the construction method in design?
- ☐ No.
  - ☐ Yes. If yes, please indicate how? \_\_\_\_\_
11. What is the estimated risk or failure probability of the group foundation design based on the safety factor you used?
- ☐ Less that 0.1%
  - ☐ Between 0.1 to 1%
  - ☐ Between 1 to 10%
  - ☐ More than 10%
  - ☐ Unknown

What is your assessment for the acceptable maximum failure probability? \_\_\_\_\_%

12. Have you ever had a pile design that ended in failure?
- ☐ No.
  - ☐ Yes. If yes, please provide some information as to what happened and why.

#### Construction Considerations

1. Do you perform static pile load test during construction?
- ☐ No.
  - ☐ Yes. What criteria are used to justify the test?

\_\_\_\_\_  
\_\_\_\_\_

What kind of test do you perform? (e.g. slow maintained to twice the design load) \_\_\_\_\_

\_\_\_\_\_

2. Do you perform dynamic pile load test during construction?
- ☐ No.
  - ☐ Yes. What are the criteria to justify the test? What percentage (%) of piles per bridge is usually subjected to dynamic load testing?
- 
3. What type of instrument is used for the dynamic load testing?
- ☐ PDA by GRL
  - ☐ Others \_\_\_\_\_
4. Which driving condition do you use to set production pile length and driving criteria?
- ☐ End of initial driving
  - ☐ Beginning of re-driving
  - ☐ Others \_\_\_\_\_
5. Do you consider pile freeze or relaxation effects in determining driving criteria?
- ☐ No.
  - ☐ Yes. How do you consider this during design?
- 
-

## DRILLED SHAFTS

### Design Considerations

1. What are design methods and/or computer programs do you use for drilled shaft design?
  - ☐  $\alpha$  - Method (Total Stress Approach) (Reese and O'Neill, 1998; Kulhawy, 1989)
  - ☐  $\beta$  - Methods (Effective Stress Approach) (Reese and O'Neill, 1988)
  - ☐ Reese and Wright (1977) Approach for side friction in cohesionless soils.
  - ☐ FHWA (O'Neill, 1996) Approach for intermediate geomaterials (soft rock)
  - ☐ Carter and Kulhawy (1988) Approach for intermediate geomaterials (soft rock)
  - ☐ Others \_\_\_\_\_

If computer programs are used in design, are they developed by?

- ☐ In-House
- ☐ FHWA
- ☐ Commercial

Others \_\_\_\_\_

2. What are the primary parameters used in your drilled shaft design and/or computer program?
  - ☐ SPT-N Value
  - ☐ CPT Data
  - ☐ Pressuremeter Data
  - ☐ Dilatometer Data
  - ☐ Friction Angle ( $\phi$ ) and Cohesion ( $c$ )
  - ☐ Others \_\_\_\_\_

3. If friction angle ( $\phi$ ) and cohesion ( $c$ ) or rock shear strength are used in design, how the design parameters are determined?

- ☐ Laboratory testing

Type of test: \_\_\_\_\_

- ☐ Correlation from in-situ testing

Type of test: \_\_\_\_\_

4. Do you consider the roughness of the borehole wall in rock socket design?

- ☐ No.
- ☐ Yes. How do you determine the roughness, by
  - ☐ Assumption
  - ☐ Field measurement?



5. Which methodology are you currently using for geotechnical and structural design?
- ☐ Allowable Stress Design (ASD)
  - ☐ AASHTO Load Factor Design (LFD)
  - ☐ AASHTO Load and Resistance Factors Design (LRFD)
  - ☐ Others \_\_\_\_\_
6. Do you apply partial safety factor on side friction and end bearing to determine allowable capacity in ASD?
- ☐ No. Using global F.S. = \_\_\_\_\_
  - ☐ Yes. F.S. = \_\_\_\_\_ for Side Friction, F.S. = \_\_\_\_\_ for End Bearing
7. Do you consider shaft settlement in design process?
- ☐ No.
  - ☐ Yes. Tolerant Settlement is \_\_\_\_\_
8. What are the lateral geotechnical/structural design methods and/or computer programs you use for driven pile design?
- ☐ Simplified methods (e.g., Broms, 1964)
  - ☐ p-y curve methods
  - ☐ Others \_\_\_\_\_
- If computer programs are used in design, are they developed by?
- ☐ In-House
  - ☐ FHWA
  - ☐ Commercial
  - ☐ Others \_\_\_\_\_
9. What are the controlling factors when designing drilled shafts subjected to lateral load?
- ☐ Lateral deflection. The tolerate deflection is \_\_\_\_\_.
  - ☐ Lateral pile capacity. The method used is \_\_\_\_\_ and the safety factor is \_\_\_\_\_.
10. Do you consider downdrag force in design?
- ☐ No.
  - ☐ Yes. Which method do you use: \_\_\_\_\_
11. Do you take into account the construction method in design?
- ☐ Yes.
  - ☐ No.

12. What is the estimated risk or failure probability of the foundation design based on the safety factor you used?
- ☐ Less than 0.1%
  - ☐ Between 0.1 to 1%
  - ☐ Between 1 to 10%
  - ☐ More than 10%
  - ☐ Unknown
- What is the acceptable maximum failure probability to you? \_\_\_\_\_%

#### Construction Considerations

1. Do you perform a static pile load test during construction?
- ☐ No.
  - ☐ Yes. What are the criteria to justify the test?
- 
2. What type of load test is used?
- ☐ Conventional static load test. If yes, what type? (slow maintained, short duration etc.)
  - ☐ Osterberg Load Cell Test
  - ☐ Statnamic Load Test
  - ☐ Dynamic Load test; Type of Test \_\_\_\_\_
  - ☐ Others \_\_\_\_\_
3. What is the method of excavation usually used in drilled shaft installation?
- ☐ Dry methods
  - ☐ Wet methods
  - ☐ Casing methods (\_\_\_ Temporary or \_\_\_ Permanent)
  - ☐ Others. \_\_\_\_\_
4. If drilled slurry is used during construction, what type of material and criteria are used?
- ☐ Mineral Slurry of Processed Attapulgite
  - ☐ Mineral Slurry of Bentonite Clays
  - ☐ Synthetic Polymers
  - ☐ Others. \_\_\_\_\_
5. What is the requirement of the shaft cleanliness?
- 
- 
6. Do you use any type of shaft inspection device to inspect the bottom of the shaft?
- ☐ No.
  - ☐ Yes. Type of Equipment \_\_\_\_\_

7. Do you use integrity testing for drilled shafts quality control?
- ☐ No
  - ☐ Yes. If yes, please specify type of tests and frequency of testing:
    - ☐ Cross Sonic Logging (CSL) ☐ Surface Reflection (Pulse Echo Method)
    - ☐ Others \_\_\_\_\_
- What percentage of caissons is tested? \_\_\_\_\_

TABLE 1 – SUMMARY OF RESPONSES TO SURVEY (as of 9/30/99)

STATE	ENGINEER	TITLE	E-MAIL
Alabama			
Alaska			
Arizona	F. Daniel Davis	State Bridge Engineer	Ddavis@dot.state.az.us
Arkansas	Edward T. Fain	Bridge Engineer	(501)569-2361
California	Tom Shantz	Senior M&R Engineer	Tom.shantz@dot.ca.gov
Colorado	Cheng-Kuang Su	Geotechnical Engineer	Cheng.su@dot.state.co.us
Connecticut	Leo Fontaine	Trans. Principal Engineer	(860)594-3180
Delaware	Douglas E. Finney	Asst. Bridge Design Engineer	Dfinney@mail.dot.state.de.us
Florida	Peter Lai	Asst. State Geot. Engineer	pwlai@ttn.net
	FL Sastry Putcha	State Construction Geot. Engr.	
	FL Chandra Samakur	District 2 Geot. Engineer	Chandra.samakur@dot.state.fl.us
	FL D. Miro	District 4 Geot. Engineer	(954) 475-4102
	FL F. Tejjidor	Dist. Turnpike Geot. Engr.	Ftejjidor@pbsi.com
Georgia	Thomas Scruggs	Geotechnical Engineer	Thomas.Scruggs@dot.state.ga.us
Hawaii	Clarence Miyashiro	State Geot. Engineer	Hdotlab@aloha.net
Idaho	R. M. Smith	Asst. M&R Engineer	Bsmith@itd.state.id.us
Illinois	Emile Samara	Chief Found. & Soil Engr.	Samara.em@mt.dot.state.il.us
Indiana	Steve Morris	Geot. Engr. Group Leader	(317)232-5280
Iowa	Frank M. Russo	Special Projects Engineer	frusso@max.state.ia.us
	IA Bob Stanley	Soil Design Engineer	Rstanley1@max.state.ia.us
Kansas	J. J. Brennan /	Soil Engineer	Brennan@ksdot.org
	G. R. Koontz	Chief Geologist	
Kentucky	Darrin Beckett	Geotechnical Engineer	Dbeckett@mail.kvtc.state.kv.us
	KY W. H. Phillips	Transp. Engr. Specialist	Hphillips@mail.kvtc.state.kv.us
Louisiana			
Maine	Laura Krusinski	Geotechnical Design Engineer	Laura.Krusinski@state.me.us
	ME John E. Buxton	Engr. & Design Manager	John.buxton@state.me.us
Maryland			
Massachusetts	Nabil Hourani	Geotechnical Engineer	Nabil.m.hourani@state.ma.us
Michigan			
Minnesota	Donald J. Flemming	State Bridge Engineer	Don.flemming@dot.state.mn.us
Mississippi			
Missouri			
Montana	W. Fullerton	Bridge Design Engineer	Wfullerton@state.mt.us
Nebraska	Omar Qudus	Geotechnical Engineer	Oqudus@dot.state.ne.us
Nevada			
New Hampshire	Mark Whitemore	Chief Design Engineer	N18mdw@dot.state.nh.us
New Jersey			
New Mexico			
New York	Don Arcari	Associate Soil Engineer	Darcari@gw.dot.state.ny.us
North Carolina	N. Abar	Soil Engineer	Nabaral@dot.state.nc.us
North Dakota	Tim Schwagler	Structural Management Engr.	(701)328-4421
	ND Blane Hoesel	Geotechnical Coordinator	Bhoesel@state.nd.us
Ohio			
Oklahoma			
Oregon	Jan Six	Geotechnical Engineer	Jan.L.Six@dot.state.or.us
Pennsylvania	Scott Christie	Chief Bridge Engr.	Rschristie@hotmail.com
Rhode Island	U. Dash	Bridge QA Engr.	Udash@dashes.com
South Carolina	Tim Adams	Bridge Geot. Engineer	Adamstn@dot.state.sc.us
South Dakota			
Tennessee	M. Leonard Oliver	Civil Engineering Manager	Loliver@mail.state.tn.us
Texas	George Odom	Geotechnical Engineer	Godom@dot.state.tx.us
Utah	Jon Bischoff	Geotechnical Engineer	(801)965-4320
Vermont	Chris Benda	Soil & Foundations Engr.	Chris.benda@state.vt.us
Virginia			
Washington	James Cuthbertson	Chief Foundation Engr.	Cuthbej@wsdot.wa.gov
Washington D.C.			
West Virginia			
Wisconsin			
Wyoming	Mike Hager /	Chief Engineering Geologist	Mhager@missc.state.wy.us
	Gregg Fredrick	Asst. State Bridge Engr.	Gfredr@missc.state.wy.us
FHWA-EFLHD	William W. Bassett	Supervisory Geot. Engr.	William.basssett@fhwa.dot.gov

## 2.2 Summary - Design and Construction Practices

### 2.2.1 General

Section 2.1 presented the questionnaire that was developed and distributed. A table summarizing the responding states as of 9/30/99 was also included.

A total of 45 surveys were returned and analyzed (43 states and 2 FHWA personnel). The analysis of the survey is presented below.

### 2.2.2 FOUNDATION ALTERNATIVES

14% of Responders primarily used shallow foundations, 75% used driven pile foundations, and 11% used drilled shaft foundations. Of those responding, 64% prefer driven pile foundations, as compared to 5% preferring drilled shaft foundations. Of those responders using driven piles, 21% primarily used prestressed concrete pile, 52% used steel H piles, 2% used open-ended steel pipe piles, and 25% used closed-end steel pipe piles.

### 2.2.3 DRIVEN PILES - Design Considerations

1. The most common methods for evaluating the static axial capacity of driven piles were: 59% for the  $\alpha$  - method (Tomlinson, 1987), 25% for the  $\beta$  - method (Esrig & Kirby, 1979), 5% for the  $\gamma$  - method (Vijayvergiya and Focht, 1972), 75% for Nordlund's method (Nordlund, 1963), 5% for Nottingham and Schmertmann's method for CPT (1975), 9% for Schmertmann's method for SPT (Sharp, 1987), 14% for Meyerhof's method (1976) modified by Zeitlen and Paikowsky (1982), and 25% for in-house methods and other less common methods. Of the computer programs used in design, 39% were developed in-house, 75% came from the FHWA and 20% from commercial vendors.
2. The most common dynamic geotechnical methods used in pile driving included: 45% using the ENR formula, 16% using Gates's equation with safety factors ranging from 2.0 to 3.5, and one (1) State using it's own dynamic formula. Wave Equation Analysis using the program GRLWEAP was used by 80% of the respondents.
3. Of the primary parameters used in design, 86% used SPT-N values, 11% used CPT data, 2% used Dilatometer data, and 77% used friction angle ( $\phi$ ) and cohesion ( $c$ ). None of the respondents reported the use of Pressuremeter data.
4. The friction angle ( $\phi$ ) and cohesion ( $c$ ) determined from laboratory testing were from Triaxial test, Direct shear test and Unconfined compression test. The In-situ tests primarily were the SPT, and less than 10% states use CPT, DMT, Vane shear test, or others.
5. The majority (more than 50%) of States used Tomlinson's method to assess the side friction coefficient in cohesive soil ( $C_A$  - adhesion), and Nordland's method in cohesionless soil ( $\delta$  - interfacial friction angle).
6. For the methodology currently used for geotechnical and structural design, 93% used Allowable Stress Design (ASD), 37% used AASHTO Load

Factor Design (LFD), and 30% used AASHTO Load and Resistance Factors Design (LRFD).

7. For those respondents using the allowable stress design (ASD) to evaluate capacity, 95% used a global safety factor ranging from 2.0 to 3.0 depending on construction control, 5% used partial safety factors with 1.5 to 2.0 for Side Friction and 3.0 for End Bearing.
8. 48% considered pile settlement in the design with tolerable settlement ranging from 0.25-1.0 inches.
9. 34% used simplified methods (e.g., Broms, 1964) in the lateral pile design methods and/or computer programs, and 88% used methods based on p-y curves.

Of the computer programs used in design, 14% were In-House, 82% were from the FHWA and 55% came from Commercial vendors.

10. In designing piles subjected to lateral load, the tolerable deflection was most often taken to lie between 0.25 to 2.0", and the lateral pile capacity safety factors ranged from 1.5 to 3.0.
11. 25% of the respondents did not consider downdrag forces in design.
12. 48% did not take into account the construction method in design.
13. The estimated risk or failure probability of the group foundation design based on the safety factor used: 27% were less than 0.1%, 4% were between 0.1 to 1%, one percent (1%) of the responses were between 1% to 10%, and 67% were unknown. The assessment for the acceptable maximum failure probability ranged from about zero (0) to 1%.
14. 14% of respondents had experienced pile failure.

#### 2.2.4 *DRIVEN PILES - Construction Considerations*

1. 77% performed static pile load test during construction, and the primary test method was the Quick Method.
2. 84% performed dynamic pile load test during construction, and about 1% to 10% of piles per bridge were usually subjected to dynamic load testing.
3. All of respondents performing dynamic load testing (86% of responses) used the PDA by GRL.
4. When setting production pile length and driving criteria, 82% used the End of Initial Driving conditions, and 52% used the Beginning of Redriving conditions.
5. 36% did not consider pile freeze or relaxation effects in determining driving criteria.

#### 2.2.5 *DRILLED SHAFTS - Design Considerations*

1. Of the design methods used in drilled shaft design, 36% used the  $\alpha$  - Method (Total Stress Approach) (Reese and O'Neill, 1998; Kulhawy, 1989), 41% used the  $\beta$  - Method (Effective Stress Approach) (Reese and O'Neill, 1988), 9% used the Reese and Wright (1977) approach for side friction in cohesionless soils, 39% used the FHWA (O'Neill, 1996) approach for intermediate geomaterials (soft rock), 11% used Carter and

Kulhawy's (1988) approach for intermediate geomaterials (soft rock), and 27% used other methods.

Of the computer programs used in design, 18% were developed In-House, 50% came from the FHWA, 29% from Commercial vendors, and 20% from others.

2. Of the primary parameters used in drilled shaft design, 70% were SPT-N values, 7% were from the CPT test, 2% were Pressuremeter Data, 2% were Dilatometer Data, and 68% were Friction Angle ( $\phi$ ) and Cohesion (c). 27% were obtained by other methods.
3. The friction angle ( $\phi$ ) and cohesion (c) or rock shear strength determined from Laboratory Testing were from the Triaxial test, Direct shear test and Unconfined compression test. The in-situ tests used were primarily the SPT, with less than 10% of States using the CPT, DMT, Vane Shear test, or others.
4. Of the 16% considering the roughness of the bore hole wall in rock socket design, all did so by assumption.
5. For the methodology currently used for geotechnical and structural design of drilled shafts, 86% used Allowable Stress Design (ASD), 32% used AASHTO Load Factor Design (LFD), and 25% used AASHTO Load and Resistance Factors Design (LRFD).
6. In the allowable capacity ASD methodology, 90% used global safety factors ranging from 2.0 to 3.0 depending on construction control, 10% used partial safety factors with 1.5 to 3.0 for side friction and 2.0 to 3.0 for end bearing.
7. 61% considered shaft settlement in the design process, with tolerable settlements ranging from 0.25 inches to 2.0 inches.
8. 27% used Simplified (e.g., Broms, 1964) lateral drilled shaft design methods and/or computer programs, and 82% used methods based on p-y curves.
9. In designing drilled shaft subjected to lateral load, the tolerate deflection ranging from 0.25 to 2.0", and the safety factor of lateral pile capacity ranging from 1.5 to 3.0.
10. 45% of respondents did not consider downdrag force in design.
11. 30% of respondents did not take into account the construction method in design.
12. Of the estimated risk or failure probability of group foundation designs based on the safety factor used, 20% were less than 0.1%, 7% were between 0.1 to 1%, 2% were between 1 to 10%, and 71% were unknown. The assessment for the acceptable maximum failure probability was from about zero (0) to 5%.

#### 2.2.6 DRILLED SHAFTS - Construction Considerations

1. 66% performed static load testing during construction.
2. The type of load test used included 32% that used conventional static load testing, 43% used an Osterberg Load Cell, 11% used the Statnamic Load Test, and 7% used Dynamic Load testing.

3. The method of excavation usually used in drilled shaft installation by respondents included 64% using Dry methods, 52% using Wet methods, and 86% using Casing methods.
4. For the drilling slurry used during construction, 25% used a Mineral Slurry of Processed Attapulgite, 52% used a Mineral Slurry of Bentonite Clays, and 36% used Synthetic Polymer slurries.
5. A majority of the States responding used AASHTO Specifications for shaft cleanliness, which requires more than 50% of base to have less than 0.5 inches of sediment, and the maximum sediment thickness to be less than 1.5 inches.
6. 54% performed inspection of the shaft bottom, in which only one State has specific inspection device. The rest performed inspection by using manual probes or an underwater camera and camcorder.
7. 16% did not perform integrity testing for drilled shaft quality control, 64% used Cross Sonic Logging (CSL), 7% used Surface Reflection (Pulse Echo Method), and 7% Gamma Ray or NX coring.



**DRILLED SHAFT ALTERNATIVE/DESIGN CONSIDERATION**  
**Design method and/or computer program used for drilled shaft design**

STATE	$\alpha$ Method	$\beta$ Method	Reese et al	FHWA	Carter et al	Others
AL						
AK						
AZ		*		*	*	
AR						*(AASHTO)
CA	*					
CO	*					
CT						*(Horvath & Kenny)
DE						NO SHAFT
FL		*		*		
GA				*		
HI						NO SHAFT
ID				*		
IL	*	*			*	*(Horvath & Kenny)
IN						
IA				*		*(AASHTO)
KS	*	*				
KY						*
LA	*	*				
ME		*				*(ASSHTO, H&K)
MD						For noise wall
MA	*	*		*	*	*(Zhang & Einstein)
MI	*	*				
MN		*		*		
MS						
MO						*(No end bearing)
MT	*	*		*	*	
NE				*		
NV	*	*				
NH		*				
NJ	*		*	*		
NM			*			
NY			*			
NC				*	*	
ND						NO SHAFT
OH				*		
OK						*
OR	*	*		*		
PA			*			
RI						
SC	*	*		*		
SD						*
TN	*	*		*		
TX						*
UT	*	*		*		
VT						NO SHAFT
VA/FHWA				*		*
WA	*	*				
DC						
WV						
WI	*	*				
WY						*(Modified Nordland)

**DRILLED SHAFT ALTERNATIVE/DESIGN CONSIDERATION**  
**Development of computer programs for axial load design**

STATE	In-House	FHWA	Commercial	Others	
AL					
AK					
AZ		*			
AR		*			
CA	*				
CO		*	*		
CT				*	
DE				*	
FL	*				
GA		*			
HI					
ID		*	*		
IL	*				
IN					
IA	*				
KS		*			
KY		*			
LA			*		
ME	*	*	*		
MD		*			
MA		*	*		
MI				*	
MN		*	*		
MS					
MO				*	
MT		*	*		
NE			*		
NV		*	*		
NH		*	*		
NJ				*	
NM					
NY		*			
NC		*	*		
ND					
OH		*	*		
OK		*			
OR			*		
PA				*	
RI					
SC		*			
SD				*	
TN		*			
TX	*				
UT	*	*			
VT					
VA/FHWA				*	
WA		*			
DC					
WV					
WI				*	
WY	*				

# DRILLED SHAFT ALTERNATIVE/DESIGN CONSIDERATION

## Primary parameters used in design and/or computer program

STATE	SPT-N	CPT	Pressuremeter	Dilatometer	C and $\phi$	Others
AL						
AK						
AZ	*				*	
AR	*				*	
CA					*	
CO	*				*	
CT						*(RQD, qu)
DE						
FL	*			*		*(RQD, qu,qt)
GA	*					
HI						
ID	*	*			*	
IL	*				*	*(RQD, Recov)
IN						
IA	*				*	*(qu)
KS	*		*		*	
KY	*				*	
LA	*				*	
ME	*				*	*(qu)
MD	*				*	
MA	*				*	*(qu)
MI	*				*	
MN						*(qu)
MS						
MO					*	*
MT	*				*	
NE	*				*	*(qu)
NV	*				*	
NH	*				*	
NJ	*	*				
NM						
NY					*	
NC	*				*	
ND						
OH	*				*	
OK	*	*				
OR	*				*	
PA	*				*	
RI						
SC	*				*	
SD						
TN	*				*	
TX						*
UT	*				*	
VT						
VA/FHWA						*(qu)
WA	*				*	
DC						
WV						
WI	*				*	*(qu)
WY	*				*	

**DRILLED SHAFT ALTERNATIVE/DESIGN CONSIDERATION**  
**Determination of friction angle ( $\phi$ ) and Cohesion (C)**

STATE	Laboratory Testing	In-situ Testing
AL		
AK		
AZ	DS	SPT
AR		SPT, RQD
CA	UU, Pocket Penet.	SPT
CO	qu	SPT
CT	qu	
DE	-	
FL	qu, qt	SPT
GA	-	
HI	-	
ID	Triaxial, DS	SPT, CPT
IL	*	
IN		
IA	Triaxial, qu	SPT, Load test
KS	qu	
KY	Triaxial, UU	SPT
LA	Triaxial, UU	SPT
ME	qu	SPT
MD	-	
MA	Point load, qu	SPT
MI	qu	SPT
MN	-	
MS		
MO	DS	SPT
MT	DS, qu	SPT
NE	qu	
NV	DS, Triaxial	
NH	qu	SPT
NJ	-	
NM		
NY	qu	
NC	*	*
ND		
OH		SPT
OK	-	
OR	Triaxial	SPT
PA	*	*
RI		
SC	Triaxial, qu	SPT
SD	DS	
TN	Triaxial	SPT
TX		Texas Cone
UT	Triaxial	SPT, CPT, Vane shear
VT	-	
VA/FHWA	qt	
WA	UU	SPT
DC		
WV		
WI	DS, Triaxial, qu, in-house rock shear	
WY	qu	SPT

**DRILLED SHAFT ALTERNATIVE/DESIGN CONSIDERATION**  
**Consideration of borehole wall roughness in rock socket design**

STATE	No	Yes/Assumption	Yes/Measurement		
AL					
AK					
AZ	*				
AR	*				
CA	*				
CO	*				
CT	*				
DE					
FL		*			
GA	*				
HI					
ID	*				
IL	*				
IN					
IA		*			
KS	*				
KY		*			
LA	*				
ME		*			
MD	*				
MA		*			
MI	*				
MN	*				
MS					
MO	*				
MT	*				
NE	*				
NV	*				
NH	*				
NJ	*				
NM					
NY		*			
NC	*				
ND					
OH	*				
OK	*				
OR	*				
PA		*			
RI					
SC	*				
SD	*				
TN	*				
TX	*				
UT	*				
VT					
VA/FHWA	*				
WA	*				
DC					
WV					
WI	*				
WY	*				

**DRILLED SHAFT ALTERNATIVE/DESIGN CONSIDERATION**  
**Methodology currently being used for geotechnical and Structure design**

STATE	ASD	LFD	LRFD	Others	
AL					
AK					
AZ	*	*			
AR	*				
CA	*				
CO	*	*	*		
CT	*		*		
DE					
FL	*	*	*		
GA	*				
HI	*				
ID	*		*		
IL	*				
IN	*				
IA	*	*			
KS	*		*		
KY	*	*			
LA	*				
ME	*				
MD		*			
MA	*	*	*		
MI		*			
MN	*	*	*		
MS	*				
MO	*	*			
MT	*				
NE	*				
NV	*				
NH	*				
NJ	*		*		
NM					
NY	*				
NC	*				
ND					
OH	*				
OK	*				
OR	*	*	*		
PA		*	*		
RI					
SC	*				
SD	*				
TN	*				
TX	*				
UT	*				
VT					
VA/FHWA	*				
WA		*	*		
DC					
WV					
WI	*				
WY	*	*			

# **DRILLED SHAFT ALTERNATIVE/DESIGN CONSIDERATION**

**Apply partial safety factor for side friction and end bearing on allowable shaft capacity**

STATE	No/ Global F.S.	Yes/Side friction/End Bearing
AL		
AK		
AZ		* 2.0 / 3.0
AR	* 2.5	
CA	* 2.0	
CO	* 3.0	
CT	* 2.0 w/ Load Test	
DE	-	
FL	* 2.5	
GA	* 2.0 to 3.0	
HI	-	
ID	* 3.0	
IL	* 3.0	
IN	* >2.0	
IA	-	
KS	-	
KY	*	
LA	* 3.0	
ME		* 3.0 / 2.0
MD	* 2.5	
MA	* 2.5 w/ load test	
MI	* 2.0 to 2.5	
MN	* 2.0	
MS		
MO	* 2.5 to 3.0	
MT	* 2.0 to 3.0	
NE	* 2.0	
NV	* 2.5	
NH	* 2.5 to 3.0	
NJ	* 3.0	
NM		
NY	* 2.0	
NC		* 2.0 / 3.0
ND	-	
OH	* 3.0	
OK	-	
OR	* 2.0 (Rock), 2.5 (Soil)	
PA	-	
RI		
SC	* 3.0	
SD		* 2.0 / No end bearing
TN	* 2.0 to 2.5	
TX	* 2.0	
UT	* 2.5	
VT	-	
VA/FHWA	*	
WA	* 2.5 to 3.0	
DC		
WV		
WI	* 2.0 to 3.0	
WY		* 1.5 / 2.0

**DRILLED SHAFT ALTERNATIVE/DESIGN CONSIDERATION**  
**Consider drilled shaft settlement in design**

STATE	No	Yes/Tolerable settlement	
AL			
AK			
AZ		* 1.0"	
AR		* AASHTO 4.4.7.2.5	
CA	*		
CO	*		
CT		* 0.25"	
DE		-	
FL		* 1.0"	
GA		* 0.5"	
HI		-	
ID	*		
IL	*		
IN			
IA		* Varies, typically 0.5"	
KS	*		
KY	*		
LA		* 0.5" @ 1.5 design load, 1" @ 2 design load	
ME		* 1.0 to 1.5"	
MD	*		
MA		* 5% Shaft Dia. In soils	
MI	*		
MN	*		
MS			
MO	*		
MT		* 1.0"	
NE		* 0.4"	
NV		* 1.0"	
NH		* Load transfer in rock socket	
NJ	*		
NM			
NY		* < 2.0"	
NC		*	
ND			
OH		* 0.5"	
OK			
OR		* Structure dependent	
PA	*		
RI			
SC		* Determined by structural engineer	
SD	*		
TN		* 0.25"	
TX	*		
UT		* Project dependent, typically <25mm	
VT			
VA/FHWA	*		
WA		* < 25mm	
DC			
WV			
WI	*		
WY	*		



# **DRILLED SHAFT ALTERNATIVE/DESIGN CONSIDERATION**

## **Design method and/or program for lateral load analysis**

STATE	Simply Method (Broms)	p-y Curve Method	Others
AL			
AK			
AZ	*	*	
AR		*	
CA		*	
CO	*	*	
CT		*	
DE		*	
FL		*	
GA		*	
HI			
ID	*	*	
IL	*	*	
IN			
IA		*	
KS		*	
KY		*	
LA		*	
ME		*	
MD		*	
MA	*	*	
MI	*	*	
MN		*	
MS			
MO		*	
MT		*	
NE		*	
NV		*	*
NH	*	*	
NJ		*	
NM			
NY	*	*	
NC		*	
ND			
OH		*	
OK			
OR		*	
PA	*	*	
RI			
SC		*	
SD			
TN	*	*	
TX		*	
UT		*	
VT			
VA/FHWA	*		
WA		*	
DC			
WV			
WI	*		
WY		*	

**DRILLED SHAFT ALTERNATIVE/DESIGN CONSIDERATION**  
**Development of computer programs for lateral load analysis**

STATE	In-House	FHWA	Commercial	Others	
AL					
AK					
AZ		*			
AR		*			
CA	*	*	*		
CO	*	*	*		
CT		*			
DE					
FL	*				
GA		*			
HI					
ID		*			
IL	*	*			
IN					
IA		*			
KS		*			
KY		*			
LA		*			
ME		*	*		
MD		*			
MA		*	*		
MI	*	*			
MN		*	*		
MS					
MO		*			
MT		*	*		
NE			*		
NV		*	*		
NH		*	*		
NJ		*		*	
NM					
NY		*			
NC		*	*		
ND					
OH		*	*		
OK					
OR		*	*		
PA		*			
RI					
SC		*	*		
SD					
TN		*			
TX		*			
UT			*		
VT					
VA/FHWA		*			
WA		*	*		
DC					
WV					
WI				*	
WY			*		

## **DRILLED SHAFT ALTERNATIVE/DESIGN CONSIDERATION**

### **Control factors of drilled shaft design subjected to lateral load**

STATE	Lateral Deflection/Tolerate Deflection	Lateral Capacity/Method used/Safety factor
AL		
AK		
AZ	* 1.0"	* 2.0
AR		* 2.5
CA	*	*
CO	* Varies	* Varies
CT	* Structure dependent	
DE		
FL	* 2.0"	
GA	*	
HI		
ID	* 0.25"	
IL	*	*
IN		
IA		* Structural reinforcement
KS		* 3.0
KY	* 0.5"	
LA	*	*
ME	* 1" or as directed by structural engineer	* 2.5
MD	* 0.5"	* 2.5
MA	Project dependent	* 1.5
MI	* Varies	
MN	* Determined by structural engineer	
MS		
MO		* 2.5
MT	* Structure dependent, typically <50 mm	
NE	* Structure dependent	
NV	* 1.0"	
NH	* Structure dependent	
NJ	* 0.5"	
NM		
NY	* 1.0"	
NC	* 1.0"	
ND		
OH	* Project dependent	
OK		
OR	* Structure dependent, typically <1.0"	*
PA	* 0.5"	
RI		
SC	* 2.0" from free head condition	
SD		* Point of fixity method
TN		*
TX	* 0.5"	
UT	* Determined by structural engineer	
VT		
VA/FHWA	* .5"	
WA	* Structure dependent	*
DC		
WV		
WI	*	
WY	* 2.0"	

# **DRILLED SHAFT ALTERNATIVE/DESIGN CONSIDERATION**

## **Consideration of downdrag force in design**

STATE	No	Yes/Methodology		
AL				
AK				
AZ		* FHWA		
AR	*			
CA	*			
CO	*			
CT	*			
DE				
FL		*		
GA	*			
HI				
ID		* $\alpha$ method		
IL		*		
IN	*			
IA	*			
KS		* FHWA, DM-7, Poulos and Daves		
KY		* DM-7		
LA	*			
ME	*			
MD	*			
MA		* DM-7		
MI	*			
MN		* Neutral plane		
MS				
MO	*			
MT	*			
NE		*		
NV		* $\alpha$ method		
NH		*		
NJ		*		
NM				
NY		*		
NC		*		
ND				
OH		*		
OK				
OR		* $\alpha$ method		
PA	*			
RI				
SC	*			
SD	*			
TN	*			
TX	*			
UT		* Fellenios		
VT				
VA/FHWA		*		
WA		*		
DC				
WV				
WI	*			
WY	*			

**DRILLED SHAFT ALTERNATIVE/DESIGN CONSIDERATION**  
**Consideration of construction method in design**

STATE	No	Yes		
AL				
AK				
AZ		*		
AR		*		
CA		*		
CO		*		
CT	*			
DE				
FL		*		
GA	*			
HI				
ID	*			
IL		*		
IN				
IA		*		
KS	*			
KY		*		
LA		*		
ME		*		
MD	*			
MA		*		
MI		*		
MN		*		
MS				
MO		*		
MT	*			
NE		*		
NV		*		
NH		*		
NJ		*		
NM				
NY		*		
NC		*		
ND				
OH	*			
OK				
OR		*		
PA		*		
RI				
SC	*			
SD	*			
TN	*			
TX	*			
UT		*		
VT				
VA		*		
WA		*		
DC				
WV				
WI	*			
WY	*			

**DRILLED SHAFT ALTERNATIVE/DESIGN CONSIDERATION**  
**Estimated risk or failure probability based on the safety factor used**

STATE	<0.1%	0.1 to 1%	1 to 10 %	>10%	Unknown	Acceptable %
AL						
AK						
AZ					*	0.1
AR					*	~0
CA					*	
CO	*				*	1.0
CT						
DE						
FL					*	1.0
GA					*	1.0
HI						
ID					*	
IL	*					0.1
IN						
IA					*	
KS	*					~0
KY			*			
LA					*	
ME		*				5.0
MD					*	
MA					*	1.0
MI		*				
MN					*	
MS						
MO					*	
MT					*	0.1 – 1.0
NE					*	0.1
NV					*	
NH					*	
NJ					*	
NM						
NY					*	
NC					*	
ND						
OH	*					
OK					*	
OR	*					0.1
PA	*					
RI					*	
SC						
SD	*					
TN	*					
TX	*					0.1
UT					*	0.1
VT						
VA/FHWA					*	
WA		*				0.5
DC						
WV						
WI					*	
WY					*	

**DRILLED SHAFT ALTERNATIVE/CONSTRUCTION CONSIDERATION**  
**Perform static load test during construction**

STATE	No	Yes/Criteria to justify	
AL			
AK			
AZ	*		
AR		* Failure of cross sonic logging	
CA		* Possible shaft defect	
CO		* Potential saving or difficult to predict	
CT		* Cost saving	
DE			
FL		*	
GA		* Friction shaft in soil or rock type previously not tested	
HI			
ID	*		
IL		* Major project	
IN			
IA		* Design phase for database	
KS	*		
KY		* Critical bridge	
LA		* Need to be verified	
ME		* Cost saving	
MD	*		
MA		* Cost saving, verify capacity	
MI		*	
MN	*		
MS			
MO		*Very rarely, only on big project w/ cost saving	
MT	*		
NE	*		
NV	*		
NH	*		
NJ		* Quality control	
NM			
NY		* High load, unknown soil conditions	
NC		*	
ND			
OH	*		
OK	*		
OR	*		
PA		*	
RI			
SC		* As necessary	
SD			
TN	*		
TX		*	
UT		*	
VT			
VA/FHWA		*	
WA	*		
DC			
WV			
WI	*		
WY		*	

# DRILLED SHAFT ALTERNATIVE/CONSTRUCTION CONSIDERATION

## Type of load test performed during construction

STATE	Conventional/Static	Osterberg	Statnamic	Dynamic	Others
AL					
AK					
AZ	*				
AR				* Controlled drop weight	
CA	*	Occasionally	Occasionally		
CO	*				
CT		*			
DE					
FL	*	*	*		
GA		*			
HI					
ID					
IL		*			
IN					
IA				* Controlled drop weight	
KS	*				
KY		*			
LA		*			
ME		*			
MD					
MA	*	*			
MI		*			
MN		* (1)			
MS					
MO	*	*	*		
MT					
NE					
NV		* (1)			
NH					
NJ		*			
NM					
NY	*	*(>700 tons)			
NC		*	*		
ND					
OH					
OK					
OR					
PA		*		*	
RI					
SC	*	*			
SD					
TN					
TX	*				
UT	*		*		
VT					
VA/FHWA	*				
WA					
DC					
WV					
WI	*				
WY	*	*			



**DRILLED SHAFT ALTERNATIVE/CONSTRUCTION CONSIDERATION**  
**Methods of shaft excavation used during installation**

STATE	Dry	Wet	Casing	Others	
AL					
AK					
AZ	*	*	* Temporary		
AR	*	*	*		
CA	*	*	*		
CO	*		* Temporary		
CT			*		
DE					
FL		*	*		
GA	*	*			
HI					
ID	*		*		
IL	*	*	*		
IN					
IA	*	*	*		
KS	*	*	*		
KY	*	*	*		
LA	*	*	*		
ME			* Permanent		
MD	*		*		
MA	*	*	*		
MI	*		* Permanent		
MN			*		
MS					
MO			*		
MT		*	*		
NE			* Permanent		
NV	*		* Temporary		
NH		*	*		
NJ		*	* Permanent		
NM					
NY	*		*		
NC	*	*	*		
ND					
OH	*	*	*		
OK	*		*		
OR	*	Rarely	*		
PA	*	*	*		
RI					
SC	*	*	*		
SD	*	*	*		
TN	*		*		
TX	*	*	*		
UT	*	*	*		
VT					
VA/FHWA	*	*	* Temporary		
WA					
DC		*	*	Oscillator	
WV					
WI			* Permanent		
WY	*		* Temporary		

# **DRILLED SHAFT ALTERNATIVE/CONSTRUCTION CONSIDERATION**

## **Type of slurry used during shaft installation**

STATE	Mineral/Processed Attapulgite	Mineral/Bentonite	Synthetic Polymers	Others
AL				
AK				
AZ	*	*		
AR		*	*	
CA	*	*	*	
CO	*	*	*	
CT	*	*	*	
DE				
FL	*			
GA		*		
HI				
ID				
IL		*		
IN				
IA			*	
KS		*	*	
KY	*	*	*	
LA	*	*	*	
ME				
MD				
MA		*	*	
MI			*	
MN		*		
MS				
MO	*	*		
MT			*	
NE		*		
NV	*			
NH		*	*	
NJ		*		
NM				
NY		*		
NC		*		
ND				
OH		*	*	
OK				
OR	*		*	
PA		*		
RI				
SC		*		
SD				
TN				
TX		*		
UT		*	*	
VT				
VA/FHWA	*		*	
WA				
DC				
WV				*
WI				*
WY				*

# **DRILLED SHAFT ALTERNATIVE/CONSTRUCTION CONSIDERATION**

## **Requirement of shaft cleanliness**

STATE		
AL		
AK		
AZ	* FHWA Specification	
AR	* 1% sand content of polymer slurry	
CA	* Cleanness of slurry for wet method, visual inspection for dry method	
CO	-	
CT	* <1.5 to 2 " sediment on bottom	
DE		
FL	* More than 50% of base <0.5", max. 1.5" sediment	
GA	* More than 50% of base <0.5", max. 1.5" sediment	
HI		
ID	* <2% sediment for end bearing shaft, <6" for friction shaft	
IL	*	
IN		
IA	* More than 50% of base <15mm, max. 35 mm sediment	
KS	* Visual inspection	
KY	* <0.5" sediment	
LA	* <0.5" for end bearing shaft, <2" for friction shaft	
ME	* More than 50% of base <0.5", max. 1.0" sediment	
MD		
MA	* <0.5" sediment on bottom, <4% sand in slurry	
MI	* <1" sediment on bottom	
MN	*	
MS		
MO	* Approved by engineer	
MT	* No standard specification	
NE	* Shaft has to be dry and clean	
NV	* Sand content <4% in slurry	
NH	* More than 50% of base <0.5", max. 1.5" sediment, AASHTO	
NJ	* Visual Inspection	
NM		
NY	*	
NC	* <1" sediment on bottom	
ND		
OH	* To be cleaned	
OK		
OR	* <50 mm for end bear shaft, < 150 mm for friction shaft	
PA	*	
RI		
SC	* < 0.5" sediment on bottom	
SD	* As approved by engineer	
TN	* No loose on bottom	
TX	* 10% max. sand content in slurry	
UT	* AASHTO	
VT		
VA		
WA	* <50 mm for end bearing shaft, <150 mm for friction pile	
DC		
WV		
WI	*	
WY	* Visual inspection ( very subjective)	

# **DRILLED SHAFT ALTERNATIVE/CONSTRUCTION CONSIDERATION**

## **Type of shaft inspection device for shaft bottom**

STATE	No	Yes	
AL			
AK			
AZ	*		
AR		* Manual probe	
CA	*		
CO	*		
CT		* Manual probe	
DE			
FL		* SID	
GA	*		
HI			
ID		* Manual probe	
IL			
IN			
IA		* Manual probe, camcorder	
KS	*		
KY		* Manual probe	
LA		* Manual probe	
ME		* Manual probe, underwater camera/video	
MD	*		
MA		* Manual probe	
MI		* Manual probe	
MN	*		
MS			
MO		* Camcorder, underwater inspection	
MT	*		
NE	*		
NV	*		
NH		* Underwater camera, downhole inspection if possible	
NJ	*		
NM			
NY		* Manual probe	
NC		* Manual probe	
ND			
OH	*		
OK	*		
OR		* Manual probe	
PA		* Camera	
RI			
SC		* Manual probe	
SD		* Manual probe	
TN		* Downhole visual inspection	
TX	*		
UT	*		
VT			
VA/FHWA	*		
WA	*		
DC			
WV			
WI	*		
WY	*		

# **DRILLED SHAFT ALTERNATIVE/CONSTRUCTION CONSIDERATION**

## **Type of integrity testing for drilled shaft quality control**

STATE	No	Cross Sonic Logging	Surface Reflection	Others	% Shaft tested
AL					
AK					
AZ		*		* Gamma Ray	100%
AR		*			100%
CA		*		* Gamma Ray	
CO		*	*		Only suspect
CT		*			10 to 20%
DE					
FL		*			?
GA		*			<5%
HI					
ID	*				
IL		*			Very small %
IN		*			100%
IA		*			100%
KS	*				
KY		*			<5%
LA		*			100%
ME		*			100%
MD	*				
MA		*	*		On 100% uncased
MI	*				
MN	*				
MS					
MO		*	*	NX coring	Project dependent
MT		*			~15%
NE	*				
NV		*			80%
NH		*(2 projects)			15 – 40%
NJ		*			100%
NM					
NY		*			100%
NC		*			100%
ND					
OH		*			1%
OK					
OR		*			1 / bent
PA	*				
RI					
SC		*			100% if 2 shafts/bent
SD		*			10%, 1 / bent
TN		*			~50%
TX		*			
UT		*			
VT					
VA					
WA					~50%
DC					
WV					
WI					
WY					

**FOUNDATION ALTERNATIVE**  
**% of foundation types used for bridge structure?**

STATE	Shallow Foundation	Driven Pile	Drilled shaft	Others	Deep Found.	Remarks
AL						
AK						
AZ	30	5	65		70	
AR	25	73	1	1	75	
CA	5	70	25		95	
CO	10	40	50		90	
CT	75	23	1	1	25	
DE	50	50	-		50	
FL	-	70	30		100	
GA	10	85	5		90	
HI	?	?	?			
ID	>15	80	<5		85	
IL	15	65	20		85	
IN	5	94	1		95	
IA	<10	>90	<1		90	
KS	35	40	25		65	
KY	50	40	10		50	
LA	-	95	5		100	
ME	68	31	<1		32	
MD	?	?	?			
MA	40	30	20	<1	60	
MI	25	75	<1		75	
MN	10	85	5		90	
MS						
MO	45	45	10		55	
MT	10	60	30		90	
NE	1	96	3		99	
NV	45	20	35		55	
NH	70	25	5		30	
NJ	44	55	1		56	
NM						
NY	37	60	2	1	62	
NC	5	55	40		95	
ND	5	95	-		95	
OH	15	75	10		85	
OK	15	35	50		85	
OR	15	70	15		85	
PA	25	70	5		75	
RI						
SC	5	60	35		95	
SD	5	75	20		95	
TN	45	50	5		55	
TX	-	20	80		100	
UT	5	80	15		85	
VT	60	40	-		40	
VA/FHWA	15	70	15		85	
WA	33	33	33		66	
DC						
WV						
WI	7	90	3		93	
WY	44	41	15		56	

**FOUNDATION ALTERNATIVE**  
**Preferred type of deep foundation**

STATE	Driven Pile	Drilled Shaft	Others		
AL					
AK					
AZ		*			
AR	*				
CA	*	*			
CO	*	*			
CT	*				
DE					
FL	*				
GA	*				
HI	*				
ID	*				
IL	*	*			
IN	*				
IA	*				
KS	*				
KY	*				
LA	*				
ME	*				
MD	*				
MA	*	*			
MI	*				
MN	*				
MS					
MO	*				
MT	*	*			
NE	*				
NV	*	*			
NH	*				
NJ	*				
NM					
NY	*				
NC	*	*			
ND	*				
OH	*	*			
OK	*				
OR	*				
PA	*				
RI					
SC	*	*			
SD	*	*			
TN	*				
TX	*	*			
UT	*				
VT	*	*			
VA/FHWA	*	*			
WA		*			
DC					
WV					
WI	*				
WY	*				

# FOUNDATION ALTERNATIVE

## Preferred type of driven pile

STATE	PSC Pile	Steel H Pile	Steel Pipe Pile/Open	Steel Pipe Pile/closed	Timber Pile	Others
AL						
AK						
AZ	6	1	3	2	6	
AR	1	2	6	3	4	
CA	1	3	2	4	6	
CO	6	1	3	2	6	
CT	4	1	3	2	5	
DE	1	4	6	2	3	
FL	1	4	2	3	6	
GA	1	2	4	3	5	
HI	1	6	6	6	6	
ID	6	1(85%)	6	2(15%)	6	
IL	6	2	6	1	6	
IN						
IA	2	1	6	6	3	
KS	3	1	4	2	6	
KY	2	1	6	6	6	
LA	1	3	2	4	5	
ME	4	1	3	2	6	
MD	5	1	2	3	4	
MA	5	1	3	2	4	
MI	6	1	6	2	3	
MN	5	2	3	1	4 (Ct. Brg.)	
MS						
MO	4	1	6	2	6	3(precast)
MT	6	2	1	4	5	3(monotube)
NE	2	1	4	3	6	
NV	3	2	6	1	6	
NH	4	1	2	3	5	
NJ	3	2	5	1	4	
NM						
NY	3	1	5	2	4	
NC	2	1	3	6	6	4(cyl. Pile)
ND	6	1	6	6	6	
OH	6	2	6	1	6	
OK	6	1	6	6	6	
OR	5	3	2	1	4	
PA	6	1	3	3	6	2(monotube)
RI						
SC	1	2	4	5	3	
SD	5	1	4	3	2	
TN	2	1	3	4	5	
TX	1	3	2	6	6	
UT	6	2	6	1	6	
VT	4	1	5	2	3	
VA/FHWA	2	1	4	3	5	
WA	5	2	3	1	4	
DC						
WV						
WI	6	2	6	1	3	
WY	6	1	6	6	6	



# DRIVEN PILE ALTERNATIVE/DESIGN CONSIDERATION

## Design method for static axial capacity

STATE	$\alpha$	$\beta$	$\gamma$	Nordlund	Nottingham/CPT	Schmertmann/SPT	Meyerhof	Others
AL								
AK								
AZ	*	*		*				
AR	*			*				
CA	*			*(sand)				
CO	*			*				
CT				*				
DE	*			*				
FL						*		
GA				*		*		
HI				*(SPILE)		*(SPT89)		
ID	*			*				
IL								*(in-house)
IN								*(In-house)
IA								
KS	*	*		*				
KY	*	*		*				
LA	*				*			*(in-house)
ME	*			*			*(End-B)	*
MD				*				
MA	*		*	*				
MI	*			*				
MN				*				
MS								
MO				*				
MT	*	*		*	*		*	
NE				*			*	
NV	*	*	*	*				
NH	*			*				
NJ	*			*			*	*(DM-7)
NM								
NY	*	*		*				
NC								*(Vesic)
ND								*(in-house)
OH	*			*			*	
OK	*	*		*				
OR	*	*		*				
PA				*				
RI								
SC	*					*	*	
SD								*
TN	*	*		*				
TX								*(in-house)
UT								*(Fellenios)
VT	*	*		*				
VA/FHWA	*			*				
WA	*	*		*				*(LCPC-cpt)
DC								
WV								
WI	*			*				
WY				*				

**DRIVEN PILE ALTERNATIVE/DESIGN CONSIDERATION**  
**Development of computer program for static capacity analysis by:**

STATE	IN-House	FHWA	Commercial	Others	
AL					
AK					
AZ		*			
AR		*			
CA	*				
CO		*	*		
CT		*			
DE		*			
FL	*				
GA		*			
HI		*			
ID		*	*		
IL	*				
IN					
IA	*				
KS		*			
KY				*	
LA	*	*			
ME	*	*			
MD		*			
MA		*	*		
MI	*				
MN		*			
MS					
MO		*			
MT		*	*		
NE		*			
NV		*	*		
NH		*			
NJ		*			
NM					
NY		*			
NC	*	*			
ND	*				
OH	*	*			
OK		*			
OR	*	*			
PA	*	*	*		
RI					
SC		*			
SD				*	
TN		*			
TX	*				
UT			*		
VT		*			
VA/FHWA		*	*		
WA	*	*	*		
DC					
WV					
WI		*			
WY	*	*			

**DRIVEN PILE ALTERNATIVE/DESIGN CONSIDERATION**  
**Dynamic formula or computer program to estimate pile capacity**

STATE	ENR/F.S.	Gates/F.S.	GRLWEAP	Others	
AL					
AK					
AZ		*3.0	*		
AR	*		*		
CA	*		*		
CO			*		
CT			*		
DE			*		
FL			*		
GA	*		*		
HI			*		
ID			*		
IL	*				
IN					
IA	*(County, City)		*		
KS			*		
KY	*		*		
LA	*	*3.5	*		
ME			*		
MD	*				
MA		*3.5	*		
MI	*		*		
MN	*(Modified)		*(Occasionally)		
MS					
MO	*				
MT	*		*		
NE	*(Modified)		*		
NV			*		
NH			*		
NJ			*		
NM					
NY			*		
NC			*		
ND	*(Modified)				
OH	*		*		
OK		*2.0			
OR		*3.0	*		
PA			*		
RI					
SC			*		
SD	*(Modified)				
TN	*				
TX	*		*		
UT			*		
VT			*		
VA/FHWA		*2.5	*		
WA			*	*(In-house)	
DC					
WV					
WI	*				
WY	*	*2.0	*		

**DRIVEN PILE ALTERNATIVE/DESIGN CONSIDERATION**  
**Primary parameters used in design and/or computer program**

STATE	SPT-N	CPT	Pressuremeter	Dilatometer	C and $\phi$	Others
AL						
AK						
AZ	*				*	
AR	*					
CA					*	
CO	*				*	
CT	*				*	
DE	*					
FL	*					
GA	*					
HI	*					
ID	*	*			*	
IL	*				*	
IN	*				*	
IA	*					
KS	*				*	
KY	*				*	
LA	*	*			*	
ME	*				*	
MD	*				*	
MA	*				*	
MI	*				*	
MN	*				*	
MS						
MO	*				*	
MT	*	*			*	
NE	*					
NV					*	
NH	*				*	
NJ	*				*	
NM						
NY					*	
NC	*				*	
ND	*				*	
OH	*	*			*	
OK	*	*		*		
OR	*				*	
PA	*				*	
RI						
SC	*				*	
SD	-					
TN	*				*	
TX						*(TX Cone)
UT	*				*	
VT	*				*	
VA/FHWA	*				*	
WA						
DC						
WV						
WI	*				*	
WY	*				*	

## DRIVEN PILE ALTERNATIVE/DESIGN CONSIDERATION

### Determination of friction angle ( $\phi$ ) and Cohesion (C)

STATE	Laboratory Testing	In-situ Testing
AL		
AK		
AZ	Direct Shear (DS)	-
AR	-	SPT
CA	UU	SPT, CPT
CO	-	SPT
CT	-	$\phi$ from gradation and relative density
DE	-	-
FL		SPT, CPT, DMT
GA	-	-
HI	Triaxial, Direct shear	
ID	Triaxial, Direct shear	SPT, CPT
IL		Field Remac compression test
IN	UU	-
IA	-	Loads test
KS	CIU, UU, DS	Vane shear, Iowa borehole shear
KY	Triaxial, qu	SPT
LA	Triaxial, qu	SPT
ME	Cu, UU, DS, Torevane, qu	SPT
MD	-	-
MA	Triaxial	SPT
MI	Transverse shear, qu	SPT
MN	UU	SPT
MS		
MO	DS, qu	SPT
MT	DS, qu	SPT
NE	-	SPT
NV	Triaxial, DS	
NH	-	SPT
NJ		SPT
NM		
NY	Triaxial	SPT
NC	*	*
ND	Triaxial, qu	-
OH	-	SPT
OK	DS	SPT
OR	CIU	SPT
PA	*	SPT
RI		
SC	Triaxial	SPT
SD	DS	-
TN	Triaxial, DS, qu	-
TX	Triaxial	-
UT	Triaxial, DS, qu	SPT, Vane shear
VT	Triaxial	Vane Shear
VA/FHWA	Triaxial, DS	-
WA	UU	SPT
DC		
WV		
WI	Triaxial, Ds, qu	-
WY	Triaxial, DS	SPT

# **DRIVEN PILE ALTERNATIVE/DESIGN CONSIDERATION**

**Assess the side friction coefficient**

STATE	$C_A$ for Cohesive Soil	$\delta$ for Cohesionless Soil	
AL			
AK			
AZ	DM-7	DM-7	
AR	FHWA	FHWA	
CA	$\alpha Su$	DM-7	
CO	Su	$\phi$	
CT	Published data		
DE	-	-	
FL	Empirical	Empirical	
GA	Triaxial	SPT	
HI	-	-	
ID	Tomlinson	Nordland	
IL	*		
IN	Tomlinson	Nordland	
IA		Load test	
KS	DM-7	DM-7	
KY	Tomlinson		
LA	-	-	
ME	Tomlinson	Nordland	
MD	-	-	
MA	-	-	
MI	In-House	DM-7	
MN	Tomlinson	Nordland	
MS			
MO	-	-	
MT	Tomlinson	Nordland	
NE	Lab test	SPT	
NV	Tomlinson	Nordland	
NH	Tomlinson	Nordland	
NJ	DM-7	DM-7	
NM			
NY	Tomlinson	Nordland	
NC	-	-	
ND	-	-	
OH	SPT	SPT	
OK	-	-	
OR	Tomlinson	Nordland	
PA	-	-	
RI			
SC	$\alpha Su$	Meyerhof	
SD	-	-	
TN	$\alpha Su$	SPT/FHWA	
TX	C, $\phi$	$\phi$	
UT	Shear test	Shear test	
VT	Tomlinson	Nordland	
VA/FHWA	-	-	
WA	Bowles	Nordland	
DC			
WV			
WI	$\alpha Su$	SPT	
WY	FHWA	FHWA	

**DRIVEN PILE ALTERNATIVE/DESIGN CONSIDERATION**  
**Methodology currently being used for geotechnical and Structure design**

STATE	ASD	LFD	LRFD	Others	
AL					
AK					
AZ	*	*			
AR	*	*			
CA	*				
CO	*	*	*		
CT	*		*		
DE			*		
FL	*	*	*		
GA	*				
HI	*				
ID	*		*		
IL	*				
IN	*				
IA	*				
KS	*		*		
KY	*	*			
LA	*				
ME	*				
MD	*				
MA	*	*	*		
MI		*			
MN	*	*	*		
MS					
MO	*	*			
MT	*				
NE	*				
NV	*				
NH	*	*			
NJ	*		*		
NM					
NY	*				
NC	*				
ND	*				
OH	*				
OK	*		*		
OR	*	*	*		
PA		*	*		
RI					
SC	*				
SD	*				
TN	*	*			
TX	*	*			
UT	*				
VT	*				
VA/FHWA	*				
WA	*	*	*		
DC					
WV					
WI	*	*			
WY	*	*			

# **DRIVEN PILE ALTERNATIVE/DESIGN CONSIDERATION**

**Apply partial safety factor for side friction and end bearing on allowable pile capacity**

STATE	No/ Global F.S.	Yes/Side friction/End Bearing
AL		
AK		
AZ		2.0 / 3.0
AR	3.0	
CA	2.0	
CO	3.0	
CT	2.0 w/ Load test	
DE	-	-
FL	2.0	
GA	3.0	
HI	3.0	
ID	3.0	
IL	3.0	
IN	2.5	
IA	2.2	
KS	3.0	
KY	*	
LA	2.0 w/Load test, 3.0	
ME	3.0, 2.25 w/PDA	
MD	2.0 – 3.5 per AASHTO	
MA	3.5, 2.75 w/WEAP, 2.25 w/PDA	
MI	2.0	
MN	3.0	
MS		
MO	3.5	
MT	2.0 – 3.0	
NE	2.0	
NV	3.0 for clay, 2.5 for sand	
NH	1.9 to 2.75	
NJ	2 to 2.75	
NM		
NY	2.0	
NC	2.0	
ND	*	
OH	2.0	
OK	3.0	
OR	2.5 – 3.0	
PA	-	
RI		
SC	3.0, 2.5 w/PDA, 2.0 w/Load test	
SD	-	
TN	2.0	
TX	2.0	
UT	2.25 w/CAPWAP	
VT	2.0 – 3.0	
VA/FHWA	*	
WA	2.5	
DC		
WV		
WI	2.0	
WY		1.5 / 3.0



## DRIVEN PILE ALTERNATIVE/DESIGN CONSIDERATION

### Consider pile settlement in design

STATE	No	Yes/Tolerable settlement	
AL			
AK			
AZ		0.75"	
AR	*		
CA	*		
CO	*		
CT		0.25"	
DE	*		
FL		1.0"	
GA	*		
HI	*		
ID	*		
IL	*		
IN		0.75"	
IA	*		
KS	*		
KY		0.5"	
LA	*		
ME		1.0"	
MD	-		
MA		Structure / soil dependent	
MI	*		
MN	*		
MS			
MO	*		
MT		Project depend	
NE	*		
NV		1.0"	
NH		*	
NJ		0.5"	
NM			
NY		<2.0"	
NC		*	
ND	*		
OH		0.5"	
OK		0.5"	
OR		Project dependent, typically <1.0"	
PA	*		
RI			
SC	*		
SD	*		
TN		0.25"	
TX	*		
UT		25 mm	
VT		1.0"	
VA/FHWA		1.0"	
WA		25 mm	
DC			
WV			
WI	*		
WY	*		

**DRIVEN PILE ALTERNATIVE/DESIGN CONSIDERATION**  
**Design method in lateral load analysis and/or program**

STATE	Simply Method (Broms)	p-y Curve Method	Others
AL			
AK			
AZ	*	*	
AR		*	
CA		*	
CO	*	*	
CT		*	
DE		*	
FL		*	
GA		*	
HI		*	
ID	*	*	
IL		*	
IN		*	
IA		* (but seldom check)	
KS		*	
KY	*		
LA		*	
ME		*	*
MD		*	
MA	*	*	
MI	*	*	
MN		*	
MS			
MO		*	
MT		*	
NE		*	
NV		*	*
NH		*	
NJ	*	*	
NM			
NY	*	*	
NC		*	
ND	*		
OH		*	
OK	*	*	
OR	* (No seismic)	* (Seismic)	
PA		*	
RI			
SC		*	
SD	-	-	
TN	*	*	
TX		*	
UT		*	
VT	*	*	
VA/FHWA	*		
WA		*	
DC			
WV			
WI	*		
WY		*	

**DRIVEN PILE ALTERNATIVE/DESIGN CONSIDERATION**  
**Development of computer programs for lateral load analysis**

STATE	In-House	FHWA	Commercial	Others	
AL					
AK					
AZ		*			
AR		*	*		
CA	*	*	*		
CO	*	*	*		
CT		*			
DE		*			
FL	*				
GA		*	*		
HI		*			
ID		*	*		
IL		*	*		
IN		*			
IA		*			
KS		*			
KY			*		
LA		*			
ME		*	*		
MD		*			
MA		*	*		
MI	*	*			
MN			*		
MS					
MO		*			
MT		*	*		
NE		*			
NV		*	*		
NH				-	
NJ		*	*		
NM		*	*		
NY		*	*	*	
NC		*	*		
ND				-	
OH		*	*		
OK		*	*		
OR		*	*		
PA		*	*		
RI					
SC		*	*		
SD				-	
TN		*			
TX		*			
UT			*		
VT				*	
VA/FHWA		*			
WA		*	*		
DC					
WV					
WI		*			
WY			*		

## **DRIVEN PILE ALTERNATIVE/DESIGN CONSIDERATION**

### **Control factors of pile design subjected to lateral load**

STATE	Lateral Deflection/Tolerate Deflection	Lateral Capacity/Method used/Safety factor
AL		
AK		
AZ	1.0"	3.0
AR	0.25"	
CA	Varies 2.0 to 6.0"	
CO	Varies	Varies
CT	Structure dependent	
DE	*	*
FL	2..0"	
GA	*	
HI	*	
ID	0.25"	
IL	*	*
IN	Typically not check	
IA	-	
KS	0.5"	
KY	0.5"	
LA	-	
ME	1.0"	
MD	-	
MA	Project dependent, usually 1.0"	1.5
MI	*	
MN	Determined by Structural Engineer	
MS		
MO		2.5
MT	Structure dependent, usually <50 mm	
NE	*	
NV	1.0"	
NH	Structure dependent	
NJ	0.5"	
NM		
NY	1.0"	
NC	1.0"	
ND		*
OH	Project dependent	
OK	-	
OR	Varies, usually <1.0"	
PA	0.5"	2.5
RI		
SC	2.0 at free head condition	
SD	-	
TN		2.0
TX	0.5"	
UT	Up to stress limit	
VT	0.5"	
VA/FHWA	0.5"	
WA	Structure dependent	Varies w/ load case
DC		
WV		
WI	Project dependent	
WY	2.0"	

**DRIVEN PILE ALTERNATIVE/DESIGN CONSIDERATION**  
**Consideration of downdrag force in design**

STATE	No	Yes/Methodology	
AL			
AK			
AZ		* FHWA	
AR	*		
CA		* (Sometimes)	
CO		* Effective Stress	
CT		* $\alpha$ method, 50% reduction w/bitumen coating	
DE		*	
FL		*	
GA		*	
HI		* PILENEG	
ID		* $\alpha$ method	
IL		*	
IN			
IA		*	
KS		* FHWA, DM-7, Poulos & Daves	
KY		* DM-7	
LA	*		
ME		* $\beta$ method per Sanford (1998)	
MD	*		
MA		* FHWA	
MI	*		
MN		* Neutral Plane method	
MS			
MO	*		
MT		* $\alpha$ Method	
NE		*	
NV		* $\alpha$ method	
NH		*	
NJ		* DM-7	
NM			
NY		* DM-7	
NC		*	
ND		*	
OH		*	
OK	*		
OR		$\alpha$ method	
PA	*		
RI			
SC		* $\alpha$ method	
SD	*		
TN	*		
TX	*		
UT		* Fellenios	
VT		*	
VA/FHWA		*	
WA		*	
DC			
WV			
WI		* FHWA	
WY	*		

**DRIVEN PILE ALTERNATIVE/DESIGN CONSIDERATION**  
**Consideration of construction method in design**

STATE	No	Yes		
AL				
AK				
AZ		*		
AR		*		
CA	*			
CO		*		
CT	*			
DE		*		
FL		*		
GA	*			
HI		*		
ID	*			
IL	*			
IN				
IA		*		
KS	*			
KY	*			
LA		*		
ME	*			
MD	*			
MA		*		
MI		*		
MN	*			
MS				
MO		*		
MT	*			
NE		*		
NV		*		
NH		*		
NJ		*		
NM				
NY		*		
NC		*		
ND	*			
OH	*			
OK	*			
OR		*		
PA	*			
RI				
SC		*		
SD	*			
TN	*			
TX	*			
UT		*		
VT	*			
VA/FHWA		*		
WA		*		
DC				
WV				
WI	*			
WY	*			

**DRIVEN PILE ALTERNATIVE/DESIGN CONSIDERATION**  
**Estimated risk or failure probability based on the safety factor used**

STATE	<0.1%	0.1 to 1%	1 to 10 %	>10%	Unknown	Acceptable %'
AL						
AK						
AZ					*	0.1
AR					*	~0
CA					*	-
CO	*					1.0
CT					*	-
DE	*					-
FL					*	1.0
GA					*	1.0
HI					*	~0
ID					*	-
IL	*					0.1
IN						
IA					*	-
KS	*					~0
KY			*			-
LA					*	-
ME					*	-
MD					*	-
MA					*	1.0
MI		*				-
MN					*	-
MS						
MO					*	-
MT					*	-
NE					*	0.1
NV					*	-
NH					*	-
NJ					*	-
NM						
NY					*	-
NC					*	-
ND					*	-
OH	*					-
OK	*					0.1
OR	*					-
PA	*					-
RI						
SC					*	-
SD	*					-
TN	*					0.1
TX	*					-
UT	*				*	0.1
VT					*	1.0
VA/FHWA					*	-
WA		*				0.5
DC						
WV						
WI					*	-
WY					*	-

## DRIVEN PILE ALTERNATIVE/DESIGN CONSIDERATION

### Experience on pile design failure

STATE	No	Yes	
AL			
AK			
AZ	*		
AR	*		
CA	*		
CO		* Scour in super flood	
CT	*		
DE	*		
FL	*		
GA	*		
HI	*		
ID	*		
IL	*		
IN	*		
IA		* Failure due to scour, landslide	
KS		* Consultant Strikes	
KY	*		
LA		*Test pile was design to plunge as close to 2X design load	
ME	*		
MD	*		
MA	*		
MI		* Extract sheet pile causing excessive pile settlement	
MN	*		
MS			
MO	*		
MT	*		
NE	*		
NV	*		
NH	*		
NJ	*		
NM			
NY	*		
NC		*	
ND	*		
OH	*		
OK	*		
OR	*		
PA	*		
RI			
SC	*		
SD	*		
TN	*		
TX	*		
UT	*		
VT	*		
VA/FHWA	*		
WA	*		
DC			
WV			
WI	*		
WY	*		



**DRIVEN PILE ALTERNATIVE/CONSTRUCTION CONSIDERATION**  
**Perform static load test during construction and type of test**

STATE	No	Yes/Criteria to justify	Type of Test
AL			
AK			
AZ	*		
AR	*		
CA		* Ptroject dependent, not meeting ENR blow count	Quick
CO		* Potential cost saving and difficult to predict	-
CT		* High end bearing pile (12ksi), most friction pile	Varies
DE		* More than 100 piles, unusual soil condition	Quick
FL		* Cost saving, unusual soil condition, high capacity design	Quick
GA		* Cost saving from using low Safet factor	Quick
HI		*Project dependent	Quick
ID	*	(Barely)	
IL		* Major project	Slow
IN			
IA		*Unusual soil condition, major structure but not now	Quick
KS		* Unusual soil condition, pile type	Quick
KY		*	Texas Quick
LA		* Cost saving, inadequate soil information	Quick
ME	*		
MD		* Project dependent	Quick/Slow
MA		* Cost saving, major project	Quick
MI		* Major project, high capacity	Slow
MN	*		
MS			
MO		*Major project, cost saving	Slow
MT		*New construction method (occasion), high capacity	Texas Quick
NE	*		
NV		* Cost saving	Quick
NH		*Generally for friction pile only	Quick
NJ		*Project dependent	Quick
NM			
NY		* Confirm Design, unknown soil condition	Quick
NC		* Project dependent	Quick
ND		* Cost saving	-
OH		* Pile over 45 tons, more 10,000 feet pile	Quick
OK	*		
OR	*		
PA		* (Sometimes)	Quick
RI			
SC		*	Texas Quick
SD	*		
TN		*	-
TX		* Major project more than 100,000 feet pile	Quick to fail
UT		*Cost saving	Quick
VT		*Large no. of friction piles	Quick
VA/FHWA		*	Quick
WA		*	Quick
DC			
WV			
WI	*		-
WY		*	Quick

## **DRIVEN PILE ALTERNATIVE/CONSTRUCTION CONSIDERATION**

Perform dynamic pile load test during construction

STATE	No	Yes/Criteria to justify	Yes/% of Pile per bridge
AL			
AK			
AZ		*	10% or mini. 2 / bridge
AR		*Relatively high capacity	1%
CA		* Hard or problem driving	
CO		* Friction pile, soft shal	1% to 5%
CT	*		
DE		*	1 / substructure unit
FL		*	On test pile, mini. 2 /bridge
GA		*	5%
HI		*	On test pile
ID		* Major structure	<5%
IL		*Major or special project	Very small %
IN		* On large project w/ ult.>240 tons	2%
IA		*Problem conditions	<2%
KS		*	
KY		* Critical bridge	10%
LA		* For driving criteria	On test pile
ME		*Cost saving from low safety factor	5% to 20%
MD	*		
MA		*QC	5% to 10%
MI		*	1 or 2 / bridge
MN		* On large project	5 %to 10%
MS			
MO		* On large project	1%
MT		* Occasion used w/ static load test	-
NE		* Major project, or not meeting ENR blow count	1 / substructure
NV	*		
NH		*	On test pile
NJ		*	On test pile
NM			
NY		*	2%
NC		*	1*
ND	*		
OH		* More than 1,500 feet piles	1 / Bridge
OK		*	-
OR		* More than 100 tons design load	-
PA		*	<10%
RI			
SC		*	<5%
SD	*		
TN	*		
TX	*		
UT		*	
VT		*	1/ substructure unit
VA/FHWA		*	1 to 2 / bridge
WA		*	<5% or 1 / bridge
DC			
WV			
WI		*	
WY		* Friction pile	10%

# DRIVEN PILE ALTERNATIVE/CONSTRUCTION CONSIDERATION

## Type of instrument used in dynamic pile load test

STATE	PDA/GRL	Others			
AL					
AK					
AZ	*				
AR	*				
CA	*				
CO	*				
CT	*				
DE	*				
FL	*				
GA	*				
HI	*				
ID	*				
IL	*				
IN	*				
IA	*				
KS	*				
KY	*				
LA	*				
ME	*				
MD			No		
MA	*				
MI	*				
MN	*				
MS					
MO	*				
MT	*				
NE	*				
NV			No		
NH	*				
NJ	*				
NM	*				
NY	*				
NC	*				
ND			No		
OH	*				
OK	*				
OR	*				
PA	*				
RI					
SC	*				
SD			No		
TN			No		
TX			No		
UT	*				
VT	*				
VA/FHWA	*				
WA	*				
DC					
WV					
WI	*				
WY	*				

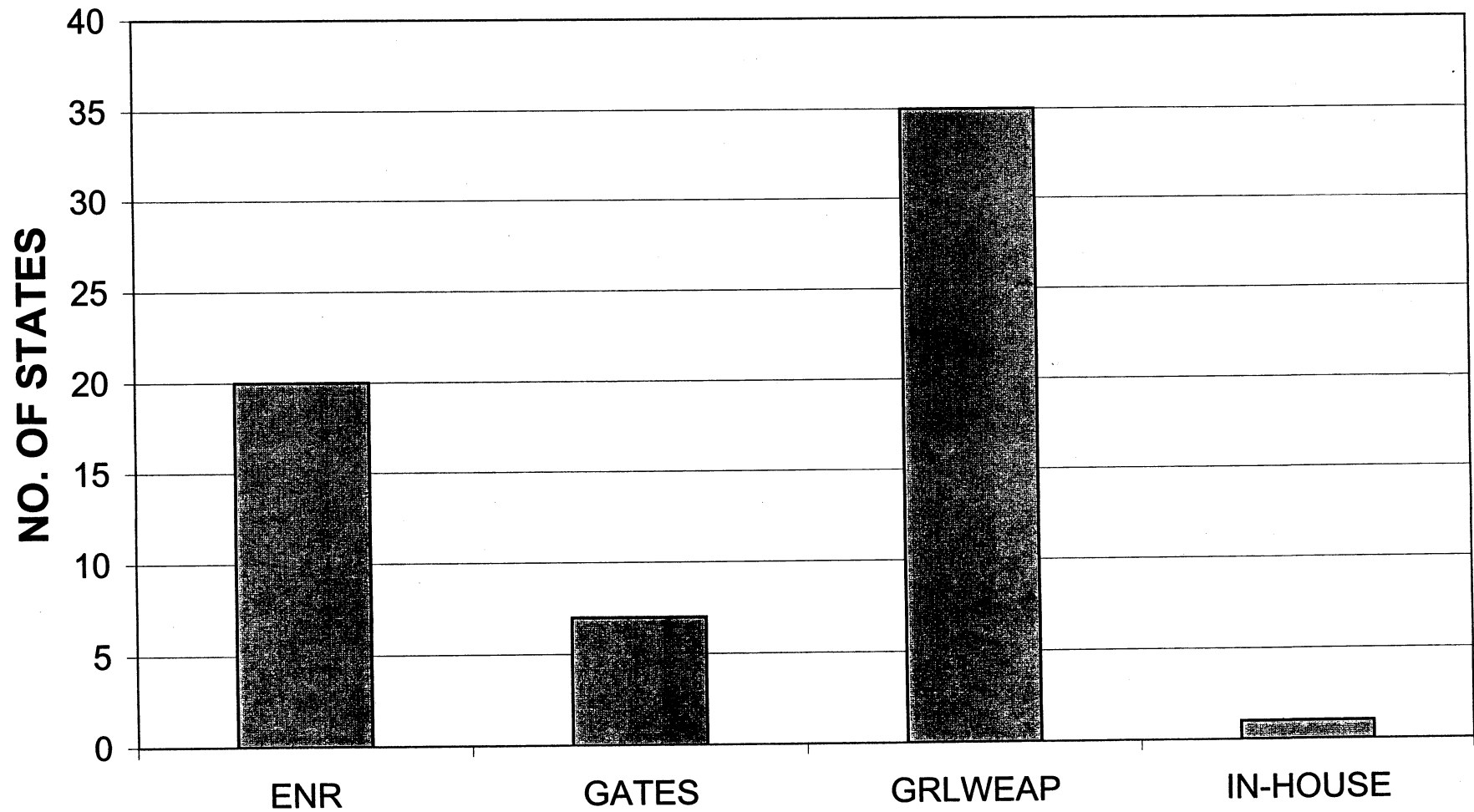
**DRIVEN PILE ALTERNATIVE/CONSTRUCTION CONSIDERATION**  
**Driving condition used to set driving criteria and production pile length**

STATE	EOD	BOR	Others		
AL					
AK					
AZ	*				
AR	*				
CA		*			
CO	*	*			
CT	* (end bearing)				
DE		*			
FL	*	*			
GA	*				
HI	*				
ID	*	* (if expected)			
IL	*				
IN	*				
IA	*	*			
KS	*				
KY	*	*			
LA	*	*			
ME		*			
MD					
MA	*	*			
MI	*				
MN	*	* (occasionally)			
MS					
MO	*	*			
MT	*	*			
NE	*	*			
NV	*				
NH	* (end bearing)	* (friction)			
NJ	*				
NM					
NY		*			
NC	*				
ND	*				
OH	*				
OK	*				
OR	*	*(In cohesive soil)			
PA	*				
RI					
SC	*	*			
SD	*				
TN	*				
TX		*			
UT		*			
VT		*			
VA/FHWA	*	*			
WA	*	*			
DC					
WV					
WI	*				
WY	*				

**DRIVEN PILE ALTERNATIVE/CONSTRUCTION CONSIDERATION**  
**Consideration of pile freeze or relaxation in setting driving criteria**

STATE	No	Yes	
AL			
AK			
AZ	*		
AR	*		
CA		*	
CO		*	
CT		* Based on experience, load test may delay for one week or more	
DE		*	
FL		*	
GA		* In loose/soft soils to avoid excessive pile length	
HI		* Project dependent	
ID	*		
IL	*		
IN		*	
IA	*		
KS		* Experience	
KY	*		
LA		*	
ME		* Relaxation	
MD	-		
MA		* Restrike after 2 to 7 days	
MI		* Specify restrike in some soil profiles	
MN	*	(In some cases)	
MS			
MO	*		
MT	*		
NE		* Experience	
NV	*		
NH		*	
NJ		*	
NM			
NY		*	
NC		*	
ND	*		
OH		*	
OK	*		
OR		*	
PA		*	
RI			
SC		*	
SD	*		
TN	*		
TX	*		
UT		*	
VT	*		
VA/FHWA		*	
WA		*	
DC			
WV			
WI		*	
WY		*	

## DYNAMIC FORMULA OR COMPUTER PROGRAM TO ESTIMATE PILE CAPACITY



NCHRP 24-17

**LOAD AND RESISTANCE FACTOR DESIGN  
(LRFD) FOR DEEP FOUNDATIONS**

**APPENDIX B  
LOAD AND RESISTANCE FACTOR DESIGN (LRFD)  
FOR DYNAMIC ANALYSES OF DRIVEN PILES**

Prepared for  
National Cooperative Highway Research Program  
Transportation Research Board  
National Research Council

Samuel G. Paikowsky and Kirk L. Stenerson  
Geotechnical Engineering Research Laboratory  
Department of Civil and Environmental Engineering  
University of Massachusetts  
Lowell, Massachusetts

July 2002

### **ACKNOWLEDGEMENT OF SPONSORSHIP**

This work was sponsored by the American Association of State Highway and Transportation Officials, in cooperation with the Federal Highway Administration, and was conducted in the National Cooperative Highway Research Program, which is administered by the Transportation Research Board of the National Research Council.

### **DISCLAIMER**

This is an uncorrected draft as submitted by the research agency. The opinions and conclusions expressed or implied in the report are those of the research agency. They are not necessarily those of the Transportation Research Board, the National Research Council, the Federal Highway Administration, the American Association of State Highway and Transportation Officials, or the individual states participating in the National Cooperative Highway Research Program.



## ABSTRACT

NCHRP Project 24-17 "LRFD Deep Foundation Design" is supported by the USA National Cooperative Highway Research Program (NCHRP) under the Transportation Research Board (TRB) of the National Academy of Science (NAS). The project is aimed at rewriting AASHTO Deep Foundation Specifications for the year 2001. The AASHTO specifications are traditionally observed on all federally aided projects and generally viewed as a national code of US Highway practice, hence influencing the construction of all the deep foundations of highway bridges throughout the USA.

The new specifications are based on Load and Resistance Factor Design (LRFD) principles with resistance factors obtained from probabilistic analysis of data. This research report presents a review of methodologies, resistance factors calculation and the application of it to the dynamic analyses of driven piles. A large database (PD/LT2000) is the backbone of the dynamic methods' performance evaluation. This database originated with the work presented by Paikowsky et al. (1994), Paikowsky and LaBelle (1994), and additional information acquired since.

A review of design methodologies is presented and the application of LRFD to Geotechnical Engineering is discussed. The process of data compilation is introduced and methods to establish pile capacity based on static load test results are evaluated for the determination of a reference static capacity. A summary and careful evaluation of PD/LT 2000 database is presented, and the parameters that control the accuracy of the dynamic predictions are analyzed. The data analysis indicates the importance of certain mechanisms associated with the pile penetration and the dynamic simulations. The most important parameters are shown to be those associated with the soil inertia, namely driving resistance and pile geometry and those associated with change of pile capacity with time, namely, time of driving, [e.g. End of Driving (EOD) and Beginning of Restrike (BOR)].

The First Order Reliability Method (FORM) is introduced and applied for LRFD of Deep Foundations. Target reliability and the associated probability of failure levels are discussed. Analyses of PD/LT2000 provide statistical details for the performance of the various dynamic methods when compared to static load testing to failure. The controlling parameters and the statistical analyses along with the recommended target reliability are then utilized for the development of the resistance factors. The final resistance factors recommended for the new specifications are extracted in a three level process; (i) detailed statistical evaluation of a wide range of cases based on the identified controlling parameters, (ii) evaluation of the resistance factors for the inclusive cases (out of the 1<sup>st</sup> stage) for three target reliability levels, and, (iii) developing the final resistance factors for the most inclusive and critical cases under the recommended target reliabilities. Two concepts are introduced for the recommended resistance factors: (a) two levels of target reliability based on the criticality of the foundation, classifying the piles as redundant and non-redundant elements and, (b) efficiency evaluation of the method of analysis in conjunction with the magnitude of the resistance factors.

The obtained parameters are evaluated against FOSM (First Order Second moment method), and the actual probability of failure. Case histories allow an evaluation of the recommended parameters in an absolute way and against WSD factors of safety. The final recommendations are comprehensive and clear providing factors for a variety of dynamic methods and means to evaluate their efficiency.

## **ACKNOWLEDGMENTS**

The American Association of State Highway and Transportation Officials (AASHTO) sponsored the presented research, under National Cooperative Highway Research Program (NCHRP) project 24-17, in cooperation with the Federal Highway Administration (FHWA). The project is supported through the Transportation Research Board (TRB) of the National Academy of Science (NAS). The panel of the research project and Mr. David Beal of the NCHRP are acknowledged for their stimulating demands. Messrs. Jerry DiMaggio, Al DiMillio and Carl Ealy of the FHWA are acknowledged for their interest, concern and support.

Dr. Gregory B. Baecher and Dr. Bilal M. Ayyub from the University of Maryland for their contributions to Chapters 2 and 9, in particular for the calculation of the presented resistance factors using FORM. Special thanks to Dr. Baecher for serving on Mr. Stenersen's M.S. thesis committee.

Dr. Frank Rausche of Goble, Rausche, Likins (GRL) and Associates for providing the data pertaining to the evaluation of GRLWEAP and for serving on Mr. Stenersen's M.S. thesis committee including the effort in traveling to the thesis defense.

Dr. John Ting from the University of Massachusetts at Lowell for serving on Mr. Stenersen's thesis committee.

Mr. Kevin O'Malley for his contributions to Chapter 7 as part of his graduate project, particularly the grueling task of compiling the data for the PD2000 database.

Dr. Michael McVay of the University of Florida for providing the data pertaining to the evaluation of the Case method in Florida.

Geosciences Testing and Research, Inc. (GTR) of North Chelmsford, Massachusetts for providing data for the research, mostly the data for the PD2000 database in Boston Blue Clay.

# TABLE OF CONTENTS

## LIST OF TABLES

## LIST OF FIGURES

### 1 INTRODUCTION

- 1.1 OVERVIEW
- 1.2 BACKGROUND
- 1.3 MANUSCRIPT LAYOUT

### 2 BACKGROUND

- 2.1 STATE OF STRESS METHODOLOGY
  - 2.1.1 Overview
  - 2.1.2 The Working Stress (WSD) Method
  - 2.1.3 The Limit States
- 2.2 LOAD AND RESISTANCE FACTOR DESIGN (LRFD) METHOD
  - 2.2.1 Reliability Based Design – History and Background
  - 2.2.2 Development of the LRFD Method for General Geotechnical Engineering
  - 2.2.3 The Principle of the LRFD Method for Deep Foundations
  - 2.2.4 Determination of Resistance Factors by Calibration
    - a) LRFD Calibration via WSD
    - b) LRFD Calibration using Reliability Theory
    - c) Reliability-Based LRFD Using Failure Point
  - 2.2.5 The Use of Limit States in LRFD
- 2.3 THE AVAILABLE AND CHOSEN DYNAMIC METHODS
  - 2.3.1 General
  - 2.3.2 Dynamic Equations
    - a) The Basic Principle
    - b) Engineering News Record Equation
    - c) Gates Equation
    - d) FHWA modified Gates Equation
  - 2.3.3 The Wave Equation
    - a) Formulation and Principles
    - b) Pre-Driving Analysis
    - c) Post-Driving Analysis – CAPWAP/TEPWAP

- 2.3.4 The Case Method
  - a) General
  - b) The Case Method Equation
  - c) Case Damping Coefficient
  - d) Case Method Variations
- 2.3.5 The Energy Approach
- 2.4 REVIEW OF THE RECOMMENDED LRFD FACTORS FOR PILE DESIGN
  - 2.4.1 Resistance Factors Recommended by AASHTO
  - 2.4.2 Resistance Factors for Dynamic Load Testing using the Case Method
  - 2.4.3 International LRFD Codes
    - a) Australian Standard, Piling-Design and Installation
    - b) 1992 AUSTROADS Bridge Design Code
    - c) Eurocode 7, Geotechnical Design
    - d) Danish Code of Practice for Foundation Engineers
    - e) Ontario Bridge Code
    - f) Canadian Bridge Code
    - g) Japanese Specifications for Highway Bridges
  - 2.4.4 Evaluation of Recommended Resistance Factors
  - 2.4.5 Evaluation of Calculated Resistance Factors
- 2.5 DIFFICULTIES OF THE EXISTING LRFD CODES
  - 2.5.1 Overview
  - 2.5.2 Construction Difficulties
    - a) General
    - b) Observations
  - 2.5.3 Deficiency in Current Geotechnical Reliability Practice for LRFD
  - 2.5.4 Calibrations Based on State-of-Practice Reliability Methodology

### **3 COMPILATION OF DATABASES**

- 3.1 GENERAL 90
- 3.2 PD/LT2000 DATABASE
  - 3.2.1 Overview
  - 3.2.2 Static Load Test Analysis
  - 3.2.3 Dynamic Measurements Analysis
    - a) Overview
    - b) Group 1 – Complete CAPWAP Analysis
    - c) Group 2 – Incomplete CAPWAP Analysis
    - d) Group 3 – TEPWAP Analysis
- 3.3 U-MASS LOWELL / UKRAINE DATABASE
- 3.4 GRLWEAP DATABASE

- 3.5 CASE METHOD DATABASE
- 3.6 PD2000
- 3.7 PD/LTT2000

#### **4 REFERENCE STATIC CAPACITY**

- 4.1 OVERVIEW
- 4.2 OBJECTIVES
- 4.3 PILE FAILURE / CAPACITY DETERMINATION
  - 4.3.1 Background
  - 4.3.2 Method of Approach
  - 4.3.3 Davisson's Criterion
  - 4.3.4 The Shape-of-Curve Method
  - 4.3.5 The Limited Total Settlement Methods
  - 4.3.6 DeBeer's log-log Method
  - 4.3.7 The Representative Static Capacity
- 4.4 PERFORMANCE EVALUATION OF THE DIFFERENT FAILURE CRITERION METHODS
  - 4.4.1 Method of Approach
  - 4.4.2 Davisson's Criterion
  - 4.4.3 The Shape-of-Curve Method
  - 4.4.4 Limiting Total Settlement to 25.4 mm
  - 4.4.5 Limiting Total Settlement to One Tenth of the Pile Diameter
  - 4.4.6 DeBeer's log-log Method
  - 4.4.7 Intermediate Conclusions
  - 4.4.8 Evaluation of a Modification for Davisson's Criterion
    - a) The Proposed Modification
    - b) The Performance of the Proposed Modification
- 4.5 STATIC LOAD TEST PROCEDURE
  - 4.5.1 Overview
  - 4.5.2 Load Test Procedures
    - a) ASTM Procedures
      - i) Standard Loading Procedure
      - ii) Cyclic Loading
      - iii) Quick Load Test Method for Individual Piles
      - iv) Constant Rate of Penetration
    - b) Massachusetts Highway Department Procedures
      - i) Short Duration Test
      - ii) Maintained Load Test
      - iii) Quick Load Test
    - c) Massachusetts Building Code Procedure
    - d) Texas Quick Test Procedure
    - e) Static-Cyclic Load Test Procedure
    - f) Summary

- 4.5.3 Performance Evaluation of the Load Test Procedures
  - a) Comparison of the Short Duration, Slow Maintained and Static Cyclic Tests
  - b) Comparison between the Static-Cyclic Load Testing and Slow Maintained Tests Using Davisson's Capacity
  - c) Intermediate Conclusions

#### 4.6 CONCLUSIONS FOR REFERENCE STATIC CAPACITY

### **5 CONTROLLING PARAMETERS OF THE DYNAMIC METHODS**

- 5.1 OVERVIEW
- 5.2 METHOD OF APPROACH
  - 5.2.1 General
  - 5.2.2 Nomenclature
  - 5.2.3 Interpretation of Statistical Results
- 5.3 THE CONTROLLING PARAMETERS
  - 5.3.1 Soil Type
    - a) General
    - b) Sand and Silt
    - c) Clay and Till
    - d) Rock
    - e) Intermediate Conclusions
  - 5.3.2 Time of Driving
  - 5.3.3 Soil Inertia Effects
    - a) Overview
    - b) Effect of Driving Resistance
    - c) Effect of Pile Type
- 5.4 INTERMEDIATE CONCLUSIONS

### **6 PERFORMANCE OF THE DYNAMIC METHODS DURING THE CONSTRUCTION STAGE**

- 6.1 OVERVIEW
- 6.2 DYNAMIC ANALYSES WITHOUT DYNAMIC MEASUREMENTS
  - 6.2.1 WEAP Analysis
  - 6.2.2 The Dynamic Equations
    - a) General
    - b) ENR Equation
    - c) Gates Equation
    - d) FHWA modified Gates Equation
    - e) The Recommended Dynamic Equation and its Performance
    - f) Summary of the Dynamic Equations Performance
- 6.3 DYNAMIC ANALYSES WITH DYNAMIC MEASUREMENTS

- 6.3.1 Overview
- 6.3.2 Performance of the Signal Matching Technique (CAPWAP or TEPWAP)
  - a) All Pile-Cases
  - b) Performance According to Time of Driving
  - c) Performance According to Driving Resistance
  - d) Performance According to Pile Type
- 6.3.3 Field Evaluation (Energy Approach)
  - a) All Pile-Cases
  - b) Performance According to Time of Driving
  - c) Performance According to Driving Resistance
  - d) Performance According to Pile Type
- 6.3.4 Field Evaluation (Case Method)
  - a) General
  - b) Evaluation of the Case-Damping Coefficient
  - c) Evaluation of the Case Method Based on Local Calibration
  - d) Summary

#### 6.4 SUMMARY AND INTERMEDIATE CONCLUSIONS

### **7 ENERGY APPROACH EOD VERSUS CAPWAP/TEPWAP BOR**

- 7.1 GENERAL
- 7.2 COMPARISON BASED ON THE PD/LT2000 DATABASE
- 7.3 COMPARISON BASED ON THE PD2000 DATABASE
  - 7.3.1 Overview
  - 7.3.2 All Pile-Cases
  - 7.3.3 Driving Resistance
  - 7.3.4 Soil Types
    - a) Overview
    - b) Clay and Till
    - c) Sand and Silt
    - d) Rock
    - e) Boston Blue Clay
  - 7.3.5 Summary
- 7.4 SUMMARY AND INTERMEDIATE CONCLUSIONS

### **8 PILE CAPACITY GAIN WITH TIME**

- 8.1 GENERAL
- 8.2 ANALYSIS OF PILE CAPACITY GAIN WITH TIME
- 8.3 INTERMEDIATE CONCLUSIONS

### **9 CALCULATION OF RESISTANCE FACTORS**

- 9.1 METHODOLOGY

- 9.2 LEVEL OF TARGET RELIABILITY
  - 9.2.1 Overview
  - 9.2.2 General Discussion
    - a) Target Reliability Levels
    - b) Calibrated Reliability Levels
  - 9.2.3 Geotechnical Perspective
- 9.3 DEAD TO LIVE LOAD RATIO
- 9.4 THE RESISTANCE FACTORS
  - 9.4.1 Initial Evaluation
  - 9.4.2 Intermediate Conclusions
  - 9.4.3 Resistance Factors for a Range of Reliability Levels
  - 9.4.4 Recommended Resistance Factors
- 9.5 EVALUATION OF THE DYNAMIC METHODS EFFICIENCY
- 9.6 EVALUATION OF THE TARGET RELIABILITY USED
  - 9.6.1 Resistance Factors Based on the Existing AASHTO Specifications
  - 9.6.2 Evaluation of the WSD Factors of Safety (AASHTO, 1997) in Light of the Obtained Results
  - 9.6.3 Evaluation of the Chosen Target Reliability
    - a) Overview
    - b) Approximate Factors of Safety
    - c) The Actual Probability of Failure
- 9.7 THE CHOSEN TARGET RELIABILITY AND RESISTANCE FACTORS

## **10 EXAMPLE CASE HISTORIES**

- 10.1 GENERAL
- 10.2 EVALUATION OF THE PROPOSED RESISTANCE FACTORS
- 10.3 INTERMEDIATE CONCLUSIONS

## **11 SUMMARY, CONCLUSIONS AND RECOMMENDATIONS**

- 11.1 SUMMARY
- 11.2 CONCLUSIONS
- 11.3 RECOMMENDATIONS

## **REFERENCES**

## **APPENDIX A - RELEVANT INFORMATION FROM DATABASES**

## **APPENDIX B - BACKGROUND CALCULATIONS FOR CASE HISTORIES PRESENTED IN CHAPTER 2**



**APPENDIX C - CALCULATED RESISTANCE FACTORS BY  
CALIBRATING TO THE STATIC LOAD TEST  
RESULTS**

**APPENDIX D - CASE HISTORY CALCULATIONS COMPARING  
THE WSD METHOD, THE LRFD METHOD AND  
THE PRESENT AASHTO CODE**

**LIST OF TABLES****PAGE**

2.1	Factor of Safety on Ultimate Axial Geotechnical Capacity Based on Level of Construction Control (AASHTO, 1997)	
2.2	Allowable Stresses in Piles (AASHTO, 1997)	
2.3	Resistance Factors for Geotechnical Strength Limit State for Axially Loaded Piles (AASHTO, 1998)	
2.4	Resistance Factors Calibrated by Fitting with WSD for $\gamma_D=1.25$ and $\gamma_L=1.75$ (After McVay et al., 1998)	
2.5	Resistance Factor for Driven Piles for Estimating the Axial Geotechnical Pile Capacity Using Reliability-Based Calibration (modified after Barker et al., 1991)	
2.6a	Relationship Between Probability of Failure and Reliability Index for Lognormal Distribution (After Withiam et al., 1997)	
2.6b	Comparison Between Rosenbleuth and Estava's Approximation and Series Expansion (Labeled "exact")	
2.7	Strength and Service Limit States for Design of Driven Pile Foundations (After Withiam et al., 1997)	
2.8	Reliability Index of Case Method Prediction (After McVay et al., 1998)	
2.9	Resistance Factor for Case Method Prediction (After McVay et al., 1998)	
2.10	Range of Values for Resistance Factors for Piles (Standard Association of Australia, 1995)	
2.11	Guide for Assessment of Resistance Factors for Piles (Standard Association of Australia, 1995)	
2.12	Material Resistance Factors for Piles (AUSTROADS, 1992)	
2.13	Typical Load and Resistance Factors for Axially Loaded Piles in Compression on Land for ULS (modified after Meyerhof, 1994)	

- 2.14 Partial Factors from Eurocode 7 and the Equivalent Resistance Factors (After Eurocode 7, 1997)
- 2.15 Piles and Anchors (From the Danish Code)
- 2.16 Resistance Factors for Deep Foundations (From Ontario Bridge Code)
- 2.17 Resistance Factors (From the Canadian Bridge Code)
- 2.18 Summary of Ultimate and Factored Loads, Test Pile # 2, Newbury Site
- 2.19 Calculated Resistance Factors Assuming that the Resistance Factor for a Static Load Test is 1.0
- 2.20 Comparison of Recommended and Calculated Resistance Factors
- 3.1 Summary of the Data in the PD/LT2000 database
- 4.1 Summary of the Interpretation Methods applied to the Static Load Test Curves in PD/LT2000
- 4.2 Summary of Static Load Test Procedures (after Paikowsky et al., 1999)
- 4.3 Summary of the Statistical Data Comparing the Slow Maintained Load Test Results using Davisson's Criterion and the Static Cyclic Load Test Results from the UMass Lowell / Ukraine Database
- 5.1 Summary of the  $K_{SW}$  Values for the Different Soil Types used for the Soil Inertia Analysis
- 5.2 Summary of the  $K_{SP}$  Values for the Different Soil Types used for the Soil Inertia Analysis
- 5.3 Summary of the Statistics showing the Importance of the Time of Driving as a Controlling Parameter
- 5.4 Summary of the Statistics showing the Importance of the Driving Resistance as a Controlling Parameter
- 5.5 Summary of the Statistics showing the Importance of the Area Ratio as a Controlling Parameter

- 6.1 Summary of the Statistical Data Evaluating the Performance of the Dynamic Equations
- 6.2 Summary of the Statistical Analyses completed for the Dynamic Equations
- 6.3 Summary of the EOD Pile-Cases for which the  $K_{sx}$  Values Were Outside Two Standard Deviations
- 6.4 Summary of the Soil Inertia Properties for PD/LT2000, Energy Approach and CAPWAP/TEPWAP vs. Static Load Test Results for the Controlling Parameters
- 6.5 Summary of the Statistical Analyses Performed in Chapter 6
- 7.1 Summary of statistical data for the Correlation between the CAPWAP/TEPWAP predictions at the BOR to the Energy Approach predictions at the EOD using the PD/LT2000 and PD2000 databases
- 8.1 Soil properties, pile type, and relevant information for dynamic capacity gain – Data Set PD/LTT2000, predominately clay embedment (Paikowsky et al., 1995)
- 8.2 Soil properties, pile type, and relevant information for dynamic capacity gain – Data Set PD/LTT2000, partially in clay embedment
- 8.3 Summary of static and dynamic based capacity gain data sets (Paikowsky et al., 1995)
- 9.1 Approximate Relationship Between Probability of Failure and Reliability Index for Lognormal Distribution, based on Rosenbleuth and Estava (1972), see Withiam et al. (1998)
- 9.2 Comparison Between Rosenbleuth and Estava's Approximation and Series Expansion (Labeled "exact")
- 9.3 Target Reliability Levels
- 9.4 Target Reliability Levels used by Ellingwood and Galambos (1982)
- 9.5 Target Reliability Values Recommended by A.S. Veritas (Lotsberg, 1991)
- 9.6 Reliability Indices for Driven Piles (Barker et al., 1991)

- 9.7 Summary of the Performance of the Dynamic Methods
- 9.8 Recommended Resistance Factors for the Critical Dynamic Cases
- 9.9 Resistance Factors for the Critical Dynamic Cases Based on FOSM using Barker et al., (1991) versus those developed through FORM (see Table 9.8)
- 9.10 Calculated Factors of Safety Based on the Resistance Factors in Table 9.8 and the Procedure Outlined by Barker et al. (1991)
- 9.11 The Probability of Failures Associated with the Critical Dynamic Methods and Their Important Categories from the PD/LT2000 Database
- 10.1 Predictions of the Dynamic Methods for Three Case History Piles
- 10.2 Summary of Design Capacity Comparisons for Three Case History Piles
- A.1 Relevant Information Pertaining to Database PD/LT2000
- A.2 Relevant Information Pertaining to Umass – Ukraine Database
- A.3 Relevant Information Pertaining to the GRLWEAP Data
- A.4 Relevant Information Pertaining to the Case Data
- A.5 Relevant Information Pertaining to Database PD2000
- A.6 Relevant Information Pertaining to Database PD/LTT2000
- D.1 Summary of Design Capacity Comparisons for Three Case History Piles

**LIST OF FIGURES****PAGE**

- 2.1 Design Basis for Spread Footings in Sand (After Peck et al., 1974)
- 2.2 An Illustration of Probability Density Functions for Load Effect and Resistance (Goble, 1999)
- 2.3 An Illustration of a Probability Density Function for R-Q (Goble, 1999)
- 2.4 An Illustration of a Probability Density Function for  $\ln(R/Q)$  (Goble, 1999)
- 2.5 Resistance vs. Displacement at the Top of the Pile
- 2.6 Smith's model simulating the hammer-pile-soil system for use with the one-dimensional wave equation (Smith, 1960)
- 2.7 Soil-pile model (left) and the corresponding elasto-plastic soil resistance-displacement relationship (after Smith, 1960)
- 2.8 Notations used for Model of Pile and Soil in TEPWAP Analysis (Paikowsky, 1982)
- 2.9 Flow Chart Describing the analysis process using TEPWAP (Paikowsky, 1982)
- 2.10 Force and Velocity Traces Showing Two Impact Peaks Indicative of Driving in Soils Capable of Large Deformations
- 2.11 Deep Foundation Design Process
- 3.1 Force and Velocity ( $V \cdot EA/C$ ) traces of pile-case 1, a steel HP12x74 that needed a force correction
- 3.2 Digitized force and velocity multiplied by the impedance ( $EA/C$ ) traces for pile-case 190 used for input into INTEGRATE
- 3.3 INTEGRATE output of pile-case 190 showing the back-calculated  $J_c$  value and the Energy Approach prediction

- 3.4 Example of the pile identification information of pile-case 189 used as input for the TEPWAP analysis
- 3.5 Example of the soil and pile properties used along the pile elements of pile-case 189 as input for the TEPWAP analysis
- 3.6 Measured force and velocity multiplied by the impedance (EA/C) traces of pile-case 189 used by the TEPWAP analysis
- 3.7 Comparison between measured force near the top of pile-case 189 and the calculated force from the TEPWAP analysis
- 3.8 Summary of the final results from TEPWAP analysis performed on pile-case 189
- 4.1 Load-settlement curve of pile-case 344 with the elastic compression line inclined at 20 degrees
- 4.2 Load-settlement curve of pile-case 344 with a scale that does not consider the elastic compression of the pile
- 4.3 Load-settlement curve of pile-case 344 with the elastic compression line inclined at approximately 20 degrees
- 4.4 Load-settlement data plotted on a logarithmic graph for pile-case 344 to determine the failure load according to DeBeer's method
- 4.5 Histogram and frequency distributions of  $K_{SD}$  for 186 PD/LT2000 pile-cases in all types of soils
- 4.6  $K_{SD}$  values vs. Pile Diameter for all PD/LT2000 pile-cases, all types of soils
- 4.7 Histogram and frequency distributions of  $K_{SC}$  for 193 PD/LT2000 pile-cases in all types of soils
- 4.8  $K_{SC}$  values vs. Pile Diameter for all PD/LT2000 pile-cases, all types of soils
- 4.9 Histogram and frequency distributions of  $K_{ST}$  for 161 PD/LT2000 pile-cases in all types of soils
- 4.10  $K_{ST}$  values vs. Pile Diameter for all PD/LT2000 pile-cases, all types of soils

- 4.11 Histogram and frequency distributions of  $K_{SL}$  for 90 PD/LT2000 pile-cases in all types of soils
- 4.12  $K_{SL}$  values vs. Pile Diameter for all PD/LT2000 pile-cases, all types of soils
- 4.13 Histogram and frequency distributions of  $K_{SB}$  for 187 PD/LT2000 pile-cases in all types of soils
- 4.14  $K_{SB}$  values vs. Pile Diameter for all PD/LT2000 pile-cases, all types of soils
- 4.15 Distribution Function Curves for the Five methods used for analysis of Static Load Test Curves based on 196 piles from PD/LT2000
- 4.16 Histogram and frequency distributions of  $K_{SD}$  and  $K_{SLD}$  for 30 and 20 PD/LT2000 pile-cases, respectively, in all types of soils
- 4.17  $K_{SLD}$  values vs. Pile Diameter for all large diameter PD/LT2000 pile-cases, all types of soils
- 4.18 Static Pile Load Testing Procedures According to ASTM (after Paikowsky et al., 1999)
- 4.19 Static Pile Load Testing Procedures According to MHD (after Paikowsky et al., 1999)
- 4.20 Comparison of the Short Duration, Slow Maintained and Static Cyclic Load Tests for Test Pile # 2 at the Newbury Site (after Paikowsky et al., 1999)
- 4.21 Comparison of the Short Duration, Slow Maintained and Static Cyclic Load Tests for Test Pile # 3 at the Newbury Site (after Paikowsky et al., 1999)
- 4.22 Comparison of the Short Duration and Slow Maintained Static Load Tests, Reduced for Creep, for Test Pile # 2 at the Newbury Site
- 4.23 Comparison of the Short Duration and Slow Maintained Static Load Tests, Reduced for Creep, for Test Pile # 3 at the Newbury Site
- 4.24 Davisson Capacity vs. Static Cyclic Load Test Capacity for 75 pile-cases from the UMass Lowell / Ukraine Database (after Paikowsky et al., 1999)



- 5.1 Static Load Test Results vs. CAPWAP or TEPWAP predictions for 382 PD/LT2000 pile-cases in all types of soils (AAA)
- 5.2 Static Load Test Results vs. Energy Approach predictions for 378 PD/LT2000 pile-cases in all types of soils (AAA)
- 5.3 Static Load Test Results vs. CAPWAP or TEPWAP predictions for 265 PD/LT2000 pile-cases in sand & silt (AAS)
- 5.4 Static Load Test Results vs. Energy Approach predictions for 260 PD/LT2000 pile-cases in sand & silt (AAS)
- 5.5 Static Load Test Results vs. CAPWAP or TEPWAP predictions for 100 PD/LT2000 pile-cases in clay & till (AAC)
- 5.6 Static Load Test Results vs. Energy Approach predictions for 101 PD/LT2000 pile-cases in clay & till (AAC)
- 5.7 Static Load Test Results vs. CAPWAP or TEPWAP predictions for 15 PD/LT2000 pile-cases in rock (AAR)
- 5.8 Static Load Test Results vs. Energy Approach predictions for 15 PD/LT2000 pile-cases in rock (AAR)
- 5.9 Static Load Test Results vs. CAPWAP or TEPWAP predictions for 377 PD/LT2000 pile-cases in all types of soils (AAA)
- 5.10 Static Load Test Results vs. CAPWAP or TEPWAP predictions for 125 PD/LT2000 pile-cases at EOD in all types of soils (AEA)
- 5.11 Static Load Test Results vs. CAPWAP or TEPWAP predictions for 162 PD/LT2000 pile-cases at BOR(last) in all types of soils (ABA)
- 5.12 Static Load Test Results vs. Energy Approach predictions for 371 PD/LT2000 pile-cases in all types of soils (AAA)
- 5.13 Static Load Test Results vs. Energy Approach predictions for 128 PD/LT2000 pile-cases at EOD in all types of soils (AEA)
- 5.14 Static Load Test Results vs. Energy Approach predictions for 153 PD/LT2000 pile-cases at BOR(last) in all types of soils (ABA)
- 5.15 Static Load Test Results vs. CAPWAP or TEPWAP predictions for 108 PD/LT2000 pile-cases with Blow Count < 16 BP10cm in all types of soils (AAA)

- 5.16 Static Load Test Results vs. CAPWAP or TEPWAP predictions for 274 PD/LT2000 pile-cases with Blow Count  $\geq 16$  BP10cm in all types of soils (AAA)
- 5.17 Static Load Test Results vs. Energy Approach predictions for 109 PD/LT2000 pile-cases with Blow Count  $< 16$  BP10cm in all types of soils (AAA)
- 5.18 Static Load Test Results vs. Energy Approach predictions for 269 PD/LT2000 pile-cases with Blow Count  $\geq 16$  BP10cm in all types of soils (AAA)
- 5.19  $K_{SW}$  versus Blow count for all pile-cases in PD/LT2000
- 5.20  $K_{SP}$  versus Blow count for all pile-cases in PD/LT2000
- 5.21 Static Load Test Results vs. CAPWAP or TEPWAP predictions for 250 PD/LT2000 pile-cases with Area Ratio  $< 350$  in all types of soils (AAA)
- 5.22 Static Load Test Results vs. CAPWAP or TEPWAP predictions for 132 PD/LT2000 pile-cases with Area Ratio  $\geq 350$  in all types of soils (AAA)
- 5.23 Static Load Test Results vs. Energy Approach predictions for 250 PD/LT2000 pile-cases with Area Ratio  $< 350$  in all types of soils (AAA)
- 5.24 Static Load Test Results vs. Energy Approach predictions for 128 PD/LT2000 pile-cases with Area Ratio  $\geq 350$  in all types of soils (AAA)
- 5.25  $K_{SW}$  versus Area Ratio for all pile-cases in PD/LT2000
- 5.26  $K_{SP}$  versus Area Ratio for all pile-cases in PD/LT2000
- 5.27  $K_{SW}$  versus Area Ratio for 71 PD/LT2000 pile-cases at EOD with Blow Count  $\geq 16$ BP10cm in all types of soils
- 6.1 Flow Chart Depicting the Various Investigated Dynamic Analyses of Driven Piles
- 6.2 Static Load Test Results vs. GRLWEAP Predictions for 99 pile-cases at EOD provided by GRL Inc., in all types of soils (AEA)

- 6.3 Static Load Test Results vs. GRLWEAP Predictions for 99 pile-cases at BOR provided by GRL Inc., all types of soils (ABA)
- 6.4 Static Load Test Results vs. ENR Equation Capacity for 384 PD/LT2000 pile-cases in all types of soils
- 6.5 Static Load Test Results vs. ENR Equation Capacity with Factor of Safety of 6 for 384 PD/LT2000 pile-cases in all types of soils
- 6.6 Static Load Test Results vs. Gates Dynamic Equation Capacity for 384 PD/LT2000 pile-cases in all types of soils
- 6.7 Static Load Test Results vs. Pile Capacity according to the FHWA Version of the Gates Equation for 384 PD/LT2000 pile-cases in all types of soils
- 6.8 Static Load Test Results vs. Pile Capacity according to the FHWA Version of the Gates Equation for 135 PD/LT2000 EOD pile-cases in all types of soils (AEA)
- 6.9 Static Load Test Results vs. Pile Capacity according to the FHWA Version of the Gates Equation for 159 PD/LT2000 BOR(last) pile-cases in all types of soils (ABA)
- 6.10 Static Load Test Results vs. Pile Capacity according to the FHWA Version of the Gates Equation for 62 PD/LT2000 pile-cases at the EOD with Blow Count  $< 16$  BP10cm in all types of soils (AEA)
- 6.11 Static Load Test Results vs. Pile Capacity according to the FHWA Version of the Gates Equation for 32 PD/LT2000 pile-cases at the BOR(last) with Blow Count  $< 16$  BP10cm in all types of soils (ABA)
- 6.12 Static Load Test Results vs. Pile Capacity according to the FHWA Version of the Gates Equation for 73 PD/LT2000 pile-cases at the EOD with Blow Count  $\geq 16$  BP10cm in all types of soils (AEA)
- 6.13 Static Load Test Results vs. Pile Capacity according to the FHWA Version of the Gates Equation for 127 PD/LT2000 pile-cases at the BOR(last) with Blow Count  $\geq 16$  BP10cm in all types of soils (ABA)

- 6.14 Static Load Test Results vs. CAPWAP or TEPWAP predictions for all 377 PD/LT2000 pile-cases at all times and in all types of soils (AAA)
- 6.15 Static Load Test Results vs. CAPWAP or TEPWAP predictions for 125 PD/LT2000 pile-cases at EOD in all types of soils (AEA)
- 6.16 Static Load Test Results vs. CAPWAP or TEPWAP predictions for 162 PD/LT2000 pile-cases at BOR (last) in all types of soils (ABA)
- 6.17 Static Load Test Results vs. CAPWAP or TEPWAP predictions for 54 PD/LT2000 pile-cases at the EOD with Blow Count < 16 BP10cm in all types of soils (AEA)
- 6.18 Static Load Test Results vs. CAPWAP or TEPWAP predictions for 71 PD/LT2000 pile-cases at the EOD with Blow Count  $\geq 16$  BP10cm in all types of soils (AEA)
- 6.19 Static Load Test Results vs. CAPWAP or TEPWAP predictions for 32 PD/LT2000 pile-cases at the BOR (last) with Blow Count < 16 BP10cm in all types of soils (ABA)
- 6.20 Static Load Test Results vs. CAPWAP or TEPWAP predictions for 130 PD/LT2000 pile-cases at the BOR (last) with Blow Count  $\geq 16$  BP10cm in all types of soils (ABA)
- 6.21 Static Load Test Results vs. CAPWAP or TEPWAP predictions for 37 PD/LT2000 pile-cases at the EOD with Blow Count < 16 BP10cm and Area Ratio < 350 in all types of soils (AEA)
- 6.22 Static Load Test Results vs. CAPWAP or TEPWAP predictions for 22 PD/LT2000 pile-cases at the EOD with Blow Count < 16 BP10cm and Area Ratio  $\geq 350$  in all types of soils (AEA)
- 6.23 Static Load Test Results vs. CAPWAP or TEPWAP predictions for 37 PD/LT2000 pile-cases at the EOD with Blow Count  $\geq 16$  BP10cm and Area Ratio < 350 in all types of soils (AEA)
- 6.24 Static Load Test Results vs. CAPWAP or TEPWAP predictions for 34 PD/LT2000 pile-cases at the EOD with Blow Count  $\geq 16$  BP10cm and Area Ratio  $\geq 350$  in all types of soils (AEA)
- 6.25 Static Load Test Results vs. CAPWAP or TEPWAP predictions for 22 PD/LT2000 pile-cases at the BOR (last) with Blow Count < 16 BP10cm and Area Ratio < 350 in all types of soils (ABA)

- 6.26 Static Load Test Results vs. CAPWAP or TEPWAP predictions for 10 PD/LT2000 pile-cases at the BOR (last) with Blow Count < 16 BP10cm and Area Ratio  $\geq 350$  in all types of soils (ABA)
- 6.27 Static Load Test Results vs. CAPWAP or TEPWAP predictions for 83 PD/LT2000 pile-cases at the BOR (last) with Blow Count  $\geq 16$  BP10cm and Area Ratio < 350 in all types of soils (ABA)
- 6.28 Static Load Test Results vs. CAPWAP or TEPWAP predictions for 47 PD/LT2000 pile-cases at the BOR (last) with Blow Count  $\geq 16$  BP10cm and Area Ratio  $\geq 350$  in all types of soils (ABA)
- 6.29 Static Load Test Results vs. Energy Approach predictions for 371 PD/LT2000 pile-cases at all times and in all types of soils (AAA)
- 6.30 Static Load Test Results vs. Energy Approach predictions for 128 PD/LT2000 pile-cases at EOD in all types of soils (AEA)
- 6.31 Static Load Test Results vs. Energy Approach predictions for 153 PD/LT2000 pile-cases at BOR(last) in all types of soils (ABA)
- 6.32 Static Load Test Results vs. Energy Approach predictions for 56 PD/LT2000 pile-cases at the EOD with Blow Count < 16 BP10cm in all types of soils (AEA)
- 6.33 Static Load Test Results vs. Energy Approach predictions for 72 PD/LT2000 pile-cases at the EOD with Blow Count  $\geq 16$  BP10cm in all types of soils (AEA)
- 6.34 Static Load Test Results vs. Energy Approach predictions for 29 PD/LT2000 pile-cases at the BOR (last) with Blow Count < 16 BP10cm in all types of soils (ABA)
- 6.35 Static Load Test Results vs. Energy Approach predictions for 124 PD/LT2000 pile-cases at the BOR (last) with Blow Count  $\geq 16$  BP10cm in all types of soils (ABA)
- 6.36 Static Load Test Results vs. Energy Approach predictions for 39 PD/LT2000 pile-cases at the EOD with Blow Count < 16 BP10cm and Area Ratio < 350 in all types of soils (AEA)
- 6.37 Static Load Test Results vs. Energy Approach predictions for 23 PD/LT2000 pile-cases at the EOD with Blow Count < 16 BP10cm and Area Ratio  $\geq 350$  in all types of soils (AEA)

- 6.38 Static Load Test Results vs. Energy Approach predictions for 39 PD/LT2000 pile-cases at the EOD with Blow Count  $\geq 16$  BP10cm and Area Ratio  $< 350$  in all types of soils (AEA)
- 6.39 Static Load Test Results vs. Energy Approach predictions for 34 PD/LT2000 pile-cases at the EOD with Blow Count  $\geq 16$  BP10cm and Area Ratio  $\geq 350$  in all types of soils (AEA)
- 6.40 Static Load Test Results vs. Energy Approach predictions for 19 PD/LT2000 pile-cases at the BOR (last) with Blow Count  $< 16$  BP10cm and Area Ratio  $< 350$  in all types of soils (ABA)
- 6.41 Static Load Test Results vs. Energy Approach predictions for 10 PD/LT2000 pile-cases at the BOR (last) with Blow Count  $< 16$  BP10cm and Area Ratio  $\geq 350$  in all types of soils (ABA)
- 6.42 Static Load Test Results vs. Energy Approach predictions for 82 PD/LT2000 pile-cases at the BOR (last) with Blow Count  $\geq 16$  BP10cm and Area Ratio  $< 350$  in all types of soils (ABA)
- 6.43 Static Load Test Results vs. Energy Approach predictions for 42 PD/LT2000 pile-cases at the BOR (last) with Blow Count  $\geq 16$  BP10cm and Area Ratio  $\geq 350$  in all types of soils (ABA)
- 6.44 Tip Soil Conditions versus calculated Case Damping Coefficient,  $J_c$ , based on Static Load Test Results for 290 PD/LT pile-cases (Paikowsky et al., 1994)
- 6.45 Static Load Test Results vs. the Case Method (RMX) predictions for 77 pile-cases with varied  $J_c$  in all types of soils, (data obtained from the University of Florida)
- 6.46 Static Load Test Results vs. the Case Method (RMX) predictions for 40 EOD pile-cases with varied  $J_c$  in all types of soils, (data obtained from the University of Florida)
- 6.47 Static Load Test Results vs. the Case Method (RMX) predictions for 40 BOR pile-cases with varied  $J_c$  in all types of soils, (data obtained from the University of Florida)
- 7.1 CAPWAP (last Restrike) Predictions vs. Energy Approach (EOD) Predictions for 83 PD/LT2000 pile-cases in all types of soils (AAA)

- 7.2 CAPWAP (last Restrike) Predictions vs. Energy Approach (EOD)  
Predictions for 47 PD/LT2000 pile-cases with Blow Count < 16  
BP10cm in all types of soils (AAA)
- 7.3 CAPWAP (last Restrike) Predictions vs. Energy Approach (EOD)  
Predictions for 36 PD/LT2000 pile-cases with Blow Count  $\geq$  16  
BP10cm in all types of soils (AAA)
- 7.4 CAPWAP (last Restrike) Predictions vs. Energy Approach (EOD)  
Predictions for 228 PD2000 pile-cases in all soil types
- 7.5 CAPWAP (last Restrike) Predictions vs. Energy Approach (EOD)  
Predictions for 43 PD2000 pile-cases with Blow Count < 16  
BP10cm in all soil types
- 7.6 CAPWAP (last Restrike) Predictions vs. Energy Approach (EOD)  
Predictions for 185 PD2000 pile-cases with Blow Count  $\geq$  16  
BP10cm in all soil types
- 7.7 CAPWAP (last Restrike) Predictions vs. Energy Approach (EOD)  
Predictions for 90 PD2000 pile-cases in clay & till
- 7.8 CAPWAP (last Restrike) Predictions vs. Energy Approach (EOD)  
Predictions for 15 PD2000 pile-cases with Blow Count < 16  
BP10cm in clay & till
- 7.9 CAPWAP (last Restrike) Predictions vs. Energy Approach (EOD)  
Predictions for 75 PD2000 pile-cases with Blow Count  $\geq$  16  
BP10cm in clay & till
- 7.10 CAPWAP (last Restrike) Predictions vs. Energy Approach (EOD)  
Predictions for 42 PD2000 pile-cases in sand & silt
- 7.11 CAPWAP (last Restrike) Predictions vs. Energy Approach (EOD)  
Predictions for 16 PD2000 pile-cases with Blow Count < 16  
BP10cm in sand & silt
- 7.12 CAPWAP (last Restrike) Predictions vs. Energy Approach (EOD)  
Predictions for 26 PD2000 pile-cases with Blow Count  $\geq$  16  
BP10cm in sand & silt
- 7.13 CAPWAP (last Restrike) Predictions vs. Energy Approach (EOD)  
Predictions for 94 PD2000 pile-cases in rock

- 7.14 CAPWAP (last Restrike) Predictions vs. Energy Approach (EOD)  
Predictions for 12 PD2000 pile-cases with Blow Count < 16  
BP10cm in rock
- 7.15 CAPWAP (last Restrike) Predictions vs. Energy Approach (EOD)  
Predictions for 82 PD2000 pile-cases with Blow Count  $\geq 16$   
BP10cm in rock
- 7.16 CAPWAP (last Restrike) Predictions vs. Energy Approach (EOD)  
Predictions for 72 PD2000 pile-cases with Boston Blue Clay
- 7.17 CAPWAP (last Restrike) Predictions vs. Energy Approach (EOD)  
Predictions for 8 PD2000 pile-cases with Blow Count < 16  
BP10cm with Boston Blue Clay
- 7.18 CAPWAP (last Restrike) Predictions vs. Energy Approach (EOD)  
Predictions for 64 PD2000 pile-cases with Blow Count  $\geq 16$   
BP10cm with Boston Blue Clay
- 8.1 Kws values vs. log – Time for PD/LTT2000 pile-cases with multiple  
Restrikes with the majority of the skin friction coming from the clay  
layers (Paikowsky et al., 1995)
- 8.2 Kws values vs. log - Time for PD/LTT2000 pile-cases with multiple  
Restrikes partially in clay
- 9.1 Resistance Factor Analysis Flow Chart (after Ayyub & Assakkaf, 1999,  
Ayyub et al., 2000)
- 9.2 Calculated Resistance Factors for the CAPWAP and Energy Approach  
General Cases showing the Influence of the Dead to Live Load Ratio
- 9.3 Flow Chart Presenting the Sub-Grouping of the Dynamic Analyses  
According to the Controlling Parameters and the Resulting Statistical  
Parameters for a Normal Distribution Function
- 9.4 Histogram and frequency distributions of  $K_{sw}$  for 377 PD/LT2000  
CAPWAP pile-cases in all types of soils (AAA)
- 9.5 Histogram and frequency distributions of  $K_{sw}$  for 125 PD/LT2000  
CAPWAP pile-cases at the EOD in all types of soils (AEA)



- 9.6 Histogram and frequency distributions of  $K_{SW}$  for 37 PD/LT2000 CAPWAP pile-cases at the EOD with Blow Counts < 16 BP10cm and Area Ratio < 350 in all types of soils (AEA)
- 9.7 Histogram and frequency distributions of  $K_{SW}$  for 162 PD/LT2000 CAPWAP pile-cases at the BOR(last) in all types of soils (ABA)
- 9.8 Histogram and frequency distributions of  $K_{SP}$  for 371 PD/LT2000 Energy Approach pile-cases in all types of soils (AAA)
- 9.9 Histogram and frequency distributions of  $K_{SP}$  for 128 PD/LT2000 Energy Approach pile-cases at the EOD in all types of soils (AEA)
- 9.10 Histogram and frequency distributions of  $K_{SP}$  for 39 PD/LT2000 Energy Approach pile-cases at the EOD with Blow Counts < 16 BP10cm and Area Ratio < 350 in all types of soils (AEA)
- 9.11 Histogram and frequency distributions of  $K_{SP}$  for 153 PD/LT2000 Energy Approach pile-cases at the BOR(last) in all types of soils (ABA)
- 9.12 Histogram and frequency distributions of  $K_{SENR}$  (without FS = 6) for 384 PD/LT2000 pile-cases in all types of soils (AAA)
- 9.13 Histogram and frequency distributions of  $K_{SENR}$  (with FS = 6) for 384 PD/LT2000 pile-cases in all types of soils (AAA)
- 9.14 Histogram and frequency distributions of  $K_{SG}$  for 384 PD/LT2000 pile-cases in all types of soils (AAA)
- 9.15 Histogram and frequency distributions of  $K_{SFG}$  for 384 PD/LT2000 pile-cases in all types of soils (AAA)
- 9.16 Histogram and frequency distributions of  $K_{SFG}$  for 135 PD/LT2000 pile-cases at the EOD in all types of soils (AAA)
- 9.17 Histogram and frequency distributions of  $K_{SFG}$  for 62 PD/LT2000 pile-cases at the EOD with Blow Counts < 16 BP10cm in all types of soils (AAA)
- 9.18 Histogram and frequency distributions of  $K_{SWP}$  for 99 PD/LT2000 GRLWEAP pile-cases at the EOD in all types of soils (AAA)
- 9.19 Histogram and frequency distributions of  $K_{SWP}$  for 99 PD/LT2000 GRLWEAP pile-cases at the BOR in all types of soils (AAA)

- B.1 Blow Count vs. Depth for Newbury Site
- B.2 Vertical Effective Stress vs. Depth for Newbury Site
- B.3 Tip Resistance vs. Depth, CPT's, Newbury Site
- B.4 Side Resistance vs. Depth, CPT's, Newbury Site
- B.5 Load vs. Deflection Curve, Compression Test, Newbury Site
- B.6 Load vs. Deflection Curve, Tension Test, Newbury Site
- D.1 Soil Profile and SPT values with Depth for the Newbury Site
- D.2 CPT data,  $f_s$  profile with Depth for the Newbury Site
- D.3 CPT data,  $q_c$  profile with Depth for the Newbury Site
- D.4 Soil Profile and SPT values with Depth for the Choctawhatchee River Project
- D.5 CPT data,  $f_s$  profile with Depth for the Choctawhatchee River Project
- D.6 CPT data,  $q_c$  profile with Depth for the Choctawhatchee River Project

# **CHAPTER 1**

## **INTRODUCTION**

### **1.1 OVERVIEW**

An ongoing project supported by the USA National Cooperative Highway Research Program (NCHRP) under the Transportation Research Board (TRB) of the National Academy of Science (NAS), is aimed at rewriting AASHTO Deep Foundation Specifications for the year 2001. The AASHTO specifications are traditionally observed on all federally aided projects and generally viewed as a national code of US Highway practice, hence influencing the construction of all the deep foundations of highway bridges throughout the USA.

The new code is based on Load and Resistance Factor Design (LRFD) principles with resistance factors obtained from probabilistic analysis of data. A large database (PD/LT2000) is the backbone of the dynamic methods' performance evaluation. This database originated with the work presented by Paikowsky et al. (1994), Paikowsky and LaBelle (1994), and additional information acquired since.

A summary and careful evaluation of the large database is presented, detailing the performance of various dynamic methods when compared to static load testing to failure. The parameters that control the accuracy of the dynamic predictions are

analyzed, suggesting the importance of certain mechanisms associated with the pile penetration and the dynamic simulations.

The controlling parameters and the statistical analyses are then utilized for the development of resistance factors to be recommended for the new specifications.

## **1.2 BACKGROUND**

National Cooperative Highway Research Program, project, NCHRP 24-17, "LRFD Deep Foundations Design" was initiated to: (i) Provide recommended revisions to the driven pile and drilled shaft portions of section 10 of AASHTO Specifications and (ii) Provide a detailed procedure for calibrating deep foundation resistance factors. The current AASHTO specifications as well as other existing codes based on Load and Resistance Factor Design (LRFD) principles were developed using insufficient data, hence they utilized mostly back-calculated factors. The main challenges of the project are therefore: (a) Compilation of large, high quality databases and (b) Framework for a procedure and data management to enable: (i) LRFD parameter evaluation and (ii) Future updates. These challenges include two requirements: (i) Organization of the factors following the design - construction - quality control sequence (i.e. independence in resistance factors according to the chronological stage and the evaluation procedure) and (ii) Overcome the generic difficulties of applying the LRFD methodology to geotechnical applications, i.e. incorporation of indirect variability, (e.g. site or parameters interpretation), judgment (e.g. previous experience), and other similar factors.

The project team, headed by Samuel G. Paikowsky, is divided into three major groups dealing with static analyses (University of Florida), probabilistic approaches and structural analyses (University of Maryland), and dynamic analyses (University of Massachusetts at Lowell). The present paper provides a background for design methodologies and the LRFD. Database PD/LT2000 is presented and analyzed. The state of practice and the selected dynamic methods are described, followed by an initial evaluation of the signal matching technique and examination of the controlling parameters. The performance of the dynamic methods is then provided, categorized according to the controlling parameters. The obtained results are used for the development of resistance factors to be recommended for the new specifications.

### **1.3 MANUSCRIPT LAYOUT**

The following is a brief description of the contents of each chapter:

**CHAPTER 2** presents a summary of the Working Stress Design (WSD) method and the Load and Resistance Factor Design (LRFD) method as they apply to Geotechnical Engineering. Also presented is a review of the recommended LRFD factors based on many international codes.

**CHAPTER 3** describes the processes that were used in compiling the data presented in each of the databases for use in the present research. The actual data is presented in Appendix A but will be discussed in detail in this chapter.

**CHAPTER 4** discusses the methodology used to determine which method of determining pile capacity based on the static load test curve should be used as the

reference static capacity when comparing the dynamic pile capacity predictions to the static load test results.

**CHAPTER 5** presents the analysis used to determine the controlling parameters that effect the pile capacity based on the dynamic methods. The controlling parameters that are analyzed are the effects of soil type, time of driving (EOD – End Of Driving and BOR – Beginning Of Restrike), and the soil inertia effects (driving resistance and pile type).

**CHAPTER 6** discusses the performance of the dynamic methods during the construction phase. The performance of the dynamic methods is analyzed for two cases, with dynamic measurements and without dynamic measurements. The analysis that is presented for the case without dynamic measurements includes the WEAP analysis and the dynamic equations. The CAPWAP method, the Energy Approach method, and the Case Method are all presented in the case with dynamic measurements.

**CHAPTER 7** presents a comparison between the Energy Approach pile capacity predictions at the EOD and the CAPWAP pile capacity predictions at the BOR based on the controlling parameters presented in Chapter 5.

**CHAPTER 8** briefly discusses the effects of pile capacity gain with time due to pore water pressure dissipation.

**CHAPTER 9** presents the methodology that was used to calculate the proposed resistance factors for the dynamic methods, which are also presented in this chapter.

**CHAPTER 10** discusses the difficulty of comparing the pile capacities determined using the LRFD method with the proposed resistance factors and previous codes. A comparison is made although it is limited due to the discussed difficulties.

**CHAPTER 11** presents the conclusions of the present research.

## **CHAPTER 2**

### **BACKGROUND**

#### **2.1 STATE OF STRESS METHODOLOGY**

##### **2.1.1 Overview**

Working Stress Design (WSD) method, also called the Allowable Stress Design (ASD) method, has been the traditional design basis in Civil Engineering since it was first introduced in the early 1800's. In the 1950's the continued demand for a more economical design of piles brought about the use of Limit States or Limit States Design (LSD). The two types of limit states are the Ultimate Limit State (ULS) and the Serviceability Limit State. Both limit states must be satisfied when using the Limit States Design method. A more detailed description of the two limit states is presented in the following sections. The material in the overview section is based primarily on Becker (1996) and Allen (1994).

The latest method of pile design to be introduced is the Load and Resistance Factor Design (LRFD) method. This method relies heavily on the use of limit states and reliability theory, which is also known as Reliability Based Design (RBD). The reliability theory introduced the determination of factors of safety based on the combined probability of load and resistance looking into the probability of pile failure or the probability of failure of the soil in bearing capacity. The most recent methods of pile design, i.e. LRFD, RBD and LSD can be utilized in a simple manner for a specific site or can be involved as need



be for more complex subsurface conditions. “Regardless of the design philosophy and approach used, the basic design criteria is that the capacity or resistance of the system must be greater than the demand or loads on the system for an acceptable or required level of safety” (Becker, 1996).

### 2.1.2 The Working Stress Design (WSD) Method

The Working Stress Design (WSD) method is aimed to ensure that when the structure is subjected to the “working” or service applied load; the induced stresses are less than the allowable stresses. The WSD method combines all of the uncertainties in the loads and the soil and accounts for them by using one factor of safety, FS. The design loads, Q, consist of the actual forces estimated to be applied directly to the structure, (Becker, 1996 and Withiam et al. 1998). This can be seen in the fundamental equation that governs WSD:

$$Q \leq Q_{all} = \frac{R_n}{FS} = \frac{Q_{ult}}{FS} \quad (2.1)$$

Where: Q = Design load (kN)  
 $Q_{all}$  = Allowable design load (kN)  
 $R_n = Q_{ult}$  = Ultimate geotechnical pile force resistance of a pile; and  
 FS = Factor of safety

Equation 2.1 can also be written as:

$$\frac{R_n}{FS} \geq \sum Q_i \quad (2.2)$$

Where:  $R_n$  = Nominal resistance  
 $\sum Q_i$  = Load effect  
 FS = Factor of safety

The factor of safety is commonly defined as the ratio of the resistance of the structure ( $R_n$ ) to the load effects ( $Q$ ) acting on the structure. The determination of the factor of safety is the most difficult part of the design process. Rearranging Equation 2.2 to solve for the factor of safety (FS), the factor of safety can be expressed as a variable or a constant. The factor of safety mostly depends on the level of control that was used in the design and construction phases. For example, if data from a subsurface exploration program is used, a static analysis is completed, and the results from a wave equation analysis are used to determine the ultimate geotechnical resistance of a pile, then the factor of safety must be greater than 2.75, (see Table 2.1). On the other hand, if more reliable methods for determining the ultimate geotechnical resistance of a pile are used, then a reduced factor of safety can be incorporated. "Traditionally, the factor of safety is applied to the resistance as in Equation 2.2. This method gives sensible results when material strength (resistance) represents the greatest uncertainty in design", (Simpson et al., 1981).

Table 2.1, after AASHTO (1997), provides different factors of safety that are used in the analysis of the ultimate geotechnical resistance of a piles. Table 2.1 relates to both design and construction phases and demonstrates that the WSD method allows the factor of safety to vary depending on the level of control. When a more reliable and consistent level of Construction Control is used, a smaller factor of safety can be implemented, leading to a more economical construction.

Equation 2.1 can also be rewritten for structural design based on allowable stress as:

$$\Sigma Q \leq \sigma_{all} A = P_{all} \quad (2.3)$$

Where:  $\sigma_{all}$  = Allowable axial stress in pile (kPa)  
 $P_{all}$  = Allowable axial structural capacity (kN); and  
 $A$  = Cross sectional area of pile (m<sup>2</sup>)

Equation 2.3 can be rewritten so as to solve for the allowable axial load,  $P_{all}$ :

$$P_{all} = \Sigma \sigma_{all} A \quad (2.4)$$

The applied load is limited by the maximum allowable load. The maximum allowable axial load that can be applied to the pile is obtained from Equation 2.4 by multiplying the allowable stress (see Table 2.2) by the cross sectional area of the pile.

In addition to axial geotechnical and structural capacity evaluation, the design of driven piles by WSD requires evaluations of pile displacements and comparisons with deformation criteria using the following:

$$\delta_i \leq \delta_n \quad (2.5)$$

Where:  $\delta_i$  = Estimated displacement (mm); and  
 $\delta_n$  = Tolerable displacement established by designer (mm).

The tolerable displacement is typically associated with the structure type and function, for example the allowable displacement of bridges depends on the structural concept (e.g., simply supported versus integral), and the type of supports that are being utilized for the superstructure.

### 2.1.3 The Limit States

Limit states are defined as the conditions under which a structure or its component members can no longer perform their intended functions. Whenever a structure or a part of it fails to satisfy one of its designated operational criteria, it is

said to have reached a limit state. The two limit states that are checked in the design of piles are the Ultimate Limit State (ULS) or Strength Limit State and the Serviceability Limit State (SLS).

Ultimate limit states pertain to structural safety and define dangerous conditions. The ULS involves the collapsing of the structure and in relation to piles the event under which the ultimate bearing capacity of the soil is exceeded. Serviceability limit states (SLS) represent the conditions that affect the function or service requirements (performance) of the structure under expected service/ working loads. These conditions can include excessive deformations and settlement or deterioration of the structure pile(s). "The serviceability limit states are checked by using a partial factor of unity on all specified or characteristic service loads and load effects", (Meyerhof, 1994).

In WSD, the term "allowable soil bearing pressure" may be controlled by either bearing capacity (ULS) or by settlement (SLS) considerations. WSD implicitly accounts for these two key limit states, but generally does not do so explicitly, (Becker, 1996). In other words, the WSD method does not require that the calculations be made to check both of the limit states, instead, there are charts that are used to show whether the designer needs to check the ultimate limit state or the serviceability limit state. Figure 2.1 is an example of the type of charts used for determining whether the design of spread footings is controlled by bearing capacity or settlement. The LRFD method for piles checks both the ultimate and serviceability

limit states explicitly. The calculations are done to insure that the design criteria have been met for both; the ultimate and serviceability limit states.

When limit states were first introduced, the design method encountered opposition because designers and engineers thought it to be too complicated for practice. The limit state design calculations and analyses can however range from estimates and back-of-the envelope calculations to three-dimensional finite element analysis. "Simple calculations that capture the essence of the behavior and promote thinking are preferred for preliminary design and checking, rather than complex computer programs", (Allen, 1994). Regardless of the complexity of the analysis and calculations, all limit states designs are carried out to satisfy the following criteria:

Ultimate limit state (ULS):

$$\text{Factored resistance} \geq \text{Factored load effects} \quad (2.6)$$

Serviceability limit state (SLS):

$$\text{Deformation} \leq \text{Tolerable deformation to remain serviceable} \quad (2.7)$$

(Becker, 1996)

According to Duncan et al. (1989) the SLS have a higher probability of occurrence than the ULS. The allowable settlement of a structure generally controls the design of shallow foundations rather than the ultimate bearing capacity of the soil. "In geotechnical design, a serviceability condition or settlement criterion frequently constitutes the primary limit state. Accordingly, the design would be based on specific SLS; the ULS would be checked subsequently", (Becker, 1996). By and large, the design of deep foundations is controlled by the ultimate limit state. However, O'Neill

(1999) suggests that this is not always the case, deep foundations need to be checked for settlement, therefore, it is required that their serviceability limit state be evaluated as well. Examples for such cases are group settlement of driven piles in certain soil/pile stiffness conditions and large diameter drilled shafts (say 4m), especially when carrying a large portion of the load at the toe of the deep foundation.

## **2.2 LOAD AND RESISTANCE FACTOR DESIGN (LRFD) METHOD**

### **2.2.1 Reliability Based Design - History and Background**

The design of a pile depends upon predicted loads and the pile's capacity to resist them. Both loads and capacity have various types and levels of uncertainty that needs to be considered in design. Historically, engineering design methods and processes have compensated for these uncertainties by experience and subjective judgment. However, with reliability technology, these uncertainties can be considered more quantitatively. Specifically, the use of probability-based design criteria, or safety check expressions, has the promise of producing better-engineered designs with consistent levels of reliability. The load and resistance factor design (LRFD) format is a commonly used reliability-based format in many areas. It consists of the requirement that a factored (reduced) strength of a pile is larger than a linear combination of factored (magnified) load effects. In this format, load effects are increased, and strength is reduced, by multiplying the corresponding characteristic (nominal) values with factors, which are called strength (resistance) and load factors, respectively. The characteristic value of some quantity is the value that is used in current design practice, and it is usually equal to a certain percentile of the probability

distribution of that quantity. The load and strength factors are different for each type of load and strength. The higher the uncertainty associated with a load, the higher the corresponding load factor. These factors are determined probabilistically so that they correspond to a prescribed safety level. It is also common to consider two classes of performance functions that correspond to ultimate strength (or simply strength) and serviceability requirements. The difference between working stress and LRFD formats is that the latter use different safety factors for each type of load and strength thereby allowing to take into account uncertainties in load and strength, and to scale their characteristic values accordingly in the design equation. Working stress formats cannot do that as it uses only one safety factor. Relative to a conventional factor of safety code, a probability-based design code has the promise of producing a better engineered structure. Experience has shown that adoption of a probability-based design code has resulted in significant savings in materials and/or an efficient use of materials. Reliability improvements are still under evaluation even though, the new codes are specifically designed so that the reliability is equal to or better than the older codes they replace. Experiences are not well documented at this time, but designers have commented that, relative to the conventional working stress code, the new AISC-LRFD (American Institute of Steel Construction) requirements are saving anywhere from 5% to 30% steel weight, with about 10% being typical. This may or may not be the case for other industries. Specific benefits in pile design include the following:

1. A more efficiently balanced design results in weight/cost savings and/or an improvement of reliability.
2. Uncertainties in the design are treated more rationally and rigorously.

3. An improved perspective of the overall design and construction process (substructure and superstructure) and the development of probability-based design procedures can stimulate advances in pile analysis and design.
4. The codes become a living document that can be easily revised to include new information reflecting statistical data on design factors.
5. The partial safety factor format used herein also provides a framework for extrapolating existing design practice to new foundation concepts and materials where experience is limited.

The concept of using the probability of failure as a criterion for structural design can be credited to the Russians N. F. Khotsialov and N. S. Streletskii who presented the idea in the late 1920s. The first exposition of the idea in the United States was made by A. M. Freudenthal in 1947. Considerable interest by many industries and engineering disciplines has evolved in developing reliability-based design codes. Reliability-based design codes using an LRFD format were developed using first-order second-moment reliability methods (Ayyub and McCuen 1997) such as by the American Institute of Steel Construction (AISC 1994, and Galambos and Ravindra 1978) and by the American Concrete Institute (ACI). An effort was made by the National Standards Institute (ANSI) to develop probability-based load criteria for buildings (Ellingwood et al. 1982a and 1982b) that was published as ASCE 7-93 (ASCE 1993). The American Petroleum Institute (API) extrapolated LRFD technology for its use in fixed offshore platforms (API 1989, and Moses (1985 and 1986)). Other efforts which provide excellent and comprehensive summaries of implementation of modern probabilistic design theory into design codes include those of Siu, et al. (1975) for the National Building Code of Canada (1977), Ellingwood et



al. (1980) for the National Bureau of Standards, and the CIRIA 63 (1977) report. Ayyub et al. (1998) provide details on LRFD rules for naval surface ship structures developed for the US Navy.

The AASHTO LRFD Bridge Design and Construction Specifications (1994) as a result of NCHRP Project 12-33 by Nowak, (1993) provide design guidance for girders. To enable uniform treatment of all bridge subsystems, this study is required to provide design and construction specifications for piles that are consistent with the AASHTO LRFD Bridge Design and Construction Specifications.

### **2.2.2 Development of the LRFD Method for General Geotechnical Engineering**

The following section is based on a comprehensive review presented by Goble, (1999). Figure 2.2 shows the probability density functions for the load effect,  $Q$ , and the resistance,  $R$ . (The term load effect refers to the load calculated to act on the particular element in question). The area where the two curves overlap illustrates the region where the load effect is greater than the resistance indicating a scenario where there is a high probability of failure. The shaded area under the probability density function for the resistance represents the probability that the resistance will have a value between  $a$  and  $b$ .

In probability-based design, a prescribed value that is based on previous case histories similar to the one that is being evaluated is chosen for the probability of failure. The probability of the failure for the specific case in question should be greater than the prescribed value.

In Figure 2.2, the probability density function for the load effect is narrower than for the resistance because the loads are usually much more deterministic than the resistances. In terms of probability and statistics, the load effect has much less variability than the resistance. This is measured by the standard deviation, which is not shown in Figure 2.2.  $\bar{Q}$  and  $\bar{R}$  as shown in the Figure 2.2 are the mean of the load effect and the mean of the resistance, respectively. The strength or resistance that is determined by the method, which is being used to evaluate the case history, is the nominal strength,  $R_n$ , shown in Figure 2.2. This strength is not necessarily the mean strength or resistance. When the probability density functions are available for both the load effect and the resistance the probability of failure can be determined directly.

There are two different approaches that are used to determine the probability of failure and they are illustrated in Figure 2.3 and Figure 2.4. Figure 2.3 shows the combined probability density function of  $R-Q$ . The probability of failure is the shaded region that is shown to the left of the y-axis. The principle of the method is that  $\overline{R - Q}$  needs to be larger than  $R-Q = 0$ . Usually the mean value is used to define the reference value and the distance of the mean above zero is taken as a multiple of the standard deviation of the distribution. The multiple of the standard deviation, shown in Figure 2.3 as  $\beta$ , is called the reliability index. Figure 2.4 shows the second approach for determining the probability of failure and this is done by using the natural log of  $R/Q$  ( $\ln R/Q$ ). The limiting condition is when  $\ln R/Q = 0$  or when  $R/Q = 1$ . The reliability index is defined the same for both approaches. The reliability

index is defined in greater detail in a later section entitled *LRFD Calibration using Reliability Theory*.

### 2.2.3 The Principle of the LRFD Method for Deep Foundations

The Load and Resistance Factor Design (LRFD) method takes into consideration the variability in the loads placed on the structure by applying a load factor ( $\gamma$ ). A resistance factor ( $\phi$ ) is applied to the resistance to take into account its variability. According to O'Neill (1995), the intent of this design method is to separate uncertainties in loading from uncertainties in resistance and to assure a prescribed margin of safety. The load and resistance factors are present in the fundamental LRFD equations used for checking the resistance and deformation of the supporting soil and rock materials as well as the structural components. Following the 1999 AASHTO LRFD Highway Bridge Design Specifications:

For the strength limit states:

$$R_r = \phi R_n \geq \eta \sum \gamma_i Q_i \quad (2.8)$$

and for the serviceability limit states:

$$\eta \sum \gamma_i \delta_i \leq \phi \delta_n \quad (2.9)$$

Where:

$$\eta = \eta_D \eta_R \eta_I > 0.95 \quad (2.10)$$

- $\eta$  = Factors to account for effects of ductility ( $\eta_D$ ), redundancy ( $\eta_R$ ), and operational importance ( $\eta_I$ ) (dimensionless)
- $\gamma_i$  = Load factor (dimensionless);
- $Q_i$  = Force effect, stress or stress resultant (F or F/A);
- $\phi$  = Resistance factor (dimensionless);
- $R_n$  = Ultimate or nominal resistance (F or F/A);
- $R_r$  = Factored resistance (F or F/A);
- $\delta_i$  = Estimated displacement (L); and

$\delta_n$  = Tolerable displacement (L).

The method for determining the ultimate geotechnical resistance ( $R_n$ ) of a single pile is basically the same for both, the LRFD and WSD methods. The difference between the methods is the resistance factors used in the LRFD method. The ultimate axial geotechnical resistance of piles subjected to axial loading,  $R_n$  is:

$$R_n = Q_{ult} = Q_p + Q_s \quad (2.11)$$

And the factored axial geotechnical resistance,  $Q_R$  is:

$$Q_R = R_r = Q_{ult} = \phi_{qp}Q_p + \phi_{ps}Q_s \quad (2.12)$$

For which:

$$Q_p = q_p A_p \quad (2.13)$$

$$Q_s = q_s A_s \quad (2.14)$$

Where:  $\phi_{qp}, \phi_{qs}$  = Resistance factors based on Barker et al. (1991), see Table 2.3  
 $Q_p, Q_s$  = Ultimate pile tip and side resistance  
 $q_p, q_s$  = Unit tip and side resistance  
 $A_p, A_s$  = Area of pile tip and side surface

(AASHTO, 1998)

The reduction multiplier factor  $\lambda_v$  as shown in Table 2.3 is to account for the level of field capacity verification. As an example, a piles capacity is calculated using the SPT-method for a site where the pile has end bearing and friction in sand, for which the corresponding resistance factor is  $0.45\lambda_v$ . If the ENR equation is used to verify the calculated capacity without stress wave measurements during driving the

corresponding reduction multiplier factor is 0.80, which results in a resistance factor of 0.36.

Various procedures can be used to determine the ultimate axial capacity of driven piles. Whenever using a design method, the resistance factor that is associated with (calibrated to) that particular design procedure, must be used. For example; when using the AASHTO LRFD Specification, only those methods referred to in Table 2.3, for which the calibrated  $\phi$ -factors have been developed, can be used (Withiam et al., 1998). The methods commonly used in practice today are briefly described below:

- Static Methods of Analysis
  - $\alpha$  – method - A semi-empirical, total stress static method of analysis for estimating the ultimate unit side resistance,  $q_s$ , and the ultimate unit tip resistance,  $q_p$ , as a function of the undrained shear strength,  $S_u$ , of cohesive soil (Drewry et al., 1977)
  - $\beta$  – method - a semi-empirical, effective stress method of analysis for estimating  $q_s$  and  $q_p$  in soil as a function of the effective overburden pressure (Burland, 1973)
  - $\lambda$  – method - A semi-empirical, effective stress method of analysis for estimating  $q_s$  in soil as a function of the passive effective lateral earth pressure (Vijayvergiva and Focht, 1972)
  - End-Bearing Pile on Rock - Semi-empirical method (Canadian Geotechnical Society, 1992) for estimating  $q_p$  as a function of the uniaxial compressive strength of the rock,  $c$ , and the spacing of discontinuities
- In-Situ Methods of Analysis
  - SPT-method - Semi-empirical developed by Meyerhof (1976) which correlates  $q_s$  with the SPT blow count for cohesionless soils
  - CPT-method - Semi-empirical method developed by Nottingham and Schmertmann (1975) which correlates  $q_s$  and  $q_p$  with CPT results for cohesionless soils

- Methods Based on Field Testing of Pile
  - Dynamic Measurements - Methods based on data obtained during pile driving for estimating total load capacity based on monitored performance of driven piles and wave equation analyses. Several methods fall under this category, among the field methods: (a) the Case method (see Goble et al., 1970 and Goble et al., 1975) and (b) the Energy Approach (Paikowsky et al. 1994) and the office method: CAPWAP (Goble et al., 1970).
  - Static Load Test - A method for determining the total load capacity based on quasi-static loading (ASTM, 1996) representative of pile, load and subsurface conditions expected for the prototype piles (AASHTO, 1997).

The above procedures are used to determine the ultimate axial geotechnical capacity of driven piles in soil using semi-empirical methods and in-situ testing, and for piles bearing on or in rock using semi-empirical methods.

The load factors that are generally used in practice range from 1.25 for structural loads (dead loads) to 1.75 for moving or live loads. AASHTO has conducted an extensive testing program to determine the load factors that should be used for the different types of loads and these general values can be found in the AASHTO manual. When using Equation 2.8 for driven pile foundation design at the Strength Limit States, the following values of  $\eta$  can normally be used:

- $\eta_D = \eta_R = 1.00$ ; and
- $\eta_I = 1.05$  for structures deemed operationally important, 1.00 for typical structures and 0.95 for relatively less important structures, (AASHTO, 1997)

The determination of the resistance factor ( $\phi$ ) is the challenging element when using LRFD. The following sections describe in detail the calibration processes that are used in conjunction with the LRFD method.

#### 2.2.4 Determination of Resistance Factors by Calibration

The resistance factor can be obtained via calibration utilizing the Working Stress Design (WSD) method (in order to achieve approximately the same factor of safety that WSD would provide) or using the Reliability Theory. The Reliability Theory emphasizes the use of probability analysis via statistical parameters. The following sections describe the calibration process using the WSD method and the reliability theory, respectively.

##### a) *LRFD Calibration via WSD*

Calibration through fitting to the WSD method is used when insufficient statistical data does not allow the performance of a calibration process by optimization, (Withiam et al., 1998). The method of calibrating by fitting with WSD is a simple process in which the fundamental LRFD equation (Eq. 2.8) is divided by the fundamental ASD equation (Eq. 2.2) to determine an equation for the resistance factor ( $\phi$ ). If an average value of 1.0 is used for the load modifier  $\eta$ , then the equation obtained is:

$$\phi \geq \frac{\sum \gamma_i Q_i}{FS \sum Q_i} \quad (2.15)$$

If only the dead loads and live loads are considered the equation becomes:

$$\phi = \frac{\gamma_D Q_D + \gamma_L Q_L}{FS(Q_D + Q_L)} \quad (2.16)$$

Dividing both the numerator and denominator by  $Q_L$  the equation becomes:

$$\phi = \frac{\frac{\gamma_D Q_D}{Q_L} + \gamma_L}{FS(\frac{Q_D}{Q_L} + 1)} \quad (2.17)$$

Where:  $\phi$  = Resistance factor  
 $\gamma_D, \gamma_L$  = Load factors for dead and live loads, respectively  
 $Q_D, Q_L$  = Force effect for dead and live loads, respectively  
 $FS$  = WSD method factor of safety

(After O'Neill, 1995)

Equation 2.17 can be used to determine the resistance factors that need to be used in the LRFD equations in order to obtain a factor of safety equal to that of the WSD method. “While the load and resistance factor design method represented by equation 8 as calibrated using Equation 2.17 provides the designer a clearer means of visualizing uncertainty than the lumped factor of safety method, use of the current load and resistance factors are not likely to result in improved design. Such can only occur if the resistance factors are evaluated directly, rather than through calibration with existing factors of safety”, (O'Neill, 1995). Table 2.4 presents values of the resistance factors using Equation 2.17 for factors of safety varying between 1.5 to 4 and average dead and live load factors of 1.25 and 1.75 respectively. The table presents the resistance factors that would be used to obtain a factor of safety of 1.5 to 4.0 (in 0.5 intervals) related to ratios of dead to live load of 1 to 9. The obtained relations provide an important scale of values, but when using the resistance factors calibrated via the WSD in the LRFD equation (2.8) it is no different from using the WSD method.



**b) LRFD Calibration using Reliability Theory**

Based on Withiam et al. (1998) the resistance factor chosen for a particular limit state must take into account: (i) the variability of the soil and rock properties, (ii) the reliability of the equations used for predicting resistance, (iii) the quality of the construction workmanship, (iv) the extent of soil exploration (little versus extensive), and (v) the consequence of failure. In order to take into account the inherent uncertainties of the resistance and load in a consistent manner, first-order, second-moment principles can be used to establish Equation 2.18 from Equation 2.8 with  $\eta = 1$ :

$$\phi = \frac{\lambda_R (\sum \gamma_i Q_i) \sqrt{\frac{1 + COV_Q^2}{1 + COV_R^2}}}{Q \exp\{\beta_T \sqrt{\ln[(1 + COV_R^2)(1 + COV_Q^2)]}\}} \quad (2.18)$$

Where:  $\lambda_R$  = Overall bias for resistance  
 $COV_Q$  = Coefficient of variation of the load  
 $COV_R$  = Coefficient of variation of the resistance  
 $\beta_T$  = Target reliability index

When just the dead and live loads are considered Equation 2.18 can be written as:

$$\phi = \frac{\lambda_R (\frac{\gamma_D Q_D}{Q_L} + \gamma_L) \sqrt{\frac{(1 + COV_{QD}^2 + COV_{QL}^2)}{(1 + COV_R^2)}}}{(\frac{\lambda_{QD} Q_D}{Q_L} + \lambda_{QL}) \exp\{\beta_T \sqrt{\ln[(1 + COV_R^2)(1 + COV_{QD}^2 + COV_{QL}^2)]}\}} \quad (2.19)$$

Where:  $\lambda_{QD}, \lambda_{QL}$  = Overall bias for the dead and live loads  
 $COV_{QD}, COV_{QL}$  = Coefficient of variation of the dead and live loads

(After Barker et. al., 1991)

Table 2.5 summarizes the calculated resistance factors for five different methods of Axial Pile Capacity. The five methods are the  $\alpha$ -method, the  $\beta$ -method, the  $\lambda$ -method, the CPT method and the SPT method. Both the  $\alpha$ -method and the  $\lambda$ -method show a Type I and a Type II method of axial pile capacity estimation. Type I refers to soils with undrained shear strength,  $S_u$ , less than 50 kPa and Type II refers to soils with  $S_u$  greater than 50 kPa. The calculations allow the examination of the way the pile's length affects the value of the resistance factor. The presented results indicate that the resistance factor does not vary much for the different pile lengths. The selected values of resistance factors for the five methods shown here are the recommended resistance factors in the LRFD AASHTO Specification for the different methods. The selected values of  $\phi$  are all relatively close to the average value of  $\phi$  that was determined, the exception being the  $\phi$  factor selected for the  $\beta$ -method. According to Withiam et al. (1998) the  $\phi$  factor for the  $\beta$ -method chosen in the LRFD AASHTO Specification is much lower than the average value based on the limited number of reported cases where the method had been used in conjunction with performance testing, and the engineering judgment of the code developers.

The following paragraphs describe in detail the different statistical parameters that are being used in the calculation of the resistance factor when calibrating utilizing the reliability theory. The coefficient of variation, bias factors, and the reliability index and its correlation with the probability of failure are described.

The coefficient of variation, COV, is a dimensionless measure of the variability of the data. The COV is defined as the standard deviation ( $\sigma$ ) divided by the mean value ( $\bar{x}$ ):

$$\text{coefficient of variation, } COV = \frac{\sigma}{\bar{x}} \quad (2.20)$$

Where, for a given set of data,  $x_i = (x_1, x_2, \dots, x_N)$  the mean ( $\bar{x}$ ) is defined by:

$$\bar{x} = \sum \frac{x_i}{N} \quad (2.21)$$

for which N is equal to the total number of data values and the standard deviation ( $\sigma$ ) is determined by:

$$\sigma = \sqrt{\frac{\sum (x_i - \bar{x})^2}{(N - 1)}} \quad (2.22)$$

The COV expresses the magnitude of the variability as a percentage or fraction of the mean value. There can be many different types of coefficients of variation including those related to the dead load, live load and the piles resistance.

The bias factor, ( $\lambda$ ), is defined as the ratio of the measured resistance to the predicted or nominal resistance. In equation form it is:

$$\text{Bias factor, } \lambda = \frac{R_m}{R_n} \quad (2.23)$$

Where:  $R_m$  = Measured resistance; and  
 $R_n$  = Predicted (nominal) resistance.

Bias factors are used for live loads, dead loads and the resistance, as can be seen in Equation 2.19.

The term  $\beta$ , the reliability index, is also determined using different statistical parameters and is defined as the number of standard deviations,  $\zeta_g$ , between the mean value,  $\bar{g}$ , and the origin (i.e.,  $\beta = \bar{g}/\zeta_g$ ). Using this definition the reliability index,  $\beta$ , can be expressed as:

$$\beta = \frac{\ln \left[ \left( \frac{R}{Q} \right) \sqrt{\frac{(1 + COV_Q^2)}{(1 + COV_R^2)}} \right]}{\sqrt{\ln \left[ \frac{(1 + COV_R^2)}{(1 + COV_Q^2)} \right]}} \quad (2.24)$$

For further detail on the derivation of this equation the reader is referred to the National Highway Institute Reference Manual and Participant Workbook, NHI Course No. 13068 by Withiam et al. (1998).

There is a correlation between the reliability index and the probability of failure for the pile or structure, presented in the following two equations:

$$p_f = 460e^{(-4.3\beta)} \quad 2 < \beta < 6 \quad (2.25)$$

$$\beta = \frac{\ln\left(\frac{460}{p_f}\right)}{4.3} \quad 10^{-1} < p_f < 10^{-9} \quad (2.26)$$

(Rosenblueth and Esteva, 1972)

Table 2.6a presents the normal PDF approximation generated using the two equations above. Table 2.6a can be used to: (i) determine the target reliability index for a prescribed maximum probability of failure in a design, and (ii) determine the probability of failure for a certain target reliability index. Rosenbleuth and Estava

base this relationship used by Withiam, Barker et al. (1991) and others, on an approximation. Unfortunately, although they say that the approximation pertains to log normal distributions (because they use the mean of the logs and the standard deviation of the logs to calculate), the approximation is not so good below  $\beta$  of about 2.5. Table 2.6b prepared by Greg Baecher provides the comparison between the "exact" numbers to the approximation and suggests significant errors, especially in our zone of interest ( $\beta = 2$  to 3). The "exact" numbers will be used in the presented research.

**c) *Reliability-Based LRFD Using Failure Point***

The First-Order Reliability Method (FORM) is conveniently used to assess the reliability of a pile according to a specified limit state. FORM also provides a means for calculating the partial safety factors  $\phi$  and  $\gamma_i$  for a specified target reliability level  $\beta_0$ . The simplicity of the FORM approach stems from the fact that this method, beside the requirement that the distribution types must be known, requires only first and second moments of the distribution, namely, the mean values and standard deviations of the respective random variables.

In design practice, there are usually two types of limit states: ultimate limit states and serviceability limit state. Each can be represented by a performance function of the form,

$$g(\mathbf{X}) = g(X_1, X_2, \dots, X_n) \quad (2.27)$$

in which  $\mathbf{X}$  is a vector of basic random variables ( $X_1, X_2, \dots, X_n$ ) for strengths and loads. The performance function  $g(\mathbf{X})$  is sometimes called the limit state function. It

relates the random variables for the limit-state of interest. The limit state is defined when  $g(\mathbf{X}) = 0$ , and therefore, failure occurs when  $g(\mathbf{X}) < 0$ . The reliability index  $\beta$  is defined as the shortest distance from the origin to the failure surface at the most probable failure point (MPFP).

As indicated earlier, the basic approach to develop a reliability-based strength standard is to determine the relative reliability of designs based on current practice. Therefore, reliability assessments of existing designs are needed to estimate representative values of the reliability index  $\beta$ . FORM is well suited to perform such a reliability assessment.

The following are computational steps for determining  $\beta$  using FORM:

1. Assume a design point  $x_i^*$  and obtain its corresponding point,  $x_i'^*$  in a reduced coordinate system using the normalizing transformation:

$$x_i'^* = \frac{x_i^* - \mu_{X_i}}{\sigma_{X_i}} \quad (2.28)$$

Where:  $\mu_{X_i}$  = mean value of the basic random variable  $X_i$ , and  
 $\sigma_{X_i}$  = standard deviation of the basic random variable.

The mean values of the basic random variables can be used as initial guesses for the design points, to be later solved for iteratively. The notation  $x^*$  and  $x'^*$  is used respectively for the design point in the regular coordinates and in the reduced (normalized) coordinates.

2. Evaluate the equivalent normal distributions for the non-normal basic random variables at the design point using the following equations:

$$\mu_X^N = x^* - \Phi^{-1}(F_X(x^*))\sigma_X^N \quad (2.29)$$

and

$$\sigma_X^N = \frac{\left(\Phi^{-1}(F_X(x^*))\right)}{f_X(x^*)} \quad (2.30)$$

where  $\mu_X^N$  = mean of the equivalent normal distribution,  $\sigma_X^N$  = standard deviation of the equivalent normal distribution,  $F_X(x^*)$  = original cumulative distribution function (CDF) of  $X_i$  evaluated at the design point,  $f_X(x^*)$  = original probability density function (PDF) of  $X_i$  evaluated at the design point,  $\Phi(\cdot)$  = CDF of the standard normal distribution, and  $\phi(\cdot)$  = PDF of the standard normal distribution.

3. Set  $x_i^* = -\alpha_i^* \beta$ , in which the  $\alpha_i^*$  are direction cosines. Compute the directional cosines ( $\alpha_i^*$ ,  $i = 1, 2, \dots, n$ ) using the equations:

$$\alpha_i^* = \frac{\left(\frac{\partial g}{\partial x_i}\right)_*}{\sqrt{\sum_{i=1}^n \left(\frac{\partial g}{\partial x_i}\right)_*^2}} \quad \text{for } i = 1, 2, \dots, n \quad (2.31)$$

Where:

$$\left(\frac{\partial g}{\partial x_i}\right)_* = \left(\frac{\partial g}{\partial x_i}\right) \sigma_{X_i}^N \quad (2.32)$$

4. With  $\alpha_i^*$ ,  $\mu_{X_i}^N$ , and  $\sigma_{X_i}^N$  now known, the following equation can be solved for  $\beta$ :

$$g[(\mu_{x_1}^N - \alpha_{x_1}^* \sigma_{x_1}^N \beta), \dots, (\mu_{x_n}^N - \alpha_{x_n}^* \sigma_{x_n}^N \beta)] = 0 \quad (2.33)$$

5. Using the  $\beta$  obtained from step 4, a new design point is obtained from:

$$x_i^* = \mu_{x_i}^N - \alpha_i^* \sigma_{x_i}^N \beta \quad (2.34)$$

6. Repeat steps 1 to 5 until a convergence of  $\beta$  is achieved. This reliability index is the shortest distance to the failure surface from the origin in the reduced coordinates.

The first-order reliability method (FORM) can be used to estimate partial safety factors such as those found in the design format. At the failure point  $(R^*, L_1^*, \dots, L_n^*)$ , the limit state is given by

$$g = R^* - L_1^* - \dots - L_n^* = 0 \quad (2.35)$$

or, in a general form

$$g(X) = g(x_1^*, x_2^*, \dots, x_n^*) = 0 \quad (2.36)$$

For given target reliability index  $\beta_0$ , probability distributions and statistics (means and standard deviations) of the load effects, and the coefficient of variation of strength, the mean value of the resistance, and the partial safety factors can be determined by the iterative solution as previously presented. The mean value of the resistance and the design point can be used to compute the mean required partial design safety factors as,



$$\phi = \frac{R^*}{\mu_R} \quad (2.37)$$

$$\gamma_i = \frac{L_i^*}{\mu_{L_i}} \quad (2.38)$$

In developing design code provisions for piles, it is sometimes necessary to follow the current design practice to insure consistent levels of reliability over various pile types. Calibrations of existing design codes are needed to make the new design formats as simple as possible and to put them in a form that is familiar to users or designers. Moreover, the partial safety factors for the new codes provide consistent levels of safety or reliability. For a given reliability index  $\beta$  and probability characteristics for the resistance and load effects, the partial safety factors determined by the FORM approach might be different for different failure modes for the same or differing component. For this reason, calibration of the calculated partial safety factors (PSF's) is important in order to maintain the same values for all loads at different failure modes.

Normally, the calibration is performed on the strength factor  $\phi$  for a given set of load factors. The following algorithm can be used to accomplish this objective:

1. For a given value of the reliability index  $\beta$ , probability distributions and statistics of the load variables, and the coefficient of variation for the strength, compute the mean of the strength  $R$  using the first-order reliability method as outlined previously.

2. With the mean value for  $R$  computed in step 1, the partial safety factor  $\phi$  can be revised as follows:

$$\phi = \frac{\sum_{i=1}^n \gamma_i \mu_{L_i}}{\mu_R} \quad (2.39)$$

Where  $\mu_{L_i}$  and  $\mu_R$  are the mean values of the loads and strength variables, respectively and  $\gamma_i, i = 1, 2, \dots, n$ , are the given set of load factors.

### 2.2.5 The Use of Limit States in LRFD

The design of driven pile foundations using LRFD requires evaluation of pile suitability at various strength limit states and the service I limit state (Withiam et al., 1997). The service I limit state is defined as the load combination relating to the normal operational use of the bridge with a 56-mph (90 km/hr) wind. For driven piles supporting bridges, two different strength limit states can be used depending on the type of loading that is applied to the pile(s). If the loading is designed for vehicles without wind then the strength I limit state is used and if the loading is a permit vehicle loading then the strength II limit state is used. Table 2.7 shows the design considerations that must be taken into account for piles that are designed at the different limit states. There are many different types of ultimate and serviceability limit states that are used in pile design with the LRFD method.

## 2.3 THE AVAILABLE AND CHOSEN DYNAMIC METHODS

### 2.3.1 General

The materials presented in this section are based on the review of the dynamic methods by Paikowsky et al., 1994 and Paikowsky, 1995. Dynamic analyses of piles are methods that predict pile capacity based on behavior during driving. The evaluation of static capacity from pile driving is based on the concept that the driving operation induces failure in the pile-soil system – in other words, a very fast load test is carried out under each blow. There are basically two methods of estimating the ultimate capacity of driven piles on the basis of dynamic driving resistance: pile-driving formulas (i.e., dynamic equations) and wave-equation analysis.

### 2.3.2 Dynamic Equations

#### a) *The Basic Principle*

The theoretical equations have been formulated around analyses that evaluate the total resistance of the pile, based on the work done by the pile during penetration. Observations of the hammer's ram stroke and the pile set are used in determining this work done by the hammer and the pile. These theoretical equation formulations assume elasto-plastic force-displacement relations (see figure 2.5). The total work is computed as:

$$W = R_u \left( S + \frac{Q}{2} \right) \quad (2.40)$$

Where:

$R_u$	=	Yield resistance
$S$	=	Pile set, denoting the permanent displacement (plastic deformation) of the pile under each hammer blow

$Q$  = Quake, denoting the elastic deformation of the pile-soil system.

**b) Engineering News Record Equation**

The Engineering New Record (ENR) Equation was developed for timber piles using a drop hammer with a factor of safety of approximately 6. Since the equation was first introduced it has been modified for different types of hammers and piles. The ENR equation is based on Wellington (1892). The following overview is also presented in Bowles, 1996 as follows (length units of  $s$  and  $h$  must be the same):

(2.41)

Where:

$P_u$	=	Ultimate pile capacity (F)
$e_h$	=	Hammer efficiency
$W_r$	=	Weight of ram (for double-acting hammers include weight of casing) (F)
$h$	=	Height of fall of ram (L)
$s$	=	Amount of point penetration per blow (L)
$C$	=	A single factor which contains all the elastic compression, $C=25$ mm or 1 inch for drop hammers and $C=2.54$ mm or 0.1 inch for all other hammers

When using the ENR equation with SI units the weight of the ram should be in kN and the set and height of fall of the ram need to be expressed in millimeters. When expressing the ultimate pile capacity in English units the weight of the ram can be in tons, kips or pounds, but the set and height of fall of the ram need to be expressed in inches.

**c) Gates Equation**

The Gates equation is empirical in nature (using sound relations of energy and resistance) based on 130 static load tests to failure. Details are not provided but it is

reasonable to assume that the data set represents different pile and soil conditions.

Recommended F.S. = 3, (Gates, 1957). The equation is presented as follows:

$$B = \frac{1}{7} \times \sqrt{E} \times (1 - \log s) \quad (2.42)$$

Where:

$B$	=	Safe load-carrying capacity of pile, in tons
$E$	=	Gross energy of pile-driving hammer, in ft-lb, times 75 percent for drop hammers, and 85 percent for all other hammers unless otherwise stated by manufacturer
$s$	=	Set per blow, in inches

#### **d) FHWA modified Gates Equation**

The FHWA version of the Gates equation was derived through corrections suggested by Olsen and Flaate, 1967 (using a small database) and then further simplified by Dick Cheney of the FHWA (DiMaggio, 2000). The FHWA modified Gates equation is presented as follows:

$$R_u = 1.75 \times \sqrt{E} \times \log 10N - 100 \quad (2.43)$$

Where:

$R_u$	=	Ultimate capacity (tons)
$E$	=	Gross energy of pile hammer, ft-lb 0.75E for drop hammers 0.85E for all other hammers
$N$	=	Number of blows per inch

### **2.3.3 The Wave Equation**

#### **a) Formulation and Principles**

Issacs (1931) concluded that many pile-driving formulas were incorrectly based on Newtonian mechanics for the pile/hammer impact and he became the first person to suggest the use of an analysis based on the one-dimensional wave equation instead. This proposed solution assumed that the toe of the pile was fixed and that no

side resistance existed (Lowery et al., 1969). Fox (1932) proposed an exact solution to Issacs formulation; however, without the aid of computers, many simplified assumptions were necessary because of the complexity of his solution (Smith, 1960).

Stress-wave propagation in a pile during driving can be described by the following one-dimensional wave equation (after Paikowsky and Whitman, 1990) modified to include frictional resistance along the pile:

$$E_p \frac{\partial^2 u}{\partial x^2} - \frac{S_p}{A_p} f_s = \rho_p \frac{\partial^2 u}{\partial t^2} \quad (2.44)$$

Where:  $E_p, \rho_p$  = Modulus of elasticity and unit density of the pile material  
 $u(x,t)$  = Longitudinal displacement of infinitesimal segment  
 $f_s$  = Frictional stress along the pile  
 $A_p, S_p$  = Pile area and circumference, respectively

The displacement ( $u$ ) causes strains in each pile element that can be used to calculate pile stresses as well as the resistance developed in the soil. This displacement can be determined with respect to time and location. The friction stresses ( $f_s$ ) are generated by the movement of the pile. When the pile is subjected to free-wave motion ( $f_s = 0$ ), the stress propagation equation becomes the familiar one-dimensional wave equation:

$$c^2 \frac{\partial^2 u}{\partial x^2} = \frac{\partial^2 u}{\partial t^2} \quad (2.45)$$

Where:  $c = \sqrt{\frac{E_p}{\rho_p}} \quad (2.46)$

$c$  = Wavespeed of the pile material  
 $E_p$  = Modulus of elasticity of the pile  
 $\rho_p$  = Density of the pile material

Among the assumptions implicit in the development of the one-dimensional wave equation are prismatic shape and homogeneity. Also, it is assumed that under loading, plane parallel cross sections remain plane and parallel and that a uniform distribution of stress exists across each plane. The assumption of uniaxial stress does not include uniaxial strain and, therefore, lateral expansions and contractions (Poisson's effect) arise from the axial stresses associated with lateral inertia (Graff, 1975). The additional friction term (after Paikowsky and Whitman, 1990) was included under the assumption that the soil is stationary (having no inertia effects), and the action of the friction forces does not violate any of the previous assumptions.

The so-called "wave equation methods" are based on a numerical solution of the one-dimensional wave equation. The numerical solution utilizes mathematical models for the pile and pile-soil system. When the one-dimensional wave equation numerical solution is used for pre-driving analysis, the driving system is also modeled.

In 1960, Smith developed a numerical model to simulate the dynamic behavior of the hammer-pile-soil system during driving. This model is represented by a series of discrete masses and springs used for solving the one-dimensional wave equation (see Figure 2.6). The soil resistance is modeled via a spring, slider, and dashpot, which represent the static and dynamic soil resistances (see Figure 2.7). The elastoplastic soil model is employed for the static soil resistance in Smith's solution. The distance traveled by the pile toe during the elastic deformation of the soil is represented by the soil quake (Smith, 1960). As the elastic limit of the soil is reached (represented by the slider in sequence with the spring), plastic deformation takes

place. The plastic deformation, or irreversible compression of the soil, is denoted by the permanent set of the soil (see Figure 2.7).

According to this model, point A represents the ground resistance buildup to the ultimate resistance,  $R_u$ . Plastic failure occurs as the ground resistance has reached its maximum and the adjacent pile segment displaces, plastically, to point B. Unloading the soil at point B produces an elastic rebound, equal to the quake, to point C. The permanent set is, therefore, equal to the distance OC, which, in turn, is equal to distance AB (Smith, 1960). The static soil resistance-displacement relationship, as presented by Smith (1960), is modeled by a spring ( $K_s$ ) and a slider, where  $W$  represents the mass of the pile element.

The dynamic component of the soil's resistance is assumed to viscous (soiltype related) and is, therefore, velocity-dependent. This dynamic resistance is modeled by a dashpot ( $J$ ) parallel to the spring (see Figure 2.7). The resisting soil force ( $R_{max}$ ) developed under each hammer blow is a combination of the static and dynamic soil resistances:

$$R_{max} = R_s + R_d \quad (2.47)$$

Where:

$R_{max}$	=	Total resistance
$R_s$	=	Static resistance
$R_d$	=	Dynamic resistance

The wave equation formulation is used in two general ways: pre-driving analysis and post-driving analysis.



***b) Pre-Driving Analysis***

The so-called "wave equation analysis" utilizes the one-dimensional wave equation to predict dynamic pile behavior before construction and models the pile-soil system and the driving system (i.e., the hammer, cushion, and capblock), as suggested by Smith (1960). This computerized solution is used for the evaluation of the penetration resistance (i.e., blow count) and the driving stresses in the modeled pile under given conditions. The static capacity is then determined by relating the computed static capacity-penetration resistance relationship for a certain energy rating to observed dynamic resistances during driving. Such analyses enable engineers to determine a suitable pile-site-equipment combination.

***c) Post-Driving Analysis - CAPWAP/TEPWAP***

Post-driving analyses utilize the measured force signal (calculated from strain readings) and the measured velocity signal (integrated from acceleration readings) obtained near the pile top during driving. These analyses model the pile-soil system as shown in Figure 2.8 with the element denoted as number 3 representing the point of measurement. The velocity signal is used as a boundary condition at that point while varying the parameters describing the soil resistance in order to match the calculated and measured force signals. These parameters include the side and tip quake, side and tip damping, the pile shaft resistance, and the pile tip resistance. Additional parameters may be used to describe soil resistance and rebound ratio for unloading different from that of loading. The process is described in the form of a flow chart in Figure 2.9. The subscripts *msd.* and *cal.* denote measured and calculated values,

respectively. Iterations are performed by changing the soil-model variables for each pile element in contact with the soil until the best match between the force signals is obtained. The results of these analyses are assumed to represent the actual distribution of the ultimate static capacity of the pile.

This procedure was first suggested by Goble, Likins, and Rausche (1970), utilizing the computer program CAPWAP. Similar analyses were developed by others (see Paikowsky, 1982 and Paikowsky and Whitman, 1989) utilizing the program code TEPWAP.

#### **2.3.4 The Case Method**

##### **a) General**

The Case method (see Goble et al., 1970 and Rausche et al., 1975), is a simple field procedure used by the PDA to estimate pile capacities. Analysis by the Case method is based on the assumptions of a uniform elastic pile, ideal plastic soil behavior, and a simplified wave propagation formulation. Employed are force and velocity measurements taken at the pile top and a correlation between the soil at the pile tip to a damping parameter.

##### **b) The Case Method Equation**

The Case method calculates the total soil resistance (*RTL*) active during pile-driving, using the following equation:

$$RTL = \frac{\left[ F(T1) + F\left(T1 + \frac{2L}{C}\right) \right]}{2} + \left[ v(T1) - v\left(T1 + \frac{2L}{C}\right) \right] \times \frac{MC}{2L} \quad (2.48)$$

Where:	$F(T1)$	=	Measured force at the time $T1$
	$F(T1+2L/C)$	=	Measured force at the time $T1$ plus $2L/C$
	$v(T1)$	=	Measured velocity at the time $T1$
	$v(T1 + 2L/C)$	=	Measured velocity at the time $T1$ plus $2L/C$
	$L, M$	=	Length and mass of the pile, respectively
	$C$	=	Speed of wave propagation in the pile

Different variations of the Case method have been developed taking  $T1$  as the time of impact or modified to include a time delay constant allowing higher  $RTL$  values to be obtained. The time  $T1$  is defined, in equation form, as:

$$T1 = TP + \delta \quad (2.49)$$

Where:	$TP$	=	Time of the impact peak
	$\delta$	=	Time delay

The time delay is required in soils capable of large deformations before achieving full resistance (see Figure 2.10). A time delay is also used in situations where the hammer impact is uneven (PDA Manual, 1999).

The total resistance calculated is a combination of the static resistance ( $S$ ) which is displacement-dependent, and the dynamic resistance ( $D$ ) which is velocitydependent. Therefore, the total resistance (Goble et al., 1975) is:

$$RTL = S + D \quad (2.50)$$

Several factors that influence the pile-soil system must be considered when the total predicted resistance is evaluated. These factors include the damping coefficient, time-dependent soil strength changes, and refusal driving when the soil's resistance is not fully mobilized under a single hammer blow.

**c) Case Damping Coefficient**

The dynamic resistance ( $D$ ) is considered to be viscous in nature, hence, a function of the velocity at the pile toe ( $V_{toe}$ ) and a damping constant ( $J$ ) where:

$$D = J \times V_{toe} \quad (2.51)$$

By applying the wave propagation theory, the pile toe velocity can be calculated as a function of the velocity at the pile top (Goble et al., 1975):

$$V_{toe} = 2V_{top} - \frac{L}{MC} RTL \quad (2.52)$$

Where:

$L$	=	Pile length
$M$	=	Pile mass
$C$	=	Wave speed of the pile material
$R$	=	Total resistance
$V_{top}$	=	Velocity at pile top

$V_{top}$  is taken as the pile top velocity at the time  $TL$ .

According to Goble et al. (1975), remolding effects cause the majority of the damping resistance to be concentrated near the pile tip. Consequently, the damping constant is determined according to the soil type at the pile tip. In most cases, the damping constant ( $J$ ) is proportional to the pile properties ( $EA/C$ ) and, therefore, is represented by a dimensionless coefficient ( $J_c$ ) using the following equation:

$$J = J_c \frac{EA}{C} \quad (2.53)$$

The recommended values for  $J_c$  are based on soil type. These recommended values can be found in the PDA Manual.

**d) Case Method Variations**

Variations of the Case method have evolved for adopting the analysis to different driving situations and soil types. The variations are similar in that they all begin with the initial total resistance prediction (*RTL*) of equation 2.48. Five distinct methods are used to employ the predicted *RTL*: Damping Factor Method (RSP), the Maximum Resistance Method (RMX), the Minimum Resistance Method (RMN), the Unloading Method (RSU), and the Automatic Method (RAU), PDA Manual (1999).

The Damping Factor Method (RSP) uses the standard Case method equation for normal driving conditions. The method utilizes damping constants empirically derived from static load tests.

The Maximum Resistance Method (RMX) is useful for short rise time impacts or large soil quakes where the full toe resistance is not activated by the time the stress wave first reaches the pile toe. RMX is often helpful for displacement piles with large end bearing. RX# can be used for  $J = 0.6$  (i.e., RX6 is RMX with  $J_c = 0.6$ ). With a fixed  $2L/C$ , time  $T_1$  is varied from  $T_p$  to  $T_p + 30$  msec to search for the maximum resistance RMX. This method is advantageous for large displacement piles with substantial end bearing (PDA Manual, 1999).

The minimum capacity (RMN) is determined using the tip reflection time. This method can be used with confidence if the blow count is less than 131 blows per meter (PDA Manual, 1999).

For long piles with high frictional resistance, the measured velocity can become negative before a reflection from the tip is observed at  $T_2$ . Under such

conditions, the upper portion of the pile experiences decreasing displacement or rebounding. This results in an unloading of the upper soil layers resistance and the computed capacities are under-predicted. The Unloading Method (RSU) compensates for this by calculating the total friction in the upper unloading layers from the force velocity difference.

The Automatic Method computes the capacity (RAU) for the first time where the computed pile toe velocity ( $V_{toe}$ ) is zero. This method, originally proposed by Goble et al. (1967), does not select a damping coefficient because damping must be zero when  $V_{toe}$  is zero; therefore, the resistance at this time is completely static. This method provides an exact solution for the end bearing for piles with no skin friction and is recommended for use on piles with very little frictional resistance.

### **2.3.5 The Energy Approach**

This review of the Energy Approach method was taken from Paikowsky and Stenersen (2000). The Energy Approach uses basic energy relations in conjunction with dynamic measurements to determine pile capacity; the concept was presented by Paikowsky (1982) and was examined on a limited scale by Paikowsky and Chernauskas (1992). Extensive studies of the Energy Approach method were carried out by Paikowsky et al. (1994), and Paikowsky and LaBelle (1994). The underlying concept of this approach is the energy balance between the total energy delivered to the pile and the work done by the pile/soil system. The basic Energy Approach equation is:

$$R_u = \frac{E_{max}}{Set + \frac{(D_{max} - Set)}{2}} \quad (2.54)$$

Where:

- $R_u$  = Maximum pile resistance
- $E_{max}$  = Measured maximum energy delivered to the pile
- $D_{max}$  = Measured maximum pile top displacement
- $Set$  = permanent displacement of the pile at the end of the analyzed blow, or 1/measured blow count

For further details regarding the Energy Approach method see Paikowsky et al. (1994) and Paikowsky (1995).

## 2.4 REVIEW OF RECOMMENDED LRFD FACTORS FOR PILE DESIGN

### 2.4.1 Resistance Factors Recommended by AASHTO

Table 2.3 presents the recommended resistance factors ( $\phi$ ) AASHTO (1998), related to the methods employed for determining the ultimate axial pile capacity, described earlier. The resistance factors shown in Table 2.3 are for the ultimate bearing resistance of single piles and are additionally multiplied by a factor  $\lambda_v$  as specified in the table. This factor is accounting for the method that was used to control the pile's installation and to verify the pile's capacity during or after driving.

### 2.4.2 Resistance Factors for Dynamic Load Testing using the Case Method

The majority of the piles installed by the Florida Department of Transportation (FDOT) require dynamic load testing using Pile Driving Analyzer (PDA) monitoring. The FDOT Standard Specifications for Road and Bridge Construction Section A455 recommends that a factor of safety of 2.5 be used for all dynamic pile capacity evaluations based on the PDA. The piles are generally monitored throughout the entire driving but the static capacity is usually evaluated for the end of driving (EOD)

and beginning of restrike (BOR) cases only. McVay et al. (1998) stated that the pile bearing capacity for the EOD case is generally underestimated when compared with the static load test results due to the freezing (set-up) effect with time. This will result in a low probability of failure for the Case method EOD case. The Case method BOR analysis usually gives a prediction that is closer to the static load test results because at the time of the restrike sufficient time has passed to allow for set-up (freezing effects) to occur. Therefore, the Case method BOR analysis will generally result in a higher probability of failure.

The dead and live load factors that are recommended in the AASHTO LRFD Bridge Design Specification (1994) are 1.25 and 1.75, respectively. Barker et al., (1991) recommended the following values be used for the bias factors for dead and live loads 1.05 and 1.15, respectively and for the coefficients of variation for dead and live loads 0.1 and 0.18, respectively. Resistance factors based on the Case method using the maximum resistance method predictions were predominantly for piles driven in Florida and were analyzed and reported by McVay et al. (1998). The pile-cases that were provided by McVay are related to different damping factors. The influence of this damping factor on the predicted static capacity depends on the reflected wave from the pile's tip, and hence on the driving resistance. It needs to be noted that because of the different damping factors that were used the presented data is not entirely reliable. Table 2.8 shows the back-calculated reliability index for a WSD factor of safety of 2.5 and the statistical parameters defined above. The reliability indices for the Case method EOD and BOR cases ranged from 3.04 to 3.14 and from



2.40 to 2.50, respectively, for dead to live load ratios from 1 to 9. The reliability analysis showed that the medians of the reliability index for the Case method EOD and BOR cases are 3.09 and 2.45, respectively. These values relate to a probability of failure of approximately  $7.8 \times 10^{-4}$  and  $1.2 \times 10^{-2}$ , respectively.

Table 2.9 shows the resistance factors that were calculated for both the Case method EOD and BOR cases for target reliability indices of 2.0, 2.5, 3.0 and dead to live load ratios from 1 to 9. Using the target reliability index of 2.5 as an example, the resistance factors ranged from 0.70 to 0.63 for the Case method EOD analysis and from 0.55 to 0.50 for the Case method BOR analysis. From Table 2.4 it can be seen that for a factor of safety of 2.5 and calibrating directly with the WSD the resistance factors ranged from 0.60 to 0.52 for dead to live load ratios from 1 to 9. As a general rule, the dead to live load ratios are in the order of 2 to 4 for the majority of highway bridges. Based on the results of the calibration by reliability analysis and ASD fitting in conjunction with the engineering judgements, a resistance factor of 0.65 is selected for using the Case method EOD condition of dynamic load test to estimate the axial compression capacity of driven pile, and 0.55 for the Case method BOR condition (McVay et al., 1998).

Table 2.8 shows the bias factor for the BOR case as 1.052, which indicates that for the average BOR condition an accurate prediction of the pile capacity is provided. The bias factor for the EOD condition was calculated as 1.552, which indicates that the Case method EOD analysis underestimates the pile capacity. A higher resistance factor was calculated for the EOD condition as compared with the BOR condition,

0.65 and 0.55, respectively. A higher risk is posed when using the Case method BOR condition than when using the Case method EOD condition because of the high uncertainty of the pile freeze effect. As a result, the recommendation by McVay et al., 1998 is that for the general procedure of piling control, the Case method EOD condition be used with a resistance factor of 0.65. The Case method BOR condition can be used with a resistance factor of 0.55 in special cases where the pile freeze effect is well documented.

### **2.4.3 International LRFD Codes**

#### ***a) Australian Standard, Piling-Design and Installation***

A review of the "Australian Standard, Piling-Design and Installation" (1995) is provided by Goble (1999). Table 2.10 presents the resistance factors recommended in the Australian Standard and Table 2.11 is used to determine the final value of the resistance factor to be used from the recommended range of resistance factors given in Table 2.10. In traditional structural design specifications, a nominal value is given and the value used is based primarily on engineering judgement and cannot exceed the nominal value. The Australian Standard is therefore a unique code providing a guide for assessing which resistance factor to use for piles. It is noted that no recommendations are given in regard to the dynamic measurements for the use of EOD or BOR and the method by which the resistance factors were generated is not provided in the code.

**b) 1992 AUSTROADS Bridge Design Code**

Table 2.12 presents the resistance factors specified by AUSTROADS (1992) for different methods used to determine the axial pile capacity. The range of resistance factors in Table 2.12 is quite large and the resistance factor that is provided for the static load test is larger than those provided by other modern codes. No explanation as to how the resistance factors were obtained is given in the specification. Goble (1999) states that the resistance factors were probably calibrated via the WSD method.

**c) Eurocode 7, Geotechnical Design**

Given in this section is the method that is used to determine the ultimate axial geotechnical resistance using Eurocode 7 (1993) and its partial factors ( $\gamma$ ). Eurocode 7 uses the LRFD method of design with one major difference, the factors used for the resistance are greater than unity and the resistances are divided by the Eurocode partial factors. Eurocode 7 also uses different symbols to describe the different terms in the resistance equations. The design bearing resistance,  $R_{cd}$ , of a pile shall be found from:

$$R_{cd} = R_{bd} + R_{sd} \quad (2.55)$$

Where:

$$R_{bd} = \frac{R_{bk}}{\gamma_b} \quad (2.56)$$

$$R_{sd} = \frac{R_{sk}}{\gamma_s} \quad (2.57)$$

In which:

$$R_{bk} = q_{bk} A_b, \text{ and} \quad (2.58)$$

$$R_{sk} = \sum q_{sik} A_{si} \quad (2.59)$$

Where the following symbols are used:

$R_{bk}$ and $R_{sk}$	the characteristic values of the base and shaft resistances
$A_b$	the nominal plan area of the base of the pile
$A_{si}$	the nominal surface area of the pile in soil layer I
$q_{bk}$	the characteristic value of the resistance per unit area of the base
$q_{sik}$	the characteristic value of the resistance per unit area of the shaft in layer i (Eurocode, 1993)

Table 2.13 provides the equivalent load and resistance factors for Eurocode 7 in comparison with the factors provided by the Canadian Geotechnical Society and AASHTO.

Table 2.14 presents the partial factors for Eurocode 7 that are to be used in Equation 2.55. The partial factors that are to be used are constant and independent of soil types or soil tests that are performed on the piles to check their ultimate capacity.

The comparison between the recommended resistance factors of Eurocode 7, the Canadian Geotechnical Society and AASHTO, (presented in Table 2.13) suggest that the load factors recommended by AASHTO, are more conservative than those of the Canadian Geotechnical Society and Eurocode 7. "It is observed that the AASHTO resistance ( $\phi$ ) factors tend to be higher than those for the other codes because they have been calibrated to generally higher load factors (O'Neill, 1995)". Fellenius (1994) reports that foundation engineers espousing LRFD have generally accepted the load factors for the superstructure and have focused on establishing resistance factors. Neither Eurocode 7 nor the Canadian Geotechnical Society provide resistance factors for bored piles. Eurocode 7 does not differentiate between resistances that are

determined using load tests or SPT tests and do not use a different resistance factor for compression and tension load tests.

***d) Danish Code of Practice for Foundation Engineers***

The Danish Code (see Goble, 1999) is similar to Eurocode 7, where partial factors are used instead of resistance factors. For easy comparison with the AASHTO parameters Table 2.15 presents the inverse of the partial coefficients from the Danish Code. In the code the use of static analysis based on soil properties as well as the use of static load tests to determine the axial pile capacity are discussed. Also discussed in the Danish Code is the Danish Formula for dynamic analysis.

The resistance factors (inverse of the partial coefficients) shown in Table 2.15 were calibrated to provide the same level of safety existing in the current practice and do not rely on actual data and its analysis.

***e) Ontario Bridge Code***

Table 2.16 presents resistance factors for deep foundations recommended by the Ontario Highway Bridge Code. No differentiation exists between the various static analysis methods and the provided resistance factors seem to be very small compared to those recommended by other codes. No information is given as to the way in which the resistance factors were obtained.

***f) Canadian Bridge Code***

The Canadian Bridge Code is brief in its design requirements for deep foundations. The three categories that are dealt with for the soil limit state in the Canadian Bridge Code are routine static load testing, dynamic testing and the

geotechnical formula (static analysis). For routine static load tests a resistance factor of 0.5 is to be used while for high-level static load tests a resistance factor of 0.6 is recommended. The two types are defined but only qualitatively. For dynamic load testing a resistance factor of 0.4 is recommended for routine testing and when the analysis is based on parameters obtained from dynamic field measurements a resistance factor of 0.5 is recommended.

In the Canadian Bridge Code the static analysis is defined as the geotechnical formula, the particular formula that is used is not given but whatever formula a designer chooses to use must be approved. When soil properties are used to determine the axial pile capacity such as the cohesion or the friction angle the resistance factors used are 0.5 and 0.8, respectively. The resistance factors presented in Table 2.17, based on pile type, are then multiplied by the pile capacity that was obtained using the soil properties modified by the resistance factors for the particular soil property. The code states that the calculated capacity shall not be greater than  $EAp/C$  or the structural nominal resistance, where  $E$  is the modulus of elasticity of the pile and  $C$  is the velocity of the stress wave propagation. The other two terms,  $\rho$  and  $A$ , are not defined in the code but represent the density of the pile's material and its average cross-sectional area, respectively. The basis for determining the resistance factors was not provided in the code.

***g) Japanese Specifications for Highway Bridges***

The Japanese Design Standards are in the process of being revised to a more generically performance based design, such as LRFD, in conformity to other

international design standards. The presented limited review is based on a report entitled "Foundation Design Standards in the World - Toward Performance-Based Design" written by Kusakabe, 1998. The current specifications for highway bridges are based on two design concepts, the allowable stress design method and the ductility method. Three limit states are considered for the allowable stress design: (i) normal conditions, (ii) at the time of a medium scaled earthquake and (iii) during the time of a storm. At the time of a large scaled earthquake the ductility design method is used. The acceptance criterion for a static load test is based on the "Standard for vertical loading of test piles (JGS, 1811)" Japanese Geotechnical Society.

#### **2.4.4 Evaluation of Recommended Resistance Factors**

A detailed test pile case history was used to evaluate the AASHTO recommended resistance factors. The relevant calculations and a summary of results are presented in Table 2.18. The test pile is part of a research test program conducted in Newbury, Massachusetts by the Geotechnical Engineering Research Laboratory at the University of Massachusetts - Lowell. Detailed reports about the site and the piles are provided by Paikowsky and Chen, (1998) and Paikowsky and Hajduk, (1999), respectively. The ultimate capacity,  $Q_{ult}$ , and the factored axial capacity,  $Q_R$ , of the pile were evaluated using the CPT, SPT, static load test results, the traditional methods based on soil properties, and a computer program, Driven 1.0, which is a windows based update to the program S-Pile.

The information presented in Table 2.18 suggests that the factored axial capacity,  $Q_R$ , for all methods is relatively equal with the exception of the results from

Driven 1.0. Driven 1.0 uses the Nordlund method to determine the static pile capacity and resulted in conservative values. A resistance factor of 0.55 was used for Driven 1.0 based on a recommendation by Withiam et al. (1998).

The designated pile capacities in Table 2.18 under the category "traditional methods" refer to calculations using soil properties to evaluate the skin friction and end bearing resistance of a pile. The designated ultimate loads under this category are an average of the ultimate loads based on a combination of many different methods. The subsurface profile for test pile # 2 consists of both sand and clay layers. For the clay layers the designated skin resistance is the average of the one obtained using the  $\alpha$  and the  $\lambda$ -methods. An average of the skin resistance found using four different methods was used as the designated skin resistance for each sand layer (refer to Appendix B for details). The methods that were used are the General Values after Mansur and Hunter (1970), the API (1989) charts, the McClelland method (McClelland et al., 1969), and Meyerhof's method using the SPT values (Meyerhof, 1956). The average skin resistance found for each of the layers was summed and this value was used as the total side friction for the pile. To determine the tip resistance the methods used were the General Values after Coyle and Castello (Coyle and Castello, 1981), the API (1989) charts, Meyerhof's method using the SPT values (Meyerhof, 1956), the Vesic-Simplified method (Vesic, 1965), the Vesic-Advanced method (Vesic, 1977), the Berezantzev method (Berezantzev et al., 1961), and the simplified SPT method (Meyerhof, 1976). The values determined by each of these methods were summed and an average was taken and this average value was used as



the tip resistance for the traditional methods. AASHTO (1997) recommends resistance factors for some of these different methods individually, but not for the case when they are combined and averaged, such as was done here. Due to the large variability of the subsurface and for illustration purposes a resistance factor of 0.35 was used. This resistance factor is translated to a factor of safety of approximately three in the Working Stress Design method.

The proposed resistance factors from AASHTO (1997) provide parity between the factored axial pile capacities when the ultimate capacity is calculated using the SPT method, CPT method, and the load test data. The problem arises when the ultimate pile capacity is calculated using the computer programs (Nordlund method), because the proposed resistance factor does not give a factored axial pile capacity that is comparable with that calculated using the other methods. Many more case histories will have to be reviewed before any conclusions can be made whether the resistance factors provided by AASHTO and the FHWA are acceptable for practice today.

#### **2.4.5 Evaluation of Calculated Resistance Factors**

Contained in this section are the resistance factors that were calculated by calibrating to the ultimate load that was determined from the static load test results, assuming that the resistance factor for a static load test is 1.00. The calculations were done using the following equations.

$$Q_R = Q_R \quad (2.60)$$

If the resistance factor for end bearing and skin friction are equal then:

$$Q_R = Q_{ult}\phi \quad (2.61)$$

$$Q_{ultA}\phi_A = Q_{ultB}\phi_B \quad (2.62)$$

Where:

- $Q_{ultA}$  = Ultimate Load calculated from static load test results
- $Q_{ultB}$  = Ultimate Load for the method that is being analyzed
- $\phi_A$  = Resistance Factor for the static load test = 1.0 (assumed)
- $\phi_B$  = Resistance Factor to be calculated for the method that is being analyzed

Rearranging Equation 2.62 to solve for  $\phi_B$ , Equation 2.63 is obtained:

$$\phi_B = \frac{Q_{ultA}}{Q_{ultB}} \quad (2.63)$$

Equation 2.60 is a fundamental equation that can be written for the LRFD method of driven pile design. The equation basically states that in the theoretical aspect of LRFD the factored axial capacity calculated using the different methods should be equal. Equation 2.62 is obtained by making the assumption that the resistance factors for both the end bearing and skin friction resistances are equal for the different methods being analyzed. Looking at Table 2.3 it can be seen that this is not an entirely incorrect assumption according to the resistance factors as recommended by AASHTO. Equation 2.63 is obtained by rearranging Equation 2.62 to solve for the resistance factor for the method that is being analyzed.

Table 2.19 shows the resistance factors that were calculated for the SPT method, the CPT method, the Nordlund method (Driven 1.0), and the traditional methods using Equation 2.63. Four different test piles were analyzed to calculate an average resistance factor for each of the four different methods shown in the table. These test piles case histories come from two different project sites, the Newbury Site Project in Newbury, Massachusetts and the West Bay Project in Bay County, Florida. These are two projects in

which the soils data and load test data were well documented, enabling for detailed calculations as presented in Appendix B. The calculations that were done to obtain the resistance factors shown in Table 2.19 are presented in Appendix C.

Table 2.19 shows that for the CPT method there is no consistency between the resistance factors calculated for the different test piles. The resistance factors that were calculated for the SPT method are approximately the same for the two test piles of each site. The problem is that there is a substantial difference between the resistance factors for the test piles of the Newbury Project and the resistance factors for the test piles of the West Bay Project. For both the Nordlund method and the traditional methods the resistance factors that were calculated for the different test piles are approximately the same.

Again referring to Table 2.19 it can be seen that the calculated resistance factor for the CPT method, for test pile # 9 at the West Bay Project is incorrect because it is greater than one (1.38). This is saying that the engineer has so much confidence in the CPT method that instead of reducing the calculated ultimate load it is increased. The resistance factors that are used for the Load and Resistance Factor Design method are all less than one, which states that an ultimate load can never be increased to obtain a factored load. A major problem arises when a resistance factor is greater than one because it essentially shows that a factor of safety that is less than one can be used in the Working Stress Design method.

A direct comparison between the recommended resistance factors and the average calculated resistance factors as well as the average calculated resistance factors multiplied by the AASHTO recommended resistance factor for a static load test of 0.80 are presented

in Table 2.20. This table shows that the average calculated resistance factors were higher (except for the Nordlund method) when compared with the recommended resistance factors. This is reasonable, as by and large the recommended resistance factors need to provide safe design capacities. The fact that the calculated resistance factor for the Nordlund method is lower than the recommended suggests that using the AASHTO specification would result in less than anticipated safe design.

Based on the presented case history calculations and keeping in mind that the resistance factor for the traditional methods is just an assumed resistance factor that provides a factor of safety of approximately three, the statement can be made that there needs to be some research done which looks into the basis for the AASHTO recommended resistance factors. The AASHTO recommended resistance factors need to be founded on large high quality databases.

## **2.5 DIFFICULTIES OF THE EXISTING LRFD CODES**

### **2.5.1 Overview**

All existing codes suffer from two major difficulties. One is the application of LRFD to geotechnical problems due to uncertainties in resistance principally manifested in site characterization, soil behavior, and construction quality. The other problem is lack of data. None of the reviewed codes and associated resistance factors were developed based on databases enabling the calculation of resistance factors from case histories.

The current AASHTO specifications encounter additional difficulty due to the irrational multiplication of the resistance factor by the modifier  $\lambda_v$ . This procedure

requires the interaction of two independent evaluations (e.g. static analysis and dynamic methods) and results in unnecessary and confusing conservatism. A clear separation of the resistance factors on the basis of design and construction is required.

### **2.5.2 Construction Difficulties**

#### ***a) General***

In geotechnical practice, uncertainties in resistance principally manifest in site characterization, soil behavior, and construction quality. The uncertainties have to do with interpreting site conditions, understanding soil behavior, and accounting for construction effects. Uncertainties in external loads are small compared with uncertainties in soil and water loads and the strength-deformation behaviors of soils. The approach for selecting load and resistance factors developed in structural practice, though a useful starting point for geotechnical applications, is not sufficient. Work is needed to incorporate in the LRFD formulation factors that are unique to geotechnical design.

Philosophically, the selection of load and resistance factors need not be made probabilistically, although in current structural practice a reliability-theory-based calibration is commonly used. This approach focuses more on load uncertainties than resistance uncertainties, and does not include many subjective factors unique to geotechnical practice. An expanded approach is needed if the full benefits of LRFD are to be achieved for foundation design.

The initial LRFD specification for driven piles uses uncertainties associated with pile capacity equations in calibrating resistance factors. In practice, engineers

use more than just the equations in designing piles. Load test results provide additional information, and quality assurance procedures are implemented on the construction process. These other factors intend to reduce uncertainty, and thus by not including them the LRFD design is more conservative than needed. The 1997 specification attempts to address this issue by introducing a parameter  $\lambda$  to be multiplied by the resistance factor,  $\phi$ . These  $\lambda$  factors are typically less than 1.0. Unfortunately, this adds a further level of conservatism, rather than giving credit to the additional information provided by load tests and construction controls.

The current specifications in the dynamic evaluation of pile capacity area are completely disassociated from (a) common design and construction procedures and (b) the understanding and utilization of the instruments and methods of analyses employed for dynamic evaluations. The specified numbers can neither be used to write specifications (i.e. contract documents) nor can they be used by a practicing engineer as a design guideline. Such critical statements call for (a) a detailed review of these specifications and (b) suggested revisions. This chapter has provided the review and suggested revisions are given in this manuscript.

***b) Observations***

The following observations are made regarding the review of the current specifications:

- (a) The provided information seems not to be founded on actual data (database) assuming unavailability at the time of the original code development.

- b) The specifications provided for the dynamic evaluation of driven piles are by and large unrelated to the actual design / QA process used in practice (see for example Figure 2.11). The methods referred to are by no means absolute (or just do not exist). For example: the performance of a wave equation analysis in the design stage requires the modeling of the pile, soil and the driving system. The obtained results can be varied markedly based on the input parameters and hence cannot be referred to as 'a' specific method without a guideline. Moreover, the reference to the pile driving analyzer (PDA) is not clear. This is an instrument that acquires data. These data can be analyzed in different ways. One method employed by the PDA most commonly used in the USA (manufactured by Pile Dynamics Inc. of Cleveland, Ohio) in analyzing the data is the Case Method (Goble et al., 1970, Rausche et al., 1975, and PDA, 1999). This method has many (at least five!) variations and is often highly dependent (related to the driving conditions) on a 'Case damping' parameter that is assumed to be associated with soil conditions, (Paikowsky, 1982, Paikowsky et al. 1994, Paikowsky and LaBelle, 1994, Paikowsky 1995, Paikowsky and Chernauskas, 1996).
- (c) The specifications seem to be concerned mostly with the structural integrity aspect of the driven piles. While being one important aspect of the construction process, the specifications provide only a qualitative unclear guideline for monitoring pile driving, (e.g. severe driving, good driving).
- (d) The methodology lumps together multiple sources of uncertainties. The oversimplification in the geotechnical approach results in a crude procedure of

questionable calibration ability. This is true for all parameter sources; superstructure loading, soil conditions, design procedure and field-testing.

- (e) A limited use of databases in conjunction with the aforementioned crude procedure results in recommended parameters that by and large mimic or parallel the WSD. As such, the LRFD approach loses its effectiveness and becomes a burden to the practicing engineer.

### **2.5.3 Deficiency in Current Geotechnical Reliability Practice for LRFD**

While the use of LRFD for the design of structures enjoyed a deep involvement of professionals in the probability area (Ellingwood et al. 1980; Ravindra and Galambos 1978), geotechnical applications of reliability in the US lag behind their counterparts in structural engineering (Meyerhof 1994). Earlier work performed in Europe as the preparation for Eurocode 7 (Baecher 1982; Standardization 1993) has been slow to make its way into American practice, and the "design point" approach to calibrating partial factors based on advanced second-moment methodology (the basis for most load factors in current LRFD codes) has yet to replace the mathematically inconsistent first-order second-moment approach in geotechnical applications. The current project presents unique opportunities to bring geotechnical implementations of LRFD into align with more advanced structural implementations.

The current literature on LRFD for deep foundations is inconsistent on the definition of reliability index as used in calibrating resistance factors, either against ASD or statistical data. FHWA publications (Barker et al. 1991; Withiam et al. 1997) define reliability index,  $\beta$ , on the logarithms of load and resistance; in other places in



the literature  $\beta$  is defined on arithmetic values (O'Neill 1995). These two definitions give different answers. A reliability index calculated on arithmetic values of logNormally distributed parameters is not consistently related to probability of failure,  $p_f$ , and the same is true of converse is true with  $\beta$  calculated on the logarithms of Normally distributed parameters. In fact, geotechnical design methods for pile resistance confound multiplicative and additive sources of uncertainty. This is especially obvious in static formulas that add tip and shaft resistance, while multiplying uncertainties having to do with soil conditions and construction effects. While current procedures incorporate extensive knowledge of geomechanics, they do not incorporate the state-of-practice in reliability analysis of data.

#### **2.5.4 Calibrations Based on State-of-Practice Reliability Methodology**

It is important that the calibrations of resistance factors for piles and shafts make use of modern methodology consistent with procedures used to calibrate load factors. If it is not based on the current approach, the calibrated resistance factors, which result run the risk of being inconsistent with corresponding load factors for bridge superstructures. Also of being internally inconsistent with respect to the statistical assumptions of distributional form, uncertainty structure, and correlation among variables on which they are based (Nowak 1999).

In the proposed work, calibrations will be performed in two, redundant ways and compared to obtain appropriate resistance factors:

- (1) Using the first-order second-moment, one-dimensional formulation discussed in current FHWA publications (Withiam et al. 1997).

- (2) Using "design-point" methodology of current reliability theory, incorporating both resistances and loads (see for example Ayyub and McCuen 1997, and Melchers 1987). By comparing and contrasting results obtained, the objective will be to take advantage of the more modern and mathematically consistent approach of advanced second-moment reliability, while at the same time attempting to ensure continuity with past practice. This redundant approach also contributes to quality assurance in the analysis.

The first-order second-moment approach reflected in current geotechnical documents combines the many sources of uncertainty that contribute to error in resistance predictions into a single variable, and then calculates a coefficient of variation for that single dimension. This approach is straightforward, and produces accurate results when the probabilistic models are sufficiently well known and simple that approximations are not required. This is, however, not the case in most predictions of pile and shaft resistance. In these cases the calculation is usually an approximation, the first order approach implicitly takes that approximation at the joint means of the uncertain qualities. This introduces well-known inaccuracies in which, for example, mechanically equivalent definitions of failure may yield different reliability indices based on the same parameter uncertainties.

Current practice in reliability theory is to represent each limiting state as a surface in the space of uncertain parameters, and to center approximations at the point  $(R^*, Q^*)$  along the limiting state surface which has the highest probability with respect to the uncertain parameters. This point is called the "design point," and is solved for

iteratively (Ayyub and McCuen 1997, Madsen et al. 1985; Melchers 1987; Thoft-Christensen and Baker 1982). Using this approach, the reliability index  $\beta$  can be defined geometrically as the vector distance between the design point in the joint means ( $m_R, m_Q$ ) of the uncertain parameters [Hasofer, 1974 #19]. The partial factors on loads and resistances can be found the ratio of the coordinate of the design point on each parameter axis divided by the respective mean of the parameter (i.e.,  $\phi = R^*/m_R$ ;  $\gamma = Q^*/m_Q$ , and so forth for resistance and load components).

The design-point methodology provides greater internal consistency among the load resistance factors calculated, better consistency with load factors (which is a not uncommon concern at the state level), and an efficient way for dealing with correlations among parameters. Uncertainties in geotechnical parameters typically exhibit substantial correlations with one another, and significant errors can be made if these are ignored, as they usually have been in past practice using the first-order second-moment approach. An important additional benefit of design-point methodology is that it allows partial factors to be calculated on the individual components of geotechnical uncertainty, providing greater insight on how the uncertainties combine (Cf., (Taylor 1948) on the appropriateness of separate factors of safety for cohesion and friction angle). One example of this is the relative contributions of uncertainty in tip resistance and skin friction in static formula calculations.

Most LRFD calibration work for resistance factor  $\phi$  addresses total pile resistance, ignoring the possibly differing uncertainties attending the components of

resistance (e.g., end bearing vs. side friction). The reasons are understandable. Only a small fraction of pile load tests have sufficient instrumentation to discriminate among resistance components, and more advanced data analysis procedures than those based on equation 2.63 are required to evaluate the data.

A sufficient number of test results exist in the database to analyze partial resistance factors for static design formulas. An analysis of these data will be made using advanced second-moment reliability to separate out partial factors on end bearing and side friction. The separately calibrated partial factors will be compared to total resistance factors calibrated using the first-order second-moment equation.

**Table 2.1.** Factor of Safety on Ultimate Axial Geotechnical Capacity  
Based on Level of Construction Control (AASHTO, 1997).

Basis for Design and Type of Construction Control	Increasing Design/Construction Control				
Subsurface Exploration	X	X	X	X	X
Static Calculation	X	X	X	X	X
Dynamic Formula	X				
Wave Equation		X	X	X	X
CAPWAP Analysis			X		X
Static Load Test				X	X
Factor of Safety (FS)	3.50	2.75	2.25	2.00 <sup>(1)</sup>	1.90

<sup>(1)</sup> For any combination of construction control that includes a static load test, FS = 2.0.

**Table 2.2.** Allowable Stresses in Piles (AASHTO, 1997).

Pile Type	Maximum Allowable Stress, $\sigma_{all}$ , (kPa)
Steel	
• Driving Damage Likely	0.25 $F_y$
• Driving Damage Unlikely	0.33 $F_y$
Concrete-Filled Steel Pipe	0.25 $F_y$ + 0.40 $f'_c$ <sup>(1)</sup>
Prestressed Concrete	0.33 $f'_c$ - 0.27 $f_{pe}$ <sup>(2)</sup>
Round Timber	
• Douglas-Fir - Coast	8.3
• Douglas-Fir - Interior	7.6
• Lodgepole Pine	5.5
• Red Oak	7.6
• Southern Pine	8.3
• Western Hemlock	6.9

<sup>(1)</sup> Applied over cross-sectional area of steel pipe and cross-sectional area of concrete;

<sup>(2)</sup> Applied over gross cross-sectional area of concrete;  $F_y$  = Yield strength of steel (kPa);  $f'_c$  = Concrete compressive strength (kPa); and  $f_{pe}$  = Concrete compressive strength due to prestressing (kPa).

**Table 2.3.** Resistance Factors for Geotechnical Strength Limit State for Axially Loaded Piles (AASHTO, 1998).

Method/Soil/Condition		Resistance Factor, $\phi$
Ultimate Bearing Resistance of Single Piles	Skin Friction: Clay	
	$\alpha$ -method	$0.70\lambda_v$
	$\beta$ -method	$0.50\lambda_v$
	$\lambda$ -method	$0.55\lambda_v$
	End Bearing: Clay and Rock	
	Clay	$0.70\lambda_v$
	Rock	$0.50\lambda_v$
	Skin Friction and End Bearing: Sand	
	SPT-method	$0.45\lambda_v$
	CPT-method	$0.55\lambda_v$
	Wave equation analysis with assumed driving resistance	$0.65\lambda_v$
	Load Test	$0.80\lambda_v$
Block Failure	Clay	0.65
Uplift Resistance of Single Piles	$\alpha$ -method	0.60
	$\beta$ -method	0.40
	$\lambda$ -method	0.45
	SPT-method	0.35
	CPT-method	0.45
	Load Test	0.80
Group Uplift Resistance	Sand	0.55
	Clay	0.55
Method of controlling installation of piles and verifying their capacity during or after driving to be specified in the contract documents		Value of $\lambda_v$
Pile Driving Formulas, e.g., ENR, equation without stress wave measurements during driving		0.80
Bearing graph from wave equation analysis without stress wave measurements during driving		0.85
Stress wave measurements on 2% to 5% of piles, capacity verified by simplified methods, e.g., the pile driving analyzer		0.90
Stress wave measurements on 2% to 5% of piles, capacity verified by simplified methods, e.g., the pile driving analyzer, and static load test to verify capacity		1.00
Stress wave measurements on 2% to 5% of piles, capacity verified by simplified methods, e.g., the pile driving analyzer, and CAPWAP analyses to verify capacity		1.00
Stress wave measurements on 10% to 70% of piles, capacity verified by simplified methods, e.g., the pile driving analyzer		1.00

**Table 2.4.** Resistance Fsfactors Calibrated by Fitting with WSD for  $\gamma_D = 1.25$  and  $\gamma_L = 1.75$  (After McVay et al., 1998).

$Q_D/Q_L$	Resistance Factor, $\phi$					
	FS=1.5	FS=2.0	FS=2.5	FS=3.0	FS=3.5	FS=4.0
1	1.00	0.75	0.60	0.50	0.43	0.38
2	0.94	0.71	0.57	0.47	0.40	0.35
3	0.92	0.69	0.55	0.46	0.39	0.34
4	0.90	0.68	0.54	0.45	0.39	0.34
5	0.89	0.67	0.53	0.44	0.38	0.33
6	0.88	0.66	0.53	0.44	0.38	0.33
7	0.88	0.66	0.53	0.44	0.38	0.33
8	0.87	0.65	0.52	0.44	0.37	0.33
9	0.87	0.65	0.52	0.43	0.37	0.33
Median	0.94	0.70	0.56	0.47	0.39	0.34
Recommended	0.90	0.65	0.55	0.45	0.35	0.30

**Table 2.5.** Resistance Factor for Driven Piles for Estimating the Axial Geotechnical Pile Capacity Using Reliability-Based Calibration (modified after Barker, et al., 1991).

Pile Length (m)	$\beta_T$	$\phi$ Values by Method of Axial Pile Capacity Estimation						
		$\alpha$		$\beta$	$\lambda$		CPT	SPT
		Type I	Type II		Type I	Type II		
10	2.0	0.78	0.92	0.79	0.53	0.65	0.59	0.48
30	2.0	0.84	0.96	0.79	0.55	0.71	0.62	0.51
10	2.5	0.65	0.69	0.68	0.41	0.56	0.48	0.36
30	2.5	0.71	0.73	0.68	0.44	0.62	0.51	0.38
Average $\phi$		0.78		0.74	0.56		0.55	0.43
Selected $\phi$		0.70		0.50	0.55		0.55	0.45

Type I refers to soils with  $S_u < 50$  kPa; Type II refers to soils with  $S_u > 50$  kPa

**Table 2.6a.** Relationship Between Probability of Failure and Reliability Index for Lognormal Distribution (After Withiam et al., 1997).

Reliability Index, $\beta$	Probability of Failure, $p_f$	Probability of Failure, $p_f$	Reliability Index, $\beta$
2.5	$0.99 \times 10^{-2}$	$1 \times 10^{-1}$	1.96
3.0	$1.15 \times 10^{-3}$	$1 \times 10^{-2}$	2.50
3.5	$1.34 \times 10^{-4}$	$1 \times 10^{-3}$	3.03
4.0	$1.56 \times 10^{-5}$	$1 \times 10^{-4}$	3.57
4.5	$1.82 \times 10^{-6}$	$1 \times 10^{-5}$	4.10
5.0	$2.12 \times 10^{-7}$	$1 \times 10^{-6}$	4.64
5.5	$2.46 \times 10^{-8}$	$1 \times 10^{-7}$	5.17

**Table 2.6b.** Comparison Between Rosenbleuth and Estava's Approximation and Series Expansion (Labeled "exact").

$\beta$	Rosenbleuth and Estavas' $p_f$	"exact" $p_f$	Percent Error
2.0	8.4689E-2	2.2750E-2	272.3%
2.5	9.8649E-3	6.2097E-3	58.9%
3.0	1.1491E-3	1.3500E-3	-14.9%
3.5	1.3385E-4	2.3267E-4	-42.5%
4.0	1.5592E-5	3.1686E-5	-50.8%
4.5	1.8162E-6	3.4008E-6	-46.6%
5.0	2.1156E-7	2.8711E-7	-26.3%
5.5	2.4643E-8	1.9036E-8	29.5%
6.0	2.8705E-9	9.9012E-10	189.9%



**Table 2.7.** Strength and Service Limit States for Design of Driven Pile Foundations  
(After Withiam et al., 1997).

Performance Limit	Strength Limit State(s)	Service I Limit State
Bearing Resistance of Single Pile/Group	X	
Pile/Group Punching	X	
Settlement of Pile Group		X
Tensile Resistance of Uplift-Loaded Piles	X	
Lateral Displacement of Pile/Group		X
Structural Capacity of Axially/Laterally-Loaded Piles	X	

**Table 2.8.** Reliability Index of Case Method Prediction (After McVay et al., 1998).

$Q_D/Q_L$	$\beta$		$COV_R$		$\lambda_R$		$COV_{QD}$	$\lambda_D$	$COV_{QL}$	$\lambda_L$	ASD FS
	EOD	BOR	EOD	BOR	EOD	BOR					
1	3.04	2.40	0.325	0.318	1.355	1.052	0.1	1.05	0.18	1.15	2.5
2	3.08	2.44	0.325	0.318	1.355	1.052	0.1	1.05	0.18	1.15	2.5
3	3.10	2.46	0.325	0.318	1.355	1.052	0.1	1.05	0.18	1.15	2.5
4	3.11	2.47	0.325	0.318	1.355	1.052	0.1	1.05	0.18	1.15	2.5
5	3.12	2.48	0.325	0.318	1.355	1.052	0.1	1.05	0.18	1.15	2.5
6	3.13	2.49	0.325	0.318	1.355	1.052	0.1	1.05	0.18	1.15	2.5
7	3.13	2.49	0.325	0.318	1.355	1.052	0.1	1.05	0.18	1.15	2.5
8	3.13	2.49	0.325	0.318	1.355	1.052	0.1	1.05	0.18	1.15	2.5
9	3.14	2.50	0.325	0.318	1.355	1.052	0.1	1.05	0.18	1.15	2.5

**Table 2.9.** Resistance Factor for Case Method Prediction (After McVay et al., 1998).

$Q_D/Q_L$	Resistance Factor, $\phi$					
	EOD			BOR		
	$\beta=2.0$	$\beta=2.5$	$\beta=3.0$	$\beta=2.0$	$\beta=2.5$	$\beta=3.0$
1	0.85	0.70	0.58	0.66	0.55	0.46
2	0.81	0.67	0.56	0.64	0.53	0.44
3	0.79	0.66	0.54	0.62	0.52	0.43
4	0.78	0.65	0.54	0.61	0.51	0.42
5	0.77	0.64	0.53	0.61	0.51	0.42
6	0.77	0.64	0.53	0.60	0.50	0.42
7	0.77	0.63	0.53	0.60	0.50	0.41
8	0.76	0.63	0.52	0.60	0.50	0.41
9	0.76	0.63	0.52	0.60	0.50	0.41

**Table 2.10.** Range of Values for Resistance Factors for Piles  
(Standard Association of Australia, 1995).

Method of Assessment of Ultimate Geotechnical Strength	Range of Values of $\phi_g$
Static load testing to failure	0.70-0.90
Static proof (not to failure) load testing <sup>1</sup>	0.70-0.90
Dynamic load testing to failure supported by signal matching <sup>2</sup>	0.65-0.85
Dynamic load testing to failure not supported by signal matching	0.50-0.70
Dynamic proof (not to failure) load testing supported by signal matching <sup>1,2</sup>	0.65-0.85
Dynamic proof (not to failure) load testing not supported by signal matching <sup>1</sup>	0.50-0.70
Static analysis using CPT data	0.45-0.65
Static analysis using SPT data in cohesionless soils	0.40-0.55
Static analysis using laboratory data for cohesive soils	0.45-0.55
Dynamic analysis using wave equation method	0.45-0.55
Dynamic analysis using driving formulae for piles in rock	0.50-0.65
Dynamic analysis using driving formulae for piles in sand	0.45-0.55
Dynamic analysis using driving formulae for piles in clay	Note 2
Measurement during installation of proprietary displacement piles, using well established in-house formulae	0.50-0.65

Notes:

<sup>1</sup> $\phi_g$  should be applied to the maximum load applied.

<sup>2</sup>Signal matching of the recorded data obtained from dynamic load testing should be undertaken on representative test piles using a full wave signal matching process.

<sup>3</sup>Caution should be exercised in the sole use of dynamic formulae (e.g., Hiley) for the determination of the ultimate geotechnical strength of piles in clays. In particular, the dynamic measurements will not measure the 'set up' which occurs after completion of driving. It is preferable that assessment be first made by other methods, with correlation then made with dynamic methods on a site-specific basis if these latter are to be used for site driving control.

For cases not covered in Table 10, values of  $\phi_g$  should be chosen using the stated values as a guide.

**Table 2.11.** Guide for Assessment of Resistance Factors for Piles  
(Standard Association of Australia, 1995).

Circumstances in Which Lower End of Range May be Appropriate	Circumstances in Which Upper End of Range May be Appropriate
Limited site investigation	Comprehensive site investigation
Simple method of calculation	More sophisticated design method
Average geotechnical properties used	Geotechnical properties chosen conservatively
Use of published correlations for design parameters	Use of site-specific correlations for design parameters
Limited construction control	Careful construction control
Less than 3 percent of piles dynamically tested	15 percent or more piles dynamically tested
Less than 1 percent of piles statically tested	3 percent or more of piles statically tested

**Table 2.12.** Material Resistance Factors for Piles  
(AUSTROADS, 1992).

Routine proof load tested	0.8
Load tested to failure	0.9
Piles analyzed by dynamic formulae or wave equation methods based on assumed driving system energy and soil parameters	0.4 - 0.5*
Piles subjected to closed-form dynamic solutions, e.g., Case method	0.5
Piles subjected to closed-form dynamic solutions correlated against static load test or dynamic load tests using measured field parameters in a wave equation analysis (e.g., CAPWAP)	0.6
Piles subjected to dynamic load tests using measured field parameters in a wave equation (e.g., CAPWAP)	0.8

\* Note: A value of 0.4 should be used for cohesive soils and structures where permanent loads dominate. In noncohesive soils and for structures where transient loads dominate, values up to 0.5 may be used.

**Table 2.13.** Typical Load and Resistance Factors for Axially Loaded Piles in Compression on Land for ULS (modified after Meyerhof, 1994).

Code Factor	Eurocode 7 (1993)	Canadian Geotechnical Society (1992)	AASHTO (1994)
Dead Load	1.1	1.25	1.3
Live Load	1.5	1.5	2.17
Resistance (driven pile with load tests)	0.4 - 0.6	0.5 - 0.6	0.80
Resistance (driven piles from SPT tests)	---	0.33 - 0.5	0.45
Resistance (bored piles with load tests)	---	---	0.80
Resistance (bored piles from static analysis)	---	---	0.45 - 0.65

**Table 2.14.** Partial Factors from Eurocode 7 and the Equivalent Resistance Factors (After Eurocode 7, 1997).

Component factors	$\gamma_b$	$\gamma_s$
Driven piles	1.30	1.30
Bored piles	1.60	1.30
CFA (Continuos flight auger) piles	1.45	1.30

**Table 2.15.** Piles and Anchors<sup>1</sup> (From the Danish Code).

Partial Coefficient	Safety Class	
	Normal	High
$\gamma_{b1}$ without test loading	0.50	0.45
$\gamma_{b2}$ with test loading	0.63	0.57
$\gamma_{b3}$ for piles and anchor actually subjected to test loading	0.71	0.65

<sup>1</sup> The  $\gamma$ -values are inverted here to more easily compare with United States practice.

**Table 2.16.** Resistance Factors for Deep Foundations  
(From Ontario Bridge Code).

Axial Load	Factor
Static analysis, compression	0.4
Static analysis, tension	0.3
Static test, compression	0.6
Static test, tension	0.4
Dynamic analysis, compression	0.4
Dynamic analysis, compression field measurements and analysis	0.5

**Table 2.17.** Resistance Factors (From the Canadian Bridge Code).

Type of Unit	Resistance Factor
Precast reinforced concrete	0.4
Cast-in-place concrete	0.4
Expanded-base concrete	0.4
Prestressed concrete	0.4
Steel H-section	0.5
Unfilled steel pipe pile	0.5
Concrete-filled steel pipe pile	0.4
Wood	0.4



**Table 2.18.** Summary of Ultimate and Factored Loads, Test Pile # 2, Newbury Site.

Method	Q <sub>p</sub> (tons)	Q <sub>s</sub> (tons)	Q <sub>ult</sub> (tons)	φ-factor	Q <sub>R</sub> (tons)
SPT	61	71	132	0.45	59
CPT	50	50	100	0.55	55
Traditional Methods	77	86	163	0.35	57
Driven 1.0 (Nordlund)	48	119	167	0.55	92
Static Load Test	28	46	74	0.80	59
Average	53	74	127	-----	64
Standard Deviation	18	30	40	-----	16

**Table 2.19.** Calculated Resistance Factors Assuming that the Resistance Factor for a Static Load Test is 1.0.

	Newbury Site Project		West Bay Project		Average $\phi$ -factor for Method
Test Pile Method	#2	#3	#9	#15	
SPT	0.56	0.51	0.79	0.75	0.65
CPT	0.74	0.62	1.38	0.88	0.91
Driven 1.0 (Nordlund)	0.44	0.33	0.42	0.40	0.40
Traditional Methods	0.45	0.41	0.53	0.51	0.48

**Table 2.20.** Comparison of Recommended and Calculated Resistance Factors.

	Calculated $\phi$ -factors	Recommended $\phi$ -factors	0.80 * Calculated $\phi$ -factors
SPT	0.65	0.45	0.52
CPT	0.91	0.55	0.73
Driven 1.0 (Nordlund)	0.40	0.55	0.32
Traditional Methods	0.48	0.35	0.38

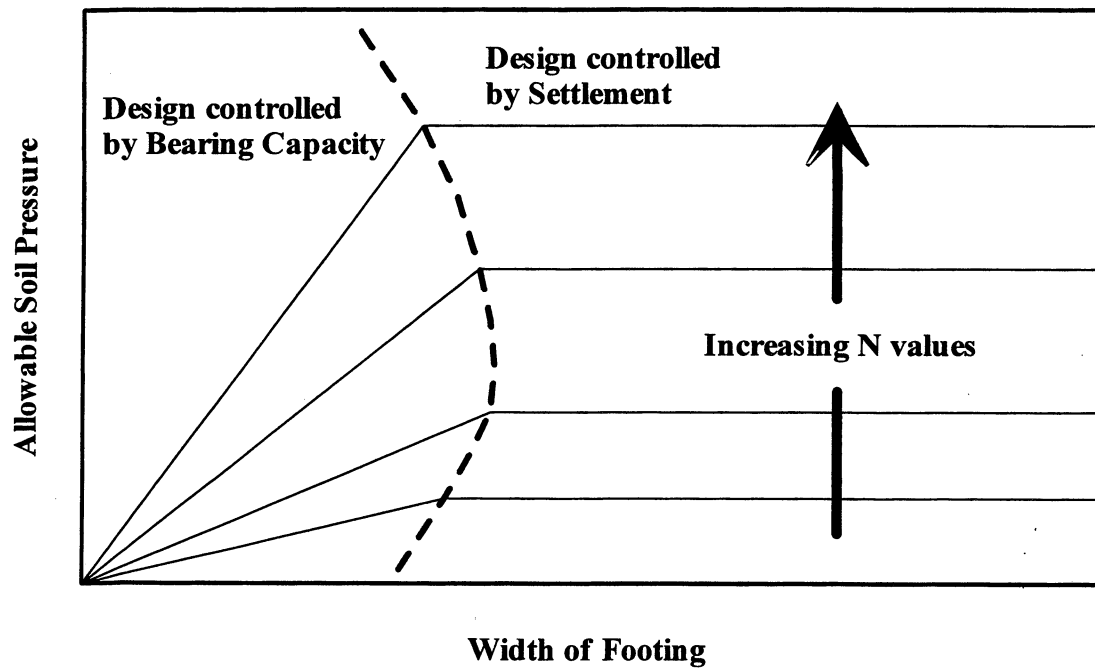


Figure 2.1. Design Basis for Spread Footings in Sand (after Peck et al., 1974).

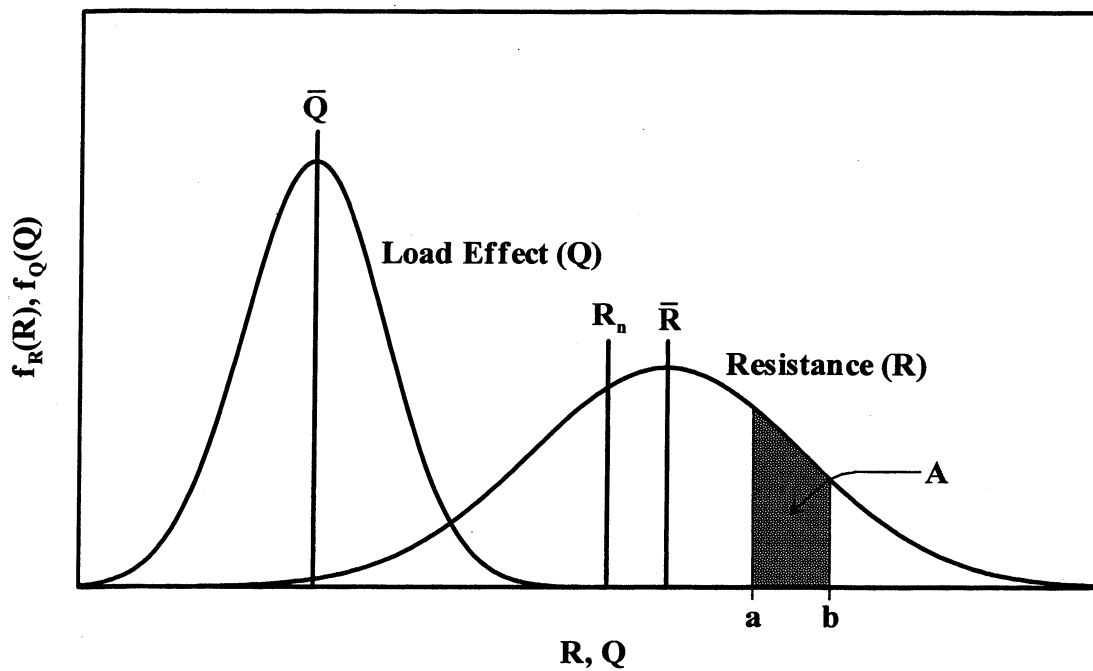
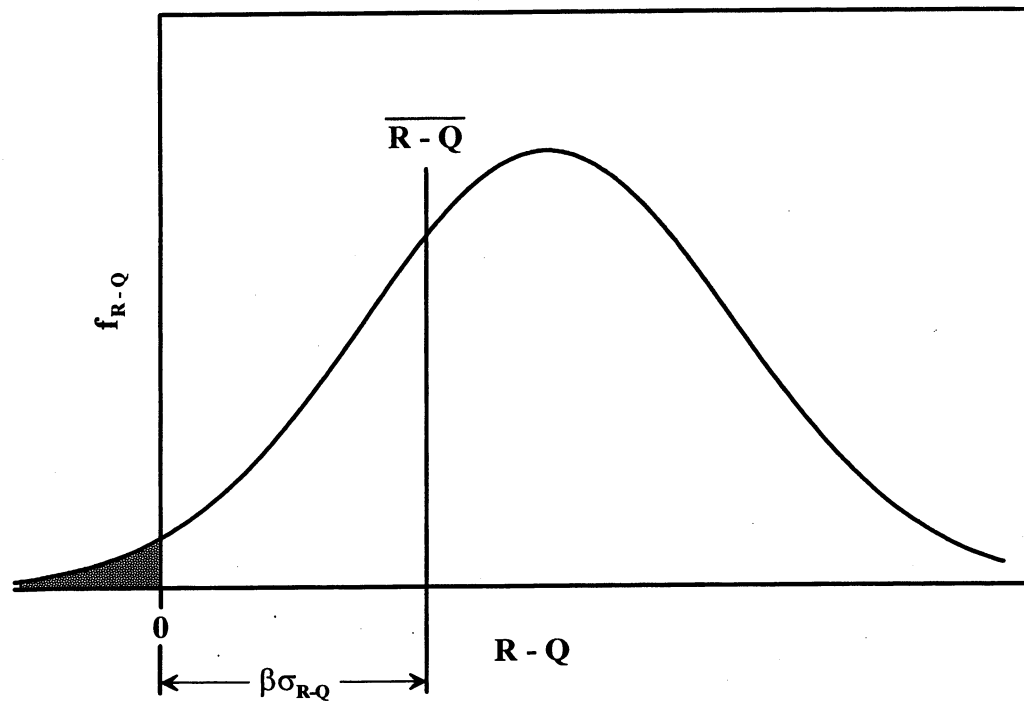
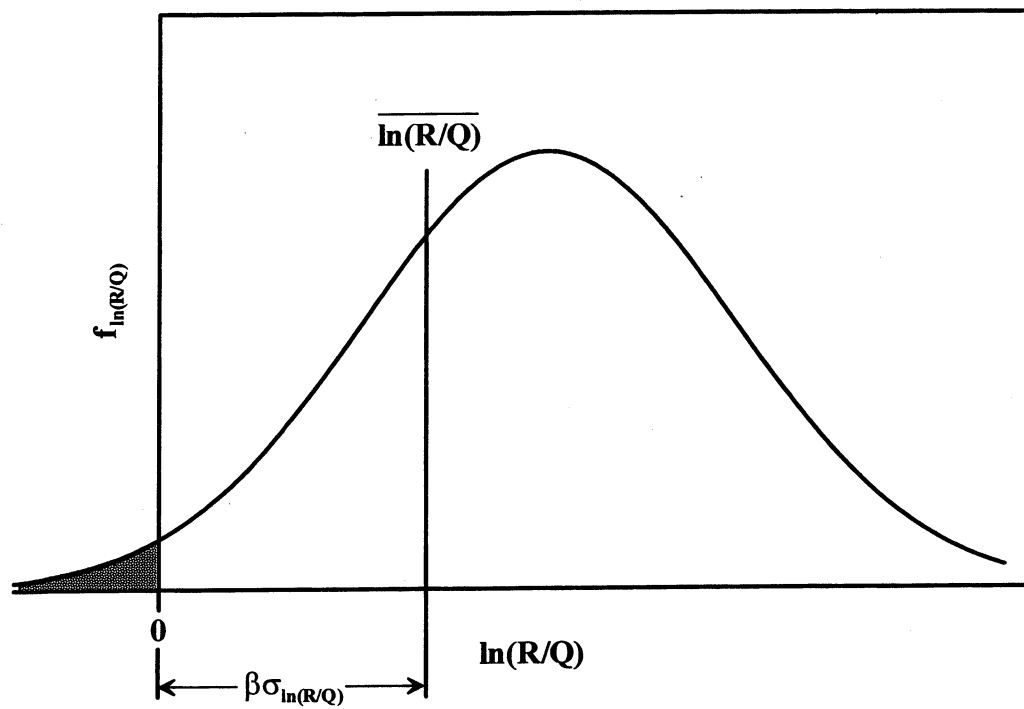


Figure 2.2. An Illustration of Probability Density Functions for Load Effect and Resistance (Goble, 1999).



**Figure 2.3.** An Illustration of a Probability Density Function for  $R - Q$  (Goble, 1999).



**Figure 2.4.** An Illustration of a Probability Density Function for  $\ln(R/Q)$  (Goble, 1999).

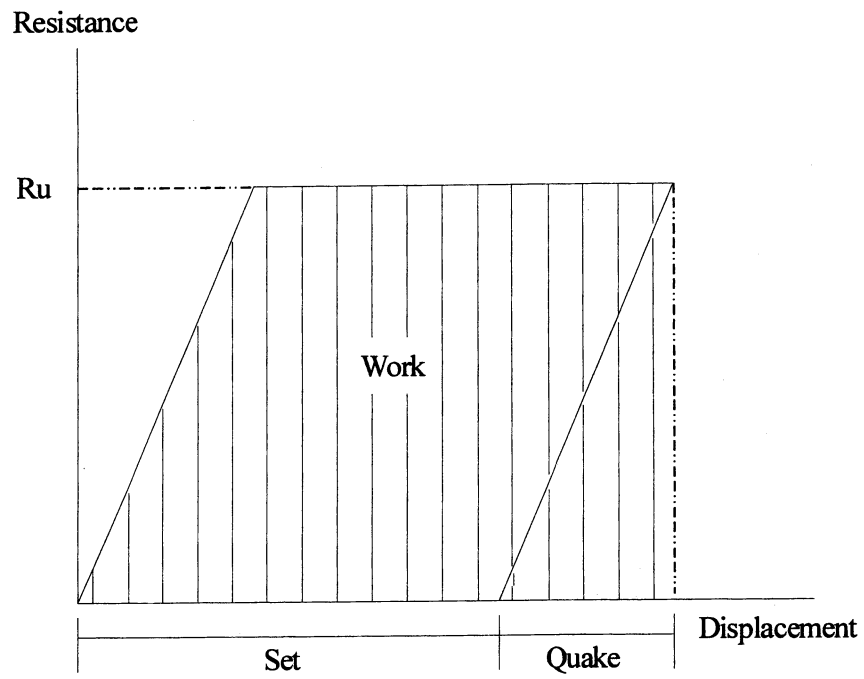


**Figure 2.5.** Resistance vs. Displacement at the Top of the Pile.

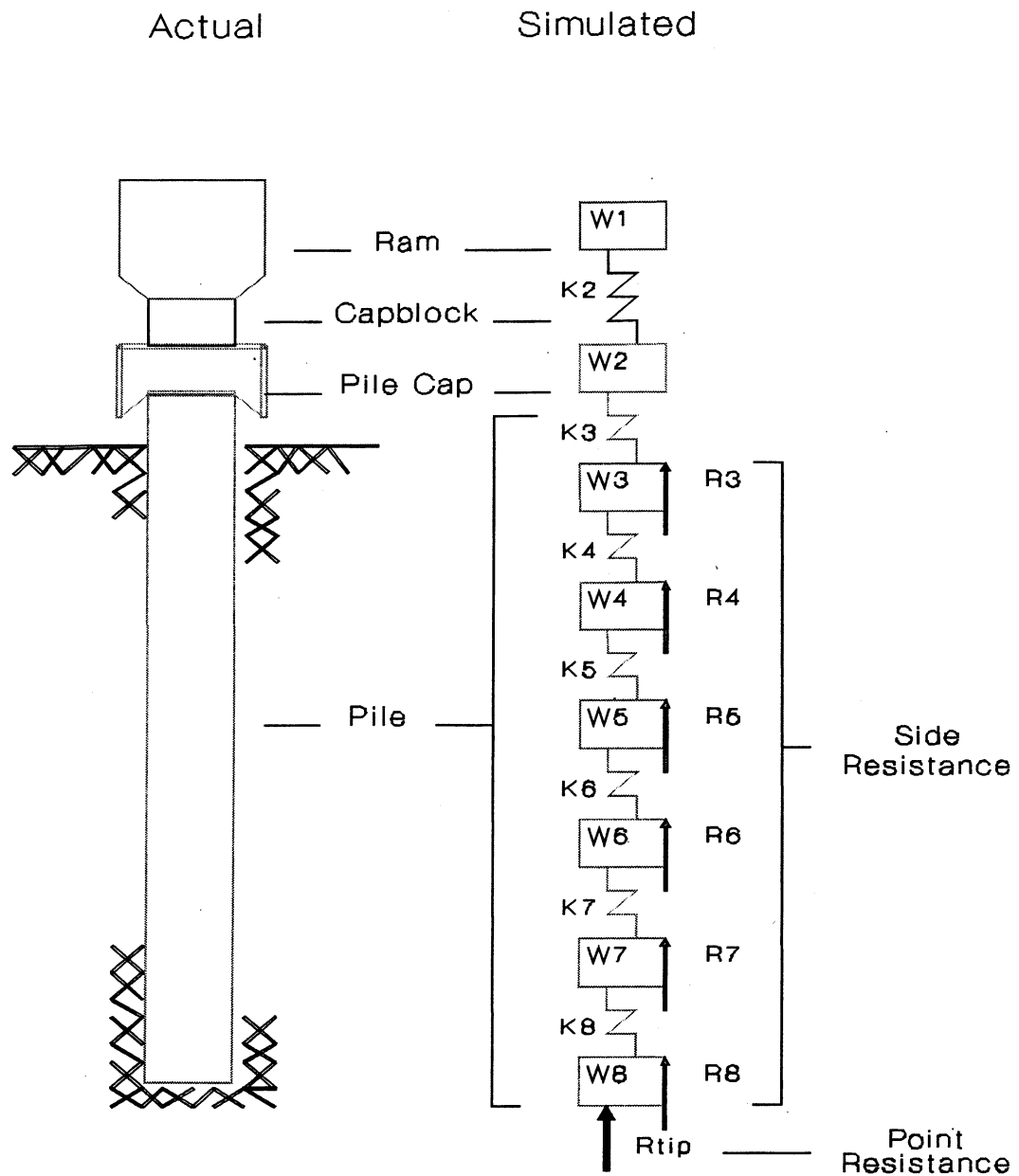


**Figure 2.6.** Smith's model simulating the hammer-pile-soil system for use with the one-dimensional wave equation (Smith, 1960).

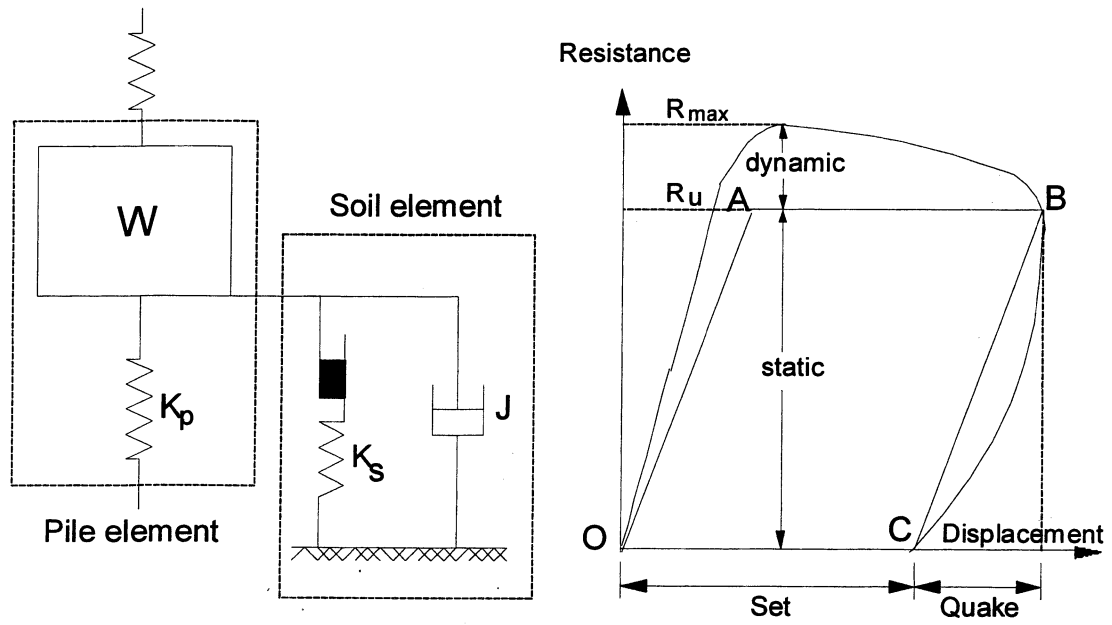


**Figure 2.7.** Soil-pile model (left) and the corresponding elasto-plastic soil resistance-displacement relationship (after Smith, 1960).

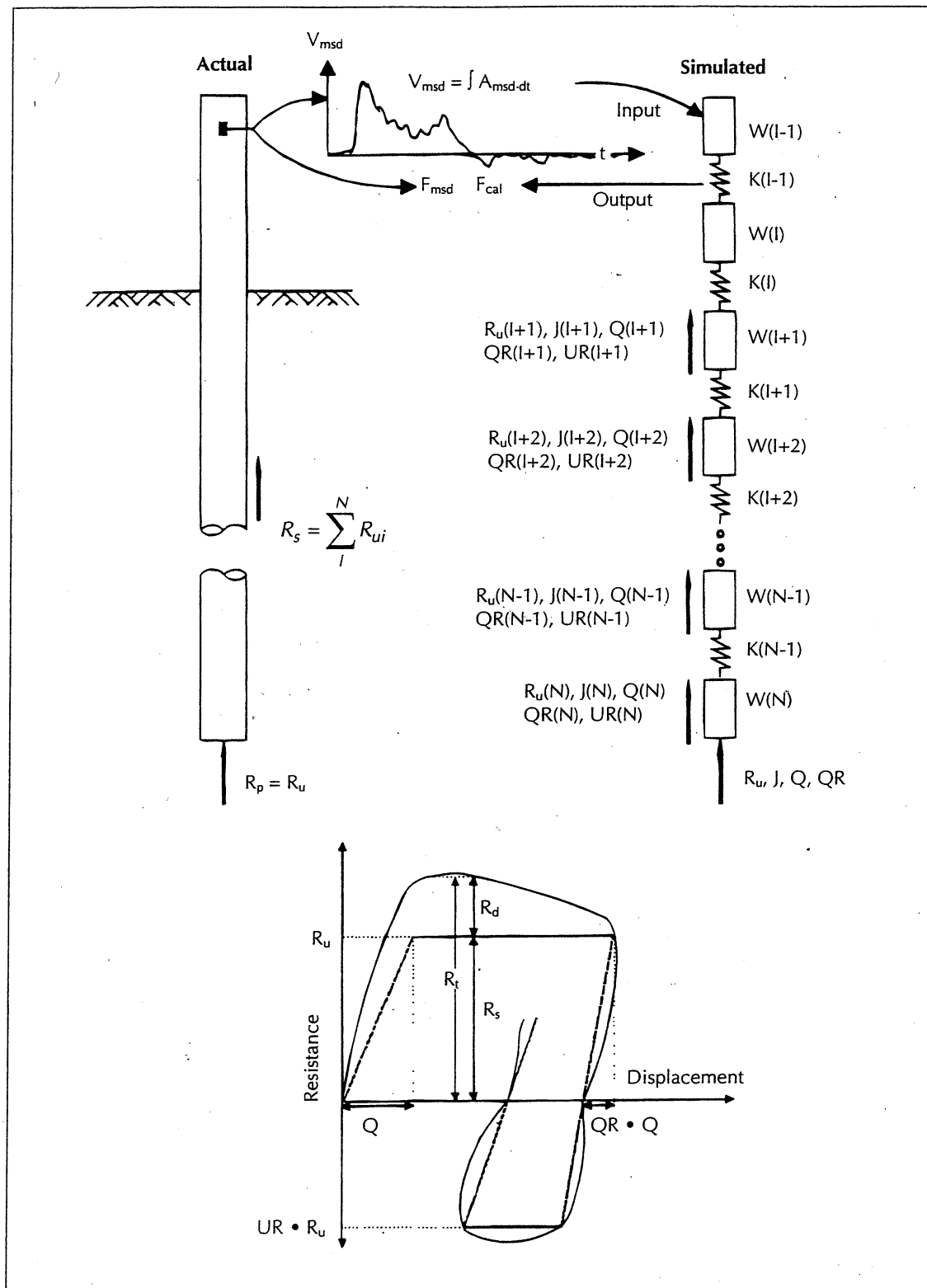


**Figure 2.8.** Notations used for Model of Pile and Soil in TEPWAP Analysis (Paikowsky, 1982)



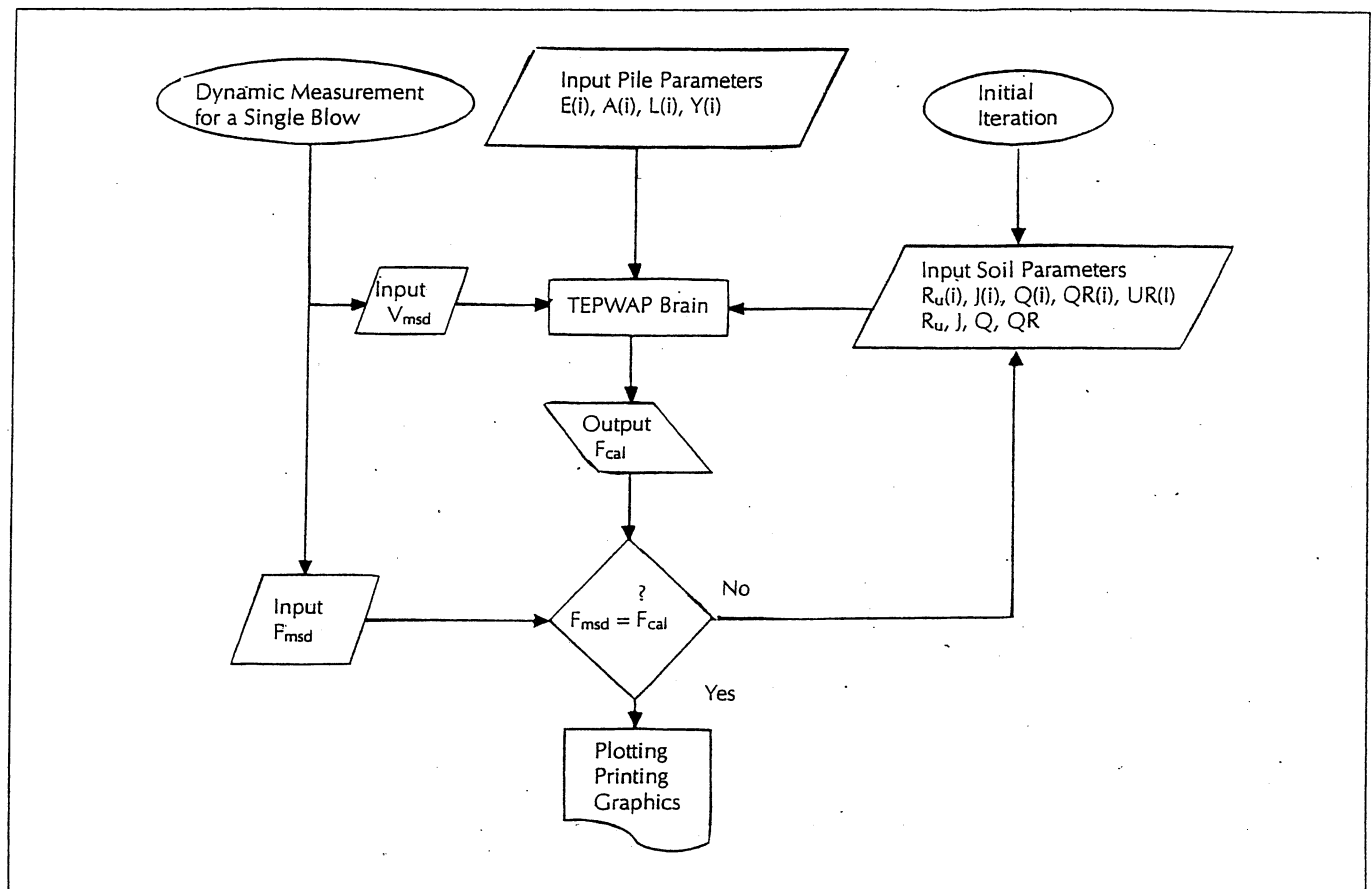


**Figure 2.9.** Flow Chart Describing the analysis process using TEPWAP (Paikowsky, 1982).

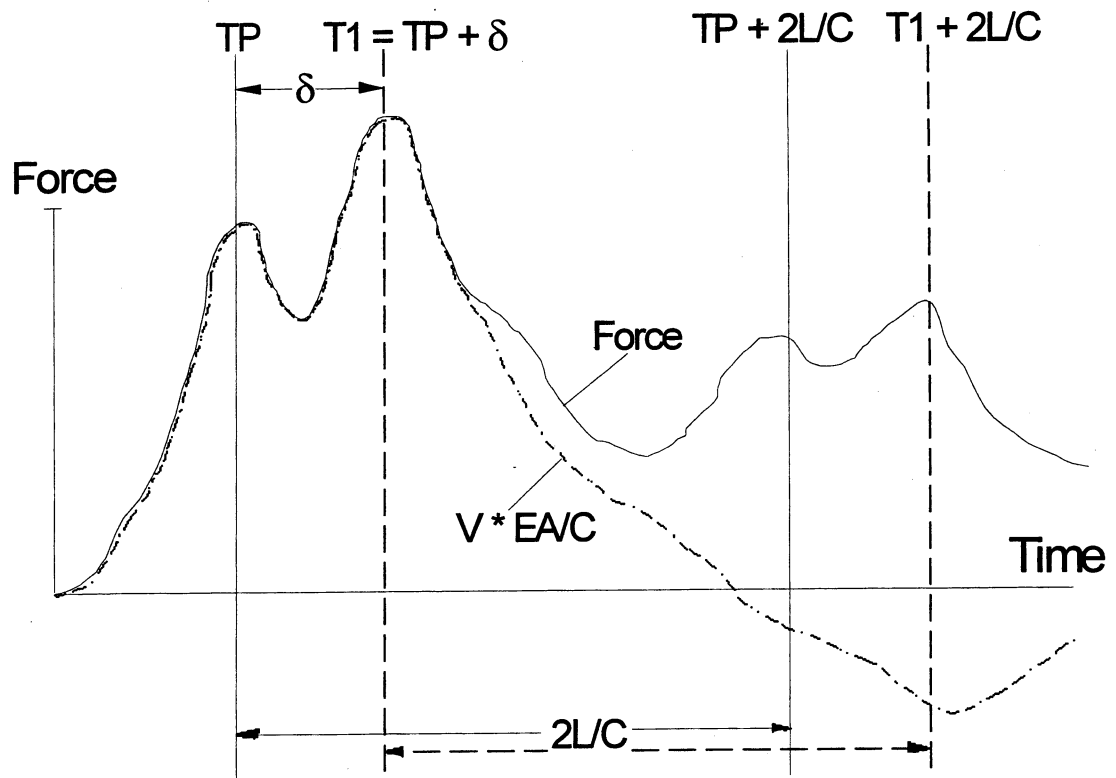


**Figure 2.10.** Force and Velocity Traces Showing Two Impact Peaks Indicative of Driving in Soils Capable of Large Deformations.

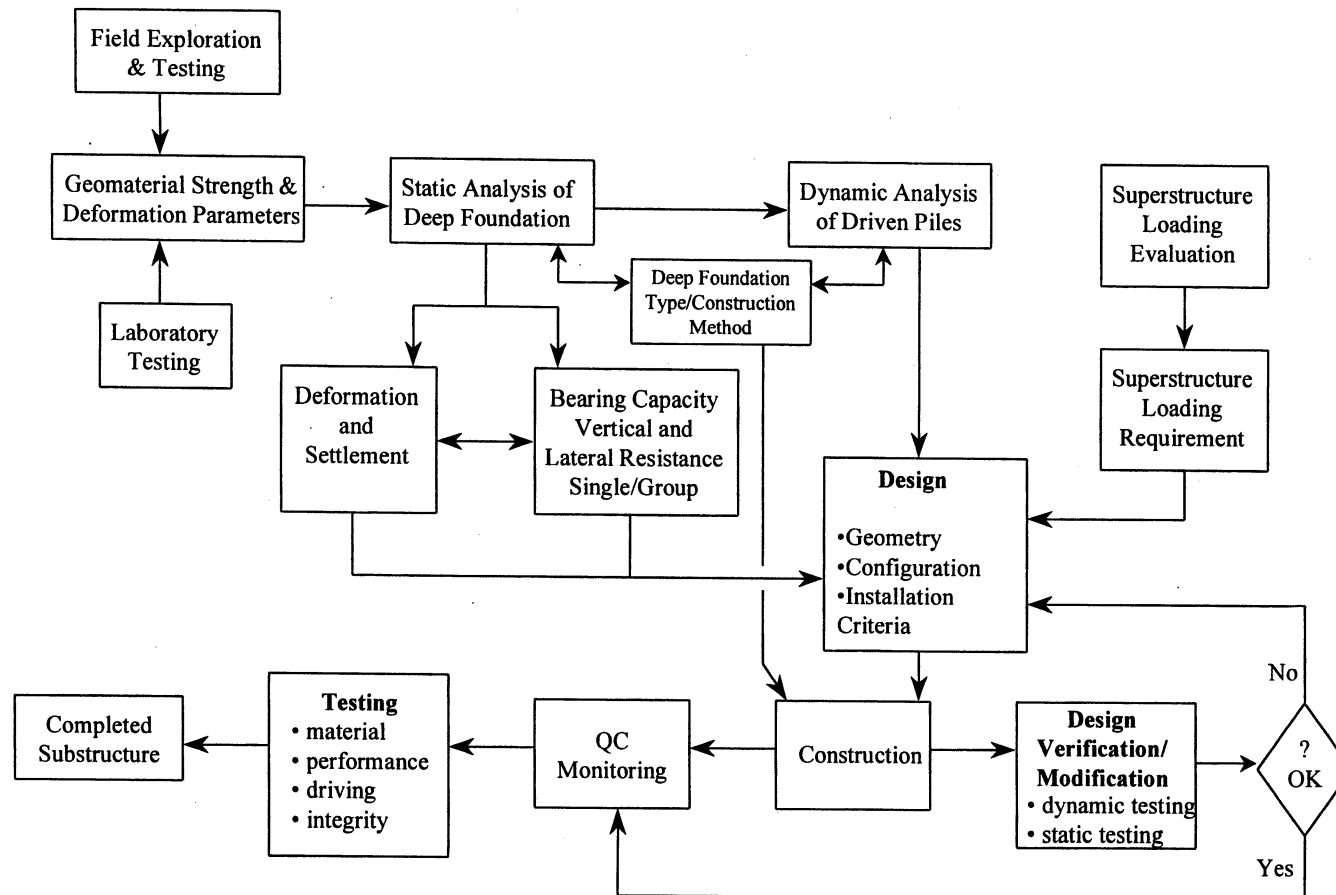


**Figure 2.11.** Deep Foundation Design Process.

## **CHAPTER 3**

### **COMPILATION OF THE DATA BASES**

#### **3.1 GENERAL**

This chapter presents the databases that were compiled to allow for the statistical analyses required in this research. Each section briefly describes the method that was used to obtain the data and the purpose for which the data were used. The five databases that were used in the presented research are the PD/LT2000 database, the U-MASS LOWELL/UKRAINE database, the GRLWEAP database, the PD2000 database, and the PD/LTT2000 database. The PD/LT2000 database is used for the majority of the dynamic analyses while the other databases are used to examine specific issues such as the influence of the type of static load test procedure on the pile's capacity, the performance of the WEAP method, the comparison of the Energy Approach End Of Driving (EOD) predictions in relation to the CAPWAP/TEPWAP Beginning Of Restrike (BOR) predictions, and the optimum time to perform a restrike to obtain the most accurate prediction of the pile's capacity.

#### **3.2 PD/LT2000 DATABASE**

##### **3.2.1 Overview**

The data found in the PD/LT2000 database is widely used throughout this thesis for analyzing the dynamic methods. In this section a detailed description of the

processes used to obtain this data will be described. Table 3.1 presents a brief summary of the types of data that make up the PD/LT2000 database. The data was sub-grouped according to pile type, geographical location, soil type along the side of the pile and at the tip of the pile, soil inertia properties based on the blow counts and area ratios, time of driving, i.e., End Of Driving (EOD and Beginning Of Restrike (BOR), and the pile capacity as determined by the static load test results. The table shows that the data was obtained from many different areas of the United States as well as from many countries around the world. The data was taken from approximately 77 different project sites around the world. A full table presenting all of the data found in PD/LT2000 is in Appendix A.

### **3.2.2 Static Load Test Analysis**

Each pile-case that was incorporated into PD/LT2000 was required to have a static load test to failure. The methodology used to analyze the load-settlement curves for each pile will be described in detail in sections 4.3.1 and 4.3.2 and therefore will not be discussed in this section.

### **3.2.3 Dynamic Measurement Analysis**

#### **(a) Overview**

This section is based on previous research completed by Paikowsky et al. (1994). The text, tables and figures were taken directly from the previous report therefore the units that are used in this section are English units with SI units in parentheses were applicable.

The analyses performed on piles in data set PD/LT employed office analysis (i.e., CAPWAP or TEPWAP) as well as several computer programs developed to process and manage force and velocity signals, including DIGITIZE, PDAP, INTEGRATE, and FILECHNG.

The dynamic analyses were performed in different ways depending on the completeness of each pile-case. In all cases, the pile geometry (i.e., type, material, length of penetration, the soil at the pile' tip and side, and the blow count) was known before any type of analysis was initiated. The individual cases were divided into three distinct groups:

- (a) Group 1 - pile-cases with complete CAPWAP summaries, including  $E_{\max}$ ,  $D_{\max}$ ,  $F1$ , and  $V1$ .
- (b) Group 2 - pile-cases with incomplete CAPWAP summaries, such as those missing  $E_{\max}$ ,  $D_{\max}$ ,  $F1$ , and/or  $V1$ .
- (c) Group 3 - pile-cases that were analyzed using TEPWAP.

**(b) *GROUP 1 – Complete CAPWAP Analyses***

Pile group 1 contains the complete cases available in data set PD/LT. The most common adjustment necessary for the pile cases in this group was a ratio correction between the force at impact ( $F1$ ) and the velocity at impact ( $V1$ ). Theoretically, the force and velocity multiplied by the pile impedance are identical under a passing disturbance, as long as no other external forces act. The ratio between these values is:

$$\frac{V1 \left( \frac{EA}{C} \right)}{F1} \quad (3.1)$$

Where:      E = modulus of elasticity of the pile material  
               A = cross-sectional area of the pile  
               C = wave speed of the pile

and should be equal to unity. An acceptable ratio was considered to be  $1.0 \pm 0.1$ . Beyond this ratio, a linear multiplier was applied to either or both parameters (force, velocity, or both) and to their byproducts, e.g., displacement and energy. The ratio between force and velocity may also be influenced by the pre-compression of a diesel hammer and hammer misalignment.

Pre-compression in a diesel hammer occurs as the air-fuel mixture is compressed by the ram just prior to combustion. This results in a force that is applied to the pile top. However, as the force is applied relatively slowly and before the actual impact between the ram and the pile top, there is not a corresponding velocity wave. This scenario results in a discrepancy between the impact force (F1) and the impact velocity ( $V1(EA/C)$ ), as shown in Figure 3.1. The force and velocity traces of pile-case 1, driven with a Delmag 30 diesel hammer, are shown in Figure 3.1. The observed relations indicate the need for a force reduction ( $\Delta_{total}$ ), which is equal to the difference between  $\Delta_k$  and  $\Delta_s$ . Prior to a correction, the ratio ( $V1(EA/C)/F1$ ) for pile-case 1 was 0.874. The factor ( $\Delta_{total}$ ) represents the number of units by which the force must be reduced in order to produce an acceptable ratio according to Equation 3.2. The magnitude of  $\Delta_{total}$  and the reduction of F1 are performed as follows:

$$\Delta_{total} = \Delta_{pk} - \Delta_{ps} = 2 \text{ units} \Rightarrow \frac{2 \text{ units}}{38.5 \text{ units}} \times 250 \text{ kips} = 13 \text{ kips (58 kN)} \quad (3.2)$$

$$F1 = F1_{uncorrected} - \Delta_{total} = 335.4 \text{ kips} - 13 \text{ kips} = F1_{corrected} = 322.4 \text{ kips (1434 kN)} \quad (3.3)$$

The corrected F1 yields a new V1(EA/C)/F1 ratio, and adjusted E<sub>max</sub>, and a corresponding uncorrected Energy Approach prediction (R<sub>u</sub>) as follows:

$$\frac{V1\left(\frac{EA}{C}\right)}{F1_{corrected}} = 0.909 \quad (3.4)$$

$$E_{mas} = 18 \text{ kip-ft} \times \frac{322.4 \text{ kips}}{335.4 \text{ kips}} = 17.3 \text{ kip-ft} \Rightarrow R_u = 362 \text{ kips (1610 kN)} \quad (3.5)$$

The procedure for correcting F1 is also performed in a similar manner for adjusting V1 and the corresponding D<sub>max</sub>, where D<sub>max</sub> = ∫V(t) dt. This is sometimes necessary when either there is a significant hammer-pile misalignment that creates disturbance in the force and velocity measurements or there is a discrepancy in the measurement itself. The correction procedure for decreasing V1(EA/C) also uses the factor Δ<sub>total</sub> as determined by the discrepancy in the F1 and V1(EA/C) measurements where Δ<sub>total</sub> is converted to units of force. Similarly, V1(EA/C) is decreased by:

$$V1\left(\frac{EA}{C}\right)_{Corrected} = V1\left(\frac{EA}{C}\right)_{uncorrected} - \Delta_{total} \quad (3.6)$$

producing a corrected ratio:

$$\frac{\left(V1\frac{EA}{C}\right)_{corrected}}{F1} \quad (3.7)$$

and an adjusted D<sub>max</sub>:

$$D_{max(corrected)} = \int V1_{corrected} dt \quad (3.8)$$

The corresponding uncorrected Energy Approach prediction is calculated using the adjusted D<sub>max</sub> as follows:



$$R_u = \frac{E_{\max}}{Set + \frac{D_{\max(\text{corrected})} - Set}{2}} \quad (3.9)$$

It should be noted that it is sometimes necessary to correct both the force and the velocity measurements given the proper circumstances. In general, very few pile-cases required correction, the majority of which needed very small adjustments. These corrections usually had an insignificant effect on the obtained  $J_c$  and  $R_u$  values.

After the static load test analysis and the dynamic analysis were completed, the Case damping coefficient ( $J_c$ ) was back-calculated using equation 6 as outlined by Goble *et al.* (1980).

**(c) GROUP 2 - Incomplete CAPWAP Analyses**

The pile cases categorized in group 2 include piles from data set PD/LT that were analyzed via CAPWAP. Difficulties associated with retrieving and accumulating complete pile data cause pile-cases to require more analysis in order to produce missing information essential for the study. Typical information missing from pile cases included  $E_{\max}$  (the maximum energy delivered to the pile top) and  $D_{\max}$  (the maximum displacement of the pile top). A typical pile-case in group 2 includes a static load test plot, subsurface site information, blow count records, and CAPWAP predictions at EOD, BOR, and/or EOR, excluding the CAPWAP summary tables. The CAPWAP summary tables include pile characteristics, Case method predictions and crucial dynamic measurements ( $V_{\max}$ ,  $V_{\text{fin}}$ ,  $V1*Z$ ,  $F1$ ,  $F_{\max}$ ,  $D_{\max}$ ,  $D_{\text{fin}}$ ,  $E_{\max}$ , and  $E_{\text{fin}}$ ). In order to determine these missing dynamic parameters, a program was developed at UMASS-Lowell called INTEGRATE (written by L. Chernauskas). This program was

specifically developed to calculate the uncorrected Energy Approach and the Case method similar to a more extensive and versatile program called PDAP (Pile Driving Analysis Program), which was developed by Paikowsky (1984). The program PDAP uses recorded field data from the PDA, enables it's manipulation and correction, and produces an Energy Approach prediction and a range of Case method predictions based on all the different variations for different  $J_c$  values.

INTEGRATE processes digitized force and velocity ( $V*EA/C$ ) traces (see Figure 3.2 for example) and, using the pile parameters as given by the user, produces the dynamic measurements listed above. INTEGRATE also calculates the uncorrected Energy Approach prediction and back-calculates the Case damping coefficient ( $J_c$ ) using the following relationship after (Goble et al., 1980):

$$J_c = \frac{RTL - FINAL R_s}{V1 \frac{EA}{C} + F1 - RTL} \quad (3.10)$$

The static load test results are denoted FINAL  $R_s$ , and must be supplied by the user. An example of the results of an INTEGRATE analysis of the force and velocity traces shown in Figure 3.2 for pile-case 192 (33P1BOR) is shown in Figure 3.3. After reviewing the force and velocity ( $EA/C$ ) traces for a given pile case and the  $(V1*EA/C)/F1$  ratio, calculated by INTEGRATE, any necessary corrections and corresponding adjustments to  $E_{max}$  and  $D_{max}$  can be made, as outlined in section 3.2.2(a); and the uncorrected Energy Approach calculations can be performed.

**(d) GROUP 3 - TEPWAP Analyses**

Several pile cases in data set PD/LT were lacking the CAPWAP office analysis and, therefore, required wave match analysis to be performed. These pile cases were categorized in group 3 and all of them were analyzed using a computer program called TEPWAP. TEPWAP (Paikowsky, 1982; Paikowsky and Whitman, 1990; and Chernauskas, 1993) utilizes a procedure somewhat similar to the CAPWAP analysis described by Goble *et al.* (1970). This program allows the input of the measured velocity at the pile top as a function of time, solving for a set of parameters describing the soil resistance (dynamic and static) along the pile. Adjustments of the matches are made until the calculated force at the top matches that measured. A good agreement between CAPWAP and TEPWAP analyses was presented by Paikowsky (1982) and further confirmed by Chernauskas (1993).

The pile cases in group 3 were initially analyzed in the same manner as those in group 2, whereby their force and velocity traces were digitized with respect to time using the program DIGITIZE and processed using INTEGRATE. After these steps were successfully completed, three data files were created for each case: an input file, an identification file, and a pile/soil file. An input file for TEPWAP is created using the program DIGPWAVE that processes digitized force and velocity traces and prepares them in the same manner as the PDA. Figures 3.4 and 3.5 show the identification file and the pile/soil file for pile-case 191, respectively. These files, along with the digitized force and velocity traces (see Figure 3.6 for example), are necessary for TEPWAP analyses. Iterations are performed, where the user is required

to adjust the soil properties (i.e., side and tip damping and quake, and side and tip resistance) until an acceptable force wave match is made. Figure 3.7 presents the comparison between the calculated forces at the top (obtained from the above procedure) to the measured force at the top of pile-case 191.

This particular pile case appears to be exhibiting pile plugging near the tip as indicated by the sudden observed force "jump" near  $2L/C$  and again near  $4L/C$ . Pile plugging is most commonly associated with open-pipe piles or H-piles. It usually refers to the phenomenon that occurs when soil enters the open-pipe pile during driving until the inner-soil cylinder develops sufficient resistance to prevent further soil intrusion (see Paikowsky et al., 1989; Paikowsky and Whitman, 1990). The development of friction along the web of an H-pile can also develop enough resistance to prevent soil intrusion, causing the H-pile to become "plugged." When an H-pile becomes plugged, it then assumes the penetration characteristics of a large displacement pile (i.e., with a closed rectangular tip). Pile plugging is shown to have the following marked effects: significant contribution to the capacity of piles driven in sand; delay in capacity gain with time for piles driven in clay; and changes in the behavior of piles during installation, causing it to differ from that described by the models commonly used to predict and analyze pile driving (Paikowsky and Whitman, 1990). Further investigation into pile-case 191 shows that the H-pile is embedded over 114 ft (35 m) into silty sand. These conditions are ideal for pile plugging to occur and, therefore, plugging can be attributed to the force match disagreement at  $2L/C$  and again at  $4L/C$  by TEPWAP as shown in Figure 3.2.

The final summary of results from TEPWAP analyses is produced for each case (see Figure 3.8 for example). These summaries allow the user to investigate the compressive and tensile stresses developed in the pile during driving (e.g., concrete piles) as well as the side and tip resistance and the measured and calculated energy delivered to the pile. All of the pile-cases that were analyzed using TEPWAP are footnoted in the data set tables found in Appendix A. The Case damping coefficients for these cases were calculated as part of the INTEGRATE output as previously stated.

It should be noted that the additional pile-cases that were added to the PD/LT and PD/LT2 databases (Paikowsky et al., 1994 and Paikowsky and LaBelle, 1994) all fell into Group 1 as described above. For each pile-case of the added data there was a complete CAPWAP analysis as well as a static load test to failure.

### **3.3 U-MASS LOWELL/UKRAINE DATABASE**

The U-Mass Lowell/Ukraine database consists of static load test data compiled by Dr. Operstein from the Research Design Institute at Dniepropetvorsk, Ukraine. Dr. Operstein, currently with the Technion, Israel Institute of Technology, revisited the research Design Institute in 1997 and obtained data and graphical results for about 176 full-scale pile cases carried out to failure. The piles were tested under the conventional static load-test method (Standard test) and the static cyclic test. The reader is referred to the research report entitled "Express Method of Pile testing by Static Cyclic Loading" by Paikowsky et al., (1999) for more detailed analysis of this database. The data from the U-Mass Lowell/Ukraine database was used to evaluate

the effect of the type of static load test that is completed on the static pile capacity that is determined from the static load test results. A total of 81 piles that had both a standard static load test completed as well as static cyclic load test were used in this analysis. The analysis of the effect of the type of static load test that is completed on the static load test results is presented in section 4.5.3. The database is presented in its entirety in Appendix A as well as in the above referenced report.

### **3.4 GRLWEAP DATABASE**

The GRLWEAP database was compiled for the sole purpose of analyzing the performance of the WEAP method for determining pile capacity at the EOD using default values. Therefore, each of the pile-cases obtained contain a static load test to failure as well as a WEAP analysis at the end of pile driving. The data were obtained from GRL Inc. and consists of 99 pile-cases that have a static load tests to failure that were analyzed using Davisson's criterion, as well standard and corrected WEAP analyses at the EOD and BOR. The evaluation of the performance of the WEAP method is presented in section 6.2.1. Table A.3 in Appendix A presents the data in the GRLWEAP database.

### **3.5 CASE METHOD DATABASE**

Similar to the GRLWEAP database the Case method database was compiled to evaluate the performance of the Case method at the EOD. The data found in this database was obtained from Mike McVay of the University of Florida. All of the piles found within the database were driven in Florida. A total of 40 piles with a Case method evaluation at the EOD and a static load test to failure are contained within the

Case database. Also found in the Case database are 37 piles with a Case method analysis at the BOR as well as a static load test to failure. The evaluation of the Case method is presented in section 6.3.4 and a table showing all of the data in the Case database is presented in Appendix A.

### **3.6 PD2000 DATABASE**

The PD2000 database was compiled by Kevin O'Malley and was compiled in such a manner that the Energy Approach results at the EOD could be compared to the CAPWAP/TEPWAP results at the BOR. The database includes pile-cases for which dynamic analysis was completed both at the EOD (Energy Approach) and the BOR (CAPWAP/TEPWAP). There was no record showing that a static load test to failure was completed on any of these piles. Chapter 7 presents the comparison between the Energy Approach predictions at the EOD and the CAPWAP/TEPWAP predictions at the BOR. A presentation of the data found in the PD2000 database is shown in Appendix A.

### **3.7 PD/LTT2000 DATABASE**

The PD/LTT2000 database consists of driven piles that had a static load test to failure as well as dynamic measurements taken at the EOD and on two or more restrikes. The data contained in this database was taken directly out of the PD/LT2000 database; it also contains two test piles that were analyzed by Edward Hajduk of the Geotechnical Engineering Research Laboratory at the University of Massachusetts Lowell (Paikowsky and Hajduk, 1999 and Paikowsky and Hajduk, 2000). The database presents the phenomenon of pile capacity gain over time for piles driven into

cohesive soils. The database was also used to evaluate the optimum time to perform restrikes on driven piles to obtain the most accurate prediction of pile capacity. The analyses that were completed using this database are presented in chapter 8. All of the data found in the PD/LTT2000 database is presented in Appendix A.



**Table 3.1.** Summary of the Data in the PD/LT2000 database.

Pile Types		Geographical Location		Soil Types			Soil Inertia			Type of Data		Pile Capacities	
Pile Type	No.	Location	No.	Soil Type	Side	Tip	Criteria	Blow Count	A <sub>R</sub>	Time	No.	Range (kN)	No.
<i>H-Pile</i>	37	<i>NE USA</i>	44	<i>Clay &amp; Till</i>	67	61	$\geq 16$ blows per 10cm	272	-----	<i>EOD &amp; BOR</i>	92	0-445	2
<i>OEP</i>	10	<i>SE USA</i>	69									445-890	6
<i>CEP</i>	61	<i>North USA</i>	24							<i>EOD &amp; BOR's</i>	30	890-1334	17
<i>Voided Conc.</i>	35	<i>South USA</i>	10									1334-1779	44
<i>Sq. Conc.</i>	254	9	<i>NW USA</i>	<i>Rock</i>	0	11	$< 16$ blows per 10cm	112	-----	<i>EOD</i>	135	1779-2224	27
	305	5	<i>SW USA</i>									2224-2669	25
	356	8	<i>Australia</i>							<i>BOR</i>	239	2669-3114	15
	406	1	<i>Brunswick</i>									3114-3559	10
	457	8	<i>Holland</i>	<i>Sand &amp; Silt</i>	140	137	$\geq 350$	-----	134	<i>EOR</i>	11	3559-4003	13
	508	8	<i>Hong Kong</i>									4003-4448	13
	610	16	<i>Israel</i>				$< 350$	-----	255	<i>DD</i>	2	4448-4893	11
	762	5	<i>Ontario</i>									4893-5338	6
<i>Octagonal Concrete</i>	3	<i>Sweden</i>	1	<i>NA</i>	3	1	<i>Unknown</i>	5	-----	<i>DR</i>	1	5338-5783	5
		<i>NA</i>	6									5783-6228	4
<i>Timber</i>	2									<i>ALT</i>	1	6228-6672	6
<i>Monotube</i>	2											>6672	6
<b>Total</b>	210	-----	210	-----	210	210	-----	389	389	-----	389	-----	210

- Notes:**
- |                                |                                    |                                       |
|--------------------------------|------------------------------------|---------------------------------------|
| 1. OEP - Open Ended Pipe Pile  | 7. DR - During Restrike            | 13. North USA - FHWA Regions 5, 7 & 8 |
| 2. CEP - Close Ended Pipe Pile | 8. ALT - Alternate measurement     | 14. South USA - FHWA Region 6         |
| 3. EOD - End of Driving        | 9. A <sub>R</sub> - Area Ratio     | 15. NE USA - FHWA Regions 1, 2 & 3    |
| 4. BOR - Beginning of Restrike | 10. No. - Number of Piles/Cases    | 16. SE USA - FHWA Region 4            |
| 5. EOR - End of Restrike       | 11. NA - Non-Applicable/Unknown    | 17. NW USA - FHWA Region 10           |
| 6. DD - During Driving         | 12. USA - United States of America | 18. SW USA - FHWA Region 9            |

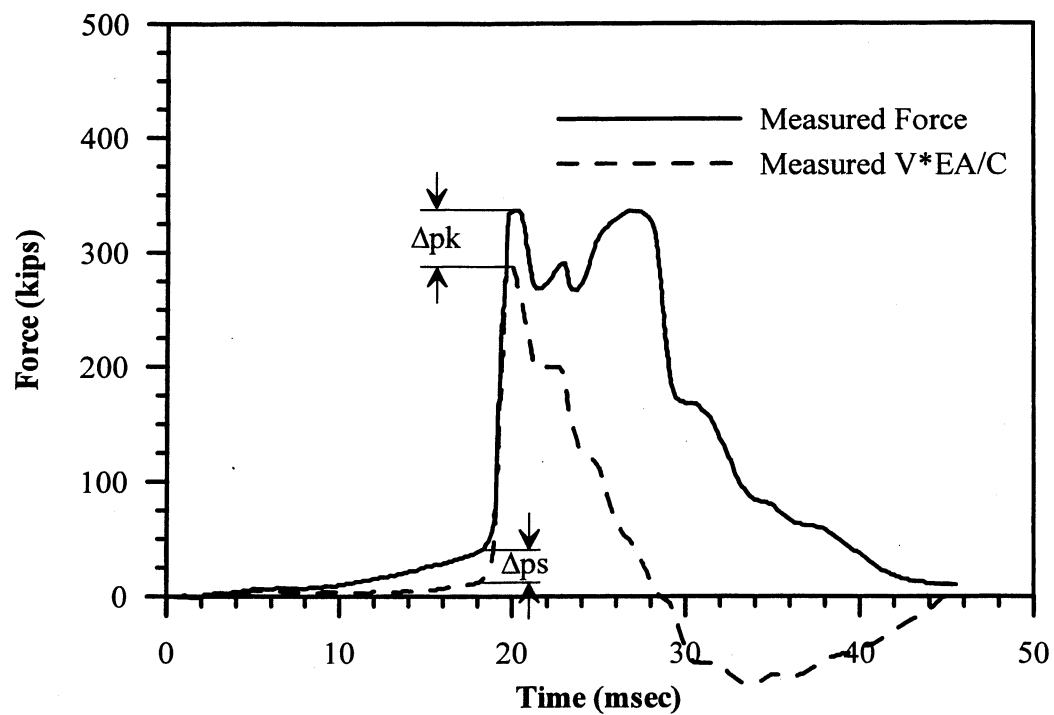


**Figure 3.1.** Force and velocity ( $V \cdot EA/C$ ) traces of pile-case 1, a steel HP12x74 that needed a force correction (not to scale).

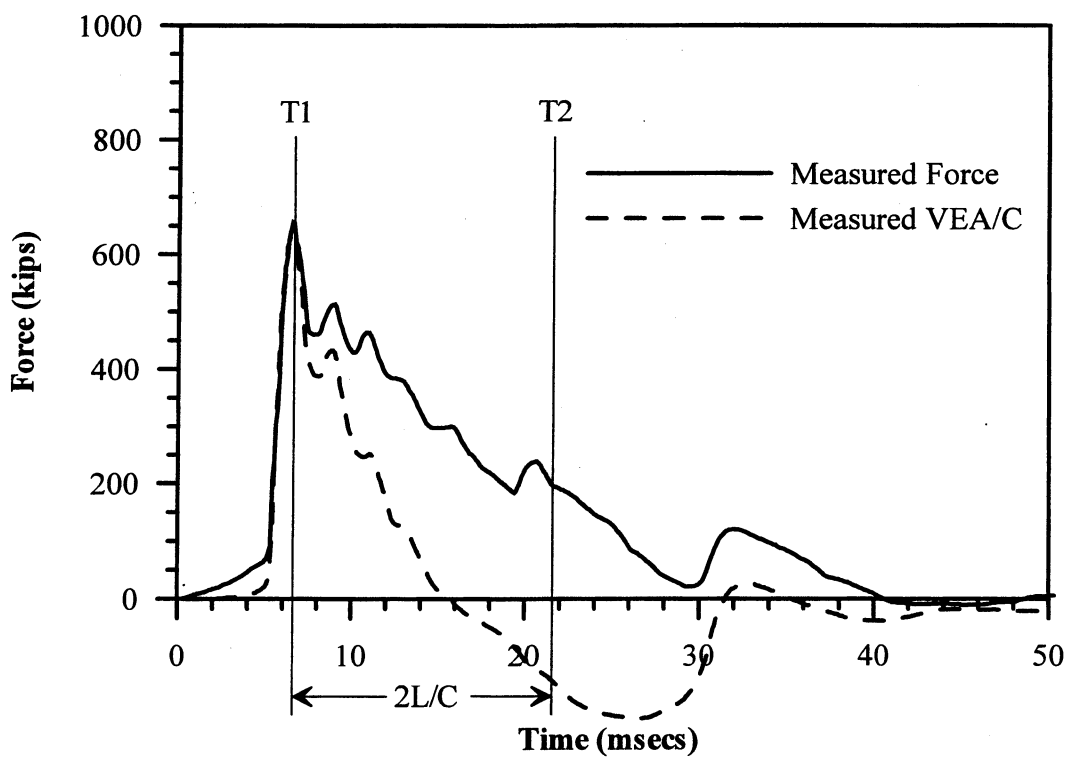


**Figure 3.2.** Digitized force and velocity multiplied by the impedance ( $EA/C$ ) traces for pile-case 190 used for input into INTEGRATE.

**UMASS-LOWELL GEOTECHNICAL ENGINEERING  
DYNAMIC PILE TESTING**

**SUMMARY OF INPUT PARAMETERS**

File .....	33P1BOR
Pile Location .....	Site 33
Date of Analysis .....	2-10-92
Pile Designation .....	33P1-BOR
Pile Type .....	HP12x74
Hammer Type .....	B-400
Nominal Energy of Hammer (ft-kips) .....	46
Penetration Depth (ft) .....	114.4
2L/C (msecs) .....	14.39
Time Interval (msecs) .....	0.1
Pile Impedance – EA/C (kip/sec/ft) .....	38.9
Final Blow Count (blows/inch) .....	16
T2 (offset from T1) (msecs) .....	14.39

**SUMMARY OF OUTPUT PARAMETERS**

D <sub>max</sub> .....	0.787
D <sub>final</sub> .....	0.164
Hammer Efficiency (%) .....	69.14
E <sub>max</sub> (kip-ft) .....	31.80
E <sub>final</sub> (kip-ft) .....	25.55
V <sub>max</sub> (ft/sec) .....	15.78
V <sub>final</sub> (ft/sec) .....	0.420
F <sub>max</sub> (kips) .....	637.38
F <sub>final</sub> (kips) .....	42.02
J .....	-0.017
F1 (kips) .....	637.38
F2 (kips) .....	192.10
V1 (ft/sec) .....	15.78
V2 (ft/sec) .....	-3.59
(V1*EA/C)/F1 .....	0.963

**PILE CAPACITY (kips)**

Davisson's Criteria .....	800
Shape of Curve .....	800
D = 0.1B .....	598
D = 1 inch .....	522
DeBeers log method .....	800
Final R <sub>s</sub> .....	800
CASE RTL .....	792
CAPWAP .....	715
Energy Approach R <sub>u</sub> (uncorrected) .....	898

**Figure 3.3.** INTEGRATE output of pile-case 190 showing the back-calculated Jc value and the Energy Approach prediction.

\*\*\*\*\*  
**UNIVERSITY OF MASSACHUSETTS - LOWELL**  
**GEOTECHNICAL ENGINEERING**  
**TEPWAP ANALYSIS**  
 \*\*\*\*\*

=====

**IDENTIFICATION DATA**

=====

Job Number ..... TP1EOD  
 Job Name ..... 33\_P  
 Date of Driving ..... 10-28-77  
 Pile Designation ..... H  
 Type of Pile ..... HP 12x74  
 Pile Length (ft) ..... 121  
 Type of Hammer ..... B-400  
 Nominal Energy of Hammer (ft-kips) ..... 46  
 Depth of Penetration (ft) ..... 114.4  
 Element Length (ft) ..... 5.26  
 Damping Model ..... Smith  
 Number of Blows per last three inches ..... 13, 13, 12  
 Date of Analysis ..... 9-16-92  
 PDA Blow # ..... 2  
 Iteration # ..... 1  
 Time Interval ..... 0.200  
 Option Number ..... 2

=====

**Figure 3.4.** Example of the pile identification information of pile-case 189 used as input for the TEPWAP analysis.

\*\*\*\*\*  
**UNIVERSITY OF MASSACHUSETTS - LOWELL**  
**GEOTECHNICAL ENGINEERING**  
**TEPWAP ANALYSIS**  
 \*\*\*\*\*

=====

**SOIL AND PILE PROPERTIES ALONG PILE ELEMENTS**

=====

element no.	dist. from gauges (ft)	area (in <sup>2</sup> )	weight (lbs)	stiffn (k/in)	resist (kips)	sum of resist (kips)	damp (s/ft)	quake (in)	quake rebnd ratio (%)	upwrd resist ratio (%)
3	5.3	21.8	390.1	10364	0.0	439.0	0.000	0.000	0.0	0.0
4	10.5	21.8	390.1	10364	5.0	434.0	0.020	0.300	100.0	-50.0
5	15.8	21.8	390.1	10364	5.0	429.0	0.020	0.300	100.0	-50.0
6	21.0	21.8	390.1	10364	5.0	424.0	0.020	0.300	100.0	-50.0
7	26.3	21.8	390.1	10364	5.0	419.0	0.020	0.300	100.0	-50.0
8	31.6	21.8	390.1	10364	5.0	414.0	0.020	0.300	100.0	-50.0
9	38.8	21.8	390.1	10364	0.0	414.0	0.010	0.300	100.0	-50.0
10	42.1	21.8	390.1	10364	0.0	414.0	0.010	0.300	100.0	-50.0
11	47.3	21.8	390.1	10364	0.0	414.0	0.010	0.300	100.0	-50.0
12	52.6	21.8	390.1	10364	0.0	414.0	0.010	0.300	100.0	-50.0
13	57.9	21.8	390.1	10364	0.0	414.0	0.010	0.300	100.0	-50.0
14	63.1	21.8	390.1	10364	5.0	409.0	0.010	0.300	100.0	-50.0
15	68.4	21.8	390.1	10364	5.0	404.0	0.010	0.300	100.0	-50.0
16	73.6	21.8	390.1	10364	8.0	396.0	0.010	0.300	100.0	-50.0
17	78.9	21.8	390.1	10364	8.0	388.0	0.010	0.300	100.0	-50.0
18	84.2	21.8	390.1	10364	8.0	380.0	0.010	0.300	100.0	-50.0
19	89.4	21.8	390.1	10364	8.0	372.0	0.010	0.300	100.0	-50.0
20	94.7	21.8	390.1	10364	8.0	364.0	0.010	0.300	100.0	-50.0
21	99.9	21.8	390.1	10364	8.0	356.0	0.010	0.300	100.0	-50.0
22	105.2	21.8	390.1	10364	8.0	348.0	0.010	0.300	100.0	-50.0
23	110.5	21.8	390.1	10364	8.0	340.0	0.010	0.300	100.0	-50.0
24	115.7	21.8	390.1	10364	80.0	260.0	0.090	0.150	100.0	-50.0
25	121.0	21.8	390.1	10364	100.0	160.0	0.080	0.150	100.0	-50.0
tip					160.0	0.0	0.080	0.150	100.0	

**Figure 3.5.** Example of the soil and pile properties used along the pile elements of pile-case 189 as input for the TEPWAP analysis.

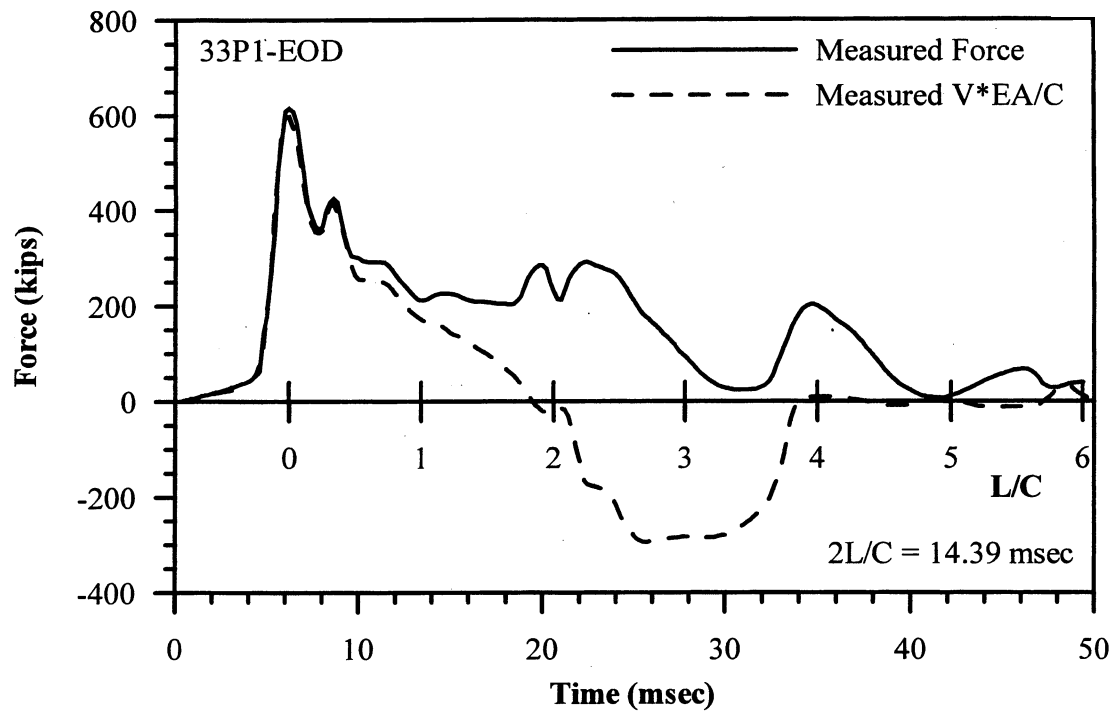


**Figure 3.6.** Measured force and velocity multiplied by the impedance (EA/C) traces of pile-case 189 used by the TEPWAP analysis.

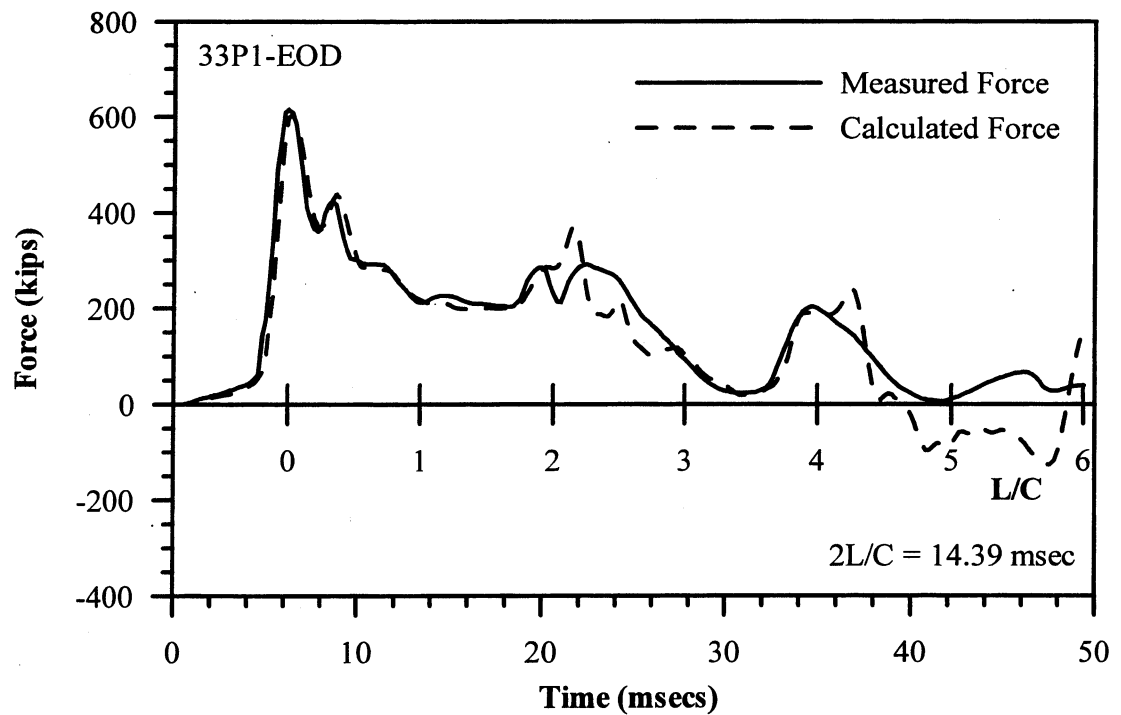


**Figure 3.7.** Comparison between measured force near the top of pile-case 189 and the calculated force from the TEPWAP analysis.

\*\*\*\*\*  
**UNIVERSITY OF MASSACHUSETTS - LOWELL**  
**GEOTECHNICAL ENGINEERING**  
**TEPWAP ANALYSIS**  
 \*\*\*\*\*

---

---

SUMMARY OF FINAL RESULTS

---

---

End Resistance	-	160.0 kips
Side Friction	-	279.0 kips
Total Capacity	-	439.0 kips

Percent in Friction	-	63.6%
---------------------	---	-------

Top Quake	-	0.79 inches
Set at Tip	-	0.32 inches

The Set Corresponds to 3 Blows Per Inch.

Maximum Calculated Energy	-	32.362 kip*ft
Maximum Measured Energy	-	32.674 kip*ft

---

---

Energy Difference (Calc – Measured)	-	-0.312 kip*ft
-------------------------------------	---	---------------

Maximum Compression force is in element #3 on iteration 32	-	636.49 kips
---	---	-------------

Maximum Tension force is in element #19 on iteration 181	-	-139.18 kips
---	---	--------------

The Maximum Stress is	-	29.20 kips/in <sup>2</sup>
The Minimum Stress is	-	-6.38 kips/in <sup>2</sup>

---

---

**Figure 3.8.** Summary of the final results from TEPWAP analysis performed on pile-case 189.

## **CHAPTER 4**

### **REFERENCE STATIC CAPACITY**

#### **4.1 OVERVIEW**

Different methods of analysis are used for the interpretation of load-settlement curves obtained from static load tests of piles. Many of the methods are subjective, resulting in a different static capacity from method to method and from engineer to engineer for the same static load test curve.

#### **4.2 OBJECTIVES**

The aim of the work presented in this chapter is to determine statistically if there is one method for analyzing pile capacity based on the static load-settlement curve that provides consistent and "correct" results. The main purposes in assigning one method for use in analyzing pile capacity are; (a) that there will be consistency in the pile capacity determination in general and (b) in the present LRFD parameter determination, predictive methods are compared to the "correct" capacity and one uniform approach is required.

#### **4.3 PILE FAILURE / CAPACITY DETERMINATION**

##### **4.3.1 Background**

A universal criterion capable of establishing the ultimate capacity of a pile is essential in improving the accuracy of static load test interpretations. Various ultimate



load criteria have been proposed and used by researchers and design organizations (see for example Vesic, 1977 and Fellenius, 1989). Significant disagreements remain among these methods as they are based on different principles and produce different values under varying pile types and sizes, load test procedures, and surrounding soils.

Vesic (1972) pointed out that interpreting a pile's ultimate load based solely on a visual examination of its load-settlement curve (i.e. shape of the curve) may be misleading and can result in different pile capacities depending on the scale used to plot the curve. Figure 4.1 and 4.2 demonstrate this point by presenting the same load-settlement relations using two different scales. Figure 4.1 shows a load-settlement curve indicating a pile capacity of approximately 4430 kN whereas the curve in Figure 4.2 suggests that the pile's displacement at 4430 kN may still be based on the elastic compression of the pile and that the pile capacity is approximately 4800 kN. One solution to this problem is to implement a common scale, based on the pile's elastic deformation. When plotting load-settlement curves, the elastic deformation of a fixed end column, (i.e., frictionless pile) is expressed as:

$$\delta = \frac{PL}{EA} \quad (4.1)$$

Where:

- $\delta$  = the calculated elastic deformation of the pile
- $P$  = the applied load
- $L$  = pile length
- $E$  = elastic modulus of the pile material
- $A$  = cross sectional area of the pile.

The elastic compression line obtained by Equation 4.1 is based on the assumption that the entire load applied to the pile top is transferred to the pile toe. To implement a

scale proportional to all load settlement curves, the elastic compression line should be inclined at an angle of approximately 20 degrees to the load axis (see Figure 4.3).

#### **4.3.2 Method of Approach**

In order to facilitate the aforementioned uniform scale, all of the load-settlement curves in the dataset PD/LT were digitized using the program DIGITIZE, developed at UMASS-Lowell by Chernauskas and Paikowsky. These curves were then replotted, using the graphics software GRAPHER, to produce curves that were proportional to each pile's elastic compression line inclined at 20 degrees.

After replotting, each load-settlement curve was analyzed using five different failure load interpretation procedures: Davisson's Criterion, the Shape of Curve method, Limited Total Settlement methods ( $\Delta = 25.4$  mm (1 inch) and  $\Delta = 0.1B$ ), and DeBeer's method.

#### **4.3.3 Davisson's Criterion**

The Davisson Criterion, (Davisson, 1972), or offset limit, defines the failure load of a pile as the load corresponding to the settlement which exceeds the elastic compression of the pile, by an offset,  $X$ , equal to 3.81 mm plus a factor equal to the diameter of the pile divided by 120. The offset is simply:

$$X = 3.81 + \frac{B}{120} \quad (4.2)$$

Where:  $B$  = the diameter of the pile in mm.

The Davisson's Criterion line is parallel to the elastic compression line and predicts the failure load at its intersection with the load-settlement curve. Figure 4.3 illustrates

the use of Davisson's failure criterion for load-settlement relations of pile-case 344, yielding a capacity of 4235 kN.

#### **4.3.4 The Shape of Curve Method**

The Shape of Curve method is a failure load approximation, which usually yields a range of values over which the pile is considered at or near failure. The boundaries of this range can be determined by examining the minimum curvature in the load-settlement curve through lines drawn tangent to the load-settlement curve (similar to the method proposed by Butler and Hoy (1977)). The failure range is relatively easy to define for load-settlement curves that exhibit general failure or plunging failure (rapid settlement with slightly increased loads) (see Figure 4.3 for example). Piles that experience local failure, or non-plunging failure, are difficult to analyze using the shape of curve method because of the uniform changes in slope of lines drawn tangent to the curve. Figure 4.3 illustrates the use of the 'shape of curve' procedure yielding an estimated capacity as a range between 4060 kN and 4800 kN.

#### **4.3.5 The Limited Total Settlement Methods**

The Limited Total Settlement methods,  $\Delta = 25.4 \text{ mm}$  and  $\Delta = 0.1B$  (Terzaghi, 1942), define the failure load as the load corresponding to settlements of 25.4 mm and 0.1B, respectively, where B is the diameter of the pile. These methods are not applicable in many cases. For example, the elastic compression for a very long steel pile often exceeds 25.4 mm and/or 0.1B without inducing any plastic deformation in the soil. Figure 4.3 shows as an example a load-settlement curve for pile-case 344, a 16" square concrete pile, that experiences a plunging failure before a displacement of

25.4 mm. Also, it is obvious that a settlement of 0.1B, or 40.64 mm in this case, does not represent the failure load of this pile and therefore is not applicable.

#### **4.3.6 DeBeer's log-log Method**

DeBeer (1970) defines the failure load as the load corresponding to the intersection of two distinct slopes created by the load-settlement data plotted using logarithmic scales. Figure 4.4 illustrates the use of DeBeer's criteria for the load-settlement curve of pile-case 344 leading to an estimated capacity as a range between 3960 kN and 4800 kN. The two slopes are especially visible for piles that experience plunging failures, yet when using DeBeer's method piles that undergo local failures, the result may be a range of values, such as illustrated here. As mentioned earlier, each load-settlement curve was digitized from the standard linear plots that they were presented on and the data was stored. This data was later plotted in logarithmic scales to utilize DeBeer's method.

#### **4.3.7 The Representative Static Capacity**

The capacity results for each method were reviewed independently based on the load-settlement curves for each pile. After considering the pile type, soil type, size of each pile and the load test procedure, unrealistic results were eliminated, and the acceptable values were averaged, yielding a final static capacity,  $R_s$ . For example, for pile-case 344 presented in Figures 4.3 and 4.4 the considered criteria were: Davisson's = 4235 kN, shape of curve = 4060 - 4800 kN, 25.4 mm settlement = 4800 kN, 0.1B settlement = NA, and DeBeer's = 3960 - 4804 kN. Excluding the 0.1B settlement

method, which is not applicable, the average of all the criteria led to a final static resistance assessment of  $R_s = 4462$  kN.

#### **4.4 PERFORMANCE EVALUATION OF THE DIFFERENT FAILURE CRITERION METHODS**

##### **4.4.1 Method of Approach**

Each of the methods described above was evaluated by comparing the capacity determined by that particular method to the representative pile capacity. The analysis was completed using 196 piles from the database PD/LT2000. The analysis used a  $K_{SX}$  value, which is the ratio of the representative capacity to the capacity determined by the method being analyzed. The subscript S in the K value corresponds to the representative static capacity. The X value is substituted for different letters depending on the method that was being analyzed. The subscripts were used as follows; D is used for the Davisson's criterion, B is used for the DeBeer method, L is used for the method of limiting the total settlement to  $\Delta = 0.1B$ , T is used for the method of limiting total settlement to 25.4 mm, and C is used for the Shape of Curve method. As an example, if the ratio is labeled  $K_{SD}$  it is the representative pile capacity divided by the Davisson's criterion capacity. A mean and standard deviation of the  $K_{SX}$  value were calculated for each of the five methods of pile capacity analysis. To evaluate each method a graph was generated presenting the normal and lognormal distributions as well as the actual data distribution in the form of a bar chart. The bar charts were generated by graphing the total number of  $K_{SX}$  values within a 0.02 interval versus that range of  $K_{SX}$  values. The graphs for all methods of analysis were plotted at the same scale so that comparisons could be made between them.

Conclusions could then be drawn, by comparing the figures, as to which method should be used in the analysis of static load test curves if the analysis is limited to one method. The following sections present the results of these analyses.

#### **4.4.2 Davisson's Criterion**

Figure 4.5 shows the normal and lognormal distributions of the  $K_{SD}$  value, which represents the ratio of the representative pile capacity to the capacity determined by Davisson's criterion. A total of 186 piles were used in the evaluation of the Davisson's criterion. For 10 piles, Davisson's criterion could not be applied. In nine (9) of these piles, the maximum settlement was less than the failure criterion and for the tenth pile; the pile capacity according to Davisson's criterion was below the the range of load in which the failure took place. The mean  $K_{SD}$  is 1.018 with a standard deviation of 0.1010 while the mean using the lognormal distribution is 1.013 with a standard deviation of 0.0892. The coefficient of variation, which is the ratio of the standard deviation to the mean, is 9.9%; statistically indicating that Davisson's criterion is a good method for use in analyzing static load test curves as it matches well the designated representative capacity. The bar chart, which shows the actual data for the  $K_{SD}$  values compares relatively well with the normal and lognormal distributions, the major exception being the large number of  $K_{SD}$  values, (40 and 36), concentrating in the ranges from 0.970 to 0.990 and 0.990 to 1.010, respectively, (total of 41% between 0.970 and 1.010). Figure 4.6 shows that there is no clear correlation between the  $K_{SD}$  value and the pile diameter. From the presented results the

Davisson's criterion method is an adequate method to use in the analysis of static load tests.

#### **4.4.3 The Shape of Curve Method**

The normal and lognormal distributions of the  $K_{SC}$  value, which is the ratio of the representative pile capacity to the capacity determined by the Shape of Curve method, are presented in Figure 4.7. A total of 193 piles were used in the evaluation of the Shape of Curve method. There were three cases for which the Shape of Curve method could not be applied; as the load settlement relationship was a gradual consistent curve without a clear point of failure. The mean  $K_{SC}$  for the 193 piles is 1.019 with a standard deviation of 0.0661 while the mean for the lognormal distribution is 1.017 with a standard deviation of 0.0596. The bar chart shows a good comparison between the actual data and the normal and lognormal distributions. The ranges from 0.990 to 1.010 and 1.010 to 1.030 show a large number of  $K_{SC}$  values, 57 and 38, respectively, (total of 49.2% between 0.990 and 1.030), which are close to the calculated mean values. This shows that for the majority of the cases the performance of the method is actually better than what is shown by the means and standard deviations. The relationships presented in Figure 4.8 suggest that there is no correlation between the  $K_{SC}$  value and the pile diameter. The obtained results indicate that the Shape of Curve method is an excellent method to use in the analysis of static load tests, with the only drawback being that the method is subjective.

#### **4.4.4 Limiting Total Settlement to 25.4 mm**

The  $K_{ST}$  value is the ratio of the representative pile capacity to the capacity determined by the load that relates to the settlement of the pile equal to 25.4 mm. There were 161 piles that met the failure criterion of  $\Delta = 25.4$  mm. There were 35 piles for which the limiting total settlement to 25.4 mm could not be applied, as the maximum settlement of the piles was smaller than the failure criterion. The normal and lognormal distributions of the  $K_{ST}$  values are shown in Figure 4.9 with a mean and standard deviation of 0.971 and 0.0981, respectively, for the normal distribution and 0.967 and 0.0959, respectively, for the lognormal distribution. There is a superior match between the bar chart, which shows the actual data, and the calculated normal and lognormal distributions. There are 4 ranges that have the highest and approximately the same number of  $K_{ST}$  values, 18 and 19, and the ranges are from 0.910 to 0.990 in 0.02 intervals, (total of 46.6% between 0.910 and 0.990). Figure 4.10 shows that there may be a correlation between the  $K_{ST}$  value and the pile diameter but there is not enough data to allow for conclusive observations. These results suggest that limiting the total settlement to 25.4 mm provides a good method to use in the analysis of static load tests, the drawback being that there are a significant number of piles that have failed before the failure criterion is reached, hence, the criterion maybe associated with the pile geometry and type of failure.

#### **4.4.5 Limiting Total Settlement to One Tenth of the Pile Diameter**

Figure 4.11 shows the normal and lognormal distributions of the  $K_{SL}$  value, which is the ratio of the representative pile capacity to the capacity determined by



taking the pile capacity as the load at a settlement equal to one tenth of the diameter of the pile. There were only 90 piles for which this method could have been applied. For 106 piles this failure criterion could not have been applied because the maximum settlement of the piles did not reach ten percent of the pile's diameter. The mean  $K_{SL}$  value for the normal distribution is 0.938 with a standard deviation of 0.1144 while the mean for the lognormal distribution is 0.932 with a standard deviation of 0.1215. The match between the bar chart, which shows the actual data, and the normal and lognormal distributions is not very good because the actual data is erratic. The highest number of  $K_{SL}$  values, 17, is in the range from 0.970 to 0.990, (total of 18.9% between 0.970 and 0.990), which is slightly higher than the mean of 0.938. Figure 4.12 in general shows that as the pile diameter increases this criterion shows more and more higher results than the designated static capacity (lower  $K_{SL}$ ). These results show that the limiting total settlement to one tenth of the pile diameter is not a good method to use in the analysis of static load tests because over half of the piles have failed before the failure criterion is reached and the statistical data is not very supportive of the method.

#### **4.4.6 DeBeer's log-log Method**

The normal and lognormal distributions of the  $K_{SB}$  value, which is the ratio of the representative pile capacity to the capacity determined by the DeBeer's method, are shown in Figure 4.13. A total of 187 piles were used in the evaluation of DeBeer's method of analysis for static load test curves. There were 9 piles for which the method could not have been applied because the load settlement relationship on a log-log scale

did not result in an identifiable change in orientation. The mean  $K_{SB}$  value for the 187 piles is 1.033 with a standard deviation of 0.0877 while the mean for the lognormal distribution is 1.030 with a standard deviation of 0.0816. These statistics show that this is a good method of analysis as the coefficient of variation is approximately 8.5%. The bar chart shows a good comparison between the actual data and the normal and lognormal distributions, the exception being the two peaks with a high number of  $K_{SB}$  values, 39 and 29, in the ranges from 0.990 to 1.010 and 1.010 to 1.030, respectively, (total of 36.4% between 0.990 and 1.030). Figure 4.14 shows that there is no correlation between the  $K_{SB}$  value and the pile diameter. The obtained results suggest that the DeBeer method is an excellent procedure to be used in the analysis of static load tests. The drawback of the DeBeer method is that it is by and large a subjective method that provides a narrow band of possible capacity outcome under the conditions of a clear general failure.

#### **4.4.7 Intermediate Conclusions**

The analyses and their graphical representation as provided in the previous section allows for an educated evaluation of the load test interpretation methods and the possible selection of a single method of analysis rather than a representative pile capacity. Table 1 provides a complete summary of the mean and standard deviation of the  $K_{SX}$  value for each of the methods as well as some other significant information for comparison purposes. Figure 4.15 shows a comparison of the normal distribution curves for the five methods used to determine the pile capacities.

The Shape of Curve and DeBeer methods show a good correlation between the normal and lognormal distributions to the actual data. The mean  $K_{SX}$  value for each of the methods is close to one with a small standard deviation. For the majority of the pile-cases using the Shape of Curve method, 179 of 193 pile-cases, the  $K_{SC}$  values fall within the range of 0.90 to 1.10. For most of the pile-cases using the DeBeer method (153 of 187 pile-cases) the  $K_{SB}$  values fall within the range of 0.90 to 1.10. According to these statistics alone the conclusion can be drawn that the Shape of Curve and DeBeer's methods are preferable methods for evaluating static load tests. The problem with these two methods (in particular the Shape of Curve) is that they are both subjective, the results can vary greatly from engineer to engineer, and therefore they cannot be recommended for evaluating static load test capacity under conditions that require objectivity and repetitiveness.

The method of determining the pile capacity using a total settlement ( $\Delta = 25.4$  mm) seems to perform well judging by the mean and standard deviations as well as the number of  $K_{ST}$  values that fall in the range of 0.90 to 1.10, 120 of 161 pile-cases. The method is objective, but 35 piles out of the examined 196 piles did not meet the failure criterion. The method of determining pile capacity by limiting the total settlement to 25.4 mm is therefore not recommended because of the above stated disadvantage.

The method of determining the pile capacity using the failure criterion of  $\Delta = 0.1B$  seemed to perform well judging by the mean and standard deviation. The number of piles that have  $K_{ST}$  values that fall within the range of 0.90 to 1.10 is also very small (59 of 90 pile-cases) compared to the other interpretation methods. These

disadvantages as well as the fact that the method could be applied to only 90 of the 196 piles that were evaluated lead to the conclusion that this method of analysis should not be used by itself (stand alone).

The intermediate conclusion of this analysis is that the one method to use in evaluating the pile capacity based on the static load test results is the Davisson's criterion. This method has a mean  $K_{SD}$  value that is close to one and the standard deviation is relatively small. In addition; for 160 of 186 pile-cases the  $K_{SD}$  value falls within the range of 0.90 to 1.10, which is satisfactory by itself. The method's major additional advantage is its objectivity so the results from the analysis should not vary much from one engineer to another. Based on the minimum and maximum  $K_{SD}$  values it is clear however that the method must be examined and judgment needs to be applied.

#### **4.4.8 Evaluation of a Modification for Davisson's Criterion**

##### ***a) The Proposed Modification***

Davisson's Criterion as concluded above is the method that should be used to analyze static load test curves if only one method of analysis needs to be used. Static load tests on large diameter piles require larger settlements to develop the toe resistance, therefore, Kyfor et al., (1992), proposed that for large diameter piles (diameter greater than 610 mm), the offset to be used for Davisson's criterion should be:

$$X = \frac{B}{30} \quad (4.3)$$

Where  $B$  is the pile diameter in the units consistent with the calculated elastic deformation. The following section presents an evaluation of the proposed criterion.

***b) The Performance of the Proposed Modification***

Thirty-one (31) piles of database PD/LT2000 belong to the large diameter pile category, for which the load-settlement curves were reanalyzed based on the modified criterion and new pile capacities were determined. Figure 4.16 presents the normal and lognormal distributions of the  $K_{SD}$  and  $K_{SLD}$  values for the large diameter piles in PD/LT2000.  $K_{SLD}$  represents the ratio of the representative pile capacity to the capacity determined by the Davisson's criterion method using the offset given in Equation 4.3 for the large diameter piles. Of the 31 piles that fall into the large diameter pile category only 20 meet the Davisson's failure criterion using the modified offset. Using the original offset there was only one pile that did not meet the Davisson's failure criterion. Using the modified offset caused ten additional cases (out of the 31) to be excluded from the Davisson's failure criterion. These were excluded because the settlement of the pile did not reach the failure criterion. This information alone raises doubts about the applicability of the modified offset for large diameter piles as it significantly decreases the number of piles that meet the failure criterion. As shown in Figure 4.16 for the thirty-one large diameter piles, the mean  $K_{SLD}$  is 0.920, while the mean  $K_{SD}$  is 0.994, which is much better. The standard deviation of the  $K_{SLD}$  values is 0.0714, which is slightly better than that of the standard deviation for the  $K_{SD}$  values, 0.0749. The lognormal distribution statistics also show that the original offset gives better results than the modified offset based on the 31

large diameter piles. The bar chart, which shows the actual data for the  $K_{SLD}$  values compares relatively well with the normal and lognormal distributions, with the exception being the two ranges from 0.970 to 0.990 and 0.990 to 1.010 with large numbers of  $K_{SLD}$  values, 36 and 31, respectively. Figure 4.17 shows that there is no correlation between the  $K_{SLD}$  value and the pile diameter. The results of this analysis has lead the authors to the conclusion that the single method of choice for analyzing static load test results is the Davisson's criterion method and the correction for large diameter piles should not be used.

## **4.5 STATIC LOAD TEST PROCEDURE**

### **4.5.1 Overview**

This section reviews common procedures used when performing a static load test in the United States. The ASTM, Massachusetts Highway Department, Massachusetts Building Code, and the Texas Quick Test procedures are described and briefly analyzed. Detailed comparisons are held between two methods; the slow maintained and short duration load tests as well as the static cyclic test. The influence of creep on the static load test results when using two different static load test procedures is examined and some new research data are presented. The material presented in this section is based on the Paikowsky et al., (1999).

### **4.5.2 Load Test Procedures**

#### ***a) ASTM Procedures***

The American Standard for Testing and Materials (ASTM) provides four static load test procedures, which include the standard loading procedure, cyclic loading,

quick load test, and constant rate of penetration. These procedures are described briefly below, for more details refer to ASTM (1998).

#### *Standard Loading Procedure*

The standard ASTM method calls for piles to be loaded to 200% of the anticipated design load, unless failure occurs first. The pile shall be loaded in increments of 25% of the total test load. Each load increment will be held until the rate of settlement is not greater than 0.25 mm/hr (0.01 inches per hour) but no longer than two hours per increment. In the event the pile has not failed, hold the total load on the test pile between 12 and 24 hours until the butt settlement is not greater than 0.25 mm/hr (0.01 inches per hour). After the settlement rates have been satisfied, remove the load in decrements of 25% of the total test load with one hour between decrements.

#### *Cyclic Loading*

The pile is loaded in a series of four cycles. The first cycle is loaded in increments of 25% of the total design load up to 50% and each load increment is held for one hour. At 50% the pile is unloaded in decrements of 25% until the entire load is removed from the pile with 20 minutes between decrements. Cycles two, three, and four are loaded to 100%, 150%, and 200%, respectively in increments of 50% of the total design load. Each load increment is held for one hour during each cycle. Once the maximum load is reached per cycle, the pile is unloaded to zero in decrements of 50% of the maximum applied load with 20 minutes between each unloading.

### *Quick Load Test Method for Individual Piles*

The load is applied in increments of 10 to 15% of the design load with a constant time interval of 2.5 minutes between loading increments. Load increments are added until continuous jacking is required to hold the test load or until the specified capacity of the loading device is reached. After one of these criteria is reached, the load is held for five minutes and the full load is removed from the pile.

### *Constant Rate of Penetration*

The pile is loaded at a constant rate of penetration 0.3 to 1.3 mm/min (0.01 to 0.05 in/min) for cohesive soils or 0.8 to 2.5 mm/hr (0.03 to 0.1 in/min) for granular soils. The pile is continually loaded until no further increase in load is necessary for the constant rate of penetration of the pile under the predetermined rate or the capacity of the pile is reached. If the pile continues to settle under the constant load, the load is held until the pile has moved at least 15% of the pile diameter and then the pile is unloaded completely. If maximum capacity of the pile is reached before failure, the total load is released.

### ***b) Massachusetts Highway Department Procedures***

The Massachusetts Highway Department uses a set of load test procedures similar to the ASTM methods. The procedures described by the Massachusetts Highway Department encompass the short duration test, maintained load test, and the quick load test. The procedures are described in detail by the Massachusetts Highway Department (1995) and briefly reviewed below.



### *Short Duration Test*

Massachusetts Highway Department requires the load to be applied up to 200% of the design load in increments of 25%. Each load increment is held for half an hour. Once the maximum applied load is achieved, it is held for one hour and until the settlement rate is less than 25 mm/hr (1 inch per hour). After both of the above criteria are met, the load is removed in decrements of 25% of the design load every 15 minutes until zero load is reached. Finally, zero load is held for one hour to complete the test.

### *Maintained Load Test*

The pile is tested under load increments equal to 50, 100, 150, 175, and 200% of the design load and maintained for a period of two hours. Once the maximum load is achieved, it is held until the settlement does not exceed 0.02 inches (0.5 millimeters) in a 12-hour time frame. After completion of the loading, the unloading is conducted in decrements not exceeding one quarter of the total test load and maintained for a period of four hours each.

### *Quick Load Test*

The test shall be applied in increments of 50 to 100 kN (11 to 22 kips) and maintained for 2.5 minutes until continuous jacking is required to maintain the test load. The final load increment shall be held for no more than five minutes and then unloaded in four equal decrements.

**c) *Massachusetts Building Code Procedure***

Massachusetts Building Code (5<sup>th</sup> Edition, 1996) requires the pile to be loaded to 200% of the design load in increments of 25% and each increment is held for half an hour. Once the maximum applied load is achieved, it is held for one hour or until the settlement rate is less than 25 mm/hr (1 inch per hour). After both of the above criteria are met, the load is removed in decrements of 25% of the design load every 15 minutes until zero load is reached. Finally, zero load shall be held for one hour to complete the test.

**d) *Texas Quick Test Procedure***

The Texas quick test (Butler and Hoy, 1977) is a modification of the Constant Rate of Penetration Test (CRP). The CRP test advances a pile into the ground at a constant penetration rate while the force required to sustain the rate is continually adjusted. Engineers at the Texas State Department of Highways and Public Transportation simplified the CRP test. The new test requires that load be applied in 44 to 89 kN (5 to 10 ton) (or 10-15% of the design load) increments while recording the load and settlement data immediately after each load increment. Each load increment is held for 2.5 minutes before the next load increment is applied. Once the maximum load is achieved, it is held for 2.5 minutes before complete removal of the load from the pile.

**e) *Static-Cyclic Load Test Procedure***

The static-cyclic approach is based on a methodology developed by Dr. Valery Operstein during her work as the Chief Engineer at Ukrspetsstroiproekt, a soils and

foundations research design institute in Dniepropetvorsk, Ukraine. A pile is loaded to failure by applying a load at a high constant rate of approximately 150 kN/min and then unloaded at a fast rate of approximately 325 kN/min. Typically a series of three load-unload cycles is performed within a time period of less than one hour. The method enables the unique determination of the ultimate pile capacity based on the load-settlement relations in the load-unload cycle, which is closely related to the fundamental physical mechanism of soil/pile interaction.

*f) Summary*

The static load test procedures discussed in the above sections are compiled in Table 4.2. The table summarizes the loading and unloading increments and hold times associated with each test. Figure 4.18 displays the ASTM procedures in a graphical format. The figure depicts the duration in minutes vs. percent of design load for each test and testing stage. Figure 4.19 shows the MHD procedures using the same format. The loading procedure (MBC) and standard tests are not displayed on any graph because they replicate the short duration test (MHD) and maintained load test (MHD), respectively. General hold times were used to complete each graph and it should be noted that the hold times for each test would vary depending on the soil conditions.

#### **4.5.3 Performance Evaluation of the Load Test Procedures**

*a) Comparison of the Short Duration, Slow Maintained and Static Cyclic Tests*

To evaluate the influence of creep on static load test results two pile case histories were analyzed. The two piles were part of a research project conducted by the University of Massachusetts Lowell Geotechnical Engineering Research

Laboratory at a bridge reconstruction site in Newbury, Massachusetts. The two test piles were labeled test pile # 2 and test pile # 3; both of these piles were tested under slow maintained, short duration and static cyclic load test procedures. The load test curves for both the slow maintained and short duration static load test types were reduced for creep and compared for both test piles.

Figure 4.20 and Figure 4.21 present the static load test curves, using the original data, for the short duration, slow maintained and static cyclic tests for test piles # 2 and # 3, respectively. In both figures it is seen that a significant creep takes place during the holding times for both the slow maintained and short duration load test types. The figures show that, even with the large settlements due to creep, the pile capacity determined by Davisson's criterion is approximately equivalent for both load test types. The static cyclic capacities, which is the load equivalent to the intersection of the load and unload curves on the load displacement graph, is approximately the same load that was determined using Davisson's criterion for both load test piles. Static cyclic load test results will be compared to pile capacities determined using Davisson's criterion on slow maintained static load tests in the following section. These two test piles load-displacement curves show that there is an insignificant influence on the load test results from the type of static load test that is completed.

To evaluate the effect of creep on the results of the load test analysis the load test curves for both test pile # 2 and # 3 were replotted using the original data reduced for creep. The new load-settlement curves are shown in Figures 4.22 and 4.23 for test piles # 2 and # 3, respectively.

Figure 4.22 presents the original short duration and slow maintained static load test curves for test pile # 2 as well as the curves that were reduced for creep. When reducing both static load test curves for creep it was apparent that the significant amount of settlement at a load of approximately 700 kN could no longer be attributed to creep but the pile had begun to plunge. The pile capacity based on Davisson's criterion for both types of static load test is approximately the same. The analysis of test pile # 2 suggests that there is no influence of the static load test results (designated failure) based on the type of static load test performed.

Figure 4.23 presents the slow maintained and short duration static load test curves using both the original data and the data reduced for creep for test pile # 3. The presented load-settlement relations suggest that test pile # 3 begins to fail by plunging at approximately 1200 kN. The settlement at this load is too large to be attributed to creep. Evaluating this pile's capacity based on Davisson's criterion and the two types of static load tests; results in a pile capacity of approximately 1200 kN with little or no influence of the load test type.

***b) Comparison between the Static-Cyclic Load Testing and Slow Maintained Tests Using Davisson's Capacity***

In order to further evaluate whether the static load test capacity is influenced by the static load test procedure, a comparison between results obtained using the static cyclic and slow maintained load tests was made. A database compiled by Dr. Valerie Operstein and the University of Massachusetts - Lowell presented by Paikowsky et al., (1999) was used. The database contains 81 piles, which were statically load tested using both methods, but there were 6 piles for which the

Davisson's criterion did not apply to the slow maintained test. Figure 4.24 shows a comparison between the pile capacity determined using Davisson's criterion for the slow maintained load test and the static cyclic capacity. The mean  $K_{SCYC}$  of 0.930 and standard deviation of 0.136 show that the results determined using each load test method are very similar and there is no significant difference. A few of the cases shown on the graph do show a fairly large discrepancy between the results from each of the load tests. This is due to limiting the analysis of the slow maintained test to a single method. As shown in Table 4.3 the statistics, the mean of 1.023 for the ratio between the representative pile capacity for the slow maintained test and the static cyclic results and its standard deviation, 0.057, show that when a representative pile capacity is used the two load test methods give almost identical results. The results of this analysis show that the load test results are not significantly influenced by the procedure of the static load test.

**c) *Intermediate Conclusions***

The influence of the static load test procedure on the chosen pile capacity based on the above two analyses is insignificant. As only a small number of pile-cases exist for which multiple types of static load tests to failure were completed the above analysis of the two piles at the Newbury site is rare but it has lead the authors to the above conclusion. The extensive research on the static-cyclic load testing procedure that was recently completed (Paikowsky et al., 1999) also shows that the static load test procedure has little to no influence on the pile capacity.

#### **4.6 CONCLUSIONS FOR REFERENCE STATIC CAPACITY**

It is recommended that the traditional Davisson's criterion will be used for determining the pile capacity based on static load-settlement curves. The correction for the large diameter piles suggested by Kyfor et al., 1992 did not prove to be worthwhile. The static capacity used for the evaluation of the dynamic methods will make use of the static pile's capacity as evaluated based on Davisson's criterion regardless of the load testing procedure.

**Table 4.1.** Summary of the Interpretation Methods applied to the Static Load Test Curves in PD/LT2000.

Interpretation Method	Number of Valid Cases	Mean Ratio $K_{SX}$	Standard Deviation	Max Value of $K_{SX}$	Min Value of $K_{SX}$	Number of Cases for the Range of $K_{SX}$ from 0.95 to 1.05	Number of Cases for the Range of $K_{SX}$ from 0.90 to 1.10	Non-Applicable Cases and Reason why they are non-applicable
Davisson's Criteria	186	1.018	0.101	1.734	0.766	111	161	9 - max settlement less than failure criterion 1 - load below the failure range
DeBeer	187	1.033	0.088	1.429	0.750	119	153	9 - no clear failure point on log - log graph of load settlement curve
$\Delta = 0.1B$	90	0.938	0.114	1.367	0.647	39	59	106 - max settlement less than failure criterion
$\Delta = 1''$	161	0.971	0.098	1.538	0.714	73	120	35 - max settlement less than failure criterion
Shape of Curve	193	1.019	0.066	1.600	0.833	145	179	3 - load settlement curve did not have a clear failure point
Representative Pile Capacity	196	1.000	0.000	1.000	1.000	196	196	0

Notes:

$K_{SX}$  – The ratio between the representative pile capacity to the capacity obtained by the examined method.



**Table 4.2.** Summary of Static Load Test Procedures (after Paikowsky et al., 1999)

Code	Test Name	Loading		Hold Time at Max. Load	Unloading		Hold time at Zero Load
		Increments	Hold Time		Increments	Hold Time	
<b>ASTM</b>	<i>Standard Loading Procedure</i>	25%	0.01 in/hr	12-24 hr	25%	1 hr & .01 in/hr	1 hr
	<i>Cyclic Loading</i>	50%	1 hr	0 hr	50%	0.33 hr	1 hr
		50%	0.33 hr	12-24 hr	25%	1 hr	0 hr
	<i>Quick Load Test</i>	10-15%	2.5 min	5 min	1 step	Instantaneous	0 hr
	<i>Constant Rate of Penetration</i>	.01 - .1 in/min	0 hr	-	-	-	-
<b>MHD</b>	<i>Short Duration</i>	25%	0.5 hr	1 hr	25%	0.25 hr	1 hr
	<i>Maintained Load Test</i>	50%	2 hr	12-24 hr	25%	4 hr	4 hr
	<i>Quick Load Test</i>	50-100kN	2.5 min	5 min	25% of max.	2.5 min	15 min
<b>MBC</b>	<i>Loading Procedure</i>	25%	0.5 hr	1 hr	25%	0.25 hr	1 hr
<b>TQT</b>	<i>Quick Load Method</i>	10-15%	2.5 min	2.5 min	1 step	Instantaneous	2.5 min
	<i>Static-Cyclic Test</i>	150 kN/min	0 hr	0 hr	325 kN/min	0 hr	0 hr

Notes:

1. ASTM – American Standard for Testing and Materials.
2. MHD – Massachusetts Highway Department.
3. MBC – Massachusetts Building Code.
4. TQT – Texas Quick Test.
5. All percentages are in percent of total design load of the pile.
6. The loading increment for the standard test is based on the assumed bearing capacity of the pile.

**Table 4.3.** Summary of the Statistical Data Comparing the Slow Maintained Load Tests Results using Davisson's Criterion and the Static Cyclic Load Test Results from the UMass Lowell / Ukraine Database.

	<u>Representative Load Test Results</u> Static Cyclic Capacity	<u>Davissons Capacity</u> Static Cyclic Capacity
Mean $K_{SC}$	1.023	0.930
Standard Deviation	0.057	0.136
Number of Cases	81	75
Maximum $K_{SC}$	1.216>1.215	
Minimum $K_{SC}$	0.893	0.577

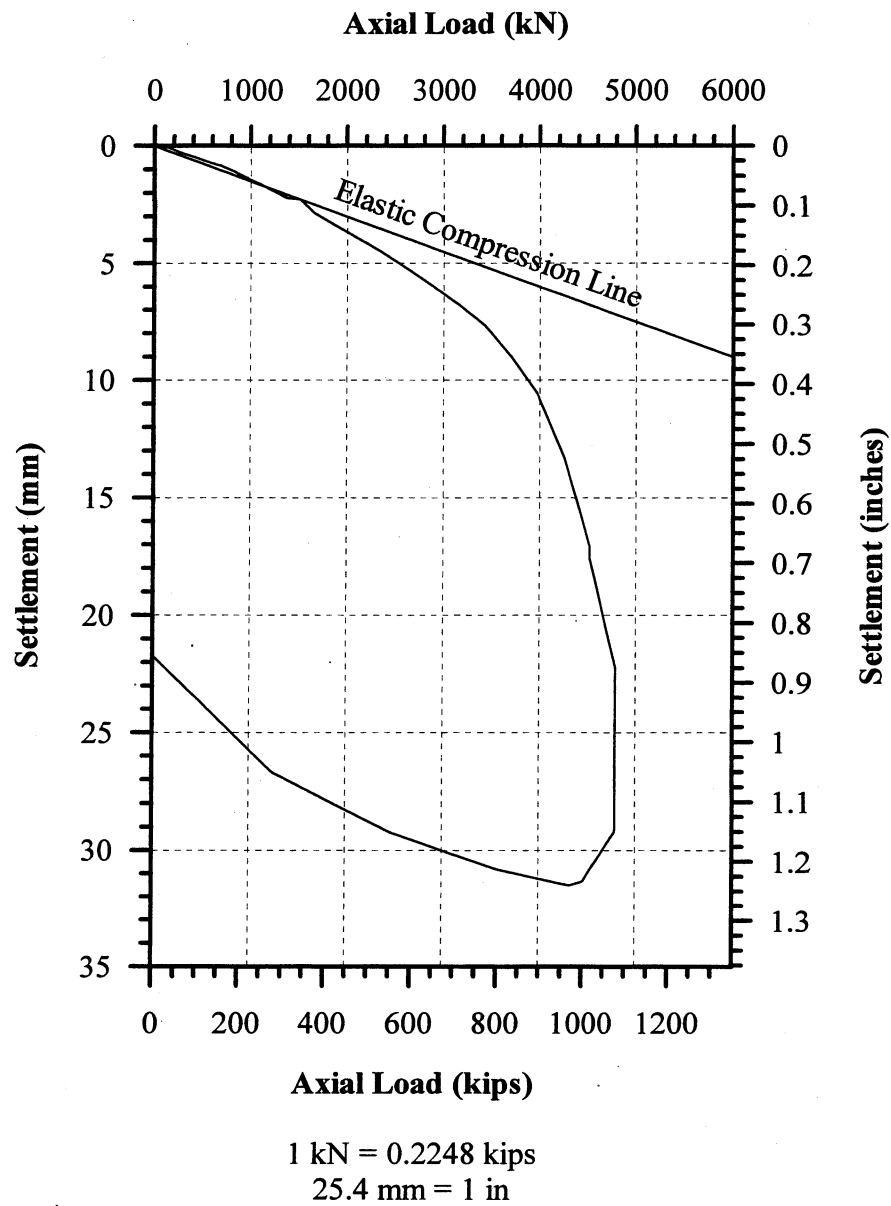


**Figure 4.1.** Load-settlement curve of pile-case 344 with the elastic compression line inclined at 20 degrees.

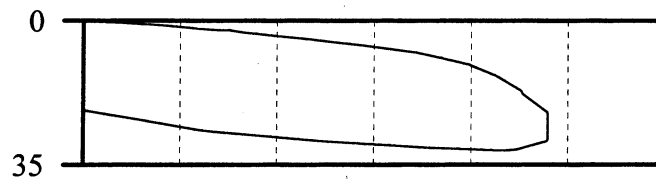


**Figure 4.2.** Load-settlement curve of pile-case 344 with a scale that does not consider the elastic compression of the pile.

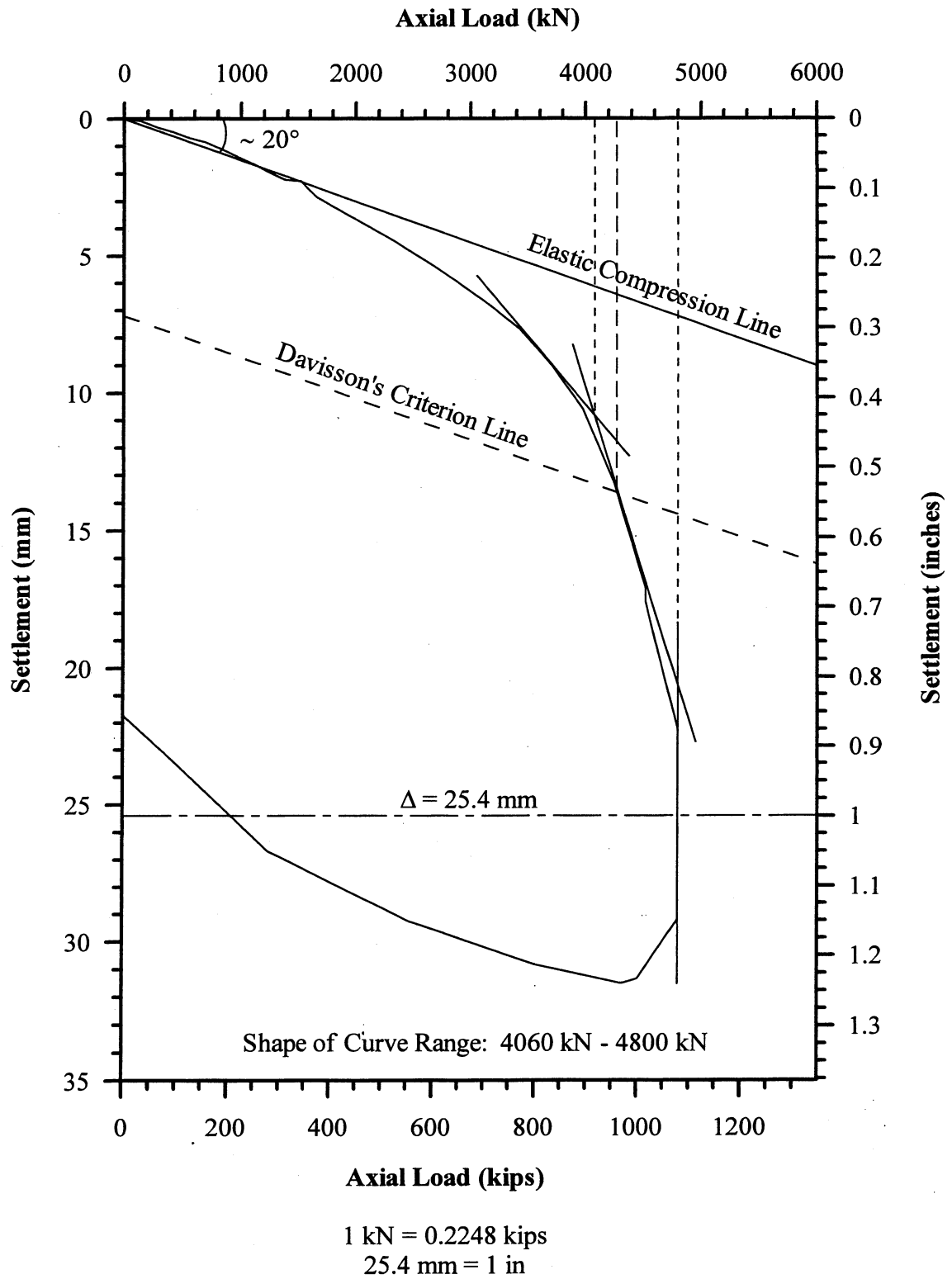


**Figure 4.3.** Load-settlement curve of pile-case 344 with the elastic compression line inclined at approximately 20 degrees.

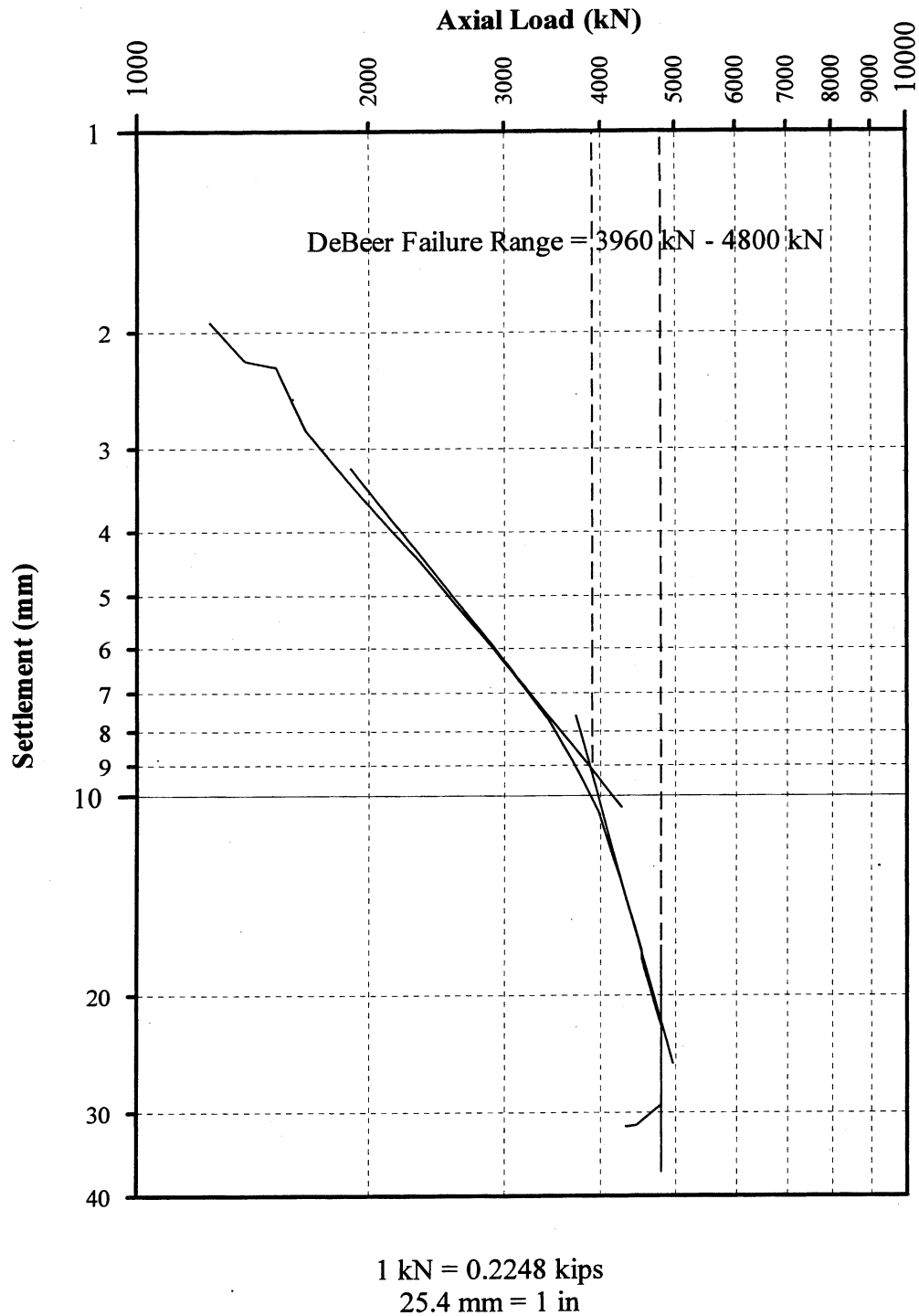


**Figure 4.4.** Load-settlement data plotted on a logarithmic graph for pile-case 344 to determine the failure load according to DeBeer's method.

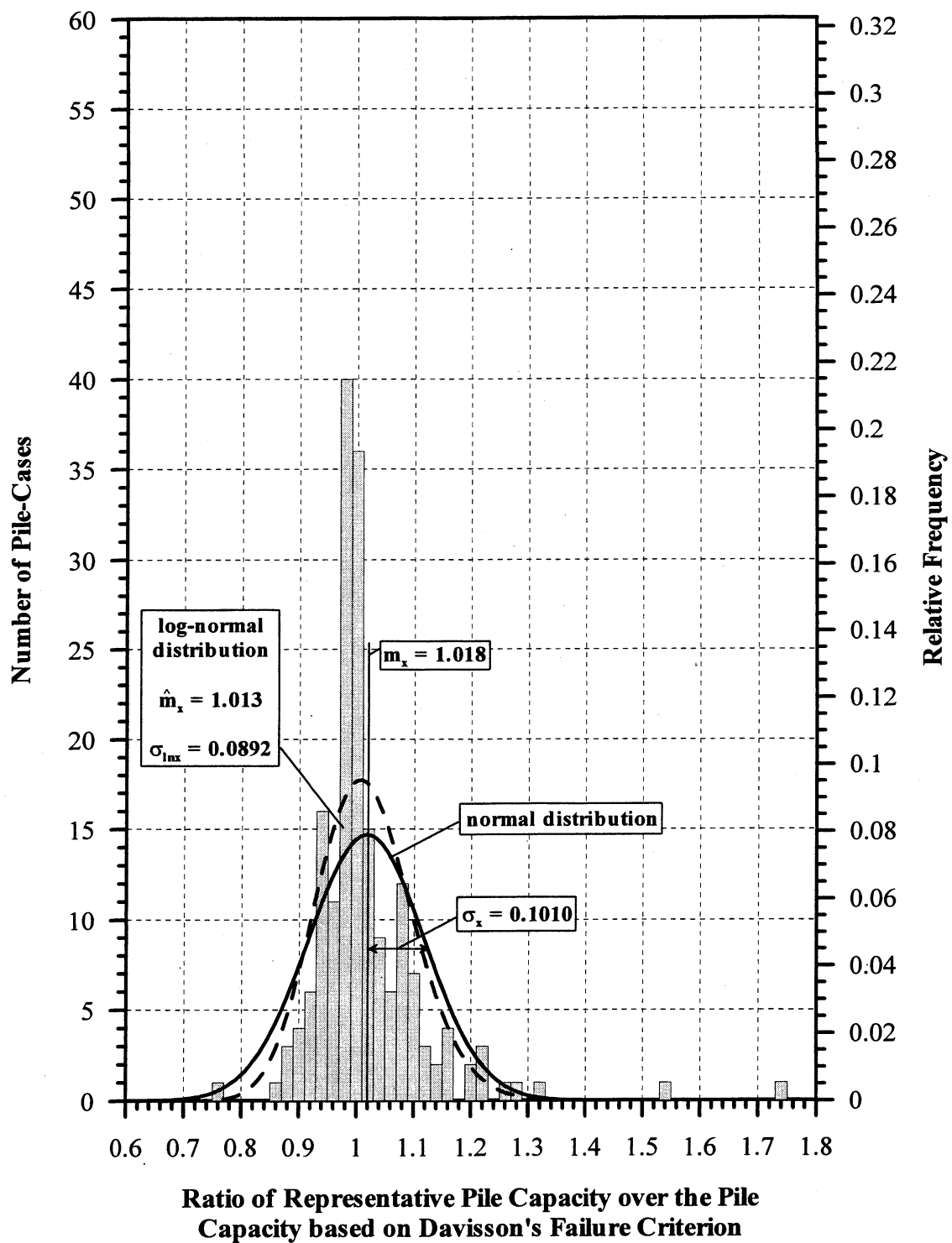


**Figure 4.5.** Histogram and frequency distributions of  $K_{SD}$  for 186 PD/LT2000 pile-cases in all types of soils.

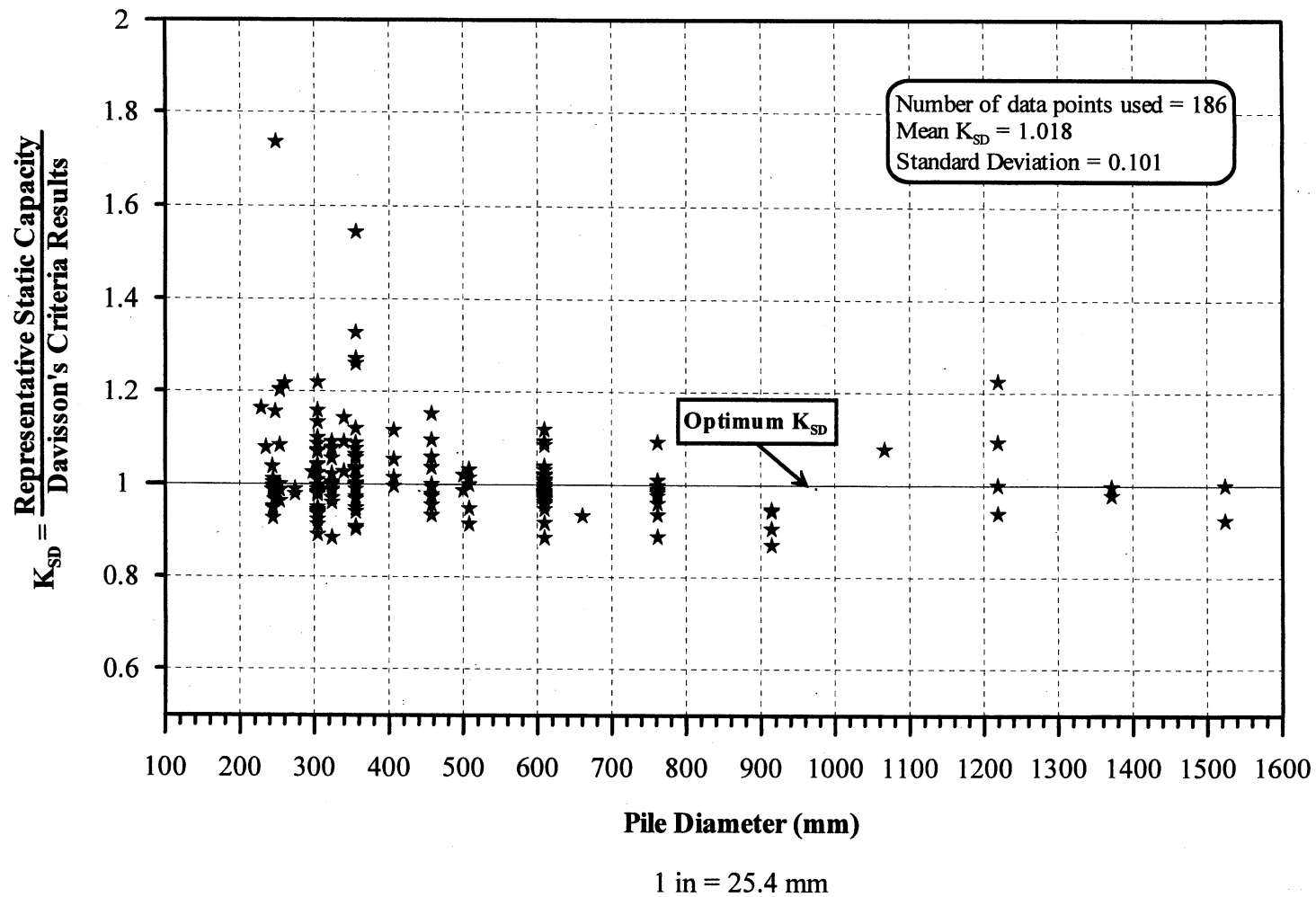


**Figure 4.6.**  $K_{SD}$  values vs. Pile Diameter for all PD/LT2000 pile-cases, all types of soils.

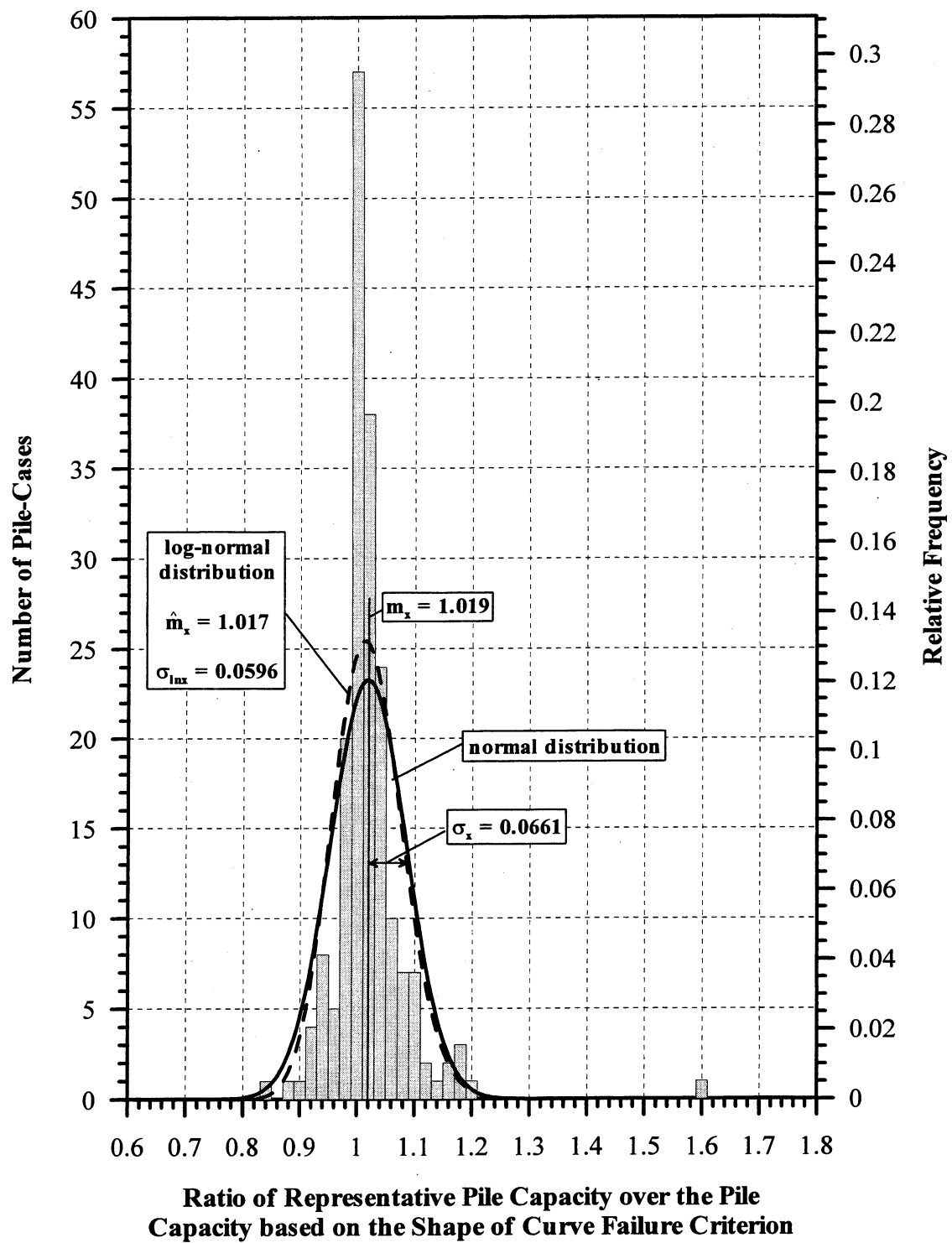


**Figure 4.7.** Histogram and frequency distributions of  $K_{sc}$  for 193 PD/LT2000 pile-cases in all types of soils.



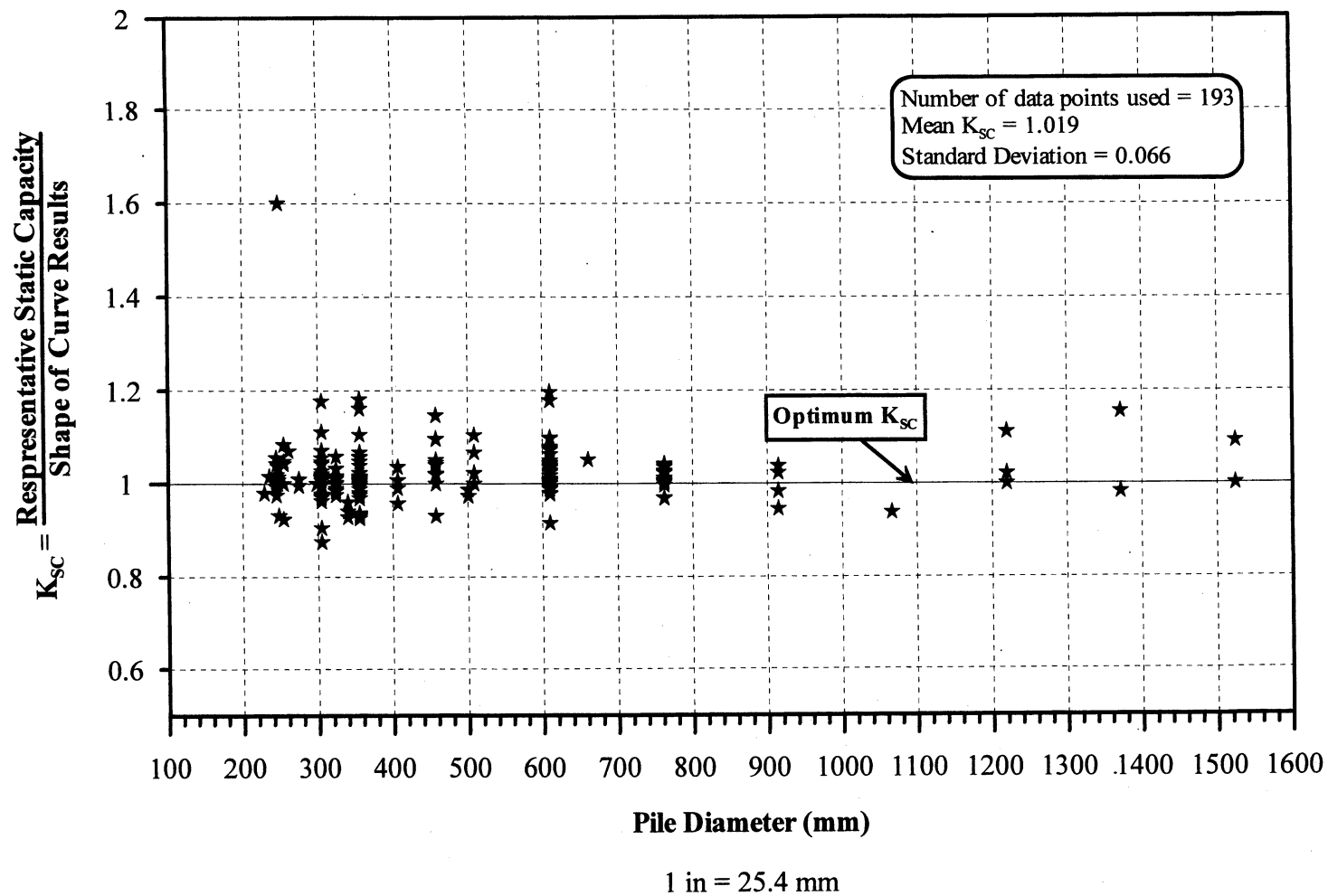


**Figure 4.8.**  $K_{sc}$  values vs. Pile Diameter for all PD/LT2000 pile-cases, all types of soils.

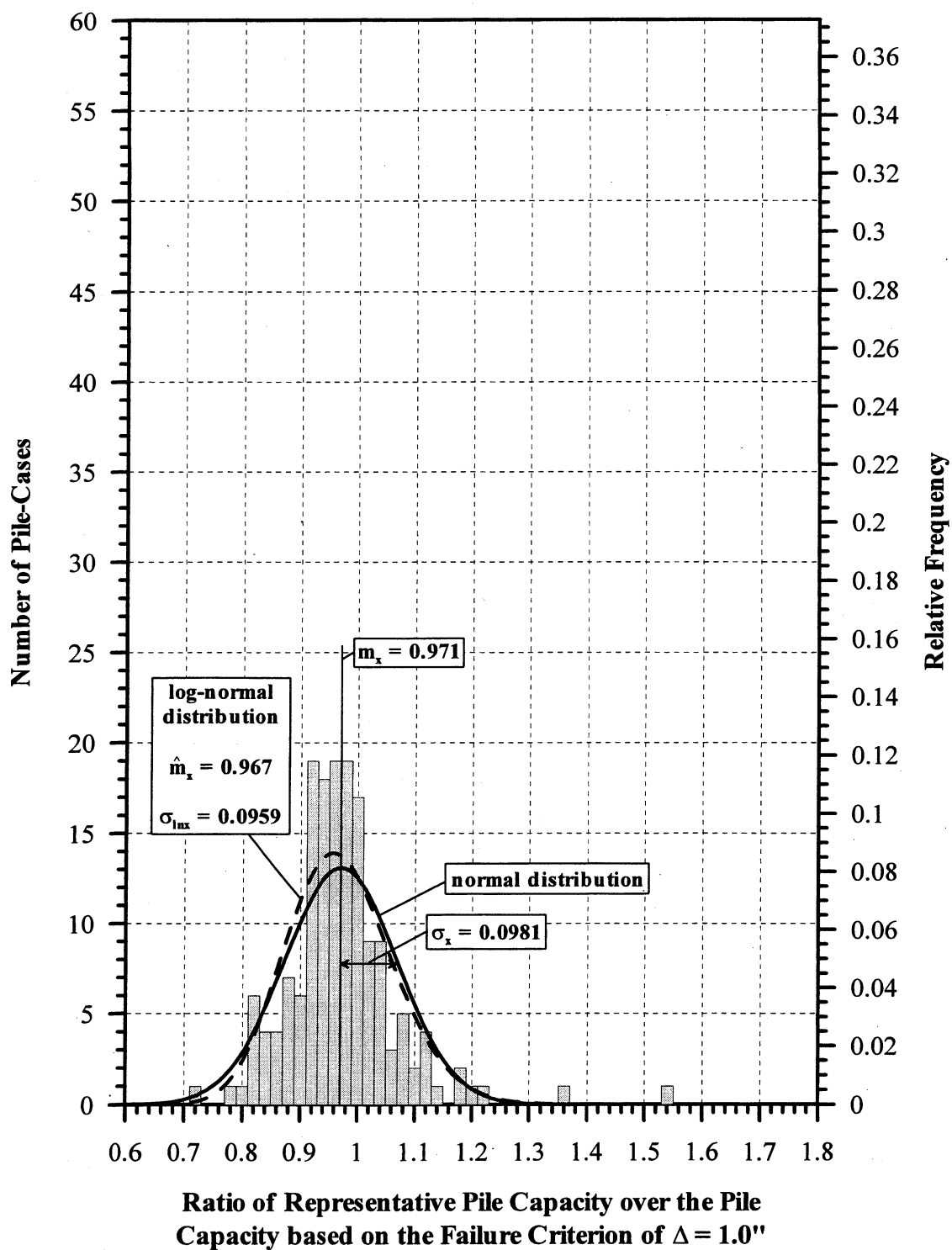


**Figure 4.9.** Histogram and frequency distributions of  $K_{ST}$  for 161 PD/LT2000 pile-cases in all types of soils.

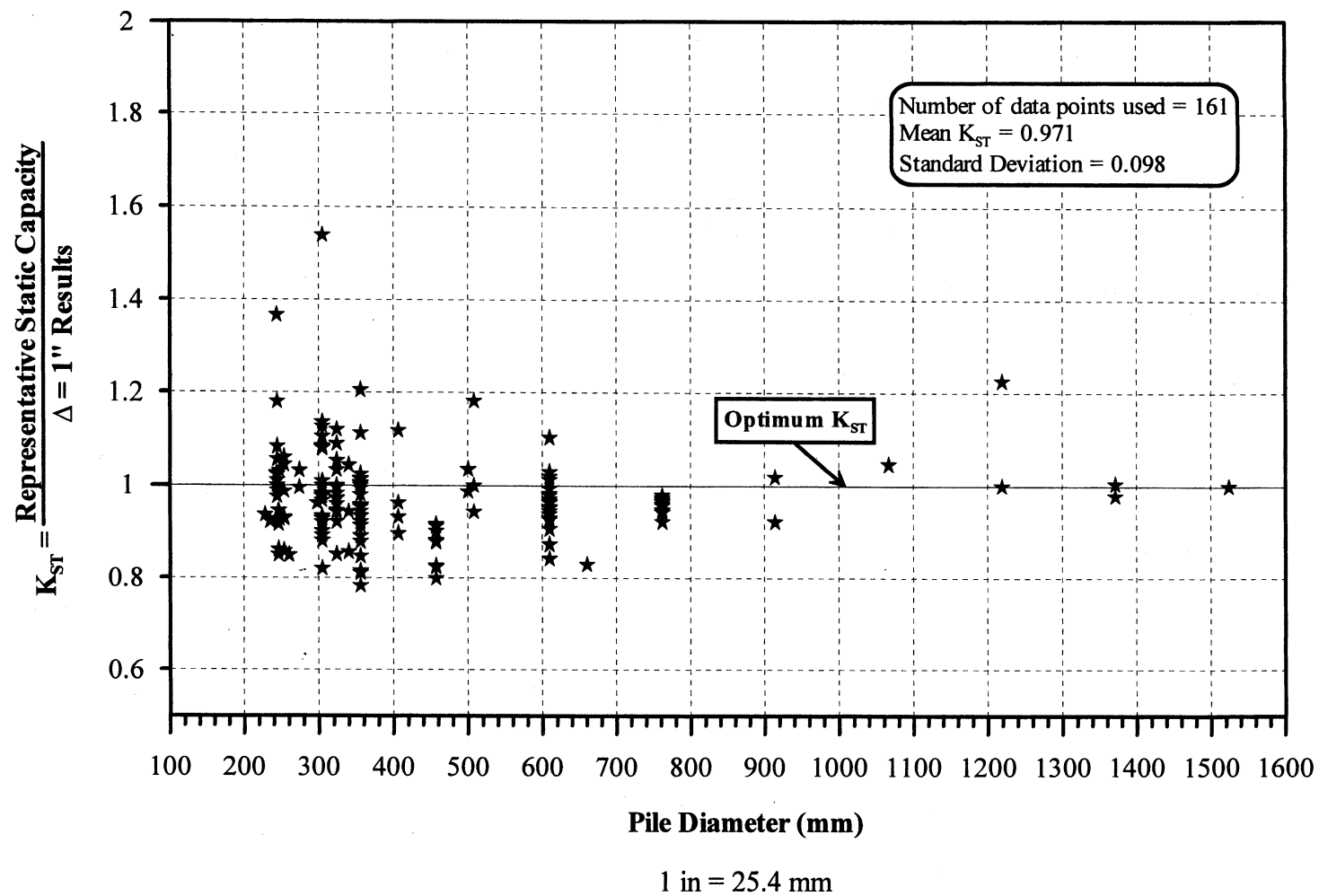


**Figure 4.10.**  $K_{ST}$  values vs. Pile Diameter for all PD/LT2000 pile-cases, all types of soils.

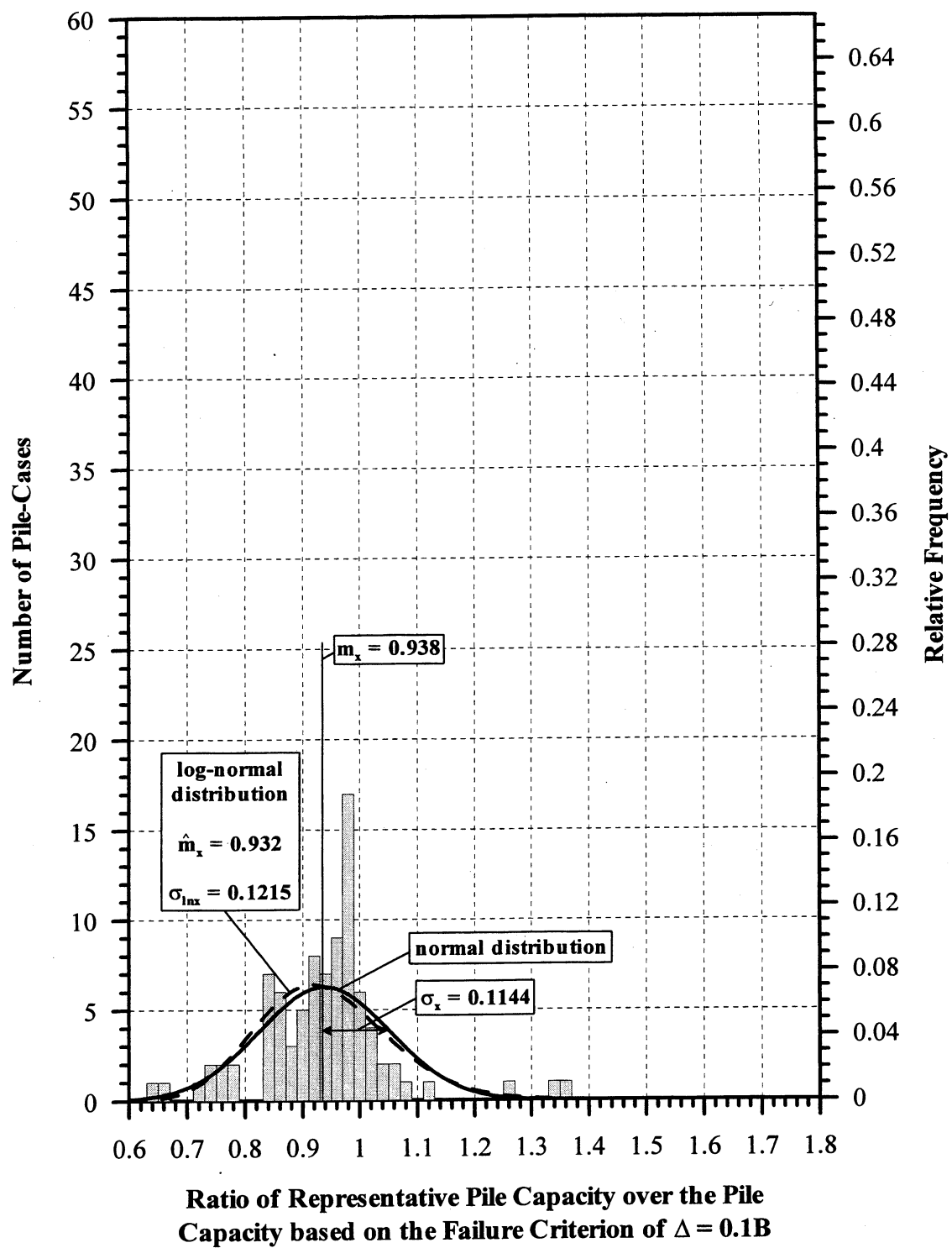


**Figure 4.11.** Histogram and frequency distributions of  $K_{SL}$  for 90 PD/LT2000 pile-cases in all types of soils.

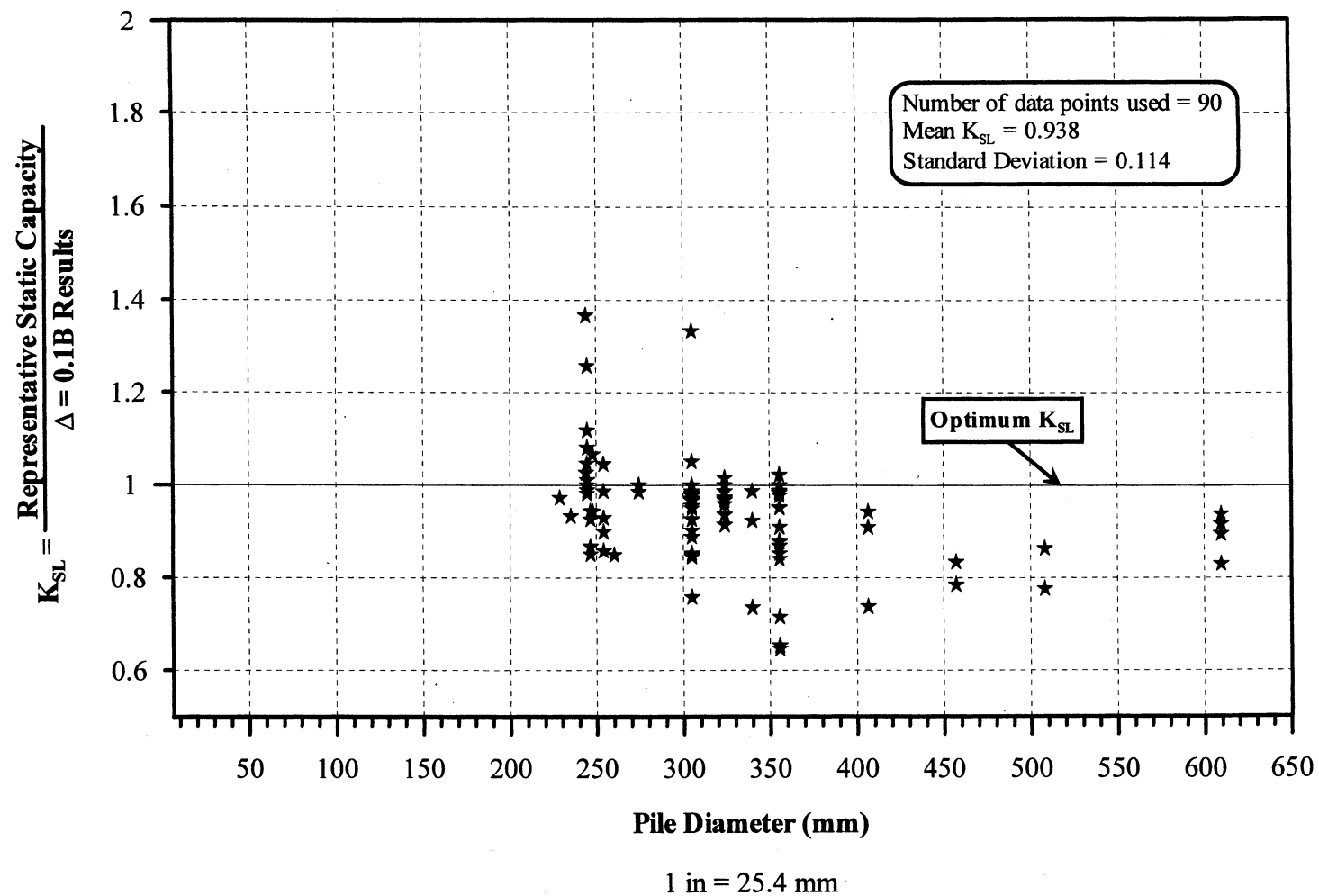


**Figure 4.12.**  $K_{SL}$  values vs. Pile Diameter for all PD/LT2000 pile-cases, all types of soils.

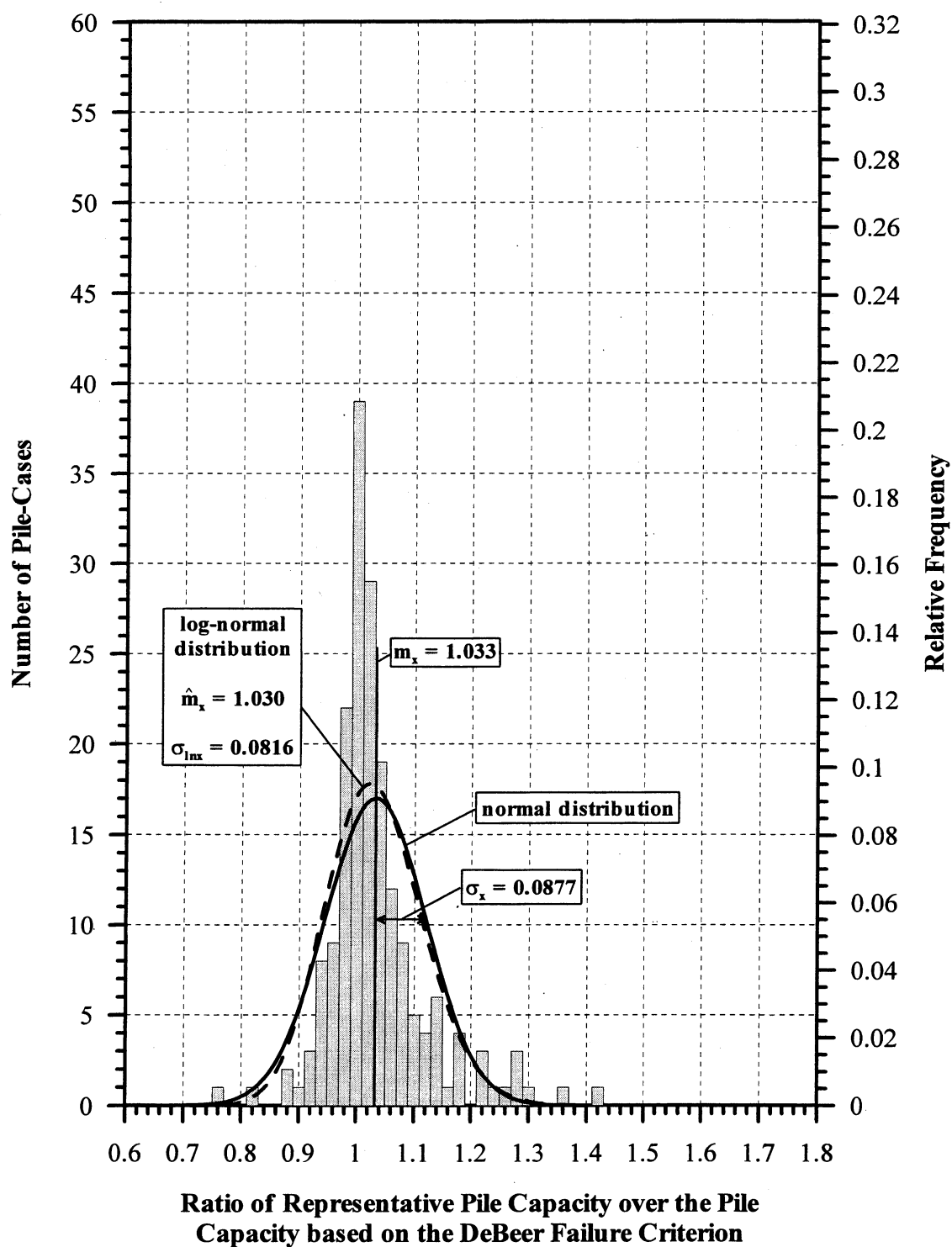


**Figure 4.13.** Histogram and frequency distributions of  $K_{SB}$  for 187 PD/LT2000 pile-cases in all types of soils.

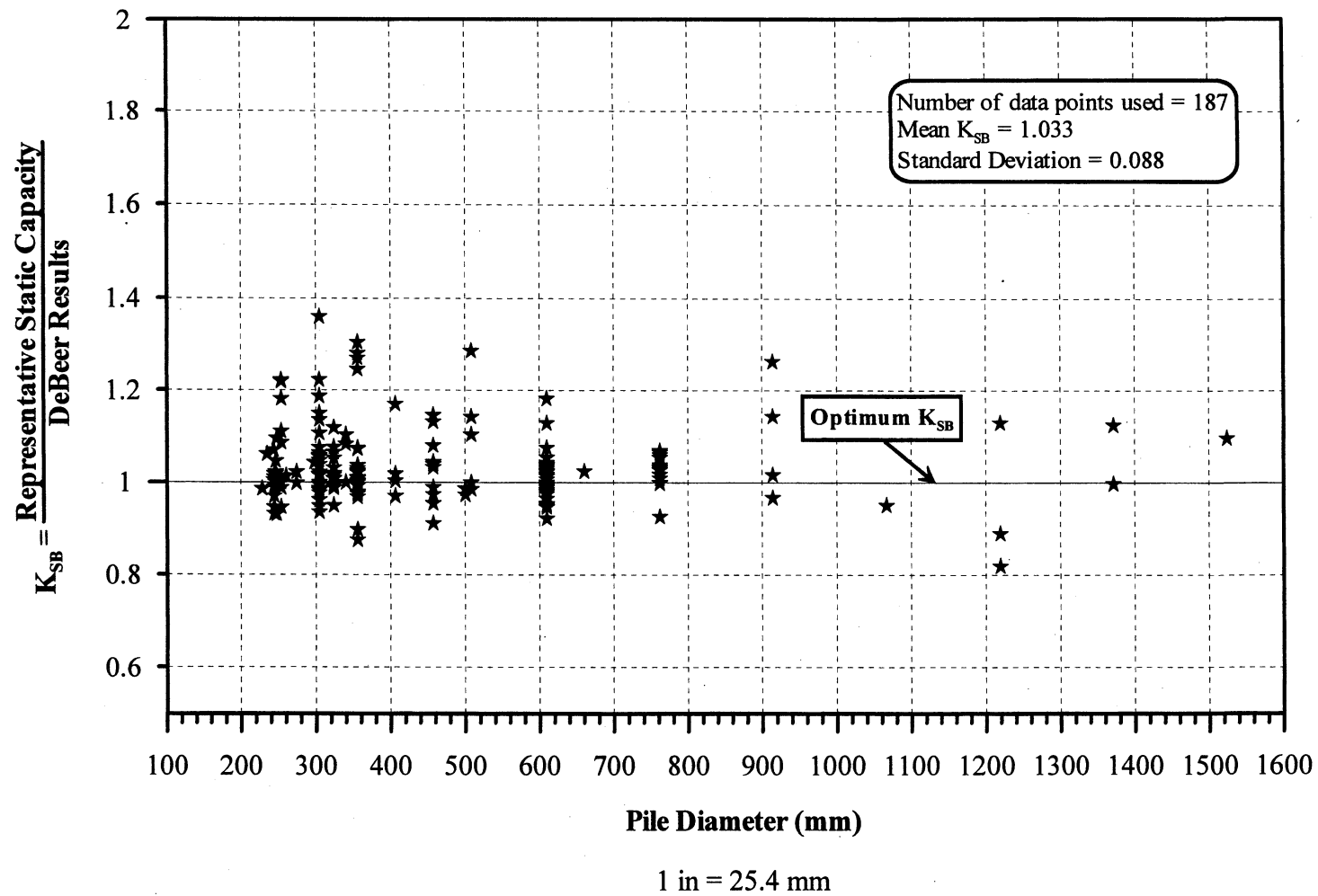


**Figure 4.14.**  $K_{SB}$  values vs. Pile Diameter for all PD/LT2000 pile-cases, all types of soils.

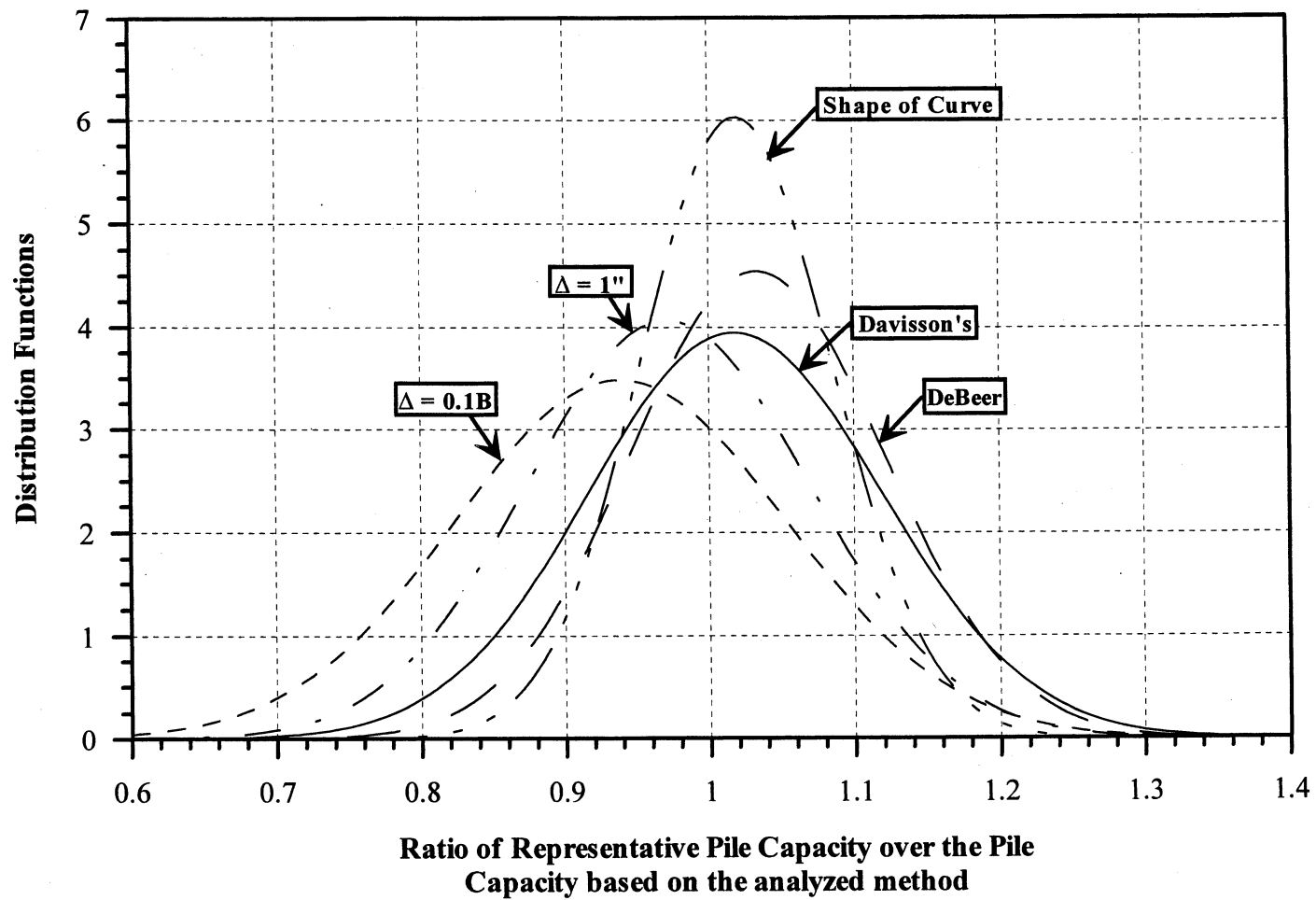
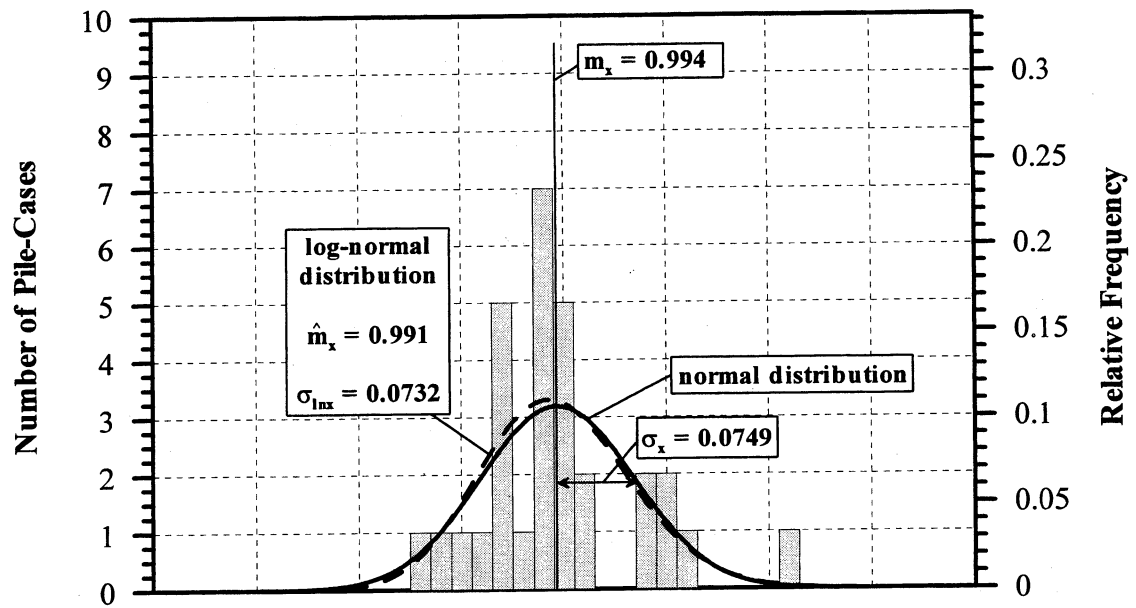
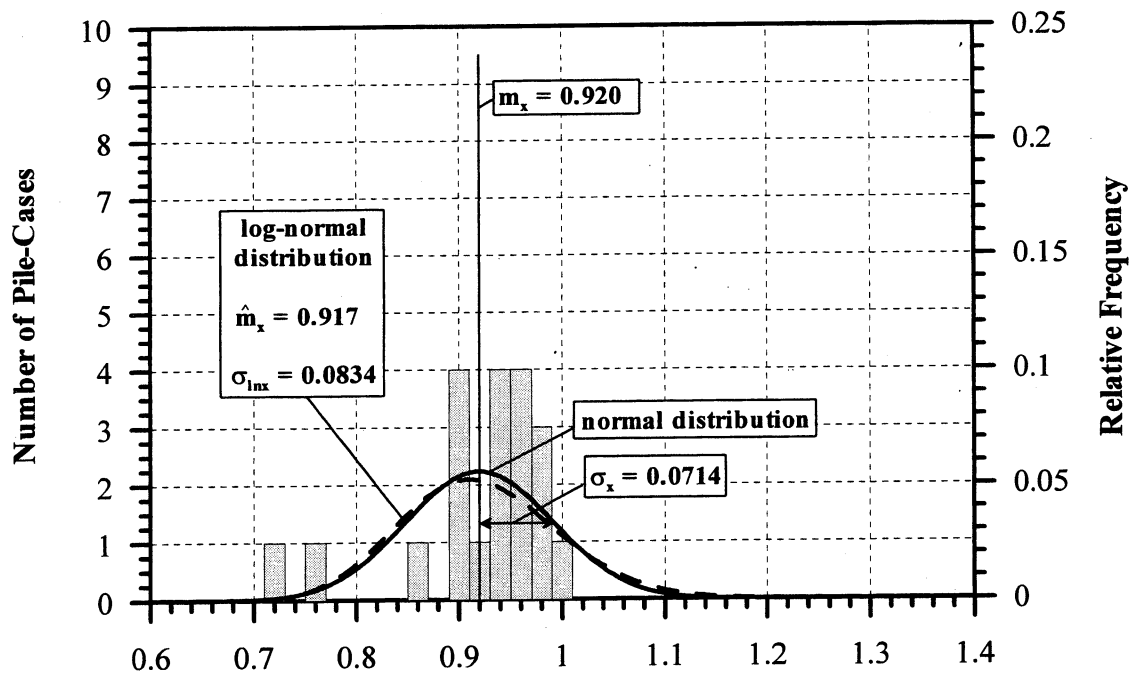


**Figure 4.15.** Distribution Function Curves for the Five methods used for analysis of Static Load Test Curves based on 196 piles from PD/LT2000.





Ratio of Representative Pile Capacity over the Pile Capacity based on Davisson's Failure Criterion with offset  $X = 3.81 + B/120$ ,  $K_{SD}$



Ratio of Representative Pile Capacity over the Pile Capacity based on Davisson's Failure Criterion with offset  $X = B/30$ ,  $K_{SLD}$

**Figure 4.16.** Histogram and frequency distributions of  $K_{SD}$  and  $K_{SLD}$  for 30 and 20 PD/LT2000 pile-cases, respectively, in all types of soils.

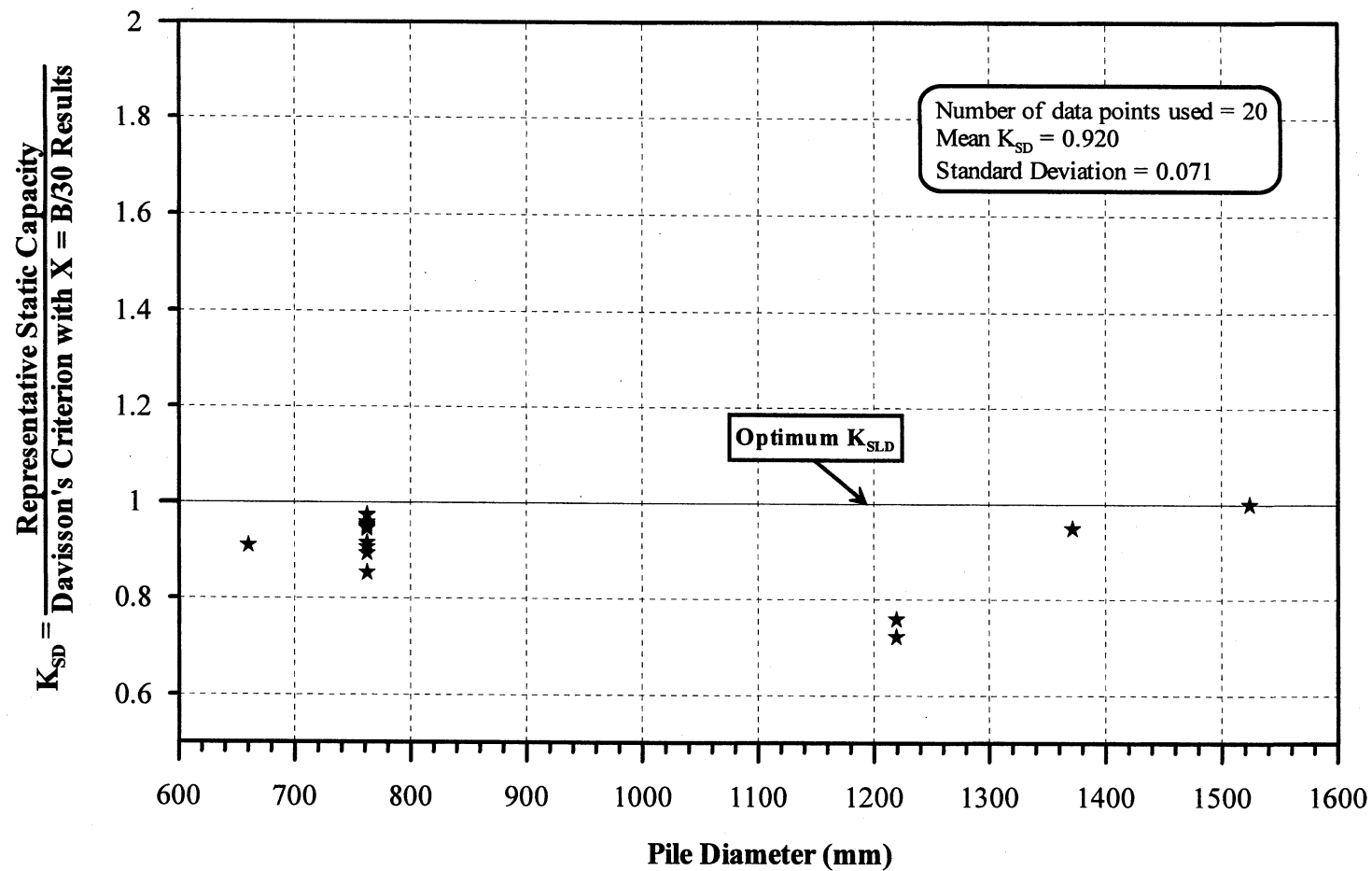


**Figure 4.17.**  $K_{SLD}$  values vs. Pile Diameter for all large diameter PD/LT2000 pile-cases, all types of soils.

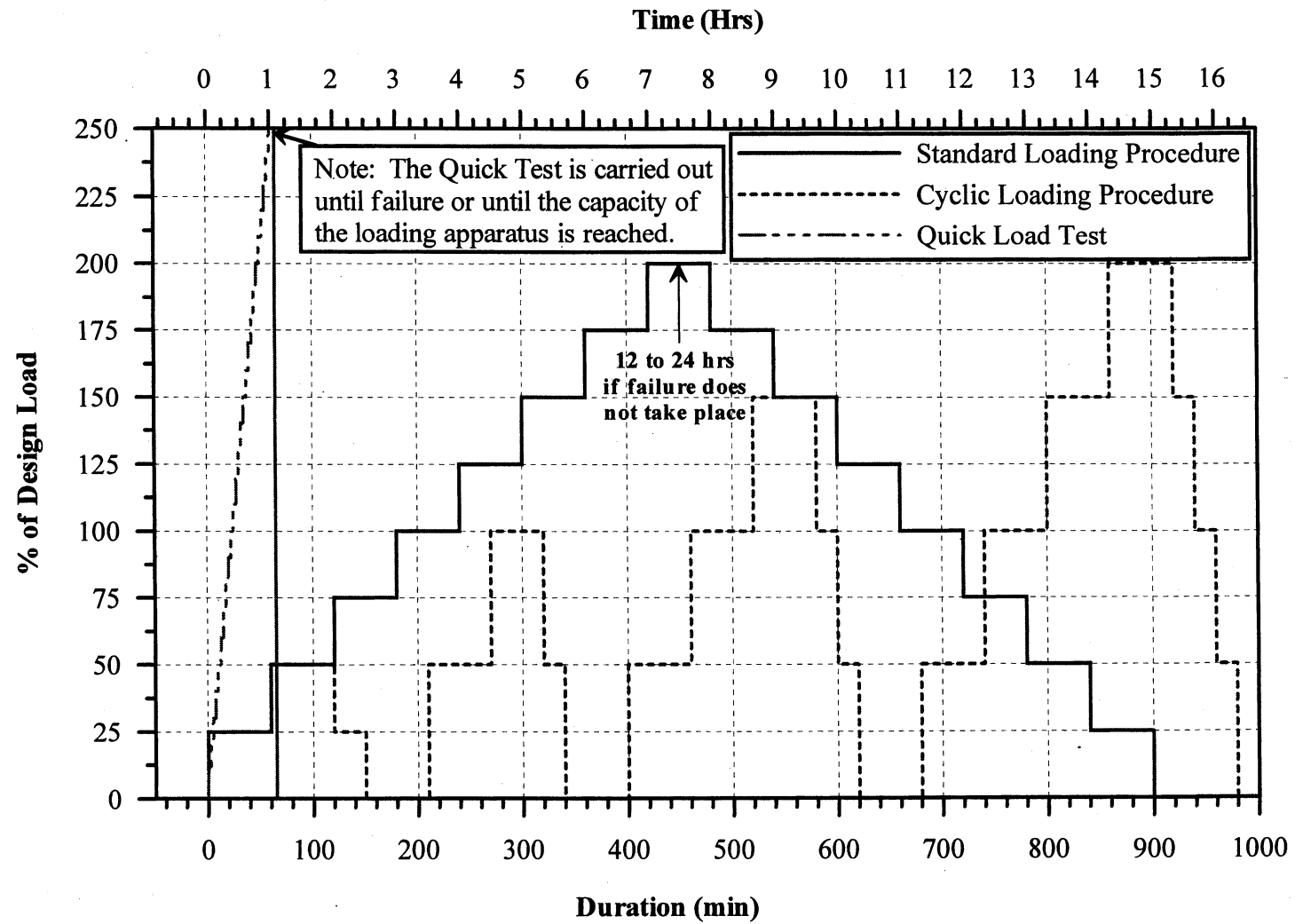


**Figure 4.18.** Static Pile Load Testing Procedures According to ASTM (after Paikowsky et al., 1999)

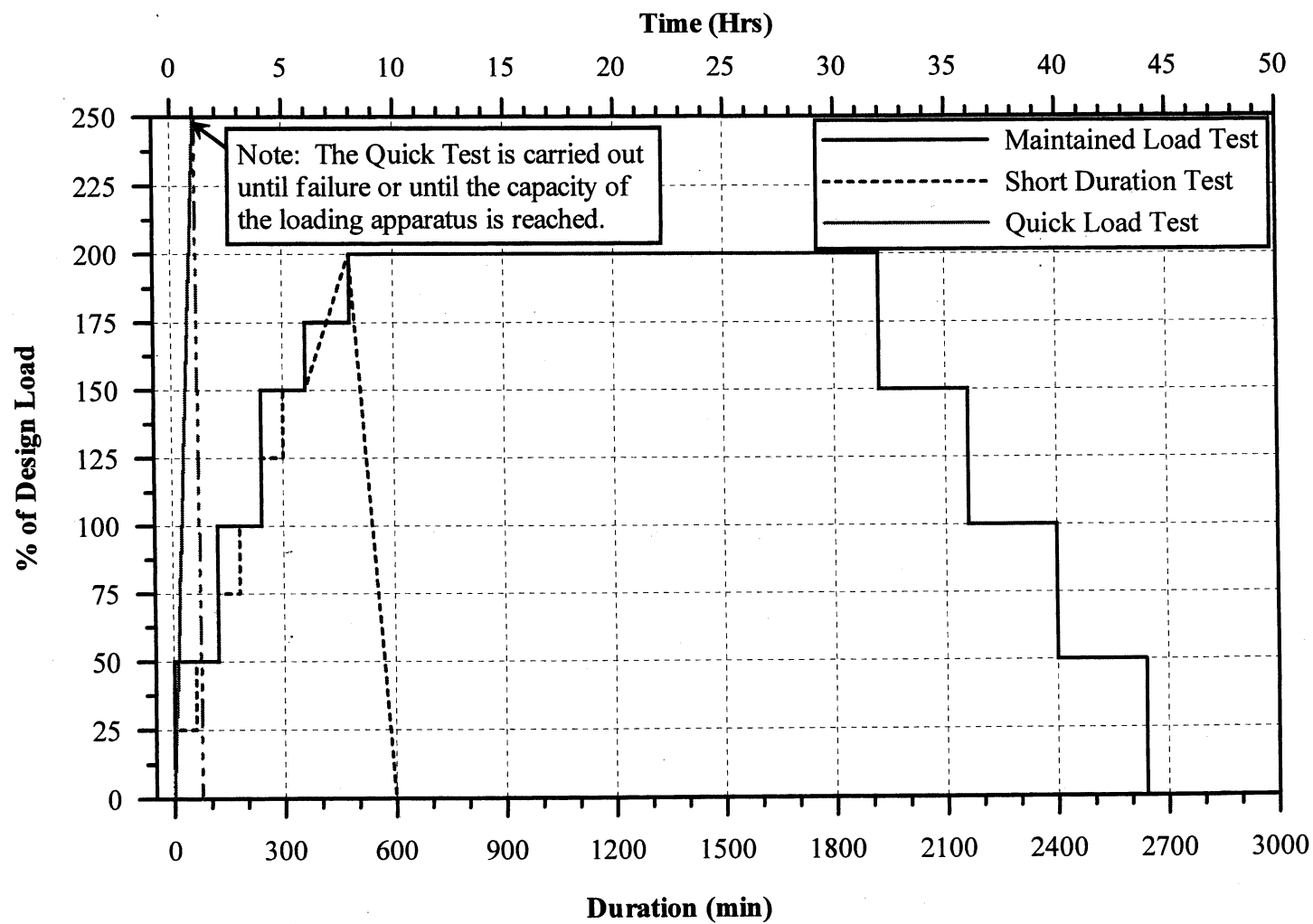


**Figure 4.19.** Static Pile Load Testing Procedures According to MHD (after Paikosky et al., 1999)

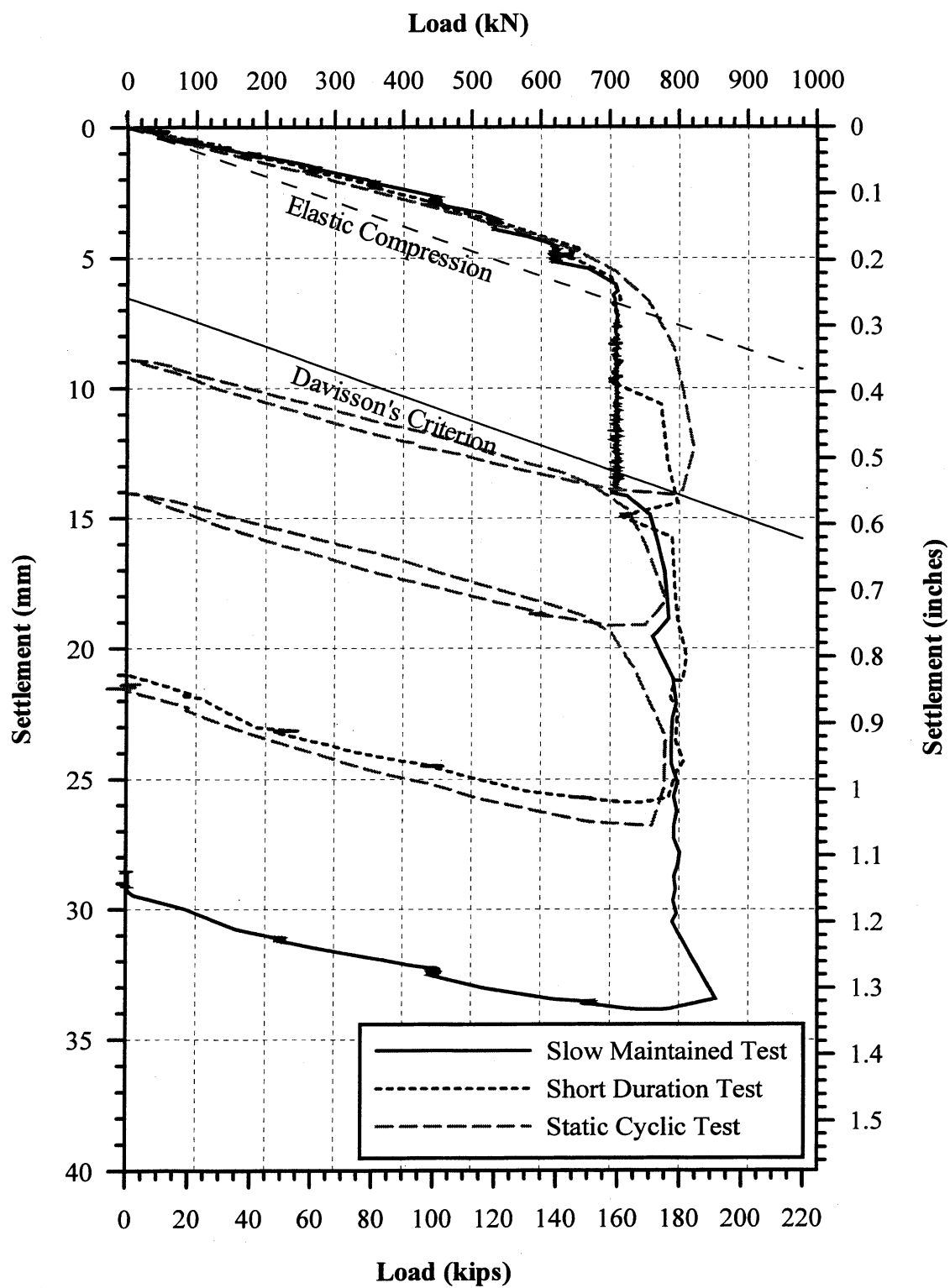


**Figure 4.20.** Comparison of the Short Duration, Slow Maintained and Static Cyclic Load Tests for Test Pile # 2 at the Newbury Site (after Paikowsky et al., 1999).

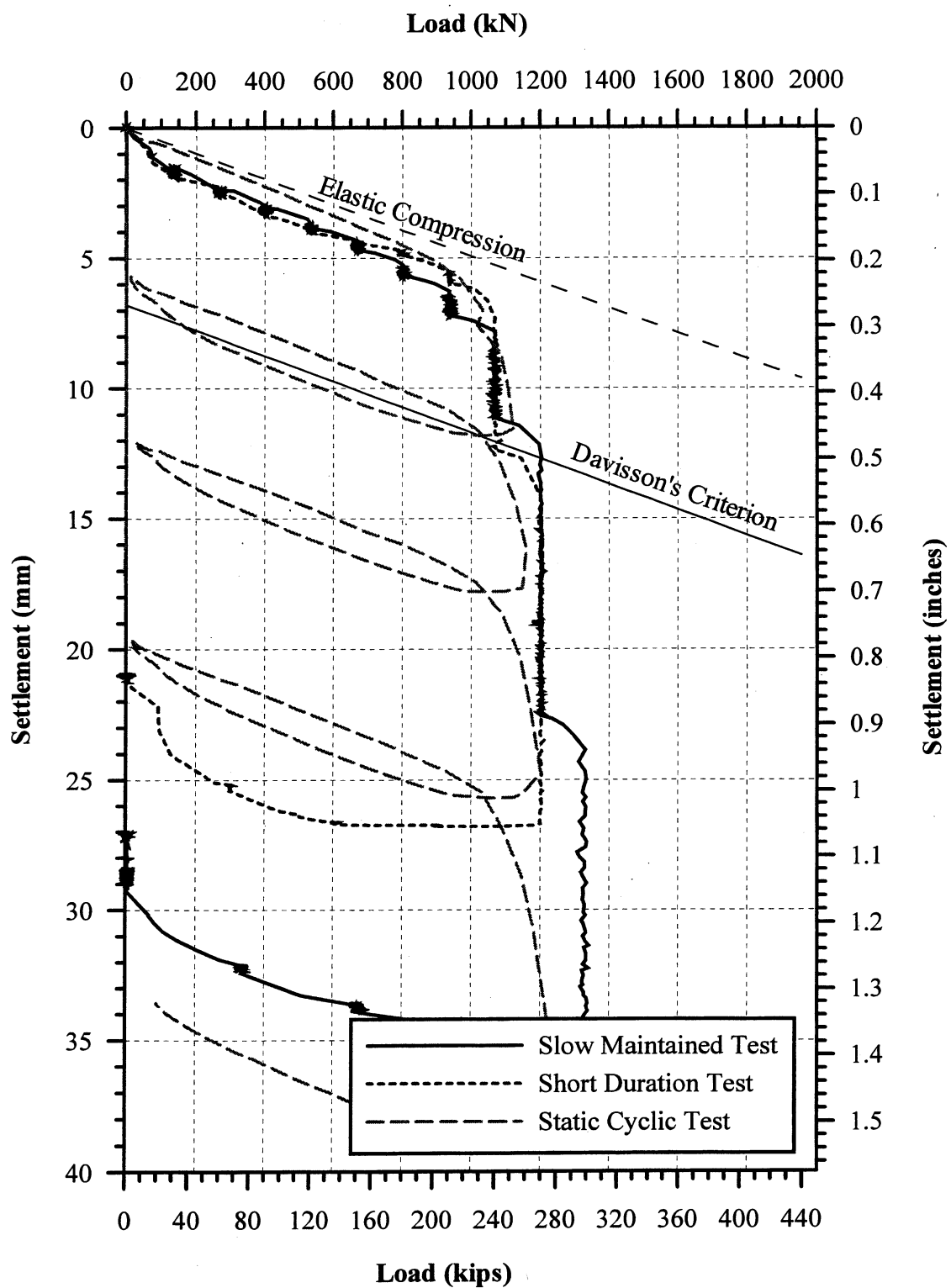


**Figure 4.21.** Comparison of the Short Duration, Slow Maintained and Static Cyclic Load Tests for Test Pile # 3 at the Newbury Site (after Paikowsky et al., 1999).

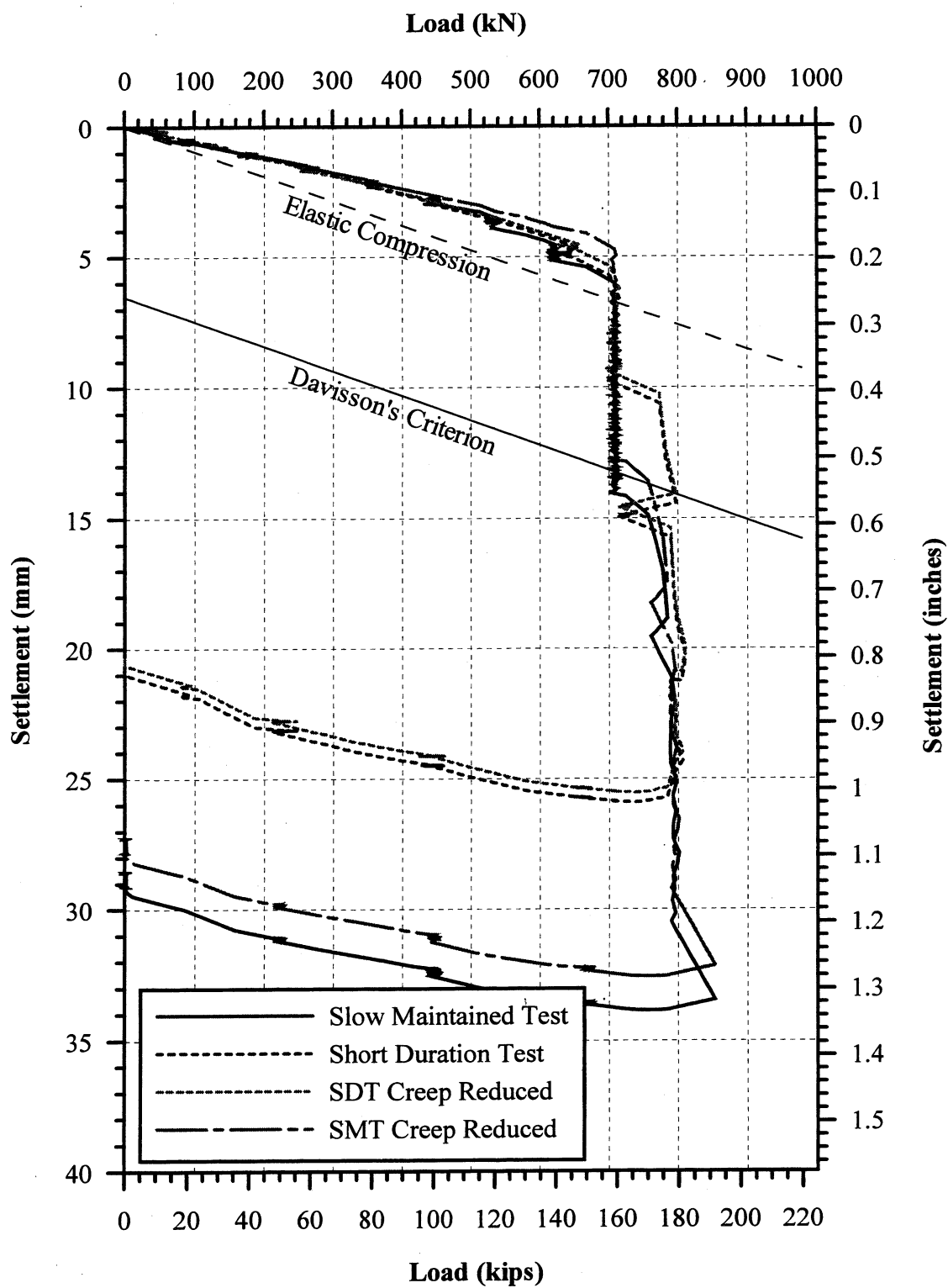


**Figure 4.22.** Comparison of the Short Duration and Slow Maintained Static Load Tests, Reduced for Creep, for Test Pile # 2 at the Newbury Site.

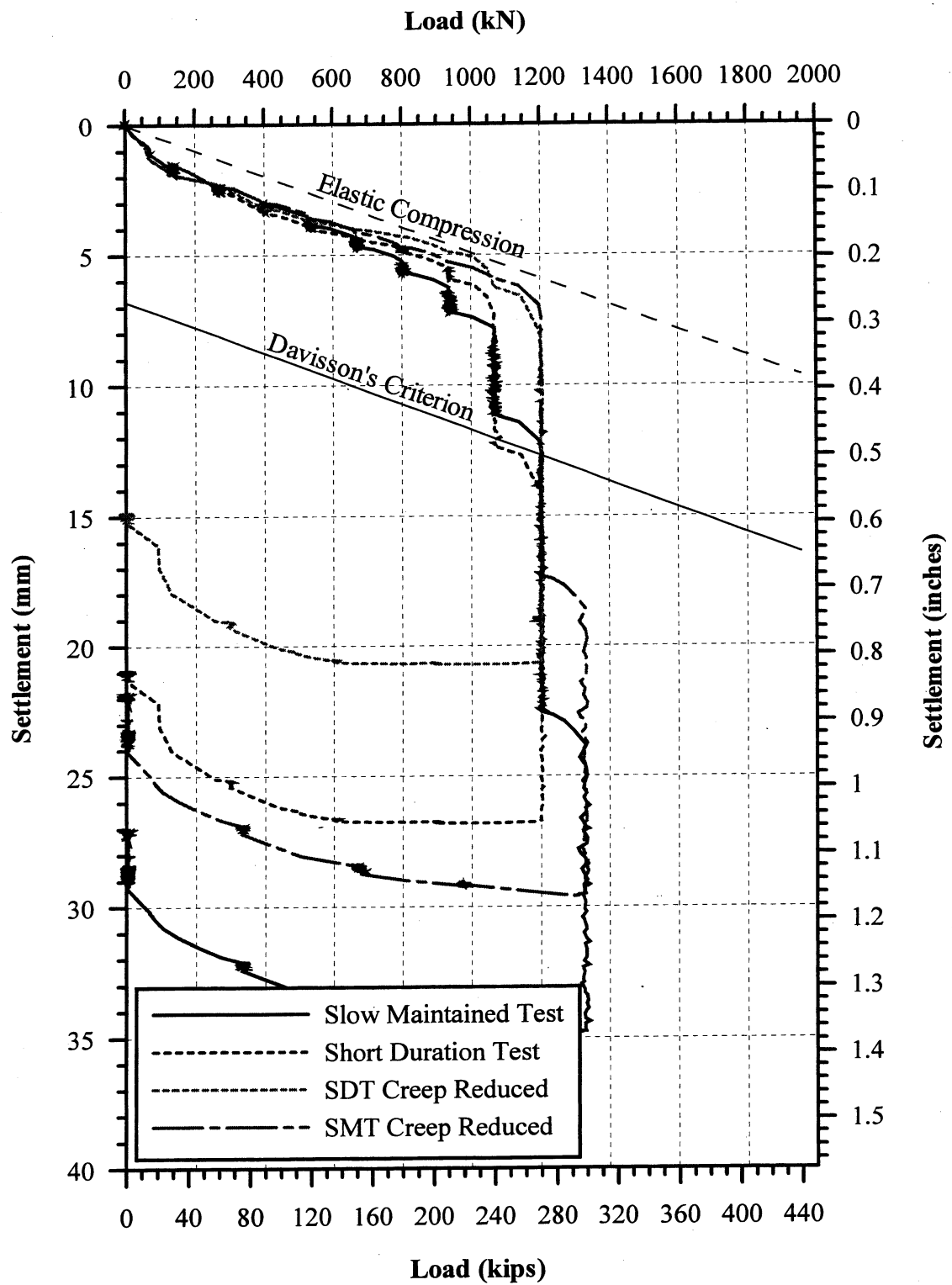
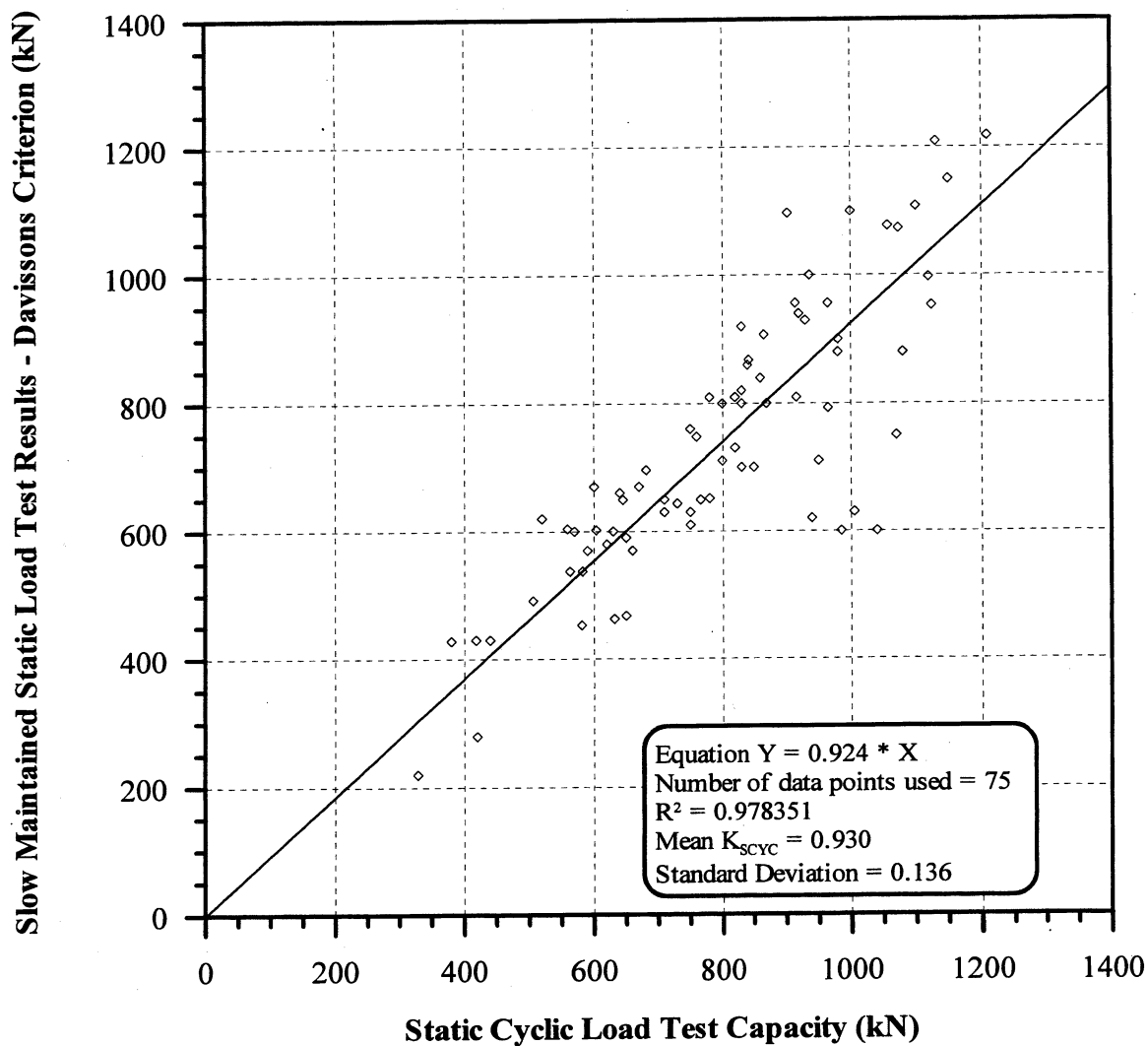


**Figure 4.23.** Comparison of the Short Duration and Slow Maintained Static Load Tests, Reduced for Creep, for Test Pile # 3 at the Newbury Site.





1 kN = 0.2248 kips

**Figure 4.24.** Davisson Capacity vs. Static Cyclic Load Test Capacity for 75 pile-cases from the UMass Lowell / Ukraine Database (after Paikowsky et al., 1999).

## **CHAPTER 5**

### **CONTROLLING PARAMETERS OF THE DYNAMIC METHODS**

#### **5.1 OVERVIEW**

The performance of the dynamic methods has been assumed to depend on the type of soil (cohesive or cohesionless) the pile is driven into, the time of driving (End of Driving - EOD or Beginning of Restrike - BOR), and the soil inertia effects (type of pile and difficulty of driving). The controlling effect of each these parameters on the dynamic predictions vary for each pile-case. In this chapter the parameters will be analyzed using the data from PD/LT2000 in an attempt to determine the significance of each parameter. The performance of the dynamic methods can then be evaluated according to the controlling parameters.

#### **5.2 METHOD OF APPROACH**

##### **5.2.1 General**

The first parameter to be analyzed is the effect of the soil type on the accuracy of the dynamic prediction. This factor has been traditionally assumed to be a major controlling parameter on the accuracy of the dynamic methods. The second controlling parameter to be evaluated is the time of driving. When a dynamic test is completed at the EOD no time has been given to allow for pile setup (freeze effects) to take place, hence, the pile resistance at the time of the measurement differs from that

exhibited at the time of a static load test. If a dynamic test is conducted, during a restrike, generally, a reasonable amount of time after driving has passed and the freeze effects are accounted for. The final parameter that is analyzed is that of the soil inertia effects. In this category are the effects contributing to the soil motion, i.e., the type of pile (small or large displacement) and the driving resistance (easy or hard driving). The analysis in this chapter will evaluate the soil inertia effect and will determine what constitutes a small vs. large displacement pile and hard vs. easy driving.

### **5.2.2 Nomenclature**

The nomenclature that is used throughout this manuscript and extensively in this chapter is based on a method we will label the XXX method. The first letter denotes the pile type, where A = all piles, L = large displacement piles and S = small displacement piles. The second letter denotes the time at which the dynamic measurements were taken, A = all times, E = End Of Driving (EOD) and B = Beginning Of Restrike (BOR). The third letter denotes the soil type along the side of the pile, where A = all soils, S = sand and silt, C = clay and till and R = rock. As an example, pile-cases labeled LES are large displacement piles with dynamic measurements taken at the EOD where the pile was driven into a sand and silt material or AAA would be all types of piles at all times of driving in all types of soils.

### **5.2.3 Interpretation of Statistical Results**

The relationship between the predicted static pile capacity and the actual measured static pile capacity (based on Davisson's criterion from the load-settlement test curves) is presented as a scatter-gram of the two values. The best-fit line (forced

through the origin) was plotted on each of the graphs comparing the actual and predicted static pile capacity. The best-fit line was forced through the origin of the axes as the predicted pile capacity is expected to be zero when the actual capacity is zero. The coefficient of determination values ( $r^2$ ) were found to be only slightly affected (lower) due to the forced best-fit line through zero, compared to those passing through the y-intercept (Paikowsky et al., 1994).

The following review of the coefficient of determination follows that presented by Paikowsky et al., (1994). The coefficient of determination ( $r^2$ ) represents the proportion of the sum of squares of deviations of the y-values about their mean, and it is a measure of the contribution of "x" in prediction "y". By definition, a scatter at higher x-values will influence this coefficient more than a scatter close to the origin of axes. The coefficient of determination varies between 0 and 1; the first indicating no correlation or contribution and the last ( $r^2 = 1$ ) is a perfect match where all the points fall on the best-fit, least-squares line. For example,  $r^2 = 0.6$  means that 60 percent of the sum of squares of deviations of the observed y-values about their mean is attributed to the linear relations between y and x (actual vs. predicted). In other words, 60 percent of the variability in y is explained by the regression equation. According to Ryan (1989), a meaningful correlation is obtained with  $r^2 \geq 0.80$ , which coincides with  $p \leq 0.0011$ ; p is the probability of obtaining an F-value as or larger than the calculated value. This value of  $r^2 = 0.80$  may be rigorous relative to correlations in geotechnical engineering. The results, therefore, may be reviewed in the following ranges (Veneziano, 1993):

$r^2 \geq 0.80$	good correlation
$0.60 \leq r^2 < 0.80$	moderate correlation
$r^2 < 0.60$	poor correlation

A second parameter that can be used to determine whether there is a good or poor correlation between data is the coefficient of variation (COV), which was defined in section 2.2.4b as the ratio of the standard deviation over the mean. Based on previous geotechnical experience the results will be reviewed in the following ranges:

$COV < 0.30$	very good correlation
$0.30 \leq COV < 0.45$	good correlation
$0.45 \leq COV < 0.60$	moderate correlation
$COV \geq 0.60$	poor correlation

### **5.3 THE CONTROLLING PARAMETERS**

#### **5.3.1 Soil Type**

##### ***a) General***

The soil type sub-groupings are based on a research report submitted to the Federal Highway Department by Paikowsky et al., 1994. The soil groupings, which refer to the soil type along the side of the pile, are as follows; clay and till, sand and silt, and rock. During the soil type analysis the question arose whether the soil groupings should not follow a more conventional sub-grouping of cohesive soils, non-cohesive soils and rock. This would lead to the sub-groupings of sand and gravel, clay and silt, and till and rock. The analysis was done comparing both sets of sub-groupings and it was found that no matter what the soil groupings were the effect of soil type on the dynamic predictions is minimal. The analysis was therefore continued using the original soil sub-groupings.

The figures used in evaluating the effect of the soil type on the performance of the dynamic predictions present the data sub-grouped according to small and large displacement piles. This is based on the definition of small displacement piles being H-piles and open-ended pipe piles (OEP) and large displacement piles being categorized as all piles that are not H-piles or OEP piles.

Figures 5.1 and 5.2 show the relationship between the static load test results compared to the CAPWAP/TEPWAP predictions and the Energy Approach predictions, respectively. The data shown are sub-grouped into soil types and type of pile as described above. Based on the  $r^2$  values of 0.542 and 0.521 the figures show that there is a poor correlation between the static load test results and the CAPWAP/TEPWAP predictions or Energy Approach predictions for both types of piles in all types of soils. The poor correlation is also shown by the large amount of scatter in both figures. To further analyze the effect of the soil types each sub-grouping was plotted separately to better see if there is any relationship between the static load test results and the dynamically predicted results.

***b) Sand and Silt***

Figure 5.3 presents a comparison between the static load test results and the CAPWAP/TEPWAP predictions. The  $r^2$  value of 0.679 for the best-fit line forced through zero shows that a moderate correlation exists between the actual and predicted pile capacities for piles that are embedded into sand and silt. A poor correlation is shown by the COV of 0.715. The change in the mean and standard deviation is minimal when compared to the mean and standard deviation for all soil types ( $1.452 \pm$

0.985 for all cases compared to  $1.517 \pm 1.085$  for cases in sand and silt). The best-fit line forced through zero shows an under-prediction ratio of 1.260 for pile-cases in sand and silt compared to 1.161 for all pile-cases. There are some cases where CAPWAP/TEPWAP under-predicts the pile capacity by as much as 90 percent, which is an under-prediction ratio of 10.

A correlation between the static load test results and the Energy Approach predictions are shown in Figure 5.4. As is shown in the figure there is a significant amount of scatter, which is also shown by the  $r^2$  value of 0.879, which shows a poor correlation between the actual and predicted results based on the sub-grouping by soil type to sand and silt. The COV of 0.518 shows a moderate correlation between the actual and predicted values. The mean and standard deviation ( $0.968 \pm 0.501$ ) has not changed significantly from that shown for all soil types in Figure 5.2 ( $0.936 \pm 0.485$ ). The graph shows that the Energy Approach over-predicts the actual static capacity of the pile by an over-prediction ratio of 0.790, this is the slope of the best-fit line forced through zero. There is no significant change here, either, from the over-prediction ratio for all cases in all types of soils. The majority of the data points do fall within the ratios of 0.40 to 2.50 (load test results over the prediction). The scatter is still fairly large and has not changed significantly from that shown in Figure 5.2 for all of the Energy Approach predictions in all types of soils.

**c) *Clay and Till***

The data shown in Figure 5.5 is a comparison between the static load test results and the CAPWAP/TEPWAP predictions for those piles embedded in clay and

till. The figure shows a poor correlation between the actual and predicted results based on the  $r^2$  value of 0.141, while based on the COV of 0.535 there is a moderate correlation. The mean and standard deviation for the piles in clay and till ( $1.352 \pm 0.723$ ) has not notably changed from that for all the piles in all types of soils ( $1.452 \pm 0.985$ ). The under-prediction ratio changed slightly from that for all the piles in all types of soils (0.988 from 1.161) but the change is insignificant when evaluating the soil types as a controlling parameter. The majority of the extreme cases where CAPWAP or TEPWAP under-predicted the pile's capacity do not fall into the category of piles in clay and till.

Figure 5.6 shows the comparison between the static load test results and the Energy Approach predictions. A poor correlation exists between the load test results and the predicted results based on the  $r^2$  value of 0.320 and a moderate correlation exists based on the COV of 0.527. The mean, 0.873, and standard deviation, 0.460, for the piles which are embedded in clay and till has not changed considerably from the mean, 0.936, and standard deviation, 0.485, for all piles embedded in all types of soils. The figure does show that there is a slight decrease in the over-prediction ratio for the piles that are in clay from the piles that are in all types of soils; the ratio decreases from 0.744 to 0.660. The upper end of the ratios, load test results over the predictions, meaning the amount that the method under-predicts, did decrease from 2.50 to 1.67.



**d)      *Rock***

The results that are presented in this section show a significant increase in the performance of each of the dynamic analysis methods, the CAPWAP/TEPWAP and the Energy Approach methods. It should be noted that there is a significant less number of pile-cases for which the piles are embedded in rock compared to the number of piles that are embedded into sand and silt and clay and till. The small number of pile-cases accounts for the increased performance as well as the fact that with the exception of one pile all 15 have a driving resistance that is greater 16 BP10cm and two thirds of the piles have area ratios greater than 350. These two parameters are determined to have a significant effect on the performance of the dynamic methods and are discussed later in this chapter.

Figure 5.7 shows the comparison between the static load test results and the CAPWAP/TEPWAP predictions, there is a good correlation between the actual and the predicted results as the mean and standard deviation have decreased from  $1.452 \pm 0.985$  for all piles in all types of soils to  $0.930 \pm 0.172$  for those piles embedded in rock. The  $r^2$  value of 0.790 shows that there is a moderate to good correlation between the actual and predicted pile capacities, while the COV of 0.185 shows a very good correlation between the data. The mean over-prediction ratio is 0.879, which has changed from an under-prediction ratio of 1.161 for all pile-cases. All of the data points fall within a fairly narrow band of ratios (load test results over the predictions); the ratios range from approximately 0.60 to 1.25 showing that there is minimal scatter when comparing the actual and predicted results for piles that are embedded in rock.

Presented in Figure 5.8 is the comparison between the static load test results and the Energy Approach predictions for all pile-cases that are embedded in rock. As is shown the Energy Approach method also performs very well for piles that are embedded in rock with a mean of 0.744 and a standard deviation of 0.154; this is a decrease from a mean of 0.936 and a standard deviation of 0.485 for all pile-cases in all types of soils. The over-prediction ratio has also decreased from 0.744 for piles in all types of soils to 0.620 for piles that are driven into rock. Again as seen in the figure the data points fall with a narrow range of ratios (load test results over the predictions); the range is from an over-prediction ratio of 0.40 to 1.00.

***e) Intermediate Conclusions***

Tables 5.1 and 5.2 summarize the statistical data for the sub-groupings according to soil types for the wave matching methods (CAPWAP/TEPWAP predictions) and the field evaluation method (Energy Approach predictions), respectively. The tables also present a summary of the statistics for the sub-groupings by time of driving and the driving resistance. The above analyses show that the soil type does not have a significant effect on the results of the dynamic analyses excluding the small pile group that are driven into rock. Later in this chapter it will be seen that the soil inertia effects (the driving resistance of the pile and the type of pile that is driven) control the performance of the dynamic methods in rock and not necessarily just the fact that the pile is driven into rock.

### 5.3.2 Time of Driving

The time of driving (EOD versus BOR) has a significant effect on the results of the dynamic analyses. This section does not detail the effect of the time of driving on each one of the dynamic methods, but establishes the need for the time of driving to be considered in any further analyses that are done. As shown in Tables 5.1 and 5.2 the statistics for the CAPWAP/TEPWAP and Energy Approach predictions drastically improve from the end of driving cases to the beginning of restrike cases. To further evaluate the effect of time of driving on the performance of the dynamic methods, the wave matching predictions and the Energy Approach predictions will be compared to the static load test results for both EOD and BOR cases.

The wave matching predictions (CAPWAP/TEPWAP) are shown in Figure 5.9 compared to the static load test results for all pile-cases with the exception of the 5 extreme pile-cases (refer to section 6.3.1 for explanation). The mean and standard deviation of the ratio of the static load test results to the CAPWAP/TEPWAP predictions are 1.368 and 0.620, respectively. The wave matching predictions under predict the pile capacity by a mean ratio (load test results over the prediction) of 1.160.

Figures 5.10 and 5.11 present the CAPWAP/TEPWAP predictions compared to the static load test results for the end of driving and beginning of restrike pile-cases, respectively. A comparison between the means and standard deviations for all cases, the EOD cases and the BOR (last) pile-cases reveals that the time of driving has a major influence on the performance of the CAPWAP/TEPWAP methods. The mean for the EOD pile-cases is 1.626 with a standard deviation of 0.797 while the mean for

the BOR (last) pile-cases is 1.158 with a standard deviation of 0.393. The BOR (last) pile-cases have a significant less amount of scatter compared to all of the pile-cases and the EOD pile-cases. The under-prediction ratio decreases from 1.284 for the EOD pile-cases to 1.104 for the BOR (last) pile-cases. The above statistics and analysis of the wave matching methods reveals that any further analysis that is completed should take into consideration the time of driving.

Figure 5.12 presents a comparison of the static load test results and the Energy Approach predictions for all pile-cases, with the exception of the 7 extreme pile-cases (refer to section 6.3.1 for details), at all driving times. The mean and standard deviation all pile-cases is 0.894 and 0.367, respectively. The scatter is fairly significant ( $r^2 = 0.542$ ) and the ratios (load test results over the predictions) range from approximately 0.40 and 2.50. The Energy Approach over-predicts the pile capacity by an average ratio of 0.743, which is the slope of the best-fit line through zero.

Presented in Figures 5.13 and 5.14 are the graphs comparing the static load test results and the Energy Approach predictions for the EOD and BOR (last) pile-cases. A comparison between the statistics for all pile-cases, the EOD pile-cases, and the BOR (last) pile-cases shows that there is a significant improvement from the EOD pile-cases to BOR (last) pile-cases. The mean for the EOD pile-cases is 1.084 with a standard deviation of 0.431, while the mean for the BOR (last) piles-cases is 0.785 with a standard deviation of 0.290. The scatter improves slightly for the BOR (last) pile-cases from the EOD pile-cases. The range of ratios (load test results over the predictions) for the BOR (last) pile-cases is 0.40 to 1.67 while for the EOD pile-cases

the range is from 0.40 to 2.50. The mean over-prediction for the EOD pile-cases is 0.926 while for the BOR (last) pile-cases it is 0.695, this shows that for the BOR (last) pile-cases the Energy Approach over-predicts by a significant amount but it consistently over-predicts so it can be corrected with a multiplying factor. The statistics for the Energy Approach also show that any further analysis that is completed needs to take into consideration the effects of the time of driving. The time of driving effects are not as obvious for the Energy Approach predictions as for the CAPWAP/TEPWAP predictions.

Table 5.3 summarizes the statistics of the data that were presented in Figures 5.9 through 5.14 for the comparison of the static load test results and the CAPWAP/TEPWAP predictions as well as the Energy Approach predictions. Based on these statistics it can be seen that the time of driving has a major influence on the performance of the dynamic methods and needs to be considered in any further analysis.

### **5.3.3 Soil Inertia Effects**

#### ***a) Overview***

Paikowsky and Chernauskas (1996) had shown that the stationary soil assumption, under which the soil/pile interaction models were developed, does not reflect the physical phenomenon that occurs during pile driving. The use of pseudo viscous damping serves as a mechanism to absorb energy, but, as it does not reflect the actual phenomenon, its correlation to physical properties (e.g. soil type) or time of driving cannot be achieved. If the motion of the displaced soil is a major factor

contributing to the energy loss during driving, a substantial portion of the dynamic resistance should be a function of two parameters: (i) mass/volume of the displaced soil that is a function of the pile geometry, namely, small vs. large displacement piles, and (ii) acceleration of the displaced soil, (especially at the tip) that can be conveniently examined as a function of the driving resistance (Paikowsky and Stenersen, 2000).

The soil inertia effects consist of the driving resistance of the pile, hard or easy driving, and the type of pile that is used, small or large displacement. This section will first show the controlling effect of the driving resistance and then present the method used to determine the dividing point between hard and easy driving.

Through analysis previously done by Paikowsky et al. 1994 it was determined that small and large displacement piles are not defined only by the type of pile (e.g. H-piles and OEP piles are small displacement) but rather they are defined by the area ratio. The area ratio is defined by Paikowsky et al., 1994, as follows:

$$A_R = \frac{A_{\text{skin}}}{A_{\text{tip}}} = \frac{\text{Surface area in contact with the soil}}{\text{Area of the pile tip}} \quad (5.1)$$

Paikowsky et al. (1994) proposed that piles that have an area ratio above 350 are small displacement piles and piles with an area ratio less than 350 are classified as large displacement piles. The controlling effect of the type of pile driven will be shown in this section, as well as a statistical analysis used to verify the area ratio boundary between small and large displacement piles.

***b) Effect of Driving Resistance***

The initial analysis in this section shows that there is a controlling effect due to driving resistance. The initial boundary between hard and easy driving is based on research by Paikowsky et al. (1994). A blow count boundary between hard and easy driving of 16 blows per 10 cm (4 blows/inch) is used in Figures 5.15 through 5.18 to show the controlling effect of driving resistance. Paikowsky et al. (1994) suggested to use 6 BPI (Blows Per Inch), (24 blows/10cm) as the boundary between easy driving and hard driving. A later study by Paikowsky and Chernauskas (1996) found that 4 BPI (16 blows/10cm) is a better indicator of that boundary. A 3 BPI (12 blows/10cm) boundary is used by GRL for such differentiation (Rausche, 2001).

Shown in Figures 5.15 and 5.16 are the comparisons between the static load test results and the CAPWAP/TEPWAP predictions for the pile-cases that fall into the categories of easy and hard driving, respectively. The mean and standard deviation of ratio of static load test results to the wave matching predictions for the easy driving case is 1.874 and 1.580, respectively, which shows that for low blow counts the wave matching methods do not perform very well. As seen in Figure 5.16 the mean ratio of the static load test results to the CAPWAP/TEPWAP predictions is 1.285 with a standard deviation of 0.528, representing a significant improvement in the performance of the wave matching methods. The scatter for both the easy and hard driving pile case is approximately the same with the ratios (load test results over the predictions) ranging from 0.60 to 2.50. The mean under-prediction for the easy driving pile-cases is 1.308 and the mean under-prediction for the hard driving pile-

cases is 1.130, which is consistent with the improvement in the mean and standard deviations. The analysis comparing the static load test results to the CAPWAP/TEPWAP predictions for the easy and hard driving pile-cases shows that the effect of driving resistance needs to be considered in any further analysis that is completed.

Figures 5.17 and 5.18 show the comparisons of the static load test results and the Energy Approach predictions for the easy and hard driving pile-cases, respectively. The figures show an improvement in the performance of the Energy Approach method from the easy driving pile-cases to the hard driving pile-cases. This is seen in the improvement of the mean and standard deviation, which for the easy driving pile-cases are 1.173 and 0.693, respectively, and for the hard driving pile-cases are 0.840 and 0.324, respectively. The scatter for both the easy and hard driving cases are similar ranging from a ratio (load test results over the predictions) of 0.40 to 2.50. The mean over-prediction decreases from 0.871 for the easy driving pile-cases to 0.720 for the hard driving pile-cases, this is consistent with the decreasing in the mean  $K_{SP}$  value. The results from analyzing the Energy Approach predictions based on blow count show that driving resistance is a parameter that controls the performance of the dynamic methods.

A summary of the above mentioned statistics analyzing the effect of the driving resistance on the performance of the dynamic methods is presented in Table 5.4. The table shows the sub-grouping of the PD/LT2000 database into the dynamic



methods according to the CAPWAP/TEPWAP predictions and the Energy Approach predictions, as well as by the blow count according to easy and hard driving.

The continuation of the analysis reexamines the boundary between easy and hard driving using a statistical analysis of the data found in PD/LT2000. Figures 5.19 and 5.20 present the method that was used to determine this boundary. The figures show the relationship between the  $K_{SW}$  and  $K_{SP}$  values, which are the ratios of the static load test results to the CAPWAP/TEPWAP and Energy Approach predictions respectively, and the blow count. From these graphs it can be seen that at low blow counts there is larger scatter between the blow count and the  $K_{SW}$  and  $K_{SP}$  values.

To determine the blow count boundary at which the CAPWAP/TEPWAP and the Energy Approach methods perform poorly for blow counts below that boundary and better for blow counts above that boundary, the means and standard deviations were taken for all  $K_{SW}$  and  $K_{SP}$  values within ranges of 8 BP10cm (2 BPI). The mean  $K_{SX}$  (the ratio of the static load test results to the CAPWAP/TEPWAP or Energy Approach predictions depending on which method is being analyzed) values for each range of blow counts were plotted versus the midpoint blow count of that specific range. Shown on the bottom graphs for each of the figures are these relationships as well as the mean for all pile cases and their standard deviations. The figures show that at blow counts less than 8 BP10cm the Energy Approach and signal-matching methods have a mean that is approximately one standard deviation (for all pile-cases) larger than the mean for all pile-cases. The mean for the pile-cases that are within the range of 8 to 16 BP10cm is approximately equal to the mean for all cases (1.472 vs.

1.368 for CAPWAP/TEPWAP and 0.975 vs. 0.894 for the Energy Approach) but the standard deviation is still large compared to that of the means for the pile-cases in the ranges above 16 BP10cm (0.765 vs. 0.528 for CAPWAP/TEPWAP and 0.478 vs. 0.324 for the Energy Approach). The standard deviations for the ranges of 8 BP10cm above a blow count of 16 BP10cm are all fairly consistent and are significantly smaller than the standard deviations for the two ranges below 16 BP10cm. The boundary between easy and hard driving is therefore taken as 16 BP10cm (4 BPI) and will subsequently be used in all analyses.

*c) Effect of Pile Type*

The second aspect of the soil inertia effects is the volume of the displaced soil, i.e., the pile type (small or large displacement piles). The preliminary analysis to determine the pile size effect on the dynamic predictions was presented by Paikowsky et al., 1994, suggesting that the boundary between small and large displacement piles is an area ratio of 350. Figures 5.21 through 5.24 use the area ratio of 350 as the boundary between small and large displacement piles demonstrating that there is a controlling effect based on the size of the driven pile.

Figures 5.21 and 5.22 show the comparisons between the static load test results and the wave matching techniques (CAPWAP/TEPWAP) for pile-cases with area ratios below and above 350, respectively. The mean and standard deviations for the two sub-groupings show that there is a significant increase in the performance of the wave matching techniques from large displacement (area ratio  $< 350$ ) piles to small displacement piles (area ratio  $\geq 350$ ). The mean and standard deviation decreases

from  $1.536 \pm 1.137$  to  $1.295 \pm 0.582$ . There is a minimal decrease in the mean under-prediction ratio from the pile-cases with area ratios less than 350 to those with area ratios above 350; the mean decreases from 1.168 to 1.150. There are a significant number of pile-cases with area ratios less than 350 for which the wave matching techniques under-predict the pile capacity by more than sixty percent. The number of pile-cases for which the wave matching techniques under-predicts the pile capacity by more than sixty percent for pile-cases with an area ratio greater than 350 is significantly less than those for pile-cases with area ratios less than 350. Based on the predictions of the wave matching techniques there is a significant effect of the pile type on the predicted pile capacity.

The comparisons between the static load test results and the Energy Approach predictions are shown in Figures 5.23 and 5.24 for pile-cases with area ratios less than 350 and greater than 350, respectively. There is no significant difference between the mean and standard deviations for these two sub-groupings,  $0.914 \pm 0.473$  for the pile-cases with an area ratio below 350 and  $0.980 \pm 0.508$  for pile-cases with an area ratio above 350. There is a slight improvement in the mean over-prediction from the pile-cases with an area ratio less than 350 to the pile-cases with an area ratio greater than 350 (0.712 to 0.832). The scatter for both sub-groupings is very similar and the prediction ratios range from approximately 0.40 to 2.50. Based on the Energy Approach predictions there is little to no effect on the predicted pile capacity due to the pile type.

The statistics that were shown in the above analyses for the effect of pile type on the pile capacities based on the wave matching techniques and the Energy Approach are summarized in Table 5.5. The conclusion from the analysis is that there is an effect on the pile capacity determined using the dynamic methods due to the pile type, which is based on the area ratio, especially for the CAPWAP/TEPWAP predictions. The continued analysis to determine the area ratio boundary, which differentiates between small and large displacement piles, will show that even for the Energy Approach method the results are affected by the pile type.

The data presented in Figures 5.25 and 5.26 is similar to the approach that was used to determine the boundary between easy and hard driving (refer to Figures 5.19 and 5.20). The top portion of each of the figures (5.25 and 5.26) presents the comparison between the  $K_{sx}$  values (the ratio of the static load test results to the CAPWAP/TEPWAP or Energy Approach predictions depending on which method is being analyzed) and the area ratio for the CAPWAP/TEPWAP and Energy Approach predictions, respectively. The data is sub-grouped by soil type and it can be seen that there is no real correlation between the  $K_{sx}$  values and the area ratio. The bottom portions of the figures were created by plotting the mean  $K_{sx}$  values and the standard deviations for the pile-cases within a range of area ratios of 175 versus the mid-point area ratio for that specific range. As is shown in Figures 5.25 and 5.26 for both the wave matching techniques and the Energy Approach predictions the mean  $K_{sx}$  value for the range of area ratios from 0 to 175 is approximately equal to the mean for all pile-cases (1.382 vs. 1.452 for CAPWAP/TEPWAP and 0.864 vs. 0.936 for the

Energy Approach) and the standard deviations are within the standard deviation for all pile-cases (0.569 vs. 0.985 for CAPWAP/TEPWAP and 0.326 vs. 0.485 for the Energy Approach). The range in which the standard deviations become drastically larger than the standard deviations for all pile-cases is from 175 to 350 (1.425 vs. 0.985 for CAPWAP/TEPWAP and 0.563 vs. 0.485 for the Energy Approach). The majority of the means and standard deviations for the ranges above 350 fall within the range of the standard deviations of all pile-cases. The boundary between small and large displacement was therefore taken at an area ratio of 350. Piles having an area ratio greater than 350 are classified as small displacement and pile having an area ratio less than 350 are classified as large displacement piles.

In an effort to examine the true influence of the area ratio three things needed to be done. The first is to isolate, to the extent possible, the influence of the acceleration on the inertia from that of the mass on the inertia, i.e., look on blow counts greater than 16 BP10cm. The second is to look at the data when the soil inertia effects most likely exist during driving, i.e., EOD, whereas, it may not be mobilized at BOR. The final thing is the method of analysis to evaluate, the CAPWAP (wave matching techniques) were chosen because of the easier influence on the method as a full analysis of the phenomenon is done. The conclusion is that in order to look closely at the influence of the area ratio the pile-cases related to the wave matching techniques at the EOD for blow counts greater than 16 BP10cm needed to be evaluated.

Figure 5.27 presents the analysis that was completed to isolate the CAPWAP/TEPWAP pile-cases at the EOD for blow counts greater than 16 BP10cm. The top portion of the figure is a comparison between the  $K_{SW}$  values and their corresponding area ratios. This graph shows that there is a point in which the  $K_{SW}$  values begin to go asymptotically towards a  $K_{SW}$  value of 1.0. The bottom graph of the figure presents the actual analysis used to verify the boundary between small and large displacement piles. The mean  $K_{SW}$  values as well as the standard deviations for a range of area ratios were plotted versus the midpoint area ratio for that range. The ranges for these pile-cases varied due to the lesser number of pile-cases compared to all of the wave matching technique pile-cases. As is shown the means for the first two ranges of area ratios, (0 - 175 and 175- 350), are slightly higher than the mean for all cases in the specific sub-grouping being analyzed. It is apparent by the standard deviations for these two ranges that the dynamic methods performance will be less accurate for piles that have an area ratio less than 350. The means for the ranges above an area ratio of 350 are significantly smaller than the mean for all pile-cases in this sub-grouping but they are approximately one as is shown in the figure. The standard deviations are relatively small for the pile-cases that have an area ratio greater than 350 compared to the overall standard deviation for all pile-cases in this sub-grouping.

The conclusion from this analysis is that there is a significant effect on the performance of the dynamic methods due to the type of pile that is driven. The boundary between poor performance (large displacement piles) and good performance

(small displacement piles) of the CAPWAP/TEPWAP and Energy Approach predictions is taken at an area ratio of 350. The analysis that is done from this point forward will incorporate the effect of the pile type.

#### **5.4 INTERMEDIATE CONCLUSIONS**

The above analyses show that the controlling parameters that have a significant effect on the pile capacity predictions are, in order of importance, the time of driving, the driving resistance and the type of pile (small or large displacement) that was driven. The analyses showed that the effect of soil type is minimal when compared to the other controlling parameters. The boundary between easy and hard driving will be taken at a blow count of 16 BP10cm (4 BPI) and the boundary between small and large displacement piles will be taken at an area ratio of 350.

**Table 5.1.** Summary of the  $K_{SW}$  Values for the Different Soil Types used for the Soil Inertia Analysis.

	Clay & Till				Sand & Silt				Rock			
<b>Mean</b>	1.352				1.517				0.930			
<b>Standard Deviation</b>	0.723				1.085				0.172			
<b>Number of Cases</b>	100				265				15			
	<b>EOD</b>		<b>BOR(last)</b>		<b>EOD</b>		<b>BOR(last)</b>		<b>EOD</b>		<b>BOR(last)</b>	
<b>Mean</b>	1.634		1.133		2.068		1.193		0.968		0.925	
<b>Standard Deviation</b>	0.899		0.444		1.765		0.391		0.132		0.203	
<b>Number of Cases</b>	45		40		77		116		7		7	
	<b>&lt; 5 BPcm</b>	<b>≥ 5 BPcm</b>	<b>&lt; 5 BPcm</b>	<b>≥ 5 BPcm</b>	<b>&lt; 5 BPcm</b>	<b>≥ 5 BPcm</b>	<b>&lt; 5 BPcm</b>	<b>≥ 5 BPcm</b>	<b>&lt; 5 BPcm</b>	<b>≥ 5 BPcm</b>	<b>&lt; 5 BPcm</b>	<b>≥ 5 BPcm</b>
<b>Mean</b>	1.725	1.315	1.254	0.985	2.191	1.458	1.126	1.283	1.070	0.952	0.960	0.879
<b>Standard Deviation</b>	0.807	1.160	0.489	0.340	1.901	0.512	0.386	0.355	-----	0.136	0.209	0.230
<b>Number of Cases</b>	35	10	22	18	64	13	74	40	1	6	4	3



**Table 5.2.** Summary of the  $K_{SP}$  Values for the Different Soil Types used for the Soil Inertia Analysis.

	Clay & Till				Sand & Silt				Rock			
<b>Mean</b>	0.873				0.968				0.744			
<b>Standard Deviation</b>	0.460				0.501				0.154			
<b>Number of Cases</b>	101				260				15			
	<b>EOD</b>		<b>BOR(last)</b>		<b>EOD</b>		<b>BOR(last)</b>		<b>EOD</b>		<b>BOR(last)</b>	
<b>Mean</b>	1.037		0.717		1.310		0.821		0.778		0.729	
<b>Standard Deviation</b>	0.588		0.231		0.670		0.314		0.092		0.207	
<b>Number of Cases</b>	46		40		81		107		7		7	
	<b>&lt; 5 BPcm</b>	<b>≥ 5 BPcm</b>	<b>&lt; 5 BPcm</b>	<b>≥ 5 BPcm</b>	<b>&lt; 5 BPcm</b>	<b>≥ 5 BPcm</b>	<b>&lt; 5 BPcm</b>	<b>≥ 5 BPcm</b>	<b>&lt; 5 BPcm</b>	<b>≥ 5 BPcm</b>	<b>&lt; 5 BPcm</b>	<b>≥ 5 BPcm</b>
<b>Mean</b>	1.127	0.750	0.686	0.751	1.345	1.122	0.789	0.863	0.645	0.801	0.772	0.671
<b>Standard Deviation</b>	0.637	0.241	0.235	0.229	0.716	0.292	0.330	0.267	-----	0.077	0.249	0.163
<b>Number of Cases</b>	35	11	21	19	68	13	72	34	1	6	4	3

**Table 5.3.** Summary of the Statistics showing the Importance of the Time of Driving as a Controlling Parameter.

<b>Dynamic Method</b>	<b>CAPWAP</b>		<b>Energy Approach</b>	
<b>Mean</b>	1.368		0.894	
<b>Standard Deviation</b>	0.620		0.367	
<b>Number of Cases</b>	377		371	
<b>Time of Driving</b>	<b>EOD</b>	<b>BOR (last)</b>	<b>EOD</b>	<b>BOR (last)</b>
<b>Mean</b>	1.626	1.158	1.084	0.785
<b>Standard Deviation</b>	0.797	0.393	0.431	0.290
<b>Number of Cases</b>	125	162	128	153

**Table 5.4.** Summary of the Statistics showing the Importance of the Driving Resistance as a Controlling Parameter.

<b>Dynamic Method</b>	<b>CAPWAP</b>		<b>Energy Approach</b>	
<b>Mean</b>	1.368		0.894	
<b>Standard Deviation</b>	0.620		0.367	
<b>Number of Cases</b>	377		371	
<b>Driving Resistance</b>	<b>&lt; 16 BP10cm</b>	<b>≥ 16 BP10cm</b>	<b>&lt; 16 BP10cm</b>	<b>≥ 16 BP10cm</b>
<b>Mean</b>	1.874	1.285	1.173	0.840
<b>Standard Deviation</b>	1.580	0.528	0.693	0.324
<b>Number of Cases</b>	108	274	109	269

**Table 5.5.** Summary of the Statistics showing the Importance of the Area Ratio as a Controlling Parameter.

<b>Dynamic Method</b>	<b>CAPWAP</b>		<b>Energy Approach</b>	
<b>Mean</b>	1.368		0.894	
<b>Standard Deviation</b>	0.620		0.367	
<b>Number of Cases</b>	377		371	
<b>Area Ratios</b>	<b>&lt; 350</b>	<b>≥ 350</b>	<b>&lt; 350</b>	<b>≥ 350</b>
<b>Mean</b>	1.536	1.295	0.914	0.980
<b>Standard Deviation</b>	1.137	0.582	0.473	0.508
<b>Number of Cases</b>	250	132	250	128

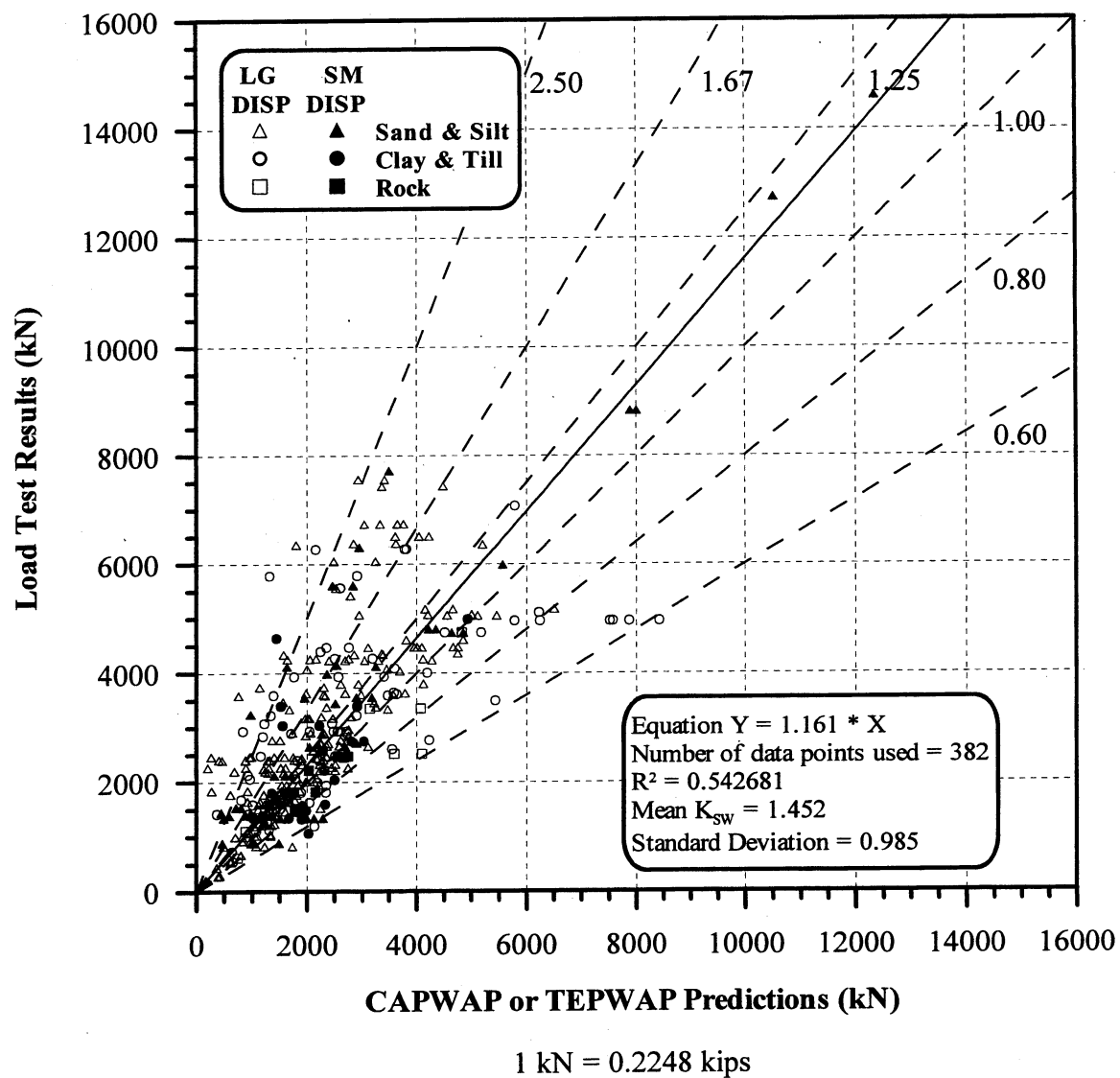


**Figure 5.1.** Static Load Test Results vs. CAPWAP or TEPWAP predictions for 382 PD/LT2000 pile-cases in all types of soils (AAA).

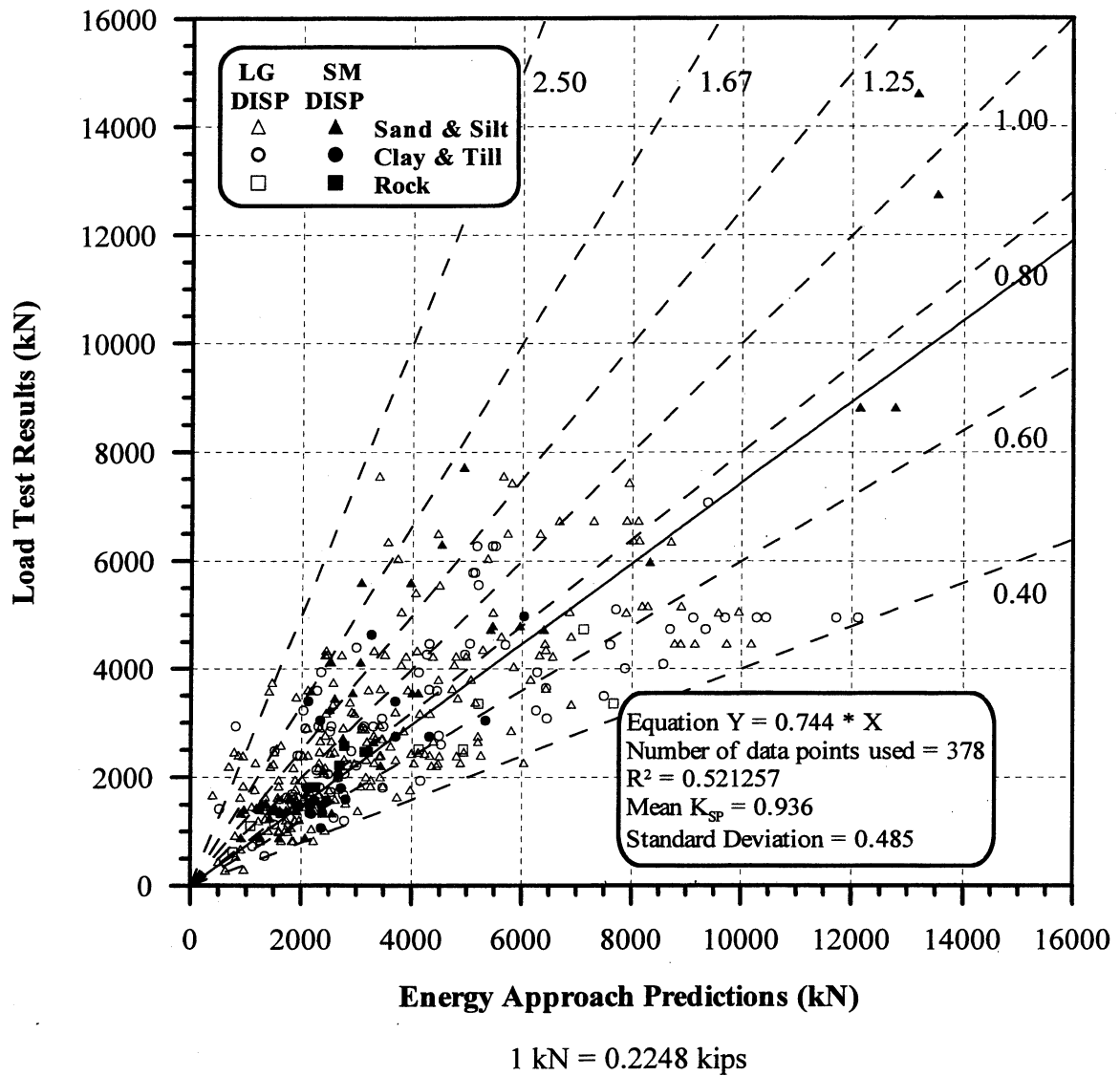


**Figure 5.2.** Static Load Test Results vs. Energy Approach predictions for 378 PD/LT2000 pile-cases in all types of soils (AAA).

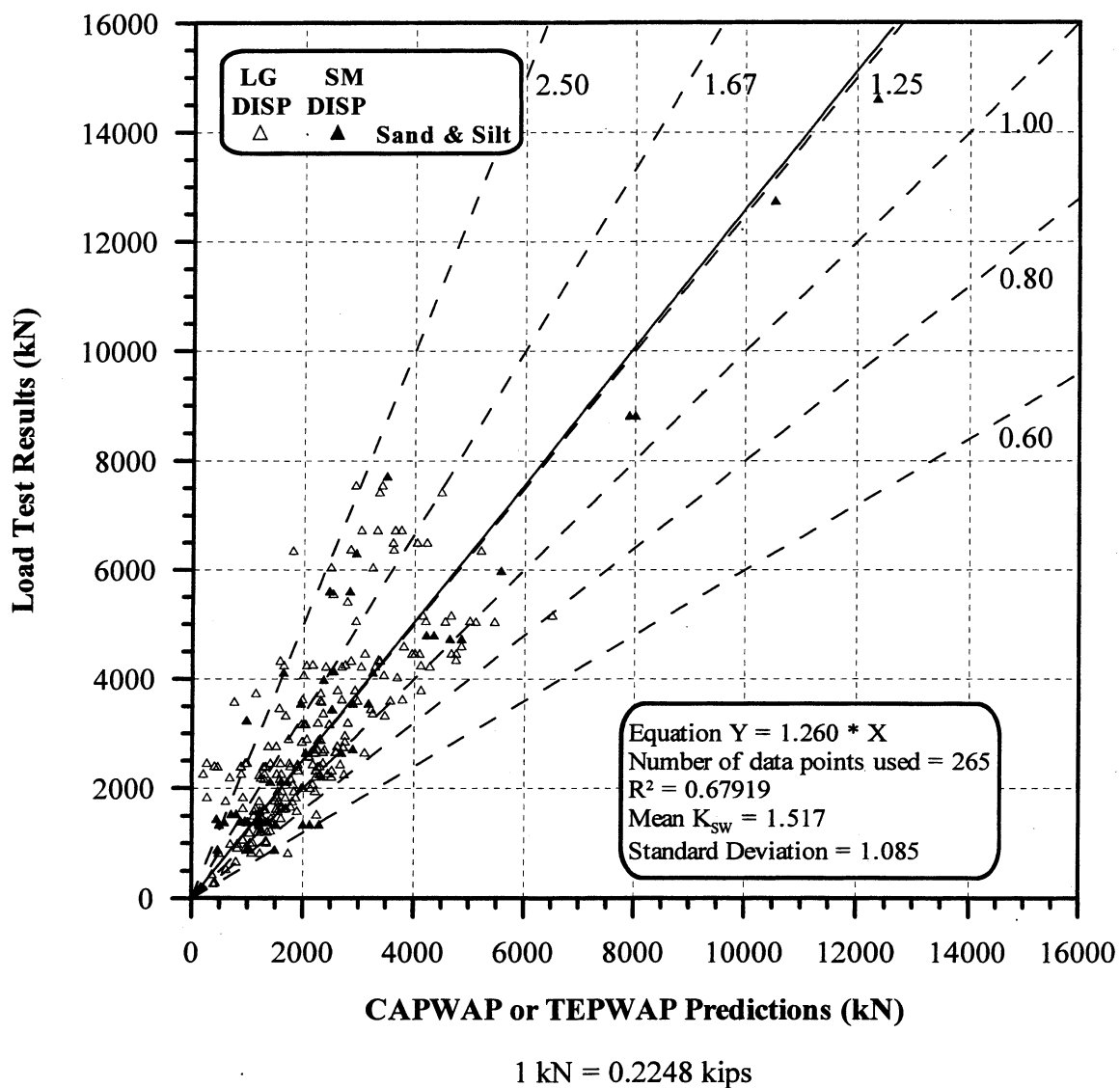


**Figure 5.3.** Static Load Test Results vs. CAPWAP or TEPWAP predictions for 265 PD/LT2000 pile-cases in sand & silt (AAS).

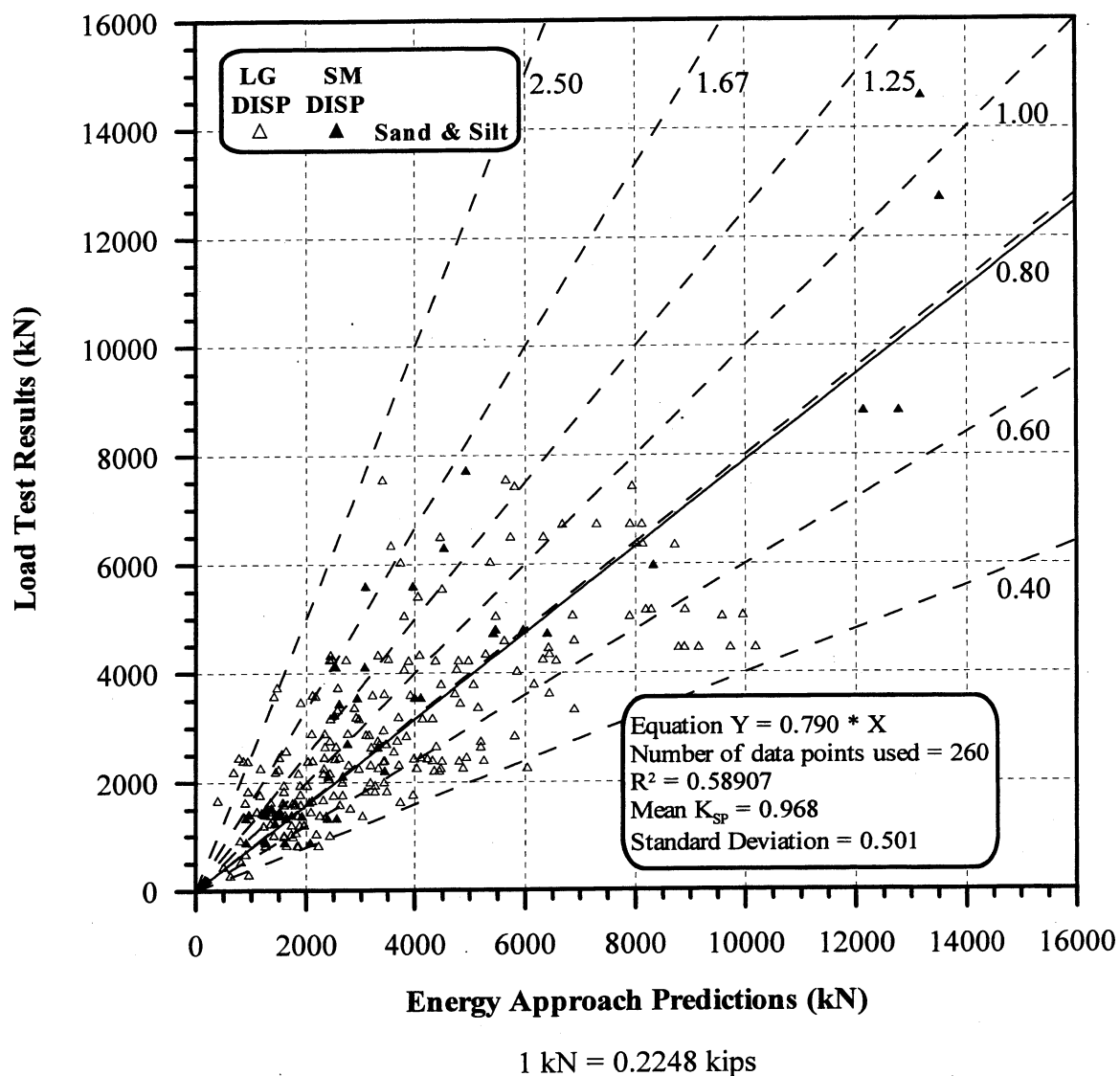


**Figure 5.4.** Static Load Test Results vs. Energy Approach predictions for 260 PD/LT2000 pile-cases in sand & silt (AAS).

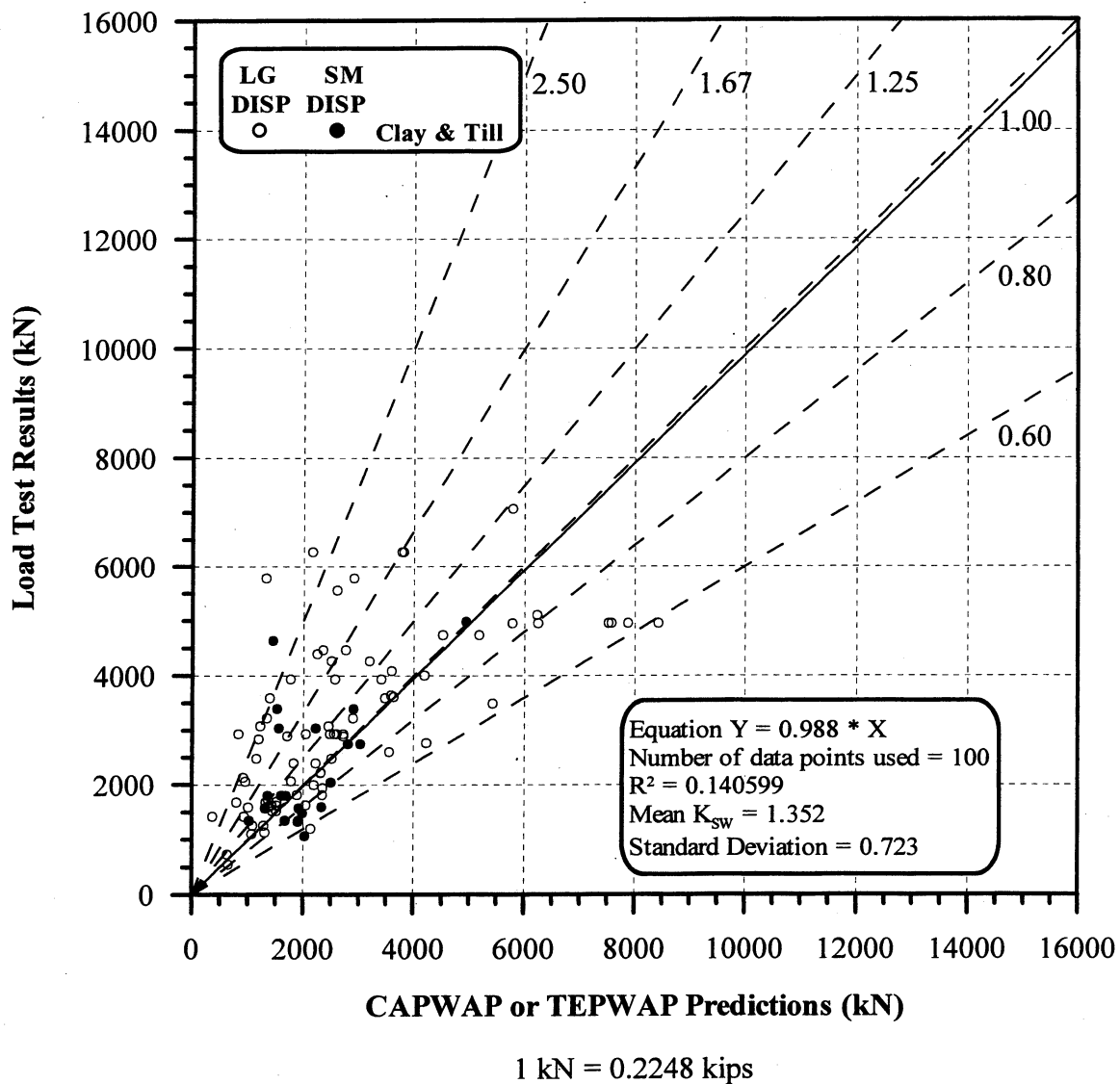


**Figure 5.5.** Static Load Test Results vs. CAPWAP or TEPWAP predictions for 100 PD/LT2000 pile-cases in clay & till (AAC).



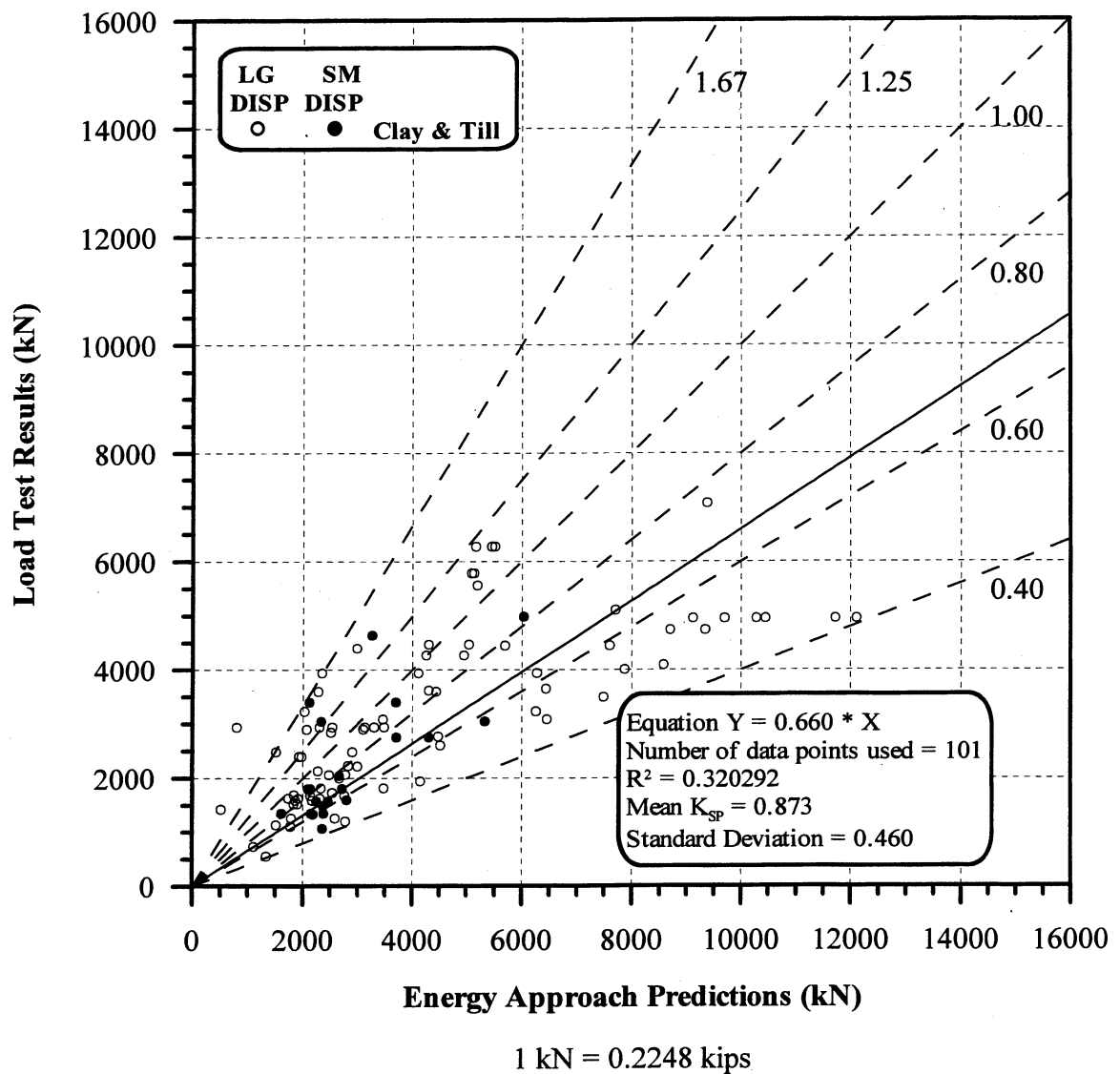


**Figure 5.6.** Static Load Test Results vs. Energy Approach predictions for 101 PD/LT2000 pile-cases in clay & till (AAC).

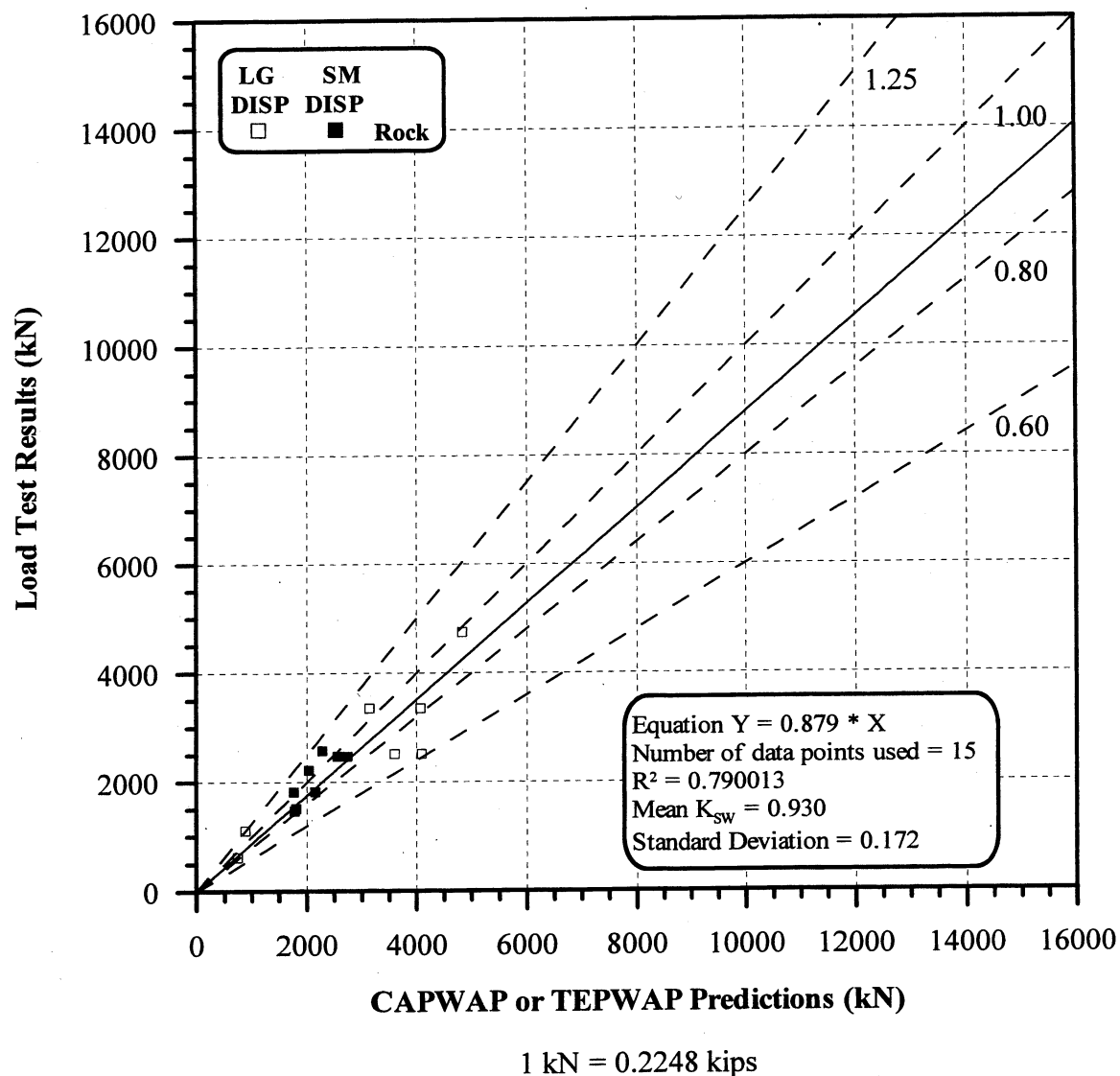


**Figure 5.7.** Static Load Test Results vs. CAPWAP or TEPWAP predictions for 15 PD/LT2000 pile-cases in rock (AAR).

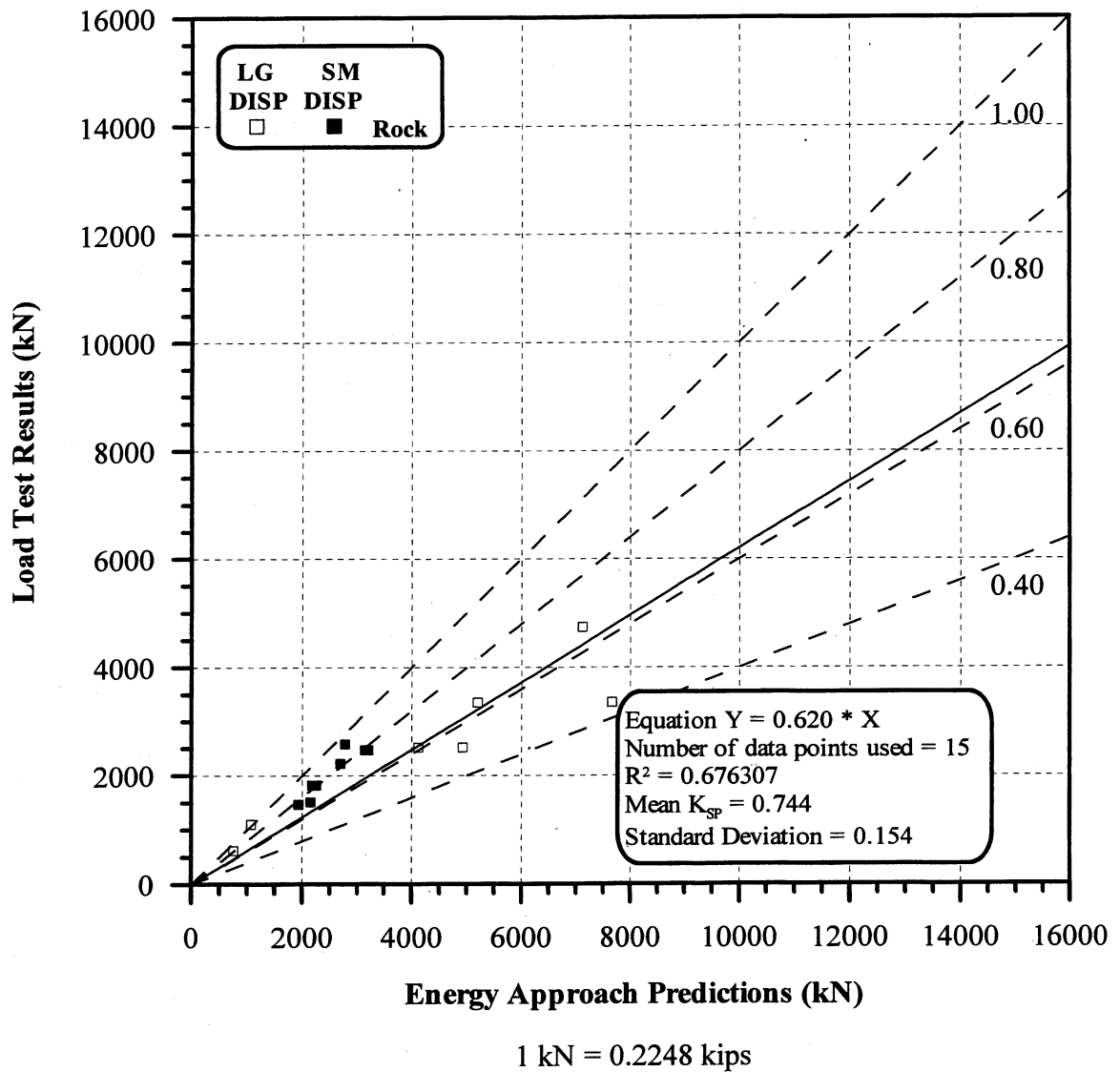


**Figure 5.8.** Static Load Test Results vs. Energy Approach predictions for 15 PD/LT2000 pile-cases in rock (AAR).

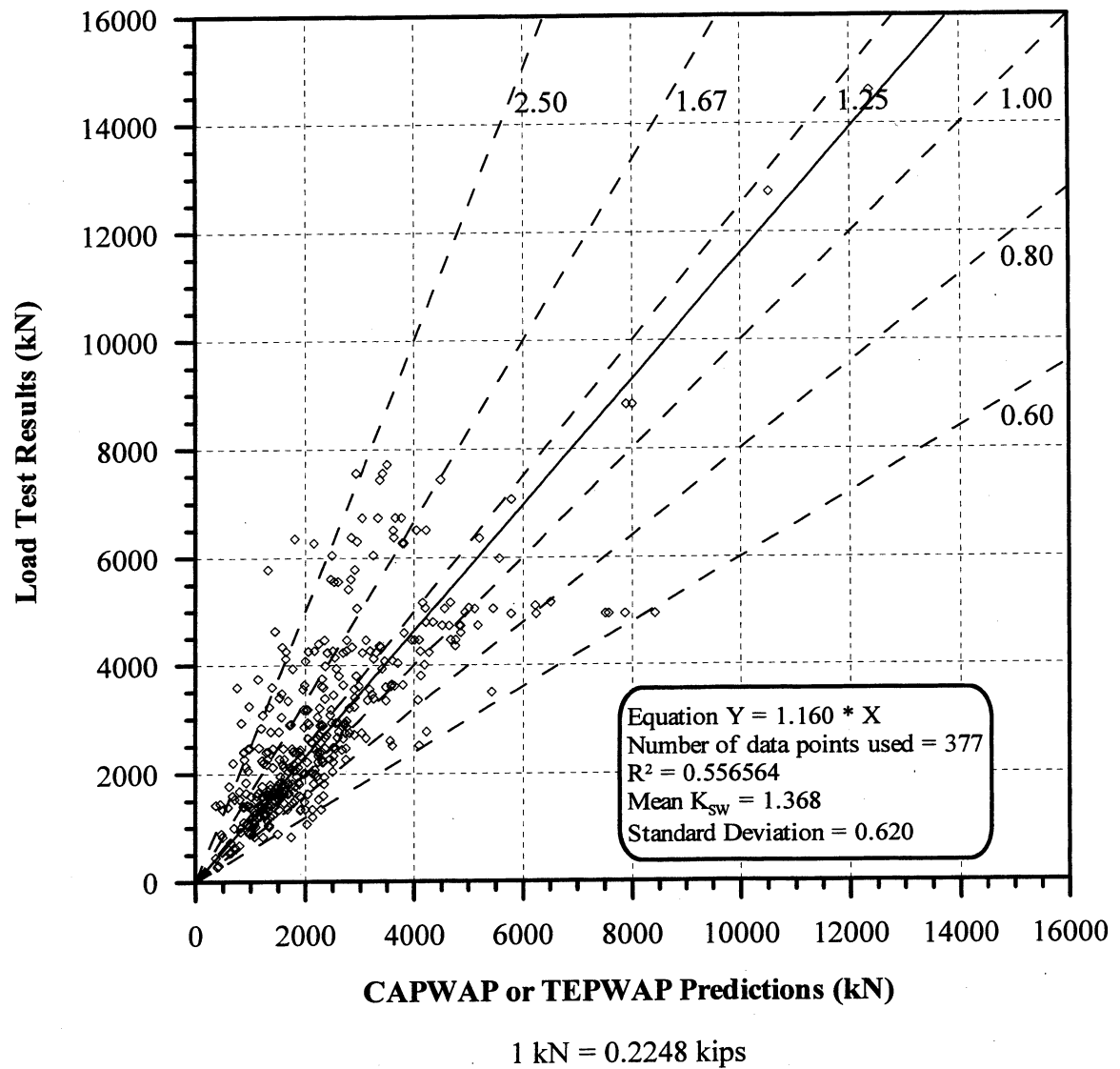


**Figure 5.9.** Static Load Test Results vs. CAPWAP or TEPWAP predictions for 377 PD/LT2000 pile-cases in all types of soils (AAA).

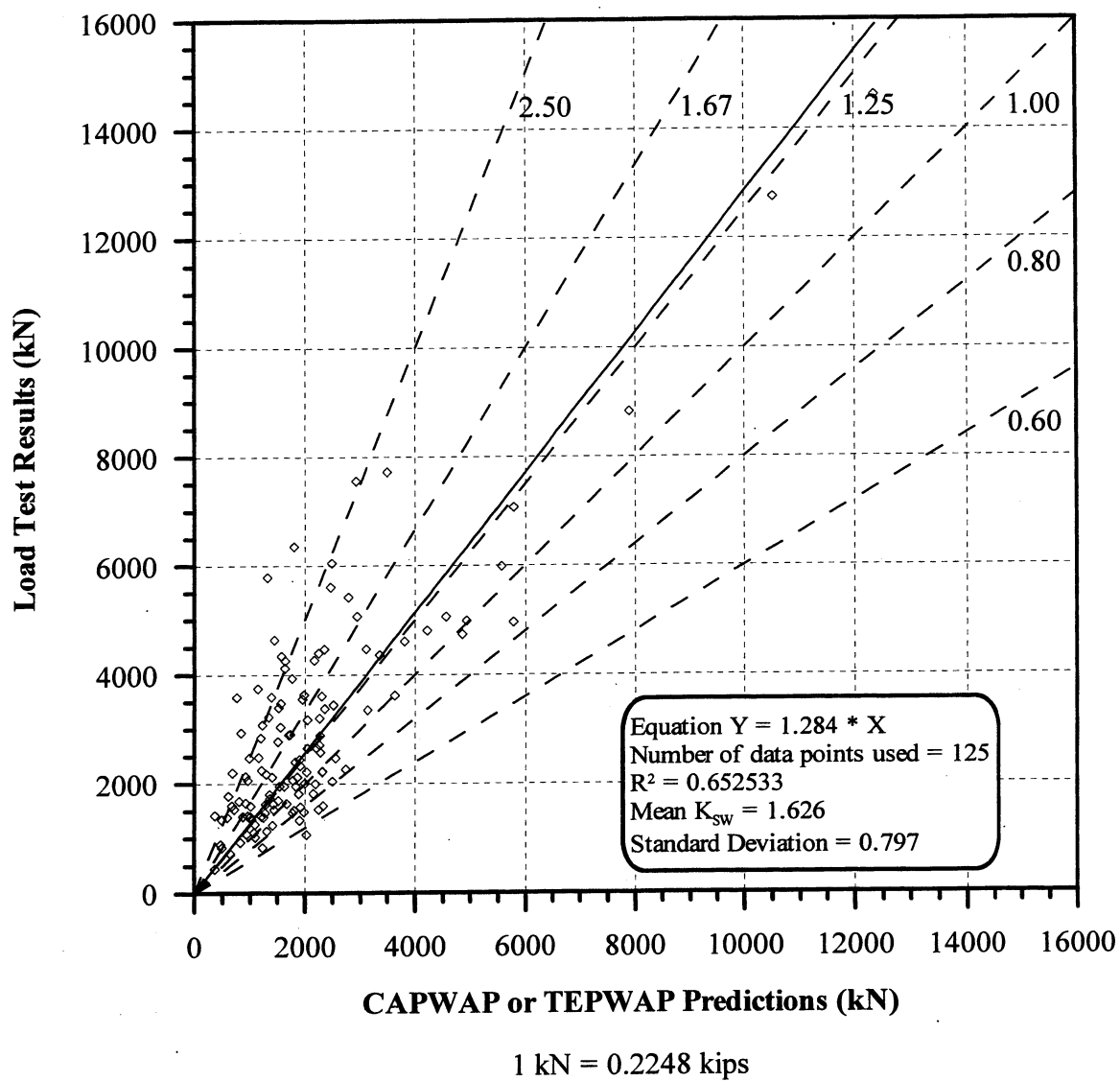


**Figure 5.10.** Static Load Test Results vs. CAPWAP or TEPWAP predictions for 125 PD/LT2000 pile-cases at EOD in all types of soils (AEA).

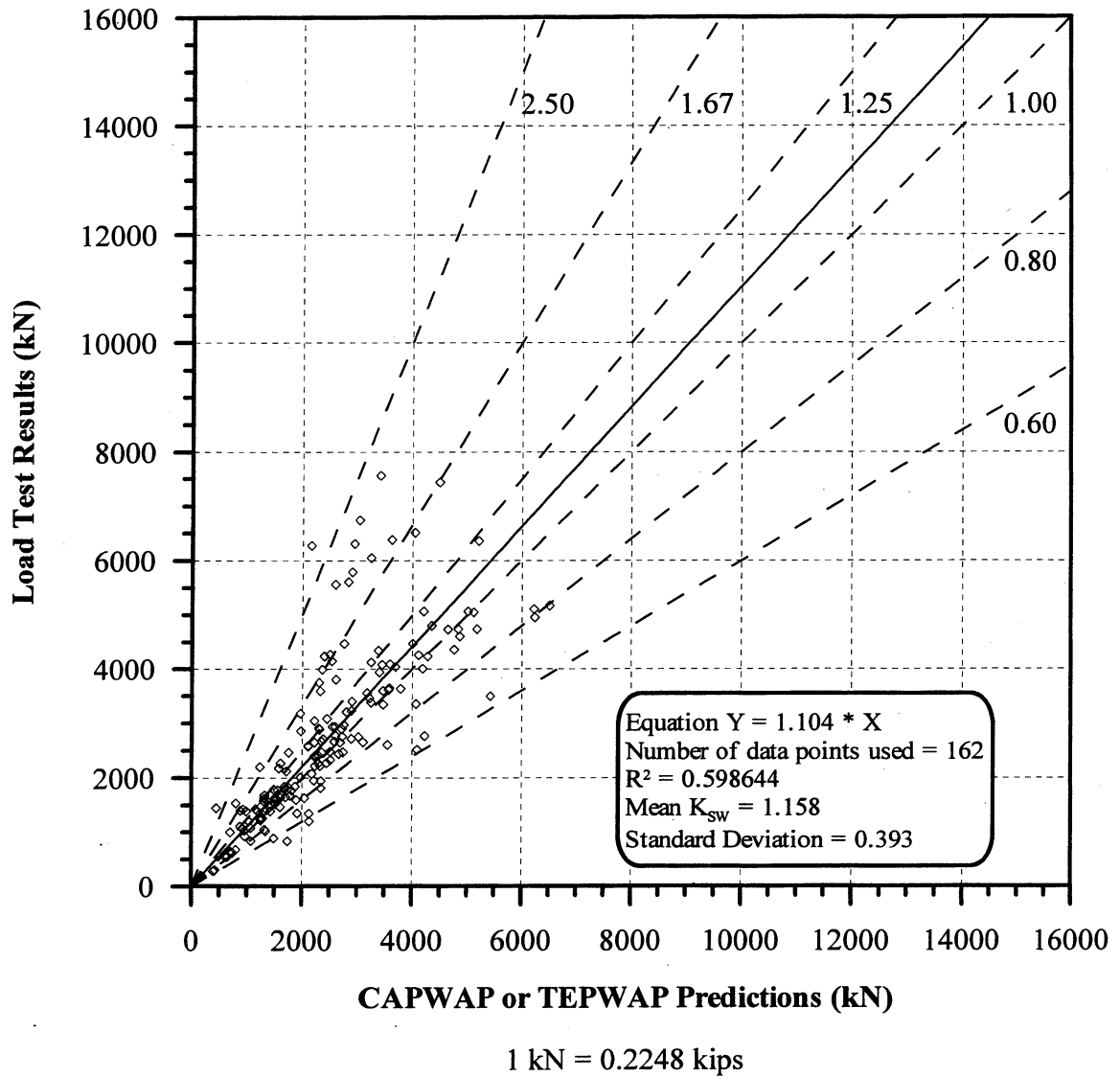


**Figure 5.11.** Static Load Test Results vs. CAPWAP or TEPWAP predictions for 162 PD/LT2000 pile-cases at BOR(last) in all types of soils (ABA).

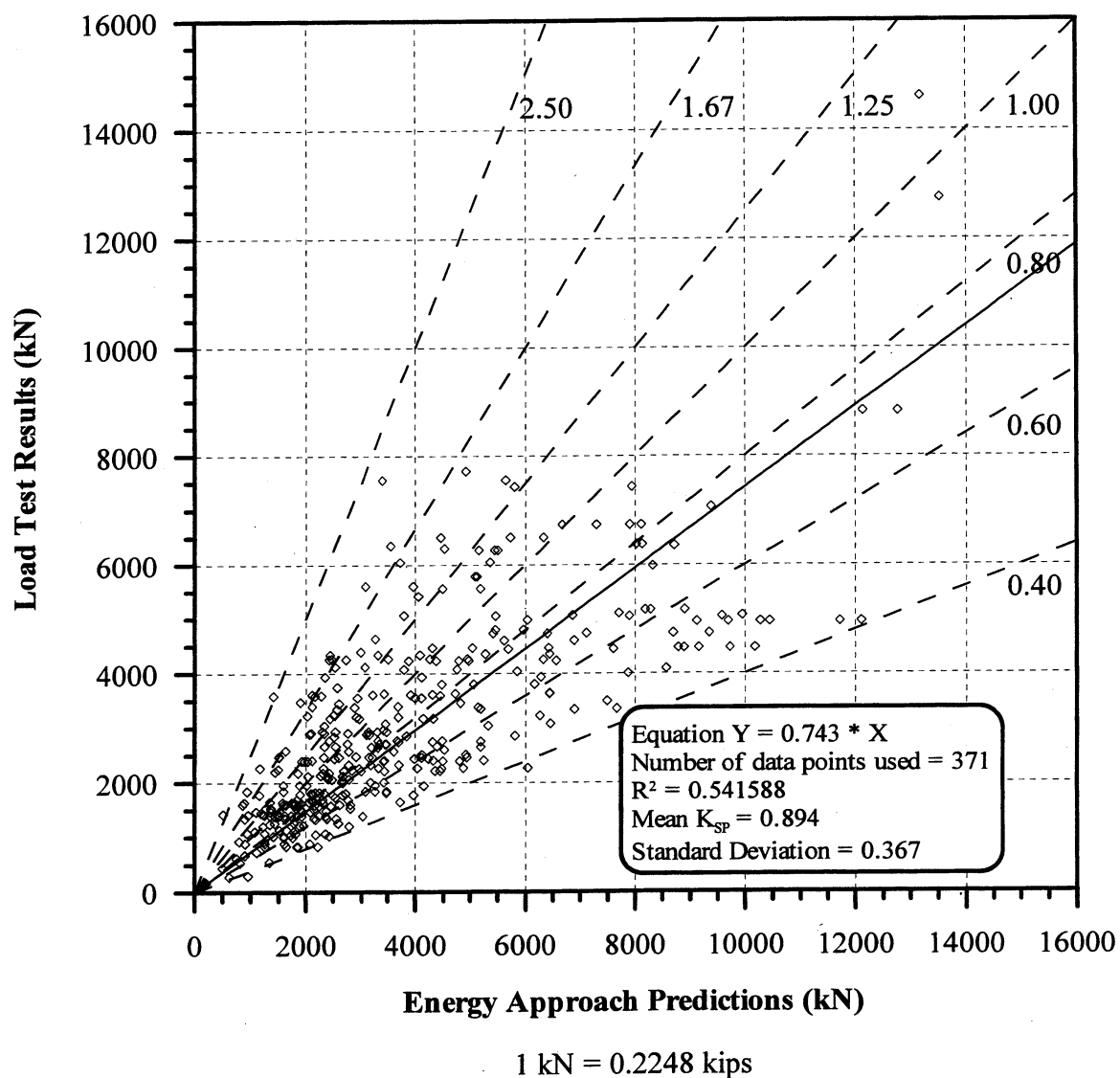


**Figure 5.12.** Static Load Test Results vs. Energy Approach predictions for 371 PD/LT2000 pile-cases in all types of soils (AAA).

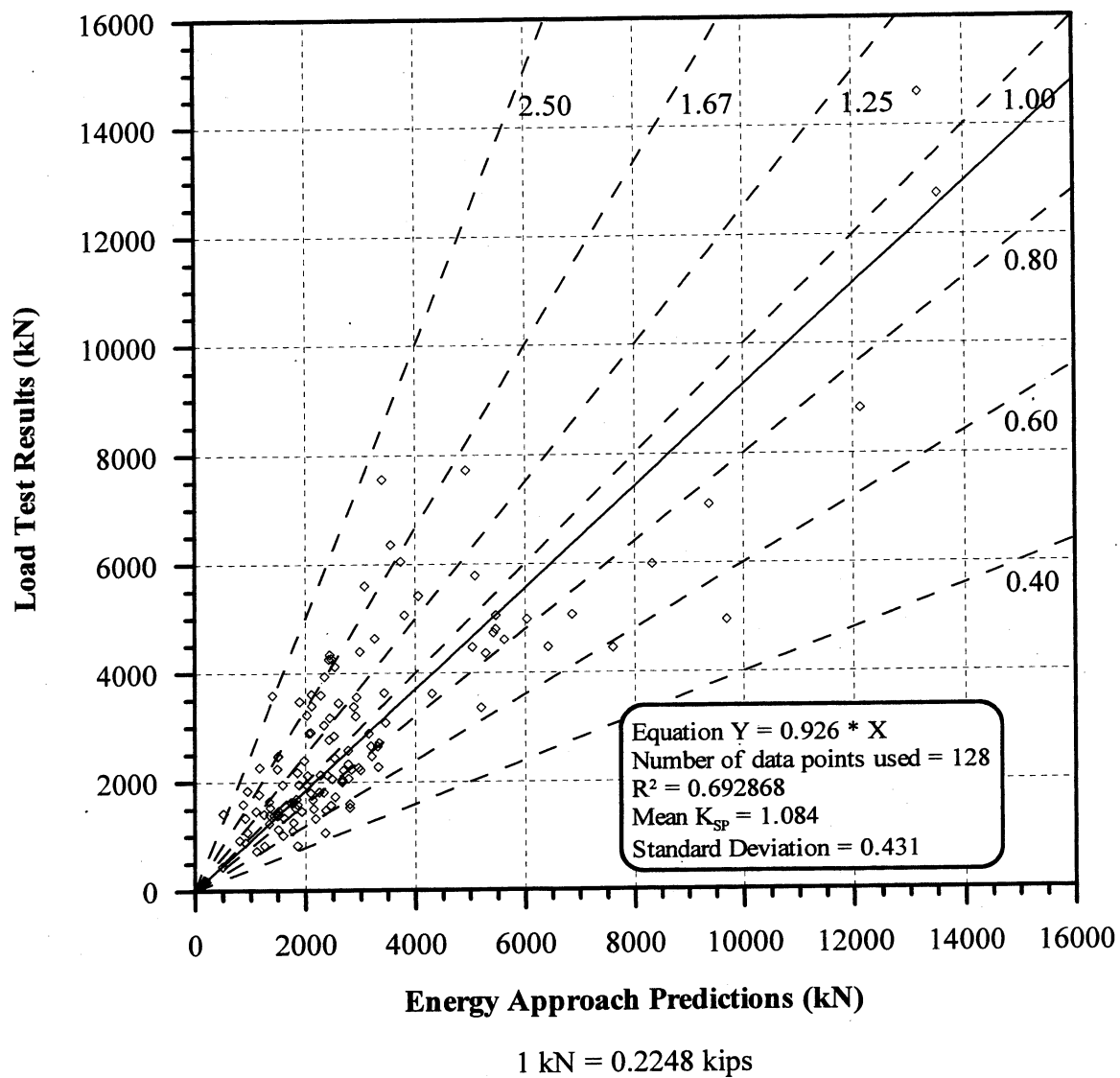


**Figure 5.13.** Static Load Test Results vs. Energy Approach predictions for 128 PD/LT2000 pile-cases at EOD in all types of soils (AEA).



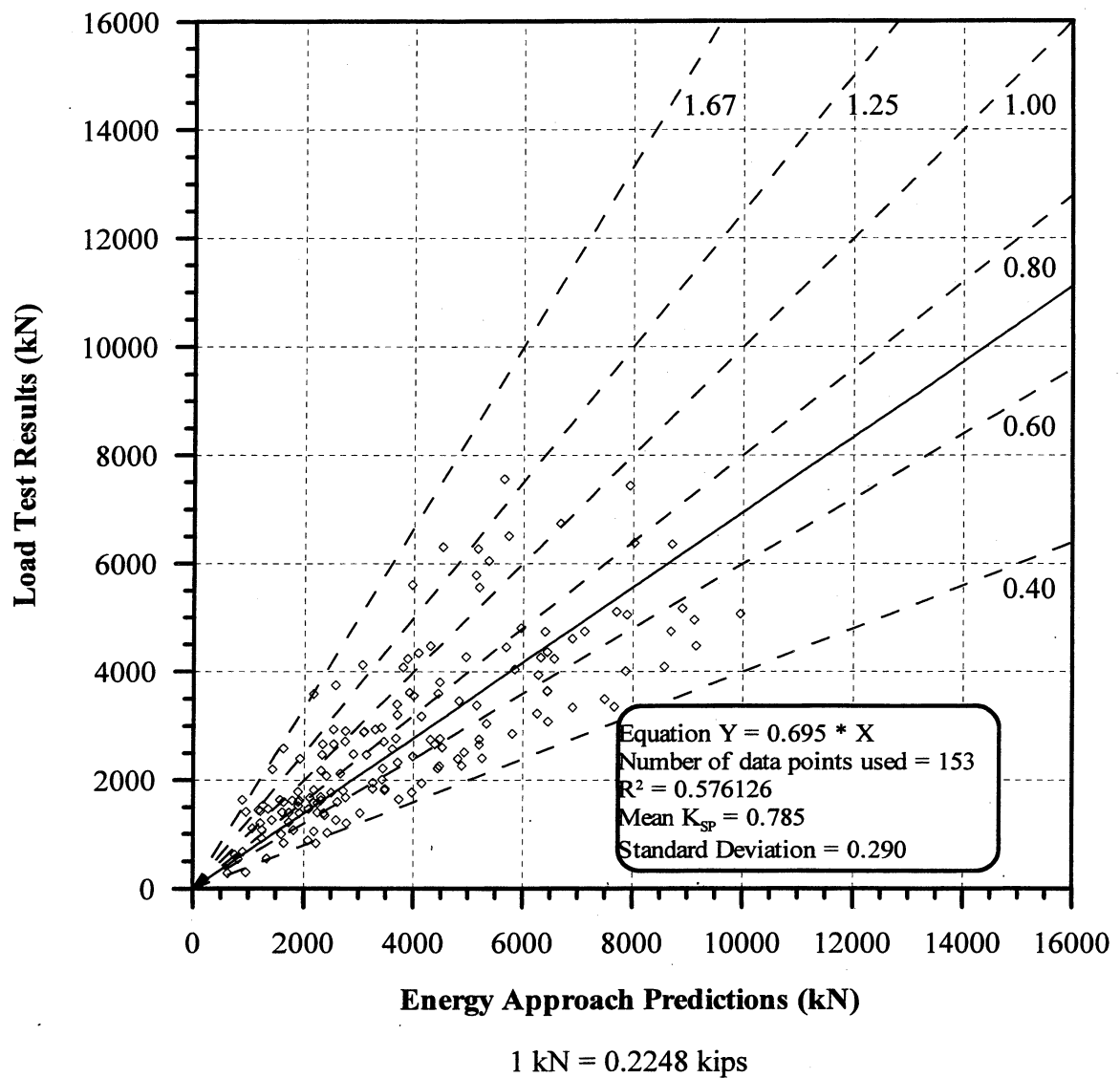
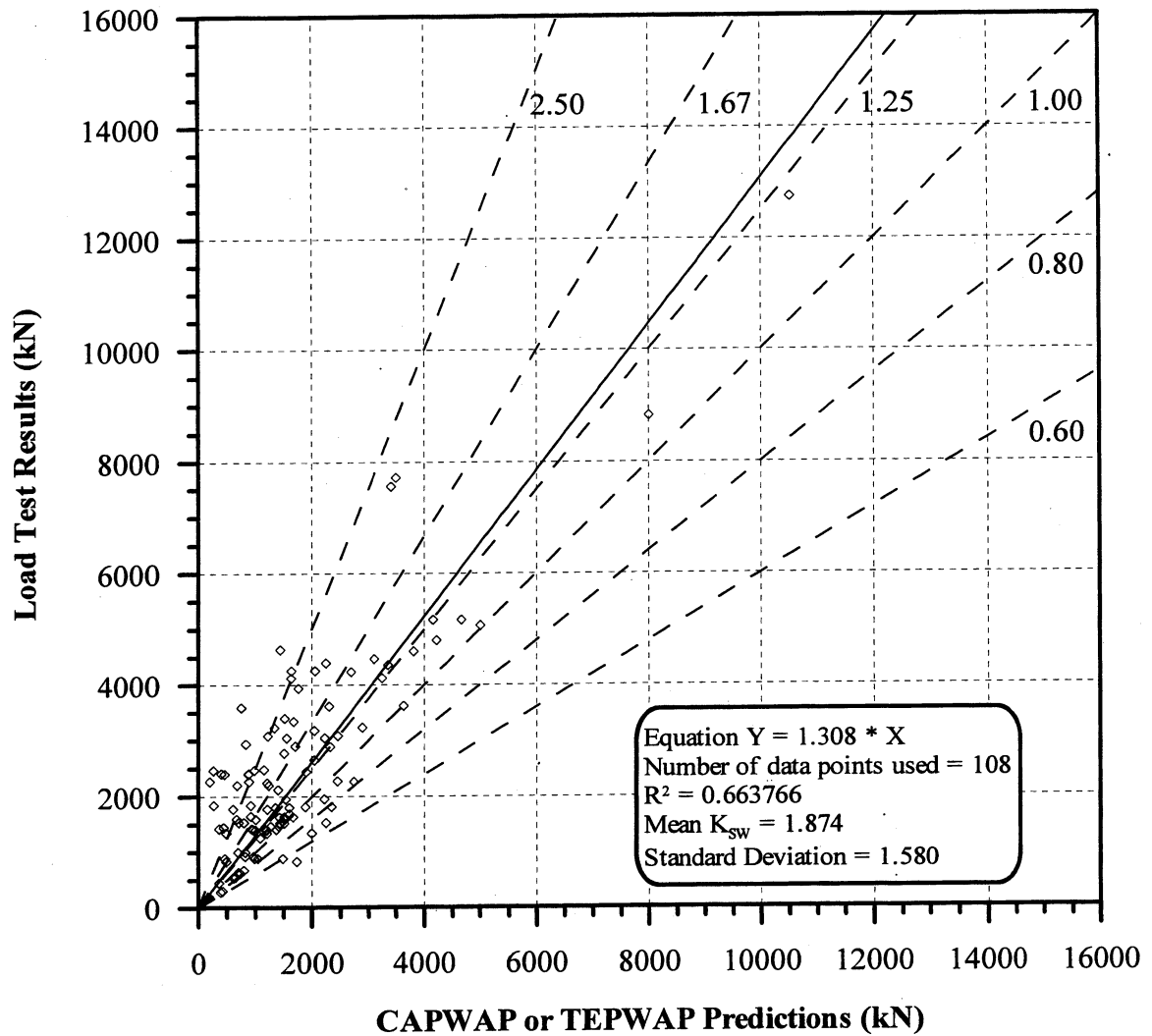
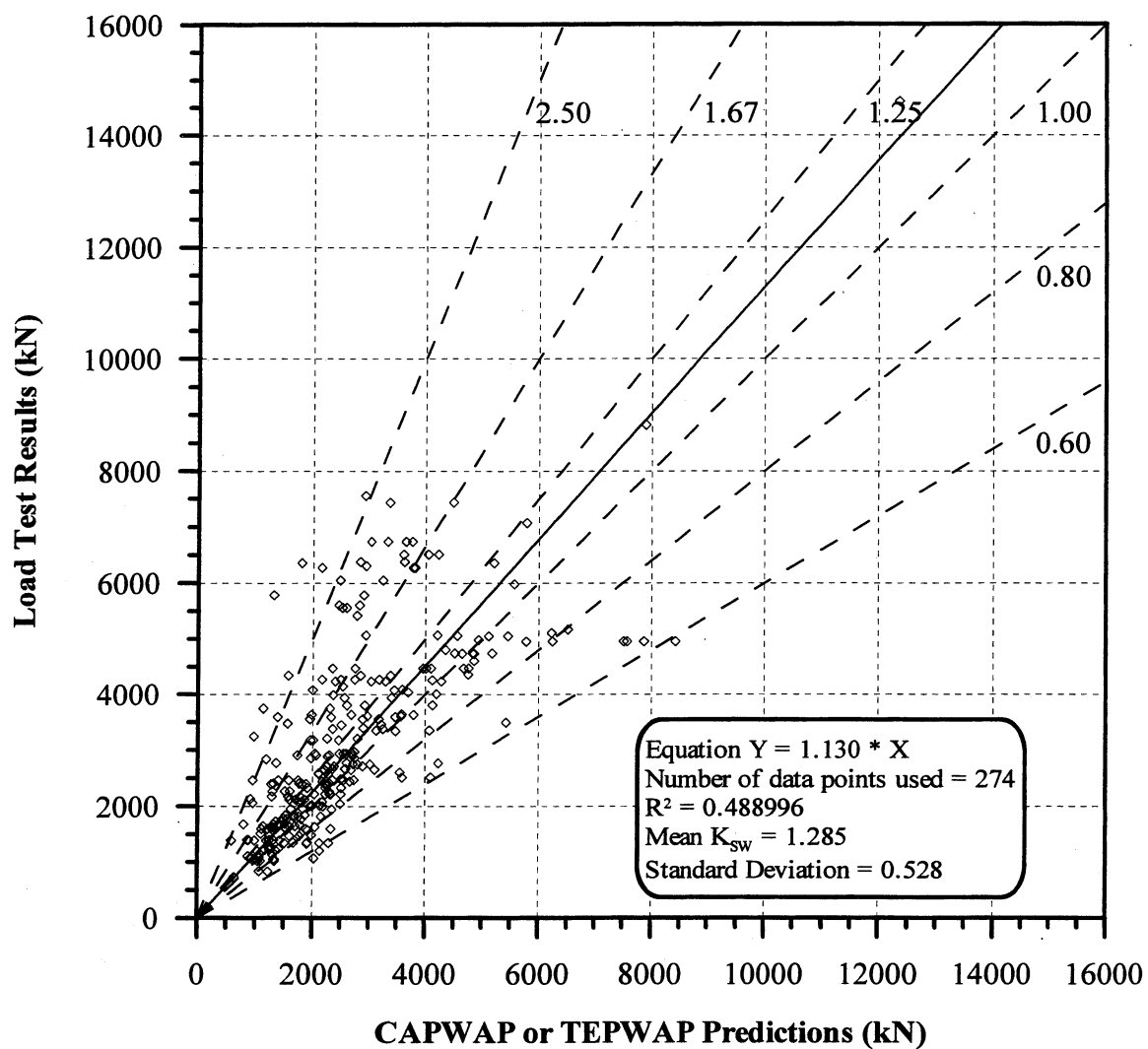


**Figure 5.14.** Static Load Test Results vs. Energy Approach predictions for 153 PD/LT2000 pile-cases at BOR(last) in all types of soils (ABA).



1 kN = 0.2248 kips

**Figure 5.15.** Static Load Test Results vs. CAPWAP or TEPWAP predictions for 108 PD/LT2000 pile-cases with Blow Count < 16 BP10cm in all types of soils (AAA).



1 kN = 0.2248 kips

**Figure 5.16.** Static Load Test Results vs. CAPWAP or TEPWAP predictions for 274 PD/LT2000 pile-cases with Blow Count  $\geq 16$  BP10cm in all types of soils (AAA).

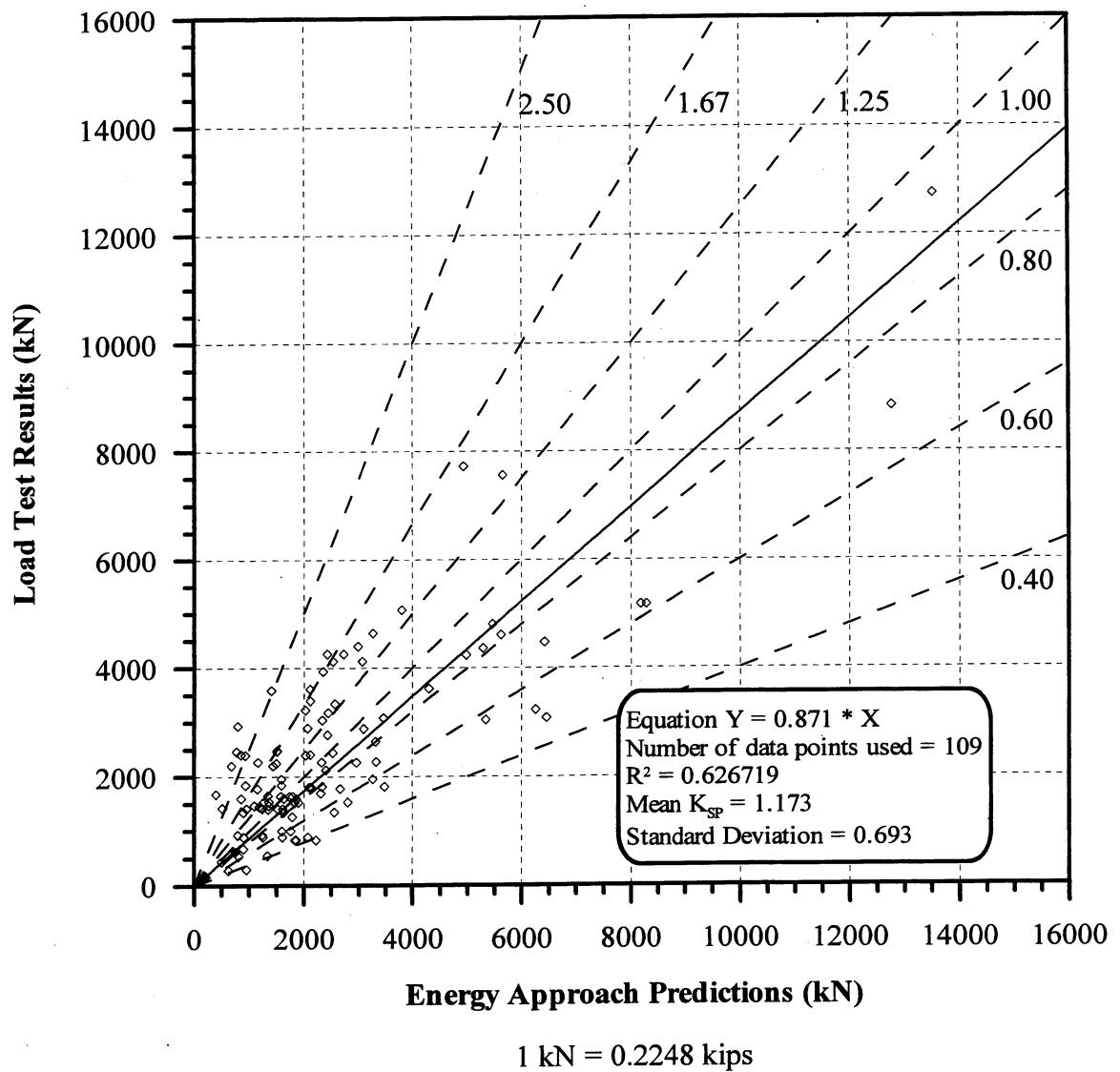


**Figure 5.17.** Static Load Test Results vs. Energy Approach predictions for 109 PD/LT2000 pile-cases with Blow Count < 16 BP10cm in all types of soils (AAA).

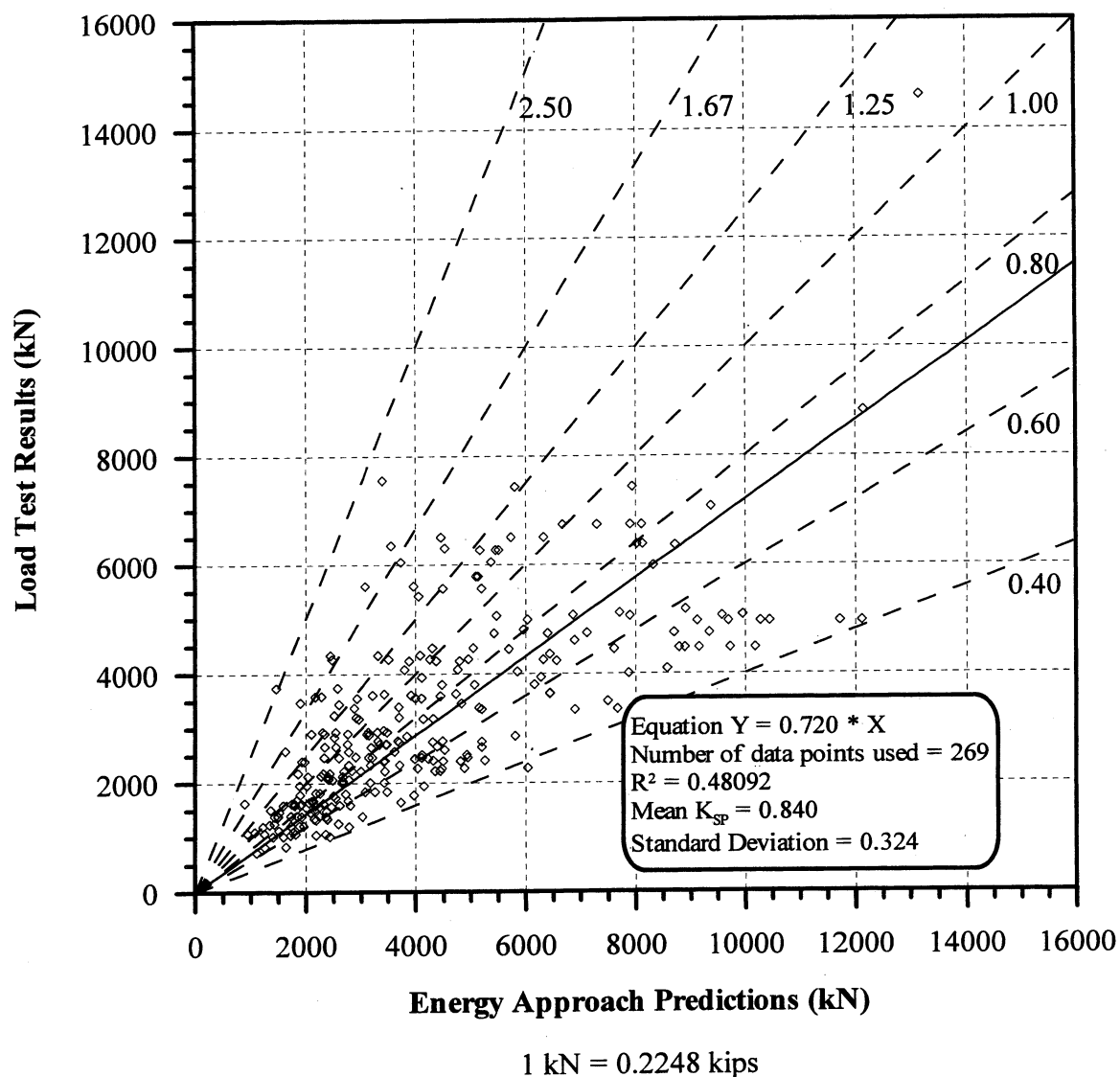


**Figure 5.18.** Static Load Test Results vs. Energy Approach predictions for 269 PD/LT2000 pile-cases with Blow Count  $\geq 16$  BP10cm in all types of soils (AAA).

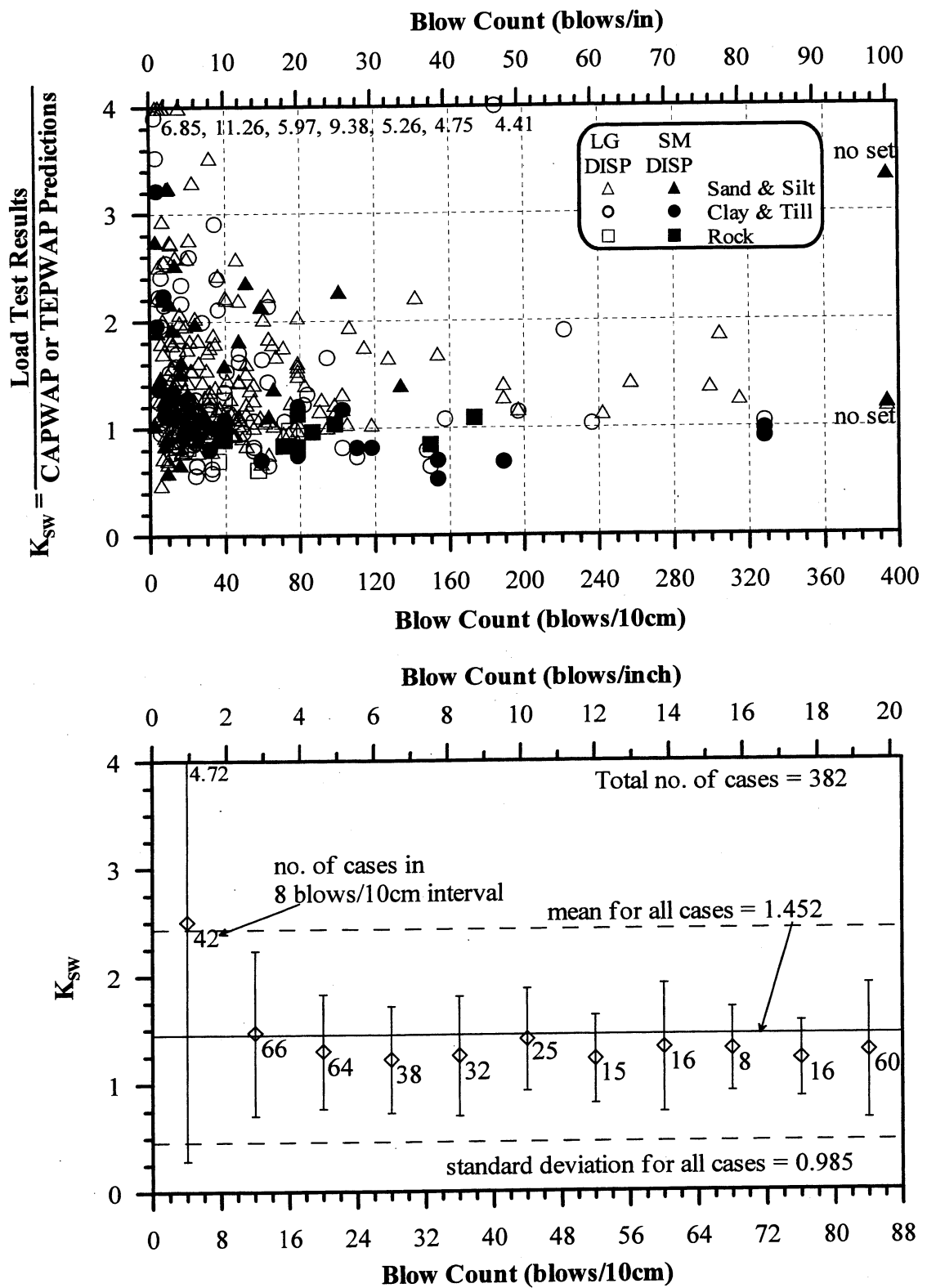


**Figure 5.19.**  $K_{sw}$  versus Blow count for all piles cases in PD/LT2000.

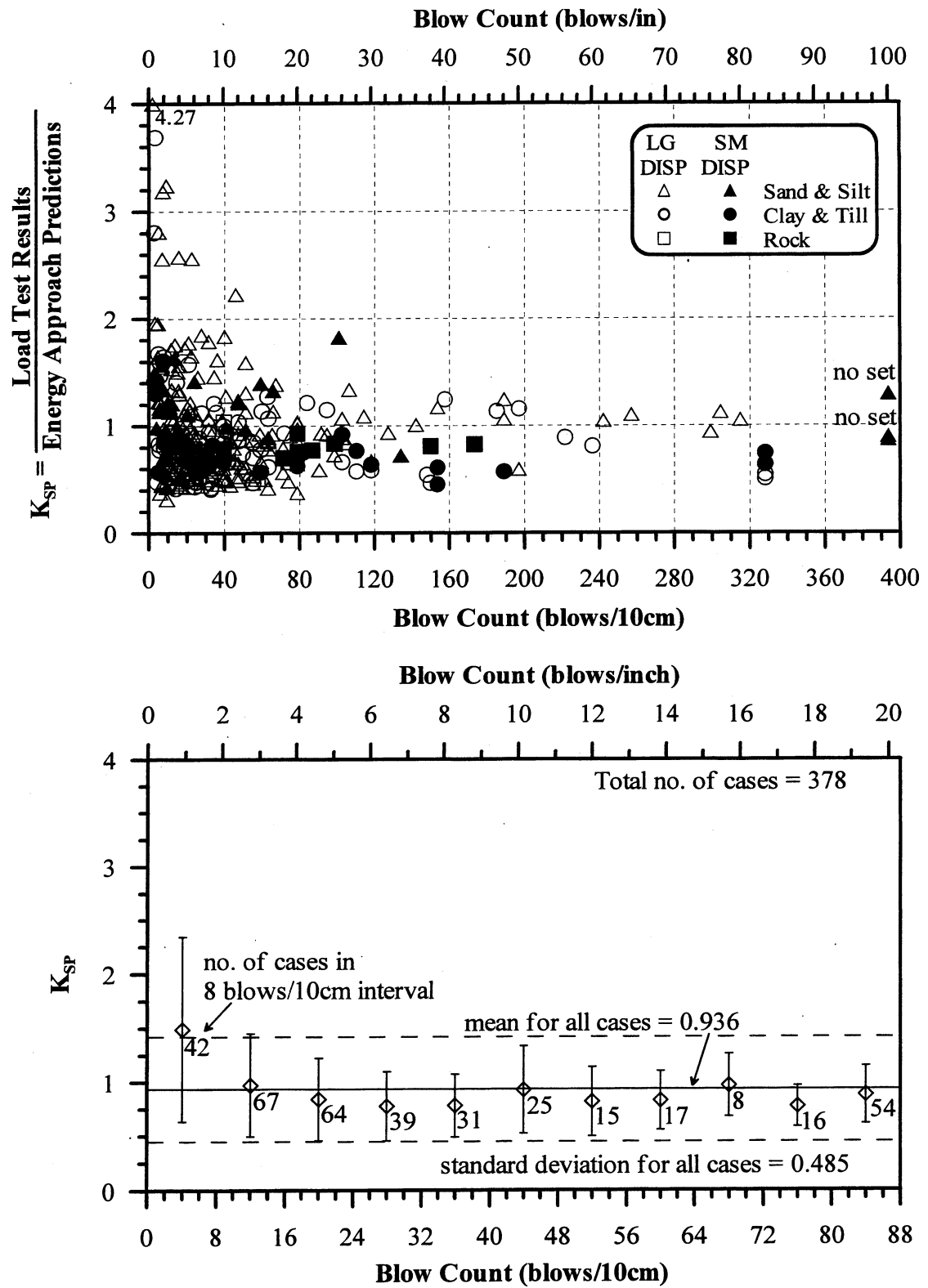


**Figure 5.20.** K<sub>SP</sub> versus Blow count for all piles cases in PD/LT2000.

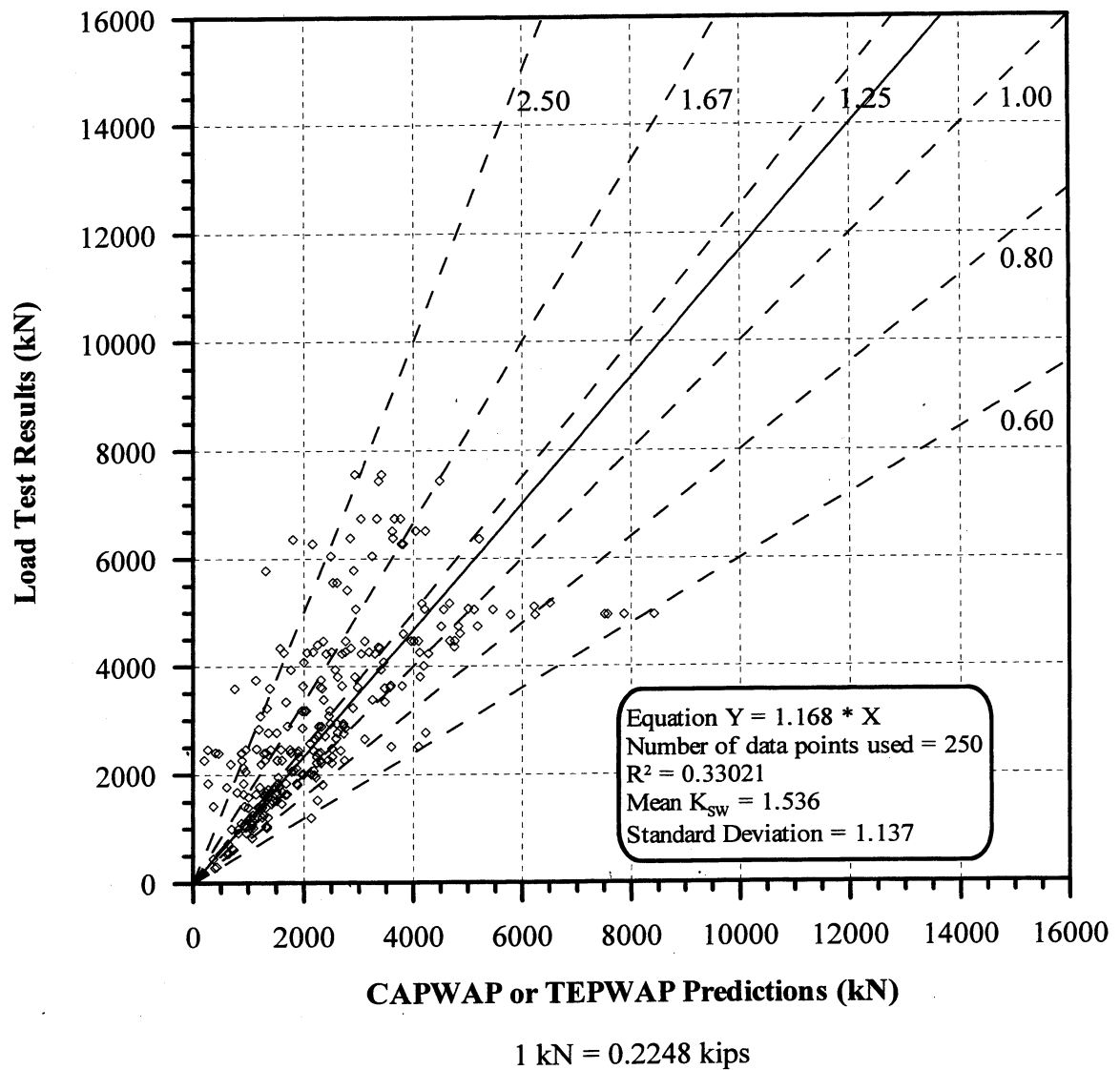
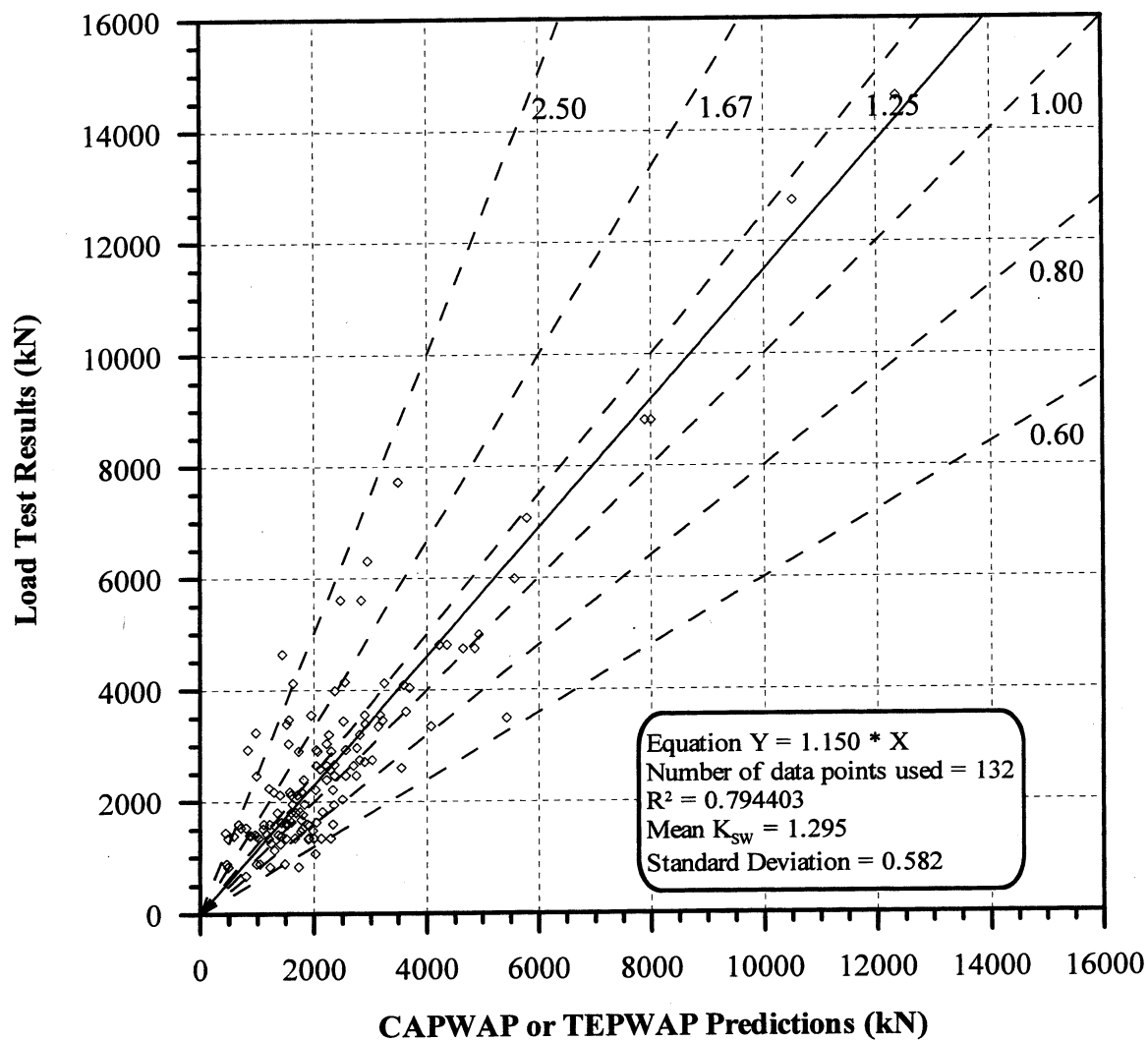


**Figure 5.21.** Static Load Test Results vs. CAPWAP or TEPWAP predictions for 250 PD/LT2000 pile-cases with Area Ratio < 350 in all types of soils (AAA).





1 kN = 0.2248 kips

**Figure 5.22.** Static Load Test Results vs. CAPWAP or TEPWAP predictions for 132 PD/LT2000 pile-cases with Area Ratio  $\geq 350$  in all types of soils (AAA).

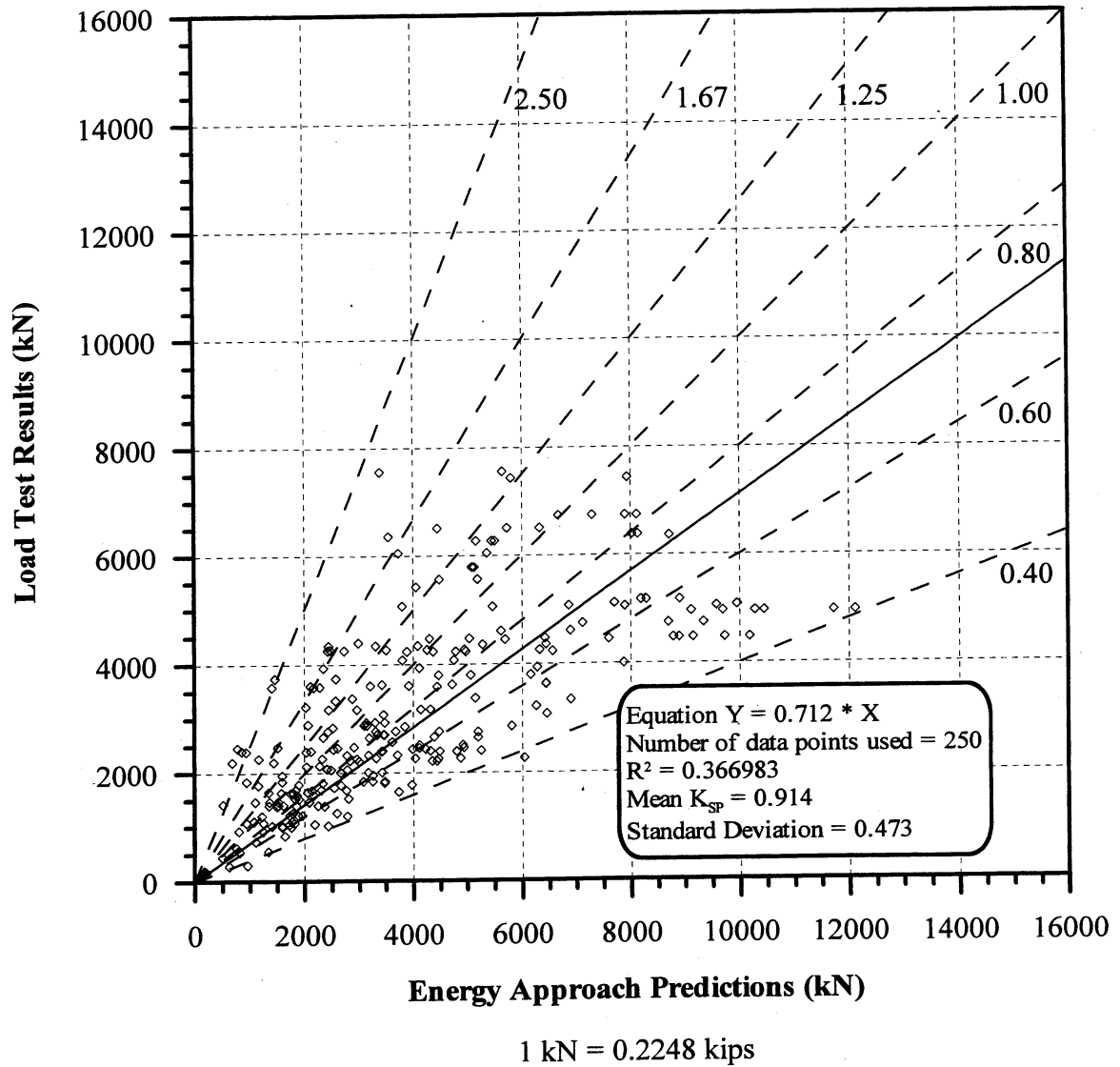


**Figure 5.23.** Static Load Test Results vs. Energy Approach predictions for 250 PD/LT2000 pile-cases with Area Ratio < 350 in all types of soils (AAA).

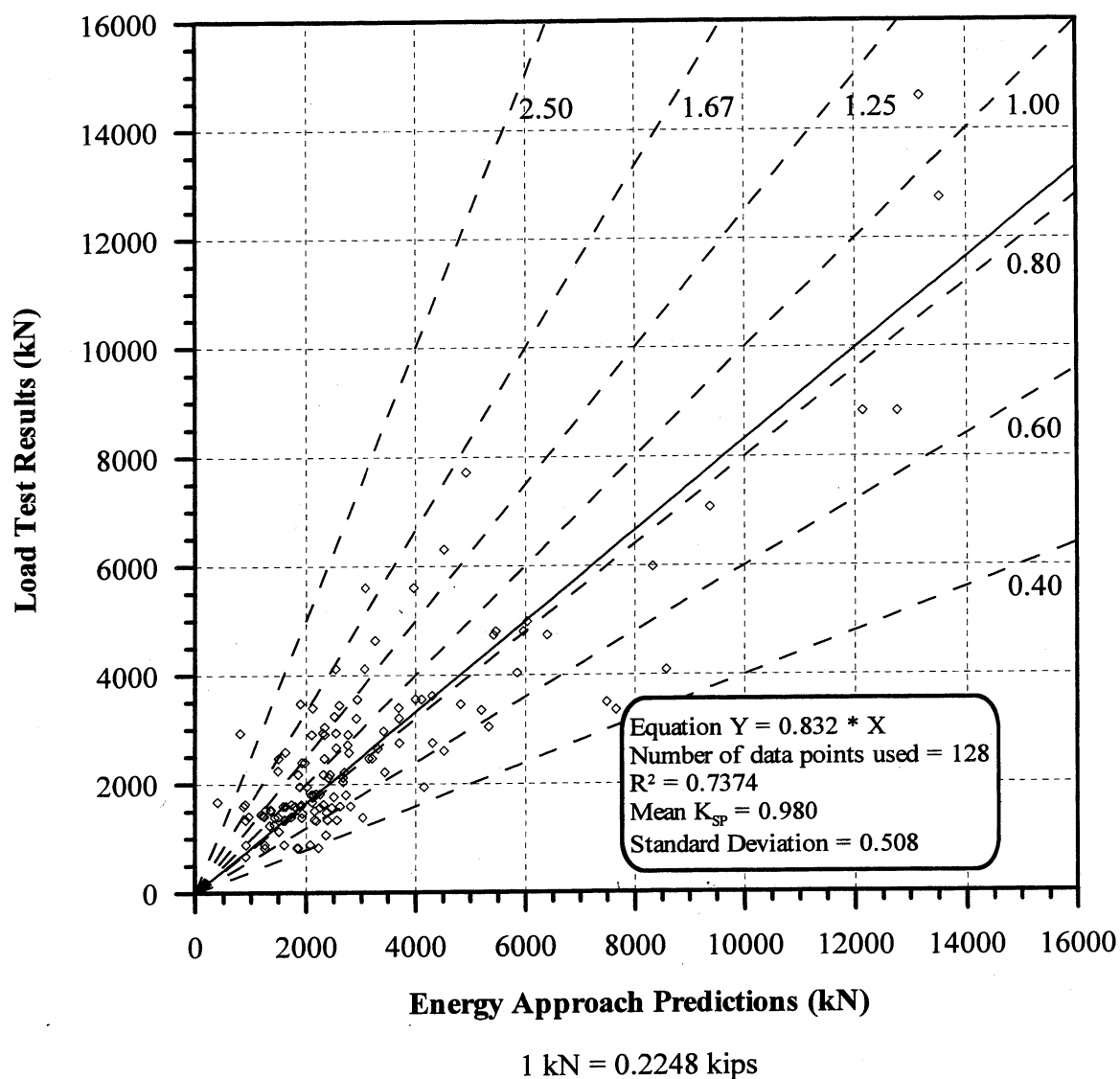


**Figure 5.24.** Static Load Test Results vs. Energy Approach predictions for 128 PD/LT2000 pile-cases with Area Ratio  $\geq 350$  in all types of soils (AAA).

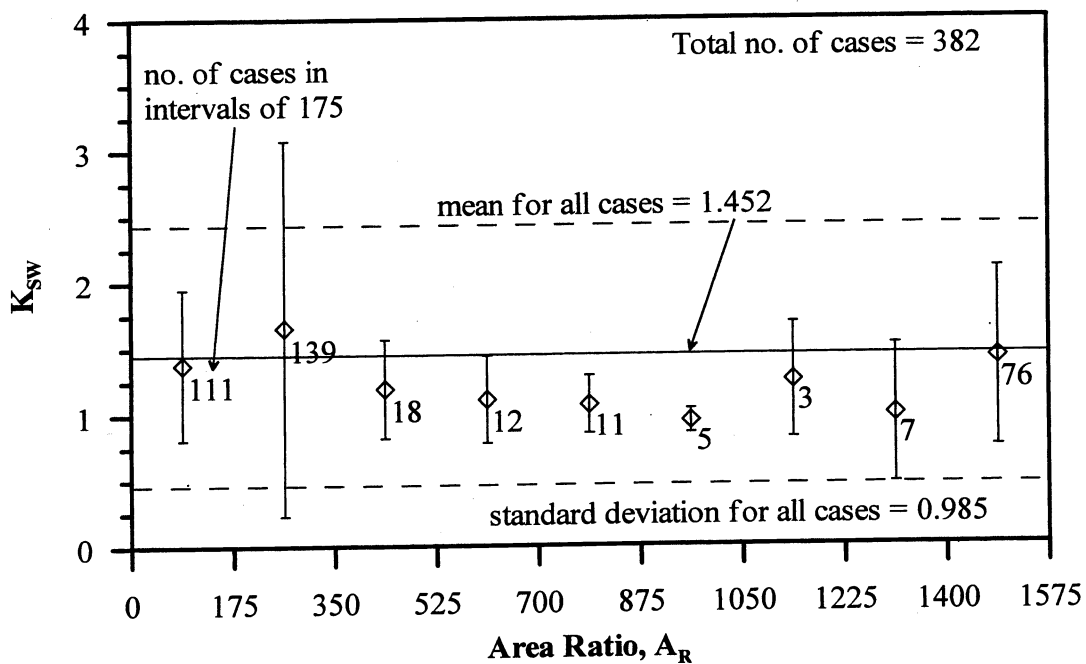
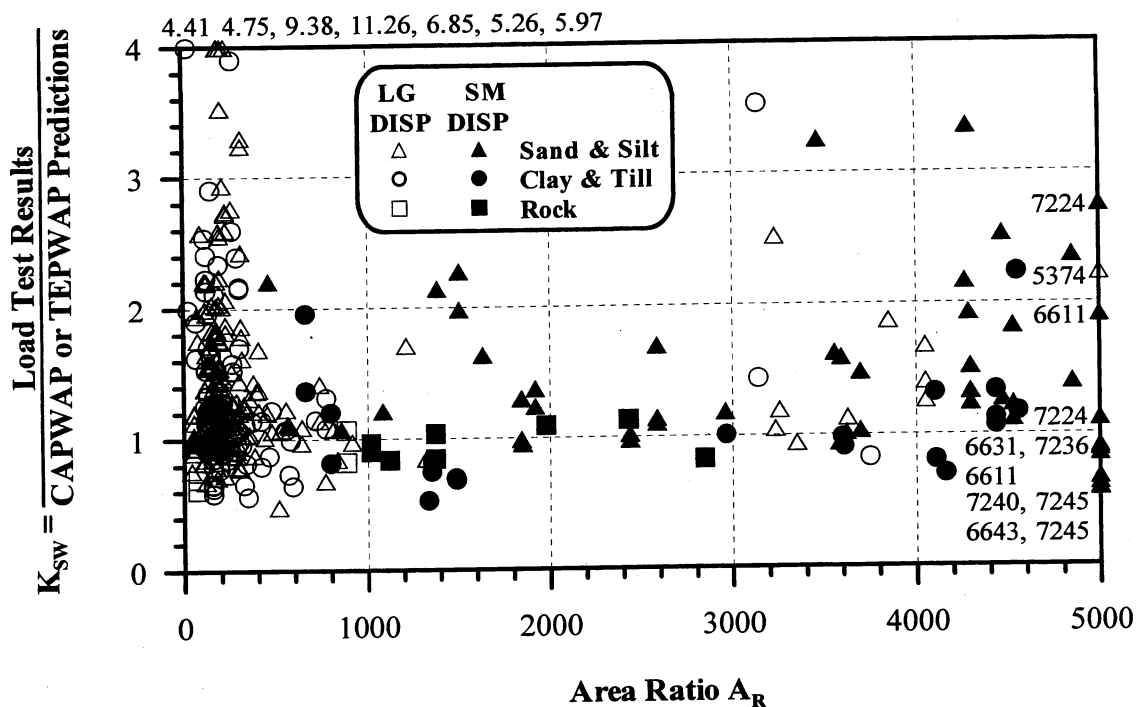


**Figure 5.25.**  $K_{SW}$  versus Area Ratio for all piles cases in PD/LT2000.

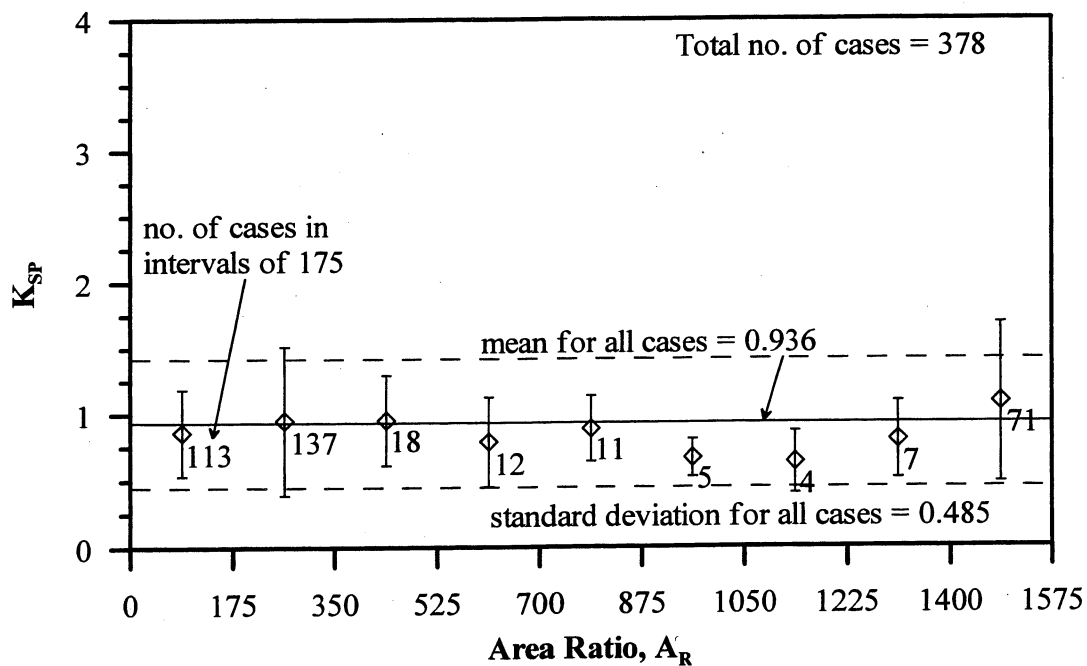
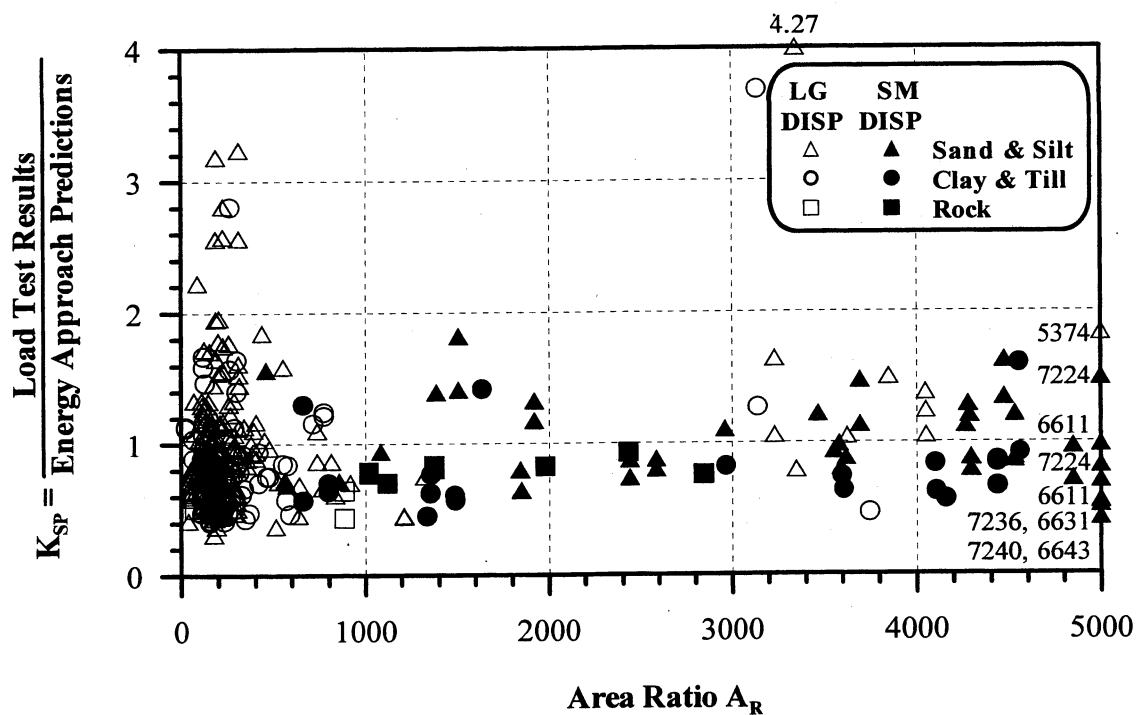


**Figure 5.26.**  $K_{SP}$  versus Area Ratio for all piles cases in PD/LT2000.

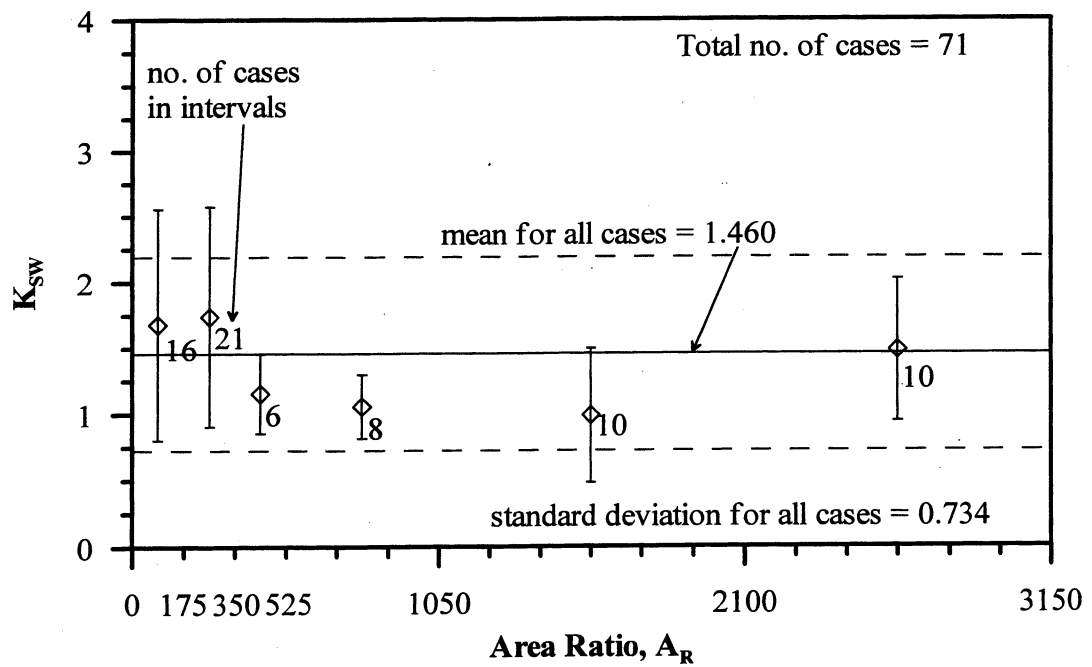
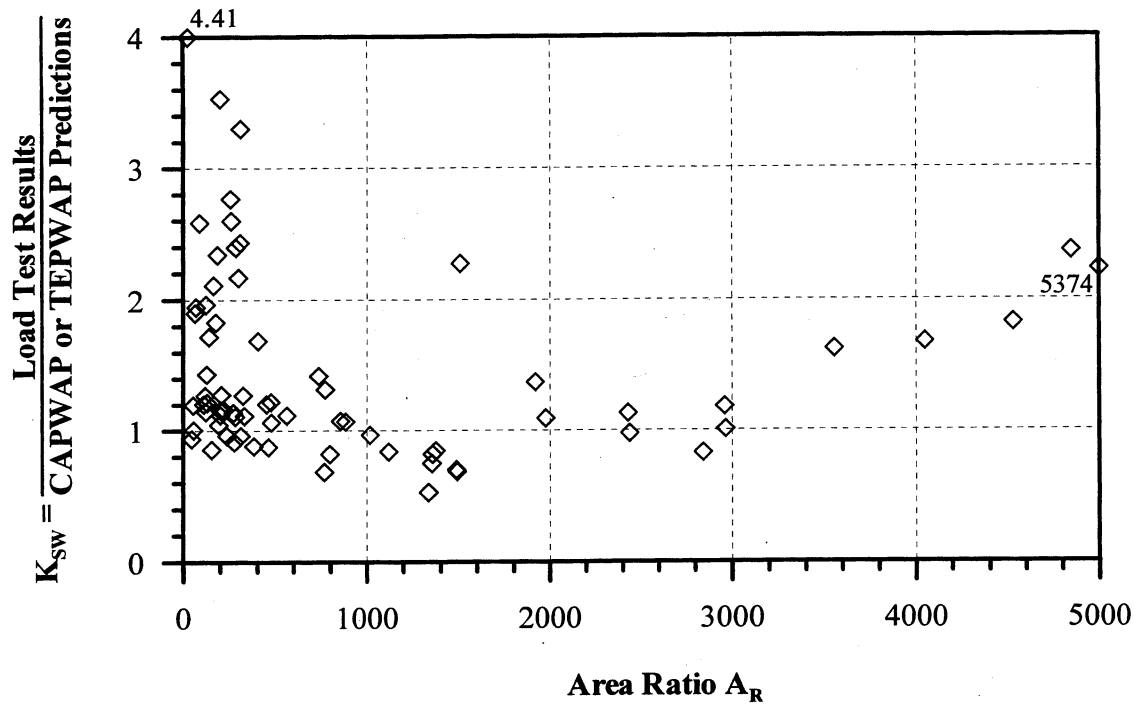


**Figure 5.27.**  $K_{sw}$  versus Area Ratio for 71 PD/LT2000 pile-cases at EOD with Blow Count  $\geq 16$  BP10cm in all types of soils.

## **CHAPTER 6**

### **PERFORMANCE OF THE DYNAMIC METHODS DURING THE CONSTRUCTION STAGE**

#### **6.1 OVERVIEW**

Figure 6.1 presents a flow chart outlining the breakdown of the dynamic analyses to be carried out. The dynamic methods can be broadly subdivided into two categories associated with the project stages: the design stage, employing a wave equation analysis (WEAP) to determine the driving system and the pile's drivability and the construction stage, in which capacity, driving criterion and quality control are required. The performance of the WEAP for drivability and pile design is highly important. The evaluation of the WEAP in pile design includes for example stress analysis, leading to load factors (see Figure 6.1). This evaluation was not included in this research. The wave equation analysis program is reviewed however in this chapter as a dynamic method for determining static pile capacity. This practice is questionable due to a high variability in the input parameters and the difficulties associated with the monitoring of the driving system without dynamic measurements. Generally, dynamic analyses are carried out using one of two methods, depending on whether dynamic measurements were recorded during pile driving. The first method, the dynamic equations, are commonly used when dynamic measurements are not recorded in the field. When dynamic measurements are taken during driving the wave

matching techniques or the field evaluation methods are used to determine the pile's capacity.

## **6.2 DYNAMIC ANALYSES WITHOUT DYNAMIC MEASUREMENTS**

### **6.2.1 WEAP Analysis**

The evaluation of WEAP (Wave Equation Analysis Program) effectiveness for capacity predictions is difficult as a large number and range of input parameters is possible, and the results are greatly affected by the actual field conditions. Examination of the method through analyses making use of default values is probably the only possible avenue. Other evaluations including WEAP analysis adjustments following dynamic measurements (e.g. matching energy) seem to be impractical in light of other available methods once dynamic measurements are performed. Such procedures lead to questionable results regarding their quality and meaning (Rausche et al., 2000 and Rausche, 2000). The wave equation analysis in this section will be evaluated using WEAP default input values and the pile's driving resistance at the End Of Driving (EOD) and Beginning Of Restrike (BOR) compared to the static load test results.

Figure 6.2 presents a comparison between the static load test results and the pile capacity prediction using the WEAP analysis at the EOD. This comparison is possible using a database obtained from GRL Inc., as described in chapter 3. The mean and standard deviation, 1.656 and 1.199, respectively, show that the WEAP analysis at the EOD performs poorly. The slope of the line forced through zero of actual results over the predicted results is 1.081. The scatter is very large as the



prediction ratios range from an under-prediction ratio of over 10 to an over-prediction ratio of about 0.6. The  $R^2$  value of 0.359 and COV of 0.724 show the poor performance of the WEAP analysis as a method for determining pile capacity at the EOD. This conclusion should not be mistaken with the importance of the use of the wave equation analysis during the design stage and its role in the determination of the driving equipment, drivability and the stresses in the pile during driving.

A comparison between the static load test results and the standard WEAP predictions at the BOR (provided by GRL, Inc.) is shown in Figure 6.3. The mean and standard deviation are 0.939 and 0.399, respectively, which results in a COV of 0.425, indicating a good correlation between the actual and predicted capacities. Based on the  $R^2$  value of 0.494 there is a poor correlation between the data and the best-fit line. It needs to be noted that this is not representative of how the WEAP method performs as an analysis program because knowledge of the specific site has generally been obtained from the initial driving of the pile and therefore, default input values are generally not used. Moreover, the hammer performance and driving system behavior is more difficult to assess at restrikes than at the EOD after a period of operation during driving.

### **6.2.2 The Dynamic Equations**

#### ***a) General***

The dynamic equations are commonly used to evaluate pile capacity when dynamic measurements are not recorded in the field at either the EOD or BOR, (see section 2.3.2). The two most commonly used dynamic equations in practice (USA)

are the Engineering News Record (ENR) equation (Wellington, 1892) and the Gates equation (Gates, 1957). These equations are evaluated in this research as well as the Federal Highway Administrations (FHWA) version of the Gates equation as suggested previously by Richard Cheney, (FHWA, 1988).

***b) ENR Equation***

The Engineering News Record (ENR) equation (Wellington, 1892) has a factor of safety of 6 incorporated directly into the equation (see section 2.3.2b). As the LRFD principles substitute for the factors of safety, the evaluation of the ENR equation was performed with and without the built in factor of safety.

Figure 6.4 presents the relationship between the static load test results and the pile capacity as calculated using the ENR equation (eliminating the factor of safety) for 384 pile-cases. The mean KSEN value, which is the ratio of the static load test results over the pile capacity prediction using the ENR equation, is 0.267 with a standard deviation of 0.243. The coefficients of variation and determination of 0.910 and 0.223, respectively, indicate the extremely poor performance of the equation. When the factor of safety of six is not incorporated into the equation the mean over-prediction ratio is 0.162 with the prediction ratios ranging from less than 0.1 to approximately 2.0. This shows that in addition to the method over-predicting by a considerable amount there is a very large amount of scatter in the prediction ratios (static load test results over the predicted results).

Figure 6.5 shows the relationship between the static load test results and the ENR equation pile capacity predictions in its typical format, with the built in factor of

safety of 6. The mean (1.600) and standard deviation (1.458) increase, logically, by a multiple of the factor of safety (6) from the case where the built in factor of safety is excluded, (Figure 6.4). The COV and  $R^2$  values remain the same whether or not the built in factor of safety is applied to the ENR equation, i.e., 0.910 and 0.223, respectively. Due to the poor performance of the ENR equation further evaluation of the prediction on the basis of sub categorization was not carried out.

**c) *Gates Equation***

A comparison between the static load test results and the pile capacity as determined by the Gates equation is presented in Figure 6.6 using 384 pile-cases from the database PD/LT2000. The mean and standard deviation of the ratio of the static load test results over the Gates equations predictions are 1.787 and 0.848, respectively. The data shows that the Gates equation performs relatively well but there is a significant bias (under-prediction) indicated by the slope of the best fit line (forced through zero), which is 1.828. There is also a large amount of scatter of the data as the prediction ratios (static load test results over the predicted results) range from approximately 0.6 to 6.0. Based on the  $R^2$  value of 0.412 and the COV of 0.475 there is poor and moderate correlation, respectively, between the actual and predicted pile capacities.

**d) *FHWA modified Gates Equation***

Figure 6.7 shows the comparison of the static load test results and the pile capacity predictions using the FHWA version of the Gates equation for 384 pile-cases from PD/LT2000. The mean  $K_{SFG}$  value, which is the ratio of the static load test

results to the pile capacity determined using the FHWA version of the Gates equation, is 0.940 with a standard deviation of 0.472. The mean over-prediction ratio, which is the ratio of the static load test results over the pile capacity, as calculated using the FHWA version of the Gates equation, is 0.922. The scatter is fairly significant ( $R^2 = 0.417$ ) with prediction ratios (static load test results over the predictions) ranging from about 0.4 to 4.0. Correcting for the bias of the original Gates equation, the FHWA version of the Gates equation performs overall better with a small over prediction (0.922), but a slightly higher COV (0.502 vs. 0.475).

***e) The Recommended Dynamic Equation and its Performance***

Table 6.1 presents a summary of the statistical data for the three evaluated dynamic equations with ENR presented with and without the built in factor of safety. The table shows that the FHWA version of the Gates equation has the smallest bias of the three dynamic equations that were reviewed. While the bias is smaller in the FHWA modified equation the coefficient of variation is slightly higher than the original Gates equation. The mean is close to one and the standard deviation is reasonably small considering that the equation does not utilize any field measurements other than the blow count. The FHWA version of the Gates equation seems to be suitable to evaluate pile capacity if no dynamic measurements are taken and is further evaluated in this section according to the controlling parameters described in chapter 5. The evaluation of the controlling parameters in chapter 5 showed that the time of driving (EOD and BOR) and the driving resistance (blow count) had the largest effect on the performance of the dynamic methods. The FHWA version of the Gates

equation is further evaluated based on the combinations of these controlling parameters.

Shown in Figure 6.8 is the comparison between the static load test results and the pile capacity predictions as obtained using the FHWA version of the Gates equation for 135 EOD pile-cases from PD/LT2000. The mean  $K_{SFG}$  value is 1.073 with a standard deviation of 0.573, which is a slight decrease in the performance of the equation compared to all pile-cases. The COV is 0.534, which shows that there is a moderate correlation between the actual and predicted results. The mean under prediction ratio (static load test results over the predicted results) is 1.048, while the scatter ranges from an over prediction ratio of approximately 0.4 to an under-prediction ratio of approximately 3.2, which shows no to little change from the scatter for all pile-cases. The  $R^2$  value of 0.412 also shows that there is a significant scatter in the data.

Figure 6.9 presents the comparison between the static load test results and the pile capacity prediction using the FHWA version of the Gates equation for 159 BOR (last) pile-cases from the PD/LT2000 database. The mean and standard deviation are 0.833 and 0.403, respectively and have decreased minimally from that for all pile-cases as shown in Figure 6.7. There is a moderate correlation between the actual and predicted pile capacities based on the COV of 0.484. The mean over-prediction ratio (static load test results over the predicted results) is 0.828, which is a slight increase from that for all pile-cases. The scatter remains approximately the same as for all pile-

cases as the prediction ratios for the BOR (last) pile-cases ranges from approximately 0.4 to 2.5 and the  $R^2$  value is 0.487.

A comparison between the static load test results and the pile capacity predictions using the FHWA version of the Gates equation for 62 PD/LT2000 pile-cases at the EOD with blow counts less than 16 BP10cm is shown in Figure 6.10. The mean  $K_{SFG}$  for these pile-cases is 1.306 with a standard deviation of 0.643, which is a significant increase from the mean and standard deviation for all pile-cases (refer to Figure 6.7). The coefficient of variation 0.492, which is approximately equal to that for all cases (0.502), shows that there is a moderate correlation between the actual and predicted results. The mean under-prediction ratio (static load test results over the predicted results) is 1.282, which is significant increase from the mean over-prediction ratio of 0.922 for all pile-cases. The amount of scatter did not change from that for all pile-cases as the prediction ratios still range from approximately 0.6 to 2.5 and the  $R^2$  value is still 0.418.

Figure 6.11 presents the comparison between the static load test results and the pile capacity prediction for 32 BOR (last) pile-cases with blow counts less than 16 BP10cm using the FHWA version of the Gates equation. The mean  $K_{SFG}$  value of 0.929 is basically the same as that for all pile-cases, 0.940, while the standard deviation has increased significantly from 0.472 for all pile-cases to 0.688 for this specific case. The COV (0.741) shows that there is a poor correlation between the actual and predicted pile capacities. The mean over-prediction ratio also basically remains unchanged, as it is 0.929. The scatter is still significant as the prediction

ratios (static load test results over the predicted results) range from approximately 0.4 to 2.0. There are a few pile-cases that do not fall within the range of scatter described above, which causes the low  $R^2$  value of 0.215, which also shows the poor correlation between the data.

The mean and standard deviation for the comparison between the static load test results and the pile capacity determined using the FHWA version of the Gates equation for 73 PD/LT2000 pile-cases at the EOD with blow count greater than 16 BP10cm as shown in Figure 6.12 is 0.876 and 0.419, respectively. This is an insignificant change from the mean and standard deviation for all pile-cases with a pile capacity prediction using the FHWA version of the Gates equation as shown in Figure 6.7. The mean over-prediction ratio has increased slightly from 0.922 for all pile-cases to 0.967 for the pile-cases at the EOD with blow counts greater than 16 BP10cm. The  $R^2$  value of 0.468 shows that there is significant scatter in the data. The prediction ratios range from 0.4 to 2.5, which also shows that there is significant scatter in the data.

Figure 6.13 presents the comparison between the static load test results and the pile capacity prediction using the FHWA version of the Gates equation for 73 pile-cases at the BOR (last) with blow counts greater than 16 BP10cm. The mean  $K_{SFG}$  value for these pile-cases is 0.809, which is a slight decrease from the mean for all pile-cases of 0.940. The standard deviation of 0.290 has decreased significantly from that for all pile-cases (0.472). There is a good correlation between the actual and predicted results based on the COV of 0.358. The mean over-prediction ratio has also

decreased from 0.922 for all pile-cases to 0.820 for these specific pile-cases. The scatter has also decreased slightly as the upper range of the prediction ratio decreased from approximately 2.5 for all pile-cases to 1.7 for the pile-cases analyzed in Figure 6.13. This decrease in scatter is also shown by the increase in the  $R^2$  value from 0.417 to 0.499.

The analysis presented in this section shows that the performance of the FHWA version of the Gates equation for all sub-groupings is approximately the same as for all pile-cases, the exceptions being for the EOD cases and the EOD cases with blow counts less than 16 blows per 10 cm.

*f) Summary of the Dynamic Equations Performance*

Table 6.2 presents a summary of the statistics representing the performance of the ENR equation (with and without the built in factor of safety), the Gates equation and the modified Gates equation. This table includes the data shown in Table 6.1 as well as the sub-categorization of the FHWA version of the Gates equation. A relatively small over-prediction exists in the FHWA version of the Gates equation for the BOR condition compared to the EOD. The data in the table shows that the FHWA version of the Gates equation performs more accurately for the BOR cases with high blow counts ( $COV = 0.358$ ) compared to those with low blow counts ( $COV = 0.741$ ).

## **6.3 DYNAMIC ANALYSES WITH DYNAMIC MEASUREMENTS**

### **6.3.1 Overview**

Three dynamic analysis methods are evaluated in this section, the wave matching techniques (CAPWAP or TEPWAP) and the field evaluation methods (the



Energy Approach and the Case method). Each of the methods is evaluated using the sub-groupings (described in chapter 5) according to the major controlling parameters.

The first step to the analysis was to evaluate the effect of the extreme pile-cases. For these cases, the ratio of the static load test results to the predicted pile capacity (using either the wave matching techniques or the Energy Approach) was either extremely small or large, relative to the overall performance of the examined method. The pile-cases for which the  $K_{SX}$  value was outside two standard deviations for all pile-cases were isolated to determine if there were any problems with the data. No problems were found with the BOR data but some difficulties that were identified with the EOD pile-cases are shown in Table 6.3. The identified EOD pile-cases are shown in Table 6.3. These data were removed from the general population and a brief explanation is provided in Table 6.3 as to why the data were removed. The extreme data that were removed from the general population of the PD/LT2000 database were kept for the area ratio sub-groupings where its extreme performance is relevant.

### **6.3.2 Performance of the Signal Matching Technique (CAPWAP or TEPWAP)**

#### ***a) All Pile-Cases***

The pile capacity predictions of the signal matching analyses are shown in Figure 6.14 compared to the static load test results for all pile-cases (377). The mean and standard deviation of the ratio of the static load test results to the CAPWAP/TEPWAP predictions are 1.368 and 0.620, respectively. The COV (0.453) shows that there is a moderate correlation between the compared data. The wave matching analyses under predict the pile capacity by a mean prediction ratio (load test

results over the prediction) of 1.368, with is the slope of the best-fit line forced through the origin being 1.160. There is a significant amount of scatter in the CAPWAP/TEPWAP predictions as the COV is 0.453 with the prediction ratios ranging from approximately 0.6 to over 4.5 and the  $R^2$  value is 0.557.

***b) Performance According to Time of Driving***

The wave matching technique predictions were sub-grouped according to the time of driving (i.e., End Of Driving, EOD, or Beginning Of Restrike, BOR). Each of these categories was then compared to the static load test results. The BOR (last) refers to the piles that had multiple restrikes; for which only the last restrike was used in the evaluation of the wave matching technique predictions. Figures 6.15 and 6.16 present the comparison between the static load test results and the wave matching technique predictions for EOD and BOR, respectively.

Shown in Figure 6.15 is the comparison between the static load test results and the CAPWAP/TEPWAP predictions at the EOD for 125 PD/LT2000 pile-cases. The statistics show that the signal matching techniques do not perform well at the EOD as the mean  $K_{SW}$  value is 1.626 with a standard deviation of 0.797, this is a significant decrease in performance from the statistics for all pile-cases as shown in Figure 6.14. The scatter is significant with the predictions ratios (static load test results over the predicted results) ranging from 0.6 to above 2.5 with a mean under-prediction ratio of 1.626 and a best line through the origin slope of 1.284. The coefficient of variation and determination are 0.490 and 0.653, respectively, which also indicate the

significant scatter and moderate to poor correlation between the actual and predicted results.

Figure 6.16 presents the comparison between the static load test results and the predicted pile capacity at the beginning of restrike (BOR) by the CAPWAP/TEPWAP wave matching techniques for 162 PD/LT2000 pile-cases. The method in this category performed very well with the mean  $K_{sw}$  value being 1.158 and a relatively small standard deviation of 0.393. The scatter ranges from approximately an over-prediction ratio 0.60 to an under prediction ratio 2.50 but the majority of the predictions (about 81%) fall within the range of predictions ratios between 0.8 and 1.67. The  $R^2$  value of 0.599 and the COV value of 0.339 indicate a moderate to good correlation between the actual and the predicted results. The mean under-prediction ratio is 1.158 and a best-fit line through the origin has a slope of 1.104, both suggest good agreement between the measured and predicted values.

The categorization according to the time of driving for the wave matching technique predictions compared to the static load test results show a significant improvement in the CAPWAP/TEPWAP methods from the end of driving cases to the beginning of restrike cases. As is shown in Figures 6.15 and 6.16 the wave matching techniques perform exceptionally well at the beginning of restrike but they perform very poorly at the end of driving.

**c)      *Performance According to Driving Resistance***

The pile capacity prediction of the CAPWAP/TEPWAP methods are analyzed by comparing the performance of the pile-cases that had a driving resistance greater

than 16 BP10cm against those with a driving resistance lower than 16 BP10cm, both at the end of driving and beginning of restrike. The four combinations of the above-described comparisons are presented in Figures 6.17 through 6.20.

Figure 6.17 shows the comparison between the static load test results and the wave matching technique predictions for 54 PD/LT2000 pile-cases at the end of driving with blow counts less than 16 BP10cm. The mean  $K_{SW}$  value and its standard deviation are 1.843 and 0.831, respectively, which have not changed significantly from the mean (1.626) and standard deviation (0.797) for all pile-cases at the end of driving. There is a moderate correlation between the actual and predicted pile capacities as is shown by the COV (0.451) and the  $R^2$  value (0.677). The mean under-prediction ratio is 1.843 with the ratios ranging from approximately 0.8 to 3.2, the slope of the best-fit line forced through the origin, is 1.388.

A comparison between the static load test results and the wave matching technique predictions for 71 PD/LT2000 pile-cases at the end of driving with blow counts greater than or equal to 16 BP10cm is presented in Figure 6.18. The mean  $K_{SW}$  for these pile-cases is 1.460, which is lower than that for the pile-cases with blow counts less than 16 BP10cm (1.843). The standard deviation is 0.734, which is approximately equal to that for pile-cases with blow counts less than 16 BP10cm (0.831). There is a moderate correlation between the actual and predicted data as shown by the COV (0.502) and the  $R^2$  value (0.647). The mean under-prediction ratio is 1.460 with the ratios ranging from approximately an over-prediction of 0.6 to an under-prediction of 3.2; the slope of the best-fit line forced through the origin is 1.236.

Figure 6.19 presents the comparison between the static load test results and the pile capacity prediction based on the signal matching techniques for 32 PD/LT2000 pile-cases at the beginning of restrike with blow counts less than 16 BP10cm. The slope of the best-fit line through the origin is 1.189. The mean  $K_{SW}$  value and its standard deviation for these pile-cases are 1.176 and 0.530, respectively, with the data ranging from  $K_{SW}$  values of approximately 0.6 to 2.5. The COV (0.451) shows a moderate to good correlation between the actual and predicted results, while the  $R^2$  value (0.717) shows a good correlation and a small amount of scatter.

Figure 6.20 presents the comparison of the static load test results and the wave matching predictions for 130 PD/LT2000 pile-cases at the beginning of restrike with blow counts greater than or equal to 16 BP10cm. The mean  $K_{SW}$  value is 1.153 with a standard deviation of 0.354, with the ratio ranging from an over-prediction ratio of approximately 0.6 to an under-prediction ratio of 2.5. The slope of the best-fit line forced through the origin, is 1.096. The COV (0.307) shows that there is a good to very good correlation between the actual and predicted results and a significant improvement over the data in Figure 6.19 (COV = 0.451). The  $R^2$  value (0.526) shows that there is a meaningful amount of scatter and a moderate to poor correlation between the data.

The figures presented in this section show that for the beginning of restrike pile-cases there is a significant effect on the performance of wave matching techniques based on the driving resistance. This effect is not as apparent for the end of driving

pile-cases and becomes clearer only when the pile type (through area ratio) is considered.

***d) Performance According to Pile Type***

The performance of the wave matching techniques based on the soil displacement / pile type, utilizes the area ratio as described in section 5.3.3a. Four combinations of cases based on driving resistance and area ratio (see Figure 6.1) are explored and presented in Figures 6.21 through 6.28.

Figure 6.21 presents the static load test results compared to the wave matching predictions for 37 PD/LT2000 pile-cases at the end of driving with blow counts less than 16 BP10cm and area ratio less than 350 (this sub-grouping includes the 5 extreme CAPWAP pile-cases, detailed in Table 6.3). The mean  $K_{SW}$  value and the standard deviation are 2.589 and 2.385, respectively; show a very poor performance of the CAPWAP/TEPWAP predictions for large displacement piles under easy driving resistance at the end of driving. The coefficients of variation and determination are 0.921 and -0.082, respectively, indicating the extremely poor performance of the method and the large scatter of the data under the analyzed conditions.

The static load test results compared to the wave matching technique predictions are presented in Figure 6.22 for 22 PD/LT2000 pile-cases at the end of driving with blow counts less than 16 BP10cm and area ratios greater than or equal to 350. The mean  $K_{SW}$  value for these pile-cases is 1.929 with a standard deviation of 0.698 resulting in a COV of 0.362. The  $R^2$  value (0.776) shows a moderate to good correlation between the actual and predicted pile capacities with the ratio ranging from

1.0 to an under-prediction ratio of approximately 2.5 with all pile-cases under-predicting the pile's capacity.

A comparison between the static load test results and the wave matching technique predictions for 37 PD/LT2000 pile-cases at the end of driving with blow counts greater than or equal to 16 BP10cm and area ratios less than 350 is presented in Figure 6.23. The mean  $K_{SW}$  value is 1.717 with a standard deviation of 0.841, resulting in a COV of 0.490, which shows a moderate correlation between the actual and predicted results. The ratio of the static load test results over the predicted capacity ranges from an over-prediction ratio of 0.8 to an under-prediction ratio of about 3.4. The  $R^2$  value (0.185) further indicates a poor correlation between the actual and predicted pile capacities.

Figure 6.24 presents a comparison between the static load test results and the wave matching technique predictions for 34 PD/LT2000 pile-cases at the end of driving with blow counts greater than or equal to 16 BP10cm and area ratios greater than or equal to 350. The mean  $K_{SW}$  value is 1.181, with a standard deviation of 0.468, resulting in a COV of 0.396; presenting a much better predictive performance than for the large displacement pile-cases shown in Figure 6.23. The  $R^2$  value (0.904) shows that there is little scatter and a good correlation to the best-fit line with a slope of 1.139 passing through the origin.

The static load test results are compared to the wave matching techniques in Figure 6.25 for 22 PD/LT2000 pile-cases at the beginning of restrike with blow counts less than 16 BP10cm and area ratios less than 350. The statistics show that for this

specific sub-category, the CAPWAP/TEPWAP method performs reasonably well with a mean  $K_{SW}$  value of 1.116 and a standard deviation of 0.362, which results in a COV of 0.324. The prediction ratios range approximately between 0.8 and 1.7, which also shows the good performance of the wave matching techniques for this specific sub-category. The  $R^2$  value (0.730) shows some scatter and a moderate correlation to the best-fit line with a slope of 1.207 passing through the origin.

Figure 6.26 presents the comparison between the static load test results and the wave matching techniques for 10 PD/LT2000 pile-cases at the beginning of restrike with blow counts less than 16 BP10cm and area ratios greater than or equal to 350. The mean  $K_{SW}$  value is 1.308 with a standard deviation 0.796, which gives a COV of 0.609, indicating a poor performance of the CAPWAP/TEPWAP methods for this specific category compared to the large displacement pile-cases as presented in Figure 6.25. The data ranges from prediction ratios of about 0.4 to 3.0. The large range in the data and the  $R^2$  value of 0.637 shows the moderate to poor performance of the CAPWAP/TEPWAP methods for this specific category.

Figure 6.27 presents the comparison of the static load test results and the wave matching technique predictions for 83 PD/LT2000 pile-cases at the beginning of restrike with blow counts greater than or equal to 16 BP10cm and area ratios less than 350. The mean  $K_{SW}$  value is 1.178 with a standard deviation of 0.379 and a COV of 0.321, which shows there is a good correlation between the actual and predicted pile capacities. The ratios range from an over-prediction ratio of 0.6 to an under-prediction ratio of about 2.9. The  $R^2$  value of 0.522 also shows the significant scatter in the data



around the best-fit line through the origin with a slope of 1.109 and a poor correlation between the actual and predicted results.

The static load test results are compared to the wave matching technique predictions for 47 PD/LT2000 pile-cases at the beginning of restrike with blow counts greater than or equal to 16 BP10cm and area ratios greater than or equal to 350 in Figure 6.28. The mean  $K_{SW}$  value is 1.110 with a standard deviation of 0.303, resulting in a COV of 0.273. The scatter is fairly significant around the best-fit line passing through the origin with a slope of 1.064. The prediction ratios range from approximately 0.6 to 2.4 and the  $R^2$  value is 0.484.

The analysis presented in this section shows that the performance of the signal matching methods (CAPWAP/TEPWAP) is affected by the pile type (small or large displacement) with the exception of the pile-cases at the beginning of restrike with blow counts greater than or equal to 16 BP10cm as presented in Figures 6.27 and 6.28.

### **6.3.3 Field Evaluation (Energy Approach)**

#### ***a) All Pile-Cases***

The Energy Approach predictions compared to the static load test results for 371 PD/LT2000 pile-cases are presented in Figure 6.29. The mean and standard deviation of the ratio of the static load test results to the Energy Approach predictions are 0.894 and 0.367, respectively, resulting in a COV of 0.411. The slope of the best-fit line forced through the origin is 0.73 and the  $R^2$  value is 0.542. The Energy Approach method for predicting pile capacity performs reasonably well overall,

however there is a significant amount of scatter in the predictions with the prediction ratios ranging from approximately 0.4 to 2.5.

***b) Performance According to Time of Driving***

To evaluate the effect of the time of driving, the Energy Approach predictions were sub-grouped according to the End Of Driving (EOD) and Beginning Of Restrike (BOR) (last) pile-cases and each of these categories were compared to the static load test results. The BOR (last) refers to the piles that had multiple restrikes; where only the last restrike was used in the evaluation of the method.

Figure 6.30 presents the comparison between the static load test results and the Energy Approach predictions at the EOD for 128 PD/LT2000 pile-cases. The mean  $K_{SP}$  value (ratio of the static load test results to the Energy Approach predictions) is 1.084 with a standard deviation of 0.431, which results in a COV of 0.398. The Energy Approach method performs very well compared to other methods for evaluating pile capacity based on the EOD data. The scatter of the data is significant with prediction ratios (static load test results over the predicted results) ranging from 0.4 to 2.5 with a best-fit line through the origin having slope of 0.926 and  $R^2$  of 0.542, indicating the significant amount of scatter in the data.

Figure 6.31 present the Energy Approach pile capacity predictions at the beginning of restrike (BOR) in comparison with the static load test results for 153 PD/LT2000 pile-cases. The mean  $K_{SP}$  value of 0.785, suggests mostly over prediction with a standard deviation of 0.290, resulting in a coefficient of variation of 0.369. The data ranges from approximately an over-prediction ratio of 0.4 to an under

prediction ratio of 1.7. The best-fit line through the origin has a slope of 0.695, which indicates a typical over prediction. The  $R^2$  value of 0.576 for this line suggests a large amount of scatter in the data in difference from the small COV.

The data in Figures 6.30 and 6.31 suggests that the Energy Approach performs reasonably well for both cases, but it significantly over predicts the piles capacity for the beginning of restrike case. It should be noted that the Energy Approach method was developed for use at the end of driving only (Paikowsky et al., 1994).

**c) *Performance According to Driving Resistance***

The performance of the Energy Approach is analyzed in this section based on the driving resistance. Hard driving is categorized as blow counts greater than or equal to 16 BP10cm and easy driving is categorized as those pile-cases with blow counts less than 16 BP10cm. The Energy Approach method is analyzed by comparing the predicted capacity to the measured capacity based on hard and easy driving pile-cases, both at the end of driving and beginning of restrike as presented in Figures 6.32 through 6.35.

Figure 6.32 shows the comparison between the static load test results and the Energy Approach predictions for 56 PD/LT2000 pile-cases at the end of driving with blow counts less than 16 BP10cm. The mean  $K_{SP}$  value and its standard deviation are 1.227 and 0.474, respectively, (COV = 0.386), which are similar to the mean (1.084) and standard deviation (0.431) for all pile-cases at the end of driving. The slope of the best-fit line forced through the origin, is 1.012 with a  $R^2$  value of 0.739 indicating that there is a moderate correlation.

A comparison between the static load test results and the Energy Approach predictions for 72 PD/LT2000 pile-cases at the end of driving with blow counts greater than or equal to 16 BP10cm is presented in Figure 6.33. The mean  $K_{SP}$  for these pile-cases is 0.972, with a standard deviation of 0.359, resulting in a COV of 0.369, indicating a good correlation between the actual and predicted pile capacities. The best-fit line through the origin has a slope of 0.885 and a  $R^2$  value of 0.680 with the scatter of data ranging from approximately a prediction ratio of 0.5 to 2.1.

Figure 6.34 presents the comparison between the static load test results and the pile capacity prediction based on the Energy Approach for 29 PD/LT2000 pile-cases at the beginning of restrike with blow counts less than 16 BP10cm. The mean  $K_{SP}$  value and its standard deviation are 0.830 and 0.352, respectively, resulting in a COV of 0.424, indicating a good correlation between the actual and predicted pile capacities. The  $R^2$  value of 0.553 suggests a significant scatter in the data around the best-fit line through the origin with a slope of 0.742.

Figure 6.35 presents the comparison of the static load test results and the Energy Approach predictions for 124 PD/LT2000 pile-cases at the beginning of restrike with blow counts greater than or equal to 16 BP10cm. The mean  $K_{SP}$  value is 0.775 with a standard deviation of 0.274, which results in a COV of 0.354. The slope of the best-fit line through the origin, 0.691, and the mean indicate that for this specific sub-category the Energy Approach over predicts the pile's capacity. The ratio ranges from an over-prediction of 0.4 to an under-prediction of approximately 1.7 with a scatter shown by the low  $R^2$  value of 0.525.

The figures presented in this section show that similarly to the signal matching analyses, the Energy Approach predicts the pile capacity for pile-cases with a hard driving resistance much more accurately than for the pile-cases with an easy driving resistance. This is shown for both the end of driving pile-cases as presented in Figures 6.32 and 6.33 as well as for the beginning or restrike pile-cases as presented in Figures 6.34 and 6.35.

**d)      *Performance According to Pile Type***

The performance of the Energy Approach method is evaluated in this section based on pile type, defining small and large displacement piles as those with area ratios greater and lower than 350, respectively. A comparison between the Energy Approach pile capacity predictions for small and large displacement piles to the static load test results is conducted for each of the analyses in the above section, i.e., eight comparisons all together, presented in Figures 6.36 through 6.43.

Figure 6.36 presents the static load test results compared to the Energy Approach predictions for 39 PD/LT2000 pile-cases at the end of driving with blow counts less than 16 BP10cm and area ratios less than 350 (this sub-grouping includes 4 of the extreme Energy Approach pile-cases, see Table 6.3). The mean  $K_{SP}$  value and its standard deviation are 1.431 and 0.727, respectively, which results in a COV of 0.508. The best-fit line through the origin has a slope of 1.018, with a large scatter shown by the range of prediction ratios from approximately 0.6 to 2.7 and a coefficient of determination,  $R^2$  of 0.134.

The static load test results compared to the Energy Approach predictions are presented in Figure 6.37 for 23 PD/LT2000 pile-cases at the end of driving with blow counts less than 16 BP10cm and area ratios greater than or equal to 350 (this sub-grouping includes 2 of the extreme Energy Approach pile-cases, see Table 6.3). The mean  $K_{SP}$  value is 1.422 with a standard deviation of 0.888, which results in a COV of 0.624. The best-fit line through the origin has a slope of 1.031 with the scatter ranging from prediction ratios of approximately 0.5 to about 3.3. The  $R^2$  value of 0.831 indicates smaller scatter mostly due to reasonably good predictions in the high capacity range.

A comparison between the static load test results and the Energy Approach predictions for 39 PD/LT2000 pile-cases at the end of driving with blow counts greater than or equal to 16 BP10cm and area ratios less than 350 is presented in Figure 6.38 (this sub-grouping includes 1 of the extreme Energy Approach pile-cases, see Table 6.3). The mean  $K_{SP}$  value for these pile-cases is 1.054 with a standard deviation of 0.459, resulting in a COV of 0.435. The best-fit line through the origin has a slope of 0.902 with the scatter ranging approximately from an over-prediction ratio of 0.5 to an under-prediction ratio of 1.8 with a coefficient of determination,  $R^2$  of 0.247 indicating the poor correlation of the method in this subcategory.

Figure 6.39 presents the comparison between the static load test results and the Energy Approach predictions for 34 PD/LT2000 pile-cases at the end of driving with blow counts greater than or equal to 16 BP10cm and area ratios greater than or equal to 350. The mean  $K_{SP}$  value is 0.926, with a standard deviation of 0.320, which results

in a COV of 0.346. The slope of the best-fit line through zero is 0.879, with the scatter ranging from ratios of approximately 0.4 to 1.8 with a coefficient of determination,  $R^2$  of 0.850 suggesting along with the COV value a relatively small amount of scatter in the data and a good performance of the Energy Approach for large displacement piles with a high driving resistance.

The static load test results are compared to the Energy Approach predictions in Figure 6.40 for 19 PD/LT2000 pile-cases at the beginning of restrike with blow counts less than 16 BP10cm and area ratios less than 350. The mean  $K_{SP}$  is 0.764 with a standard deviation of 0.318, resulting in a COV of 0.416. The Energy Approach method overall over predicts the pile capacity during restrike as also indicated by the slope of the best-fit line through zero, 0.736. There is a significant amount of scatter shown by the range of prediction ratios of approximately 0.4 to 1.4 with  $R^2$  value of 0.600.

Figure 6.41 presents the comparison between the static load test results and the Energy Approach predictions for 10 PD/LT2000 pile-cases at the beginning of restrike with blow counts less than 16 BP10cm and area ratios greater than or equal to 350. The mean  $K_{SP}$  value is 0.954 with a standard deviation 0.396, which results in a COV of 0.415. The slope of the best-fit line through the origin is 0.761 with a significant scatter shown by the  $R^2$  value of 0.334 and the range in prediction ratios of approximately 0.4 to 1.3. The amount of data is small and hence the information derived from it is limited.

Shown in Figure 6.42 is the comparison of the static load test results and the Energy Approach predictions for 82 PD/LT2000 pile-cases at the beginning of restrike with blow counts greater than or equal to 16 BP10cm and area ratios less than 350. The mean  $K_{SP}$  value is 0.736 with a standard deviation of 0.249, which results in a COV of 0.338. The Energy Approach method performs well for this sub-category, with over prediction of the pile capacity shown by the mean and by the slope of the best-fit line through zero of 0.685. The scatter ranges from an over-prediction ratio of 0.4 to an under-prediction ratio of about 1.8 and by the coefficient of determination,  $R^2$  of 0.573.

The static load test results are compared to the Energy Approach predictions for 42 PD/LT2000 pile-cases at the beginning of restrike with blow counts greater than or equal to 16 BP10cm and area ratios greater than or equal to 350 in Figure 6.43. The mean  $K_{SP}$  value is 0.851 with a standard deviation of 0.305, which results in a COV of 0.358. Again the Energy Approach method performs well for this specific category with the exception of the consistent over-prediction. The mean slope of the best-fit line through the origin is 0.712, while the scatter ranges from a prediction ratio of about 0.4 to 1.7 with a coefficient of determination,  $R^2$  of 0.269 indicating a large amount of scatter in the data.

The analysis presented in this section shows that the performance of the Energy Approach method is not affected by the pile type (small or large displacement) as much as the wave matching techniques. There is a slight effect on the Energy



Approach predictions based on pile type but none that are significant enough to require different resistance factors based on pile type.

#### **6.3.4 Field Evaluation (Case Method)**

##### ***a) General***

A background of the Case method is presented in section 2.3.4 (Goble et al., 1970 and Rausche et al., 1975). The method is often used in field evaluations, as it is built into Pile Dynamics Inc.'s Pile Driving Analyzer (PDA), and is commonly used in the USA. The method is based on a simplified pile and soil behavior assumptions (free end and plastic soil), resulting in a closed form solution related to the impact and its reflection from the tip. With the years, the method has evolved to be implemented into at least five different variations (GRL, 1999). The Case method utilizes a damping coefficient ( $J_c$ ) that is assumed to be associated with soil type. The influence of this factor on the predicted static capacity depends on the reflected wave from the pile's tip, and hence on the driving resistance. The case-damping coefficient was investigated through back calculation (to match the measured static capacity). The results, described in the next section, suggest no correlation between the soil type and the case-damping coefficient. The common recommended practice suggests the use of the method based on a specific site/area calibration (GRL, 1999).

##### ***b) Evaluation of the Case-Damping Coefficient***

A comparison between the back-calculated case-damping coefficient,  $J_c$ , based on the static load test result and the soil type at the pile tip is presented in Figure 6.44.  $J_c$  was calibrated using the static capacity  $R_s$  and the "standard" Case method, as

outlined by Goble et al. (1975). Paikowsky et al., (1994) originally presented this figure that shows data for 290 PD/LT pile-cases. The data in the figure shows that there is no correlation between the  $J_c$  value and the soil type at the tip as commonly assumed. The negative  $J_c$  values, which were back calculated from matching the load test results to the dynamic measurements, have no physical meaning and only demonstrate the limitations of the  $J_c$  coefficient.

**c) *Evaluation of the Case Method Based on Local Calibration***

A statistical examination of local calibration (in Florida) was performed by McVay et al. (2000). The results of this analysis suggested that for 48 cases, the ratio between the static pile capacities to the Case method predictions at the end of driving was  $1.344 \pm 0.443$  (mean  $\pm$  1 standard deviation). The data was obtained by the Geotechnical Engineering Research Laboratory at the University of Massachusetts Lowell from Professor Michael McVay of the UFL (see section 3.5). The data contained 40 EOD cases as well as 37 BOR cases. The RMX variation of the Case method was used to determine the static pile capacity and the  $J_c$  values that were used in each of the analyses range from 0.02 to 0.44. It should be noted that the presented data was obtained from 13 different sites throughout the state of Florida; and although considered as a local calibration, the use of the varied  $J_c$  leaves the analysis questionable.

Presented in Figure 6.45 is a comparison between the static load test results and the Case method predictions for 77 pile-cases at both the EOD and BOR. The mean  $K_{SCASE}$  value, which is the ratio of the static load test results over the case

predictions, is 1.183 with a standard deviation of 0.403, which results in a COV of 0.341. There is a large amount of scatter indicated by the  $R^2$  value of 0.361 and the range of prediction ratios from 0.6 to 2.7 while the slope of the best fit-line through the origin is 1.049.

Figure 6.46 presents the comparison between the static load test results and the Case method predictions for 40 EOD pile-cases. The mean  $K_{SCASE}$  value is 1.334 with a standard deviation of 0.438, which results in a COV of 0.328. These statistics are similar to that observed for the data presented in Figure 6.45 for all piles-cases. The scatter of the ratio ranges from approximately 0.6 to 3.1 and the  $R^2$  value is 0.470. The slope of the best-fit line through the origin is 1.165.

The comparison between the static load test results and the Case method predictions for 37 BOR pile-cases are shown in Figure 6.47. The statistics show a significant improvement in the performance of the case method for the BOR pile-cases as the mean is approximately one (1.019) and the standard deviation is relatively small (0.285) resulting in a COV of 0.280 which is also small compared to the COV for the EOD pile-cases. The best-fit line through the origin has a slope of 0.957 with a scatter shown by the  $R^2$  value of 0.366 and a range of ratios from an over-prediction ratio of 0.6 to an under-prediction ratio of 1.6.

**d) Summary**

The data presented in Figures 6.45 through 6.47 suggest that the Case method performs reasonably well under local conditions for both the EOD and BOR cases. The method performs better for the BOR cases than for the EOD pile-cases. The Case

method application in the maximum resistance form (RMX) has proven therefore effective for local conditions. Accumulated experience on extensive number of sites in the Boston area (e.g., GTR, 1997, 1998) has demonstrated the effectiveness of the Case method, when locally calibrated. As the data from Florida represents varied  $J_c$  and no generic conditions exist for the use of the Case method, international or national calibrations are not possible at this time. The projection of local calibration (of good experience and practice) beyond the geographical location and under non-uniform  $J_c$  is at this time impossible; hence, resistance factors will not be calibrated for the Case method.

#### **6.4 SUMMARY AND INTERMEDIATE CONCLUSIONS**

The evaluation of the dynamic methods used during the construction stage (indicator and production piles), was presented in this chapter. Figure 6.1 presented a flow chart that outlines the analysis methods and the conditions under which they were examined. A statistical evaluation was completed for each of the sub-categories presented in Figure 6.1 excluding the development of load factors for the stress evaluation of WEAP analyses.

The wide spread use of the WEAP analysis for pile capacity predictions has required the statistical evaluation of this method. The statistics presented in section 6.2.1 showed the use of the WEAP method for evaluating pile capacity is very limited at the EOD and somehow better at the BOR. Resistance factors are presented in Chapter 9 for these WEAP cases due to its wide spread use and demand of the research project panel.

A summary of the statistics describing the performance of the dynamic equations was presented in Table 6.2. The obtained results show that the FHWA version of the Gates equation had the lowest bias and the evaluation of this method was therefore carried out to examine its performance under different times of driving and driving resistances.

Table 6.4 presents a summary of the statistical evaluation of the methods that use dynamic measurements, namely the signal matching methods (CAPWAP/TEPWAP) and the Energy Approach method with their subcategories based on the controlling parameters. The statistics show that the Energy Approach performs the best as a construction control during driving (for the EOD pile-cases) while the signal matching methods perform the best for overall accuracy verification when used for the last BOR pile-cases. Also shown by the statistics is that both methods perform better for pile-cases with blow counts that are greater than 16 blows per 10cm than for pile-cases with blow counts less than 16 blows per 10cm. The extreme pile-cases that were discussed in section 6.3.1 result in Table 6.4 in a poor performance for the category of low driving resistance and low area ratio (large displacement piles). The most unreliable performance is that of the signal matching related to the sub-category of EOD pile-cases with blow counts of less than 16 blows per 10cm and area ratios less than 350. The EOD cases with blow count less than 16 blows per 10cm and area ratio greater than 350 resulted in a large bias but a good coefficient of variation. The unreliable categories for the Energy Approach method are the EOD pile-cases with blow counts less than 16 blows per 10cm and area ratios both less than and greater

than 350. The moderate to poor performance of the Energy Approach is therefore very noticeable for blow counts less than 16 blows per 10cm. However, its bias in these cases is on the safe side and hence would result with resistance factors similar to other categories (to be discussed in Chapter 9). The following cases for the Energy Approach and CAPWAP/TEPWAP methods are recommended to have resistance factors calculated:

1. For the CAPWAP/TEPWAP methods, the general case, the EOD case, the BOR case and the EOD case with blow counts less than 16 blows per 10cm and area ratios less than 350.
2. For the Energy Approach method, the general case, the EOD case, the BOR case and the EOD case with blow counts less than 16 blows per 10cm and area ratios less than 350.

These are only the preliminary recommended cases to have resistance factors evaluated and may not necessarily be the final cases that have recommended resistance factors assigned for them.

A resistance factor will not be calculated for the Case method for two reasons: (a) the Case method performs really well for local calibrations, but calibration based on a national scale (beyond the local geographical conditions) could not be evaluated and (b) the presented assessment of the Case method although uses a uniform interpretation methodology (RMX) used different  $J_c$  values for each case. The reevaluation of the capacity based on a uniform application of the method (i.e., RMX,

say with  $J_c = 0.6$ ) requires data not available in this study and may be a well-justified expansion of this research in the future.

Table 6.5 is a summary of the statistics that were calculated for each of the sub-categories presented in this chapter. For each sub-category the number of cases, the mean K value, the standard deviation, the coefficient of variation, the slope of the best-fit line through the origin, and the coefficient of determination are presented.

**Table 6.1.** Summary of the Statistical Data Evaluating the Performance of the Dynamic Equations.

	<u>ENR Equation</u> Load Test Results	<u>ENR Equation (w/FS)</u> Load Test Results	<u>Gates Formula</u> Load Test Results	<u>FHWA Version</u> Load Test Results
Mean $K_{SX}$	0.267	1.600	1.787	0.940
Standard Deviation	0.243	1.458	0.848	0.472
Coefficient of Variation	0.910	0.911	0.475	0.502
Minimum $K_{SX}$	0.058	0.347	0.374	0.223
Maximum $K_{SX}$	2.208	13.249	7.063	3.907
No. of Cases	384	384	384	384



**Table 6.2.** Summary of the Statistical Analyses Performed for the Dynamic Equations.

Method	ENR Equation	ENR Equation (w/FS)	Gates Equation	FHWA Version of Gates Equation			
$\mu_{K_{SX}}$	0.267	1.600	1.787	0.940			
$\sigma_{K_{SX}}$	0.243	1.458	0.848	0.472			
COV	0.910	0.911	0.475	0.502			
No.	384	384	384	384			
Time of Driving	----	----	----	EOD	BOR (last)		
$\mu_{K_{SX}}$	----	----	----	1.073	0.833		
$\sigma_{K_{SX}}$	----	----	----	0.573	0.403		
COV	----	----	----	0.534	0.484		
No.	----	----	----	135	159		
Blow Count	----	----	----	< 16 BP10cm	≥ 16 BP10cm	< 16 BP10cm	≥ 16 BP10cm
$\mu_{K_{SX}}$	----	----	----	1.306	0.876	0.929	0.809
$\sigma_{K_{SX}}$	----	----	----	0.643	0.419	0.688	0.290
COV	----	----	----	0.492	0.478	0.741	0.358
No.	----	----	----	62	73	32	127

NOTES: COV = Coefficient of Variation     $K_{SX}$  = Static Load Test Results over the Dynamic Equation Prediction.  
EOD = End of Driving    BOR = Beginning of Restrike     $\mu$  = mean value     $\sigma$  = standard deviation

**Table 6.3.** Summary of the EOD Pile-Cases for which the  $K_{SX}$  Values Were Outside Two Standard Deviations.

Energy Approach Pile-Cases						
No.	Pile-Case Number	Location	Area Ratio	Blow Count (BP10cm)	K <sub>SP</sub>	Reason for Removal
226	CH39-EOD	Jones Island, WI	3142	3.3	3.687	Blow Counts were measured in BPF and not BPI at the EOD. D <sub>max</sub> is less than the measured set.
229	CH6-5B-EOD	Jones Island, WI	3349	2.0	4.273	
286	DD22-EOD	Orlando, FL	309	22.3	2.567	Blow Counts were measured in BPF and not BPI at the EOD.
288	DD23-EOD	Orlando, FL	309	8.9	3.242	
300	LB5-EOD	Kenner, LA	189	7.2	3.188	See reason below for this same site.
305	LB6-EOD	Kenner, LA	226	4.9	2.813	
310	LB7-EOD	Kenner, LA	225	15.5	2.580	
CAPWAP Pile-Cases						
No.	Pile-Case Number	Location	Area Ratio	Blow Count (BP10cm)	K <sub>SW</sub>	Reason for Removal
291	LB3-EOD	Kenner, LA	203	3.3	6.854	Pile-cases are all from the same site and all have very low blow counts and very low area ratios. These 5 pile-cases fall into the category of Blow Count less than 16 BP10cm (4 BPI) and Area Ratio less than 350, and were retained for that specific combination of the analysis.
295	LB4-EOD	Kenner, LA	189	4.6	11.256	
300	LB5-EOD	Kenner, LA	189	7.2	9.375	
305	LB6-EOD	Kenner, LA	226	4.9	5.969	
310	LB7-EOD	Kenner, LA	225	15.5	5.258	

Notes: EOD = End of Driving  
 $K_{SP}$  = Ratio of Static Load Test Results to Energy Approach Predictions  
 $K_{SW}$  = Ratio of Static Load Test Results to CAPWAP Predictions

BP10cm = Blows per 10 centimeters  
BPI = Blows per inch  
BPF = Blows per foot

**Table 6.4. Summary of the Soil Inertia Properties for PD/LT2000, Energy Approach and CAPWAP/TEPWAP vs. Static Load Test Results for the Controlling Parameters.**

Method	CAPWAP/TEPWAP								Energy Approach							
$\mu_{K_{SX}}$	1.368								0.894							
$\sigma_{K_{SX}}$	0.620								0.367							
COV	0.453								0.411							
No.	377								371							
Time	EOD				BOR (last)				EOD				BOR (last)			
$\mu_{K_{SX}}$	1.626				1.158				1.084				0.785			
$\sigma_{K_{SX}}$	0.797				0.393				0.431				0.290			
COV	0.490				0.339				0.398				0.369			
No.	125				162				128				153			
Bl. Count	< 16 BP10cm		≥ 16 BP10cm		< 16 BP10cm		≥ 16 BP10cm		< 16 BP10cm		≥ 16 BP10cm		< 16 BP10cm		≥ 16 BP10cm	
$\mu_{K_{SX}}$	1.843		1.460		1.176		1.153		1.227		0.972		0.830		0.775	
$\sigma_{K_{SX}}$	0.831		0.734		0.530		0.354		0.474		0.359		0.352		0.274	
COV	0.451		0.503		0.451		0.307		0.386		0.369		0.424		0.354	
No.	54		71		32		130		56		72		29		124	
$A_R$	< 350	≥ 350	< 350	≥ 350	< 350	≥ 350	< 350	≥ 350	< 350	≥ 350	< 350	≥ 350	< 350	≥ 350	< 350	≥ 350
$\mu_{K_{SX}}$	2.589	1.929	1.717	1.181	1.116	1.308	1.178	1.110	1.431	1.422	1.054	0.926	0.764	0.954	0.736	0.851
$\sigma_{K_{SX}}$	2.385	0.698	0.841	0.468	0.362	0.796	0.379	0.303	0.727	0.888	0.459	0.320	0.318	0.396	0.249	0.305
COV	0.921	0.362	0.490	0.396	0.324	0.609	0.446	0.273	0.508	0.624	0.435	0.346	0.416	0.415	0.338	0.358
No.	37	22	37	34	22	10	83	47	39	23	39	34	19	10	82	42

**NOTES:** COV = Coefficient of Variation       $K_{SX}$  = Static Load Test Results over the CAPWAP/TEPWAP or Energy Approach Predictions.  
EOD = End of Driving      BOR = Beginning of Restrike       $\mu$  = mean       $\sigma$  = standard deviation

**Table 6.5.** Summary of the Statistical Analyses Performed in Chapter 6.

Method	No.	Mean K <sub>sx</sub>	Standard Deviation	COV	m <sub>0</sub>	R <sup>2</sup>
GRLWEAP, EOD	99	1.656	1.199	0.724	1.081	0.359
GRLWEAP, BOR	99	0.939	0.399	0.425	0.803	0.495
ENR w/out FS	384	0.267	0.243	0.910	0.162	0.223
ENR w/FS	384	1.600	1.458	0.910	0.972	0.223
Gates, General	384	1.787	0.848	0.475	1.828	0.412
FHWA, General	384	0.940	0.472	0.502	0.922	0.417
FHWA, EOD	135	1.073	0.573	0.534	1.048	0.413
FHWA, BOR	159	0.833	0.403	0.484	0.828	0.487
FHWA, EOD, ED	62	1.306	0.643	0.492	1.282	0.419
FHWA, BOR, ED	32	0.929	0.688	0.741	0.929	0.215
FHWA, EOD, HD	73	0.876	0.419	0.478	0.967	0.468
FHWA, BOR, HD	127	0.809	0.290	0.358	0.820	0.499
CAPWAP, General	377	1.368	0.620	0.453	1.160	0.557
CAPWAP, EOD	125	1.626	0.797	0.490	1.284	0.653
CAPWAP, BOR	162	1.158	0.393	0.339	1.104	0.599
CAPWAP, EOD, ED	54	1.843	0.831	0.451	1.388	0.677
CAPWAP, EOD, HD	71	1.460	0.734	0.503	1.236	0.647
CAPWAP, BOR, ED	32	1.176	0.530	0.451	1.189	0.717
CAPWAP, BOR, HD	130	1.153	0.354	0.307	1.096	0.526
CAPWAP, EOD, ED, LD	37	2.589	2.385	0.921	1.467	-0.082
CAPWAP, EOD, ED, SD	22	1.929	0.698	0.362	1.360	0.776
CAPWAP, EOD, HD, LD	37	1.717	0.841	0.490	1.479	0.185
CAPWAP, EOD, HD, SD	34	1.181	0.468	0.396	1.139	0.904

Notes: K<sub>sx</sub> = Ratio of Static Load Test Results to the Predicted Results  
m<sub>0</sub> = Slope of the best-fit line forced through the origin  
No. = Number of pile-cases  
R<sup>2</sup> = coefficient of determination  
BOR = Beginning of Restrike  
ED = Easy Driving  
LD = Large Displacement  
EA = Energy Approach  
COV = Coefficient of Variation  
EOD = End of Driving  
FS = Factor of Safety  
HD = Hard Driving  
SD = Small Displacement

**Table 6.5 (con't). Summary of the Statistical Analyses Performed in Chapter 6**

<b>Method</b>	<b>No.</b>	<b>Mean K<sub>sx</sub></b>	<b>Standard Deviation</b>	<b>COV</b>	<b>m<sub>0</sub></b>	<b>R<sup>2</sup></b>
<b>CAPWAP, BOR, ED, LD</b>	22	1.116	0.362	0.324	1.207	0.730
<b>CAPWAP, BOR, ED, SD</b>	10	1.308	0.796	0.609	1.133	0.638
<b>CAPWAP, BOR, HD, LD</b>	83	1.178	0.379	0.322	1.109	0.522
<b>CAPWAP, BOR, HD, SD</b>	47	1.110	0.303	0.273	1.064	0.484
<b>EA, General</b>	371	0.894	0.367	0.411	0.743	0.542
<b>EA, EOD</b>	128	1.084	0.431	0.398	0.926	0.693
<b>EA, BOR</b>	153	0.785	0.290	0.369	0.695	0.576
<b>EA, EOD, ED</b>	56	1.227	0.474	0.386	1.012	0.739
<b>EA, EOD, HD</b>	72	0.972	0.359	0.369	0.885	0.680
<b>EA, BOR, ED</b>	29	0.830	0.352	0.424	0.742	0.554
<b>EA, BOR, HD</b>	124	0.775	0.274	0.354	0.691	0.525
<b>EA, EOD, ED, LD</b>	39	1.431	0.727	0.508	1.018	0.134
<b>EA, EOD, ED, SD</b>	23	1.422	0.888	0.624	1.031	0.831
<b>EA, EOD, HD, LD</b>	39	1.054	0.459	0.435	0.902	0.247
<b>EA, EOD, HD, SD</b>	34	0.926	0.320	0.346	0.879	0.850
<b>EA, BOR, ED, LD</b>	19	0.764	0.318	0.416	0.736	0.600
<b>EA, BOR, ED, SD</b>	10	0.954	0.396	0.415	0.761	0.334
<b>EA, BOR, HD, LD</b>	82	0.736	0.249	0.338	0.685	0.573
<b>EA, BOR, HD, SD</b>	42	0.851	0.305	0.358	0.712	0.269
<b>Case, General</b>	77	1.183	0.403	0.341	1.049	0.361
<b>Case, EOD</b>	40	1.334	0.438	0.328	1.165	0.470
<b>Case, BOR</b>	37	1.019	0.285	0.280	0.957	0.366

Notes: K<sub>sx</sub> = Ratio of Static Load Test Results to the Predicted Results  
m<sub>0</sub> = Slope of the best-fit line forced through the origin  
No. = Number of pile-cases      COV = Coefficient of Variation  
R<sup>2</sup> = coefficient of determination      EOD = End of Driving  
BOR = Beginning of Restrike      FS = Factor of Safety  
ED = Easy Driving      HD = Hard Driving  
LD = Large Displacement      SD = Small Displacement  
EA = Energy Approach

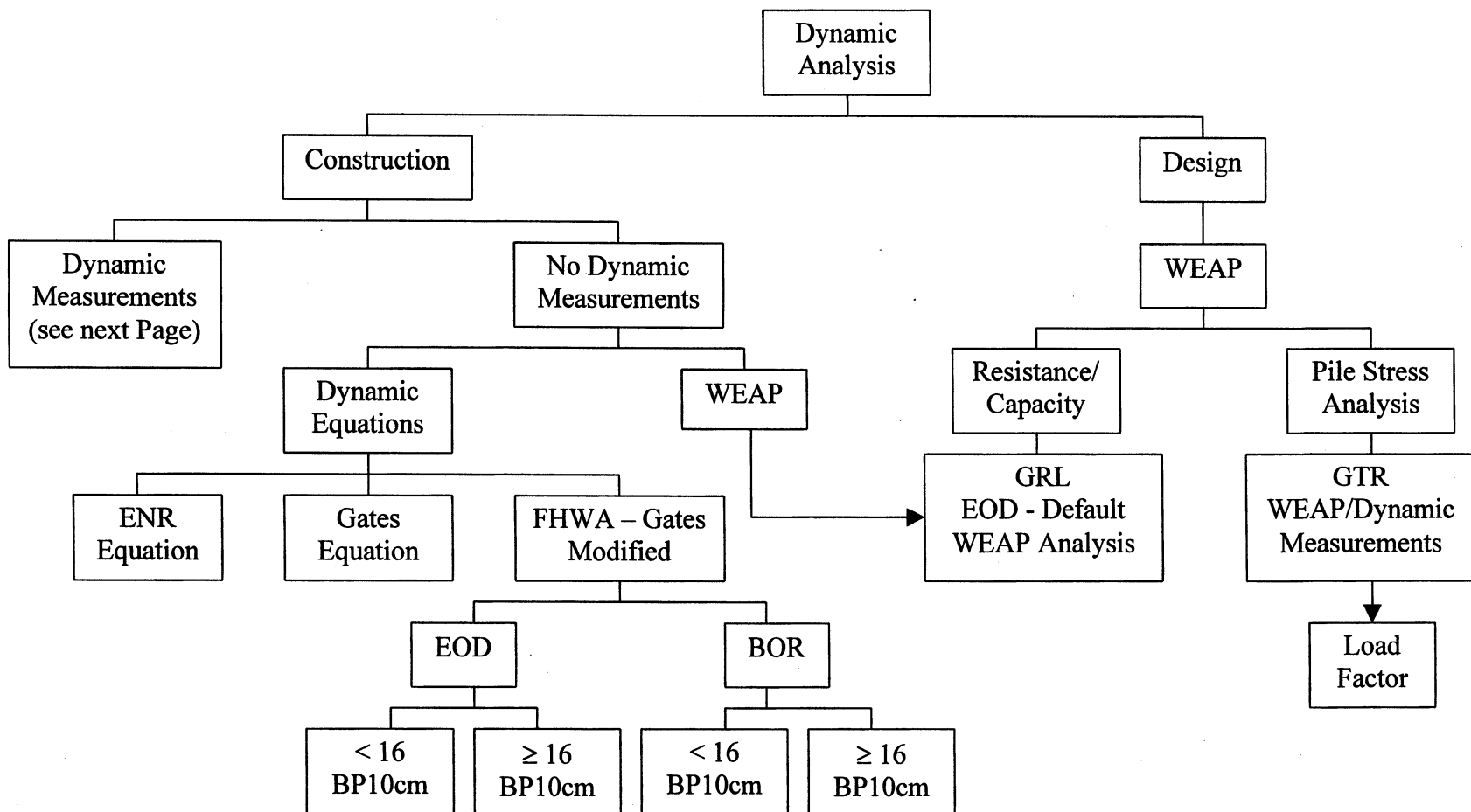


**Figure 6.1.** Flow Chart Depicting the Various Investigated Dynamic Analyses of Driven Piles (Pile Stress Analysis Excluded)

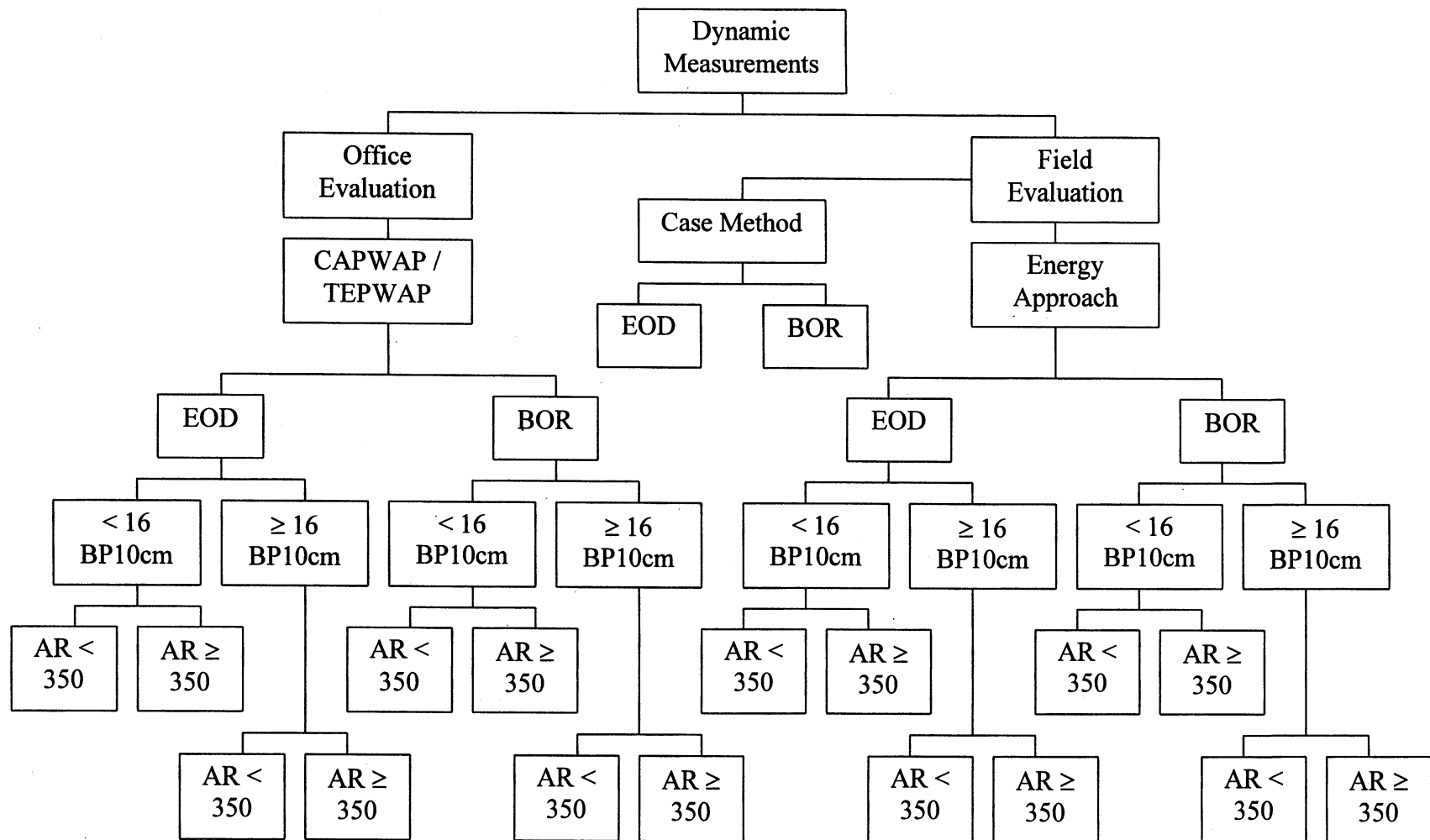


**Figure 6.1 (con't).** Flow Chart Depicting the Various Investigated Dynamic Analyses of Driven Piles (Pile Stress Analysis Excluded).

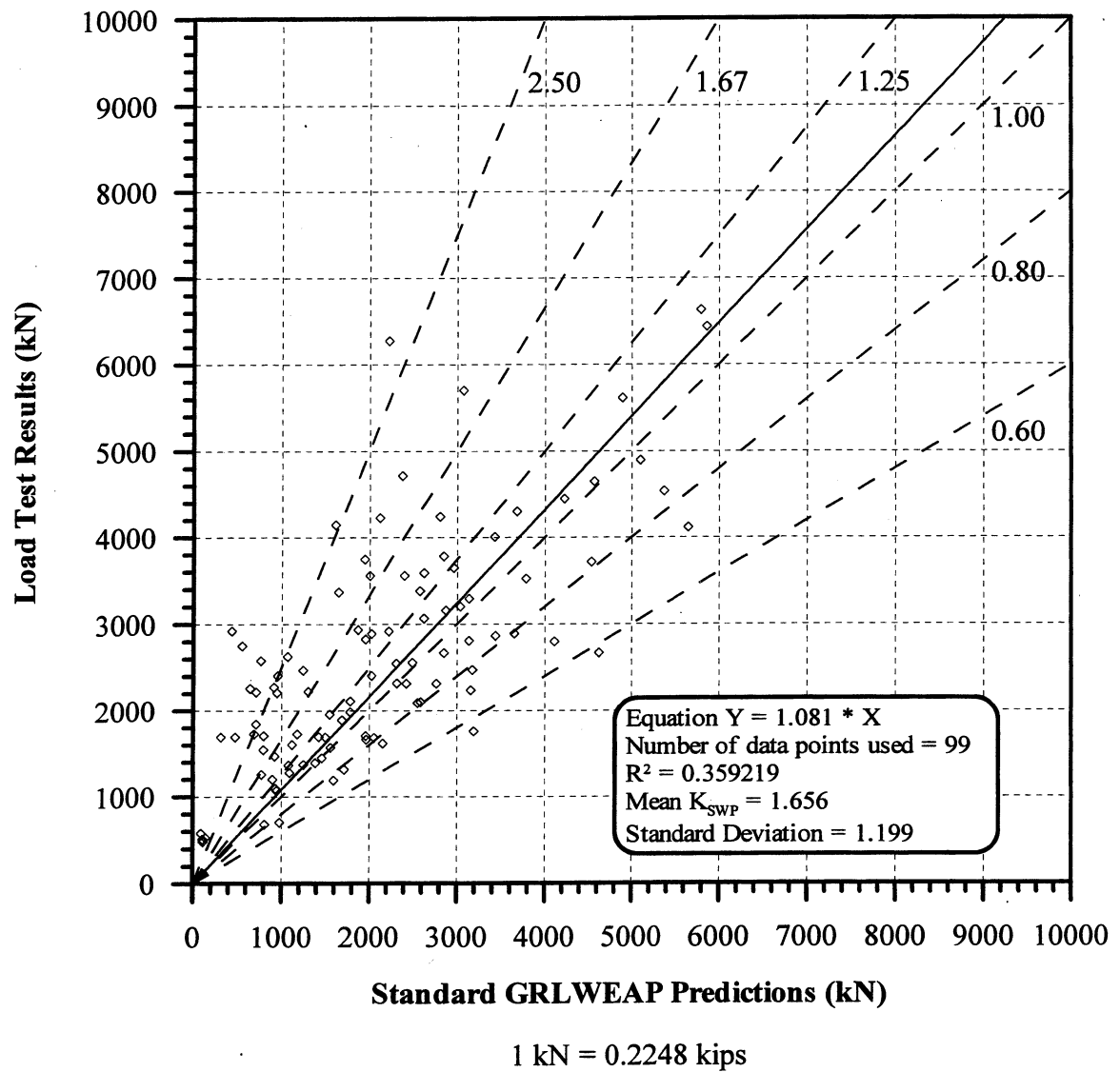


**Figure 6.2.** Static Load Test Results vs. GRLWEAP Predictions for 99 pile-cases at EOD provided by GRL Inc., in all types of soils (AEA).



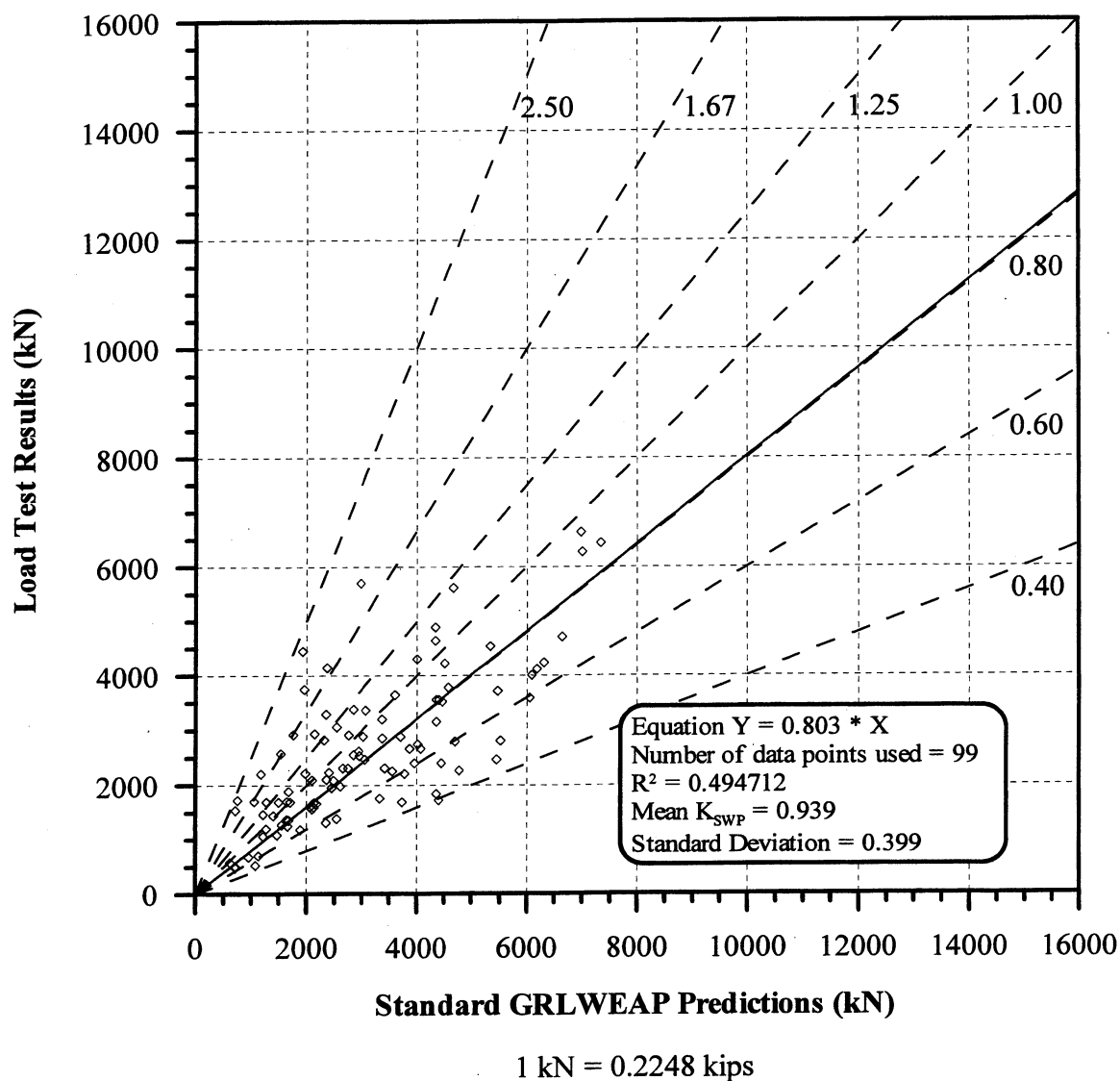


**Figure 6.3.** Static Load Test Results vs. GRLWEAP Predictions for 99 pile-cases at BOR provided by GRL Inc., all types of soils (ABA).

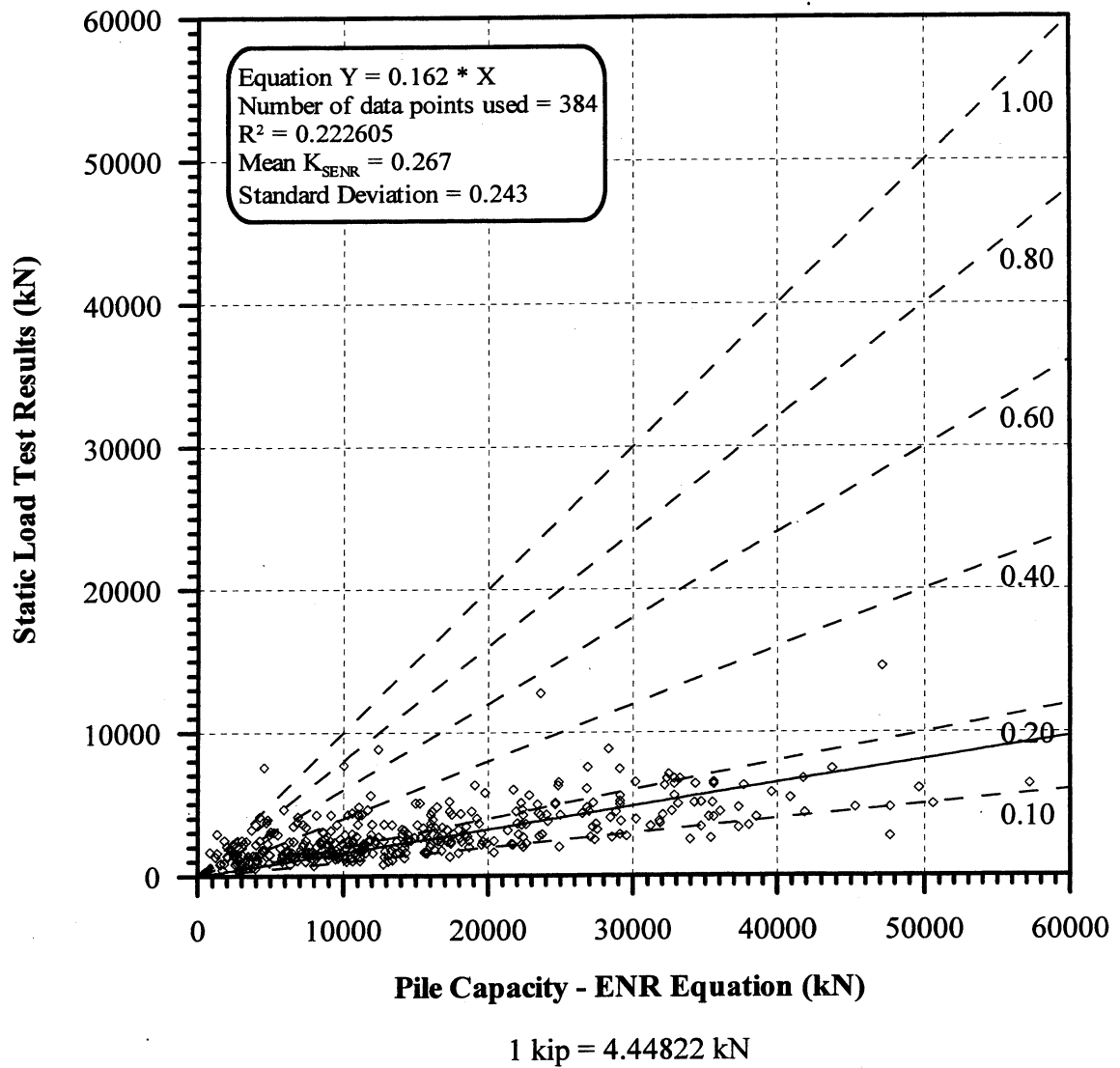


**Figure 6.4.** Static Load Test Results vs. ENR Equation Capacity for 384 PD/LT2000 pile-cases at all times and in all types of soils (AAA).

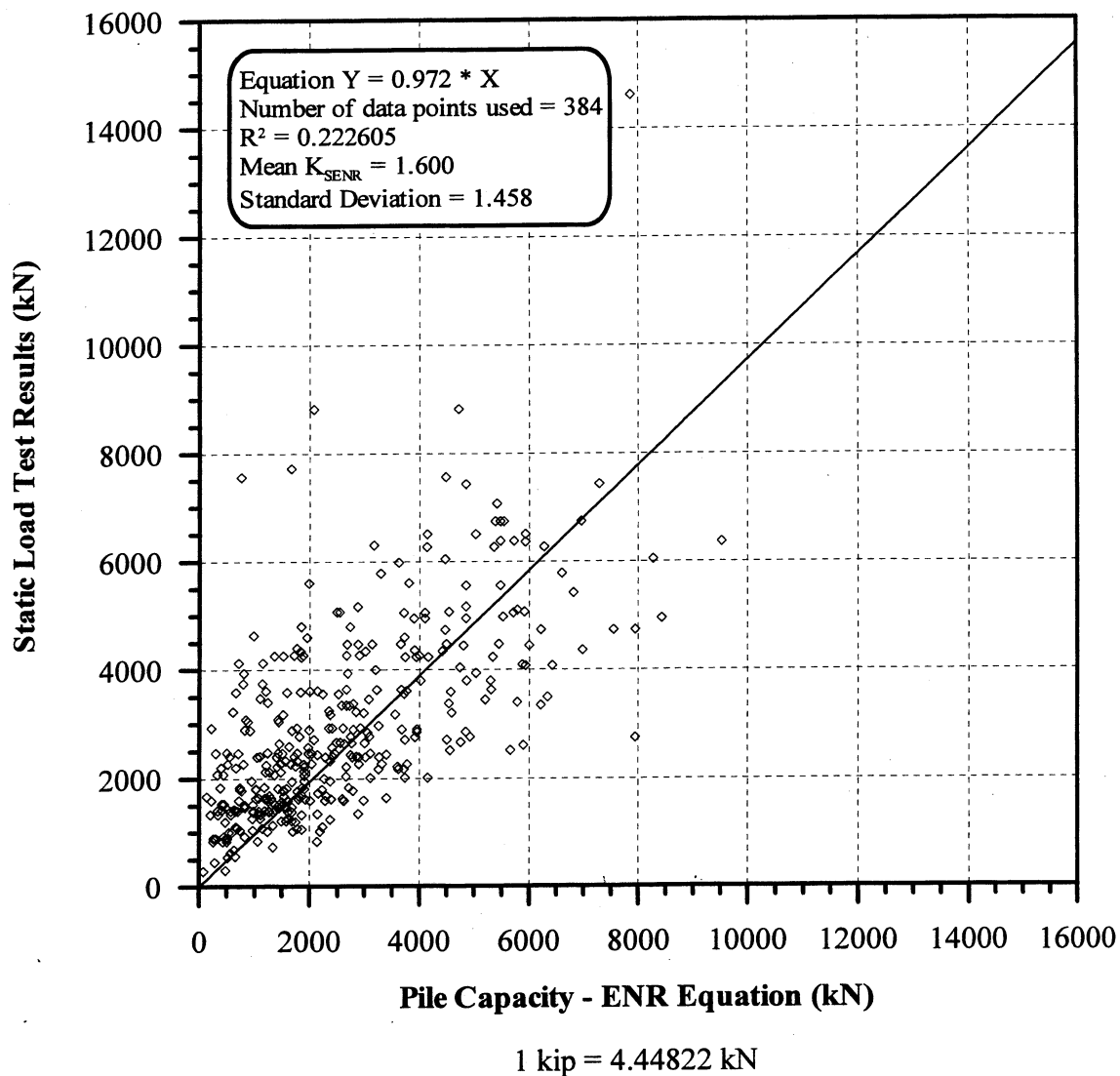


**Figure 6.5.** Static Load Test Results vs. ENR Equation Capacity with Factor of Safety of 6 for 384 PD/LT2000 pile-cases at all times and in all types of soils (AAA).

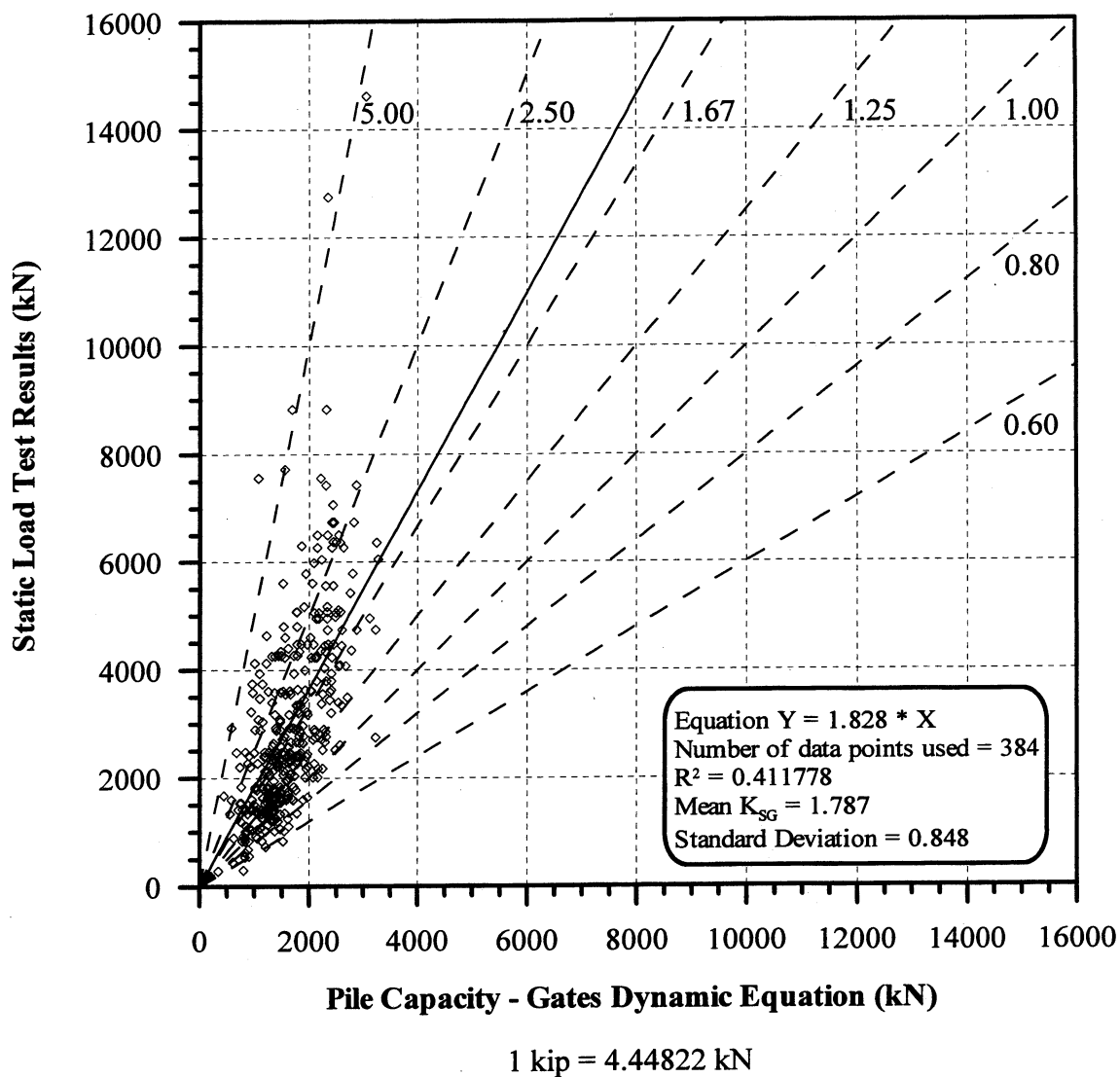
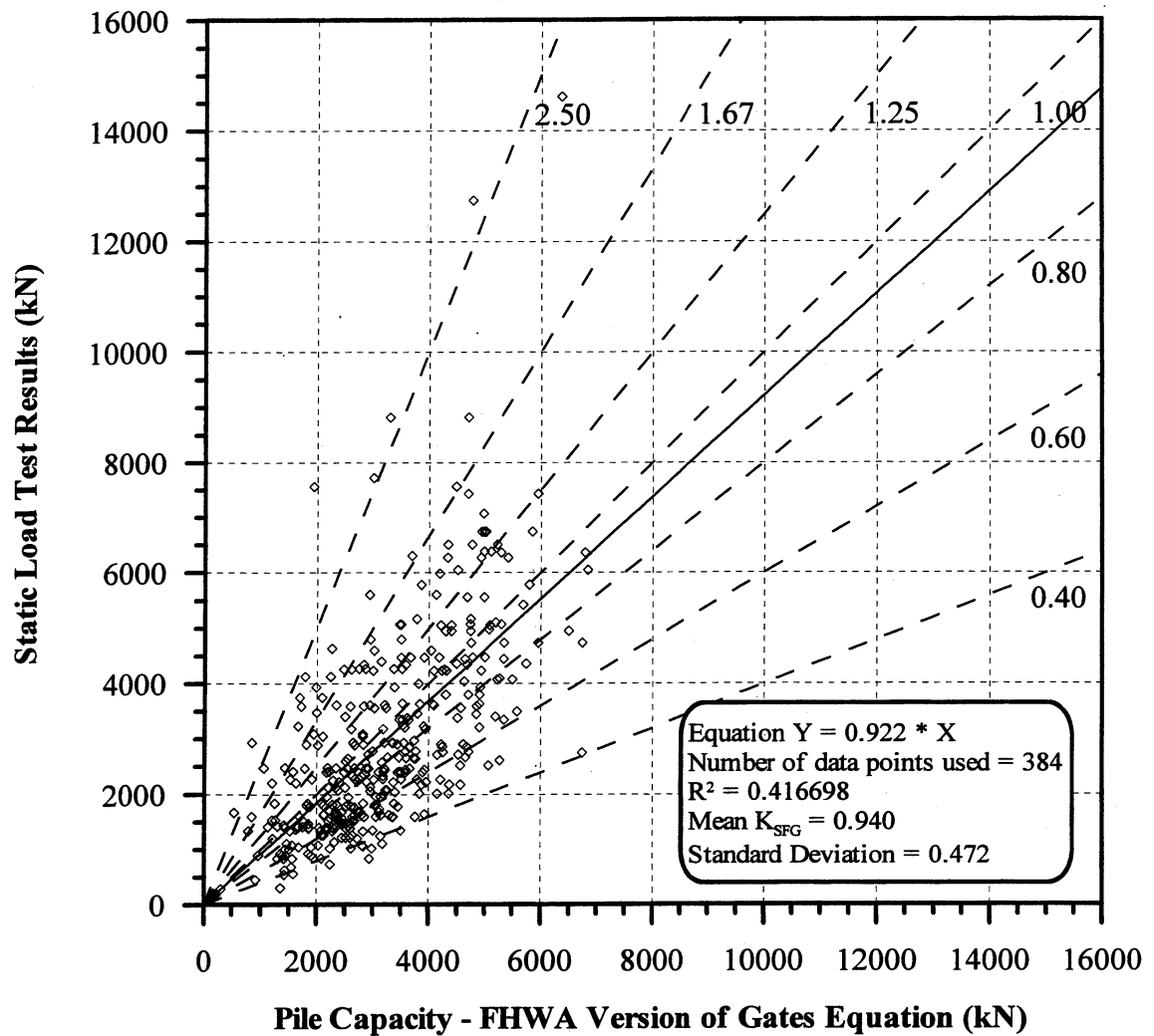


**Figure 6.6.** Static Load Test Results vs. Gates Dynamic Equation Capacity for 384 PD/LT2000 pile-cases at all times and in all types of soils (AAA).



1 kip = 4.44822 kN

**Figure 6.7.** Static Load Test Results vs. Pile Capacity according to the FHWA Version of the Gates Equation for 384 PD/LT2000 pile-cases at all times and in all types of soils (AAA).

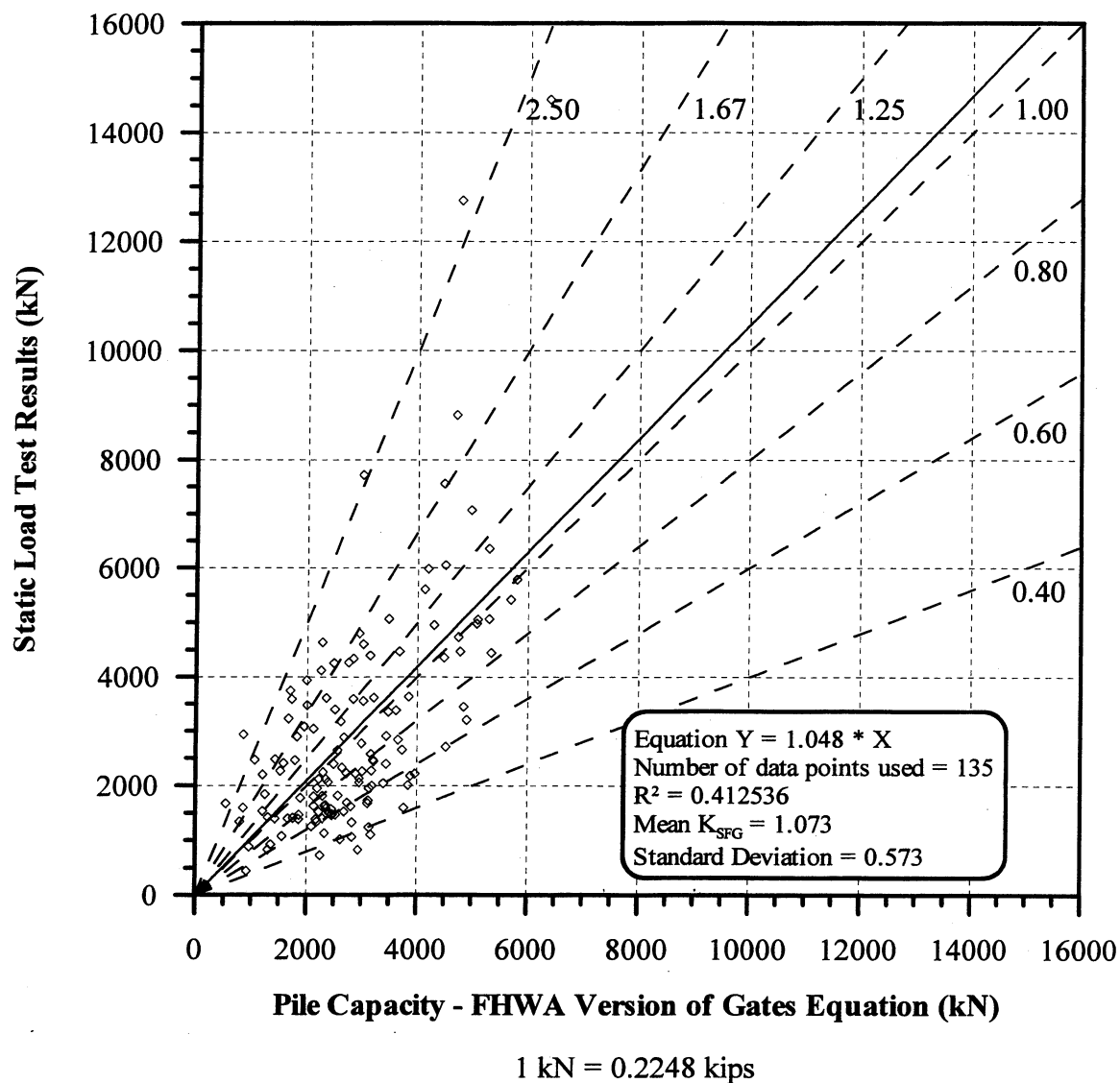


**Figure 6.8.** Static Load Test Results vs. Pile Capacity according to the FHWA Version of the Gates Equation for 135 PD/LT2000 EOD pile-cases in all types of soils (AEA)

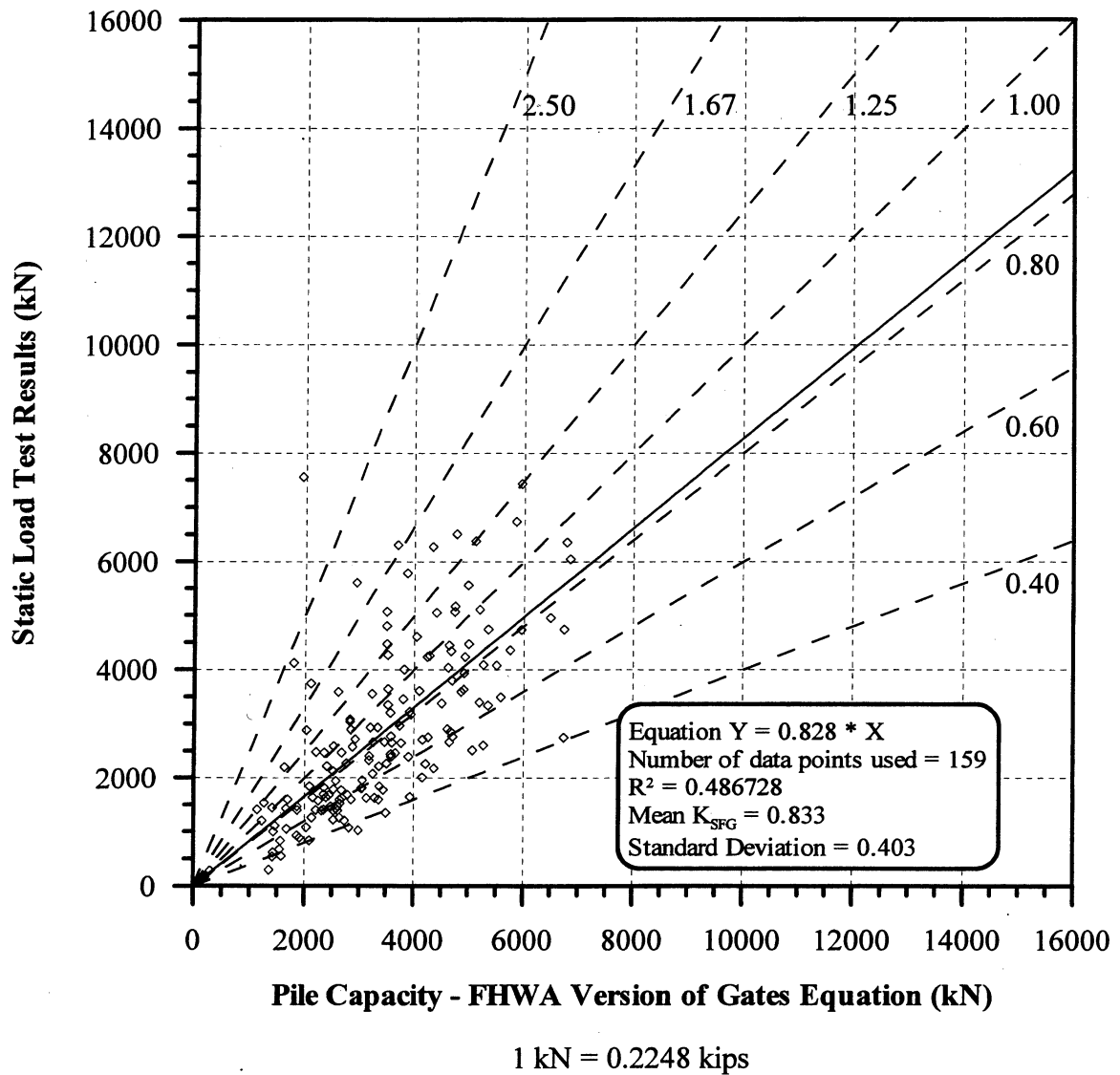


**Figure 6.9.** Static Load Test Results vs. Pile Capacity according to the FHWA Version of the Gates Equation for 159 PD/LT2000 BOR(last) pile-cases in all types of soils (ABA).

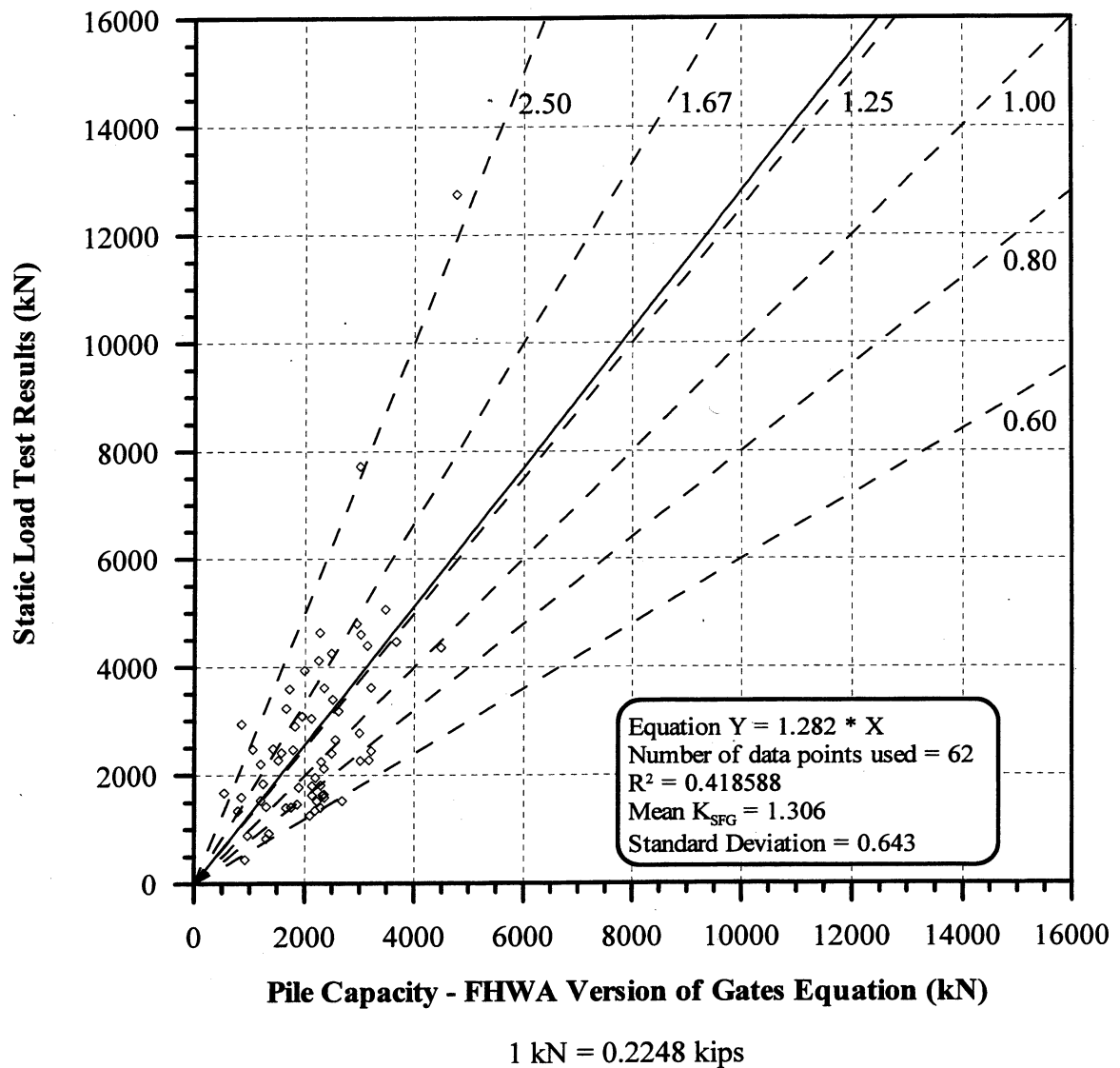
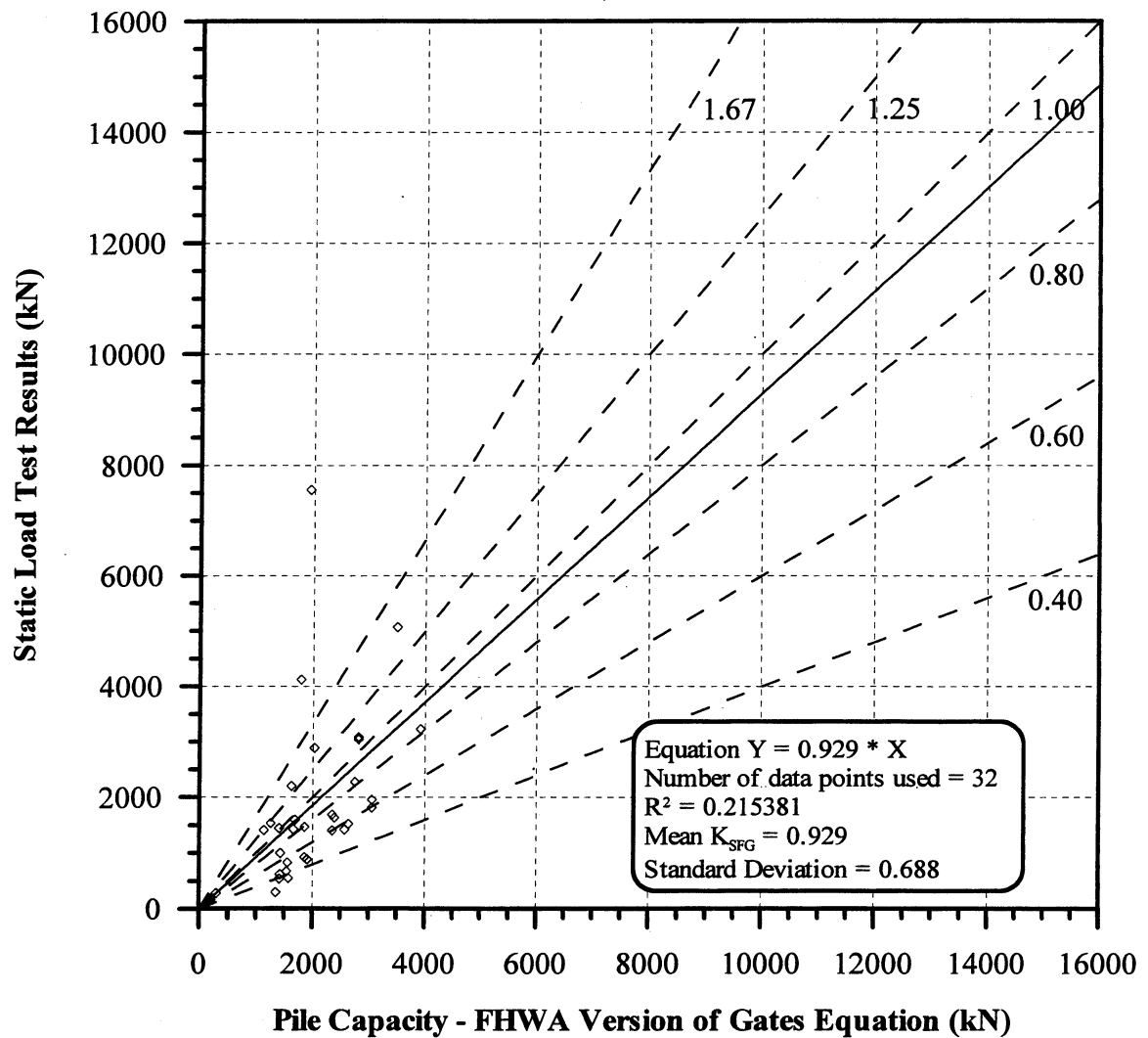


**Figure 6.10.** Static Load Test Results vs. Pile Capacity according to the FHWA Version of the Gates Equation for 62 PD/LT2000 pile-cases at the EOD with Blow Count < 16 BP10cm in all types of soils (AEA).





1 kN = 0.2248 kips

**Figure 6.11.** Static Load Test Results vs. Pile Capacity according to the FHWA Version of the Gates Equation for 32 PD/LT2000 pile-cases at the BOR (last) with Blow Count < 16 BP10cm in all types of soils (ABA).

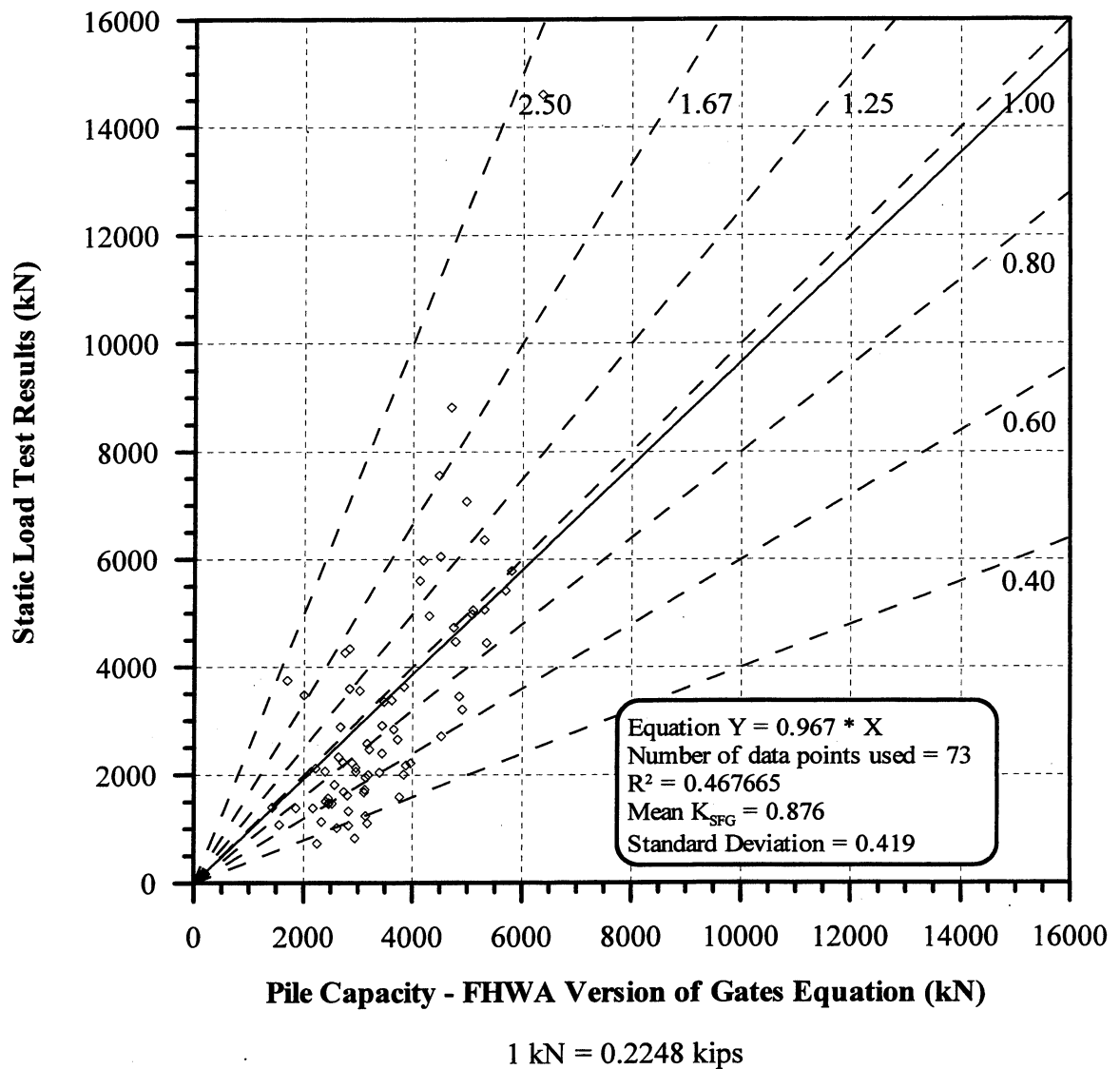


**Figure 6.12.** Static Load Test Results vs. Pile Capacity according to the FHWA Version of the Gates Equation for 73 PD/LT2000 pile-cases at the EOD with Blow Count  $\geq 16$  BP10cm in all types of soils (AEA).

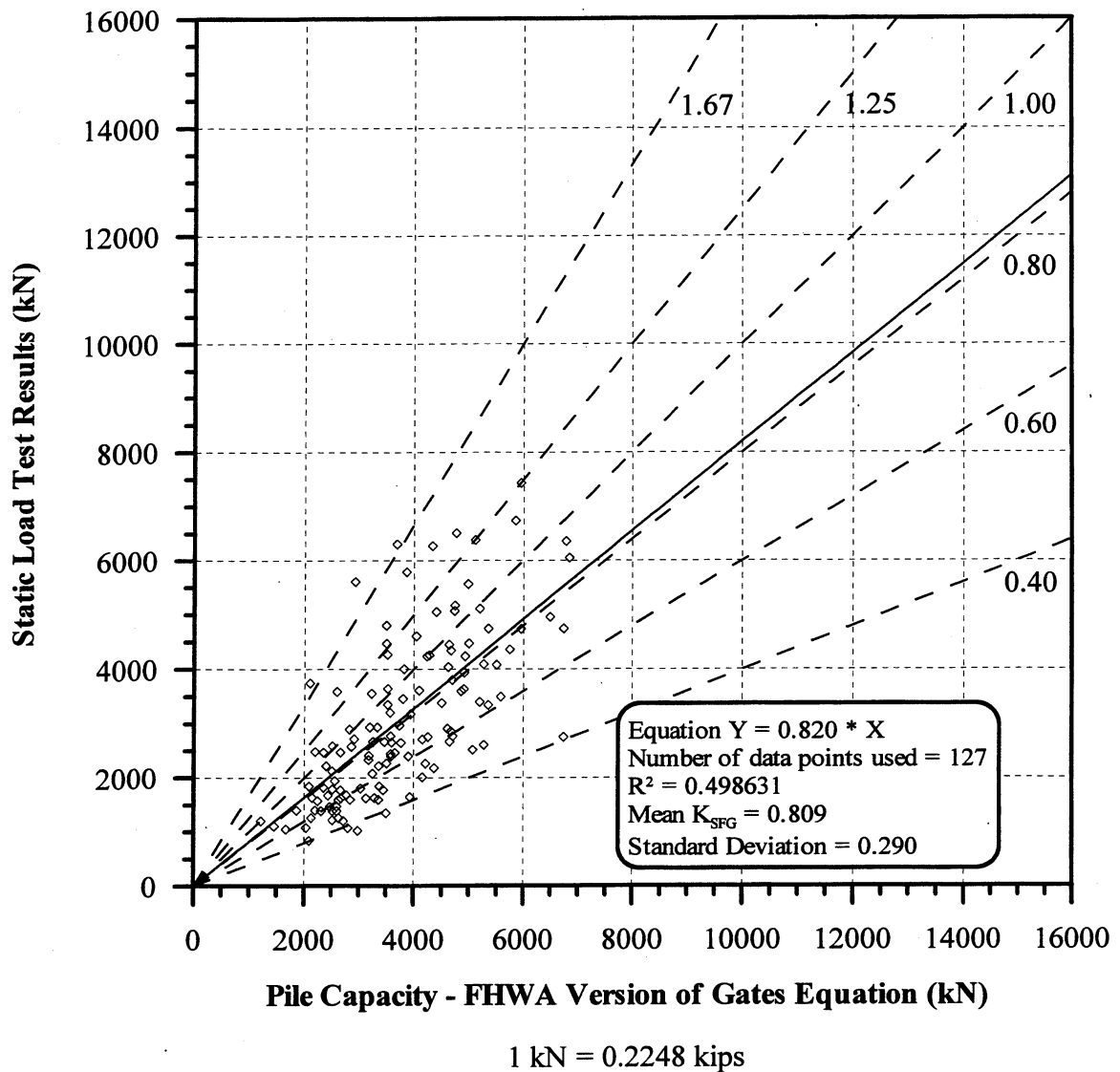
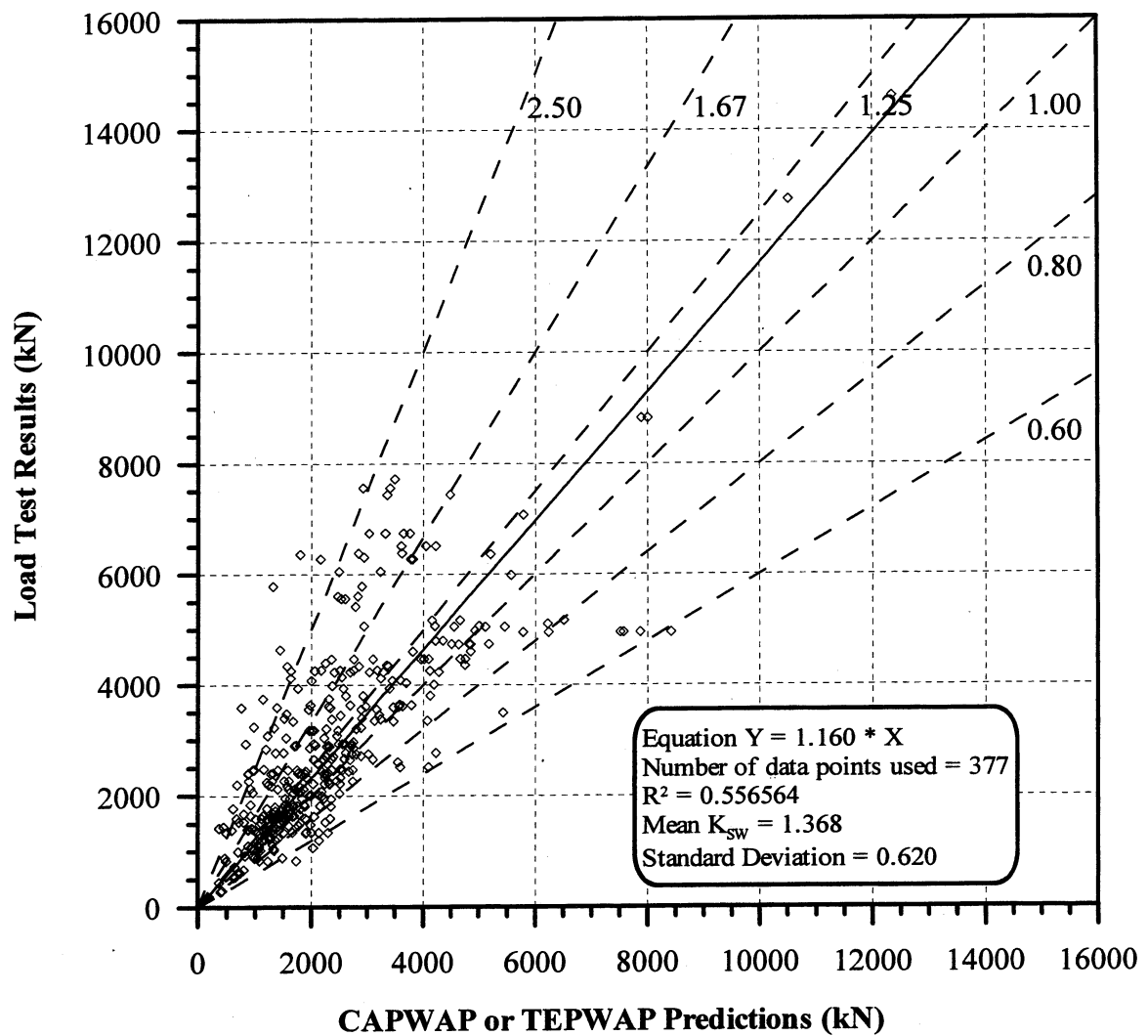


**Figure 6.13.** Static Load Test Results vs. Pile Capacity according to the FHWA Version of the Gates Equation for 127 PD/LT2000 pile-cases at the BOR (last) with Blow Count  $\geq 16$  BP10cm in all types of soils (ABA).



1 kN = 0.2248 kips

**Figure 6.14.** Static Load Test Results vs. CAPWAP or TEPWAP predictions for all 377 PD/LT2000 pile-cases at all times and in all types of soils (AAA).

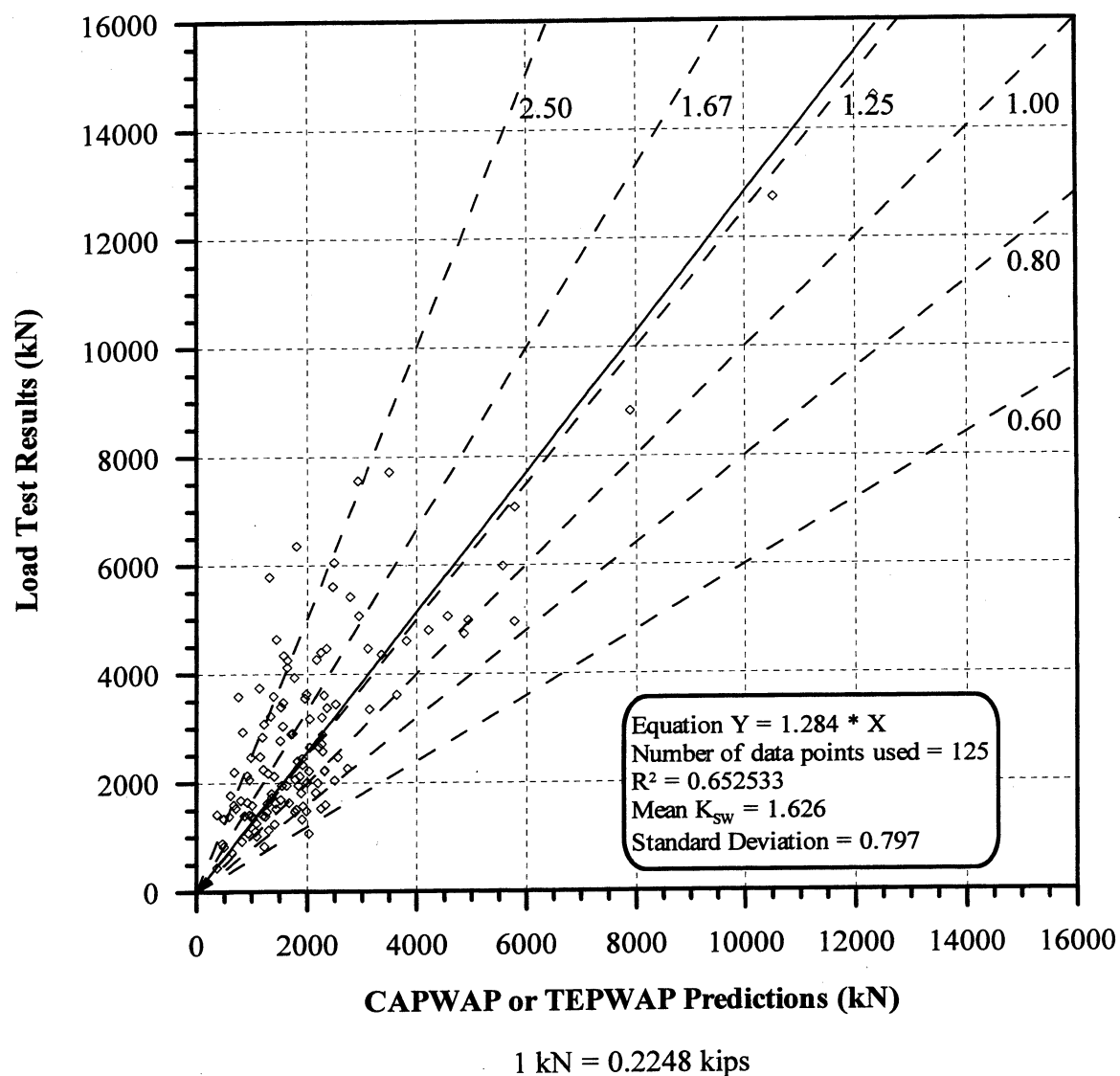


**Figure 6.15.** Static Load Test Results vs. CAPWAP or TEPWAP predictions for 125 PD/LT2000 pile-cases at EOD in all types of soils (AEA).

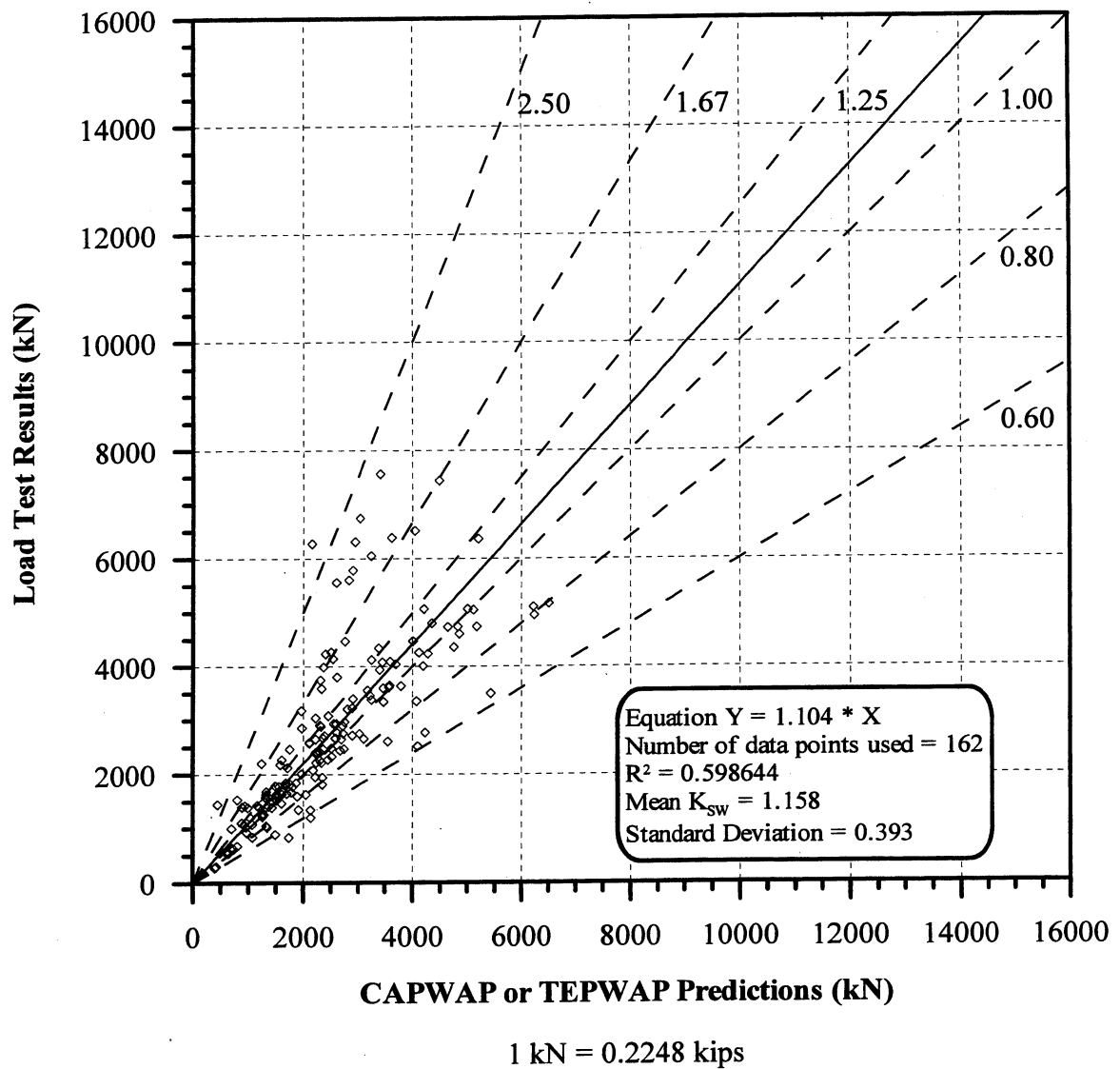


**Figure 6.16.** Static Load Test Results vs. CAPWAP or TEPWAP predictions for 162 PD/LT2000 pile-cases at BOR(last) in all types of soils (ABA).

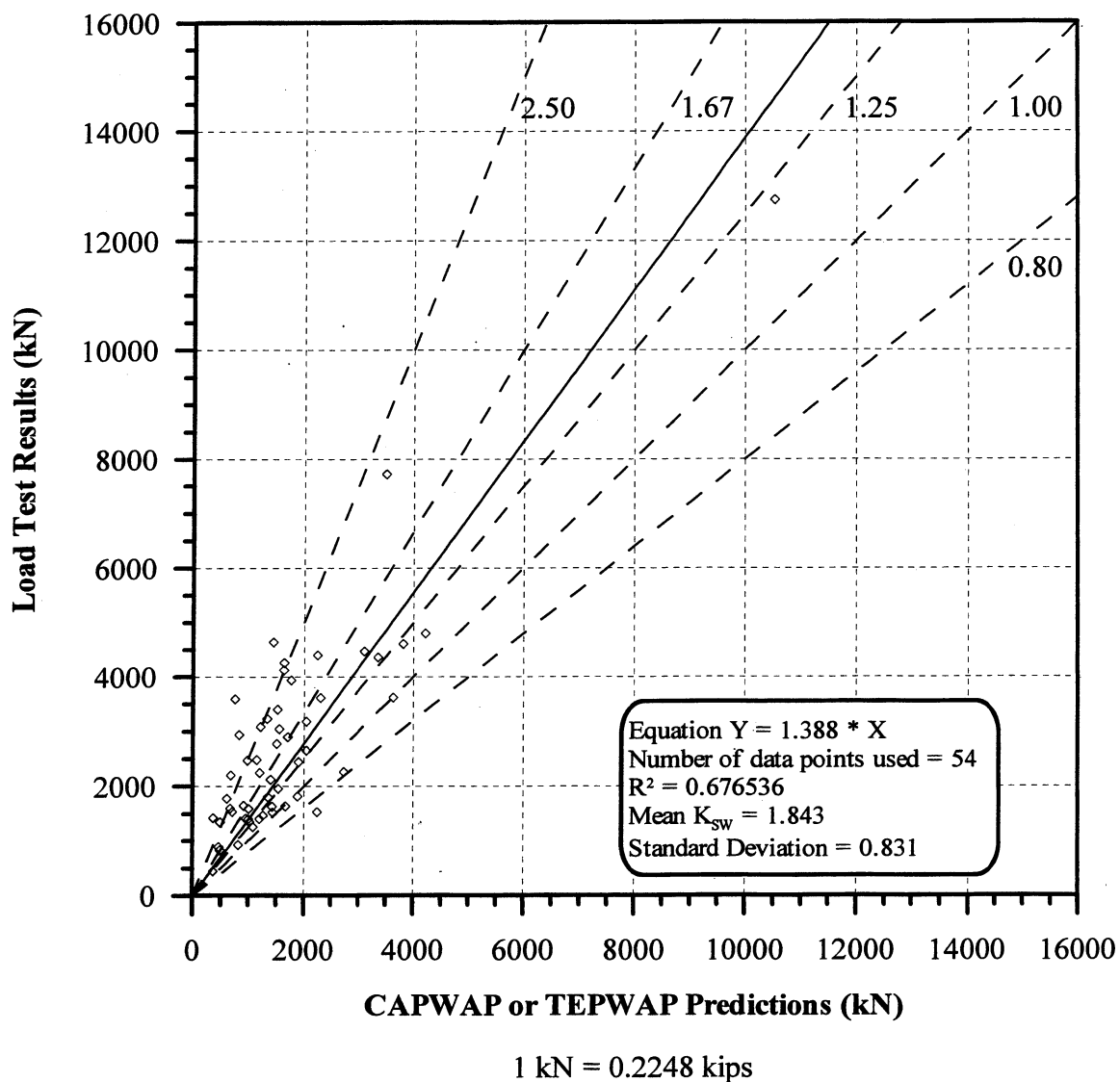
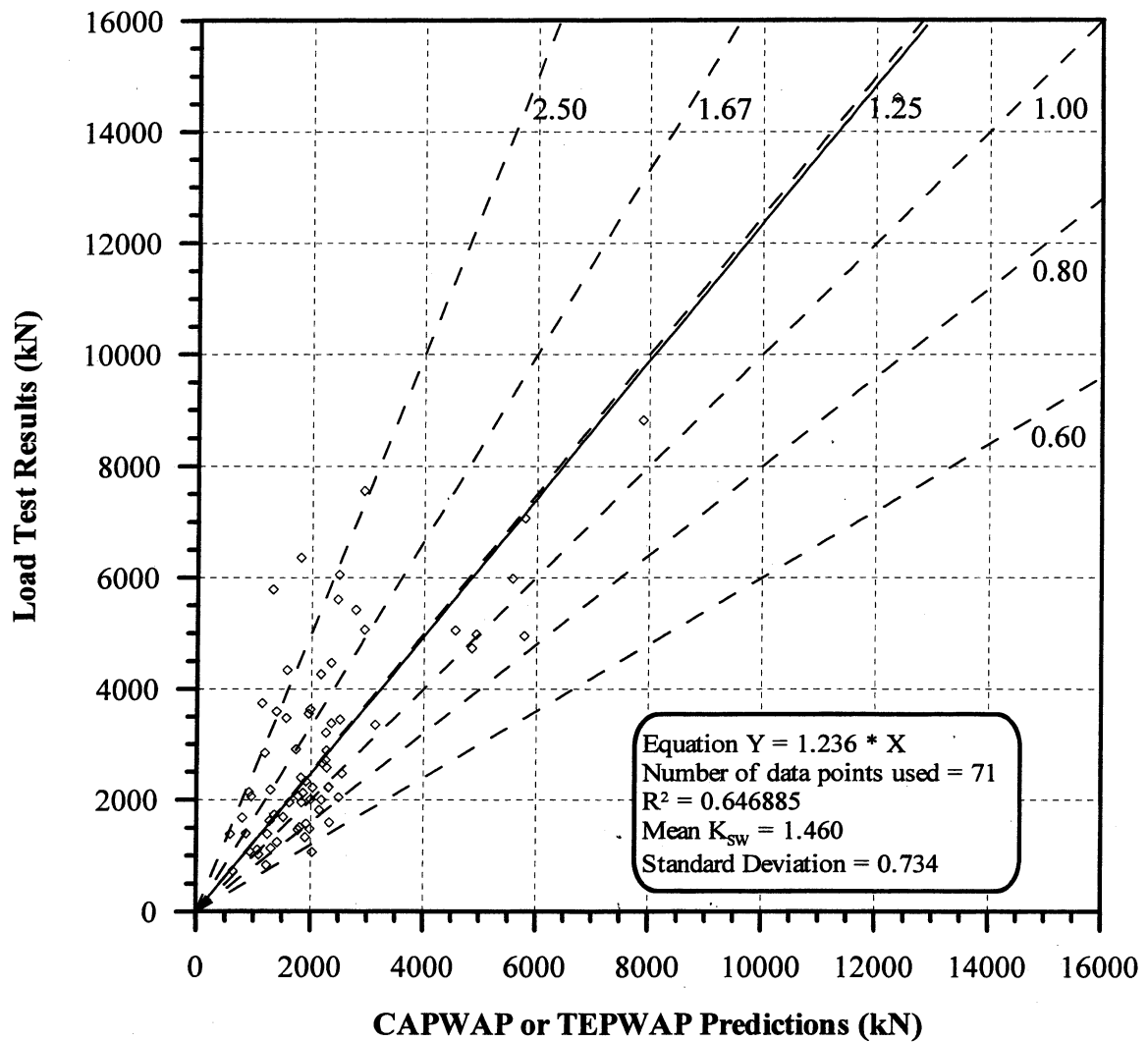


**Figure 6.17.** Static Load Test Results vs. CAPWAP or TEPWAP predictions for 54 PD/LT2000 pile-cases at the EOD with Blow Count < 16 BP10cm in all types of soils (AEA).



1 kN = 0.2248 kips

**Figure 6.18.** Static Load Test Results vs. CAPWAP or TEPWAP predictions for 71 PD/LT2000 pile-cases at the EOD with Blow Count  $\geq 16$  BP10cm in all types of soils (AEA).



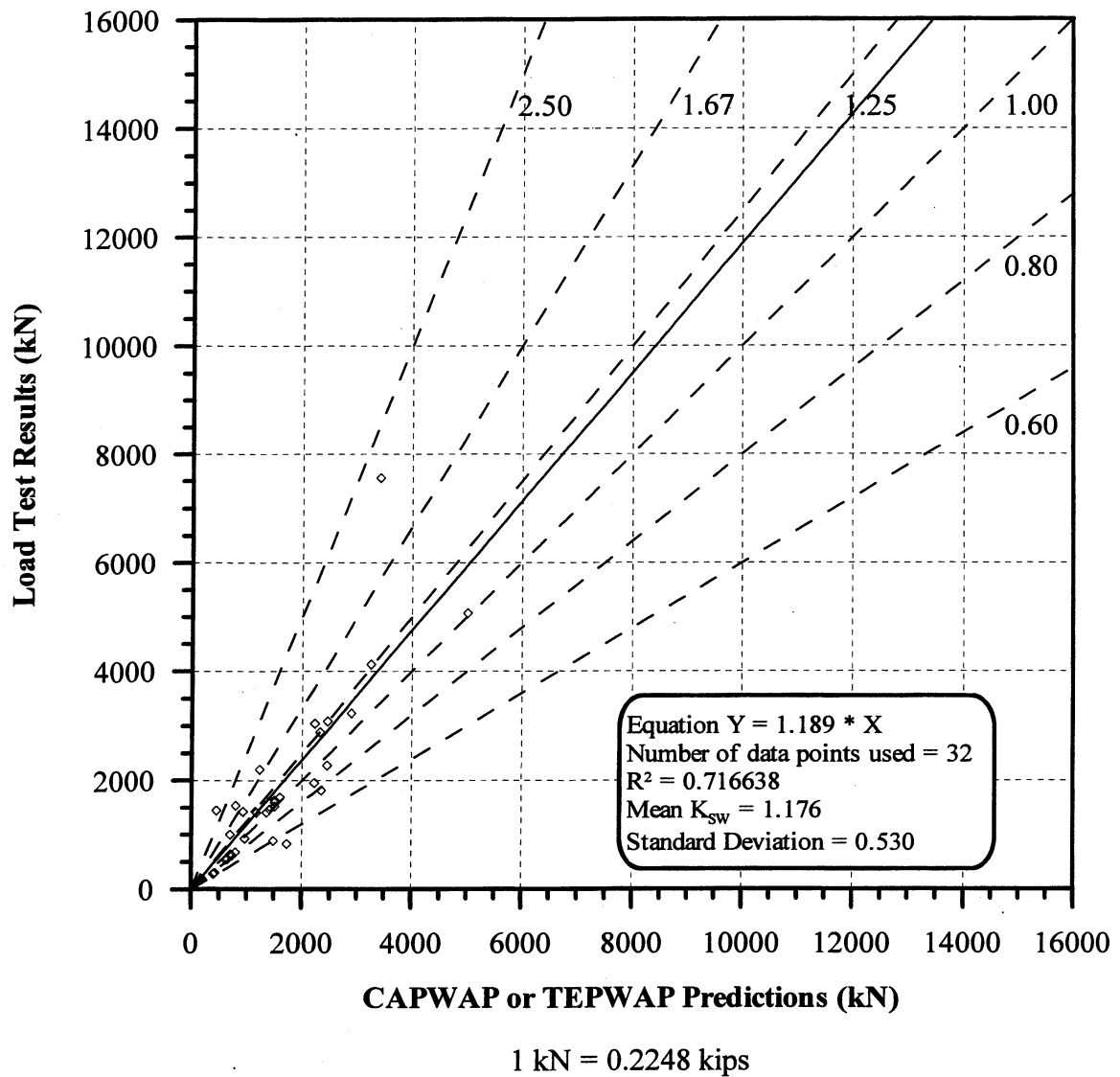


**Figure 6.19.** Static Load Test Results vs. CAPWAP or TEPWAP predictions for 32 PD/LT2000 pile-cases at the BOR(last) with Blow Count < 16 BP10cm in all types of soils (ABA).

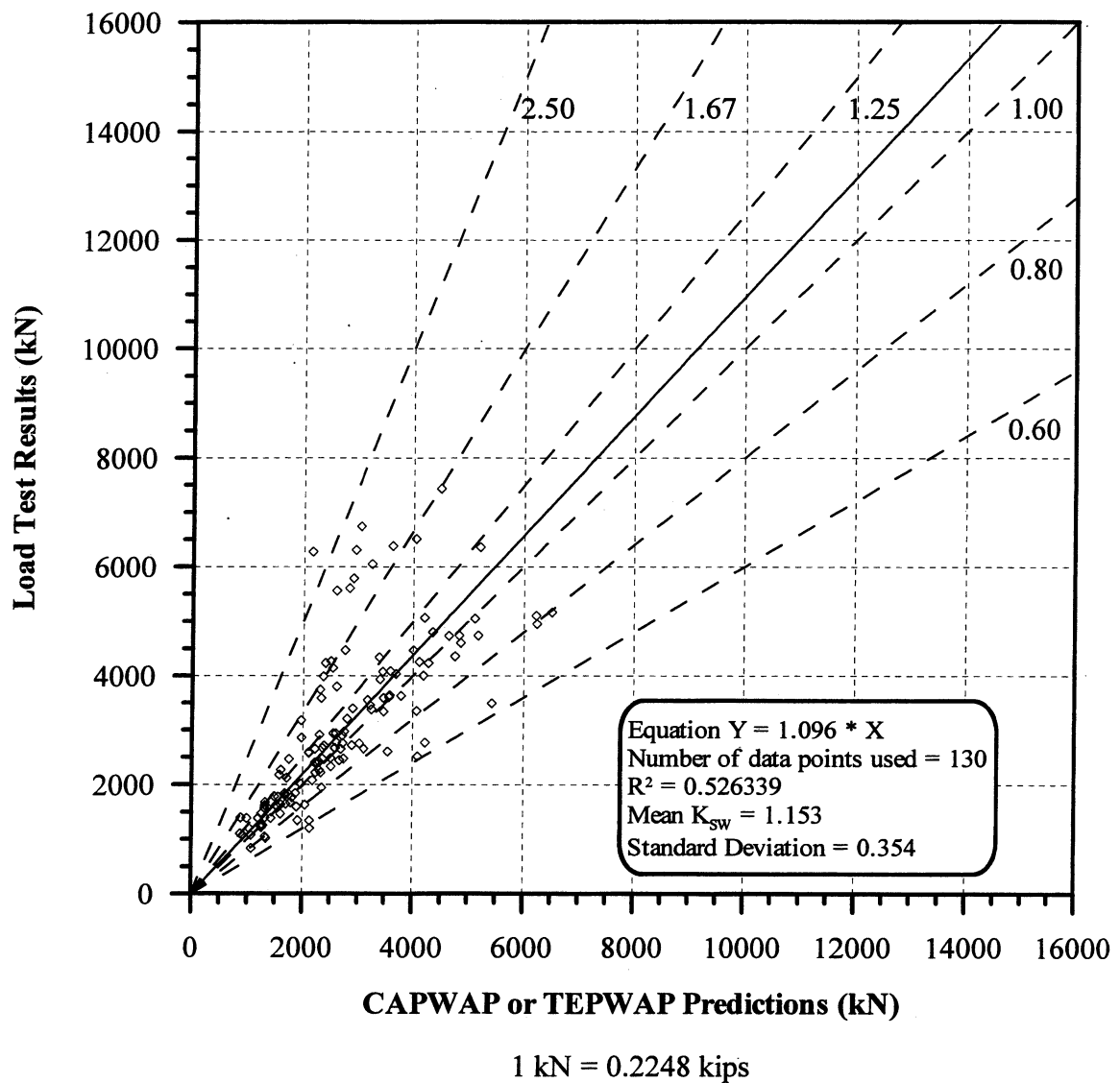


**Figure 6.20.** Static Load Test Results vs. CAPWAP or TEPWAP predictions for 130 PD/LT2000 pile-cases at the BOR(last) with Blow Count  $\geq 16$  BP10cm in all types of soils (ABA).

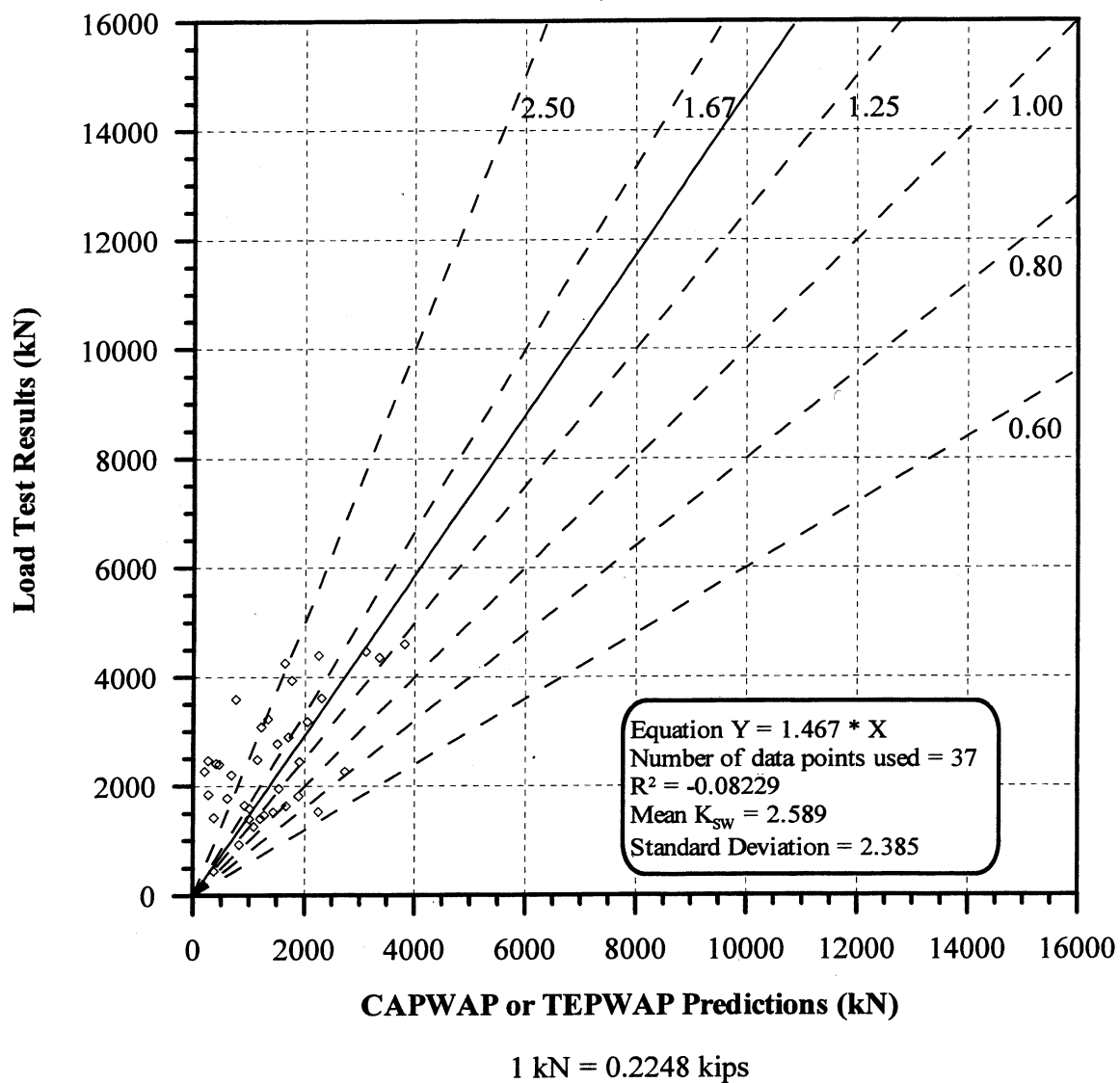


**Figure 6.21.** Static Load Test Results vs. CAPWAP or TEPWAP predictions for 37 PD/LT2000 pile-cases at the EOD with Blow Count < 16 BP10cm and Area Ratio < 350 in all types of soils (AEA).

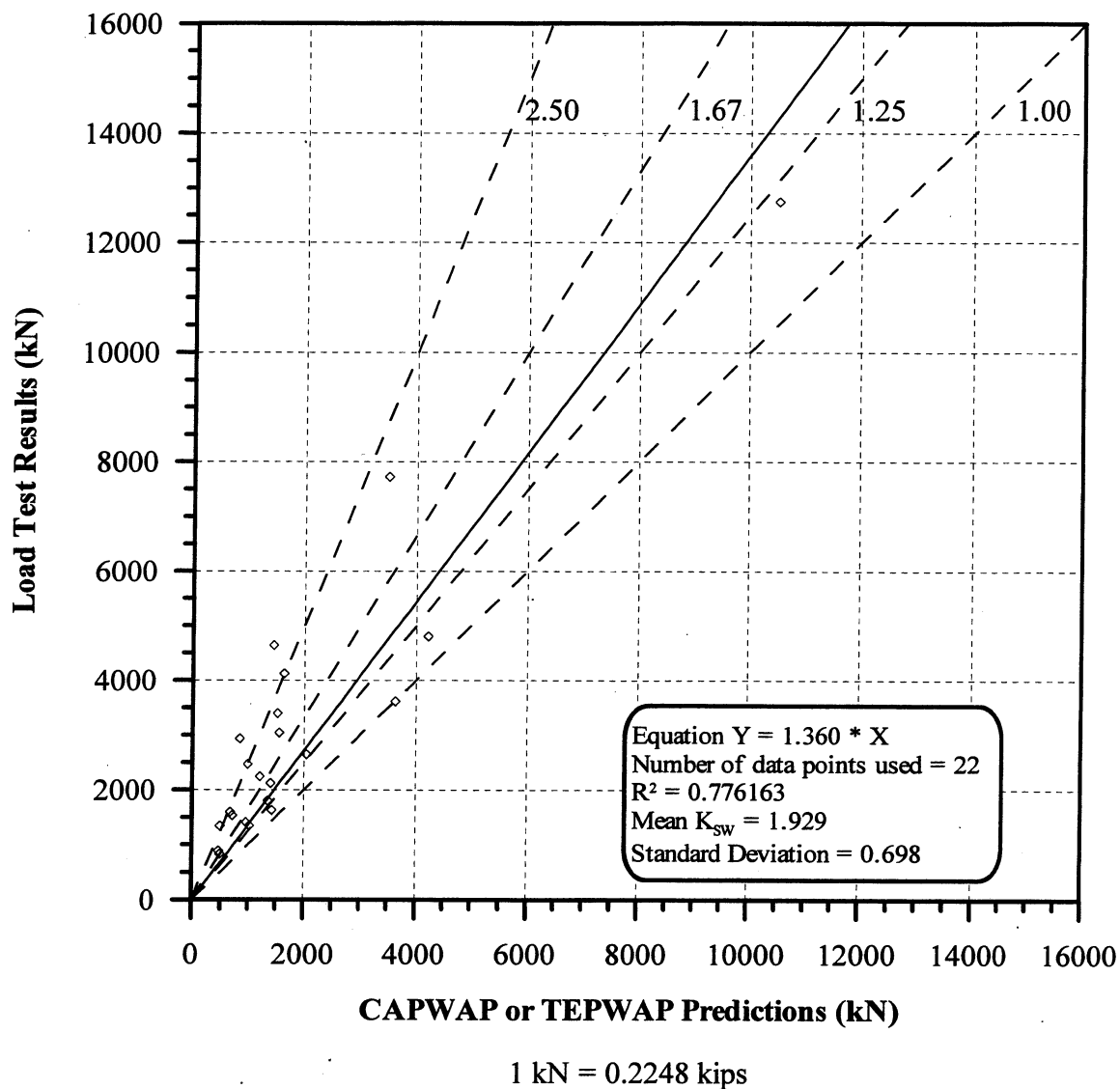


**Figure 6.22.** Static Load Test Results vs. CAPWAP or TEPWAP predictions for 22 PD/LT2000 pile-cases at the EOD with Blow Count < 16 BP10cm and Area Ratio  $\geq 350$  in all types of soils (AEA).

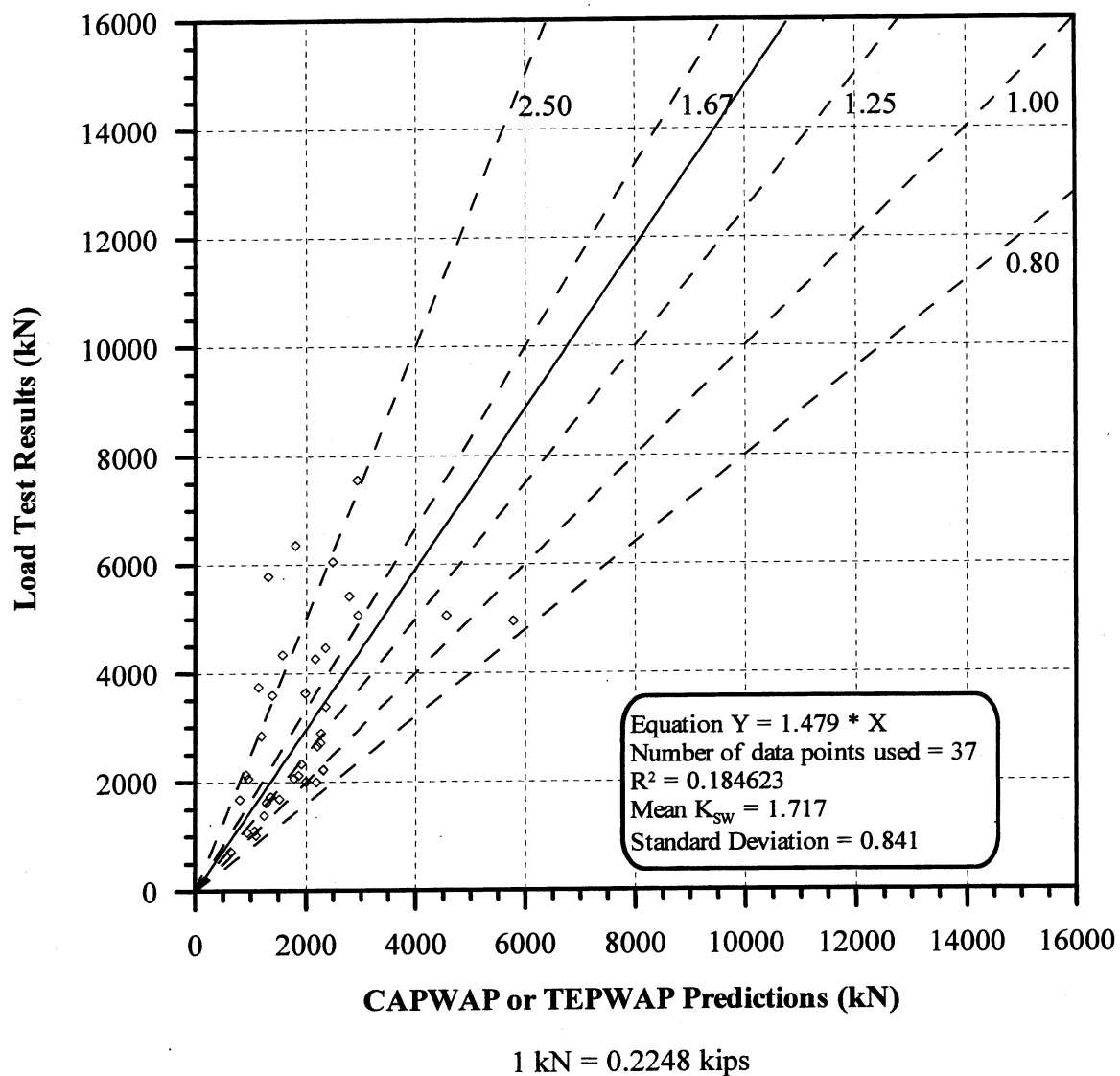


**Figure 6.23.** Static Load Test Results vs. CAPWAP or TEPWAP predictions for 37 PD/LT2000 pile-cases at the EOD with Blow Count  $\geq 16$  BP10cm and Area Ratio  $< 350$  in all types of soils (AEA).

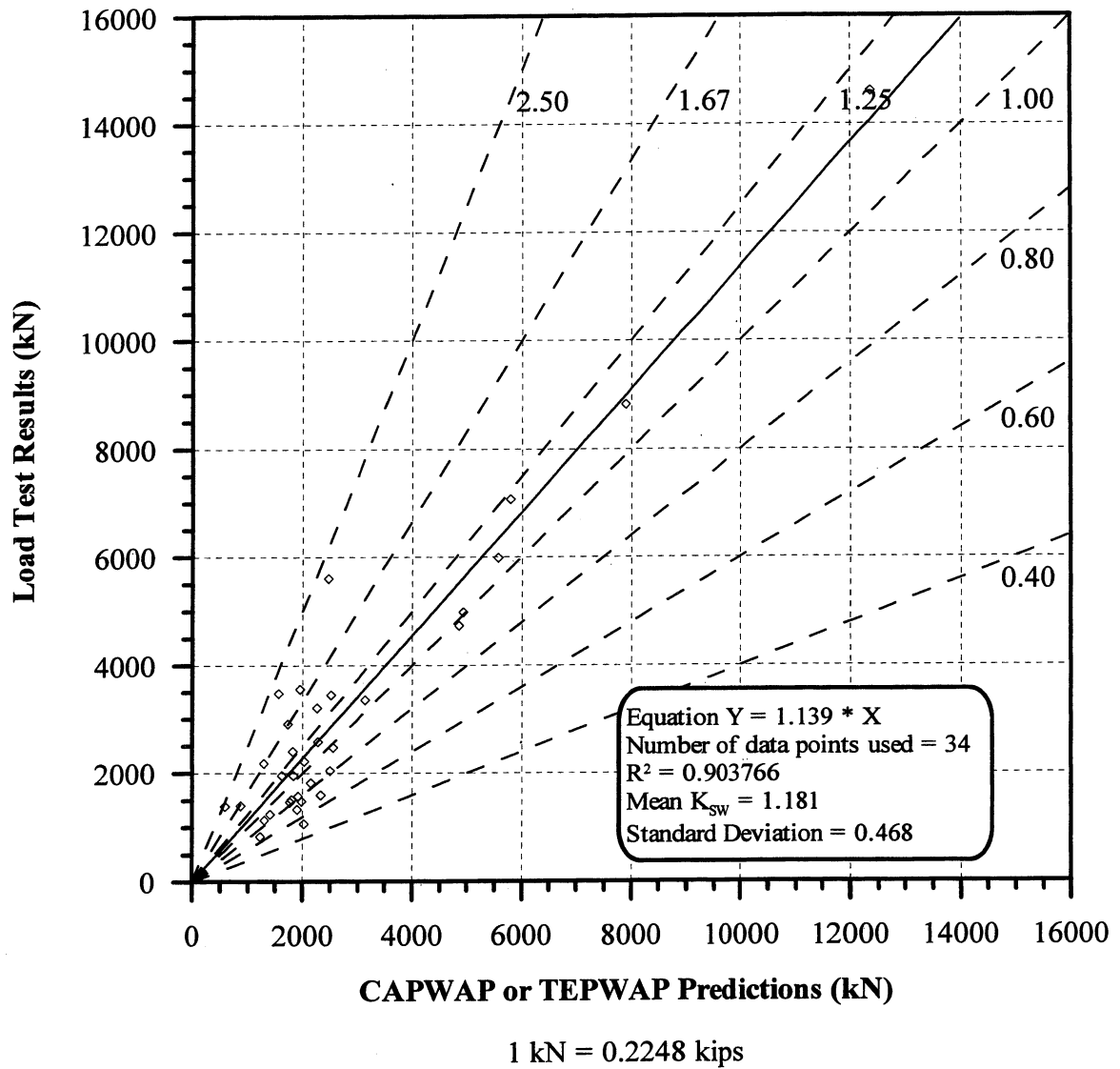


**Figure 6.24.** Static Load Test Results vs. CAPWAP or TEPWAP predictions for 34 PD/LT2000 pile-cases at the EOD with Blow Count  $\geq 16$  BP10cm and Area Ratio  $\geq 350$  in all types of soils (AEA).

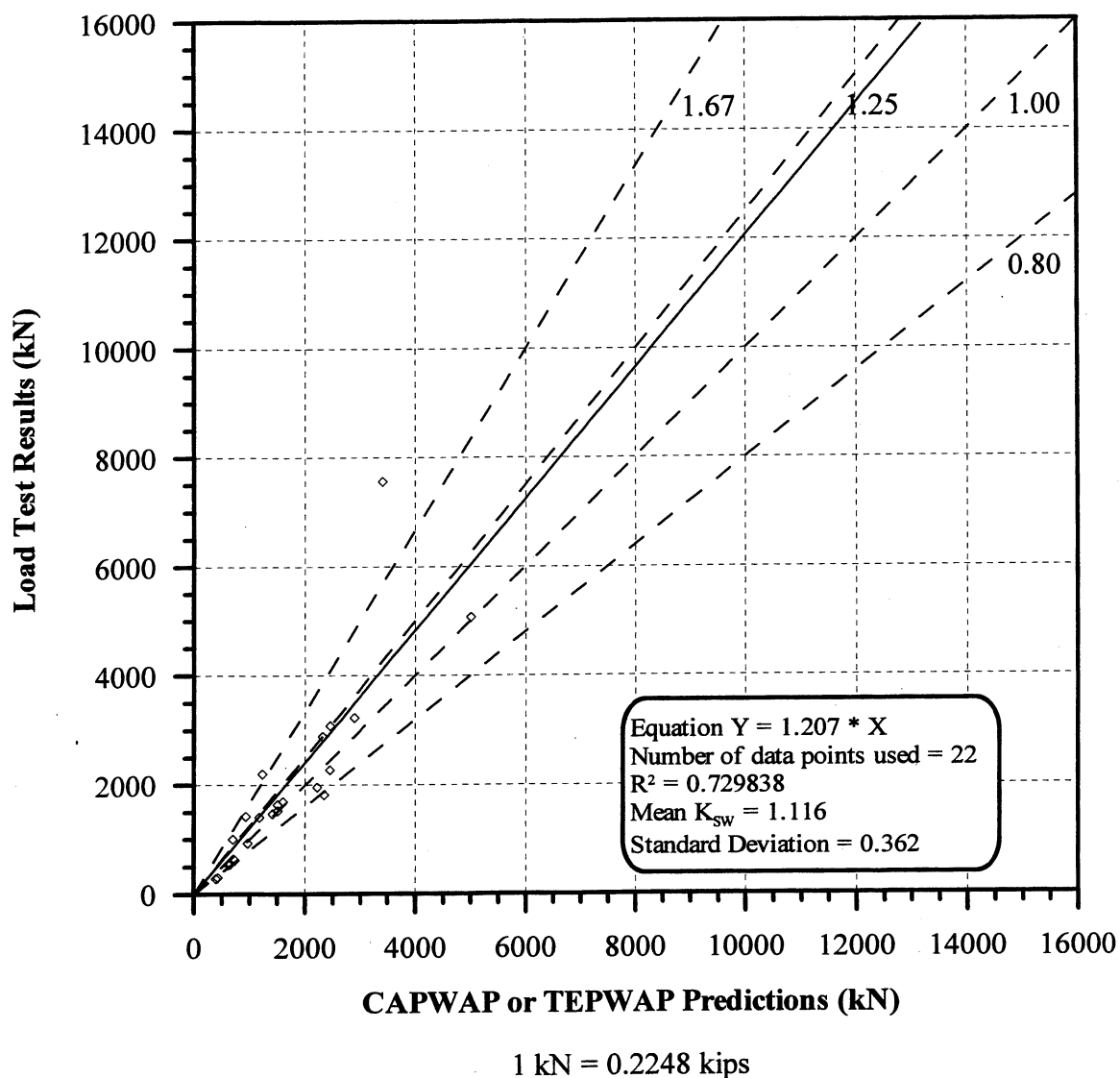


**Figure 6.25.** Static Load Test Results vs. CAPWAP or TEPWAP predictions for 22 PD/LT2000 pile-cases at the BOR (last) with Blow Count < 16 BP10cm and Area Ratio < 350 in all types of soils (ABA).

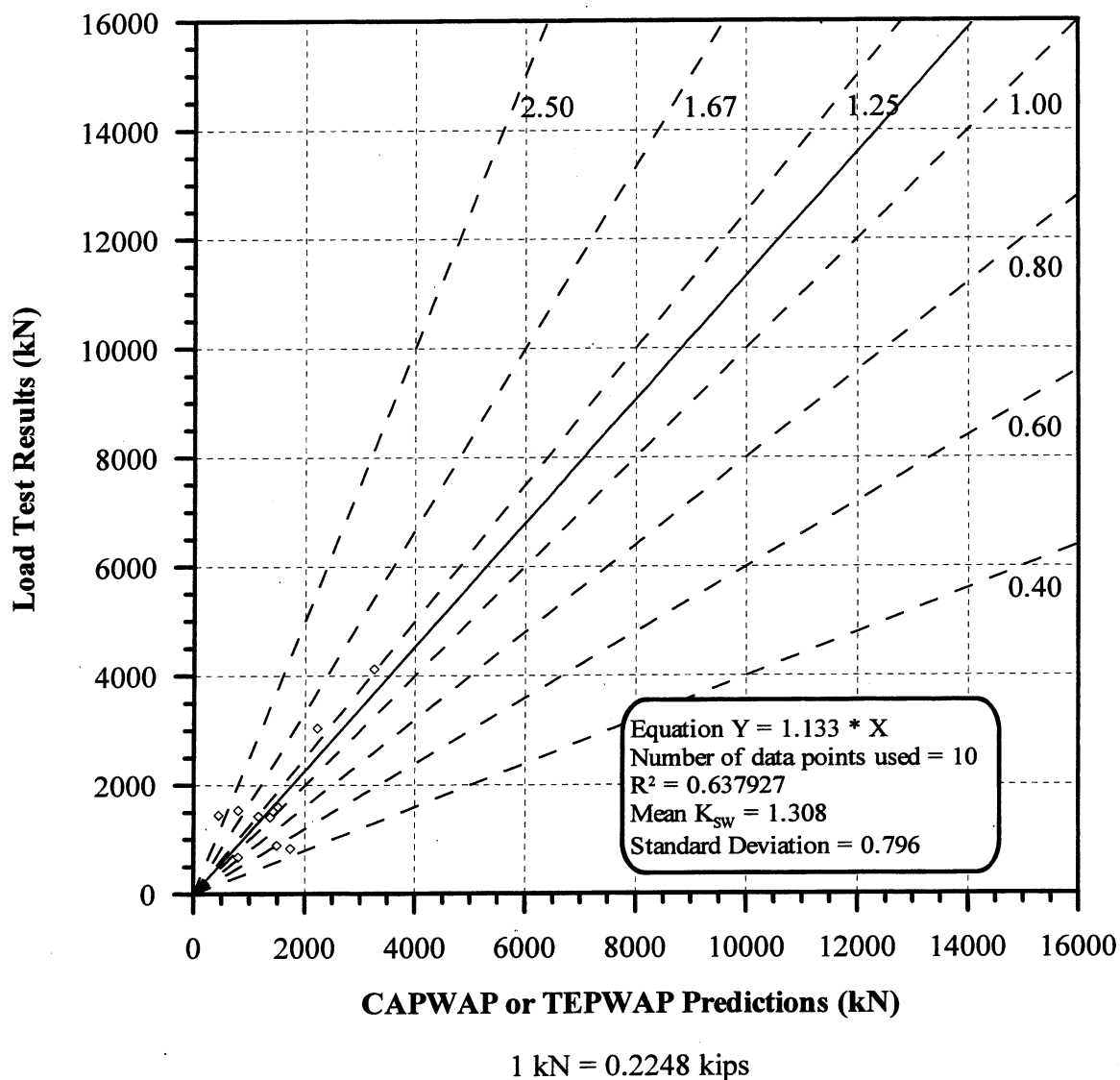


**Figure 6.26.** Static Load Test Results vs. CAPWAP or TEPWAP predictions for 10 PD/LT2000 pile-cases at the BOR (last) with Blow Count < 16 BP10cm and Area Ratio  $\geq 350$  in all types of soils (ABA).



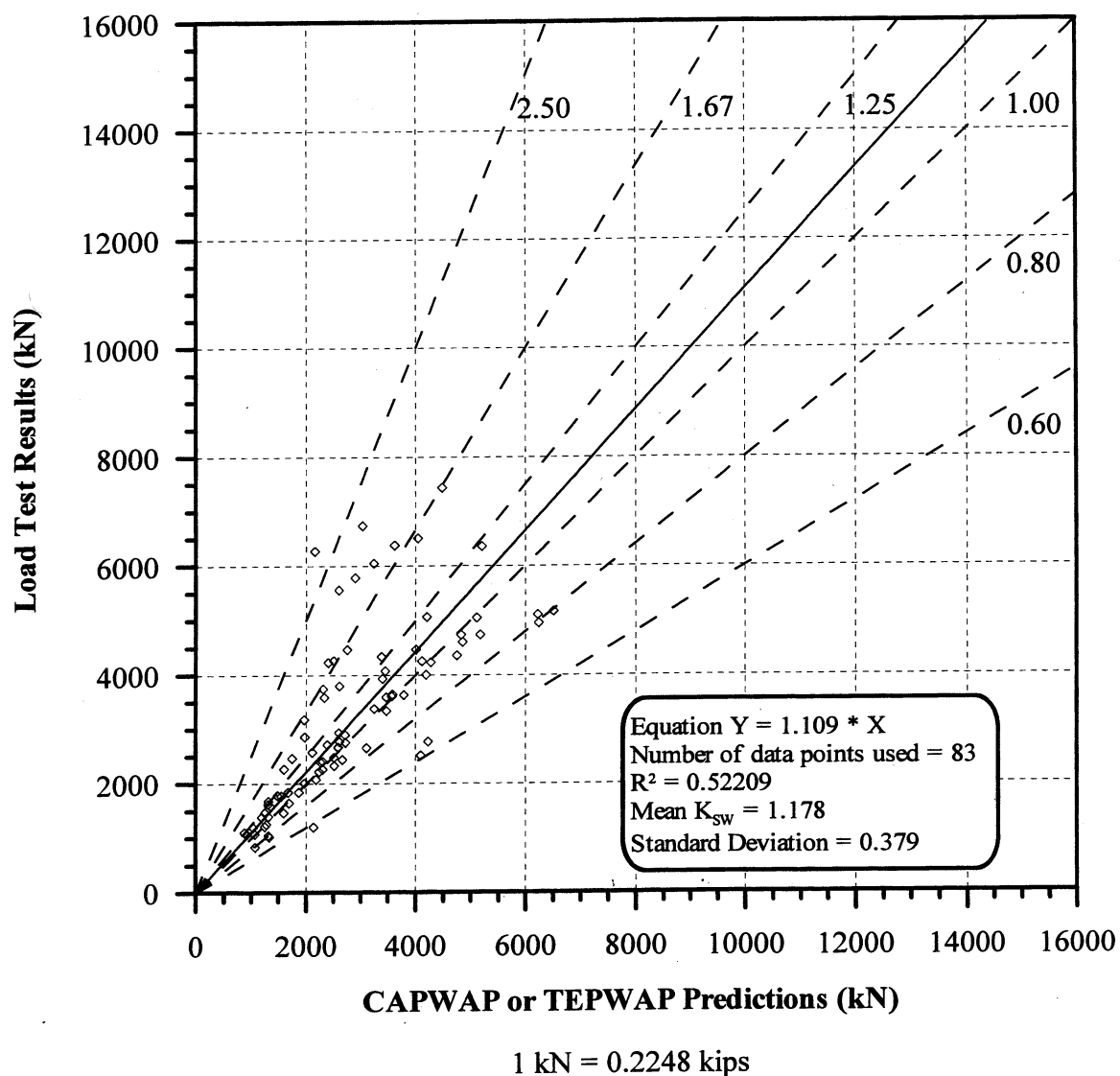


**Figure 6.27.** Static Load Test Results vs. CAPWAP or TEPWAP predictions for 83 PD/LT2000 pile-cases at the BOR (last) with Blow Count  $\geq 16$  BP10cm and Area Ratio  $< 350$  in all types of soils (ABA).

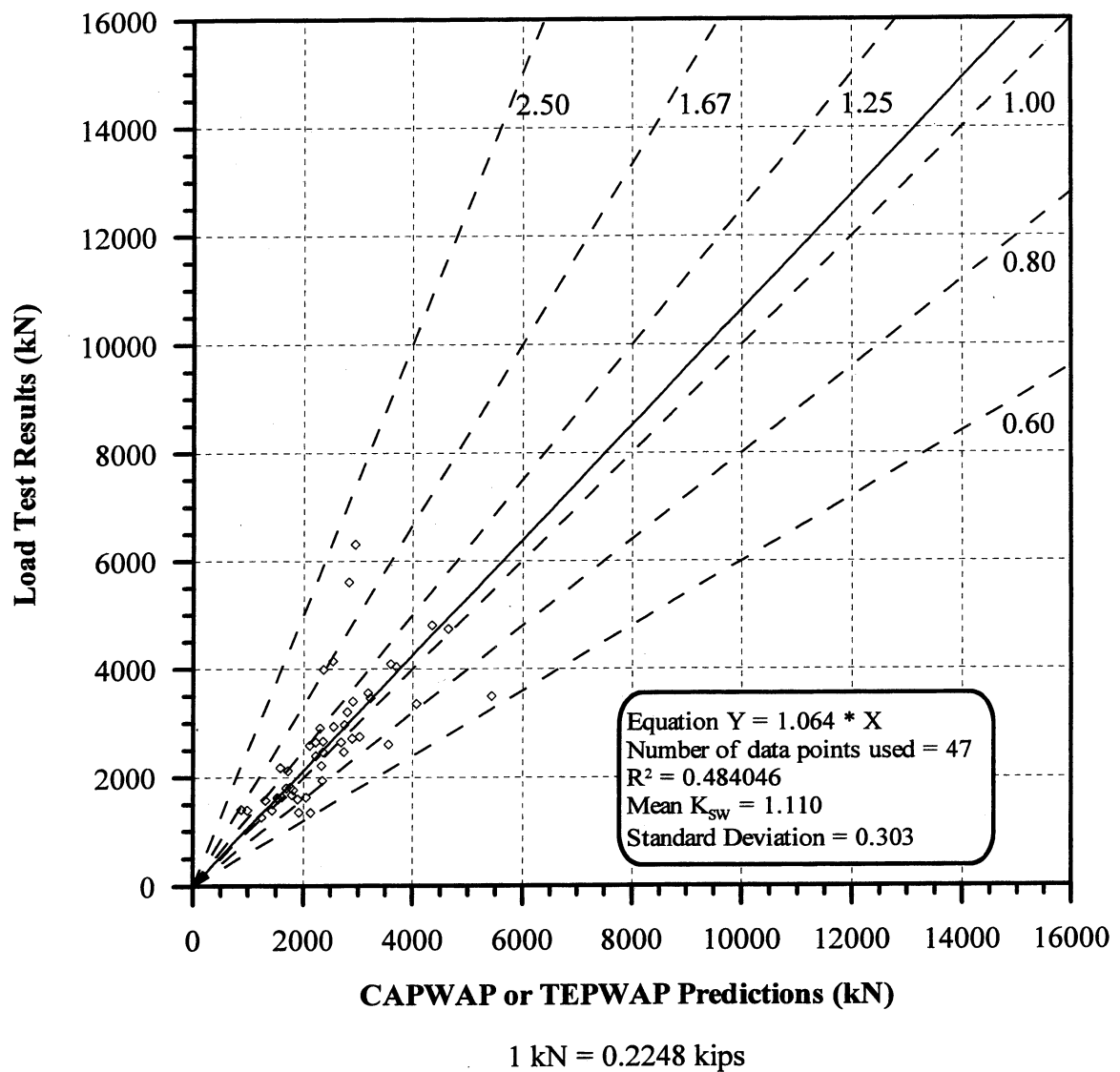


**Figure 6.28.** Static Load Test Results vs. CAPWAP or TEPWAP predictions for 47 PD/LT2000 pile-cases at the BOR (last) with Blow Count  $\geq 16$  BP10cm and Area Ratio  $\geq 350$  in all types of soils (ABA).

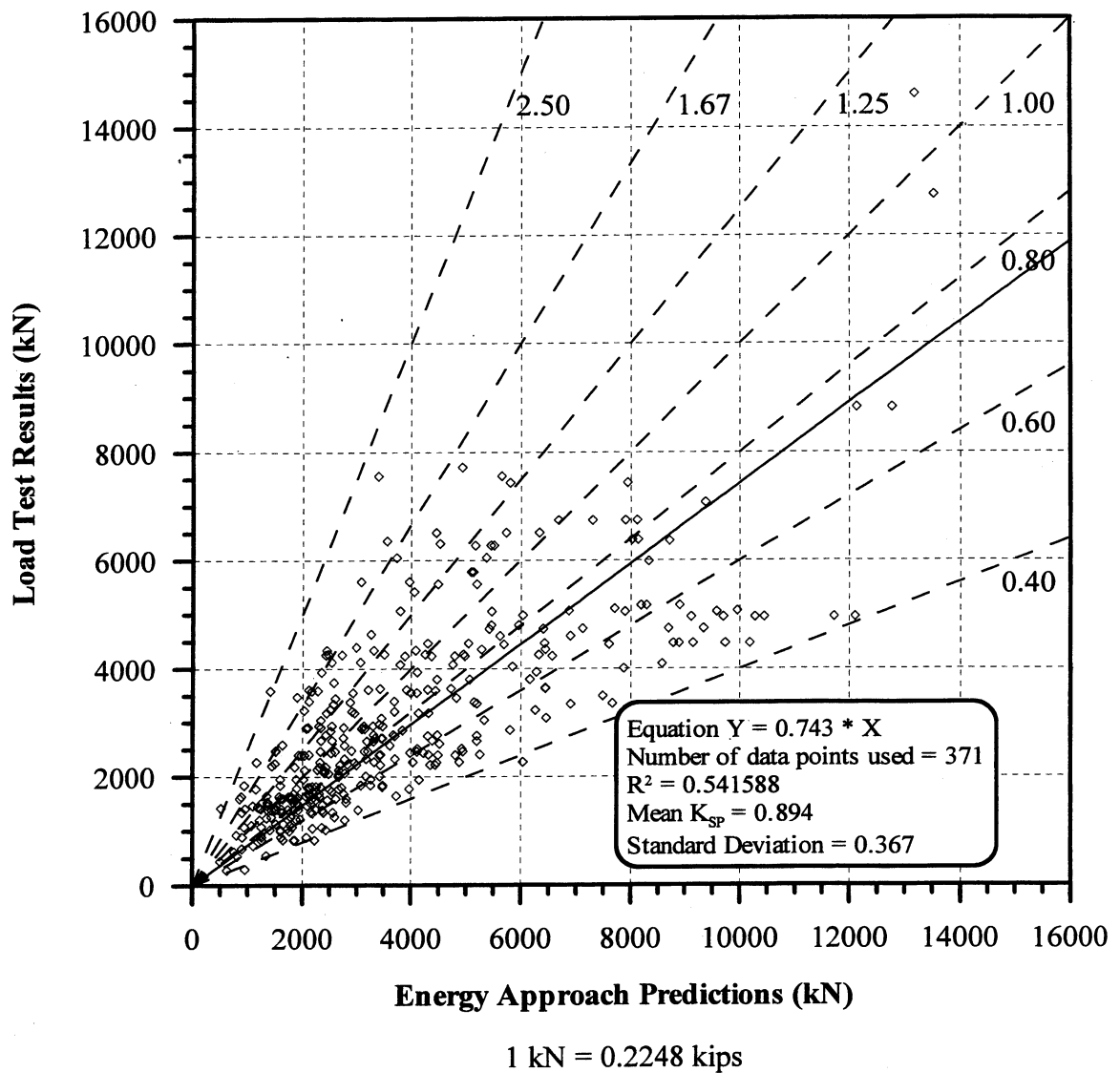


**Figure 6.29.** Static Load Test Results vs. Energy Approach predictions for 371 PD/LT2000 pile-cases at all times and in all types of soils (AAA).

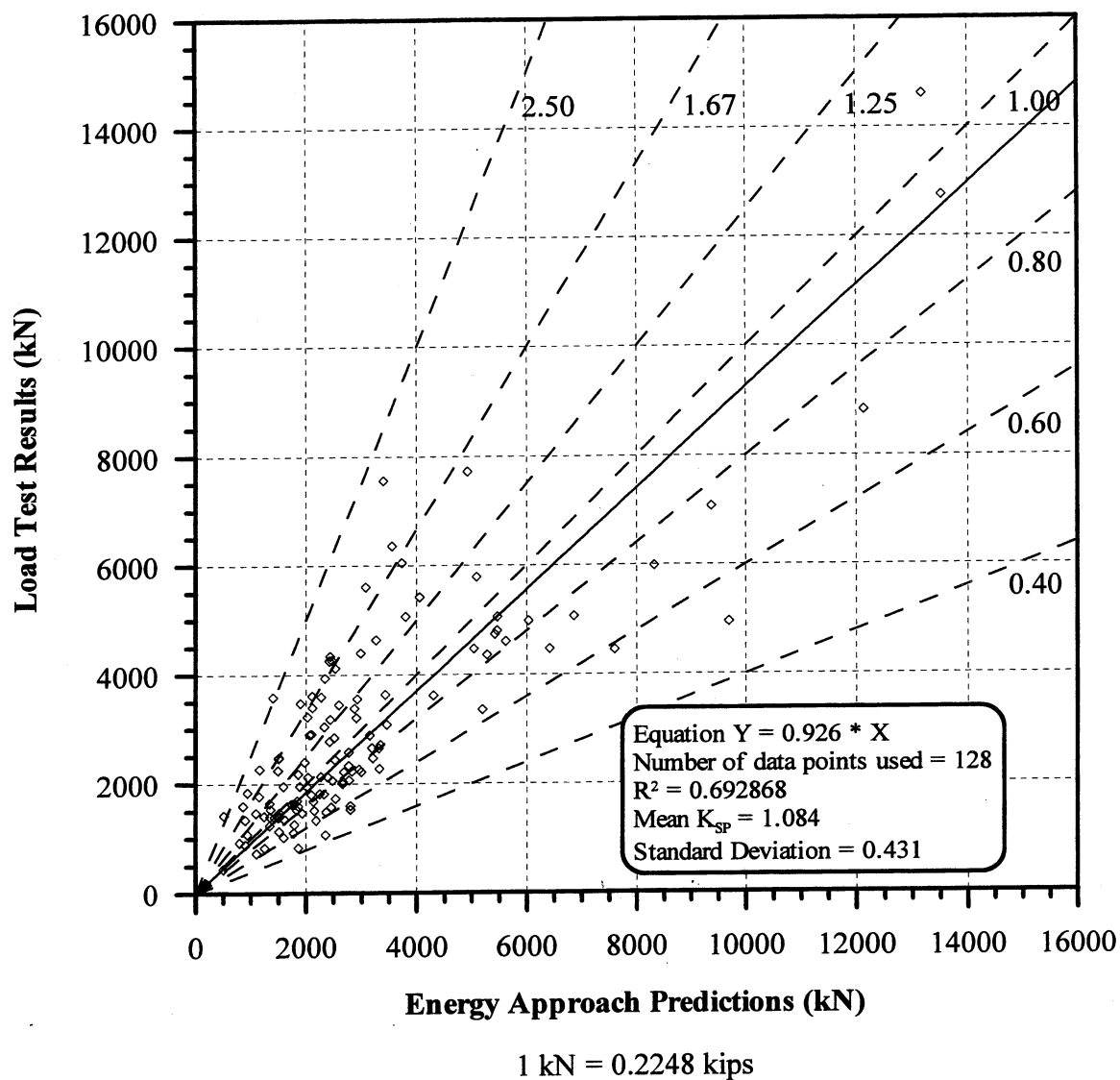


**Figure 6.30.** Static Load Test Results vs. Energy Approach predictions for 128 PD/LT2000 pile-cases at EOD in all types of soils (AEA).

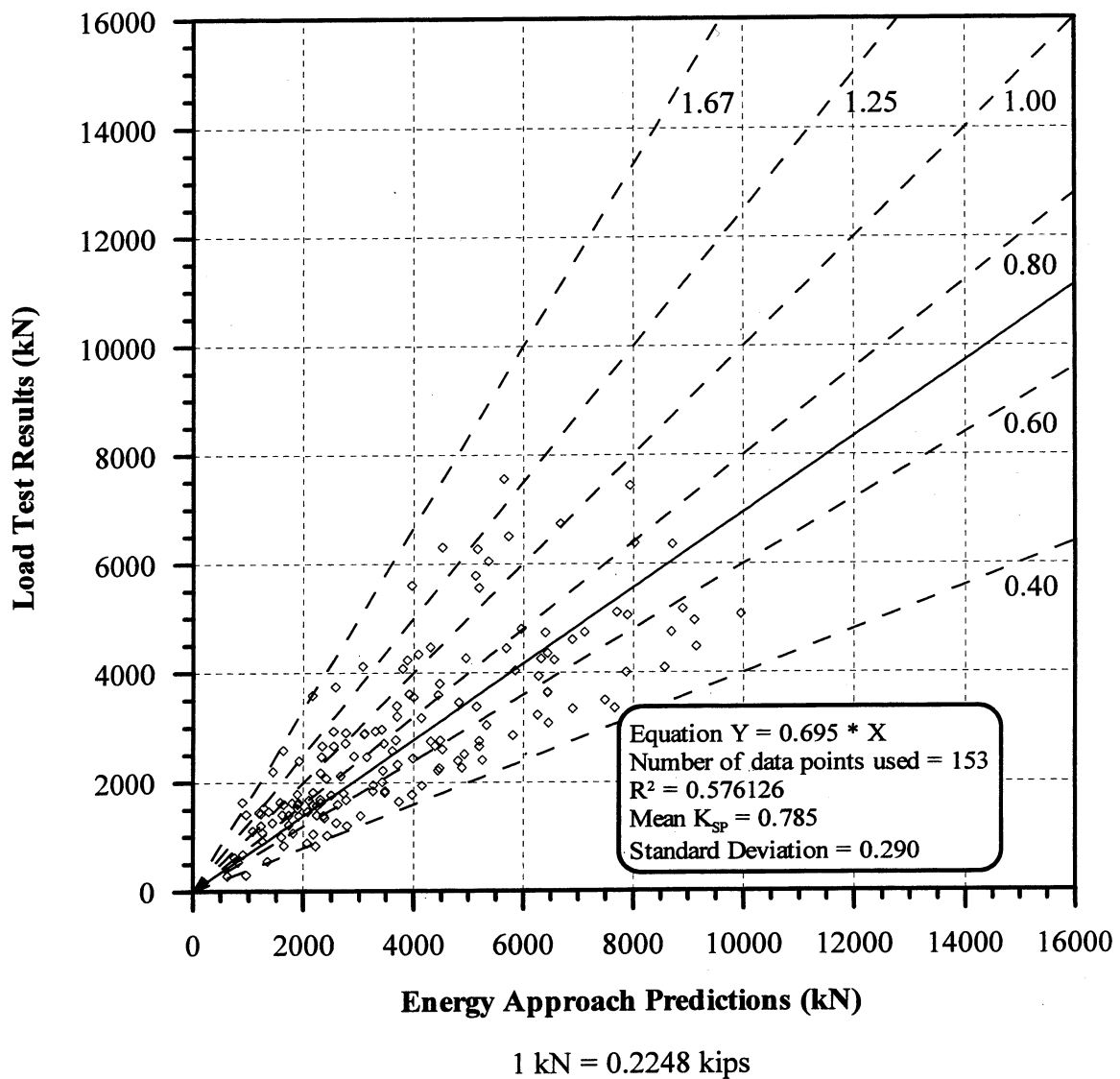


**Figure 6.31.** Static Load Test Results vs. Energy Approach predictions for 153 PD/LT2000 pile-cases at BOR (last) in all types of soils (ABA).

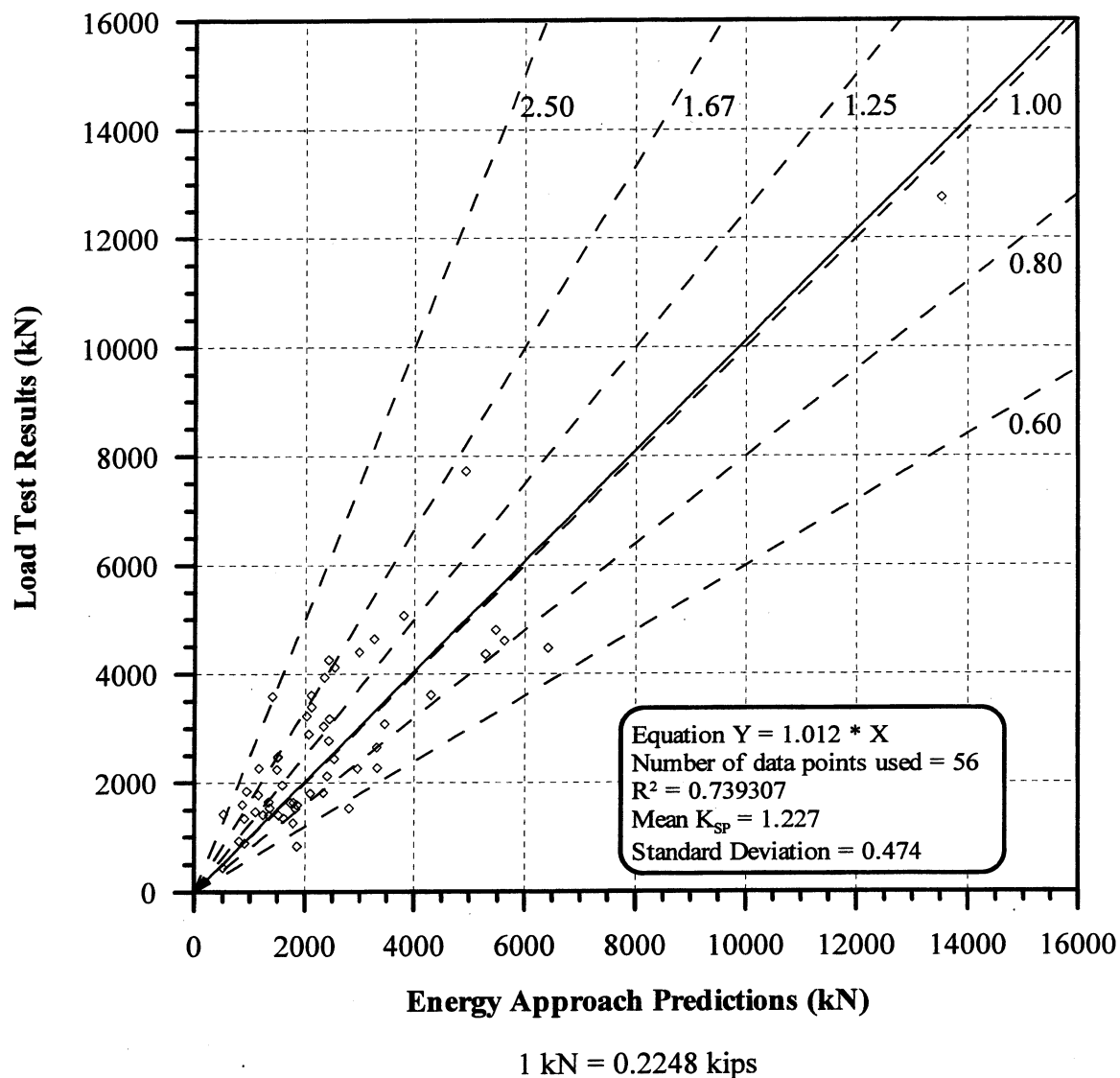


**Figure 6.32.** Static Load Test Results vs. Energy Approach predictions for 56 PD/LT2000 pile-cases at the EOD with Blow Count < 16 BP10cm in all types of soils (AEA).

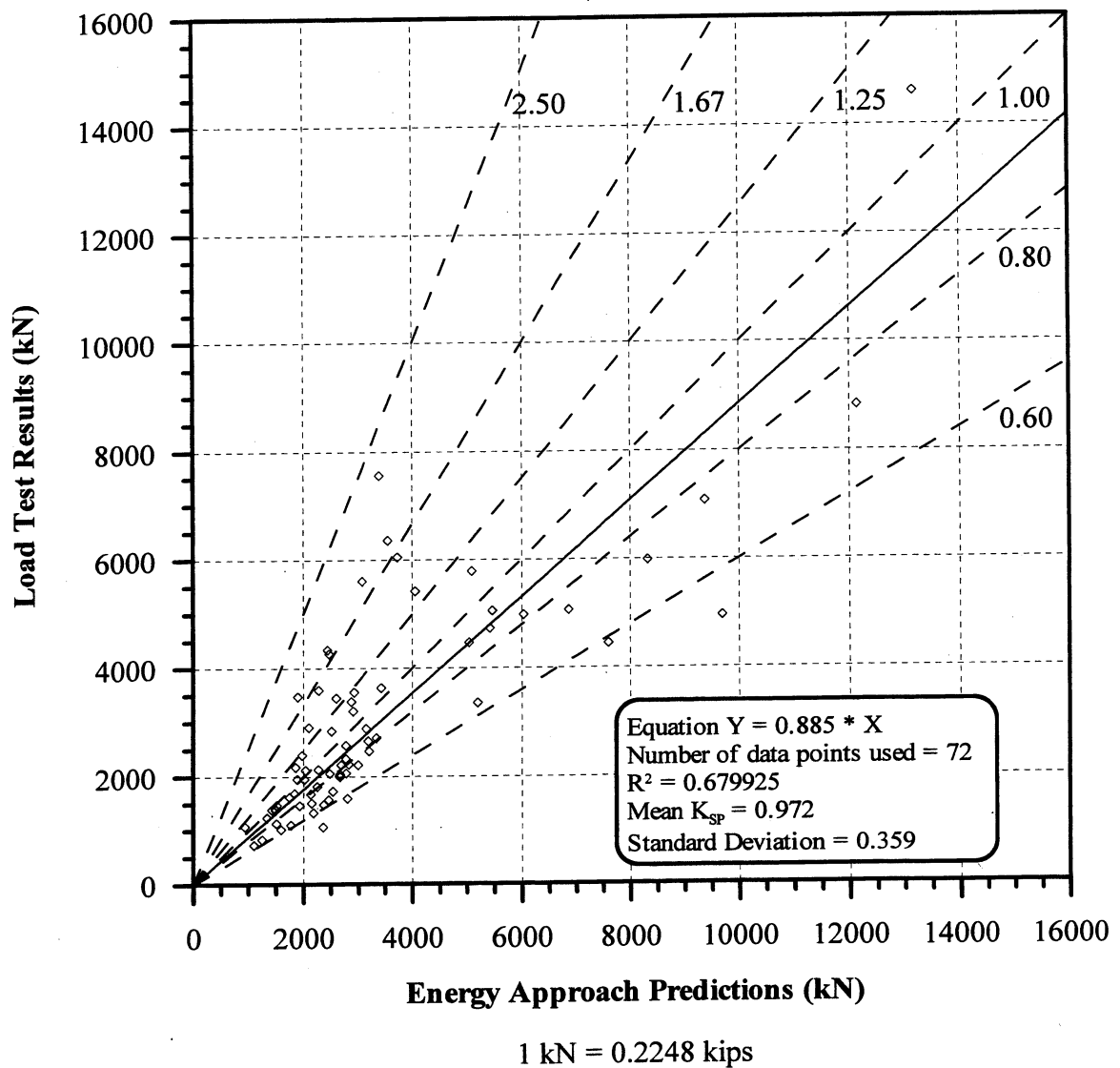


**Figure 6.33.** Static Load Test Results vs. Energy Approach predictions for 72 PD/LT2000 pile-cases at the EOD with Blow Count  $\geq 16$  BP10cm in all types of soils (AEA).

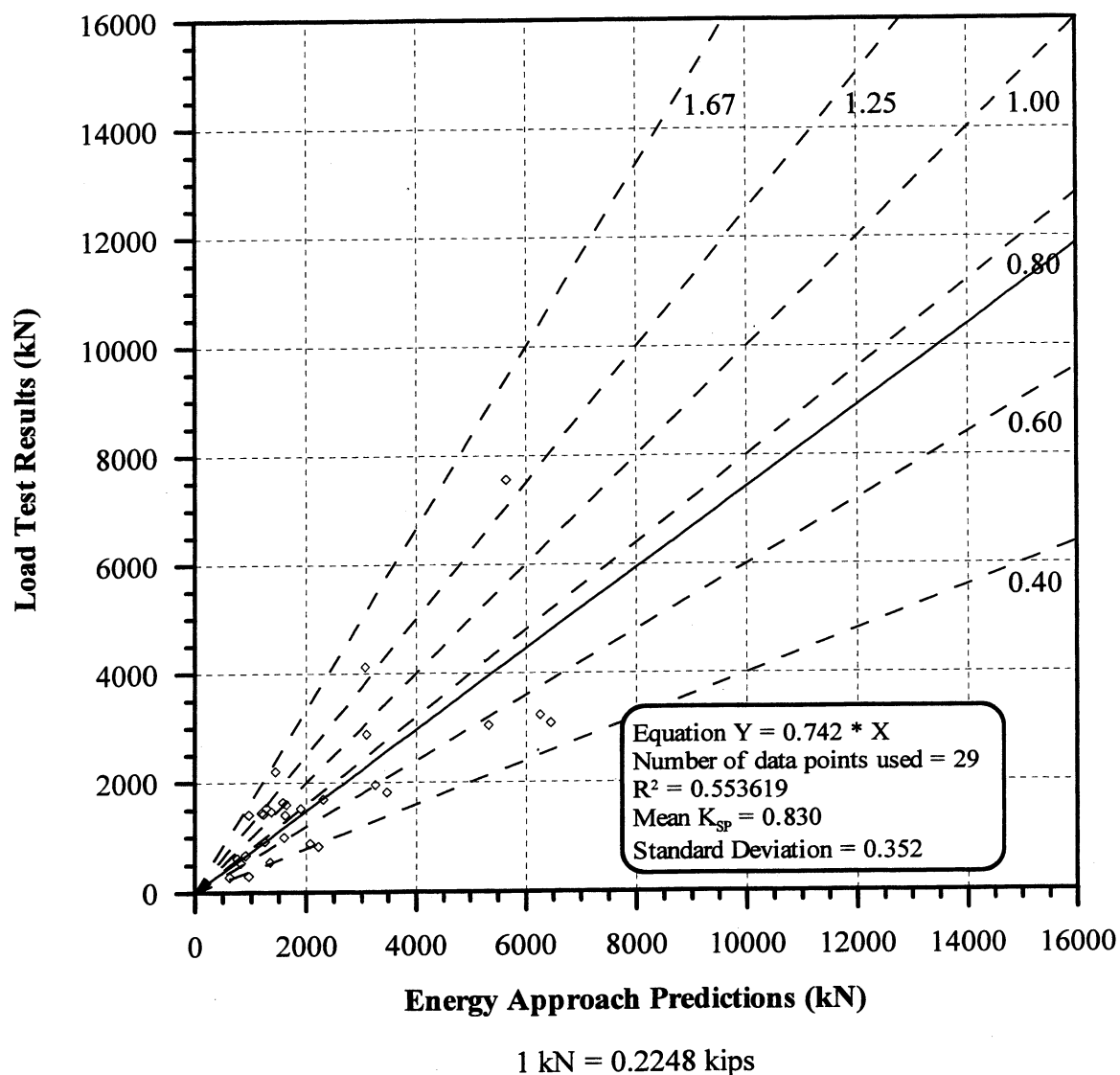


**Figure 6.34.** Static Load Test Results vs. Energy Approach predictions for 29 PD/LT2000 pile-cases at the BOR (last) with Blow Count < 16 BP10cm in all types of soils (ABA).



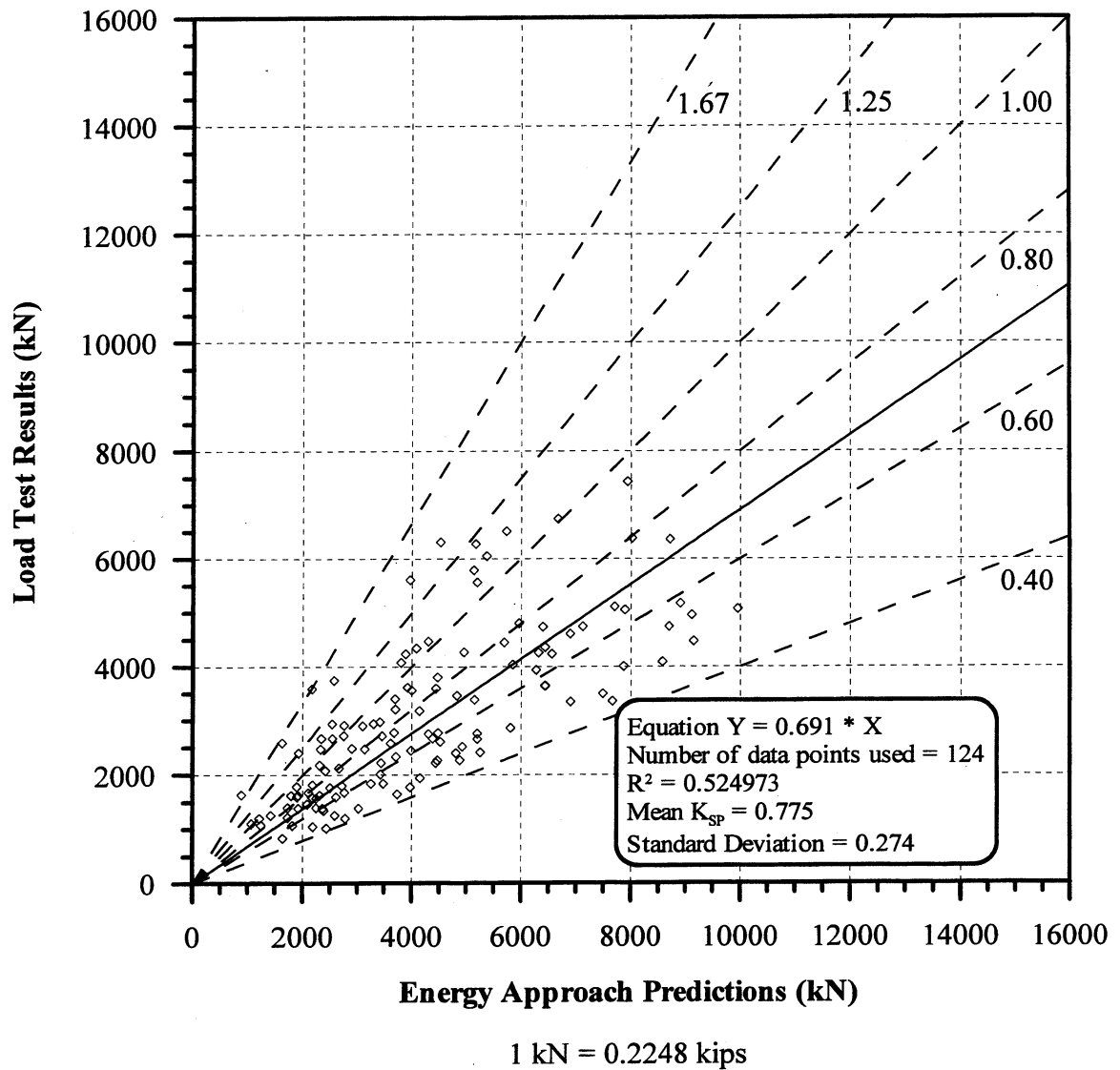


**Figure 6.35.** Static Load Test Results vs. Energy Approach predictions for 124 PD/LT2000 pile-cases at the BOR (last) with Blow Count  $\geq 16$  BP10cm in all types of soils (ABA).

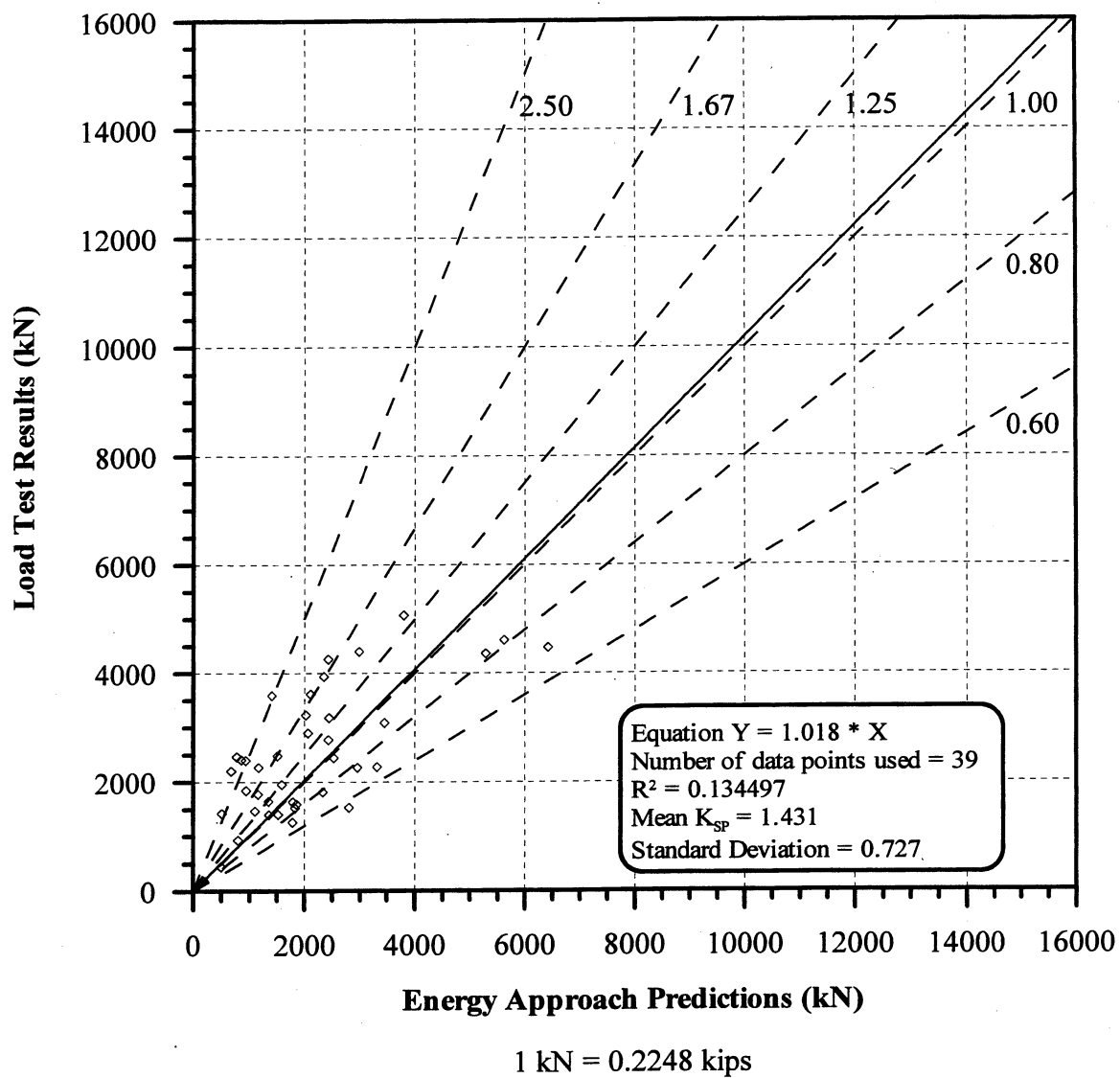


**Figure 6.36.** Static Load Test Results vs. Energy Approach predictions for 39 PD/LT2000 pile-cases at the EOD with Blow Count < 16 BP10cm and Area Ratio < 350 in all types of soils (AEA).

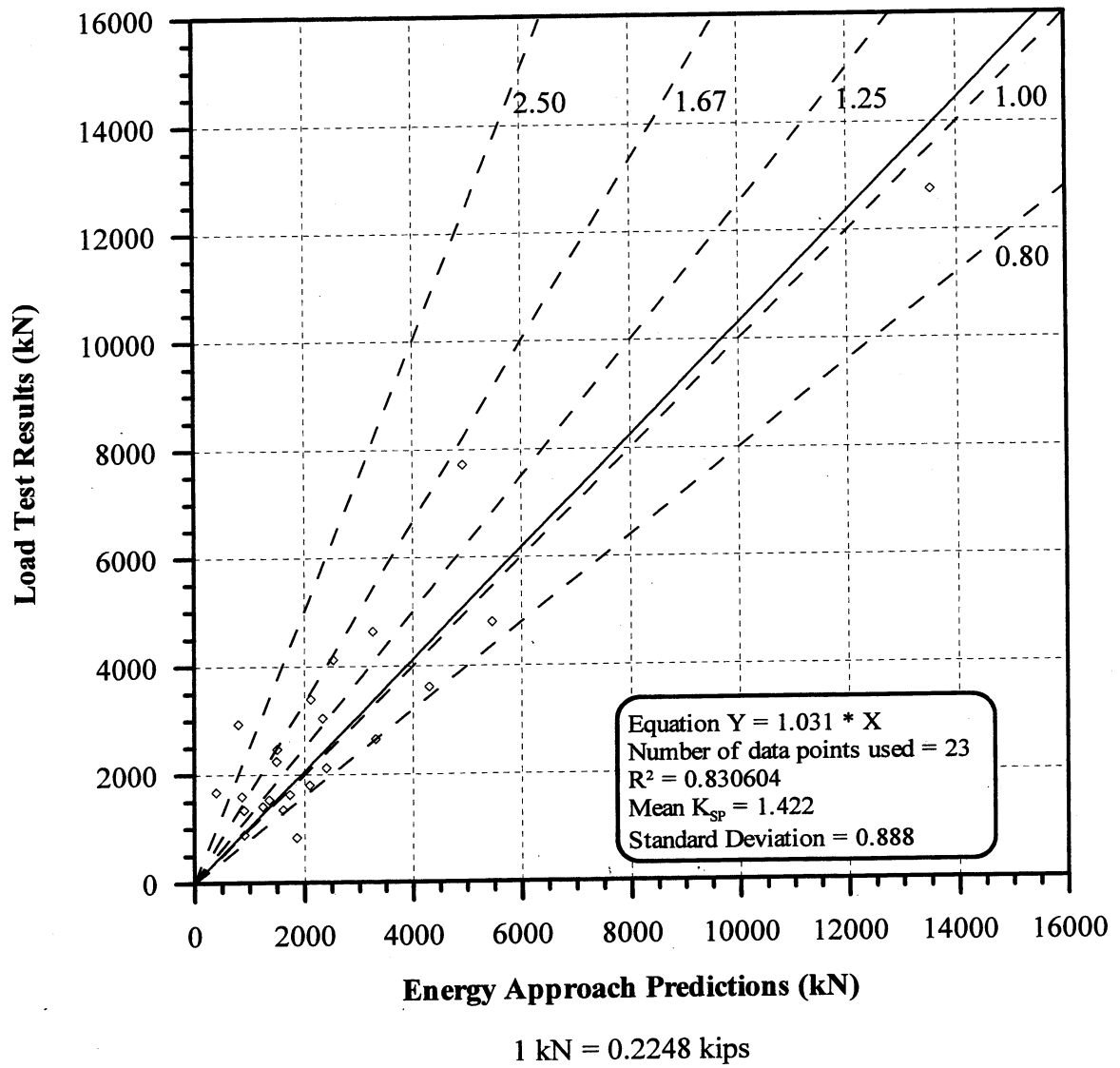


**Figure 6.37.** Static Load Test Results vs. Energy Approach predictions for 23 PD/LT2000 pile-cases at the EOD with Blow Count < 16 BP10cm and Area Ratio  $\geq 350$  in all types of soils (AEA).

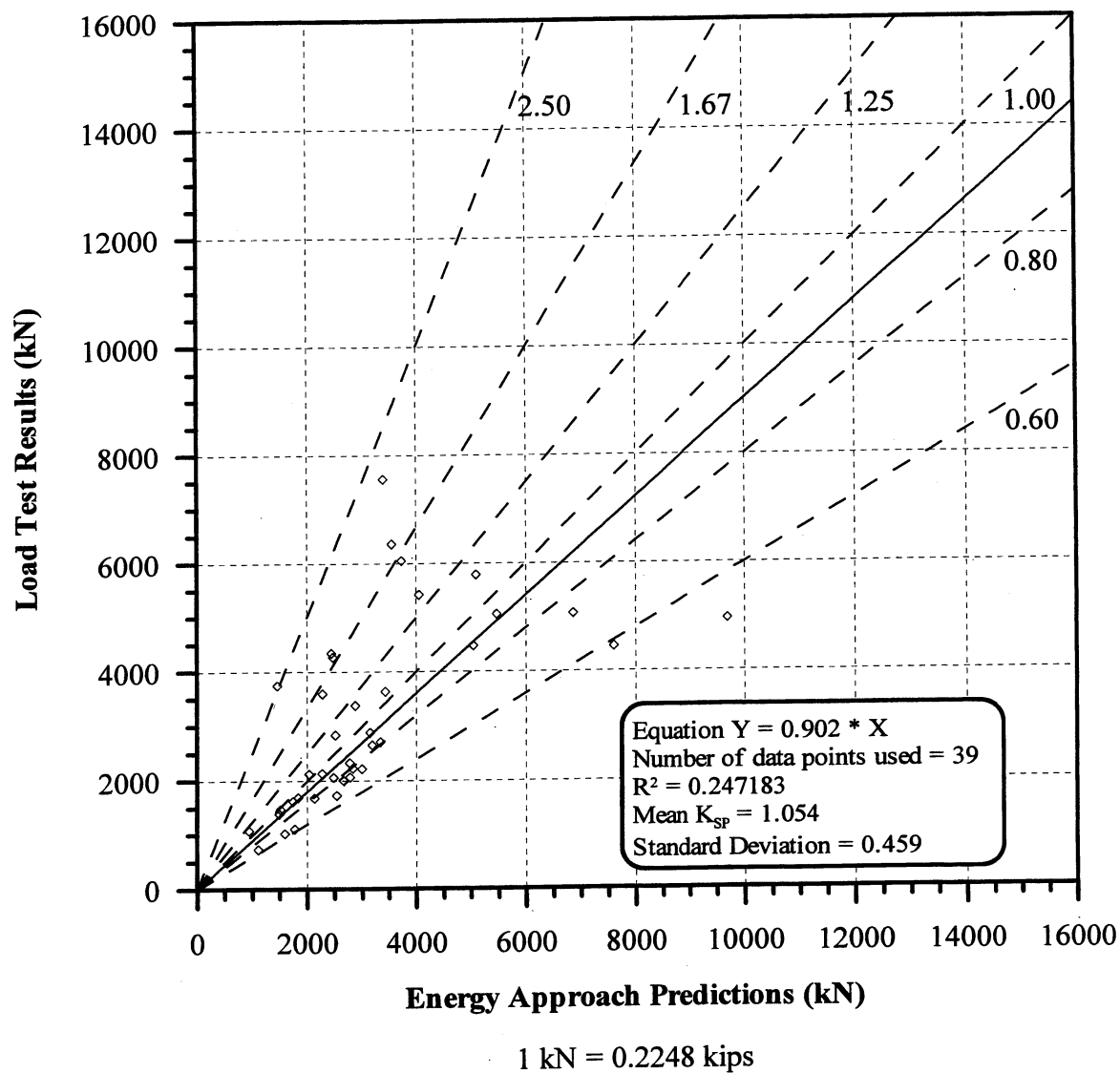


**Figure 6.38.** Static Load Test Results vs. Energy Approach predictions for 39 PD/LT2000 pile-cases at the EOD with Blow Count  $\geq 16$  BP10cm and Area Ratio  $< 350$  in all types of soils (AEA).

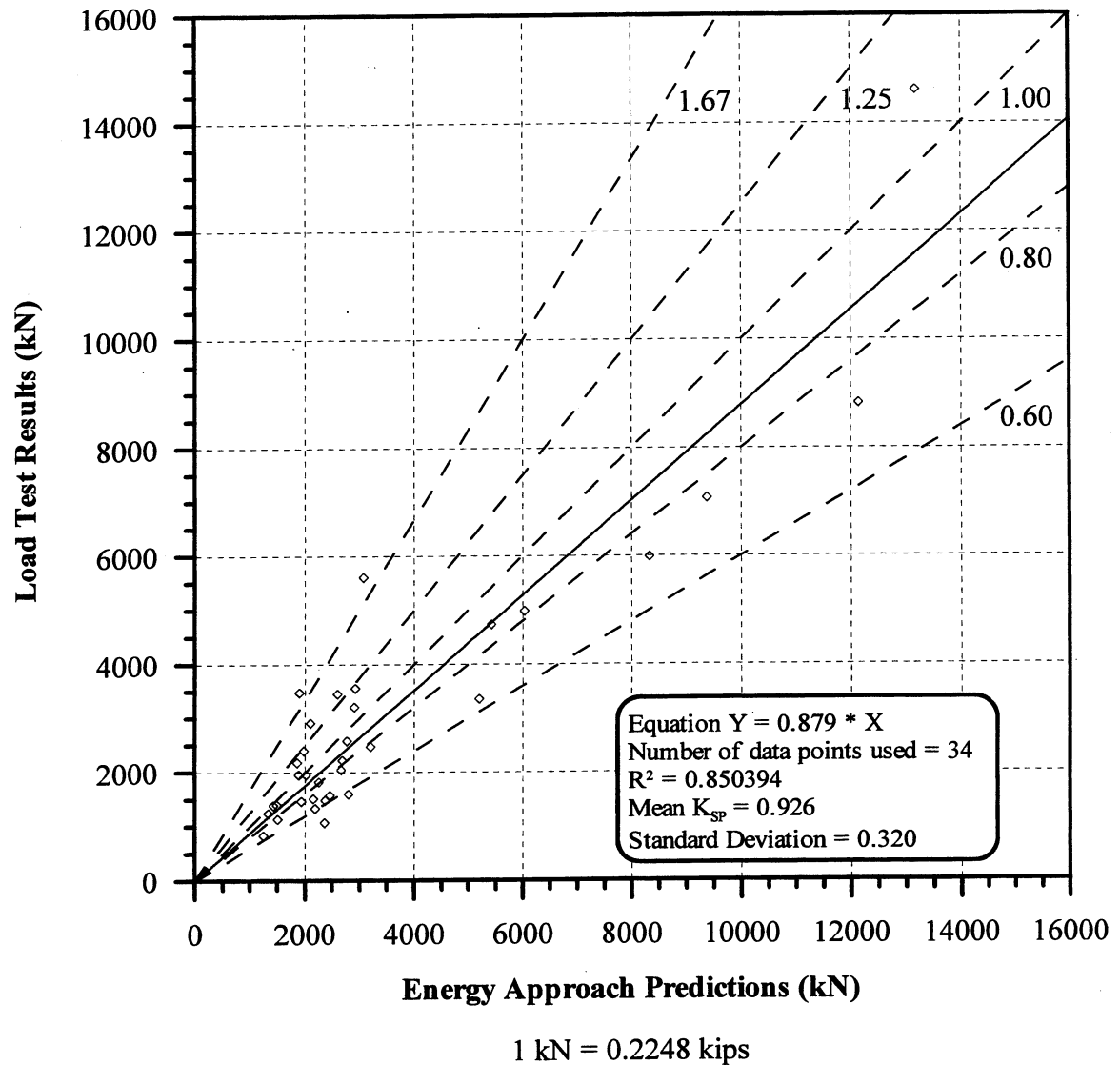


**Figure 6.39.** Static Load Test Results vs. Energy Approach predictions for 34 PD/LT2000 pile-cases at the EOD with Blow Count  $\geq 16$  BP10cm and Area Ratio  $\geq 350$  in all types of soils (AEA).

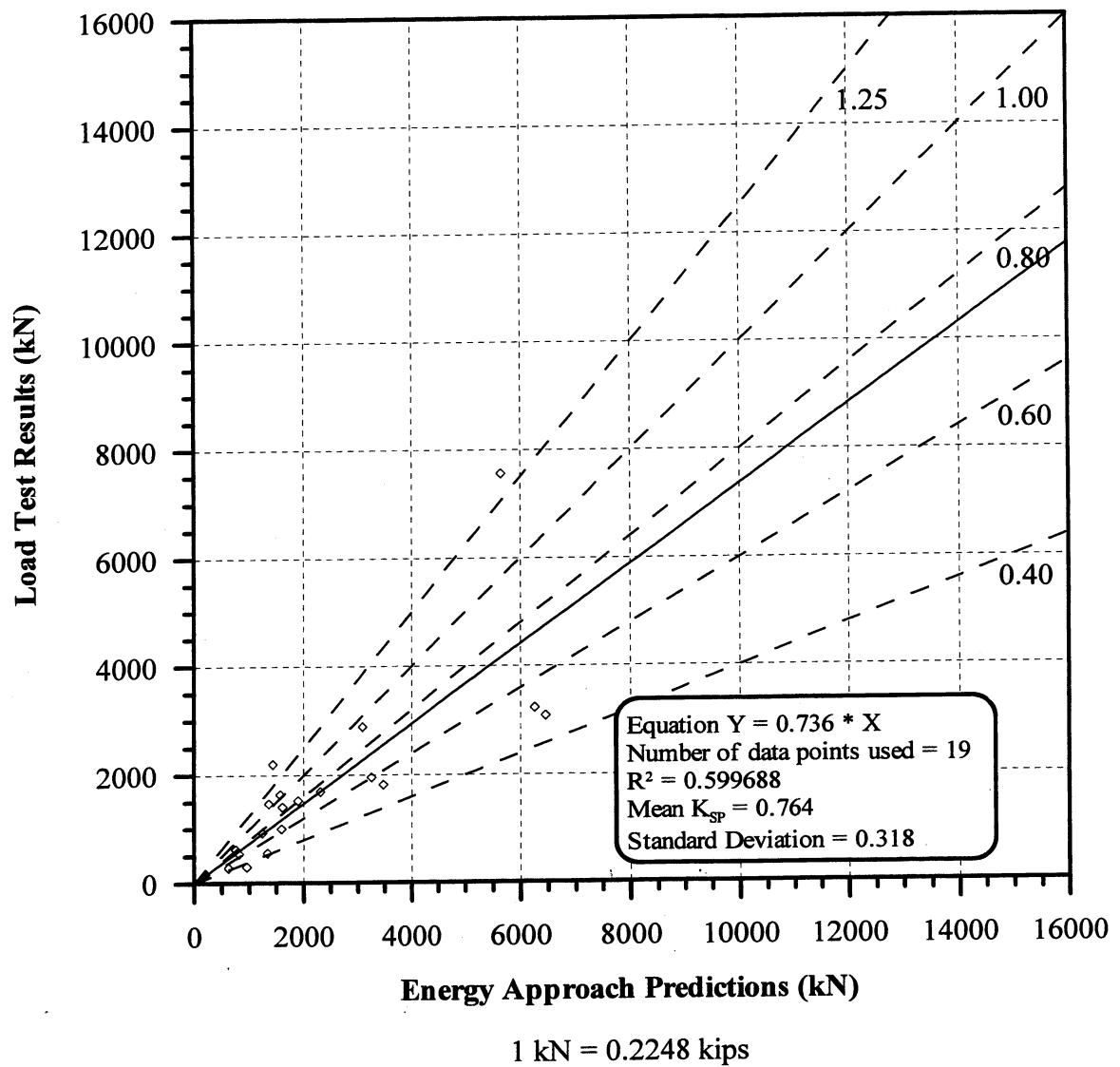


**Figure 6.40.** Static Load Test Results vs. Energy Approach predictions for 19 PD/LT2000 pile-cases at the BOR (last) with Blow Count < 16 BP10cm and Area Ratio < 350 in all types of soils (ABA).

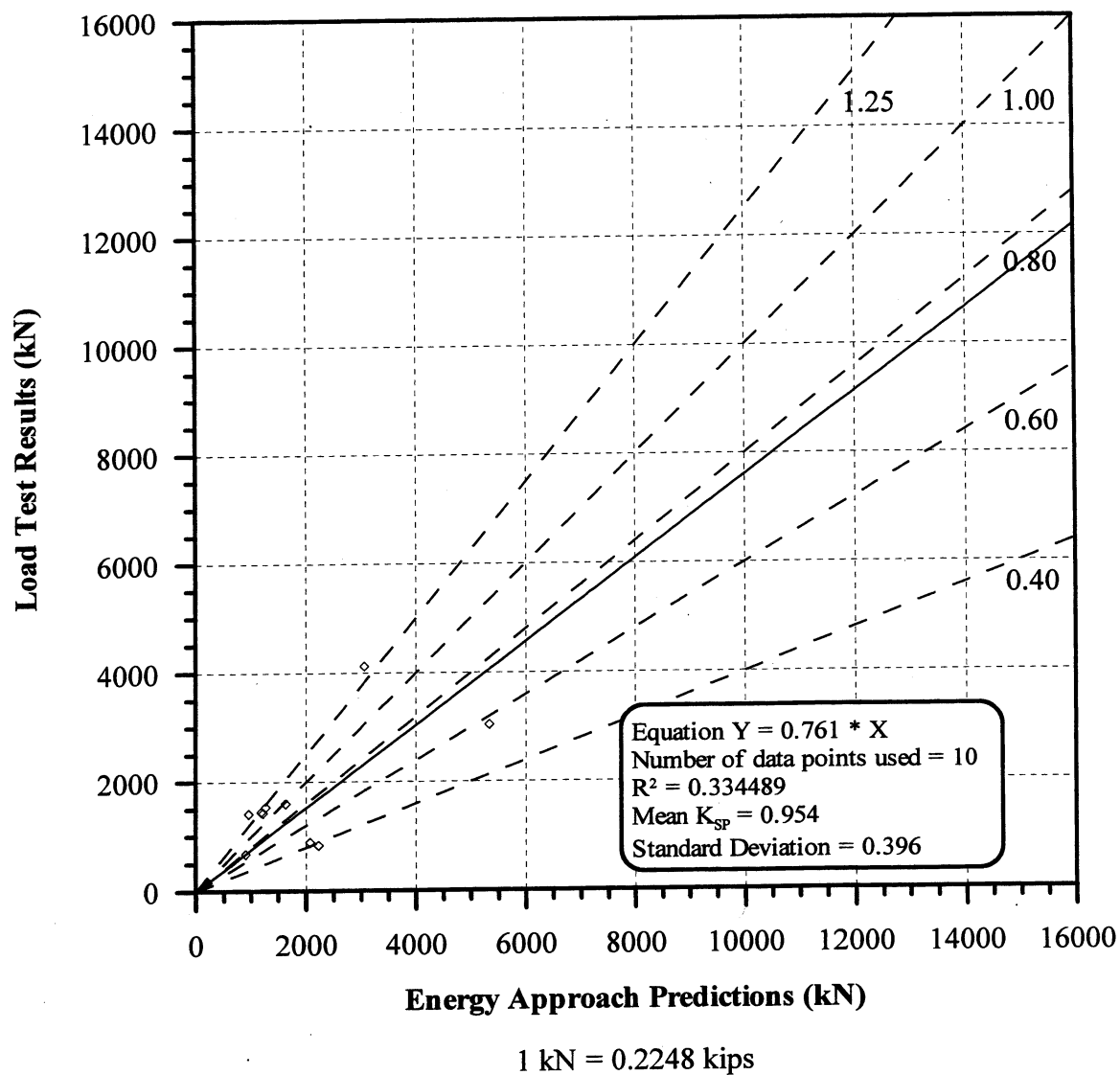


**Figure 6.41.** Static Load Test Results vs. Energy Approach predictions for 10 PD/LT2000 pile-cases at the BOR (last) with Blow Count < 16 BP10cm and Area Ratio  $\geq 350$  in all types of soils (ABA).

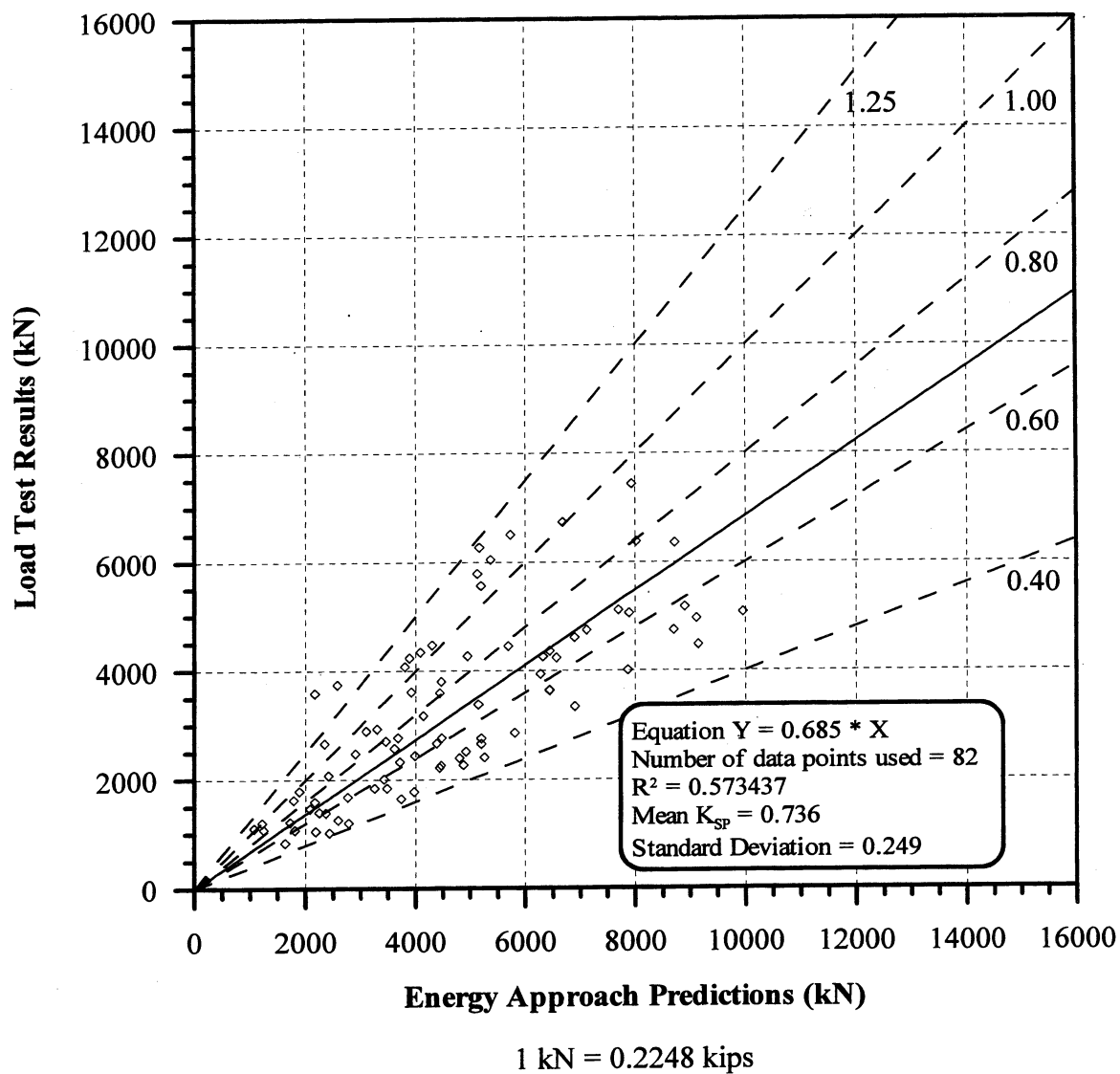


**Figure 6.42.** Static Load Test Results vs. Energy Approach predictions for 82 PD/LT2000 pile-cases at the BOR (last) with Blow Count  $\geq 16$  BP10cm and Area Ratio  $< 350$  in all types of soils (ABA).



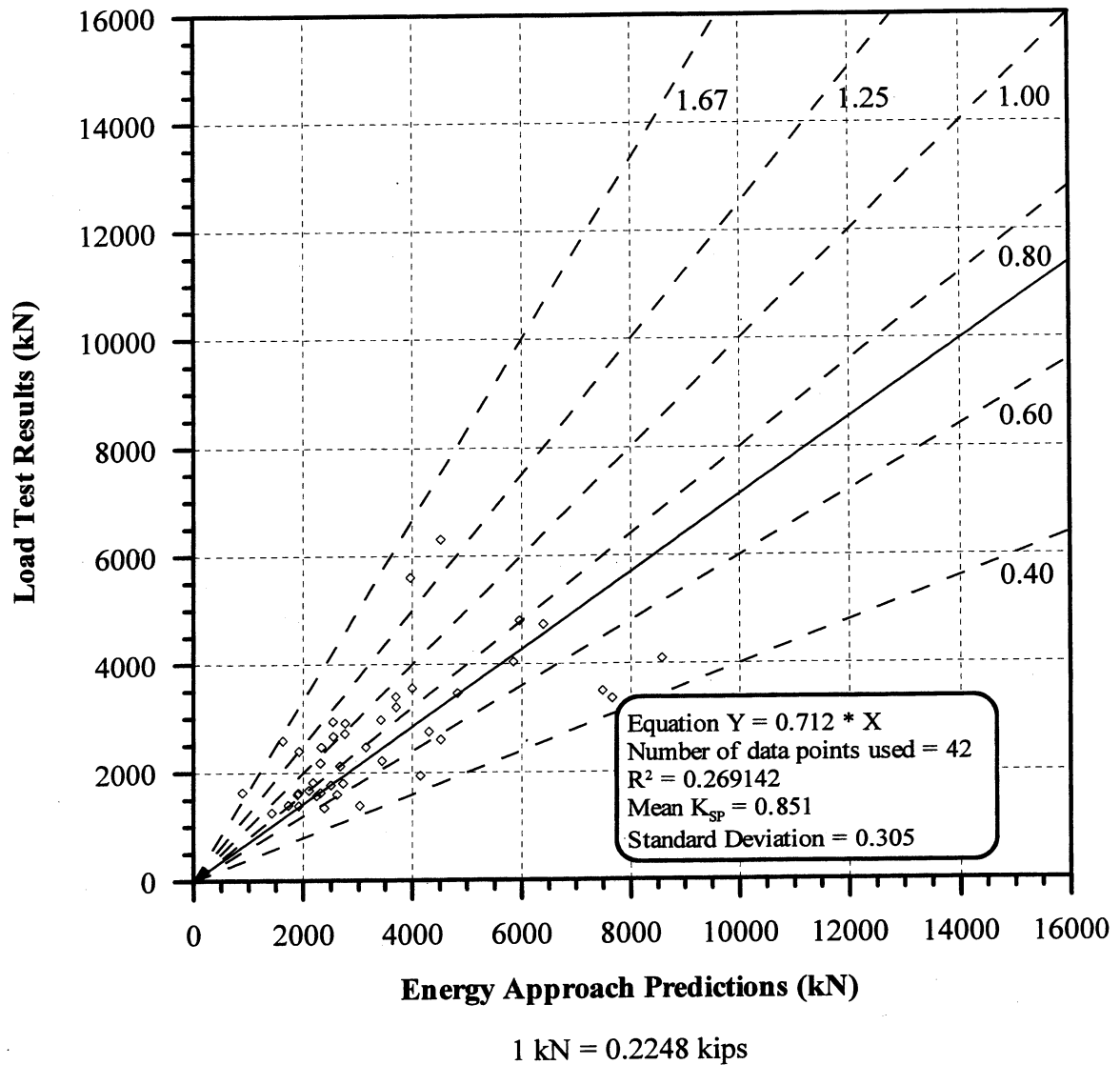


**Figure 6.43.** Static Load Test Results vs. Energy Approach predictions for 42 PD/LT2000 pile-cases at the BOR (last) with Blow Count  $\geq 16$  BP10cm and Area Ratio  $\geq 350$  in all types of soils (ABA).

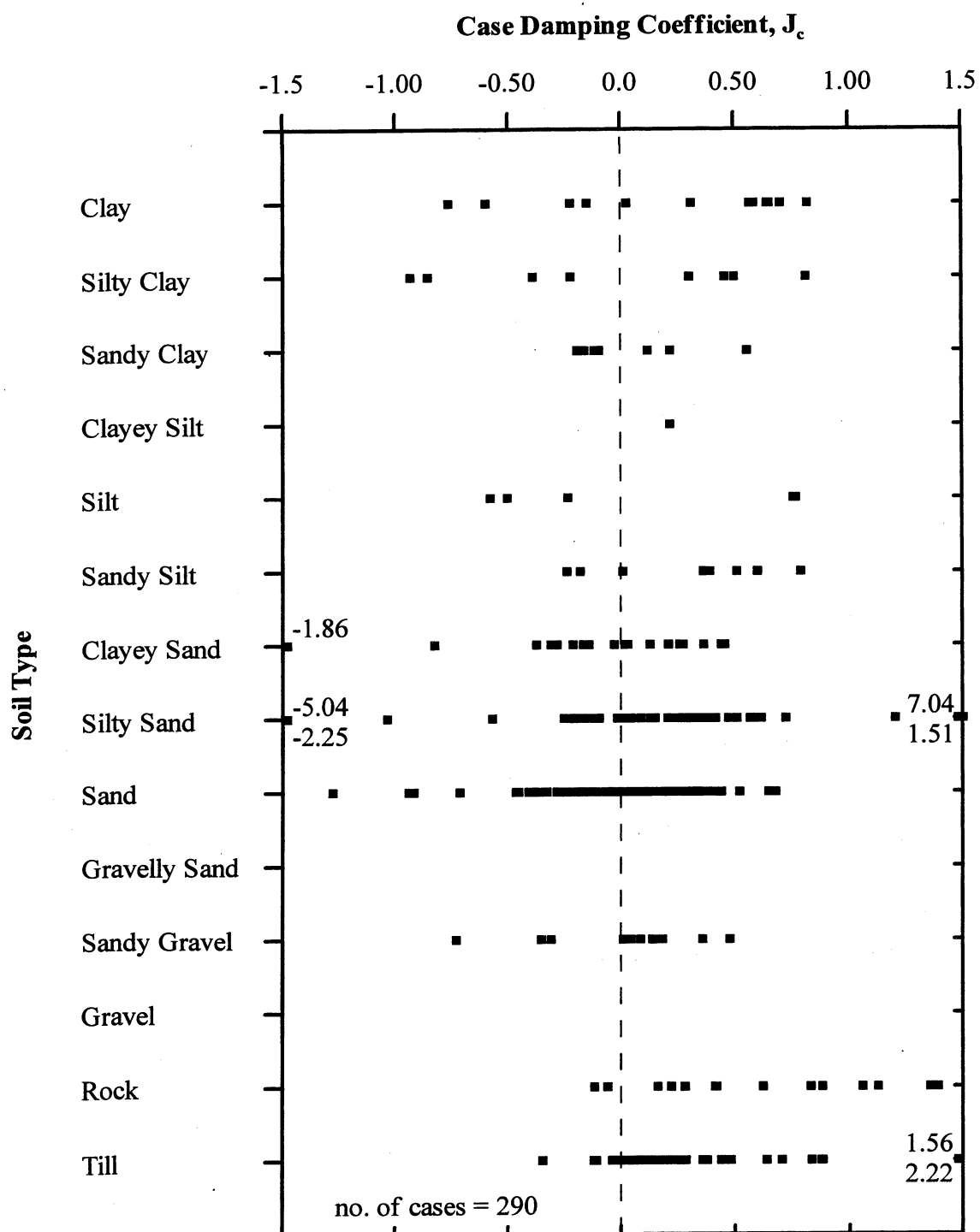
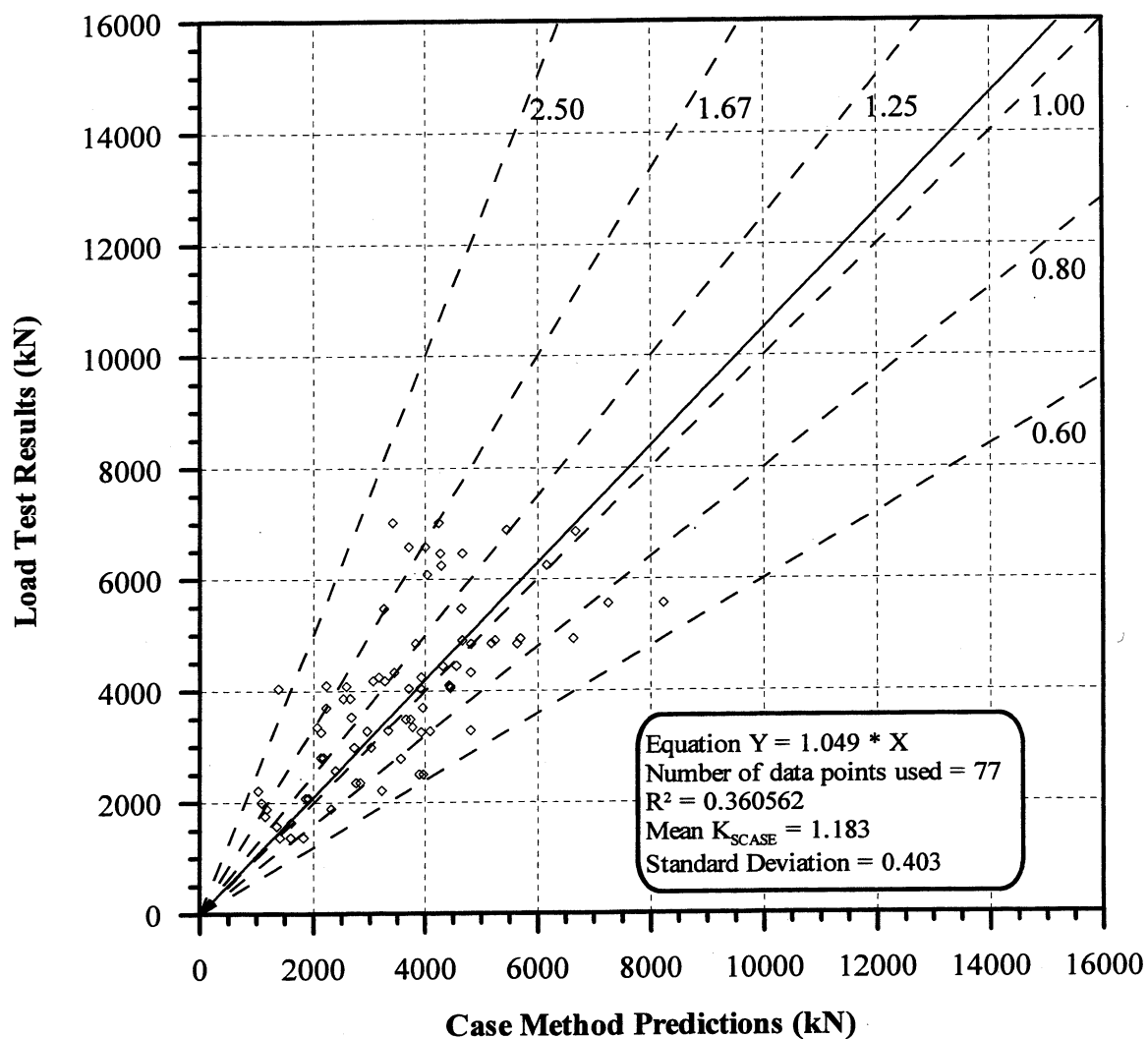


**Figure 6.44.** Tip Soil Conditions versus calculated Case Damping Coefficient,  $J_c$ , based on Static Load Test Results for 290 PD/LT pile-cases (Paikowsky et al., 1994).



1 kN = 0.2248 kips

**Figure 6.45.** Static Load Test Results vs. the Case Method (RMX) predictions for 77 pile-cases in Florida with varied  $J_c$  in all types of soils, (data obtained from the University of Florida).

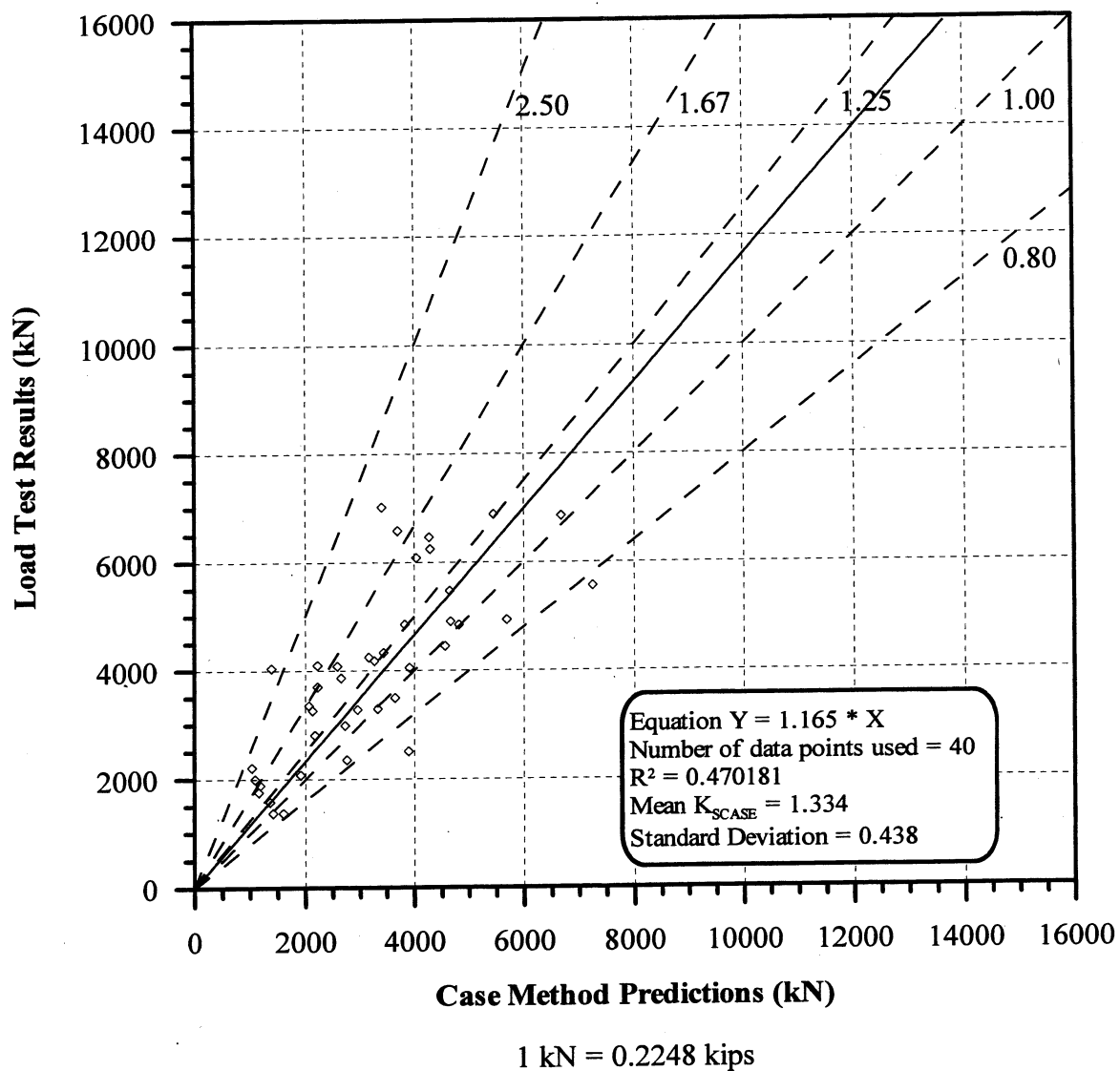


**Figure 6.46.** Static Load Test Results vs. the Case Method (RMX) predictions for 40 EOD pile-cases in Florida with varied  $J_c$  in all types of soils, (data obtained from the University of Florida).

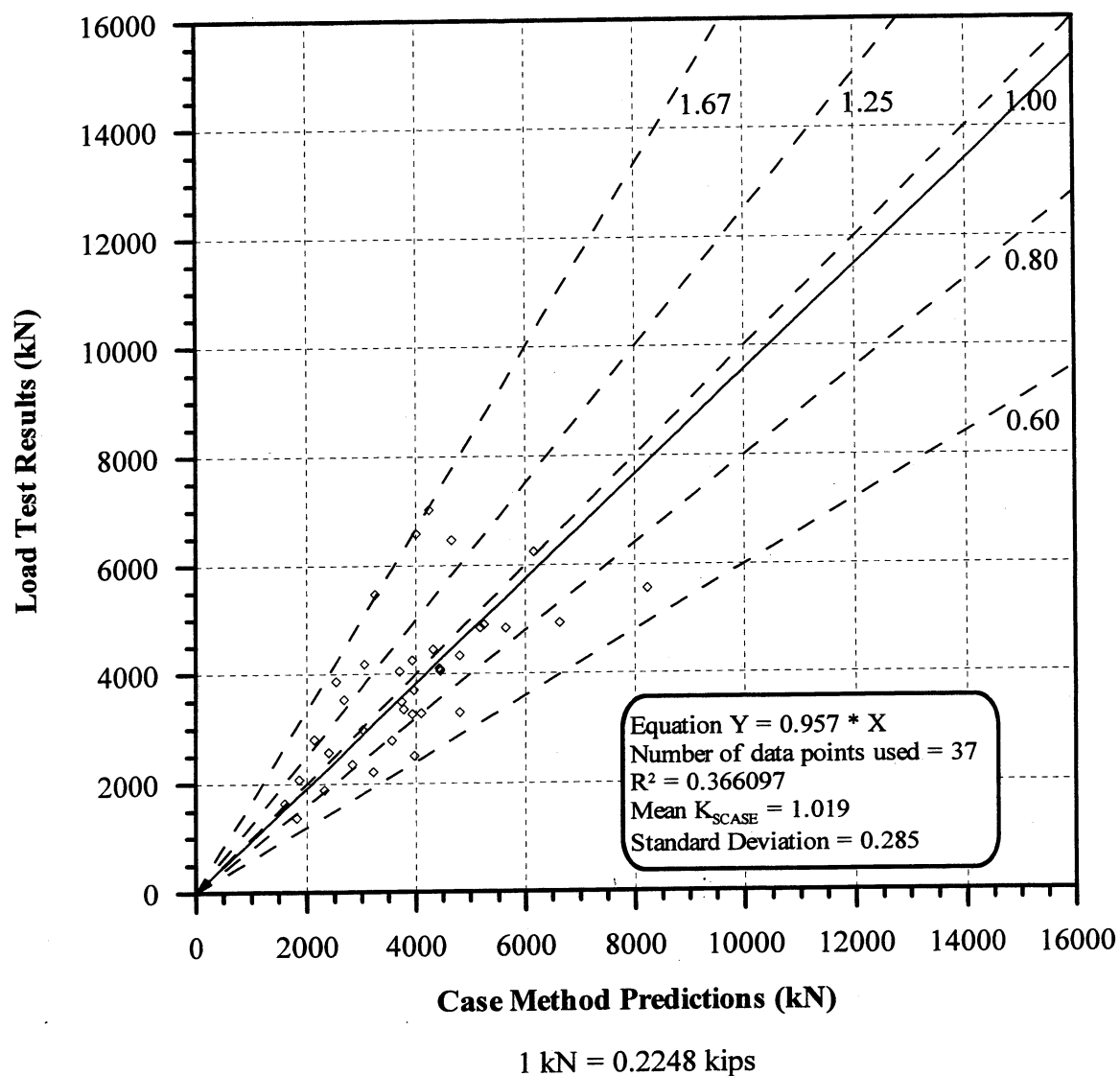


**Figure 6.47.** Static Load Test Results vs. the Case Method (RMX) predictions for 37 BOR pile-cases in Florida with varied  $J_c$  in all types of soils, (data obtained from the University of Florida).

## **CHAPTER 7**

### **ENERGY APPROACH EOD VERSUS CAPWAP / TEPWAP BOR**

#### **7.1 GENERAL**

The statistics presented in Chapter 6 confirmed the findings of previous studies; high accuracy of predictions for the signal matching analyses (e.g. CAPWAP) when performed at the BOR (Beginning of Restrike) and for the Energy Approach, when carried out during driving as indicated by the EOD (End of Driving) analyses. This chapter evaluates the practicality of using the Energy Approach method at the EOD in conjunction with or instead of performing a CAPWAP analysis at the BOR. The performance of the Energy Approach method at the EOD and the CAPWAP/TEPWAP methods at the BOR are presented compared to the static load test results. A comparison between the Energy Approach predictions at the EOD to the CAPWAP/TEPWAP predictions at the BOR is then made using 83 pile-cases from PD/LT2000 for which both analyses were available for the same piles. The evaluation comparing the two methods is continued using the database PD2000, which contains 228 pile-cases that have both an Energy Approach analysis at the EOD and a CAPWAP analysis at the BOR without static load test results, this data was compiled by Mr. Kevin O'Malley using data provided by Geosciences Testing and Research

Inc, (GTR). In all BOR analyses the CAPWAP predictions of the last restrike are utilized.

## **7.2 COMPARISON BASED ON THE PD/LT2000 DATABASE**

A comparison between the static load test results and the Energy Approach predictions at the EOD was presented in Figure 6.30. The mean  $K_{SP}$  value, which is the ratio of the static load test results over the Energy Approach predictions, is 1.084 with a standard deviation of 0.431. These statistics show a fairly high accuracy of the Energy Approach predictions at the EOD. The CAPWAP/TEPWAP predictions at the BOR also show a high accuracy as was presented in Figure 6.16, where the mean  $K_{SW}$  value (static load test results over the CAPWAP/TEPWAP predictions) is 1.158 with a standard deviation of 0.393.

The accuracy of both the Energy Approach at the EOD and the CAPWAP/TEPWAP methods at the BOR improve when the blow counts are greater than 16 blows per 10cm (see Chapter 6). The mean  $K_{SP}$  value and its standard deviation for the Energy Approach at the EOD with blow counts less than 16 blows per 10cm are 1.227 and 0.474, respectively, while for blow counts greater than 16 blows per 10cm the mean  $K_{SP}$  value is 0.972 with a standard deviation of 0.359. For the CAPWAP/TEPWAP methods at the BOR with blows counts less than 16 blows per 10cm the mean  $K_{SW}$  value is 1.176 with a standard deviation of 0.530, while for the pile-cases with blow counts greater than 16 blows per 10cm the mean  $K_{SW}$  value and its standard deviation are 1.153 and 0.354, respectively. The presented statistics

show that both methods provide more accurate results for pile-cases in which the blow counts are greater than 16 blows per 10cm.

The relationship between the CAPWAP/TEPWAP predictions at the BOR and the Energy Approach predictions at the EOD is presented in Figure 7.1 for 83 PD/LT2000 pile-cases. The figure shows a good correlation between the results of the two methods at the different driving times as the mean  $K_{WP}$  value (ratio of the CAPWAP/TEPWAP predictions at the BOR over the Energy Approach predictions at the EOD) is 1.054 with a standard deviation of 0.370, which results in a COV of 0.351. The slope of the best-fit line forced through the origin for the presented data is 0.861 with a coefficient of determination ( $R^2$ ) of 0.484, which shows a poor correlation between the two predictions. The  $R^2$  value shows that there is significant scatter in the data. The ratios between the two predictions (CAPWAP/TEPWAP predictions over the Energy Approach predictions) ranges from approximately 0.50 to 2.5, which also shows significant scatter in the data.

Figure 7.2 presents the relationship between the CAPWAP/TEPWAP predictions at the BOR and the Energy Approach predictions at the EOD for 47 PD/LT2000 pile-cases with blow counts less than 16 blows per 10cm. The correlation is approximately the same as that for all pile-cases as the mean  $K_{WP}$  value increased slightly to 1.180, the standard deviation increased slightly to 0.400 and the COV decreased slightly to 0.339. The slope of the best-fit line forced through the origin increased to 0.958. The  $R^2$  value (0.464) suggests that the scatter remained approximately the same as that for all pile-cases presented in Figure 7.1.



The relationship between the CAPWAP/TEPWAP predictions at the BOR and the Energy Approach predictions at the EOD for 36 PD/LT2000 pile-cases with blow counts greater than 16 blows per 10cm is presented in Figure 7.3. As is expected, the statistics have improved from that for all pile-cases, (presented in Figure 7.1), with the mean  $K_{WP}$  value being 0.890 with a standard deviation of 0.248, which results in a COV of 0.279. The slope of the best-fit line forced through the origin is 0.795, with  $R^2 = 0.571$ , which shows a significant amount of scatter in the data. The scatter is also shown by the prediction ratios that range from approximately 0.5 to 1.4.

The statistical information presented in this section suggests a high correlation between the Energy Approach at the EOD and CAPWAP during the BOR. The relationship suggests that from the construction point of view in many cases the use of the Energy Approach at the EOD can be much more cost effective than conducting dynamic testing and completing a complex CAPWAP or TEPWAP analysis at the BOR. This is less true for pile-cases where the blow counts at the end of driving are less than 16 blows per 10cm as the Energy Approach methods performance is more limited under such conditions with possible significant pile capacity gain with time.

### **7.3 COMPARISON BASED ON THE PD2000 DATABASE**

#### **7.3.1 Overview**

Presented in this section are the comparisons between the CAPWAP predictions at the BOR and the Energy Approach predictions at the EOD for the pile-cases contained in database PD2000. The above comparison is made for all pile-cases as well as for the pile-cases with blow counts less and greater than 16 blows per 10cm.

The analysis is continued by comparing the two predictions based on the soil type at the tip of the pile for both cases where the blow count is less than and greater than 16 blows per 10cm.

### **7.3.2 All Pile-Cases**

The comparison between the CAPWAP predictions at the BOR and the Energy Approach predictions at the EOD for the 228 pile-cases in PD2000 is presented in Figure 7.4. The figure shows a very good correlation between the two predictions as the mean  $K_{WP}$  value, (CAPWAP predictions over the Energy Approach predictions), is 0.962 with a standard deviation of 0.269. The data is plotted according to soil type at the tip with no clear correlation for any specific soil type. The slope of the best-fit line forced through the origin, which is an indicator of the accuracy of the correlation between the two prediction methods, is 0.901, with a coefficient of determination ( $R^2$ ) of 0.738. These measures indicate a moderate correlation between the predicted capacities using the two different methods at different times of driving. The scatter is relatively insignificant as shown by the  $R^2$  value and the prediction ratios (CAPWAP predictions over Energy Approach predictions), which range from approximately 0.5 to approximately 1.7.

### **7.3.3 Driving Resistance**

Figure 7.5 presents the comparison between the CAPWAP predictions at the BOR and the Energy Approach predictions at the EOD for 43 PD2000 pile-cases with blow counts less than 16 blows per 10cm. The data is plotted according to soil type with no clear correlation for any specific soil type at the pile tip. The mean and

standard deviation are 1.167 and 0.434, respectively, have increased from that for all PD2000 EOD pile-cases. The COV (0.372) also increased from that for all EOD PD2000 pile-cases, but still shows that there is a good correlation between the prediction methods. The slope of the best-fit line is 0.979, with a coefficient of determination ( $R^2$ ) of 0.556, which shows a significant scatter in the data as shown also by the ratios of the CAPWAP predictions to the Energy Approach predictions ranging from approximately 0.7 to 1.8.

Figure 7.6 presents a comparison between the CAPWAP predictions at the BOR and the Energy Approach predictions at the EOD for 185 PD2000 pile-cases with blow counts greater than 16 blows per 10cm. The plotted data according to soil type at the tip suggests that a larger scatter exists for the piles in clay and till but no clear correlation was established based on a specific soil type. The mean  $K_{WP}$  value is 0.915 with a standard deviation of 0.185, which is a significant improvement from the statistics for all pile-cases as was shown in Figure 7.4 or those for the EOD case in easy driving (Figure 7.5). An excellent correlation exists between the predictions using the two dynamic methods with the slope of the best-fit line forced through zero being 0.895, and a coefficient of determination ( $R^2$ ) of 0.725. The scatter is small based on the  $R^2$  and COV values and the small range of ratios of CAPWAP predictions over Energy Approach predictions (approximately 0.5 to 1.5, with only 5 pile-cases falling above the ratio of 1.25 or below 0.6).

The statistics presented in this section showed that the correlation between the two methods for pile-cases with blow counts greater than 16 blows per 10cm is

excellent while the correlation is not so good for pile-cases with blow counts less than 10 blows per 10cm. This again leads to the conclusion that if the blow counts are less than 16 blows per 10cm at the EOD then a restrrike and a signal matching analysis may be advantageous. The data for each of the presented figures was plotted according to soil types at the tip and from these figures it appears that there is no clear correlation based on soil types. The next section will examine the correlation between the CAPWAP predictions at the BOR and the Energy Approach predictions at the EOD based on soil type.

#### **7.3.4 Soil Type**

##### ***a) Overview***

This section presents the correlations between the CAPWAP predictions at the BOR and the Energy Approach predictions at the EOD based on the type of soil at the pile's tip. The correlation is also shown for a special group of pile-cases driven through Boston Blue Clay. Each of the correlations based on soil type are also sub-grouped according to the driving resistance distinguishing between less and greater than 16 blows per 10cm.

##### ***b) Clay and Till***

The comparison between the CAPWAP predictions at the BOR and the Energy Approach predictions at the EOD for 90 PD2000 pile-cases embedded in clay and till is presented in Figure 7.7. The mean  $K_{WP}$  value is 0.999 with a standard deviation of 0.293, which results in a COV of 0.293 suggesting a very good correlation between the two dynamic method predictions for piles embedded in clay and till. The slope of

the best-fit line forced through the origin is 0.943, with a coefficient of determination of 0.820, which also shows the good correlation between the two dynamic method predictions. The scatter of data is relatively small as the data ranges from ratios of CAPWAP predictions to Energy Approach predictions of approximately 0.6 to approximately 1.8 and the  $R^2$  value is greater than 0.8.

Figure 7.8 presents the comparison between the CAPWAP predictions at the BOR and the Energy Approach predictions at the EOD for 15 PD2000 pile-cases embedded in clay and till with blow counts less than 16 blows per 10cm. Based on the mean  $K_{WP}$  value of 1.272 and a standard deviation of 0.539, the COV is 0.424, which shows a reasonably good correlation between the two prediction methods. The slope of the best-fit line forced through the origin is 1.037, with a coefficient of determination ( $R^2$ ) of 0.608, indicating a borderline moderate correlation (to poor) between the predictions based on the two dynamic methods for pile-cases embedded in clay and till with blow counts less than 16 blows per 10cm. The ratios of the CAPWAP predictions over the Energy Approach predictions range from 0.7 to above 2.4 and with the marginal  $R^2$  value and only 15 pile-cases in this category, the correlation of the method in this case is rather limited.

Figure 7.9 presents the comparison between the CAPWAP predictions at the BOR and the Energy Approach predictions at the EOD for 75 PD2000 pile-cases with blow counts greater than 16 blows per 10cm embedded in clay and till. The mean  $K_{WP}$  value is 0.944 with a standard deviation of 0.173, which results in a COV of 0.183. These statistics show a very good correlation between the two dynamic method

predictions, as does the slope of the best-fit line forced through the origin, 0.939 and the coefficient of determination,  $R^2$  value of 0.800. The ratios of the CAPWAP predictions over the Energy Approach predictions range from approximately 0.6 to 1.5 with only 2 pile-cases falling above the ratio of 1.25.

**c) *Sand and Silt***

Figure 7.10 presents a comparison between the CAPWAP predictions at the BOR and the Energy Approach predictions at the EOD for 42 PD2000 pile-cases of piles embedded in sand and silt. The mean  $K_{WP}$  value, which is the ratio of the CAPWAP predictions over the Energy Approach prediction, is 1.028 with a standard deviation of 0.333, which results in a COV of 0.324. The slope of the best-fit line forced through the origin is 0.871; with a coefficient of determination ( $R^2$ ) of 0.721. These statistics show a good correlation between the two dynamic methods at the different times of driving with the ratios (CAPWAP predictions over the Energy Approach predictions) ranging from approximately 0.6 to 1.7 and the  $R^2$  value suggests moderate to good correlation.

Presented in Figure 7.11 is the comparison between the CAPWAP predictions at the BOR and the Energy Approach predictions at the EOD for 16 PD2000 pile-cases with blow counts of less than 16 blows per 10cm embedded in sand and silt. Based on the COV of 0.320 the performance in this category has not changed from that for all pile-cases in sand and silt, although the mean  $K_{WP}$  value, 1.254, and the standard deviation of 0.401 have increased. The standard deviation (0.401) has also increased. The slope of the best-fit line is 1.148, with a coefficient of determination

( $R^2$ ) of 0.441 shows a poor correlation between the pile capacity predictions using the two methods. The scatter is fairly significant as it ranges from ratios of CAPWAP predictions over Energy Approach predictions of approximately 0.8 to 1.7.

The comparison between the CAPWAP predictions at the BOR and the Energy Approach predictions at the EOD for 26 PD2000 pile-cases with blows counts greater than 16 blows per 10cm embedded in sand and silt is presented in Figure 7.12. The data in the figure shows a good correlation between the pile capacity predictions based on the two dynamic methods, as the mean  $K_{WP}$  value is 0.888 with a standard deviation of 0.179, which results in a COV of 0.202. The slope of the best-fit line is 0.837, with a coefficient of determination ( $R^2$ ) of 0.804, which shows a small amount of scatter and a good correlation between the predictions.

**d) Rock**

Figure 7.13 presents a comparison between the CAPWAP predictions at the BOR and the Energy Approach predictions at the EOD for 94 PD2000 pile-cases embedded in rock. The mean  $K_{WP}$  value is 0.906 with a standard deviation of 0.187, which results in a COV of 0.206, suggesting an excellent correlation between the pile capacity predictions using the two dynamic methods. The slope of the best-fit line forced through the origin is 0.902; with a  $R^2$  value of 0.708. The ratios of the CAPWAP predictions over the Energy Approach predictions range from approximately 0.5 to 1.3, which shows a small amount of scatter and a moderate correlation between the two methods predictions.

Figure 7.14 presents the comparison between the CAPWAP predictions at the BOR and the Energy Approach predictions at the EOD for 12 PD2000 pile-cases with blow counts less than 16 blows per 10cm embedded in rock. The statistics have not changed from that presented for all pile-cases. The mean  $K_{WP}$  value is 0.918 with a standard deviation of 0.188, which results in a COV of 0.205. The slope of the best-fit line forced through the origin is 0.887, with a  $R^2$  value of 0.590, suggesting a significant amount of scatter in the data and a moderate to poor correlation between the predictions using these two dynamic methods at different times of driving. These conclusions are subjected however to the small sample size of 12 cases only.

The comparison between the CAPWAP predictions at the BOR and the Energy Approach predictions at the EOD for 82 PD2000 pile-cases with blow counts greater than 16 blows per 10cm embedded in rock is presented in Figure 7.15. Again the mean and standard deviation did not change from that for all pile-cases embedded in rock. The mean  $K_{WP}$  value is 0.905 with a standard deviation of 0.188, which results in a COV of 0.208 and the slope of the best-fit line forced through the origin is 0.904, with a  $R^2$  value of 0.713. The ratios of the CAPWAP predictions to the Energy Approach predictions range from approximately 0.5 to 1.5, which along with the other parameters suggests a moderate correlation between the pile capacity predictions based on the two dynamic methods.

***e) Boston Blue Clay***

The comparison between the CAPWAP predictions at the BOR and the Energy Approach predictions at the EOD for 72 PD2000 pile-cases with Boston blue clay as



the major soil type along the side of the pile is presented in Figure 7.16. The mean  $K_{WP}$  value, 0.920, and its standard deviation, 0.178, result in a COV of 0.193, which shows an excellent correlation between the pile capacity predictions based on the two dynamic methods. The slope of the best-fit line forced through the origin, 0.940, with a  $R^2$  value of 0.821, which also suggests a good correlation between the predictions. The scatter is relatively small based on the ratios of the CAPWAP predictions over the Energy Approach predictions, which range from approximately 0.5 to 1.5 with only 3 pile-cases having a ratio greater than 1.25.

Presented in Figure 7.17 is the comparison between the CAPWAP predictions at the BOR and the Energy Approach predictions at the EOD for 8 PD2000 pile-cases with blow counts less than 16 blows per 10cm and with Boston blue clay as the major soil type along the side of the pile. The mean  $K_{WP}$  value is 0.845 with a standard deviation of 0.136, which results in COV of 0.161, which shows a very good correlation between the pile capacity predictions using the two dynamic methods. The slope of the best-fit line forced through the origin is 0.841, with a  $R^2$  value of 0.144. The small sample size of this category provides limited ability to conclude decisively regarding the meaning of the data.

Figure 7.18 presents the comparison between the CAPWAP predictions at the BOR and the Energy Approach predictions at the EOD for 64 PD2000 pile-cases with blow counts greater than 16 blow per 10cm and with Boston blue clay as the major soil type along the side of the pile. The mean  $K_{WP}$  value, 0.930, and its standard deviation, 0.181, result in a COV of 0.195 which is approximately the same as the

COV for all pile-cases with Boston blue clay as the major soil type along the side of the pile. These values again suggest an excellent correlation between the predictions of the two dynamic methods. The slope of the best-fit line is 0.947; with an  $R^2$  value of 0.825 also remained relatively unchanged. The relatively small change between this case to the total case is expected as 64 out of the 72 cases of Figure 7.16 relate to a blow count greater than 16 BP10cm.

### **7.3.5 Summary**

As the best performing dynamic methods for BOR and EOD, the correlation between the CAPWAP predictions (at the BOR) and the Energy Approach predictions (at the EOD) was evaluated using the database PD2000. The conclusion from the presented analyses is that if the blow counts at the end of driving are less than 16 blows per 10cm, it is wise to complete a CAPWAP analysis at the beginning of a restrike. Chapter 8 will discuss a way to evaluate the time required to perform a restrike after the end of driving to obtain the most accurate predictions of the pile capacity. If the blow count at the end of driving is greater than 16 blows per 10cm the high accuracy of the Energy Approach and the good correlation between the methods suggest that it is much more cost effective to complete a quick field evaluation of the pile capacity using the Energy Approach rather than performing a delayed and more expensive wave matching technique evaluation in the office. The correlation developed in this section also showed that the soil type has a minimal effect on the accuracy of the direct correlation between the CAPWAP predictions at the BOR and the Energy Approach predictions at the EOD. Piles that are driven into cohesive soils

such as Boston blue clay often exhibit a significant gain of capacity with time. The analysis based on the criteria that all pile-cases have Boston blue clay as the major soil type along the side of the pile showed that the pile capacity gain with time does not affect the proposed correlation with the Energy Approach at the EOD matching well with CAPWAP results at the BOR. Demonstrating again the high accuracy of the Energy Approach for the long-term pile capacity.

#### **7.4 SUMMARY AND INTERMEDIATE CONCLUSIONS**

The analysis presented in this chapter has shown that there is a very good correlation between the CAPWAP predictions at the BOR and the Energy Approach predictions at the EOD. A summary of the analyses that were performed is presented in Table 7.1. The statistical data of Table 7.1 suggests the following:

- (i) Soil type has a minimal effect on the accuracy of the correlation between the pile capacity predictions using the two dynamic methods at different times of driving.
- (ii) A better correlation exists between the two dynamic method predictions for pile-cases with blow counts greater than 16 blows per 10cm compared to those with blow counts less than 16 blows per 10cm.
- (iii) A reasonable practical suggestion is therefore to use the Energy Approach method to evaluate the pile capacity at the end of driving unless the recorded blow counts are less than 16 blows per 10cm. If the blow count is smaller than 16 blows per 10cm a CAPWAP analysis should be completed for a restrike performed some time after the driving of the pile, to be discussed in Chapter 8.

**Table 7.1.** Summary of statistical data for the Correlation between the CAPWAP/TEPWAP predictions at the BOR to the Energy Approach predictions at the EOD using the PD/LT2000 and PD2000 databases.

	Ratios	All Cases	Blow Count < 16 BP10cm	Blow Count $\geq$ 16 BP10cm
PD/LT2000 Database	$K_{SP}$ (all soil types) End of Driving	$\mu = 1.084$ $\sigma = 0.431$ no. = 128	$\mu = 1.227$ $\sigma = 0.474$ no. = 56	$\mu = 0.972$ $\sigma = 0.359$ no. = 72
	$K_{SW}$ (all soil types) Beginning of Restrike	$\mu = 1.158$ $\sigma = 0.393$ no. = 162	$\mu = 1.176$ $\sigma = 0.530$ no. = 32	$\mu = 1.153$ $\sigma = 0.354$ no. = 130
	$K_{WP}$ (all soil types)	$\mu = 1.054$ $\sigma = 0.370$ no. = 83	$\mu = 1.180$ $\sigma = 0.400$ no. = 47	$\mu = 0.890$ $\sigma = 0.248$ no. = 36
PD2000 Database	$K_{WP}$ (all soil types)	$\mu = 0.962$ $\sigma = 0.269$ no. = 228	$\mu = 1.167$ $\sigma = 0.434$ no. = 43	$\mu = 0.915$ $\sigma = 0.185$ no. = 185
	$K_{WP}$ (clay & till)	$\mu = 0.999$ $\sigma = 0.293$ no. = 90	$\mu = 1.272$ $\sigma = 0.539$ no. = 15	$\mu = 0.944$ $\sigma = 0.173$ no. = 75
	$K_{WP}$ (sand & silt)	$\mu = 1.028$ $\sigma = 0.333$ no. = 42	$\mu = 1.254$ $\sigma = 0.401$ no. = 16	$\mu = 0.888$ $\sigma = 0.179$ no. = 26
	$K_{WP}$ (rock)	$\mu = 0.906$ $\sigma = 0.187$ no. = 94	$\mu = 0.918$ $\sigma = 0.188$ no. = 12	$\mu = 0.905$ $\sigma = 0.188$ no. = 82
	$K_{WP}$ (BBC side)	$\mu = 0.920$ $\sigma = 0.178$ no. = 72	$\mu = 0.845$ $\sigma = 0.136$ no. = 8	$\mu = 0.930$ $\sigma = 0.181$ no. = 64

- Notes:
1. The soil types are the soil types at the tip.
  2. BBC side – pile cases with Boston Blue Clay as the major soil type on the side of the pile.
  3.  $K_{SP}$  – ratio of static load test results to the Energy Approach predictions at the EOD.
  4.  $K_{SW}$  – ratio of static load test results to the CAPWAP/TEPWAP predictions at the BOR.
  5.  $K_{WP}$  – ratio of the CAPWAP/TEPWAP predictions at the BOR to the Energy Approach predictions at the EOD.
  6. EOD – End of Driving
  7. BOR – Beginning of Restrike and in this instance is the last restrike.
  8. 16 BP10cm is approximately 4 BPI.
  9. Two pile-cases had unknown soil types at the tip.

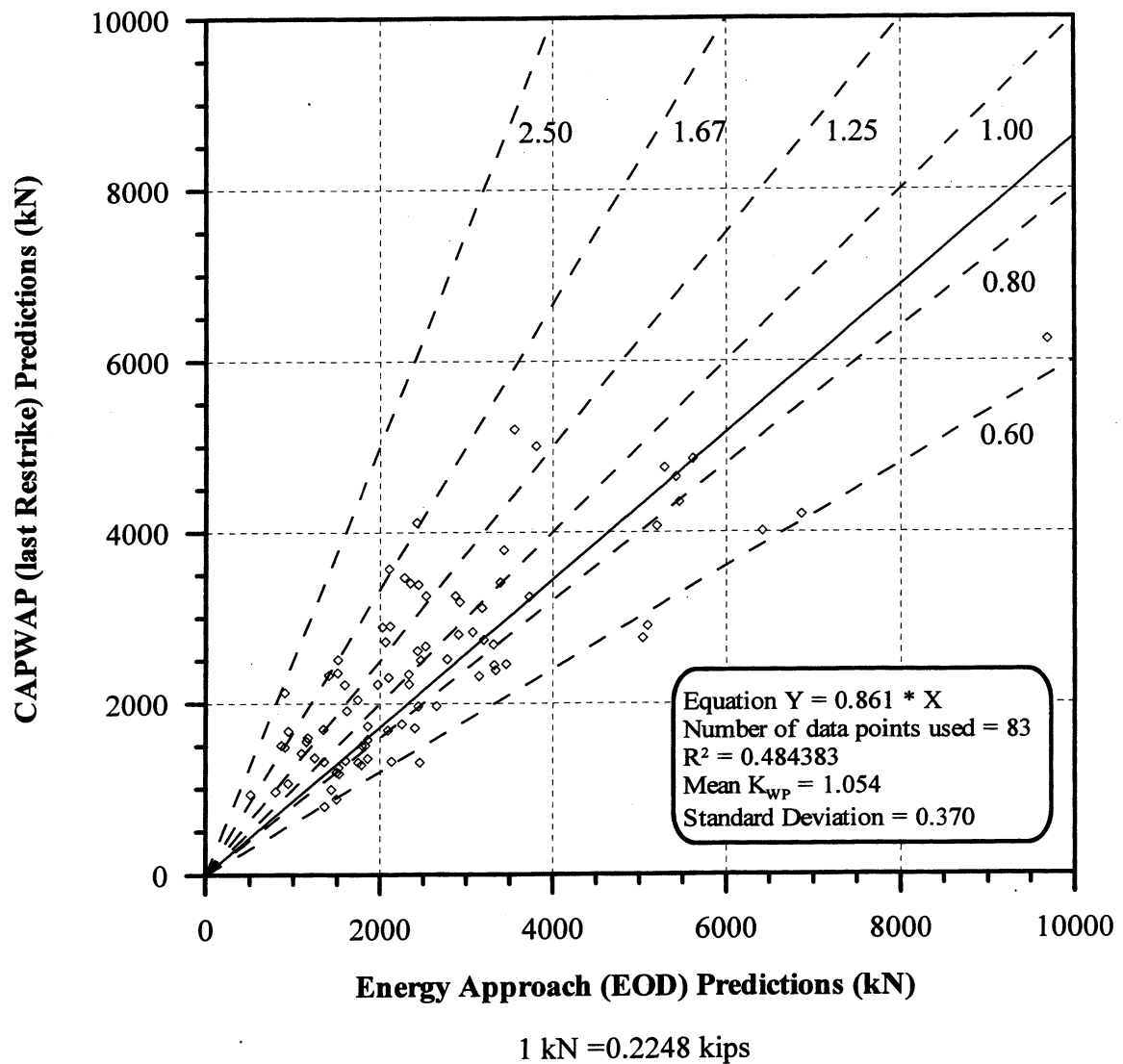


**Figure 7.1.** CAPWAP (last Restrike) Predictions vs. Energy Approach (EOD) Predictions for 83 PD/LT2000 pile-cases in all types of soils (AAA).

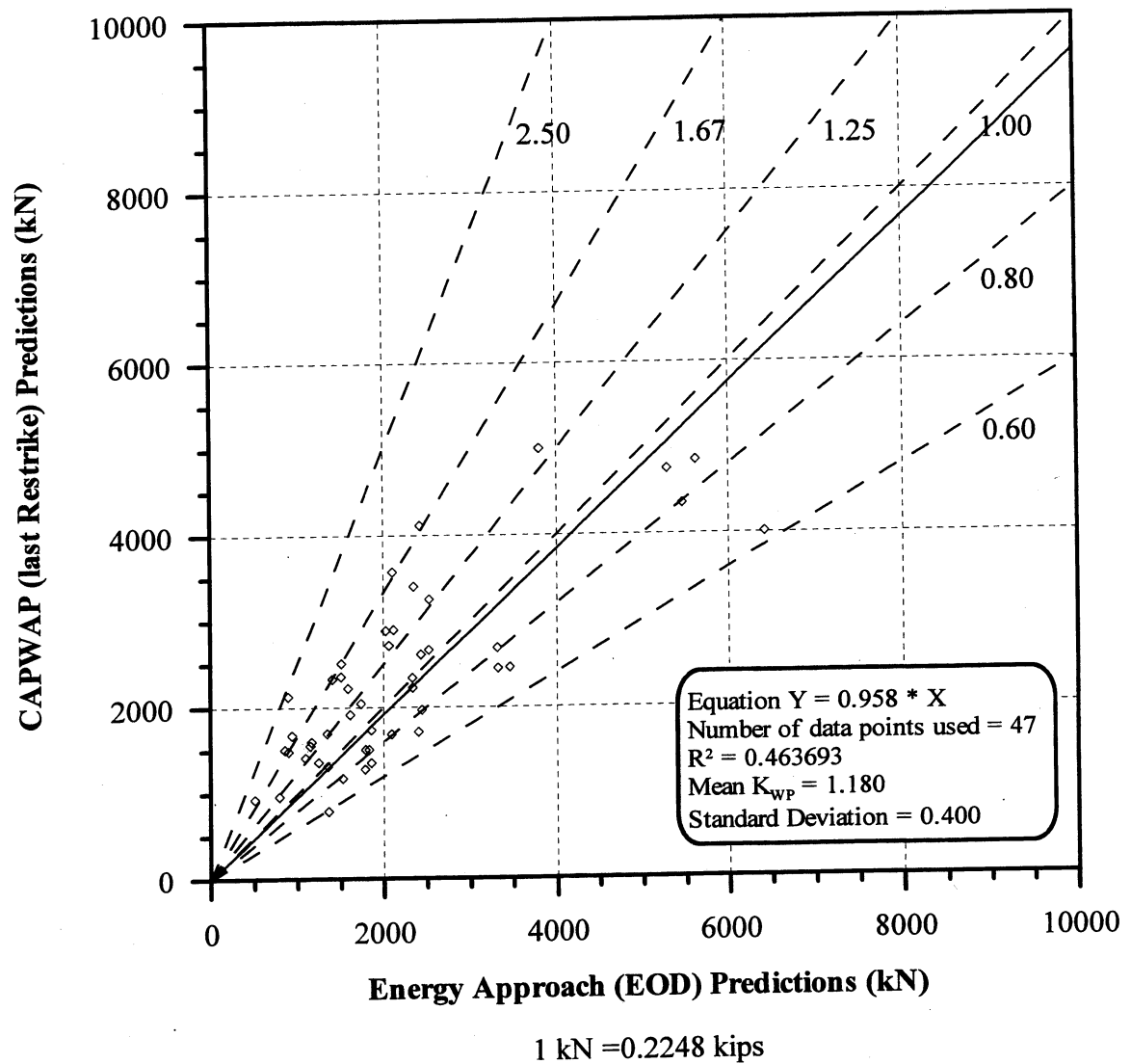


**Figure 7.2.** CAPWAP (last Restrike) Predictions vs. Energy Approach (EOD) Predictions for 47 PD/LT2000 pile-cases with Blow Count < 16 BP10cm in all types of soils (AAA).

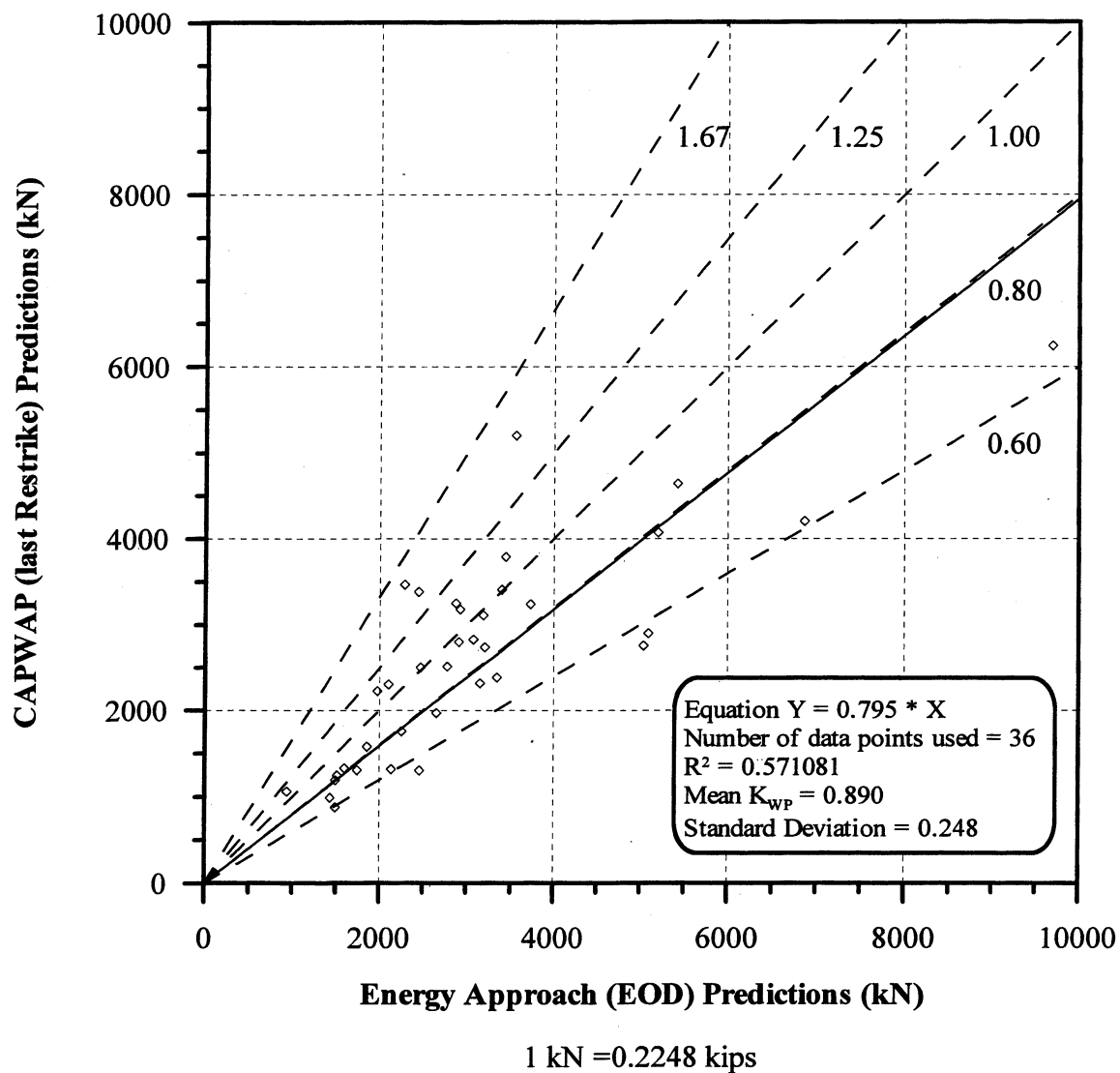


**Figure 7.3.** CAPWAP (last Restrike) Predictions vs. Energy Approach (EOD) Predictions for 36 PD/LT2000 pile-cases with Blow Count  $\geq 16$  BP10cm in all types of soils (AAA).

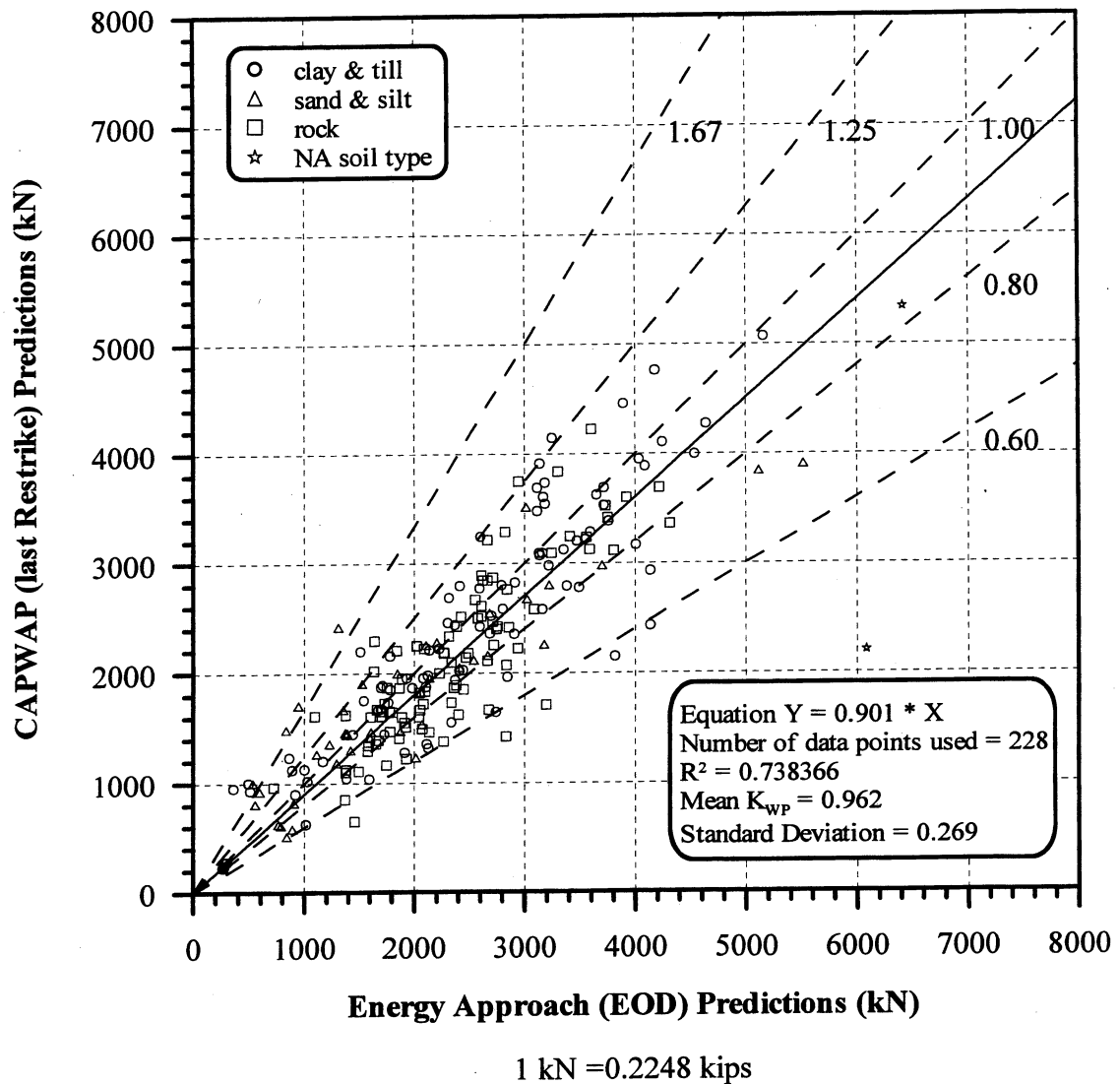


**Figure 7.4.** CAPWAP (last Restrike) Predictions vs. Energy Approach (EOD) Predictions for 228 PD2000 pile-cases in all soil types.



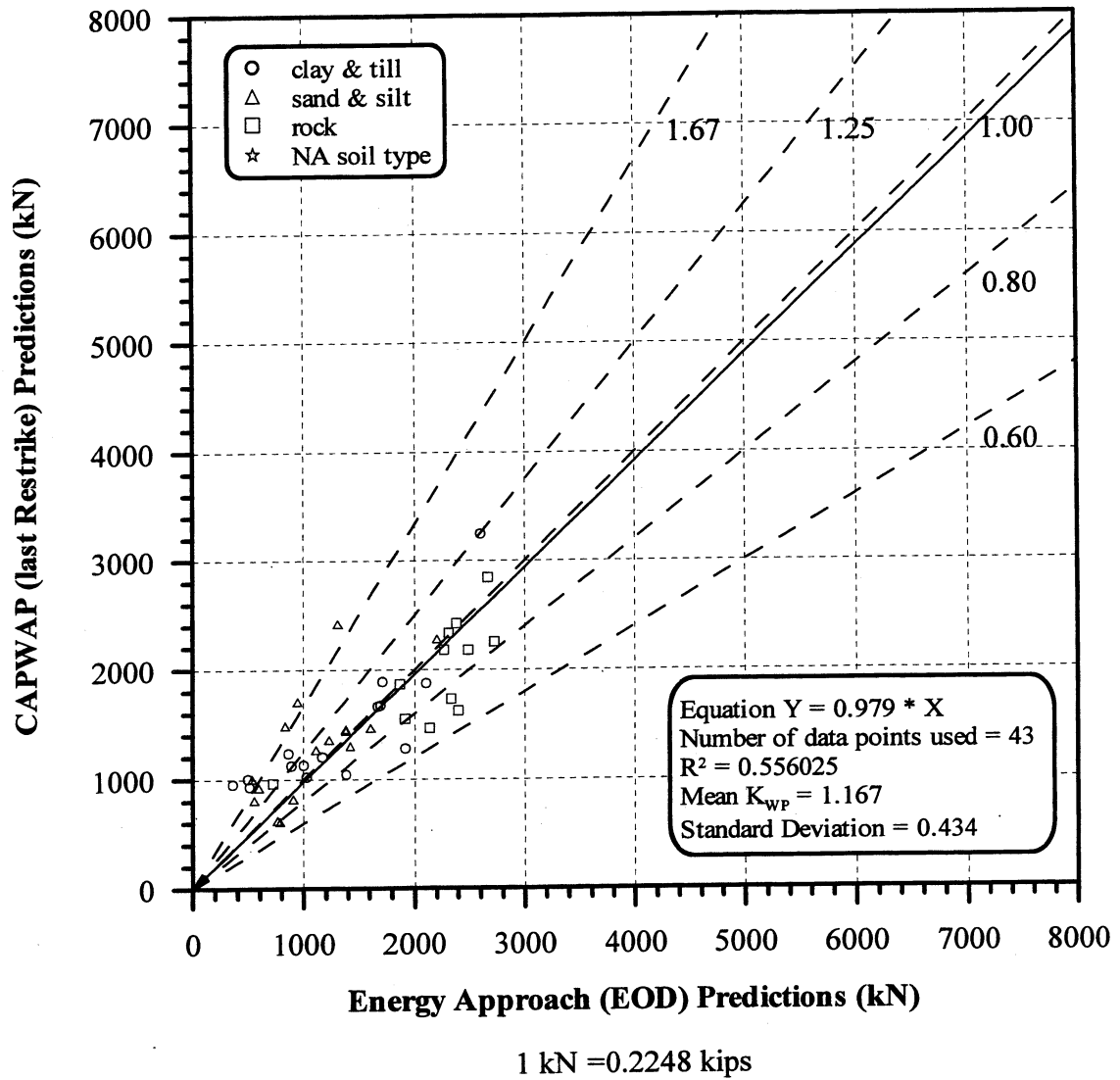


**Figure 7.5.** CAPWAP (last Restrike) Predictions vs. Energy Approach (EOD) Predictions for 43 PD2000 pile-cases with Blow Count < 16 BP10cm in all soil types.

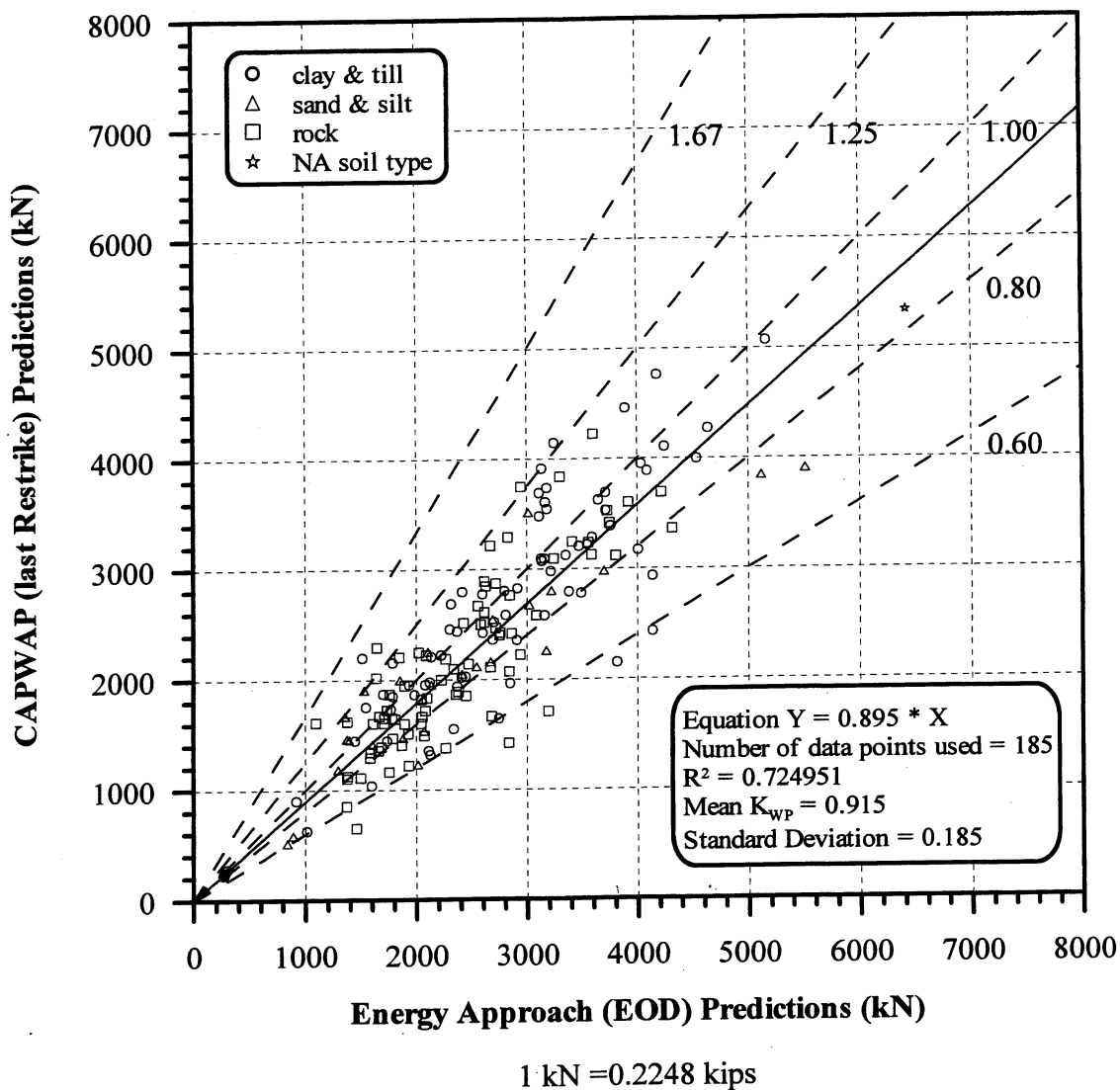


**Figure 7.6.** CAPWAP (last Restrike) Predictions vs. Energy Approach (EOD) Predictions for 185 PD2000 pile-cases with Blow Count  $\geq 16$  BP10cm in all soil types.

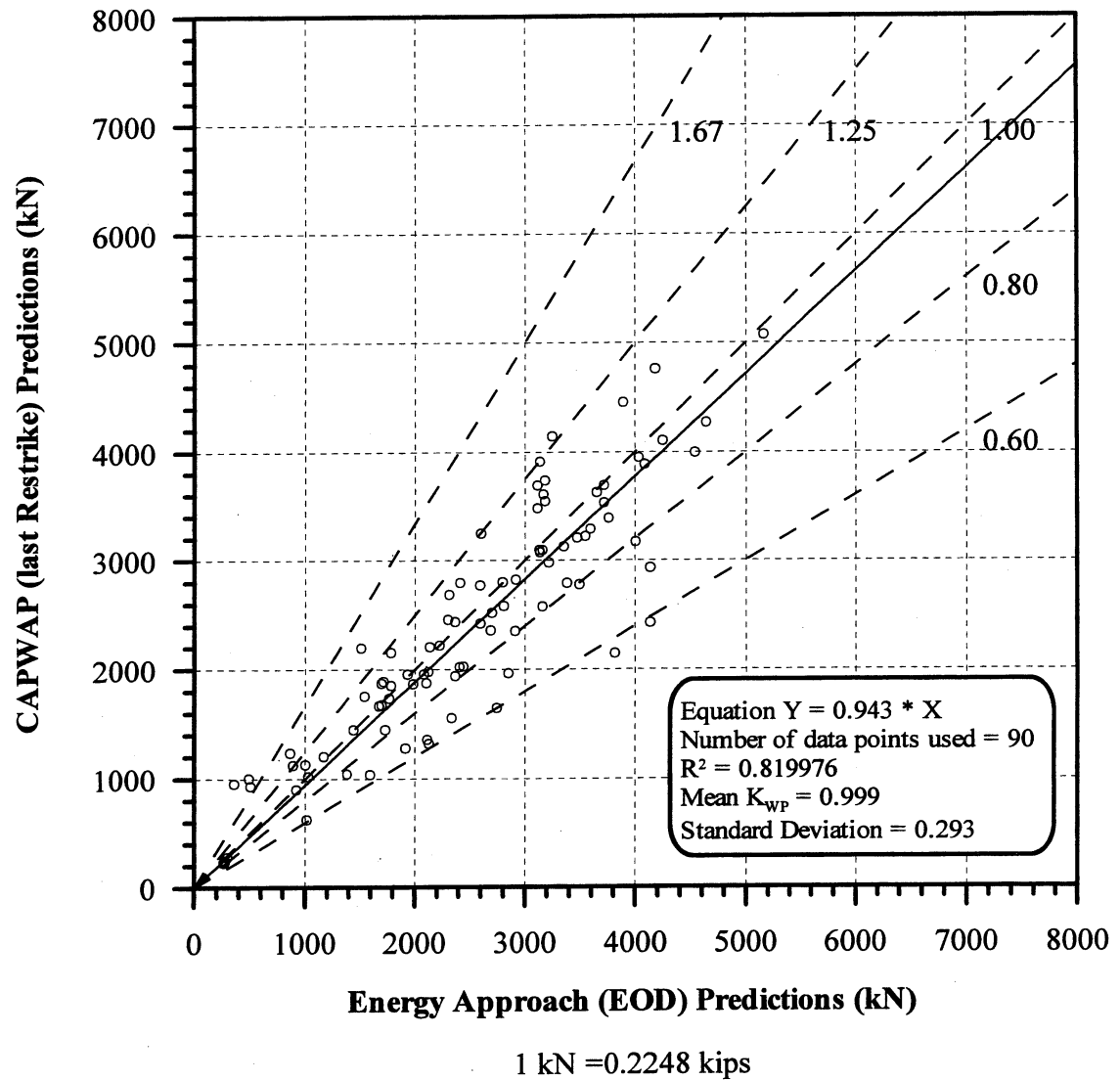


**Figure 7.7.** CAPWAP (last Restrike) Predictions vs. Energy Approach (EOD) Predictions for 90 PD2000 pile-cases in clay & till.

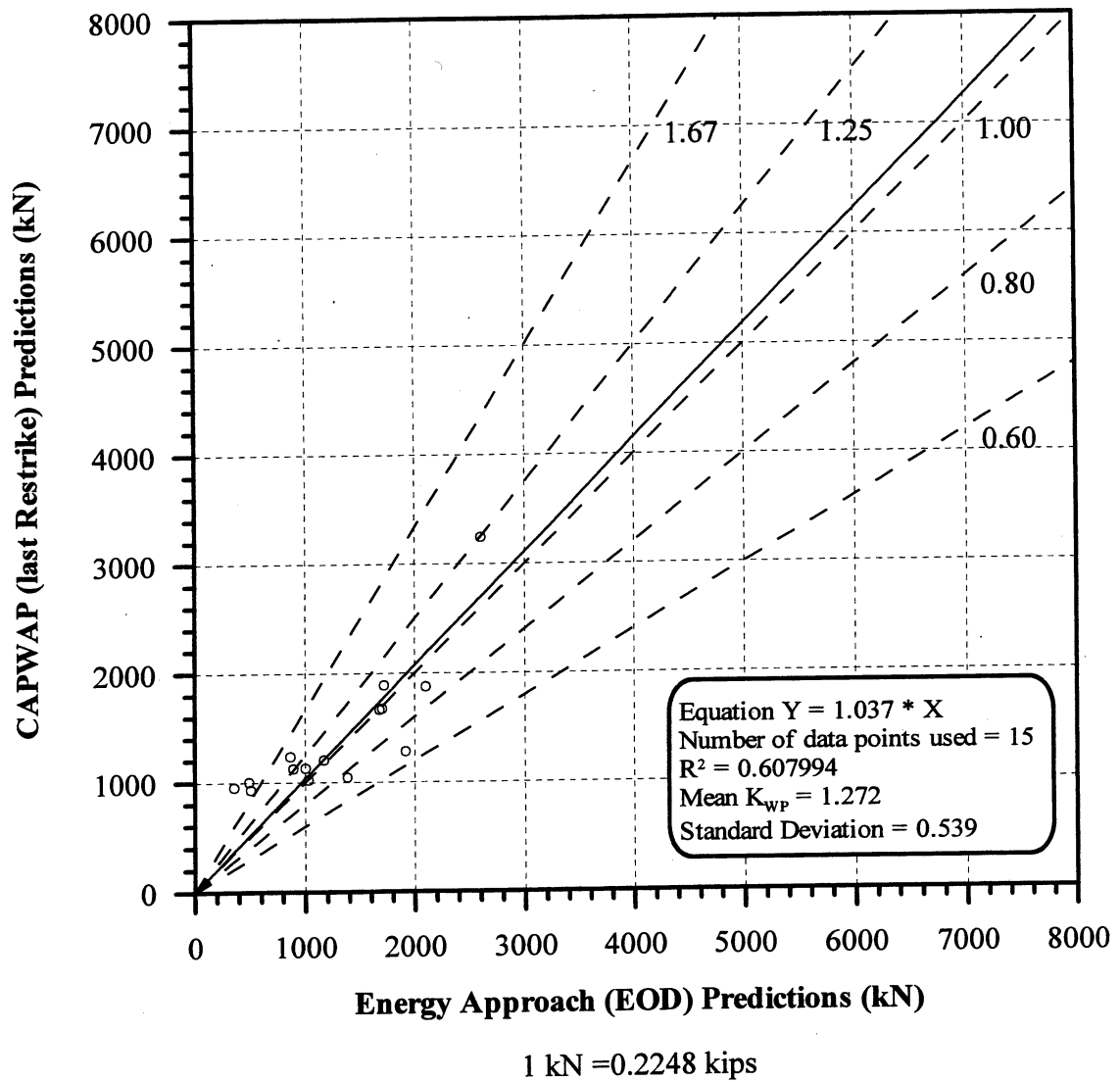


**Figure 7.8.** CAPWAP (last Restrike) Predictions vs. Energy Approach (EOD) Predictions for 15 PD2000 pile-cases with Blow Count < 16 BP10cm in clay & till.

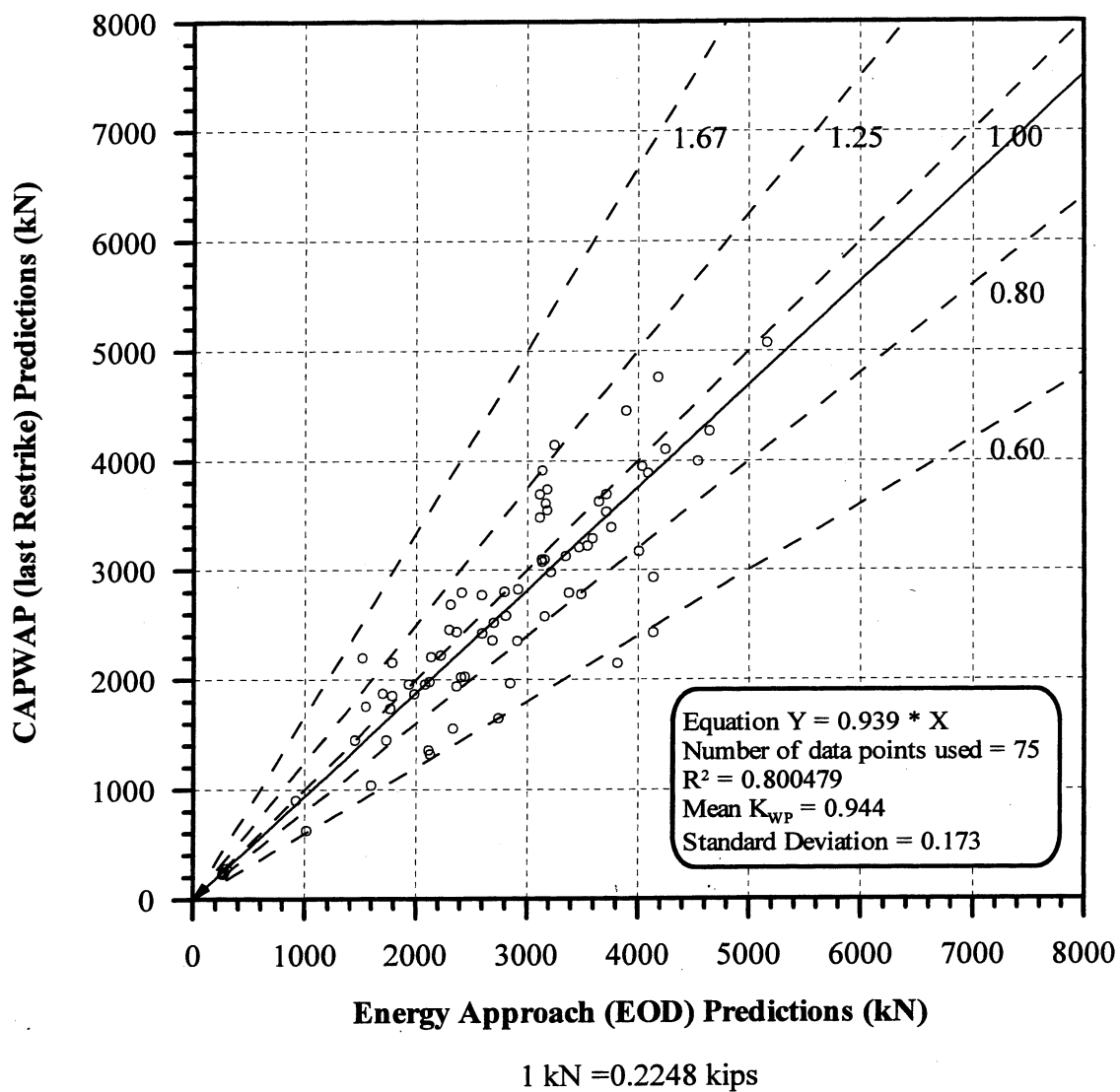


**Figure 7.9.** CAPWAP (last Restrike) Predictions vs. Energy Approach (EOD) Predictions for 75 PD2000 pile-cases with Blow Count  $\geq 16$  BP10cm in clay & till.

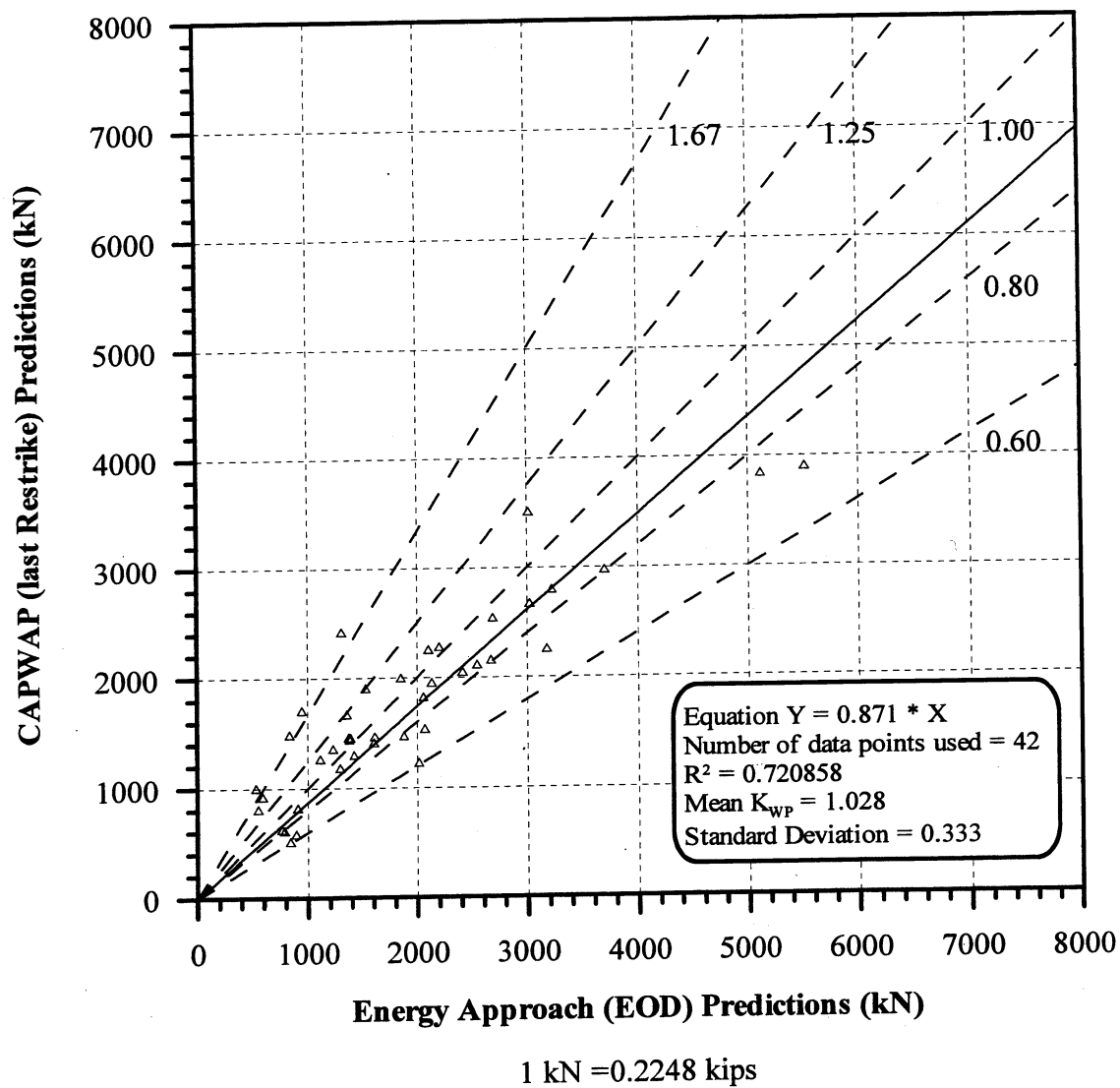


**Figure 7.10.** CAPWAP (last Restrike) Predictions vs. Energy Approach (EOD) Predictions for 42 PD2000 pile-cases in sand & silt.

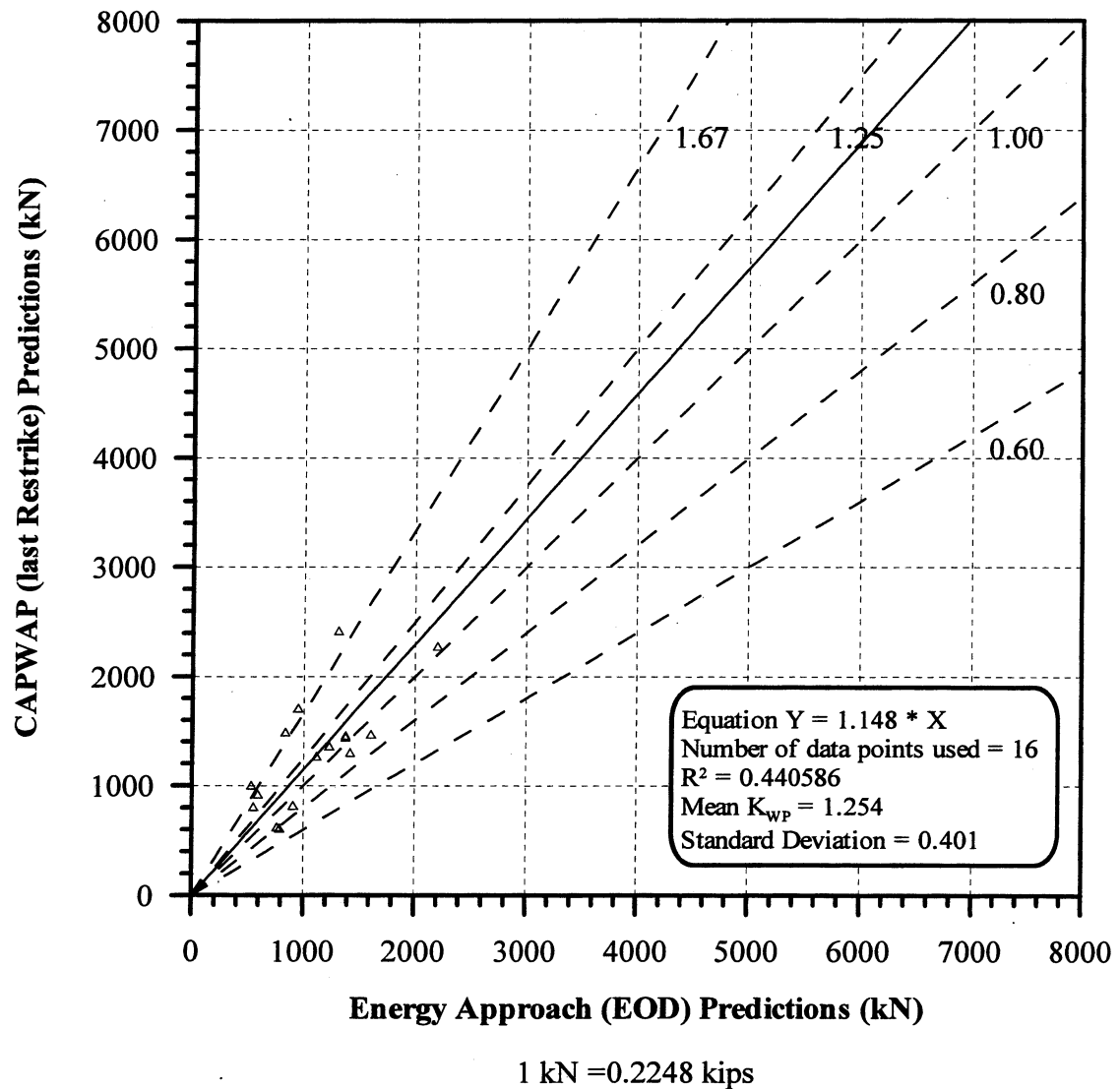


**Figure 7.11.** CAPWAP (last Restrike) Predictions vs. Energy Approach (EOD) Predictions for 16 PD2000 pile-cases with Blow Count < 16 BP10cm in sand & silt.

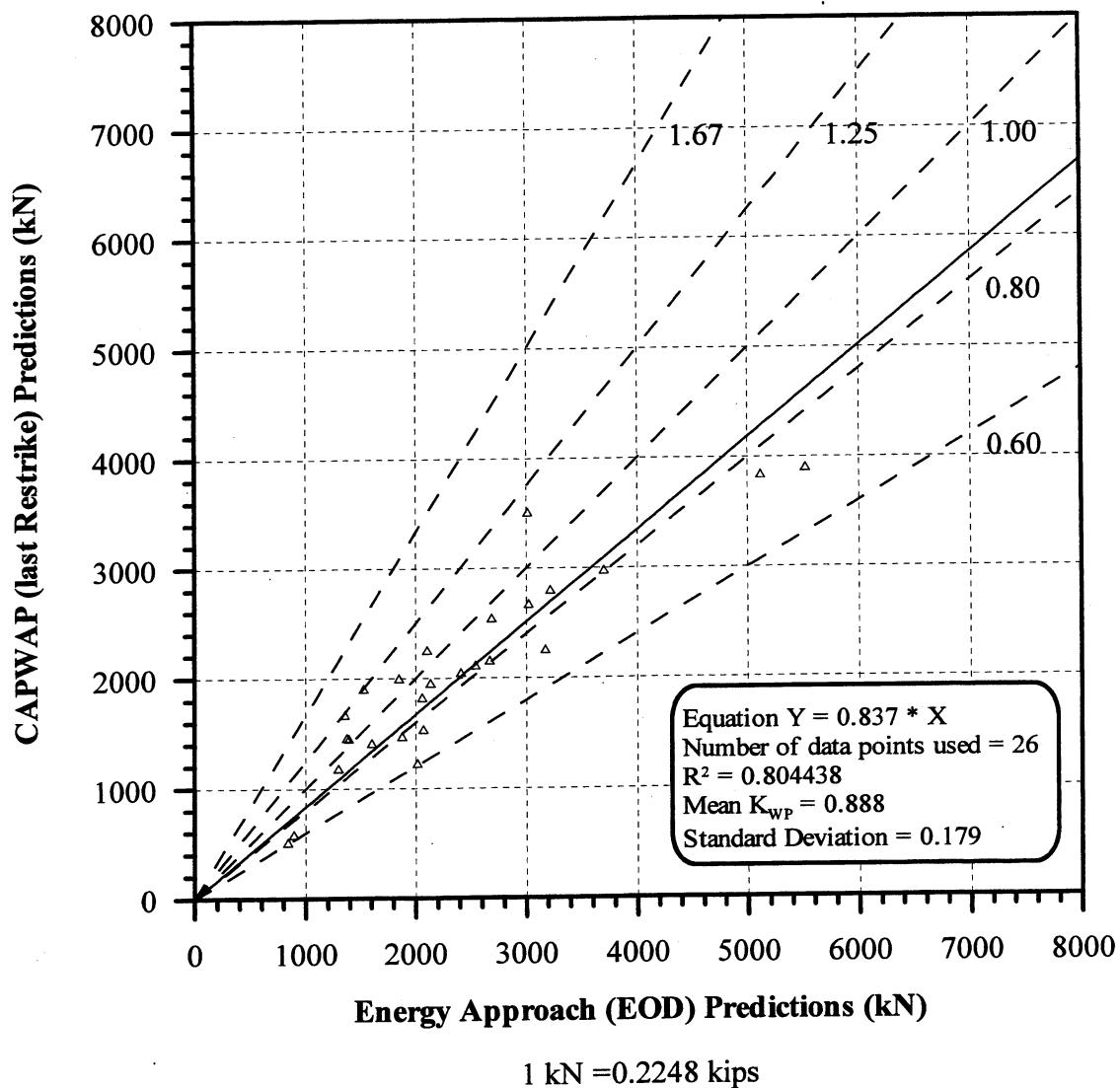


**Figure 7.12.** CAPWAP (last Restrike) Predictions vs. Energy Approach (EOD) Predictions for 26 PD2000 pile-cases with Blow Count  $\geq 16$  BP10cm in sand & silt.



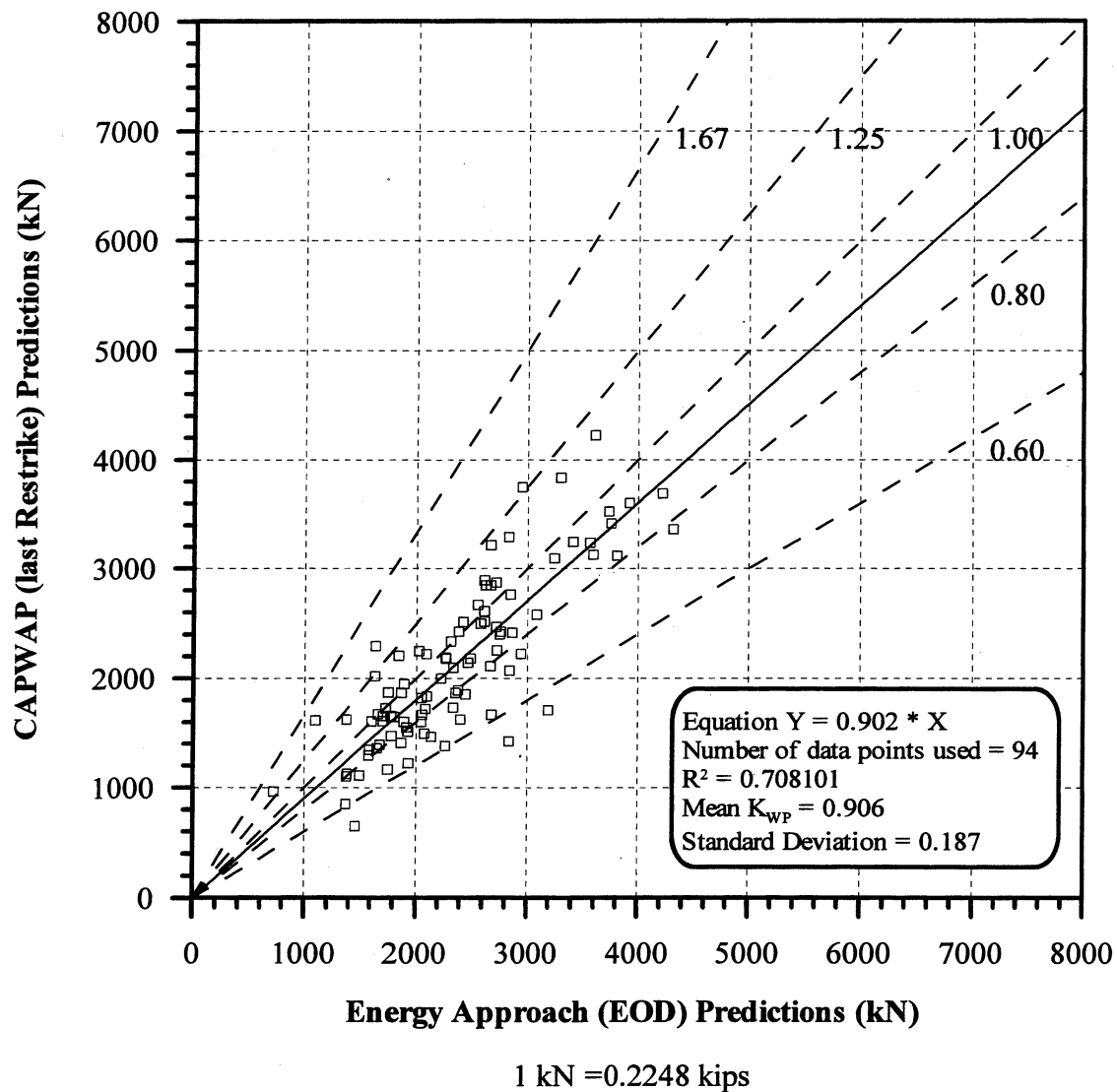


**Figure 7.13.** CAPWAP (last Restrike) Predictions vs. Energy Approach (EOD) Predictions for 94 PD2000 pile-cases in rock.

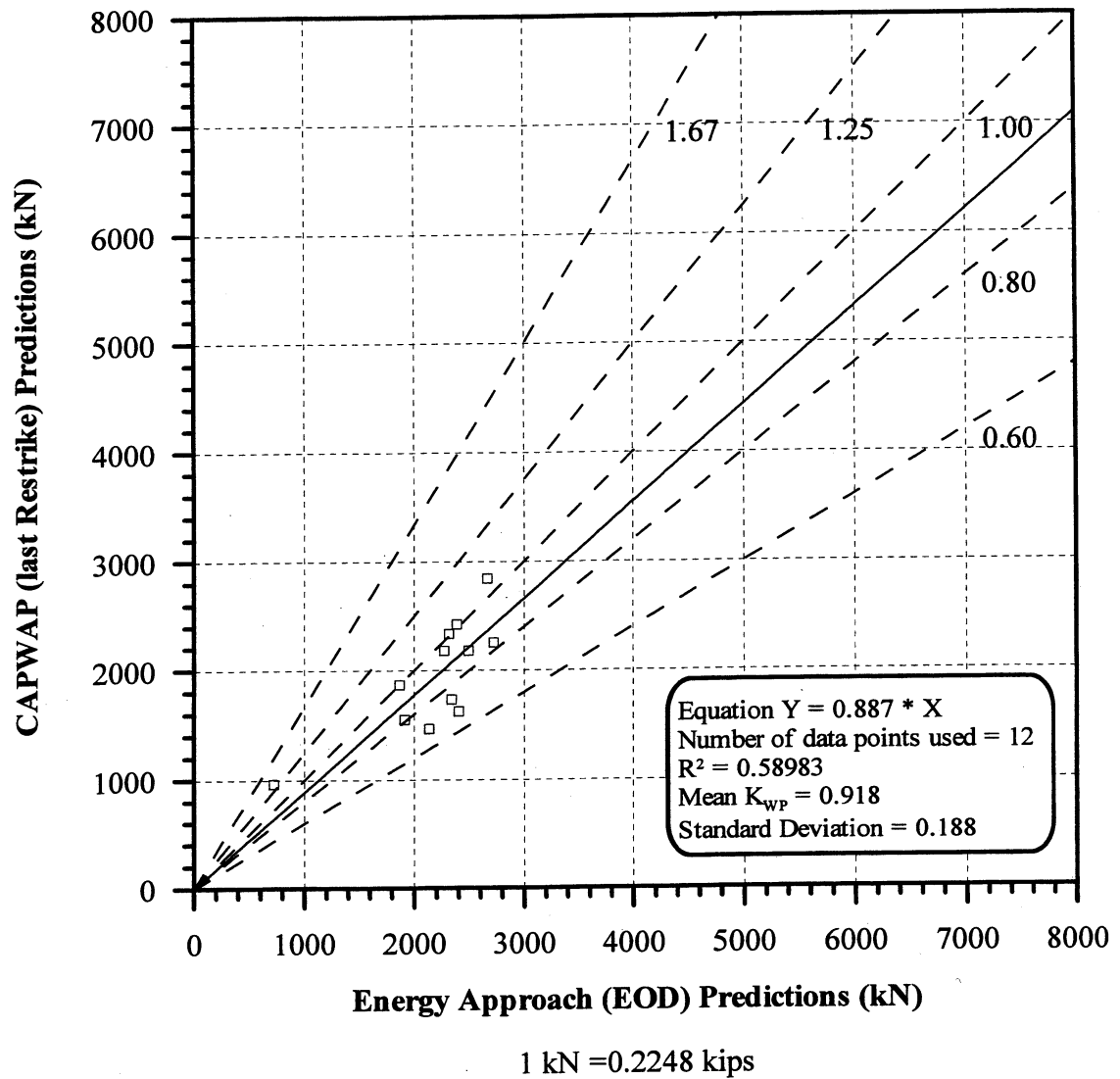


**Figure 7.14.** CAPWAP (last Restrike) Predictions vs. Energy Approach (EOD) Predictions for 12 PD2000 pile-cases with Blow Count < 16 BP10cm in rock.

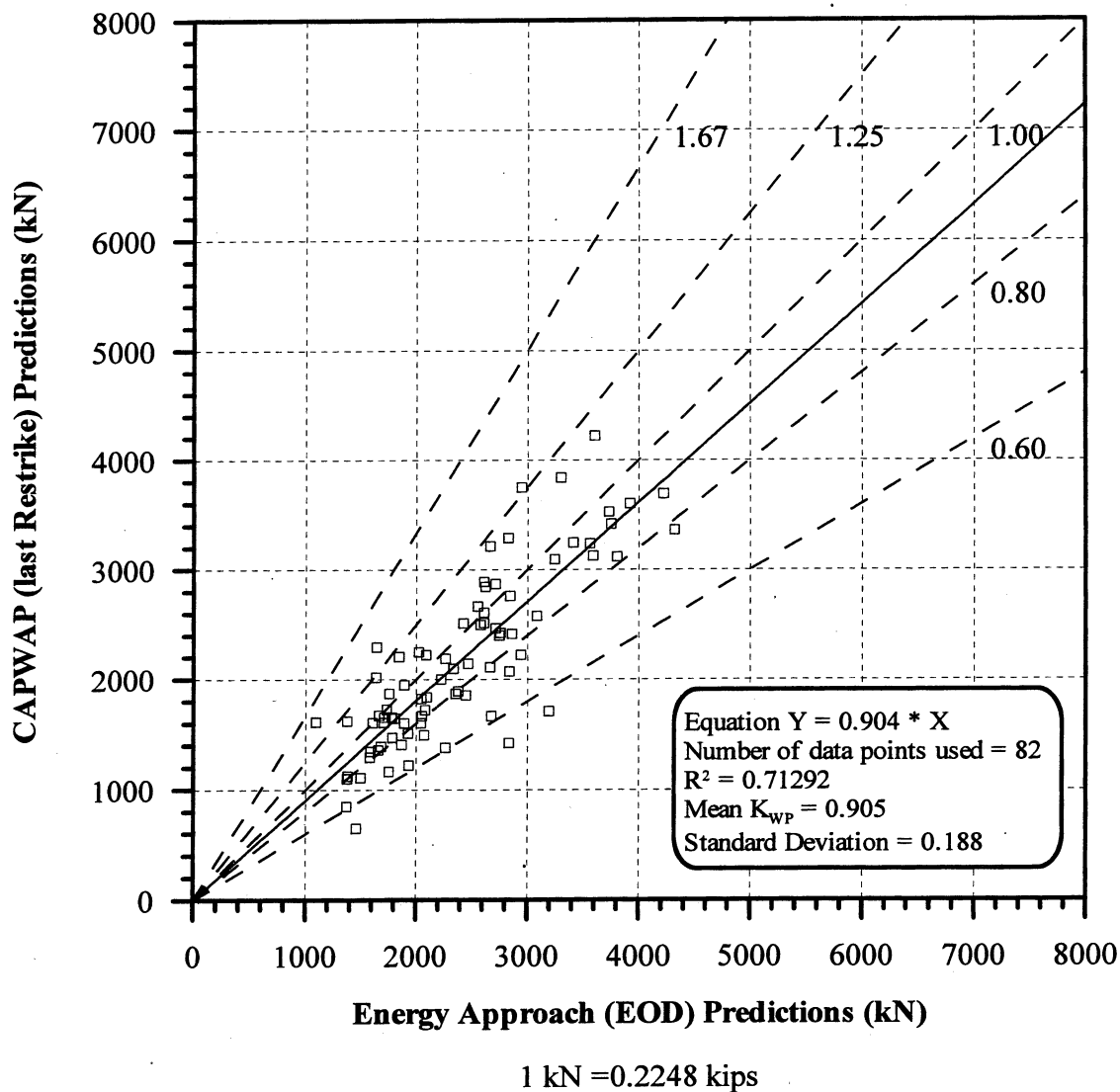


**Figure 7.15.** CAPWAP (last Restrike) Predictions vs. Energy Approach (EOD) Predictions for 82 PD2000 pile-cases with Blow Count  $\geq 16$  BP10cm in rock.

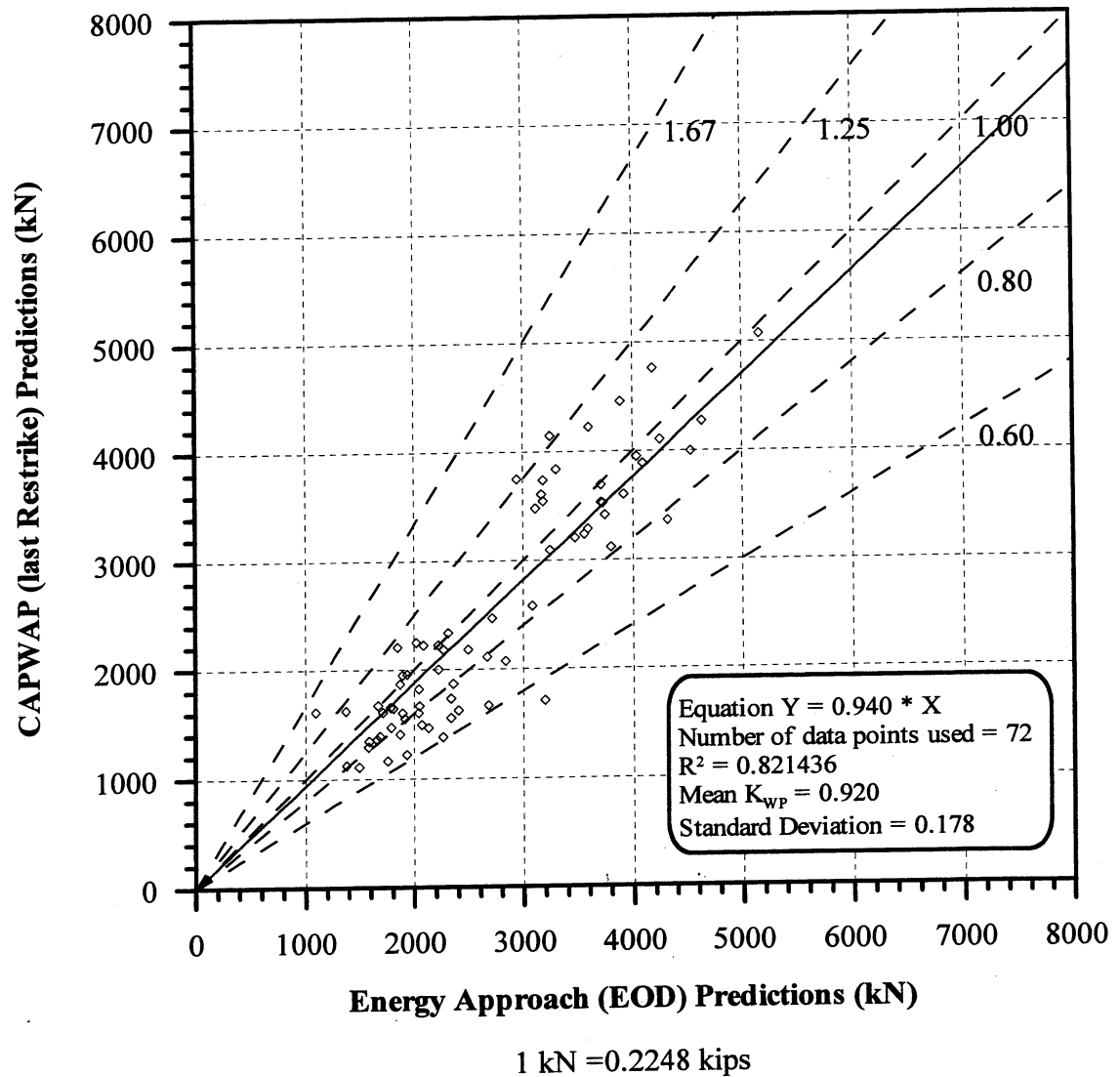


**Figure 7.16.** CAPWAP (last Restrike) Predictions vs. Energy Approach (EOD) Predictions for 72 PD2000 pile-cases with Boston Blue Clay.

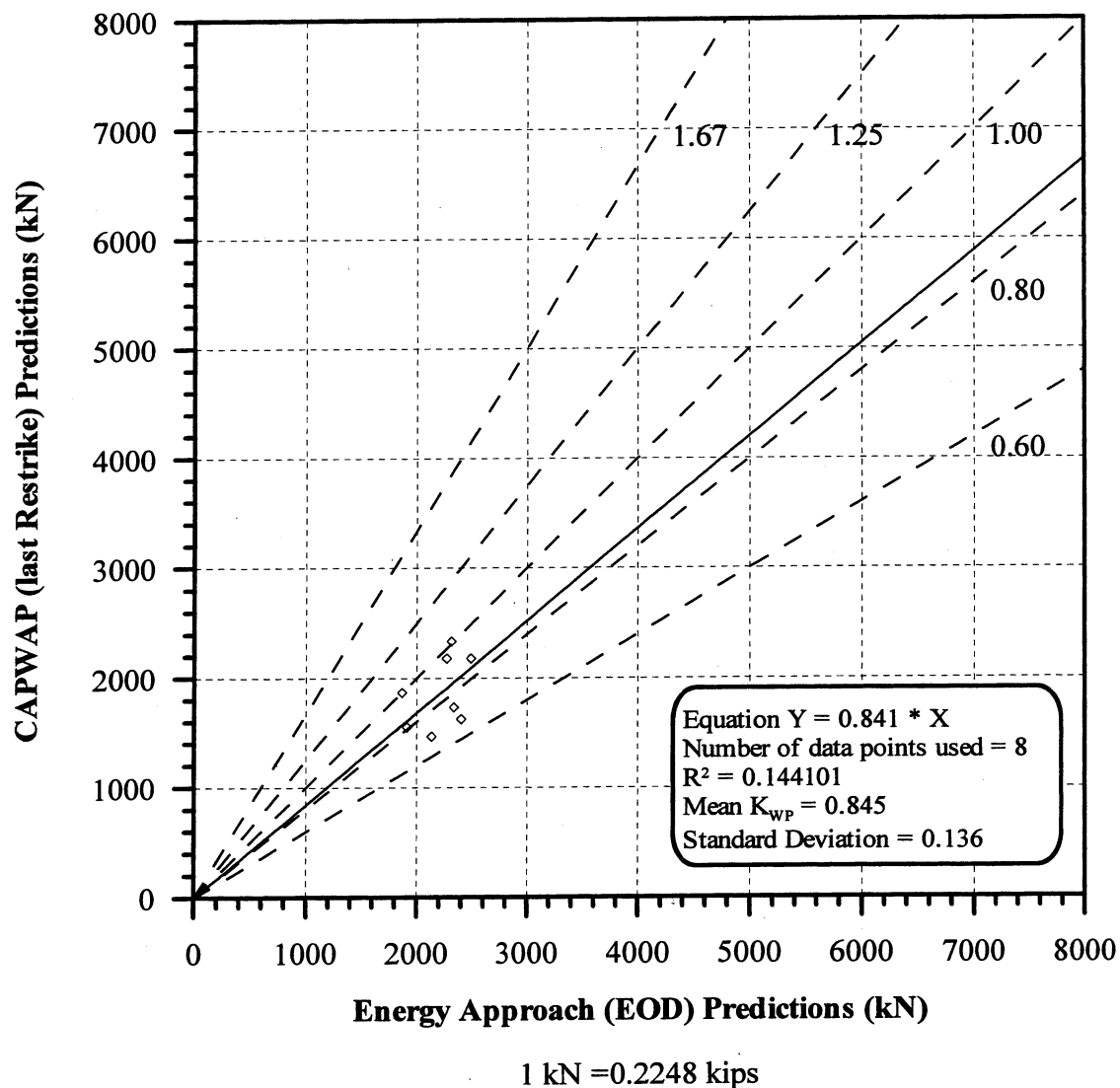


**Figure 7.17.** CAPWAP (last Restrike) Predictions vs. Energy Approach (EOD) Predictions for 8 PD2000 pile-cases with Blow Count < 16 BP10cm with Boston Blue Clay.

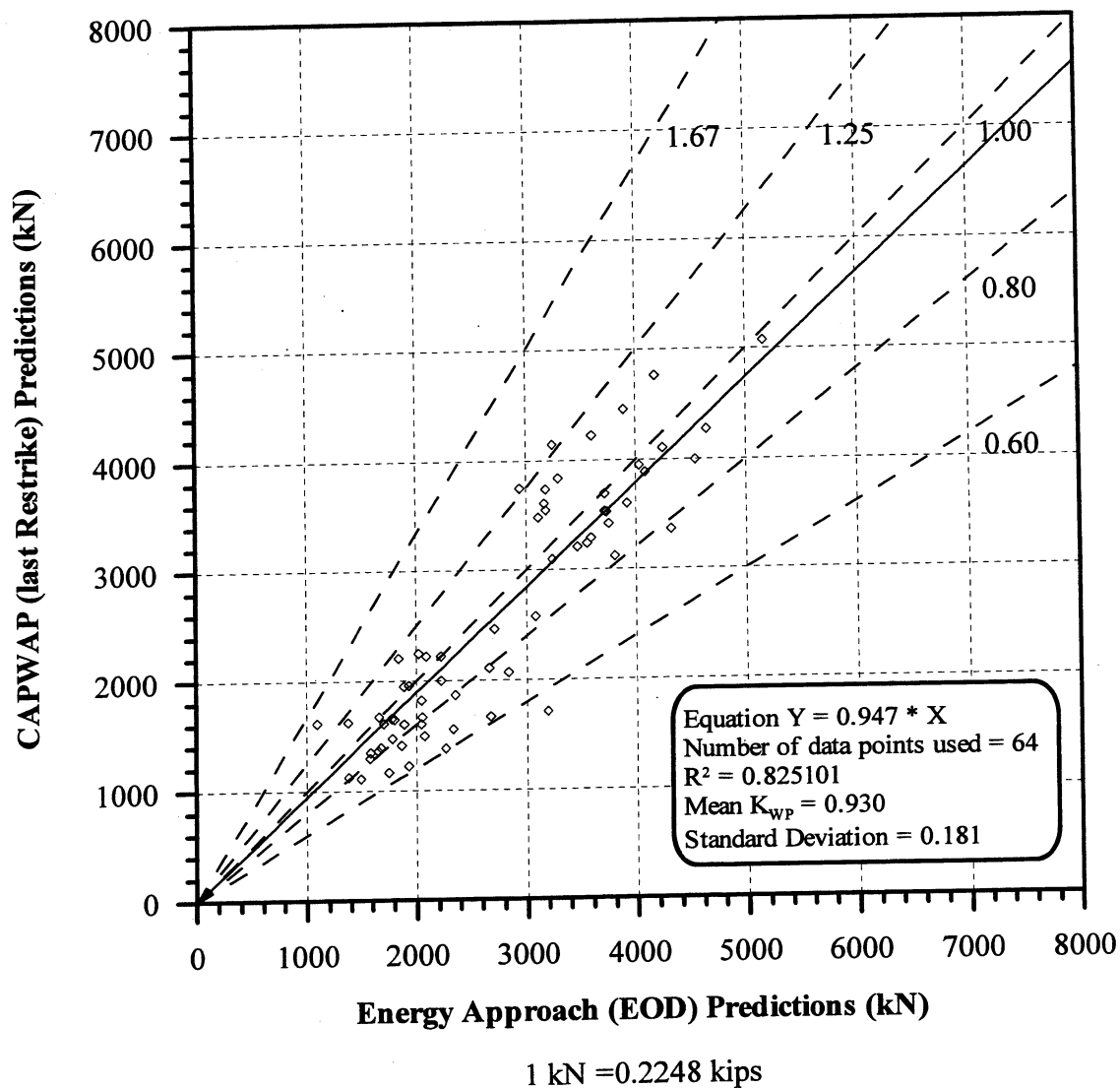


**Figure 7.18.** CAPWAP (last Restrike) Predictions vs. Energy Approach (EOD) Predictions for 64 PD2000 pile-cases with Blow Count  $\geq 16$  BP10cm with Boston Blue Clay.

## **CHAPTER 8**

### **PILE CAPACITY GAIN WITH TIME**

#### **8.1 GENERAL**

The concepts and information presented in this chapter makes use of data accumulated at the Geotechnical Engineering Research Laboratory under a long-term research project that investigates the gain of pile capacity with time. This work is not yet completed and thus far has been reported by Paikowsky et al. (1995), Paikowsky et al. (1996) and Paikowsky and Hart (1998). This chapter presents the relevant information concerning the pile capacity gain for design. For further details on the principles and procedures the reader is referred to one or all of the above references.

Data set PD/LTT2000 was initially reported by Paikowsky et al. (1995) as PD/LTT, has been modified in this work. The database contains fifteen piles that were dynamically monitored over time (EOD - End Of Driving and/or BOR - Beginning Of Restrike) and one load test to failure. Eight of the piles are pre-stressed concrete (PSC) ranging in widths from 250mm to 914mm, four of the piles are H-piles, two HP310×93 piles and two HP310×110 piles, and three of the piles are closed ended pipe piles (CEP) ranging in diameters from 245mm to 324mm. Table 8.1 and Table 8.2 summarize all the relevant data for the PD/LTT2000 pile cases, subdivided according to piles embedded predominately in clay (Table 8.1) and partially in clay

(Table 8.2). All dynamic capacities were determined through CAPWAP analysis (Case Pile Wave Analysis Program, Goble et al. 1970, GRL Inc., 1995). To allow comparison between the different cases, the data were presented in the form of capacity ratio versus the time on a logarithmic scale. The capacity ratio was determined by dividing the obtained CAPWAP capacity by the static load test capacity based on Davisson's failure criterion. The static load test capacity was not necessarily the maximum capacity, especially for the cases where the pile was dynamically monitored after the load test.

## **8.2 ANALYSIS OF PILE CAPACITY GAIN WITH TIME**

Penetration of piles in fine-grained soils causes compression and disturbance, resulting in soil resistance during driving that differs from the long-term pile capacity. Although factors such as thixotropy and aging contribute to this phenomenon, the most significant cause for gain of capacity with time is associated with the migration of pore water. Measurements carried out on a model (Paikowsky & Hart 2000) and full-scale piles (Paikowsky & Hajduk 1999, 2000) show that pore pressure at magnitudes similar to the total soil pressures create in clays around the pile's shaft zones of about zero effective stresses, resulting in almost a complete loss of frictional resistance. Paikowsky et al. (1995, 1996) examined the static and dynamic gain of capacity with time based on radial consolidation; a normalization process was followed, allowing for a comparison between different pile sizes. Table 8.3 presents a summary of parameters describing the pile capacity gain with time based on static and dynamic testing. The presented data shows that while the rate of capacity gain



(normalized to the maximum capacity vs. time on log scale) is similar when based on static or dynamic measurements ( $C_{gt} = 0.389$  and  $C_{gtd} = 0.348$ , respectively). The associated time for achieving 75% of the maximum capacity (normalized for all piles to 254mm (1ft) diameter) is about 20 times greater for the static data compared to the dynamic based data. In other words, dynamic testing (namely CAPWAP) while following the physical behavior of capacity gain, exhibit this gain much faster than the actual gain monitored by the static load test results.

Figure 8.1 presents the capacity gain curves based on dynamic measurements for the seven piles embedded in mostly clay, adjusted according to pile size. Also included on this graph are the equations of the best-fit lines, their corresponding coefficient of determination, and the number of points used for each curve. The slopes of the best-fit lines, termed  $C_{gtd}$ , represent the rate at which the pile gains capacity. The pile from Denmark (DN1) drastically shifted outside of the expected band. This pile was first load tested 29 days after its installation. This is a significant amount of time that elapsed between driving and testing for a 250mm square PSC pile. The data available, therefore, captures only the end of the capacity gain process and not the major event. As a result it is believed that the  $t_{75}$  value (the time needed for 75% of the capacity gain to be reached) does not reflect the actual time needed for this pile to gain 75% of its capacity. The  $t_{75}$  values ranged from 12.4 hours to 189.8 hours (8 days) with a mean value of 45.4 hours and a standard deviation of 64.1 hours. After eliminating the data from Denmark, the standard deviation substantially decreases to 7.9 hours with a mean of 21.3 hours.

The capacity gain curves for the eight piles partially embedded in clay are presented in Figure 8.2, adjusted according to pile size. Also included on this graph are the equations of the best-fit lines where the slope represents the rate at which the pile gains capacity, their corresponding coefficient of determination, and the number of points used for each curve. The  $t_{75}$  values ranged from 2.2 hours to 83.2 hours (3.5 days) with a mean value of 25.0 hours and a standard deviation of 28.4 hours. The two piles with  $t_{75}$  values of zero, also shown in Table 8.2, are not realistic. The unrealistic results are due to a combination of two factors. The first being that the dynamic tests over predicted the pile capacity compared to the actual static load test results, which causes a shift of the best-fit line upward. The other cause is that the rate at which the pile gains capacity is high, possibly due to the fast drainage through the sand and silt layers, which in turn creates a problem when attempting to linear interpolate back to the  $t_{75}$  value, at an adjusted time of one hour the  $K_{SW}$  value is greater than 0.75. This means that the time for the pile to gain 75 percent of the actual pile capacity is less than one hour. In a practical way, when the pile is embedded in mixed layers the sand and silt layers diminish the pile capacity gain with time phenomenon and need to be evaluated in a more detailed approach than the one presented.

### **8.3 INTERMEDIATE CONCLUSIONS**

Since this data set is of limited size (especially if the two open-ended 36"  $\times$  5" (0.914 m  $\times$  0.127 m) PSC cylindrical piles (TP6 and TP7) are eliminated), it is difficult to make definitive conclusions regarding the applicability of the size/time

adjustment process based solely on the presented data. The practical conclusions offered for the presented data are:

- (i) actual gain of capacity is much slower than that exhibited by the dynamic methods,
- (ii) scheduling of construction or testing based on capacity gain should consider the reason for time evaluation (i.e. static loading in early construction or dynamic testing as part of quality control), and,
- (iii) at present, the dynamic methods evaluation should concentrate on the long term pile capacity.

Considering all of the above the following simplified relationships can be offered to determine the time elapsed from driving to the time for 75% of the maximum capacity:

For piles embedded completely in clay:

- For static testing purpose:  $t_{75\%} = 1540 \times r^2$  (8.1)

- For dynamic testing purpose:  $t_{75\%} = 85 \times r^2$  (8.2)

For piles embedded in alternating soil conditions (granular and cohesive):

- For dynamic testing purpose:  $t_{75\%} = 39 \times r^2$  (8.3)

Where:  $t_{75\%}$  = time to reach 75% of maximum capacity in hours  
 $r$  = pile radius in feet.

For example a 1 ft diameter pile in a clay deposit requires approximately a 1-day (21 hrs) delay for a restrike to present about 75% of the maximum capacity. A 2ft diameter pile will require a 3.5-day delay for a restrike under similar conditions.

The relationships for the piles embedded completely in clay were calculated using the  $t_{75}$  values presented in Table 8.3. The  $t_{75}$  value for the piles embedded in alternating soil conditions was determined by passing the best-fit line through all of the data points plotted in Figure 8.2 and using the resulting equation of that line. The obtained slope of the best-fit line ( $C_{gtd}$ ) was 0.255 with a y-intercept of 0.499. The calculated  $t_{75}$  value was therefore 9.65 hours. The above relationships (equations 8.1-8.3) were determined by using the equation proposed by Paikowsky and Whitman (1990):

$$\frac{t_1}{t_2} = \left( \frac{r_1}{r_2} \right)^2 \quad (8.4)$$

Where:

$t_1$	=	elapsed time since driving for a pile of interest
$r_1$	=	radius of pile of interest
$t_2$	=	actual time since driving for a known pile
$r_2$	=	radius of known pile

For piles other than closed circular shapes, an equivalent radius ( $r_2$ ) can be determined. In the presented analysis, the radius of open-ended pipe piles was taken as one-half of the outside diameter. For the square box shape, half of one side represents the radius. The depth from the outer edge of one flange to the outer edge of the other flange was considered the equivalent radius for H-piles.

**Table 8.1.** Soil properties, pile type, and relevant information for dynamic capacity gain - Data Set PD/LTT2000, predominately clay embedment (Paikowsky et al., 1995).

Location	Soil Type		Pile Type	Depth (m)	Davisson Capacity (kN)	$t_{75}^*$ (hrs)	$C_{gtd}$
	Shaft	Tip					
Baton Rouge, LA	silty clay	silty sand	PSC 61 cm sq	25.7	1779	12.4	0.243
Denmark	sandy clay	clayey chalk	PSC 25cm sq	21.0	1250	189.8	0.332
Kenner, LA	clay	sand	PSC 61 cm sq	25.0	1842	29.3	0.332
Kenner, LA	clay	sand	PSC 76 cm sq	25.3	2273	32.7	0.341
Kenner, LA	clay	sand	PSC 76 cm sq	25.3	2469	19.5	0.315
Kenner, LA	clay	sand	91.4 cm ×; 12.7 cm PSC cyl	25.0	2411	16.4	0.431
Kenner, LA	clay	sand	91.4 cm ×; 12.7 cm PSC cyl	24.7	2402	17.6	0.439
Avg:						45.4	0.348
Stdev:						64.1	0.068
w/out Denmark, Avg:						21.3	
w/out Denmark, Stdev:						7.9	

**Table 8.2.** Soil properties, pile type, and relevant information for dynamic capacity gain - Data Set PD/LTT2000, partially in clay embedment.

Location	Soil Type		Pile Type	Depth (m)	Davisson Capacity (kN)	t <sub>75</sub> (hrs)	C <sub>gtd</sub>
	Shaft	Tip					
Jones Is., WI	sa-si-clay	silty sand	HP310×;93	47.5	1343	25.6	0.396
Jones Is., WI	sa-si-clay	silty sand	HP310×;93	43.5	890	0*	0.171
Newbury, MA	sa-si-clay	sand	CEP 324mm	21.1	667	41.2	0.455
Newbury, MA	sa-si-clay	sand	PSC 356mm sq	21.3	783	0*	0.134
Jones Is., WI	silty clay	silty clay	CEP 245mm	43.4	2936	83.2	0.139
Jones Is., WI	sa-si-clay	silty sand	CEP 324mm	37.5	2909	34.4	0.255
Newbury, MA	sa-si-clay	glacial till	HP310×;110	34.1	1806	2.2	0.103
Newbury, MA	sa-si-clay	silty sand	HP310×;110	33.1	2126	13.7	0.158
Avg:						25.0	0.226
Stdev:						28.4	0.131

\*These two pile-cases are ones in which the dynamic predictions were considerably larger than the static load test results.

**Table 8.3.** Summary of static and dynamic based capacity gain data sets (Paikowsky et al. 1995).

	Static Data Sets LTT and PUT/LTT		Dynamic Data Set PD/LTT		All Data	
	$C_{gtd}$	$t_{75}^*$	$C_{gtd}$	$t_{75}^{**}$	$C_{gtd}$	$t_{75}^{**}$
No.	15	5	7	6	22	11
Average	0.389	385.0	0.348	21.3	0.376	186.6
Standard Deviation	0.119	226.3	0.068	7.9	0.106	237.9

\* closed-ended piles only

\*\* excluding the case from Denmark

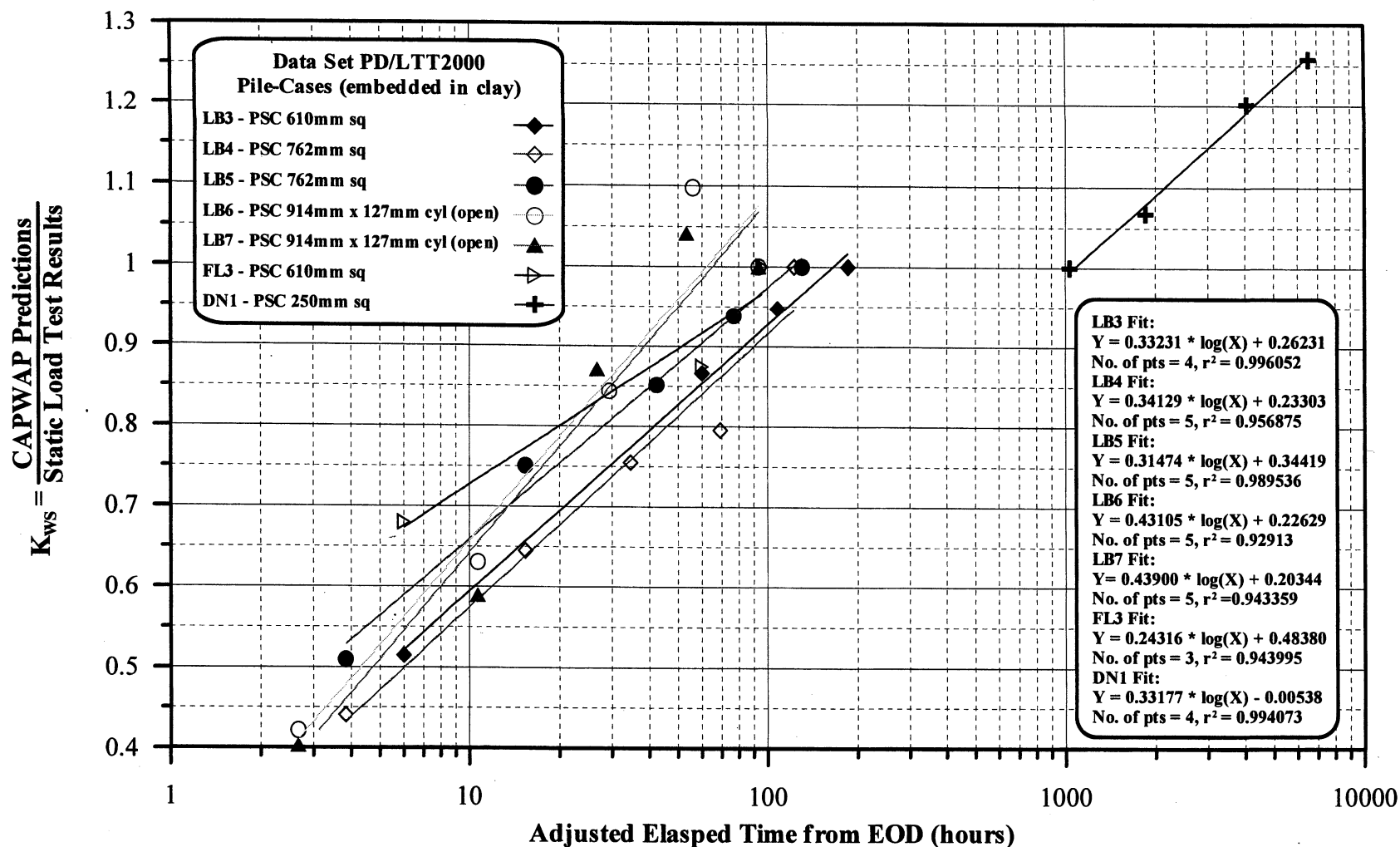


**Figure 8.1.**  $K_{ws}$  values vs. log - Time for PD/LTT2000 pile-cases with multiple Restrikes with the majority of the skin friction coming from the clay layers (Paikowsky et al., 1995).



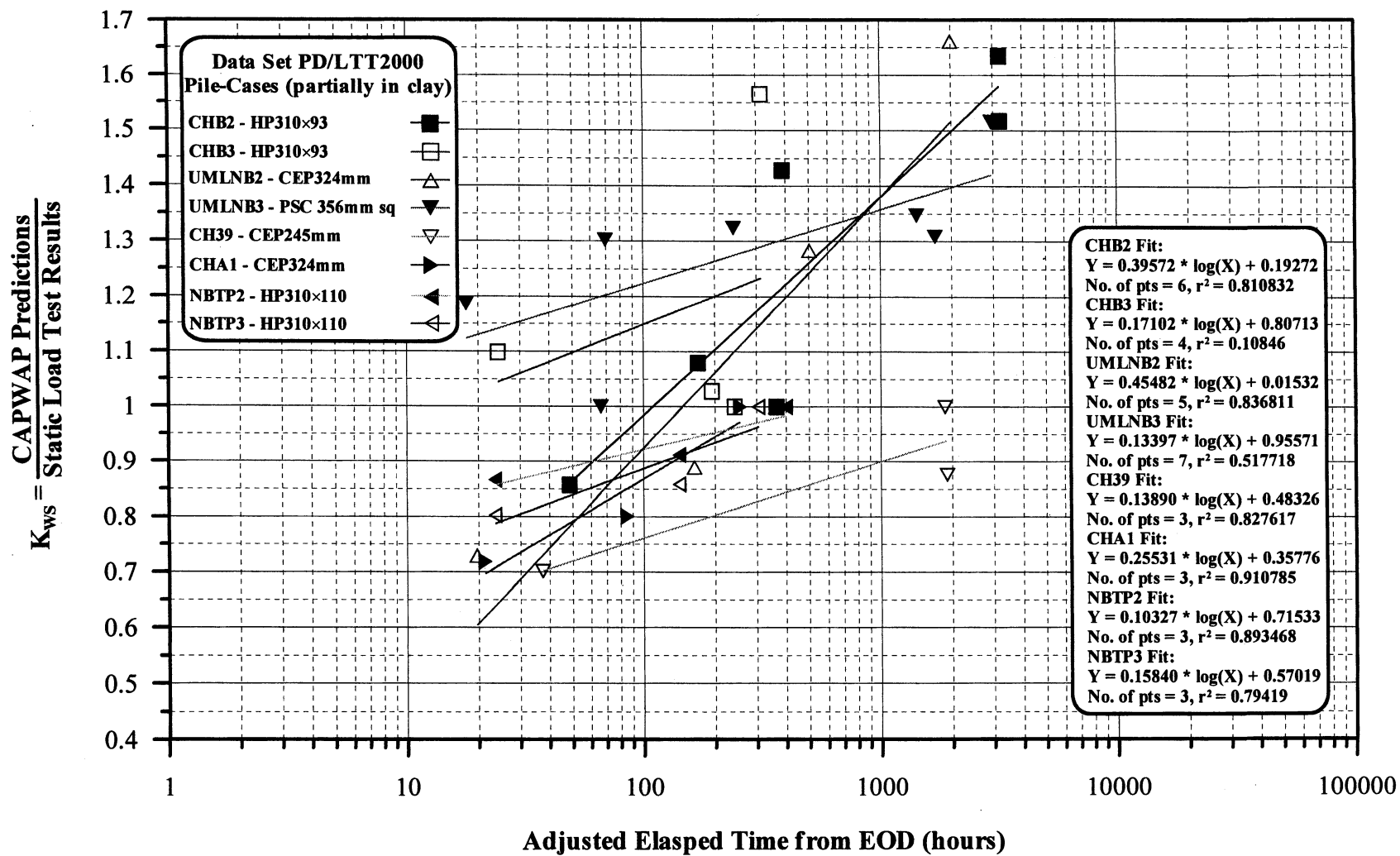


**Figure 8.2.**  $K_{ws}$  values vs. log - Time for PD/LTT2000 pile-cases with multiple Restrikes partially in clay.

## CHAPTER 9

### CALCULATION OF RESISTANCE FACTORS

#### 9.1 METHODOLOGY

This section is based on contributions provided by Professor Bilal M. Ayyub and Gregory B. Baecher of the Department of Civil Engineering at the University of Maryland. The present project calibrates LRFD partial safety factors using the First-Order Reliability Method (FORM), (Hasofer and Lind, 1974). FORM can be used to assess the reliability of a pile with respect to specified limit states, and provides a means for calculating partial safety factors  $\phi$  and  $\gamma_i$  for resistance and loads, respectively, against target reliability levels,  $\beta_0$ . FORM requires only the first and second moment information on resistances and loads (i.e., means and standard deviations), and an assumption of distribution type (e.g., Normal, lognormal, etc.). The entire calibration process is presented in Figure 9.1.

In design practice, there are usually two types of limit states: ultimate limit states and serviceability limit state. Each can be represented by a performance function of the form,

$$g(X) = g(X_1, X_2, \dots, X_n) \quad (9.1)$$

in which  $X$  is a vector of basic random variables ( $X_1, X_2, \dots, X_n$ ) for strengths and loads. The performance function  $g(X)$  is sometimes called the limit state function. It relates

the random variables for the limit-state of interest. The limit state is defined when  $g(X) = 0$ , and therefore, failure occurs when  $g(X) < 0$ . The reliability index  $\beta$  is defined as the distance from the origin of the space of basic random variables ( $X_1, X_2, \dots, X_n$ ) to the failure surface at the most probable failure point. The most probable failure point is that point on the limit state function at which the probability density of the basic random variables is greatest. This is also called, the design point. This relationship can also be used to back calculate representative values of the reliability index  $\beta$  from current design practice.

The computational scheme for determining  $\beta$  using FORM is the following:

1. Assume a design point  $x_i^*$  and obtain its corresponding point,  $x_i'^*$  in a reduced coordinate system using the normalizing transformation:

$$x_i'^* = \frac{x_i^* - \mu_{X_i}}{\sigma_{X_i}} \quad (9.2)$$

where  $\mu_{X_i}$  = mean value of the basic random variable  $X_i$ , and  $\sigma_{X_i}$  = standard deviation. The mean values of the basic random variables are often used as initial guesses for the design points,

2. For non-normal basic random variables, evaluate the equivalent normal distributions at the design point using:

$$\mu_X^N = x^* - \Phi^{-1}(F_X(x^*))\sigma_X^N \quad (9.3)$$

and

$$\sigma_X^N = \frac{\left( \Phi^{-1} \left( F_X(x^*) \right) \right)}{f_X(x^*)} \quad (9.4)$$

where  $\mu_X^N$  = mean of the equivalent normal distribution,  $\sigma_X^N$  = standard deviation of the equivalent normal distribution,  $F_X(x^*)$  = original cumulative distribution function (CDF) of  $X_i$  evaluated at the design point,  $f_X(x^*)$  = original probability density function (PDF) of  $X_i$  evaluated at the design point,  $\Phi(\cdot)$  = CDF of the standard normal distribution, and  $\phi(\cdot)$  = PDF of the standard normal distribution.

3. Set  $x_i^* = -\alpha_i^* \beta$ , in which the  $\alpha_i^*$  are direction cosines computed as,

$$\alpha_i^* = \frac{\left( \frac{\partial g}{\partial x_i} \right)_*}{\sqrt{\sum_{i=1}^n \left( \frac{\partial g}{\partial x_i} \right)_*^2}} \quad \text{for } i = 1, 2, \dots, n \quad (9.5)$$

where

$$\left( \frac{\partial g}{\partial x_i} \right)_* = \left( \frac{\partial g}{\partial x_i} \right)_* \sigma_{X_i}^N \quad (9.6)$$

4. With  $\alpha_i^*$ ,  $\mu_{X_i}^N$ , and  $\sigma_{X_i}^N$  now known solve for  $\beta$  in the limit state function,

$$g \left[ (\mu_{X_1}^N - \alpha_{X_1}^* \sigma_{X_1}^N \beta), \dots, (\mu_{X_n}^N - \alpha_{X_n}^* \sigma_{X_n}^N \beta) \right] = 0 \quad (9.7)$$

5. Using the  $\beta$  obtained from step 4, a new design point is obtained from:

$$x_i^* = \mu_{X_i}^N - \alpha_i^* \sigma_{X_i}^N \beta \quad (9.8)$$

6. Repeat steps 1 to 5 until it converges. This reliability index is the shortest distance to the failure surface from the origin in the reduced coordinates.

To estimate partial safety factors on resistance and loads, such as those found in the design format, consider that at the failure point  $(R^*, L_1^*, \dots, L_n^*)$ , the limit state is given by

$$g = R^* - L_1^* - \dots - L_n^* = 0 \quad (9.9)$$

or, in a general form

$$g(X) = g(x_1^*, x_2^*, \dots, x_n^*) = 0 \quad (9.10)$$

For given target reliability index  $\beta_0$ ; probability distributions, means and standard deviations of load effects; and probability distribution, mean and coefficient of variation of resistance; partial safety factors can be determined by the iterative solution. The mean value of the resistance and the design point are then used to compute the mean required partial design safety factors as,

$$\phi = \frac{R^*}{\mu_R} \quad (9.11)$$

$$\gamma_i = \frac{L_i^*}{\mu_{L_i}} \quad (9.12)$$

In developing design code provisions for piles, it is necessary to follow the current design practice to ensure consistent levels of reliability over various pile types. Calibrations of existing design codes are needed to make the new design formats as simple as possible and to put them in a form that is familiar to users or designers. For

a given reliability index  $\beta$  and probability characteristics for the resistance and load effects, the partial safety factors determined by the FORM approach might be different for different failure modes for the same or differing component. For this reason, calibration of the calculated partial safety factors (PSF's) is important in order to maintain the same values for all loads at different failure modes. In the case of geotechnical codes, the calibration of resistance factors is performed for a set of load factors already specified in the structural code. Thus, the load factors are fixed. In this case, the following algorithm is used to determine resistance factors:

1. For a given value of the reliability index  $\beta$ , probability distributions and moments of the load variables, and the coefficient of variation for the resistance, compute mean resistance  $R$  using FORM
2. With the mean value for  $R$  computed in step 1, the partial safety factor  $\phi$  is revised as:

$$\phi = \frac{\sum_{i=1}^n \gamma_i \mu_{L_i}}{\mu_R} \quad (9.13)$$

where  $\mu_{L_i}$  and  $\mu_R$  are the mean values of the loads and strength variables, respectively, and  $\gamma_i, i = 1, 2, \dots, n$ , are the given set of load factors.

## 9.2 LEVEL OF TARGET RELIABILITY

### 9.2.1 Overview

The utilization of the LRFD method requires the discussion of a target reliability which determines the probability of failure and hence the magnitude of the

resistance factors. The probability of failure represents the probability for the condition in which the resistance multiplied by the resistance factor will be less than the load multiplied by the load factors. An approximate relationship between the two for a lognormal distribution was presented by Rosenbleuth and Estava (1972):  $p_f = 460 \exp(-4.3)$  and is presented in Table 9.1. Unfortunately, although Rosenbleuth and Estava say that the approximation pertains to log normal distributions (because they use the mean of the logs and the standard deviation of the logs to calculate  $\beta$ ), the approximation is not so accurate below  $\beta$  of about 2.5. Table 9.2 prepared by Professor Gregory B. Baecher provides the comparison between the "exact" numbers to the approximation and suggests significant errors, especially in our zone of interest ( $\beta = 2$  to 3). The "exact" numbers will be used in this research.

## **9.2.2 General Discussion**

### ***a) Target Reliability Levels***

The discussion presented in this section was contributed by Professor Bilal M. Ayyub. Both codified and direct reliability-based design requires that a set of target reliability levels be defined. The selection of these levels is a difficult task (Payer *et al.* 1994). These values are not readily available and need to be generated or selected. Also, these levels might vary from one industry to another due to factors such as the implied reliability levels in currently used design practices by industries, failure consequences, public and media sensitivity, or response to failures that can depend on the industry type, types of users or owners, design life of a structure, and other political, economic, and societal factors. Two approaches for generating target

reliability levels were used by other industries. These approaches are: 1) calibrated reliability levels that are implied in currently used codes, and 2) cost benefit analysis.

The first approach was commonly used to develop reliability-based codified design such as the LRFD format. The target reliability levels according to this approach are based on calibrated values of implied levels in a currently used design practice. The argument behind this approach is that a code represents a documentation of an accepted practice. Therefore, since it is accepted, it can be used as a launching point for code revision and calibration. Any adjustments in the implied levels should be for the purpose of creating consistency in reliability among the resulting designs according to the reliability-based code. Using the same argument, it can be concluded that target reliability levels used in one industry might not be fully applicable to another industry.

The second approach is based on cost-benefit analysis. This approach was used effectively in dealing with designs for which failures result in only economic losses and consequences. Since structural failures might result in human injury or loss, this method might be very difficult to use because of its need for assigning a monetary value to human life. Although this method is logical on an economic basis, its main shortcoming is its need to measure the value of human life. Consequently, the first approach is favored for this study and is discussed further in the following sections.



**b)      *Calibrated Reliability Levels***

A number of efforts in which target reliability levels (i.e., safety indices or  $\beta$  values) were developed for the purpose of calibrating a new generation structural design code to an existing code have been completed.

According to *Structural Reliability: Analysis and Prediction*, Melchers (1987), the general methodology for code calibration based on specific reliability theories, using second-moment reliability concepts, is discussed by Allen (1975), Baker (1976), CIRIA (1977), Hawrenenk and Rackwitz (1976), Guiffre and Pinto (1976), Skov (1976), Ravindra and Galambos (1978), Ellingwood *et al.* (1980), Lind (1976), and Ravindra *et al.* (1969). The key steps in the process, following the discussion in Melchers (1987), are as follows. First, the scope of the design situation must be identified (e.g., material, loads, structural type) and narrowed to fit the specific situation. Next, a design space reflecting all key variables (nominal yield stresses, range of applied loads, continuity conditions, etc.) is chosen and divided into discrete zones. These zones are used to develop typical designs using existing codes. Next, performance functions for the failure modes, expressed in terms of the basic variables, are defined. The statistical properties (distributions, means, variances, and averagepoint-in-time values) of the basic variables are used for the determination of the  $\beta$  indices using a specified method for reliability analysis (e.g., moment methods).

Next, each of the designs obtained above, together with the performance functions and the statistical data derived above, are used to determine  $\beta$  for each zone. Repeated analyses will yield the variation of  $\beta$ . From these data, a weighted  $\beta$  is

obtained and used as a target reliability level  $\beta_t$ . Melchers notes that frequently the information is insufficient for this determination and one must make a "semi-intuitive" judgment in selecting  $\beta_t$  values. For example, recognizing a different  $\beta$  value is used for dead, live, and snow load combinations as compared to, dead, live, and wind load combinations or dead, live, and earthquake load combinations. Divergent  $\beta_t$  values should be corrected by means of the partial factor(s) on material strength or resistance (e.g., through the strength reduction factor).

While the specific reliabilities will be a function of the strength criteria needed for specific materials and load combinations within designated structures, it is useful to have an indication of the range of possible target reliability levels. Ellingwood *et al.* (1980) present ranges for reliability levels for metal structures, reinforced and prestressed concrete structures, heavy timber structures, and masonry structures, as well as discussions of issues that should be considered when making the calibrations. Table 9.3 provides typical values for target reliability levels. This table was developed based on values provided by Ellingwood *et al.* (1980). The target reliability levels shown in Table 9.4 were also used by Ellingwood and Galambos (1982) to demonstrate the development of partial safety factors.

Reed and Brown (1992) provide a summary of the target reliability levels used in the AISC LRFD specifications. In addition to the values provided in Tables 9.3 and 9.4, values for high strength bolts in tension and shear were given as 5.0 to 5.1, and 5.9 to 6.0, respectively. Also, a value for fillet welds of 4.4 is given. Detailed information about these values are provided by Galambos (1989).

Moses and Verma (1987) suggested target reliability levels in calibrating bridge codes (i.e. AASHTO Specifications). Assuming that bridge spans of less than 100 ft are most common, a  $\beta_t$  of 2.5 to 2.7 is suggested for redundant bridges, and a  $\beta_t$  of 3.5 for non-redundant bridges.

Wirsching (1984) estimated the safety index implied by the API specifications API RP2A (1989) for fixed offshore structures in fatigue of tubular welded joints to be 2.5. He reported that this value is on the low end, because of the reference wave values.

Madsen *et al.* (1986) discuss target reliability levels that were used by the National Building Code of Canada (1977) for hot-rolled steel structures. The target reliability values were selected as follows:  $\beta_t = 4.00$  for yielding in tension and flexure,  $\beta_t = 4.75$  for compression and buckling failure, and  $\beta_t = 4.25$  for shear failures. These values are larger than the values in Tables 9.3 and 9.4 because they reflect different environmental loading conditions and possibly different design life. Also, the Canadian Standard Association presented the following target failure probabilities for developing design criteria for offshore installation in Canadian waters (Mansour *et al.* 1994):  $10^{-5}$  per year for failures that result in great loss of life or a high potential for environmental damage; and  $10^{-3}$  per year for failures that result in small risk to life or a low potential for environmental damage.

Madsen *et al.* (1986) also discuss target reliability levels that were used by the Nordic Building Code Committee (1978). The target reliability values were selected depending on the failure consequences of a building in the following ranges:  $\beta_t = 3.1$

for less serious failure consequences,  $\beta_t = 5.2$  for very serious failure consequences, and  $\beta_t = 4.265$  for common cases.

For ship structures, A. S. Veritas (Lotsberg, 1991), a subsidiary of Det Norske Veritas, recommended target safety indices that depend on failure consequences and failure types. Table 9.5 provides a summary of these values. These values are annual probabilities. Therefore, they need to be multiplied by a design life to obtain the needed target values.

### 9.2.3 Geotechnical Perspective

The review provided in section 9.2.2 suggests that typical target reliability for members and structures relevant to bridge construction varies between 1.75 to 3.0 with a target reliability of 2.5 to 2.7 for relevant bridges.

Barker et al. (1991) have provided the following regarding target reliability index for driven piles (p.A-51): *"Meyerhof (1970) showed that the probability of failure of foundations should be between  $10^{-3}$  and  $10^{-4}$ , which corresponds to values of  $\beta$  between 3 and 3.6. The reliability index of offshore piles reported by Wu, et al. (1989) is between 2 and 3. They calculated that the reliability index for pile systems is somewhat higher and is approximately 4.0, corresponding to a lifetime probability of failure of 0.00005. Tang et al. (1990) reported that offshore piles have a reliability index ranging from 1.4 to 3.0.*

*Reliability indices for driven piles are summarized in Table 5.4 (see Table 9.6). Values of  $\beta$  between 1.5 and 2.8 are generally obtained for the lognormal procedure. Thus a target value of  $\beta$  between 2.5 to 3 may be appropriate. However,*

*piles are usually used in groups. Failure of one pile does not necessarily imply that the pile group will fail. Because of this redundancy in pile groups, it is felt that the target reliability index for driven piles can be reduced from 2.5 to 3.0 to a value between 2.0 and 2.5."*

Zhang et al. (2001) presented a method to evaluate the reliability of axially loaded pile groups designed using the traditional concept of group efficiency, along the line of load and resistance factor design (LRFD). Group effects and system effects were identified to be the major causes that led to a significantly greater observed reliability of pile foundations than calculated reliability of single piles. In group effect Zhang et al. referred to the combined action of any number of piles vs. a single pile. A system effect is the contribution of the superstructure to the load distribution and resistance as related to the stiffness of that structure. The calculated probability of failure of pile groups was found to be one to four orders of magnitude smaller than that of single piles, depending on significance of system effects. Based on their study Zhang et al. (2001) state that the target reliability index,  $\beta_T$ , for achieving a specified reliability level should be different for an isolated single pile, an isolated pile group, and a pile system. They give the following recommendations based on their research:

- (i) A  $\beta_T$  value as low as 1.7 may be adopted for design of pile groups if a system bias factor,  $\lambda_x$ , of 2.0 is justifiable.
- (ii) A  $\beta_T$  value in the range of 2.0 to 2.5 may be sufficient for pile groups with a  $\lambda_x$  factor not smaller than 1.5.

- (iii) A  $\beta_T$  value not smaller than 3.0 is required for pile groups without any system effect.

In presenting the resistance factors for driven piles, Barker et al. (1991) related to a target reliability between 2.0 to 2.5 and dead to live load ratio of 3.69. The following results were obtained based on the questionnaire distributed by the research team for this project: The estimated risk or failure probability of the group foundation design based on the safety factor used: 27% were less than 0.1%, 4% were between 0.1 to 1%, one percent (1%) of the responses were between 1% to 10%, and 67% were unknown. The assessment for the acceptable maximum failure probability ranged from about zero (0) to 1%. 14% of respondents had experienced pile failures.

Based on the presented review and data it seems reasonable to establish the target reliability for the dynamic analyses between 2.0 to 2.5 for pile groups, possibly in the middle, and as high as 3.0 for single piles. The evaluation of the resistance factors was carried out by using reliability indices of 2.0, 2.5, and 3.0. This provided a reasonable range before final target reliability values were set.

### **9.3 DEAD TO LIVE LOAD RATIO**

Figure 9.2 presents examples of the resistance factors calculated based on the FORM procedure for the general CAPWAP and Energy Approach cases. Before exact target reliability was established, the resistance factors were evaluated for target reliability values of 2, 2.5, and 3.0 associated with probability of failure values of 2.3%, 0.62%, and 0.14%, respectively. The factors were evaluated using load factors of 1.25 and 1.75 for Dead Load (DL) and Live Load (LL), respectively, and for DL to

LL ratios ranging from 1 to 4. The obtained results presented in Figure 9.2 suggest very little sensitivity of the resistance factors to the DL to LL ratio. A parametric study was carried out for a generic coefficient of variation of 0.40 and dead to live load ratios ranging from 1 to 10. The large dead to live ratios represent a wide possibility of bridge construction, typically associated with very long bridge spans. No significant influence of the dead to live load ratio on the calculated resistance factors was found.

## **9.4 THE RESISTANCE FACTORS**

### **9.4.1 Initial Evaluation**

Figure 9.3 presents a flow chart that summarizes the parameters of the normal distribution (number of cases, mean and standard deviation) for all the dynamic analysis methods and their sub-categories established in Chapter 6. The statistical analysis presented in Figure 9.3 allows for the identification of the critical cases that require calibration and development into resistance factors. For example, the CAPWAP cases include (i) all data, (ii) EOD, (iii) BOR, and (iv) the worst combination of soil inertia (Blow count < 16 BP10cm and  $A_R < 350$ ).

Table 9.7 presents a summary of the major categories of the dynamic methods that are identified from Figure 9.3 as the cases that require calibration for a resistance factor. The Case method was not included for the reasons discussed in section 6.3.4 and as it refers to a limited database (Florida), utilizing the RMX version of the method with variable Case damping coefficients,  $J_c$ .

Histogram and frequency distributions were prepared for the identified critical cases, presented in Table 9.7. This visual information enables to examine the match between the actual data and the probability distribution functions. Figure 9.4 through 9.19 present the data along with the calculated normal and lognormal distributions.

#### **9.4.2 Intermediate Conclusions**

This section presents the conclusions derived from the observed statistical performance. It is placed here for clarity and completeness. The data presented in Chapter 5 and summarized in Table 9.7 and Figures 9.3 through 9.19 lead to several preliminary conclusions:

- (i) The signal matching procedure generally under-predicts the pile's capacity. The method performs very well for the BOR (last restrike) cases.
- (ii) The simple Energy Approach provides excellent prediction for evaluating the pile's capacity during driving (EOD).
- (iii) The above suggests that construction delays due to restrike and costly signal matching analyses need to be examined in light of capacity time dependency and economical factors.
- (iv) The FHWA modified gates equation provides very reasonable predictions for evaluating the pile's capacity when dynamic methods are not carried out.
- (v) A reasonably good match exists for most cases between the calculated lognormal distribution and the observed data. For this reason lognormal functions were used in calibration procedures of the resistance factors.



#### **9.4.3 Resistance Factors for a Range of Reliability Indices**

Table 9.7 summarizes the resistance factors that were calculated for the critical investigated cases of the dynamic analyses. The resistance factors were calculated for reliability indices of 2.0, 2.5 and 3.0 and load factors of 1.25 and 1.75 for Dead Load (DL) and Live Load (LL), respectively, and for ratios of  $DL/LL = 1$  and  $DL/LL = 4$ . The range of the reliability indices ( $\beta = 2.0$  to  $3.0$ ) covers the expected range of probability of failure ( $p_f = 2.28\%$  to  $p_f = 0.14\%$ ) adequate for the dynamic methods. The obtained resistance factors presented in Table 9.7 allow (i) to assess the range of the obtained values and its sensitivity to the reliability index and (ii) reevaluate the 'critical' cases such that subcategories with similar resistance factors can be combined; e.g., Energy Approach EOD case and Energy Approach EOD for  $A_R < 350$  and Blow Count  $< 16$  BP10cm.

#### **9.4.4 Recommended Resistance Factors**

Based on the resistance factors presented in Table 9.7 the critical dynamic cases were reevaluated resulting in smaller number of categories, encompassing others, e.g., five versus eight for the methods of the dynamic measurements. The selected methods, their important categories and the recommended factors are presented in Table 9.8. Following review of existing common practice in probability of failure, review of the obtained parameters (to be presented in the following section) and discussion with the NCHRP 24-17 project panel, the following reliability indices and probability of failure are recommended:

- (i) For redundant piles, defined as five or more piles per pile cap, the recommended probability of failure is  $p_f = 1\%$ , corresponding to a reliability index of  $\beta = 2.33$ .
- (ii) For non-redundant piles, defined as four or less piles per pile cap, the recommended probability of failure is  $p_f = 0.1\%$ , corresponding to a reliability index of  $\beta = 3.00$ .

The obtained resistance factors for the methods that utilize dynamic measurements, range from 0.41 to 0.65 for the redundant pile cases and 0.23 to 0.51 for the non-redundant pile cases with typical decrease of about 25% in the resistance factor when moving from one category to the other. This practically means that the use of four piles with non-redundant resistance factors will be approximately equivalent to the use of five piles with redundant resistance factors.

The magnitude of the resistance factors by itself is not a measure that indicates the performance or economical value of the method. A comparison requires therefore an "efficiency" measure, discussed in the following section.

## **9.5 EVALUATION OF THE DYNAMIC METHODS EFFICIENCY**

In the same way that a factor of safety alone is not a representative of the efficiency of a method, the resistance factors alone do not provide a measure for the evaluation of the efficiency of the dynamic methods. Such efficiency can be evaluated through the bias factor (mean of the ratio of the measured over predicted), its coefficient of variation (see Table 9.7) or the ratio of the resistance factor to the bias factor, i.e.  $\phi/\text{mean } K_{sx}$ , as proposed by McVay et al. (2000). This ratio is provided for

the final selected cases in Table 9.8. The efficiency values in Table 9.8 suggest that overall the higher efficiency is obtained by the signal matching analyses for the last restrike, followed by the Energy Approach at the end of driving (0.561 vs. 0.489 and 0.440 vs. 0.369 for redundant and non-redundant cases, respectively).

## **9.6 EVALUATION OF THE CHOSEN TARGET RELIABILITY AND RECOMMENDED RESISTANCE FACTORS**

### **9.6.1 Resistance Factors Based on the Existing AASHTO Specifications**

Utilizing the statistical parameters of the critical cases presented in Table 9.8, the same data and reliability indices were used to calculate the resistance factors based on the existing AASHTO methodology as presented by Barker et al. (1991) and reviewed in section 2.2.4b of this manuscript. Table 9.9 follows the format of Table 9.8 with the resistance factors from FORM compared with those of FOSM calculated using the existing AASHTO methodology as proposed by Barker et al. (1991).

The resistance factors obtained using FOSM (the existing AASHTO methodology) are approximately 10% lower than those obtained using FORM. In principle this shows that the methodology for calculating resistance factors using the existing AASHTO methodology is slightly more conservative than the method used to calculate the proposed resistance factors for the 2001 AASHTO code, assuming the same statistical data available for both.

### **9.6.2 Evaluation of the WSD Factors of Safety (AASHTO, 1997) in Light of the Obtained Results**

The traditional WSD factors of safety presented in Table 2.1 can now be evaluated in light of the available data. For example, the coefficient of variation for

the WEAP analysis at the EOD is 0.724, which practically means that the method is unsuitable for the purpose of capacity prediction. The reduction in the factor of safety from 3.50 to 2.75 in Table 2.1 when adding WEAP analysis to static calculations is therefore unfounded. Moreover, considering the mean bias of the WEAP at EOD, ( $K_{sx} = 1.656$ ), the F.S. = 2.75 actually means an average factor of safety of 4.55 ( $2.55 \times 1.656$ ), which is by no means of any "savings", compared to the static methods predictions assuming those to be accurate. The use of unspecified CAPWAP (general case) again does not justify the reduction of the factor of safety to 2.25 even though the average prediction is conservative (mean over prediction ratio of 1.368) and hence for the mean case with a F.S. = 2.25, the actual factor of safety is 3.1 ( $1.368 \times 2.25$ ). In comparison, the use of F.S. = 2.25 with a specified CAPWAP at the BOR is reasonable and is associated with an acceptable probability of failure for single pile application (approximately 1.85%, see Figure 9.7).

The conclusions of the above are:

- (i) The common wisdom accepting the recommended traditional factors of safety as accumulation of a long term knowledge must be evaluated in light of actual performance, hence the use of databases is as important for WSD as for LRFD, and
- (ii) The specific factors of safety recommended by AASHTO (1997) though seem to be logical and progressive (decrease of F.S. with increase of knowledge), are not so anymore when considering the bias of each method.

### **9.6.3 Evaluation of the Chosen Target Reliability**

#### ***a) Overview***

The chosen target reliability and probability of failure presented in section 9.4.4 need to be examined. The most desired method to determine the target reliability is by a calibration of accepted practice as described in Section 9.2.2. This is not possible in the case of the dynamic methods, due to the following reasons:

1. A large-scale analysis of the methods to produce calibration through design is beyond the scope of this work.
2. No direct relationship exist between the resistance factors calculated in this study and back calculated Factors of Safety.
3. The existing LRFD AASHTO specifications suggest in the case of the dynamic methods to multiply the resistance factor based on the static analysis by an additional factor ( $\lambda$ ). There is not therefore a relationship between the current AASHTO resistance factor used for the dynamic methods and the one developed in the present study.
4. WSD Factors of Safety as used by AASHTO until 1997 (see Table 2.1 in Chapter 2) are questionable in light of the statistics presented in Table 9.7 (see section 9.6.2).

As a result of the above, two approaches have been adopted for evaluating the adequacy of the proposed target reliability in addition to the previously discussed material and comparisons. These approaches are described in the following sections.

**(b) Approximate Factors of Safety**

Barker et al. (1991) suggested calibration by fitting the resistance factors of the LRFD with WSD factors of safety, utilizing the following equation:

$$\phi \geq \frac{\gamma_D \frac{Q_D}{Q_L} + \gamma_L}{FS \left( \frac{Q_D}{Q_L} + 1 \right)} \quad (9.14)$$

This equation is not compatible with the FORM calibration procedure presented in section 9.1 but was used in order to obtain indicative factors of safety. The close agreement between FOSM and FORM presented in section 9.6.1 further supports this approach. Table 9.10 was developed using the load factors  $\gamma_L=1.75$   $\gamma_D=1.25$ , and the resistance factors corresponding to  $\beta=2.33$  and  $\beta=3.0$ , presented in Table 9.8. In reviewing these factors of safety one should consider the bias factors as well. For example, the average F.S. for CAPWAP under the general case for non-redundant piles is 3.32, however the bias of the method under the general case is 1.368 (see Table 9.7) hence the “actual mean” factor of safety is 4.54 ( $3.32 \times 1.37$ ). Similarly the FS for the Energy Approach at EOD is 3.57, the bias is 1.084 hence the “actual mean” factor of safety is 3.87. The columns describing the actual mean F.S. in Table 9.10 describe therefore the “true” average F.S. considering the bias of the method.

**(c) The Actual Probability of Failure**

In this procedure the database was used directly (not through the calculated distribution function) to calculate the probability of failure when applying a certain

F.S. For example, if F.S.=2.0 would have been applied to the results of the Energy Approach analyses, in 9.16% of the cases, the obtained capacity would be still higher than the actual ultimate capacity. The results of this analysis are shown in Table 9.11, for factors of safety ranging from 2.00 to 4.00 in intervals of 0.25. Five factors are noticed when reviewing the data presented in Table 9.11:

1. The percent values are actual numbers from counting the cases for each category under certain F.S., with the total number of cases for each category provide in the table.
2. The prediction is compared to static analysis utilizing Davisson's failure criterion, which by itself, is not absolute. The meaning of "failure" in this regard is usually associated with larger settlement but not necessarily mean catastrophic failure or even structural damage.
3. When reviewing the obtained factors of safety one needs to consider the application of a factor of safety for the loads (or load factors) where as in the described analysis, the load is the actual failure load, i.e., the applied F.S. or  $\gamma$  is one. As a result the probability of failure presented in Table 9.11 is different than that discussed earlier, and in fact higher than the one actually expected in the field.
4. The factors of safety should again be judged in relation to the bias of the method as discussed earlier in relation to Table 9.10, e.g., a F.S. = 2.0 for the CAPWAP general case represents average actual F.S. = 2.736 or a F.S.

= 1.788 for the general case of the Energy Approach (bias of 1.368 and 0.894 for CAPWAP and Energy Approach, respectively).

## **9.7 THE CHOSEN TARGET RELIABILITY AND RESISTANCE FACTORS**

Based on the presented material in this chapter the target reliability of 2.33 for pile groups and 3.0 for single piles seem to be adequate and compatible with existing and past work. These values are used therefore to calculate the resistance factors for the critical dynamic analysis methods and the obtained results are presented in Table 9.8. The resistance factors presented in Table 9.8 are therefore recommended to be used in the new AASHTO specifications and the ratio of evaluating the method's efficiency (comparison) is recommended to be used in conjunction with the resistance factors or as part of the commentary.



**Table 9.1.** Approximate Relationship Between Probability of Failure and Reliability Index for Lognormal Distribution, based on Rosenbleuth and Estava (1972), see Withiam et al. (1998).

Reliability Index, $\beta$	Probability of Failure, $p_f$	Probability of Failure, $p_f$	Reliability Index, $\beta$
2.0	$8.47 \times 10^{-2}$	$1 \times 10^{-1}$	1.96
2.5	$9.86 \times 10^{-2}$	$1 \times 10^{-2}$	2.50
3.0	$1.15 \times 10^{-3}$	$1 \times 10^{-3}$	3.03
3.5	$1.34 \times 10^{-4}$	$1 \times 10^{-4}$	3.57
4.0	$1.56 \times 10^{-5}$	$1 \times 10^{-5}$	4.10
4.5	$1.82 \times 10^{-6}$	$1 \times 10^{-6}$	4.64
5.0	$2.12 \times 10^{-7}$	$1 \times 10^{-7}$	5.17

**Table 9.2.** Comparison Between Rosenbleuth and Estava's Approximation and Series Expansion (Labeled "exact").

$\beta$	Rosenbleuth and Estavas' $p_f$	"exact" $p_f$	Percent Error
2.0	8.4689E-2	2.2750E-2	272.3%
2.5	9.8649E-3	6.2097E-3	58.9%
3.0	1.1491E-3	1.3500E-3	-14.9%
3.5	1.3385E-4	2.3267E-4	-42.5%
4.0	1.5592E-5	3.1686E-5	-50.8%
4.5	1.8162E-6	3.4008E-6	-46.6%
5.0	2.1156E-7	2.8711E-7	-26.3%
5.5	2.4643E-8	1.9036E-8	29.5%
6.0	2.8705E-9	9.9012E-10	189.9%

**Table 9.3.** Target Reliability Levels.

Structural Type	Target Reliability Level ( $\beta_t$ )
Metal structures for buildings (dead, live, and snow loads)	3
Metal structures for buildings (dead, live, and wind loads)	2.5
Metal structures for buildings (dead, live, snow, and earthquake loads)	1.75
Metal connections for buildings (dead, live, and snow loads)	4 to 4.5
Reinforced concrete for buildings (dead, live, and snow loads)	
- ductile failure	3
- brittle failure	3.5

The  $\beta_t$  values are for structural members designed for 50 years of service.

**Table 9.4.** Target Reliability Levels used by Ellingwood and Galambos (1982).

Member, Limit State	Target Reliability Level ( $\beta_t$ )
Structural Steel	
Tension member, yield	3.0
Beams in flexure	2.5
Beams in shear	3.0
Column, intermediate slenderness	3.5
Reinforced Concrete	
Beam in flexure	3.0
Beam in shear	3.0
Tied column, compressive failure	3.5
Masonry, unreinforced	
Wall in compression, uninspected	5.0
Wall in compression, inspected	7.5

The  $\beta_t$  values are for structural members designed for 50 years of service.

**Table 9.5.** Target Reliability Values Recommended  
by A.S. Veritas (Lotsberg, 1991).

Failure Consequences	Failure Type		
	Ductile Failure with reserve capacity	Ductile failure without reserve capacity	Brittle fracture with instability
<u>Not serious:</u> Small possibility of human injury, pollution, or economic consequences	3.09	3.71	4.26
<u>Serious:</u> Possibility of human injury or fatality, pollution, or significant economic consequences	3.71	4.26	4.75
<u>Very serious:</u> Possibility of human injury or fatality, significant pollution, or very large economic consequences	4.26	4.75	5.20

**Table 9.6.** Reliability Indices for Driven Piles (Barker et al., 1991).

Dead to Live Load Ratio	Reliability Index, $\beta$	
	Lognormal	Advanced
1.00	1.6 – 2.8	1.6 – 3.0
3.69	1.7 – 3.1	1.8 – 3.3

**Table 9.7. Summary of the Performance of the Dynamic Methods.**

Method		Case	No. of Cases	Mean $K_{SX}$	Standard Deviation	COV	Preliminary Resistance Factors for given Reliability Index, $\beta$		
							2.0	2.5	3.0
Dynamic Measurements	CAPWAP	General	377	1.368	0.620	0.453	0.68	0.54	0.43
		EOD	125	1.626	0.797	0.490	0.75	0.59	0.46
		EOD - AR < 350 & Bl. Ct. < 16 BP10cm	37	2.589	2.385	0.921	0.52	0.35	0.23
		BOR	162	1.158	0.393	0.339	0.73	0.61	0.51
	Energy Approach	General	371	0.894	0.367	0.411	0.48	0.39	0.32
		EOD	128	1.084	0.431	0.398	0.60	0.49	0.40
		EOD - AR < 350 & Bl. Ct. < 16 BP10cm	39	1.431	0.727	0.508	0.63	0.49	0.39
		BOR	153	0.785	0.290	0.369	0.46	0.38	0.32
Dynamic Equations	ENR	General w/o FS = 6	384	0.267	0.243	0.910	0.04	0.03	0.02
	ENR	General w/ FS = 6	384	1.602	1.458	0.910	0.33	0.22	0.15
	Gates	General	384	1.787	0.848	0.475	0.85	0.67	0.53
	FHWA modified Gates	General	384	0.940	0.472	0.502	0.42	0.33	0.26
		EOD	135	1.073	0.573	0.534	0.45	0.35	0.27
		EOD Bl. Ct. < 16BP10cm	62	1.306	0.643	0.492	0.60	0.47	0.37
	WEAP	EOD	99	1.656	1.199	0.724	0.48	0.34	0.25
WEAP		BOR	99	0.939	0.399	0.425	0.49	0.40	0.32

See Notes on Table 9.8

**Table 9.8.** Recommended Resistance Factors for the Critical Dynamic Cases.

Method		Case	Resistance factor, $\phi$		$\phi$ /Mean $K_{SX}$	
			Redundant $\beta = 2.33$ $p_f = 1.0\%$	Non-Redundant $\beta = 3.0$ $p_f = 0.1\%$	Redundant $\beta = 2.33$ $p_f = 1.0\%$	Non-Redundant $\beta = 3.0$ $p_f = 0.1\%$
Dynamic Measurements	Signal Matching	General	0.59	0.43	0.431	0.314
		EOD, AR<350, Bl. Ct.<16BP10cm	0.41	0.23	0.158	0.089
		BOR	0.65	0.51	0.561	0.440
	Energy Approach	General	0.42	0.32	0.470	0.358
		EOD	0.53	0.40	0.489	0.369
Dynamic Equations	ENR	General w/ FS = 6	0.26	0.15	0.162	0.094
	Gates	General	0.73	0.53	0.409	0.297
	FHWA modified	General	0.36	0.26	0.383	0.277
WEAP		EOD	0.39	0.25	0.236	0.151

Notes:  $\beta$  = Reliability Index       $p_f$  = Probability of Failure      COV = Coefficient of Variation  
EOD = End of Driving      BOR = Beginning of Restrike      ENR = Engineering News Record Equation  
AR = Area Ratio      Bl. Ct. = Blow Count  
BP10cm = Blows per 10cm       $K_{SX}$  = Ratio of the Static Load Test Results to the predicted capacity  
Redundant = Five piles or more under one pile cap.  
Non-Redundant = Less than five piles under one pile cap.

**Table 9.9.** Resistance Factors for the Critical Dynamic Cases Based on FOSM using Barker et al., (1991) versus those developed through FORM (see Table 9.8).

Method		Case	Resistance factor, $\phi$ $\beta = 2.33, p_f = 1.0\%$		Resistance factor, $\phi$ $\beta = 3.00, p_f = 0.1\%$	
			FORM	FOSM	FORM	FOSM
Dynamic Measurements	Signal Matching	General	0.59	0.54	0.43	0.39
		EOD, AR<350, Bl. Ct.<16BP10cm	0.41	0.38	0.23	0.22
		BOR	0.65	0.56	0.51	0.45
	Energy Approach	General	0.42	0.39	0.32	0.29
		EOD	0.53	0.48	0.40	0.36
Dynamic Equations	ENR	General w/ FS = 6	0.26	0.24	0.15	0.14
	Gates	General	0.73	0.67	0.53	0.48
	FHWA modified	General	0.36	0.33	0.26	0.24
WEAP		EOD	0.39	0.37	0.25	0.23

Notes:  $\beta$  = Reliability Index  
EOD = End of Driving  
AR = Area Ratio  
BP10cm = Blows per 10cm  
FORM = First Order Reliability Method  
 $p_f$  = Probability of Failure  
BOR = Beginning of Restrike  
Bl. Ct. = Blow Count  
ENR = Engineering News Record Equation  
FOSM = First Order Second Moment

**Table 9.10.** Calculated Factors of Safety Based on the Resistance Factors in Table 9.8 and the Procedure Outlined by Barker et al. (1991).

Dynamic Method for Capacity Evaluation	Resistance Factor, $\phi$		Factor of Safety (FS); $\gamma_L = 1.75, \gamma_D = 1.25$							
			Redundant - $\beta = 2.33$				Non-Redundant - $\beta = 3.0$			
	$\beta = 2.33$	$\beta = 3.00$	$\frac{DL}{LL} = 1$	$\frac{DL}{LL} = 4$	Mean FS	"Actual mean" FS	$\frac{DL}{LL} = 1$	$\frac{DL}{LL} = 4$	Mean FS	"Actual mean" FS
<b>CAPWAP - General</b>	0.59	0.43	2.54	2.29	2.42	3.31	3.49	3.14	3.32	4.54
<b>CAPWAP - EOD, AR&lt;350, Bl. Ct.&lt;16 BP10cm</b>	0.41	0.23	3.66	3.29	3.48	9.01	6.52	5.87	6.20	16.05
<b>CAPWAP - BOR</b>	0.65	0.51	2.31	2.08	2.20	2.55	2.94	2.65	2.80	3.24
<b>Energy Approach - General</b>	0.42	0.32	3.57	3.21	3.39	3.03	4.69	4.22	4.46	3.99
<b>Energy Approach - EOD</b>	0.53	0.40	2.88	2.60	2.74	2.97	3.75	3.38	3.57	3.87
<b>ENR – General w/ FS = 6</b>	0.26	0.15	5.77	5.19	5.48	8.78	10.00	9.00	9.50	15.21
<b>Gates - General</b>	0.73	0.53	2.05	1.85	1.95	3.48	2.83	2.55	2.69	4.81
<b>FHWA - General</b>	0.36	0.26	4.17	3.75	3.96	3.72	5.77	5.19	5.48	5.15
<b>WEAP - EOD</b>	0.39	0.25	3.85	3.46	3.66	6.06	6.00	5.40	5.70	9.44

Notes:  $\beta$  = Reliability Index      DL/LL = Dead Load to Live Load Ratio      AR = Area Ratio  
 "Actual mean FS" = Mean FS  $\times$  Mean  $K_{SX}$       Bl. Ct. = Blow Count

**Table 9.11.** The Probability of Failures Associated with the Critical Dynamic Methods and Their Important Categories from the PD/LT2000 Database.

Factor of Safety	Probability of Failure - Risk							
	CAPWAP			Energy Approach		Gates	FHWA	WEAP
	General	BOR	EOD - AR<350 Bl. Ct. <16 BP10cm	General	EOD	General	General	EOD
<b>2.00</b>	0.27%	0%	2.70%	9.16%	1.56%	0.26%	10.42%	0%
<b>2.25</b>	0%	0%	0%	3.23%	0%	0.26%	5.47%	0%
<b>2.50</b>	0%	0%	0%	0.81%	0%	0.26%	3.13%	0%
<b>2.75</b>	0%	0%	0%	0.27%	0%	0%	1.56%	0%
<b>3.00</b>	0%	0%	0%	0.27%	0%	0%	0.78%	0%
<b>3.25</b>	0%	0%	0%	0%	0%	0%	0.52%	0%
<b>3.50</b>	0%	0%	0%	0%	0%	0%	0.52%	0%
<b>3.75</b>	0%	0%	0%	0%	0%	0%	0.26%	0%
<b>4.00</b>	0%	0%	0%	0%	0%	0%	0.26%	0%
<b>No. of Cases</b>	377	162	37	371	128	384	384	99

Notes: AR = Area Ratio  
Bl. Ct. = Blow Count  
EOD = End of Driving  
BOR = Beginning of Restrike



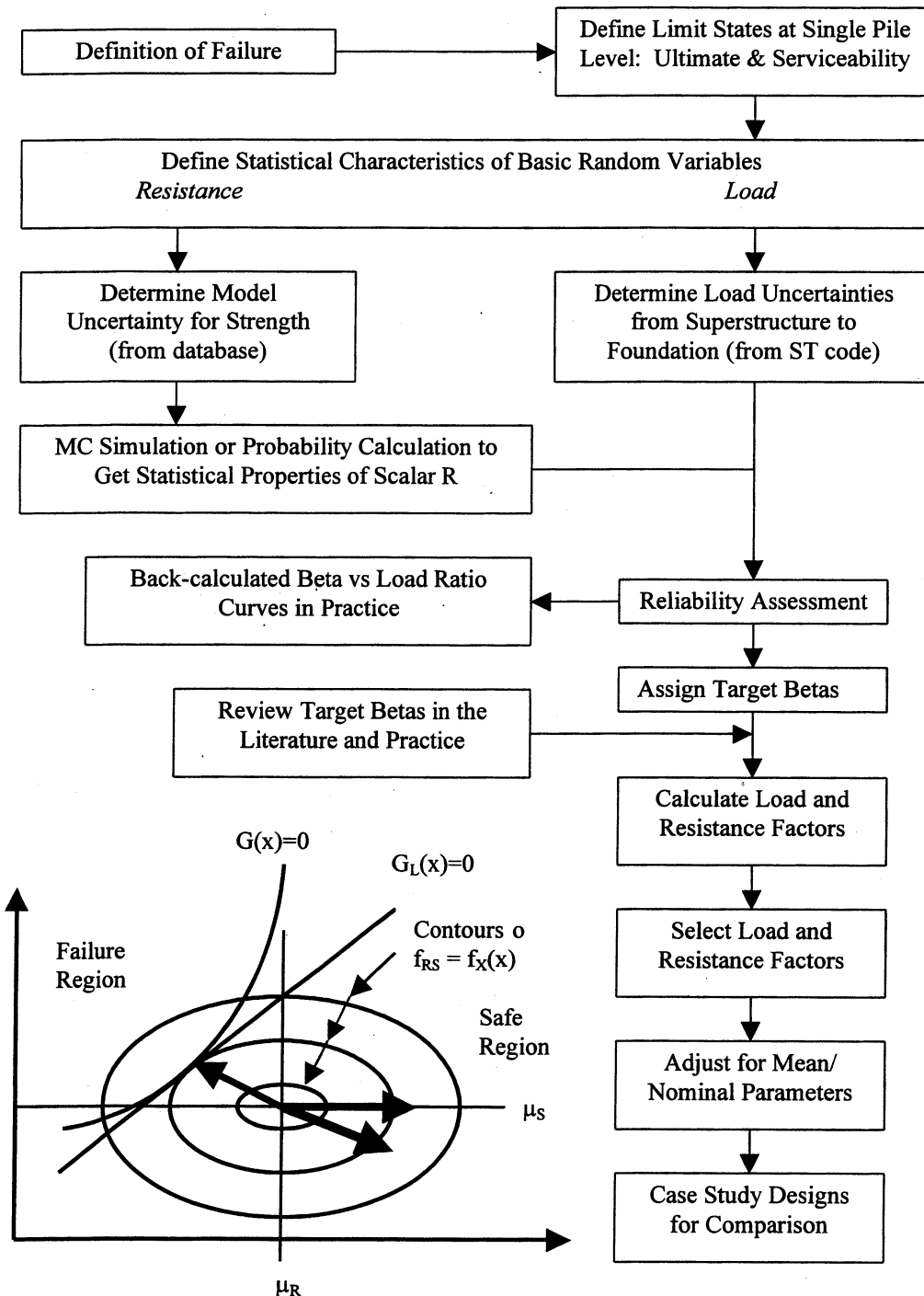


**Figure 9.1.** Resistance Factor Analysis Flow Chart (after Ayyub & Assakkaf, 1999, Ayyub et al., 2000).

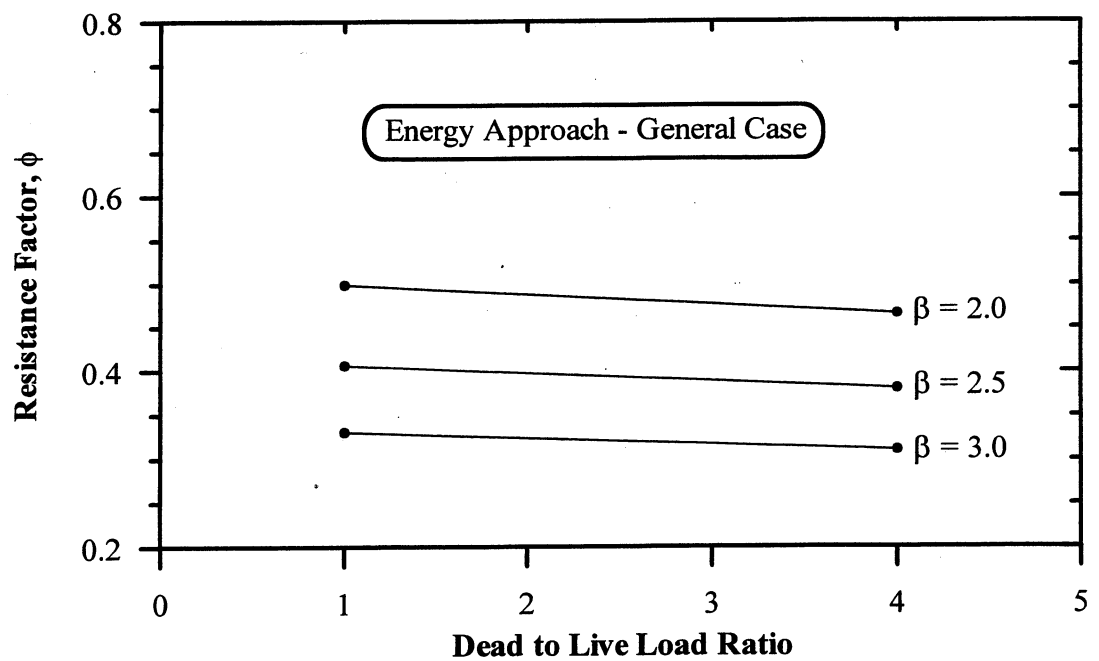
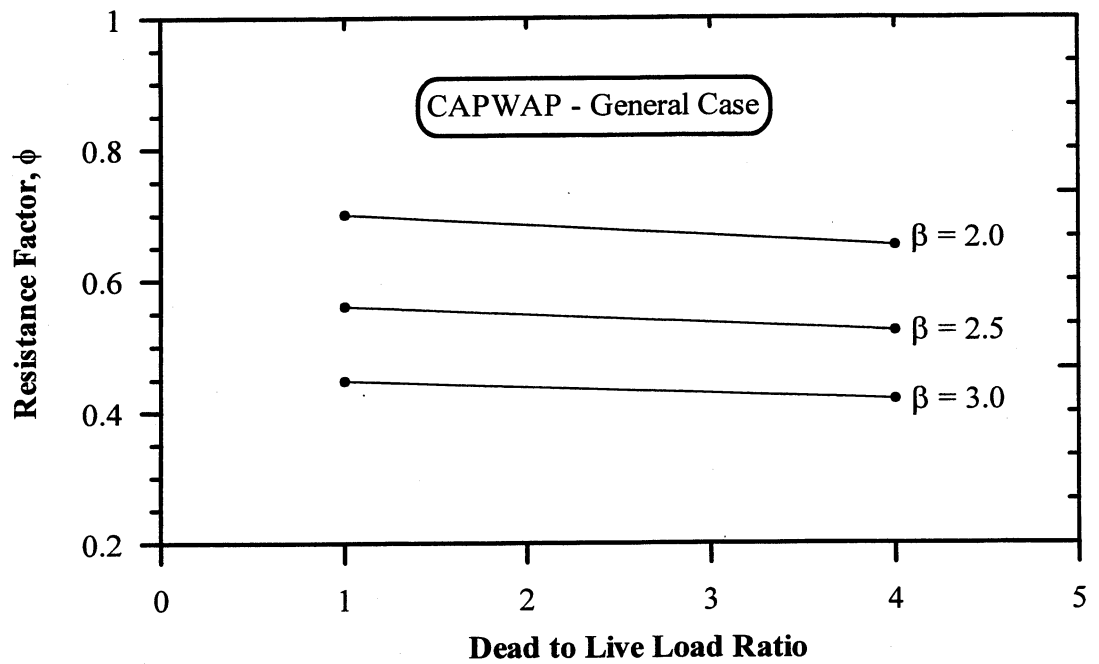


**Figure 9.2.** Calculated Resistance Factors for the CAPWAP and Energy Approach General Cases showing the Influence of the Dead to Live Load Ratio.

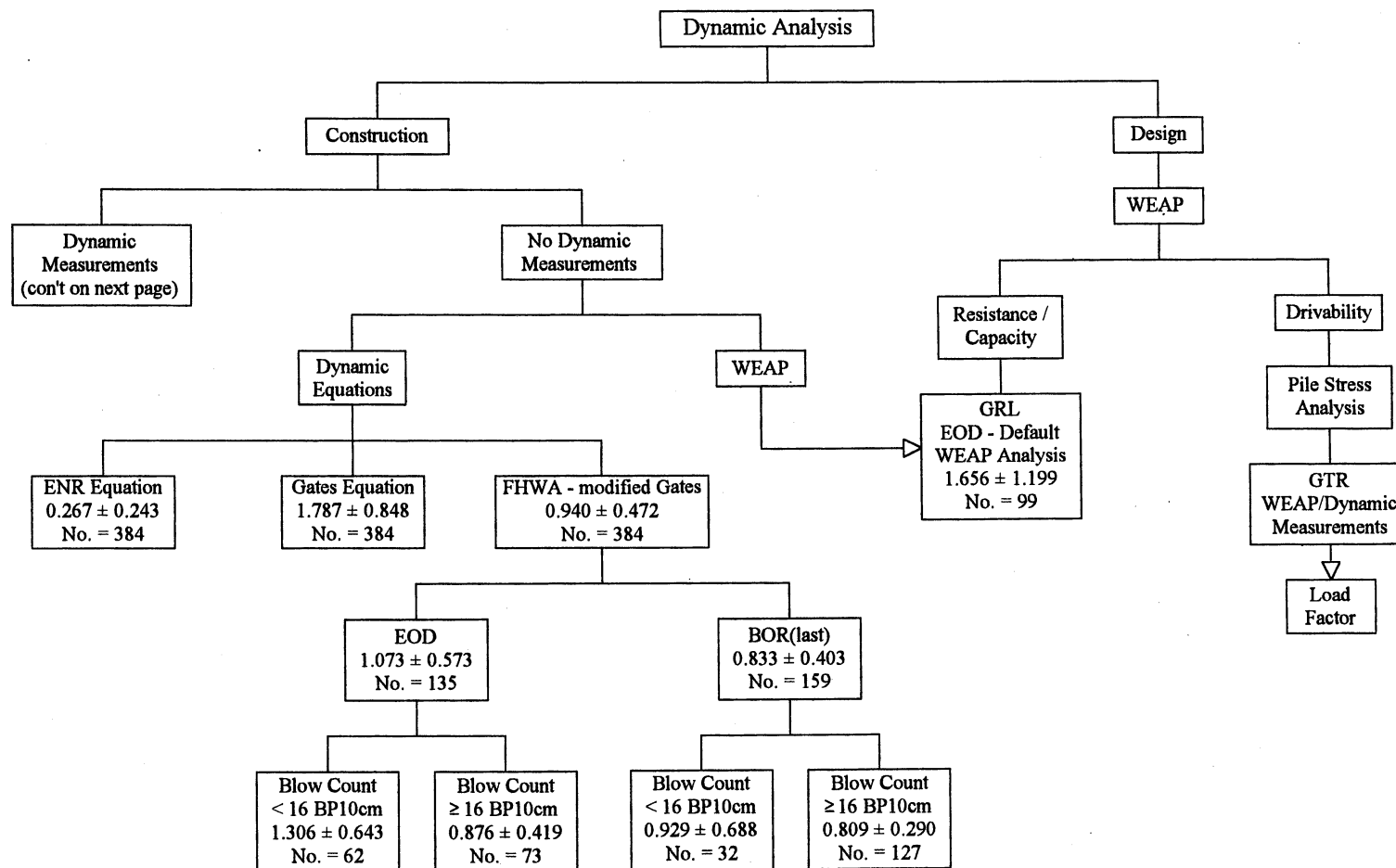


**Figure 9.3.** Flow Chart Presenting the Sub-Grouping of the Dynamic Analyses According to the Controlling Parameters and the Resulting Statistical Parameters for a Normal Distribution Function.

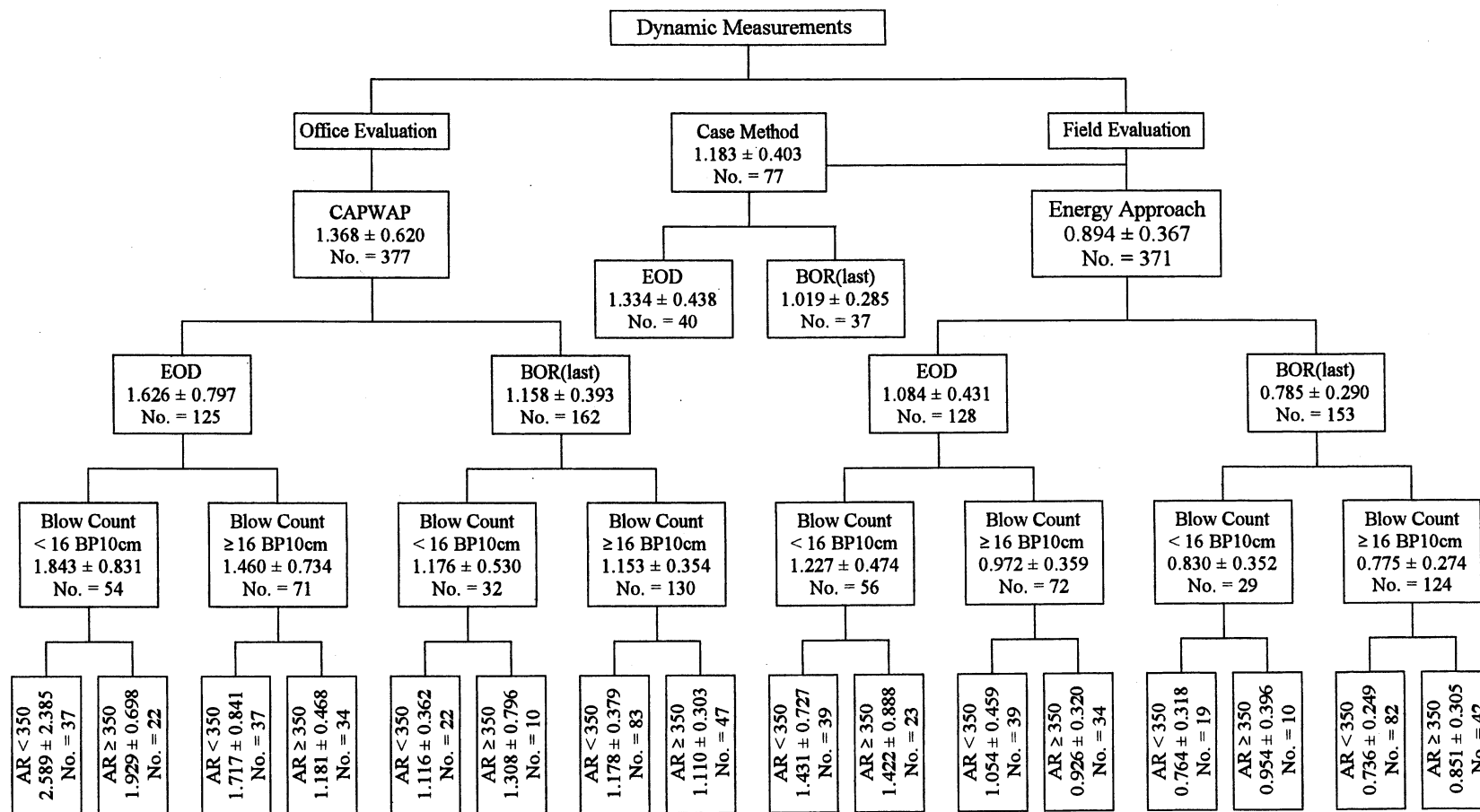


**Figure 9.3 (con't).** Flow Chart Presenting the Sub-Grouping of the Dynamic Analyses According to the Controlling Parameters and the Resulting Statistical Parameters for a Normal Distribution Function.

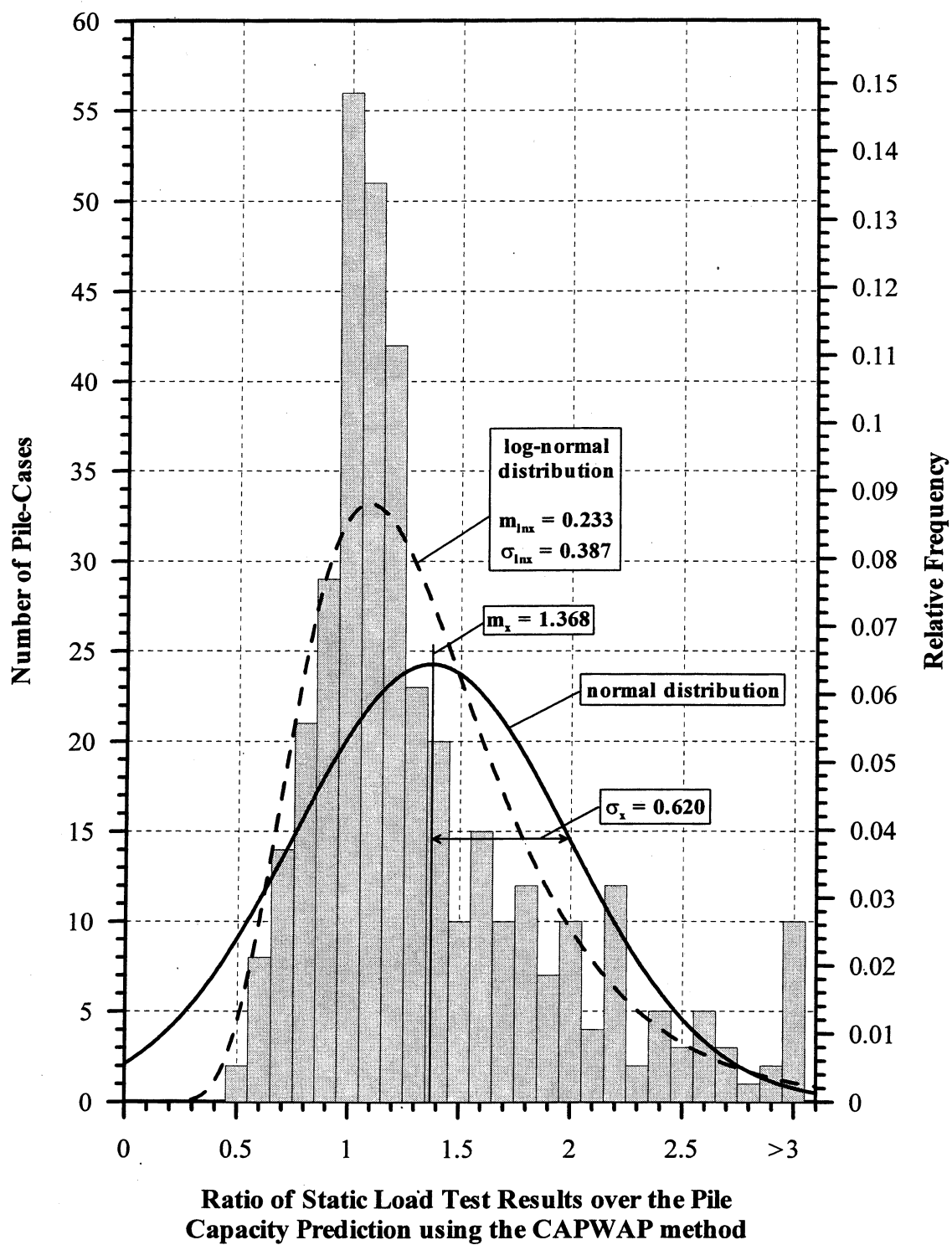


**Figure 9.4.** Histogram and frequency distributions of  $K_{sw}$  for 377 PD/LT2000 CAPWAP pile-cases in all types of soils (AAA).

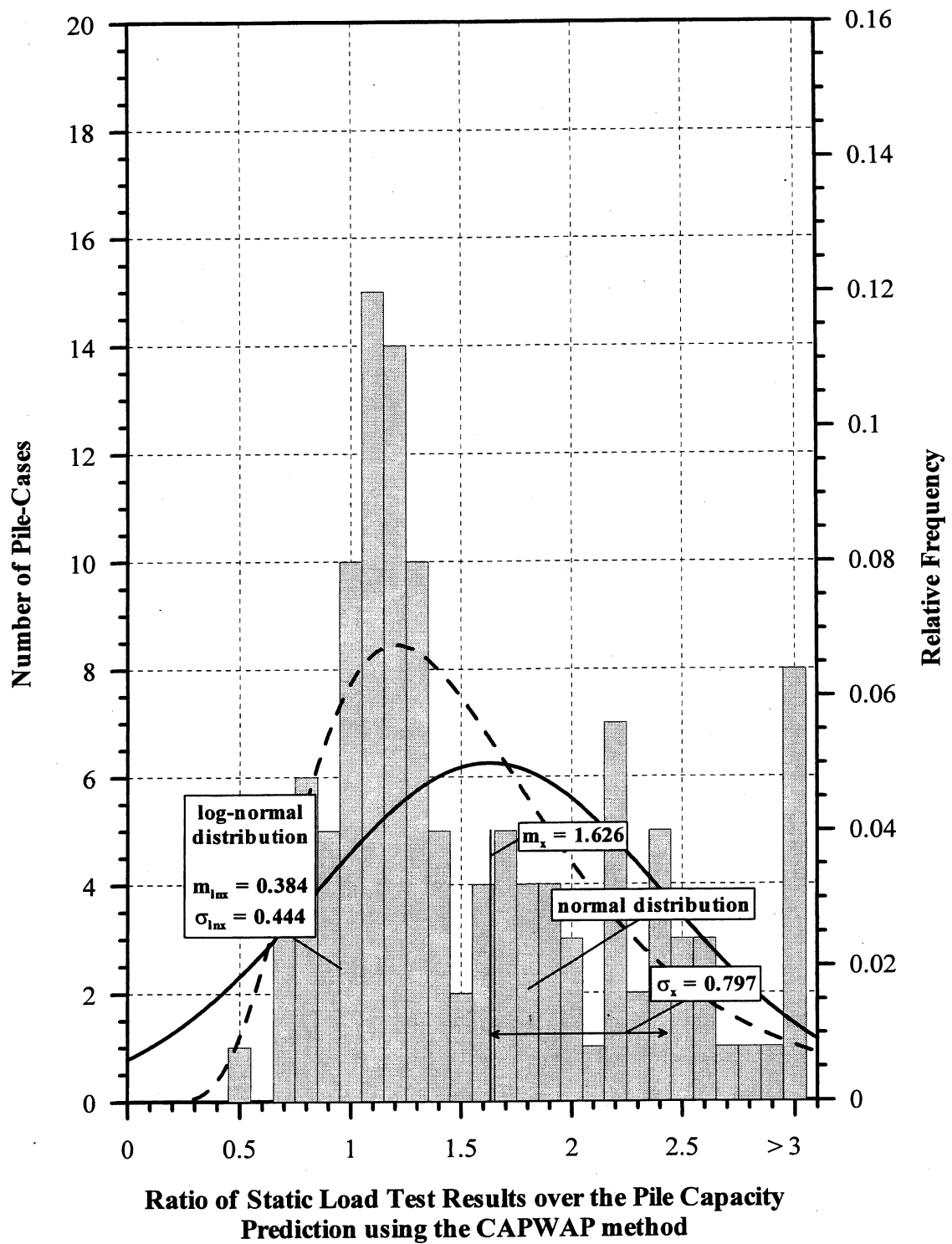


**Figure 9.5.** Histogram and frequency distributions of  $K_{sw}$  for 125 PD/LT2000 CAPWAP pile-cases at the EOD in all types of soils (AEA).

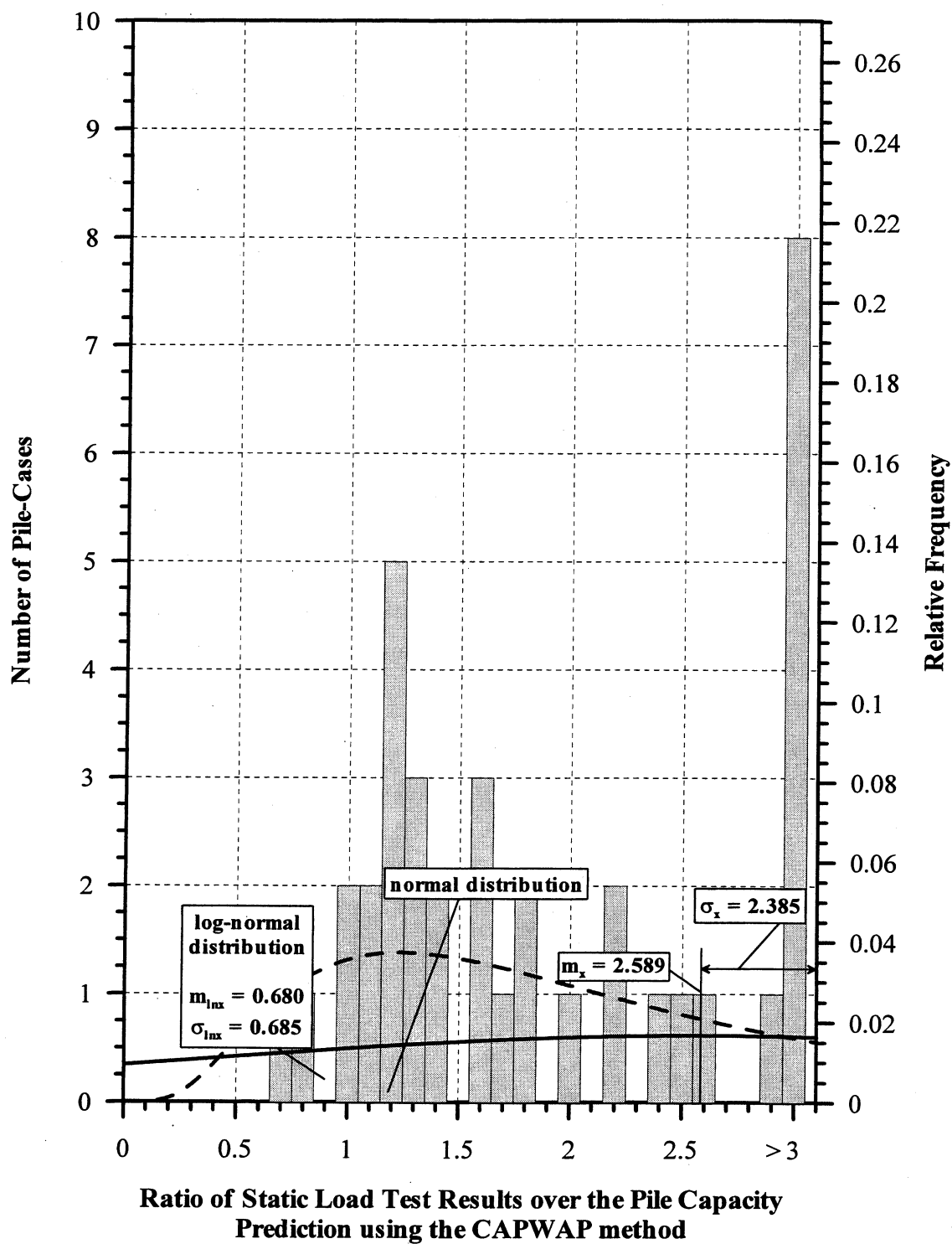


**Figure 9.6.** Histogram and frequency distributions of  $K_{sw}$  for 37 PD/LT2000 CAPWAP pile-cases at the EOD with Blow Counts < 16 BP10cm and Area Ratio < 350 in all types of soils (AEA).

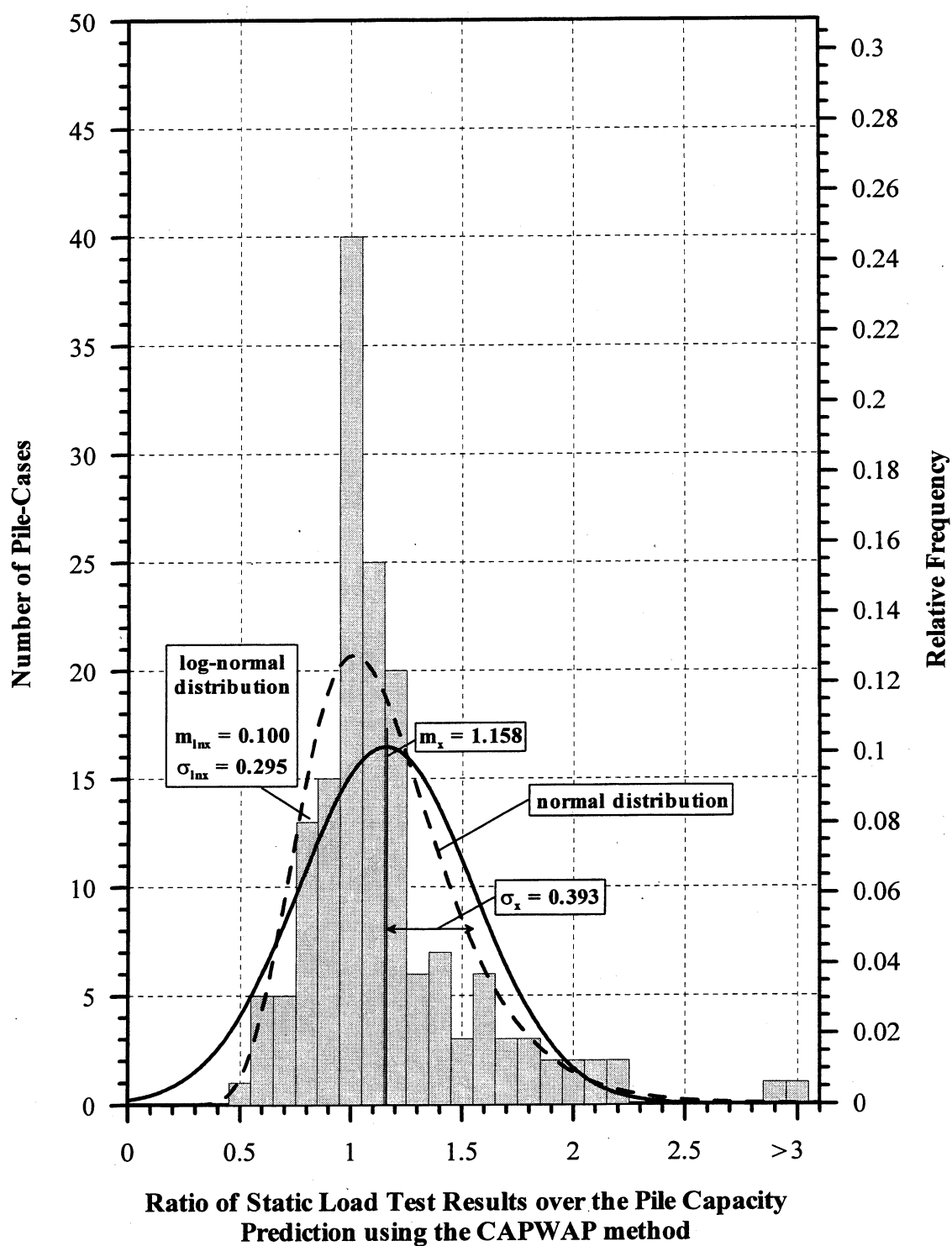


**Figure 9.7.** Histogram and frequency distributions of  $K_{sw}$  for 162 PD/LT2000 CAPWAP pile-cases at the BOR(last) in all types of soils (ABA).



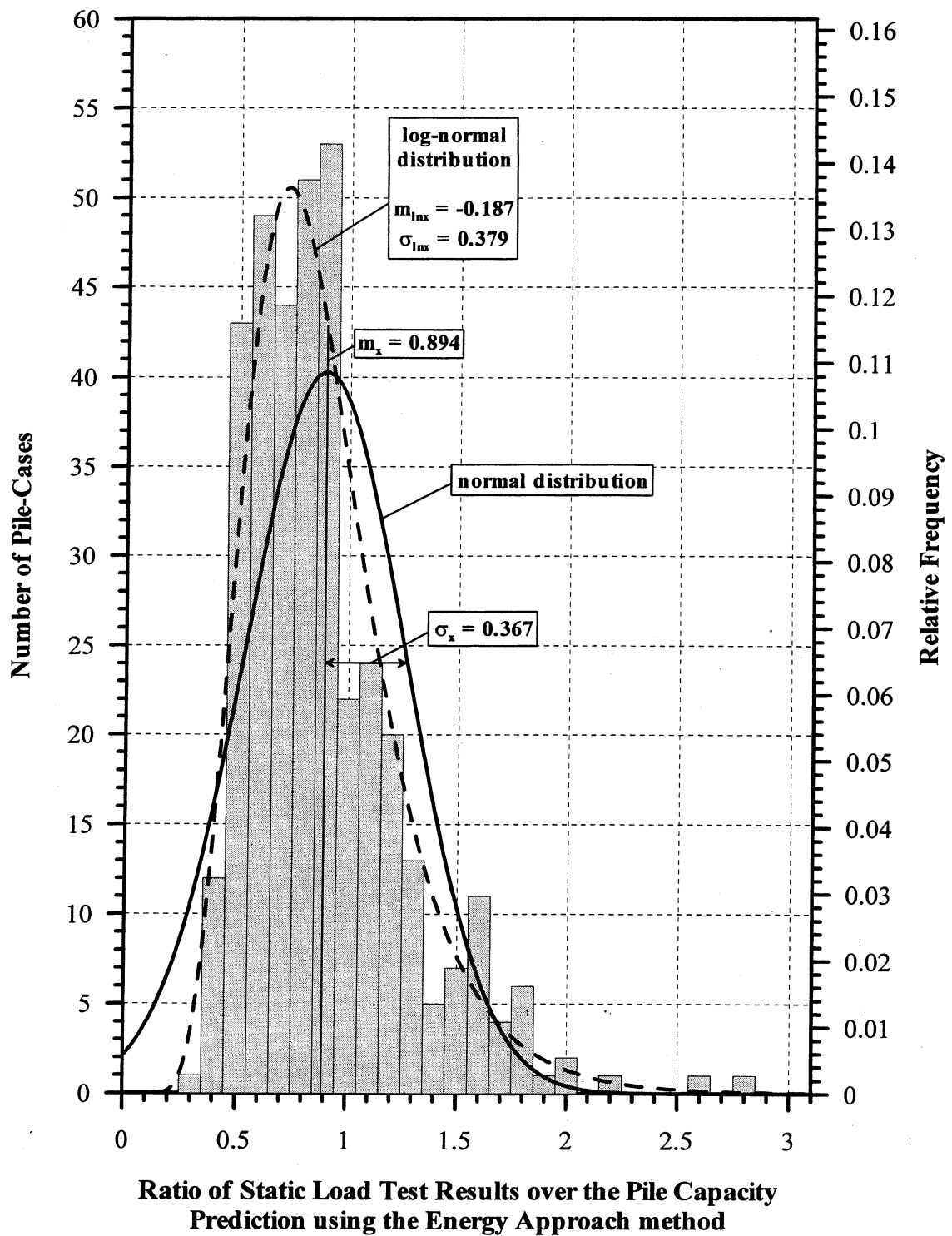


**Figure 9.8.** Histogram and frequency distributions of  $K_{SP}$  for 371 PD/LT2000 Energy Approach pile-cases in all types of soils (AAA).

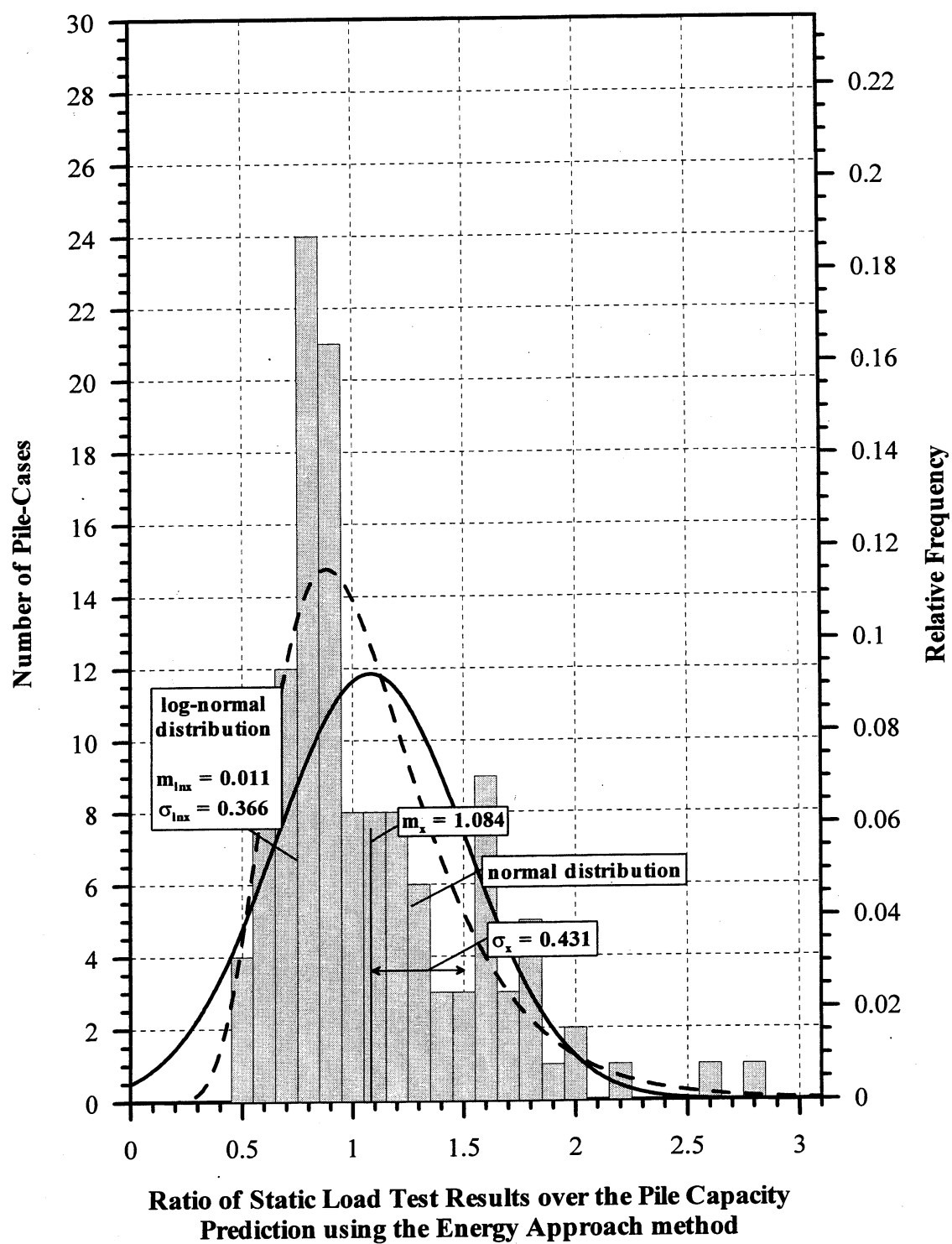


**Figure 9.9.** Histogram and frequency distributions of  $K_{SP}$  for 128 PD/LT2000 Energy Approach pile-cases at the EOD in all types of soils (AEA).

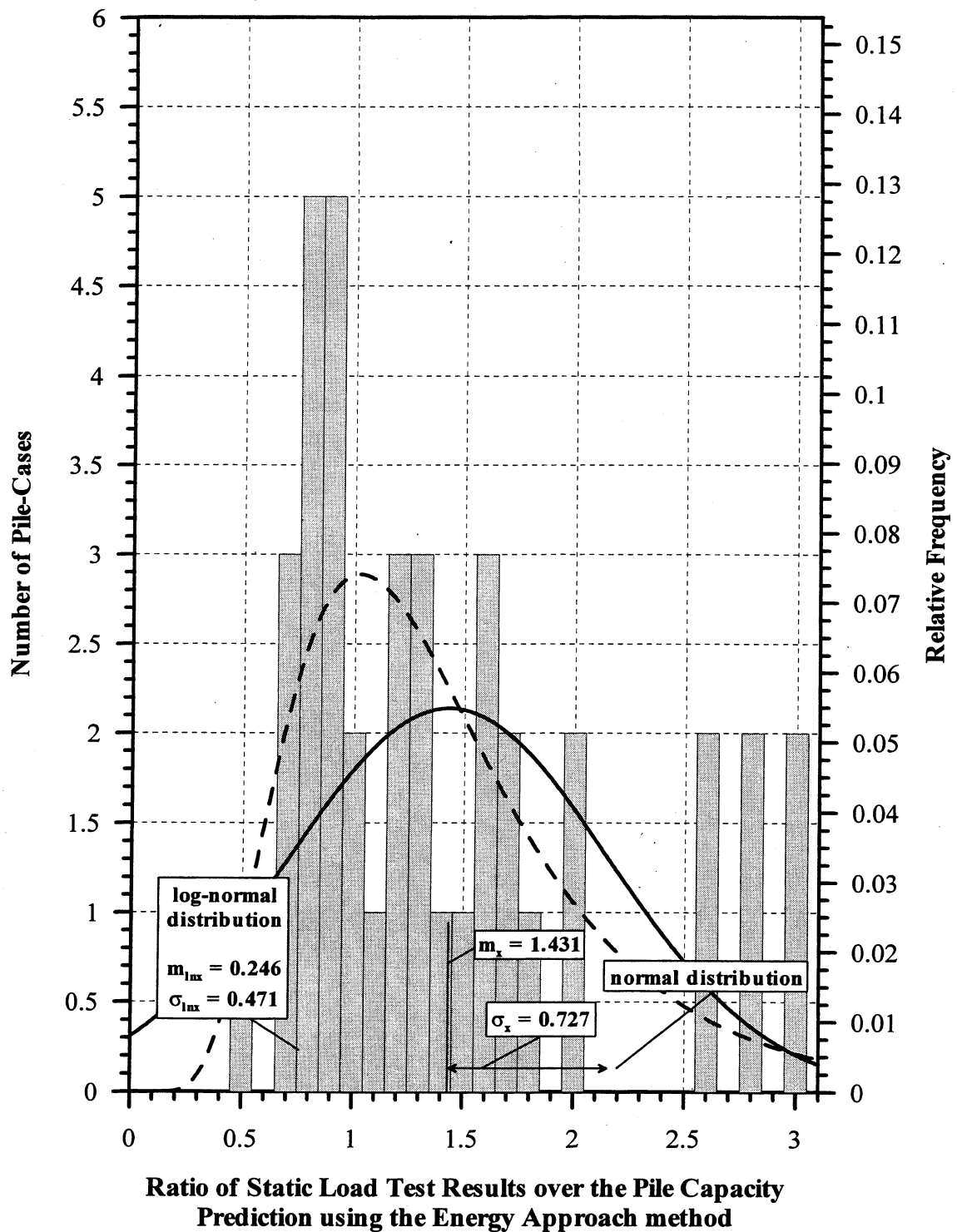


**Figure 9.10.** Histogram and frequency distributions of  $K_{sp}$  for 39 PD/LT2000 Energy Approach pile-cases at the EOD with Blow Counts < 16BP10cm and Area Ratio < 350 in all types of soils (AEA).

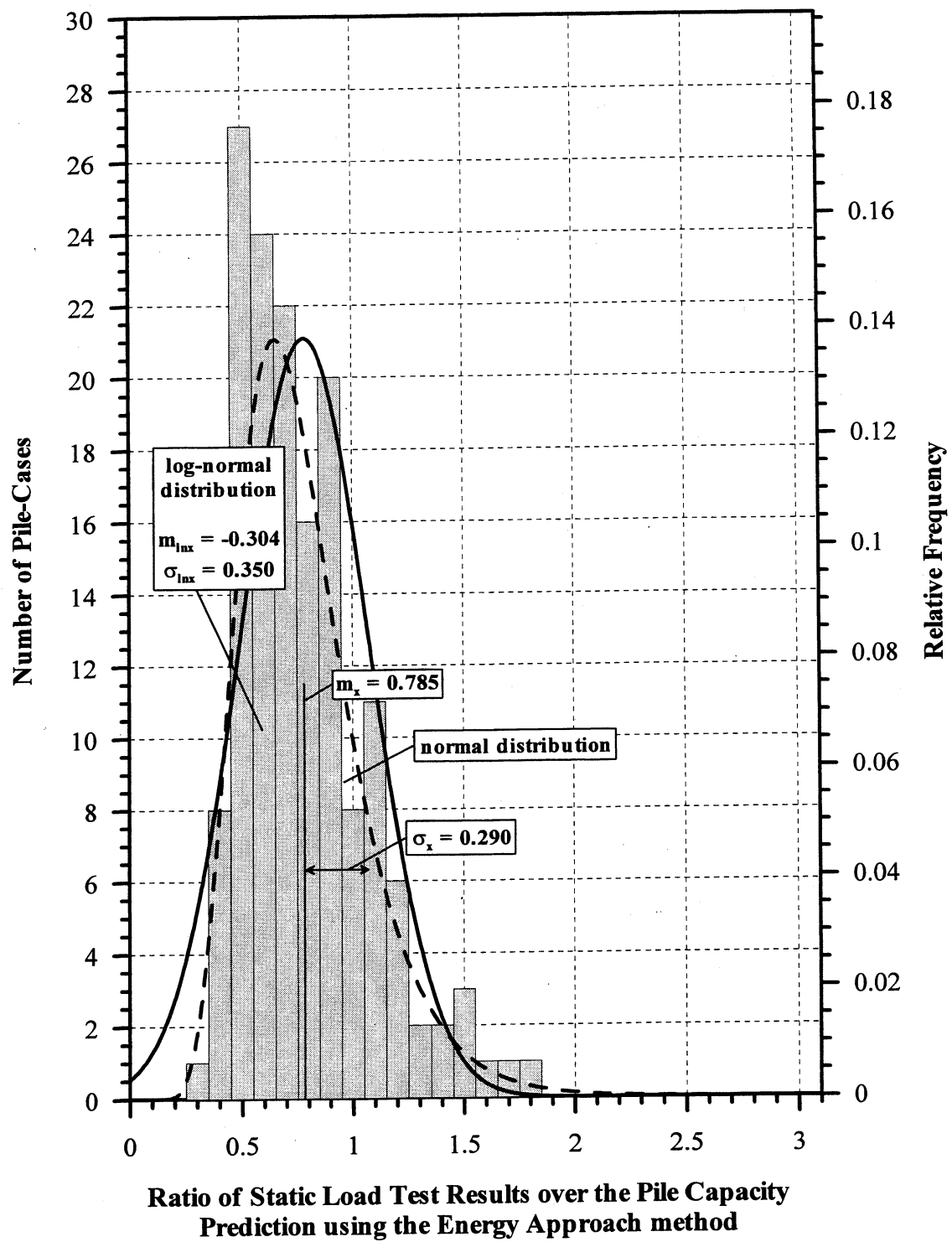


**Figure 9.11.** Histogram and frequency distributions of  $K_{SP}$  for 153 PD/LT2000 Energy Approach pile-cases at the BOR(last) in all types of soils (ABA).

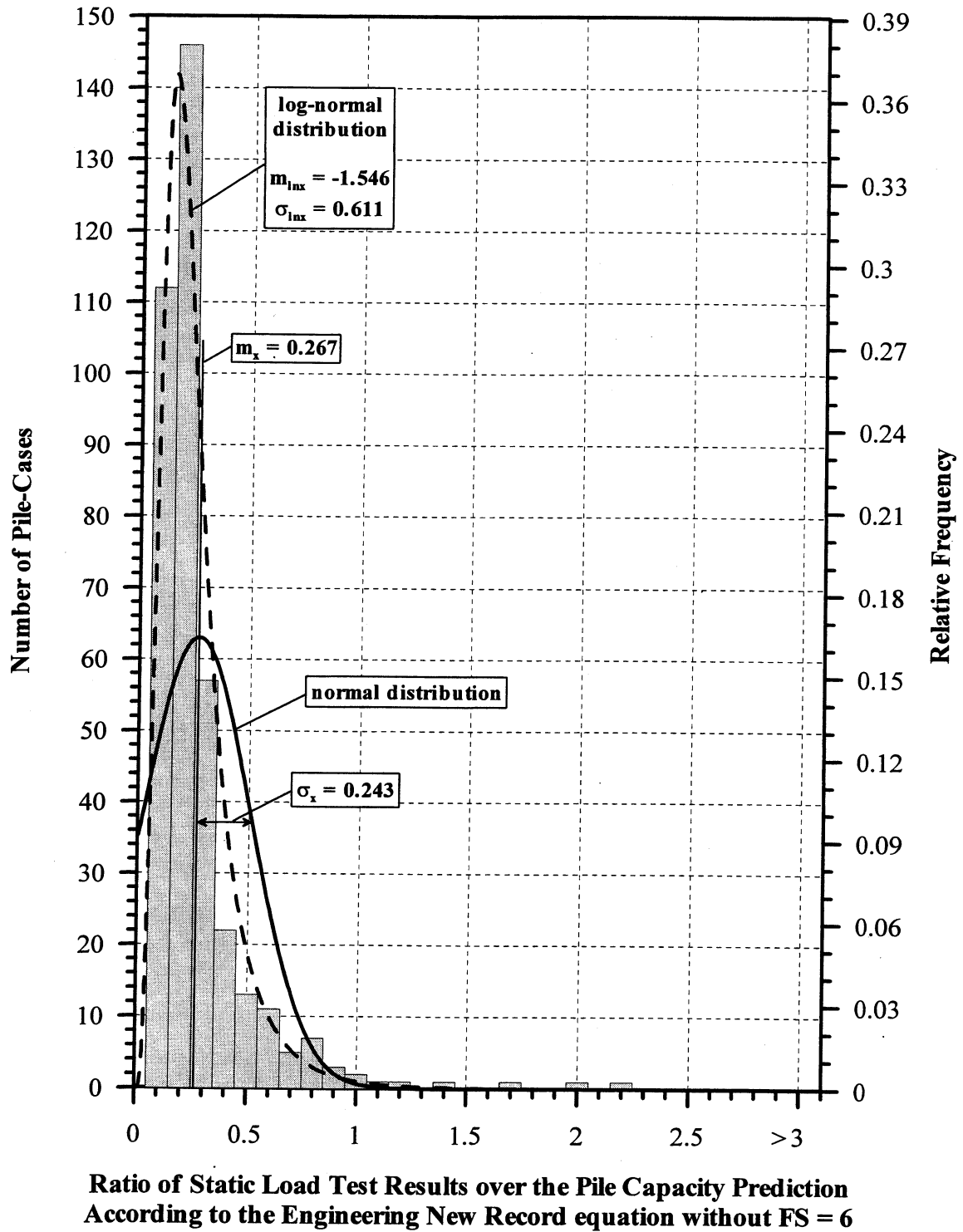


**Figure 9.12.** Histogram and frequency distributions of  $K_{SENR}$  (without FS = 6) for 384 PD/LT2000 pile-cases in all types of soils (AAA).

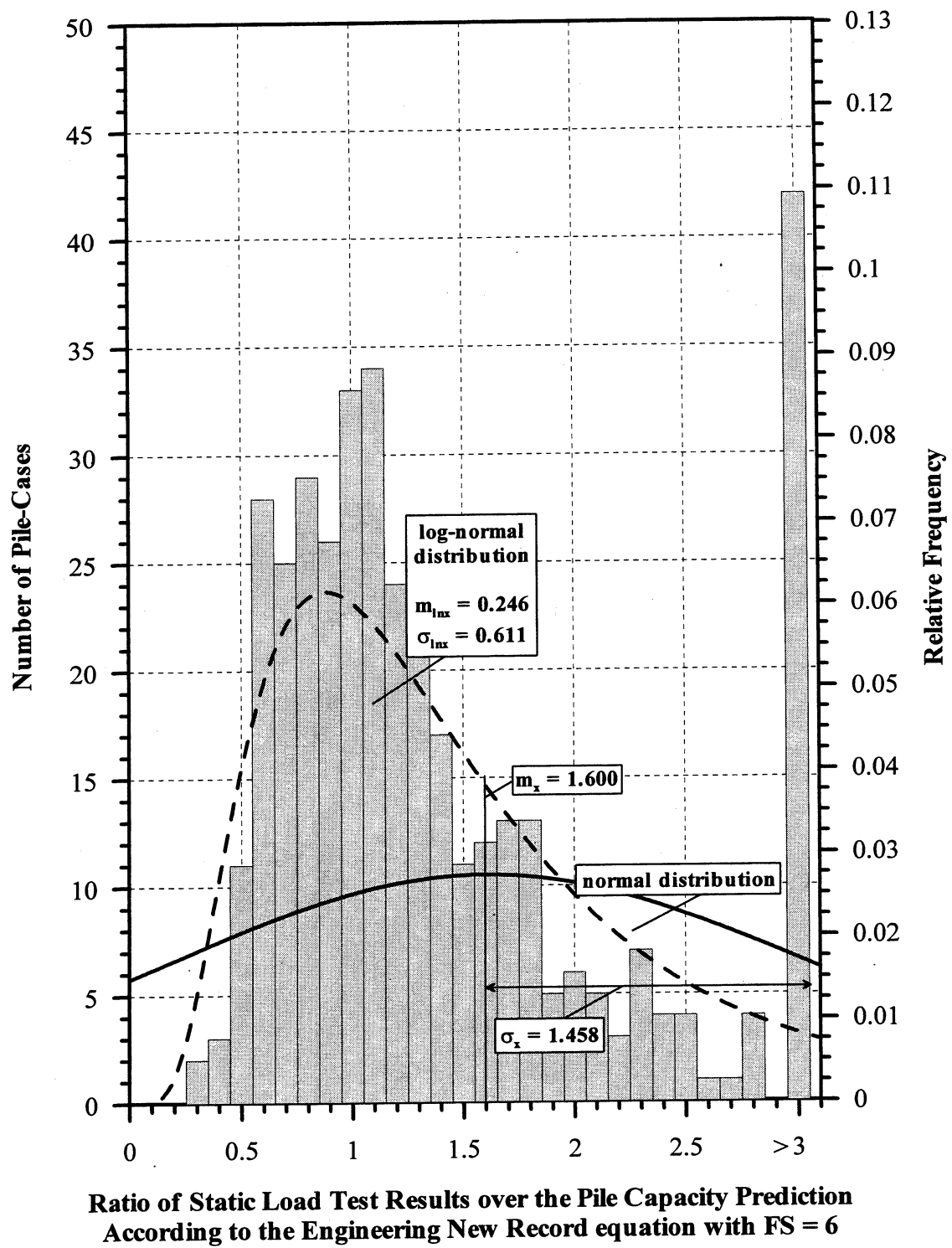


**Figure 9.13.** Histogram and frequency distributions of  $K_{SNER}$  (with FS = 6) for 384 PD/LT2000 pile-cases in all types of soils (AAA).

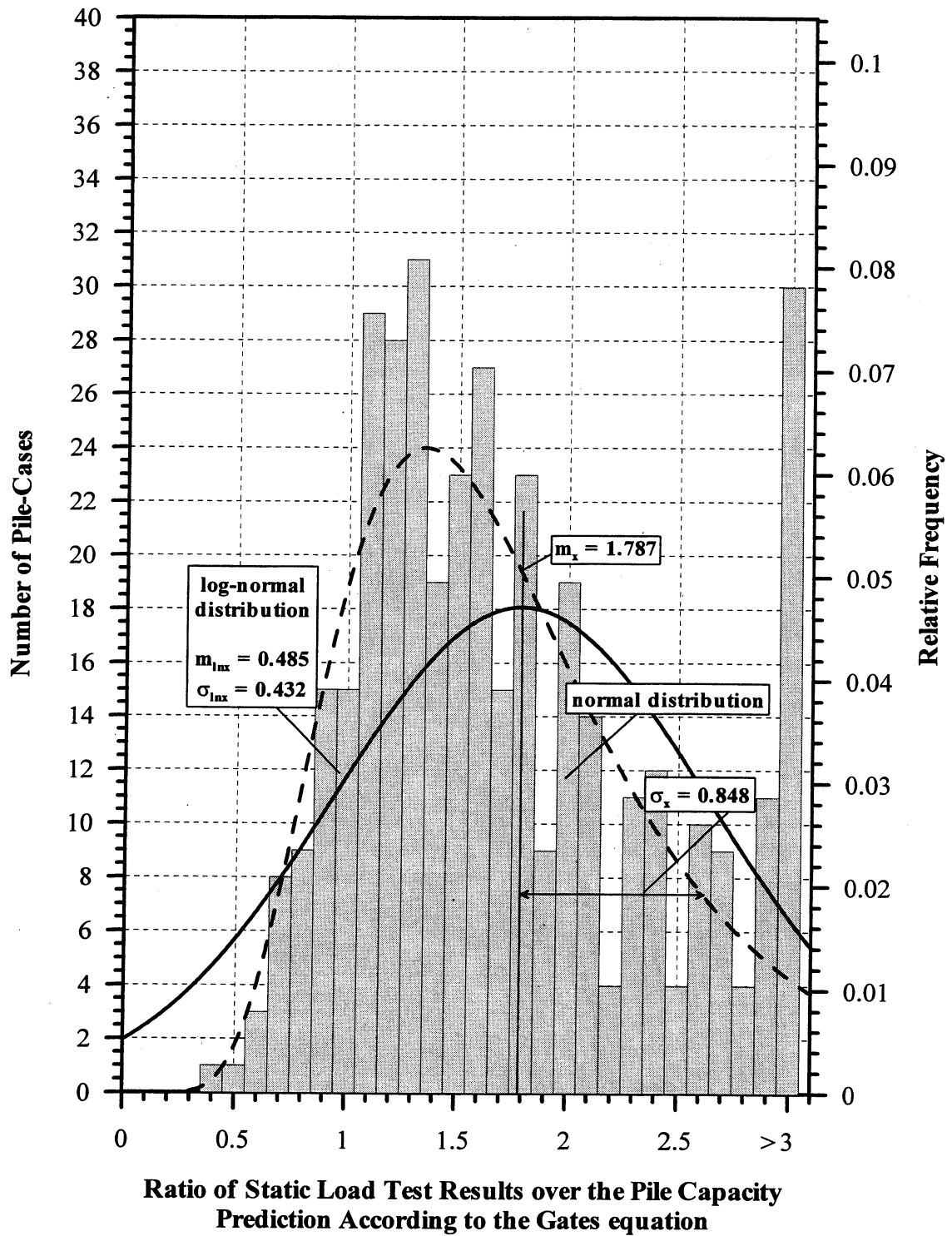


**Figure 9.14.** Histogram and frequency distributions of  $K_{SG}$  for 384 PD/LT2000 pile-cases in all types of soils (AAA).

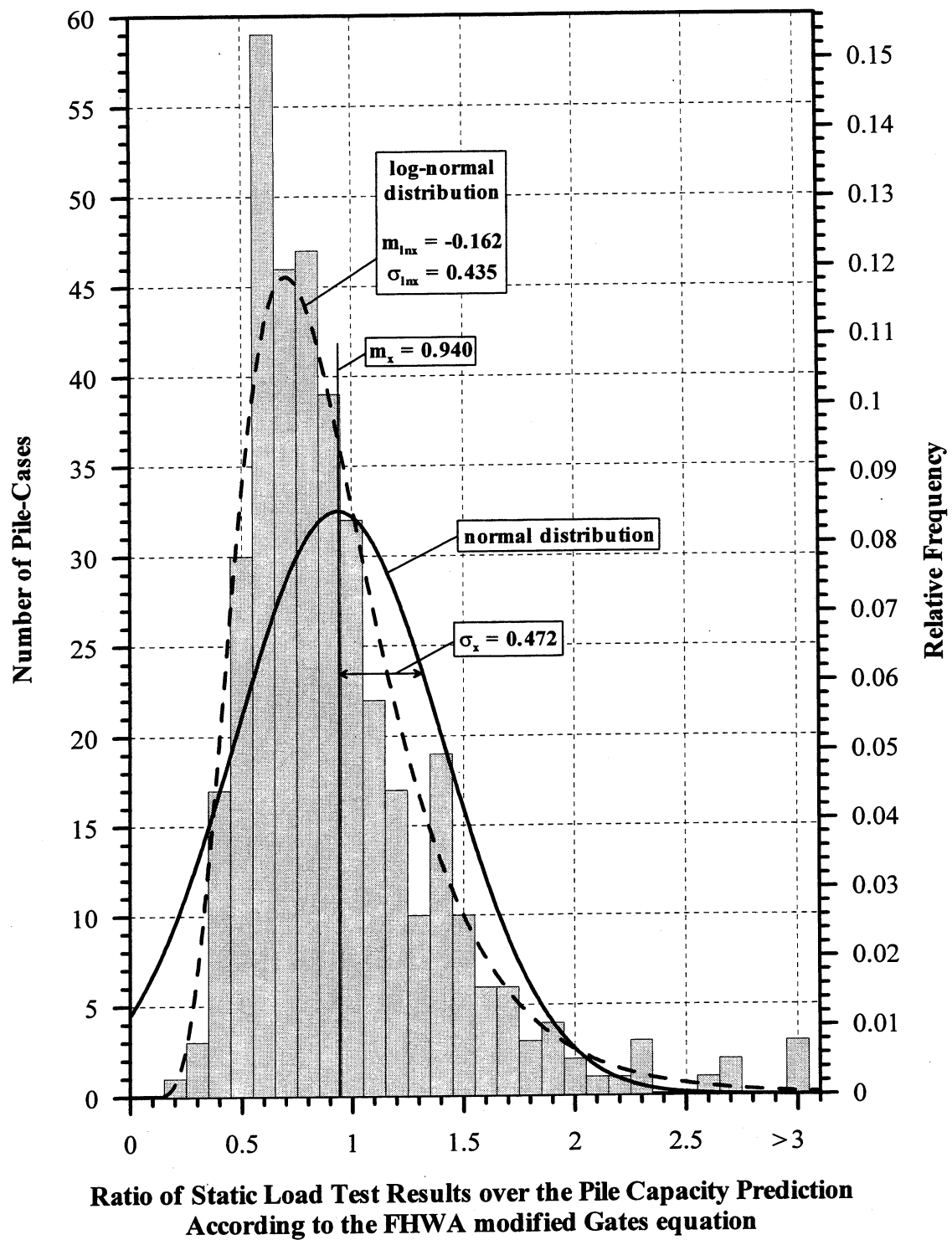


**Figure 9.15.** Histogram and frequency distributions of  $K_{SFG}$  for 384 PD/LT2000 pile-cases in all types of soils (AAA).



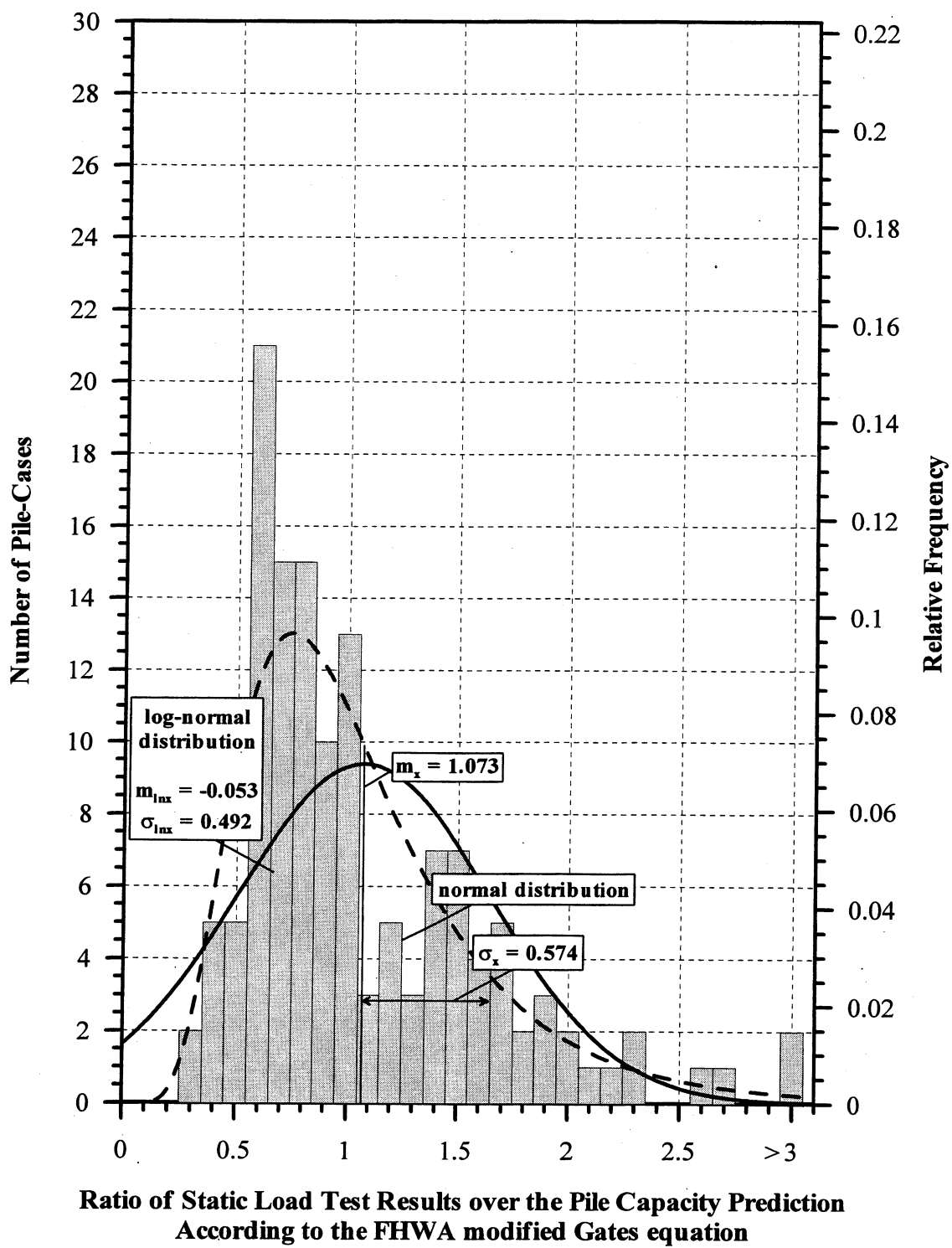


**Figure 9.16.** Histogram and frequency distributions of  $K_{SFG}$  for 135 PD/LT2000 pile-cases at the EOD in all types of soils (AAA).

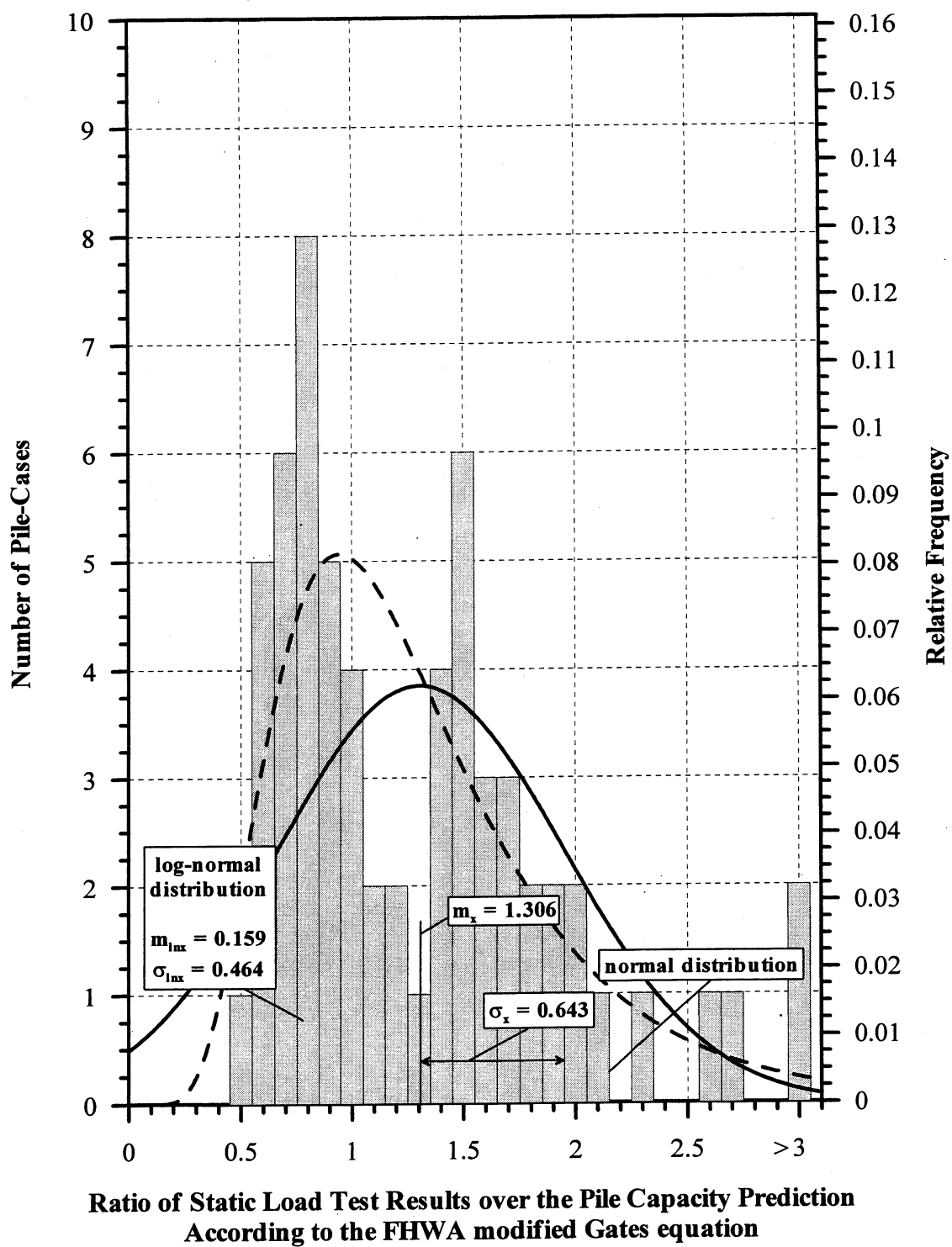


**Figure 9.17.** Histogram and frequency distributions of  $K_{SFG}$  for 62 PD/LT2000 pile-cases at the EOD with Blow Counts < 16 BP10cm in all types of soils (AAA).

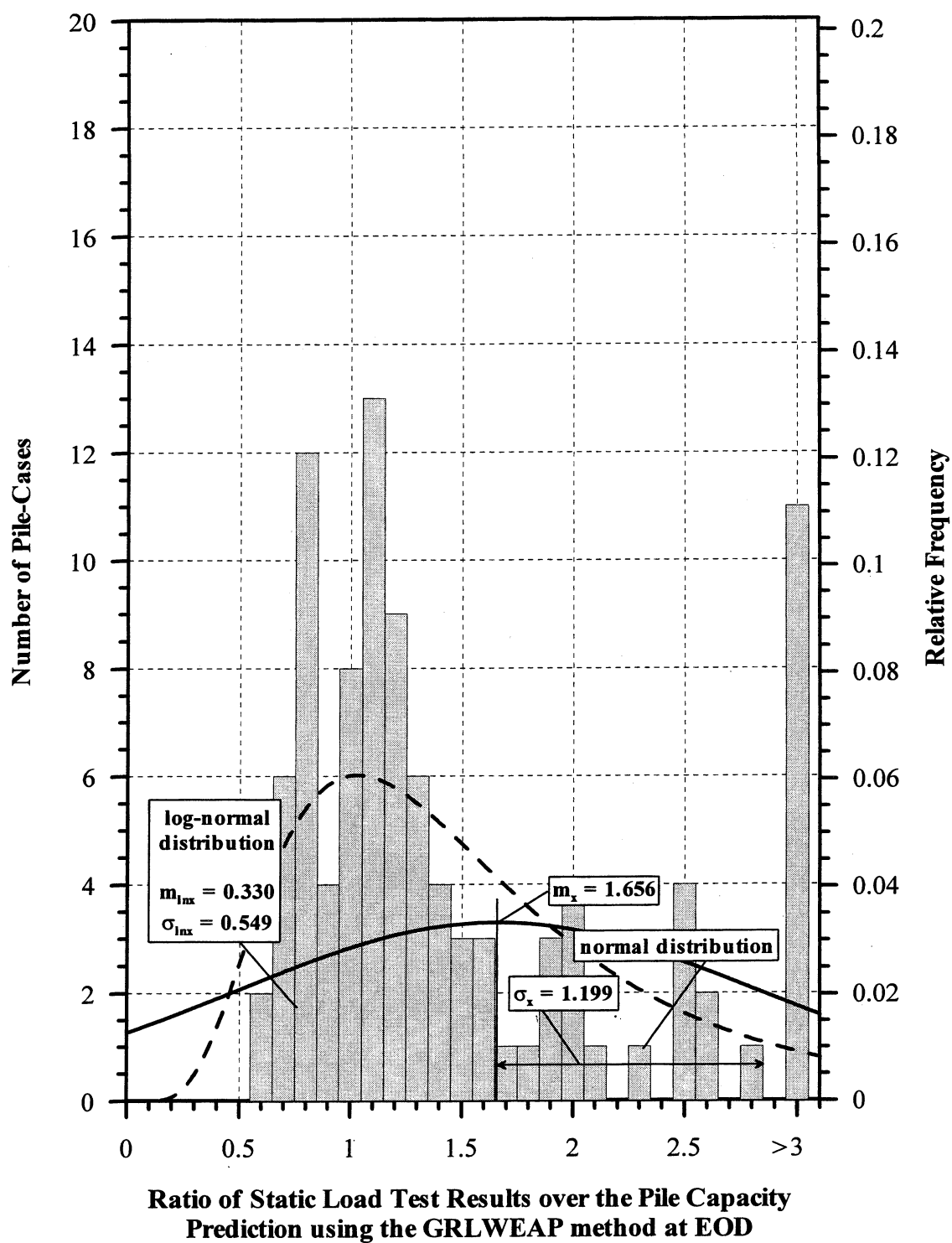


**Figure 9.18.** Histogram and frequency distributions of  $K_{swp}$  for 99 PD/LT2000 GRLWEAP pile-cases at the EOD in all types of soils.

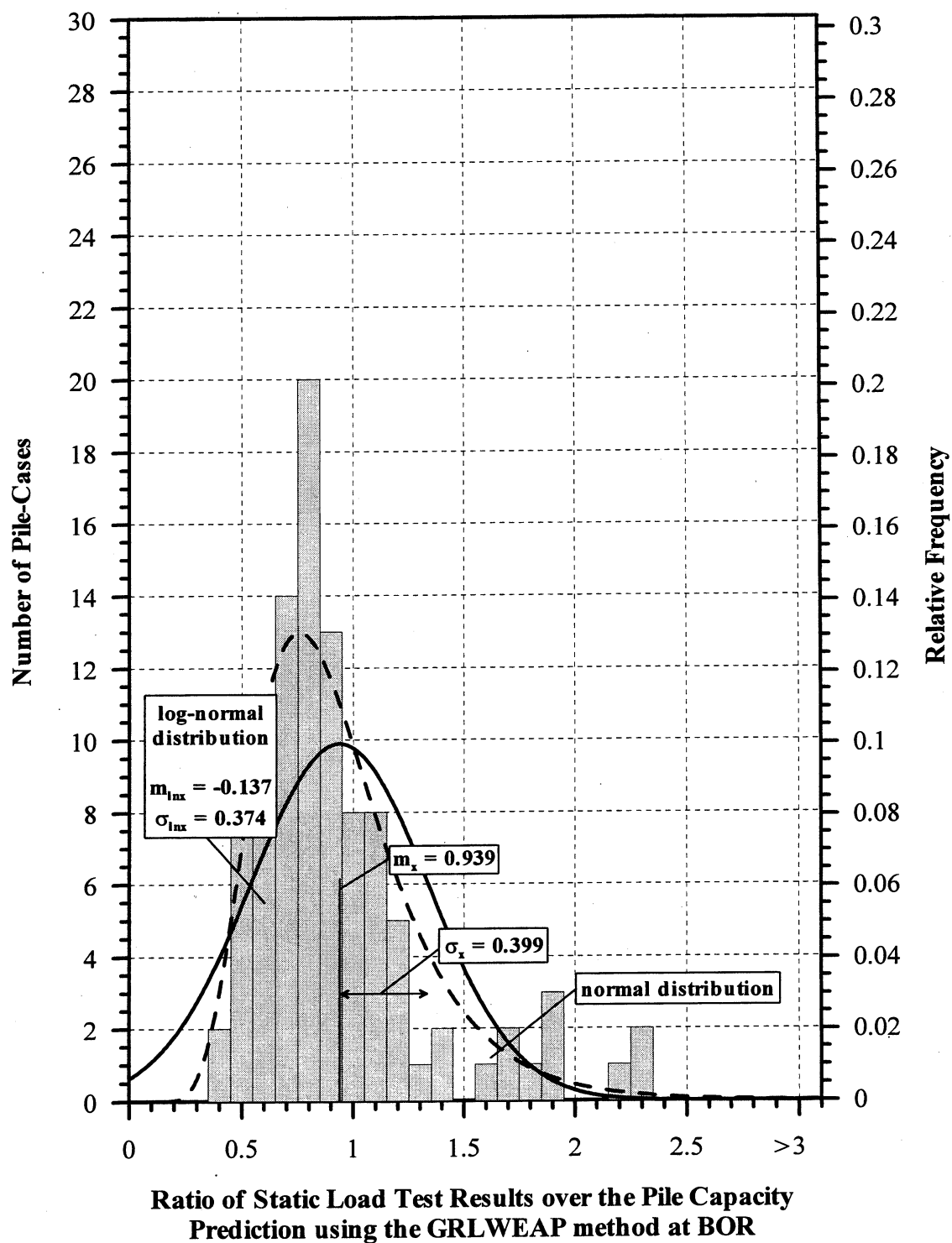


**Figure 9.19.** Histogram and frequency distributions of  $K_{SWP}$  for 99 PD/LT2000 GRLWEAP pile-cases at the BOR in all types of soils.

## **CHAPTER 10**

### **EXAMPLE CASE HISTORIES**

#### **10.1 GENERAL**

This chapter attempts to make a comparison between the LRFD method using the presented resistance factors, the 1998 AASHTO code and the Working Stress Design (WSD). This is a difficult task because there is no direct way to compare the 1998 AASHTO code with the proposed resistance factors as the code combines the static and dynamic methods for evaluating pile capacity. Appendix D presents the calculations for three test piles, two friction piles and one end bearing pile.

#### **10.2 EVALUATION OF THE PROPOSED RESISTANCE FACTORS**

The two test piles from Newbury, MA are considered friction piles, driven into a subsurface consisting of mostly clay as well as some sand and silt. The third test pile from the Choctawhatchee River project in Florida was driven into a sandy soil and is an end-bearing pile.

Table 10.1 summarizes the ultimate static pile capacities obtained for the three case history piles using a variety of the dynamic methods. Table 10.2 summarizes the allowed (design) pile capacities based on the different codes for the three case history piles. The pile capacities that are shown under the WSD headings were obtained by applying the appropriate factor of safety for each of the four methods used to

determine the piles' capacity (CAPWAP, Energy Approach, Gates formula, and the FHWA version of the Gates formula). The factors of safety that were used are 2.25 for the CAPWAP method, 3.50 for the two dynamic equations, and 2.75 for the Energy Approach. The determination of the pile capacities based on the 1998 AASHTO code is a challenge as the code uses static capacity methods to determine the pile's capacity and if specific dynamic methods are used to verify that pile capacity then the appropriate resistance factors can be used in conjunction with the static analysis results. The resistance factors based on the dynamic method used to verify pile capacities are 1.00 for CAPWAP verification, 0.90 for the Energy Approach verification, and 0.80 for the dynamic equation verification. For example the pile capacity for the Energy Approach method for test pile 2 was obtained by calculating the static pile capacity using the CPT method to be 883 kN, then applying a static resistance factor of 0.55 for the CPT method and finally applying the  $\lambda$  factor of 0.90 to the CPT prediction, resulting in 437 kN. The pile capacities listed under the heading Ch 9  $\phi$ 's are those capacities that were determined using the recommended resistance factors for non-redundant piles in Table 9.8. The pile capacities that were determined by each of the methods shown in Table 10.1 were simply multiplied by the appropriate resistance factor for that method, e.g., for the Energy Approach at the EOD for test pile 2, the predicted value was 792 kN, the resistance factor for non-redundant pile is  $\phi = 0.40$  resulting in a design capacity of 320 kN, which represents an actual factor of safety of 2.06 in this case.

### **10.3 INTERMEDIATE CONCLUSIONS**

Due to the different types of methods that were used to determine these pile capacities it is difficult to state whether the proposed resistance factors for the LRFD method are an improvement over the 1998 AASHTO code based strictly on pile capacities. Comparing between the existing code (AASHTO, 1998) and the recommended parameters obtained in this study is difficult. The comparison between the WSD factored capacities and the recommended parameters shows overall a very good agreement between the two, fully rationalizing the recommended resistance factors. The major improvement remains in the methodology, the ability to adopt the resistance factors to variable conditions (e.g. redundant versus non-redundant) and the method in which the load factors are determined and applied. The current concept is an immeasurable improvement compared to the existing AASHTO parameter application, separating the static and dynamic methods and their relevant resistance factors.

**Table 10.1.** Predictions of the Dynamic Methods for Three Case History Piles.

Type of Analysis	Method	Q <sub>ult</sub> (kN)		
		Friction Piles		End Bearing Pile
		Newbury TP # 2	Newbury TP # 3	Choctawhatchee Pier 5
CAPWAP Analyses	CAPWAP EOD	418	738	-----
	CAPWAP BOR	-----	-----	2527
	CAPWAP BORL	1112	1228	2598
Simplified Methods	EA EOD	792	1228	-----
	EA BOR	-----	-----	4484
	EA BORL	1432	4075	5187
Dynamic Equations	ENR w/ FS = 6, EOD	347	409	-----
	ENR w/ FS = 6, BOR	-----	-----	4857
	ENR w/ FS = 6, BORL	1041	2527	5480
	Gates EOD	721	783	-----
	Gates BOR	-----	-----	2304
	Gates BORL	1219	1708	2447
	FHWA EOD	1157	1299	-----
	FHWA BOR	-----	-----	4680
	FHWA BORL	2251	3354	4982
Static Load Test Results		Q <sub>ult</sub> = 658 kN	Q <sub>ult</sub> = 872 kN	Q <sub>ult</sub> = 5560 kN

Note: 1 ton = 8.896 kN



**Table 10.2.** Summary of Design Capacity Comparisons for Three Case History Piles.

Type of Analysis	Method	Q <sub>all</sub> (kN)								
		Friction Piles						End Bearing Pile		
		Newbury TP # 2			Newbury TP # 3			Choctawhatchee Peir 5		
		WSD	AASHTO	Ch 9 ϕ's	WSD	AASHTO	Ch 9 ϕ's	WSD	AASHTO	Ch 9 ϕ's
Wave Matching	CAPWAP EOD	187	667	178	329	943	320	-----	1246	-----
	CAPWAP BOR	-----		-----	-----		1121	1290		
	CAPWAP BORL	489		569	543		623	1157		1326
Simplified Methods	EA EOD	285	605	320	445	854	489	-----	1121	-----
	EA BOR	-----		-----	-----		1628	1432		
	EA BORL	525		463	1486		1308	1886		1664
Dynamic Equations	ENR EOD	98	534	53	116	756	62	-----	996	-----
	ENR BOR	-----		-----	-----		-----	1388		730
	ENR BORL	294		160	721		383	1566		818
	Gates EOD	205		383	222		418	-----		-----
	Gates BOR	-----		-----	-----		-----	658		1219
	Gates BORL	347		649	489		907	703		1299
	FHWA EOD	329		302	374		338	-----		-----
	FHWA BOR	-----		-----	-----		-----	1334		1219
	FHWA BORL	641		587	961		872	1423		1299
Static Load Test Results		Q <sub>ult</sub> = 658 kN			Q <sub>ult</sub> = 872 kN			Q <sub>ult</sub> = 5560 kN		

Note: The wave matching techniques are not recommended by GRL to be used at the EOD (Rausche, 2001) and the Energy Approach is not recommended to be used during restrike.

## CHAPTER 11

### SUMMARY, CONCLUSIONS, AND RECOMMENDATIONS

#### 11.1 SUMMARY

1. A summary of the principles of the Load and Resistance Factor Design (LRFD) method was provided. The intent of the LRFD method is to separate the uncertainties in loading from uncertainties in resistance and to assure a prescribed margin of safety. The principle of the LRFD method for piles is that the ultimate resistance ( $R_u$ ) multiplied by a resistance factor ( $\phi$ ), which is equal to the factored resistance ( $R_f$ ), must be greater than or equal to the summation of the loads ( $Q_i$ ) multiplied by a modifier ( $\eta_i$ ) and load factor ( $\gamma_i$ ), (Refer to Chapter 2).
2. Six datasets were compiled as part of the presented research: PD/LT2000, U-Mass Lowell / Ukraine, GRLWEAP, Case method, PD2000, and PD/LTT2000. The methods and standards that were used in compiling the data for each of the databases used in the LRFD research are presented (Chapter 3) and the relevant information pertaining to each of the databases is presented in Appendix A.
3. In order to evaluate the performance of each of the dynamic methods, the actual static pile capacity needs to be determined. A comparison study between

different bearing capacity interpretation methods had shown that the most reasonable method for determining pile capacity using static load test loadsettlement curves was Davisson's criterion, (Chapter 4). It was also determined that the type of static load test performed, i.e., a slow maintained, short duration, or static cyclic does not greatly affect the representative pile capacity determined from the load test curves.

4. The controlling parameters of the dynamic methods were evaluated based on soil type, time of driving, and soil inertia effects. The effect of soil type was examined by determining the accuracy of the predictive methods relative to the soil type. The time of driving effect was examined by comparing the static load test results to the dynamic predictions at the End Of Driving (EOD) and the Beginning Of Restrike (BOR). The soil inertia effects are represented by the driving resistance and the displaced soil volume, which is defined by the area ratio, (Chapter 5). The driving resistance can be categorized as hard or easy depending on the blow count. The dividing blow count between easy and hard driving was determined to be 16 blows per 10 centimeters (4 blows per inch). The pile types categorized as small displacement and large displacement with the quantitative boundary of  $A_R = 350$ . This criterion was proposed by Paikowsky et al. (1994) and was confirmed in this research. Using the controlling parameters for the dynamic methods as described above, resistance factors for each of the important sub-categories were calculated.

## 11.2 CONCLUSIONS

Based on the presented data the following conclusions are derived:

1. The compilation of a large database allows for the evaluation of the dynamic methods, the examination of the Working Stress Design (WSD) methodology (e.g. validity of the assigned factors of safety), and the development of new methodologies such as the Load and Resistance Factor Design (LRFD).
2. The dynamic methods performance is controlled by the time of driving and soil inertia, which in turn is controlled by the driving resistance and the ratio of the soil displaced by the pile's tip to the area of the soil along the shaft of the pile.
3. The most commonly known dynamic equation, the Engineering News Record (ENR) equation, is shown to be completely unreliable and unreasonable for use. In contrast, the Gates equation and its variation, modified by the Federal Highway Administration (FHWA), seem to provide a reasonable assessment of the pile's capacity considering the absence of dynamic measurements.
4. The wave equation analysis performs poorly when used for pile capacity evaluation. However, this conclusion should not be mistaken with the importance of the wave equation analysis during the design stage. The drivability study and pile stress analysis often determine the pile type, geometry and the adequacy of the proposed equipment.
5. Signal matching techniques (e.g. CAPWAP) prove to be most reliable for long-term restrike measurements. However, when evaluated by its efficiency ( $\phi / \text{mean } K_{sx}$ ), the application of the signal matching on restrikes seem to be

marginal compared to the Energy Approach at the End of Driving (EOD). These conclusions though representative of most cases, cannot be based on statistical data alone. For example, sites that exhibit a significant but highly variable setup may economically justify consistent and long-term restrikes along with signal matching analysis.

6. The field application of the Energy Approach provides an exceptionally efficient evaluation of pile capacity during driving.
7. The recommended resistance factors for the dynamic methods that performed reasonably well range from 0.42 to 0.73 for redundant piles ( $p_f = 1\%$ ) and from 0.32 to 0.53 for non-redundant piles ( $p_f = 0.1\%$ ).
8. The development of resistance factors based on FOSM as used by Barker et al. (1991) and the statistical data of this research resulted in resistance factors of about 10% lower than those obtained through FORM, used in this study.
9. A back calculated factors of safety from the obtained resistance factors and an evaluation of the actual risk suggested that the proposed resistance factors and the probability of failure they are based on are reasonable and compatible with common practice.
10. Examination of three case histories suggests good agreement between the recommended resistance factors and the traditional factors of safety of the WSD methodology.
11. The framework for the development of resistance factors as part of the LRFD methodology seem to facilitate a design which is better suitable for

geotechnical applications. The presented work is only an initial stage in that direction.

### **11.3 RECOMMENDATIONS**

1. The presented research refers to single pile analysis while in reality pile groups are most commonly used. Additional data and research are needed for evaluating the reliability of pile groups in comparison to single piles and hence determine resistance factors based on the probability of failure of pile groups.
2. Soil inertia greatly affects the performance of the dynamic analyses. This suggests the need for development of new methods of dynamic analyses that will correctly account for the soil inertia during pile penetration.
3. A complete code based on LRFD needs to consider factors associated with subsurface variability, site-specific technology and previous experience, as well as amount and type of testing during construction. The gathering of data and the development of parameters considering such factors would greatly enhance Geotechnical design.

## REFERENCES

AASHTO, 1994. *LRFD Highway Bridge Design Specifications*. American Association of State Highway and Transportation Officials, Washington D.C.

AASHTO, 1997. *Standard Specifications for Highway Bridges*, American Association of State Highway and Transportation Officials, Washington D.C., 16<sup>th</sup> Edition (1996 with 1997 interims).

AASHTO, 1998. *Standard Specifications for Highway Bridges*, American Association of State Highway and Transportation Officials, Washington D.C.

AISC, 1994. Load and Resistance Factor Design, *Manual of Steel Construction*, American Institute of Steel Construction, Chicago, IL.

Allen, D.E., 1975. Limit States Design - A Probabilistic Study, *Canadian Journal of Civil Engineering*, Vol. 2, No. 1, pp. 36-49.

Allen, D.E., 1994, *The History and Future of Limit States Design*, Journal of Thermal Insulation and Building Envelopes, Vol. 18: pp. 3-20

American Society for Testing and Materials (ASTM), 1996. Annual Book of ASTM Standards, Volume 04.08, Soil and Rock (I): D 420 - D 4914, Philadelphia, PA, p. 1,000.

American Society for Testing and Materials (ASTM), 1998. Standard Test Method for Individual Piles Under Static Axial Compressive Load. *Annual Book of ASTM Standards*, 4.08, Philadelphia.

API, 1989. Draft Recommended Practice for Planning, Designing and Constructing Fixed Offshore Platforms - Load and Resistance Factor Design. *API RP2A-LRFD*, American Petroleum Institute, Dallas, TX.

ASCE, 1993. Minimum Design Loads for Buildings and Other Structures. *ASCE 7-93 (formerly ANSI A58.1)*.

AUSTROADS, 1992. *AUSTROADS Bridge Design Code*, National Office, AUSTROADS, Surry Hills, NSW, Australia.

Ayyub, B. and Assakkaf, I., 1999. LRFD Rules for naval Surface Ship Structures: Reliability-Based Load and Resistance Factor Design Rules. Naval Surface Warfare Center, Carderock Division, U.S. Navy.

Ayyub, B.M., Assakkaf, I., and Atua, K., 1998. Development of LRFD Rules for Naval Surface Ship Structures: Reliability-Based Load and Resistance Factor Design Rules, Part III - Stiffened and Gross Panels. Naval Surface Warfare Center, Carderock Division, U.S. Navy.

Ayyub, B., Assakkaf, I., and Atua, K., 2000. Reliability-Based Load and Resistance Factor Design (LRFD) of Hull Girders for Surface Ships. *Naval Engineers Journal*, ASNE, May 2000.

Ayyub, B.M., Assakkaf, I., Atua, K.I., Melton, W., and Hess, P., 1997, "LRFD Rules for Naval Surface Ship Structures: Reliability-Based Load and Resistance Factor Design Rules," U.S. Navy, Naval Sea System Command, Washington, DC.

Ayyub, B.M., and Atua, K., 1996, "Development of LRFD Rules for Naval Surface Ship Structures: Reliability-Based Load and Resistance Factor Design Rules, Part I - Hull Girder Bending," Naval Surface Warfare Center, Carderock Division, U.S. Navy.

Ayyub, B.M., Beach, J., and Packard, T., 1995, "Methodology for the Development of Reliability-Based Design Criteria for Surface Ship Structures," *Naval Engineers Journal*, ASNE, 107(1), Jan. 1995, 45-61.

Ayyub, B.M. and McCuen, R.H., 1997, Probability, Statistics and Reliability for Engineers, CRC Press, FL.

Baecher, G.B., 1998. Personal Communication.

Baecher, G. and Rackwitz, R., 1982. Factors of Safety of Pile Load Tests, *Journal of Numerical and Analytical Methods in Geomechanics*, Vol. 6, pp. 409-424.

Baker, M.J., 1976. Evaluation of Partial Safety Factors for Level I Codes.

Barker, R.M., Duncan, J.M., Rojiani, K.B., Ooi, P.S.K., Tan, C.K., and Kim, S.G., 1991. *Manuals for the Design of Bridge Foundations*, NCHRP Report 343. Transportation Research Board, National Research Council, Washington, DC.

Becker, D.E., 1996. Eighteenth Canadian Geotechnical Colloquium: *Limit States Design for Foundations. Part I. An Overview of the Foundation Design Process*. Canadian Geotechnical Journal, Vol. 32: pp. 956-983.



Berezantzev, V. G., Khristoforov, V. and Golubkov, V., 1961. Load Bearing Capacity and Deformation of Piled Foundations. *Proceedings 5<sup>th</sup> International Conference*. S.M. & F.E., Vol. 2, pp. 11-15.

Bowles, J.E., 1996. Foundation Analysis and Design, 5<sup>th</sup> Edition. McGraw-Hill, USA.

Burland, J. B., 1973. Shaft friction of piles in clay - A simple fundamental approach. *Ground Engineering*, Vol. 6, No. 3, pp. 30-42.

Butler, H.D. and Hoy, H.E., 1977. *Users Manual for the Texas Quick-Load Method for Foundation Load Testing*. Federal Highway Administration, Office of Development, Report No. FHWA-IP-77-8, Washington DC.

Canadian Geotechnical Society, 1992. *Canadian Foundation Engineering Manual*, 3<sup>rd</sup> Edition, Bi-Tech publishers, Ltd., Richmond, British Columbia, Canada.

Chernauskas, L.R., 1993. Dynamic Analysis of Plugged Piles in Clay. *Master of Science Thesis submitted to the Department of Civil Engineering*, University of Massachusetts-Lowell, 1993.

CIRIA 63, 1977. Rationalization of Safety and Serviceability Factors in Structural Codes. Construction Industry Research and Information Association, SWIP 3AU, Report 63, London.

Coyle, H. M. and Castello, R.R., 1981. New Design Correlations for Piles in Sand. *J. Geotech. Eng. Div.*, Proc. ASCE, Vol. 107, No. GT7, pp. 965-986.

Danish Geotechnical Institute, 1985. Code of Practice for Foundation Engineering. DGI Bulletin 36, 1 Maglebjergvej, DK-2800 Lyngby, Denmark.

Davisson, M.T., 1972. High Capacity Piles. *Proceedings, Soil Mechanics Lecture Series on Innovations in Foundation Construction*. American Society of Civil Engineers, Illinois Section, Chicago, pp. 81-112.

DeBeer, E.E., 1970. Proefondervindelijke bijdrage tot de studie van het grandsdraagvermogen van zand onder funderinger op staal. English version, *Geotechnique*, Vol. 20, No. 4, pp. 387-411.

DiMaggio, 2000. Personal Communication.

Drewry, J. M., Weidler, J. B. and Hwong, S. T., 1977. Predicting axial pile capacities for offshore platforms, *Petroleum Engineer*, Vol. 41.

Duncan, J.M., Tan, C.K., Barker, R.M., and Rojiani, K.B., 1989, Load and Resistance Factor Design of Bridge Structures. *In the Proceedings of the Symposium on Limit States Design in Foundation Engineering. Canadian Geotechnical Society Southern Ontario Section*, Toronto, May 26 - 27, pp. 47 - 63.

Ellingwood, B. and Galambos, T.V., 1982. Probability-Based Criteria for Structural Design, *Structural Safety*, 1, pp. 15-26.

Ellingwood, B., Galambos, T., MacGregor, J. and Cornell, C. 1980. Development of a Probability-Based Load Criterion for American National Standard A58. *National Bureau of Standards Publication 577*, Washington, DC.

Ellingwood, B., Galambos, T., MacGregor, J. and Cornell, C. 1982a. Probability Based Load Criteria - Assessment of Current Design Practices. *Journal of the Structural Division*, ASCE, Vol. 108, ST5, pp. 959-977.

Ellingwood, B., Galambos, T., MacGregor, J. and Cornell, C. 1982b. Probability Based Load Criteria - Load Factors and Load Combinations. *Journal of the Structural Division*, ASCE, Vol. 108, ST5, pp. 978-997.

Eurocode 7, 1993. *Geotechnical Design, General Rules*, European Committee for Standardization. Pre-standard. Danish Geotechnical Institute, Copenhagen.

Fellenius, H.B., 1989. Guidelines for the Interpretation and Analysis of the Static Loading Test. Deep Foundations Institute.

Fellenius, H.B., 1994. Limit States Design for Deep Foundations. *Proceedings, U.S. DOT International Conference on Deep Foundations*, Orlando, FL, December 1994, p. 12.

FHWA, 1988. FHWA Guide Specifications for Driven Piles. Federal Highway Administration.

Freudenthal, A.M. 1947. Safety of Structures. *Transactions of the ASCE*. Vol. 112, pp. 125-180.

Fox, E., 1932. Stress Phenomena Occurring in Pile Driving. *Engineering Journal*, London, England, Vol. 134.

Galambos, T.V., 1989. Present and Future Developments in Steel Design Codes, *Proceedings 5<sup>th</sup> International Conference on Structural Safety and Reliability*, Ang, A., et al. (eds.), ASCE, New York, pp. 2011-2018.

Galambos, T.V. and Ravindra, M.K. 1978. Properties of Steel for Use in LRFD. *Journal of Structural Engineering, ASCE*, Vol. 104, No. 9, pp. 1459-1468.

Gates, 1957. Empirical Formula for Predicting Pile Bearing Capacity. *Civil Engineering*, Vol. 27, No. 3, pp. 65-66.

Goble, G., 1999. Geotechnical Related Development and Implementation of Load and Resistance Factor Design (LRFD) Methods. *NCHRP Report 276*, Transportation Research Board, Washington, DC, pp. 10-36.

Goble, G. G., Likens, G., and Rausche, F., 1970. Dynamic Studies on the Bearing Capacity of Piles - Phase III, Report No. 48. *Division of Solid Mechanics, Structures, and Mechanical Design*. Case Western Reserve University.

Goble, G. G., Likens, G. and Rausche, F., 1975. Bearing Capacity of Piles from Dynamic Measurements, Final Report, Ohio Department of Transportation, Ohio DOT-05-75.

Goble, G.G., Rausche, F. and Likins, G., 1980. The Analysis of Pile-Driving: A State of the Art. *Proceedings from the 2<sup>nd</sup> Conference on the Application of Stress-Wave Theory on Piles*, Stockholm, Sweden, June 1980, pp. 1-34.

Goble, Rausche, Likens and Associates, Inc. (GRL), 1996. "Design and Construction of Driven Pile Foundations," Volume I, NHI Course Nos. 13221 and 13222, US Department of Transportation, Federal Highway Administration, Washington DC.

Goble, G.G., Scanlan, R.H. and Tomko, J.J., 1967. Dynamic Studies on the Bearing Capacity of Piles, Phase II. Vol. I and II, Case Institute of Technology.

Graff, K.F., 1975. Wave Motion in Elastic Solids. Ohio State University Press, Columbus, Ohio.

GRL, 1999. *Pile-Driving Analyzer, PAK Users Manual*. Goble, Rausche, Likins and Associates, Inc.

GTR, 1997. *Dynamic Pile Testing Report, Central Artery/Tunnel Project C07D2, I-90/Airport Interchange Arrivals Tunnel - Phase I, East Boston, MA*. Geosciences Testing and Research, Inc., North Chelmsford, MA.

GTR, 1998. *Dynamic Pile Testing Report, Central Artery/Tunnel Project C07D2, I-90/Airport Interchange Toll Plaza, East Boston, MA*. Geosciences Testing and Research, Inc., North Chelmsford, MA.

Guiffre, N. and Pinto, P.E., 1976. Discretization from a Level II Method, Information Bulletin No. 112, CIB Joint Committee on Structural Safety, Paris, France, pp. 158-189.

Hasofer, A.M. and Lind, N.C., 1974. An Exact and Invariant First-Order Reliability Format. *Journal of Engineering Mechanics*, ASCE, Vol. 100, No. EM1, pp. 111-121.

Hawrenek, R. and Rackwitz, R., 1976. Reliability Calculations for Steel Columns, Information Bulletin No. 112, CIB Joint Committee on Structural Safety, Paris, France, pp. 125-157.

Isaacs, D. 1931. Reinforced Concrete Pile Formula. *Transactions of the Institute of Engineers*, Australia, Vol. 12, pp. 312-323.

Kusakabe, Osamu, 1998. Foundation Design Standards in the World - Toward Performance-Based Design. *Japanese Geotechnical Society*, September 1998.

Kyfor, Z.G., Schnore, A.S., Carlo, T.A. and Baily, D.F., 1992. Static Testing of Deep Foundations. Report No. FHWA-SA-91-042, U.S. Department of Transportation, Federal Highway Administration, Office of Technology Applications, Washington DC., p. 174.

Lind, N.C., 1976. Application to Design of Level I Codes, Information Bulletin No. 112, CIB Joint Committee on Structural Safety, Paris, France, pp. 73-89.

Lotsberg, I., 1991. Target Reliability Index, A Literature Survey, Report No. 91-2023, A.S. Veritas Research, Norway.

Lowery, L.L., Hirsh, T.J., Edwards, T.C., Coyle, H.M. and Samson, C.H., 1969. Pile-Driving Analysis - State of the Art, Research Report 33-13 (Final). Texas Highway Department, Research Study No. 2-5-62-33.

Madsen, H.O., Krenk, S. and Lind, N.C., 1986. *Methods of Structural Safety*. Prentice Hall, Englewood Cliffs, New Jersey.

Mansour, A.E., Wirsching, P.H., Ayyub, B.M. and White, G.J., 1994. Probability Based Ship Design Implementation of Design Guidelines for Ships, Ship Structures Committee Draft Report, U.S. Coast Guard, Washington, D.C.

Mansur, C.I. and Hunter, A.H., 1970. Pile Tests - Arkansas River Project. *JSMFD*, ASCE, Vol. 96, SM 5, September, pp. 1545-1582.

Massachusetts Highway Department, (Section 940), 1995. Driven Piles. *1995 Standard Specifications for Highways and Bridges*, Metric Edition, pp. 257-271.

McClelland, B., Focht, J. A., & Emrich, W. J., 1969. Problems in Design and Installation of Offshore Piles. *JSMFD*, ASCE, Vol.95, SM6, pp. 1419-1514.

McVay, M., Birgisson, B., Zhang, L., Perez, A. and Putcha, S., 2000. Load and Resistance Factor Design (LRFD) for Driven Piles Using Dynamic Methods - A Florida Perspective. *Geotechnical Testing Journal*, ASTM, Vo. 23, No. 1, pp. 55-66.

McVay, M.C., Ching, K.L., and Singletary, W.A., 1998. Calibrating Resistance Factors in the Load and Resistance Factor Design for Florida Foundations. Final Report, Department of Civil Engineering, University of Florida, Submitted to the Florida Department of Transportation, December 1998.

Melchers, R.E., 1987. Structural Reliability Analysis and Prediction. Ellis Horwood Limited, UK

Meyerhof, G.G., 1956. Penetration Tests and Bearing Capacity of Cohesionless Soils. *JSMFD*, ASCE, Vol. 85, SM6, pp. 1-29.

Meyerhof, G.G., 1970. Safety Factors in Soil Mechanics. *Canadian Geotechnical Journal*, Vol. 7, No. 4, pp. 349-355.

Meyerhof, G.G., 1976. Bearing Capacity and Settlement of Pile Foundations. *J. Geotech, Div.*, ASCE, Vol. 102, No. GT 3, pp. 197-228.

Meyerhof, G.G., 1994, Evolution of Safety Factors and Geotechnical Limit State Design. *Spencer J. Buchanan Lecture, Texas A and M University*, Nov. 4, pp. 32

Moses, F., 1985. Implementation of a Reliability-Based API RP2A Format, Final Report. *API PRAC 83-22*. American Petroleum Institute.

Moses, F., 1986. Development of Preliminary Load and Resistance Factor Design Document for Fixed Offshore Platforms, Final Report. *API-PRAC 95-22*. American Petroleum Institute.

Moses, F. and Verma, D., 1987. Load Capacity Evaluation of Existing Bridges, NCHRP Report 301, Transportation Research Board, Washington, D.C.

National Research Council of Canada, 1977. *National Building Code of Canada*. Ottawa.

Nordic Building Code Committee, 1978. Recommendations for Loading and Safety Regulations for Structural Design, Report No. 36, Copenhagen, Denmark, p. 148.

Nottingham, L. and Schmertmann, J., 1975. An Investigation of Pile Capacity Design Procedures, Final Report D629 to Florida Department of Transportation from the Department of Civil Engineering, University of Florida, p. 159.

Nowak, A.S., 1993. Calibration of LRFD Bridge Design Code. Department of Civil and Environmental Engineering Report UMCE 92-25, University of Michigan, NCHRP 12-33.

Nowak, A.S., 1999. Calibration of LRFD Bridge Design Code. Department of Civil and Environmental Engineering Report UMCE 92-25. University of Michigan, NCHRP 12-33.

Olsen, R. and Flaate, K., 1967. Pile Driving Formulas for Friction Piles in Sand. *ASCE JSMFC*, Vol. 93, SM6, November 1967, pp. 279-297.

Ontario Ministry of Transportation and Communication, 1992. Ontario Highway Bridge Design Code and Commentary, 3<sup>rd</sup> ed.

O'Neill, Michael W., 1999. Personal Communication.

O'Neill, Michael W., 1995. LRFD Factors for Deep Foundations through Direct Experimentation. *In Proceedings of US/Taiwan Geotechnical Engineering Collaboration Workshop*. Sponsored by the National Science Foundation (USA) and the National Science Council (Taiwan, ROC) Taipei, January 1995, pp. 100 - 114.

Paikowsky, S., 1982. Use of Dynamic Measurements to Predict Pile Capacity Under Local Conditions. M.Sc. Thesis, Dept. of Civil Engineering Technion-Israel Institute of Technology.

Paikowsky, S., 1984. Use of Dynamic Measurements for Pile Analysis. Including PDAP-Pile-Driving Analysis Program, GZA Inc., Newton, MA.

Paikowsky, S., 1995. Using Dynamic Measurements for the Capacity Evaluation of Driven Piles. *Civil Engineering Practice, Journal of the Boston Society of Civil Engineers Section / ASCE*. Vol. 10, No. 2, pp. 61-76.

Paikowsky, S.G. and Chen, Y.L., 1998. Field and Laboratory Study of the Physical Characteristics and Engineering Parameters of the Subsurface at the Newbury Bridge Site. *Research Report submitted to the Massachusetts Highway Department, January 1998*, Boston, Massachusetts.

Paikowsky, S. and Chernauskas, L., 1992. Energy Approach for Capacity Evaluation of Driven Piles. *4<sup>th</sup> International Conference on the Application of Stress-Wave Theory to Piles*. The Hague, Netherlands, pp. 595-601.

Paikowsky, S. and Chernauskas, L., 1996. Soil Inertia and the Use of Pseudo Viscous Damping Parameters. *5<sup>th</sup> International Conference on the Application of Stress-Wave Theory to Piles*. Orlando, FL, pp. 203-216.

Paikowsky, S.G. and Hajduk, E.L., 1999. Design and Construction of an Instrumented Test Pile Cluster. *Research Report submitted to the Massachusetts Highway Department, Geotechnical Section, September 1999*, Boston, Massachusetts.

Paikowsky, S.G. and Hajduk, E.L., 2000. Theoretical Evaluation and Full Scale Field Testing Examination of Pile Capacity Gain with Time. *Research Report to be submitted to the Massachusetts Highway Department, December 2000*. Boston, MA.

Paikowsky, S. and Hart, L., 2000. Development and Field Testing of Multiple Deployment Model Pile (MDMP). *Research Report to be submitted to the Federal Highway Administration, April 2000*. FHWA-RD-99-194, Washington DC.

Paikowsky, S. and LaBelle, V. 1994. Examination of the Energy Approach for Capacity Evaluation of Driven Piles. *US FHWA International Conference on Design and Construction of Deep Foundations. December 6-8, 1994*. Orlando, FL. Vol. II, pp. 1133-1149.

Paikowsky, S., LaBelle, V. and Hourani, N., 1996. Dynamic Analyses and Time Dependent Pile Capacity. *5<sup>th</sup> International Conference on the Application of Stress-Wave Theory to Piles*. Orlando, FL, pp. 325-339.

Paikowsky, S., LaBelle, V. and Mynampaty, R., 1995. Static and Dynamic Time Dependent Pile Behavior. *Research Report submitted to the Massachusetts Highway Department, November 1995*. Boston, MA.

Paikowsky, S., Operstein, V. and Bachand, M., 1999. Express Method of Pile Testing by Static Cyclic Loading. *Research Report submitted to the Massachusetts Highway Department, October 1999*. Boston, MA.

Paikowsky, S. G., Regan, J. E., and McDowell, J. J., 1994. A Simplified Field Method for Capacity Evaluation of Driven Piles. *FHWA Report No. FHWA-RD-94-042, September 1994*. Washington DC.

Paikowsky, S.G. and Stenersen, K.L., 2000. The performance of the dynamic methods, their controlling parameters and deep foundation specifications. *6<sup>th</sup> International Conference on the Application of Stress-Wave Theory to Piles*. São Paulo, Brazil, September 2000, Editors; S. Niyama and J. Beim.

Paikowsky, S. and Whitman, R., 1990. The Effect of Plugging on Pile Performance and Design. *Canadian Geotechnical Journal*, Vol. 27, No. 4, pp. 429-440.

Paikowsky, S., Whitman, R. and Baligh, M., 1989. A New Look at the Phenomenon of Offshore Pile Plugging. *Marine Geotechnology*, Vol. 8, No. 3, pp. 213-230.

Payer, H.G., Huppmann, H., Jochum, C., Madsen, H.o.< Nittinger, K., Shibata, H., Wild, W., and Wingender, H. J., 1994. Plenary Panel Discussion on How Safe is Safe Enough? *Structural Safety and Reliability*, Schueller, Shinozuka and Yao (eds.), Balkema, Rotterdam, Netherlands, pp. 57-74.

PDA Manual, 1999. Pile Dynamics, Inc., Model PAK, Cleveland, Ohio.

Peck, R.P., Hanson, W.E., and Thornburn, T.H., 1974. *Foundation Engineering*, 2<sup>nd</sup> ed. John Wiley & Sons, Inc., New York.

Rausche, F., 2000. Personal Communication. February 2000.

Rausche, F., 2001. Personal Communication. February 2001.

Rausche, F., Goble, G. and Likens, G., 1975. Bearing Capacity of Piles from Dynamic Measurements, Final Report, Ohio Department of Transportation, Ohio DOT-05-75.

Ravindra, M.K. and Galambos, T.V., 1978. Load and Resistance Factor Design for Steel. *Journal of the Structural Division*, Proceedings of the American Society of Civil Engineers, New York, N.Y., Vol. 104, No. 9, pp. 1337-1354.

Ravindra, M.K., Heany, A.C. and Lind, N.C., 1969. Probabilistic Evaluation of Safety Factors, Final Report, Symposium on Concepts of Safety of Structures and Methods of Designs, IABSE, London, pp. 36-46.

Reed, D.A. and Brown, C.B., 1992. Reliability in the Context of Design, *Structural Safety*, 11, pp. 109-119.

Rosenblueth, E. and L. Esteva, 1972. Reliability Basis for Some Mexican Codes. *ACI Publication SP-31*, American Concrete Institute, Detroit, MI.

Ryan, T.P., 1989. Linear Regression. Chapter 13 of *Handbook of Statistical Methods for Engineers and Scientists*, H.M. Wadsworth, editor. McGraw-Hill.

Simpson, B., Pappin, J.W., and Croft, D.D. 1981. An Approach to Limit State Calculations in Geotechnics, *Ground Engineering*, Vol. 14(6): pp. 21 - 28.

Siu, W.W.C., Parimi, S.R., and Lind, N.C., 1975. Practical Approach to Code Calibration. *Journal of the Structural Division*. ASCE, Vol. 101, No. ST7, pp. 1469-1480.



Smith, E., 1960. Pile Driving Analysis by the Wave Equation. *Journal of Soil Mechanics and Foundations, American Society of Civil Engineers*, August 1960, pp. 35-61.

Standards Association of Australia, 1995. Australian Standards, Piling-Design and Installation. Homebush, NSW.

Tang, W.H., Woodford, D.L. and Pelletier, J.J., 1990. Performance Reliability of Offshore Pile. *22<sup>nd</sup> Annual Offshore Technology Conference*, Paper No. OTC 6379, Houston, TX.

Taylor, D.W., 1948. *Fundamentals of Soil Mechanics*. John Wiley & Sons, New York, p. 700.

Terzaghi, K., 1942. Discussion of the Progress Report of the Committee on the Bearing Value of Pile Foundations. *Proceedings, ASCE*. Vol. 68, pp. 311-323.

The Massachusetts State Building Code, (Section 1213.0), 1996. Pile Foundations. *The Massachusetts Building Code 5<sup>th</sup> Edition*, 780 CMR, pp. 14-25.

Thoft-Christensen, P. and Baker, M.J., 1982. Structural Reliability Theory and Its Application. Springer-Verlag, New York.

Veneziano, D., 1993. Personal Communication.

Vesic, A. S., 1965. Ultimate Loads and Settlements of Deep Foundations in Sands. *Proceedings of the Symposium on Bearing Capacity and Settlement of Foundations*. Duke University, Durham, NC, pp. 53-68.

Vesic, A. S., 1977. Design of Pile Foundations. Transportation Research Board, National Research Council, Washington, DC.

Vijayvergiya, V. N. and Focht Jr., J. A., 1972. A new way to predict capacity of piles in clay. *Proceedings, 4<sup>th</sup> Offshore Technology Conference*, Houston, TX, Vol. 2, pp. 856-874.

Wellington, 1892. Discussion of "the Iron Wharf at Fort Monroe, VA." By J.B. Cuncklee. *Transactions, ASCE* Vol. 27, paper No. 543, August 1892, pp. 129-137.

Wirsching, P.H., 1984. Fatigue Reliability for Offshore Structures. *Journal of Structural Engineering*, American Society of Civil Engineers, New York, Vol. 110, No. 10, pp. 2340-2356.

Withiam, J. L., Voytko, E.P., Barker, R.M., Duncan, M.J., Kelly, B.C., Musser, S.C. and Elias, V., 1997. Load and Resistance Factor Design (LRFD) of Highway Bridge Substructures. Washington D.C.: U.S. DOT Federal Highway Administration.

Withiam, J. L., Voytko, E.P., Barker, R.M., Duncan, M.J., Kelly, B.C., Musser, S.C. and Elias, V., 1998. Load and Resistance Factor Design (LRFD) of Highway Bridge Substructures. *FHWA Publication No. HI-98-032*, July 1998. Washington D.C.

Wu, T.H., Tang, W.H., Sangrey, D.A. and Baecher, G.B., 1989. Reliability of Offshore Foundations - State of the Art. *Journal of Geotechnical Engineering*, ASCE, Vol. 115, No. 2, pp. 157-178.

Yoon, Gil and O'Neill, Michael, 1997. Resistance Factors for Single Driven Piles from Experiments. Transportation Research Board, 76<sup>th</sup> Annual Meeting, January 12-16. Washington DC.

NCHRP 24-17

**LOAD AND RESISTANCE FACTOR DESIGN  
(LRFD) FOR DEEP FOUNDATIONS**

**APPENDIX B  
LOAD AND RESISTANCE FACTOR DESIGN (LRFD)  
FOR DYNAMIC ANALYSES OF DRIVEN PILES  
APPENDICES A - D**

Prepared for  
National Cooperative Highway Research Program  
Transportation Research Board  
National Research Council

Samuel G. Paikowsky and Kirk L. Stenerson  
Geotechnical Engineering Research Laboratory  
Department of Civil and Environmental Engineering  
University of Massachusetts  
Lowell, Massachusetts

July 2002

### **ACKNOWLEDGEMENT OF SPONSORSHIP**

This work was sponsored by the American Association of State Highway and Transportation Officials, in cooperation with the Federal Highway Administration, and was conducted in the National Cooperative Highway Research Program, which is administered by the Transportation Research Board of the National Research Council.

### **DISCLAIMER**

This is an uncorrected draft as submitted by the research agency. The opinions and conclusions expressed or implied in the report are those of the research agency. They are not necessarily those of the Transportation Research Board, the National Research Council, the Federal Highway Administration, the American Association of State Highway and Transportation Officials, or the individual states participating in the National Cooperative Highway Research Program.

## **APPENDIX A**

### **RELEVANT INFORMATION FROM DATABASES**

**Table A.1.** Relevant Information Pertaining to Database PD/LT2000.

No.	Pile-Case Number	Refer. No.	Location	Pile Type	Pile Area	Length Below Gauges	Penetr Depth	Area Ratio	Soil Type	
					(mm <sup>2</sup> )	(m)	(m)	AR	Side	Tip
1	FN1-EOD	I-480	Omaha NE	HP10x42	8000	21.95	21.95	4102	silty clay	till
2	FN1-BOR1	I-480	Omaha NE	HP10x42	8000	21.95	21.98	4108	silty clay	till
3	FN1-BOR2	I-480	Omaha NE	HP10x42	8000	21.95	22.25	4159	silty clay	till
4	FN2-EOD	I-480	Omaha NE	PSC12"sq	92903	18.90	19.81	260	silty clay	till
5	FN2-BOR	I-480	Omaha NE	PSC12"sq	92903	18.90	19.81	260	silty clay	till
6	FN3-EOD	I-480	Omaha NE	PSC14"sq	126451	18.90	17.07	165	silty clay	till
7	FN3-BOR	I-480	Omaha NE	PSC14"sq	126451	18.90	17.07	165	silty clay	till
8	FN4-EOD	I-480	Omaha NE	CEP12.75"	12387	20.12	20.12	248	silty clay	till
9	FN4-BOR	I-480	Omaha NE	CEP12.75"	12387	20.12	20.12	248	silty clay	till
10	FIA-EOD	Site 1	Iowa	HP14x89	16839	35.81	34.78	4470	clayey sand	sand
11	FIA-BOR	Site 1	Iowa	HP14x89	16839	35.81	34.78	4470	clayey sand	sand
12	FIB-EOD	Site 1	Iowa	CEP 14"	13677	29.72	28.68	323	clayey sand	sand
13	FIB-BOR	Site 1	Iowa	CEP 14"	13677	29.72	28.68	323	clayey sand	sand
14	FO1-EOD	Cim S-1	Oklahoma	CEP 26"	43677	18.38	18.35	111	silty sand	silty sand
15	FO1-BOR	Cim S-1	Oklahoma	CEP 26"	43677	18.38	18.35	111	silty sand	silty sand
16	FO2-EOD	Cim S-1	Oklahoma	PSC24"oct	303806	18.75	19.20	128	silty sand	silty sand
17	FO2-BOR	Cim S-1	Oklahoma	PSC24"oct	303806	18.75	19.23	128	silty sand	silty sand
18	FO3-EOD	Cim S-2	Oklahoma	HP14x117	22194	33.53	19.42	1919	sa-si-clay	clayey sand
19	FO4-EOD	Cim S-2	Oklahoma	RC24"sq	371612	18.38	13.72	90	sa-si-clay	clayey sand
20	FO4-BOR	Cim S-2	Oklahoma	RC24"sq	371612	18.38	17.01	112	sa-si-clay	clayey sand
21	FOR1-EOD	Alsea	Oregon	PSC20"sq	253548	39.93	38.25	307	sand & silt	siltstone
22	FOR1-BOR	Alsea	Oregon	PSC20"sq	253548	39.93	38.28	307	sand & silt	siltstone
23	FM5-EOD	Site A	Maine	CEP 18"	17742	35.75	30.18	264	clay & sand	sand
24	FM5-BOR	Site A	Maine	CEP 18"	17742	30.78	30.21	264	clay & sand	sand
25	FM17-EOD	Site B	Maine	CEP 18"	17742	23.71	21.67	190	till	till

**Table A.1 (con't). Relevant Information Pertaining to Database PD/LT2000.**

No.	Pile-Case Number	Refer. No.	Location	Pile Type	Pile Area	Length Below Gauges	Penetr Depth	Area Ratio	Soil Type	
					(mm <sup>2</sup> )	(m)	(m)	AR	Side	Tip
26	FM17-BOR	Site B	Maine	CEP 18"	17742	23.71	21.73	190	till	till
27	FM23-EOD	Site B	Maine	CEP 18"	17742	17.31	15.45	135	till	till
28	FM23-BOR	Site B	Maine	CEP 18"	17742	17.31	15.48	135	till	till
29	FC1-EOD	Crook	Colorado	CEP12.75"	6335	10.21	10.21	126	sand	sand
30	FC1-BOR	Crook	Colorado	CEP12.75"	6335	10.21	10.33	128	sand	sand
31	FC2-EOD	Crook	Colorado	CEP12.75"	6335	8.38	8.08	100	sand	sand
32	FC2-BOR	Crook	Colorado	CEP12.75"	6335	8.38	8.20	101	sand	sand
33	FMI1-EOD	Rt. 115	Missouri	CEP 14"	10387	25.30	25.30	285	sand-gravel	sand
34	FMI1-BOR	Rt. 115	Missouri	CEP 14"	10387	25.30	25.33	285	sand-gravel	sand
35	FMI2-EOD	Rt. 115	Missouri	CEP 14"	10387	18.75	18.59	209	sand-gravel	sand
36	FMI2-BOR	Rt. 115	Missouri	CEP 14"	10387	18.75	18.59	209	sand-gravel	sand
37	FWA-EOD	3rd lake	Washingtn	CEP 48"	71806	46.33	7.56	25	till-gravel	till
38	FWA-BOR	3rd lake	Washingtn	CEP 48"	71806	46.33	7.59	25	till-gravel	till
39	FWB-EOD	3rd lake	Washingtn	CEP 48"	71806	42.67	33.22	109	till-gravel	till
40	FWB-BOR	3rd lake	Washingtn	CEP 48"	71806	42.67	33.31	109	till-gravel	till
41	FA1-EOD	I-165	Alabama	PSC 18"sq	209032	19.20	19.51	171	silty sand	silty sand
42	FA1-BOR1	I-165	Alabama	PSC 18"sq	209032	19.20	19.66	172	silty sand	silty sand
43	FA1-BOR2	I-165	Alabama	PSC 18"sq	209032	19.20	19.75	173	silty sand	silty sand
44	FA2-EOD	I-165	Alabama	PSC 18"sq	209032	22.25	22.86	200	silty sand	silty sand
45	FA2-BOR1	I-165	Alabama	PSC 18"sq	209032	22.25	22.95	201	silty sand	silty sand
46	FA2-BOR2	I-165	Alabama	PSC 18"sq	209032	22.25	23.01	201	silty sand	silty sand
47	FA3-EOD	I-165	Alabama	PSC 24"sq	315483	19.20	19.51	151	silty sand	silty sand
48	FA3-BOR1	I-165	Alabama	PSC 24"sq	315483	19.20	19.54	151	silty sand	silty sand
49	FA3-BOR2	I-165	Alabama	PSC 24"sq	315483	19.20	19.66	152	silty sand	silty sand
50	FA4-EOD	I-165	Alabama	PSC 24"sq	315483	22.25	22.86	177	silty sand	silty sand

**Table A.1 (con't).** Relevant Information Pertaining to Database PD/LT2000.

No.	Pile-Case Number	Refer. No.	Location	Pile Type	Pile Area	Length Below Gauges	Penetr Depth	Area Ratio	Soil Type	
					(mm <sup>2</sup> )	(m)	(m)	AR	Side	Tip
51	FA4-BOR1	I-165	Alabama	PSC 24"sq	315483	22.25	22.89	177	silty sand	silty sand
52	FA4-BOR2	I-165	Alabama	PSC 24"sq	315483	22.25	22.92	177	silty sand	silty sand
53	FA5-EOD	I-165	Alabama	PSC 36"sq	579354	21.34	22.25	140	silty sand	silty sand
54	FA5-BOR	I-165	Alabama	PSC 36"sq	579354	21.34	22.28	141	silty sand	silty sand
55	FV15-EOD	WRJ	Vermont	HP14x73	13806	28.04	22.86	3556	silt-d.sand	sand gravel
56	FV15-BOR	WRJ	Vermont	HP14x73	13806	28.04	23.10	3594	silt-d.sand	sand gravel
57	FV10-EOD	WRJ	Vermont	HP14x73	13806	28.04	27.43	4267	silt-d.sand	sand gravel
58	FV10-BOR	WRJ	Vermont	HP14x73	13806	28.04	27.55	4286	silt-d.sand	sand gravel
59	FMN2-EOD	Rt. 18	Minnesota	HP14x73	13806	29.57	29.26	4551	sa-si-clay	fat clay
60	FMN2-BOR	Rt. 18	Minnesota	HP14x73	13806	29.57	29.29	4556	sa-si-clay	fat clay
61	FP5-EOD	Tioga	Penn.	Monotube	4516	10.52	7.19	202	sandy grvl	sandy grvl
62	FP5-BOR	Tioga	Penn.	Monotube	4516	10.52	7.25	204	sandy grvl	sandy grvl
63	FKG-EOD	Rt.27	Kentucky	PSC14"sq	126451	21.95	10.58	119	soft clay	dense
64	FKG-BOR	Rt.27	Kentucky	PSC14"sq	126451	21.95	10.58	119	soft clay	dense
65	FL3-EOD	Rt.415	Louisiana	PSC24"sq	298709	30.48	25.69	210	silty clay	silty sand
66	FL3-BOR1	Rt.415	Louisiana	PSC24"sq	298709	30.48	25.69	210	silty clay	silty sand
67	FL3-BOR2	Rt.415	Louisiana	PSC24"sq	298709	30.48	25.69	210	silty clay	silty sand
68	CA1-EOD	Site C-L	O.S. Ont	CEP 9.6"	9948	52.43	47.03	771	si-sa-clay	si-sa-till
69	CA1-BOR	Site C-L	O.S. Ont	CEP 9.6"	9948	52.43	47.03	771	si-sa-clay	si-sa-till
70	CA2-BOR	Site C-L	O.S. Ont	CEP 9.6"	9948	34.29	33.56	550	si-sa-clay	si-sa-clay
71	CA5-BOR1	Site A	N.Y. Ont	CEP11.73"	7729	20.42	19.26	259	fill-sand	sand
72	CA5-BOR2	Site A	N.Y. Ont	CEP11.73"	7729	20.42	19.99	268	fill-sand	sand
73	CA3/8-BOR	Marina	Bar. Ont	CEP10.24"	5639	22.49	19.63	302	sand-silt	silt
74	CA24-BOR	Site D	Tor. Ont	CEP12.75"	9381	11.77	11.77	145	sand	sand
75	CA6-BOR1	Site E	Ham. Ont	CEP12.75"	9381	18.35	16.46	203	sa-si-till	silt-till



**Table A.1 (con't).** Relevant Information Pertaining to Database PD/LT2000.

No.	Pile-Case Number	Refer. No.	Location	Pile Type	Pile Area  (mm <sup>2</sup> )	Length Below Gauges (m)	Penetr Depth (m)	Area Ratio  AR	Soil Type	
									Side	Tip
76	CA6-BOR2	Site E	Ham. Ont	CEP12.75"	9381	18.35	16.46	203	sa-si-till	silt-till
77	CA6-EOR	Site E	Ham. Ont	CEP12.75"	8742	18.35	16.46	203	sa-si-till	silt-till
78	WC3-EOD	White	Florida	PSC24"sq	371612	14.75	8.32	55	ls.-d.sand	dense
79	WC3-BOR1	White	Florida	PSC24"sq	371612	14.75	8.38	55	ls.-d.sand	dense
80	WC3-BOR2	White	Florida	PSC24"sq	371612	11.43	8.38	55	ls.-d.sand	dense
81	WC6-EOD	White	Florida	PSC24"sq	371612	12.04	8.63	57	ls.-d.sand	dense
82	WC6-BOR1	White	Florida	PSC24"sq	371612	12.04	8.69	57	ls.-d.sand	dense
83	WC6-BOR2	White	Florida	PSC24"sq	371612	8.53	8.38	55	ls.-d.sand	dense
84	WB9-BOR	West	Florida	PSC30"sq	416451	39.62	39.17	287	clayey sand	clayey
85	WB15-BOR	West	Florida	PSC30"sq	416451	32.00	31.58	231	sand	silt-clay
86	T1/A-EOD	offshore	Israel	OEP 60"	136774	42.21	16.09	563	clcr sand	sand
87	T1/A-ALT	offshore	Israel	OEP 60"	136774	53.00	16.40	574	clcr sand	sand
88	T1/B-EOD	offshore	Israel	OEP 60"	136774	65.90	31.00	1085	clcr sand	sand
89	T2/A-EOD	offshore	Israel	OEP 48"	71826	35.69	16.00	853	clcr sand	sand
90	T2/B-EOD	offshore	Israel	OEP 48"	71826	79.40	55.50	2960	clcr sand	sand
91	35-1-BOR	C.N.R.	Toronto	HP12x74	14064	18.32	14.78	1920	cl-sa-silt	silty sand
92	35-4-BOR	C.N.R.	Toronto	CEP12.75"	6323	15.91	14.69	181	cl-sa-silt	silty sand
93	35-5-BOR	C.N.R.	Toronto	HP12x74	14064	30.54	27.58	3582	cl-sa-silt	silty sand
94	35-6-BOR	C.N.R.	Toronto	CEP12.75"	6323	32.13	27.43	339	cl-sa-silt	silty sand
95	35-7-BOR	C.N.R.	Toronto	T.Timber	101290	13.53	12.68	284	cl-sa-silt	silty sand
96	35-10-BOR	C.N.R.	Toronto	PSC 12"sq	92903	15.24	14.63	192	cl-sa-silt	silty sand
97	E2-BOR	DFI	Raleigh	PSC 12"sq	92903	13.26	13.56	178	cl-sa-silt	cl-sa-silt
98	63S-BOR	Mahonig	Penn.	HP12x53	10000	20.97	20.12	3621	sand-silt	silt
99	LB21-BOR	Site A	NA	PSC 20"sq	258064	10.97	10.97	86	silt-sand	silt-sand
100	LB20-BOR	Site B	NA	PSC 20"sq	258064	15.54	16.76	132	sand	sand

**Table A.1 (con't).** Relevant Information Pertaining to Database PD/LT2000.

No.	Pile-Case Number	Refer. No.	Location	Pile Type	Pile Area	Length Below Gauges	Penetr Depth	Area Ratio	Soil Type	
					(mm <sup>2</sup> )	(m)	(m)	AR	Side	Tip
101	LC3-BOR	Site C	NA	PSC 20"sq	258064	35.05	26.21	206	cl-sa-silt	cl-sa-silt
102	LIN16-BOR	Site D	NA	PSC 20"sq	258064	47.24	28.65	226	cl-sa-silt	cl-sa-silt
103	LE37-BOR	Site E	NA	PSC 10"sq	64516	18.29	15.24	240	cl-sa-silt	limestone
104	LE64-BOR	Site F	NA	PSC 10"sq	64516	18.29	17.68	278	cl-sa-silt	sa-cl-silt
105	ST1-EOD	Site H	Florida	PSC 18"sq	209032	20.12	13.41	117	-	carb sand
106	ST2-EOD	Site P	Florida	PSC 18"sq	209032	18.90	12.19	107	-	carb sand
107	ST9-BOR	I-664	Virginia	PSC 54"sq	496773	39.93	33.22	367	-	silt-clay
108	ST46-EOD	Castletn	New York	CEP 10"	3742	12.19	11.58	182	silt-sand	silt-sand
109	GZA3-EOD	Civic	Prov. RI	CEP13.38"	13097	43.59	38.25	451	silt-sand	gr-sa-silt
110	GZA5-EOD	Civic	Prov. RI	CEP 9.75"	10000	42.06	28.59	462	silt-sand	till-shale
111	GZA6-EOD	Civic	Prov. RI	CEP 9.75"	10000	52.12	47.55	768	silt-sand	gr-sa-silt
112	GZBBC-EOD	Civic	Prov. RI	CEP 10"	11871	35.36	30.33	478	silt-sand	silt
113	GZBP2-EOD	Civic	Prov. RI	CEP13.38"	13097	43.80	32.31	380	silt-sand	gr-sa-silt
114	GZB6-EOD	Civic	Prov. RI	CEP13.38"	13097	29.57	28.13	331	silt-sand	si-sa-till
115	GZZ5-EOD	Deer Is.	Boston MA	CEP 14"	13677	26.52	26.52	298	till-clay	till
116	GZO5-EOD	Deer Is.	Boston MA	CEP 14"	13677	26.52	16.46	185	till-clay	till
117	GZCC5-EOD	Deer Is.	Boston MA	CEP 14"	13677	35.66	24.38	274	till-clay	till
118	GZL2-EOD	Deer Is.	Boston MA	CEP 14"	13677	35.66	25.30	285	till-clay	till
119	GZP14-EOD	Deer Is.	Boston MA	CEP 14"	13677	32.00	18.44	207	till-clay	till
120	GZP11-EOD	Deer Is.	Boston MA	CEP 14"	13677	32.00	17.22	194	till-clay	till
121	GZP12-EOD	Deer Is.	Boston MA	CEP 14"	13677	35.20	21.03	237	till-clay	till
122	GZB22-EOD	NWS	Colt Neck	OEP 36"	34839	42.06	35.97	2966	sand-clay	silt-clay
123	GZW1-EOR	Water	Vermont	CP12.75"	9419	38.40	30.33	375	silty sand	sand
124	A54-EOD	HICC	Australia	RC10.8"sq	75626	20.70	20.60	299	silty clay	clay
125	A54-BOR	HICC	Australia	RC10.8"sq	75626	20.70	20.60	299	silty clay	clay

**Table A.1 (con't).** Relevant Information Pertaining to Database PD/LT2000.

No.	Pile-Case Number	Refer. No.	Location	Pile Type	Pile Area  (mm <sup>2</sup> )	Length Below Gauges  (m)	Penetr Depth  (m)	Area Ratio  AR	Soil Type	
									Side	Tip
126	A147-EOD	HICC	Australia	RC10.8"sq	75626	20.70	20.60	299	silty clay	clay
127	A147-BOR	HICC	Australia	RC10.8"sq	75626	20.70	20.60	299	silty clay	clay
128	GF19-EOD	Site 1	Pgh. PA	HP10x42	7935	17.83	15.09	2843	grvl-snd-slt	shale
129	GF110-EOD	Site 1	Pgh. PA	HP12x74	14000	17.37	15.15	1976	grvl-snd-slt	shale
130	GF222-EOD	Site 2	Pgh. PA	HP12x74	14000	20.42	18.62	2430	grvl-snd-slt	shale
131	GF224-EOD	Site 2	Pgh. PA	Monotube	6258	16.15	9.02	270	grvl-snd-slt	grvl-snd-slt
132	GF312-EOD	Site 3	Pgh. PA	HP12x74	14000	10.06	8.60	1121	snd-grvl-shl	shale
133	GF313-EOD	Site 3	Pgh. PA	HP10x57	10774	10.67	9.60	1352	snd-grvl-shl	claystone
134	GF412-EOD	Site 4	Pgh. PA	HP12x74	14000	14.78	10.24	1336	grvl-snd-slt	claystone
135	GF413-EOD	Site 4	Pgh. PA	HP10x57	10774	10.42	10.55	1486	grvl-snd-slt	claystone
136	GF414-EOD	Site 4	Pgh. PA	HP10x57	10774	14.48	10.58	1490	grvl-snd-slt	claystone
137	GF415-EOD	Site 4	Pgh. PA	HP12x74	14000	14.48	10.39	1356	grvl-snd-slt	claystone
138	EF62-EOD	Ottawa	Canada	CP 9.625"	10026	-	18.99	311	si-sa-clay	till
139	EF167-BOR	Ottawa	Canada	CP 9.625"	10026	-	21.00	343	si-sa-clay	till
140	A3-EOD2	Apalach	Florida	VC 24"sq	298645	28.65	27.52	225	clayey sand	sand
141	A3-BOR2	Apalach	Florida	VC 24"sq	298645	28.65	27.55	225	clayey sand	sand
142	A3-BOR3	Apalach	Florida	VC 24"sq	298645	27.22	27.61	225	clayey sand	clayey sand
143	A14-DD1	Apalach	Florida	VC 24"sq	298645	32.61	13.72	112	sandy clay	sand
144	A14-DD2	Apalach	Florida	VC 24"sq	298645	32.61	14.33	117	sandy clay	sand
145	A14-BOR1	Apalach	Florida	VC 24"sq	298645	32.61	17.83	146	clayey sand	sand
146	A14-BOR2	Apalach	Florida	VC 24"sq	298645	22.86	17.92	82	clayey sand	sand
147	A25-EOD	Apalach	Florida	VC 24"sq	298645	32.31	16.79	137	clayey sand	sand
148	A25-BOR1	Apalach	Florida	VC 24"sq	298645	32.31	16.82	137	clayey sand	sand
149	A25-BOR2	Apalach	Florida	VC 24"sq	298645	18.07	16.89	138	clayey sand	sand
150	A25-BOR3	Apalach	Florida	VC 24"sq	298645	18.07	16.92	138	clayey sand	sand

**Table A.1 (con't).** Relevant Information Pertaining to Database PD/LT2000.

No.	Pile-Case Number	Refer. No.	Location	Pile Type	Pile Area	Length Below Gauges	Penetr Depth	Area Ratio	Soil Type	
					(mm <sup>2</sup> )	(m)	(m)	AR	Side	Tip
151	A16-EOD	Apalach	Florida	PSC18"sq	209032	19.81	18.47	162	sandy clay	sand
152	A16-BOR1	Apalach	Florida	PSC18"sq	209032	19.81	18.47	162	sandy clay	sand
153	A16-BOR2	Apalach	Florida	PSC18"sq	209032	18.96	18.59	163	sandy clay	sand
154	A41-EOD	Apalach	Florida	VC 24"sq	298645	27.74	15.85	129	clay	sand
155	A41-BOR1	Apalach	Florida	VC 24"sq	298645	27.74	15.85	129	clay	sand
156	A41-BOR2	Apalach	Florida	VC 24"sq	298645	18.75	16.09	131	clay	sand
157	A101-EOD	Apalach	Florida	VC 24"sq	298645	26.82	18.84	154	clay	clayey sand
158	A101-BOR1	Apalach	Florida	VC 24"sq	298645	26.82	18.84	154	clay	clayey sand
159	A101-BOR2	Apalach	Florida	VC 24"sq	298645	21.79	18.93	155	clay	clayey sand
160	A133-EOD	Apalach	Florida	VC 24"sq	298645	39.62	31.67	259	clayey sand	sandy clay
161	A133-BOR	Apalach	Florida	VC 24"sq	298645	35.27	31.97	261	clayey sand	sandy clay
162	A145-EOD	Apalach	Florida	VC 24"sq	298645	40.23	31.36	256	clayey sand	sand
163	A145-BOR1	Apalach	Florida	VC 24"sq	298645	40.23	31.36	256	clayey sand	sand
164	A145-BOR2	Apalach	Florida	VC 24"sq	298645	35.08	31.39	256	clayey sand	sand
165	CB3-BOR	Choctw	Florida	PSC24"sq	371612	23.74	23.47	154	clayey sand	sand
166	CB3-BORL	Choctw	Florida	PSC24"sq	371612	24.35	23.71	156	clayey sand	sand
167	CB5-BOR	Choctw	Florida	VC 30"sq	416470	26.52	16.18	118	clayey sand	sand
168	CB5-BORL	Choctw	Florida	VC 30"sq	416470	18.62	16.46	120	clayey sand	sandy clay
169	CB11-BORL	Choctw	Florida	VC 30"sq	416470	29.75	26.12	191	clayey sand	clayey sand
170	CB11-EORL	Choctw	Florida	VC 30"sq	416470	29.75	26.15	191	clayey sand	clayey sand
171	CB17-BOR1	Choctw	Florida	VC 30"sq	416470	29.57	23.68	173	clayey sand	clayey sand
172	CB17-BOR2	Choctw	Florida	VC 30"sq	416470	29.57	23.71	174	clayey sand	clayey sand
173	CB17-BORL	Choctw	Florida	VC 30"sq	416470	27.43	23.74	174	clayey sand	clayey sand
174	CB17-DRL	Choctw	Florida	VC 30"sq	416470	27.43	23.84	174	clayey sand	clayey sand
175	CB23-BOR	Choctw	Florida	VC 30"sq	416470	29.26	24.48	179	clayey sand	sand

**Table A.1 (con't). Relevant Information Pertaining to Database PD/LT2000.**

No.	Pile-Case Number	Refer. No.	Location	Pile Type	Pile Area  (mm <sup>2</sup> )	Length Below Gauges  (m)	Penetr Depth  (m)	Area Ratio  AR	Soil Type	
									Side	Tip
176	CB23-BORL	Choctw	Florida	VC 30"sq	416470	29.26	25.21	184	clayey sand	sand
177	CB29-BORL	Choctw	Florida	VC 30"sq	416470	28.99	25.76	188	clayey sand	clayey sand
178	CB29-EORL	Choctw	Florida	VC 30"sq	416470	28.99	25.76	188	clayey sand	clayey sand
179	CB35-BOR1	Choctw	Florida	VC 30"sq	416470	29.60	23.93	175	clayey sand	clayey sand
180	CB35-BOR2	Choctw	Florida	VC 30"sq	416470	29.60	24.05	176	clayey sand	clayey sand
181	CB35-BORL	Choctw	Florida	VC 30"sq	416470	27.16	24.11	176	clayey sand	clayey sand
182	CB41-EOR	Choctw	Florida	VC 30"sq	416470	31.18	19.72	144	sandy clay	sandy clay
183	CB41-BOR	Choctw	Florida	VC 30"sq	416470	30.88	19.72	144	sandy clay	sandy clay
184	CB41-BORL	Choctw	Florida	VC 30"sq	416470	24.08	19.93	146	sandy clay	sandy clay
185	CB26-EOD	Choctw	Florida	PSC24"sq	371612	24.41	19.05	125	clayey sand	sand
186	CB26-BOR	Choctw	Florida	PSC24"sq	371612	24.41	19.08	125	clayey sand	sand
187	CB26-EOR	Choctw	Florida	PSC24"sq	371612	24.41	19.75	130	clayey sand	sandy clay
188	CB26-BOR2	Choctw	Florida	PSC24"sq	371612	19.81	19.81	130	sandy clay	sandy clay
189	33P1-EOD	Site P	Ontario	HP 12x74	14064	36.85	34.87	4528	cl-sa-silt	silty sand
190	33P1-BOR	Site P	Ontario	HP 12x74	14064	36.85	34.87	4528	cl-sa-silt	silty sand
191	33P1-EOR	Site P	Ontario	HP 12x74	14064	36.85	34.87	4528	cl-sa-silt	silty sand
192	33P2-EOD	Site P	Ontario	CP 12.75"	6323	45.60	32.67	404	cl-sa-silt	silty sand
193	33P2-BOR	Site P	Ontario	CP 12.75"	6323	33.83	32.67	404	cl-sa-silt	silty sand
194	33P2-EOR	Site P	Ontario	CP 12.75"	6323	33.83	32.67	404	cl-sa-silt	silty sand
195	33P4-EOD	Site P	Ontario	PSC 12"sq	92903	19.81	16.52	217	cl-sa-silt	cl-silt-till
196	33P5-EOD	Site P	Ontario	#14 Timber	93484	13.11	8.66	123	cl-sa-silt	cl-silt-till
197	TRD22-EOD	Site R	Ontario	HP 12x74	14064	6.86	6.13	796	sand	till
198	TRD22-BOR	Site R	Ontario	HP 12x74	14064	6.86	6.13	796	sand	till
199	TRE22-EOD	Site R	Ontario	HP 12x74	14064	9.14	7.83	1017	sand	rock
200	TRE22-BOR	Site R	Ontario	HP 12x74	14064	9.14	7.83	1017	sand	rock

**Table A.1 (con't).** Relevant Information Pertaining to Database PD/LT2000.

No.	Pile-Case Number	Refer. No.	Location	Pile Type	Pile Area	Length Below Gauges	Penetr Depth	Area Ratio	Soil Type	
					(mm <sup>2</sup> )	(m)	(m)	AR	Side	Tip
201	TRP5X-EOD	Site R	Ontario	HP 12x53	10064	7.62	7.68	1374	sand	rock
202	TRP5X-BOR	Site R	Ontario	HP 12x53	10064	7.62	7.68	1374	sand	rock
203	TR131-BOR	Site R	Ontario	CP 7.063"	5097	8.17	NA	183	sand	rock
204	TRAH-EOR	Site S	Brunswick	HP 12x89	17097	42.06	38.40	4279	clayey silt	sandy gravel
205	TRBH-BOR	Site S	Brunswick	HP 12x89	17097	34.84	31.12	3468	clayey silt	sandy gravel
206	TRBP-EOR	Site S	Brunswick	CP 12.75"	8000	33.53	31.70	391	clayey silt	sandy gravel
207	CHA1-EOD	Jones Is.	Wisconsin	CEP 12.75"	9419	42.00	37.49	4048	sa-si clay	silty sand
208	CHA1-BOR1	Jones Is.	Wisconsin	CEP 12.75"	9419	42.00	37.52	4052	sa-si clay	silty sand
209	CHA1-BOR2	Jones Is.	Wisconsin	CEP 12.75"	9419	42.25	37.52	4053	sa-si clay	silty sand
210	CHA4-EOD	Jones Is.	Wisconsin	CEP 12.75"	9419	37.64	35.66	3852	sa-si clay	silty sand
211	CHB2-EOD	Jones Is.	Wisconsin	HP12x63	11871	47.95	47.34	7224	sa-si clay	silty sand
212	CHB2-BOR1	Jones Is.	Wisconsin	HP12x63	11871	47.95	47.34	7224	sa-si clay	silty sand
213	CHB2-BOR3	Jones Is.	Wisconsin	HP12x63	11871	47.95	47.40	7236	sa-si clay	silty sand
214	CHB2-BOR4	Jones Is.	Wisconsin	HP12x63	11871	47.67	47.43	7240	sa-si clay	silty sand
215	CHB2-BOR5a	Jones Is.	Wisconsin	HP12x63	11871	46.45	47.46	7245	sa-si clay	silty sand
216	CHB2-BOR5b	Jones Is.	Wisconsin	HP12x63	11871	46.45	47.46	7245	sa-si clay	silty sand
217	CHB3-EOD	Jones Is.	Wisconsin	HP12x63	11871	44.10	43.31	6611	sa-si clay	silty sand
218	CHB3-BOR1	Jones Is.	Wisconsin	HP12x63	11871	44.10	43.31	6611	sa-si clay	silty sand
219	CHB3-BOR2	Jones Is.	Wisconsin	HP12x63	11871	44.10	43.43	6631	sa-si clay	silty sand
220	CHB3-BOR3	Jones Is.	Wisconsin	HP12x63	11871	44.10	43.53	6643	sa-si clay	silty sand
221	CHC3-EOD	Jones Is.	Wisconsin	CEP14"	43548	47.70	47.30	1213	sa-si clay	silty sand
222	CHC3-BOR	Jones Is.	Wisconsin	CEP14"	43548	47.70	47.30	1213	sa-si clay	silty sand
223	CHC3-BORL	Jones Is.	Wisconsin	CEP14"	102774?	47.70	47.34	515	sa-si clay	silty sand
224	CH4-EOD	Jones Is.	Wisconsin	CEP9.63"	10064	49.65	43.43	3315	silty clay	
225	CH4-BOR	Jones Is.	Wisconsin	CEP9.63"	10064	49.65	43.43	3315	silty clay	

**Table A.1 (con't).** Relevant Information Pertaining to Database PD/LT2000.

No.	Pile-Case Number	Refer. No.	Location	Pile Type	Pile Area  (mm <sup>2</sup> )	Length Below Gauges (m)	Penetr Depth (m)	Area Ratio  AR	Soil Type	
									Side	Tip
226	CH39-EOD	Jones Is.	Wisconsin	CEP9.63"	10581	44.81	43.28	3142	silty clay	silty clay
227	CH39-BOR	Jones Is.	Wisconsin	CEP9.63"	10581	44.81	43.28	3142	silty clay	silty clay
228	CH39-BORL	Jones Is.	Wisconsin	CEP9.63"	46581	44.81	43.37	715	silty clay	silty clay
229	CH6-5B-EOD	Jones Is.	Wisconsin	CEP9.63"	10064	46.24	43.89	3349	silty clay	silty sand
230	CH6-5B-BOR	Jones Is.	Wisconsin	CEP9.63"	10064	46.02	43.89	3349	silty clay	silty sand
231	CH95B-EOD	Jones Is.	Wisconsin	CEP9.63"	10064	49.68	42.37	3233	silty clay	sand & grvl
232	CH95B-BOR	Jones Is.	Wisconsin	CEP9.63"	10064	49.68	42.37	3233	silty clay	sand & grvl
233	CH256-BOR3	Jones Is.	Wisconsin	CEP9.63"	10064	44.20	42.67	3256	si-sa clay	si-sa & grvl
234	CH351-BOR2	Jones Is.	Wisconsin	CEP9.63"	10064	48.16	47.55	3629	si-sa clay	si-sa & grvl
235	PO2-BOR1	Port Orng	Florida	PSC18"sq	209032	26.52	5.73	50	sand	dense sand
236	PO2-BOR2	Port Orng	Florida	PSC18"sq	209032	26.52	6.07	53	sand	dense sand
237	PO2-BORL	Port Orng	Florida	PSC18"sq	209032	9.27	6.28	55	sand	dense sand
238	PO19-BOR	Port Orng	Florida	PSC18"sq	209032	26.52	4.63	41	sand	dense sand
239	PO19-EOD	Port Orng	Florida	PSC18"sq	209032	26.52	5.24	46	sand	dense sand
240	PO19-EORL	Port Orng	Florida	PSC18"sq	209032	9.51	5.36	47	sand	dense sand
241	ER5-BOR1	Escambia	Florida	PSC24"sq	371612	31.70	25.97	170	sand	sand
242	ER5-BOR2	Escambia	Florida	PSC24"sq	371612	31.70	26.03	171	sand	sand
243	ER5-BORL	Escambia	Florida	PSC24"sq	371612	26.82	26.15	172	sand	sand
244	ER77-BOR	Escambia	Florida	PSC24"sq	371612	29.84	18.56	122	clayey sand	cl-si-sand
245	ER77-BORL	Escambia	Florida	PSC24"sq	371612	18.59	18.68	123	clayey sand	cl-si-sand
246	BB13-EOD	Duval Cnty	Florida	VC 30"sq	481289	43.86	28.29	179	clayey sand	sand
247	BB13-BOR1a	Duval Cnty	Florida	VC 30"sq	481289	43.86	28.32	179	clayey sand	sand
248	BB13-BOR1b	Duval Cnty	Florida	VC 30"sq	481289	43.86	28.32	179	clayey sand	sand
249	BB13-BOR2a	Duval Cnty	Florida	VC 30"sq	481289	43.86	28.71	182	clayey sand	sand
250	BB13-BOR2b	Duval Cnty	Florida	VC 30"sq	481289	43.86	28.71	182	clayey sand	sand

**Table A.1 (con't).** Relevant Information Pertaining to Database PD/LT2000.

No.	Pile-Case Number	Refer. No.	Location	Pile Type	Pile Area	Length Below Gauges	Penetr Depth	Area Ratio	Soil Type	
					(mm <sup>2</sup> )	(m)			Side	Tip
251	BB13-BORL	Duval Cnty	Florida	VC 30"sq	481289	33.83	28.80	182	clayey sand	sand
252	BB19-BORa	Duval Cnty	Florida	VC 30"sq	481289	46.30	27.13	172	sand	sand
253	BB19-BORb	Duval Cnty	Florida	VC 30"sq	481289	46.30	27.13	172	sand	sand
254	BB19-BORL	Duval Cnty	Florida	VC 30"sq	481289	32.74	27.19	172	sand	sand
255	BB24-EOD	Duval Cnty	Florida	VC 30"sq	481289	43.86	24.44	155	sand	clay
256	BB24-BOR1a	Duval Cnty	Florida	VC 30"sq	481289	43.86	24.48	155	sand	clay
257	BB24-BOR1b	Duval Cnty	Florida	VC 30"sq	481289	43.86	24.48	155	sand	clay
258	BB24-BOR2a	Duval Cnty	Florida	VC 30"sq	481289	43.86	24.63	156	sand	clay
259	BB24-BOR2b	Duval Cnty	Florida	VC 30"sq	481289	43.86	24.63	156	sand	clay
260	BB24-BORL	Duval Cnty	Florida	VC 30"sq	481289	30.97	24.69	156	sand	clay
261	BB29-BOR	Duval Cnty	Florida	VC 30"sq	481289	43.86	23.90	151	sand	sand
262	BB29-BORL	Duval Cnty	Florida	VC 30"sq	481289	29.26	23.96	152	sand	sand
263	ABF6-BOR	Jacksonvil	Florida	PSC 24" sq	371612	21.64	17.54	115	si/clayey sand	clayey sand
264	ABF6-BORL	Jacksonvil	Florida	PSC 24" sq	371612	19.20	17.84	117	si/clayey sand	clayey sand
265	ABG13-BORL	Jacksonvil	Florida	PSC 24" sq	371612	17.68	14.08	92	clayey sand	limestone
266	ABH2-BOR	Jacksonvil	Florida	PSC 24" sq	371612	12.47	10.90	72	silt/silty clay	limestone
267	ABH2-BORL	Jacksonvil	Florida	PSC 24" sq	371612	10.64	10.96	72	silt/silty clay	limestone
268	BC79-EOD	Beaufort	S.Carolina	PSC 24" oct	307741		23.47	186	si-cl-sand	calcar sand
269	BC79-BORL	Beaufort	S.Carolina	PSC 24" oct	307741	23.93	23.50	186	si-cl-sand	calcar sand
270	BC64-EOD	Beaufort	S.Carolina	PSC 24" oct	307741		18.59	147	si-cl-sand	calcar sand
271	BC64-BORL	Beaufort	S.Carolina	PSC 24" oct	307741	19.35	18.62	148	si-cl-sand	calcar sand
272	D1-BOR1	Delft	Holland	PSC 9.7"sq	60903	10.91	10.91	177	clay-sand	sand
273	D2-BOR1	Delft	Holland	PSC 9.7"sq	60903	14.30	14.30	231	clay-sand	clay
274	D3-BORa	Delft	Holland	PSC 9.7"sq	60903	18.29	18.29	296	clay-sand	sand
275	D3-BORb	Delft	Holland	PSC 9.7"sq	60903	18.29	18.29	296	clay-sand	sand



**Table A.1 (con't). Relevant Information Pertaining to Database PD/LT2000.**

No.	Pile-Case Number	Refer. No.	Location	Pile Type	Pile Area  (mm <sup>2</sup> )	Length Below Gauges  (m)	Penetr Depth  (m)	Area Ratio  AR	Soil Type	
									Side	Tip
276	D5-BORa	Delft	Holland	PSC 9.7"sq	60903	18.29	18.29	296	clay-sand	sand
277	D5-BORb	Delft	Holland	PSC 9.7"sq	60903	18.29	18.29	296	clay-sand	sand
278	MB1-EOD	Myrtle Bch	S. Carolina	PSC 16"sq	165161	18.90	18.90	186	sand	silty sand
279	MB1-BOR	Myrtle Bch	S. Carolina	PSC 16"sq	165161	18.90	19.20	189	sand	silty sand
280	MB2-BOR	Myrtle Bch	S. Carolina	HP14x89	16839	23.47	20.12	2586	silty sand	calcar. silt
281	MB3-BOR	Myrtle Bch	S. Carolina	OEP 16"	15710	23.47	20.12	1635	silty sand	calcar. silt
282	S1-EOD	Socastee	S. Carolina	OEP 24"	25806	24.69	24.84	1843	clayey sand	sandy silt
283	S1-BOR	Socastee	S. Carolina	OEP 24"	25806	24.69	24.84	1843	clayey sand	sandy silt
284	S2-EOD	Socastee	S. Carolina	HP14x73	13806	24.32	23.77	3698	clayey sand	sandy silt
285	S2-BOR	Socastee	S. Carolina	HP14x73	13806	24.14	23.77	3698	clayey sand	sandy silt
286	DD22-EOD	Orlando	Florida	PSC 14"sq	126451	32.92	27.43	309	clay	sand
287	DD22-BOR	Orlando	Florida	PSC 14"sq	126451	32.92	27.74	312	clay	sand
288	DD23-EOD	Orlando	Florida	CEP 12.75	82387	29.57	24.99	309	clay	sand
289	DD23-BOR	Orlando	Florida	CEP 12.75	82387	25.91	25.09	310	clay	sand
290	JR17-EOD	James River	Richmond, VA	PSC 24" sq	371612	11.28	10.76	71	cl-si-sand	silty sand
291	LB3-EOD	Luling Bridge	Kenner, LA	PSC 24" sq	298645	24.38	24.84	203	clay	Sand
292	LB3-BOR1	Luling Bridge	Kenner, LA	PSC 24" sq	298645	24.38	24.99	204	clay	Sand
293	LB3-BOR2	Luling Bridge	Kenner, LA	PSC 24" sq	298645	24.38	24.99	204	clay	Sand
294	LB3-BOR3	Luling Bridge	Kenner, LA	PSC 24" sq	298645	24.38	24.99	204	clay	Sand
295	LB4-EOD	Luling Bridge	Kenner, LA	PSC 30" sq	403483	24.38	24.99	189	clay	Sand
296	LB4-BOR1	Luling Bridge	Kenner, LA	PSC 30" sq	403483	24.38	25.21	190	clay	Sand
297	LB4-BOR2	Luling Bridge	Kenner, LA	PSC 30" sq	403483	24.38	25.27	191	clay	Sand
298	LB4-BOR3	Luling Bridge	Kenner, LA	PSC 30" sq	403483	24.38	25.30	191	clay	Sand
299	LB4-BOR4	Luling Bridge	Kenner, LA	PSC 30" sq	403483	24.38	25.30	191	clay	Sand
300	LB5-EOD	Luling Bridge	Kenner, LA	PSC 30" sq	403483	24.38	24.99	189	clay	Sand

**Table A.1 (con't).** Relevant Information Pertaining to Database PD/LT2000.

No.	Pile-Case Number	Refer. No.	Location	Pile Type	Pile Area	Length	Penetr	Area Ratio	Soil Type	
						Below Gauges	Depth		Side	Tip
					(mm <sup>2</sup> )	(m)	(m)	AR		
301	LB5-BOR1	Luling Bridge	Kenner, LA	PSC 30" sq	403483	24.38	24.99	189	clay	Sand
302	LB5-BOR2	Luling Bridge	Kenner, LA	PSC 30" sq	403483	24.38	24.99	189	clay	Sand
303	LB5-BOR3	Luling Bridge	Kenner, LA	PSC 30" sq	403483	24.38	25.30	191	clay	Sand
304	LB5-BOR4	Luling Bridge	Kenner, LA	PSC 30" sq	403483	24.38	25.30	191	clay	Sand
305	LB6-EOD	Luling Bridge	Kenner, LA	PSC 36" cyl	314193	24.38	24.69	226	clay	Sand
306	LB6-BOR1	Luling Bridge	Kenner, LA	PSC 36" cyl	314193	24.38	24.69	226	clay	Sand
307	LB6-BOR2	Luling Bridge	Kenner, LA	PSC 36" cyl	314193	24.38	24.69	226	clay	Sand
308	LB6-BOR3	Luling Bridge	Kenner, LA	PSC 36" cyl	314193	24.38	24.99	229	clay	Sand
309	LB6-BOR4	Luling Bridge	Kenner, LA	PSC 36" cyl	314193	24.38	24.99	229	clay	Sand
310	LB7-EOD	Luling Bridge	Kenner, LA	PSC 36" cyl	314193	24.38	24.60	225	clay	Sand
311	LB7-BOR1	Luling Bridge	Kenner, LA	PSC 36" cyl	314193	24.38	24.69	226	clay	Sand
312	LB7-BOR2	Luling Bridge	Kenner, LA	PSC 36" cyl	314193	24.38	24.69	226	clay	Sand
313	LB7-BOR3	Luling Bridge	Kenner, LA	PSC 36" cyl	314193	24.38	24.69	226	clay	Sand
314	LB7-BOR4	Luling Bridge	Kenner, LA	PSC 36" cyl	314193	24.38	24.69	226	clay	Sand
315	DI221-EOD	Deer Island	Massachusetts	PSC 14" sq	126451	26.21	19.20	216	sa-si-clay	fine sand & silt
316	DI221-2DR	Deer Island	Massachusetts	PSC 14" sq	126451	26.21	19.20	216	sa-si-clay	fine sand & silt
317	TW488-EOD	MBTA Project	Massachusetts	PSC 14" sq	126451	23.77	23.16	261	stiff clay	stiff clay
318	TW488-3DR	MBTA Project	Massachusetts	PSC 14" sq	126451	23.77	23.16	261	stiff clay	stiff clay
319	NBTP2-EOD	Newbury	Massachusetts	HP12X74	14064	35.51	34.14	4433	si-sa-clay	glacial till
320	NBTP2-1DR	Newbury	Massachusetts	HP12X74	14064	35.51	34.14	4433	si-sa-clay	glacial till
321	NBTP2-6DR	Newbury	Massachusetts	HP12X74	14064	35.51	34.14	4433	si-sa-clay	glacial till
322	NBTP3-EOD	Newbury	Massachusetts	HP12X74	14064	35.51	33.07	4295	si-sa-clay	silty sand
323	NBTP3-1DR	Newbury	Massachusetts	HP12X74	14064	35.51	33.07	4295	si-sa-clay	silty sand
324	NBTP3-6DR	Newbury	Massachusetts	HP12X74	14064	35.51	33.07	4295	si-sa-clay	silty sand
325	NBTP5-EOD	Newbury	Massachusetts	CEP12.75"	9406	35.72	33.83	418	si-sa-clay	glacial till

**Table A.1 (con't).** Relevant Information Pertaining to Database PD/LT2000.

No.	Pile-Case Number	Refer. No.	Location	Pile Type	Pile Area	Length Below Gauges	Penetr Depth	Area Ratio	Soil Type	
					(mm <sup>2</sup> )	(m)	(m)	AR	Side	Tip
326	NBTP5-3DR	Newbury	Massachusetts	CEP12.75"	9406	35.72	33.83	418	si-sa-clay	glacial till
327	PR1-BOR1	Pagan River	Virginia	PSC 24" sq	371612	32.31	31.88	209	sand & silt	silty sand
328	DD29-EOD	Orlando	Florida	CEP 12.75"	9406	52.73	49.68	5374	clayey sand	clayey sand
329	ND50-BOR1	Norwood	Ohio	CEP 12"	4852	12.34	6.71	1324	silty clay	si-clayey sand
330	NZ12-BOR1	Natchez	Mississippi	HP14X73	13806	11.03	11.89	1849	silt	silt
331	DW1-BOR1	Dawhoo	S. Carolina	PSC 24" sq	371612	26.52	27.46	180	silty clay	silty clay
332	DW1-BOR2	Dawhoo	S. Carolina	PSC 24" sq	371612	26.52	27.52	181	silty clay	silty clay
333	DW2-BOR1	Dawhoo	S. Carolina	HP14X73	16387	26.52	27.46	3599	si-sa-clay	silty clay
334	DW2-BOR2	Dawhoo	S. Carolina	HP14X73	16387	26.52	27.52	3607	si-sa-clay	silty clay
335	DS1-BOR1	Daughty St.	S. Carolina	PSC 12" sq	92903	27.22	26.82	352	cl-si-sand	calcar sand
336	DS1-BOR2	Daughty St.	S. Carolina	PSC 12" sq	92903	27.22	26.85	352	cl-si-sand	calcar sand
337	PX2-BOR1	Phoenix	Arizona	HP14X117	22194	14.94	14.02	1386	clay & sand	sa-gr-cobble
338	PX3-EOD	Phoenix	Arizona	HP14X117	22194	19.51	15.24	1506	clay & sand	sa-gr-cobble
339	PX3-BOR1	Phoenix	Arizona	HP14X117	22194	16.46	15.24	1506	clay & sand	sa-gr-cobble
340	PX4-EOD	Phoenix	Arizona	CEP 14"	10355	8.84	6.83	737	clay & sand	clayey sand
341	PX4-BOR1	Phoenix	Arizona	CEP 14"	10355	8.84	6.83	737	clay & sand	clayey sand
342	PX5-BOR1	Phoenix	Arizona	CEP 14"	10355	8.84	7.53	812	clay & sand	clayey sand
343	PX6-BOR1	Phoenix	Arizona	PSC 16" sq	152490	9.08	7.01	75	clay & sand	clayey sand
344	PX7-EOD	Phoenix	Arizona	PSC 16" sq	152490	7.32	6.10	65	clay & sand	clay
345	PX7-BOR1	Phoenix	Arizona	PSC 16" sq	152490	7.32	6.10	65	clay & sand	clay
346	CH11-42-BOR1	Jones Island	Wisconsin	CEP 12.75"	7865	29.78	28.99	3750	sa-cl-silt	silty clay
347	SSTPD-5DR	Stockholm	Sweden	PSC 9.25" sq	55226	13.20	12.80	218	silty sand	silty sand
348	TSW/D62/1-EOD	Site 2	Hong Kong	PSC 19.69" cyl	125703	23.00	22.70	284	sa-cl-silt	sandy silt
349	TSW/D62/1-BOR	Site 2	Hong Kong	PSC 19.69" cyl	125703	23.00	22.70	284	sa-cl-silt	sandy silt
350	TSW/HHK9/1-EOD	Site 2	Hong Kong	PSC 19.69" cyl	125703	23.00	23.60	295	sa-cl-silt	sandy silt

**Table A.1 (con't).** Relevant Information Pertaining to Database PD/LT2000.

No.	Pile-Case Number	Refer. No.	Location	Pile Type	Pile Area  (mm <sup>2</sup> )	Length Below Gauges (m)	Penetr Depth (m)	Area Ratio  AR	Soil Type	
									Side	Tip
351	TSW/HHK9/1-BOR	Site 2	Hong Kong	PSC 19.69" cyl	125703	23.00	23.60	295	sa-cl-silt	sandy silt
352	TSW/D62/2-EOD	Site 3	Hong Kong	HP12X120?	22929	35.00	29.70	2438	sa-cl-silt	sandy silt
353	TSW/D62/2-BOR	Site 3	Hong Kong	HP12X120?	22929	35.00	29.70	2438	sa-cl-silt	sandy silt
354	TSW/HHK9/2-EOD	Site 3	Hong Kong	HP12X120?	22929	35.00	31.50	2586	sa-cl-silt	sandy silt
355	TSW/HHK9/2-BOR	Site 3	Hong Kong	HP12X120?	22929	35.00	31.50	2586	sa-cl-silt	sandy silt
356	OD1J-EOD	Site 1	Oakland, CA	OEP 24"	35342	9.14	8.47	459	silty sand	silty clayey sand
357	OD2P-EOD	Site 2	Oakland, CA	OEP 24"	35342	12.22	12.19	661	silty sand	silty sandy clay
358	OD2P-BOR	Site 2	Oakland, CA	OEP 24"	35342	12.22	12.19	661	silty sand	silty sandy clay
359	OD2T-EOD	Site 2	Oakland, CA	CEP 24"	35342	12.19	10.67	578	silty sand	silty sand & clay
360	OD3H-EOD	Site 3	Oakland, CA	OEP 42"	62703	30.78	30.63	1637	stiff clay	clay w/ sa-si-gr
361	OD4L-EOD	Site 4	Oakland, CA	CEP 24"	23813	21.40	19.51	128	sandy clay	silty sandy clay
362	OD4P-EOD	Site 4	Oakland, CA	CEP 24"	23813	21.34	17.07	112	silty clay	silty sandy clay
363	OD4P-BOR	Site 4	Oakland, CA	CEP 24"	23813	21.34	17.07	112	silty clay	silty sandy clay
364	OD4T-EOD	Site 4	Oakland, CA	CEP 24"	23813	21.34	18.29	120	sandy clay	silty sandy clay
365	OD4T-BOR	Site 4	Oakland, CA	CEP 24"	23813	21.34	18.29	120	sandy clay	silty sandy clay
366	OD4W-EOD	Site 4	Oakland, CA	CEP 24"	23813	21.40	18.29	120	sandy clay	silty sandy clay
367	OD4W-BOR2	Site 4	Oakland, CA	CEP 24"	23813	21.40	18.29	120	sandy clay	silty sandy clay
368	OD4W-BOR3	Site 4	Oakland, CA	CEP 24"	23813	21.40	18.38	121	sandy clay	silty sandy clay
369	QC3-EOD	Queens County	New York	PSC 54" cyl	496573	27.13	23.01	200	sand	dense sand
370	QC3-14DR	Queens County	New York	PSC 54" cyl	496573	27.13	23.01	200	sand	dense sand
371	QC14-EOD	Queens County	New York	PSC 14" cyl	126451	25.91	22.86	202	sand	dense sand
372	QC14-30DR	Queens County	New York	PSC 14" cyl	126451	25.91	22.86	202	sand	dense sand
373	NYSP-EOD	SE New York	New York	HP10X42	10329	35.51	33.50	4849	silty sand	silty sand w/gr
374	NYSP-BOR	SE New York	New York	HP10X42	10323	33.89	33.50	4849	silty sand	silty sand w/gr
375	UFSS1A - BOR	Sunshine Skyway	Florida	PSC 24" sq	371612	0.00	15.00	590	cl-si-sand	silty clay

**Table A.1 (con't).** Relevant Information Pertaining to Database PD/LT2000.

No.	Pile-Case Number	Refer. No.	Location	Pile Type	Pile Area  (mm <sup>2</sup> )	Length Below Gauges  (m)	Penetr Depth  (m)	Area Ratio  AR	Soil Type	
									Side	Tip
376	UFSS1B - BOR	Sunshine Skyway	Florida	PSC 20" sq	258064	0.00	14.42	568	cl-si-sand	silty clay
377	UFSS10 - BOR	Sunshine Skyway	Florida	PSC 24" sq	371612	0.00	8.50	335	sa-si-clay	silty clay
378	UFSS13B - BOR	Sunshine Skyway	Florida	PSC 24" sq	371612	0.00	8.20	323	sa-si-clay	silty clay
379	BIT20 - BOR	Jacksonville	Florida	PSC 20" sq	258064	0.00	14.08	554	silty sand	sand
380	BIT21 - BOR	Jacksonville	Florida	PSC 20" sq	258064	10.97	11.09	437	cl-si-sand	silty sand
381	HFLS3 - EOD	Tampa Bay	Florida	PSC 30" sq	580644	0.00	12.07	475	sa-si-clay	sandy clay
382	HFLS4L - EOD	Tampa Bay	Florida	PSC 30" sq	580644	0.00	22.40	882	cl-si-limestone-sand	limerock
383	HFLS4L - BOR	Tampa Bay	Florida	PSC 30" sq	580644	0.00	22.40	882	cl-si-limestone-sand	limerock
384	RBA30 - BOR	Stuart	Florida	PSC 30" sq	580644	21.34	16.28	641	silty sand	silty sand
385	RBB30W - BOR	Stuart	Florida	PSC 30" sq	580644	18.59	13.35	526	silty sand	silty sand
386	CC6 - BOR	Cape Canaveral	Florida	PSC 18" sq	209032	23.47	16.18	637	silty sand	sand
387	CC7 - BOR	Cape Canaveral	Florida	PSC 14" sq	126451	23.47	23.23	914	cl-si-sand	silty sand
388	CC14 - BOR	Cape Canaveral	Florida	PSC 14" sq	126451	23.47	21.18	834	cl-si-sand	silty sand
389	49SB37 - EOD	Clearwater	Florida	PSC 30" sq	580644	16.46	7.13	281	sandy clay	silty limestone

**Table A.1 (con't). Relevant Information Pertaining to Database PD/LT2000.**

No.	Pile-Case Number	Hammer Type	Rated Hammer Energy (kN-m)	Delivered Energy (kN-m)	Blow Count (BP10cm)	Impedence EA/C (kN/m/s)	Vimp (m/s)	Fimp (kN)	VEA/C F	Dmax (mm)	2L/C (ms)	Tip Quake (mm)	Side Quake (mm)	Tip Damping (sec/m)	Side Damping (sec/m)
1	FN1-EOD	D-30	73.49	23.46	11.1	323.0	4.04	1434	0.909	20.1	8.57	5.08	2.54	0.230	0.558
2	FN1-BOR1	D-30	73.49	24.97	31.5	323.0	4.04	1402	0.930	20.7	8.57	2.54	2.54	1.312	0.427
3	FN1-BOR2	D-30	73.49	27.32	59.1	323.0	3.97	1374	0.934	21.3	8.57	2.54	2.54	1.903	0.361
4	FN2-EOD	D-30	73.49	17.22	13.8	882.8	2.24	2055	0.963	11.3	9.55	5.08	5.59	0.164	0.886
5	FN2-BOR	D-30	73.49	16.74	19.7	882.8	2.55	2264	0.994	10.4	9.55	2.03	3.81	0.328	1.083
6	FN3-EOD	D-30	73.49	13.42	36.1	1253.5	1.87	2482	0.946	9.8	9.55	3.05	1.52	0.951	1.969
7	FN3-BOR	D-30	73.49	21.96	23.6	1253.5	2.40	3074	0.979	11.7	9.55	5.33	1.78	1.115	1.017
8	FN4-EOD	D-30	73.49	21.08	9.8	500.0	3.95	2128	0.929	13.5	7.85	3.81	3.05	0.164	0.492
9	FN4-BOR	D-30	73.49	23.59	19.7	500.0	4.03	2116	0.953	13.1	7.85	2.54	2.79	0.164	0.591
10	FIA-EOD	K-25	69.82	31.70	13.1	680.1	4.54	2971	1.039	17.4	13.98	7.62	4.32	1.572	0.161
11	FIA-BOR	K-25	69.82	25.60	7.2	680.1	4.57	2925	1.062	14.2	13.98	1.27	2.54	1.959	0.180
12	FIB-EOD	K-25	69.82	34.44	23.0	551.6	4.60	2470	1.027	17.5	11.59	5.08	3.81	0.217	0.194
13	FIB-BOR	K-25	69.82	30.47	9.8	551.6	4.66	2439	1.054	17.1	11.59	3.81	2.54	0.423	0.223
14	FO1-EOD	DE110	126.77	24.51	22.3	1762.9	1.65	3508	0.827	10.5	7.17	7.11	2.54	0.456	0.446
15	FO1-BOR	DE110	126.77	50.80	19.7	1762.9	2.71	5443	0.878	13.7	7.17	7.11	2.54	0.302	0.302
16	FO2-EOD	DE110	126.77	24.78	20.0	2905.6	1.19	3585	0.963	11.5	9.41	5.84	2.54	0.161	0.607
17	FO2-BOR	DE110	126.77	42.53	47.2	2905.6	1.74	4955	1.018	11.4	9.41	6.35	2.54	0.128	0.545
18	FO3-EOD	DE110	126.77	22.24	65.6	896.1	2.01	2177	0.828	15.9	13.08	1.27	2.03	2.215	0.269
19	FO4-EOD	DE110	126.77	13.30	45.9	3131.9	0.76	2559	0.933	6.8	10.48	3.30	2.54	0.377	0.417
20	FO4-BOR	DE110	126.77	30.82	3.9	3131.9	1.43	4500	0.997	9.2	10.48	5.08	3.05	0.801	0.633
21	FOR1-EOD	D-46-23	142.36	40.82	36.1	2320.4	1.86	4208	1.025	21.3	20.96	9.65	6.35	0.197	0.587
22	FOR1-BOR	D-46-23	142.36	32.23	304.4	2320.4	1.77	4084	1.004	11.7	20.96	5.59	5.59	0.807	0.607
23	FM5-EOD	K-45	125.82	36.61	5.1	716.3	3.27	2449	0.957	26.2	13.96	8.13	2.54	0.135	0.282
24	FM5-BOR	K-45	125.82	54.50	11.8	716.3	4.05	2928	0.992	24.9	12.02	9.91	2.54	0.318	0.243
25	FM17-EOD	K-45	125.82	53.55	5.6	716.3	3.40	2628	0.926	28.1	9.26	13.46	2.29	0.253	0.249

**Table A.1 (con't). Relevant Information Pertaining to Database PD/LT2000.**

No.	Pile-Case Number	Hammer Type	Rated Hammer Energy (kN-m)	Delivered Energy (kN-m)	Blow Count (BP10cm)	Impedence EA/C (kN/m/s)	Vimp (m/s)	Fimp (kN)	VEA/C F	Dmax (mm)	2L/C (ms)	Tip Quake (mm)	Side Quake (mm)	Tip Damping (sec/m)	Side Damping (sec/m)
26	FM17-BOR	K-45	125.82	49.49	11.8	716.3	4.01	3104	0.926	20.0	9.26	5.08	2.54	0.164	0.466
27	FM23-EOD	K-45	125.82	45.15	5.2*	716.3	3.47	2487	0.998	30.2	6.75	10.16	2.03	0.135	1.490
28	FM23-BOR	K-45	125.82	42.03	7.9	716.3	3.22	2260	1.021	31.7	6.75	25.40	5.33	0.148	0.295
29	FC1-EOD	KC-25	69.82	20.97	13.8*	256.0	4.08	1213	0.862	20.3	3.98	7.62	3.99	0.118	0.118
30	FC1-BOR	KC-25	69.82	21.95	15.0*	256.0	4.08	1229	0.851	20.5	3.98	8.38	3.56	0.098	0.105
31	FC2-EOD	KC-25	69.82	24.50	14.4*	256.0	4.54	1290	0.901	20.5	3.27	8.38	3.76	0.135	0.085
32	FC2-BOR	KC-25	69.82	18.52	15.7*	256.0	3.99	1193	0.857	17.3	3.14	8.38	3.81	0.095	0.079
33	FMI1-EOD	ICE-640	54.23	14.91	11.8*	419.3	2.47	1113	0.919	18.7	9.87	2.54	2.54	0.167	0.154
34	FMI1-BOR	ICE-640	54.23	16.27	11.8	419.3	2.68	1354	0.830	16.1	9.87	3.81	2.54	0.315	0.056
35	FMI2-EOD	ICE-640	54.23	15.81	5.6*	419.3	2.16	1024	0.886	21.9	7.32	3.56	2.54	0.098	0.197
36	FMI2-BOR	ICE-640	54.23	18.41	11.8	419.3	2.74	1271	0.905	21.2	7.32	3.81	2.54	0.180	0.098
37	FWA-EOD	Con300	122.02	60.88	185.0	2898.6	2.99	8563	1.011	23.4	18.08	12.70	6.60	0.312	0.994
38	FWA-BOR	Con300	122.02	45.15	27.6	2898.6	2.68	7598	1.023	14.0	18.08	7.65	6.38	0.620	0.449
39	FWB-EOD	Con300	122.02	63.99	118.1	2898.6	2.59	7629	0.990	16.0	16.66	-	-	-	-
40	FWB-BOR	Con300	122.02	53.28	59.1	2898.6	2.32	6744	0.996	17.0	16.66	-	-	-	-
41	FA1-EOD	K-45	125.82	23.77	5.9*	2126.6	1.33	2797	1.013	18.5	9.40	2.54	2.54	0.404	0.768
42	FA1-BOR1	K-45	125.82	12.46	27.6	2126.6	1.10	2437	0.957	8.5	9.07	5.08	1.52	1.201	1.204
43	FA1-BOR2	K-45	125.82	29.61	27.6	2126.6	2.23	4777	0.990	12.2	9.07	6.35	2.54	1.191	1.056
44	FA2-EOD	K-45	125.82	28.77	13.8*	2126.6	1.21	2842	0.908	15.5	10.51	10.67	2.54	0.322	0.705
45	FA2-BOR1	K-45	125.82	30.74	27.6	2050.7	2.10	4555	0.946	10.9	10.90	6.35	2.54	0.925	0.673
46	FA2-BOR2	K-45	125.82	28.20	19.7	2126.6	2.04	4559	0.952	9.1	10.51	4.32	3.30	1.060	1.073
47	FA3-EOD	K-45	125.82	30.90	11.1*	3233.0	1.01	3243	1.006	16.4	9.16	8.89	2.54	0.600	1.079
48	FA3-BOR1	K-45	125.82	20.64	23.6	3210.5	1.04	3480	0.959	8.2	9.06	5.08	1.78	1.683	1.306
49	FA3-BOR2	K-45	125.82	22.11	19.7	3233.0	1.62	5333	0.979	7.0	9.00	5.21	2.03	1.014	1.296
50	FA4-EOD	K-45	125.82	25.84	25.3*	3233.0	1.09	3480	1.007	11.1	10.43	6.35	2.54	0.502	0.974

**Table A.1 (con't). Relevant Information Pertaining to Database PD/LT2000.**

No.	Pile-Case Number	Hammer Type	Rated Hammer Energy (kN-m)	Delivered Energy (kN-m)	Blow Count (BP10cm)	Impedence EA/C (kN/m/s)	Vimp (m/s)	Fimp (kN)	VEA/C F	Dmax (mm)	2L/C (ms)	Tip Quake (mm)	Side Quake (mm)	Tip Damping (sec/m)	Side Damping (sec/m)
51	FA4-BOR1	K-45	125.82	22.80	31.5	3209.6	1.58	4929	1.030	6.5	10.51	3.05	1.52	1.096	1.280
52	FA4-BOR2	K-45	125.82	27.69	70.9	3209.6	2.06	6530	1.013	7.2	10.51	3.81	2.54	0.925	1.168
53	FA5-EOD	D-62-22	207.71	50.25	30.2*	5894.2	1.55	9368	0.978	11.3	10.07	8.38	3.05	1.296	0.991
54	FA5-BOR	D-62-22	207.71	61.70	19.7	5894.2	2.26	13416	0.991	7.3	10.45	6.10	1.78	1.299	1.296
55	FV15-EOD	MKT-35B	29.83	13.56	16.4*	557.3	3.17	1794	0.985	12.1	10.95	7.62	2.54	0.459	0.335
56	FV15-BOR	MKT-35B	29.83	16.58	35.4	557.3	4.33	2326	1.037	16.3	10.95	7.62	2.54	1.391	0.292
57	FV10-EOD	MKT-35B	29.83	14.89	10.5*	557.3	3.26	1858	0.978	12.4	10.95	7.62	2.54	1.237	0.663
58	FV10-BOR	MKT-35B	29.83	18.93	7.9	557.3	4.97	2709	1.022	17.1	10.95	8.64	3.18	0.906	0.538
59	FMN2-EOD	ICE-90S	122.02	38.36	7.2*	557.3	4.57	2792	0.913	22.3	11.19	12.70	4.06	0.259	0.341
60	FMN2-BOR	ICE-90S	122.02	39.51	98.4	557.3	5.03	3005	0.932	20.4	11.19	3.81	3.86	0.279	0.374
61	FP5-EOD	D-12	29.83	10.25	21.3*	182.3	4.21	789	0.972	17.2	4.10	5.08	1.02	0.121	0.299
62	FP5-BOR	D-12	29.83	10.24	51.2	182.3	4.54	856	0.967	14.5	4.10	4.83	1.14	0.098	0.289
63	FKG-EOD	LB-520	42.03	11.27	91.5*	1170.9	1.30	1572	0.971	11.8	11.39	6.35	2.29	0.341	0.840
64	FKG-BOR	LB-520	42.03	10.52	70.9	1170.9	1.39	1661	0.978	10.3	11.39	3.56	1.52	0.371	0.925
65	FL3-EOD	Vul-020	81.35	19.79	6.6*	2973.4	1.00	3017	0.985	19.2	15.04	10.16	2.54	0.807	0.883
66	FL3-BOR1	Vul-020	81.35	23.09	15.7	2973.4	1.13	3609	0.929	11.0	15.04	6.35	3.81	1.240	1.286
67	FL3-BOR2	Vul-020	81.35	19.56	43.3	2973.4	1.13	3538	0.948	7.5	15.04	6.35	3.15	1.716	1.663
68	CA1-EOD	B-400	62.37	27.55	84.0	406.7	4.80	1923	1.016	26.7	20.47	3.56	3.56	0.292	0.272
69	CA1-BOR	B-400	62.37	25.71	157.5	406.7	4.40	1903	0.941	26.0	20.47	3.30	3.30	0.292	0.246
70	CA2-BOR	B-400	62.37	22.70	55.1	406.7	4.60	1886	0.992	21.9	13.39	2.54	2.54	0.318	0.344
71	CA5-BOR1	35kdrop	52.5min	41.30	98.4	312.0	4.60	1520	0.944	33.3	7.97	9.19	2.54	0.039	0.289
72	CA5-BOR2	49kdrop	73.5min	42.63	43.3	312.0	4.10	1367	0.936	33.0	7.97	8.31	5.51	0.115	0.079
73	CA3/8-BOR	ICE 40S	54.23	25.80	16.7	227.7	4.70	1226	0.873	25.4	8.78	9.50	7.01	0.315	0.387
74	CA24-BOR	D-12	32.54	11.97	196.9	196.1	4.30	959	0.879	12.7	4.59	4.50	3.00	0.371	0.253
75	CA6-BOR1	D-30-13	89.48	55.90	39.4	378.4	5.28	2199	0.909	29.6	7.16	8.99	7.01	0.157	0.164



**Table A.1 (con't).** Relevant Information Pertaining to Database PD/LT2000.

No.	Pile-Case Number	Hammer Type	Rated Hammer Energy (kN-m)	Delivered Energy (kN-m)	Blow Count (BP10cm)	Impedence EA/C (kN/m/s)	Vimp (m/s)	Fimp (kN)	VEA/C F	Dmax (mm)	2L/C (ms)	Tip Quake (mm)	Side Quake (mm)	Tip Damping (sec/m)	Side Damping (sec/m)
76	CA6-BOR2	D-30-13	89.48	57.87	26.3	378.4	5.46	2236	0.924	31.2	7.16	10.01	6.50	0.154	0.171
77	CA6-EOR	D-30-13	89.48	50.98	31.5	378.4	5.13	1858	1.045	29.4	7.16	8.51	6.50	0.121	0.203
78	WC3-EOD	Delmag	142.36	23.73	36.7	3922.1	1.29	4994	1.013	11.5	6.80	10.16	2.54	0.551	0.217
79	WC3-BOR1	Delmag	142.36	22.91	36.7	3922.1	1.30	5247	0.968	10.5	6.80	8.89	3.30	0.118	0.643
80	WC3-BOR2	Delmag	142.36	24.26	26.3	3922.1	1.06	4637	0.895	10.2	5.36	8.13	2.03	0.285	0.449
81	WC6-EOD	Delmag	142.36	23.86	19.7	3880.2	1.36	5298	0.998	12.9	5.54	10.67	2.54	0.387	0.469
82	WC6-BOR1	Delmag	142.36	24.73	31.5	3880.2	1.37	5448	0.977	12.4	5.54	11.96	2.03	0.417	0.696
83	WC6-BOR2	Delmag	142.36	35.63	26.3	3880.2	1.54	5917	1.007	16.9	3.93	15.49	2.54	0.157	1.020
84	WB9-BOR	Con300	122.02	54.06	26.3	3962.5	1.96	7776	0.997	9.7	20.00	6.60	1.27	1.421	0.823
85	WB15-BOR	Con300	122.02	47.05	19.7	3933.1	1.78	6822	1.025	9.5	16.28	5.72	1.52	0.794	1.594
86	T1/A-EOD	D-55	169.48	61.00	29.0	5524.8	2.44	13198	1.022	6.6	16.49	3.81	1.27	0.230	0.377
87	T1/A-ALT	D-55	169.48	205.41	9.0	5524.8	3.81	19674	1.070	21.1	20.70	5.08	2.54	0.515	0.259
88	T1/B-EOD	M-2500	NA	234.19	8.0	5524.8	3.87	21294	1.004	22.1	25.74	1.52	1.52	0.069	0.154
89	T2/A-EOD	D-55	169.48	82.19	19.0	2900.5	2.87	8412	0.988	14.5	13.94	3.81	1.02	0.771	0.285
90	T2/B-EOD	M-2500	NA	228.70	20.0	2900.5	4.15	12517	0.961	29.7	31.01	1.78	1.78	0.505	0.108
91	35-1-BOR	B-400	62.37	17.76	7.2*	568.1	3.11	1882	0.939	15.2	7.15	6.35	2.54	0.374	0.141
92	35-4-BOR	B-400	62.37	31.46	21.9*	255.4	5.47	1677	0.833	25.7	6.21	7.62	2.54	0.079	0.108
93	35-5-BOR	B-400	62.37	24.00	40.6*	568.1	4.42	2598	0.967	15.0	11.93	1.02	1.02	0.138	0.207
94	35-6-BOR	B-400	62.37	35.39	65.6*	255.4	5.67	1655	0.875	28.7	12.55	2.54	1.52	0.003	0.305
95	35-7-BOR	B-225	39.32	13.42	10.0*	276.8	3.26	965	0.935	23.1	8.88	5.08	2.54	0.131	0.154
96	35-10-BOR	B-400	62.37	15.05	23.6	883.8	2.77	2322	1.055	11.7	7.69	6.35	1.02	0.062	0.272
97	E2-BOR	Conm65	35.93	20.35	39.4	936.9	2.43	2347	0.968	10.0	6.31	6.60	2.54	0.394	0.574
98	63S-BOR	ICE-640	54.23	16.45	17.7	442.8	3.31	1455	1.006	15.2	8.19	7.11	2.54	0.089	0.866
99	LB21-BOR	VUL-510	67.79	18.26	15.7*	2472.2	1.40	3655	0.948	9.5	5.50	7.87	2.54	0.420	0.554
100	LB20-BOR	VUL-510	67.79	20.03	31.5	2361.3	1.80	4297	0.988	7.9	7.91	5.84	3.05	0.692	0.692

**Table A.1 (con't). Relevant Information Pertaining to Database PD/LT2000.**

No.	Pile-Case Number	Hammer Type	Rated Hammer Energy (kN-m)	Delivered Energy (kN-m)	Blow Count (BP10cm)	Impedence EA/C (kN/m/s)	Vimp (m/s)	Fimp (kN)	VEA/C F	Dmax (mm)	2L/C (ms)	Tip Quake (mm)	Side Quake (mm)	Tip Damping (sec/m)	Side Damping (sec/m)
101	LC3-BOR	D-46-23	145.07	53.42	27.6	2362.8	2.53	6392	0.935	16.9	20.31	8.89	6.35	0.630	0.449
102	LIN16-BOR	D-46-23	145.07	37.96	39.4*	2362.8	1.80	4835	0.879	14.7	24.50	5.59	3.05	0.961	1.106
103	LE37-BOR	VUL-01	20.34	7.32	39.4	566.2	1.75	1007	0.977	11.0	10.00	3.56	2.03	0.594	2.133
104	LE64-BOR	VUL-01	20.34	9.36	21.7	566.2	1.86	1100	0.957	10.7	10.00	2.67	1.78	0.486	0.433
105	ST1-EOD	D-36-13	113.89	44.92	9.5*	1795.0	2.53	4606	0.986	21.5	11.52	7.62	2.03	0.177	0.200
106	ST2-EOD	D-36-13	113.89	44.78	13.5*	1929.3	1.93	3830	0.973	22.8	9.96	15.24	2.03	0.056	0.066
107	ST9-BOR	CN5300	203.37	61.96	30.9*	4948.8	1.86	9235	0.996	11.2	24.19	5.59	2.54	1.056	0.486
108	ST46-EOD	VUL-1	20.34	7.46	10.5*	151.0	3.05	456	1.010	20.1	4.52	10.16	3.81	0.108	0.138
109	GZA3-EOD	ICE-640	54.23	21.86	78.7	528.3	3.29	1611	1.079	21.9	17.00	8.38	3.81	0.174	0.164
110	GZA5-EOD	ICE-640	54.23	23.54	23.6	405.7	3.11	1338	0.942	27.0	16.50	8.13	3.81	0.098	0.164
111	GZA6-EOD	ICE-640	54.23	18.17	59.1	404.3	2.47	978	1.021	27.3	20.37	6.35	3.18	0.387	0.174
112	GZBBC-EOD	ICE-640	54.23	23.96	78.7	551.6	2.71	1611	0.929	22.5	13.79	1.47	1.27	0.299	0.246
113	GZBP2-EOD	ICE-640	54.23	12.98	78.7	528.3	2.07	1151	0.952	18.0	17.08	1.02	1.27	0.167	0.423
114	GZB6-EOD	ICE-640	54.23	21.57	43.3	404.3	3.32	1532	0.876	21.2	11.56	6.10	3.05	0.200	0.210
115	GZZ5-EOD	ICE1070	98.43	38.95	16.5	551.6	4.05	2374	0.942	25.4	10.34	11.43	8.89	0.561	0.781
116	GZO5-EOD	ICE1070	98.43	32.15	16.5	551.6	4.33	2527	0.945	22.3	10.34	14.73	2.54	0.194	2.657
117	GZCC5-EOD	ICE1070	98.43	46.17	21.3	551.6	4.45	2627	0.934	30.0	13.91	10.92	5.59	0.095	0.384
118	GZL2-EOD	ICE1070	98.43	34.99	35.4	551.6	3.93	2227	0.974	25.0	13.91	13.46	8.13	0.449	0.801
119	GZP14-EOD	ICE1070	98.43	34.82	19.7	551.6	3.47	2234	0.858	22.4	12.48	11.43	2.54	0.253	0.335
120	GZP11-EOD	ICE1070	98.43	21.87	20.9	551.6	3.41	2097	0.898	19.9	12.48	2.54	2.54	0.207	0.584
121	GZP12-EOD	ICE1070	98.43	46.97	49.6	551.6	3.87	2222	0.961	29.3	13.73	2.79	4.32	0.125	0.610
122	GZB22-EOD	MH72B	183.04	74.80	33.5	1619.9	3.54	5899	0.971	21.8	18.71	1.65	1.65	0.679	0.413
123	GZW1-EOR	K-25	63.72	17.34	47.2	380.9	3.72	1509	0.939	19.7	15.02	4.32	2.54	0.387	0.466
124	A54-EOD	Banut-6	47.07	28.54	14.3	741.7	2.66	1810	1.090	21.9	12.07	3.51	2.51	0.653	0.331
125	A54-BOR	Banut	47.07	34.80	71.4*	741.7	3.17	2184	1.077	21.0	12.07	2.54	8.71	0.289	0.358

**Table A.1 (con't).** Relevant Information Pertaining to Database PD/LT2000.

No.	Pile-Case Number	Hammer Type	Rated Hammer Energy (kN-m)	Delivered Energy (kN-m)	Blow Count (BP10cm)	Impedence EA/C (kN/m/s)	Vimp (m/s)	Fimp (kN)	VEA/C F	Dmax (mm)	2L/C (ms)	Tip Quake (mm)	Side Quake (mm)	Tip Damping (sec/m)	Side Damping (sec/m)
126	A147-EOD	Banut	47.07	26.70	7.7*	706.9	2.48	1798	0.976	22.4	11.18	16.99	2.54	0.190	0.367
127	A147-BOR	Banut	47.07	34.30	26.3*	688.8	2.79	1945	0.987	19.8	10.89	5.56	2.54	0.246	0.328
128	GF19-EOD	LB-520	NA	12.74	78.7	434.9	3.22	1525	0.918	11.9	9.45	2.79	2.54	0.115	0.203
129	GF110-EOD	LB-520	NA	13.78	173.2	565.2	3.18	1997	0.900	9.7	6.79	4.06	2.79	0.112	0.384
130	GF222-EOD	ICE-640	NA	22.51	78.7	565.2	3.84	2237	0.969	15.0	7.97	3.56	3.30	0.213	0.256
131	GF224-EOD	ICE-640	NA	28.47	19.7	252.6	4.79	1152	1.050	22.9	6.30	2.03	0.76	0.151	0.075
132	GF312-EOD	LB-520	NA	9.30	70.9	565.2	2.79	1762	0.899	7.2	3.93	3.05	2.03	0.377	0.187
133	GF313-EOD	LB-520	NA	13.63	78.7	434.9	3.29	1566	0.915	10.2	4.16	3.81	2.03	0.436	0.141
134	GF412-EOD	LB-520	NA	11.51	153.5	565.2	2.93	1818	0.911	9.1	5.78	3.05	3.05	0.190	0.085
135	GF413-EOD	LB-520	NA	12.30	153.5	434.9	3.27	1603	0.888	10.6	4.07	2.54	3.05	0.210	0.095
136	GF414-EOD	ICE-640	NA	22.33	189.0	434.9	3.45	1655	0.907	15.4	5.65	3.05	2.79	0.141	0.039
137	GF415-EOD	ICE-640	NA	16.61	110.2	565.2	3.17	1969	0.909	11.6	5.66	3.30	2.54	0.184	0.089
138	EF62-EOD	D30-32	70.50	37.00	24.0	407.9	5.18	2370	0.886	22.0	-	-	-	-	-
139	EF167-BOR	D30-32	70.50	34.99	24.0	408.5	4.66	2134	0.892	21.0	-	-	-	-	-
140	A3-EOD2	Vul-020	81.35	25.56	13.5	3059.8	1.04	3509	0.904	13.7	13.43	6.35	3.81	0.525	0.591
141	A3-BOR2	Vul-020	81.35	22.87	15.7	3059.8	0.94	2984	0.966	10.5	13.43	0.51	2.03	0.492	0.853
142	A3-BOR3	Vul-020	81.35	29.73	118.1	3059.8	1.11	3351	1.010	8.6	12.76	4.32	2.54	0.853	0.722
143	A14-DD1	Con-300	122.02	40.42	34.4	4247.8	1.07	4574	0.996	15.6	15.35	9.91	2.54	0.427	0.919
144	A14-DD2	Con-300	122.02	41.91	42.6	4247.8	1.32	5421	1.034	15.2	15.35	9.40	3.56	0.361	0.919
145	A14-BOR1	Con-300	122.02	55.41	11.8	4247.8	1.91	7471	1.085	13.8	15.35	2.54	3.05	0.722	0.722
146	A14-BOR2	Con-300	122.02	30.68	78.7	4247.8	0.96	4283	0.955	8.1	10.76	5.08	3.81	0.394	0.755
147	A25-EOD	Vul-020	81.35	30.53	15.7	3026.8	1.10	3231	1.031	18.7	15.31	8.89	3.05	0.262	0.394
148	A25-BOR1	Vul-020	81.35	25.84	31.5	3026.8	0.95	2897	0.994	14.3	15.31	8.13	2.54	0.328	0.361
149	A25-BOR2	Vul-020	81.35	30.10	78.7	3026.8	1.16	3413	1.033	12.7	15.31	9.65	6.86	1.017	0.328
150	A25-BOR3	Vul-020	81.35	30.00	78.7	3026.8	1.15	3353	1.040	13.2	15.31	9.65	6.35	0.853	0.623

**Table A.1 (con't).** Relevant Information Pertaining to Database PD/LT2000.

No.	Pile-Case Number	Hammer Type	Rated Hammer Energy	Delivered Energy	Blow Count	Impedence EA/C	Vimp	Fimp	VEA/C F	Dmax	2L/C	Tip Quake	Side Quake	Tip Damping	Side Damping
			(kN-m)	(kN-m)	(BP10cm)	(kN/m/s)	(m/s)	(kN)		(mm)	(ms)	(mm)	(mm)	(sec/m)	(sec/m)
151	A16-EOD	Vul-010	44.06	15.62	12.5	2197.1	1.21	2540	1.049	15.2	9.05	5.84	2.54	0.492	0.328
152	A16-BOR1	Vul-010	44.06	14.62	23.6	2197.1	1.10	2375	1.015	11.6	9.05	8.38	2.54	0.525	0.328
153	A16-BOR2	Vul-010	44.06	12.26	30.2	2197.1	0.97	2033	1.051	7.6	8.66	6.10	2.03	2.133	0.525
154	A41-EOD	Vul-002	81.35	29.75	16.4*	3005.9	1.14	3508	0.977	15.3	13.24	7.37	2.03	0.492	0.262
155	A41-BOR1	Vul-020	81.35	34.45	19.7	3005.9	1.31	3684	1.072	16.6	13.24	9.40	2.29	0.459	0.295
156	A41-BOR2	Vul-020	81.35	29.31	31.5	3005.9	1.29	3851	1.004	12.6	8.95	8.89	2.54	0.427	0.328
157	A101-EOD	Vul-020	81.35	28.40	11.5*	3040.5	1.12	3133	1.088	18.2	12.65	10.16	3.05	0.131	1.017
158	A101-BOR1	Vul-020	81.35	28.74	23.6	3040.5	1.19	3311	1.089	13.7	12.65	3.05	2.03	0.394	0.525
159	A101-BOR2	Vul-020	81.35	19.98	94.5	3040.5	0.94	2864	0.997	9.1	10.28	2.54	2.29	0.656	0.689
160	A133-EOD	Vul-020	81.35	24.46	20.7	3103.0	1.31	3701	1.096	16.6	18.31	8.89	4.57	0.853	0.689
161	A133-BOR	Vul-020	81.35	20.91	236.2	3103.0	1.06	3363	0.976	9.0	16.30	3.30	3.30	0.689	0.623
162	A145-EOD	Vul-020	81.35	25.31	20.7	3104.3	1.13	3430	1.026	15.9	18.59	4.83	2.29	0.492	0.787
163	A145-BOR1	Vul-020	81.35	23.73	51.2	3104.3	0.92	2900	0.982	12.4	18.59	4.32	4.32	0.558	0.886
164	A145-BOR2	Vul-020	81.35	22.40	189.0	3104.3	1.09	3330	1.020	10.4	16.21	4.06	3.56	0.689	0.689
165	CB3-BOR	Vul-020	81.35	22.44	39.4	3722.6	0.94	3411	1.025	7.8	11.38	4.83	2.54	1.847	1.040
166	CB3-BORL	Vul-020	81.35	21.49	39.4	3722.6	1.03	3596	1.063	7.1	11.67	4.83	2.79	1.729	1.243
167	CB5-BOR	ICE200S	135.58	20.80	47.2	4260.7	1.01	3993	1.077	7.2	12.45	3.56	2.54	1.030	3.048
168	CB5-BORL	ICE200S	135.58	33.85	63.0	4260.7	1.30	5735	0.962	11.5	8.74	7.62	2.54	0.745	1.329
169	CB11-BORL	ICE200S	135.58	38.45	70.9	4642.3	1.55	7272	0.992	8.2	12.81	3.56	4.57	4.380	0.817
170	CB11-EORL	ICE200S	135.58	39.48	63.0	4642.3	1.55	7253	0.989	8.1	12.81	3.05	4.32	2.165	1.765
171	CB17-BOR1	ICE200S	135.58	39.58	63.0	4336.7	1.51	6600	0.991	8.4	13.63	3.30	5.33	1.355	0.846
172	CB17-BOR2	ICE200S	135.58	49.60	60.4	4336.7	1.87	8107	1.003	10.6	13.63	6.35	4.06	1.043	0.909
173	CB17-BORL	ICE200S	135.58	27.79	141.7	4336.7	1.28	5591	0.995	7.6	12.65	5.59	0.76	1.148	0.410
174	CB17-DRL	ICE200S	135.58	36.40	65.0	4336.7	1.41	6753	0.908	8.4	12.65	6.35	0.25	1.076	0.102
175	CB23-BOR	ICE200S	135.58	19.08	31.5	4520.2	0.80	3745	0.971	6.8	12.95	3.56	3.30	2.159	0.932

**Table A.1 (con't). Relevant Information Pertaining to Database PD/LT2000.**

No.	Pile-Case Number	Hammer Type	Rated Hammer Energy (kN-m)	Delivered Energy (kN-m)	Blow Count (BP10cm)	Impedence EA/C (kN/m/s)	Vimp (m/s)	Fimp (kN)	VEA/C F	Dmax (mm)	2L/C (ms)	Tip Quake (mm)	Side Quake (mm)	Tip Damping (sec/m)	Side Damping (sec/m)
176	CB23-BORL	ICE200S	135.58	31.02	47.2	4520.2	1.36	6261	0.979	8.6	12.95	1.27	4.32	5.492	1.755
177	CB29-BORL	ICE200S	135.58	12.05	102.4	4207.1	0.64	2844	0.951	5.4	13.78	2.29	2.54	2.320	1.585
178	CB29-EORL	ICE200S	135.58	22.94	78.7	4207.1	1.07	4530	0.994	8.4	13.78	5.08	2.54	0.423	2.664
179	CB35-BOR1	ICE200S	135.58	42.48	34.4*	4290.5	1.57	6203	1.084	16.2	13.79	6.10	2.54	0.371	0.312
180	CB35-BOR2	ICE200S	135.58	30.78	78.7	4290.5	1.46	5962	1.048	8.5	13.79	4.57	2.54	0.371	1.421
181	CB35-BORL	ICE200S	135.58	26.57	51.2	4290.5	1.28	5484	0.999	7.3	12.66	2.29	4.32	2.297	0.741
182	CB41-EOR	ICE200S	135.58	43.63	59.7	4410.3	1.53	6689	1.011	14.2	14.14	6.60	2.54	0.463	0.686
183	CB41-BOR	ICE200S	135.58	36.73	94.5	4410.3	1.59	6917	1.016	12.4	14.00	6.60	2.79	0.417	0.650
184	CB41-BORL	ICE200S	135.58	29.15	34.3	4410.3	1.41	6452	0.963	8.4	10.92	3.56	3.30	1.152	1.286
185	CB26-EOD	Vul-020	81.35	21.06	18.7	3821.3	0.87	3355	0.996	11.7	11.40	5.33	3.05	0.249	0.344
186	CB26-BOR	Vul-020	81.35	30.74	21.5	3821.3	1.10	4214	1.001	12.9	11.40	6.86	2.79	0.325	0.194
187	CB26-EOR	Vul-020	81.35	34.44	39.4	3821.3	1.17	4600	0.970	13.6	11.40	8.38	2.29	0.184	0.184
188	CB26-BOR2	Vul-020	81.35	28.38	47.2	3821.3	1.07	4172	0.977	9.3	9.25	5.84	2.54	0.577	2.415
189	33P1-EOD	B-400	62.37	44.29	47.2	567.7	4.69	2737	0.972	28.2	14.39	3.81	7.62	0.262	0.033
190	33P1-BOR	B-400	62.37	43.12	63.0	567.7	4.81	2835	0.963	20.0	14.39	1.52	1.02	0.098	0.125
191	33P1-EOR	B-400	62.37	44.06	no set	567.7	5.06	2918	0.984	21.5	14.39	2.54	2.54	0.039	0.092
192	33P2-EOD	B-400	62.37	44.53	153.5	256.0	5.01	1251	1.025	47.2	17.81	10.16	5.08	0.492	0.066
193	33P2-BOR	B-400	62.37	41.99	299.2	256.0	5.08	1410	0.922	36.0	13.21	7.62	7.62	0.157	0.151
194	33P2-EOR	B-400	62.37	42.36	no set	256.0	5.27	1502	0.885	34.9	13.21	7.62	7.62	0.033	0.108
195	33P4-EOD	B-400	62.37	33.18	19.7	958.5	3.33	3511	0.964	17.4	10.45	2.54	0.64	0.328	0.164
196	33P5-EOD	B-225	39.32	8.69	42.0	358.4	2.67	1072	0.892	13.4	6.94	2.29	2.54	0.131	0.131
197	TRD22-EOD	D-12	30.51	13.26	118.1	564.8	3.20	1756	1.005	9.9	2.68	3.81	2.54	0.049	0.735
198	TRD22-BOR	D-12	30.51	10.62	78.7	564.8	2.93	1825	0.886	8.2	2.68	4.06	2.54	0.348	0.709
199	TRE22-EOD	D-22	54.23	20.59	86.6	564.8	4.06	2235	1.003	11.7	3.53	2.54	2.54	0.328	0.328
200	TRE22-BOR	D-22	54.23	20.58	39.4	564.8	4.35	2676	0.896	10.5	3.53	6.35	2.54	0.059	0.443

**Table A.1 (con't).** Relevant Information Pertaining to Database PD/LT2000.

No.	Pile-Case Number	Hammer Type	Rated Hammer Energy (kN-m)	Delivered Energy (kN-m)	Blow Count (BP10cm)	Impedence EA/C (kN/m/s)	Vimp (m/s)	Fimp (kN)	VEA/C F	Dmax (mm)	2L/C (ms)	Tip Quake (mm)	Side Quake (mm)	Tip Damping (sec/m)	Side Damping (sec/m)
201	TRP5X-EOD	D-12	30.51	12.43	149.6	405.7	3.96	1673	0.960	10.4	2.94	3.81	2.54	0.066	0.364
202	TRP5X-BOR	D-12	30.51	13.15	98.4	405.7	3.70	1608	0.933	11.0	2.94	3.81	2.54	0.043	0.420
203	TR131-BOR	D-12	30.51	9.63	15.7	205.8	3.38	703	0.991	19.3	3.15	7.62	7.62	0.112	0.771
204	TRAH-EOR	B-225	39.32	12.88	no set	681.5	3.14	2175	0.990	10.3	16.24	5.08	2.54	0.082	2.470
205	TRBH-BOR	B-225	39.32	16.95	9.8	683.0	3.38	2366	0.974	18.5	13.40	1.27	1.27	3.412	0.676
206	TRBP-EOR	B-225	39.32	11.66	18.4	318.1	3.93	1361	0.919	11.9	12.94	0.64	2.54	0.656	0.328
207	CHA1-EOD	Vul-200C	67.79	47.29	66.9	367.3	3.29	1208	1.000	43.6	16.40	3.81	2.54	0.131	0.331
208	CHA1-BOR1	Vul-200C	67.79	41.81	189.0	367.3	3.68	1352	1.000	35.3	16.40	1.02	1.02	0.023	1.411
209	CHA1-BOR2	Vul-200C	67.79	49.95	315.0	367.3	4.12	1512	1.000	35.9	16.50	0.76	0.76	0.023	0.180
210	CHA4-EOD	Vul-200C	67.79	31.17	14.8	367.3	2.84	1139	0.920	35.0	14.70	19.05	2.03	0.213	0.171
211	CHB2-EOD	Vul-010	44.06	34.30	3.0	489.9	4.05	2046	0.970	42.4	18.73	3.05	3.05	0.282	0.233
212	CHB2-BOR1	Vul-010	44.06	24.81	9.8	489.9	3.57	1819	0.960	20.3	18.73	3.05	3.05	0.276	0.262
213	CHB2-BOR3	Vul-010	44.06	28.74	24.6	489.9	3.84	2015	0.930	20.1	18.73	3.05	3.05	0.262	0.259
214	CHB2-BOR4	8tndrp	65.08	47.32	15.7	489.9	3.26	1868	0.860	30.7	18.62	3.05	3.05	0.210	0.213
215	CHB2-BOR5a	Vul-010	44.06	40.54	?	489.9	5.17	2064	0.914	28.4	18.14	3.05	3.05	0.413	2.493
216	CHB2-BOR5b	Vul-010	44.06	29.83	?	489.9	6.01	2309	0.950	29.5	18.14	2.29	2.29	2.133	0.226
217	CHB3-EOD	Vul-010	44.06	25.49	3.9	489.2	3.84	1944	0.970	31.0	17.22	2.54	2.54	0.377	0.394
218	CHB3-BOR1	Vul-010	44.06	19.12	7.9	489.2	3.17	1544	1.000	17.8	17.22	2.54	2.54	0.285	0.358
219	CHB3-BOR2	Vul-010	44.06	25.49	8.6	489.2	3.69	1806	1.000	20.1	17.22	2.54	2.03	0.299	0.381
220	CHB3-BOR3	8tndrp	65.08	38.37	9.4	489.2	3.20	1713	0.910	26.4	17.22	3.05	3.05-5.59	0.223	0.341
221	CHC3-EOD	Vul-010	44.06	32.40	6.9	1759.1	2.44	4310	1.000	20.3	20.71	1.02	2.54	2.461	0.328
222	CHC3-BOR	Vul-010	44.06	30.91	8.3	1759.1	2.68	4150	1.140	21.6	20.71				
223	CHC3-BORL	8tndrp	65.08	51.93	5.9	939.8?	2.68	2825	0.890	29.7	25.04?	12.70	3.05	0.121	0.249
224	CH4-EOD	Vul-010	44.06	29.68	3.3	420.2	4.14	1721	1.010	38.7	20.11	20.32	3.81	0.348	0.164
225	CH4-BOR	Vul-010	44.06	22.87	13.1	420.2	3.54	1561	0.950	20.4	20.11	5.59	3.81	0.883	0.085

**Table A.1 (con't). Relevant Information Pertaining to Database PD/LT2000.**

No.	Pile-Case Number	Hammer Type	Rated Hammer Energy (kN-m)	Delivered Energy (kN-m)	Blow Count (BP10cm)	Impedence EA/C (kN/m/s)	Vimp (m/s)	Fimp (kN)	VEA/C F	Dmax (mm)	2L/C (ms)	Tip Quake (mm)	Side Quake (mm)	Tip Damping (sec/m)	Side Damping (sec/m)
226	CH39-EOD	Vul-010	44.06	21.15	3.3	427.5	3.99	1793	0.950	22.6	17.50	3.81	3.81	0.436	0.075
227	CH39-BOR	Vul-010	44.06	26.71	62.6	427.5	4.36	1819	1.020	21.6	17.50	3.56	3.56	0.210	0.210
228	CH39-BORL	Vul-010	44.06	19.66	196.9	651.9	2.90	1877	1.010	15.0	22.54	3.30	3.81	0.102	0.128
229	CH6-5B-EOD	Vul-010	44.06	18.51	2.0	406.6	4.76	1548	1.060	43.5	18.10				
230	CH6-5B-BOR	Vul-010	44.06	24.27	44.7	405.7	3.51	1406	1.010	20.8	18.02	2.03	3.05	1.178	0.279
231	CH95B-EOD	Vul-010	44.06	42.78	4.6	406.6	4.22	1815	0.940	35.1	19.45	6.35	3.68	0.427	0.397
232	CH95B-BOR	Vul-010	44.06	33.22	38.6	403.7	4.15	1677	1.000	25.9	19.39	1.27	1.93	0.564	0.325
233	CH256-BOR3	Vul-010	44.06	25.62	23.6/0	404.0	3.90	1601	0.980	22.4	17.26	2.54	2.54	0.131	0.108
234	CH351-BOR2	Vul-010	44.06	26.03	242.1	404.0	3.90	1659	0.950	20.1	18.81	1.27	1.52-3.81	0.279	0.098
235	PO2-BOR1	ICE-640	54.23	14.41	35.4	2008.1	1.46	2933	1.000	11.9	13.26	3.56	0.51	0.538	0.187
236	PO2-BOR2	ICE-640	54.23	13.31	28.6	2008.1	1.65	3333	0.990	10.7	13.26	5.33	0.38	0.463	0.361
237	PO2-BORL	ICE-640	54.23	13.02	31.5	2008.1	1.25	2534	1.000	11.9	4.63	7.11	1.27	0.207	0.243
238	PO19-BOR	ICE-640	54.23	15.77	63.0	1989.1	1.46	2927	0.990	11.4	13.39	4.70	0.15	0.722	0.318
239	PO19-EOD	ICE-640	54.23	9.99	36.1	1989.1	1.10	2209	0.990	9.7	13.39	3.18	0.64	0.784	0.344
240	PO19-EORL	ICE-640	54.23	11.05	21.0	1989.1	1.10	2423	0.910	11.0	4.80	6.10	0.41	0.423	0.131
241	ER5-BOR1	D46-23	145.34	24.69	28.7	3950.3	1.31	5349	0.970	6.3	14.33	5.33	1.14	0.325	1.037
242	ER5-BOR2	D46-23	145.34	28.23	49.2	3948.8	1.37	5650	0.960	7.1	14.33	4.06	1.14	0.325	1.007
243	ER5-BORL	D46-23	145.34	19.93	40.9	3948.7	1.01	4140	0.960	6.5	12.13	5.59	1.27	0.778	1.004
244	ER77-BOR	D46-23	145.34	29.76	40.7	3672.8	1.49	5509	1.000	7.8	14.50	5.84	2.54	0.502	0.886
245	ER77-BORL	D46-23	145.34	29.83	127.4	3672.8	1.58	6048	0.960	6.7	9.04	4.83	3.81	0.748	0.814
246	BB13-EOD	Con300	162.70	76.85	13.2	4548.6	1.89	9052	0.950	16.6	22.29	7.16	1.78	0.561	0.853
247	BB13-BOR1a	Con300	162.70	93.28	20.5	4548.3	2.31	10698	0.980	16.1	22.30	5.97	1.02	0.361	0.541
248	BB13-BOR1b	Con300	162.70	90.26	20.5	4548.6	2.25	10545	0.970	15.7	22.29	5.72	0.51	0.351	0.623
249	BB13-BOR2a	Con300	162.70	98.30	16.4	4573.6	2.64	12064	1.000	14.1	22.17	4.83	2.57	0.427	0.636
250	BB13-BOR2b	Con300	162.70	105.40	16.4	4580.7	2.73	12569	1.000	14.6	22.14	6.35	1.78	0.719	0.354

**Table A.1 (con't).** Relevant Information Pertaining to Database PD/LT2000.

No.	Pile-Case Number	Hammer Type	Rated Hammer Energy (kN-m)	Delivered Energy (kN-m)	Blow Count (BP10cm)	Impedence EA/C (kN/m/s)	Vimp (m/s)	Fimp (kN)	VEA/C F	Dmax (mm)	2L/C (ms)	Tip Quake (mm)	Side Quake (mm)	Tip Damping (sec/m)	Side Damping (sec/m)
251	BB13-BORL	Con300	162.70	76.69	41.0	4548.6	1.65	7746	0.970	14.3	17.20	5.08	1.85	0.499	0.997
252	BB19-BORa	Con300	162.70	88.18	14.6	4615.9	2.11	9900	0.980	14.7	23.19	4.57	2.54	0.367	1.093
253	BB19-BORb	Con300	162.70	89.36	14.6	4615.9	2.21	10401	0.980	14.7	23.19	6.73	3.18	0.377	0.538
254	BB19-BORL	Con300	162.70	78.03	32.8	4615.9	1.80	8280	1.000	14.5	17.85	9.14	2.54	0.463	0.554
255	BB24-EOD	Con300	162.70	87.78	22.6*	4568.3	2.26	10502	0.980	13.7	22.20	6.73	0.25	0.377	0.758
256	BB24-BOR1a	Con300	162.70	90.11	24.6	4550.2	2.47	11601	0.970	13.2	22.29	6.38	0.48	0.512	0.312
257	BB24-BOR1b	Con300	162.70	88.52	24.6	4579.1	2.44	11314	0.990	13.2	22.15	7.49	1.04	0.328	0.482
258	BB24-BOR2a	Con300	162.70	98.87	32.8	4615.9	2.66	12550	0.980	13.3	22.73	4.70	0.89	0.505	0.833
259	BB24-BOR2b	Con300	162.70	91.54	32.8	4552.7	2.65	12302	0.980	12.6	22.10	6.12	1.91	0.328	0.604
260	BB24-BORL	Con300	162.70	54.40	147.6	4550.2	1.34	6121	1.000	11.3	15.74	5.08	2.54	0.794	0.758
261	BB29-BOR	Con 300	162.70	90.37	21.0*	4554.3	2.23	10226	0.990	14.1	21.89				
262	BB29-BORL	Con 300	162.70	78.26	24.6*	4604.7	1.78	8190	1.000	15.8	14.69	9.02	2.03	0.243	0.902
263	ABF6-BOR	D46-32	145.34	30.70	15.7	3455.3	1.18	4323	0.950	17.6	11.18	15.24	2.87	0.161	0.482
264	ABF6-BORL	D46-32	145.34	28.50	73.8	3455.3	1.24	4656	0.920	6.9	9.92	5.08	3.96	1.814	0.899
265	ABG13-BORL	D46-32	145.34	33.85	73.8	3618.1	1.33	5183	0.930	8.2	9.32	5.84	3.30	0.472	0.538
266	ABH2-BOR	D46-32	145.34	29.42	36.1	3618.4	1.35	4797	1.020	11.5	6.15	9.27	1.19	0.115	0.505
267	ABH2-BORL	D46-32	145.34	29.49	57.4	3673.1	1.43	4869	1.080	10.2	5.17	8.28	2.79	0.161	0.764
268	BC79-EOD	Vul 320/520	135.58	41.66	11.7		2.05	5256	1.020	16.5	13.10				
269	BC79-BORL	Vul 320/520	135.58	50.63	7.9		2.02	5595	1.020	20.4	12.57	11.43	2.03	0.230	0.249
270	BC64-EOD	Vul 320/520	135.58	36.35	15.4		1.54	3970	0.990	12.6	10.60				
271	BC64-BORL	Vul 320/520	135.58	58.73	15.7		2.19	6297	1.000	14.5	9.85	7.11	4.32	0.344	0.210
272	D1-BOR1	IHC	38.00	11.46	9.4	566.1	2.17	1516	0.810	15.4	5.74	3.18	1.27	0.164	0.492
273	D2-BOR1	IHC	38.00	11.47	14.1	566.1	2.02	1449	0.790	11.6	7.53	4.45	1.02	0.164	0.656
274	D3-BORa	IHC	38.00	19.92	12.4	566.1	3.22	1958	0.930	14.6	9.64	1.27	2.54	0.492	0.656
275	D3-BORb	IHC	38.00	19.73	10.9	566.1	3.32	1991	0.940	15.5	9.64	0.64	2.54	0.492	0.656



**Table A.1 (con't).** Relevant Information Pertaining to Database PD/LT2000.

No.	Pile-Case Number	Hammer Type	Rated Hammer Energy (kN-m)	Delivered Energy (kN-m)	Blow Count (BP10cm)	Impedence EA/C (kN/m/s)	Vimp (m/s)	Fimp (kN)	VEA/C F	Dmax (mm)	2L/C (ms)	Tip Quake (mm)	Side Quake (mm)	Tip Damping (sec/m)	Side Damping (sec/m)
276	D5-BORa	IHC	38.00	14.11	25.0	566.1	2.14	1355	0.890	12.8	9.64	6.60	5.08	0.033	0.656
277	D5-BORb	IHC	38.00	21.22	16.7	566.1	3.55	2190	0.920	13.4	9.64	3.81	3.81	0.492	0.820
278	MB1-EOD	Con100E	67.79	33.07	6.9*	1571.9	2.04	3276	0.980	32.6	9.78	28.35	1.60	0.207	0.745
279	MB1-BOR	Con100E	67.79	15.36	22.0*	1571.9	1.26	2000	0.990	9.6	9.54	3.05	1.78	0.489	0.994
280	MB2-BOR	Con100E	67.79	31.36		679.1	3.50	2477	0.960	17.8	9.17	3.05	2.57	0.325	0.607
281	MB3-BOR	Con100E	67.79	26.94		633.5	3.02	2005	0.950	18.7	9.17	2.72	3.94	0.276	0.410
282	S1-EOD	Vul 512	81.35	40.93	14.8*	1041.7	3.21	3487	0.960	17.9	9.64	11.18	3.43	0.381	0.696
283	S1-BOR	Vul 512	81.35	47.17		1039.1	3.60	3953	0.950	16.4	9.64	6.40	5.46	1.207	0.692
284	S2-EOD	Vul 512	81.35	23.33	5.6*	557.5	2.79	1767	0.880	19.6	9.50	14.55	1.65	0.430	0.761
285	S2-BOR	Vul 512	81.35	26.45	2.6*	556.0	3.57	2223	0.890	17.3	9.40	14.55	1.65	0.430	0.761
286	DD22-EOD	Vul 80C	33.19	12.61	22.3	1096.0	1.55	1866	0.910	12.8	15.65	6.60	3.30	0.249	0.955
287	DD22-BOR	Vul 010	44.06	24.24	25.6	1274.0	1.92	2391	1.020	14.9	15.65	3.56	2.29	0.558	0.361
288	DD23-EOD	Vul 80C	33.19	13.15	8.9	255.4	3.47	923	0.960	27.3	11.54	6.86	3.30	0.154	0.259
289	DD23-BOR	Vul 010	44.06	26.79	11.8	255.4	4.36	1112	1.000	28.8	10.11	4.57	6.35	0.200	0.131
290	JR17-EOD	D-46	142.36	40.00	106.3	3437.2	2.32	7985	1.000	18.8	5.93	9.53	1.78	0.128	0.230
291	LB3-EOD	D46-13	75.84	34.13	3.3	3029.7	1.16	3545	0.990	42.2	11.55	13.97	13.97	1.329	0.669
292	LB3-BOR1	D46-13	75.84	28.43	6.9	3029.7	1.19	3817	0.940	21.2	11.55	3.05	3.05	1.404	0.367
293	LB3-BOR2	D46-13	75.84	23.77	23.6	2927.5	1.31	4148	0.930	11.2	11.95	4.57	3.30	1.243	0.696
294	LB3-BOR3	D46-13	75.84	19.77	47.2	2927.5	1.46	4209	1.020	9.2	11.95	4.83	4.83	0.909	0.955
295	LB4-EOD	D46-13	75.84	31.39	4.6	3954.9	1.92	6155	1.230	32.2	11.95	20.32	5.08	1.388	1.388
296	LB4-BOR1	D46-13	75.84	37.79	7.6	3954.9	1.65	6710	0.970	19.3	11.95	19.05	3.05	1.427	1.004
297	LB4-BOR2	D46-13	75.84	42.88	19.7	3954.9	1.80	7434	0.960	16.2	11.95	7.62	5.08	1.191	1.309
298	LB4-BOR3	D46-13	75.84	43.97	78.7	3954.9	1.86	7699	0.960	13.3	11.95	7.62	4.45	1.109	1.519
299	LB4-BOR4	D46-13	75.84	30.90	55.1	3954.9	1.25	5188	0.950	10.8	11.95	9.40	3.56	1.135	1.578
300	LB5-EOD	D46-13	70.01	15.24	7.2	3954.9	0.82	3517	0.930	26.1	11.95	17.78	5.08	0.331	0.331

**Table A.1 (con't).** Relevant Information Pertaining to Database PD/LT2000.

No.	Pile-Case Number	Hammer Type	Rated Hammer Energy (kN-m)	Delivered Energy (kN-m)	Blow Count (BP10cm)	Impedence EA/C (kN/m/s)	Vimp (m/s)	Fimp (kN)	VEA/C F	Dmax (mm)	2L/C (ms)	Tip Quake (mm)	Side Quake (mm)	Tip Damping (sec/m)	Side Damping (sec/m)
301	LB5-BOR1	D46-13	70.01	31.03	19.4	3954.9	1.19	4842	0.970	18.7	11.95	17.78	5.08	0.666	1.473
302	LB5-BOR2	D46-13	70.01	31.01	31.5	3954.9	1.16	5093	0.900	11.9	11.95	10.67	5.08	1.093	1.552
303	LB5-BOR3	D46-13	70.01	32.87	29.8	3954.9	1.19	5363	0.880	10.0	11.95	8.89	4.32	1.562	1.608
304	LB5-BOR4	D46-13	70.01	27.88	>78.7	3954.9	1.13	4943	0.900	9.9	11.95	9.53	5.84	1.404	1.178
305	LB6-EOD	D46-13	75.84	20.69	4.9	3131.9	1.28	4002	1.000	28.0	11.43	22.86	2.54	0.328	0.522
306	LB6-BOR1	D46-13	75.84	27.56	11.1	3079.3	1.34	4304	0.960	17.0	11.43	13.97	5.08	0.919	0.965
307	LB6-BOR2	D46-13	75.84	27.40	21.0	3079.3	1.43	4674	0.940	11.2	11.43	3.81	3.81	0.909	1.378
308	LB6-BOR3	D46-13	75.84	20.30	53.1	3079.3	1.31	4432	0.910	7.5	11.43	6.73	3.05	0.981	1.106
309	LB6-BOR4	D46-13	75.84	27.58	37.1	3079.3	1.52	4973	0.940	7.8	11.43	7.24	3.05	0.591	0.823
310	LB7-EOD	D46-13	75.84	9.17	15.5	3079.3	1.19	2894	1.260	13.1	11.85	6.35	3.81	0.577	0.758
311	LB7-BOR1	D46-13	75.84	27.05	10.5	3079.3	1.34	4785	0.860	17.1	11.94	15.24	7.62	1.165	0.896
312	LB7-BOR2	D46-13	75.84	23.78	33.5	3079.3	1.31	4759	0.850	10.9	12.31	8.13	7.62	0.623	1.135
313	LB7-BOR3	D46-13	75.84	25.16	55.1	3079.3	1.43	5150	0.860	9.4	12.31	9.78	5.59	1.014	0.686
314	LB7-BOR4	D46-13	75.84	24.80	61.0	3079.3	1.43	5033	0.880	8.7	12.31	7.11	5.08	0.833	0.827
315	DI221-EOD	ICE 640	54.23	23.18	31.5	1179.8	1.83	2318	0.931	27.4	13.49	---	---	---	---
316	DI221-2DR	ICE 640	54.23	20.74	35.4	1179.8	1.95	2647	0.870	16.8	13.49	14.48	2.03	0.558	0.384
317	TW488-EOD	D30-32	99.87	20.20	2.6*	1202.9	1.77	1824	1.166	44.7	12.15	7.62	7.62	2.110	0.479
318	TW488-3DR	D30-32	99.87	27.66	10.5*	1202.9	2.07	2758	0.904	19.8	12.15	17.78	6.35	0.988	0.801
319	NBTP2-EOD	HPSI 1000	67.79	39.86	11.8	567.8	4.94	2900	0.967	30.0	13.86	1.27	5.72	0.039	0.138
320	NBTP2-1DR	HPSI 1000	67.79	45.56	7.9	567.8	5.39	3087	0.992	30.0	13.86	1.27	5.33	0.046	0.135
321	NBTP2-6DR	HPSI 1000	67.79	39.05	39.4	567.8	4.91	2798	0.996	26.4	13.86	1.27	6.35	0.066	0.135
322	NBTP3-EOD	HPSI 1000	67.79	43.93	15.7	567.8	5.30	3060	0.984	29.7	13.86	6.60	1.27	0.305	0.092
323	NBTP3-1DR	HPSI 1000	67.79	38.78	19.7	567.8	5.06	2847	1.009	27.7	13.86	6.35	1.27	0.285	0.056
324	NBTP3-6DR	HPSI 1000	67.79	45.83	19.7	567.8	5.36	3065	0.994	28.7	13.86	6.86	1.27	0.289	0.062
325	NBTP5-EOD	HPSI 1000	67.79	34.57	11.8	379.7	4.66	1882	0.941	31.0	13.94	13.97	1.27	0.200	0.230

**Table A.1 (con't).** Relevant Information Pertaining to Database PD/LT2000.

No.	Pile-Case Number	Hammer Type	Rated Hammer Energy (kN-m)	Delivered Energy (kN-m)	Blow Count (BP10cm)	Impedence EA/C (kN/m/s)	Vimp (m/s)	Fimp (kN)	VEA/C F	Dmax (mm)	2L/C (ms)	Tip Quake (mm)	Side Quake (mm)	Tip Damping (sec/m)	Side Damping (sec/m)
326	NBTP5-3DR	HPSI 1000	67.79	32.81	55.1	379.7	5.00	2068	0.918	25.9	13.94	3.81	2.54	0.279	0.240
327	PR1-BOR1	D 46-32	153.42	33.35	23.6	3184.3	1.31	4644	0.899	10.7	15.14	8.13	1.52	0.755	1.837
328	DD29-EOD	Vul - 80C	33.15	26.44	40.0	379.7	4.08	1535	1.011	25.4	24.71	3.56	3.56	0.217	0.719
329	ND50-BOR1	FEC 1500	36.73	10.17	14.1	195.8	3.03	885	0.671	15.6	5.79	3.05	1.63	0.174	0.236
330	NZ12-BOR1	D 19-32	57.49	23.46	23.6	557.7	3.87	2958	0.730	9.4	5.17	6.35	1.52	0.574	0.728
331	DW1-BOR1	Vul - 520	135.58	46.64	328.1	3388.2	1.72	6099	0.953	9.7	12.43	5.84	6.60	1.060	0.823
332	DW1-BOR2	Vul - 520	135.58	42.30	328.1	3388.2	1.41	6067	0.786	9.4	12.43	4.34	5.33	0.259	1.152
333	DW2-BOR1	Vul - 520	135.58	31.86	328.1	661.5	3.19	2660	0.793	16.9	12.43	2.36	3.76	0.745	0.433
334	DW2-BOR2	Vul - 520	135.58	47.72	328.1	661.5	3.86	3065	0.834	21.9	12.43	3.81	3.99	0.502	0.499
335	DS1-BOR1	ICE - 640	55.07	8.95	102.4	850.1	1.36	1299	0.890	9.0	12.76	3.89	3.51	0.823	0.774
336	DS1-BOR2	ICE - 640	55.07	10.44	105.0	850.1	1.56	1423	0.930	10.0	12.76	3.30	3.30	0.761	0.761
337	PX2-BOR1	MKTDE70B	80.67	27.93	59.1	896.5	3.90	3946	0.886	10.7	7.00	6.86	3.30	0.072	0.161
338	PX3-EOD	MKTDE70B	80.67	12.07	100.7	896.5	2.23	2420	0.824	6.9	9.14	3.05	2.29	0.089	0.217
339	PX3-BOR1	MKTDE70B	80.67	29.01	23.6	896.5	3.90	4003	0.874	10.4	7.71	1.78	1.78	0.072	0.207
340	PX4-EOD	MKTDE70B	80.67	16.81	256.9	418.3	3.72	2331	0.667	11.2	4.14	4.57	2.54	0.108	0.302
341	PX4-BOR1	MKTDE70B	80.67	34.17	51.2	418.3	5.21	3011	0.724	16.5	4.14	7.62	3.81	0.089	0.112
342	PX5-BOR1	MKTDE70B	80.67	28.34	63.0	418.3	4.85	2687	0.754	15.0	4.14	6.60	4.06	0.072	0.180
343	PX6-BOR1	MKTDE70B	80.67	16.00	114.2	1365.7	2.41	3345	0.983	7.4	4.26	3.81	2.54	0.213	0.285
344	PX7-EOD	MKTDE70B	80.67	20.34	221.5	1365.7	1.71	3599	0.648	7.6	3.43	5.59	5.08	0.190	0.256
345	PX7-BOR1	MKTDE70B	80.67	30.23	47.2	1365.7	3.32	4435	1.023	11.9	3.43	7.62	6.35	0.144	0.171
346	CH11-42-BOR1	Vul - 010	44.06	31.05	55.1	380.3	2.99	3256	0.349	13.2	13.96	4.83	3.81	0.554	0.623
347	SSTPD-5DR	SECH	8.00	9.10	6.9	552.1	1.84	1090	0.930	14.8	6.60	3.91	2.57	0.833	0.627
348	TSW/D62/1-EOD	D62	223.71	86.80	14.3	1224.4	4.78	5770	1.010	25.9	11.80	14.20	1.27	0.098	0.456
349	TSW/D62/1-BOR	D62	223.71	67.60	35.7	1236.8	4.25	5628	0.930	18.2	11.68	3.84	2.54	0.833	0.394
350	TSW/HHK9/1-EOD	JunHHK9	105.89	82.89	15.4	1236.8	4.05	4842	1.030	23.0	11.68	10.21	1.88	0.141	0.328

**Table A.1 (con't).** Relevant Information Pertaining to Database PD/LT2000.

No.	Pile-Case Number	Hammer Type	Rated Hammer Energy (kN-m)	Delivered Energy (kN-m)	Blow Count (BP10cm)	Impedence EA/C (kN/m/s)	Vimp (m/s)	Fimp (kN)	VEA/C F	Dmax (mm)	2L/C (ms)	Tip Quake (mm)	Side Quake (mm)	Tip Damping (sec/m)	Side Damping (sec/m)
351	TSW/HHK9/1-BOR	JunHHK9	105.89	78.60	45.5	1236.8	3.94	4943	0.990	20.6	11.68	2.11	1.70	1.299	0.161
352	TSW/D62/2-EOD	D62	223.71	90.89	17.2	940.0	5.60	5619	0.940	27.7	13.66	3.51	3.38	0.082	0.246
353	TSW/D62/2-BOR	D62	223.71	98.88	41.7	939.4	5.70	5854	0.910	28.5	13.67	3.51	2.54	10.102	0.135
354	TSW/HHK9/2-EOD	JunHHk9	105.89	98.89	14.3	939.4	5.52	5315	0.980	29.2	13.67	3.58	4.93	0.417	0.213
355	TSW/HHK9/2-BOR	JunHHk9	105.89	87.04	25.6	939.4	5.30	5260	0.950	25.3	13.67	3.51	2.57	0.722	0.217
356	OD1J-EOD	D62-22	178.15	96.13	6.6	1426.6	4.37	6777	0.919	23.8	3.57	23.22	0.64	0.118	0.390
357	OD2P-EOD	D62-22	158.36	72.67	3.6	1426.6	3.77	5744	0.936	34.5	4.77	1.91	3.43	0.066	0.289
358	OD2P-BOR	D62-23	197.95	157.95	4.9	1426.6	6.05	9204	0.938	38.9	4.77	12.70	1.50	0.253	0.233
359	OD2T-EOD	D46-32	123.79	76.74	14.1	1426.6	4.49	6602	0.971	28.6	4.76	23.90	1.57	0.144	0.105
360	OD3H-EOD	D62-22	178.15	89.35	3.6	2531.2	4.16	10574	0.996	27.1	12.02	1.65	1.27	0.062	0.568
361	OD4L-EOD	D62-22	217.74	90.70	5.6	961.3	4.65	4475	1.000	42.7	8.35	33.76	1.63	0.174	0.482
362	OD4P-EOD	D30-32	71.75	40.13	8.5	961.3	3.21	3244	0.951	29.8	8.33	21.69	2.03	0.217	0.846
363	OD4P-BOR	D62-22	217.74	133.82	4.4	961.3	5.72	5623	0.978	44.6	8.33	34.29	2.54	0.089	0.417
364	OD4T-EOD	D30-32	71.75	38.37	5.9	961.3	3.26	3419	0.915	20.9	8.33	11.05	4.09	0.066	0.653
365	OD4T-BOR	D62-22	217.74	119.18	9.8	961.3	5.37	5805	0.890	27.9	8.33	24.49	4.67	0.082	0.636
366	OD4W-EOD	D46-32	110.01	71.32	4.9	961.3	4.31	4215	0.982	40.4	8.35	34.32	3.18	0.157	0.689
367	OD4W-BOR2	D30-32	80.73	40.27	40.7	961.3	3.52	3647	0.929	17.1	8.35	10.52	6.99	0.466	0.400
368	OD4W-BOR3	D62-22	197.95	95.72	24.9	961.3	5.10	5178	0.947	26.5	8.35	22.86	5.08	0.430	0.348
369	QC3-EOD	Con5300	203.37	25.49	31.5	4902.4	0.88	4302	1.010	11.2	13.20	7.11	0.76	1.745	0.696
370	QC3-14DR	Con5300	203.37	42.03	98.4	4916.2	1.20	6179	0.960	8.6	13.16	5.08	0.76	0.564	1.253
371	QC14-EOD	MKT S-8	35.25	7.86	47.2	1004.9	1.34	1339	1.010	8.4	15.29	3.35	0.99	2.060	0.653
372	QC14-30DR	MKT S-8	35.25	11.52	90.6	1280.9	1.51	1899	1.020	8.7	12.00	5.51	1.27	1.942	0.636
373	NYSP-EOD	Vulcan 06	26.44	13.29	51.2	416.9	3.07	1204	1.060	16.6	13.86	3.56	1.27	0.325	0.640
374	NYSP-BOR	Vulcan 06	26.44	15.19	133.9	416.4	3.59	1390	1.080	15.1	13.24	3.73	1.57	1.135	0.869
375	UFSS1A - BOR	ConC300	122.02	46.23	149.6	3317.2				11.7					

**Table A.1 (con't).** Relevant Information Pertaining to Database PD/LT2000.

No.	Pile-Case Number	Hammer Type	Rated Hammer Energy (kN-m)	Delivered Energy (kN-m)	Blow Count (BP10cm)	Impedence EA/C (kN/m/s)	Vimp (m/s)	Fimp (kN)	VEA/C F	Dmax (mm)	2L/C (ms)	Tip Quake (mm)	Side Quake (mm)	Tip Damping (sec/m)	Side Damping (sec/m)
376	UFSS1B - BOR	ConC300	122.02	21.56	110.2	2304.4				8.6					
377	UFSS10 - BOR	ConC300	122.02	50.71	102.4	3285.1				12.2					
378	UFSS13B - BOR	ConC300	122.02	32.00	63.0	3285.1				12.7					
379	BIT20 - BOR	Vulcan 510	44.06	6.55	51.2	2286.9				6.1					
380	BIT21 - BOR	Vulcan 510	44.06	5.60	27.6	2472.2	1.40	3655	0.948	9.0	5.50	7.87	2.54	0.420	0.554
381	HFLS3 - EOD	ConC300	122.02	56.94	82.0	5205.6				10.9		7.37	3.56	0.190	0.167
382	HFLS4L - EOD	ConC300	122.02	48.81	18.7	5205.6				13.4		9.65	3.81	0.233	0.650
383	HFLS4L - BOR	ConC300	122.02	59.66	19.7	5205.6				10.5		5.08	2.54	0.676	0.138
384	RBA30 - BOR	ICE 200S	135.58	34.44	44.9	5442.1	1.43	7800	0.997	9.6	10.94	7.16	3.81	0.823	1.237
385	RBB30W - BOR	ICE 200S	135.58	39.05	20.9	5439.1	1.33	7481	0.968	11.4	9.53	9.58	3.81	1.273	0.525
386	CC6 - BOR	ICE 640	54.23	18.17	35.4	1878.2	1.68	3291	0.957	9.2	12.71	5.69	3.30	0.646	1.398
387	CC7 - BOR	ICE 640	54.23	15.19	39.4	1125.2	1.58	2076	0.857	9.6	12.84	3.56	3.56	0.515	0.751
388	CC14 - BOR	ICE 640	54.23	15.32	51.2	1125.2	1.71	2185	0.879	9.8	12.84	4.83	4.32	0.594	0.771
389	49SB37 - EOD	D62-32	145.34	13.79	58.7	5611.4	1.55	8151	1.070	9.9	8.18	5.84	2.54	0.610	0.384

**Table A.1 (con't).** Relevant Information Pertaining to Database PD/LT2000.

No.	Pile-Case Number	Load Test Type	Davisson's Criteria  (kN)	Shape of Curve (kN)	Average Shape of Curve (kN)	$\Delta=1''$ (kN)	$\Delta=0.1B$ (kN)	DeBeer (kN)	Average DeBeer (kN)	Static Resist Rs (kN)	CAPWAP TEPWAP (kN)	Energy Appr. Ru (kN)	Ksp Rs Ru
1	FN1-EOD	Q	1352	1334	1334	1352	1352	1334	1334	1334	1023	1610	0.829
2	FN1-BOR1	Q	1352	1334	1334	1352	1352	1334	1334	1334	1668	2153	0.620
3	FN1-BOR2	Q	1352	1334	1334	1352	1352	1334	1334	1334	1917	2380	0.561
4	FN2-EOD	Q	1592	1575	1575	1610	1628	1584	1584	1575	1005	1859	0.847
5	FN2-BOR	Q	1592	1575	1575	1610	1628	1584	1584	1575	1357	2166	0.727
6	FN3-EOD	Q	1681	1646	1646	1699	1748	1628	1628	1664	796	2135	0.779
7	FN3-BOR	Q	1681	1646	1646	1699	1748	1628	1628	1664	1321	2762	0.602
8	FN4-EOD	Q	1263	1246	1246	1281	1299	1254	1254	1246	1085	1784	0.698
9	FN4-BOR	Q	1263	1246	1246	1281	1299	1254	1254	1246	1281	2589	0.481
10	FIA-EOD	Q	4128	4155	4155	3434	4048	4092	4092	4137	1632	2531	1.634
11	FIA-BOR	Q	4128	4155	4155	3434	4048	4092	4092	4137	3252	3065	1.349
12	FIB-EOD	Q	2891	2135-2847	2491	2891	NA	2882	2882	2891	2273	3149	0.918
13	FIB-BOR	Q	2891	2135-2847	2491	2891	NA	2882	2882	2891	2318	3096	0.934
14	FO1-EOD	Q	2660	2224-2491	2358	2989	NA	2420	2420	2478	2206	3185	0.811
15	FO1-BOR	Q	2660	2224-2491	2358	2989	NA	2420	2420	2478	3114	5200	0.476
16	FO2-EOD	Q	3381	3336	3336	3470	3559	3354	3354	3336	2358	2874	1.161
17	FO2-BOR	Q	3381	3336	3336	3470	3559	3354	3354	3336	3252	5151	0.648
18	FO3-EOD	Q	3452	3114-3781	3447	3630	3834	3648	3648	3648	2518	2598	1.404
19	FO4-EOD	Q	7562	6228	6228	7633	8007	7402	7402	7340	2927	3394	2.163
20	FO4-BOR	Q	7562	6228	6228	7633	8007	7402	7402	7340	3412	5645	1.300
21	FOR1-EOD	Q	6050	6005	6005	5196	7117	6228	6228	6139	2487	3732	1.651
22	FOR1-BOR	Q	6050	6005	6005	5196	7117	6228	6228	6139	3243	5369	1.143
23	FM5-EOD	Q	1957	1601-1957	1779	2340	NA	2051	2051	1868	1539	1588	1.176
24	FM5-BOR	Q	1957	1601-1957	1779	2340	NA	2051	2051	1868	2220	3265	0.572
25	FM17-EOD	Q	1815	1668-1957	1815	2406	NA	1913	1913	1988	1886	2331	0.853

**Table A.1 (con't).** Relevant Information Pertaining to Database PD/LT2000.

No.	Pile-Case Number	Load Test Type	Davisson's Criteria (kN)	Shape of Curve (kN)	Average Shape of Curve (kN)	$\Delta=1''$ (kN)	$\Delta=0.1B$ (kN)	DeBeer (kN)	Average DeBeer (kN)	Static Resist Rs (kN)	CAPWAP TEPWAP (kN)	Energy Appr. Ru (kN)	Ksp Rs Ru
26	FM17-BOR	Q	1815	1668-1957	1815	2406	NA	1913	1913	1988	2340	3474	0.572
27	FM23-EOD	Q	1521	1290-1468	1379	1681	NA	1584	1584	1512	1437	1833	0.825
28	FM23-BOR	Q	1521	1290-1468	1379	1681	NA	1584	1584	1512	1512	1895	0.798
29	FC1-EOD	Q	1406	1423-1601	1512	1646	1655	1592	1592	1512	1201	1521	0.994
30	FC1-BOR	Q	1406	1423-1601	1512	1646	1655	1592	1592	1512	1179	1615	0.937
31	FC2-EOD	Q	1637	1557-1779	1668	1966	NA	1495	1495	1673	1668	1788	0.935
32	FC2-BOR	Q	1637	1557-1779	1668	1966	NA	1495	1495	1673	1512	1570	1.065
33	FMI1-EOD	Q	1468	1281-1410	1348	1481	NA	1423	1423	1379	1268	1094	1.260
34	FMI1-BOR	Q	1468	1281-1410	1348	1481	NA	1423	1423	1379	1419	1361	1.013
35	FMI2-EOD	Q	930	712	712	NA	NA	560	560	712	818	796	0.894
36	FMI2-BOR	Q	930	712	712	NA	NA	560	560	712	965	1241	0.573
37	FWA-EOD	SM	5783	5783	5783	5783	NA	5115	5115	5783	1312	5093	1.135
38	FWA-BOR	SM	5783	5783	5783	5783	NA	5115	5115	5783	2900	5133	1.127
39	FWB-EOD	SM	4448	5338	5338	4448	NA	6659	6659	5449	plug	7598	0.717
40	FWB-BOR	SM	4448	5338	5338	4448	NA	6659	6659	5449	plug	5694	0.957
41	FA1-EOD	S	1646	1446-1557	1503	1864	NA	1486	1486	1535	912	1343	1.142
42	FA1-BOR1	S	1646	1446-1557	1503	1864	NA	1486	1486	1535	1143	2055	0.747
43	FA1-BOR2	S	1646	1446-1557	1503	1864	NA	1486	1486	1535	1699	3737	0.411
44	FA2-EOD	S	2447	2135-2447	2291	2616	NA	2406	2406	2380	1904	2527	0.942
45	FA2-BOR1	S	2447	2135-2447	2291	2616	NA	2406	2406	2380	2175	4226	0.563
46	FA2-BOR2	S	2447	2135-2447	2291	2616	NA	2406	2406	2380	2664	3986	0.597
47	FA3-EOD	S	2780	2224-2847	2535	3020	NA	2882	2882	2731	1512	2433	1.122
48	FA3-BOR1	S	2780	2224-2847	2535	3020	NA	2882	2882	2731	1366	3309	0.825
49	FA3-BOR2	S	2780	2224-2847	2535	3020	NA	2882	2882	2731	2611	3674	0.743
50	FA4-EOD	S	3634	3047-3670	3358	3946	NA	3327	3327	3438	1984	3434	1.001

**Table A.1 (con't).** Relevant Information Pertaining to Database PD/LT2000.

No.	File-Case Number	Load Test Type	Davisson's Criteria (kN)	Shape of Curve (kN)	Average Shape of Curve (kN)	$\Delta=1"$ (kN)	$\Delta=0.1B$ (kN)	DeBeer (kN)	Average DeBeer (kN)	Static Resist Rs (kN)	CAPWAP TEPWAP (kN)	Energy Appr. Ru (kN)	Ksp Rs Ru
51	FA4-BOR1	S	3634	3047-3670	3358	3946	NA	3327	3327	3438	2687	4724	0.728
52	FA4-BOR2	S	3634	3047-3670	3358	3946	NA	3327	3327	3438	3790	6441	0.534
53	FA5-EOD	S	5071	4671	4671	5196	NA	4177	4177	4777	2945	6864	0.696
54	FA5-BOR	S	5071	4671	4671	5196	NA	4177	4177	4777	4204	9955	0.480
55	FV15-EOD	Q	1401	1334-1557	1446	1655	1957	1094	1094	1401	863	1495	0.938
56	FV15-BOR	Q	1401	1334-1557	1446	1655	1957	1094	1094	1401	881	1730	0.810
57	FV10-EOD	Q	1535	1023-1334	1179	1779	2153	1068	1068	1392	707	1357	1.026
58	FV10-BOR	Q	1535	1023-1334	1179	1779	2153	1068	1068	1392	796	1268	1.098
59	FMN2-EOD	Q	3403	3203-3292	3247	3212	3345	3221	3221	3292	1521	2117	1.555
60	FMN2-BOR	Q	3403	3203-3292	3247	3212	3345	3221	3221	3292	2900	3696	0.890
61	FP5-EOD	Q	1081	979-1045	1014	NA	NA	939	939	1010	934	939	1.076
62	FP5-BOR	Q	1081	979-1045	1014	NA	NA	939	939	1010	1063	1246	0.811
63	FKG-EOD	Q	1628	2135-2313	2224	2358	NA	2113	2113	2068	1281	1744	1.186
64	FKG-BOR	Q	1628	2135-2313	2224	2358	NA	2113	2113	2068	1312	1793	1.154
65	FL3-EOD	LLT	1779	1779	1779	NA	NA	1779	1779	1779	605	1148	1.550
66	FL3-BOR1	LLT	1779	1779	1779	NA	NA	1779	1779	1779	1210	2660	0.669
67	FL3-BOR2	LLT	1779	1779	1779	NA	NA	1779	1779	1779	1557	3972	0.448
68	CA1-EOD	S	2402	2224-2491	2358	1735	1735	2358	2358	2371	1824	1975	1.200
69	CA1-BOR	S	2402	2224-2491	2358	1735	1735	2358	2358	2371	2224	1926	1.231
70	CA2-BOR	S	1628	1423-1779	1601	1646	1646	1579	1579	1690	1521	1913	0.884
71	CA5-BOR1	S	2082	2046-2224	2135	2224	NA	2046	2046	2135	1819	2402	0.888
72	CA5-BOR2	S	2082	2046-2224	2135	2224	NA	2046	2046	2135	2175	2415	0.883
73	CA3/8-BOR	Q	841	890-1023	956	1205	1205	1010	1010	1023	1072	1641	0.623
74	CA24-BOR	S	1076	979-1157	1068	NA	NA	1094	1094	1081	921	1815	0.595
75	CA6-BOR1	S	2936	2758-2936	2847	2624	2891	2847	2847	2936	2713	3479	0.844



**Table A.1 (con't).** Relevant Information Pertaining to Database PD/LT2000.

No.	Pile-Case Number	Load Test Type	Davisson's Criteria (kN)	Shape of Curve (kN)	Average Shape of Curve (kN)	$\Delta=1''$ (kN)	$\Delta=0.1B$ (kN)	DeBeer (kN)	Average DeBeer (kN)	Static Resist Rs (kN)	CAPWAP TEPWAP (kN)	Energy Appr. Ru (kN)	Ksp Rs Ru
76	CA6-BOR2	S	2936	2758-2936	2847	2624	2891	2847	2847	2936	2598	3301	0.889
77	CA6-EOR	S	2936	2758-2936	2847	2624	2891	2847	2847	2936	2482	3132	0.938
78	WC3-EOD	FQ	2713	2447-2891	2669	NA	NA	2758	2758	2713	2264	3341	0.812
79	WC3-BOR1	FQ	2713	2447-2891	2669	NA	NA	2758	2758	2713	2251	3474	0.781
80	WC3-BOR2	FQ	2713	2447-2891	2669	NA	NA	2758	2758	2713	2384	3456	0.785
81	WC6-EOD	FQ	2015	1979-2424	2202	NA	NA	2389	2389	2202	2002	2656	0.829
82	WC6-BOR1	FQ	2015	1979-2424	2202	NA	NA	2389	2389	2202	2135	3172	0.694
83	WC6-BOR2	FQ	2015	1979-2424	2202	NA	NA	2389	2389	2202	1971	3434	0.641
84	WB9-BOR	FQ	4003	3692-3914	3803	4115	NA	3803	3803	3932	4186	7869	0.500
85	WB15-BOR	FQ	3648	3292-3514	3403	3705	NA	3412	3412	3407	3581	6441	0.529
86	T1/A-EOD	SM	8825	8825	8825	8825	NA	8042	8042	8825	7896	12139	0.726
87	T1/A-ALT	SM	8825	8825	8825	8825	NA	8042	8042	8825	8007	12766	0.690
88	T1/B-EOD	SM	12749*	10787	10787	NA	NA	8238	8238	11770	10524	13531	0.871
89	T2/A-EOD	SM	5983	5885	5885	NA	NA	7357	7357	6539	5569	8327	0.785
90	T2/B-EOD	SM	14612	>9804	>9804	NA	NA	NA	NA	13701#	12357	13185	1.040
91	35-1-BOR	S	1432	1423-1557	1490	1575	1628	1415	1415	1446	1157	1219	1.184
92	35-4-BOR	S	1468	1334-1468	1401	1486	1521	1397	1397	1423	1601	2082	0.684
93	35-5-BOR	S	2722	2580-2758	2669	2669	2705	2669	2669	2669	2891	2749	0.971
94	35-6-BOR	S	2669	2224-2447	2335	2358	2438	2340	2340	2358	2580	2340	1.007
95	35-7-BOR	S	543	534-756	645	676	649	641	641	632	618	814	0.776
96	35-10-BOR	S	1788	1646-1868	1757	1922	1975	1681	1681	1779	1486	1890	0.941
97	E2-BOR	Q	1846	1668-1757	1713	NA	NA	1641	1641	1735	1868	3256	0.533
98	63S-BOR	CRP	1263	1112-1210	1161	1299	NA	1148	1148	1192	1241	1423	0.838
99	LB21-BOR	S	1690	1601	1601	NA	2064	1246	1246	1601	1606	2309	0.694
100	LB20-BOR	S	2580	2135	2135	NA	NA	2135	2135	2358	2108	3616	0.652

**Table A.1 (con't).** Relevant Information Pertaining to Database PD/LT2000.

No.	Pile-Case Number	Load Test Type	Davisson's Criteria (kN)	Shape of Curve (kN)	Average Shape of Curve (kN)	$\Delta=1''$ (kN)	$\Delta=0.1B$ (kN)	DeBeer (kN)	Average DeBeer (kN)	Static Resist Rs (kN)	CAPWAP TEPWAP (kN)	Energy Appr. Ru (kN)	Ksp Rs Ru
101	LC3-BOR	S	2758	2669	2669	3025	NA	2491	2491	2847	2722	5200	0.547
102	LIN16-BOR	S	2669	2669	2669	2669	NA	2669	2669	2669	2589	4381	0.609
103	LE37-BOR	S	1112	1068	1068	1201	NA	1023	1023	1112	876	1072	1.037
104	LE64-BOR	S	1201	1068	1068	NA	NA	979	979	1157	1032	1219	0.949
105	ST1-EOD	S	1530	1246-1423	1334	NA	NA	1334	1334	1530	2246	2802	0.546
106	ST2-EOD	S	2269	2402	2402	NA	NA	2224	2224	2402	2740	2958	0.812
107	ST9-BOR	S	4092	3203-3737	3470	4092	NA	3559	3559	4003	3590	8572	0.467
108	ST46-EOD	S	NA	463	463	NA	NA	463	463	463	365	503	0.920
109	GZA3-EOD	Q	1957	2224	2224	2046	2313	2135	2135	2135	1624	1886	1.132
110	GZA5-EOD	Q	1139	712-934	823	1423	1397	1201	1201	1317	1303	1508	0.873
111	GZA6-EOD	Q	836	1557	1557	1406	1361	1557	1557	1450	1223	1250	1.160
112	GZBBC-EOD	Q	1957	2224-2491	2358	2224	2624	2491	2491	2358	1837	2015	1.169
113	GZBP2-EOD	Q	1246	1512	1512	1512	1441	1290	1290	1423	1410	1343	1.059
114	GZB6-EOD	Q	1690	1868	1868	2028	2358	1601	1601	1735	1517	1837	0.944
115	GZZ5-EOD	Q	2064	1868-2091	1979	2402	NA	1824	1824	1957	952	2478	0.790
116	GZO5-EOD	Q	2135	1957-2135	2046	2669	NA	2180	2180	2162	912	2273	0.951
117	GZCC5-EOD	Q	2002	2135-2313	2224	2313	3336	NA	NA	2180	2189	2664	0.818
118	GZL2-EOD	Q	2847	2669-2936	2802	3069	3381	2358	2358	2936	1188	2518	1.167
119	GZP14-EOD	Q	1735	1601-1779	1690	1957	2224	2135	2135	1868	1357	2535	0.737
120	GZP11-EOD	Q	1112	1512-1868	1690	1690	1957	1913	1913	1717	1063	1775	0.967
121	GZP12-EOD	Q	2224	2669	2669	2802	NA	NA	NA	2491	2313	2998	0.831
122	GZB22-EOD	Q	4982	4982	4982	4626	NA	3737	3737	4715	4933	6036	0.781
123	GZW1-EOR	Q	1601	1490-1779	1637	1797	1850	1570	1570	1690	1112	1588	1.064
124	A54-EOD	CRP	2900	2802-2900	2851	2749	2838	2842	2842	2838	1704	2064	1.437
125	A54-BOR	CRP	2900	2802-2900	2851	2749	2838	2842	2842	2838	2718	3105	0.914

**Table A.1 (con't).** Relevant Information Pertaining to Database PD/LT2000.

No.	Pile-Case Number	Load Test Type	Davisson's Criteria (kN)	Shape of Curve (kN)	Average Shape of Curve (kN)	$\Delta=1''$ (kN)	$\Delta=0.1B$ (kN)	DeBeer (kN)	Average DeBeer (kN)	Static Resist Rs (kN)	CAPWAP TEPWAP (kN)	Energy Appr. Ru (kN)	Ksp Rs Ru
126	A147-EOD	CRP	2482	2433	2433	2469	2491	2402	2402	2455	1152	1508	1.628
127	A147-BOR	CRP	2482	2433	2433	2469	2491	2402	2402	2455	2509	2905	0.845
128	GF19-EOD	Q	1468	1779-2046	1913	1690	1690	1446	1446	1766	1770	1931	0.915
129	GF110-EOD	Q	2224	2224-2669	2447	2491	2491	2002	2002	2447	2033	2691	0.909
130	GF222-EOD	Q	2580	2402-2669	2535	2624	2624	2402	2402	2535	2277	2771	0.916
131	GF224-EOD	Q	NA	2002-2091	2046	NA	NA	2068	2068	2060	1864	2037	1.011
132	GF312-EOD	Q	1512	1334-1379	1357	NA	NA	1246	1246	1379	1802	2148	0.642
133	GF313-EOD	Q	1486	1423-1468	1401	NA	NA	1486	1486	1468	1984	2366	0.620
134	GF412-EOD	Q	1068	1068-1246	1157	1308	1308	890	890	1210	2024	2358	0.513
135	GF413-EOD	Q	1334	1246-1423	1334	1557	1557	1201	1201	1334	1904	2184	0.611
136	GF414-EOD	Q	1601	1601-1868	1735	1868	1868	1423	1423	1735	2331	2802	0.619
137	GF415-EOD	Q	2046	2046-2313	2180	2402	2402	1957	1957	2224	2495	2664	0.835
138	EF62-EOD	Q	2233	1957-2269	2113	2073	2028	2135	2135	2122	2322	2829	0.750
139	EF167-BOR	Q	1205	1188	1188	1241	1232	1188	1188	1210	2131	2780	0.436
140	A3-EOD2	FQ	4261	3781-4181	3981	4270	NA	4261	4261	4177	1637	2424	1.723
141	A3-BOR2	FQ	4261	3781-4181	3981	4270	NA	4261	4261	4177	2055	2722	1.534
142	A3-BOR3	FQ	4261	3781-4181	40012	4270	NA	4261	4261	4177	4115	6321	0.661
143	A14-DD1	FQ	NA	3825-4204	4017	NA	NA	4039	4039	4026	3043	4368	0.922
144	A14-DD2	FQ	NA	3825-4204	4017	NA	NA	4039	4039	4026	3296	4786	0.841
145	A14-BOR1	FQ	NA	3825-4204	4017	NA	NA	4039	4039	4026	2687	4973	0.809
146	A14-BOR2	FQ	NA	3825-4204	4017	NA	NA	4039	4039	4026	4279	6566	0.613
147	A25-EOD	FQ	3180	3336-3737	3536	3737	NA	3759	3759	3559	2042	2442	1.457
148	A25-BOR1	FQ	3180	3336-3737	3536	3737	NA	3759	3759	3559	2469	2958	1.203
149	A25-BOR2	FQ	3180	3336-3737	3536	3737	NA	3759	3759	3559	2011	4315	0.825
150	A25-BOR3	FQ	3180	3336-3737	3536	3737	NA	3759	3759	3559	1966	4137	0.860

**Table A.1 (con't).** Relevant Information Pertaining to Database PD/LT2000.

No.	Pile-Case Number	Load Test Type	Davisson's Criteria (kN)	Shape of Curve (kN)	Average Shape of Curve (kN)	$\Delta=1''$ (kN)	$\Delta=0.1B$ (kN)	DeBeer (kN)	Average DeBeer (kN)	Static Resist Rs (kN)	CAPWAP TEPWAP (kN)	Energy Appr. Ru (kN)	Ksp Rs Ru
151	A16-EOD	FQ	1401	1223-1401	1312	1557	NA	1210	1210	1370	996	1348	1.017
152	A16-BOR1	FQ	1401	1223-1401	1312	1557	NA	1210	1210	1370	1254	1846	0.742
153	A16-BOR2	FQ	1401	1223-1401	1312	1557	NA	1210	1210	1370	1317	2246	0.610
154	A41-EOD	FQ	2331	2224-2335	2282	2402	NA	2384	2384	2358	1917	2776	0.849
155	A41-BOR1	FQ	2331	2224-2335	2282	2402	NA	2384	2384	2358	2237	3180	0.741
156	A41-BOR2	FQ	2331	2224-2335	2282	2402	NA	2384	2384	2358	2513	3710	0.635
157	A101-EOD	FQ	3612	3559-3737	3648	NA	NA	3559	3559	3603	2300	2108	1.709
158	A101-BOR1	FQ	3612	3559-3737	3648	NA	NA	3559	3559	3603	2976	3212	1.122
159	A101-BOR2	FQ	3612	3559-3737	3648	NA	NA	3559	3559	3603	3572	3919	0.919
160	A133-EOD	FQ	3594	3470-3825	3648	3603	NA	3852	3852	3674	1383	2282	1.610
161	A133-BOR	FQ	3594	3470-3825	3648	3603	NA	3852	3852	3674	3470	4439	0.828
162	A145-EOD	FQ	4341	3825-4226	4026	4337	NA	4061	4061	4181	1570	2442	1.712
163	A145-BOR1	FQ	4341	3825-4226	4026	4337	NA	4061	4061	4181	2851	3314	1.262
164	A145-BOR2	FQ	4341	3825-4226	4026	4337	NA	4061	4061	4181	3385	4083	1.024
165	CB3-BOR	FQ	2224	2171-2224	2197	2091	NA	2100	2100	2153	2509	4350	0.495
166	CB3-BORL	FQ	2224	2171-2224	2197	2091	NA	2100	2100	2153	2233	4439	0.485
167	CB5-BOR	FQ	5560	5516	5516	5894	NA	5204	5204	5542	2527	4484	1.236
168	CB5-BORL	FQ	5560	5516	5516	5894	NA	5204	5204	5542	2598	5191	1.068
169	CB11-BORL	FQ	6383	6094	6094	6361	NA	6067	6067	6228	3621	8020	0.776
170	CB11-EORL	FQ	6383	6094	6094	6361	NA	6067	6067	6228	2842	8127	0.766
171	CB17-BOR1	FQ	6739	6228	6228	6672	NA	6228	6228	6463	3648	7900	0.818
172	CB17-BOR2	FQ	6739	6228	6228	6672	NA	6228	6228	6463	3332	8114	0.797
173	CB17-BORL	FQ	6739	6228	6228	6672	NA	6228	6228	6463	3038	6677	0.968
174	CB17-DRL	FQ	6739	6228	6228	6672	NA	6228	6228	6463	3759	7300	0.885
175	CB23-BOR	FQ	2860	2847-3603	3225	3256	NA	3372	3372	3123	2753	3843	0.813

**Table A.1 (con't). Relevant Information Pertaining to Database PD/LT2000.**

No.	Pile-Case Number	Load Test Type	Davisson's Criteria (kN)	Shape of Curve (kN)	Average Shape of Curve (kN)	$\Delta=1''$ (kN)	$\Delta=0.1B$ (kN)	DeBeer (kN)	Average DeBeer (kN)	Static Resist Rs (kN)	CAPWAP TEPWAP (kN)	Energy Appr. Ru (kN)	Ksp Rs Ru
176	CB23-BORL	FQ	2860	2847-3603	3225	3256	NA	3372	3372	3123	1975	5809	0.538
177	CB29-BORL	FQ	4079	3870-4270	4070	4270	NA	4048	4048	4119	3452	3803	1.083
178	CB29-EORL	FQ	4079	3870-4270	4070	4270	NA	4048	4048	4119	1997	4755	0.866
179	CB35-BOR1	FQ	6508	6228	6228	6628	NA	6228	6228	6392	3612	4453	1.436
180	CB35-BOR2	FQ	6508	6228	6228	6628	NA	6228	6228	6392	4221	6325	1.011
181	CB35-BORL	FQ	6508	6228	6228	6628	NA	6228	6228	6392	4043	5734	1.115
182	CB41-EOR	FQ	6272	6139	6139	6383	NA	6036	6036	6210	3812	5507	1.128
183	CB41-BOR	FQ	6272	6139	6139	6383	NA	6036	6036	6210	3781	5449	1.140
184	CB41-BORL	FQ	6272	6139	6139	6383	NA	6036	6036	6210	2157	5169	1.201
185	CB26-EOD	FQ	4270	3781-4226	4003	4448	NA	4448	4448	4293	2171	2469	1.739
186	CB26-BOR	FQ	4270	3781-4226	4003	4448	NA	4448	4448	4293	2753	3505	1.225
187	CB26-EOR	FQ	4270	3781-4226	4003	4448	NA	4448	4448	4293	3185	4257	1.008
188	CB26-BOR2	FQ	4270	3781-4226	4003	4448	NA	4448	4448	4293	2504	4951	0.867
189	33P1-EOD	S	>3559	3559	3559	2313	2669	3559	3559	3559	1953	2922	1.218
190	33P1-BOR	S	>3559	3559	3559	2313	2669	3559	3559	3559	3180	3995	0.891
191	33P1-EOR	S	>3559	3559	3559	2313	2669	3559	3559	3559	2891	4106	0.867
192	33P2-EOD	S	2180	2002-2224	2113	2002	2180	2046	2046	2180	1290*	1859	1.172
193	33P2-BOR	S	2180	2002-2224	2113	2002	2180	2046	2046	2180	1579	2313	0.942
194	33P2-EOR	S	2180	2002-2224	2113	2002	2180	2046	2046	2180	1784	2429	0.897
195	33P4-EOD	S	2073	1557-2224	1890	2473	2633	2091	2091	2224	1779*	2780	0.800
196	33P5-EOD	S	730	712-890	801	1085	1174	890	890	890	636*	1103	0.806
197	TRD22-EOD	S	1575	1557	1557	NA	NA	1584	1584	1557	1922	2460	0.633
198	TRD22-BOR	S	1575	1557	1557	NA	NA	1584	1584	1557	1308	2242	0.694
199	TRE22-EOD	S	2473	2535	2535	NA	NA	2535	2535	2535	2558*	3203	0.792
200	TRE22-BOR	S	2473	2535	2535	NA	NA	2535	2535	2535	2740	3145	0.806

**Table A.1 (con't).** Relevant Information Pertaining to Database PD/LT2000.

No.	Pile-Case Number	Load Test Type	Davisson's Criteria (kN)	Shape of Curve (kN)	Average Shape of Curve (kN)	$\Delta=1''$ (kN)	$\Delta=0.1B$ (kN)	DeBeer (kN)	Average DeBeer (kN)	Static Resist Rs (kN)	CAPWAP TEPWAP (kN)	Energy Appr. Ru (kN)	Ksp Rs Ru
201	TRP5X-EOD	S	1824	2224-2447	2335	2269	2491	1779	1779	2113	2153	2251	0.939
202	TRP5X-BOR	S	1824	2224-2447	2335	2269	2491	1779	1779	2113	1757	2180	0.969
203	TR131-BOR	S	623	712-890	801	934	890	890	890	667	738	752	0.888
204	TRAH-EOR	S	3247	2891-3114	3003	2669	2891	2847	2847	2891	970	2509	1.152
205	TRBH-BOR	S	1446	1223-1334	1281	1499	1566	1352	1352	1334	445	1183	1.128
206	TRBP-EOR	S	1512	>1334	>1334	1512	1512	1446	1446	1468	1103*	1361	1.078
207	CHA1-EOD	Q	2909	2785-3034	2909	2785	2918	2669-3034	2851	2878	1735	2100	1.370
208	CHA1-BOR1	Q	2909	2785-3034	2909	2785	2918	2669-3034	2851	2878	2068	2335	1.230
209	CHA1-BOR2	Q	2909	2785-3034	2909	2785	2918	2669-3034	2851	2878	2304	2758	1.040
210	CHA4-EOD	Q	2251	2171-2251	2211	2251	2242	2251	2251	2242	1205	1495	1.500
211	CHB2-EOD	Q	1343	1246-1957	1601	1246	1334	1174-1779	1477	1401	489	899	1.560
212	CHB2-BOR1	Q	1343	1246-1957	1601	1246	1334	1174-1779	1477	1401	1201	1628	0.860
213	CHB2-BOR3	Q	1343	1246-1957	1601	1246	1334	1174-1779	1477	1401	1512	2384	0.590
214	CHB2-BOR4	Q	1343	1246-1957	1601	1246	1334	1174-1779	1477	1401	2002	2553	0.550
215	CHB2-BOR5a	Q	1343	1246-1957	1601	1246	1334	1174-1779	1477	1401	2291		
216	CHB2-BOR5b	Q	1343	1246-1957	1601	1246	1334	1174-1779	1477	1401	2126		
217	CHB3-EOD	Q	890	783-1094	939	943	996	827	827	952	467	903	1.050
218	CHB3-BOR1	Q	890	783-1094	939	943	996	827	827	952	1045	1254	0.760
219	CHB3-BOR2	Q	890	783-1094	939	943	996	827	827	952	979	1606	0.590
220	CHB3-BOR3	Q	890	783-1094	939	943	996	827	827	952	1490	2073	0.460
221	CHC3-EOD	Q	836	890-1357	1125	1050	1237	890-1157	1023	1054	489*	1859	0.570
222	CHC3-BOR	Q	836	890-1357	1125	1050	1237	890-1157	1023	1054		1837	0.570
223	CHC3-BORL	Q	836	890-1357	1125	1050	1237	890-1157	1023	1054	1735	2224	0.470
224	CH4-EOD	Q	1601	1592-1668	1632	1601	1601	1668	1668	1619	667	859	1.890
225	CH4-BOR	Q	1601	1592-1668	1632	1601	1601	1668	1668	1619	1512	1632	0.990

**Table A.1 (con't). Relevant Information Pertaining to Database PD/LT2000.**

No.	Pile-Case Number	Load Test Type	Davisson's Criteria  (kN)	Shape of Curve (kN)	Average Shape of Curve (kN)	$\Delta=1''$ (kN)	$\Delta=0.1B$ (kN)	DeBeer (kN)	Average DeBeer (kN)	Static Resist Rs (kN)	CAPWAP TEPWAP (kN)	Energy Appr. Ru (kN)	Ksp Rs Ru
226	CH39-EOD	Q	2936	2829-2936	2882	2473	2322	2936	2936	2918	832	796	3.660
227	CH39-BOR	Q	2936	2829-2936	2882	2473	2322	2936	2936	2918	2046	2304	1.270
228	CH39-BORL	Q	2936	2829-2936	2882	2473	2322	2936	2936	2918	2558	2535	1.150
229	CH6-5B-EOD	Q	1673	1503-1673	1588	1673	1673	1673	1673	1655		391	4.230
230	CH6-5B-BOR	Q	1673	1503-1673	1588	1673	1673	1673	1673	1655	1779	2104	0.790
231	CH95B-EOD	Q	2473	2464	2464	2464	2464	2438	2438	2464	983*	1503	1.640
232	CH95B-BOR	Q	2473	2464	2464	2464	2464	2438	2438	2464	2358	2331	1.060
233	CH256-BOR3	Q	2651	2384-2651	2518	2269	2197	2633	2633	2455	2224		
234	CH351-BOR2	Q	2669	2420-2660	2540	2393	2340	2669	2669	2527	2358	2544	0.990
235	PO2-BOR1	mQ	1219	1228-1486	1357	1441	1610	1210	1210	1263	1352	1962	0.640
236	PO2-BOR2	mQ	1219	1228-1486	1357	1441	1610	1210	1210	1263	1174	1882	0.670
237	PO2-BORL	mQ	1219	1228-1486	1357	1441	1610	1210	1210	1263	1250	1730	0.730
238	PO19-BOR	mQ	1023	1068-1246	1157	1290	1415	1210	1210	1179	1334	2433	0.480
239	PO19-EOD	mQ	1023	1068-1246	1157	1290	1415	1210	1210	1179	1090	1597	0.740
240	PO19-EORL	mQ	1023	1068-1246	1157	1290	1415	1210	1210	1179	1045	1406	0.840
241	ER5-BOR1	mQ	3803	3123-3714	3421	3981	NA	3559	3559	3692	2927	5062	0.730
242	ER5-BOR2	mQ	3803	3123-3714	3421	3981	NA	3559	3559	3692	4123	6156	0.600
243	ER5-BORL	mQ	3803	3123-3714	3421	3981	NA	3559	3559	3692	2611	4470	0.830
244	ER77-BOR	mQ	7433	6303-7126	6717	NA	NA	5107-6001	5556	6570	3363	5805	1.130
245	ER77-BORL	mQ	7433	6303-7126	6717	NA	NA	5107-6001	5556	6570	4484	7936	0.830
246	BB13-EOD	mQ	4475	4003-4688	4346	4644	NA	4110	4110	4395	3114	6419	0.680
247	BB13-BOR1a	mQ	4475	4003-4688	4346	4644	NA	4110	4110	4395	4092	8892	0.490
248	BB13-BOR1b	mQ	4475	4003-4688	4346	4644	NA	4110	4110	4395	3959	8785	0.500
249	BB13-BOR2a	mQ	4475	4003-4688	4346	4644	NA	4110	4110	4395	4760	9728	0.450
250	BB13-BOR2b	mQ	4475	4003-4688	4346	4644	NA	4110	4110	4395	4671	10186	0.430

**Table A.1 (con't).** Relevant Information Pertaining to Database PD/LT2000.

No.	Pile-Case Number	Load Test Type	Davisson's Criteria (kN)	Shape of Curve (kN)	Average Shape of Curve (kN)	$\Delta=1''$ (kN)	$\Delta=0.1B$ (kN)	DeBeer (kN)	Average DeBeer (kN)	Static Resist Rs (kN)	CAPWAP TEPWAP (kN)	Energy Appr. Ru (kN)	Ksp Rs Ru
251	BB13-BORL	mQ	4475	4003-4688	4346	4644	NA	4110	4110	4395	4008	9150	0.480
252	BB19-BORa	mQ	5169	4448-5498	4973	5418	NA	4333-5338	4835	5098	4155	8185	0.620
253	BB19-BORb	mQ	5169	4448-5498	4973	5418	NA	4333-5338	4835	5098	4666	8287	0.620
254	BB19-BORL	mQ	5169	4448-5498	4973	5418	NA	4333-5338	4835	5098	6512	8905	0.570
255	BB24-EOD	mQ	4955	4448-4893	4671	5000	NA	4822	4822	4866	5783	9693	0.500
256	BB24-BOR1a	mQ	4955	4448-4893	4671	5000	NA	4822	4822	4866	7517	10449	0.470
257	BB24-BOR1b	mQ	4955	4448-4893	4671	5000	NA	4822	4822	4866	7571	10280	0.470
258	BB24-BOR2a	mQ	4955	4448-4893	4671	5000	NA	4822	4822	4866	8420	12108	0.400
259	BB24-BOR2b	mQ	4955	4448-4893	4671	5000	NA	4822	4822	4866	7873	11721	0.420
260	BB24-BORL	mQ	4955	4448-4893	4671	5000	NA	4822	4822	4866	6241	9119	0.530
261	BB29-BOR	mQ	5053	5062	5062	5338	NA	4760	4760	5044	5458	9581	0.530
262	BB29-BORL	mQ	5053	5062	5062	5338	NA	4760	4760	5044	5115	7891	0.640
263	ABF6-BOR	Q	3345	2758-3309	3034	3879	4057	3817	3817	3630	1677	2567	1.410
264	ABF6-BORL	Q	3345	2758-3309	3034	3879	4057	3817	3817	3630	3474	6899	0.530
265	ABG13-BORL	Q	4742	3870-4644	4257	5560	NA	3639-4653	4146	4680	4826	7122	0.660
266	ABH2-BOR	Q	2518	2162-2669	2415	2980	NA	2189-2793	2491	2598	3594	4115	0.630
267	ABH2-BORL	Q	2518	2162-2669	2415	2980	NA	2189-2793	2491	2598	4092	4924	0.530
268	BC79-EOD	Q	2277	2224-2464	2344	2562	NA	2277	2277	2366		3323	0.700
269	BC79-BORL	Q	2277	2224-2464	2344	2562	NA	2277	2277	2366	2447		
270	BC64-EOD	Q	5071	4662	4662	5480	NA	4608	4608	4955		3803	1.300
271	BC64-BORL	Q	5071	4662	4662	5480	NA	4608	4608	4955	5004		
272	D1-BOR1	S	302	298	298	316	316	285	285	298	423*	956	0.310
273	D2-BOR1	S	556	547	547	649	649	552	552	552	654*	1339	0.410
274	D3-BORa	S	1005	979	979	1085	1072	974	974	992	818*	1757	0.570
275	D3-BORb	S	1005	979	979	1085	1072	974	974	992	694*	1597	0.620



**Table A.1 (con't).** Relevant Information Pertaining to Database PD/LT2000.

No.	Pile-Case Number	Load Test Type	Davisson's Criteria (kN)	Shape of Curve (kN)	Average Shape of Curve (kN)	$\Delta=1"$ (kN)	$\Delta=0.1B$ (kN)	DeBeer (kN)	Average DeBeer (kN)	Static Resist Rs (kN)	CAPWAP TEPWAP (kN)	Energy Appr. Ru (kN)	Ksp Rs Ru
276	D5-BORa	S	1050	979	979	1179	1170	992	992	1014	1334*	1726	0.590
277	D5-BORb	S	1050	979	979	1179	1170	992	992	1014	1317*	2184	0.460
278	MB1-EOD	Q	3590	3430-4172	3803	4075	NA(4938)	3114	3114	3643	756	1401	2.600
279	MB1-BOR	Q	3590	3430-4172	3803	4075	NA(4938)	3114	3114	3643	2326	2166	1.680
280	MB2-BOR	Q	3990	3857	3857	3492	4266	3870	3870	3879	2362		
281	MB3-BOR	Q	4146	4168	4168	3696	4381	4252	4252	4128	2540		
282	S1-EOD	Q	2651	2518	2518	2767	NA(3140)	2473	2473	2607	2046	3314	0.790
283	S1-BOR	Q	2651	2518	2518	2767	NA(3140)	2473	2473	2607	2687		
284	S2-EOD	Q	1415	1326	1326	1539	1486	1317	1317	1415	956	1241	1.140
285	S2-BOR	Q	1415	1326	1326	1539	1486	1317	1317	1415	1366*	956	1.480
286	DD22-EOD		NA(3745)	2936-3576	3256	3625	NA	2922-3599	3261	3381	1134	1459	2.317
287	DD22-BOR		NA(3745)	2936-3576	3256	3625	NA	2922-3599	3261	3381	2309	2571	1.315
288	DD23-EOD		2206	2002	2002	2251	NA	1824-2193	2011	2117	681	681	3.111
289	DD23-BOR		2206	2002	2002	2251	NA	1824-2193	2011	2117	1232	1437	1.474
290	JR17-EOD	Q	5422	5187-5845	5516	NA	NA	NA	NA	5471	2785	4052	1.350
291	LB3-EOD		1842	1761	1761	NA	NA	1779	1779	1770	269	939	1.880
292	LB3-BOR1		1842	1761	1761	NA	NA	1779	1779	1770	912	1592	1.110
293	LB3-BOR2		1842	1761	1761	NA	NA	1779	1779	1770	1534	3075	0.580
294	LB3-BOR3		1842	1761	1761	NA	NA	1779	1779	1770	1677	3479	0.510
295	LB4-EOD		2273	2002	2002	NA	NA	2015	2015	2015	202	1163	1.730
296	LB4-BOR1		2273	2002	2002	NA	NA	2015	2015	2015	887	2325	0.870
297	LB4-BOR2		2273	2002	2002	NA	NA	2015	2015	2015	1299	4039	0.500
298	LB4-BOR3		2273	2002	2002	NA	NA	2015	2015	2015	1521	6042	0.330
299	LB4-BOR4		2273	2002	2002	NA	NA	2015	2015	2015	1603	4881	0.410
300	LB5-EOD		NA	1926	1926	NA	NA	1810	1810	1868	263	774	2.410

**Table A.1 (con't).** Relevant Information Pertaining to Database PD/LT2000.

No.	Pile-Case Number	Load Test Type	Davisson's Criteria  (kN)	Shape of Curve (kN)	Average Shape of Curve (kN)	$\Delta=1''$ (kN)	$\Delta=0.1B$ (kN)	DeBeer (kN)	Average DeBeer (kN)	Static Resist Rs (kN)	CAPWAP TEPWAP (kN)	Energy Appr. Ru (kN)	Ksp Rs Ru
301	LB5-BOR1		NA	1926	1926	NA	NA	1810	1810	1868	952	2601	0.720
302	LB5-BOR2		NA	1926	1926	NA	NA	1810	1810	1868	1402	4110	0.450
303	LB5-BOR3		NA	1926	1926	NA	NA	1810	1810	1868	1591	4940	0.380
304	LB5-BOR4		NA	1926	1926	NA	NA	1810	1810	1868	1752	?	?
305	LB6-EOD		2411	2019	2019	NA	NA	2166	2166	2095	404	857	2.440
306	LB6-BOR1		2411	2019	2019	NA	NA	2166	2166	2095	883	2119	0.990
307	LB6-BOR2		2411	2019	2019	NA	NA	2166	2166	2095	1322	3443	0.610
308	LB6-BOR3		2411	2019	2019	NA	NA	2166	2166	2095	1767	4318	0.490
309	LB6-BOR4		2411	2019	2019	NA	NA	2166	2166	2095	2300	5256	0.400
310	LB7-EOD		2402	2206	2206	NA	NA	2135	2135	2171	457	931	2.330
311	LB7-BOR1		2402	2206	2206	NA	NA	2135	2135	2171	875	2033	1.070
312	LB7-BOR2		2402	2206	2206	NA	NA	2135	2135	2171	1279	3419	0.630
313	LB7-BOR3		2402	2206	2206	NA	NA	2135	2135	2171	1891	4489	0.480
314	LB7-BOR4		2402	2206	2206	NA	NA	2135	2135	2171	2260	4803	0.450
315	DI221-EOD	SD	1477	1601	1601	NA	NA	1601	1601	1561	---	1517	1.029
316	DI221-2DR	SD	1477	1601	1601	NA	NA	1601	1601	1561	1250	---	---
317	TW488-EOD	Q	1423	1388-1423	1406	NA	NA	1415-1441	1428	1419	365	507	2.798
318	TW488-3DR	Q	1423	1388-1423	1406	NA	NA	1415-1441	1428	1419	934	---	---
319	NBTP2-EOD	SD	1806	1806-1993	1899	1713	1904	1922	1922	1849	1352	2091	0.884
320	NBTP2-1DR	SD	1806	1806-1993	1899	1713	1904	1922	1922	1849	1601	2135	0.866
321	NBTP2-6DR	SD	1806	1806-1993	1899	1713	1904	1922	1922	1849	1686	2713	0.681
322	NBTP3-EOD	SD	2126	NA	NA	1757	2100	NA	NA	1994	1401	2402	0.830
323	NBTP3-1DR	SD	2126	NA	NA	1757	2100	NA	NA	1994	1601	2402	0.830
324	NBTP3-6DR	SD	2126	NA	NA	1757	2100	NA	NA	1994	1713	2669	0.747
325	NBTP5-EOD	SD	1632	1824	1824	1886	NA	NA	NA	1781	1423	1735	1.026

**Table A.1 (con't).** Relevant Information Pertaining to Database PD/LT2000.

No.	Pile-Case Number	Load Test Type	Davisson's Criteria  (kN)	Shape of Curve (kN)	Average Shape of Curve (kN)	$\Delta=1''$ (kN)	$\Delta=0.1B$ (kN)	DeBeer (kN)	Average DeBeer (kN)	Static Resist Rs (kN)	CAPWAP TEPWAP (kN)	Energy Appr. Ru (kN)	Ksp  Rs Ru
326	NBTP5-3DR	SD	1632	1824	1824	1886	NA	NA	NA	1781	2046	2313	0.770
327	PR1-BOR1	Q	NA	2068-2237	2153	NA	NA	2224	2224	2189	2304	4469	0.490
328	DD29-EOD	Q	NA	3318-3336	3327	3114	3367	3305	3305	3278	1561	1895	1.730
329	ND50-BOR1	S	676	658-676	667	801	NA	672	672	704	796	898	0.784
330	NZ12-BOR1	Q	2224	2224	2224	2224	2224	2224	2224	2224	2331	3441	0.646
331	DW1-BOR1	Q	4742	4448-4706	4577	4849	NA	4644	4644	4703	4515	9345	0.503
332	DW1-BOR2	Q	4742	4448-4706	4577	4849	NA	4644	4644	4703	5178	8697	0.541
333	DW2-BOR1	Q	2753	2722-2749	2736	2709	2807	2722	2722	2745	2798	3706	0.741
334	DW2-BOR2	Q	2753	2722-2749	2736	2709	2807	2722	2722	2745	3025	4305	0.638
335	DS1-BOR1	Q	1601	1579	1579	1637	NA	1570	1570	1597	1214	1800	0.887
336	DS1-BOR2	Q	1601	1579	1579	1637	NA	1570	1570	1597	1535	1901	0.840
337	PX2-BOR1	Q	NA	6050-6308	6179	6107	NA	NA	NA	6143	2945	4519	1.359
338	PX3-EOD	Q	NA	5476	5476	NA	NA	5547	5547	5511	2464	3074	1.793
339	PX3-BOR1	Q	NA	5476	5476	NA	NA	5547	5547	5511	2829	3962	1.391
340	PX4-EOD	Q	3207	3278-3456	3367	3745	NA	3327	3327	3412	2260	2907	1.174
341	PX4-BOR1	Q	3207	3278-3456	3367	3745	NA	3327	3327	3412	2802	3701	0.922
342	PX5-BOR1	Q	2971	4199-4315	4257	4141	4479	3861	3861	3942	2749	3420	1.153
343	PX6-BOR1	Q	4235	4061-4800	4430	4800	NA	3959-4804	4381	4462	2406	3882	1.149
344	PX7-EOD	Q	4475	4822	4822	5196	5498	4978	4978	4994	2353	5039	0.991
345	PX7-BOR1	Q	4475	4822	4822	5196	5498	4978	4978	4994	2758	4302	1.161
346	CH11-42-BOR1	Q	1948	2117-2153	2135	2140	2246	1988-2086	2037	2101	2349	4148	0.507
347	SSTPD-5DR		285	302	302	334	329	289	289	307	389	623	0.490
348	TSW/D62/1-EOD		4359	4568	4568	4297	NA	4568	4568	4448	3358	5284	0.842
349	TSW/D62/1-BOR		4359	4568	4568	4297	NA	4568	4568	4448	4755	6441	0.691
350	TSW/HHK9/1-EOD		NA(4604)	4604	4604	4604	NA	4604	4604	4542	3812	5618	0.808

**Table A.1 (con't).** Relevant Information Pertaining to Database PD/LT2000.

No.	Pile-Case Number	Load Test Type	Davisson's Criteria (kN)	Shape of Curve (kN)	Average Shape of Curve (kN)	$\Delta=1''$ (kN)	$\Delta=0.1B$ (kN)	DeBeer (kN)	Average DeBeer (kN)	Static Resist Rs (kN)	CAPWAP TEPWAP (kN)	Energy Appr. Ru (kN)	Ksp Rs Ru
351	TSW/HHK9/1-BOR		NA(4604)	4604	4604	4604	NA	4604	4604	4542	4853	6895	0.659
352	TSW/D62/2-EOD		4737	3594-4804	4199	4159	4591	4804	4804	4497	4853	5422	0.829
353	TSW/D62/2-BOR		4737	3594-4804	4199	4159	4591	4804	4804	4497	4644	6401	0.703
354	TSW/HHK9/2-EOD		4804	4804	4804	4252	4804	4804	4804	4693	4212	5462	0.859
355	TSW/HHK9/2-BOR		4804	4804	4804	4252	4804	4804	4804	4693	4350	5961	0.787
356	OD1J-EOD	STM	7722	7393	7393	7571	NA	7397	7397	7522	3496	4924	1.528
357	OD2P-EOD	STM	3047	2607-2980	2793	2829	NA	2989	2989	2914	1557	2335	1.248
358	OD2P-BOR	STM	3047	2607-2980	2793	2829	NA	2989	2989	2914	2224	5333	0.546
359	OD2T-EOD	STM	3616	3020	3020	NA	NA	NA	NA	3314	3634	4301	0.770
360	OD3H-EOD	STM	4639	5329	5329	4777	NA	5258	5258	5000	1441	3261	1.533
361	OD4L-EOD	STM	4399	4150	4150	4346	NA	4172	4172	4266	2242	2989	1.427
362	OD4P-EOD	STM	3087	2914	2914	3203	NA	2971	2971	3043	1214	3461	0.879
363	OD4P-BOR	STM	3087	2914	2914	3203	NA	2971	2971	3043	2455	6454	0.471
364	OD4T-EOD	STM	3229	3154-3367	3261	3412	NA	3269	3269	3292	1339	2028	1.623
365	OD4T-BOR	STM	3229	3154-3367	3261	3412	NA	3269	3269	3292	2891	6263	0.526
366	OD4W-EOD	STM	3937	4057	4057	3968	NA	4101	4101	4017	1766	2349	1.710
367	OD4W-BOR2	STM	3937	4057	4057	3968	NA	4101	4101	4017	2567	4110	0.977
368	OD4W-BOR3	STM	3937	4057	4057	3968	NA	4101	4101	4017	3403	6276	0.640
369	QC3-EOD	Q	6361	6574	6574	6428	NA	6477	6477	6459	1802	3554	0.457
370	QC3-14DR	Q	6361	6574	6574	6428	NA	6477	6477	6459	5204	8710	0.186
371	QC14-EOD	Q	1392	1450	1450	1450	1459	1450	1450	1441	1241	1495	0.229
372	QC14-30DR	Q	1392	1450	1450	1450	1459	1450	1450	1441	1197	2362	0.145
373	NYSP-EOD	TQT	1388	302-340	1428	1357	1357	304-340	1432	1392	587	1432	0.972
374	NYSP-BOR	TQT	1388	302-340	1428	1357	1357	304-340	1432	1392	992	1922	0.725
375	UFSS1A - BOR		3496	682-1102	3968	4706	NA	1120-1196	5151	4333	5427	7486	0.579

**Table A.1 (con't).** Relevant Information Pertaining to Database PD/LT2000.

No.	Pile-Case Number	Load Test Type	Davisson's Criteria (kN)	Shape of Curve (kN)	Average Shape of Curve (kN)	$\Delta=1''$ (kN)	$\Delta=0.1B$ (kN)	DeBeer (kN)	Average DeBeer (kN)	Static Resist Rs (kN)	CAPWAP TEPWAP (kN)	Energy Appr. Ru (kN)	Ksp Rs Ru
376	UFSS1B - BOR		2611	476-600	2393	NA	NA	430-600	2291	2433	3554	4519	0.538
377	UFSS10 - BOR		5107	1008-1148	4795	NA	NA	NA	NA	4951	6228	7700	0.643
378	UFSS13B - BOR		2771	787-1002	3981	4880	NA	963-1199	4809	4110	4226	4479	0.918
379	BIT20 - BOR		2593	2375	2375	NA	NA	2358	2358	2442	2108	1628	1.500
380	BIT21 - BOR		1637	378-448	1837	2060	NA	1326	1326	1717	1606	885	1.940
381	HFLS3 - EOD		7073	7962	7962	8852	NA	8087	8087	7993	5787	9377	0.852
382	HFLS4L - EOD		3354	3919	3919	4075	6010	3901	3901	3812	3136	5200	0.733
383	HFLS4L - BOR		3354	3919	3919	4075	6010	3901	3901	3812	4070	7664	0.497
384	RBA30 - BOR		4039	4573	4573	5022	NA	4635	4635	4568	3692	5849	0.781
385	RBB30W - BOR		3461	685-861	3438	4123	NA	3732	3732	3732	3225	4822	0.774
386	CC6 - BOR		1388	1357	1357	NA	NA	1352	1352	1366	1423	3025	0.451
387	CC7 - BOR		1770	1726	1726	NA	NA	1713	1713	1735	1810	2500	0.694
388	CC14 - BOR		1601	1557	1557	1699	1726	1535	1535	1624	1890	2611	0.622
389	49SB37 - EOD		5058	978-1276	5013	6147	NA	5289	5289	5378	4559	5467	0.984

**Table A.2.** Relevant Information Pertaining to Umass - Ukraine Database.

Case No.	Location	Pile designation	Cyclic Bearing Capacity	Davison's Criteria	Shape of Curve	De Beer	$\Delta=1''$	$\Delta=0.1B$	Representative Static Resistance	Ratio of $P_s$ divided by $P_{CYCL}$	Ratio of $P_D$ divided by $P_{CYCL}$
			$P_{CYCL}$	$P_D$ (kN)	$P_2$ (kN)	$P_3$ (kN)	$P_4$ (kN)	$P_5$ (kN)	$P_s$ (kN)	$P_s/P_{CYCL}$	$P_D/P_{CYCL}$
1	Herson	1/1	903	1097	858-1056	780-970	1081	1094	916	1.014	1.215
2		1/2	866	907	830-890	900	988	990	880	1.016	1.047
3	Dnepropetrovsk	2/1a	418	430	373-433	350-420	418	418	418	1.000	1.029
4	Press.	2/1b	640	660	600-700	610-680	760	780	650	1.016	1.031
5		2/1c	1073	1073	950-1260	1220	1271	1275	1125	1.048	1.000
6		2/2	936	1000	900-1000	900	-	-	950	1.015	1.068
7		2/3	842	868	770-854	860	938	955	847	1.006	1.031
8	Dnepropetrovsk	3/13	380	428	390-503	380-490	500	500	438	1.153	1.126
9	Str.Januar	3/13a	650	468	694-800	700-800	800	815	748	1.151	0.720
10		3/14	329	220	400	400	426	441	400	1.216	0.669
11		3/15	632	463	568-716	700	718	719	670	1.060	0.733
12		3/15a	780	651	790-950	920	964	965	887	1.137	0.835
13	Zaporogie	4/2	840	860	880-900	-	951	967	880	1.048	1.024
14	Zaporogie	5/1	1040	600	1000-1060	-	1030	1080	1030	0.990	0.577
15	A 7050	5/2	506	492	400-469	400-500	602	602	452	0.893	0.972
16		5/2a	760	748	706-790	690-780	852	862	743	0.978	0.984
17		5/3	420	280	415	-	450	460	415	0.988	0.667
18		5/3a	750	630	680-700	-	730	750	700	0.933	0.840
19	Herson	6/2	1057	1077	1032-1120	1180	1200	1200	1102	1.043	1.019
20	Kindy Road	6/3	915	956	920-970	-	1118	1119	945	1.033	1.045
21		6/1	1100	1108	1107-1200	1200	1220	1220	1158	1.053	1.007
22	Zaporogie	8/1	645	649	640-650	650	756	756	647	1.003	1.006
23		8/2	1005	630	920-1080	-	1100	1130	1000	0.995	0.627
24		8/3	950	710	970-900	-	995	1010	980	1.032	0.747
25		8/4	750	760	670-780		790	795	743	0.991	1.013

**Table A.2 (con't).** Relevant Information Pertaining to Umass - Ukraine Database.

Case No.	Location	Pile designation	Cyclic Bearing Capacity	Davison's Criteria	Shape of Curve	De Beer	$\Delta=1''$	$\Delta=0.1B$	Representative Static Resistance	Ratio of $P_S$ divided by PCYCL	Ratio of $P_D$ divided by PCYCL
			$P_{CYCL}$	$P_D$ (kN)	$P_2$ (kN)	$P_3$ (kN)	$P_4$ (kN)	$P_5$ (kN)	$P_S$ (kN)	$P_S/P_{CYCL}$	$P_D/P_{CYCL}$
26		8/5	603	602	600-620	-	660	680	612	1.015	0.998
27	Zaporogie	9/1	1110	-	1200	-	-	-	1200	1.081	---
28	Techn.school	9/2	920	940	1050-1020	-	-	-	1035	1.125	1.022
29		9/3	1120	-	1030-1200	-	-	-	1115	0.996	---
30	A 3438	10/1	810		800-900	-	9210	920	850	1.049	---
31	A 3438	10/10	710	650	680-780	-	740	752	690	0.972	0.915
32	A 3438	10/10a	930	930	930		960	970	930	1.000	1.000
33	A 3438	10/12a	980	900	1000-1050	-	-	-	1025	1.046	0.918
34	A 3438	10/14	860	840	800-860	-	915	930	835	0.971	0.977
35	A 3438	10/15	1150	1150	1100-1200	-	-	-	1150	1.000	1.000
36	A 3438	10/16	1131	1209	1145-1200	1187	1225	1226	1185	1.048	1.069
37	A 3438	10/17a	830	920	900	-	1050	1070	910	1.096	1.108
38	A 3438	10/3	1000	1100	900-1300	-	-	-	1100	1.100	1.100
39	A 3438	10/6	1200	-	1000-1300	-	-	-	1200	1.000	---
40	A 3438	10/9	1070	750	1000-1120	-	1160	1180	1100	1.028	0.701
41	A3438/1	11/8	830	800	800	-	830	840	800	0.964	0.964
42	A3438/2	12/1	520	620	500-580	-	630	640	540	1.038	1.192
43	A3438/2	12/1a	780	810	820	-	825	835	800	1.026	1.038
44	A3438/2	12/2	980	880	980	-	1000	1020	980	1.000	0.898
45	A3438/2	12/3	766	649	600-893	650-700			698	0.911	0.847
46		12/4	830	820	800-860	-	-	-	828	0.998	0.988
47	Dnepropetrovsk	13/1	830	700	800-880	-	940	960	840	1.012	0.843
48	Novopolozk	14/9a	820	730	850-900	-	950	960	875	1.067	0.890
49		14/9b	1080	880	1000-1200	-	1230	1250	1100	1.019	0.815
50		14/11	800	710	780-820	-	830	900	800	1.000	0.888

**Table A.2 (con't).** Relevant Information Pertaining to Umass - Ukraine Database.

Case No.	Location	Pile designation	Cyclic Bearing Capacity	Davison's Criteria	Shape of Curve	De Beer	$\Delta=1''$	$\Delta=0.1B$	Representative Static Resistance	Ratio of $P_s$ divided by	Ratio of $P_D$ divided by
			$P_{CYCL}$	$P_D$ (kN)	$P_2$ (kN)	$P_3$ (kN)	$P_4$ (kN)	$P_5$ (kN)	$P_s$ (kN)	$P_s/P_{CYCL}$	$P_D/P_{CYCL}$
51	Dnepropetrovsk	15/1	681	696	600-800	650-700	746	765	689	1.012	1.022
52	#60F4	15/1a	1124	953	1000-1097	1063	1126	1155	1028	0.915	0.848
53		15/2	550	-	550	-	600	600	560	1.018	---
54		15/3	670	670	650-690	-	710	720	670	1.000	1.000
55	Odessa	16/1	800	800	800	-	820	825	800	1.000	1.000
56	OPZ	16/2	870	800	820-920	-	910	950	870	1.000	0.920
57		16/3	820	810	820	-	850	860	820	1.000	0.988
58		16/4	440	430	430-510	-	530	540	456	1.036	0.977
59		16/6a	710	630	700	-	710	715	660	0.930	0.887
60		16/6b	750	610	800	-	810	820	800	1.067	0.813
61	Dnepropetrovsk	17/1	965	793	800-987	980	1028	1050	890	0.922	0.822
62		17/3	1245	-	1100-1300	1050	-	-	1150	0.924	---
63	Herson	18/1	985	600	1030-1050	-	1065	1075	1040	1.056	0.609
64		18/2	730	643	722-800	780	816	831	767	1.051	0.881
65	A7460	19/1a	581	453	453-558	580-600	634	649	530	0.912	0.780
66		19/1b	1209	1218	1218-1290	1259	1309	1327	1246	1.031	1.007
67		19/2	563	538	550-687	670-700	712	725	578	1.027	0.956
68		19/2a	965	956	902-1028	1060	1065	1083	986	1.022	0.991
69	Zaporogie	22/4	1119	997	1017-1200	1202	1200	1200	1104	0.987	0.891
70	Belgorod,#231	23/1	650	590	650-690	-	700	730	650	1.000	0.908
71		23/2	630	600	600-700	-	710	720	633	1.005	0.952
72		23/3a	582	538	587	650	675	681	592	1.017	0.924
73		23/3b	939	620	977	1000	1033	1052	988	1.052	0.660
74		23/5	559	604	603-630	670	709	720	626	1.120	1.081
75		23/7	660	570	670-700	-	715	725	685	1.038	0.864



**Table A.2 (con't).** Relevant Information Pertaining to Umass - Ukraine Database.

Case No.	Location	Pile designation	Cyclic Bearing Capacity	Davison's Criteria	Shape of Curve	De Beer	$\Delta=1''$	$\Delta=0.1B$	Representative Static Resistance	Ratio of $P_s$ divided by PCYCL	Ratio of $P_D$ divided by PCYCL
			$P_{CYCL}$	$P_D$ (kN)	$P_2$ (kN)	$P_3$ (kN)	$P_4$ (kN)	$P_5$ (kN)	$P_s$ (kN)	$P_s/P_{CYCL}$	$P_D/P_{CYCL}$
76		23/8a	620	580	580-700	-	710	722	620	1.000	0.935
77		23/8b	916	810	900-1000	-	1010	1020	950	1.037	0.884
78		23/9	570	600	570-660	-	715	725	610	1.070	1.053
79		23/10a	590	570	570-700	-	720	735	613	1.039	0.966
80		23/10b	850	700	1030-1050	-	1060	1080	926	1.089	0.824
81		23/11	600	670	660-680	-	750	760	670	1.117	1.117

**Table A.3.** Relevant Information Pertaining to the GRL WEAP Data.

ID #	Site	SLT Results	Standard EOD WEAP	<u>WEAP</u> SLT	Standard BOR WEAP	<u>WEAP</u> SLT	Adjusted EOD WEAP	<u>WEAP</u> SLT	Adjusted BOR WEAP	<u>WEAP</u> SLT
		(kN)	(kN)		(kN)		(kN)		(kN)	
1	Appalachi., FL	4226	2117	1.996	4515	0.936	2091	2.021	5872	0.720
2	Appalachi., FL	4239	2802	1.513	6316	0.671	2802	1.513	6228	0.681
3	Appalachi., FL	3158	2869	1.101	4359	0.724	3172	0.996	5026	0.628
4	Appalachi., FL	2313	2429	0.952	3425	0.675	2647	0.874	4137	0.559
5	Appalachi., FL	3559	2002	1.778	4404	0.808	2358	1.509	4404	0.808
6	Appalachi., FL	3559	2402	1.481	4359	0.816	2580	1.379	4381	0.812
8	Pagan River, VA	2260	645	3.503	3559	0.635	845	2.674	3559	0.635
9	Charles River, MA	2313	2767	0.836	2745	0.843	2398	0.965	2144	1.079
10	West Bay Brg., FL	4115	5649	0.728	6183	0.665	4960	0.830	5983	0.688
11	West Bay Brg., FL	3714	4537	0.819	5471	0.679	3581	1.037	4893	0.759
12	Mobile Tunnel, AL	1695	1423	1.191	3737	0.454	1090	1.555	3247	0.522
13	Mobile Tunnel, AL	2544	2313	1.100	2949	0.863	2189	1.163	2482	1.025
14	Mobile Tunnel, AL	2891	2024	1.429	3705	0.780	2006	1.441	2891	1.000
15	Mobile Tunnel, AL	3781	2847	1.328	4582	0.825	2691	1.405	4003	0.944
16	Mobile Tunnel, AL	4893	5098	0.960	4337	1.128	4751	1.030	4537	1.078
17	Omaha, NE	1361	1081	1.259	1677	0.812	970	1.404	1544	0.882
18	Omaha, NE	1690	1499	1.128	1499	1.128	1499	1.128	1392	1.214
19	Omaha, NE	1704	1957	0.870	1650	1.032	1957	0.870	2024	0.842
20	Omaha, NE	1277	1090	1.171	1557	0.820	1001	1.276	1410	0.905
22	Portland ,ME	1984	1779	1.115	2602	0.762	1401	1.416	2447	0.811
23	Portland ,ME	1957	1548	1.264	2447	0.800	1535	1.275	2313	0.846
24	Portland ,ME	1570	1557	1.009	2091	0.751	1415	1.110	1735	0.905
26	White City, VT	1468	925	1.587	1214	1.209	907	1.618	1361	1.078
27	White City, VT	1726	689	2.503	756	2.282	734	2.352	890	1.940
28	W.B. Rouge, LA	1726	1179	1.464	4404	0.392	854	2.021	3114	0.554

**Table A.3 (con't).** Relevant Information Pertaining to the GRL WEAP Data.

ID #	Site	SLT Results	Standard EOD WEAP	<u>WEAP</u> SLT	Standard BOR WEAP	<u>WEAP</u> SLT	Adjusted EOD WEAP	<u>WEAP</u> SLT	Adjusted BOR WEAP	<u>WEAP</u> SLT
		(kN)	(kN)		(kN)		(kN)		(kN)	
29	GRL, MB-AL	1201	899	1.337	1277	0.941	899	1.337	867	1.385
30	GRL, MB-AL	3381	2580	1.310	2847	1.188	1908	1.772	2380	1.421
31	Turnpike, PA	1254	774	1.621	1659	0.756	623	2.014	1321	0.949
32	Choctawhat., FL	3590	2624	1.368	6050	0.593	2624	1.368	6601	0.544
33	Seattle, WA	5614	4893	1.147	4671	1.202	4559	1.231	3114	1.803
34	Orlando, FL	3745	1944	1.927	1957	1.914	1597	2.345	2580	1.452
35	Orlando, FL	2211	947	2.333	1179	1.875	623	3.550	1223	1.807
37	Dubuque, IA	4146	1610	2.575	2362	1.755	1753	2.365	2304	1.799
38	Dubuque, IA	2936	1868	1.571	2144	1.369	2091	1.404	2068	1.419
41	Cleveland, OH	2473	3176	0.779	3060	0.808	2758	0.897	2945	0.840
42	Cleveland, OH	3203	3034	1.056	3372	0.950	2936	1.091	2882	1.111
43	Cleveland, OH	1370	1250	1.096	1646	0.832	1272	1.077	1744	0.786
44	Norwood, OH	681	810	0.841	956	0.712	810	0.841	685	0.994
45	Hennipin, MN	3367	1646	2.046	3069	1.097	1388	2.426	2567	1.312
46	Choctawhat., FL	2215	712	3.113	3781	0.586	712	3.113	3737	0.593
47	Choctawhat., FL	6272	2224	2.820	7006	0.895	2224	2.820	9030	0.695
48	Choctawhat., FL	6632	5792	1.145	6984	0.950	5792	1.145	7451	0.890
49	Choctawhat., FL	2811	3136	0.896	5516	0.510	3136	0.896	6050	0.465
50	Choctawhat., FL	4003	3425	1.169	6094	0.657	3425	1.169	3225	1.241
51	Choctawhat., FL	6437	5858	1.099	7340	0.877	5858	1.099	5961	1.080
54	Natchez, MS	2224	1303	1.706	1979	1.124	1303	1.706	1979	1.124
55	Cimarron, OK	2669	4626	0.577	3870	0.690	2326	1.147	3692	0.723
56	Cimarron, OK	3523	3781	0.932	4470	0.788	3038	1.160	4982	0.707
59	Route 115, MO	1446	1459	0.991	1401	1.032	1157	1.250	1125	1.285
60	Route 115, MO	1094	934	1.171	1468	0.745	685	1.597	1157	0.946

**Table A.3 (con't).** Relevant Information Pertaining to the GRL WEAP Data.

ID #	Site	SLT Results	Standard EOD WEAP	<u>WEAP</u> SLT	Standard BOR WEAP	<u>WEAP</u> SLT	Adjusted EOD WEAP	<u>WEAP</u> SLT	Adjusted BOR WEAP	<u>WEAP</u> SLT
		(kN)	(kN)		(kN)		(kN)		(kN)	
61	Bailey fork, TN	1188	1592	0.746	1890	0.628	965	1.230	1557	0.763
62	White City, FL	2891	3648	0.793	3025	0.956	3648	0.793	2891	1.000
63	White City, FL	2100	2589	0.811	2100	1.000	2157	0.973	2447	0.858
66	SR 15 Tioga, PA	1068	943	1.132	1214	0.879	721	1.481	867	1.231
67	Annacis, Canada	1757	3194	0.550	3336	0.527	2455	0.716	2914	0.603
68	Dawhoo, SC	4715	2380	1.981	6650	0.709	3087	1.527	8363	0.564
69	Dawhoo, SC	2624	1068	2.458	2945	0.891	1068	2.458	3381	0.776
70	Dawhoo, SC	2749	556	4.944	4012	0.685	418	6.574	2660	1.033
71	Socastee, SC	1392	1388	1.003	2535	0.549	756	1.841	2002	0.696
72	Socastee, SC	2669	2851	0.936	4070	0.656	2442	1.093	4048	0.659
74	Doughty St., SC	1601	1121	1.429	2135	0.750	1121	1.429	1761	0.909
75	Battery Cr., SC	2237	3158	0.708	2402	0.931	2949	0.759	2936	0.762
76	Battery Cr., SC	4648	4568	1.018	4337	1.072	4568	1.018	5649	0.823
78	Phoenix, AZ	5698	3069	1.857	2980	1.912	1882	3.028	2980	1.912
79	Phoenix, AZ	3292	3136	1.050	2344	1.404	2211	1.489	2491	1.321
80	Phoenix, AZ	3065	2624	1.168	2535	1.209	2624	1.168	2433	1.260
82	Phoenix, AZ	4448	4226	1.053	1935	2.299	4226	1.053	2802	1.587
83	Franklin Br., FL	4301	3679	1.169	4003	1.074	4404	0.977	4448	0.967
84	Franklin Br., FL	3648	2963	1.231	3603	1.012	3381	1.079	4537	0.804
85	Port of LA, CA	4537	5373	0.844	5338	0.850	4217	1.076	6744	0.673
87	Jones Island, WI	2918	2224	1.312	2758	1.058	2068	1.411	3198	0.912
88	Jones Island, WI	2091	2553	0.819	2482	0.842	1979	1.056	2847	0.734
89	Jones Island, WI	2580	765	3.372	1535	1.681	832	3.102	1548	1.667
90	Jones Island, WI	1690	311	5.429	1708	0.990	311	5.429	1699	0.995
92	Jones Island, WI	2922	436	6.704	1761	1.659	378	7.729	2291	1.276

**Table A.3 (con't). Relevant Information Pertaining to the GRL WEAP Data.**

ID #	Site	SLT Results	Standard EOD WEAP	<u>WEAP</u> SLT	Standard BOR WEAP	<u>WEAP</u> SLT	Adjusted EOD WEAP	<u>WEAP</u> SLT	Adjusted BOR WEAP	<u>WEAP</u> SLT
		(kN)	(kN)		(kN)		(kN)		(kN)	
93	Jones Island, WI	1690	476	3.551	1281	1.319	503	3.363	1210	1.397
101	Newport, KY	1615	2157	0.748	2068	0.781	2002	0.807	1913	0.844
102	N/A	1664	1966	0.846	2180	0.763	1570	1.059	1868	0.890
103	N/A	2318	2318	1.000	2647	0.876	2011	1.153	2277	1.018
104	N/A	1681	2055	0.818	2135	0.788	1735	0.969	1681	1.000
105	Boston, MA	2825	1953	1.446	2313	1.221	1779	1.588	1864	1.516
118	Kontich, Belgium	2108	1779	1.185	2358	0.894	1766	1.194	2380	0.886
119	Kontich, Belgium	1317	1713	0.769	2349	0.561	1686	0.781	2424	0.543
120	Kontich, Belgium	2558	2495	1.025	2847	0.898	2469	1.036	3158	0.810
126	Arutmin, Indonesia	2798	4115	0.680	4702	0.595	4115	0.680	3710	0.754
185	Duluth, MN	1890	1686	1.121	1677	1.127	1419	1.332	1339	1.412
187	New Orleans, LA	485	111	4.360	712	0.681	98	4.955	520	0.932
188	New Orleans, LA	578	93	6.190	618	0.935	93	6.190	467	1.238
189	New Orleans, LA	529	138	3.839	1076	0.492	138	3.839	689	0.768
190	New Orleans, LA	507	107	4.750	712	0.713	89	5.700	520	0.974
191	Jakarta, Indonesia	2865	3434	0.834	3381	0.847	3434	0.834	2865	1.000
192	McDuffie Island, AL	703	979	0.718	1134	0.620	872	0.806	1268	0.554
193	McDuffie Island, AL	1544	796	1.939	712	2.169	716	2.155	712	2.169
194	McDuffie Island, AL	1704	801	2.128	1059	1.609	947	1.798	1143	1.490
196	Luling Brdg., LA	1842	712	2.588	4359	0.422	689	2.671	3603	0.511
197	Luling Brdg., LA	2273	912	2.493	4782	0.475	872	2.607	5160	0.441
198	Luling Brdg., LA	2469	1241	1.989	5449	0.453	859	2.876	5560	0.444
199	Luling Brdg., LA	2406	956	2.516	3959	0.608	703	3.424	3959	0.608
200	Luling Brdg., LA	2406	2024	1.189	4448	0.541	1059	2.273	4724	0.509

**Table A.4. Relevant Information Pertaining to the Case Data**

DB #	LOCATION	Time of Driving	Average Set (IN)	Blow Count (BPI)	Davisson Capacity R <sub>D</sub> (kips)	TEST DATE	R <sub>MAX</sub> (kips)	SMITH DAMPING FACTOR	CASE DAMPING FACTOR	K <sub>SC</sub> R <sub>D</sub> R <sub>max</sub>
1	HOWARD FRANKLAND/LS1	BOR	0.14	7.22	1000	05/20/86	970	0.04	0.20	1.031
2	HOWARD FRANKLAND/LS3	BOR	N/A	NA	1549	N/A	NA	NA	NA	
3	HOWARD FRANKLAND/LS4 - SHORT	BOR	N/A	NA	1542	N/A	NA	NA	NA	
4	HOWARD FRANKLAND/LS4 - LONG	BOR	0.20	5.00	740	05/19/86	1080	0.07	0.20	0.686
5	APPALACHICOLA RIVER BRIDGE/PIER 3	BOR	0.03	30.00	922	09/17/86	996	0.06	0.29	0.926
6	APPALACHICOLA RIVER BRIDGE/PIER 14	BOR	0.05	20.00	NA	09/11/86	1144	0.10	0.40	
7	APPALACHICOLA RIVER BRIDGE/PIER 25	BOR	0.05	20.00	672	10/01/86	680	0.06	0.20	0.988
8	APPALACHICOLA RIVER BRIDGE/FSB16	BOR	0.13	7.67	308	10/30/86	410	0.05	0.13	0.752
9	APPALACHICOLA BAY BRIDGE/BENT 41	BOR	0.13	8.00	530	10/13/86	636	0.06	0.20	0.834
10	APPALACHICOLA BAY BRIDGE/BENT 101	BOR	0.04	24.00	739	10/23/86	920	0.03	0.12	0.803
11	APPALACHICOLA BAY BRIDGE/BENT 133	BOR	0.02	56.00	734	12/05/86	884	0.05	0.20	0.830
12	APPALACHICOLA BAY BRIDGE/BENT 145	BOR	0.02	48.00	955	12/16/86	884	0.05	0.20	1.080
13	APPALACHICOLA BAY BRIDGE/FSB22	BOR	0.08	12.00	425	09/17/86	520	0.11	0.39	0.818
14	BLOUNT ISLAND TERMINAL/B-20	BOR	0.08	13.00	579	04/23/87	538	0.12	0.40	1.077
15	BLOUNT ISLAND TERMINAL/B-21	BOR	0.14	7.00	369	04/21/87	362	0.02	0.04	1.020
16	ORLANDO/D-22	BOR	0.25	4.00	835	02/02/88	NA	NA	NA	
17	DODGE ISLAND BRIDGE/3-E-18	BOR	0.38	2.67	NA	10/03/88	720	0.25	0.50	
18	DODGE ISLAND BRIDGE/4-E-18	BOR	0.38	2.67	NA	10/10/88	770	0.23	0.50	
19	DODGE ISLAND BRIDGE/6-E-20	BOR	0.14	7.08	NA	10/07/88	1050	0.17	0.50	
20	DODGE ISLAND BRIDGE/8-E-20	BOR	0.07	15.00	NA	09/30/88	1830	0.10	0.50	
21	DODGE ISLAND BRIDGE/9-E-20	BOR	0.05	21.00	NA	09/30/88	1780	0.10	0.50	
22	DODGE ISLAND BRIDGE/LTP	BOR	0.05	18.67	1250	10/14/88	1850	0.10	0.50	0.676
23	CHOCTAWHATCHEE/FSB-3	BOR	0.10	10.00	497	12/21/88	724	0.14	0.40	0.687
24	CHOCTAWHATCHEE/P-5	BOR	0.06	16.00	1231	05/12/87	732	NA	NA	1.681
25	CHOCTAWHATCHEE/P-11	BOR	0.06	18.00	1405	04/17/89	1384	0.09	0.40	1.015

**Table A.4 (con't). Relevant Information Pertaining to the Case Data**

DB #	LOCATION	Time of Driving	Average Set (IN)	Blow Count (BPI)	Davisson Capacity R <sub>D</sub> (kips)	TEST DATE	R <sub>MAX</sub> (kips)	SMITH DAMPING FACTOR	CASE DAMPING FACTOR	K <sub>SC</sub> R <sub>D</sub> R <sub>max</sub>
26	CHOCTAWHATCHEE/P-17	BOR	0.03	36.00	1481	04/06/89	900	0.13	0.40	1.645
27	CHOCTAWHATCHEE/P-23	BOR	0.08	12.00	626	03/10/89	800	0.15	0.40	0.783
28	CHOCTAWHATCHEE/P-29	BOR	0.04	26.00	910	02/07/89	832	0.14	0.40	1.093
29	CHOCTAWHATCHEE/P-35	BOR	0.05	22.00	1453	01/25/89	1048	0.11	0.40	1.387
30	CHOCTAWHATCHEE/P-41	BOR	0.12	8.70	1368	01/13/89	NA	NA	NA	
31	CHOCTAWHATCHEE/FSB-26	BOR	0.06	16.00	940	12/16/88	688	0.15	0.40	1.366
32	CHOCTAWHATCHEE/TP-26	BOR	0.10	10.00	794	11/12/91	601	0.22	0.50	1.322
33	CAPE CANAVERAL/T-1	BOR	0.03	36.00	451	07/24/89	NA	NA	NA	
34	CAPE CANAVERAL/T-6	BOR	0.11	9.00	309	07/24/89	NA	NA	NA	
35	CAPE CANAVERAL/T-7	BOR	0.10	10.00	395	07/24/89	NA	NA	NA	
36	CAPE CANAVERAL/T-14	BOR	0.08	13.00	355	07/24/89	NA	NA	NA	
37	WHITE CITY BRIDGE/TP1	BOR	N/A	NA	NA	N/A	NA	NA	NA	
38	WHITE CITY BRIDGE/TP2	BOR	0.12	8.33	NA	03/22/90	590	0.19	0.41	
39	WHITE CITY BRIDGE/TP3	BOR	0.15	6.67	632	03/30/90	480	0.29	0.52	1.317
40	WHITE CITY BRIDGE/TP4	BOR	0.18	5.67	NA	03/22/90	480	0.23	0.41	
41	WHITE CITY BRIDGE/TP5	BOR	0.15	6.67	NA	03/13/90	470	0.18	0.32	
42	WHITE CITY BRIDGE/TP6	BOR	0.15	6.67	468	04/06/90	420	0.25	0.40	1.114
43	WHITE CITY BRIDGE/TP7	BOR	0.06	16.00	NA	03/13/90	570	0.15	0.32	
44	WHITE CITY BRIDGE/TP8	BOR	0.13	8.00	NA	03/13/90	490	0.18	0.32	
45	ACOSTA BRIDGE/PIER F6	BOR	0.06	18.00	754	04/19/90	848	0.12	0.40	0.889
46	ACOSTA BRIDGE/PIER G13	BOR	0.06	18.00	1090	05/03/90	1164	0.09	0.40	0.936
47	ACOSTA BRIDGE/PIER H2	BOR	0.07	14.00	563	05/30/90	892	0.11	0.40	0.631
48	WEST BAY BRIDGE/TP-9	BOR	0.15	6.67	919	03/07/91	1000	0.11	0.40	0.919
49	WEST BAY BRIDGE/TP-15	BOR	0.20	5.00	832	01/23/91	890	0.12	0.40	0.935
50	ESCAMBIA RIVER/BENT 5	BOR	0.10	10.00	869	11/21/92	568	0.19	0.40	1.529

**Table A.4 (con't). Relevant Information Pertaining to the Case Data**

DB #	LOCATION	Time of Driving	Average Set (IN)	Blow Count (BPI)	Davisson Capacity R <sub>D</sub> (kips)	TEST DATE	R <sub>MAX</sub> (kips)	SMITH DAMPING FACTOR	CASE DAMPING FACTOR	K <sub>SC</sub> R <sub>D</sub> Rmax
51	ESCAMBIA RIVER/BENT 77	BOR	0.03	33.25	1578	12/14/91	954	0.11	0.40	1.654
52	ROOSEVELT BRIDGE SITE/A-30	BOR	0.09	11.43	910	01/20/92	1000	0.21	0.55	0.910
53	ROOSEVELT BRIDGE SITE/B-30-W	BOR	0.19	5.33	786	01/20/92	840	0.24	0.55	0.936
54	BUCKMAN BRIDGE/TS-13	BOR	0.10	10.00	974	05/11/93	1080	0.12	0.40	0.902
55	BUCKMAN BRIDGE/TS-19	BOR	0.17	6.00	1089	06/21/93	1268	0.10	0.40	0.859
56	BUCKMAN BRIDGE/TS-24	BOR	0.03	29.00	1110	07/14/93	1492	0.08	0.40	0.744
57	BUCKMAN BRIDGE/TS-29	BOR	0.16	6.25	1103	05/29/93	1178	0.11	0.40	0.936
1	HOWARD FRANKLAND/LS1	EOD	0.01	79.17	1000	05/12/86	1025	0.04	0.20	0.976
2	HOWARD FRANKLAND/LS3	EOD	0.05	19.40	1549	N/A	1225	0.06	0.20	1.264
3	HOWARD FRANKLAND/LS4 - SHORT	EOD	0.03	29.17	1542	N/A	1500	0.05	0.20	1.028
4	HOWARD FRANKLAND/LS4 - LONG	EOD	0.21	4.76	740	04/24/86	750	0.10	0.20	0.987
5	APPALACHICOLA RIVER BRIDGE/PIER 3	EOD	0.29	3.42	922	09/04/86	500	0.18	0.43	1.844
6	APPALACHICOLA RIVER BRIDGE/PIER 14	EOD	0.33	3.00	NA	08/22/86	788	0.13	0.36	
7	APPALACHICOLA RIVER BRIDGE/PIER 25	EOD	0.25	4.00	672	09/19/86	612	0.05	0.14	1.097
8	APPALACHICOLA RIVER BRIDGE/FSB16	EOD	0.32	3.17	308	10/13/86	318	0.09	0.20	0.969
9	APPALACHICOLA BAY BRIDGE/BENT 41	EOD	0.24	4.17	530	09/12/86	620	0.05	0.14	0.855
10	APPALACHICOLA BAY BRIDGE/BENT 101	EOD	0.34	2.91	739	09/29/86	664	0.06	0.18	1.112
11	APPALACHICOLA BAY BRIDGE/BENT 133	EOD	0.19	5.25	734	11/11/86	480	0.17	0.39	1.529
12	APPALACHICOLA BAY BRIDGE/BENT 145	EOD	0.19	5.25	955	11/07/86	712	0.06	0.20	1.341
13	APPALACHICOLA BAY BRIDGE/FSB22	EOD	0.24	4.17	425	09/04/86	266	0.10	0.19	1.598
14	BLOUNT ISLAND TERMINAL/B-20	EOD	0.13	8.00	579	N/A	NA	NA	NA	
15	BLOUNT ISLAND TERMINAL/B-21	EOD	0.26	3.92	369	N/A	NA	NA	NA	
16	ORLANDO/D-22	EOD	0.18	5.67	835	01/26/88	NA	NA	NA	
17	DODGE ISLAND BRIDGE/3-E-18	EOD	0.11	9.00	NA	09/30/88	1180	0.15	0.50	
18	DODGE ISLAND BRIDGE/4-E-18	EOD	0.38	2.67	NA	10/06/88	660	0.27	0.50	



**Table A.4 (con't). Relevant Information Pertaining to the Case Data**

DB #	LOCATION	Time of Driving	Average Set (IN)	Blow Count (BPI)	Davisson Capacity R <sub>D</sub> (kips)	TEST DATE	R <sub>MAX</sub> (kips)	SMITH DAMPING FACTOR	CASE DAMPING FACTOR	K <sub>SC</sub> R <sub>D</sub> Rmax
19	DODGE ISLAND BRIDGE/6-E-20	EOD	0.20	5.00	NA	10/06/88	910	0.20	0.50	
20	DODGE ISLAND BRIDGE/8-E-20	EOD	0.05	22.00	NA	09/29/88	1840	0.10	0.50	
21	DODGE ISLAND BRIDGE/9-E-20	EOD	0.05	19.00	NA	09/28/88	1790	0.10	0.50	
22	DODGE ISLAND BRIDGE/LTP	EOD	0.09	11.00	1250	10/13/88	1630	0.11	0.50	0.767
23	CHOCTAWHATCHEE/FSB-3	EOD	1.00	1.00	497	12/08/88	232	0.44	0.40	2.144
24	CHOCTAWHATCHEE/P-5	EOD	0.08	12.00	1231	02/06/89	1044	NA	NA	1.179
25	CHOCTAWHATCHEE/P-11	EOD	0.59	1.69	1405	03/09/89	964	0.13	0.40	1.457
26	CHOCTAWHATCHEE/P-17	EOD	0.07	14.17	1481	03/06/89	832	0.14	0.40	1.780
27	CHOCTAWHATCHEE/P-23	EOD	0.27	3.67	626	02/28/89	NA	NA	0.40	
28	CHOCTAWHATCHEE/P-29	EOD	0.50	2.00	910	01/05/89	312	0.37	0.40	2.916
29	CHOCTAWHATCHEE/P-35	EOD	0.11	8.73	1453	12/30/89	960	0.12	0.40	1.514
30	CHOCTAWHATCHEE/P-41	EOD	0.06	17.00	1368	12/20/88	908	0.13	0.40	1.506
31	CHOCTAWHATCHEE/FSB-26	EOD	0.18	5.45	940	12/02/88	736	0.14	0.40	1.277
32	CHOCTAWHATCHEE/TP-26	EOD	0.33	3.00	794	10/16/91	NA	NA	NA	
33	CAPE CANAVERAL/T-1	EOD	0.40	2.50	451	07/22/89	245	0.13	0.40	1.839
34	CAPE CANAVERAL/T-6	EOD	0.13	7.50	309	07/22/89	360	0.14	0.40	0.859
35	CAPE CANAVERAL/T-7	EOD	0.50	2.00	395	07/22/89	260	0.12	0.40	1.521
36	CAPE CANAVERAL/T-14	EOD	0.18	5.50	355	07/20/89	305	0.10	0.40	1.164
37	WHITE CITY BRIDGE/TP1	EOD	0.02	53.00	NA	03/26/91	510	NA	NA	
38	WHITE CITY BRIDGE/TP2	EOD	0.13	7.83	NA	03/22/90	580	0.19	0.41	
39	WHITE CITY BRIDGE/TP3	EOD	0.11	9.33	632	03/22/90	490	0.22	0.41	1.290
40	WHITE CITY BRIDGE/TP4	EOD	0.19	5.29	NA	03/22/90	480	0.23	0.41	
41	WHITE CITY BRIDGE/TP5	EOD	0.14	7.17	NA	03/12/90	440	0.19	0.32	
42	WHITE CITY BRIDGE/TP6	EOD	0.20	5.00	468	03/13/90	430	0.20	0.32	1.088
43	WHITE CITY BRIDGE/TP7	EOD	0.09	10.67	NA	03/13/90	550	0.16	0.32	

**Table A.4 (con't).** Relevant Information Pertaining to the Case Data

DB #	LOCATION	Time of Driving	Average Set (IN)	Blow Count (BPI)	Davisson Capacity R <sub>p</sub> (kips)	TEST DATE	R <sub>MAX</sub> (kips)	SMITH DAMPING FACTOR	CASE DAMPING FACTOR	K <sub>SC</sub> R <sub>D</sub> Rmax
44	WHITE CITY BRIDGE/TP8	EOD	0.15	6.67	NA	03/13/90	470	0.18	0.32	
45	ACOSTA BRIDGE/PIER F6	EOD	0.25	4.00	754	03/28/90	464	0.21	0.40	1.626
46	ACOSTA BRIDGE/PIER G13	EOD	0.14	7.00	1090	04/20/90	860	0.12	0.40	1.267
47	ACOSTA BRIDGE/PIER H2	EOD	0.11	8.83	563	05/11/90	876	0.11	0.40	0.643
48	WEST BAY BRIDGE/TP-9	EOD	0.20	5.00	919	03/07/91	580	0.24	0.50	1.584
49	WEST BAY BRIDGE/TP-15	EOD	0.30	3.33	832	01/23/91	500	0.21	0.40	1.665
50	ESCAMBIA RIVER/BENT 5	EOD	0.14	7.00	869	10/29/92	596	0.18	0.40	1.457
51	ESCAMBIA RIVER/BENT 77	EOD	0.06	18.00	1578	11/23/91	768	0.14	0.40	2.055
52	ROOSEVELT BRIDGE SITE/A-30	EOD	0.12	8.58	910	01/15/92	880	0.23	0.55	1.034
53	ROOSEVELT BRIDGE SITE/B-30-W	EOD	0.23	4.33	786	01/17/92	820	0.25	0.55	0.959
54	BUCKMAN BRIDGE/TS-13	EOD	0.29	3.42	974	04/08/93	774	0.16	0.40	1.258
55	BUCKMAN BRIDGE/TS-19	EOD	0.19	5.25	1089	04/26/93	1082	0.11	0.40	1.007
56	BUCKMAN BRIDGE/TS-24	EOD	0.18	5.50	1110	04/13/93	1280	0.09	0.40	0.867
57	BUCKMAN BRIDGE/TS-29	EOD	0.17	6.00	1103	04/29/93	1048	0.12	0.40	1.052

**Table A.5. Relevant Information Pertaining to Database PD2000.**

Ref. No.	Pile-Case Number	Refer. Time	Location	Pile Type	Pile Area	Length Below Gauges	Penetr Depth	Soil Type	
					(in <sup>2</sup> )	(ft)	(ft)	Side	Tip
1	96-104-1W-D	EOD	Newbury Brdg (N-10-15)	HP 12x74	21.8	137	131.5	Clay (BB)	Till/Rock
2	96-104-1W-D	1 DR	Newbury Brdg (N-10-15)	HP 12x74	21.8	137		Clay (BB)	Till/Rock
3	96-104-1W-I	EOD	Newbury Brdg (N-10-15)	HP 12x74	21.8	137	125.0	Clay (BB)	Till/Rock
4	96-104-1W-I	1 DR	Newbury Brdg (N-10-15)	HP 12x74	21.8	126		Clay (BB)	Till/Rock
5	96-104-2E-K	EOD	Newbury Brdg (N-10-15)	HP 12x74	21.8	133	134.0	Clay (BB)	Till/Rock
6	96-104-2E-K	1 DR	Newbury Brdg (N-10-15)	HP 12x74	21.8	133		Clay (BB)	Till/Rock
7	96-104-2W-R	EOD	Newbury Brdg (N-10-15)	HP 12x74	21.8	141	130.0	Clay (BB)	Till/Rock
8	96-104-2W-R	1 DR	Newbury Brdg (N-10-15)	HP 12x74	21.8	142		Clay (BB)	Till/Rock
9	96-104-3E-A	EOD	Newbury Brdg (N-10-15)	HP 12x74	21.8	111.5	108.0	Clay (BB)	Till/Rock
10	96-104-3E-A	1 DR	Newbury Brdg (N-10-15)	HP 12x74	21.8	111.5		Clay (BB)	Till/Rock
11	96-104-3W-G	EOD	Newbury Brdg (N-10-15)	HP 12x74	21.8	117	103.0	Clay (BB)	Till/Rock
12	96-104-3W-G	1 DR	Newbury Brdg (N-10-15)	HP 12x74	21.8	102		Clay (BB)	Till/Rock
13	96-104-5W-F	EOD	Newbury Brdg (N-10-15)	HP 12x74	21.8	112	105.0	Clay (BB)	Till/Rock
14	96-104-5W-F	4 DR	Newbury Brdg (N-10-15)	HP 12x74	21.8	112		Clay (BB)	Till/Rock
15	96-104-NA-4	EOD	Newbury Brdg (N-10-15)	HP 12x74	21.8	112	105.0	Clay (BB)	Till/Rock
16	96-104-NA-4	1 DR	Newbury Brdg (N-10-15)	HP 12x74	21.8	112		Clay (BB)	Till/Rock
17	96-104-NA-53	EOD	Newbury Brdg (N-10-15)	HP 12x74	21.8	117	111.0	Clay (BB)	Till/Rock
18	96-104-NA-53	1 DR	Newbury Brdg (N-10-15)	HP 12x74	21.8	117		Clay (BB)	Till/Rock
19	96-104-TP1	EOD	Newbury Brdg (N-10-15)	12-3/4x3/8 Pipe	14.6	57.5	58.0	Clay (BB)	Silty Clay
20	96-104-TP1	1 DR	Newbury Brdg (N-10-15)	12-3/4x3/8 Pipe	14.6	57.5		Clay (BB)	Silty Clay
21	96-104-TP4	EOD	Newbury Brdg (N-10-15)	HP12x74	21.8		105.5	Clay (BB)	Till/Rock
22	96-104-TP4	1 DR	Newbury Brdg (N-10-15)	HP12x74	21.8	116.5		Clay (BB)	Till/Rock
23	96-104-TP4	7 DR	Newbury Brdg (N-10-15)	HP12x74	21.8	116.5		Clay (BB)	Till/Rock
24	96-104-W1-V26	EOD	Newbury Brdg (N-10-15)	12.75x3/8" Pipe	14.6	34	18.0	Clay (BB)	Clay (BB)
25	96-104-W1-V26	1 DR	Newbury Brdg (N-10-15)	12.75x3/8" Pipe	14.6	23		Clay (BB)	Clay (BB)

**Table A.5 (con't). Relevant Information Pertaining to Database PD2000.**

Ref. No.	Pile-Case Number	Refer. Time	Location	Pile Type	Pile Area	Length Below Gauges	Penetr Depth	Soil Type	
								Side	Tip
26	96-104-W2-V13	EOD	Newbury Brdg (N-10-15)	12.75x3/8" Pipe	14.6	73.5	57.5	Clay (BB)	Silty Clay
27	96-104-W2-V13	1 DR	Newbury Brdg (N-10-15)	12.75x3/8" Pipe	14.6	73.5		Clay (BB)	Silty Clay
28	96-104-W4-B36	EOD	Newbury Brdg (N-10-15)	12.75x3/8" Pipe	14.6	136.5	135.0	Clay (BB)	Till/Rock
29	96-104-W4-B36	3 DR	Newbury Brdg (N-10-15)	12.75x3/8" Pipe	14.6	136.5		Clay (BB)	Till/Rock
30	96-104-W4-V24	EOD	Newbury Brdg (N-10-15)	12.75x3/8" Pipe	14.6	132	123.0	Clay (BB)	Till/Rock
31	96-104-W4-V24	3 DR	Newbury Brdg (N-10-15)	12.75x3/8" Pipe	14.6	132		Clay (BB)	Till/Rock
32	96-104-W5-3	EOD	Newbury Brdg (N-10-15)	12.75x3/8" Pipe	14.6	118	115.0	Clay (BB)	Till/Rock
33	96-104-W5-3	1 DR	Newbury Brdg (N-10-15)	12.75x3/8" Pipe	14.6	118		Clay (BB)	Till/Rock
34	96-104-W5-8	EOD	Newbury Brdg (N-10-15)	12.75x3/8" Pipe	14.6	148	118.0	Clay (BB)	Till/Rock
35	96-104-W5-8	1 DR	Newbury Brdg (N-10-15)	12.75x3/8" Pipe	14.6	117		Clay (BB)	Till/Rock
36	96-104-W5-V27	EOD	Newbury Brdg (N-10-15)	12.75x3/8" Pipe	14.6	125.5	121.0	Clay (BB)	Till/Rock
37	96-104-W5-V27	1 DR	Newbury Brdg (N-10-15)	12.75x3/8" Pipe	14.6	125.5		Clay (BB)	Till/Rock
38	96-104-W5-V28	EOD	Newbury Brdg (N-10-15)	12.75x3/8" Pipe	14.6	123.5	121.0	Clay (BB)	Till/Rock
39	96-104-W5-V28	1 DR	Newbury Brdg (N-10-15)	12.75x3/8" Pipe	14.6	123.5		Clay (BB)	Till/Rock
40	96-115-3	EOD	Airport Toll Plaza	HP14x73	21.4	137	121.5	Clay (BB)	Till/Rock
41	96-115-3	1 DR	Airport Toll Plaza	HP14x73	21.4	137		Clay (BB)	Till/Rock
42	96-115-7	EOD	Airport Toll Plaza	HP14x73	21.4	129.5	121.0	Clay (BB)	Till/Rock
43	96-115-7	6 DR	Airport Toll Plaza	HP14x73	21.4	129.5		Clay (BB)	Till/Rock
44	96-115-106	EOD	Abut. 1A/D	16" PPC Ind. Piles	256	174	158.3	Clay (BB)	Till/Rock
45	96-115-106	41 DR	Abut. 1A/D	16" PPC Ind. Piles	256	174	-	Clay (BB)	Till/Rock
46	96-115-109	EOD	Abut. 1A/D	16" PPC Ind. Piles	256	174	169.6	Clay (BB)	Till/Rock
47	96-115-109	41 DR	Abut. 1A/D	16" PPC Ind. Piles	256	174	-	Clay (BB)	Till/Rock
48	96-115-117	EOD	Arrivals Tunnel	16" PPC Ind. Piles	256	88	89.0	Clay (BB)	Clay (BB)
49	96-115-117	14 DR	Arrivals Tunnel	16" PPC Ind. Piles	256	88	-	Clay (BB)	Clay (BB)
50	96-115-157	EOD	Arrivals Tunnel	16" PPC Ind. Piles	256	83.5	81.5	Clay (BB)	Clay (BB)

**Table A.5 (con't). Relevant Information Pertaining to Database PD2000.**

Ref. No.	Pile-Case Number	Refer. Time	Location	Pile Type	Pile Area	Length	Penetr	Soil Type	
						Below Gauges	Depth		
					(in <sup>2</sup> )	(ft)	(ft)	Side	Tip
51	96-115-157	7 DR	Arrivals Tunnel	16" PPC Ind. Piles	256	83.5	-	Clay (BB)	Clay (BB)
52	96-115-158	EOD	Arrivals Tunnel	16" PPC Ind. Piles	256	83.5	83.5	Clay (BB)	Clay (BB)
53	96-115-158	7 DR	Arrivals Tunnel	16" PPC Ind. Piles	256	83.5	-	Clay (BB)	Clay (BB)
54	96-115-163	EOD	Arrivals Tunnel	16" PPC Ind. Piles	256	82	83.0	Clay (BB)	Clay (BB)
55	96-115-163	3 DR	Arrivals Tunnel	16" PPC Ind. Piles	256	82	83.0	Clay (BB)	Clay (BB)
56	96-115-182	EOD	Arrivals Tunnel	16" PPC Ind. Piles	256	83	83.0	Clay (BB)	Clay (BB)
57	96-115-182	14 DR	Arrivals Tunnel	16" PPC Ind. Piles	256	81	-	Clay (BB)	Clay (BB)
58	96-115-258	EOD	Arrivals Tunnel	16" PPC Ind. Piles	256		72.0	Clay (BB)	Clay (BB)
59	96-115-258	22 DR	Arrivals Tunnel	16" PPC Ind. Piles	256	72	72.0	Clay (BB)	Clay (BB)
60	96-115-279	EOD	Arrivals Tunnel	16" PPC Ind. Piles	256	78	69.0	Clay (BB)	Clay (BB)
61	96-115-279	3 DR	Arrivals Tunnel	Rev. Criteria	256	78		Clay (BB)	Clay (BB)
62	96-115-279	54 DR	Arrivals Tunnel	Rev. Criteria	256			Clay (BB)	Clay (BB)
63	96-115-357	EOD	Arrivals Tunnel	16" PPC Ind. Piles	256	82	60.5	Clay (BB)	Clay (BB)
64	96-115-357	5 DR	Arrivals Tunnel	16" PPC Ind. Piles	256	82	60.5	Clay (BB)	Clay (BB)
65	96-115-375	EOD	Arrivals Tunnel	16" PPC Ind. Piles	256	81	54.5	Clay (BB)	Clay (BB)
66	96-115-375	7 DR	Arrivals Tunnel	16" PPC Ind. Piles	256	59	54.5	Clay (BB)	Clay (BB)
67	96-115-414	EOD	Arrivals Tunnel	16" PPC Ind. Piles	256	81	65.0	Clay (BB)	Clay (BB)
68	96-115-414	14 DR	Arrivals Tunnel	16" PPC Ind. Piles	256	81	65.0	Clay (BB)	Clay (BB)
69	96-115-806	EOD	Abut. TA/D	16" PPC Ind. Piles	256	159	129.3	Clay (BB)	Till/Rock
70	96-115-806	55 DR	Abut. TA/D	16" PPC Ind. Piles	256	159	-	Clay (BB)	Till/Rock
71	96-115-816	EOD	Abut. TA/D	16" PPC Ind. Piles	256	159	131.5	Clay (BB)	Till/Rock
72	96-115-816	56 DR	Abut. TA/D	16" PPC Ind. Piles	256	159	-	Clay (BB)	Till/Rock
73	96-115-910	EOD	Toll Plaza	16" PPC Ind. Piles	256	131	125.5	Clay (BB)	Till/Rock
74	96-115-910	41 DR	Toll Plaza	16" PPC Ind. Piles	256	123.8		Clay (BB)	Till/Rock
75	96-115-916	EOD	Toll Plaza	16" PPC Ind. Piles	256	141	121.5	Clay (BB)	Till/Rock

**Table A.5 (con't).** Relevant Information Pertaining to Database PD2000.

Ref. No.	Pile-Case Number	Refer. Time	Location	Pile Type	Pile Area	Length Below Gauges	Penetr Depth	Soil Type	
								Side	Tip
76	96-115-916	39 DR	Toll Plaza	16" PPC Ind. Piles	256	123.1		Clay (BB)	Till/Rock
77	96-115-919	EOD	Toll Plaza	16" PPC Ind. Piles	256	131	125.1	Clay (BB)	Till/Rock
78	96-115-919	39 DR	Toll Plaza	16" PPC Ind. Piles	256	121.4		Clay (BB)	Till/Rock
79	96-115-926	EOD	Toll Plaza	16" PPC Ind. Piles	256	131	125.8	Clay (BB)	Till/Rock
80	96-115-926	39 DR	Toll Plaza	16" PPC Ind. Piles	256	122.2		Clay (BB)	Till/Rock
81	96-115-937	EOD	Toll Plaza	16" PPC Ind. Piles	256	131	126.3	Clay (BB)	Till/Rock
82	96-115-937	39 DR	Toll Plaza	16" PPC Ind. Piles	256	125.8		Clay (BB)	Till/Rock
83	96-115-940	EOD	Toll Plaza	16" PPC Ind. Piles	256	141	122.5	Clay (BB)	Till/Rock
84	96-115-940	41 DR	Toll Plaza	16" PPC Ind. Piles	256	125.1		Clay (BB)	Till/Rock
85	96-115-3111	EOD	Arrivals Tunnel	Rev. Criteria	256	60	58.5	Clay (BB)	Clay (BB)
86	96-115-3111	14 DR	Arrivals Tunnel	Rev. Criteria	256	60	-	Clay (BB)	Clay (BB)
87	96-115-3115	EOD	Arrivals Tunnel	Rev. Criteria	256	60	53.5	Clay (BB)	Clay (BB)
88	96-115-3115	14 DR	Arrivals Tunnel	Rev. Criteria	256	55.5	-	Clay (BB)	Clay (BB)
89	96-115-3117	EOD	Arrivals Tunnel	Rev. Criteria	256	60	53.0	Clay (BB)	Clay (BB)
90	96-115-3117	14 DR	Arrivals Tunnel	Rev. Criteria	256	60	-	Clay (BB)	Clay (BB)
91	96-115-3118	EOD	Arrivals Tunnel	Rev. Criteria	256	60	59.0	Clay (BB)	Clay (BB)
92	96-115-3118	14 DR	Arrivals Tunnel	Rev. Criteria	256	60	-	Clay (BB)	Clay (BB)
93	96-115-3181	EOD	Arrivals Tunnel	16" PPC Ind. Piles	256	84	79.0	Clay (BB)	Clay (BB)
94	96-115-3181	33 DR	Arrivals Tunnel	16" PPC Ind. Piles	256	77	-	Clay (BB)	Clay (BB)
95	96-115-3220	EOD	Arrivals Tunnel	16" PPC Ind. Piles	256	75	61.5	Clay (BB)	Clay (BB)
96	96-115-3220	4 DR	Arrivals Tunnel	16" PPC Ind. Piles	256	75	61.5	Clay (BB)	Clay (BB)
97	96-115-3259	EOD	Arrivals Tunnel	16" PPC Ind. Piles	256	82	66.5	Clay (BB)	Clay (BB)
98	96-115-3259	5 DR	Arrivals Tunnel	16" PPC Ind. Piles	256	82	66.5	Clay (BB)	Clay (BB)
99	96-116-9	EOD	Amesbury, MA Brdg	14"x1/2" Pipe Piles	21.2	106	97.5	F. Sand	Till/Rock
100	96-116-9	1 DR	Amesbury, MA Brdg	14"x1/2" Pipe Piles	21.2	106	97.5	F. Sand	Till/Rock

**Table A.5 (con't). Relevant Information Pertaining to Database PD2000.**

Ref. No.	Pile-Case Number	Refer. Time	Location	Pile Type	Pile Area	Length	Penetr	Soil Type	
						Below Gauges	Depth	Side	Tip
					(in <sup>2</sup> )	(ft)	(ft)		
101	96-116-12	EOD	Amesbury, MA Brdg	14"x1/2" Pipe Piles	21.2	106	98.0	F. Sand	Till/Rock
102	96-116-12	1 DR	Amesbury, MA Brdg	14"x1/2" Pipe Piles	21.2	106	98.0	F. Sand	Till/Rock
103	96-117-A4	EOD	Tewksbury, MA Brdg	12.75x3/8 Pipe Pile	14.6	32	20.0	SW	SW/Till
104	96-117-A4	Res.	Tewksbury, MA Brdg	12.75x3/8 Pipe Pile	14.6	32	-	SW	SW/Till
105	97-102-TP2	EOD	U. S. Air Terminal Add.	14" PPC Test Piles	196	111.5	109.0	Silt/Clay	Rock
106	97-102-TP2	6 DR	U. S. Air Terminal Add.	14" PPC Test Piles	196	111.5	109.0	Silt/Clay	Rock
107	97-104-TP1 (#7)	EOD	Whatley Brdg	HP 12x53 Test Piles	15.5	173	162.0	Silt/Clay	SW
108	97-104-TP1 (#7)	31 DR	Whatley Brdg	HP 12x53 Test Piles	15.5	167	162.0	Silt/Clay	SW
109	97-104-TP2 (#18)	EOD	Whatley Brdg	HP 12x53 Test Piles	15.5	101	80.0	Silt/Clay	Clay
110	97-104-TP2 (#18)	3 DR	Whatley Brdg	HP 12x53 Test Piles	15.5	101	80.5	Silt/Clay	Clay
111	97-104-TP2 (#18)	34 DR	Whatley Brdg	HP 12x53 Test Piles	15.5	101	80.8	Silt/Clay	Clay
112	97-106-TP1	EOD	96" Diam. Force Main	12" PPC Ind. Piles	144	51	42.5	Silty Clay	Till
113	97-106-TP1	8 DR	96" Diam. Force Main	12" PPC Ind. Piles	144	51	42.5	Silty Clay	Till
114	97-106-TP2	EOD	96" Diam. Force Main	12" PPC Ind. Piles	144	51	35.5	Silty Clay	Till
115	97-106-TP2	8 DR	96" Diam. Force Main	12" PPC Ind. Piles	144	51	35.5	Silty Clay	Till
116	97-106-TP3	EOD	96" Diam. Force Main	12" PPC Ind. Piles	144	51	40.5	Silty Clay	Till
117	97-106-TP3	7 DR	96" Diam. Force Main	12" PPC Ind. Piles	144	51	40.5	Silty Clay	Till
118	97-108-#7	EOD	South Harbor Garage	13.75"x5/8" Pipe Piles	25.8	42.5	36.0	Silty Clay	Till
119	97-108-#7	1 DR	South Harbor Garage	13.75"x5/8" Pipe Piles	25.8	42.5	36.0	Silty Clay	Till
120	97-108-#106	EOD	South Harbor Garage	13.75"x5/8" Pipe Piles	25.8	42	43.5	Silty Clay	Till
121	97-108-#106	1 DR	South Harbor Garage	13.75"x5/8" Pipe Piles	25.8	42	43.5	Silty Clay	Till
122	97-108-#77	EOD	South Harbor Garage	13.75"x5/8" Pipe Piles	25.8	40	39.0	Silty Clay	Till
123	97-108-#77	1 DR	South Harbor Garage	13.75"x5/8" Pipe Piles	25.8	40	39.0	Silty Clay	Till
124	97-108-#69	EOD	South Harbor Garage	13.75"x5/8" Pipe Piles	25.8	43	42.5	Silty Clay	Till
125	97-108-#69	Res.	South Harbor Garage	13.75"x5/8" Pipe Piles	25.8	43	43.0	Silty Clay	Till

**Table A.5 (con't).** Relevant Information Pertaining to Database PD2000.

Ref. No.	Pile-Case Number	Refer. Time	Location	Pile Type	Pile Area	Length Below Gauges	Penetr Depth	Soil Type	
					(in <sup>2</sup> )	(ft)	(ft)	Side	Tip
126	97-108-#27	EOD	South Harbor Garage	13.75"x5/8" Pipe Piles	25.8	43.5	39.5	Silty Clay	Till
127	97-108-#27	1 DR	South Harbor Garage	13.75"x5/8" Pipe Piles	25.8	43.5	39.5	Silty Clay	Till
128	97-109-A10#64 (TP5)	EORD	Logan Walkways	HP14x89	26.2		119.0	Sand/Clay	Till
129	97-109-A10#64 (TP5)	2nd Res.	Logan Walkways	HP14x89	26.2	127	119'-1"	Sand/Clay	Till
130	97-109-A3#20 (TP6)	EORD	Logan Walkways	HP14x89	26.2		98.0	Sand/Clay	Till
131	97-109-A3#20 (TP6)	1st Res.	Logan Walkways	HP14x89	26.2	107	105.0	Sand/Clay	Till
132	97-109-A3#28 (TP1)	EORD	Logan Walkways	HP14x89	26.2		102.0	Sand/Clay	Till
133	97-109-A3#28 (TP1)	2nd Res.	Logan Walkways	HP14x89	26.2	107	102'-1"	Sand/Clay	Till
134	97-109-AE#42 (TP2)	EORD	Logan Walkways	HP14x89	26.2		117.0	Sand/Clay	Till
135	97-109-AE#42 (TP2)	2nd Res.	Logan Walkways	HP14x89	26.2		117'-1"	Sand/Clay	Till
136	97-109-AF#73 (TP4)	EORD	Logan Walkways	HP14x89	26.2		126'-6"	Sand/Clay	Till
137	97-109-AF#73 (TP4)	2nd Res.	Logan Walkways	HP14x89	26.2	142	126'-6"	Sand/Clay	Till
138	97-109-AG/A4 #31 (TP2)	EORD	Logan Walkways	HP14x89	26.2		117.0	Sand/Clay	Till
139	97-109-AG/A4 #31 (TP2)	2nd Res.	Logan Walkways	HP14x89	26.2	142	117'-1"	Sand/Clay	Till
140	97-109-AH#96 (TP3)	EORD	Logan Walkways	HP14x89	26.2		128'-4"	Sand/Clay	Till
141	97-109-AH#96 (TP3)	2nd Res.	Logan Walkways	HP14x89	26.2	147	128'-4"	Sand/Clay	Till
142	97-109-LAETP8 N. Node #21	EOD	Logan Walkways	HP14x89	26.2	117	92.0	Sand/Clay	Till
143	97-109-LAETP8 N. Node #21	3 DR	Logan Walkways	HP14x89	26.2	97	-	Sand/Clay	Till
144	97-109-LETP10 S. Node #78	EOD	Logan Walkways	HP14x89	26.2	146.5	132.0	Sand/Clay	Till
145	97-109-LETP10 S. Node #78	2 DR	Logan Walkways	HP14x89	26.2	137	-	Sand/Clay	Till
146	97-109-LETP11 N. Node #11	EOD	Logan Walkways	HP14x89	26.2	87	86.0	Sand/Clay	Till
147	97-109-LETP11 N. Node #11	3 DR	Logan Walkways	HP14x89	26.2	87	-	Sand/Clay	Till
148	97-109-LETP12 E3-106	EOD	Logan Walkways	HP14x89	26.2	151.5	141.5	Sand/Clay	Till
149	97-109-LETP12 E3-106	2 DR	Logan Walkways	HP14x89	26.2	142.5	-	Sand/Clay	Till
150	97-109-LETP15 E4-86	EOD	Logan Walkways	HP14x89	26.2	133	131.0	Sand/Clay	Till



**Table A.5 (con't).** Relevant Information Pertaining to Database PD2000.

Ref. No.	Pile-Case Number	Refer. Time	Location	Pile Type	Pile Area	Length Below Gauges	Penetr Depth	Soil Type	
					(in <sup>2</sup> )	(ft)	(ft)	Side	Tip
151	97-109-LETP15 E4-86	4 DR	Logan Walkways	HP14x89	26.2	133	-	Sand/Clay	Till
152	97-109-Strs#112 (TP7)	EOD	Logan Walkways	HP 14x89 (100 TDL)	26.2	107	106.0	Sand/Clay	Till
153	97-109-Strs#112 (TP7)	BOR	Logan Walkways	HP 14x89 (100 TDL)	26.2	107	106.0	Sand/Clay	Till
154	97-114-HBTP1	EOD	Chapin Rd. Repl. Brdg	HP12x84 Test Pile	24.6	27	23.7	Sand	Rock
155	97-114-HBTP1	5 DR	Chapin Rd. Repl. Brdg	HP12x84 Test Pile	24.6	27	-	Sand	Rock
156	97-117-UMG-TP4	EOD	UM Park. Gar. VT	HP 14x73 A-67 SE	21.4	48.1	43.9	Sand/Clay	Clay/Till
157	97-117-UMG-TP4	1 DR	UM Park. Gar. VT	HP 14x73 A-67 SE	21.4	48.1	-	Sand/Clay	Clay/Till
158	97-117-UMG-TP4	2 DR	UM Park. Gar. VT	HP 14x73 A-67 SE	21.4	44	-	Sand/Clay	Clay/Till
159	97-117-UMG-TP8	EOD	UM Park. Gar. VT	HP 14x73 E-5 S	21.4	41.4	39.0	Sand/Clay	Clay
160	97-117-UMG-TP8	14 DR	UM Park. Gar. VT	HP 14x73 E-5 S	21.4	41.4	-	Sand/Clay	Clay
161	97-120-MPTP1 (B-2)	EOD	Metro. Pipe Addition	12.75 x 0.375 Pipe Piles	14.6	59	54.0	Sand/Clay	Till
162	97-120-MPTP1 (B-2)	8 DR	Metro. Pipe Addition	12.75 x 0.375 Pipe Piles	14.6	49.5	54.0	Sand/Clay	Till
163	97-120-MPTP2 (D-3)	EOD	Metro. Pipe Addition	12.75 x 0.375 Pipe Piles	14.6	57	48.5	Sand/Clay	Till
164	97-120-MPTP2 (D-3)	8 DR	Metro. Pipe Addition	12.75 x 0.375 Pipe Piles	14.6	45	48.5	Sand/Clay	Till
165	97-123-B-12	EOD	6 Cambridge Center	14" PPC Ind. Piles	196	78	75.0	Sand/Clay	Till/Rock
166	97-123-B-12	7 DR	6 Cambridge Center	14" PPC Ind. Piles	196	74.5	-	Sand/Clay	Till/Rock
167	98-105-TP1 (E. Abut.)	EOD	Vill. Hill Rd Brdg Williamsburg	HP 14x89	26.1	42.9	33.0	SM w/Grav	Rock
168	98-105-TP1 (E. Abut.)	3 DR	Vill. Hill Rd Brdg Williamsburg	HP 14x89	26.1	42.9	-	SM w/Grav	Rock
169	98-105-TP6 (W. Abut.)	EOD	Vill. Hill Rd Brdg Williamsburg	HP 14x89	26.1	32.3	21.5	SM w/Grav	Rock
170	98-105-TP6 (W. Abut.)	EOD	Vill. Hill Rd Brdg Williamsburg	HP 14x89	26.1	32.3	24.5	SM w/Grav	Rock
171	98-105-TP6 (W. Abut.)	3 DR	Vill. Hill Rd Brdg Williamsburg	HP 14x89	26.1	32.3	-	SM w/Grav	Rock
172	98-106-#1	EOD	Portland St.	Timber Test Piles	121	29	25.0	Org. Silt	H. Clay
173	98-106-#1	11 DR	Portland St.	Timber Test Piles	121	29	-	Org. Silt	H. Clay
174	98-106-#2	EOD	Portland St.	Timber Test Piles	121	30	26.0	Org. Silt	H. Clay
175	98-106-#2	11 DR	Portland St.	Timber Test Piles			-	Org. Silt	H. Clay

**Table A.5 (con't). Relevant Information Pertaining to Database PD2000.**

Ref. No.	Pile-Case Number	Refer. Time	Location	Pile Type	Pile Area	Length Below Gauges	Penetr Depth	Soil Type	
					(in <sup>2</sup> )	(ft)	(ft)	Side	Tip
176	98-106-#3	EOD	Portland St.	Timber Test Piles	134	28	25.5	Org. Silt	H. Clay
177	98-106-#3	11 DR	Portland St.	Timber Test Piles	134	28	-	Org. Silt	H. Clay
178	98-106-#4	EOD	Portland St.	Timber Test Piles	127	28	26.5	Org. Silt	H. Clay
179	98-106-#4	11 DR	Portland St.	Timber Test Piles	127	28	-	Org. Silt	H. Clay
180	98-107-LCTP1 (#6)	EOD	CA/T C19E5	12" Timber Test Piles	121	27	23.0	Sand/Clay	Till
181	98-107-LCTP1 (#6)	1 DR	CA/T C19E5	12" Timber Test Piles	121	27	-	Sand/Clay	Till
182	98-107-LCTP3 (#27)	EOD	CA/T C19E5	12" Timber Test Piles			28.0	Sand/Clay	Till
183	98-107-LCTP3 (#27)	EOD	CA/T C19E5	12" Timber Test Piles	121	29	28.0	Sand/Clay	Till
184	98-107-LCTP3 (#27)	1 DR	CA/T C19E5	12" Timber Test Piles	121	29	-	Sand/Clay	Till
185	98-109-C19TP1	EOD	CA/T C19B1 Boston	16" PPC Piles	256	60	44.0	Sand/Clay	SM/Till
186	98-109-C19TP1	7 DR	CA/T C19B1 Boston	16" PPC Piles	256	60	-	Sand/Clay	SM/Till
187	98-109-C19TP2	EOD	CA/T C19B1 Boston	16" PPC Piles	256	60	59.0	Sand/Clay	SM/Rock
188	98-109-C19TP2	6 DR	CA/T C19B1 Boston	16" PPC Piles	256	60	-	Sand/Clay	SM/Rock
189	98-109-C19TP3	EOD	CA/T C19B1 Boston	16" PPC Piles	256	60	42.0	Sand/Clay	SM/Till
190	98-109-C19TP3	5 DR	CA/T C19B1 Boston	16" PPC Piles	256	60	-	Sand/Clay	SM/Till
191	98-109-C19TP3	Redrive	CA/T C19B1 Boston	16" PPC Piles	256	60	47.0	Sand/Clay	SM/Till
192	98-109-C19TP4	EOD	CA/T C19B1 Boston	16" PPC Piles	256	66	68.0	Sand/Clay	SM/Rock
193	98-109-C19TP4	46 DR	CA/T C19B1 Boston	16" PPC Piles	256	67	-	Sand/Clay	SM/Rock
194	98-109-C19TP5	EOD	CA/T C19B1 Boston	16" PPC Piles	256	75	56.0	Sand/Clay	SM/Till
195	98-109-C19TP5	43 DR	CA/T C19B1 Boston	16" PPC Piles	256	75	-	Sand/Clay	SM/Till
196	98-109-C19TP6	EOD	CA/T C19B1 Boston	12" PPC Piles	144	66	58.0	Sand/Clay	SM/Till
197	98-109-C19TP6	43 DR	CA/T C19B1 Boston	12" PPC Piles	144	66	-	Sand/Clay	SM/Till
198	98-109-260	EOD	CA/T C19B1 Boston	16" PPC Piles	256	72	50.5	Sand/Clay	SM/Till
199	98-109-260	1 DR	CA/T C19B1 Boston	16" PPC Piles	256	52	-	Sand/Clay	SM/Till
200	98-109-1099	EOD	CA/T C19B1 Boston	16" PPC Piles	256	72	37.0	Sand/Clay	Clay/SM

**Table A.5 (con't).** Relevant Information Pertaining to Database PD2000.

Ref. No.	Pile-Case Number	Refer. Time	Location	Pile Type	Pile Area	Length	Penetr	Soil Type	
						Below Gauges	Depth	Side	Tip
					(in <sup>2</sup> )	(ft)	(ft)		
201	98-109-1099	1 DR	CA/T C19B1 Boston	16" PPC Piles	256	42	-	Sand/Clay	Clay/SM
202	98-109-1043	EOD	CA/T C19B1 Boston	16" PPC Piles	256	72	45.5	Sand/Clay	SM/Till
203	98-109-1043	1 DR	CA/T C19B1 Boston	16" PPC Piles	256	50	-	Sand/Clay	SM/Till
204	98-109-1050	EOD	CA/T C19B1 Boston	16" PPC Piles	256	65	42.5	Sand/Clay	SM/Till
205	98-109-1050	2 DR	CA/T C19B1 Boston	16" PPC Piles	256	65	-	Sand/Clay	SM/Till
206	98-109-1201	EOD	CA/T C19B1 Boston	16" PPC Piles	256	65	44.0	Sand/Clay	SM/Till
207	98-109-1201	2 DR	CA/T C19B1 Boston	16" PPC Piles	256	65	-	Sand/Clay	SM/Till
208	98-109-Test 1	EOD	CA/T C19B1 Boston	16" PPC Piles	256	76.5	75.0	Sand/Clay	SM/Rock
209	98-109-Test 1	1 DR	CA/T C19B1 Boston	16" PPC Piles	256	76.5	-	Sand/Clay	SM/Rock
210	98-109-AC-4	EOD	CA/T C19B1 Boston	12" PPC Piles	144	57	52.0	Sand/Clay	SM/Till
211	98-109-AC-4	7 DR	CA/T C19B1 Boston	12" PPC Piles	144	57	-	Sand/Clay	SM/Till
212	98-109-IND-1	EOD	CA/T C19B1 Boston	12" PPC Piles	144	52	41.0	Sand/Clay	SM/Till
213	98-109-IND-1	1 DR	CA/T C19B1 Boston	12" PPC Piles	144	52	-	Sand/Clay	SM/Till
214	98-109-IND-2	EOD	CA/T C19B1 Boston	12" PPC Piles	144	52	46.0	Sand/Clay	SM/Till
215	98-109-IND-2	1 DR	CA/T C19B1 Boston	12" PPC Piles	144	52	-	Sand/Clay	SM/Till
216	98-109-IND-3	EOD	CA/T C19B1 Boston	12" PPC Piles	144	52	39.0	Sand/Clay	Clay/SM
217	98-109-IND-3	1 DR	CA/T C19B1 Boston	12" PPC Piles	144	52	-	Sand/Clay	Clay/SM
218	98-110-TP1 (9049)	EOD	CA/T C0702 Temp. Detour	HP 10x42 Test Piles	12.2	67.5	63.0	Fill/Clay	S. Clay/Till
219	98-110-TP1 (9049)	1 DR	CA/T C0702 Temp. Detour	HP 10x42 Test Piles	12.2	67.5	-	Fill/Clay	S. Clay/Till
220	98-110-TP2 (9032)	EOD	CA/T C0702 Temp. Detour	HP 10x42 Test Piles	12.2	67.5	65.0	Fill/Clay	S. Clay/Till
221	98-110-TP2 (9032)	1 DR	CA/T C0702 Temp. Detour	HP 10x42 Test Piles	12.2	67.5	-	Fill/Clay	S. Clay/Till
222	98-110-3	EOD	CA/T C0702 Toll Plaza	HP 14x73 Test Piles	21.4	137	121.5	Fill/Clay	Rock
223	98-110-3	1 DR	CA/T C0702 Toll Plaza	HP 14x73 Test Piles	21.4	137	-	Fill/Clay	Rock
224	98-110-7	EOD	CA/T C0702 Toll Plaza	HP 14x73 Test Piles	21.4	129.5	121.0	Fill/Clay	Rock
225	98-110-7	6 DR	CA/T C0702 Toll Plaza	HP 14x73 Test Piles	21.4	129.5	-	Fill/Clay	Rock

**Table A.5 (con't).** Relevant Information Pertaining to Database PD2000.

Ref. No.	Pile-Case Number	Refer. Time	Location	Pile Type	Pile Area	Length	Penetr	Soil Type	
						Below Gauges	Depth		
					(in <sup>2</sup> )	(ft)	(ft)	Side	Tip
226	98-112-LSTP2 (D10)	EOD	Lafayette Sch. Everett, MA	14" PPC Ind. Piles	196	85	65.0	Clay	Till
227	98-112-LSTP2 (D10)	8 DR	Lafayette Sch. Everett, MA	14" PPC Ind. Piles	196	85	-	Clay	Till
228	98-112-LSTP3 (G10)	EOD	Lafayette Sch. Everett, MA	14" PPC Ind. Piles	196	89	66.0	Clay	Till
229	98-112-LSTP3 (G10)	8 DR	Lafayette Sch. Everett, MA	14" PPC Ind. Piles	196	89	-	Clay	Till
230	98-112-LSTP4 (A10)	EOD	Lafayette Sch. Everett, MA	14" PPC Ind. Piles	196	85	67.0	Clay	Till
231	98-112-LSTP4 (A10)	8 DR	Lafayette Sch. Everett, MA	14" PPC Ind. Piles	196	85	-	Clay	Till
232	98-112-LSTP5 (A6)	EOD	Lafayette Sch. Everett, MA	14" PPC Ind. Piles	196	75	61.0	Clay	Till
233	98-112-LSTP5 (A6)	8 DR	Lafayette Sch. Everett, MA	14" PPC Ind. Piles	196	75	-	Clay	Till
234	98-112-LSTP6 (G1)	EOD	Lafayette Sch. Everett, MA	14" PPC Ind. Piles	196	71	46.0	Clay	Clay/Till
235	98-112-LSTP6 (G1)	7 DR	Lafayette Sch. Everett, MA	14" PPC Ind. Piles	196	71	-	Clay	Clay/Till
236	98-112-LSTP7 (C1)	EOD	Lafayette Sch. Everett, MA	14" PPC Ind. Piles	196	71	53.0	Clay	Till
237	98-112-LSTP7 (C1)	7 DR	Lafayette Sch. Everett, MA	14" PPC Ind. Piles	196	71	-	Clay	Till
238	98-112-LSTP9 (A1)	EOD	Lafayette Sch. Everett, MA	14" PPC Ind. Piles	196	68	52.0	Clay	Till
239	98-112-LSTP9 (A1)	7 DR	Lafayette Sch. Everett, MA	14" PPC Ind. Piles	196	68	-	Clay	Till
240	98-112-LSTP10 (G5.1)	EOD	Lafayette Sch. Everett, MA	14" PPC Ind. Piles	196	83	69.0	Clay	Till
241	98-112-LSTP10 (G5.1)	5 DR	Lafayette Sch. Everett, MA	14" PPC Ind. Piles	196	83	-	Clay	Till
242	98-113-152	EOD	CA/T C01A3 MBTA	14" PPC Fric. Test Piles	196	79	78.0	Sand/Clay	Clay
243	98-113-152	1 DR	CA/T C01A3 MBTA	14" PPC Fric. Test Piles	196	79	-	Sand/Clay	Clay
244	98-113-222	EOD	CA/T C01A3 MBTA	14" PPC Fric. Test Piles	196	61	60.0	Sand/Clay	Clay
245	98-113-222	4 DR	CA/T C01A3 MBTA	14" PPC Fric. Test Piles	196	61	-	Sand/Clay	Clay
246	98-113-306	EOD	CA/T C01A3 MBTA	14" PPC Fric. Test Piles	196	61	60.0	Sand/Clay	Clay
247	98-113-306	4 DR	CA/T C01A3 MBTA	14" PPC Fric. Test Piles	196	61	-	Sand/Clay	Clay
248	98-113-488	EOD	CA/T C01A3 MBTA	14" PPC Fric. Test Piles	196	78	76.0	Clay	Clay
249	98-113-488	3 DR	CA/T C01A3 MBTA	14" PPC Fric. Test Piles	196	78	-	Clay	Clay
250	98-118-NB11	EOD	Rt 146 (W-44-146) N. Abut.	HP 14x102	29.85	74	56.0	Fill/MH	SW

**Table A.5 (con't).** Relevant Information Pertaining to Database PD2000.

Ref. No.	Pile-Case Number	Refer. Time	Location	Pile Type	Pile Area	Length Below Gauges	Penetr Depth	Soil Type	
					(in <sup>2</sup> )	(ft)	(ft)	Side	Tip
251	98-118-NB11	1 DR	Rt 146 (W-44-146) N. Abut.	HP 14x102	29.85	74	-	Fill/MH	SW
252	98-118-SB26	EOD	Rt 146 (W-44-146) N. Abut.	HP 14x102	29.85	79.5	60.0	Fill/MH	SW
253	98-118-SB26	1 DR	Rt 146 (W-44-146) N. Abut.	HP 14x102	29.85		-	Fill/MH	SW
254	98-118-29	EOD	Rt 146 (W-44-146) S. Abut.	HP 14x102	29.85	57.5	54.0	Fill/MH	SW
255	98-118-29	1 DR	Rt 146 (W-44-146) S. Abut.	HP 14x102	29.85	57.5	-	Fill/MH	SW
256	98-118-44	EOD	Rt 146 (W-44-146) S. Abut.	HP 14x102	29.85	67.5	65.0	Fill/MH	SW
257	98-118-44	1 DR	Rt 146 (W-44-146) S. Abut.	HP 14x102	29.85	67.5	-	Fill/MH	SW
258	98-118-TP30	EOD	Rt 146 (W-44-147)	HP 14x102	29.85	57.2	43.0	SW	Rock
259	98-118-TP30	1 DR	Rt 146 (W-44-147)	HP 14x102	29.85	48	-	SW	Rock
260	98-118-TP31	EOD	Rt 146 (W-44-147)	HP 14x102	29.85	57.2	35.0	SW	Rock
261	98-118-TP31	1 DR	Rt 146 (W-44-147)	HP 14x102	29.85	40.5	-	SW	Rock
262	98-118-TP34	EOD	Rt 146 (W-44-147) N. Abut.	HP 14x102	29.85	57.2	53.0	SW	Rock
263	98-118-TP34	1 DR	Rt 146 (W-44-147) N. Abut.	HP 14x102	29.85	57.2	-	SW	Rock
264	98-118-TP35	EOD	Rt 146 (W-44-147) N. Abut.	HP 14x102	29.85	57.2	46.5	SW	SW/Rock
265	98-118-TP35	1 DR	Rt 146 (W-44-147) N. Abut.	HP 14x102	29.85	51	-	SW	SW/Rock
266	98-118-TP52	EOD	Rt 146 (W-44-147)	HP 14x102	29.85	57.2	28.0	SW	Rock
267	98-118-TP52	1 DR	Rt 146 (W-44-147)	HP 14x102	29.85	33	-	SW	Rock
268	98-118-TP62	EOD	Rt 146 (W-44-147) N. Abut.	HP 14x102	29.85	57.2	44.5	SW	SW/Rock
269	98-118-TP62	1 DR	Rt 146 (W-44-147) N. Abut.	HP 14x102	29.85	49	-	SW	SW/Rock
270	98-118-TP8	EOD	Rt 146 (W-44-147)	HP 14x102	29.85	57.2	30.0	SW	Rock
271	98-118-TP8	1 DR	Rt 146 (W-44-147)	HP 14x102	29.85	35	-	SW	Rock
272	98-118-TP8	EOD	Rt 146 (W-44-147) N. Abut.	HP 14x102	29.85	57.2	45.0	SW	SW/Rock
273	98-118-TP8	1 DR	Rt 146 (W-44-147) N. Abut.	HP 14x102	29.85	49	-	SW	SW/Rock
274	98-129-CHTP1	EOD	Chelsea St. Brdg Boston	HP 12x53	15.5	83	85.0	GW/Clay	Rock
275	98-129-CHTP1	1 DR	Chelsea St. Brdg Boston	HP 12x53	15.5	83	-	GW/Clay	Rock

**Table A.5 (con't).** Relevant Information Pertaining to Database PD2000.

Ref. No.	Pile-Case Number	Refer. Time	Location	Pile Type	Pile Area	Length	Penetr	Soil Type	
						Below Gauges	Depth		
					(in <sup>2</sup> )	(ft)	(ft)	Side	Tip
276	98-129-CHTP2	EOD	Chelsea St. Brdg Boston	HP 12x53	15.5	83	84.0	GW/Clay	Rock
277	98-129-CHTP2	1 DR	Chelsea St. Brdg Boston	HP 12x53	15.5	83	-	GW/Clay	Rock
278	98-131-Bent 1, #3	EOD	Dover/Sherborn Brdg	12.75"x 3/8" Pipe	14.6	60.5	42.5	SW/SM	SM
279	98-131-Bent 1, #3	4 DR	Dover/Sherborn Brdg	12.75"x 3/8" Pipe	14.6	60.5		SW/SM	SM
280	98-131-Bent 2, #1	EOD	Dover/Sherborn Brdg	12.75"x 3/8" Pipe	14.6	57	45.0	SW/SM	SM
281	98-131-Bent 2, #1	1 DR	Dover/Sherborn Brdg	12.75"x 3/8" Pipe	14.6	57		SW/SM	SM
282	98-138-17	EOD	Bridge St, N. Abut. Eastham	10.75" Pipe Piles	11.9	83.2	80.0	F. Sand	F. Sand
283	98-138-17	1 DR	Bridge St, N. Abut. Eastham	10.75" Pipe Piles	11.9	83.2	-	F. Sand	F. Sand
284	98-138-5	EOD	Bridge St, N. Abut. Eastham	10.75" Pipe Piles	11.9	89	81.5	F. Sand	F. Sand
285	98-138-5	1 DR	Bridge St, N. Abut. Eastham	10.75" Pipe Piles	11.9	89	-	F. Sand	F. Sand
286	98-138-9	EOD	Bridge St, S. Abut. Eastham	10.75" Pipe Piles	11.9	84.5	65.0	F. Sand	F. Sand
287	98-138-9	1 DR	Bridge St, S. Abut. Eastham	10.75" Pipe Piles	11.9	84.5	-	F. Sand	F. Sand
288	98-138-18	EOD	Bridge St, S. Abut. Eastham	10.75" Pipe Piles	11.9	82.5	64.0	F. Sand	F. Sand
289	98-138-18	1 DR	Bridge St, S. Abut. Eastham	10.75" Pipe Piles	11.9	82.5	-	F. Sand	F. Sand
290	99-112-1	EOD	Tage Inn Somerville, MA	12" PPC Piles	144	92	88.0	Clay/Till	Till/Rock
291	99-112-1	4 DR	Tage Inn Somerville, MA	12" PPC Piles	144	92	-	Clay/Till	Till/Rock
292	99-112-13	EOD	Tage Inn Somerville, MA	12" PPC Piles	144	82	62.3	Clay/Till	Till/Rock
293	99-112-13	4 DR	Tage Inn Somerville, MA	12" PPC Piles	144	82	-	Clay/Till	Till/Rock
294	99-112-159	EOD	Tage Inn Somerville, MA	12" PPC Piles	144	82	72.5	Clay/Till	Till/Rock
295	99-112-159	4 DR	Tage Inn Somerville, MA	12" PPC Piles	144	82	-	Clay/Till	Till/Rock
296	99-114-D-2 (2)	EOD	Harborlights Boston, MA	12.75" Pipe Piles	14.6	93	85.0	Clay/Till	Till/Rock
297	99-114-D-2 (2)	4 DR	Harborlights Boston, MA	12.75" Pipe Piles	14.6	93	-	Clay/Till	Till/Rock
298	99-114-B-2 (2)	EOD	Harborlights Boston, MA	12.75" Pipe Piles	14.6	93	84.0	Clay/Till	Till/Rock
299	99-114-B-2 (2)	4 DR	Harborlights Boston, MA	12.75" Pipe Piles	14.6	93	-	Clay/Till	Till/Rock
300	99-117-3	EOD	Channel Food Boston, MA	12.75" Pipe Piles	9.82	155	117.0	OL/Clay	SW

**Table A.5 (con't). Relevant Information Pertaining to Database PD2000.**

Ref. No.	Pile-Case Number	Refer. Time	Location	Pile Type	Pile Area	Length Below Gauges	Penetr Depth	Soil Type	
					(in <sup>2</sup> )	(ft)	(ft)	Side	Tip
301	99-117-3	EOD	Channel Food Boston, MA	12.75" Pipe Piles	9.82	155	-	OL/Clay	SW
302	99-117-3	3 DR	Channel Food Boston, MA	12.75" Pipe Piles	9.82	155	-	OL/Clay	SW
303	99-117-5	EOD	Channel Food Boston, MA	12.75" Pipe Piles	9.82	153	116.0	OL/Clay	SW
304	99-117-5	3 DR	Channel Food Boston, MA	12.75" Pipe Piles	9.82	153	-	OL/Clay	SW
305	99-123-100	EOD	Lewis School	14" PPC Ind. Piles	196	87	68.0	Clay/Till	Till/Rock
306	99-123-100	2 DR	Lewis School	14" PPC Ind. Piles	196	87	-	Clay/Till	Till/Rock
307	99-123-113	EOD	Lewis School	14" PPC Ind. Piles	196	80	53.0	Clay/Till	Till/Rock
308	99-123-113	3 DR	Lewis School	14" PPC Ind. Piles	196	80	-	Clay/Till	Till/Rock
309	99-123-172	EOD	Lewis School	14" PPC Ind. Piles	196	93	71.0	Clay/Till	Till/Rock
310	99-123-172	2 DR	Lewis School	14" PPC Ind. Piles	196	93	-	Clay/Till	Till/Rock
311	99-123-184	EOD	Lewis School	14" PPC Ind. Piles	196	73	59.0	Clay/Till	Till/Rock
312	99-123-184	3 DR	Lewis School	14" PPC Ind. Piles	196	73	-	Clay/Till	Till/Rock
313	99-123-227	EOD	Lewis School	14" PPC Ind. Piles	196	73	56.0	Clay/Till	Till/Rock
314	99-123-227	3 DR	Lewis School	14" PPC Ind. Piles	196	77	-	Clay/Till	Till/Rock
315	99-123-281	EOD	Lewis School	14" PPC Ind. Piles	196	96	82.0	Clay/Till	Till/Rock
316	99-123-281	2 DR	Lewis School	14" PPC Ind. Piles	196	96	-	Clay/Till	Till/Rock
317	99-123-293	EOD	Lewis School	14" PPC Ind. Piles	196	87	67.0	Clay/Till	Till/Rock
318	99-123-293	1 DR	Lewis School	14" PPC Ind. Piles	196	87	-	Clay/Till	Till/Rock
319	99-123-303	EOD	Lewis School	14" PPC Ind. Piles	196	80	67.0	Clay/Till	Till/Rock
320	99-123-303	EOD	Lewis School	14" PPC Ind. Piles	196	80	68.0	Clay/Till	Till/Rock
321	99-123-303	1 DR	Lewis School	14" PPC Ind. Piles	196	80	-	Clay/Till	Till/Rock
322	99-124-N1	EOD	Lyman St Brdg Waltham	HP 12x74	21.8	77.5	60.0	Sand	Sand
323	99-124-N1	Redrive	Lyman St Brdg Waltham	HP 12x74	21.8	77.5	79.0	Sand	Sand
324	99-124-N1	Redrive	Lyman St Brdg Waltham	HP 12x74	21.8	77.5	79.0	Sand	Sand
325	99-124-N4	EOD	Lyman St Brdg Waltham	HP 12x74	21.8	62.5	64.0	Sand	Sand

**Table A.5 (con't).** Relevant Information Pertaining to Database PD2000.

Ref. No.	Pile-Case Number	Refer. Time	Location	Pile Type	Pile Area	Length Below Gauges	Penetr Depth	Soil Type	
					(in <sup>2</sup> )	(ft)	(ft)	Side	Tip
326	99-124-N4	6 DR	Lyman St Brdg Waltham	HP 12x74	21.8	62.5	64.5	Sand	Sand
327	99-126-TP1	EOD	Marina Bay Quincy, MA BA-B9	12.75"x 0.25" Pipe	9.8	57	61.0	Clay/Till	Till/Rock
328	99-126-TP1	3 DR	Marina Bay Quincy, MA BA-B9	12.75"x 0.25" Pipe	9.8	57	-	Clay/Till	Till/Rock
329	99-126-TP2	EOD	Marina Bay Quincy, MA AJ-A2	12.75"x 0.25" Pipe	9.8	57	60.0	Clay/Till	Till/Rock
330	99-126-TP2	3 DR	Marina Bay Quincy, MA AJ-A2	12.75"x 0.25" Pipe	9.8	57	-	Clay/Till	Till/Rock
331	97-110-P105-S93	EOD	Deer Is. Batt C	PPC 14	196	51	35.5	Clay (BB)	Till/Rock
332	97-110-P105-S93	3 DR	Deer Is. Batt C	PPC 14	196	51	35.5	Clay (BB)	Till/Rock
333	97-110-P16-S93	EOD	Deer Is. Batt C	PPC 14	196	51	28.0	Clay (BB)	Till/Rock
334	97-110-P16-S93	6 DR	Deer Is. Batt C	PPC 14	196	32	35.5	Clay (BB)	Till/Rock
335	97-110-P332-S7	EOD	Deer Is. Batt C	PPC 14	196	51	48.5	Clay (BB)	Till/Rock
336	97-110-P332-S7	3 DR	Deer Is. Batt C	PPC 14	196	51	35.5	Clay (BB)	Till/Rock
337	97-110-P566-S6	EOD	Deer Is. Batt C	PPC 14	196	86	61.5	Clay (BB)	Till/Rock
338	97-110-P566-S6	3 DR	Deer Is. Batt C	PPC 14	196	86	61.5	Clay (BB)	Till/Rock
339	97-110-P56-S7	EOD	Deer Is. Batt C	PPC 14	196	86	70.0	Clay (BB)	Till/Rock
340	97-110-P56-S7	3 DR	Deer Is. Batt C	PPC 14	196	86	70.0	Clay (BB)	Till/Rock
341	97-110-P86-S7	EOD	Deer Is. Batt C	PPC 14	196	86	64.5	Clay (BB)	Till/Rock
342	97-110-P86-S7	3 DR	Deer Is. Batt C	PPC 14	196	86	70.0	Clay (BB)	Till/Rock
343	97-110-P212-S7	EOD	Deer Is. Batt C	PPC 14	196	86	70.0	Clay (BB)	Till/Rock
344	97-110-P212-S7	3 DR	Deer Is. Batt C	PPC 14	196	86	70.0	Clay (BB)	Till/Rock
345	97-110-P350-S6	EOD	Deer Is. Batt C	PPC 14	196	81	56.5	Clay (BB)	Till/Rock
346	97-110-P350-S6	2 DR	Deer Is. Batt C	PPC 14	196	81	56.5	Clay (BB)	Till/Rock
347	97-110-P499-S8	EOD	Deer Is. Batt C	PPC 14	196	76	50.5	Clay (BB)	Till/Rock
348	97-110-P499-S8	2 DR	Deer Is. Batt C	PPC 14	196	76	50.5	Clay (BB)	Till/Rock
349	97-110-P30-S8	EOD	Deer Is. Batt C	PPC 14	196	86	64.5	Clay (BB)	Till/Rock
350	97-110-P30-S8	2 DR	Deer Is. Batt C	PPC 14	196	86	64.5	Clay (BB)	Till/Rock



**Table A.5 (con't). Relevant Information Pertaining to Database PD2000.**

Ref. No.	Pile-Case Number	Refer. Time	Location	Pile Type	Pile Area	Length Below Gauges	Penetr Depth	Soil Type	
					(in <sup>2</sup> )	(ft)	(ft)	Side	Tip
351	97-110-P320-S7	EOD	Deer Is. Batt C	PPC 14	196	86	69.5	Clay (BB)	Till/Rock
352	97-110-P320-S7	2 DR	Deer Is. Batt C	PPC 14	196	86	69.5	Clay (BB)	Till/Rock
353	97-110-P333-S6	EOD	Deer Is. Batt C	PPC 14	196	51	27.5	Clay (BB)	Till/Rock
354	97-110-P333-S6	5 DR	Deer Is. Batt C	PPC 14	196	34	27.5	Clay (BB)	Till/Rock
355	97-110-P553-S6	EOD	Deer Is. Batt C	PPC 14	196	66	49.0	Clay (BB)	Till/Rock
356	97-110-P553-S6	5 DR	Deer Is. Batt C	PPC 14	196	66	49.0	Clay (BB)	Till/Rock
357	97-110-P341-S6	EOD	Deer Is. Batt C	PPC 14	196	71	43.5	Clay (BB)	Till/Rock
358	97-110-P341-S6	5 DR	Deer Is. Batt C	PPC 14	196	71	43.5	Clay (BB)	Till/Rock
359	97-110-P21-S8	EOD	Deer Is. Batt C	PPC 14	196	81	62.5	Clay (BB)	Till/Rock
360	97-110-P21-S8	5 DR	Deer Is. Batt C	PPC 14	196	81	62.5	Clay (BB)	Till/Rock
361	97-110-P168-S8	EOD	Deer Is. Batt C	PPC 14	196	86	70.0	Clay (BB)	Till/Rock
362	97-110-P168-S8	5 DR	Deer Is. Batt C	PPC 14	196	86	70.0	Clay (BB)	Till/Rock
363	97-110-P382-S8	EOD	Deer Is. Batt C	PPC 14	196	76	60.5	Clay (BB)	Till/Rock
364	97-110-P382-S8	5 DR	Deer Is. Batt C	PPC 14	196	76	60.5	Clay (BB)	Till/Rock
365	97-110-P12-S8	EOD	Deer Is. Batt C	PPC 14	196	61	46.5	Clay (BB)	Till/Rock
366	97-110-P12-S8	5 DR	Deer Is. Batt C	PPC 14	196	61	46.5	Clay (BB)	Till/Rock
367	97-110-P6-S8	EOD	Deer Is. Batt C	PPC 14	196	51	39.5	Clay (BB)	Till/Rock
368	97-110-P6-S8	4 DR	Deer Is. Batt C	PPC 14	196	44	39.5	Clay (BB)	Till/Rock
369	97-110-P2-S6	EOD	Deer Is. Batt C	PPC 14	196	51	22.0	Clay (BB)	Till/Rock
370	97-110-P2-S6	3 DR	Deer Is. Batt C	PPC 14	196	51	22.0	Clay (BB)	Till/Rock
371	97-110-P492-S8	EOD	Deer Is. Batt C	PPC 14	196	71	60.5	Clay (BB)	Till/Rock
372	97-110-P492-S8	3 DR	Deer Is. Batt C	PPC 14	196	71	60.5	Clay (BB)	Till/Rock
373	97-110-P159-S8	EOD	Deer Is. Batt C	PPC 14	196	81	58.5	Clay (BB)	Till/Rock
374	97-110-P159-S8	3 DR	Deer Is. Batt C	PPC 14	196	81	58.5	Clay (BB)	Till/Rock
375	97-110-P485-S8	EOD	Deer Is. Batt C	PPC 14	196	81	47.5	Clay (BB)	Till/Rock

**Table A.5 (con't).** Relevant Information Pertaining to Database PD2000.

Ref. No.	Pile-Case Number	Refer. Time	Location	Pile Type	Pile Area	Length Below Gauges	Penetr Depth	Soil Type	
					(in <sup>2</sup> )	(ft)	(ft)	Side	Tip
376	97-110-P485-S8	3 DR	Deer Is. Batt C	PPC 14	196	81	47.5	Clay (BB)	Till/Rock
377	97-110-P522-S8	EOD	Deer Is. Batt C	PPC 14	196	75	52.5	Clay (BB)	Till/Rock
378	97-110-P522-S8	3 DR	Deer Is. Batt C	PPC 14	196	75	52.5	Clay (BB)	Till/Rock
379	PD-TP4	EOD		CEP 12.75	9.82		57.0	Sand/Silt	Sand
380	PD-TP4	BOR		CEP 12.75	9.82		57.0	Sand/Silt	Sand
381	PD-PN3	EOD		CEP 12x0.6	14.6		60.0	Silt/Grav	Sand/Silt
382	PD-PN3	BOR		CEP 12x0.6	14.6		60.0	Silt/Grav	Sand/Silt
383	PD-PN317	EOD		CEP 14x0.37	16.05		125.0	Silt	Sand/Grav
384	PD-PN317	BOR		CEP 14x0.37	16.05		124.0	Silt	Sand/Grav
385	PD-PN12	EOD		CEP 16	16.8		77.0	Sand	Sand
386	PD-PN12	BOR		CEP 16	16.8		77.0	Sand	Sand
387	PD-PN7	EOD		CEPIPE24	54.8		60.3	Clay/Sand	Clay/Sand
388	PD-PN7	BOR		CEPIPE24	54.8		60.3	Clay/Silt	Clay/Silt
389	PD-T1	EOD		HP 10x42	12.4		72.0	Clay/Silt	Clay
390	PD-T1	BOR		HP 10x42	12.4		72.0	Clay/Silt	Clay
391	PD-SHD1	EOD		HP 12x53	15.5		82.0	Clay/Sand	Limestone
392	PD-SHD1	BOR		HP 12x53	15.5		82.0	Clay/Sand	Limestone
393	PD-R1	EOD		HP 14x73	21.4		71.0	Clay/Silt	Clay
394	PD-R1	BOR		HP 14x73	21.4		71.0	Clay/Silt	Clay
395	PD-R10	EOD		HP 14x73	21.4		72.0	Clay/Silt	Clay
396	PD-R10	BOR		HP 14x73	21.4		72.0	Clay/Silt	Clay
397	PD-TP4	EOD		HP 14x73	21.4		27.0	Clay	Clay
398	PD-TP4	BOR		HP 14x73	21.4		27.0	Clay	Clay
399	PD-TP2	EOD		HP14x73	21.4		42.1	Clay/Silt	Clay/Silt
400	PD-TP2	BOR		HP14x73	21.4		42.1	Clay/Silt	Clay/Silt

**Table A.5 (con't). Relevant Information Pertaining to Database PD2000.**

Ref. No.	Pile-Case Number	Refer. Time	Location	Pile Type	Pile Area  (in <sup>2</sup> )	Length Below Gauges (ft)	Penetr Depth (ft)	Soil Type	
								Side	Tip
401	PD-PN13	EOD		PSC 12	144		30.0	Clay/Silt	Sand/Silt
402	PD-PN13	BOR		PSC 12	144		30.0	Clay/Silt	Sand/Silt
403	PD-PN6	EOD		MONO 11	8.14		38.0	Sand	Silt/Clay
404	PD-PN6	RES		MONO 11	8.14		38.0	Sand	Clay/Silt
405	PD-TP23	EOD		MONO14 NU	8.14		42.0	Sand	Clay/Silt
406	PD-TP23	BOR		MONO14 NU	8.14		42.0	Sand	Clay/Silt
407	PD-PN4	EOD		OEP 12x0.6	14.6		60.0	Silt/Grav	Sand/Silt
408	PD-PN4	BOR		OEP 12x0.6	14.6		60.0	Silt/Grav	Sand/Silt
409	PD-T4	EOD		PIPE 12.75	19.2		66.0	Clay/Silt	Clay
410	PD-T4	BOR		PIPE 12.75	19.2		66.0	Clay/Silt	Clay
411	PD-J31	EOD		PIPE 14"	31.2		91.0	Clay/Silt	Rock
412	PD-J31	BOR		PIPE 14"	31.2		91.0	Clay/Silt	Rock
413	PD-TP1799	EOD		PSC	96.5		70.0	Sand/Silt	Clay
414	PD-TP1799	RES		PSC	96.5		73.0	Sand/Silt	Clay
415	PD-TP1799	X		PSC	96.5		70.0	Silt	Sand
416	PD-T2	EOD		PSC 12	144		62.0	Clay/Silt	Clay
417	PD-T2	BOR		PSC 12	144		62.0	Clay/Silt	Clay
418	PD-TP6	EOD		PSC 12	144		53.0	Sand/Silt	Clay/Silt
419	PD-TP6	BOR		PSC 12	144		53.0	Sand/Silt	Clay/Silt
420	PD-PNH20	EOD		PSC 12	144		58.0	Clay/Sand	Clay/Sand
421	PD-PNH20	BOR		PSC 12	144		58.0	Clay/Sand	Clay/Sand
422	PD-T3	EOD		PSC 14	196		62.0	Clay/Silt	Clay
423	PD-T3	BOR		PSC 14	196		62.0	Clay/Silt	Clay
424	PD-PN110	EOD		PSC 16	256		35.0	Sand/Clay	Clay/Silt
425	PD-PN110	BOR		PSC 16	256		35.0	Sand/Clay	Clay/Silt

**Table A.5 (con't).** Relevant Information Pertaining to Database PD2000.

Ref. No.	Pile-Case Number	Refer. Time	Location	Pile Type	Pile Area  (in <sup>2</sup> )	Length Below Gauges (ft)	Penetr Depth (ft)	Soil Type	
								Side	Tip
426	PD-PN111	EOD		PSC 16	256		35.0	Sand/Clay	Clay/Silt
427	PD-PN111	BOR		PSC 16	256		35.0	Sand/Clay	Clay/Silt
428	PD-TP3	EOD		PSC 18	324		77.0	Sand	Sandstone
429	PD-TP3	BOR		PSC 18	324		77.0	Sand	Sandstone
430	PD-TP21	EOD		PSC 36	487		63.0	Sand/Silt	Sand
431	PD-TP21	BOR		PSC 36	487		63.0	Sand/Silt	Sand
432	PD-TP11	EOD		PSC 36	487		47.0	Silt/Grav	Sand/Silt
433	PD-TP11	BOR		PSC 36	487		47.0	Sand/Silt	Sand
434	PD-TP11	BOR		PSC 36	487		47.0	Silt/Grav	Sand/Silt
435	PD-151	EOD		PSC12	144		42.0	Clay/Sand	Sand
436	PD-151	BOR		PSC12	144		42.0	Clay/Silt	Sand
437	PD-P3T1	EOD		PIPE 12.75	14.58		75.0	Sand/Silt	Rock
438	PD-P3T1	BOR		PIPE 12.75	14.58		75.0	Sand/Silt	Rock
439	PD-TP1	EOD		HP 14x73	21.4		60.3	Sand Clay	Sand Clay
440	PD-TP1	BOR		HP 14x73	21.4		60.3	Sand Clay	Sand Clay
441	PD-PN126	EOD		PSC 14	196		70.0	Clay	G. Till
442	PD-PN126	BOR		PSC 14	196		70.0	Clay	G. Till
443	PD-TP26	EOD		PSC 12	144		62.0	Sand/Silt	Sand/Silt
444	PD-TP26	BOR		PSC 12	144		64.0	Sand/Silt	Sand/Silt
445	PD-TP114	EOD		PSC 12	144		64.0	Sand/Silt	Sand/Silt
446	PD-TP114	BOR		PSC 12	144		64.0	Sand/Silt	Sand/Silt
447	PD-PN177	EOD		PSC 14	196		70.0	Clay	G. Till
448	PD-PN177	BOR		PSC 14	196		72.0	Clay	G. Till
449	PD-TP1	EOD		CEPIPE 1	12.4		72.3	Sand	Sand/Till
450	PD-TP1	BOR		E\CEPIPE	12.4		72.3	Sand	Sand/Till

**Table A.5 (con't). Relevant Information Pertaining to Database PD2000.**

Ref. No.	Pile-Case Number	Refer. Time	Location	Pile Type	Pile Area  (in <sup>2</sup> )	Length Below Gauges (ft)	Penetr Depth (ft)	Soil Type	
								Side	Tip
451	PD-D418	EOD		OEP 9.6	16		45.0	Clay/Shale	DOLOM
452	PD-D418	BOR		OEP 9.6	16		45.0	Clay/Shale	DOLOM
453	PD-PN2	EOD		MONO	8.14		43.0	Sand	Silt
454	PD-PN2	RES		MONO 12	8.96		43.0	Sand	Sand
455	PD-PN26	EOD		PSC 12	144		32.0	Clay/Silt	Sand/Silt
456	PD-PN26	BOR		PSC 12	144		32.0	Clay/Silt	Sand/Silt
457	PD-PN49	EOD		PSC 12	144		30.0	Clay/Silt	Sand/Silt
458	PD-PN49	BOR		PSC 12	144		30.0	Clay/Silt	Sand/Silt
459	PD-PN6	EOD		PSC	900		134.0	NA	NA
460	PD-PN6	RES		PSC 14	196		107.0	Sand/Silt	Sand/Silt
461	PD-TP1	EOD		PSC 14	196		77.0	Sand	Sandstone
462	PD-TP1	BOR		PSC 14	196		77.0	Sand	Sandstone
463	PD-TP2	EOD		PSC 12	144		57.0	Sand/Silt	Rock
464	PD-TP2	BOR		PSC 12	144		64.0	Sand/Silt	Sand/Silt
465	PD-TP8	EOD		PSC 14	196		77.0	Sand	Sandstone
466	PD-TP8	BOR		PSC 14	196		77.0	Sand	Sandstone
467	PD-PN7E3	EOD		PSC 30	900		125.0	NA	NA
468	PD-PN7E	BOR		PSC 30	900		116.0	Sand	Sandstone

**Table A.5 (con't). Relevant Information Pertaining to Database PD2000.**

Ref. No.	Pile-Case Number	Hammer Type	Rated Hammer Energy (kip-ft)	Delivered Energy (max) (EMX) (kip-ft)	Blow Count (BPI)	WS "C" (ft/s)	EM "E" (KSI)	Impedence EA/C "Z" (kips/ft/s)	Vimp VMX (ft/s)	Fimp FMX (kips)	VEA/C F	Dmax DMX (in)	2L/C (ms)
1	96-104-1W-D	HPSI 1000	35	28.4	5.0	16810	30000	38.91	15.4	605	0.990	1.13	16.30
2	96-104-1W-D	HPSI 1000	35	26.7	10.0	16810	30000	38.91	14.9	585	0.991	1.00	16.30
3	96-104-1W-I	HPSI 1000	35	30.8	3.0	16810	30000	38.91	16.7	668	0.973	1.21	16.30
4	96-104-1W-I	HPSI 1000	35	31.7	2.5	16810	30000	38.91	19.2	719	1.039	1.15	14.99
5	96-104-2E-K	HPSI 1000	35	30.9	8.0	16810	30000	38.91	17.5	686	0.992	1.06	15.82
6	96-104-2E-K	HPSI 1000	35	27.7	10.7	16810	30000	38.91	16.5	632	1.016	0.96	15.82
7	96-104-2W-R	HPSI 1000	35	25.7	4.0	16810	30000	38.91	15.4	597	1.004	1.11	16.78
8	96-104-2W-R	HPSI 1000	35	28.9	4.5	16810	30000	38.91	16.6	656	0.984	1.18	16.89
9	96-104-3E-A	HPSI 1000	35	27.7	6.0	16810	30000	38.91	16.5	657	0.977	1.15	13.27
10	96-104-3E-A	HPSI 1000	35	25.8	5.0	16810	30000	38.91	16	641	0.971	1.03	13.27
11	96-104-3W-G	HPSI 1000	35	29.5	4.0	16810	30000	38.91	17.4	653	1.037	1.05	13.92
12	96-104-3W-G	HPSI 1000	35	25.9	8.0	16810	30000	38.91	14.7	587	0.974	0.86	12.14
13	96-104-5W-F	HPSI 1000	35	28.4	4.0	16810	30000	38.91	17.1	659	1.010	1.06	13.33
14	96-104-5W-F	HPSI 1000	35	29.6	6.7	16810	30000	38.91	17.2	647	1.034	1.04	13.33
15	96-104-NA-4	HPSI 1000	35	28.5	4.0	16810	30000	38.91	17.5	651	1.046	0.98	13.33
16	96-104-NA-4	HPSI 1000	35	30.3	12.0	16810	30000	38.91	17.5	639	1.065	0.94	13.33
17	96-104-NA-53	HPSI 1000	35	29.2	4.0	16810	30000	38.91	17	630	1.050	1.09	13.92
18	96-104-NA-53	HPSI 1000	35	26.8	5.3	16810	30000	38.91	16.7	615	1.056	1.00	13.92
19	96-104-TP1	HPSI 1000	50	13.7	>20	16810	30000	26.06	13.6	535	0.662	0.66	6.84
20	96-104-TP1	HPSI 1000	50	14.5	>20	16810	30000	26.06	12	509	0.614	0.60	6.84
21	96-104-TP4	HPSI 1000	50	30.5	3.0	16810	30000	38.91					0.00
22	96-104-TP4	HPSI 1000	50	29.3	8.0	16810	30000	38.91	17.6	661	1.036	0.95	13.86
23	96-104-TP4	HPSI 1000	50	27.4	10.0	16810	30000	38.91	17	643	1.029	0.94	13.86
24	96-104-W1-V26	HPSI 1000	40	13.6	7.2	16810	30000	26.06	12.3	389	0.824	0.62	4.05
25	96-104-W1-V26	HPSI 1000	40	15.2	7.0	16810	30000	26.06	13.5	433	0.812	0.54	2.74

**Table A.5 (con't). Relevant Information Pertaining to Database PD2000.**

Ref. No.	File-Case Number	Hammer Type	Rated Hammer Energy (kip-ft)	Delivered Energy (max) (EMX) (kip-ft)	Blow Count (BPI)	WS "C" (ft/s)	EM "E" (KSI)	Impedence EA/C "Z" (kips/ft/s)	Vimp VMX (ft/s)	Fimp FMX (kips)	VEA/C F	Dmax DMX (in)	2L/C (ms)
26	96-104-W2-V13	HPSI 1000	40	17.7	6.4	16810	30000	26.06	14.3	533	0.699	0.66	8.74
27	96-104-W2-V13	HPSI 1000	40	16.1	9.0	16810	30000	26.06	12.7	429	0.771	0.82	8.74
28	96-104-W4-B36	HPSI 1000	30	17.5	6.0	16810	30000	26.06	15.1	442	0.890	0.81	16.24
29	96-104-W4-B36	HPSI 1000	30	17.7	20.0	16810	30000	26.06	14.9	449	0.865	0.78	16.24
30	96-104-W4-V24	HPSI 1000	30	22.7	5.7	16810	30000	26.06	15.8	495	0.832	0.96	15.70
31	96-104-W4-V24	HPSI 1000	30	23.8	10.0	16810	30000	26.06	16.9	589	0.748	0.78	15.70
32	96-104-W5-3	HPSI 1000	30	27.3	3.0	16810	30000	26.06	16.3	459	0.925	1.21	14.04
33	96-104-W5-3	HPSI 1000	30	26.2	13.3	16810	30000	26.06	15.6	443	0.918	1.08	14.04
34	96-104-W5-8	HPSI 1000	30	27.2	5.0	16810	30000	26.06	17.9	470	0.992	1.44	17.61
35	96-104-W5-8	HPSI 1000	30	24.1	20.0	16810	30000	26.06	16.4	435	0.982	1.12	13.92
36	96-104-W5-V27	HPSI 1000	30	19.4	5.0	16810	30000	26.06	14.9	473	0.821	0.84	14.93
37	96-104-W5-V27	HPSI 1000	30	18.4	32.0	16810	30000	26.06	15.2	449	0.882	0.85	14.93
38	96-104-W5-V28	HPSI 1000	30	21.2	5.2	16810	30000	26.06	15.1	478	0.823	0.92	14.69
39	96-104-W5-V28	HPSI 1000	30	21.5	36.0	16810	30000	26.06	14.7	436	0.878	0.96	14.69
40	96-115-3	ICE 640	40	13.8	14.7	16810	30000	38.19	9.2	404	0.870	0.69	16.30
41	96-115-3	ICE 640	40	16.1	14.5	16810	30000	38.19	11.9	501	0.907	0.74	16.30
42	96-115-7	ICE 640	40	13.8	12.3	16810	30000	38.19	8.5	425	0.764	0.63	15.41
43	96-115-7	ICE 640	40	20.3	20.0	16810	30000	38.19	11.8	514	0.877	0.74	15.41
44	96-115-106	HPSI 2000	80	29	11.0	13000	5467	107.66		670	0.000	0.97	26.77
45	96-115-106	HPSI 2000	80	36	52.0	13000	5467	107.66		780	0.000	0.92	26.77
46	96-115-109	HPSI 2000	80	40	8.0	13000	5467	107.66		820	0.000	1.08	26.77
47	96-115-109	HPSI 2000	80	46	56.0	13000	5467	107.66		910	0.000	0.97	26.77
48	96-115-117	HPSI 2000	80	33	12.0	13000	5467	107.66	6.8	770	0.951	0.76	13.54
49	96-115-117	HPSI 2000	80	36	20<1"	13000	5467	107.66	6.8	710	1.031	0.77	13.54
50	96-115-157	HPSI 2000	80	31	15.2	13000	5467	107.66	6.1	660	0.995	0.78	12.85

**Table A.5 (con't). Relevant Information Pertaining to Database PD2000.**

Ref. No.	Pile-Case Number	Hammer Type	Rated Hammer Energy (kip-ft)	Delivered Energy (max) (EMX) (kip-ft)	Blow Count (BPI)	WS "C" (ft/s)	EM "E" (KSI)	Impedence EA/C "Z" (kips/ft/s)	Vimp VMX (ft/s)	Fimp FMX (kips)	VEA/C F	Dmax DMX (in)	2L/C (ms)
51	96-115-157	HPSI 2000	80	55	14<1"	13000	5467	107.66	10.6	1120	1.019	0.89	12.85
52	96-115-158	HPSI 2000	80	31	11.5	13000	5467	107.66	6.2	660	1.011	0.77	12.85
53	96-115-158	HPSI 2000	80	38	17<1"	13000	5467	107.66	7.8	820	1.024	0.75	12.85
54	96-115-163	HPSI 2000	80	26	18.0	13000	5467	107.66	6.3	670	1.012	0.81	12.62
55	96-115-163	HPSI 2000	80	41	16 per 4 in	13000	5467	107.66	8.9	880	1.089	0.85	12.62
56	96-115-182	HPSI 2000	80	36	14.5	13000	5467	107.66	7.2	770	1.007	0.76	12.77
57	96-115-182	HPSI 2000	80	34	20<1"	13000	5467	107.66	6.4	770	0.895	0.69	12.46
58	96-115-258	HPSI 2000	80	47	13.7	13000	5467	107.66			#VALUE!		0.00
59	96-115-258	HPSI 2000	80	46	20<1"	13000	5467	107.66	7.4	910	0.875	0.78	11.08
60	96-115-279	HPSI 2000	80	32	10.0	13000	5467	107.66	6.5	720	0.972	1.01	12.00
61	96-115-279	HPSI 2000	80	46	10.0	13000	5467	107.66	8.2	860	1.027	0.96	12.00
62	96-115-279	HPSI 2000	80	35	15.0	13000	5467	107.66			#VALUE!		0.00
63	96-115-357	HPSI 2000	80	39	18.0	13000	5467	107.66	6.9	820	0.906	0.88	12.62
64	96-115-357	HPSI 2000	80	42	40 per 4 in	13000	5467	107.66	7.7	910	0.911	0.82	12.62
65	96-115-375	HPSI 2000	80	37	39.0	13000	5467	107.66	6	720	0.897	0.92	12.46
66	96-115-375	HPSI 2000	80	40	20.0	13000	5467	107.66	7.6	860	0.951	0.80	9.08
67	96-115-414	HPSI 2000	80	34	20.0	13000	5467	107.66	6.2	710	0.940	0.87	12.46
68	96-115-414	HPSI 2000	80	35	15 < 1"	13000	5467	107.66	6	760	0.850	0.78	12.46
69	96-115-806	HPSI 2000	80	37	10.7	13000	5467	107.66		750	0.000	0.93	24.46
70	96-115-806	HPSI 2000	80	37	80.0	13000	5467	107.66	6.6	800	0.888	0.88	24.46
71	96-115-816	HPSI 2000	80	36	12.3	13000	5467	107.66		860	0.000	0.94	24.46
72	96-115-816	HPSI 2000	80	45	16.7	13000	5467	107.66	7.3	940	0.836	0.94	24.46
73	96-115-910	HPSI 2000	80	30	10.0	13000	5467	107.66		720	0.000	0.87	20.15
74	96-115-910	HPSI 2000	80	35	20.0	13000	5467	107.66		680	0.000	0.90	19.05
75	96-115-916	HPSI 2000	80	32	6.2	13000	5467	107.66		770	0.000	0.92	21.69



**Table A.5 (con't). Relevant Information Pertaining to Database PD2000.**

Ref. No.	Pile-Case Number	Hammer Type	Rated Hammer Energy (kip-ft)	Delivered Energy (max) (EMX) (kip-ft)	Blow Count (BPI)	WS "C" (ft/s)	EM "E" (KSI)	Impedence EA/C "Z" (kips/ft/s)	Vimp VMX (ft/s)	Fimp FMX (kips)	VEA/C F	Dmax DMX (in)	2L/C (ms)
76	96-115-916	HPSI 2000	80	30	13.5	13000	5467	107.66		660	0.000	0.85	18.94
77	96-115-919	HPSI 2000	80	36	9.2	13000	5467	107.66		940	0.000	0.82	20.15
78	96-115-919	HPSI 2000	80	33	9.0	13000	5467	107.66		660	0.000	0.88	18.68
79	96-115-926	HPSI 2000	80	36	9.3	13000	5467	107.66		820	0.000	0.93	20.15
80	96-115-926	HPSI 2000	80	33	8.3	13000	5467	107.66		690	0.000	0.89	18.80
81	96-115-937	HPSI 2000	80	39	13.3	13000	5467	107.66		850	0.000	0.94	20.15
82	96-115-937	HPSI 2000	80	33	16.8	13000	5467	107.66		640	0.000	0.93	19.35
83	96-115-940	HPSI 2000	80	34	9.7	13000	5467	107.66		770	0.000	1.00	21.69
84	96-115-940	HPSI 2000	80	29	16.7	13000	5467	107.66		620	0.000	0.83	19.25
85	96-115-3111	HPSI 2000	80	41	10.5	13000	5467	107.66	6.4	860	0.801	1.12	9.23
86	96-115-3111	HPSI 2000	80	34	9.5	13000	5467	107.66	6	980	0.659	0.58	9.23
87	96-115-3115	HPSI 2000	80	45	7.7	13000	5467	107.66	6.6	1010	0.704	1.23	9.23
88	96-115-3115	HPSI 2000	80	49	6.5	13000	5467	107.66	8.3	1070	0.835	0.85	8.54
89	96-115-3117	HPSI 2000	80	41	8.3	13000	5467	107.66	6.1	870	0.755	1.29	9.23
90	96-115-3117	HPSI 2000	80	53	13.0	13000	5467	107.66	8	1180	0.730	0.84	9.23
91	96-115-3118	HPSI 2000	80	35	12.0	13000	5467	107.66	4.8	840	0.615	1.11	9.23
92	96-115-3118	HPSI 2000	80	40	8.5	13000	5467	107.66	6.7	1150	0.627	0.63	9.23
93	96-115-3181	HPSI 2000	80	32	20.0	13000	5467	107.66	5.4	620	0.938	0.84	12.92
94	96-115-3181	HPSI 2000	80	36	8.0	13000	5467	107.66	6.7	790	0.913	0.71	11.85
95	96-115-3220	HPSI 2000	80	26	10.0	13000	5467	107.66	5.9	640	0.992	0.84	11.54
96	96-115-3220	HPSI 2000	80	39	14.0	13000	5467	107.66	7	760	0.992	0.86	11.54
97	96-115-3259	HPSI 2000	80	23	13.0	13000	5467	107.66	4.6	570	0.869	0.78	12.62
98	96-115-3259	HPSI 2000	80	40	10.0	13000	5467	107.66	7.8	890	0.944	0.79	12.62
99	96-116-9	ICE 60S	60	27	10.0	16810	30000	37.83	14.6	600	0.921	0.90	12.61
100	96-116-9	ICE 60S	60	35.1	14.5	16810	30000	37.83	16.1	681	0.894	0.89	12.61

**Table A.5 (con't).** Relevant Information Pertaining to Database PD2000.

Ref. No.	Pile-Case Number	Hammer Type	Rated Hammer Energy (kip-ft)	Delivered Energy (max) (EMX) (kip-ft)	Blow Count (BPI)	WS "C" (ft/s)	EM "E" (KSI)	Impedence EA/C "Z" (kips/ft/s)	Vimp VMX (ft/s)	Fimp FMX (kips)	VEA/C F	Dmax DMX (in)	2L/C (ms)
101	96-116-12	ICE 60S	60	24.2	9.0	16810	30000	37.83	15.6	606	0.974	0.93	12.61
102	96-116-12	ICE 60S	60	33.6	13<1"	16810	30000	37.83	19	791	0.909	1.01	12.61
103	96-117-A4	ICE 42S	42	15.7	4.8	16810	30000	26.06	14.5	400	0.945	0.74	3.81
104	96-117-A4	ICE 42S	42	17.1	6.7	16810	30000	26.06	15.5	448	0.901	0.73	3.81
105	97-102-TP2	ICE 640	40	18.6	10.0	12670	5193	80.33	6.2	541	0.921	0.68	17.60
106	97-102-TP2	ICE 640	40	21.5	15.0	12670	5193	80.33	8.5	773	0.883	0.44	17.60
107	97-104-TP1 (#7)	ICE 42S	42	13.2	3.5	16810	30000	27.66	14.1	413	0.944	0.79	20.58
108	97-104-TP1 (#7)	ICE 42S	42	13.5	5.0	16810	30000	27.66	13.5	387	0.965	0.72	19.87
109	97-104-TP2 (#18)	ICE 42S	42	12.8	0.5	16810	30000	27.66	13.9	334	1.151	1.87	12.02
110	97-104-TP2 (#18)	ICE 42S	42	12.5	1.3	16810	30000	27.66	12.9	390	0.915	0.67	12.02
111	97-104-TP2 (#18)	ICE 42S	42	15	7.3	16810	30000	27.66			#VALUE!		12.02
112	97-106-TP1	ICE 80S	80	15.73	8.0	13000	5467	60.56			#VALUE!	0.53	7.85
113	97-106-TP1	ICE 80S	80	26.6	13.3	13000	5467	60.56	10.6	688	0.933	0.60	7.85
114	97-106-TP2	ICE 80S	80	11.83	7.3	13000	5467	60.56			#VALUE!	0.44	7.85
115	97-106-TP2	ICE 80S	80	25.2	13.3	13000	5467	60.56	9.8	671	0.884	0.59	7.85
116	97-106-TP3	ICE 80S	80	7.33	8.5	13000	5467	60.56			#VALUE!	0.36	7.85
117	97-106-TP3	ICE 80S	80	18.4	10.0	13000	5467	60.56	8.2	535	0.928	0.56	7.85
118	97-108-#7	ICE 60S	60	27.3	4.8	16810	29983	46.02			#VALUE!		5.06
119	97-108-#7	ICE 60S	60	28.3	12.0	16810	29983	46.02	15.3	788	0.893	0.73	5.06
120	97-108-#106	ICE 60S	60	22.4	3.7	16810	29983	46.02			#VALUE!		5.00
121	97-108-#106	ICE 60S	60	30.1	13.0	16810	29983	46.02	16.6	789	0.968	0.68	5.00
122	97-108-#77	ICE 60S	60	23	4.3	16810	29983	46.02			#VALUE!		4.76
123	97-108-#77	ICE 60S	60	30.2	12.0	16810	29983	46.02	15.8	861	0.844	0.60	4.76
124	97-108-#69	ICE 60S	60	28.6	6.0	16810	29983	46.02			#VALUE!		5.12
125	97-108-#69	ICE 60S	60	26.6	9.0	16810	29983	46.02	15.7	772	0.936	0.71	5.12

**Table A.5 (con't).** Relevant Information Pertaining to Database PD2000.

Ref. No.	Pile-Case Number	Hammer Type	Rated Hammer Energy (kip-ft)	Delivered Energy (max) (EMX) (kip-ft)	Blow Count (BPI)	WS "C" (ft/s)	EM "E" (KSI)	Impedence EA/C "Z" (kips/ft/s)	Vimp VMX (ft/s)	Fimp FMX (kips)	VEA/C F	Dmax DMX (in)	2L/C (ms)
126	97-108-#27	ICE 60S	60	24.6	6.5	16810	29983	46.02			#VALUE!		5.18
127	97-108-#27	ICE 60S	60	29.3	8.0	16810	29983	46.02	15.6	788	0.911	0.73	5.18
128	97-109-A10#64 (TP5)	HPSI 1000	50	43.7 to 45.2	50.0	16810	29983	46.73			#VALUE!	1.06	0.00
129	97-109-A10#64 (TP5)	ICE 80S	99.2	44	20<1"	16810	29983	46.73	18.5	861	1.004	1.03	15.11
130	97-109-A3#20 (TP6)	ICE 80S	99.2	17.85	4.2	16810	29983	46.73			#VALUE!	0.55	0.00
131	97-109-A3#20 (TP6)	ICE 80S	99.2	45	20<1"	16810	29983	46.73	17.1	868	0.921	0.91	12.73
132	97-109-A3#28 (TP1)	ICE 60S	60	20 to 25	14.2	16810	29983	46.73			#VALUE!	0.71	0.00
133	97-109-A3#28 (TP1)	ICE 60S	60	37.9	20<1"	16810	29983	46.73	16.1	789	0.954	0.91	12.73
134	97-109-AE#42 (TP2)			23 to 27	19.2	16810	29983	46.73			#VALUE!	0.80	0.00
135	97-109-AE#42 (TP2)			43.4	20/<1"	16810	29983	46.73			#VALUE!	1.07	0.00
136	97-109-AF#73 (TP4)	D-30-32	73.7	15.7 to 23.8	11.1	16810	29983	46.73			#VALUE!	0.73	0.00
137	97-109-AF#73 (TP4)	ICE 80S	99.2	27.6	20<1"	16810	29983	46.73	12.8	634	0.943	0.83	16.89
138	97-109-AG/A4 #31 (TP2)	ICE 60S	60	23 to 27	19.2	16810	29983	46.73			#VALUE!	0.80	0.00
139	97-109-AG/A4 #31 (TP2)	ICE 60S	60	43.4	20/<1"	16810	29983	46.73	18.3	867	0.986	1.07	16.89
140	97-109-AH#96 (TP3)	HPSI 1000	50	42.6 to 44.4	14.9	16810	29983	46.73			#VALUE!	1.05	0.00
141	97-109-AH#96 (TP3)	ICE 60S	60	44.3	20<1"	16810	29983	46.73	19.4	883	1.027	1.10	17.49
142	97-109-LAETP8 N. Node #21	HPSI 1000	50	36.7 [42.3]	7.0	16810	30000	46.76	17.8	796	1.046	1.12	13.92
143	97-109-LAETP8 N. Node #21	HPSI 1000	50	37.8	13<1"	16810	30000	46.76	18	834	1.009	0.93	11.54
144	97-109-LETP10 S. Node #78	HPSI 1000	50	43.3 [44.8]	8.0	16810	30000	46.76	18.8	876	1.003	1.18	17.43
145	97-109-LETP10 S. Node #78	HPSI 1000	50	40.2	5<1"	16810	30000	46.76	18.5	846	1.022	1.00	16.30
146	97-109-LETP11 N. Node #11	HPSI 1000	50	40.5	5.8	16810	29983	46.73	18.1	861	0.982	1.03	10.35
147	97-109-LETP11 N. Node #11	HPSI 1000	50	40.7	10<1/2"	16810	30000	46.76	19.1	881	1.014	0.98	10.35
148	97-109-LETP12 E3-106	HPSI 1000	50	40.5	12.0	16810	30000	46.76	18.7	786	1.112	1.17	18.02
149	97-109-LETP12 E3-106	HPSI 1000	50	38.1	20 < 1"	16810	30000	46.76	18.1	825	1.026	0.99	16.95
150	97-109-LETP15 E4-86	HPSI 1000	50	40	8.8	16810	30000	46.76	18.8	847	1.038	1.12	15.82

**Table A.5 (con't).** Relevant Information Pertaining to Database PD2000.

Ref. No.	Pile-Case Number	Hammer Type	Rated Hammer Energy (kip-ft)	Delivered Energy (max) (EMX) (kip-ft)	Blow Count (BPI)	WS "C" (ft/s)	EM "E" (KSI)	Impedence EA/C "Z" (kips/ft/s)	Vimp VMX (ft/s)	Fimp FMX (kips)	VEA/C F	Dmax DMX (in)	2L/C (ms)
151	97-109-LETP15 E4-86	HPSI 1000	50	41.2	22 < 1"	16810	30000	46.76	17.8	825	1.009	1.05	15.82
152	97-109-Strs#112 (TP7)	HPSI 1000	50	41.7	5.7	16810	30000	46.76	18	853	0.987	0.99	12.73
153	97-109-Strs#112 (TP7)	HPSI 1000	50	36.9	14.0	16810	30000	46.76	12.8	624	0.959	0.92	12.73
154	97-114-HBTP1	D-19-32	42.8	15.6	9.0	16810	30000	43.90	12.4	598	0.910	0.45	3.21
155	97-114-HBTP1	D-19-32	42.8	14.4	13.3	16810	30000	43.90	12.6	581	0.952	0.42	3.21
156	97-117-UMG-TP4	ICE 660	51.6	9.7	< 1"	16810	30000	38.19		#VALUE!		0.43	5.72
157	97-117-UMG-TP4	ICE 660	51.6	14.9	< 1"	16810	30000	38.19	11.4	487	0.894	0.49	5.72
158	97-117-UMG-TP4	HPH-2400	17.4	12.2	< 1"	16810	30000	38.19	14.7	589	0.953	0.43	5.23
159	97-117-UMG-TP8	HPH-2400	17.4	13.9	12.8	16810	30000	38.19	16.5	646	0.975	0.45	4.93
160	97-117-UMG-TP8	B-3505		17.2	< 1/4"	16810	30000	38.19	15.5	587	1.008	0.53	4.93
161	97-120-MPTP1 (B-2)	ICE-42S	42	18.1	10.0	16810	30000	26.06	16.9	468	0.941	0.81	7.02
162	97-120-MPTP1 (B-2)	ICE-42S	42	18.1	-	16810	30000	26.06	17	454	0.976	0.73	5.89
163	97-120-MPTP2 (D-3)	ICE-42S	42	16	10.3	16810	30000	26.06	15.4	439	0.914	0.72	6.78
164	97-120-MPTP2 (D-3)	ICE-42S	42	20.4	-	16810	30000	26.06	16.6	472	0.916	0.70	5.35
165	97-123-B-12	ICE-640	40	21.6	20.0	13000	5467	82.43		616	0.000	0.82	12.00
166	97-123-B-12	ICE-640	40	21.9	26.7	13000	5467	82.43		818	0.000	0.51	11.46
167	98-105-TP1 (E. Abut.)	B 2505	35.4471732	8.5	4.8	16810	30000	46.58	NA	NA	#VALUE!	0.33	5.10
168	98-105-TP1 (E. Abut.)	B 2505	35.4471732	8.5	10.8	16810	30000	46.58	NA	NA	#VALUE!	0.29	5.10
169	98-105-TP6 (W. Abut.)	B 2505	35.4471732	8.7	5.7	16810	30000	46.58	NA	NA	#VALUE!		3.84
170	98-105-TP6 (W. Abut.)	B 2505	35.4471732	7.6	9.8	16810	30000	46.58	NA	NA	#VALUE!	0.36	3.84
171	98-105-TP6 (W. Abut.)	B 2505	35.4471732	8.3	10.3	16810	30000	46.58	NA	NA	#VALUE!	0.31	3.84
172	98-106-#1	MKT 7	4.15	0.7	30.0	12333	1788	17.54	NA	122	0.000	0.23	4.70
173	98-106-#1	MKT 9B3	8.75	2.2	14.0	12333	1788	17.54	NA	139	0.000	0.32	4.70
174	98-106-#2	MKT 7	4.15	0.7	30.0	12333	1788	17.54	NA	89	0.000	0.21	4.86
175	98-106-#2	MKT 9B3	8.75	2.4	46.7	12333	1788	0.00	NA	?	#VALUE!	?	0.00

**Table A.5 (con't).** Relevant Information Pertaining to Database PD2000.

Ref. No.	Pile-Case Number	Hammer Type	Rated Hammer Energy (kip-ft)	Delivered Energy (max) (EMX) (kip-ft)	Blow Count (BPI)	WS "C" (ft/s)	EM "E" (KSI)	Impedence EA/C "Z" (kips/ft/s)	Vimp VMX (ft/s)	Fimp FMX (kips)	VEA/C F	Dmax DMX (in)	2L/C (ms)
176	98-106-#3	MKT 7	4.15	0.5	44.0	11700	1609	18.43	NA	90	0.000	0.16	4.79
177	98-106-#3	MKT 9B3	8.75	1.9	42.7	11700	1609	18.43	NA	115	0.000	0.31	4.79
178	98-106-#4	MKT 7	4.15	0.9	30.0	13000	1986	19.40	NA	173	0.000	0.27	4.31
179	98-106-#4	MKT 9B3	8.75	2.2	33.3	13000	1986	19.40	NA	137	0.000	0.30	4.31
180	98-107-LCTP1 (#6)	MKT 10B3	13.1	5.6	20.0	12000	1739	17.53	13.5	163	1.452	0.61	4.50
181	98-107-LCTP1 (#6)	MKT 10B3	13.1	5.4	34.0	12000	1739	17.53	14	177	1.387	0.50	4.50
182	98-107-LCTP3 (#27)	MKT 10B3	13.1	5.5	5.0	12000	1739	0.00			#VALUE!	0.54	0.00
183	98-107-LCTP3 (#27)	MKT 10B3	13.1	5.7	20.0	12000	1739	17.53	14.2	214	1.164	0.55	4.83
184	98-107-LCTP3 (#27)	MKT 10B3	13.1	4.3	48.0	12000	1739	17.53	13	183	1.246	0.46	4.83
185	98-109-C19TP1	HPSI 1000	50	20	11.2	13000	5467	107.66	6	690	0.936	0.56	9.23
186	98-109-C19TP1	HPSI 1000	50	18	26.0	13000	5467	107.66	5.9	680	0.934	0.44	9.23
187	98-109-C19TP2	HPSI 1000	50	15	6.5	13000	5467	107.66	5.7	630	0.974	0.61	9.23
188	98-109-C19TP2	HPSI 1000	50	16	11.2	13000	5467	107.66	5.9	670	0.948	0.44	9.23
189	98-109-C19TP3	HPSI 1000	50	18	1.1	13000	5467	107.66	7.4	700	1.138	1.23	9.23
190	98-109-C19TP3	HPSI 1000	50	17	3.4	13000	5467	107.66	5.7	630	0.974	0.62	9.23
191	98-109-C19TP3	HPSI 1000	50	21	2.6	13000	5467	107.66	7.3	728	1.080	0.92	9.23
192	98-109-C19TP4	HPSI 1000	50	17	9.5	13000	5467	107.66	NA	730	0.000	0.58	10.15
193	98-109-C19TP4	HPSI 1250	50	27	40.0	13000	5467	107.66	NA	810	0.000	0.54	10.31
194	98-109-C19TP5	HPSI 1000	50	14	4.8	13000	5467	107.66	NA	600	0.000	0.67	11.54
195	98-109-C19TP5	HPSI 1250	50	26	10.0	13000	5467	107.66	NA	630	0.000	0.72	11.54
196	98-109-C19TP6	HPSI 1000	50	12.6	7.0	13000	5467	60.56	NA	368	0.000	0.68	10.15
197	98-109-C19TP6	HPSI 1250	50	16.7	24.0	13000	5467	60.56	NA	481	0.000	0.60	10.15
198	98-109-260	HPSI 1000	50	25	9.3	13000	5540	109.10	NA	834	0.000	0.72	11.08
199	98-109-260	HPSI 1000	50	20	18.0	13000	5467	107.66	NA	620	0.000	0.51	8.00
200	98-109-1099	HPSI 1000	50	16	5.0	13000	5540	109.10	NA	640	0.000	0.57	11.08

**Table A.5 (con't). Relevant Information Pertaining to Database PD2000.**

Ref. No.	Pile-Case Number	Hammer Type	Rated Hammer Energy (kip-ft)	Delivered Energy (max) (EMX) (kip-ft)	Blow Count (BPI)	WS "C" (ft/s)	EM "E" (KSI)	Impedence EA/C "Z" (kips/ft/s)	Vimp VMX (ft/s)	Fimp FMX (kips)	VEA/C F	Dmax DMX (in)	2L/C (ms)
201	98-109-1099	HPSI 1000	50	30	8.0	13000	5467	107.66	NA	980	0.000	0.67	6.46
202	98-109-1043	HPSI 1000	50	19	4.0	13000	5540	109.10	NA	700	0.000	0.91	11.08
203	98-109-1043	HPSI 1000	50	22	7.3	13000	5467	107.66	NA	840	0.000	0.57	7.69
204	98-109-1050	HPSI 1000	50	17	4.8	13000	5467	107.66	5.9	580	1.095	1.04	10.00
205	98-109-1050	HPSI 1000	50	44	5.0	13000	5467	107.66	11.2	1240	0.972	1.03	10.00
206	98-109-1201	HPSI 1000	50	18	4.3	13000	5467	107.66	6.1	660	0.995	0.66	10.00
207	98-109-1201	HPSI 1000	50	30	6.7	13000	5467	107.66	7.4	800	0.996	0.69	10.00
208	98-109-Test 1	HPSI 1250	50	20	6.8	13000	5467	107.66	NA	600	0.000	0.81	11.77
209	98-109-Test 1	HPSI 1250	50	39	5 < 1"	13000	5540	109.10	NA	1100	0.000	0.72	11.77
210	98-109-AC-4	HPSI 1000	50	11.9	6.0	13000	5467	60.56	4.2	302	0.842	0.56	8.77
211	98-109-AC-4	HPSI 1000	50	8.7	9.3	13000	5467	60.56	3.8	276	0.834	0.50	8.77
212	98-109-IND-1	HPSI 1000	50	15.2	4.3	13000	5467	60.56	7.1	394	1.091	0.81	8.00
213	98-109-IND-1	HPSI 1000	50	24.1	12.0	13000	5467	60.56	8.3	575	0.874	0.73	8.00
214	98-109-IND-2	HPSI 1000	50	17.5	4.0	13000	5467	60.56	8.2	521	0.953	0.85	8.00
215	98-109-IND-2	HPSI 1000	50	19.3	12.0	13000	5467	60.56	6.8	473	0.871	0.67	8.00
216	98-109-IND-3	HPSI 1000	50	12.6	5.0	13000	5467	60.56	5.9	365	0.979	0.56	8.00
217	98-109-IND-3	HPSI 1000	50	21.6	20.0	13000	5467	60.56	7.8	527	0.896	0.65	8.00
218	98-110-TP1 (9049)	ICE 640	40	17.1	10bpf+20bpi	16810	30000	21.77	NA	389	0.000	0.91	8.03
219	98-110-TP1 (9049)	ICE 640	40	18.8	18 < 1"	16810	30000	21.77	11.9	NA	#VALUE!	0.87	8.03
220	98-110-TP2 (9032)	ICE 640	40	11.8	8.3	16810	30000	21.77	NA	345	0.000	0.71	8.03
221	98-110-TP2 (9032)	ICE 640	40	19.7	20 < 1"	16810	30000	21.77	NA	419	0.000	0.90	8.03
222	98-110-3	ICE 640	40	12	14.7	16810	30000	38.19	9.2	404	0.870	0.69	16.30
223	98-110-3	ICE 640	40	16.1	14.5	16810	30000	38.19	11.9	501	0.907	0.74	16.30
224	98-110-7	ICE 640	40	14	12.3	16810	30000	38.19	8.5	425	0.764	0.63	15.41
225	98-110-7	ICE 640	40	20.3	20.0	16810	30000	38.19	11.8	514	0.877	0.74	15.41

**Table A.5 (con't).** Relevant Information Pertaining to Database PD2000.

Ref. No.	Pile-Case Number	Hammer Type	Rated Hammer Energy (kip-ft)	Delivered Energy (max) (EMX) (kip-ft)	Blow Count (BPI)	WS "C" (ft/s)	EM "E" (KSI)	Impedence EA/C "Z" (kips/ft/s)	Vimp VMX (ft/s)	Fimp FMX (kips)	VEA/C F	Dmax DMX (in)	2L/C (ms)
226	98-112-LSTP2 (D10)	ICE 640	40	14.5	10.7	13000	5467	82.43	4.9	488	0.828	0.56	13.08
227	98-112-LSTP2 (D10)	ICE 640	40	15.7	13.6	13000	5467	82.43	5.5	541	0.838	0.50	13.08
228	98-112-LSTP3 (G10)	ICE 640	40	13.2	10.0	13000	5467	82.43	4.8	457	0.866	0.53	13.69
229	98-112-LSTP3 (G10)	ICE 640	40	18.7	11.3	13000	5467	82.43	6.4	593	0.890	0.55	13.69
230	98-112-LSTP4 (A10)	ICE 640	40	15.1	11.0	13000	5467	82.43	5	513	0.803	0.53	13.08
231	98-112-LSTP4 (A10)	ICE 640	40	16.2	10.0	13000	5467	82.43	5.6	555	0.832	0.50	13.08
232	98-112-LSTP5 (A6)	ICE 640	40	15.1	10.0	13000	5467	82.43	5.1	532	0.790	0.49	11.54
233	98-112-LSTP5 (A6)	ICE 640	40	15.3	9.3	13000	5467	82.43	5.6	565	0.817	0.46	11.54
234	98-112-LSTP6 (G1)	ICE 640	40	16.3	10.0	13000	5467	82.43	5.7	565	0.832	0.52	10.92
235	98-112-LSTP6 (G1)	ICE 640	40	18.3	15.6	13000	5467	82.43	6	584	0.847	0.53	10.92
236	98-112-LSTP7 (C1)	ICE 640	40	16.3	9.0	13000	5467	82.43	5.6	554	0.833	0.56	10.92
237	98-112-LSTP7 (C1)	ICE 640	40	17.3	11.3	13000	5467	82.43	5.8	579	0.826	0.50	10.92
238	98-112-LSTP9 (A1)	ICE 640	40	15.7	10.0	13000	5467	82.43	5.3	542	0.806	0.50	10.46
239	98-112-LSTP9 (A1)	ICE 640	40	16.3	16.0	13000	5467	82.43	6.1	609	0.826	0.46	10.46
240	98-112-LSTP10 (G5.1)	ICE 640	40	12.7	14.0	13000	5467	82.43	4	408	0.808	0.52	12.77
241	98-112-LSTP10 (G5.1)	ICE 640	40	17.8	12.8	13000	5467	82.43	5.7	564	0.833	0.53	12.77
242	98-113-152	D-30-32	73.66	16.9	1.2	13000	5467	82.43	NA	597	0.000	1.04	12.15
243	98-113-152	D-30-32	73.66	9	14.7	13000	5467	82.43	NA	518	0.000	0.27	12.15
244	98-113-222	D-30-32	73.66	18.7	1.0	13000	5467	82.43	NA	621	0.000	1.04	9.38
245	98-113-222	D-30-32	73.66	26.4	1.6	13000	5467	82.43	NA	737	0.000	0.85	9.38
246	98-113-306	D-30-32	73.66	15.8	1.2	13000	5467	82.43	NA	562	0.000	0.88	9.38
247	98-113-306	D-30-32	73.66	25.4	1.3	13000	5467	82.43	NA	734	0.000	0.84	9.38
248	98-113-488	D-30-32	73.66	14.9	0.7	13000	5467	82.43	NA	410	0.000	1.76	12.00
249	98-113-488	D-30-32	73.66	20.4	2.7	13000	5467	82.43	NA	620	0.000	0.78	12.00
250	98-118-NB11	D-30-32	73.4	39.5	5.0	16810	30000	53.27	NA	905	0.000	0.94	8.80

**Table A.5 (con't).** Relevant Information Pertaining to Database PD2000.

Ref. No.	Pile-Case Number	Hammer Type	Rated Hammer Energy (kip-ft)	Delivered Energy (max) (EMX) (kip-ft)	Blow Count (BPI)	WS "C" (ft/s)	EM "E" (KSI)	Impedence EA/C "Z" (kips/ft/s)	Vimp VMX (ft/s)	Fimp FMX (kips)	VEA/C F	Dmax DMX (in)	2L/C (ms)
251	98-118-NB11	D-30-32	73.4	39.6	5.0	16810	30000	53.27	NA	905	0.000	0.95	8.80
252	98-118-SB26	D-30-32	73.4	35.6	5.0	16810	30000	53.27	NA	841	0.000	0.99	9.46
253	98-118-SB26	D-30-32	73.4	37.6	5.0	16810	30000	53.27	NA	871	0.000	1.01	0.00
254	98-118-29	D-30-32	73.4	25.4	4.5	16810	30000	53.27	NA	740	0.000	0.63	6.84
255	98-118-29	D-30-32	73.4	26.8	12.0	16810	30000	53.27	NA	796	0.000	0.60	6.84
256	98-118-44	D-30-32	73.4	26.4	4.3	16810	30000	53.27	NA	770	0.000	0.69	8.03
257	98-118-44	D-30-32	73.4	38.3	20.0	16810	30000	53.27	NA	902	0.000	0.83	8.03
258	98-118-TP30	D-30-32	73.4	32.1	10.0	16810	30000	53.27	NA	899	0.000	0.72	6.81
259	98-118-TP30	D-30-32	73.4	32.4	10 per 0"	16810	30000	53.27	15.3	899	0.907	0.71	5.71
260	98-118-TP31	D-30-32	73.4	28.1	6.0	16810	30000	53.27	NA	811	0.000	0.69	6.81
261	98-118-TP31	D-30-32	73.4	30.2	6.0	16810	30000	53.27	14.6	848	0.917	0.67	4.82
262	98-118-TP34	D-30-32	73.4	20.5	4.0	16810	30000	53.27	NA	625	0.000	0.71	6.81
263	98-118-TP34	D-30-32	73.4	29.6	5.0	16810	30000	53.27	15.5	774	1.067	0.86	6.81
264	98-118-TP35	D-30-32	73.4	20.7	5.0	16810	30000	53.27	NA	675	0.000	0.63	6.81
265	98-118-TP35	D-30-32	73.4	27.5	7.0	16810	30000	53.27	NA	798	0.000	0.68	6.07
266	98-118-TP52	D-30-32	73.4	25.7	5.0	16810	30000	53.27	NA	831	0.000	0.70	6.81
267	98-118-TP52	D-30-32	73.4	28.8	4.0	16810	30000	53.27	14.5	866	0.892	0.69	3.93
268	98-118-TP62	D-30-32	73.4	27.3	7.3	16810	30000	53.27	NA	754	0.000	0.74	6.81
269	98-118-TP62	D-30-32	73.4	40.8	7.0	16810	30000	53.27	16.1	877	0.978	0.95	5.83
270	98-118-TP8	D-30-32	73.4	26.6	4.0	16810	30000	53.27	NA	785	0.000	0.76	6.81
271	98-118-TP8	D-30-32	73.4	23.2	5.0	16810	30000	53.27	13.2	760	0.925	0.65	4.16
272	98-118-TP8	D-30-32	73.4	26	4.0	16810	30000	53.27	NA	744	0.000	0.76	6.81
273	98-118-TP8	D-30-32	73.4	30.4	4.0	16810	30000	53.27	NA	899	0.000	0.77	5.83
274	98-129-CHTP1	ICE 640	40.6	15.3	36.0	16810	30000	27.66	NA	315	0.000	0.81	9.88
275	98-129-CHTP1	ICE 640	40.6	18.7	3.0	16810	30000	27.66	NA	342	0.000	1.18	9.88



**Table A.5 (con't). Relevant Information Pertaining to Database PD2000.**

Ref. No.	Pile-Case Number	Hammer Type	Rated Hammer Energy (kip-ft)	Delivered Energy (max) (EMX) (kip-ft)	Blow Count (BPI)	WS "C" (ft/s)	EM "E" (KSI)	Impedence EA/C "Z" (kips/ft/s)	Vimp VMX (ft/s)	Fimp FMX (kips)	VEA/C F	Dmax DMX (in)	2L/C (ms)
276	98-129-CHTP2	ICE 640	40.6	18	33.0	16810	30000	27.66	NA	340	0.000	0.91	9.88
277	98-129-CHTP2	ICE 640	40.6	15.8	2.0	16810	30000	27.66	NA	270	0.000	1.25	9.88
278	98-131-Bent 1, #3	D-19-32	42.4	25.4	9.0	16810	30000	26.06	NA	503	0.000	1.01	7.20
279	98-131-Bent 1, #3	D-19-32	42.4	23.3	14.0	16810	30000	26.06	NA	522	0.000	0.97	7.20
280	98-131-Bent 2, #1	D-19-32	42.4	26.2	30.0	16810	30000	26.06	18	610	0.769	0.93	6.78
281	98-131-Bent 2, #1	D-19-32	42.4	27.3	16.0	16810	30000	26.06	19.4	593	0.852	0.93	6.78
282	98-138-17	HPH 1200	8.68	5	4.7	16810	30000	21.24	13.5	264	1.086	0.42	9.90
283	98-138-17	HPH 1200	8.68	5.9	4.5	16810	30000	21.24	15.1	287	1.117	0.47	9.90
284	98-138-5	HPH 1200	8.68	5.7	5.0	16810	30000	21.24	14.9	306	1.034	0.48	10.59
285	98-138-5	HPH 1200	8.68	5.8	5.0	16810	30000	21.24	15.1	288	1.113	0.41	10.59
286	98-138-9	HPH 1200	8.68	5.7	4.0	16810	30000	21.24	NA	302	0.000	0.51	10.05
287	98-138-9	HPH 1200	8.68	5.7	4.8	16810	30000	21.24	NA	283	0.000	0.44	10.05
288	98-138-18	HPH 1200	8.68	5.1	4.0	16810	30000	21.24	NA	291	0.000	0.44	9.82
289	98-138-18	HPH 1200	8.68	5.3	4.0	16810	30000	21.24	NA	283	0.000	0.38	9.82
290	99-112-1	ICE 640	40	9.1	12.0	13000	5467	60.56	NA	335	0.000	0.47	14.15
291	99-112-1	ICE 640	40	11.6	19.0	13000	5467	60.56	NA	440	0.000	0.40	14.15
292	99-112-13	ICE 640	40	9	11.3	13000	5467	60.56	NA	312	0.000	0.51	12.62
293	99-112-13	ICE 640	40	11.5	19.0	13000	5467	60.56	NA	432	0.000	0.42	12.62
294	99-112-159	ICE 640	40	10.8	7.8	13000	5467	60.56	NA	453	0.000	0.54	12.62
295	99-112-159	ICE 640	40	13.5	20.0	13000	5467	60.56	NA	500	0.000	0.42	12.62
296	99-114-D-2 (2)	B3505	47.2	18.7	7.3	16810	30000	26.06	NA	456	0.000	1.08	11.06
297	99-114-D-2 (2)	B3505	47.2	20.6	20 <1"	16810	30000	26.06	NA	545	0.000	0.71	11.06
298	99-114-B-2 (2)	B3505	47.2	24.2	8.0	16810	30000	26.06	NA	508	0.000	0.94	11.06
299	99-114-B-2 (2)	B3505	47.2	23.6	16.7	16810	30000	26.06	NA	504	0.000	0.87	11.06
300	99-117-3	HPSI 200	80	17.3	6.3	16810	30000	17.53	NA	233	0.000	1.48	18.44

**Table A.5 (con't).** Relevant Information Pertaining to Database PD2000.

Ref. No.	Pile-Case Number	Hammer Type	Rated Hammer Energy (kip-ft)	Delivered Energy (max) (EMX) (kip-ft)	Blow Count (BPI)	WS "C" (ft/s)	EM "E" (KSI)	Impedence EA/C "Z" (kips/ft/s)	Vimp VMX (ft/s)	Fimp FMX (kips)	VEA/C F	Dmax DMX (in)	2L/C (ms)
301	99-117-3	HPSI 200	80	26.6	14.7	16810	30000	17.53	NA	310	0.000	1.79	18.44
302	99-117-3	HPSI 200	80	44.1	-	16810	30000	17.53	NA	405	0.000	2.17	18.44
303	99-117-5	HPSI 200	80	25.7	5.8	16810	30000	17.53	NA	273	0.000	1.80	18.20
304	99-117-5	HPSI 200	80	30	-	16810	30000	17.53	NA	309	0.000	1.84	18.20
305	99-123-100	ICE 640	40	16.8	11.7	13000	5467	82.43	NA	546	0.000	0.61	13.38
306	99-123-100	ICE 640	40	16.3	26.0	13000	5467	82.43	NA	616	0.000	0.50	13.38
307	99-123-113	ICE 640	40	15	10.3	13000	5467	82.43	NA	524	0.000	0.56	12.31
308	99-123-113	ICE 640	40	15	20.0	13000	5467	82.43	NA	528	0.000	0.49	12.31
309	99-123-172	ICE 640	40	16.6	12.7	13000	5467	82.43	NA	551	0.000	0.56	14.31
310	99-123-172	ICE 640	40	15.8	18.0	13000	5467	82.43	NA	597	0.000	0.46	14.31
311	99-123-184	ICE 640	40	19.2	9.0	13000	5467	82.43	NA	643	0.000	0.67	11.23
312	99-123-184	ICE 640	40	17.5	22.0	13000	5467	82.43	NA	615	0.000	0.51	11.23
313	99-123-227	ICE 640	40	17.1	10.7	13000	5467	82.43	NA	571	0.000	0.57	11.23
314	99-123-227	ICE 640	40	14.5	17.5	13000	5467	82.43	NA	558	0.000	0.44	11.85
315	99-123-281	ICE 640	40	16.4	8.7	13000	5467	82.43	NA	566	0.000	0.56	14.77
316	99-123-281	ICE 640	40	14.7	13.0	13000	5467	82.43	NA	583	0.000	0.44	14.77
317	99-123-293	ICE 640	40	16	9.3	13000	5467	82.43	NA	536	0.000	0.53	13.38
318	99-123-293	ICE 640	40	16.5	25.0	13000	5467	82.43	NA	586	0.000	0.49	13.38
319	99-123-303	ICE 640	40	17.7	9.0	13000	5467	82.43	NA	606	0.000	0.60	12.31
320	99-123-303	ICE 640	40	17.6	11.3	13000	5467	82.43	NA	585	0.000	0.69	12.31
321	99-123-303	ICE 640	40	15.9	13.3	13000	5467	82.43	NA	599	0.000	0.45	12.31
322	99-124-N1	ICE 422	22.5	5.2	2.7	16810	30000	38.91	NA	238	0.000	0.56	9.22
323	99-124-N1	ICE 422	22.5	7.9	5.0	16810	30000	38.91	NA	264	0.000	0.53	9.22
324	99-124-N1	ICE 422	22.5	7.1	4.3	16810	30000	38.91	NA	228	0.000	0.52	9.22
325	99-124-N4	ICE 422	22.5	5.5	2.3	16810	30000	38.91	NA	238	0.000	0.62	7.44

**Table A.5 (con't).** Relevant Information Pertaining to Database PD2000.

Ref. No.	Pile-Case Number	Hammer Type	Rated Hammer Energy (kip-ft)	Delivered Energy (max) (EMX) (kip-ft)	Blow Count (BPI)	WS "C" (ft/s)	EM "E" (KSI)	Impedence EA/C "Z" (kips/ft/s)	Vimp VMX (ft/s)	Fimp FMX (kips)	VEA/C F	Dmax DMX (in)	2L/C (ms)
326	99-124-N4	ICE 422	22.5	6.2	5.5	16810	30000	38.91	NA	336	0.000	0.33	7.44
327	99-126-TP1	D-19-32	42.4	25.8	69-84	16810	30000	17.49	NA	337	0.000	1.23	6.78
328	99-126-TP1	D-19-32	42.4	25.3	6.0	16810	30000	17.49	NA	352	0.000	1.08	6.78
329	99-126-TP2	D-19-32	42.4	20.4	113-135	16810	30000	17.49	NA	316	0.000	1.18	6.78
330	99-126-TP2	D-19-32	42.4	18.8	11.0	16810	30000	17.49	NA	446	0.000	0.86	6.78
331	97-110-P105-S93	ICE 640	40	17.7	8.0	13000	5467	82.43	6.2	508	1.006	1.24	7.85
332	97-110-P105-S93	ICE 640	40	17.7	8.0	13000	5467	82.43	8	705	0.935	0.84	7.85
333	97-110-P16-S93	ICE 640	40	14.1	9.0	13000	5467	82.43	5.7	419	1.121	1.25	7.85
334	97-110-P16-S93	ICE 640	40	17.7	8.0	12750	5259	80.84	6.9	596	0.936	0.75	5.02
335	97-110-P332-S7	ICE 640	40	17.1	8.0	13000	5467	82.43	6	570	0.868	0.82	7.85
336	97-110-P332-S7	ICE 640	40	17.7	8.0	13000	5467	82.43	6.5	607	0.883	0.46	7.85
337	97-110-P566-S6	ICE 640	40	20	8.0	13000	5467	82.43	6.6	599	0.908	0.90	13.23
338	97-110-P566-S6	ICE 640	40	17.9	8.0	12750	5259	80.84	7	655	0.864	0.56	13.49
339	97-110-P56-S7	ICE 640	40	17.5	8.0	13000	5467	82.43	6.2	511	1.000	1.23	13.23
340	97-110-P56-S7	ICE 640	40	15	8.0	12750	5259	80.84	6.5	514	1.022	0.81	13.49
341	97-110-P86-S7	ICE 640	40	19.5	8.0	13000	5467	82.43	6.4	601	0.878	1.05	13.23
342	97-110-P86-S7	ICE 640	40	15	8.0	12750	5259	80.84	6.5	584	0.900	0.57	13.49
343	97-110-P212-S7	ICE 640	40	17	8.0	13000	5467	82.43	6.4	575	0.917	1.02	13.23
344	97-110-P212-S7	ICE 640	40	15.6	9.0	12750	5259	80.84	6.8	615	0.894	0.50	13.49
345	97-110-P350-S6	ICE 640	40	18.9	8.0	12750	5259	80.84	6.7	578	0.937	0.92	12.71
346	97-110-P350-S6	ICE 640	40	18.9	8.0	12750	5259	80.84	7.1	576	0.997	0.60	12.71
347	97-110-P499-S8	ICE 640	40	18.2	8.0	12750	5259	80.84	6.6	566	0.943	1.05	11.92
348	97-110-P499-S8	ICE 640	40	18.2	8.0	12750	5259	80.84	6.6	570	0.936	0.48	11.92
349	97-110-P30-S8	ICE 640	40	18.6	8.0	12750	5259	80.84	6.3	545	0.935	1.10	13.49
350	97-110-P30-S8	ICE 640	40	18.6	8.0	12750	5259	80.84	6.8	622	0.884	0.74	13.49

**Table A.5 (con't).** Relevant Information Pertaining to Database PD2000.

Ref. No.	Pile-Case Number	Hammer Type	Rated Hammer Energy (kip-ft)	Delivered Energy (max) (EMX) (kip-ft)	Blow Count (BPI)	WS "C" (ft/s)	EM "E" (KSI)	Impedence EA/C "Z" (kips/ft/s)	Vimp VMX (ft/s)	Fimp FMX (kips)	VEA/C F	Dmax DMX (in)	2L/C (ms)
351	97-110-P320-S7	ICE 640	40	15.8	8.0	12750	5259	80.84	6.3	537	0.948	0.98	13.49
352	97-110-P320-S7	ICE 640	40	15.8	8.0	12750	5259	80.84	7.1	615	0.933	0.56	13.49
353	97-110-P333-S6	ICE 640	40	19.1	9.0	12750	5259	80.84	6.6	633	0.843	0.61	8.00
354	97-110-P333-S6	ICE 640	40	13.4	9.0	12750	5259	80.84	7.1	630	0.911	0.34	5.33
355	97-110-P553-S6	ICE 640	40	19.5	8.0	12750	5259	80.84	7	622	0.910	0.60	10.35
356	97-110-P553-S6	ICE 640	40	19.5	8.0	12750	5259	80.84	7.3	675	0.874	0.42	10.35
357	97-110-P341-S6	ICE 640	40	19.5	8.0	12750	5259	80.84	6.7	583	0.929	0.71	11.14
358	97-110-P341-S6	ICE 640	40	19.5	8.0	12750	5259	80.84	6.1	563	0.876	0.41	11.14
359	97-110-P21-S8	ICE 640	40	21.7	8.0	12750	5259	80.84	6.9	639	0.873	0.92	12.71
360	97-110-P21-S8	ICE 640	40	21.7	8.0	12750	5259	80.84	6.9	629	0.887	0.42	12.71
361	97-110-P168-S8	ICE 640	40	19.4	8.0	12750	5259	80.84	6.9	634	0.880	1.05	13.49
362	97-110-P168-S8	ICE 640	40	19.4	8.0	12750	5259	80.84	6.8	640	0.859	0.46	13.49
363	97-110-P382-S8	ICE 640	40	18.1	9.0	12750	5259	80.84	6.7	602	0.900	1.05	11.92
364	97-110-P382-S8	ICE 640	40	18.1	9.0	12750	5259	80.84	8.5	776	0.886	0.46	11.92
365	97-110-P12-S8	ICE 640	40	22.1	20.0	12750	5259	80.84	7.5	683	0.888	0.67	9.57
366	97-110-P12-S8	ICE 640	40	22.1	20.0	12750	5259	80.84	9.3	867	0.867	0.46	9.57
367	97-110-P6-S8	ICE 640	40	20.6	8.0	12750	5259	80.84	7.2	714	0.815	0.52	8.00
368	97-110-P6-S8	ICE 640	40	14.5	10.0	12750	5259	80.84	7.1	617	0.930	0.40	6.90
369	97-110-P2-S6	ICE 640	40	16.6	8.0	12750	5259	80.84	6.2	547	0.916	0.93	8.00
370	97-110-P2-S6	ICE 640	40	16.6	8.0	12750	5259	80.84	6.5	558	0.942	0.55	8.00
371	97-110-P492-S8	ICE 640	40	17.6	8.0	12750	5259	80.84	6.2	609	0.823	0.91	11.14
372	97-110-P492-S8	ICE 640	40	17.6	8.0	12750	5259	80.84	8.2	750	0.884	0.63	11.14
373	97-110-P159-S8	ICE 640	40	18.1	9.0	12750	5259	80.84	7.4	660	0.906	0.57	12.71
374	97-110-P159-S8	ICE 640	40	18.1	9.0	12750	5259	80.84	7.2	655	0.889	0.45	12.71
375	97-110-P485-S8	ICE 640	40	16.8	9.0	12750	5259	80.84	6.5	588	0.894	0.82	12.71

**Table A.5 (con't).** Relevant Information Pertaining to Database PD2000.

Ref. No.	Pile-Case Number	Hammer Type	Rated Hammer Energy (kip-ft)	Delivered Energy (max) (EMX) (kip-ft)	Blow Count (BPI)	WS "C" (ft/s)	EM "E" (KSI)	Impedence EA/C "Z" (kips/ft/s)	Vimp VMX (ft/s)	Fimp FMX (kips)	VEA/C F	Dmax DMX (in)	2L/C (ms)
376	97-110-P485-S8	ICE 640	40	16.8	9.0	12750	5259	80.84	8.3	731	0.918	0.54	12.71
377	97-110-P522-S8	ICE 640	40	18.6	9.0	12750	5259	80.84	6.9	603	0.925	0.94	11.76
378	97-110-P522-S8	ICE 640	40	18.6	9.0	12750	5259	80.84	8.4	746	0.910	0.54	11.76
379	PD-TP4	VUL 506		11.01	10.0		30000		11.8	256		0.81	
380	PD-TP4	VUL 506		11.95	11.0		30000		12.7	264		0.84	
381	PD-PN3	ICE 520		10	10.7		30000		10	296		0.70	
382	PD-PN3	ICE 520		15.18	19.0		30000		12.6	401		0.71	
383	PD-PN317	MH 35		34.61	3.0		30000		15	465		1.34	
384	PD-PN317	MH 35		34.18	10.0		30000		15.3	523		1.17	
385	PD-PN12	K25		15.72	36.2		30000		10.9	368		0.79	
386	PD-PN12	K25		14.07	70.8		30000		11.1	359		0.73	
387	PD-PN7	K35		17.0947	13.5		30000		9.0336	854.213		0.50	
388	PD-PN7	K35		17.0947	13.5		30000		9.0336	854.213		0.50	
389	PD-T1	D30		17.99	2.8		30000		13.2	336		0.79	
390	PD-T1	D30		19.51	8.0		30000		14	392		0.81	
391	PD-SHD1	ICE 640		11.27	1.3		30000		7.2	224		0.92	
392	PD-SHD1	ICE 640		11.92	2.0		30000		8.3	271		0.72	
393	PD-R1	D30		16.92	3.2		30000		12.4	511		0.54	
394	PD-R1	D30		19.48	8.0		30000		13.3	548		0.58	
395	PD-R10	D30		14.75	6.7		30000		12	498		0.50	
396	PD-R10	D30		21.44	10.0		30000		13.8	583		0.60	
397	PD-TP4	KOBE 25		9.4327	4.0		30000		9.7839	398.4295		0.48	
398	PD-TP4	KOBE 25		10.7105	4.3		30000		10.7189	433.7605		0.49	
399	PD-TP2	K25		18.0686	2.3		30000		13.299	506.2578		0.77	
400	PD-TP2	K25		18.0686	2.3		30000		13.299	506.2578		0.77	

**Table A.5 (con't). Relevant Information Pertaining to Database PD2000.**

Ref. No.	Pile-Case Number	Hammer Type	Rated Hammer Energy (kip-ft)	Delivered Energy (max) (EMX) (kip-ft)	Blow Count (BPI)	WS "C" (ft/s)	EM "E" (KSI)	Impedence EA/C "Z" (kips/ft/s)	Vimp VMX (ft/s)	Fimp FMX (kips)	VEA/C F	Dmax DMX (in)	2L/C (ms)
401	PD-PN13	D30-23		19.12	1.3		4400		8.6	556		1.08	
402	PD-PN13	D30-23		19.6	1.7		4400		7.8	574		0.63	
403	PD-PN6	D22-02		11.54	3.3		30000		10.5	244		0.75	
404	PD-PN6	D22-02		20.56	3.2		30000		12.8	316		1.04	
405	PD-TP23	D22		7.47	1.7		30000		11.3	143		0.90	
406	PD-TP23	D22		14.96	2.8		30000		12.5	278		0.85	
407	PD-PN4	ICE 520		12.86	7.9		30000		12	340		0.73	
408	PD-PN4	ICE 520		11.88	15.0		30000		11.8	339		0.68	
409	PD-T4	D30		16.72	2.5		30000		13	514		0.53	
410	PD-T4	D30		17.43	5.0		30000		13.5	502		0.52	
411	PD-J31	KOBE K-3		35.2413	20.0		30000		11.6454	681.6792		1.00	
412	PD-J31	KOBE K-3		27.1798	58.3		30000		15.1662	860.7398		0.65	
413	PD-TP1799	MKT DE33		5.22	1.8		6190		4	223		0.59	
414	PD-TP1799	MKT DE33		2.66	14.4		6190		3.1	192		0.23	
415	PD-TP1799	MKT DE33		6.84	2.7		6190		4.9	251		0.60	
416	PD-T2	D30		12.74	5.0		5452		7.4	476		0.44	
417	PD-T2	D30		12.56	5.0		5452		8.6	541		0.41	
418	PD-TP6	VUL 01		6.18	100.0		6116		5.9	385		0.32	
419	PD-TP6	VUL 01		3.02	833.3		6116		3.2	219		0.23	
420	PD-PNH20	VUL 06		11.59	2.0		5120		8.2	426		0.86	
421	PD-PNH20	VUL 06		11.16	5.0		5120		7.9	472		0.46	
422	PD-T3	D30		9.86	9.2		5934		6.1	558		0.39	
423	PD-T3	D30		16.16	7.0		5934		8.1	717		0.46	
424	PD-PN110	CON 65		4.16	25.3		5220		2.9	424		0.18	
425	PD-PN110	CON 65		4.3	52.3		5220		3.6	451		0.15	

**Table A.5 (con't). Relevant Information Pertaining to Database PD2000.**

Ref. No.	Pile-Case Number	Hammer Type	Rated Hammer Energy (kip-ft)	Delivered Energy (max) (EMX) (kip-ft)	Blow Count (BPI)	WS "C" (ft/s)	EM "E" (KSI)	Impedence EA/C "Z" (kips/ft/s)	Vimp VMX (ft/s)	Fimp FMX (kips)	VEA/C F	Dmax DMX (in)	2L/C (ms)
426	PD-PN111	CON 65		1.83	44.7		5057		1.9	248		0.12	
427	PD-PN111	CON 65		4.56	166.7		5057		3.3	435		0.15	
428	PD-TP3	ICE 640		10.92	13.0		4720		4.7	665		0.38	
429	PD-TP3	ICE 640		8.76	28.5		4767		4.4	608		0.24	
430	PD-TP21	CON 300E		26.87	8.7		6782		4.6	1081		0.45	
431	PD-TP21	CON 300E		33.97	8.0		6782		5.6	1390		0.47	
432	PD-TP11	CON 300E		23.99	19.6		6720		4.5	1068		0.41	
433	PD-TP11	CON 300E		31.8	10.0		6720		5.5	1287		0.46	
434	PD-TP11	CON 300E		32	10.0		6720		5.5	1287		0.46	
435	PD-151	MKT DE40		12.4082	10.6		6230		7.7704	531.7198		0.40	
436	PD-151	MKT DE40		10.4016	19.0		6230		6.6882	490.4773		0.33	
437	PD-P3T1	VUL 06		12.13	5.0		30000		12.5	331		0.74	
438	PD-P3T1	VUL 06		9.09	8.3		30000		10.3	276		0.55	
439	PD-TP1	K25		12.9738	5.0		30000		12.1064	464.3501		0.58	
440	PD-TP1	K25		12.8662	8.0		30000		10.693	434.9394		0.55	
441	PD-PN126	VUL 140C		19.73	11.0		4000		6.7	520		0.65	
442	PD-PN126	VUL 140C		11.84	21.0		4000		5.8	434		0.43	
443	PD-TP26	D30-23		23.21	1.3		4660		10.2	592		1.00	
444	PD-TP26	D30-23		26.04	4.0		4661		10	654		0.66	
445	PD-TP114	D30-23		28.02	1.1		4583		9.3	591		1.24	
446	PD-TP114	D30-23		34.86	3.0		4583		11.8	694		0.95	
447	PD-PN177	VUL 140C		19.22	12.0		3920		6.1	476		0.67	
448	PD-PN177	VUL 140C		11.51	15.0		4000		5.6	413		0.45	
449	PD-TP1	D16-32		15.9774	6.7		30000		15.7606	408.2024		0.76	
450	PD-TP1	D16-32		15.0187	13.3		30000		15.3736	413.6971		0.64	

**Table A.5 (con't). Relevant Information Pertaining to Database PD2000.**

Ref. No.	Pile-Case Number	Hammer Type	Rated Hammer Energy (kip-ft)	Delivered Energy (max) (EMX) (kip-ft)	Blow Count (BPI)	WS "C" (ft/s)	EM "E" (KSI)	Impedence EA/C "Z" (kips/ft/s)	Vimp VMX (ft/s)	Fimp FMX (kips)	VEA/C F	Dmax DMX (in)	2L/C (ms)
451	PD-D418	RAY 150C		12.26	90.0		30000		9.7	454		0.52	
452	PD-D418	RAY 150C		10.13	47.0		30000		7.5	468		0.46	
453	PD-PN2	D16-32		13.97	2.3		30000		14.1	284		0.78	
454	PD-PN2	ICE 520		7.27	18.0		30000		10	304		0.45	
455	PD-PN26	D30-23		20.33	1.1		4400		8.7	470		1.37	
456	PD-PN26	D30-23		13.69	2.7		4400		6.7	504		0.40	
457	PD-PN49	D30-23		16.54	1.0		4400		8	436		1.11	
458	PD-PN49	D30-23		9.41	2.2		4400		5.3	440		0.32	
459	PD-PN6	CON 300		34.77			5057		3.9	1463		0.49	
460	PD-PN6	VUL 506		10.34	12.0		5171		4.9	422		0.42	
461	PD-TP1	ICE 640		13.56	2.5		4720		5.5	494		0.71	
462	PD-TP1	ICE 640		10.98	36.0		4720		5.7	517		0.35	
463	PD-TP2	CON 65E5		17.16	15.0		5057		10.3	601		0.58	
464	PD-TP2	D30-23		26.07	3.0		4583		11.2	670		0.64	
465	PD-TP8	ICE 640		13.57	6.0		4720		5.5	509		0.52	
466	PD-TP8	ICE 640		19.72	14.0		4720		6.2	765		0.49	
467	PD-PN7E3	CON 300		29.81	8.0		5554		4.2	1652		0.37	
468	PD-PN7E	CON 300		28.41	15.0		5288		3.5	1319		0.37	



**Table A.5 (con't). Relevant Information Pertaining to Database PD2000.**

Ref. No.	Pile-Case Number	Quake Tip	Side	Damping Tip	Side	CAPWAP TEPWAP	Energy Appr. Ru	Kwe CAPWAP/Ru
		(in)	(in)	(s/ft)	(s/ft)	(kips)	(kips)	
1	96-104-1W-D					--	500	--
2	96-104-1W-D					450	--	0.900
3	96-104-1W-I					--	480	--
4	96-104-1W-I					330	--	0.688
5	96-104-2E-K					--	610	--
6	96-104-2E-K					555	--	0.910
7	96-104-2W-R					--	430	--
8	96-104-2W-R					349	--	0.812
9	96-104-3E-A					--	530	--
10	96-104-3E-A					420	--	0.792
11	96-104-3W-G					--	540	--
12	96-104-3W-G					365	--	0.676
13	96-104-5W-F					--	520	--
14	96-104-5W-F					525	--	1.010
15	96-104-NA-4					--	560	--
16	96-104-NA-4					490	--	0.875
17	96-104-NA-53					--	525	--
18	96-104-NA-53					390	--	0.743
19	96-104-TP1	0.100	0.100	0.088	0.068	--	500	--
20	96-104-TP1	0.100	0.100	0.063	0.052	500	--	1.000
21	96-104-TP4	0.350	0.100	0.053	0.040	--	510	--
22	96-104-TP4	0.260	0.050	0.058	0.056	550	--	1.078
23	96-104-TP4	0.310	0.050	0.111	0.050	490	--	0.961
24	96-104-W1-V26					--	435	--
25	96-104-W1-V26					440	--	1.011

**Table A.5 (con't).** Relevant Information Pertaining to Database PD2000.

Ref. No.	Pile-Case Number	Quake		Damping		CAPWAP		Energy	Kwe CAPWAP/Ru
		Tip	Side	Tip	Side	TEPWAP	Appr. Ru		
		(in)	(in)	(s/ft)	(s/ft)	(kips)	(kips)		
26	96-104-W2-V13					--	525	--	
27	96-104-W2-V13					350	--	0.667	
28	96-104-W4-B36					--	415	--	
29	96-104-W4-B36					496	--	1.195	
30	96-104-W4-V24					--	455	--	
31	96-104-W4-V24					506	--	1.112	
32	96-104-W5-3					--	420	--	
33	96-104-W5-3					420	--	1.000	
34	96-104-W5-8					--	400	--	
35	96-104-W5-8					372	--	0.930	
36	96-104-W5-V27					--	470	--	
37	96-104-W5-V27					500	--	1.064	
38	96-104-W5-V28					--	460	--	
39	96-104-W5-V28					410	--	0.891	
40	96-115-3	0.320	0.150	0.155	0.061	--	420	--	
41	96-115-3	0.330	0.170	0.110	0.123	317	--	0.755	
42	96-115-7	0.140	0.220	0.433	0.043	--	466	--	
43	96-115-7	0.300	0.060	0.144	0.189	336	--	0.721	
44	96-115-106	0.210	0.050	0.359	0.359	--	662	--	
45	96-115-106	0.190	0.100	0.234	0.155	843	--	1.273	
46	96-115-109	0.380	0.100	0.093	0.389	--	810	--	
47	96-115-109	0.110	0.070	0.154	0.180	949	--	1.172	
48	96-115-117	.30/.35	0.090	.301/.082	0.209	--	954	--	
49	96-115-117	.20/.25	0.100	.054/.191	0.238	923	--	0.968	
50	96-115-157	.30/.21	0.090	.376/.079	0.191	--	907	--	

**Table A.5 (con't).** Relevant Information Pertaining to Database PD2000.

Ref. No.	Pile-Case Number	Quake		Damping		CAPWAP		Energy	Kwe
		Tip	Side	Tip	Side	TEPWAP	Appr.	Ru	CAPWAP/Ru
		(in)	(in)	(s/ft)	(s/ft)	(kips)	(kips)		
51	96-115-157	.15/.38	0.156	.054/.092	0.190	888	--		0.979
52	96-115-158	.30/.32	0.080	.300/.086	0.236	--	919		--
53	96-115-158	.15/.26	0.100	.161/.071	0.243	874	--		0.951
54	96-115-163	.20/.40	0.300	.036/.063	0.412	--	835		--
55	96-115-163	.20/.38	0.100	.024/.079	0.163	794	--		0.951
56	96-115-182	.25/.37	0.100	.250/.098	0.241	--	1043		--
57	96-115-182	.15/.19	0.100	.065/.082	0.191	960	--		0.920
58	96-115-258	.35/.42	0.050	.014/.015	0.440	--	1160		--
59	96-115-258	.25/.22	0.070	.021/.072	0.113	1140	--		0.983
60	96-115-279	.80/.75	0.700	.018/.167	0.097	--	715		--
61	96-115-279	.40/.60	0.100	.022/.122	0.075	625	--		0.874
62	96-115-279	.30/.32	0.110	.070/.161	0.120	797	--		1.115
63	96-115-357	.40/.50	0.070	.017/.074	0.075	--	1020		--
64	96-115-357	.40/.45	0.400	.020/.098	0.067	898	--		0.880
65	96-115-375	.40/.47	0.250	.019/.02	0.099	--	940		--
66	96-115-375	.35/.34	0.200	.02/.061	0.067	1070	--		1.138
67	96-115-414	.45/.36	0.120	.057/.048	0.106	--	875		--
68	96-115-414	.20/.26	0.070	.048/.063	0.054	1002	--		1.145
69	96-115-806	0.410	0.130	0.143	0.161	--	843		--
70	96-115-806	0.330	0.050	0.147	0.123	768	--		0.911
71	96-115-816	0.430	0.051	0.128	0.170	--	838		--
72	96-115-816	0.330	0.060	0.103	0.264	793	--		0.946
73	96-115-910	0.320	0.200	0.088	0.123	--	742		--
74	96-115-910	0.280	0.210	0.166	0.063	863	--		1.163
75	96-115-916	0.350	0.100	0.224	0.103	--	729		--

**Table A.5 (con't).** Relevant Information Pertaining to Database PD2000.

Ref. No.	File-Case Number	Quake		Damping		CAPWAP		Energy	Kwe
		Tip	Side	Tip	Side	TEPWAP	Appr.	Ru	CAPWAP/Ru
		(in)	(in)	(s/ft)	(s/ft)	(kips)	(kips)		
76	96-115-916	0.340	0.140	0.219	0.049	696	--		0.955
77	96-115-919	0.500	0.250	0.131	0.054	--	970		--
78	96-115-919	0.270	0.270	0.229	0.021	756	--		0.779
79	96-115-926	0.400	0.100	0.149	0.035	--	855		--
80	96-115-926	0.400	0.210	0.161	0.061	701	--		0.820
81	96-115-937					--	881		--
82	96-115-937	0.220	0.080	0.204	0.080	810	--		0.919
83	96-115-940	0.500	0.250	0.162	0.050	--	800		--
84	96-115-940	0.300	0.250	0.252	0.044	728	--		0.910
85	96-115-3111	1.00/1.00	0.200	.024/.166	0.240	--	807		--
86	96-115-3111	.35/.40	0.050	.043/.541	0.033	739	--		0.916
87	96-115-3115	1.20/1.00	0.050	.036/.032	0.224	--	780		--
88	96-115-3115	.70/.81	0.050	.031/.186	0.151	721	--		0.924
89	96-115-3117	1.20/1.20	0.050	.043/.036	0.332	--	700		--
90	96-115-3117	.70/.70	0.100	.021/.150	0.185	782	--		1.117
91	96-115-3118	1.00/.95	0.040	.022/.022	0.303	--	712		--
92	96-115-3118	.40/.54	0.050	.021/.205	0.139	811	--		1.139
93	96-115-3181	.50/.53	0.050	.032/.077	0.035	--	835		--
94	96-115-3181	.3/.37	0.120	.022/.158	0.096	830	--		0.994
95	96-115-3220	.40/.40	0.050	.043/.064	0.040	--	715		--
96	96-115-3220	.40/.34	0.050	.018/.064	0.065	840	--		1.175
97	96-115-3259	.30/.34	0.300	.022/.090	0.094	--	730		--
98	96-115-3259	.30/.25	0.200	.022/.062	0.178	932	--		1.277
99	96-116-9	0.280	0.250	0.050	0.034	--	635		--
100	96-116-9	0.050	0.080	0.095	0.085	740	--		1.165

**Table A.5 (con't).** Relevant Information Pertaining to Database PD2000.

Ref. No.	Pile-Case Number	Quake		Damping		CAPWAP		Energy	Kwe CAPWAP/Ru
		Tip	Side	Tip	Side	TEPWAP	Appr. Ru	Appr. Ru	
		(in)	(in)	(s/ft)	(s/ft)	(kips)	(kips)	(kips)	
101	96-116-12	0.370	0.340	0.066	0.024	--	574	--	
102	96-116-12	0.210	0.100	0.063	0.168	600	--	1.045	
103	96-117-A4	0.500	0.100	0.065	0.046	--	390	--	
104	96-117-A4	0.520	0.100	0.065	0.047	326	--	0.836	
105	97-102-TP2	0.100	0.300	0.113	0.042	--	550	--	
106	97-102-TP2	0.250	0.250	0.887	0.073	417	--	0.758	
107	97-104-TP1 (#7)	0.250	0.200	0.146	0.113	--	320	--	
108	97-104-TP1 (#7)	0.100	0.050	0.152	0.096	293	--	0.916	
109	97-104-TP2 (#18)	0.050	0.050	0.079	0.051	--	80	--	
110	97-104-TP2 (#18)	0.400	0.050	0.166	0.158	110	--	1.375	
111	97-104-TP2 (#18)	0.370	0.050	0.276	0.162	215	--	2.688	
112	97-106-TP1					--	604	--	
113	97-106-TP1	0.300	0.100	0.103	0.182	531	--	0.879	
114	97-106-TP2					--	532	--	
115	97-106-TP2	0.300	0.100	0.121	0.188	436	--	0.820	
116	97-106-TP3					--	382	--	
117	97-106-TP3	0.300	0.100	0.092	0.187	421	--	1.102	
118	97-108-#7					--	655	--	
119	97-108-#7	0.480	0.290	0.062	0.017	635	--	0.969	
120	97-108-#106					--	585	--	
121	97-108-#106	0.420	0.250	0.049	0.021	730	--	1.248	
122	97-108-#77					--	705	--	
123	97-108-#77	0.080	0.150	0.049	0.033	880	--	1.248	
124	97-108-#69					--	785	--	
125	97-108-#69	0.430	0.270	0.046	0.043	625	--	0.796	

**Table A.5 (con't). Relevant Information Pertaining to Database PD2000.**

Ref. No.	File-Case Number	Quake		Damping		CAPWAP		Energy	Kwe
		Tip	Side	Tip	Side	TEPWAP	Appr.	Ru	
		(in)	(in)	(s/ft)	(s/ft)	(kips)	(kips)		CAPWAP/Ru
126	97-108-#27					--	710	--	
127	97-108-#27	0.390	0.280	0.076	0.019	580	--		0.817
128	97-109-A10#64 (TP5)					--	930	--	
129	97-109-A10#64 (TP5)	0.120	0.310	0.238	0.104	546	--		0.587
130	97-109-A3#20 (TP6)					--	542	--	
131	97-109-A3#20 (TP6)	0.100	0.235	0.156	0.184	629	--		1.160
132	97-109-A3#28 (TP1)					--	700	--	
133	97-109-A3#28 (TP1)	0.070	0.170	0.072	0.061	830	--		1.186
134	97-109-AE#42 (TP2)					--	704	--	
135	97-109-AE#42 (TP2)	0.200	0.320	0.060	0.091	696	--		0.989
136	97-109-AF#73 (TP4)					--	705	--	
137	97-109-AF#73 (TP4)	0.070	0.100	0.056	0.102	691	--		0.980
138	97-109-AG/A4 #31 (TP2)					--	710	--	
139	97-109-AG/A4 #31 (TP2)	0.200	0.320	0.060	0.091	696	--		0.980
140	97-109-AH#96 (TP3)					--	930	--	
141	97-109-AH#96 (TP3)	0.150	0.290	0.050	0.155	659	--		0.709
142	97-109-LAETP8 N. Node #21					--	753	--	
143	97-109-LAETP8 N. Node #21	0.100	0.275	0.097	0.048	703	--		0.934
144	97-109-LETP10 S. Node #78					--	845	--	
145	97-109-LETP10 S. Node #78	0.121	0.210	0.179	0.065	762	--		0.902
146	97-109-LETP11 N. Node #11					--	900	--	
147	97-109-LETP11 N. Node #11	0.040	0.330	0.176	0.071	713	--		0.792
148	97-109-LETP12 E3-106					--	797	--	
149	97-109-LETP12 E3-106	0.096	0.190	0.120	0.053	724	--		0.908
150	97-109-LETP15 E4-86					--	821	--	

**Table A.5 (con't).** Relevant Information Pertaining to Database PD2000.

Ref. No.	Pile-Case Number	Quake		Damping		CAPWAP		Energy	Kwe
		Tip	Side	Tip	Side	TEPWAP	Appr.	Ru	CAPWAP/Ru
		(in)	(in)	(s/ft)	(s/ft)	(kips)	(kips)		
151	97-109-LETP15 E4-86	0.080	0.240	0.120	0.068	815	--		0.994
152	97-109-Strs#112 (TP7)					--	858		--
153	97-109-Strs#112 (TP7)	0.250	0.490	0.066	0.345	483	--		0.563
154	97-114-HBTP1					--	639		--
155	97-114-HBTP1	0.287	0.100	0.038	0.053	621	--		0.972
156	97-117-UMG-TP4					--	541		--
157	97-117-UMG-TP4	0.140	0.120	0.161	0.262	550	--		1.017
158	97-117-UMG-TP4	0.140	0.050	0.067	0.208	455	--		0.841
159	97-117-UMG-TP8	0.120	0.070	0.056	0.079	461	654		--
160	97-117-UMG-TP8	0.210	0.150	0.177	0.073	530	--		0.810
161	97-120-MPTP1 (B-2)					--	477		--
162	97-120-MPTP1 (B-2)	0.350	0.100	0.021	0.042	445	--		0.933
163	97-120-MPTP2 (D-3)					--	468		--
164	97-120-MPTP2 (D-3)	0.390	0.060	0.045	0.052	440	--		0.941
165	97-123-B-12	0.530	0.400	0.099	0.100	--	610		--
166	97-123-B-12	0.240	0.100	0.080	0.112	646	--		1.059
167	98-105-TP1 (E. Abut.)	0.220	0.050	0.163	0.137	--	385		--
168	98-105-TP1 (E. Abut.)	0.190	0.050	0.129	0.122	372	--		0.966
169	98-105-TP6 (W. Abut.)					--	380		--
170	98-105-TP6 (W. Abut.)	0.270	0.050	0.145	0.161	--	468		--
171	98-105-TP6 (W. Abut.)	0.200	0.050	0.106	0.187	387	--		0.827
172	98-106-#1					--	59		--
173	98-106-#1					51	--		0.864
174	98-106-#2					--	62		--
175	98-106-#2					53	--		0.855

**Table A.5 (con't).** Relevant Information Pertaining to Database PD2000.

Ref. No.	Pile-Case Number	Quake		Damping		CAPWAP	Energy	Kwe
		Tip	Side	Tip	Side	TEPWAP	Appr. Ru	CAPWAP/Ru
		(in)	(in)	(s/ft)	(s/ft)	(kips)	(kips)	
176	98-106-#3					--	62	--
177	98-106-#3					56	--	0.903
178	98-106-#4					--	67	--
179	98-106-#4					63	--	0.940
180	98-107-LCTP1 (#6)	0.270	0.080	0.044	0.191	--	207	--
181	98-107-LCTP1 (#6)	0.160	0.070	0.040	0.105	203	--	0.980
182	98-107-LCTP3 (#27)	0.220	0.070	0.033	0.149	--	178	--
183	98-107-LCTP3 (#27)	0.165	0.050	0.115	0.121	--	228	--
184	98-107-LCTP3 (#27)					141	--	0.618
185	98-109-C19TP1	0.360	0.120	0.101	0.164	--	760	--
186	98-109-C19TP1					628	--	0.826
187	98-109-C19TP2	0.500	0.100	0.154	0.229	--	471	--
188	98-109-C19TP2					413	--	0.877
189	98-109-C19TP3	0.700	0.300	0.170	0.283	--	194	--
190	98-109-C19TP3					278	--	1.433
191	98-109-C19TP3					-	386	-
192	98-109-C19TP4	0.430	0.040	0.086	0.249	--	587	--
193	98-109-C19TP4	0.250	0.080	0.117	0.308	650	--	1.107
194	98-109-C19TP5	0.540	0.090	0.173	0.103	--	401	--
195	98-109-C19TP5	0.500	0.100	0.047	0.260	485	--	1.209
196	98-109-C19TP6	0.380	0.100	0.146	0.097	--	340	--
197	98-109-C19TP6	0.170	0.100	0.128	0.220	495	--	1.456
198	98-109-260	0.450	0.200	0.134	0.203	--	723	--
199	98-109-260	0.300	0.150	0.144	0.087	670	--	0.927
200	98-109-1099	0.400	0.100	0.142	0.220	--	480	--



**Table A.5 (con't).** Relevant Information Pertaining to Database PD2000.

Ref. No.	Pile-Case Number	Quake		Damping		CAPWAP		Energy	Kwe CAPWAP/Ru
		Tip	Side	Tip	Side	TEPWAP	Appr.	Ru	
		(in)	(in)	(s/ft)	(s/ft)	(kips)	(kips)		
201	98-109-1099	0.550	0.200	0.172	0.113	440	--		0.917
202	98-109-1043	0.800	0.100	0.211	0.164	--	386		--
203	98-109-1043	0.400	0.100	0.135	0.163	425	--		1.101
204	98-109-1050	0.980	0.150	0.119	0.250	--	325		--
205	98-109-1050	0.900	0.100	0.062	0.182	326	--		1.003
206	98-109-1201	0.455	0.070	0.140	0.214	--	480		--
207	98-109-1201	0.470	0.100	0.114	0.205	497	--		1.035
208	98-109-Test 1	0.500	0.150	0.206	0.054	--	509		--
209	98-109-Test 1	0.500	0.150	0.190	0.125	492	--		0.967
210	98-109-AC-4	0.450	0.050	0.208	0.243	--	359		--
211	98-109-AC-4	0.360	0.060	0.192	0.149	234	--		0.652
212	98-109-IND-1	0.710	0.130	0.158	0.325	--	347		--
213	98-109-IND-1	0.470	0.150	0.095	0.202	395	--		1.138
214	98-109-IND-2	0.760	0.120	0.287	0.151	--	382		--
215	98-109-IND-2	0.430	0.130	0.108	0.150	377	--		0.987
216	98-109-IND-3	0.297	0.050	0.068	0.095	--	416		--
217	98-109-IND-3	0.270	0.070	0.081	0.170	450	--		1.082
218	98-110-TP1 (9049)	0.100	0.150	0.187	0.100	--	446		--
219	98-110-TP1 (9049)	0.120	0.150	0.100	0.048	420	--		0.942
220	98-110-TP2 (9032)	0.050	0.080	0.187	0.145	--	401		--
221	98-110-TP2 (9032)	0.110	0.110	0.100	0.054	417	--		1.040
222	98-110-3	0.320	0.150	0.155	0.061	--	420		--
223	98-110-3	0.330	0.170	0.110	0.123	317	--		0.755
224	98-110-7	0.140	0.220	0.433	0.043	--	466		--
225	98-110-7	0.300	0.060	0.144	0.189	336	--		0.721

**Table A.5 (con't).** Relevant Information Pertaining to Database PD2000.

Ref. No.	Pile-Case Number	Quake		Damping		CAPWAP		Energy	Kwe
		Tip	Side	Tip	Side	TEPWAP	Appr.	Ru	CAPWAP/Ru
		(in)	(in)	(s/ft)	(s/ft)	(kips)	(kips)		
226	98-112-LSTP2 (D10)					--	532	--	
227	98-112-LSTP2 (D10)	0.290	0.200	0.068	0.067	548	--	1.030	
228	98-112-LSTP3 (G10)					--	517	--	
229	98-112-LSTP3 (G10)	0.350	0.200	0.085	0.066	553	--	1.070	
230	98-112-LSTP4 (A10)					--	584	--	
231	98-112-LSTP4 (A10)	0.290	0.200	0.093	0.077	545	--	0.933	
232	98-112-LSTP5 (A6)					--	607	--	
233	98-112-LSTP5 (A6)	0.275	0.100	0.055	0.236	567	--	0.934	
234	98-112-LSTP6 (G1)					--	631	--	
235	98-112-LSTP6 (G1)	0.290	0.070	0.095	0.113	581	--	0.921	
236	98-112-LSTP7 (C1)					--	583	--	
237	98-112-LSTP7 (C1)	0.250	0.100	0.038	0.180	624	--	1.070	
238	98-112-LSTP9 (A1)					--	628	--	
239	98-112-LSTP9 (A1)	0.212	0.142	0.045	0.293	630	--	1.003	
240	98-112-LSTP10 (G5.1)					--	520	--	
241	98-112-LSTP10 (G5.1)	0.287	0.100	0.093	0.195	604	--	1.162	
242	98-113-152	0.600	0.200	0.176	0.223	--	200	--	
243	98-113-152	0.180	0.050	0.156	0.665	253	--	1.265	
244	98-113-222	0.300	0.250	0.266	0.113	--	225	--	
245	98-113-222	0.850	0.150	0.045	0.159	254	--	1.129	
246	98-113-306	0.300	0.250	0.213	0.185	--	231	--	
247	98-113-306	0.850	0.170	0.165	0.183	230	--	0.996	
248	98-113-488	0.300	0.300	0.643	0.146	--	114	--	
249	98-113-488	0.700	0.250	0.301	0.244	210	--	1.842	
250	98-118-NB11	0.450	0.100	0.067	0.006	--	832	--	

**Table A.5 (con't).** Relevant Information Pertaining to Database PD2000.

Ref. No.	Pile-Case Number	Quake		Damping		CAPWAP		Energy	Kwe
		Tip	Side	Tip	Side	TEPWAP	Appr.	Ru	
		(in)	(in)	(s/ft)	(s/ft)	(kips)	(kips)		CAPWAP/Ru
251	98-118-NB11	0.480	0.100	0.073	0.043	670	--		0.805
252	98-118-SB26	0.500	0.070	0.053	0.161	--	724		--
253	98-118-SB26	0.520	0.080	0.050	0.139	630	--		0.870
254	98-118-29	0.200	0.100	0.062	0.102	--	678		--
255	98-118-29	0.150	0.100	0.059	0.078	790	--		1.165
256	98-118-44	0.400	0.100	0.072	0.073	--	680		--
257	98-118-44	0.400	0.070	0.069	0.092	601	--		0.884
258	98-118-TP30	0.274	0.100	0.076	0.063	--	948		--
259	98-118-TP30	0.260	0.100	0.058	0.084	830	--		0.876
260	98-118-TP31	0.290	0.100	0.069	0.164	--	766		--
261	98-118-TP31	0.290	0.100	0.047	0.107	730	--		0.953
262	98-118-TP34	0.450	0.100	0.111	0.048	--	536		--
263	98-118-TP34	0.500	0.100	0.073	0.073	545	--		1.017
264	98-118-TP35	0.330	0.050	0.103	0.065	--	587		--
265	98-118-TP35	0.380	0.200	0.103	0.087	587	--		1.000
266	98-118-TP52	0.420	0.090	0.056	0.083	--	661		--
267	98-118-TP52	0.540	0.080	0.082	0.075	500	--		0.756
268	98-118-TP62	0.420	0.150	0.099	0.157	--	643		--
269	98-118-TP62	0.600	0.100	0.110	0.152	543	--		0.844
270	98-118-TP8	0.500	0.101	0.098	0.072	--	612		--
271	98-118-TP8	0.450	0.100	0.076	0.052	507	--		0.828
272	98-118-TP8	0.480	0.100	0.106	0.032	--	599		--
273	98-118-TP8	0.400	0.150	0.099	0.056	640	--		1.068
274	98-129-CHTP1	0.480	0.060	0.037	0.087	--	308		--
275	98-129-CHTP1	0.351	0.110	0.147	0.031	191	--		0.620

**Table A.5 (con't).** Relevant Information Pertaining to Database PD2000.

Ref. No.	Pile-Case Number	Quake		Damping		CAPWAP		Energy	Kwe
		Tip	Side	Tip	Side	TEPWAP	Appr. Ru	CAPWAP/Ru	
		(in)	(in)	(s/ft)	(s/ft)	(kips)	(kips)		
276	98-129-CHTP2	0.610	0.060	0.111	0.071	--	328	--	
277	98-129-CHTP2	0.400	0.150	0.146	0.048	146	--	0.445	
278	98-131-Bent 1, #3	0.430	0.150	0.080	0.051	--	542	--	
279	98-131-Bent 1, #3	0.340	0.150	0.087	0.058	461	--	0.851	
280	98-131-Bent 2, #1	0.230	0.070	0.069	0.260	--	604	--	
281	98-131-Bent 2, #1	0.246	0.070	0.059	0.186	572	--	0.947	
282	98-138-17	0.250	0.100	0.085	0.141	--	189	--	
283	98-138-17	0.200	0.150	0.064	0.154	116	--	0.613	
284	98-138-5	0.360	0.100	0.074	0.111	--	201	--	
285	98-138-5	0.310	0.080	0.073	0.140	131	--	0.652	
286	98-138-9	0.380	0.090	0.067	0.068	--	177	--	
287	98-138-9	0.270	0.150	0.062	0.145	138	--	0.780	
288	98-138-18	0.330	0.090	0.186	0.075	--	172	--	
289	98-138-18	0.272	0.090	0.076	0.164	141	--	0.820	
290	99-112-1					--	395	--	
291	99-112-1	0.190	0.100	0.149	0.133	421	--	1.066	
292	99-112-13					--	361	--	
293	99-112-13	0.200	0.100	0.082	0.218	362	--	1.001	
294	99-112-159					--	390	--	
295	99-112-159	0.200	0.100	0.117	0.277	389	--	0.997	
296	99-114-D-2 (2)					--	369	--	
297	99-114-D-2 (2)	0.120	0.075	0.053	0.089	516	--	1.398	
298	99-114-B-2 (2)	0.220	0.090	0.054	0.104	--	525	--	
299	99-114-B-2 (2)	0.200	0.090	0.059	0.126	472	--	0.899	
300	99-117-3					--	253	--	

**Table A.5 (con't). Relevant Information Pertaining to Database PD2000.**

Ref. No.	Pile-Case Number	Quake		Damping		CAPWAP		Energy	Kwe CAPWAP/Ru
		Tip	Side	Tip	Side	TEPWAP	Appr.		
		(in)	(in)	(s/ft)	(s/ft)	(kips)	Ru (kips)		
301	99-117-3					--	344	--	
302	99-117-3	0.171	0.100	0.047	0.090	429	--	1.247	
303	99-117-5					--	313	--	
304	99-117-5	0.100	0.100	0.068	0.172	328	--	1.048	
305	99-123-100					--	580	--	
306	99-123-100	0.200	0.100	0.063	0.164	562	--	0.969	
307	99-123-113					--	545	--	
308	99-123-113	0.200	0.100	0.088	0.215	565	--	1.037	
309	99-123-172					--	620	--	
310	99-123-172	0.200	0.100	0.035	0.171	545	--	0.879	
311	99-123-184					--	590	--	
312	99-123-184	0.230	0.100	0.056	0.196	640	--	1.085	
313	99-123-227					--	618	--	
314	99-123-227	0.170	0.100	0.091	0.145	540	--	0.874	
315	99-123-281					--	587	--	
316	99-123-281	0.190	0.100	0.062	0.260	566	--	0.964	
317	99-123-293					--	599	--	
318	99-123-293	0.130	0.100	0.080	0.205	723	--	1.207	
319	99-123-303					--	597	--	
320	99-123-303					--	535	--	
321	99-123-303	0.290	0.100	0.085	0.230	425	--	0.794	
322	99-124-N1					--	133	--	
323	99-124-N1	0.400	0.160	0.124	0.067	208	250	1.564	
324	99-124-N1					--	221	--	
325	99-124-N4					--	124	--	

**Table A.5 (con't).** Relevant Information Pertaining to Database PD2000.

Ref. No.	Pile-Case Number	Quake		Damping		CAPWAP TEPWAP	Energy	Kwe
		Tip	Side	Tip	Side		Appr. Ru	CAPWAP/Ru
		(in)	(in)	(s/ft)	(s/ft)	(kips)	(kips)	
326	99-124-N4	0.200	0.080	0.077	0.241	182	--	1.468
327	99-126-TP1	--	--	--	--	--	433	--
328	99-126-TP1	0.390	0.100	0.027	0.247	340	--	0.785
329	99-126-TP2	--	--	--	--	--	368	--
330	99-126-TP2	0.050	0.100	0.070	0.215	454	--	1.234
331	97-110-P105-S93	--	--	--	--	--	309	--
332	97-110-P105-S93	0.680	0.080	0.094	0.406	365	--	1.181
333	97-110-P16-S93	--	--	--	--	--	246	--
334	97-110-P16-S93	0.630	0.070	0.164	0.201	363	--	1.476
335	97-110-P332-S7	--	--	--	--	--	406	--
336	97-110-P332-S7	0.360	0.040	0.087	0.495	370	--	0.911
337	97-110-P566-S6	--	--	--	--	--	461	--
338	97-110-P566-S6	0.410	0.040	0.223	0.105	375	--	0.813
339	97-110-P56-S7	--	--	--	--	--	310	--
340	97-110-P56-S7	0.650	0.150	0.123	0.167	253	--	0.816
341	97-110-P86-S7	--	--	--	--	--	394	--
342	97-110-P86-S7	0.530	0.130	0.351	0.149	262	--	0.665
343	97-110-P212-S7	--	--	--	--	--	356	--
344	97-110-P212-S7	0.450	0.100	0.302	0.118	291	--	0.817
345	97-110-P350-S6	--	--	--	--	--	434	--
346	97-110-P350-S6	0.480	0.150	0.291	0.330	275	--	0.634
347	97-110-P499-S8	--	--	--	--	--	372	--
348	97-110-P499-S8	0.410	0.040	0.244	0.187	306	--	0.823
349	97-110-P30-S8	--	--	--	--	--	357	--
350	97-110-P30-S8	0.560	0.080	0.175	0.086	303	--	0.849

**Table A.5 (con't). Relevant Information Pertaining to Database PD2000.**

Ref. No.	Pile-Case Number	Quake		Damping		CAPWAP		Energy	Kwe CAPWAP/Ru
		Tip	Side	Tip	Side	TEPWAP	Appr. Ru	(kips)	
		(in)	(in)	(s/ft)	(s/ft)	(kips)			
351	97-110-P320-S7	--	--	--	--	--	337	--	--
352	97-110-P320-S7	0.540	0.130	0.404	0.090	250	--	--	0.742
353	97-110-P333-S6	--	--	--	--	--	602	--	--
354	97-110-P333-S6	0.290	0.050	0.266	0.254	375	--	--	0.623
355	97-110-P553-S6	--	--	--	--	--	599	--	--
356	97-110-P553-S6	0.240	0.040	0.357	0.150	475	--	--	0.793
357	97-110-P341-S6	--	--	--	--	--	509	--	--
358	97-110-P341-S6	0.340	0.180	0.500	0.237	310	--	--	0.609
359	97-110-P21-S8	--	--	--	--	--	459	--	--
360	97-110-P21-S8	0.370	0.120	0.159	0.241	361	--	--	0.786
361	97-110-P168-S8	--	--	--	--	--	384	--	--
362	97-110-P168-S8	0.370	0.120	0.195	0.151	362	--	--	0.943
363	97-110-P382-S8	--	--	--	--	--	374	--	--
364	97-110-P382-S8	0.390	0.100	0.242	0.179	376	--	--	1.005
365	97-110-P12-S8	--	--	--	--	--	693	--	--
366	97-110-P12-S8	0.240	0.100	0.147	0.109	580	--	--	0.837
367	97-110-P6-S8	--	--	--	--	--	718	--	--
368	97-110-P6-S8	0.160	0.100	0.199	0.107	385	--	--	0.536
369	97-110-P2-S6	--	--	--	--	--	378	--	--
370	97-110-P2-S6	0.450	0.080	0.210	0.125	313	--	--	0.828
371	97-110-P492-S8	--	--	--	--	--	401	--	--
372	97-110-P492-S8	0.510	0.040	0.183	0.131	331	--	--	0.825
373	97-110-P159-S8	--	--	--	--	--	638	--	--
374	97-110-P159-S8	0.090	0.180	0.248	0.107	466	--	--	0.730
375	97-110-P485-S8	--	--	--	--	--	425	--	--

**Table A.5 (con't).** Relevant Information Pertaining to Database PD2000.

Ref. No.	Pile-Case Number	Quake Tip	Side	Damping Tip	Side	CAPWAP TEPWAP	Energy Appr. Ru	Kwe CAPWAP/Ru
		(in)	(in)	(s/ft)	(s/ft)	(kips)	(kips)	
376	97-110-P485-S8	0.290	0.100	0.138	0.062	438	--	1.031
377	97-110-P522-S8	--	--	--	--	--	425	--
378	97-110-P522-S8	0.420	0.100	0.282	0.069	361	--	0.849
379	PD-TP4	0.320	0.060	0.481	0.320	262	291	--
380	PD-TP4	0.250	0.100	0.707	0.183	267	308	0.916
381	PD-PN3	0.250	0.150	0.220	0.170	312	304	--
382	PD-PN3	0.300	0.150	0.198	0.254	376	475	1.236
383	PD-PN317	0.430	0.150	0.180	0.550	383	496	--
384	PD-PN317	0.153	0.134	0.735	0.800	513	646	1.035
385	PD-PN12	0.160	0.060	0.348	0.620	438	463	--
386	PD-PN12	0.100	0.060	0.759	0.462	411	456	0.887
387	PD-PN7	0.330	0.075	0.116	0.240	507	714	--
388	PD-PN7	0.330	0.075	0.116	0.240	507	714	0.710
389	PD-T1	0.270	0.100	0.047	1.631	230	377	--
390	PD-T1	0.100	0.086	0.301	2.058	375	499	0.995
391	PD-SHD1	0.450	0.080	0.067	0.323	148	162	--
392	PD-SHD1	0.300	0.100	0.042	0.319	217	234	1.340
393	PD-R1	0.120	0.140	0.196	0.898	285	473	--
394	PD-R1	0.110	0.110	0.198	1.644	422	666	0.892
395	PD-R10	0.100	0.160	0.052	1.508	316	549	--
396	PD-R10	0.100	0.150	0.050	1.669	456	733	0.831
397	PD-TP4	0.200	0.060	0.090	0.330	226	311	--
398	PD-TP4	0.350	0.050	0.150	0.400	235	353	0.755
399	PD-TP2	0.320	0.090	0.208	0.240	326	362	--
400	PD-TP2	0.320	0.100	0.276	0.400	331	362	0.912



**Table A.5 (con't). Relevant Information Pertaining to Database PD2000.**

Ref. No.	Pile-Case Number	Quake		Damping		CAPWAP	Energy	Kwe
		Tip	Side	Tip	Side	TEPWAP	Appr.	
		(in)	(in)	(s/ft)	(s/ft)	(kips)	Ru (kips)	CAPWAP/Ru
401	PD-PN13	0.300	0.080	0.030	0.250	132	250	--
402	PD-PN13	0.400	0.060	0.025	0.470	285	383	1.138
403	PD-PN6	0.390	0.100	0.070	0.490	208	263	--
404	PD-PN6	0.530	0.100	0.100	0.600	271	365	1.031
405	PD-TP23	0.500	0.150	0.250	0.300	124	120	--
406	PD-TP23	0.300	0.110	0.044	0.637	226	298	1.885
407	PD-PN4	0.230	0.120	0.300	0.250	345	360	--
408	PD-PN4	0.170	0.100	0.500	0.250	318	383	0.882
409	PD-T4	0.180	0.120	0.025	0.950	244	431	--
410	PD-T4	0.100	0.110	0.055	1.298	288	583	0.668
411	PD-J31	0.385	0.090	0.081	0.359	705	806	--
412	PD-J31	0.229	0.078	0.250	0.550	703	976	0.872
413	PD-TP1799	0.620	0.040	0.080	0.250	101	111	--
414	PD-TP1799	0.100	0.100	0.330	0.580	226	212	2.043
415	PD-TP1799	0.450	0.050	0.150	0.250	137	168	--
416	PD-T2	0.200	0.220	0.032	0.838	226	475	--
417	PD-T2	0.200	0.150	0.080	1.400	305	495	0.642
418	PD-TP6	0.133	0.100	0.651	0.037	393	454	--
419	PD-TP6	0.070	0.070	0.773	0.091	277	309	0.611
420	PD-PNH20	0.620	0.500	0.059	0.258	89	204	--
421	PD-PNH20	0.160	0.150	0.115	0.509	185	404	0.906
422	PD-T3	0.310	0.060	0.247	0.750	179	478	--
423	PD-T3	0.360	0.069	0.400	0.700	297	644	0.621
424	PD-PN110	0.140	0.070	0.150	0.550	282	466	--
425	PD-PN110	0.090	0.080	0.540	0.920	346	629	0.743

**Table A.5 (con't). Relevant Information Pertaining to Database PD2000.**

Ref. No.	File-Case Number	Quake		Damping		CAPWAP TEPWAP	Energy	Kwe
		Tip	Side	Tip	Side		Appr. Ru	CAPWAP/Ru
		(in)	(in)	(s/ft)	(s/ft)	(kips)	(kips)	
426	PD-PN111	0.072	0.044	0.170	0.840	237	308	--
427	PD-PN111	0.110	0.100	0.100	1.100	329	702	1.067
428	PD-TP3	0.260	0.100	0.254	0.102	357	571	--
429	PD-TP3	0.118	0.134	0.172	0.965	476	756	0.834
430	PD-TP21	0.300	0.170	0.321	0.360	850	1151	--
431	PD-TP21	0.300	0.125	0.300	0.388	864	1363	0.751
432	PD-TP11	0.250	0.130	0.415	0.312	786	1241	
433	PD-TP11	0.330	0.160	0.370	0.277	976	1353	0.787
434	PD-TP11	0.330	0.140	0.344	0.280	878	1362	0.708
435	PD-151	0.179	0.085	0.350	0.350	499	600	--
436	PD-151	0.142	0.085	0.385	0.380	486	650	0.809
437	PD-P3T1	0.200	0.080	0.400	0.120	281	309	--
438	PD-P3T1	0.080	0.080	0.500	0.200	248	324	0.802
439	PD-TP1	0.280	0.080	0.750	0.250	353	397	--
440	PD-TP1	0.170	0.080	0.838	0.550	390	457	0.983
441	PD-PN126	0.331	0.366	0.514	0.300	530	640	--
442	PD-PN126	0.218	0.326	0.530	0.350	442	595	0.691
443	PD-TP26	0.200	0.100	0.037	0.250	206	310	--
444	PD-TP26	0.350	0.100	0.109	0.887	328	687	1.057
445	PD-TP114	0.370	0.100	0.039	0.159	250	310	--
446	PD-TP114	0.600	0.100	0.065	0.547	325	651	1.047
447	PD-PN177	0.340	0.120	0.500	0.100	489	616	--
448	PD-PN177	0.174	0.318	0.650	0.320	370	539	0.600
449	PD-TP1	0.250	0.100	0.440	0.640	269	422	--
450	PD-TP1	0.080	0.080	0.346	1.265	332	504	0.785

**Table A.5 (con't).** Relevant Information Pertaining to Database PD2000.

Ref. No.	Pile-Case Number	Quake		Damping		CAPWAP		Energy	Kwe
		Tip	Side	Tip	Side	TEPWAP	Appr.	Ru	CAPWAP/Ru
		(in)	(in)	(s/ft)	(s/ft)	(kips)	(kips)		
451	PD-D418	0.080	0.100	0.971	0.514	490	555	--	
452	PD-D418	0.050	0.080	0.473	0.458	482	507	0.868	
453	PD-PN2	0.170	0.050	0.080	0.800	229	277	--	
454	PD-PN2	0.020	0.036	0.250	1.250	306	342	1.107	
455	PD-PN26	0.300	0.070	0.070	0.180	110	213	--	
456	PD-PN26	0.170	0.150	0.050	1.000	385	426	1.808	
457	PD-PN49	0.500	0.150	0.030	0.200	127	188	--	
458	PD-PN49	0.100	0.100	0.200	0.650	335	290	1.782	
459	PD-PN6	0.280	0.100	0.180	0.180	1211	1368	--	
460	PD-PN6	0.060	0.060	0.138	1.430	495	495	0.362	
461	PD-TP1	0.500	0.100	0.065	0.157	234	295	--	
462	PD-TP1	0.100	0.120	0.049	1.621	544	694	1.847	
463	PD-TP2	0.290	0.050	0.650	0.120	386	637	--	
464	PD-TP2	0.150	0.130	0.210	0.991	320	642	0.502	
465	PD-TP8	0.340	0.100	0.135	0.311	354	474	--	
466	PD-TP8	0.140	0.150	0.208	0.927	507	846	1.071	
467	PD-PN7E3	0.254	0.108	0.311	0.030	1090	1442	--	
468	PD-PN7E	0.080	0.090	0.628	0.200	1200	1547	0.832	

**Table A.6. Relevant Information Pertaining to Database PD/LTT2000.**

No.	Pile-Case Number	Driving Time	Time after Initial Driving	Time after Initial Driving	t <sub>1</sub> corrected time	Refer. No.	Location	Pile Type	Pile Diameter	Pile Area	Length Below Gauges	Penetr Depth	Area Ratio
			(days)	(hrs)	(hrs)				(mm)	(mm <sup>2</sup> )	(m)	(m)	AR
1	FN1-EOD	EOD	---	0	0.0	I-480	Omaha NE	HP250x62	254.0	8000	21.95	21.95	4102
2	FN1-BOR1	BOR	2	48	73.5	I-480	Omaha NE	HP250x62	254.0	8000	21.95	21.98	4108
3	FN1-BOR2	BOR	12	288	440.8	I-480	Omaha NE	HP250x62	254.0	8000	21.95	22.25	4159
65	FL3-EOD	EOD	---	0	0.0	Rt.415	Louisiana	PSC 610mm sq	609.6	298709	30.48	25.69	210
66	FL3-BOR1	BOR	1	24	6.0	Rt.415	Louisiana	PSC 610mm sq	609.6	298709	30.48	25.69	210
67	FL3-BOR2	BOR	9	216	54.0	Rt.415	Louisiana	PSC 610mm sq	609.6	298709	30.48	25.69	210
207	CHA1-EOD	EOD	0	0	0.0	Jones Is.	Wisconsin	CEP 324mm	323.9	9419	42.00	37.49	4048
208	CHA1-BOR1	BOR	2	24	21.3	Jones Is.	Wisconsin	CEP 324mm	323.9	9419	42.00	37.52	4052
209	CHA1-BOR2	BOR	4	96	85.0	Jones Is.	Wisconsin	CEP 324mm	323.9	9419	42.25	37.52	4053
211	CHB2-EOD	EOD	0	0	0.0	Jones Is.	Wisconsin	HP310x93	304.8	11871	47.95	47.34	7224
212	CHB2-BOR1	BOR	2	48	48.5	Jones Is.	Wisconsin	HP310x93	304.8	11871	47.95	47.34	7224
213	CHB2-BOR3	BOR	7	168	169.7	Jones Is.	Wisconsin	HP310x93	304.8	11871	47.95	47.40	7236
214	CHB2-BOR4	BOR	16	384	387.9	Jones Is.	Wisconsin	HP310x93	304.8	11871	47.67	47.43	7240
215	CHB2-BOR5a	BOR	132	3168	3199.9	Jones Is.	Wisconsin	HP310x93	304.8	11871	46.45	47.46	7245
216	CHB2-BOR5b	BOR	132	3168	3199.9	Jones Is.	Wisconsin	HP310x93	304.8	11871	46.45	47.46	7245
217	CHB3-EOD	EOD	0	0	0.0	Jones Is.	Wisconsin	HP310x93	304.8	11871	44.10	43.31	6611
218	CHB3-BOR1	BOR	1	24	24.2	Jones Is.	Wisconsin	HP310x93	304.8	11871	44.10	43.31	6611
219	CHB3-BOR2	BOR	8	192	193.9	Jones Is.	Wisconsin	HP310x93	304.8	11871	44.10	43.43	6631
220	CHB3-BOR3	BOR	13	312	315.1	Jones Is.	Wisconsin	HP310x93	304.8	11871	44.10	43.53	6643
226	CH39-EOD	EOD	0	0	0.0	Jones Is.	Wisconsin	CEP 245mm	244.6	10581	44.81	43.28	3142
227	CH39-BOR	BOR	1	24	37.3	Jones Is.	Wisconsin	CEP 245mm	244.6	10581	44.81	43.28	3142
228	CH39-BORL	BOR	51	1224	1900.6	Jones Is.	Wisconsin	CEP 245mm	244.6	46581	44.81	43.37	715
291	LB3-EOD	EOD	0	0	0.0	Luling Bridge	Kenner, LA	PSC 610mm sq	609.6	298645	24.38	24.84	203
292	LB3-BOR1	BOR	1	24	6.0	Luling Bridge	Kenner, LA	PSC 610mm sq	609.6	298645	24.38	24.99	204
293	LB3-BOR2	BOR	10	240	60.0	Luling Bridge	Kenner, LA	PSC 610mm sq	609.6	298645	24.38	24.99	204

**Table A.6 (con't).** Relevant Information Pertaining to Database PD/LTT2000.

No.	Pile-Case Number	Driving Time	Time after Initial Driving (days)	Time after Initial Driving (hrs)	t <sub>1</sub> corrected time (hrs)	Refer. No.	Location	Pile Type	Pile Diameter (mm)	Pile Area (mm <sup>2</sup> )	Length Below Gauges (m)	Penetr Depth (m)	Area Ratio AR
294	LB3-BOR3	BOR	18	432	108.0	Luling Bridge	Kenner, LA	PSC 610mm sq	609.6	298645	24.38	24.99	204
295	LB4-EOD	EOD	0	0	0.0	Luling Bridge	Kenner, LA	PSC 762mm sq	762.0	403483	24.38	24.99	189
296	LB4-BOR1	BOR	1	24	3.8	Luling Bridge	Kenner, LA	PSC 762mm sq	762.0	403483	24.38	25.21	190
297	LB4-BOR2	BOR	4	96	15.4	Luling Bridge	Kenner, LA	PSC 762mm sq	762.0	403483	24.38	25.27	191
298	LB4-BOR3	BOR	9	216	34.6	Luling Bridge	Kenner, LA	PSC 762mm sq	762.0	403483	24.38	25.30	191
299	LB4-BOR4	BOR	18	432	69.1	Luling Bridge	Kenner, LA	PSC 762mm sq	762.0	403483	24.38	25.30	191
300	LB5-EOD	EOD	0	0	0.0	Luling Bridge	Kenner, LA	PSC 762mm sq	762.0	403483	24.38	24.99	189
301	LB5-BOR1	BOR	1	24	3.8	Luling Bridge	Kenner, LA	PSC 762mm sq	762.0	403483	24.38	24.99	189
302	LB5-BOR2	BOR	4	96	15.4	Luling Bridge	Kenner, LA	PSC 762mm sq	762.0	403483	24.38	24.99	189
303	LB5-BOR3	BOR	11	264	42.2	Luling Bridge	Kenner, LA	PSC 762mm sq	762.0	403483	24.38	25.30	191
304	LB5-BOR4	BOR	20	480	76.8	Luling Bridge	Kenner, LA	PSC 762mm sq	762.0	403483	24.38	25.30	191
305	LB6-EOD	EOD	0	0	0.0	Luling Bridge	Kenner, LA	PSC 914mm cyl	914.4	314193	24.38	24.69	226
306	LB6-BOR1	BOR	1	24	2.7	Luling Bridge	Kenner, LA	PSC 914mm cyl	914.4	314193	24.38	24.69	226
307	LB6-BOR2	BOR	4	96	10.7	Luling Bridge	Kenner, LA	PSC 914mm cyl	914.4	314193	24.38	24.69	226
308	LB6-BOR3	BOR	11	264	29.3	Luling Bridge	Kenner, LA	PSC 914mm cyl	914.4	314193	24.38	24.99	229
309	LB6-BOR4	BOR	21	504	56.0	Luling Bridge	Kenner, LA	PSC 914mm cyl	914.4	314193	24.38	24.99	229
310	LB7-EOD	EOD	0	0	0.0	Luling Bridge	Kenner, LA	PSC 914mm cyl	914.4	314193	24.38	24.60	225
311	LB7-BOR1	BOR	1	24	2.7	Luling Bridge	Kenner, LA	PSC 914mm cyl	914.4	314193	24.38	24.69	226
312	LB7-BOR2	BOR	4	96	10.7	Luling Bridge	Kenner, LA	PSC 914mm cyl	914.4	314193	24.38	24.69	226
313	LB7-BOR3	BOR	10	240	26.7	Luling Bridge	Kenner, LA	PSC 914mm cyl	914.4	314193	24.38	24.69	226
314	LB7-BOR4	BOR	20	480	53.3	Luling Bridge	Kenner, LA	PSC 914mm cyl	914.4	314193	24.38	24.69	226
319	NBTP2-EOD	EOD	0	0	0.0	Newbury	Massachusetts	HP310X110	304.8	14064	35.51	34.14	4433
320	NBTP2-1DR	BOR	1	24	23.5	Newbury	Massachusetts	HP310X110	304.8	14064	35.51	34.14	4433
321	NBTP2-6DR	BOR	6	144	140.9	Newbury	Massachusetts	HP310X110	304.8	14064	35.51	34.14	4433
322	NBTP3-EOD	EOD	0	0	0.0	Newbury	Massachusetts	HP310X110	304.8	14064	35.51	33.07	4295

**Table A.6 (con't). Relevant Information Pertaining to Database PD/LTT2000.**

No.	Pile-Case Number	Driving Time	Time after Initial Driving	Time after Initial Driving	$t_1$ corrected time	Refer. No.	Location	Pile Type	Pile Diameter	Pile Area	Length Below Gauges	Penetr Depth	Area Ratio
			(days)	(hrs)	(hrs)				(mm)	(mm <sup>2</sup> )	(m)	(m)	AR
323	NBTP3-1DR	BOR	1	24	23.5	Newbury	Massachusetts	HP310X110	304.8	14064	35.51	33.07	4295
324	NBTP3-6DR	BOR	6	144	140.9	Newbury	Massachusetts	HP310X110	304.8	14064	35.51	33.07	4295
390	UMLNB2-EOD	EOD	0	0	0.0	Newbury	Massachusetts	CEP 324mm	323.9	12413	23.16	20.51	354
391	UMLNB2-BOR1	BOR	1	22.17	19.6	Newbury	Massachusetts	CEP 324mm	323.9	12413	23.16	20.63	356
392	UMLNB2-BOR2	BOR	8	184.44	163.4	Newbury	Massachusetts	CEP 324mm	323.9	12413	23.16	20.86	360
393	UMLNB2-BOR3	BOR	24	567.41	502.6	Newbury	Massachusetts	CEP 324mm	323.9	12413	23.16	11.78	203
394	UMLNB2-BOR4	BOR	94	2249.98	1993.1	Newbury	Massachusetts	CEP 324mm	323.9	12413	23.16	21.11	365
395	UMLNB3-EOD	EOD	0	0	0.0	Newbury	Massachusetts	PSC 356mm sq	355.6	126451	23.16	20.42	230
396	UMLNB3-BOR1	BOR	1	24.2	17.8	Newbury	Massachusetts	PSC 356mm sq	355.6	126451	23.47	20.57	231
397	UMLNB3-BOR2	BOR	4	94.61	69.5	Newbury	Massachusetts	PSC 356mm sq	355.6	126451	23.47	20.67	232
398	UMLNB3-BOR3	BOR	14	327.91	240.9	Newbury	Massachusetts	PSC 356mm sq	355.6	126451	23.16	20.70	233
399	UMLNB3-BOR4	BOR	33	787.53	578.6	Newbury	Massachusetts	PSC 356mm sq	355.6	126451	23.16	20.79	234
400	UMLNB3-BOR5	BOR	81	1939.13	1424.7	Newbury	Massachusetts	PSC 356mm sq	355.6	126451	23.16	20.82	234
401	UMLNB3-BOR6	BOR	97	2322.53	1706.3	Newbury	Massachusetts	PSC 356mm sq	355.6	126451	23.16	20.85	235
402	UMLNB3-BOR7	BOR	167	4004.09	2941.8	Newbury	Massachusetts	PSC 356mm sq	355.6	126451	23.16	21.34	240
x	DN1-EOD	EOD	0	0	0.0	Alborg	Denmark	PSC 25mm sq	25.0	625			
x	DN1-BOR1	BOR	52	1248	287.5	Alborg	Denmark	PSC 25mm sq	25.0	625			
x	DN1-BOR2	BOR	114	2736	630.4	Alborg	Denmark	PSC 25mm sq	25.0	625			
x	DN1-BOR3	BOR	184	4416	1017.4	Alborg	Denmark	PSC 25mm sq	25.0	625			

**Table A.6 (con't).** Relevant Information Pertaining to Database PD/LTT2000.

No.	Pile-Case	Soil Type			Hammer	Rated	Delivered	Blow	Impedence	Vimp	Fimp	VEA/C	Dmax	2L/C
	Number		Side	Tip	Type	Hammer	Energy	Count	EA/C			F		
			used in		used in		Energy							
		Side	Analysis	Tip	Analysis		(kN-m)	(kN-m)	(BP10cm)	(kN/m/s)	(m/s)	(kN)		(mm) (ms)
1	FN1-EOD	silty clay	clay & till	till	clay & till	D-30	73.5	23.5	11.1	323.0	4.04	1434.1	0.909	20.1 8.57
2	FN1-BOR1	silty clay	clay & till	till	clay & till	D-30	73.5	25.0	31.5	323.0	4.04	1402.1	0.930	20.7 8.57
3	FN1-BOR2	silty clay	clay & till	till	clay & till	D-30	73.5	27.3	59.1	323.0	3.97	1374.1	0.934	21.3 8.57
65	FL3-EOD	silty clay	clay & till	silty sand	sand & silt	Vul-020	81.3	19.8	6.6*	2973.4	1.00	3017.2	0.985	19.2 15.04
66	FL3-BOR1	silty clay	clay & till	silty sand	sand & silt	Vul-020	81.3	23.1	15.7	2973.4	1.13	3609.3	0.929	11.0 15.04
67	FL3-BOR2	silty clay	clay & till	silty sand	sand & silt	Vul-020	81.3	19.6	43.3	2973.4	1.13	3538.1	0.948	7.5 15.04
207	CHA1-EOD	sa-si clay	clay & till	silty sand	sand & silt	Vul-200C	67.8	47.3	66.9	367.3	3.29	1208.1	1.000	43.6 16.40
208	CHA1-BOR1	sa-si clay	clay & till	silty sand	sand & silt	Vul-200C	67.8	41.8	189.0	367.3	3.68	1351.8	1.000	35.3 16.40
209	CHA1-BOR2	sa-si clay	clay & till	silty sand	sand & silt	Vul-200C	67.8	49.9	315.0	367.3	4.12	1511.9	1.000	35.9 16.50
211	CHB2-EOD	sa-si clay	clay & till	silty sand	sand & silt	Vul-010	44.1	34.3	3.0	489.9	4.05	2046.2	0.970	42.4 18.73
212	CHB2-BOR1	sa-si clay	clay & till	silty sand	sand & silt	Vul-010	44.1	24.8	9.8	489.9	3.57	1819.3	0.960	20.3 18.73
213	CHB2-BOR3	sa-si clay	clay & till	silty sand	sand & silt	Vul-010	44.1	28.7	24.6	489.9	3.84	2015.0	0.930	20.1 18.73
214	CHB2-BOR4	sa-si clay	clay & till	silty sand	sand & silt	8tndrp	65.1	47.3	15.7	489.9	3.26	1868.3	0.860	30.7 18.62
215	CHB2-BOR5a	sa-si clay	clay & till	silty sand	sand & silt	Vul-010	44.1	40.5	?	489.9	5.17	2064.0	0.914	28.4 18.14
216	CHB2-BOR5b	sa-si clay	clay & till	silty sand	sand & silt	Vul-010	44.1	29.8	?	489.9	6.01	2308.6	0.950	29.5 18.14
217	CHB3-EOD	sa-si clay	clay & till	silty sand	sand & silt	Vul-010	44.1	25.5	3.9	489.2	3.84	1943.9	0.970	31.0 17.22
218	CHB3-BOR1	sa-si clay	clay & till	silty sand	sand & silt	Vul-010	44.1	19.1	7.9	489.2	3.17	1543.5	1.000	17.8 17.22
219	CHB3-BOR2	sa-si clay	clay & till	silty sand	sand & silt	Vul-010	44.1	25.5	8.6	489.2	3.69	1806.0	1.000	20.1 17.22
220	CHB3-BOR3	sa-si clay	clay & till	silty sand	sand & silt	8tndrp	65.1	38.4	9.4	489.2	3.20	1712.6	0.910	26.4 17.22
226	CH39-EOD	silty clay	clay & till	silty clay	clay & till	Vul-010	44.1	21.2	3.3	427.5	3.99	1792.6	0.950	22.6 17.50
227	CH39-BOR	silty clay	clay & till	silty clay	clay & till	Vul-010	44.1	26.7	62.6	427.5	4.36	1819.3	1.020	21.6 17.50
228	CH39-BORL	silty clay	clay & till	silty clay	clay & till	Vul-010	44.1	19.7	196.9	651.9	2.90	1877.1	1.010	15.0 22.54
291	LB3-EOD	clay	clay & till	Sand	sand & silt	D46-13	75.8	34.1	3.3	3029.7	1.16	3545.2	0.990	42.2 11.55
292	LB3-BOR1	clay	clay & till	Sand	sand & silt	D46-13	75.8	28.4	6.9	3029.7	1.19	3817.5	0.940	21.2 11.55
293	LB3-BOR2	clay	clay & till	Sand	sand & silt	D46-13	75.8	23.8	23.6	2927.5	1.31	4148.0	0.930	11.2 11.95

**Table A.6 (con't). Relevant Information Pertaining to Database PD/LTT2000.**

No.	Pile-Case Number	Soil Type				Hammer Type	Rated Hammer Energy (kN-m)	Delivered Energy (kN-m)	Blow Count (BP10cm)	Impedence EA/C (kN/m/s)	Vimp (m/s)	Fimp (kN)	VEA/C F	Dmax (mm)	2L/C (ms)
		Side		Tip											
		used in Analysis	Tip Analysis												
294	LB3-BOR3	clay	clay & till	Sand	sand & silt	D46-13	75.8	19.8	47.2	2927.5	1.46	4208.9	1.020	9.2	11.95
295	LB4-EOD	clay	clay & till	Sand	sand & silt	D46-13	75.8	31.4	4.6	3954.9	1.92	6154.6	1.230	32.2	11.95
296	LB4-BOR1	clay	clay & till	Sand	sand & silt	D46-13	75.8	37.8	7.6	3954.9	1.65	6709.7	0.970	19.3	11.95
297	LB4-BOR2	clay	clay & till	Sand	sand & silt	D46-13	75.8	42.9	19.7	3954.9	1.80	7433.9	0.960	16.2	11.95
298	LB4-BOR3	clay	clay & till	Sand	sand & silt	D46-13	75.8	44.0	78.7	3954.9	1.86	7699.4	0.960	13.3	11.95
299	LB4-BOR4	clay	clay & till	Sand	sand & silt	D46-13	75.8	30.9	55.1	3954.9	1.25	5188.0	0.950	10.8	11.95
300	LB5-EOD	clay	clay & till	Sand	sand & silt	D46-13	70.0	15.2	7.2	3954.9	0.82	3517.2	0.930	26.1	11.95
301	LB5-BOR1	clay	clay & till	Sand	sand & silt	D46-13	70.0	31.0	19.4	3954.9	1.19	4842.3	0.970	18.7	11.95
302	LB5-BOR2	clay	clay & till	Sand	sand & silt	D46-13	70.0	31.0	31.5	3954.9	1.16	5092.8	0.900	11.9	11.95
303	LB5-BOR3	clay	clay & till	Sand	sand & silt	D46-13	70.0	32.9	29.8	3954.9	1.19	5362.8	0.880	10.0	11.95
304	LB5-BOR4	clay	clay & till	Sand	sand & silt	D46-13	70.0	27.9	>78.7	3954.9	1.13	4942.9	0.900	9.9	11.95
305	LB6-EOD	clay	clay & till	Sand	sand & silt	D46-13	75.8	20.7	4.9	3131.9	1.28	4002.1	1.000	28.0	11.43
306	LB6-BOR1	clay	clay & till	Sand	sand & silt	D46-13	75.8	27.6	11.1	3079.3	1.34	4304.1	0.960	17.0	11.43
307	LB6-BOR2	clay	clay & till	Sand	sand & silt	D46-13	75.8	27.4	21.0	3079.3	1.43	4674.2	0.940	11.2	11.43
308	LB6-BOR3	clay	clay & till	Sand	sand & silt	D46-13	75.8	20.3	53.1	3079.3	1.31	4431.8	0.910	7.5	11.43
309	LB6-BOR4	clay	clay & till	Sand	sand & silt	D46-13	75.8	27.6	37.1	3079.3	1.52	4973.1	0.940	7.8	11.43
310	LB7-EOD	clay	clay & till	Sand	sand & silt	D46-13	75.8	9.2	15.5	3079.3	1.19	2894.5	1.260	13.1	11.85
311	LB7-BOR1	clay	clay & till	Sand	sand & silt	D46-13	75.8	27.0	10.5	3079.3	1.34	4785.0	0.860	17.1	11.94
312	LB7-BOR2	clay	clay & till	Sand	sand & silt	D46-13	75.8	23.8	33.5	3079.3	1.31	4758.7	0.850	10.9	12.31
313	LB7-BOR3	clay	clay & till	Sand	sand & silt	D46-13	75.8	25.2	55.1	3079.3	1.43	5149.7	0.860	9.4	12.31
314	LB7-BOR4	clay	clay & till	Sand	sand & silt	D46-13	75.8	24.8	61.0	3079.3	1.43	5033.2	0.880	8.7	12.31
319	NBTP2-EOD	si-sa-clay	clay & till	glacial till	clay & till	HPSI 1000	67.8	39.9	11.8	567.8	4.94	2900.2	0.967	30.0	13.86
320	NBTP2-1DR	si-sa-clay	clay & till	glacial till	clay & till	HPSI 1000	67.8	45.6	7.9	567.8	5.39	3087.1	0.992	30.0	13.86
321	NBTP2-6DR	si-sa-clay	clay & till	glacial till	clay & till	HPSI 1000	67.8	39.0	39.4	567.8	4.91	2797.9	0.996	26.4	13.86
322	NBTP3-EOD	si-sa-clay	clay & till	silty sand	sand & silt	HPSI 1000	67.8	43.9	15.7	567.8	5.30	3060.4	0.984	29.7	13.86



**Table A.6 (con't).** Relevant Information Pertaining to Database PD/LTT2000.

No.	Pile-Case Number	Soil Type				Hammer	Rated	Delivered	Blow	Impedence	Vimp	Fimp	VEA/C	Dmax	2L/C
		Side	Side	Tip	Tip	Type	Hammer	Energy	Count	EA/C			F		
		used in	used in	used in	used in		Energy								
		Side	Analysis	Tip	Analysis		(kN-m)	(kN-m)	(BP10cm)	(kN/m/s)	(m/s)	(kN)		(mm)	(ms)
323	NBTP3-1DR	si-sa-clay	clay & till	silty sand	sand & silt	HPSI 1000	67.8	38.8	19.7	567.8	5.06	2846.9	1.009	27.7	13.86
324	NBTP3-6DR	si-sa-clay	clay & till	silty sand	sand & silt	HPSI 1000	67.8	45.8	19.7	567.8	5.36	3064.8	0.994	28.7	13.86
390	UMLNB2-EOD	sa-si-clay	clay & till	sand	sand & silt	D19-32	57.5	23.6	3.9	501.2	1.51	698.4	1.083	34.0	9.04
391	UMLNB2-BOR1	sa-si-clay	clay & till	sand	sand & silt	D19-32	57.5	27.3	6.5	501.2	5.24	2606.7	1.008	24.4	8.05
392	UMLNB2-BOR2	sa-si-clay	clay & till	sand	sand & silt	D19-32	57.5	14.4	9.8	501.2	3.87	1765.9	1.099	15.0	8.14
393	UMLNB2-BOR3	sa-si-clay	clay & till	sand	sand & silt	D19-32	57.5	22.9	12.7	501.2	1.68	742.9	1.135	17.5	8.17
394	UMLNB2-BOR4	sa-si-clay	clay & till	sand	sand & silt	D30-32	99.9	20.3	7.4	501.2	3.90	2228.6	0.877	15.0	8.24
395	UMLNB3-EOD	sa-si-clay	clay & till	sand	sand & silt	HPSI-1000	67.8	34.0	3.9	1198.2	2.41	2931.4	0.984	30.0	11.40
396	UMLNB3-BOR1	sa-si-clay	clay & till	sand	sand & silt	HPSI-1000	67.8	14.5	22.0	1198.2	1.22	1645.8	0.888	12.7	11.55
397	UMLNB3-BOR2	sa-si-clay	clay & till	sand	sand & silt	HPSI-1000	67.8	27.8	11.6	1198.2	1.98	2593.3	0.915	18.3	11.55
398	UMLNB3-BOR3	sa-si-clay	clay & till	sand	sand & silt	HPSI-1000	67.8	23.5	17.1	1198.2	1.55	2161.8	0.862	15.5	11.40
399	UMLNB3-BOR4	sa-si-clay	clay & till	sand	sand & silt	HPSI-1000	67.8	21.7	20.7	1198.2	1.71	2473.2	0.827	14.2	11.40
400	UMLNB3-BOR5	sa-si-clay	clay & till	sand	sand & silt	D19-32	58.0	15.6	21.9	1198.2	2.26	3220.5	0.839	7.4	11.40
401	UMLNB3-BOR6	sa-si-clay	clay & till	sand	sand & silt	D19-32	58.0	17.8	56.3	1198.2	2.35	3136.0	0.897	9.1	11.40
402	UMLNB3-BOR7	sa-si-clay	clay & till	sand	sand & silt	D30-32	99.9	40.7	24.6	1198.2	3.47	4759.6	0.875	16.3	11.40
x	DN1-EOD	sand & clay	clay & till	sand	sand & silt	UDD H5H	15.0								
x	DN1-BOR1	sand & clay	clay & till	sand	sand & silt	UDD H5H	30.0								
x	DN1-BOR2	sand & clay	clay & till	sand	sand & silt	UDD H5H	30.0								
x	DN1-BOR3	sand & clay	clay & till	sand	sand & silt	UDD H5H	40.0								

**Table A.6 (con't). Relevant Information Pertaining to Database PD/LTT2000.**

No.	Pile-Case Number	Tip Quake	Side Quake	Tip Damping	Side Damping	Load Test Type	Davisson's Criteria	Shape of Curve	Average Shape of Curve	$\Delta=1''$	$\Delta=0.1B$	DeBeer	Average DeBeer	Static Resist Rs
		(mm)	(mm)	(sec/m)	(sec/m)		(kN)	(kN)	(kN)	(kN)	(kN)	(kN)	(kN)	(kN)
1	FN1-EOD	5.080	2.540	0.230	0.558	Q	1352	1334	1334	1352	1352	1334	1334	1334
2	FN1-BOR1	2.540	2.540	1.312	0.427	Q	1352	1334	1334	1352	1352	1334	1334	1334
3	FN1-BOR2	2.540	2.540	1.903	0.361	Q	1352	1334	1334	1352	1352	1334	1334	1334
65	FL3-EOD	10.160	2.540	0.807	0.883	LLT	1779	1779	1779	NA	NA	1779	1779	1779
66	FL3-BOR1	6.350	3.810	1.240	1.286	LLT	1779	1779	1779	NA	NA	1779	1779	1779
67	FL3-BOR2	6.350	3.150	1.716	1.663	LLT	1779	1779	1779	NA	NA	1779	1779	1779
207	CHA1-EOD	3.810	2.540	0.131	0.331	Q	2909	2785-3034	2909	2785	2918	2669-3034	2851	2878
208	CHA1-BOR1	1.016	1.016	0.023	1.411	Q	2909	2785-3034	2909	2785	2918	2669-3034	2851	2878
209	CHA1-BOR2	0.762	0.762	0.023	0.180	Q	2909	2785-3034	2909	2785	2918	2669-3034	2851	2878
211	CHB2-EOD	3.048	3.048	0.282	0.233	Q	1343	1246-1957	1601	1246	1334	1174-1779	1477	1401
212	CHB2-BOR1	3.048	3.048	0.276	0.262	Q	1343	1246-1957	1601	1246	1334	1174-1779	1477	1401
213	CHB2-BOR3	3.048	3.048	0.262	0.259	Q	1343	1246-1957	1601	1246	1334	1174-1779	1477	1401
214	CHB2-BOR4	3.048	3.048	0.210	0.213	Q	1343	1246-1957	1601	1246	1334	1174-1779	1477	1401
215	CHB2-BOR5a	3.048	3.048	0.413	2.493	Q	1343	1246-1957	1601	1246	1334	1174-1779	1477	1401
216	CHB2-BOR5b	2.286	2.286	2.133	0.226	Q	1343	1246-1957	1601	1246	1334	1174-1779	1477	1401
217	CHB3-EOD	2.540	2.540	0.377	0.394	Q	890	783-1094	939	943	996	827	827	952
218	CHB3-BOR1	2.540	2.540	0.285	0.358	Q	890	783-1094	939	943	996	827	827	952
219	CHB3-BOR2	2.540	2.032	0.299	0.381	Q	890	783-1094	939	943	996	827	827	952
220	CHB3-BOR3	3.048	3.05-5.59	0.223	0.341	Q	890	783-1094	939	943	996	827	827	952
226	CH39-EOD	3.810	3.810	0.436	0.075	Q	2936	2829-2936	2882	2473	2322	2936	2936	2918
227	CH39-BOR	3.556	3.556	0.210	0.210	Q	2936	2829-2936	2882	2473	2322	2936	2936	2918
228	CH39-BORL	3.302	3.810	0.102	0.128	Q	2936	2829-2936	2882	2473	2322	2936	2936	2918
291	LB3-EOD	13.970	13.970	1.329	0.669		1842	1761	1761	NA	NA	1779	1779	1770
292	LB3-BOR1	3.048	3.048	1.404	0.367		1842	1761	1761	NA	NA	1779	1779	1770
293	LB3-BOR2	4.572	3.302	1.243	0.696		1842	1761	1761	NA	NA	1779	1779	1770

**Table A.6 (con't).** Relevant Information Pertaining to Database PD/LTT2000.

No.	Pile-Case Number	Tip Quake	Side Quake	Tip Damping	Side Damping	Load Test Type	Davisson's Criteria (kN)	Shape of Curve (kN)	Average Shape of Curve (kN)	$\Delta=1"$ (kN)	$\Delta=0.1B$ (kN)	DeBeer (kN)	Average DeBeer (kN)	Static Resist Rs (kN)
294	LB3-BOR3	4.826	4.826	0.909	0.955		1842	1761	1761	NA	NA	1779	1779	1770
295	LB4-EOD	20.320	5.080	1.388	1.388		2273	2002	2002	NA	NA	2015	2015	2015
296	LB4-BOR1	19.050	3.048	1.427	1.004		2273	2002	2002	NA	NA	2015	2015	2015
297	LB4-BOR2	7.620	5.080	1.191	1.309		2273	2002	2002	NA	NA	2015	2015	2015
298	LB4-BOR3	7.620	4.445	1.109	1.519		2273	2002	2002	NA	NA	2015	2015	2015
299	LB4-BOR4	9.398	3.556	1.135	1.578		2273	2002	2002	NA	NA	2015	2015	2015
300	LB5-EOD	17.780	5.080	0.331	0.331		2469	1926	1926	NA	NA	1810	1810	1868
301	LB5-BOR1	17.780	5.080	0.666	1.473		2469	1926	1926	NA	NA	1810	1810	1868
302	LB5-BOR2	10.668	5.080	1.093	1.552		2469	1926	1926	NA	NA	1810	1810	1868
303	LB5-BOR3	8.890	4.318	1.562	1.608		2469	1926	1926	NA	NA	1810	1810	1868
304	LB5-BOR4	9.525	5.842	1.404	1.178		2469	1926	1926	NA	NA	1810	1810	1868
305	LB6-EOD	22.860	2.540	0.328	0.522		2411	2019	2019	NA	NA	2166	2166	2095
306	LB6-BOR1	13.970	5.080	0.919	0.965		2411	2019	2019	NA	NA	2166	2166	2095
307	LB6-BOR2	3.810	3.810	0.909	1.378		2411	2019	2019	NA	NA	2166	2166	2095
308	LB6-BOR3	6.731	3.048	0.981	1.106		2411	2019	2019	NA	NA	2166	2166	2095
309	LB6-BOR4	7.239	3.048	0.591	0.823		2411	2019	2019	NA	NA	2166	2166	2095
310	LB7-EOD	6.350	3.810	0.577	0.758		2402	2206	2206	NA	NA	2135	2135	2171
311	LB7-BOR1	15.240	7.620	1.165	0.896		2402	2206	2206	NA	NA	2135	2135	2171
312	LB7-BOR2	8.128	7.620	0.623	1.135		2402	2206	2206	NA	NA	2135	2135	2171
313	LB7-BOR3	9.779	5.588	1.014	0.686		2402	2206	2206	NA	NA	2135	2135	2171
314	LB7-BOR4	7.112	5.080	0.833	0.827		2402	2206	2206	NA	NA	2135	2135	2171
319	NBTP2-EOD	1.270	5.715	0.039	0.138	SD	1806	1806-1993	1899	1713	1904	1922	1922	1849
320	NBTP2-IDR	1.270	5.334	0.046	0.135	SD	1806	1806-1993	1899	1713	1904	1922	1922	1849
321	NBTP2-6DR	1.270	6.350	0.066	0.135	SD	1806	1806-1993	1899	1713	1904	1922	1922	1849
322	NBTP3-EOD	6.604	1.270	0.305	0.092	SD	2126	NA	NA	1757	2100	NA	NA	1994

**Table A.6 (con't).** Relevant Information Pertaining to Database PD/LTT2000.

No.	Pile-Case Number	Tip Quake	Side Quake	Tip Damping	Side Damping	Load Test Type	Davisson's Criteria	Shape of Curve	Average Shape of Curve	$\Delta=1''$	$\Delta=0.1B$	DeBeer	Average DeBeer	Static Resist Rs
		(mm)	(mm)	(sec/m)	(sec/m)		(kN)	(kN)	(kN)	(kN)	(kN)	(kN)	(kN)	(kN)
323	NBTP3-1DR	6.350	1.270	0.285	0.056	SD	2126	NA	NA	1757	2100	NA	NA	1994
324	NBTP3-6DR	6.858	1.270	0.289	0.062	SD	2126	NA	NA	1757	2100	NA	NA	1994
390	UMLNB2-EOD	23.774	1.270	0.226	0.761	SM	667	667	667	667	667	667	667	667
391	UMLNB2-BOR1	13.411	1.016	0.167	0.820	SM	667	667	667	667	667	667	667	667
392	UMLNB2-BOR2	8.255	2.032	0.505	0.669	SM	667	667	667	667	667	667	667	667
393	UMLNB2-BOR3	11.227	1.626	0.427	0.262	SM	667	667	667	667	667	667	667	667
394	UMLNB2-BOR4	12.446	2.032	0.397	0.000	SM	667	667	667	667	667	667	667	667
395	UMLNB3-EOD	7.366	3.048	0.157	0.679	SM	783	667-783	778	876	NA	801	801	810
396	UMLNB3-BOR1	10.668	0.991	0.200	1.102	SM	783	667-784	778	876	NA	801	801	810
397	UMLNB3-BOR2	16.688	1.016	0.423	0.663	SM	783	667-785	778	876	NA	801	801	810
398	UMLNB3-BOR3	10.897	2.616	0.787	0.817	SM	783	667-786	778	876	NA	801	801	810
399	UMLNB3-BOR4			0.000	0.000	SM	783	667-787	778	876	NA	801	801	810
400	UMLNB3-BOR5	6.350	2.540	0.705	1.106	SM	783	667-788	778	876	NA	801	801	810
401	UMLNB3-BOR6	6.147	1.041	0.981	1.056	SM	783	667-789	778	876	NA	801	801	810
402	UMLNB3-BOR7	7.798	6.350	0.489	1.378	SM	783	667-790	778	876	NA	801	801	810
x	DN1-EOD													1250
x	DN1-BOR1													1250
x	DN1-BOR2													1250
x	DN1-BOR3													1250

**Table A.6 (con't).** Relevant Information Pertaining to Database PD/LTT2000.

No.	Pile-Case Number	CAPWAP TEPWAP	Energy Appr.	Ksp	Ksw	Kws
		Rc (kN)	Ru (kN)	Rd Ru	Rd Rc	Rc Rs
1	FN1-EOD	1023	1610	0.840	1.322	0.767
2	FN1-BOR1	1668	2153	0.628	0.811	1.250
3	FN1-BOR2	1917	2380	0.568	0.705	1.437
65	FL3-EOD	605	1148	1.550	2.941	0.340
66	FL3-BOR1	1210	2660	0.669	1.471	0.680
67	FL3-BOR2	1557	3972	0.448	1.143	0.875
207	CHA1-EOD	1735	2100	1.386	1.677	0.603
208	CHA1-BOR1	2068	2335	1.246	1.406	0.719
209	CHA1-BOR2	2304	2758	1.055	1.263	0.801
211	CHB2-EOD	489	899	1.495	2.745	0.349
212	CHB2-BOR1	1201	1628	0.825	1.119	0.857
213	CHB2-BOR3	1512	2384	0.563	0.888	1.079
214	CHB2-BOR4	2002	2553	0.526	0.671	1.429
215	CHB2-BOR5a	2291			0.586	1.635
216	CHB2-BOR5b	2126			0.632	1.517
217	CHB3-EOD	467	903	0.985	1.905	0.491
218	CHB3-BOR1	1045	1254	0.709	0.851	1.098
219	CHB3-BOR2	979	1606	0.554	0.909	1.028
220	CHB3-BOR3	1490	2073	0.429	0.597	1.565
226	CH39-EOD	832	796	3.687	3.529	0.285
227	CH39-BOR	2046	2304	1.274	1.435	0.701
228	CH39-BORL	2558	2535	1.158	1.148	0.877
291	LB3-EOD	269	939	1.960	6.854	0.152
292	LB3-BOR1	912	1592	1.157	2.020	0.515
293	LB3-BOR2	1534	3075	0.599	1.200	0.867

**Table A.6 (con't).** Relevant Information Pertaining to Database PD/LTT2000.

No.	Pile-Case Number	CAPWAP TEPWAP	Energy Appr.	Ksp	Ksw	Kws
		Rc (kN)	Ru (kN)	Rd Ru	Rd Rc	Rc Rs
294	LB3-BOR3	1677	3479	0.529	1.098	0.947
295	LB4-EOD	202	1163	1.954	11.256	0.100
296	LB4-BOR1	887	2325	0.978	2.561	0.440
297	LB4-BOR2	1299	4039	0.563	1.749	0.645
298	LB4-BOR3	1521	6042	0.376	1.495	0.755
299	LB4-BOR4	1603	4881	0.466	1.418	0.796
300	LB5-EOD	263	774	3.188	9.375	0.141
301	LB5-BOR1	952	2601	0.949	2.593	0.510
302	LB5-BOR2	1402	4110	0.601	1.761	0.750
303	LB5-BOR3	1591	4940	0.500	1.552	0.851
304	LB5-BOR4	1752	?		1.409	0.938
305	LB6-EOD	404	857	2.813	5.969	0.193
306	LB6-BOR1	883	2119	1.138	2.730	0.421
307	LB6-BOR2	1322	3443	0.700	1.824	0.631
308	LB6-BOR3	1767	4318	0.558	1.365	0.843
309	LB6-BOR4	2300	5256	0.459	1.048	1.098
310	LB7-EOD	457	931	2.580	5.258	0.210
311	LB7-BOR1	875	2033	1.181	2.744	0.403
312	LB7-BOR2	1279	3419	0.702	1.878	0.589
313	LB7-BOR3	1891	4489	0.535	1.270	0.871
314	LB7-BOR4	2260	4803	0.500	1.063	1.041
319	NBTP2-EOD	1352	2091	0.864	1.336	0.731
320	NBTP2-1DR	1601	2135	0.846	1.128	0.866
321	NBTP2-6DR	1686	2713	0.666	1.071	0.912
322	NBTP3-EOD	1401	2402	0.885	1.517	0.703

**Table A.6 (con't).** Relevant Information Pertaining to Database PD/LTT2000.

No.	Pile-Case Number	CAPWAP TEPWAP	Energy Appr.	Ksp	Ksw	Kws
		Rc (kN)	Ru (kN)	Rd Ru	Rd Rc	Rc Rs
323	NBTP3-1DR	1601	2402	0.885	1.328	0.803
324	NBTP3-6DR	1713	2669	0.797	1.242	0.859
390	UMLNB2-EOD	414	792	0.843	1.613	0.620
391	UMLNB2-BOR1	487	1370	0.487	1.371	0.729
392	UMLNB2-BOR2	593	1139	0.586	1.124	0.889
393	UMLNB2-BOR3	857	1806	0.369	0.779	1.284
394	UMLNB2-BOR4	1108	1432	0.466	0.602	1.661
395	UMLNB3-EOD	737	1228	0.638	1.062	0.910
396	UMLNB3-BOR1	960	1650	0.474	0.815	1.186
397	UMLNB3-BOR2	1055	2064	0.379	0.742	1.303
398	UMLNB3-BOR3	1072	2206	0.355	0.730	1.325
399	UMLNB3-BOR4		2273	0.344		
400	UMLNB3-BOR5	1091	2602	0.301	0.717	1.348
401	UMLNB3-BOR6	1060	3567	0.219	0.739	1.309
402	UMLNB3-BOR7	1228	4075	0.192	0.638	1.516
x	DN1-EOD	600				0.480
x	DN1-BOR1	1335				1.068
x	DN1-BOR2	1502				1.202
x	DN1-BOR3	1572				1.258

## **APPENDIX B**

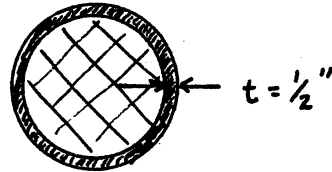
### **BACKGROUND CALCULATIONS FOR CASE HISTORIES PRESENTED IN CHAPTER 2**



# NEWBURY SITE PROJECT, TEST PILE # 2

## Pile Dimensions

Steel Pipe Pile:



Embedment Length,  $D_b, D_b'$

$$D_b = 80 \text{ ft}$$

$$D_b' = 80 \text{ ft} - 9 \text{ ft} = 71 \text{ ft}$$

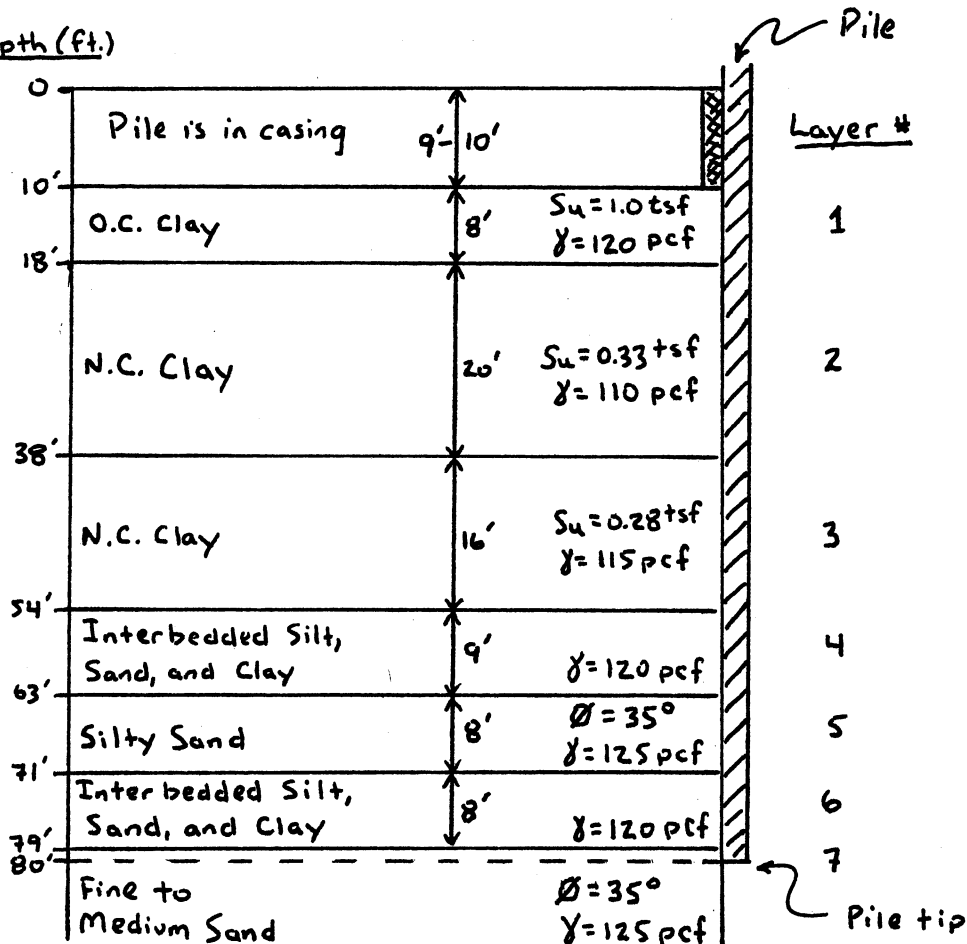
↑ casing

$$B = 12 \frac{3}{4} \text{ inches} = 1.0625 \text{ ft}$$

$$A_p = \pi (12.75 \text{ in})^2 / 4 = 127.7 \text{ in}^2 = 0.8866 \text{ ft}^2$$

## Soil Profile:

Depth (ft.)



Calculations to determine  $Q_{ult}$  using traditional methods:

$$\phi_{@tip} = 35^\circ$$

$$\begin{aligned} \sigma'_{v@tip} = q_{@tip} = & 125 \frac{lb}{ft^3} \times 5.4 ft + (125 - 62.4) \frac{lb}{ft^3} \times 2.6 ft \\ & + (101 - 62.4) \frac{lb}{ft^3} \times 1 ft + (120 - 62.4) \frac{lb}{ft^3} \times 9 ft + (110 - 62.4) \frac{lb}{ft^3} \times 20 ft \\ & + (115 - 62.4) \frac{lb}{ft^3} \times 16 ft + (120 - 62.4) \frac{lb}{ft^3} \times 9 ft + (125 - 62.4) \frac{lb}{ft^3} \times 8 ft \\ & + (120 - 62.4) \frac{lb}{ft^3} \times 8 ft + (125 - 62.4) \frac{lb}{ft^3} \times 1 ft \end{aligned}$$

$$= 4,731.0 \frac{lb}{ft^2} = 2.37 tsf$$

\*Find  $Q_p$ :

General Values:

- Coyle & Castello:

$$\left. \begin{aligned} D_c/B &= 80 ft / 1.0625 ft = 75 \\ \phi_{@tip} &= 35^\circ \end{aligned} \right\} \Rightarrow q_p = \underline{125 tsf}$$

- API:

$$\begin{aligned} q_{pmax} &= 200 \frac{K}{ft^2} = 100 tsf ; N_q = 40 \\ q_p &= 2.37 tsf \times 40 = \underline{95 tsf} < 100 tsf \quad O.K. \end{aligned}$$

Meyerhof:  $q_p = \sigma'_v \cdot N_q \leq \sigma'_v(@D_c) \cdot N_q$

$$\sigma'_v = 2.37 tsf$$

$$D_c/B = 11 \Rightarrow D_c = 12 ft$$

$$\text{from chart with } \phi = 35^\circ \Rightarrow N_q = 48$$

$$\begin{aligned} \sigma'_v(@12ft) &= 125 \frac{lb}{ft^3} \times 5.5 ft + (125 - 62.4) \frac{lb}{ft^3} \times 2.5 ft + (101 - 62.4) \frac{lb}{ft^3} \times 1 ft \\ &+ (120 - 62.4) \frac{lb}{ft^3} \times 3 ft \end{aligned}$$

$$= 1,055.4 \frac{lb}{ft^2} = 0.53 tsf$$

$$q_p = 2.37 tsf \times 48 = 114 tsf \leq 0.53 tsf \times 48 = \underline{25 tsf}$$

Vesic - Simplified:  $q_p = \sigma_o \cdot N_q$

$\phi = 35^\circ \rightarrow$  from chart  $N_q = 60$

$$K_o = 1 - \sin \phi = 1 - \sin 35^\circ = 0.43$$

$$\sigma_o = q \cdot \frac{(1 + 2 \cdot K_o)}{3} = 2.37^{tsf} \cdot \frac{(1 + 2 \cdot 0.43)}{3} = 1.47^{tsf}$$

$$q_p = 1.47^{tsf} \times 60 = \underline{88^{tsf}}$$

Vesic - Advanced:  $q_p = N_o \cdot \sigma_o$

from above  $\sigma_o = 1.47^{tsf}$

from table  $I_r \approx 125$

$$\text{say } E_{vmin} = 10\% = \Delta \Rightarrow I_{rr} = \frac{125}{1 + 125 \times 0.1} \approx 10$$

maximum boundary  $I_r = I_{rr} = 125$

from graph for  $\phi = 35^\circ$

for  $I_{rr} = 10 \Rightarrow N_o = 34$

for  $I_{rr} = 125 \Rightarrow N_o = 95$

$$\left. \begin{array}{l} q_{p(min)} = 34 \times 1.47^{tsf} = 50 \\ q_{p(max)} = 95 \times 1.47^{tsf} = 140 \end{array} \right\} \Rightarrow q_{p(avg)} = \underline{95^{tsf}}$$

Berezantzev:  $q_p = N_q (\sigma'_v \cdot \alpha_T)$

$D/B = 75 > 25 \therefore$  use 25 with  $\phi = 35^\circ$

from table  $\alpha_T = 0.65$

from graph with  $\phi = 35^\circ \Rightarrow N_q = 75$

$$q_p = 75 (2.37^{tsf} \times 0.65) = \underline{116^{tsf}}$$

SPT:  $q_p = 0.4 \cdot N_{corr} \times D/B \leq 4 \cdot N_{corr}$

$$N_{\phi tip} = 24; \quad \sigma'_{v \phi tip} = 2.37^{tsf}$$

$$N_{corr} = N \cdot \sqrt{\frac{1}{\sigma'_v}} = 24 \cdot \sqrt{\frac{1}{2.37^{tsf}}} = 15.6$$

$$q_p = 0.4 \times 15.6 \times \frac{80^{ft}}{1.0625^{ft}} = 470^{tsf} \leq 4 \times 15.6 = \underline{62^{tsf}}$$

Summary of  $q_p$  to get  $Q_p$ :

<u>Method</u>	<u><math>q_p</math></u>
Coyle & Castello	125 tsf
API	95 tsf
Meyerhof	25 tsf
Vesic - Simplified	88 tsf
Vesic - Advanced	95 tsf
Berezantsev	116 tsf
SPT	62 tsf

$$\Sigma = 606 \text{ tsf}$$

$$q_{p(\text{avg})} = \frac{606 \text{ tsf}}{7} = \underline{\underline{87 \text{ tsf}}}$$

$$Q_p = q_p \cdot A_p$$

$$= 87 \text{ tsf} \times 0.8866 \text{ ft}^2 = \underline{\underline{77 \text{ tons}}}$$

\* Find  $Q_s$ : (break up into layers according to different soil types, see Soil Profile)

Layer #1 O.C. Clay  $S_u = 1.0 \text{ tsf}$

$\alpha$  method:  $f_s = \alpha \cdot S_u$

$\sigma'_v(\text{@ midpoint}) = 0.58 \text{ tsf}$  (from Eff. Stress vs. Depth graph)

$$\psi = \frac{S_u}{\sigma'_v} = \frac{1.0 \text{ tsf}}{0.58 \text{ tsf}} = 1.72 > 1.0$$

$$\therefore \alpha = 0.5 \cdot \psi^{-0.25}$$

$$\alpha = 0.5 (1.72)^{-0.25} = 0.44 < 1.0 \text{ o.k.}$$

$$q_s = f_s = 0.44 \times 1.0 \text{ tsf} = 0.44 \text{ tsf}$$

$$Q_{s(1)} = f_s \cdot A_s = 0.44 \text{ tsf} \times (\pi \times 1.0625 \text{ ft} \times 8 \text{ ft})$$

$$Q_{s(1)} = \underline{12 \text{ tons}}$$

$\lambda$  method:  $f_s = \lambda (\sigma'_v + 2 \cdot S_u)$

$$\sigma'_{v_m} = 0.58 \text{ tsf} \text{ (from above)}$$

from figure with  $D_b = 80 \text{ ft} \Rightarrow \lambda = 0.15$

$$q_s = f_s = 0.15 (0.58 \text{ tsf} + 2 \times 1.0 \text{ tsf}) = 0.39 \text{ tsf}$$

$$Q_{s(1)} = f_s \cdot A_s = 0.39 \text{ tsf} \times (\pi \times 1.0625 \text{ ft} \times 8 \text{ ft})$$

$$Q_{s(1)} = \underline{10 \text{ tons}}$$

Summary of Layer 1:

$$Q_{s(1)} = \frac{12 \text{ tons} + 10 \text{ tons}}{2} = \underline{\underline{11 \text{ tons}}}$$

Layer #2      Soft N.C. Clay       $S_u = 0.33 \text{ tsf}$

$\alpha$  method:       $f_s = \alpha \cdot S_u$

$$\bar{\sigma}'_v (\text{@ midpoint}) = 0.94 \text{ tsf (from Eff. Stress vs. Depth graph)}$$

$$\psi = \frac{S_u}{\bar{\sigma}'_v} = \frac{0.33 \text{ tsf}}{0.94 \text{ tsf}} = 0.35 < 1.0$$

$$\therefore \alpha = 0.5 \cdot \psi^{-0.5}$$

$$\alpha = 0.5 (0.35)^{-0.5} = 0.85 < 1.0 \quad \text{o.k.}$$

$$q_s = f_s = 0.85 \times 0.33 \text{ tsf} = 0.28 \text{ tsf}$$

$$Q_s(z) = f_s \cdot A_s = 0.28 \text{ tsf} \times (\pi \times 1.0625 \text{ ft} \times 20 \text{ ft})$$

$$Q_s(z) = \underline{19 \text{ tons}}$$

$\lambda$  method:       $f_s = \lambda (\bar{\sigma}'_v + 2 \cdot S_u)$

$$\bar{\sigma}'_{vm} = 0.94 \text{ tsf (from above)}$$

$$\text{from figure with } D_b = 80 \text{ ft} \Rightarrow \lambda = 0.15$$

$$q_s = f_s = 0.15 (0.94 \text{ tsf} + 2 \times 0.33 \text{ tsf}) = 0.24 \text{ tsf}$$

$$Q_s(z) = f_s \cdot A_s = 0.24 \text{ tsf} \times (\pi \times 1.0625 \text{ ft} \times 20 \text{ ft})$$

$$Q_s(z) = \underline{16 \text{ tons}}$$

Summary of Layer 2:

$$Q_s(z) = \frac{19 \text{ tons} + 16 \text{ tons}}{2} = \boxed{17.5 \text{ tons}}$$

Layer #3 N.C. Clay  $S_u = 0.28 \text{ tsf}$

$\alpha$  method:  $f_s = \alpha \cdot S_u$

$$\sigma_v'(\text{@ midpoint}) = 1.38 \text{ tsf (from Eff. Stress vs. Depth graph)}$$

$$\psi = \frac{S_u}{\sigma_v'} = \frac{0.28 \text{ tsf}}{1.38 \text{ tsf}} = 0.20 < 1.0$$

$$\therefore \alpha = 0.5 \cdot \psi^{-0.5}$$

$$\alpha = 0.5 (0.20)^{-0.5} = 1.12 > 1.0 \text{ use } 1.0$$

$$q_s = f_s = 1.0 \times 0.28 \text{ tsf} = 0.28 \text{ tsf}$$

$$Q_s(3) = f_s \cdot A_s = 0.28 \text{ tsf} \times (\pi \times 1.0625 \text{ ft} \times 16 \text{ ft})$$

$$Q_s(3) = \underline{15 \text{ tons}}$$

$\lambda$  method:  $f_s = \lambda (\sigma_v' + 2 \cdot S_u)$

$$\sigma_{v'm} = 1.38 \text{ tsf (from above)}$$

$$\text{from figure with } D_b = 80' \Rightarrow \lambda = 0.15$$

$$q_s = f_s = 0.15 (1.38 \text{ tsf} + 2 \times 0.28 \text{ tsf}) = 0.29 \text{ tsf}$$

$$Q_s(3) = f_s \cdot A_s = 0.29 \text{ tsf} \times (\pi \times 1.0625 \text{ ft} \times 16 \text{ ft})$$

$$Q_s(3) = 15 \text{ tons}$$

Summary of Layer 3:

$$Q_s(3) = \frac{15 \text{ tons} + 15 \text{ tons}}{2} = \underline{\underline{15 \text{ tons}}}$$

Layer #4

Interbedded Silt, Sand, and Clay

Calculate both as clay with  $S_u = 0.30 \text{ tsf}$  & Sand with  $\phi = 35^\circ$

- As Clay:  $S_u = 0.30 \text{ tsf}$

$\alpha$  method:  $f_s = \alpha \cdot S_u$

$\sigma'_{v@midpoint} = 1.72 \text{ tsf}$  (from Eff. Stress vs. Depth graph)

$$\psi = \frac{S_u}{\sigma'_{v}} = \frac{0.30 \text{ tsf}}{1.72 \text{ tsf}} = 0.17 < 1.0$$

$$\therefore \alpha = 0.5 \psi^{-0.5}$$

$$\alpha = 0.5 (0.17)^{-0.5} = 1.21 > 1.0 \text{ use } 1.0$$

$$q_s = f_s = 1.0 \times 0.30 \text{ tsf} = 0.30 \text{ tsf}$$

$$Q_s(4) = f_s \cdot A_s = 0.30 \text{ tsf} \times (\pi \times 1.0625 \text{ ft} \times 9 \text{ ft})$$

$$Q_s(4) = \underline{9 \text{ tons}}$$

$\lambda$  method:  $f_s = \lambda (\sigma'_v + 2 \cdot S_u)$

$$\sigma'_{vm} = 1.72 \text{ tsf} \text{ (from above)}$$

$$\text{from figure with } D_b = 30' \Rightarrow \lambda = 0.15$$

$$q_s = f_s = 0.15 (1.72 \text{ tsf} + 2 \times 0.30 \text{ tsf}) = 0.35 \text{ tsf}$$

$$Q_s(4) = f_s \cdot A_s = 0.35 \text{ tsf} \times (\pi \times 1.0625 \text{ ft} \times 9 \text{ ft})$$

$$Q_s(4) = \underline{11 \text{ tons}}$$

Summary assuming layer 4 is clay with  $S_u = 0.30 \text{ tsf}$

$$Q_s(4) = \frac{9 \text{ tons} + 11 \text{ tons}}{2} = \underline{\underline{10 \text{ tons}}}$$



- A<sub>s</sub> Sand:  $\phi = 35^\circ$

General Values:  $f_s = \sigma_v' \cdot K \cdot \tan \delta$

after Mansur & Hunter (1970) use  $K = 1.25$

$$\delta = \frac{2}{3}\phi = \frac{2}{3}(35^\circ) = 23.3^\circ$$

considering critical depth for  $\phi = 35^\circ \Rightarrow D_c/B = 12$

$$\therefore D_c = 12 \times 1.0625 \text{ ft} = 13 \text{ ft} \text{ for which } \sigma_v' = 0.56 \text{ tsf}$$

from  $\sigma_v'$  vs. Depth graph

$$P_s = \pi \times 1.0625 \text{ ft} [9 \text{ ft} \times 0.56 \text{ tsf}] \times 1.25 \times \tan(23.3^\circ)$$

$$Q_s(4) = P_s = \underline{9 \text{ tons}}$$

API: (using charts)

$$K = 1.0; \quad \delta = 25^\circ; \quad f_{s\max} = 1.85 \frac{1}{4} \text{ ft}^2 = 0.925 \text{ tsf}$$

$$P_s = \pi \times 1.0625 \text{ ft} \left[ 9 \text{ ft} \times \left( \frac{1.59 \text{ tsf} + 1.85 \text{ tsf}}{2} \right) \right] \times 1.0 \times \tan 25^\circ$$

$$Q_s(4) = P_s = \underline{24 \text{ tons}}$$

$$\text{check } f_{s\max} = 1.85 \text{ tsf} \times 1.0 \times \tan 25^\circ = 0.86 \text{ tsf} < 0.925 \text{ tsf} \text{ o.k.}$$

$$\therefore Q_s(4) = \underline{24 \text{ tons}}$$

McClelland:

same as general values above, only use  $\delta = \phi = 35^\circ$

$$P_s = \pi \times 1.0625 \text{ ft} [9 \text{ ft} \times 0.56 \text{ tsf}] \times 1.25 \times \tan 35^\circ$$

$$Q_s(4) = P_s = \underline{15 \text{ tons}}$$

Meyerhof:  $f_s = N_{55}/50 \text{ (tsf)}$

from SPT calculations  $N_{avg} = 19$  for layer

take correction factor for the midpoint of layer  $\sigma_v' = 1.72 \text{ tsf}$

$$N_{corr} = N \cdot \sqrt{\frac{1}{\sigma_v'}} = 19 \cdot \sqrt{\frac{1}{1.72 \text{ tsf}}} = 14$$

$$N_{55} = \frac{70}{55} \times 14 = 18$$

$$f_s = \frac{18}{50} = 0.36 \text{ tsf}$$

$$P_s = f_s \cdot A_s = 0.36 \text{ tsf} \times (\pi \times 1.0625 \text{ ft} \times 9 \text{ ft})$$

$$Q_s(4) = P_s = \underline{11 \text{ tons}}$$

Summary assuming layer 4 is sand with  $\phi = 35^\circ$

$$Q_{s(4)} = \frac{9 \text{ tons} + 24 \text{ tons} + 15 \text{ tons} + 11 \text{ tons}}{4} = \underline{\underline{15 \text{ tons}}}$$

Summary of Layer 4:

Assuming layer is half silty sand and half Clay

$$Q_{s(4)} = \frac{10 \text{ tons} + 15 \text{ tons}}{2} = \boxed{\underline{12 \text{ tons}}}$$

Layer # 5 Silty Sand  $\phi = 35^\circ$

General Values:  $f_s = \sigma_v' \cdot K \cdot \tan \delta$

after Mansur & Hunter (1970) use  $K \approx 1.25$

$$\delta = \frac{2}{3}\phi = \frac{2}{3}(35^\circ) = 23.3^\circ$$

considering critical depth for  $\phi = 35^\circ \Rightarrow D_c/B = 12$

$$\therefore D_c = 12 \times 1.0625 \text{ ft} = 13 \text{ ft} \Rightarrow \text{for which } \sigma_v' = 0.56 \text{ tsf}$$

using  $\sigma_v'$  vs. depth graph

$$P_s = \pi \times 1.0625 \text{ ft} \times [8 \text{ ft} \times 0.56 \text{ tsf}] \times 1.25 \times \tan(23.3^\circ)$$

$$Q_s(s) = P_s = \underline{8 \text{ tons}}$$

API: (using charts)

$$K = 1.0; \delta = 28^\circ; f_{s\max} = 1.88 \text{ k/ft}^2 = 0.94 \text{ tsf}$$

$$P_s = \pi \times 1.0625 \text{ ft} \times \left[ 8 \text{ ft} \times \frac{(1.35 \text{ tsf} + 2.10 \text{ tsf})}{2} \right] \times 1.0 \times \tan 28^\circ$$

$$Q_s(s) = P_s = 28 \text{ tons}$$

$$\text{check } f_{s\max} = 2.10 \text{ tsf} \times 1.0 \times \tan 28^\circ = 1.12 > 0.94 \text{ tsf No Good!}$$

$\therefore$  max  $\sigma_v'$  to be used is:

$$\sigma_v' \times 1.0 \times \tan 28^\circ = 0.94 \text{ tsf} \Rightarrow \sigma_v' = 1.77 \text{ tsf which occurs @ } 60 \text{ ft}$$

$$\text{so, } P_s = \pi \times 1.0625 \text{ ft} \times [8 \text{ ft} \times 1.77 \text{ tsf}] \times 1.0 \times \tan 28^\circ$$

$$Q_s(s) = P_s = \underline{25 \text{ tons}}$$

McClelland:

same as general values above just use  $\delta = \phi = 35^\circ$

$$P_s = \pi \times 1.0625 \text{ ft} \times [8 \text{ ft} \times 0.56 \text{ tsf}] \times 1.25 \times \tan 35^\circ$$

$$Q_s(s) = P_s = \underline{13 \text{ tons}}$$

Meyerhof:  $f_s = N_{ss}/50 \text{ (tsf)}$

from SPT calculations  $N_{avg} = 34$  for layer

take correction factor for midpoint of layer  $\sigma_v' = 1.97 \text{ tsf}$

$$N_{corr} = N \cdot \sqrt{1/\sigma_v'} = 34 \cdot \sqrt{1/1.97 \text{ tsf}} = 24$$

$$N_{ss} = 70/55 \times 24 = 31$$

$$f_s = 31/50 = 0.62 \text{ tsf}$$

$$P_s = f_s \cdot A_s = 0.62 \text{ tsf} \times [\pi \times 1.0625 \text{ ft} \times 8 \text{ ft}]$$

$$Q_s(s) = P_s = \underline{17 \text{ tons}}$$

Summary of Layer 5:

$$Q_{s(5)} = \frac{8 \text{ tons} + 25 \text{ tons} + 13 \text{ tons} + 17 \text{ tons}}{4}$$

$$= \boxed{16 \text{ tons}}$$

Layer #6 Interbedded Silt, Sand, and Clay

Calculate both as clay with  $S_u = 0.30 \text{ tsf}$  and Sand with  $\phi = 35^\circ$

- As Clay:  $S_u = 0.30 \text{ tsf}$

$\alpha$  method:  $f_s = \alpha \cdot S_u$

$\sigma'_v(\text{@midpoint}) = 2.22 \text{ tsf}$  (from  $\sigma'_v$  vs. Depth graph)

$$\psi = \frac{S_u}{\sigma'_v} = \frac{0.30 \text{ tsf}}{2.22 \text{ tsf}} = 0.14 < 1.0$$

$$\therefore \alpha = 0.5 \psi^{-0.5} \\ = 0.5 (0.14)^{-0.5} = 1.34 > 1.0 \text{ use } 1.0$$

$$q_s = f_s = \alpha \cdot S_u = 1.0 \times 0.30 \text{ tsf} = 0.30 \text{ tsf}$$

$$Q_{s(6)} = f_s A_s = 0.30 \text{ tsf} \times (\pi \times 1.0625 \text{ ft} \times 8 \text{ ft})$$

$$Q_{s(6)} = \underline{8 \text{ tons}}$$

$\lambda$  method:  $f_s = \lambda (\sigma'_v + 2 \cdot S_u)$

$\sigma'_{vm} = 2.22 \text{ tsf}$  (from above)

from figure with  $D_b = 80' \Rightarrow \lambda = 0.15$

$$q_s = f_s = 0.15 (2.22 \text{ tsf} + 2 \times 0.30 \text{ tsf}) = 0.42 \text{ tsf}$$

$$Q_{s(6)} = f_s A_s = 0.42 \text{ tsf} \times (\pi \times 1.0625 \text{ ft} \times 8 \text{ ft})$$

$$Q_{s(6)} = \underline{11 \text{ tons}}$$

Summary assuming layer 6 is Clay with  $S_u = 0.30 \text{ tsf}$ :

$$Q_{s(6)} = \frac{8 \text{ tons} + 11 \text{ tons}}{2} = \underline{9 \text{ tons}}$$

- As Sand:  $\phi = 35^\circ$

General Values:  $f_s = \sigma_v' \cdot K \cdot \tan \delta$

after Mansur & Hunter (1970) use  $K = 1.25$

$$\delta = \frac{2}{3} \phi = \frac{2}{3} (35^\circ) = 23.3^\circ$$

considering critical depth for  $\phi = 35^\circ \Rightarrow D_c/B = 12$

$$\therefore D_c = 12 \times 1.0625 \text{ ft} = 13 \text{ ft for which } \sigma_v' = 0.56 \text{ tsf}$$

from  $\sigma_v'$  vs. Depth graph

$$P_s = \pi \times 1.0625 \text{ ft} \times (8 \text{ ft} \times 0.56 \text{ tsf}) \times 1.25 \times \tan(23.3^\circ)$$

$$Q_s(6) = P_s = \underline{8 \text{ tons}}$$

API: (using charts)

$$K = 1.0; \delta = 28^\circ; f_{s \max} = 1.88 \frac{\text{tsf}}{\text{ft}^2} = 0.94 \text{ tsf}$$

$$P_s = \pi \times 1.0625 \text{ ft} \times \left[ 8 \text{ ft} \times \frac{(2.10 \text{ tsf} + 2.33 \text{ tsf})}{2} \right] \times 1.0 \times \tan 28^\circ$$

$$Q_s(6) = P_s = \underline{31 \text{ tons}}$$

$$\text{check } f_{s \max} = 2.33 \text{ tsf} \times 1.0 \times \tan 28^\circ = 1.24 \text{ tsf} > 0.94 \text{ tsf} \quad \text{No! Good!}$$

$\therefore$  max  $\sigma_v'$  to be used is:

$$\sigma_v' \times 1.0 \times \tan 28^\circ = 0.94 \text{ tsf} \Rightarrow \sigma_v' = 1.77 \text{ tsf which occurs @ } 60 \text{ ft}$$

$$\text{so, } P_s = \pi \times 1.0625 \text{ ft} \times (8 \text{ ft} \times 1.77 \text{ tsf}) \times 1.0 \times \tan 28^\circ$$

$$Q_s(6) = P_s = \underline{25 \text{ tons}}$$

McClelland:

same as general values above, only use  $\delta = \phi = 35^\circ$

$$P_s = \pi \times 1.0625 \text{ ft} \times (8 \text{ ft} \times 0.56 \text{ tsf}) \times 1.25 \times \tan(35^\circ)$$

$$Q_s(6) = P_s = \underline{13 \text{ tons}}$$

Meyerhof:  $f_s = N_{55}/50 \text{ (tsf)}$

from SPT calculations  $N_{avg} = 41$  for layer

take correction factor for the midpoint of layer,  $\sigma_v' = 2.23 \text{ tsf}$

$$N_{corr} = N \cdot \sqrt{1/\sigma_v'} = 41 \sqrt{1/2.23 \text{ tsf}} = 27$$

$$N_{55} = 70/55 \times 27 = 35$$

$$f_s = 35/50 = 0.70 \text{ tsf}$$

$$P_s = f_s \cdot A_s = 0.70 \text{ tsf} \times (\pi \times 1.0625 \text{ ft} \times 8 \text{ ft})$$

$$Q_s(6) = P_s = \underline{19 \text{ tons}}$$

Summary assuming Layer 6 is sand with  $\phi = 35^\circ$

$$Q_{s(6)} = \frac{8 \text{ tons} + 25 \text{ tons} + 13 \text{ tons} + 19 \text{ tons}}{4} = \underline{\underline{16 \text{ tons}}}$$

Summary of Layer 6:

Assuming layer is half silty sand and half clay:

$$Q_{s(6)} = \frac{9 \text{ tons} + 16 \text{ tons}}{2} = \underline{\underline{13 \text{ tons}}}$$

Layer # 7 Fine to Medium Sand  $\phi = 35^\circ$

General Values:  $f_s = \sigma_v' \cdot K \cdot \tan \delta$

after Mansur & Hunter (1970) use  $K = 1.25$

$$\delta = \frac{2}{3} \phi = \frac{2}{3} (35^\circ) = 23.3^\circ$$

considering critical depth for  $\phi = 35^\circ = D_c/B = 12$

$$\therefore D_c = 12 \times 1.0625 \text{ ft} = 13 \text{ ft for which } \sigma_v' = 0.56 \text{ tsf}$$

using  $\sigma_v'$  vs. depth graph

$$P_s = \pi \times 1.0625 \text{ ft} \times (1 \text{ ft} \times 0.56 \text{ tsf}) \times 1.25 \times \tan(23.3^\circ)$$

$$Q_s(z) = P_s = \underline{1 \text{ ton}}$$

API: (using charts)

$$K = 1.0; \delta = 30^\circ; f_{s\max} = 2.0 \text{ k/ft}^2 = 1.0 \text{ tsf}$$

$$P_s = \pi \times 1.0625 \text{ ft} \times \left[ 1 \text{ ft} \times \frac{(2.33 \text{ tsf} + 2.36 \text{ tsf})}{2} \right] \times 1.0 \times \tan(30^\circ)$$

$$Q_s(z) = P_s = 5 \text{ tons}$$

$$\text{check } f_{s\max} = 2.37 \text{ tsf} \times 1.0 \times \tan 30^\circ = 1.36 \text{ tsf} > 1.0 \text{ tsf} \text{ No Good!}$$

$\therefore$  max  $\sigma_v'$  to be used is:

$$\sigma_v' \times 1.0 \times \tan 30^\circ = 1.0 \text{ tsf} \Rightarrow \sigma_v' = 1.73 \text{ tsf which occurs @ } 58 \text{ ft}$$

$$\text{so, } P_s = \pi \times 1.0625 \text{ ft} \times (1 \text{ ft} \times 1.73 \text{ tsf}) \times 1.0 \times \tan(30^\circ)$$

$$Q_s(z) = P_s = \underline{3 \text{ tons}}$$

McClelland:

same as general values above, only use  $\delta = \phi = 35^\circ$

$$P_s = \pi \times 1.0625 \text{ ft} \times (1 \text{ ft} \times 0.56 \text{ tsf}) \times 1.25 \times \tan(35^\circ)$$

$$Q_s(z) = P_s = \underline{2 \text{ tons}}$$

Meyerhof:  $f_s = N_{55}/50 \text{ (tsf)}$

from SPT calculations  $N_{avg} = 23$  for layer

take correction factor for the midpoint of layer  $\sigma_v' = 2.35 \text{ tsf}$

$$N_{corr} = N \cdot \sqrt{1/\sigma_v'} = 23 \times \sqrt{1/2.35 \text{ tsf}} = 19$$

$$N_{55} = \frac{70}{55} \times 15 = 19$$

$$f_s = 19/50 = 0.38 \text{ tsf}$$

$$P_s = f_s \cdot A_s = 0.38 \text{ tsf} \times (\pi \times 1.0625 \text{ ft} \times 1 \text{ ft})$$

$$Q_s(z) = P_s = \underline{1 \text{ ton}}$$



Summary of layer 7:

$$Q_s(7) = \frac{1 \text{ ton} + 3 \text{ tons} + 2 \text{ tons} + 1 \text{ ton}}{4}$$

$$= \boxed{2 \text{ tons}}$$

## SUMMARY OF $Q_{ULT}$ BY TRADITIONAL METHODS:

$$Q_p = 77 \text{ tons}$$

$Q_s$ :

<u>Layer i</u>	<u>Material</u>	<u><math>Q_{si}</math></u>
1	O.C. Clay	11 tons
2	Soft N.C. Clay	17 tons
3	N.C. Clay	15 tons
4	Silt, Sand, & Clay	12 tons
5	Silty Sand	16 tons
6	Silt, Sand, & Clay	13 tons
7	Fine to Med. Sand	<u>2 tons</u>

$$\Sigma = Q_s = \underline{86 \text{ tons}}$$

$Q_{ult} = ?$

$$Q_{ult} = Q_p + Q_s$$

$$= 77 \text{ tons} + 86 \text{ tons}$$

$$= \boxed{\underline{\underline{163 \text{ tons}}}}$$

## Calculations using SPT data to obtain $Q_{ult}$ :

$$Q_{ult} = Q_p + Q_s$$

where:  $Q_p = q_p \cdot A_p$

$$Q_s = q_s \cdot A_s$$

$$q_p = \frac{0.4 \cdot N_{corr} \cdot D_b}{D} \leq 4 \cdot N_{corr} \quad (\text{AASHTO 10.7.3.2.4.2a-1})$$

$$N_{corr} = [0.77 \cdot \log_{10}(\frac{20}{\sigma_v'})] \cdot N_{@tip} \quad (\text{AASHTO 10.7.3.2.4.2a-2})$$

$D$  = diameter of pile @ tip

$D_b$  = embedded length

$\sigma_v'$  = effective vertical stress @ tip in tsf

$$q_s = \frac{\bar{N}}{50} \text{ (tsf)} \quad (\text{AASHTO 10.7.3.2.4.2b-1})$$

$\bar{N}$  = average  $N$  along pile

\* Find  $Q_p$ :

$$N_{@tip} = 24$$

$$\begin{aligned} \sigma_v'_{@tip} = & 125 \frac{\text{lb}}{\text{ft}^2} \times 5.5 \text{ ft} + (125 - 62.4) \frac{\text{lb}}{\text{ft}^3} \times 2.5 \text{ ft} + (101 - 62.4) \frac{\text{lb}}{\text{ft}^3} \times 1 \text{ ft} \\ & + (120 - 62.4) \frac{\text{lb}}{\text{ft}^3} \times 9 \text{ ft} + (110 - 62.4) \frac{\text{lb}}{\text{ft}^3} \times 20 \text{ ft} + (115 - 62.4) \frac{\text{lb}}{\text{ft}^3} \times 16 \text{ ft} \\ & + (120 - 62.4) \frac{\text{lb}}{\text{ft}^3} \times 9 \text{ ft} + (125 - 62.4) \frac{\text{lb}}{\text{ft}^3} \times 8 \text{ ft} + (120 - 62.4) \frac{\text{lb}}{\text{ft}^3} \times 8 \text{ ft} \\ & + (125 - 62.4) \frac{\text{lb}}{\text{ft}^3} \times 1 \text{ ft} \end{aligned}$$

$$= 4,737.2 \frac{\text{lb}}{\text{ft}^2} = 2.37 \text{ tsf}$$

$$N_{corr} = [0.77 \cdot \log_{10}(\frac{20}{2.37 \text{ tsf}})] \times 24 = 17.12$$

$$q_p = \frac{0.4 \times 17.12 \times 71 \text{ ft}}{1.0625 \text{ ft}} = 453 \text{ tsf} \leq 4 \times 17.12 = \underline{68.5 \text{ tsf}}$$

$$A_p = \frac{\pi (12.75 \text{ in})^2}{4} = 127.7 \text{ in}^2 = 0.8866 \text{ ft}^2$$

$$Q_p = 68.5 \text{ tsf} \times 0.8866 \text{ ft}^2$$

$$= \underline{\underline{61 \text{ tons}}}$$

\* Find  $Q_s$ :

$$\begin{aligned}\bar{N} &= \left[ 4 \text{ ft} \times \left( \frac{13+26}{2} \right) + 10 \text{ ft} \times \left( \frac{26+0}{2} \right) + 25 \text{ ft} \times (0) + 5 \text{ ft} \times \left( \frac{0+22}{2} \right) \right. \\ &\quad + 5 \text{ ft} \times \left( \frac{22+16}{2} \right) + 5 \text{ ft} \times \left( \frac{16+22}{2} \right) + 10 \text{ ft} \times \left( \frac{22+54}{2} \right) + 5 \text{ ft} \times \left( \frac{54+21}{2} \right) \\ &\quad \left. + 2 \text{ ft} \times \left( \frac{21+24}{2} \right) \right] / 71 \text{ ft} \\ &= 15.01\end{aligned}$$

$$q_s = \frac{15.01}{50} = 0.3002 \text{ tsf}$$

$$A_s = \pi \times 1.0625^4 \times 71 \text{ ft} = 237.0 \text{ ft}^2$$

$$Q_s = 0.3002 \text{ tsf} \times 237.0 \text{ ft}^2 = \underline{\underline{71 \text{ tons}}}$$

Summary of  $Q_{ult}$  using SPT:

$$Q_p = \underline{\underline{61 \text{ tons}}}$$

$$Q_s = \underline{\underline{71 \text{ tons}}}$$

\* Find  $Q_{ult}$ :

$$Q_{ult} = 61 \text{ tons} + 71 \text{ tons}$$

$$= \underline{\underline{132 \text{ tons}}}$$

### Calculations using CPT data to obtain $Q_{ult}$ :

$$Q_{ult} = Q_p + Q_s$$

where:  $Q_p = q_p \cdot A_p$

$$Q_s = K_s \left[ \sum_{i=1}^{N_1} \left( \frac{L_i}{8D_i} \right) \cdot f_{s_i} \cdot a_{s_i} \cdot h_i + \sum_{i=N_1}^{N_2} f_{s_i} \cdot a_{s_i} \cdot h_i \right] \quad \left( \begin{array}{c} \text{AASHTO} \\ 10.7.3.4.3c-1 \end{array} \right)$$

$$q_p = \frac{q_{c1} + q_{c2}}{2} \quad (\text{AASHTO } 10.7.3.4.3b-1)$$

\*Find  $Q_p$ :

$$8D = 8(1.0625 \text{ ft}) = 8.5 \text{ ft}$$

$$4D = 4(1.0625 \text{ ft}) = 4.25 \text{ ft}$$

$$q_{c2} = (40^{tsf} \times 4 \text{ ft} + 105^{tsf} \times 4 \text{ ft} + 75^{tsf} \times 0.5 \text{ ft}) / 8.5 \text{ ft} = 72.65^{tsf}$$

$$q_{c1}(\text{min @ } 2 \text{ ft}) = (40^{tsf} \times 2 \text{ ft}) / 2 \text{ ft} = 40^{tsf}$$

$$q_p = \frac{72.65^{tsf} + 40^{tsf}}{2} = 56.33^{tsf}$$

$$A_p = \pi \times (12.75 \text{ in})^2 / 4 = 127.7 \text{ in}^2 = 0.8866 \text{ ft}^2$$

$$Q_p = 56.33^{tsf} \times 0.8866 \text{ ft}^2 = \underline{\underline{50 \text{ tons}}}$$

\*Find  $Q_s$ :

From figure 10.7.3.4.3c-1 of AASHTO with  
 $\gamma_D = 80 \text{ ft} / 1.0625 \text{ ft} = 75 \Rightarrow K_s = 0.30$

Pile Segment <u>i</u>	<u><math>L_i</math></u> (ft)	<u><math>D_i</math></u> (ft)	<u><math>f_{s_i}</math></u> (tsf)	<u><math>a_{s_i}</math></u> (ft <sup>2</sup> /ft)	<u><math>h_i</math></u> (ft)	<u><math>Q_{s_i}</math></u> (tons)
1	4.25	1.0625	0.05	3.338	8.5	0.2
2	N/A	N/A	0.05	3.338	1.5	0.1
3	N/A	N/A	1.70	3.338	5	8.5
4	N/A	N/A	0.10	3.338	31	3.1
5	N/A	N/A	0.70	3.338	9	5.6
6	N/A	N/A	0.95	3.338	4	3.9
7	N/A	N/A	0.60	3.338	5	3.0
8	N/A	N/A	1.60	3.338	15	24.0
9	N/A	N/A	0.60	3.338	2	1.2

Example calculations to get  $Q_s$ :

- pile segment 1:

$$Q_{s1} = 0.30 \times \left( \frac{4.25 \text{ ft}}{8 \times 1.0625 \text{ ft}} \right) \times 0.05 \text{ tsf} \times 3.338 \frac{\text{ft}^2}{\text{ft}} \times 8.5 \text{ ft} = 0.2 \text{ tons}$$

- pile segment 9:

$$Q_{s9} = 0.30 \times 0.60 \text{ tsf} \times 3.338 \frac{\text{ft}^2}{\text{ft}} \times 2 \text{ ft} = 1.2 \text{ tons}$$

$$\begin{aligned} Q_s &= \sum Q_{si} \\ &= 0.2 \text{ tons} + 0.1 \text{ tons} + 8.5 \text{ tons} + 3.1 \text{ tons} + 5.6 \text{ tons} + 3.8 \text{ tons} + 3.0 \text{ tons} \\ &\quad + 24.0 \text{ tons} + 1.2 \text{ tons} \\ &= \underline{\underline{50 \text{ tons}}} \end{aligned}$$

Summary of  $Q_{ult}$  using CPT:

$$Q_p = \underline{\underline{50 \text{ tons}}}$$

$$Q_s = \underline{\underline{50 \text{ tons}}}$$

\* Find  $Q_{ult}$ :

$$Q_{ult} = 50 \text{ tons} + 50 \text{ tons}$$

$$= \boxed{\underline{\underline{100 \text{ tons}}}}$$

## Analysis of Static Load Test Results:

### \* Analysis of compression static load test to find $Q_{ult}$ :

#### Limiting Total Settlement: (to 1.0 inch)

from compression test curve

$$Q_{ult} = \underline{75 \text{ tons}}$$

#### Limiting Plastic Settlement: (use Mass. Building Code $\frac{1}{2}$ inch)

from compression test curve

$$Q_{ult} = \underline{75 \text{ tons}}$$

#### Limiting Ratio: $0.01 \text{ inch/ton} \rightarrow$ too large ; $0.03 \text{ inch/ton}$

from compression test curve

$$Q_{ult} = 70 \text{ tons}$$

#### Davison's Criteria:

$$\Delta = \Delta_{\text{plastic}} + \Delta_{\text{elastic}}$$

$$\Delta_{\text{plastic}} = 0.15'' + \frac{B(\text{inch})}{120} = 0.15'' + \frac{12.75''}{120} = 0.26 \text{ in}$$

$$\Delta_{\text{elastic}} = \frac{PL}{EA} = \frac{P \cdot 80 \text{ ft} \times 12 \text{ in/ft}}{29,000 \text{ ksi} \times 19.24 \text{ in}^2 \times 1 \text{ ton}/2 \text{ kip}} = P \times 0.003441 \frac{\text{inch}}{\text{ton}}$$

$$\text{where } A = \frac{\pi(12.75 \text{ in})^2}{4} - \frac{\pi(12.75 \text{ in} - 2 \times 0.5 \text{ in})^2}{4} = 19.24 \text{ in}^2$$

$$\Delta = 0.26 \text{ in} + P \times 0.003441 \text{ in/ton}$$

from compression test curve

$$Q_{ult} = P = \underline{74 \text{ tons}}$$

#### Shape of Curve:

from compression test curve

$$Q_{ult} = \underline{74 \text{ tons}}$$

$$Q_{ult(\text{avg})} = \frac{75 \text{ tons} + 75 \text{ tons} + 70 \text{ tons} + 74 \text{ tons} + 74 \text{ tons}}{5} = \underline{\underline{74 \text{ tons}}}$$

\* Analysis of tension static load test to find  $Q_s$ :

Limiting Total Movement: (to 1.0 inch)

from tension test curve

$$Q_s = \underline{48 \text{ tons}}$$

Limiting Plastic Movement: (use Mass. Building Code  $\frac{1}{2}$  inch)

from tension test curve

$$Q_s = \underline{48 \text{ tons}}$$

Limiting Ratio: ~~0.01 inch/ton~~  $\rightarrow$  too large;  $0.03 \text{ in/ton}$

from tension test curve

$$Q_s = \underline{42 \text{ tons}}$$

Davisson's Criteria:  $\Delta = \Delta_{\text{plastic}} + \Delta_{\text{elastic}}$

$$\Delta_{\text{plastic}} = 0.15" + \frac{B(\text{inch})}{120} = 0.15" + \frac{12.75"}{120} = 0.26 \text{ in}$$

$$\Delta_{\text{elastic}} = \frac{PL}{EA} = \frac{P \times 80 \text{ ft} \times 12 \frac{\text{in}}{\text{ft}}}{29,000 \frac{\text{ksi}}{\text{in}^2} \times 19.24 \text{ in}^2 \times 1 \frac{\text{ton}}{2 \text{ kips}}} = P \times 0.003441 \frac{\text{in}}{\text{ton}}$$

$$\text{where } A = \frac{\pi (12.75 \text{ in})^2}{4} - \frac{\pi (12.75 \text{ in} - 2 \times 0.5 \text{ in})^2}{4} = 19.24 \text{ in}^2$$

$$\Delta = 0.26 \text{ in} + P \times 0.003441 \text{ in/ton}$$

from tension test curve

$$Q_s = P = \underline{45 \text{ tons}}$$

Shape of Curve:

from tension test curve

$$Q_s = \underline{47 \text{ tons}}$$

$$Q_{s(\text{avg})} = \frac{48 \text{ tons} + 48 \text{ tons} + 42 \text{ tons} + 45 \text{ tons} + 47 \text{ tons}}{5} = \underline{\underline{46 \text{ tons}}}$$



Summary of  $Q_{ult}$  by Static Load Test Results:

$$Q_{ult} = \boxed{\underline{\underline{74 \text{ tons}}}}$$

$$Q_s = \underline{\underline{46 \text{ tons}}}$$

$$Q_p = Q_{ult} - Q_s = 74 \text{ tons} - 46 \text{ tons}$$

$$Q_p = \underline{\underline{28 \text{ tons}}}$$

Figure B-1  
Blow Count vs. Depth for Newbury Site

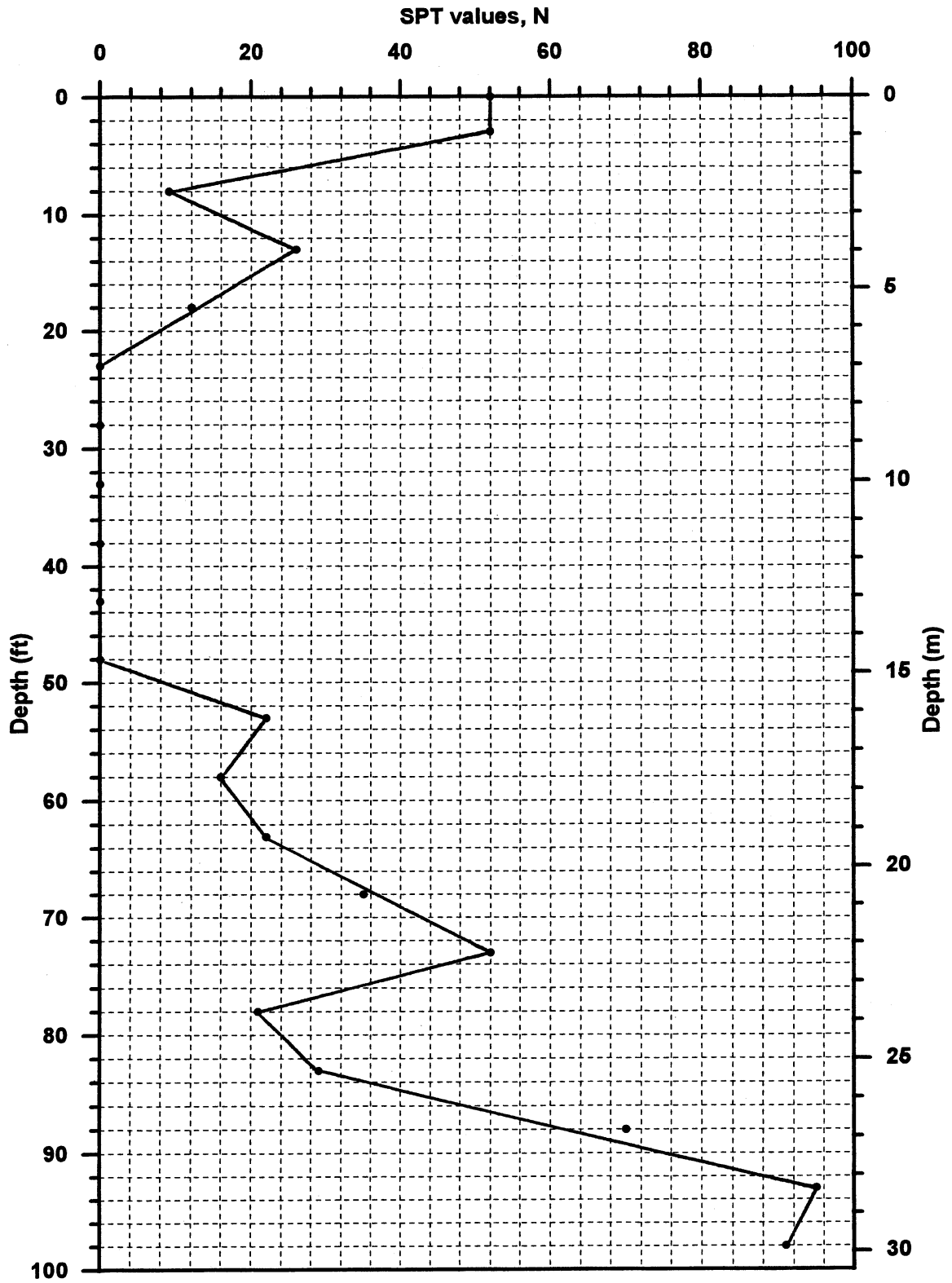


**Figure B-2**  
**Vertical Effective Stress vs Depth for Newbury Site**

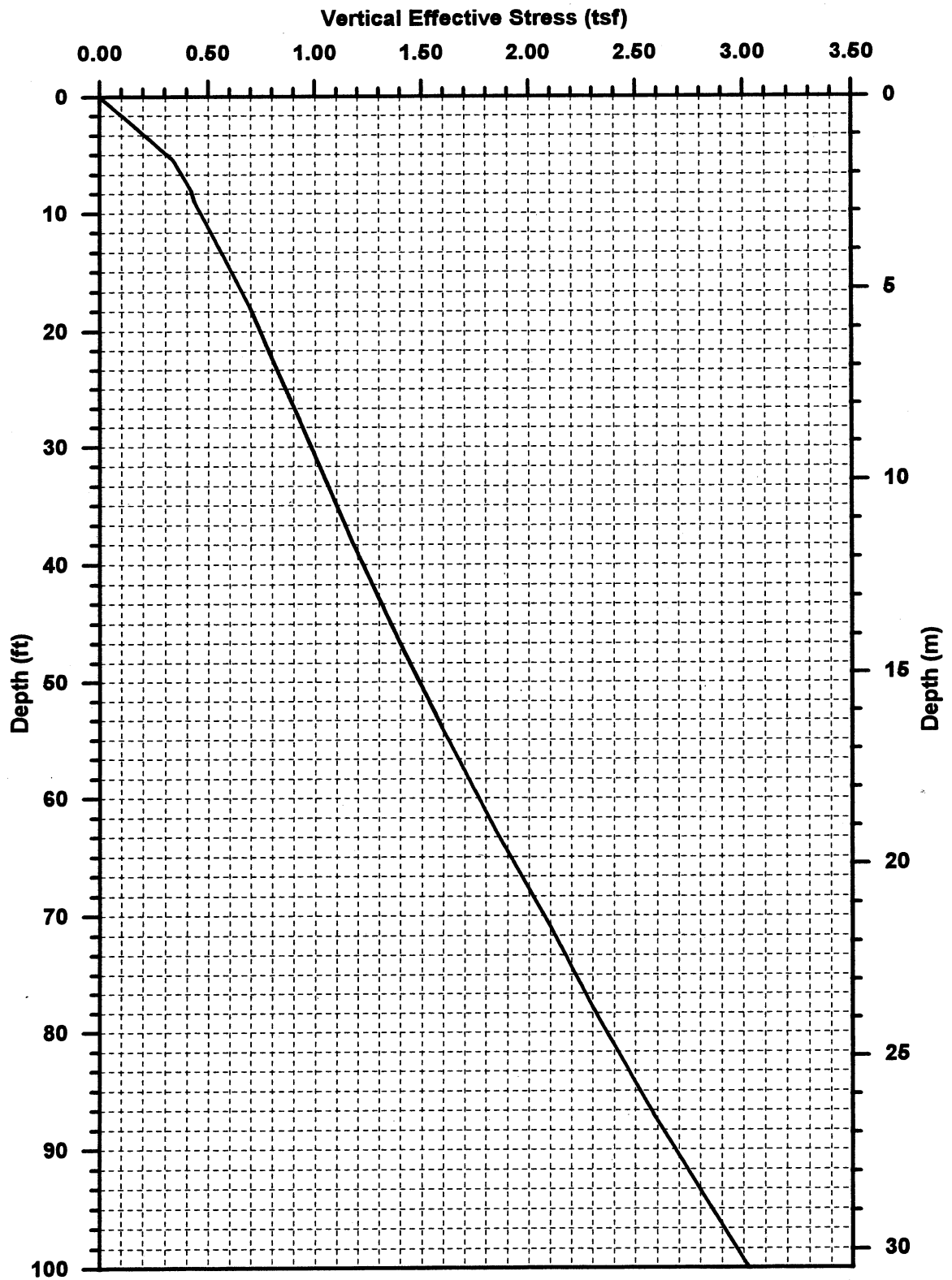


Figure B-3  
Tip Resistance vs Depth, CPT's, Newbury Site

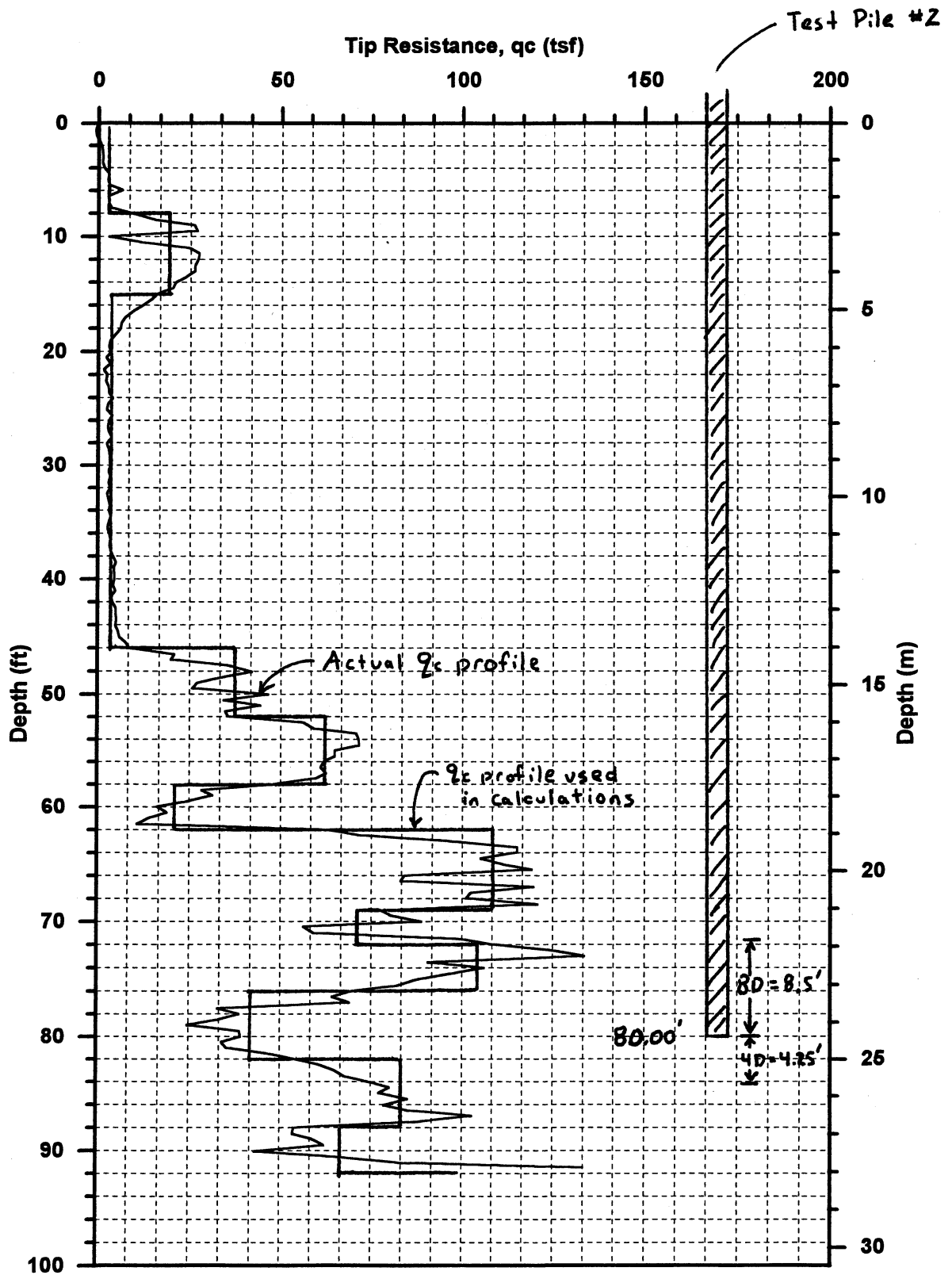


Figure B-4  
Side Resistance vs Depth, CPT's, Newbury Site

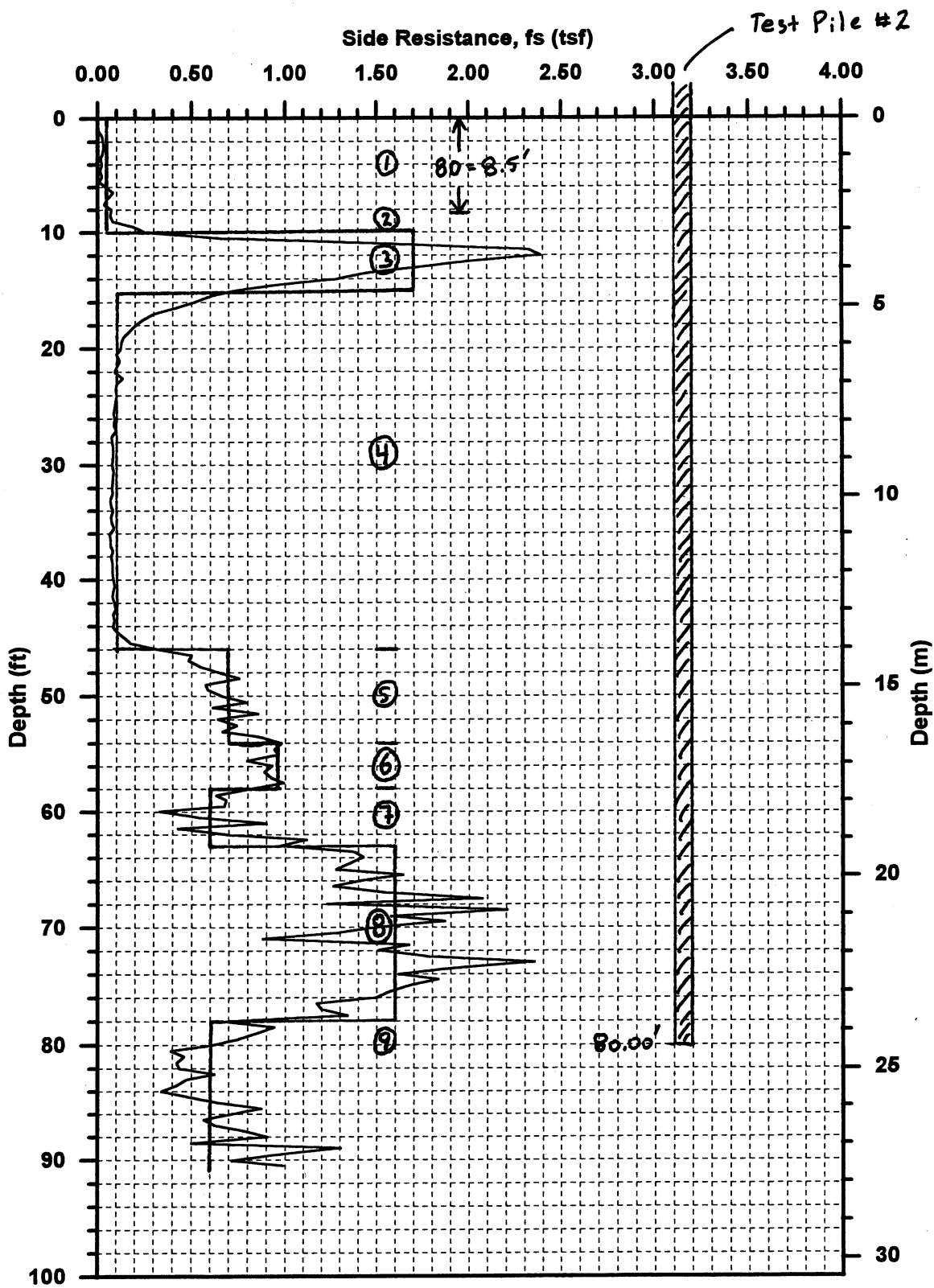


Figure B-5  
Load vs Deflection Curve, Compression Test, Newbury Site

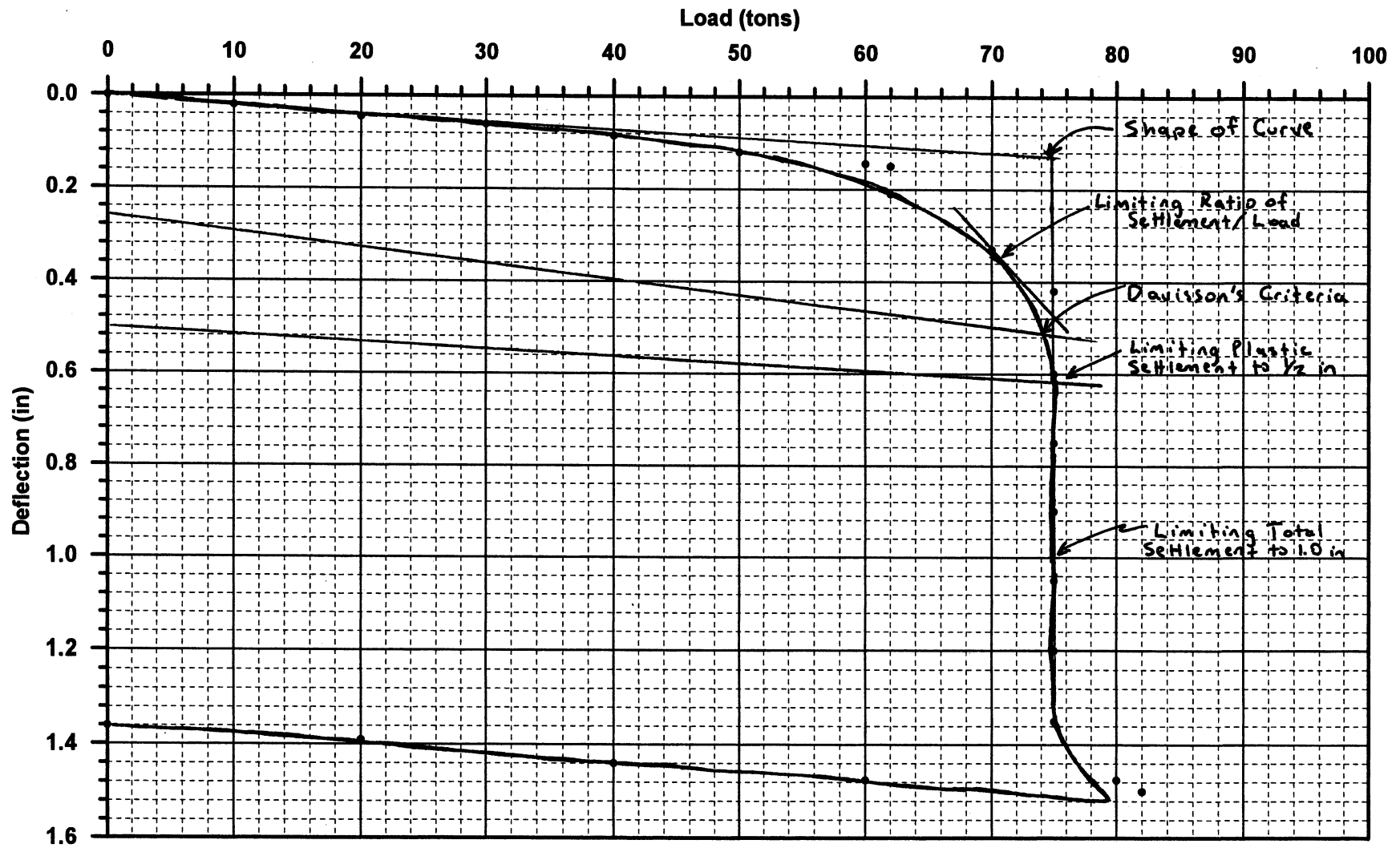
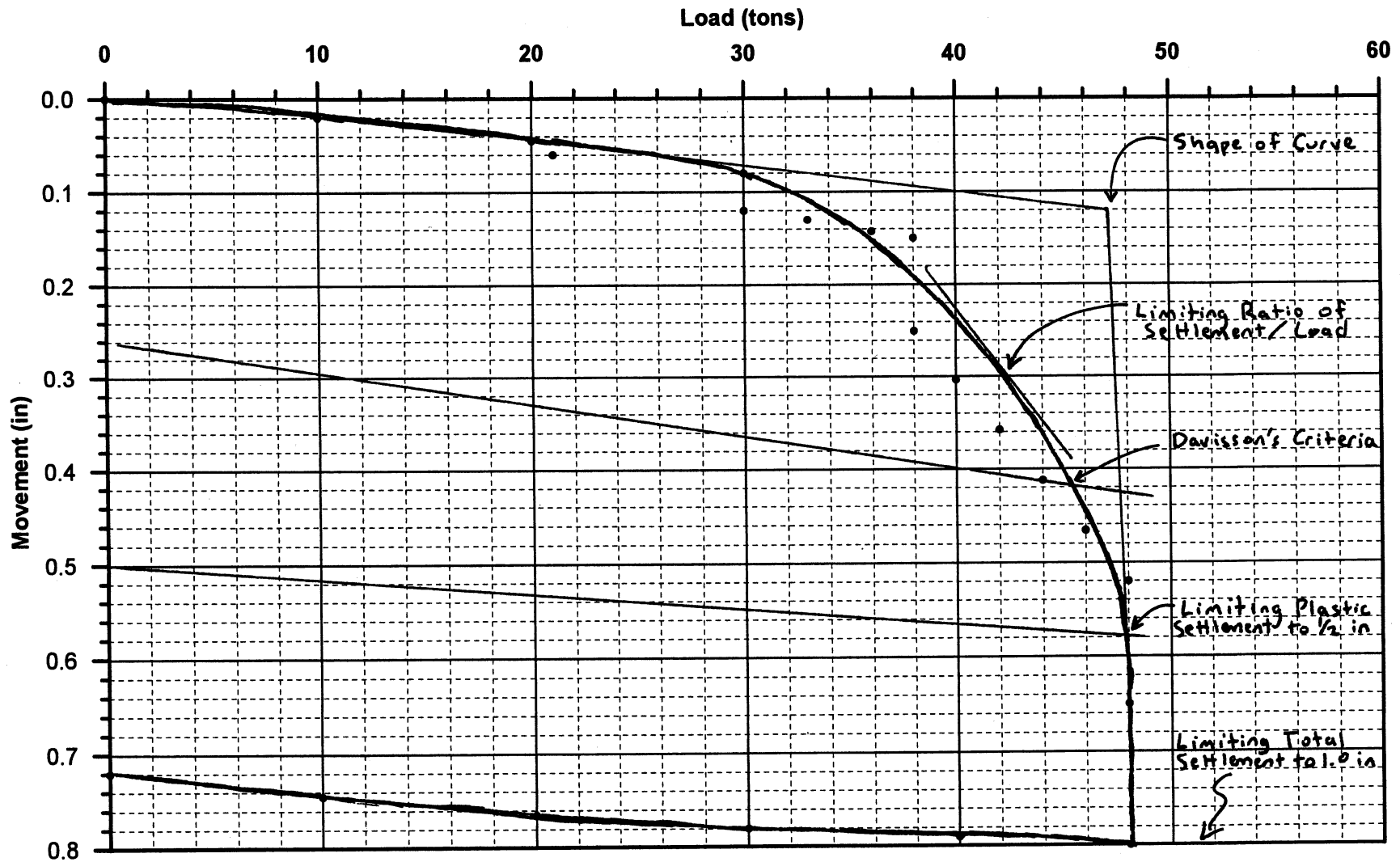


Figure B-6  
Load vs Deflection Curve, Tension Test, Newbury Site



## **APPENDIX C**

### **CALCULATED RESISTANCE FACTORS BY CALIBRATING TO THE STATIC LOAD TEST RESULTS**



### Calculated Resistance Factors:

$$Q_R = \phi \times Q_{ult} = \text{constant (for any method)}$$

$$\phi_A \times Q_{ult A} = \phi_B \times Q_{ult B}$$

$$\phi_B = 1.0 = \phi_{\text{load test (assumed)}}$$

$$\therefore \phi_A = \frac{Q_{ult B}}{Q_{ult A}}$$

### Newbury Site Project, Test Pile #2:

$$Q_{ult} (\text{load test}) = 74 \text{ tons}$$

$$Q_{ult} (\text{SPT}) = 132 \text{ tons}$$

$$Q_{ult} (\text{CPT}) = 100 \text{ tons}$$

$$Q_{ult} (\text{Nordlund}) = 167 \text{ tons}$$

$$Q_{ult} (\text{Traditional Methods}) = 163 \text{ tons}$$

- SPT Method:

$$\phi_{\text{SPT}} = \frac{74 \text{ tons}}{132 \text{ tons}} = \underline{\underline{0.56}}$$

- CPT Method:

$$\phi_{\text{CPT}} = \frac{74 \text{ tons}}{100 \text{ tons}} = \underline{\underline{0.74}}$$

- Driven 1.0 (Nordlund Method):

$$\phi_{\text{Nordlund}} = \frac{74 \text{ tons}}{167 \text{ tons}} = \underline{\underline{0.44}}$$

- Traditional Methods:

$$\phi_{\text{T.M.}} = \frac{74 \text{ tons}}{163 \text{ tons}} = \underline{\underline{0.45}}$$

Newbury Site Project, Test Pile #3:

$$Q_{ult}(\text{load test}) = 98 \text{ tons}$$

$$Q_{ult}(\text{SPT}) = 192 \text{ tons}$$

$$Q_{ult}(\text{CPT}) = 158 \text{ tons}$$

$$Q_{ult}(\text{Nordlund}) = 300 \text{ tons}$$

$$Q_{ult}(\text{Traditional Methods}) = 241 \text{ tons}$$

- SPT Method:

$$\phi_{\text{SPT}} = \frac{98 \text{ tons}}{192 \text{ tons}} = \underline{\underline{0.51}}$$

- CPT Method:

$$\phi_{\text{CPT}} = \frac{98 \text{ tons}}{192 \text{ tons}} = \underline{\underline{0.62}}$$

- Driven I.O (Nordlund Method):

$$\phi_{\text{Nordlund}} = \frac{98 \text{ tons}}{300 \text{ tons}} = \underline{\underline{0.33}}$$

- Traditional Methods:

$$\phi_{\text{T.M.}} = \frac{98 \text{ tons}}{241 \text{ tons}} = \underline{\underline{0.41}}$$

## West Bay Project, Test Pile #9

$$Q_{ult}(\text{load test}) = 468 \text{ tons}$$

$$Q_{ult}(\text{SPT}) = 590 \text{ tons}$$

$$Q_{ult}(\text{CPT}) = 340 \text{ tons}$$

$$Q_{ult}(\text{Nordlund}) = 1124 \text{ tons}$$

$$Q_{ult}(\text{Traditional Methods}) = 881 \text{ tons}$$

- SPT Method:

$$\phi_{\text{SPT}} = \frac{468 \text{ tons}}{590 \text{ tons}} = \underline{\underline{0.79}}$$

- CPT Method:

$$\phi_{\text{CPT}} = \frac{468 \text{ tons}}{340 \text{ tons}} = \underline{\underline{1.38}}$$

- Driven 1.0 (Nordlund Method)

$$\phi_{\text{Nordlund}} = \frac{468 \text{ tons}}{1124 \text{ tons}} = \underline{\underline{0.42}}$$

- Traditional Methods:

$$\phi_{\text{T.M.}} = \frac{468 \text{ tons}}{881 \text{ tons}} = \underline{\underline{0.53}}$$

West Bay Project, Test Pile #15:

$$Q_{ult} \text{ (load test)} = 423 \text{ tons}$$

$$Q_{ult} \text{ (SPT)} = 564 \text{ tons}$$

$$Q_{ult} \text{ (CPT)} = 481 \text{ tons}$$

$$Q_{ult} \text{ (Nordlund)} = 1048 \text{ tons}$$

$$Q_{ult} \text{ (Traditional Methods)} = 830 \text{ tons}$$

- SPT Method:

$$\phi_{SPT} = \frac{423 \text{ tons}}{564 \text{ tons}} = \underline{\underline{0.75}}$$

- CPT Method:

$$\phi_{CPT} = \frac{423 \text{ tons}}{481 \text{ tons}} = \underline{\underline{0.88}}$$

- Driven I.O (Nordlund Method):

$$\phi_{Nordlund} = \frac{423 \text{ tons}}{1048 \text{ tons}} = \underline{\underline{0.40}}$$

- Traditional Methods:

$$\phi_{T.M.} = \frac{423 \text{ tons}}{830 \text{ tons}} = \underline{\underline{0.51}}$$

**APPENDIX D**

**CASE HISTORY CALCULATIONS COMPARING**

**THE WSD METHOD, THE LRFD METHOD AND**

**THE PRESENT AASHTO CODE**

## Static Pile Capacity Calculations

The presented calculations will compare the pile capacity predictions based on the Working Stress Design (WSD), the present AASHTO code, and the resistance factors as recommended in Chapter 9.

### Working Stress Design Method:

$$Q_{all} = \frac{Q_{ult}}{FS}$$

for which:

$$Q_{ult} = Q_s + Q_p$$

where:

$$Q_s = q_s \times A_s$$

$$Q_p = q_p \times A_p$$

$Q_{all}$  = allowable or factored bearing resistance (F)

$Q_{ult}$  = bearing resistance of a single pile (F)

$Q_s$  = pile shaft resistance (F)

$Q_p$  = pile tip resistance (F)

$q_s$  = unit shaft resistance of pile (F/L<sup>2</sup>)

$q_p$  = unit tip resistance of pile (F/L<sup>2</sup>)

$A_s$  = surface area of pile shaft (L<sup>2</sup>)

$A_p$  = area of pile tip (L<sup>2</sup>)

### Present AASHTO Code (1998):

$$Q_{all} = \phi_q \times Q_{ult} = \phi_{qs} \times Q_s + \phi_{qp} \times Q_p$$

for which:

$$Q_s = q_s \times A_s$$

$$Q_p = q_p \times A_p$$

where:

- $Q_{all}$  = factored bearing resistance
- $Q_{ult}$  = bearing resistance of a single pile (F)
- $Q_s$  = pile shaft resistance (F)
- $Q_p$  = pile tip resistance (F)
- $q_s$  = unit shaft resistance of pile (F/L<sup>2</sup>)
- $q_p$  = unit tip resistance of pile (F/L<sup>2</sup>)
- $A_s$  = surface area of pile shaft (L<sup>2</sup>)
- $A_p$  = area of pile tip (L<sup>2</sup>)
- $\phi_q$  = resistance factor for those methods that do not separate the resistance of a pile into contributions from the tip and shaft resistance.
- $\phi_{qs}$  = resistance factor for shaft resistance specified in Table 10.5.5-2 of the 1998 AASHTO code for those method that separate the resistance of a pile into contributions from tip resistance and shaft resistance.
- $\phi_{qp}$  = resistance factor for tip resistance specified in Table 10.5.5-2 of the 1998 AASHTO code for those method that separate the resistance of a pile into contributions from tip resistance and shaft resistance.

#### **Recommended Resistance Factors:**

The recommendation is to use the same process as described above and in the present AASHTO code, only using the resistance factors that were calculated in Chapter 9 and as presented in Table 9.6.

The process used for comparing predicted allowable pile capacities using the dynamic methods and the different codes and recommendations is a difficult one, as a direct comparison cannot be made. The problem lies in the present AASHTO code, which does not have recommended resistance factors for the dynamic methods. The method that is recommended is to calculate the pile capacity using the static methods and then if using a dynamic method to verify the pile capacity the static methods resistance factor can be multiplied by a  $\lambda$  factor. Therefore, the first step in comparing

the different codes and the recommendations is to calculate the pile capacity using the static methods as described in the 1998 AASHTO code.

**Static methods to be used:**

***For the cohesive layers:***

**$\alpha$  – method:**

$$q_s = \alpha \times S_u$$

where:  $S_u$  = mean undrained shear strength (tsf)  
 $\alpha$  = adhesion factor

**$\beta$  – method:**

$$q_s = \beta \times \sigma'_v$$

where:  $\sigma'_v$  = vertical effective stress (tsf)  
 $\beta$  = skin friction factor

**$\lambda$  – method:**

$$q_s = \lambda \times (\sigma'_v + 2 \times S_u)$$

where:  $\sigma'_v + 2S_u$  = passive lateral earth pressure (tsf)  
 $\lambda$  = an empirical coefficient

***For the Cohesionless layers:***

**SPT – method:**

$$q_p = \frac{0.4 \times N_{corr} \times D_b}{D} \leq q_t$$

for which:

$$N_{corr} = \left[ 0.77 \times \log_{10} \left( \frac{20}{\sigma'_v} \right) \right] \times N$$



where:

- $N_{corr}$  = representative SPT blow count near the pile tip corrected for overburden pressure  $\sigma'_v$  (blows/ft)  
 $N$  = measured SPT blow count (blows/ft)  
 $D$  = pile width or diameter (ft)  
 $D_b$  = depth of penetration in bearing strata (ft)  
 $q_l$  = limiting point resistance taken as  $4N_{corr}$  for sands and  $3N_{corr}$  for nonplastic silt (tsf)

$$q_s = \frac{\bar{N}}{50} \text{ for driven displacement piles}$$

$$q_s = \frac{\bar{N}}{100} \text{ for nondisplacement pile (e.g., steel H-piles)}$$

where:

- $q_s$  = unit skin friction for driven piles  
 $\bar{N}$  = average (uncorrected) SPT-blow count along the pile shaft (blows/ft)

***Applied to all layers:***

CPT – method:

$$q_p = \frac{q_{c1} + q_{c2}}{2}$$

where:

- $q_{c1}$  = average  $q_c$  over a distance of  $yD$  below the pile tip (see AASHTO code for details).  
 $q_{c2}$  = average  $q_c$  over a distance of  $8D$  above the pile tip (see AASHTO code for details)

$$Q_s = K_{s,c} \left[ \sum_{i=1}^{N_1} \left( \frac{L_i}{8D_i} \right) f_{si} a_{si} h_i + \sum_{i=1}^{N_2} f_{si} a_{si} h_i \right]$$

where:

- $K_{s,c}$  = correction factors:  $K_c$  for clays and  $K_s$  for sands from Figure 10.7.3.4.3c-1 of AASHTO code (DIM).
- $L_i$  = depth to middle of length interval at the point considered (ft).
- $D_i$  = pile width or diameter at the point considered (ft).
- $f_{si}$  = unit local sleeve friction resistance from CPT at the point considered (tsf).
- $a_{si}$  = pile perimeter at the point considered (ft).
- $h_i$  = length interval at the point considered (ft).
- $N_1$  = number of intervals between the ground surface and a point 8D below the ground surface.
- $N_2$  = number of intervals between 8D below the ground surface and the tip of the pile.

**Newbury Test Site (2 friction piles):**

**Soil Layers (see also Figure D.1):**

Layer 1:	Overconsolidated Clay	$\gamma = 120 \text{ pcf}$	$S_u = 1.0 \text{ tsf}$
Layer 2:	Soft Normally Consolidated Clay	$\gamma = 110 \text{ pcf}$	$S_u = 0.33 \text{ tsf}$
Layer 3:	Normally Consolidated Clay	$\gamma = 115 \text{ pcf}$	$S_u = 0.28 \text{ tsf}$
Layer 4:	Interbedded Sand, Silt, and Clay	$\gamma = 120 \text{ pcf}$	$N' = 14.3$
	Therefore, from Bowles, 1996		$\phi = 34^\circ$
Layer 5:	Silty Sand	$\gamma = 125 \text{ pcf}$	$\phi = 35^\circ$
Layer 6:	Interbedded Sand, Silt, and Clay	$\gamma = 120 \text{ pcf}$	$N' = 25.5$
	Therefore, from Bowles, 1996		$\phi = 36^\circ$
Layer 7:	Fine to Medium Sand	$\gamma = 125 \text{ pcf}$	$\phi = 35^\circ$

Note: It is assumed that the two interbedded layers act as a Cohesionless soil.

**Test Pile # 2 (12.75" closed ended steel pipe pile driven 80ft, top 10 ft is encased):**

**Skin Friction:**

**Layer 1 (8 ft thick layer):**

$$A_s = \pi \times 12.75 \text{ in} \times 8 \text{ ft} \times \frac{1 \text{ ft}}{12 \text{ in}} = 26.704 \text{ ft}^2$$

**$\alpha$  – method:**

from Figure 10.7.3.3.2a-1 of 1998 AASHTO code with  $S_u = 1.0 \text{ tsf}$ ,  $\alpha = 0.90$

$$q_s = 0.90 \times 1.0 = 0.90 \text{ tsf}$$

$$Q_s = 0.90 \text{ tsf} \times 26.704 \text{ ft}^2 = 24.03 \text{ tons}$$

**$\beta$  – method:**

From Paikowsky and Chen (1998),  $\text{OCR} \approx 9$  at 14 ft, therefore from Figure 10.7.3.3.2b-1 of 1998 AASHTO code  $\beta = 1.3$ .  $\sigma'_v = 0.582 \text{ tsf}$  at 14 ft (midpoint of layer).

$$q_s = 1.3 \times 0.582 \text{ tsf} = 0.756 \text{ tsf}$$

$$Q_s = 0.756 \text{tsf} \times 26.704 \text{ft}^2 = 20.19 \text{tons}$$

$\lambda$  - method:

From Figure 10.7.3.3.2c-1 of the 1998 AASHTO,  $\lambda = 0.15$

$$q_s = 0.15 \times (0.582 \text{tsf} + 2 \times 1.0 \text{tsf}) = 0.387 \text{tsf}$$

$$Q_s = 0.387 \text{tsf} \times 26.704 \text{ft}^2 = 10.33 \text{tons}$$

Layer 2 (20 ft thick layer):

$$A_s = \pi \times 12.75 \text{in} \times 20 \text{ft} \times \frac{1 \text{ft}}{12 \text{in}} = 66.759 \text{ft}^2$$

$\alpha$  - method:

from Figure 10.7.3.3.2a-1 of 1998 AASHTO code with  $S_u = 0.33 \text{tsf}$ ,  $\alpha = 0.97$

$$q_s = 0.97 \times 0.33 = 0.320 \text{tsf}$$

$$Q_s = 0.320 \text{psf} \times 66.759 \text{ft}^2 = 21.36 \text{tons}$$

$\beta$  - method:

From Paikowsky and Chen (1998),  $\text{OCR} \approx 1$  at 28 ft, therefore from Figure 10.7.3.3.2b-1 of 1998 AASHTO code  $\beta = 0.3$ .  $\sigma'_v = 0.935 \text{tsf}$  at 28 ft (midpoint of layer).

$$q_s = 0.3 \times 0.935 \text{tsf} = 0.281 \text{tsf}$$

$$Q_s = 0.281 \text{tsf} \times 66.759 \text{ft}^2 = 18.76 \text{tons}$$

$\lambda$  - method:

From Figure 10.7.3.3.2c-1 of the 1998 AASHTO,  $\lambda = 0.15$

$$q_s = 0.15 \times (0.935 \text{tsf} + 2 \times 0.33 \text{tsf}) = 0.239 \text{tsf}$$

$$Q_s = 0.239 \text{tsf} \times 66.759 \text{ft}^2 = 15.96 \text{tons}$$

Layer 3 (16 ft thick layer):

$$A_s = \pi \times 12.75 \text{ in} \times 16 \text{ ft} \times \frac{1 \text{ ft}}{12 \text{ in}} = 53.407 \text{ ft}^2$$

$\alpha$  – method:

from Figure 10.7.3.3.2a-1 of 1998 AASHTO code with  $S_u = 0.28 \text{ tsf}$ ,  $\alpha = 0.98$

$$q_s = 0.98 \times 0.28 = 0.274 \text{ tsf}$$

$$Q_s = 0.274 \text{ tsf} \times 53.407 \text{ ft}^2 = 14.63 \text{ tons}$$

$\beta$  – method:

From Paikowsky and Chen (1998),  $\text{OCR} \approx 1$  at 46 ft, therefore from Figure 10.7.3.3.2b-1 of 1998 AASHTO code  $\beta = 0.3$ .  $\sigma'_v = 1.384 \text{ tsf}$  at 46 ft (midpoint of layer).

$$q_s = 0.3 \times 1.384 \text{ tsf} = 0.415 \text{ tsf}$$

$$Q_s = 0.415 \text{ psf} \times 53.407 \text{ ft}^2 = 22.16 \text{ tons}$$

$\lambda$  - method:

From Figure 10.7.3.3.2c-1 of the 1998 AASHTO,  $\lambda = 0.15$

$$q_s = 0.15 \times (1.384 \text{ tsf} + 2 \times 0.28 \text{ tsf}) = 0.292 \text{ tsf}$$

$$Q_s = 0.292 \text{ tsf} \times 53.407 \text{ ft}^2 = 15.59 \text{ tons}$$

Layer 4 (9 ft layer):

$$A_s = \pi \times 12.75 \text{ in} \times 9 \text{ ft} \times \frac{1 \text{ ft}}{12 \text{ in}} = 30.041 \text{ ft}^2$$

SPT method:

$$\bar{N} = 18.5$$

$$q_s = \frac{18.5}{50} = 0.370tsf$$

$$Q_s = 0.370tsf \times 30.041ft^2 = 11.12 tons$$

Layer 5 (8 ft layer):

$$A_s = \pi \times 12..75in \times 8ft \times \frac{1ft}{12in} = 26.704ft^2$$

SPT method:

$$\overline{N} = 32.9$$

$$q_s = \frac{32.9}{50} = 0.658tsf$$

$$Q_s = 0.658tsf \times 26.704ft^2 = 17.57 tons$$

Layer 6 (8 ft layer):

$$A_s = \pi \times 12..75in \times 8ft \times \frac{1ft}{12in} = 26.704ft^2$$

SPT method:

$$\overline{N} = 38.1$$

$$q_s = \frac{38.1}{50} = 0.762tsf$$

$$Q_s = 0.762tsf \times 26.704ft^2 = 20.35 tons$$

Layer 7 (1 ft layer):

$$A_s = \pi \times 12..75in \times 1ft \times \frac{1ft}{12in} = 3.338ft^2$$

SPT method:

$$\overline{N} = 23.4$$

$$q_s = \frac{23.4}{50} = 0.468 \text{ tsf}$$

$$Q_s = 0.468 \text{ tsf} \times 3.338 \text{ ft}^2 = 1.56 \text{ tons}$$

***Tip of Pile:***

$$A_p = \pi \times \left( \frac{12.75}{2} \right)^2 = 127.68 \text{ in}^2 = 0.8866 \text{ ft}^2$$

SPT method:

$\sigma'_v = 2.365 \text{ tsf}$  and  $N = 24.2$  at the tip, i.e., depth of 80 ft.

$$N_{corr} = \left[ 0.77 \times \log_{10} \left( \frac{20}{2.365} \right) \right] \times 24.2 = 17.3$$

$$D = 12.75 \text{ in} = 1.0625 \text{ ft}, D_b = 80 \text{ ft}$$

$$q_p = \frac{0.4 \times 17.3 \times 80 \text{ ft}}{1.0625 \text{ ft}} = 521 \text{ tsf} \leq 4 \times 17.3 = 69.2 \text{ tsf}$$

therefore,

$$q_p = 69.2 \text{ tsf}$$

$$Q_p = 69.2 \text{ tsf} \times 0.8866 \text{ ft}^2 = 61.35 \text{ tons}$$

***CPT method:***

Skin Friction:

$8D = 8.5 \text{ ft}$ , therefore, the first term in calculating the skin friction is not needed as the pile is cased to 10 ft.

$$\frac{L}{D} = \frac{80 \text{ ft}}{1.0625 \text{ ft}} = 75, \text{ from Figure 10.7.3.4.3c-1 of AASHTO code } K_s = 0.30$$

Set up Table using segments shown in Figure D.2.

Pile Segment, <i>i</i>	$f_{si}$ (tsf)	$a_{si}$ (ft <sup>2</sup> /ft)	$h_i$ (ft)	$Q_{si}$ (tons)
1	1.70	3.338	5	8.51
2	0.10	3.338	31	3.10
3	0.70	3.338	8	5.61
4	0.95	3.338	4	3.81
5	0.60	3.338	5	3.00
6	1.60	3.338	15	24.03
7	0.60	3.338	2	1.20
Total $Q_s$ =				49.26 tons

Example for pile segment 3:

$$Q_{si} = 0.30 \times 0.70 \text{tsf} \times 3.338 \text{ft} \times 8 \text{ft} = 5.61 \text{tons}$$

Tip Resistance:

$$A_p = \pi \times \left( \frac{12.75 \text{in}}{4} \right)^2 = 127.68 \text{in}^2 = 0.8866 \text{ft}^2$$

$$8D = 8 \times 1.0625 \text{ft} = 8.5 \text{ft}$$

$$4D = 4 \times 1.0625 \text{ft} = 4.25 \text{ft}$$

Using the data presented in Figure D.3:

$$q_{c2} = \frac{40 \text{tsf} \times 4 \text{ft} + 105 \text{tsf} \times 4 \text{ft} + 75 \text{tsf} \times 0.5 \text{ft}}{8.5 \text{ft}} = 72.65 \text{tsf}$$

$$q_{c1(\min @ 2 \text{ft})} = \frac{40 \text{tsf} \times 2 \text{ft}}{2 \text{ft}} = 40 \text{tsf}$$

$$q_p = \frac{40 \text{tsf} + 72.65 \text{tsf}}{2} = 56.33 \text{tsf}$$



$$Q_p = 56.33tsf \times 0.8866 ft^2 = 49.94 tons$$

### **Comparisons for Test Pile # 2:**

#### **Ultimate Calculated Loads:**

CAPWAP prediction @ EOD:	47 tons
CAPWAP prediction @ BOR(last):	125 tons
Energy Approach prediction @ EOD:	89 tons
Energy Approach prediction @ BOR(last):	161 tons
ENR prediction with FS = 6 @ EOD:	39 tons
ENR prediction with FS = 6 @ BOR(last):	117 tons
Gates Equation prediction @ EOD:	81 tons
Gates Equation prediction @ BOR(last):	137 tons
FHWA version of the Gates equation prediction @ EOD:	130 tons
FHWA version of the Gates equation prediction @ BOR(last):	253 tons

#### **Working Stress Design Method:**

Assuming that no static load test was completed the following are the recommended factors of safety for use.

CAPWAP	2.25
Dynamic Equations	3.50
Energy Approach	No recommendation, so use 2.75 for comparison sake

#### ***CAPWAP EOD:***

$$Q_{all} = \frac{47 tons}{2.25} = 20.67 tons$$

#### ***CAPWAP BOR (last):***

$$Q_{all} = \frac{125 tons}{2.25} = 55.38 tons$$

#### ***Energy Approach EOD:***

$$Q_{all} = \frac{89 tons}{2.75} = 32.36 tons$$

*Energy Approach BOR (last):*

$$Q_{all} = \frac{161 \text{ tons}}{2.75} = 58.55 \text{ tons}$$

*ENR with FS = 6 EOD:*

$$Q_{all} = \frac{39 \text{ tons}}{3.50} = 11.14 \text{ tons}$$

*ENR with FS = 6 BOR (last):*

$$Q_{all} = \frac{117 \text{ tons}}{3.50} = 33.43 \text{ tons}$$

*Gates Equation EOD:*

$$Q_{all} = \frac{81 \text{ tons}}{3.50} = 23.14 \text{ tons}$$

*Gates Equation BOR (last):*

$$Q_{all} = \frac{137 \text{ tons}}{3.50} = 39.14 \text{ tons}$$

*FHWA version of the Gates Equation EOD:*

$$Q_{all} = \frac{130 \text{ tons}}{3.50} = 37.14 \text{ tons}$$

*FHWA version of the Gates Equation BOR (last):*

$$Q_{all} = \frac{253 \text{ tons}}{3.50} = 72.29 \text{ tons}$$

Present AASHTO Code:

Summary of Static Analysis:

	Layer Number, <i>i</i>	$\phi \times Q_{si}$ $\alpha$ – method $\phi = 0.70$ (tons)	$\phi \times Q_{si}$ $\beta$ – method $\phi = 0.50$ (tons)	$\phi \times Q_{si}$ $\lambda$ – method $\phi = 0.55$ (tons)	CPT – method $\phi = 0.55$ (tons)
Clay Layers	1	16.82	10.10	5.68	-----
	2	14.95	9.38	8.78	-----
	3	10.24	11.08	8.57	-----
		$\phi \times Q_{si}$ , SPT – method, $\phi = 0.45$ (tons)			-----
Sand Layers	4	5.00	5.00	5.00	-----
	5	7.91	7.91	7.91	-----
	6	9.16	9.16	9.16	-----
	7	0.70	0.70	0.70	-----
	$\Sigma \phi \times Q_{si}$	64.78	53.33	45.80	27.09
Tip	$\phi \times Q_p$	27.61	27.61	27.61	27.47
	$Q_{all}$	92.39	80.94	73.41	54.56

$\alpha$  – method / SPT – method:

with CAPWAP verification,  $\lambda_v = 1.00$ :

$$Q_{all} = 1.00 \times 92.39 \text{ tons} = 92.39 \text{ tons}$$

with Energy Approach verification,  $\lambda_v = 0.90$ :

$$Q_{all} = 0.90 \times 92.39 \text{ tons} = 83.15 \text{ tons}$$

with dynamic equation verification,  $\lambda_v = 0.80$ :

$$Q_{all} = 0.80 \times 92.39 \text{ tons} = 73.91 \text{ tons}$$

$\beta$  – method / SPT – method:

with CAPWAP verification,  $\lambda_v = 1.00$ :

$$Q_{all} = 1.00 \times 80.94 \text{ tons} = 80.94 \text{ tons}$$

*with Energy Approach verification,  $\lambda_v = 0.90$ :*

$$Q_{all} = 0.90 \times 80.94 \text{ tons} = 72.85 \text{ tons}$$

*with dynamic equation verification,  $\lambda_v = 0.80$ :*

$$Q_{all} = 0.80 \times 80.94 \text{ tons} = 64.75 \text{ tons}$$

*$\lambda$  – method / SPT – method:*

*with CAPWAP verification,  $\lambda_v = 1.00$ :*

$$Q_{all} = 1.00 \times 73.41 \text{ tons} = 73.41 \text{ tons}$$

*with Energy Approach verification,  $\lambda_v = 0.90$ :*

$$Q_{all} = 0.90 \times 73.41 \text{ tons} = 66.07 \text{ tons}$$

*with dynamic equation verification,  $\lambda_v = 0.80$ :*

$$Q_{all} = 0.80 \times 73.41 \text{ tons} = 58.73 \text{ tons}$$

*CPT – method:*

*with CAPWAP verification,  $\lambda_v = 1.00$ :*

$$Q_{all} = 1.00 \times 54.56 \text{ tons} = 54.56 \text{ tons}$$

*with Energy Approach verification,  $\lambda_v = 0.90$ :*

$$Q_{all} = 0.90 \times 54.56 \text{ tons} = 49.10 \text{ tons}$$

*with dynamic equation verification,  $\lambda_v = 0.80$ :*

$$Q_{all} = 0.80 \times 54.56 \text{ tons} = 43.65 \text{ tons}$$

Recommended Resistance Factors (Non-Redundant Pile):

*CAPWAP EOD,  $\phi = 0.43$ :*

$$Q_{all} = 0.43 \times 47 \text{ tons} = 20.21 \text{ tons}$$

*CAPWAP BOR (last),  $\phi = 0.51$ :*

$$Q_{all} = 0.51 \times 125 \text{ tons} = 63.75 \text{ tons}$$

*Energy Approach EOD,  $\phi = 0.40$ :*

$$Q_{all} = 0.40 \times 89 \text{ tons} = 35.60 \text{ tons}$$

*Energy Approach BOR (last),  $\phi = 0.32$ :*

$$Q_{all} = 0.32 \times 161 \text{ tons} = 51.52 \text{ tons}$$

*ENR with FS = 6 EOD,  $\phi = 0.15$*

$$Q_{all} = 0.15 \times 39 \text{ tons} = 5.85 \text{ tons}$$

*ENR with FS = 6 BOR (last),  $\phi = 0.15$*

$$Q_{all} = 0.15 \times 117 \text{ tons} = 17.55 \text{ tons}$$

*Gates Equation EOD,  $\phi = 0.53$ :*

$$Q_{all} = 0.53 \times 81 \text{ tons} = 42.93 \text{ tons}$$

*Gates Equation BOR (last),  $\phi = 0.53$ :*

$$Q_{all} = 0.53 \times 137 \text{ tons} = 72.61 \text{ tons}$$

*FHWA version of Gates Equation EOD,  $\phi = 0.26$ :*

$$Q_{all} = 0.26 \times 130 \text{ tons} = 33.80 \text{ tons}$$

*FHWA version of Gates Equation BOR (last),  $\phi = 0.26$ :*

$$Q_{all} = 0.26 \times 253 \text{ tons} = 65.78 \text{ tons}$$

**Test Pile # 3 (14" square concrete pile driven 80ft, top 10 ft is encased):**

**Skin Friction:**

Layer 1 (8 ft thick layer):

$$A_s = 4 \times 14 \text{ in} \times 8 \text{ ft} \times \frac{1 \text{ ft}}{12 \text{ in}} = 37.333 \text{ ft}^2$$

$\alpha$  – method:

from Figure 10.7.3.3.2a-1 of 1998 AASHTO code with  $S_u = 1.0 \text{ tsf}$ ,  $\alpha = 0.90$

$$q_s = 0.90 \times 1.0 = 0.90 \text{ tsf}$$

$$Q_s = 0.90 \text{ tsf} \times 37.333 \text{ ft}^2 = 33.60 \text{ tons}$$

$\beta$  – method:

From Paikowsky and Chen (1998),  $\text{OCR} \approx 9$  at 14 ft, therefore from Figure 10.7.3.3.2b-1 of 1998 AASHTO code  $\beta = 1.3$ .  $\sigma'_v = 0.582 \text{ tsf}$  at 14 ft (midpoint of layer).

$$q_s = 1.3 \times 0.582 \text{ tsf} = 0.756 \text{ tsf}$$

$$Q_s = 0.756 \text{ tsf} \times 37.333 \text{ ft}^2 = 28.22 \text{ tons}$$

$\lambda$  – method:

From Figure 10.7.3.3.2c-1 of the 1998 AASHTO,  $\lambda = 0.15$

$$q_s = 0.15 \times (0.582 \text{ tsf} + 2 \times 1.0 \text{ tsf}) = 0.387 \text{ tsf}$$

$$Q_s = 0.387 \text{ tsf} \times 37.333 \text{ ft}^2 = 14.45 \text{ tons}$$

Layer 2 (20 ft thick layer):

$$A_s = 4 \times 14 \text{ in} \times 20 \text{ ft} \times \frac{1 \text{ ft}}{12 \text{ in}} = 93.333 \text{ ft}^2$$

$\alpha$  – method:

from Figure 10.7.3.3.2a-1 of 1998 AASHTO code with  $S_u = 0.33$  tsf,  $\alpha = 0.97$

$$q_s = 0.97 \times 0.33 = 0.320 \text{ tsf}$$

$$Q_s = 0.320 \text{ psf} \times 93.333 \text{ ft}^2 = 29.87 \text{ tons}$$

$\beta$  – method:

From Paikowsky and Chen (1998),  $\text{OCR} \approx 1$  at 28 ft, therefore from Figure 10.7.3.3.2b-1 of 1998 AASHTO code  $\beta = 0.3$ .  $\sigma'_v = 0.935$  tsf at 28 ft (midpoint of layer).

$$q_s = 0.3 \times 0.935 \text{ tsf} = 0.281 \text{ tsf}$$

$$Q_s = 0.281 \text{ tsf} \times 93.333 \text{ ft}^2 = 26.23 \text{ tons}$$

$\lambda$  – method:

From Figure 10.7.3.3.2c-1 of the 1998 AASHTO,  $\lambda = 0.15$

$$q_s = 0.15 \times (0.935 \text{ tsf} + 2 \times 0.33 \text{ tsf}) = 0.239 \text{ tsf}$$

$$Q_s = 0.239 \text{ tsf} \times 93.333 \text{ ft}^2 = 22.31 \text{ tons}$$

Layer 3 (16 ft thick layer):

$$A_s = 4 \times 14 \text{ in} \times 16 \text{ ft} \times \frac{1 \text{ ft}}{12 \text{ in}} = 74.667 \text{ ft}^2$$

$\alpha$  – method:

from Figure 10.7.3.3.2a-1 of 1998 AASHTO code with  $S_u = 0.28$  tsf,  $\alpha = 0.98$

$$q_s = 0.98 \times 0.28 = 0.274 \text{ tsf}$$

$$Q_s = 0.274 \text{ tsf} \times 74.667 \text{ ft}^2 = 20.46 \text{ tons}$$

$\beta$  – method:

From Paikowsky and Chen (1998),  $OCR \approx 1$  at 46 ft, therefore from Figure 10.7.3.3.2b-1 of 1998 AASHTO code  $\beta = 0.3$ .  $\sigma'_v = 1.384$  tsf at 46 ft (midpoint of layer).

$$q_s = 0.3 \times 1.384 \text{ tsf} = 0.415 \text{ tsf}$$

$$Q_s = 0.415 \text{ psf} \times 74.667 \text{ ft}^2 = 30.99 \text{ tons}$$

$\lambda$  - method:

From Figure 10.7.3.3.2c-1 of the 1998 AASHTO,  $\lambda = 0.15$

$$q_s = 0.15 \times (1.384 \text{ tsf} + 2 \times 0.28 \text{ tsf}) = 0.292 \text{ tsf}$$

$$Q_s = 0.292 \text{ tsf} \times 74.667 \text{ ft}^2 = 21.80 \text{ tons}$$

Layer 4 (9 ft layer):

$$A_s = 4 \times 14 \text{ in} \times 9 \text{ ft} \times \frac{1 \text{ ft}}{12 \text{ in}} = 42.000 \text{ ft}^2$$

SPT method:

$$\bar{N} = 18.5$$

$$q_s = \frac{18.5}{50} = 0.370 \text{ tsf}$$

$$Q_s = 0.370 \text{ tsf} \times 42.000 \text{ ft}^2 = 15.54 \text{ tons}$$

Layer 5 (8 ft layer):

$$A_s = 4 \times 14 \text{ in} \times 8 \text{ ft} \times \frac{1 \text{ ft}}{12 \text{ in}} = 37.333 \text{ ft}^2$$

SPT method:

$$\bar{N} = 32.9$$



$$q_s = \frac{32.9}{50} = 0.658 \text{ tsf}$$

$$Q_s = 0.658 \text{ tsf} \times 37.333 \text{ ft}^2 = 24.57 \text{ tons}$$

Layer 6 (8 ft layer):

$$A_s = 4 \times 14 \text{ in} \times 8 \text{ ft} \times \frac{1 \text{ ft}}{12 \text{ in}} = 37.333 \text{ ft}^2$$

SPT method:

$$\bar{N} = 38.1$$

$$q_s = \frac{38.1}{50} = 0.762 \text{ tsf}$$

$$Q_s = 0.762 \text{ tsf} \times 37.333 \text{ ft}^2 = 28.45 \text{ tons}$$

Layer 7 (1 ft layer):

$$A_s = 4 \times 14 \text{ in} \times 1 \text{ ft} \times \frac{1 \text{ ft}}{12 \text{ in}} = 4.667 \text{ ft}^2$$

SPT method:

$$\bar{N} = 23.4$$

$$q_s = \frac{23.4}{50} = 0.468 \text{ tsf}$$

$$Q_s = 0.468 \text{ tsf} \times 4.667 \text{ ft}^2 = 2.18 \text{ tons}$$

**Tip of Pile:**

$$A_p = (14 \text{ in})^2 = 196 \text{ in}^2 = 1.3611 \text{ ft}^2$$

SPT method:

$\sigma'_v = 2.365 \text{ tsf}$  and  $N = 24.2$  at the tip, i.e., depth of 80ft.

$$N_{corr} = \left[ 0.77 \times \log_{10} \left( \frac{20}{2.365} \right) \right] \times 24.2 = 17.3$$

$$D = 14 \text{ in} = 1.1667 \text{ ft}, D_b = 80 \text{ ft}$$

$$q_p = \frac{0.4 \times 17.3 \times 80 \text{ ft}}{1.1667 \text{ ft}} = 475 \text{ tsf} \leq 4 \times 17.3 = 69.2 \text{ tsf}$$

therefore,

$$q_p = 69.2 \text{ tsf}$$

$$Q_p = 69.2 \text{ tsf} \times 1.1667 \text{ ft}^2 = 80.74 \text{ tons}$$

***CPT method:***

*Skin Friction:*

$8D = 9.33 \text{ ft}$ , therefore, the first term in calculating the skin friction is not needed as the pile is cased to 10 ft.

$$\frac{L}{D} = \frac{80 \text{ ft}}{1.1667 \text{ ft}} = 69, \text{ from Figure 10.7.3.4.3c-1 of AASHTO code } K_s = 0.35$$

Set up Table using segments shown in Figure D.2.

Pile Segment, <i>i</i>	$f_{si}$ (tsf)	$a_{si}$ (ft <sup>2</sup> /ft)	$h_i$ (ft)	$Q_{si}$ (tons)
1	1.70	4.667	5	13.88
2	0.10	4.667	31	5.06
3	0.70	4.667	8	9.15
4	0.95	4.667	4	6.21
5	0.60	4.667	5	4.90
6	1.60	4.667	15	39.20
7	0.60	4.667	2	1.96
Total $Q_s$ =				80.36 tons

Example for pile segment 3:

$$Q_{si} = 0.35 \times 0.70 \text{ tsf} \times 4.667 \text{ ft} \times 8 \text{ ft} = 9.15 \text{ tons}$$

Tip Resistance:

$$A_p = (14 \text{ in})^2 = 196 \text{ in}^2 = 1.3611 \text{ ft}^2$$

$$8D = 8 \times 1.1667 \text{ ft} = 9.33 \text{ ft}$$

$$4D = 4 \times 1.1667 \text{ ft} = 4.67 \text{ ft}$$

Using the data presented in Figure D.3:

$$q_{c2} = \frac{40 \text{ tsf} \times 4 \text{ ft} + 105 \text{ tsf} \times 4 \text{ ft} + 75 \text{ tsf} \times 1.33 \text{ ft}}{9.33 \text{ ft}} = 72.86 \text{ tsf}$$

$$q_{c1(\text{min}@2ft)} = \frac{40 \text{ tsf} \times 2 \text{ ft}}{2 \text{ ft}} = 40 \text{ tsf}$$

$$q_p = \frac{40 \text{ tsf} + 72.86 \text{ tsf}}{2} = 56.43 \text{ tsf}$$

$$Q_p = 56.43 \text{ tsf} \times 1.3611 \text{ ft}^2 = 76.81 \text{ tons}$$

### **Comparisons for Test Pile # 3:**

#### **Ultimate Calculated Loads:**

CAPWAP prediction @ EOD:	83 tons
CAPWAP prediction @ BOR(last):	138 tons
Energy Approach prediction @ EOD:	138 tons
Energy Approach prediction @ BOR(last):	458 tons
ENR prediction with FS = 6 @ EOD:	46 tons
ENR prediction with FS = 6 @ BOR (last):	284 tons
Gates Equation prediction @ EOD:	88 tons
Gates Equation prediction @ BOR(last):	192 tons
FHWA version of the Gates equation prediction @ EOD:	146 tons
FHWA version of the Gates equation prediction @ BOR(last):	377 tons

#### **Working Stress Design Method:**

Assuming that no static load test was completed the following are the recommended factors of safety for use.

CAPWAP	2.25
Dynamic Equations	3.50
Energy Approach	No recommendation, so use 2.75 for comparison sake

#### ***CAPWAP EOD:***

$$Q_{all} = \frac{83 \text{ tons}}{2.25} = 36.89 \text{ tons}$$

#### ***CAPWAP BOR (last):***

$$Q_{all} = \frac{138 \text{ tons}}{2.25} = 61.33 \text{ tons}$$

#### ***Energy Approach EOD:***

$$Q_{all} = \frac{138 \text{ tons}}{2.75} = 50.18 \text{ tons}$$

*Energy Approach BOR (last):*

$$Q_{all} = \frac{458 \text{ tons}}{2.75} = 166.55 \text{ tons}$$

*ENR with FS = 6 EOD:*

$$Q_{all} = \frac{46 \text{ tons}}{3.50} = 13.14 \text{ tons}$$

*ENR with FS = 6 BOR (last):*

$$Q_{all} = \frac{284 \text{ tons}}{3.50} = 81.14 \text{ tons}$$

*Gates Equation EOD:*

$$Q_{all} = \frac{88 \text{ tons}}{3.50} = 25.14 \text{ tons}$$

*Gates Equation BOR (last):*

$$Q_{all} = \frac{192 \text{ tons}}{3.50} = 54.86 \text{ tons}$$

*FHWA version of the Gates Equation EOD:*

$$Q_{all} = \frac{146 \text{ tons}}{3.50} = 41.71 \text{ tons}$$

*FHWA version of the Gates Equation BOR (last):*

$$Q_{all} = \frac{377 \text{ tons}}{3.50} = 107.71 \text{ tons}$$

Present AASHTO Code:

Summary of Static Analysis:

	Layer Number, <i>i</i>	$\phi \times Q_{si}$ $\alpha$ – method $\phi = 0.70$ (tons)	$\phi \times Q_{si}$ $\beta$ – method $\phi = 0.50$ (tons)	$\phi \times Q_{si}$ $\lambda$ – method $\phi = 0.55$ (tons)	CPT – method $\phi = 0.55$ (tons)
Clay Layers	1	23.52	14.11	7.95	-----
	2	20.91	13.12	12.27	-----
	3	14.32	15.50	11.99	-----
		$\phi \times Q_{si}$ , SPT – method, $\phi = 0.45$ (tons)			-----
Sand Layers	4	6.99	6.99	6.99	-----
	5	11.06	11.06	11.06	-----
	6	12.80	12.80	12.80	-----
	7	0.98	0.98	0.98	-----
	$\Sigma \phi \times Q_{si}$	90.58	74.56	64.04	44.20
Tip	$\phi \times Q_p$	36.33	36.33	36.33	42.25
	$Q_{all}$	126.91	110.89	100.37	86.45

$\alpha$  – method / SPT – method:

with CAPWAP verification,  $\lambda_v = 1.00$ :

$$Q_{all} = 1.00 \times 126.91 \text{ tons} = 126.91 \text{ tons}$$

with Energy Approach verification,  $\lambda_v = 0.90$ :

$$Q_{all} = 0.90 \times 126.91 \text{ tons} = 114.22 \text{ tons}$$

with dynamic equation verification,  $\lambda_v = 0.80$ :

$$Q_{all} = 0.80 \times 126.91 \text{ tons} = 101.53 \text{ tons}$$

$\beta$  – method / SPT – method:

with CAPWAP verification,  $\lambda_v = 1.00$ :

$$Q_{all} = 1.00 \times 110.89 \text{ tons} = 110.89 \text{ tons}$$

*with Energy Approach verification,  $\lambda_v = 0.90$ :*

$$Q_{all} = 0.90 \times 110.89 \text{ tons} = 99.80 \text{ tons}$$

*with dynamic equation verification,  $\lambda_v = 0.80$ :*

$$Q_{all} = 0.80 \times 110.89 \text{ tons} = 88.71 \text{ tons}$$

*$\lambda$  – method / SPT – method:*

*with CAPWAP verification,  $\lambda_v = 1.00$ :*

$$Q_{all} = 1.00 \times 100.37 \text{ tons} = 100.37 \text{ tons}$$

*with Energy Approach verification,  $\lambda_v = 0.90$ :*

$$Q_{all} = 0.90 \times 100.89 \text{ tons} = 90.33 \text{ tons}$$

*with dynamic equation verification,  $\lambda_v = 0.80$ :*

$$Q_{all} = 0.80 \times 100.89 \text{ tons} = 80.30 \text{ tons}$$

*CPT – method:*

*with CAPWAP verification,  $\lambda_v = 1.00$ :*

$$Q_{all} = 1.00 \times 86.45 \text{ tons} = 86.45 \text{ tons}$$

*with Energy Approach verification,  $\lambda_v = 0.90$ :*

$$Q_{all} = 0.90 \times 86.45 \text{ tons} = 77.81 \text{ tons}$$

*with dynamic equation verification,  $\lambda_v = 0.80$ :*

$$Q_{all} = 0.80 \times 86.45 \text{ tons} = 69.16 \text{ tons}$$

Recommended Resistance Factors:

*CAPWAP EOD,  $\phi = 0.43$ :*

$$Q_{all} = 0.43 \times 83 \text{ tons} = 35.69 \text{ tons}$$

*CAPWAP BOR (last),  $\phi = 0.51$ :*

$$Q_{all} = 0.51 \times 138 \text{ tons} = 70.38 \text{ tons}$$

*Energy Approach EOD,  $\phi = 0.40$ :*

$$Q_{all} = 0.40 \times 138 \text{ tons} = 55.20 \text{ tons}$$

*Energy Approach BOR (last),  $\phi = 0.32$ :*

$$Q_{all} = 0.32 \times 458 \text{ tons} = 146.56 \text{ tons}$$

*ENR with FS = 6 EOD,  $\phi = 0.15$*

$$Q_{all} = 0.15 \times 46 \text{ tons} = 6.90 \text{ tons}$$

*ENR with FS = 6 BOR (last),  $\phi = 0.15$*

$$Q_{all} = 0.15 \times 284 \text{ tons} = 42.60 \text{ tons}$$

*Gates Equation EOD,  $\phi = 0.53$ :*

$$Q_{all} = 0.53 \times 88 \text{ tons} = 46.64 \text{ tons}$$

*Gates Equation BOR (last),  $\phi = 0.53$ :*

$$Q_{all} = 0.53 \times 192 \text{ tons} = 101.76 \text{ tons}$$

*FHWA version of Gates Equation EOD,  $\phi = 0.26$ :*

$$Q_{all} = 0.26 \times 146 \text{ tons} = 37.96 \text{ tons}$$

*FHWA version of Gates Equation BOR (last),  $\phi = 0.26$ :*

$$Q_{all} = 0.26 \times 377 \text{ tons} = 98.02 \text{ tons}$$



**Choctawhatchee River Project (1 end bearing pile):**

**Soil Layers (see also Figure D.4):**

Layer 1:	Silty Sand	$\gamma = 127.2 \text{ pcf}$	$\phi = 44^\circ$
Layer 2:	Sand	$\gamma = 107.3 \text{ pcf}$	$\phi = 32^\circ$
Layer 3:	Sand	$\gamma = 107.3 \text{ pcf}$	$\phi = 26^\circ$
Layer 4:	Clay/Silt	$\gamma = 101.2 \text{ pcf}$	$S_u = 0.126 \text{ tsf}$
Layer 5:	Clay/Silty Clay	$\gamma = 101.2 \text{ pcf}$	$S_u = 0.197 \text{ tsf}$
Layer 6:	Silty Sand	$\gamma = 113.4 \text{ pcf}$	$\phi = 34^\circ$
Layer 7:	Sand	$\gamma = 119.6 \text{ pcf}$	$\phi = 37^\circ$

**Test Pile # P5 (30" square concrete pile with 18" center void, driven 53.96 ft):**

**Skin Friction:**

**Layer 1 (11.5 ft thick layer):**

$$A_s = 4 \times 30 \text{ in} \times 11.5 \text{ ft} \times \frac{1 \text{ ft}}{12 \text{ in}} = 115 \text{ ft}^2$$

**SPT method:**

$$\bar{N} = 10.5$$

$$q_s = \frac{10.5}{50} = 0.210 \text{ tsf}$$

$$Q_s = 0.210 \text{ tsf} \times 115 \text{ ft}^2 = 24.15 \text{ tons}$$

**Layer 2 (8 ft thick layer):**

$$A_s = 4 \times 30 \text{ in} \times 8 \text{ ft} \times \frac{1 \text{ ft}}{12 \text{ in}} = 80 \text{ ft}^2$$

**SPT method:**

$$\bar{N} = 2.8$$

$$q_s = \frac{2.8}{50} = 0.056 \text{ tsf}$$

$$Q_s = 0.056 \text{tsf} \times 80 \text{ft}^2 = 4.48 \text{tons}$$

Layer 3 (4 ft thick layer):

$$A_s = 4 \times 30 \text{in} \times 4 \text{ft} \times \frac{1 \text{ft}}{12 \text{in}} = 40 \text{ft}^2$$

SPT method:

$$\bar{N} = 1.4$$

$$q_s = \frac{1.4}{50} = 0.028 \text{tsf}$$

$$Q_s = 0.028 \text{tsf} \times 40 \text{ft}^2 = 1.12 \text{tons}$$

Layer 4 (3.5 ft layer):

$$A_s = 4 \times 30 \text{in} \times 3.5 \text{ft} \times \frac{1 \text{ft}}{12 \text{in}} = 35 \text{ft}^2$$

$\alpha$  – method:

from Figure 10.7.3.3.2a-1 of 1998 AASHTO code with  $S_u = 0.126 \text{tsf}$ ,  $\alpha = 1.00$

$$q_s = 1.00 \times 0.126 \text{tsf} = 0.126 \text{tsf}$$

$$Q_s = 0.126 \text{tsf} \times 35 \text{ft}^2 = 4.41 \text{tons}$$

$\beta$  – method:

OCR  $\approx 1$  at 25.25 ft, therefore from Figure 10.7.3.3.2b-1 of 1998 AASHTO code  $\beta = 0.3$ .  $\sigma'_v = 0.844 \text{tsf}$  at 25.25 ft (midpoint of layer).

$$q_s = 0.3 \times 0.844 \text{tsf} = 0.253 \text{tsf}$$

$$Q_s = 0.253 \text{tsf} \times 35 \text{ft}^2 = 8.86 \text{tons}$$

$\lambda$  - method:

From Figure 10.7.3.3.2c-1 of the 1998 AASHTO,  $\lambda = 0.19$

$$q_s = 0.19 \times (0.844 \text{ tsf} + 2 \times 0.126 \text{ tsf}) = 0.208 \text{ tsf}$$

$$Q_s = 0.208 \text{ tsf} \times 35 \text{ ft}^2 = 7.28 \text{ tons}$$

Layer 5 (9 ft layer):

$$A_s = 4 \times 30 \text{ in} \times 9 \text{ ft} \times \frac{1 \text{ ft}}{12 \text{ in}} = 90 \text{ ft}^2$$

$\alpha$  - method:

from Figure 10.7.3.3.2a-1 of 1998 AASHTO code with  $S_u = 0.197 \text{ tsf}$ ,  $\alpha = 1.00$

$$q_s = 1.00 \times 0.197 \text{ tsf} = 0.197 \text{ tsf}$$

$$Q_s = 0.197 \text{ tsf} \times 90 \text{ ft}^2 = 17.73 \text{ tons}$$

$\beta$  - method:

OCR  $\approx 1$  at 31.5 ft, therefore from Figure 10.7.3.3.2b-1 of 1998 AASHTO code  $\beta = 0.3$ .  $\sigma'_v = 0.966 \text{ tsf}$  at 14 ft (midpoint of layer).

$$q_s = 0.3 \times 0.966 \text{ tsf} = 0.290 \text{ tsf}$$

$$Q_s = 0.290 \text{ tsf} \times 90 \text{ ft}^2 = 26.10 \text{ tons}$$

$\lambda$  - method:

From Figure 10.7.3.3.2c-1 of the 1998 AASHTO,  $\lambda = 0.19$

$$q_s = 0.19 \times (0.966 \text{ tsf} + 2 \times 0.197 \text{ tsf}) = 0.258 \text{ tsf}$$

$$Q_s = 0.258 \text{ tsf} \times 90 \text{ ft}^2 = 23.22 \text{ tons}$$

Layer 6 (11 ft layer):

$$A_s = 4 \times 30in \times 11ft \times \frac{1ft}{12in} = 110 ft^2$$

SPT method:

$$\bar{N} = 4.1$$

$$q_s = \frac{4.1}{50} = 0.082tsf$$

$$Q_s = 0.082tsf \times 110 ft^2 = 9.02 tons$$

Layer 7 (6.96 ft layer):

$$A_s = 4 \times 30in \times 6.96ft \times \frac{1ft}{12in} = 69.6 ft^2$$

SPT method:

$$\bar{N} = 8.6$$

$$q_s = \frac{8.6}{50} = 0.172tsf$$

$$Q_s = 0.172tsf \times 69.6 ft^2 = 11.97 tons$$

**Tip of Pile:**

$$A_p = (30in)^2 - \pi \times \left(\frac{18in}{2}\right)^2 = 645.53in^2 = 4.4829 ft^2$$

SPT method:

$\sigma'_v = 1.533$  tsf and  $N = 12$  at the tip, i.e., depth of 53.96 ft.

$$N_{corr} = \left[ 0.77 \times \log_{10} \left( \frac{20}{1.533} \right) \right] \times 12 = 10.3$$

$$D = 30 \text{ in} = 2.500 \text{ ft}, D_b = 53.96 \text{ ft}$$

$$q_p = \frac{0.4 \times 10.3 \times 53.96 \text{ ft}}{2.500 \text{ ft}} = 88.92 \text{ tsf} \leq 4 \times 10.3 = 41.2 \text{ tsf}$$

therefore,

$$q_p = 41.2 \text{ tsf}$$

$$Q_p = 41.2 \text{ tsf} \times 4.4829 \text{ ft}^2 = 184.70 \text{ tons}$$

***CPT method:***

*Skin Friction:*

$$8D = 20 \text{ ft}$$

$$\frac{L}{D} = \frac{53.96 \text{ ft}}{2.50 \text{ ft}} = 22, \text{ from Figure 10.7.3.4.3c-1 of AASHTO code } K_s = 0.41$$

Set up Table using segments shown in Figure D.5.

File Segment, $i$	$L_i$ (ft)	$D_i$ (ft)	$f_{si}$ (tsf)	$a_{si}$ (ft <sup>2</sup> /ft)	$h_i$ (ft)	$Q_{si}$ (tons)
1	4	2.5	1.8	10	8	11.81
2	12	2.5	1.1	10	8	21.65
3	18	2.5	0.3	10	4	4.43
4	N/A	N/A	0.3	10	4	4.92
5	N/A	N/A	1.8	10	5	36.90
6	N/A	N/A	0.4	10	4	6.56
7	N/A	N/A	0.2	10	5	4.10
8	N/A	N/A	0.8	10	8	26.24
9	N/A	N/A	1.4	10	3	17.22
10	N/A	N/A	2.2	10	3	27.06
11	N/A	N/A	1.8	10	1.96	14.46
Total $Q_s =$						175.35 tons

Example for pile segment 3:

$$Q_{si} = 0.41 \times \left( \frac{18}{8 \times 2.5} \right) \times 0.30 \text{ tsf} \times 10 \text{ ft} \times 4 \text{ ft} = 4.43 \text{ tons}$$

Tip Resistance:

$$A_p = (30 \text{ in})^2 - \pi \times \left( \frac{18 \text{ in}}{2} \right)^2 = 645.53 \text{ in}^2 = 4.4829 \text{ ft}^2$$

$$8D = 8 \times 2.500 \text{ ft} = 20 \text{ ft}$$

$$4D = 4 \times 2.500 \text{ ft} = 10 \text{ ft}$$

Using the data presented in Figure D.6:

$$q_{c2} = \frac{10tsf \times 8.04 ft + 30tsf \times 4 ft + 70tsf \times 7.96 ft}{20 ft} = 37.88tsf$$

$$q_{c1(min@ 4.04 ft)} = \frac{40tsf \times 4.04 ft}{4.04 ft} = 40tsf$$

$$q_p = \frac{40tsf + 37.88tsf}{2} = 38.94tsf$$

$$Q_p = 38.94tsf \times 4.4829 ft^2 = 174.56 tons$$

### **Comparisons for Test Pile # P5:**

#### **Ultimate Calculated Loads:**

CAPWAP prediction @ 1 day BOR:	284 tons
CAPWAP prediction @ BOR (last):	292 tons
Energy Approach prediction @ 1 day BOR:	504 tons
Energy Approach prediction @ BOR (last):	583 tons
ENR prediction with FS = 6 @ BOR:	546 tons
ENR prediction with FS = 6 @ BOR (last):	616 tons
Gates Equation prediction @ 1 day BOR:	259 tons
Gates Equation prediction @ BOR (last):	275 tons
FHWA version of the Gates equation prediction @ 1 day BOR:	526 tons
FHWA version of the Gates equation prediction @ BOR (last):	560 tons

#### **Working Stress Design Method:**

Assuming that no static load test was completed the following are the recommended factors of safety for use.

CAPWAP	2.25
Dynamic Equations	3.50
Energy Approach	No recommendation, so use 2.75 for comparison sake

*CAPWAP 1 day BOR:*

$$Q_{all} = \frac{284 tons}{2.25} = 126.22 tons$$

*CAPWAP BOR (last):*

$$Q_{all} = \frac{292 \text{ tons}}{2.25} = 129.78 \text{ tons}$$

*Energy Approach 1 day BOR:*

$$Q_{all} = \frac{504 \text{ tons}}{2.75} = 183.27 \text{ tons}$$

*Energy Approach BOR (last):*

$$Q_{all} = \frac{583 \text{ tons}}{2.75} = 212.00 \text{ tons}$$

*ENR with FS = 6, 1 day BOR:*

$$Q_{all} = \frac{546 \text{ tons}}{3.50} = 156.00 \text{ tons}$$

*ENR with FS = 6 BOR (last):*

$$Q_{all} = \frac{616 \text{ tons}}{3.50} = 176.00 \text{ tons}$$

*Gates Equation 1 day BOR:*

$$Q_{all} = \frac{259 \text{ tons}}{3.50} = 74.00 \text{ tons}$$

*Gates Equation BOR (last):*

$$Q_{all} = \frac{275 \text{ tons}}{3.50} = 78.57 \text{ tons}$$

*FHWA version of the Gates Equation 1 day BOR:*

$$Q_{all} = \frac{526 \text{ tons}}{3.50} = 150.29 \text{ tons}$$

*FHWA version of the Gates Equation BOR (last):*

$$Q_{all} = \frac{560 \text{ tons}}{3.50} = 160 \text{ tons}$$



Present AASHTO Code:

Summary of Static Analysis:

	Layer Number, <i>i</i>	$\phi \times Q_{si}$ $\alpha$ – method $\phi = 0.70$ (tons)	$\phi \times Q_{si}$ $\beta$ – method $\phi = 0.50$ (tons)	$\phi \times Q_{si}$ $\lambda$ – method $\phi = 0.55$ (tons)	CPT – method $\phi = 0.55$ (tons)
Clay Layers	4	3.09	4.43	4.00	-----
	5	12.41	13.05	12.77	-----
		$\phi \times Q_{si}$ , SPT – method, $\phi = 0.45$ (tons)			-----
Sand Layers	1	10.87	10.87	10.87	-----
	2	2.02	2.02	2.02	-----
	3	0.50	0.50	0.50	-----
	6	4.06	4.06	4.06	-----
	7	5.39	5.39	5.39	-----
	$\Sigma \phi \times Q_{si}$	38.34	40.32	39.61	96.44
Tip	$\phi \times Q_p$	83.12	83.12	83.12	96.01
	$Q_{all}$	121.46	123.44	122.73	192.45

$\alpha$  – method / SPT – method:

with CAPWAP verification,  $\lambda_v = 1.00$ :

$$Q_{all} = 1.00 \times 121.46 \text{ tons} = 121.46 \text{ tons}$$

with Energy Approach verification,  $\lambda_v = 0.90$ :

$$Q_{all} = 0.90 \times 121.46 \text{ tons} = 109.31 \text{ tons}$$

with dynamic equation verification,  $\lambda_v = 0.80$ :

$$Q_{all} = 0.80 \times 121.46 \text{ tons} = 97.17 \text{ tons}$$

$\beta$  – method / SPT – method:

with CAPWAP verification,  $\lambda_v = 1.00$ :

$$Q_{all} = 1.00 \times 123.44 \text{ tons} = 123.44 \text{ tons}$$

with Energy Approach verification,  $\lambda_v = 0.90$ :

$$Q_{all} = 0.90 \times 123.44 \text{ tons} = 111.10 \text{ tons}$$

with dynamic equation verification,  $\lambda_v = 0.80$ :

$$Q_{all} = 0.80 \times 123.44 \text{ tons} = 98.75 \text{ tons}$$

$\lambda$  – method / SPT – method:

with CAPWAP verification,  $\lambda_v = 1.00$ :

$$Q_{all} = 1.00 \times 122.73 \text{ tons} = 122.73 \text{ tons}$$

with Energy Approach verification,  $\lambda_v = 0.90$ :

$$Q_{all} = 0.90 \times 122.73 \text{ tons} = 110.46 \text{ tons}$$

with dynamic equation verification,  $\lambda_v = 0.80$ :

$$Q_{all} = 0.80 \times 122.73 \text{ tons} = 98.18 \text{ tons}$$

CPT – method:

with CAPWAP verification,  $\lambda_v = 1.00$ :

$$Q_{all} = 1.00 \times 192.45 \text{ tons} = 192.45 \text{ tons}$$

with Energy Approach verification,  $\lambda_v = 0.90$ :

$$Q_{all} = 0.90 \times 192.45 \text{ tons} = 173.21 \text{ tons}$$

with dynamic equation verification,  $\lambda_v = 0.80$ :

$$Q_{all} = 0.80 \times 192.45 \text{ tons} = 153.96 \text{ tons}$$

Recommended Resistance Factors:

*CAPWAP 1 day BOR,  $\phi = 0.51$ :*

$$Q_{all} = 0.51 \times 284 \text{ tons} = 144.84 \text{ tons}$$

*CAPWAP BOR (last),  $\phi = 0.51$ :*

$$Q_{all} = 0.51 \times 292 \text{ tons} = 148.92 \text{ tons}$$

*Energy Approach 1 day BOR,  $\phi = 0.32$ :*

$$Q_{all} = 0.32 \times 504 \text{ tons} = 161.28 \text{ tons}$$

*Energy Approach BOR (last),  $\phi = 0.32$ :*

$$Q_{all} = 0.32 \times 583 \text{ tons} = 186.56 \text{ tons}$$

*ENR with FS = 6, 1 day BOR,  $\phi = 0.15$ :*

$$Q_{all} = 0.15 \times 546 \text{ tons} = 81.90 \text{ tons}$$

*ENR with FS = 6 BOR (last),  $\phi = 0.15$ :*

$$Q_{all} = 0.15 \times 616 \text{ tons} = 92.40 \text{ tons}$$

*Gates Equation 1 day BOR,  $\phi = 0.53$ :*

$$Q_{all} = 0.53 \times 259 \text{ tons} = 137.27 \text{ tons}$$

*Gates Equation BOR (last),  $\phi = 0.53$ :*

$$Q_{all} = 0.53 \times 275 \text{ tons} = 145.75 \text{ tons}$$

*FHWA version of Gates Equation 1 day BOR,  $\phi = 0.26$ :*

$$Q_{all} = 0.26 \times 526 \text{ tons} = 136.76 \text{ tons}$$

*FHWA version of Gates Equation BOR (last),  $\phi = 0.26$ :*

$$Q_{all} = 0.26 \times 560 \text{ tons} = 145.60 \text{ tons}$$

**Table D.1.** Summary of Design Capacity Comparisons for Three Case History Piles.

Type of Analysis	Method	Q <sub>all</sub> (kN)								
		Friction Piles						End Bearing Pile		
		Newbury TP # 2			Newbury TP # 3			Choctawhatchee Peir 5		
		WSD	AASHTO	Ch 9 ϕ's	WSD	AASHTO	Ch 9 ϕ's	WSD	AASHTO	Ch 9 ϕ's
Wave Matching	CAPWAP EOD	187	667	178	329	943	320	-----	1246	-----
	CAPWAP BOR	-----		-----	-----		1121	1290		
	CAPWAP BORL	489		569	543		623	1157		1326
Simplified Methods	EA EOD	285	605	320	445	854	489	-----	1121	-----
	EA BOR	-----		-----	-----		1628	1432		
	EA BORL	525		463	1486		1308	1886		1664
Dynamic Equations	ENR EOD	98	534	53	116	756	62	-----	996	-----
	ENR BOR	-----		-----	-----		-----	1388		730
	ENR BORL	294		160	721		383	1566		818
	Gates EOD	205		383	222		418	-----		-----
	Gates BOR	-----		-----	-----		-----	658		1219
	Gates BORL	347		649	489		907	703		1299
	FHWA EOD	329		302	374		338	-----		-----
	FHWA BOR	-----		-----	-----		-----	1334		1219
	FHWA BORL	641		587	961		872	1423		1299
Static Load Test Results		Q <sub>ult</sub> = 658 kN			Q <sub>ult</sub> = 872 kN			Q <sub>ult</sub> = 5560 kN		

Note: The wave matching techniques are not recommended by GRL to be used at the EOD (Rausche, 2001) and the Energy Approach is not recommended to be used during restrike.

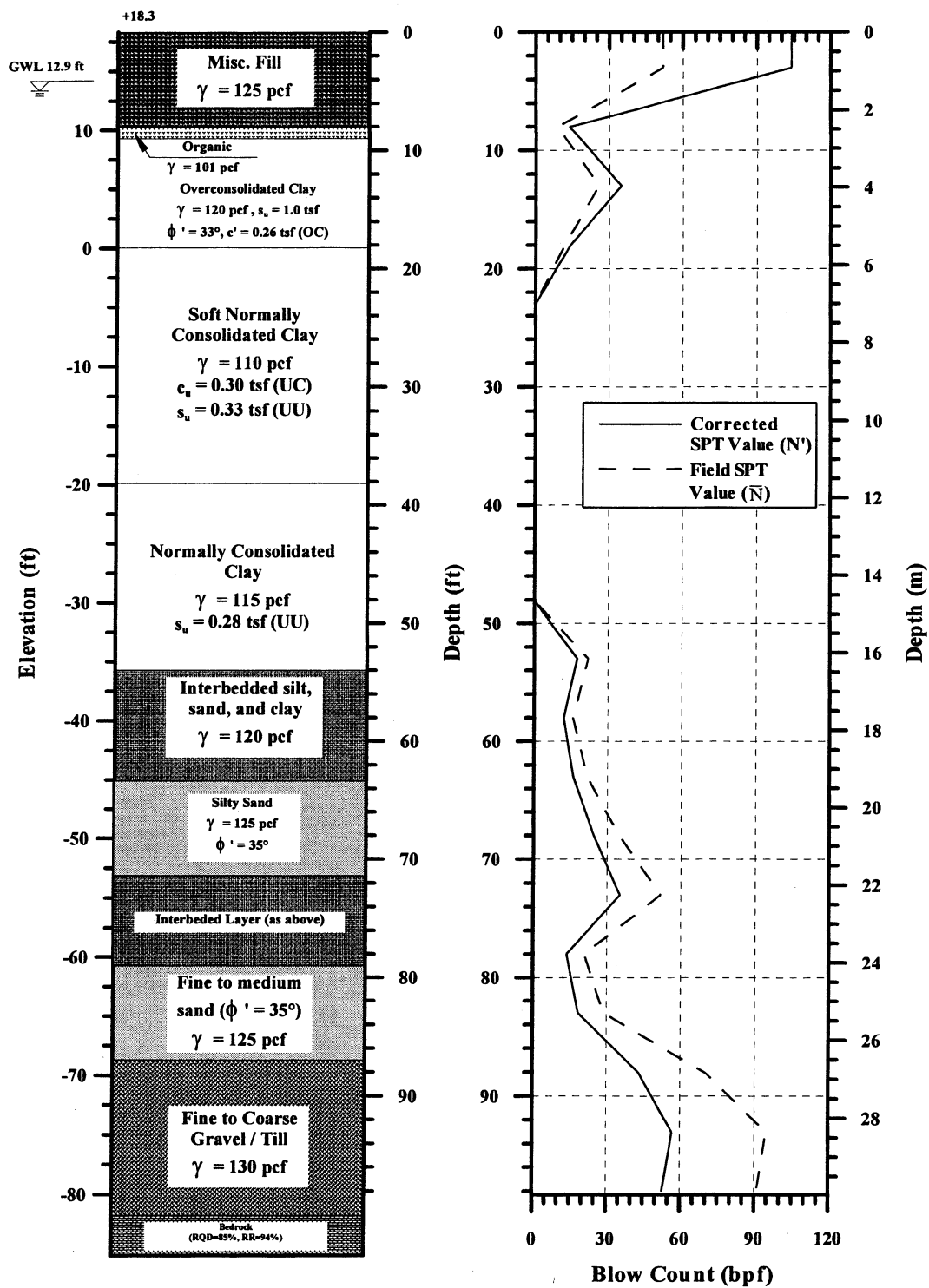


**Figure D.1.** Soil Profile and SPT values with Depth for the Newbury Site.

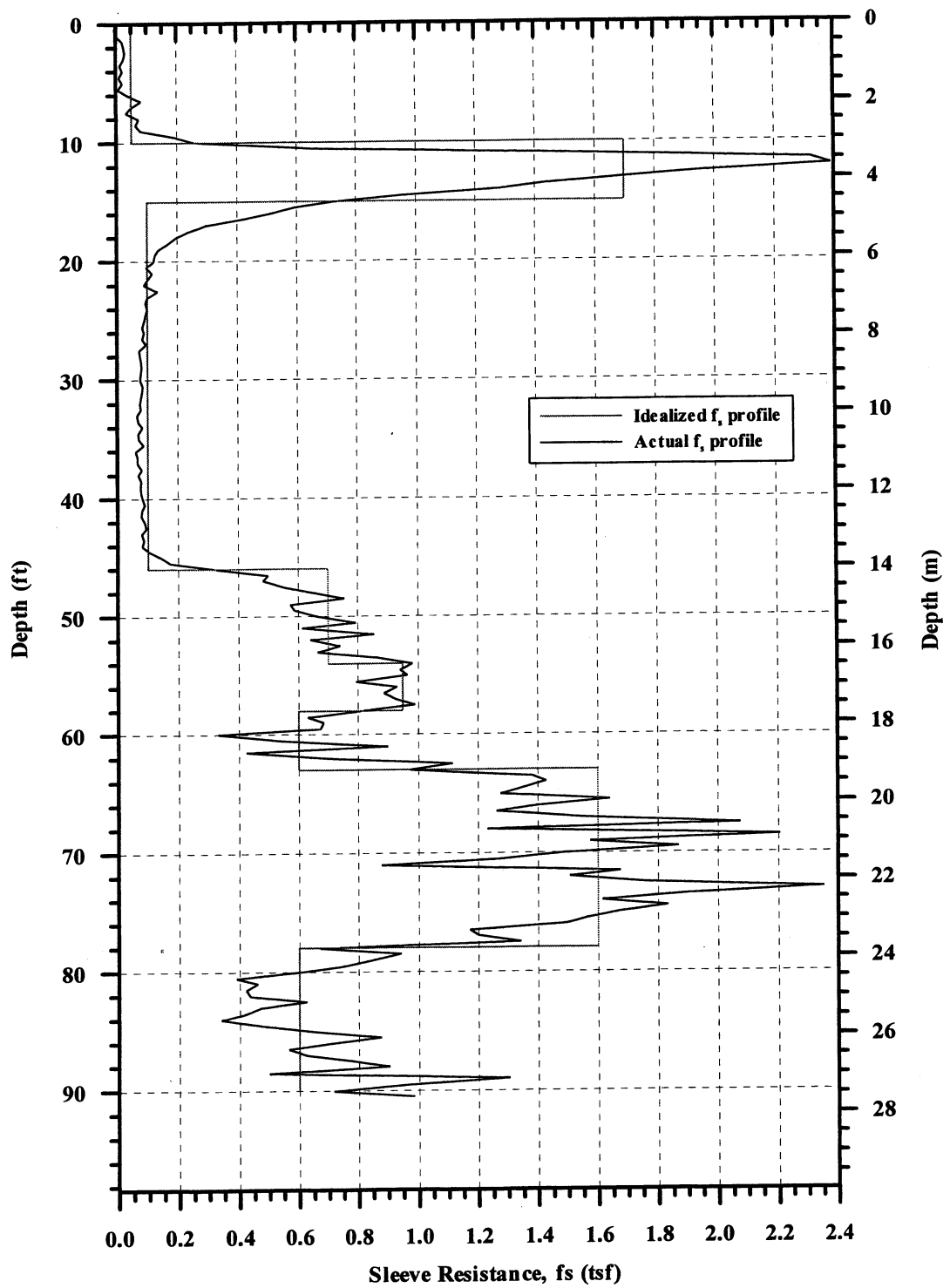


**Figure D.2.** CPT data,  $f_s$  profile with Depth for the Newbury Site.

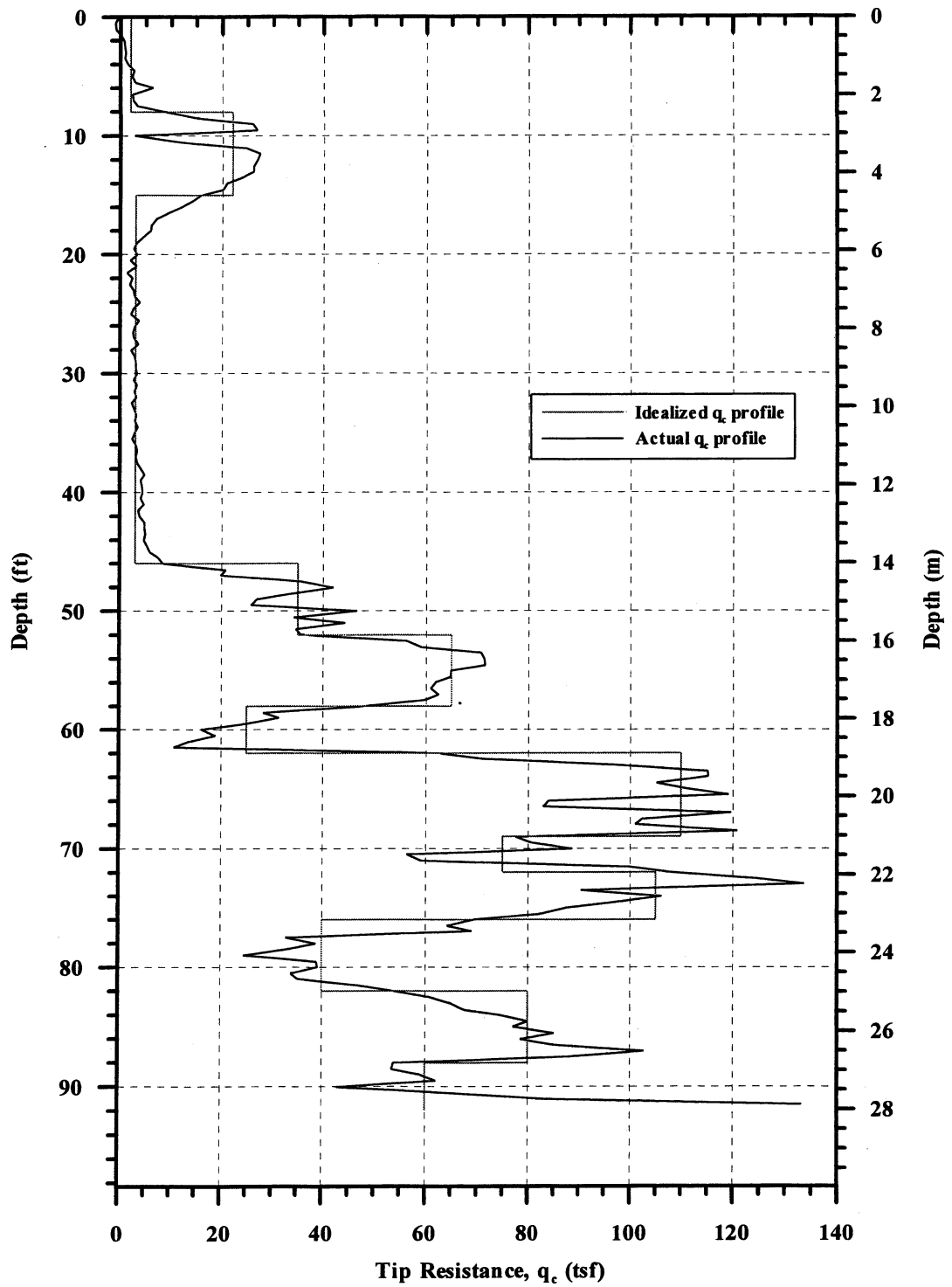


**Figure D.3.** CPT data,  $q_c$  profile with Depth for the Newbury Site.

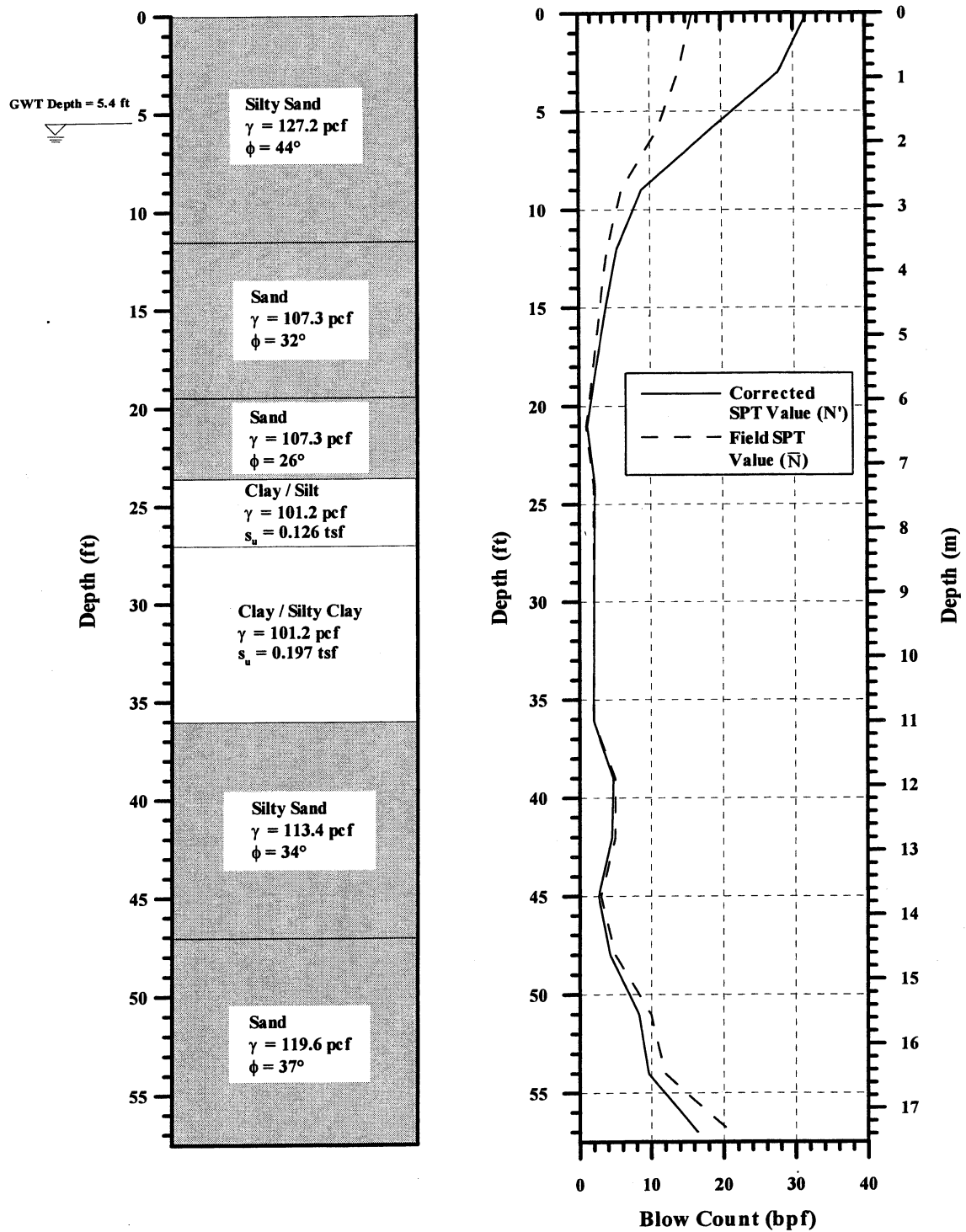


**Figure D.4.** Soil Profile and SPT values with Depth for the Choctawhatchee River Project.



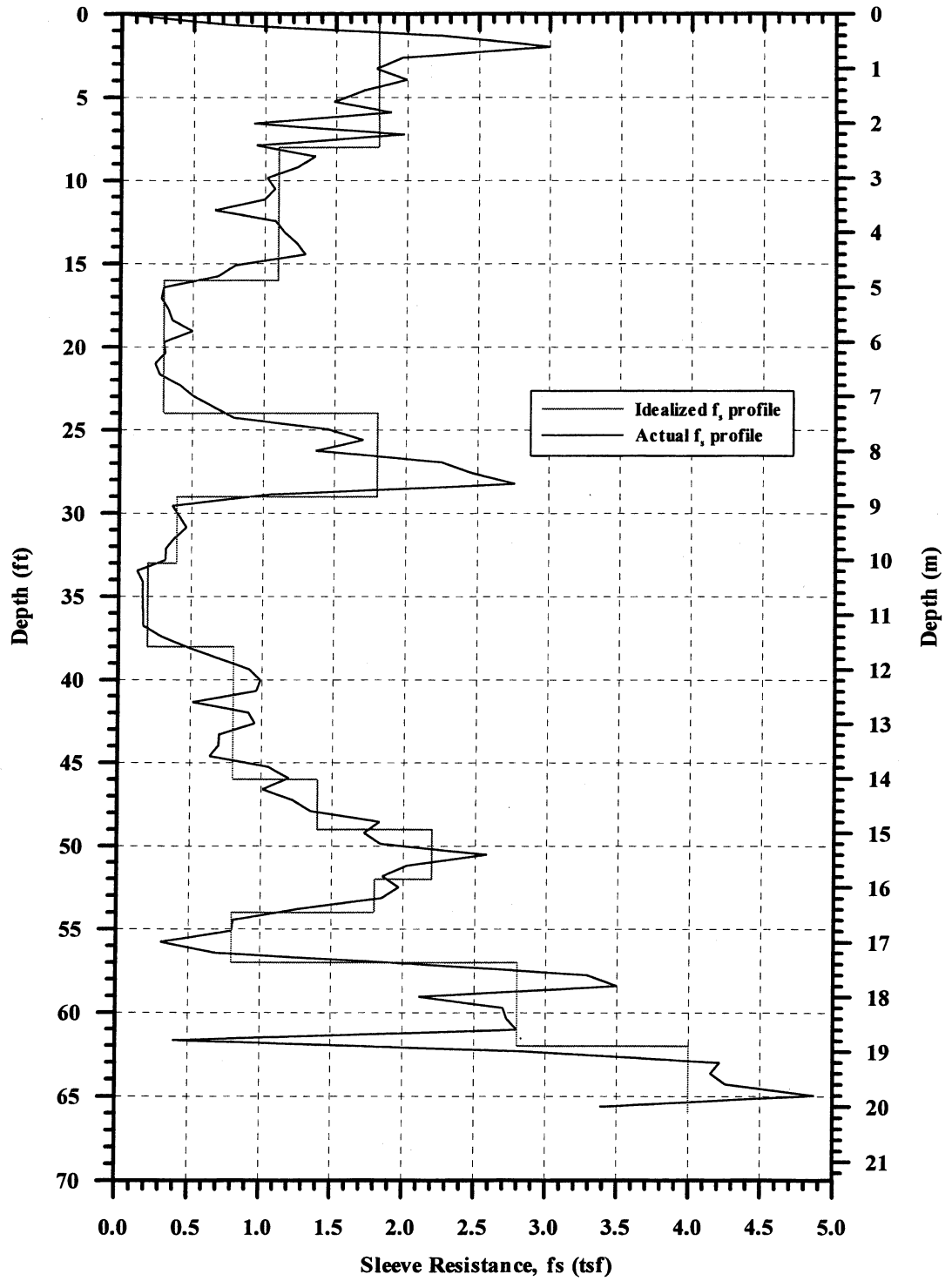


**Figure D.5.** CPT data,  $f_s$  profile with Depth for the Choctawhatchee River Project.

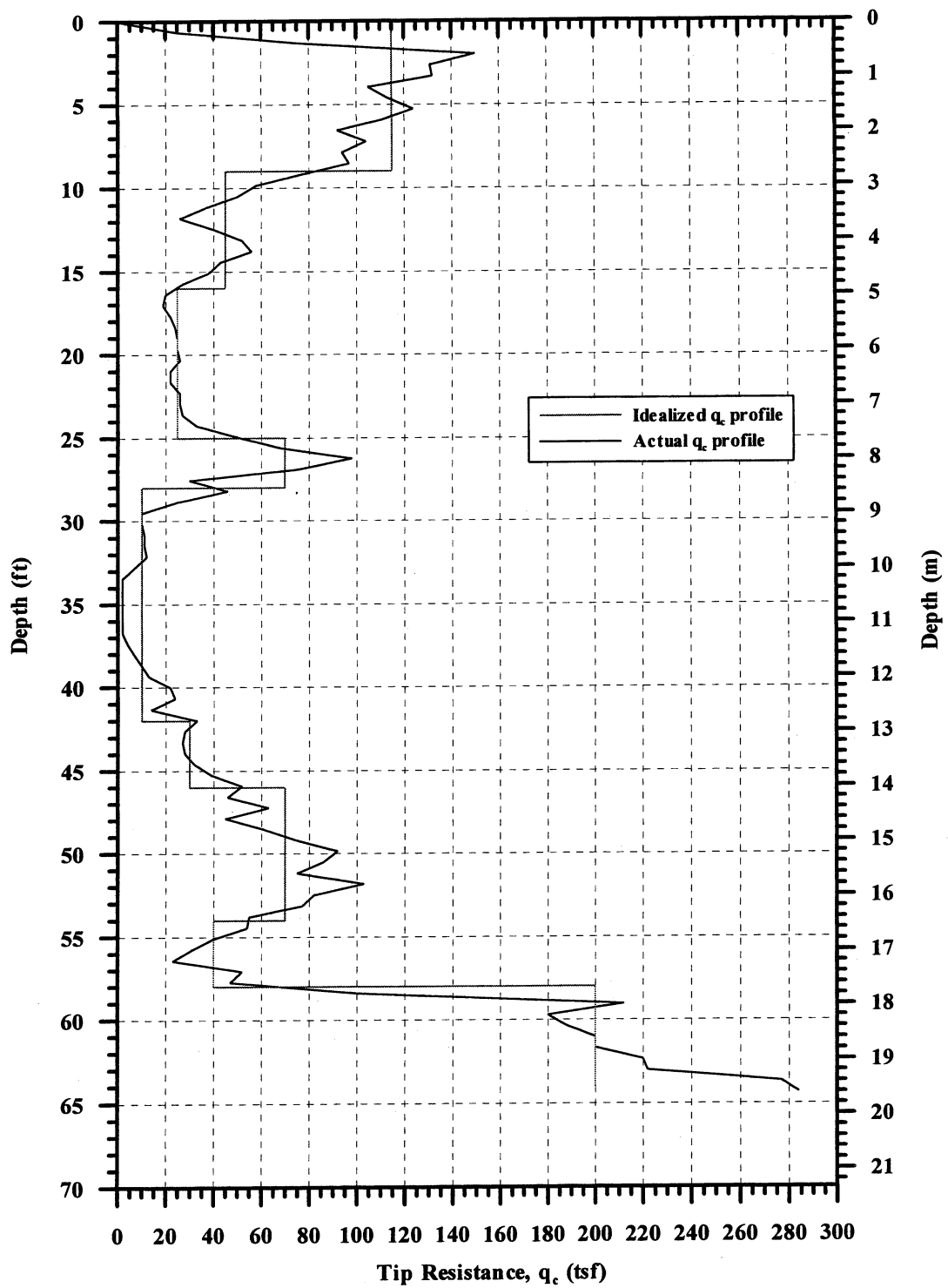


**Figure D.6.** CPT data,  $q_c$  profile with Depth for the Choctawhatchee River Project.

NCHRP 24-17

**LOAD AND RESISTANCE FACTOR DESIGN  
(LRFD) FOR DEEP FOUNDATIONS**

**APPENDIX C  
STATIC ANALYSES OF DRIVEN PILES AND  
DRILLED SHAFTS**

Prepared for National Cooperative Highway Research  
Program  
Transportation Research Board  
National Research Council

Ching L. Kuo  
Geostructures Corp.  
2713 Falling Leaves Drive, Valrico, FL 33594

Bjorn Birgisson and Michael McVay  
Department of Civil Engineering  
University of Florida  
Gainesville, FL 32611-6580

Samuel G. Paikowsky  
Geotechnical Engineering Research Laboratory  
Department of Civil and Environmental Engineering  
University of Massachusetts  
Lowell, Massachusetts

July 2002

### **ACKNOWLEDGEMENT OF SPONSORSHIP**

This work was sponsored by the American Association of State Highway and Transportation Officials, in cooperation with the Federal Highway Administration, and was conducted in the National Cooperative Highway Research Program, which is administered by the Transportation Research Board of the National Research Council.

### **DISCLAIMER**

This is an uncorrected draft as submitted by the research agency. The opinions and conclusions expressed or implied in the report are those of the research agency. They are not necessarily those of the Transportation Research Board, the National Research Council, the Federal Highway Administration, the American Association of State Highway and Transportation Officials, or the individual states participating in the National Cooperative Highway Research Program.

## TABLE OF CONTENTS

1. Overview / Static Analyses
  - 1.1 Scope of Attached Appendix
  - 1.2 Appendix Layout
  - 1.3 Calculated vs. Measured Capacities
    - 1.3.1 Driven Piles
    - 1.3.2 Drilled Shafts
2. LRFD for Static Analyses of Driven Piles and Drilled Shafts  
Driven Piles Static Analysis
  - Part I - Summary table of the obtained Resistance Factors
  - Part II - Detailed of analysis results and Statistics supporting the data summarized in Part I.
  - Part III - Description of Evaluation Methods - detailed descriptions of the methods used to statically evaluate the capacity of the driven piles
3. Drilled Shafts Static Analysis
  - Part I - Summary table of the obtained Resistance Factors
  - Part II - Detailed of analysis results and Statistics supporting the data summarized in Part I.
  - Part III - Description of Evaluation Methods - detailed descriptions of the methods used to statically evaluate the capacity of the drilled shaft.

## **1. Overview / Static Analyses**

### **1.1 Scope of Attached Appendix**

The attached appendix provides the full information regarding databases, methods of analysis, results of analyses and calculated resistance factors for drilled shafts and driven piles based on static methods of analysis.

### **1.2 Appendix Layout**

The appendix is divided into two major parts, Driven Piles and Drilled Shafts. Each part is divided into three major chapters in the following format:

Part I - Summary table of the obtained Resistance Factors

Part II - Detailed of analysis results and Statistics supporting the data summarized in Part I.

Part III - Description of Evaluation Methods - detailed descriptions of the methods used to statistically evaluate the capacity of the driven piles or the drilled shaft, respectively.

### **1.3 Calculated vs. Measured Capacities**

#### ***1.3.1 Driven Piles***

Davisson's failure criterion was used as the representative static capacity of the pile. A discussion and evaluation of the issue is provided in the report and additional details are provided in Appendix B. Note, the maximum load and settlement of each pile load test are provided as part of tables A2 & A3 of the appendix. Davisson's failure criterion is provided as part of the capacity evaluation of each pile type (e.g., Table 50, p. 108 for plugged H piles).

#### ***1.3.2 Drilled Shafts***

FHWA failure criterion was used for the capacity evaluation of the drilled shafts, i.e., the load associated with 5% of the shaft's diameter (0.05B), was taken as the shaft's capacity. As no significant amount of data are available to separate side skin from tip (end) resistances, the following procedure was used for the evaluation of the "measured" skin capacities:

The shape of the load-displacement curves was evaluated and the shafts for which more than 80% of the total capacity was mobilized in a displacement less than 2% of the shaft's diameter, were considered as those in which the resistance is based on friction and comparisons were held with the shaft resistance calculated values. See for example, the drilled shaft table of resistance factors related to skin resistance alone.

## **DRIVEN PILES - STATIC ANALYSIS**

### **SUMMARY TABLES OF RESISTANCE FACTORS**

**Table 1: All Relevant Factors**

**Table 1A: Compressed Summary (initial Evaluation)**

**Table 2: Summary of Correlation Used**

**Table 3: Soil Properties Correlation from SPT**

**Table 4: Soil Properties Correlation from CPT**

winword\research\ongoing\lrfd\databases\florida\drivenpiles10.16.01\cover page for summary tables

**Table 1 – Summary of Recommended Resistance Factors for Static Analysis of Driven Piles  
(Skin or Skin and Tip Resistances)**

Soil/Method/Condition				Correlation Used (See Table 2)	Resistance Factor					
					$\beta = 2.0$		$\beta = 2.5$		$\beta = 3.0$	
					$\phi$	$\phi/\lambda$	$\phi$	$\phi/\lambda$	$\phi$	$\phi/\lambda$
Clay	H-Piles	$\beta$ -Method	N = 4	11.5 B; T&P(2)	0.23	0.38	0.18	0.29	0.13	0.22
		$\lambda$ -Method	N = 17	11.5B; T&P(2) 2B; T&P(5)	0.43	0.54	0.34	0.44	0.28	0.36
		$\alpha$ -Tomlinson	N = 17	2B; T&P(2)	0.47	0.57	0.38	0.46	0.31	0.38
		$\alpha$ -API	N = 17	2B; T&P(5)	0.49	0.51	0.39	0.41	0.31	0.32
		Schmertmann's SPT-97	N = 9		0.45	0.35	0.33	0.26	0.25	0.19
	Concrete Piles	$\lambda$ -Method	N = 19	2B; Hara (5h)	0.52	0.66	0.44	0.56	0.37	0.47
		$\alpha$ -API	N = 19	2B; Hara (5h)	0.56	0.62	0.46	0.52	0.38	0.43
		$\beta$ -Method	N = 8	2B; Hara (5h)	0.38	0.47	0.30	0.37	0.23	0.29
		$\alpha$ -Tomlinson	N = 19	2B; Hara (5h)	0.41	0.43	0.32	0.34	0.24	0.26
	Pipe Piles	$\alpha$ -Tomlinson	N = 20	2B; T&P (1)	0.28	0.36	0.21	0.27	0.15	0.20
		$\alpha$ -API	N = 20	2B; T&P (1)	0.29	0.32	0.22	0.24	0.16	0.17
		$\beta$ -Method	N = 13	2B; T&P (1)	0.15	0.28	0.11	0.20	0.08	0.14
		$\lambda$ -Method	N = 20	2B; T&P (1)	0.26	0.34	0.19	0.26	0.14	0.19
Sand	H-Piles	Nordlund	N = 19	36; 11.5B; P(6)	0.53	0.56	0.43	0.46	0.35	0.37
		Meyerhof	N = 19		0.46	0.53	0.37	0.43	0.30	0.35
		$\beta$ -Method	N = 19	36; 2B; P(5)	0.36	0.46	0.29	0.36	0.22	0.29
		Schmertmann SPT-97	N = 19		0.73	0.51	0.58	0.41	0.46	0.33
	Concrete Piles	Nordlund Method	N = 37	36; 11.5B; P(6)	0.48	0.45	0.37	0.35	0.29	0.27
		$\beta$ -Method	N = 37	36; 2B; P(5)	0.57	0.47	0.45	0.39	0.36	0.31
		Meyerhof Method	N = 37		0.22	0.35	0.17	0.26	0.12	0.19
		Schmertmann's SPT97	N = 37		0.6	0.48	0.47	0.38	0.37	0.30
	Pipe Piles	Nordlund	N = 20	36; 2B P(5)	0.65	0.41	0.5	0.31	0.38	0.24
		$\beta$ -Method	N = 20	36; 2B P(5)	0.45	0.38	0.34	0.29	0.26	0.22
		Meyerhof	N = 20		0.37	0.39	0.28	0.30	0.21	0.22
		Schmertmann's SPT97	N = 20		0.70	0.41	0.54	0.31	0.41	0.24
Mixed Soils	H-Piles	$\alpha$ -Tomlinson/Nordlund/Thurman	N = 22	36; 2B; P(5)	0.25	0.35	0.19	0.26	0.14	0.20
		$\alpha$ -API/Nordlund/Thurman	N = 37	36; 2B; P(5)	0.35	0.38	0.27	0.29	0.20	0.22
		$\beta$ -Method/Thurman	N = 35	36; 2B; P(5)	0.20	0.36	0.15	0.30	0.11	0.20
		Schmertmann's SPT-97	N = 41		0.64	0.51	0.51	0.41	0.41	0.32
	Concrete Piles	$\alpha$ -Tomlinson/Nordlund/Thurman	N = 34	36; 2B; P; Hara(5h)	0.45	0.45	0.35	0.35	0.27	0.27
		$\alpha$ -API/Nordland/Thurman	N = 85	36; 11.5B; Sch; T&P	0.42	0.45	0.33	0.35	0.26	0.27
		$\beta$ -Method/Thurman	N = 85	36; 11.5B; Sch; T&P	0.43	0.49	0.34	0.39	0.27	0.31
		DRIVEN	N = 34		0.43	0.26	0.30	0.18	0.21	0.13
		Schmertmann's SPT97	N = 74		0.75	0.38	0.56	0.29	0.43	0.22
		Schmertmann's CPT	N = 32		0.52	0.58	0.43	0.47	0.35	0.39
	Pipe Piles	All Methods			0.25	--	0.20	--	0.15	--

NOTE: Uplift Capacity to be taken as 0.75 of Compression Capacity



**Table 1A – Compressed Summary of Recommended Resistance Factors for Static Analysis of Driven Piles (Skin or Skin and Tip Resistances)**

Soil/Method/Condition				Correlation Used (See Table 2)	Resistance Factor		
					$\beta = 2.0$	$\beta = 2.5$	$\beta = 3.0$
					$\phi$	$\phi$	$\phi$
Clay	H-Piles	$\beta$ -Method	N = 4	11.5 B; T&P(2)	0.23	0.18	0.13
		$\lambda$ -Method Schmertmann's SPT-97	N = 17 N = 9	11.5B; T&P(2) 2B; T&P(5)	0.44	0.33	0.26
		$\alpha$ -Tomlinson $\alpha$ -API	N = 17 N = 17	2B; T&P(2) 2B; T&P(5)	0.48	0.38	0.30
	Concrete Piles	$\lambda$ -Method $\alpha$ -API	N = 19 N = 19	2B; Hara (5h) 2B; Hara (5h)	0.54	0.45	0.37
		$\beta$ -Method $\alpha$ -Tomlinson	N = 8 N = 19	2B; Hara (5h) 2B; Hara (5h)	0.40	0.31	0.27
	Pipe Piles	$\alpha$ -Tomlinson $\alpha$ -API $\lambda$ -Method	N = 20 N = 20 N = 20	2B; T&P (1) 2B; T&P (1) 2B; T&P (1)	0.30	0.20	0.15
		$\beta$ -Method	N = 13	2B; T&P (1)	0.15	0.11	0.08
	Sand	H-Piles	Nordlund	N = 19	36; 11.5B, P(6)	0.53	0.43
Meyerhof			N = 19		0.46	0.37	0.30
$\beta$ -Method			N = 19	36; 2B; P(5)	0.36	0.29	0.22
Schmertmann SPT-97			N = 19		0.73	0.58	0.46
Concrete Piles		$\beta$ -Method Schmertmann's SPT97	N = 37 N = 37	36; 2B; P(5)	0.58	0.46	0.36
		Nordlund Method	N = 37	36; 11.5B; P(6)	0.48	0.37	0.29
		Meyerhof Method	N = 37		0.22	0.17	0.12
Pipe Piles		Nordlund Schmertmann's SPT97	N = 20 N = 20	36; 2B P(5)	0.65	0.50	0.39
		$\beta$ -Method	N = 20	36; 2B P(5)	0.45	0.34	0.26
		Meyerhof	N = 20		0.37	0.28	0.21
Mixed Soils		H-Piles	$\alpha$ -Tomlinson/Nordlund/ Thurman	N = 22	36; 2B; P(5)	0.20	0.15
	$\beta$ -Method/Thurman		N = 35	36; 2B; P(5)			
	$\alpha$ -API/Nordlund/Thurman		N = 37	36; 2B; P(5)	0.35	0.27	0.20
	Schmertmann's SPT-97		N = 41		0.64	0.51	0.41
	Concrete Piles	$\alpha$ -Tomlinson/Nordlund/ Thurman	N = 34	36; 2B; P; Hara(5h)	0.43	0.33	0.26
		$\alpha$ -API/Nordland/ Thurman	N = 85	36; 11.5B; Sch; T&P			
		$\beta$ -Method/Thurman	N = 85	36; 11.5B; Sch; T&P			
		DRIVEN	N = 34		0.43	0.30	0.21
		Schmertmann's SPT97	N = 74		0.75	0.56	0.43
		Schmertmann's CPT	N = 32		0.52	0.43	0.35
	Pipe Piles	All Methods	---		0.25	0.20	0.15

NOTE: Uplift Capacity to be taken as 0.75 of Compression Capacity

**Table 2: Summary of Correlations Used**

Symbol	(1)	(2)	(3)	(4)	(5)	(6)	(7)	(8)
limit $\phi$ below	40 <sup>0</sup>				36 <sup>0</sup>			
contributed zone to tip resistance	2B	11.5B	2B	11.5B	2B	11.5B	2B	11.5B
$\phi$ , if from SPT, is correlated by	Peck, Hanson and Thornburn <sup>(1)</sup>		Schmertmann <sup>(1)</sup>		Peck, Hanson and Thornburn <sup>(1)</sup>		Schmertmann <sup>(1)</sup>	
$S_u$ , if from SPT, is correlated by	Terzaghi and Peck							

Symbol	(1h)	(2h)	(3h)	(4h)	(5h)	(6h)	(7h)	(8h)
limit $\phi$ below	$40^0$				$36^0$			
contributed zone to tip resistance	2B	11.5B	2B	11.5B	2B	11.5B	2B	11.5B
$\phi$ , if from SPT, is correlated by	Peck, Hanson and Thornburn <sup>(1)</sup>		Schmertmann <sup>(1)</sup>		Peck, Hanson and Thornburn <sup>(1)</sup>		Schmertmann <sup>(1)</sup>	
$S_u$ , if from SPT, is correlated by	Hara <sup>(1)</sup>							

(1) See Tables 3 and 4 for Correlation Details

**Table 3: Correlations of soil properties from SPT**

Properties	From SPT	Reference	
$\phi$	Peck, Hanson and Thornburn: $\approx 54 - 27.6034 \exp(-0.014N')$	Figure 4.12	Kulhawy and Mayne, 1990
	Schmertmann $\phi'$ $\approx \tan^{-1} [ N / (12.2 + 20.3 \sigma') ]^{0.34}$	Figure 4.13 and Equation 4.11	
$S_u$ (bar)	Terzaghi and Peck (1967): $0.06 N$	Equation 4.59	
	Hara 1974: $0.29 N^{0.72}$	Equation 4.60	
OCR for clay	Mayne and Kemper $\approx 0.5 N / \sigma'_o$ ( $\sigma'_o$ in bar)	Figures 3.9 and 3.18	
Dr	Gibbs and Holtz's Figures	Figures 2.13 and 2.14	

**Table 4. Correlations of soil properties from CPT**

Properties	From CPT	Reference	
$\phi$	Robertson and Campanella: $\text{atan}(0.1+0.38*\text{Log}(q_c/\sigma'))$	Figure 4.14 and Equation 4.12	Kulhawy and Mayne, 1990
$S_u$ (bar)	Theoretical: $(q_c - \sigma_o) / Nk$ $q_c$ and $\sigma_o$ in bars.	Equation 4.61	
OCR for clay	Mayne: $0.29 q_c / \sigma'_o$ $q_c$ and $\sigma_o$ in bars.	Figure 3.10	
Dr	Jamiolkowski: $68 \log(q_{cn}) - 68$ $q_{cn} = \frac{q'_c}{\sqrt{P_a \sigma'_o}}$ (dimensionless) $q'_c = q_c / K_q$ $K_q = 0.9 + Dr/300$ $q_c$ and $\sigma'_o$ in bars.	Figure 2.24 and Equation 2.20	

Phi values for driven piles mod 10-18-01.do

# **DRIVEN PILES - STATIC ANALYSIS**

## **RESULTS AND STATISTICS**

winword\research\ongoing\lrfd\libraries\florida\drivenpiles10.16mod.2001

## TABLE OF CONTENTS

### THE LRFD CALIBRATION RESULTS AND ANALYSIS

- 1.1. Capacity--Results for Concrete Piles
  - 1.1.1. Figures of Capacity Prediction--Concrete Piles in Cohesionless Soils (1)
  - 1.1.2. Figures of Capacity Prediction--Concrete Piles in Cohesive Soils (1)
  - 1.1.3. Figures of Capacity Prediction--Concrete Piles in Mixed Soils (1)
  - 1.1.4. Histogram--Concrete Piles in Cohesionless Soils (5)
  - 1.1.5. Histogram--Concrete Piles in Cohesive Soils (5h)
  - 1.1.6. Histogram--Concrete Piles in Mixed Soils (5h)
- 1.2. Capacity--Results for Pipe Piles
  - 1.2.1. Figures of Capacity Prediction--Pipe Piles in Cohesionless Soils (1)
  - 1.2.2. Figures of Capacity Prediction--Pipe Piles in cohesive soil (1)
  - 1.2.3. Figures of Capacity Prediction--Pipe Piles in mixed soils (1):
  - 1.2.4. Histogram--Pipe Piles in Cohesionless Soils (5)
  - 1.2.5. Histogram--Pipe Piles in Cohesive Soils (5h)
  - 1.2.6. Histogram--Pipe Piles in Mixed Soils (5)
- 1.3. Capacity--Results for Plugged H Piles
  - 1.3.1. Figures of Capacity Prediction--Plugged H piles in Cohesionless Soils (5)
  - 1.3.2. Figures of Capacity Prediction--Plugged H piles in Cohesive Soils (5)
  - 1.3.3. Figures of Capacity Prediction--Plugged H piles in Mixed Soils (5)
  - 1.3.4. Histogram--Plugged H piles in Cohesionless Soils (5)
  - 1.3.5. Histogram--Plugged H piles in Cohesive Soils (5)
  - 1.3.6. Histogram--Plugged H piles in Mixed Soils (5)
- 1.4. Statistical Results
- 1.5. Analysis and Discussion of Results

### APPENDICES

#### A. LISTS OF PILES IN THE DATABASE

- A.1. Summary of the Driven Pile Database
- A.2. Concrete Piles
- A.3. Pipe Piles

#### B. SUB-CATEGORY OF CONCRETE PILES

- B.1. Side Resistance Only
- B.2. Total Capacity

#### C. AXIAL CAPACITIES--CONCRETE PILES

#### D. BIAS FACTORS--CONCRETE PILES

#### E. SUB-CATEGORY OF PIPE PILES

- E.1. Side Resistance Only
- E.2. Total Capacity

#### F. AXIAL CAPACITIES--PIPE PILES

#### G. BIAS FACTORS--PIPE PI

H. AXIAL CAPACITIES--PLUGGED H PILES

I. BIAS FACTORS--PLUGGED H PILES

LIST OF REFERENCES

#### LIST OF TABLES

1. Summary of the methods
2. Correlations of soil properties from SPT
3. Correlations of soil properties from CPT
4. Symbols represented the soil parameters used
5. Statistics for Concrete Piles
6. Statistics for Pipe Piles
7. Statistics for Plugged H piles
8. Statistics for Unplugged H piles
9. General observations on the parameters for concrete piles
10. General observations on the parameters for pipe piles
11. General observations on the parameters for H piles
12. Total Cases of Static Load Tests on Concrete Piles in Soils
13. The Data for Side Resistance (S) Concrete Piles
14. The Data for Side and Tip Resistance (ST) Concrete Piles
15. The Data for All Concrete Piles
16. COHESIVE SOILS: Summary of Populations by Analysis Method used to Obtain *Side Resistance Only for Concrete Piles*
17. MIXED SOILS: Summary of Populations by Analysis Method used to Obtain *Side Resistance Only for Concrete Piles*
18. ALL SOILS: Analysis methods for Concrete Piles with *Side Resistance Only*

19. COHESIONLESS SOILS: Summary of Populations by Analysis Method used to Obtain *Total Capacity for Concrete Piles*
20. COHESIVE SOILS: Summary of Populations by Analysis Method used to Obtain *Total Capacity for Concrete Piles*
21. MIXED SOILS: Summary of Populations by Analysis Method used to Obtain *Total Capacity for Concrete Piles*
22. MIXED SOILS and ROCKS: Summary of Populations by Analysis Method used to Obtain *Total Capacity for Concrete Piles*
23. ALL SOILS: Summary of Populations by Analysis Method used to Obtain *Total Capacity for Concrete Piles*
24. ALL SOILS and ROCKS: Summary of Populations by Analysis Method used to Obtain *Total Capacity for Concrete Piles*
25. Axial capacities (KN): Concrete Piles in Cohesionless soils
26. Axial capacities (KN): Concrete Piles in Cohesive soils
27. Axial capacities (KN): Concrete Piles in Mixed soils
28. Bias factor: Concrete Piles in Cohesionless soils
29. Bias factor: Concrete Piles in Cohesive soils
30. Bias factor: Concrete Piles in Mixed soils
31. Total Cases of Static Load Tests on Pipe Piles in Soils
32. The Data for Side Resistance (S) Pipe Piles
33. The Data for Side and Tip Resistance (ST) Pipe Piles
34. The Data for All Pipe Piles
35. COHESIVE SOILS: Summary of Populations by Analysis Method used to Obtain *Side Resistance Only for Pipe Piles*
36. MIXED SOILS: Summary of Populations by Analysis Method used to Obtain *Side Resistance Only for Pipe Piles*
37. ALL SOILS: Summary of Populations by Analysis Method used to Obtain *Side Resist Only for Pipe Piles*
38. COHESIONLESS SOILS: Summary of Populations by Analysis Method used to Obtain *Total Capacity for Pipe Piles*

39. COHESIVE SOILS: Summary of Populations by Analysis Method used to Obtain *Total Capacity for Pipe Piles*
40. MIXED SOILS: Summary of Populations by Analysis Method used to Obtain *Total Capacity for Pipe Piles*
41. MIXED SOILS and ROCKS: Summary of Populations by Analysis Method used to Obtain *Total Capacity for Pipe Piles*
42. ALL SOILS: Summary of Populations by Analysis Method used to Obtain *Total Capacity for Pipe Piles*
43. ALL SOILS and ROCKS: Summary of Populations by Analysis Method used to Obtain *Total Capacity for Concrete Piles*
44. Axial capacities (KN): Pipe Piles in Cohesionless soils
45. Axial capacities (KN): Pipe Piles in Cohesive soils
46. Axial capacities (KN): Pipe Piles in Mixed soils
47. Bias factor: Pipe Piles in Cohesionless soils
48. Bias factor: Pipe Piles in Cohesive soils
49. Bias factor: Pipe Piles in Mixed soils
50. Axial capacities (KN): Plugged H piles in Cohesionless soils
51. Axial capacities (KN): Plugged H piles in Cohesive soils
52. Axial capacities (KN): Plugged H piles in Mixed soils
53. Bias factor: Plugged H piles in Cohesionless soils
54. Bias factor: Plugged H piles in Cohesive soils
55. Bias factor: Plugged H piles in Mixed soils



Table 1: Summary of the methods

Methods	Side resistance	Tip resistance	Parameters required	Constraints
$\alpha$ -Tomlinson (Tomlinson, 1980/1995)	$q_s = \alpha S_u$	$q_p = 9 S_u$	$S_u$ ; $D_b$ (bearing embedment)	+Bearing layer must be stiff cohesive + Number of soil layers $\leq 2$
$\alpha$ -API (Reese et al., 1998)			$S_u$	
$\beta$ in cohesive (AASHTO, 1996/2000)	$q_s = \beta \sigma'$		OCR	
$\lambda$ (US Army Corps of Engineers, 1992)	$q_s = \lambda(\sigma' + 2S_u)$		$S_u$	Only for cohesive soils
$\beta$ in cohesionless (Bowles, 1996)	$\beta \sigma'$		$D_r$	
Nordlund and Thurman (Hannigan et al., 1995)	$q_s = K_\delta C_F \sigma' \frac{\sin(\delta + \varpi)}{\cos \varpi}$	$q_p =$ $\alpha_t N'_q \sigma'$	$\phi$	
Meyerhof SPT (Meyerhof, 1976/1981)	$q_s = k N$	$q_p =$ $0.4D/BN'$	N	+ For cohesionless soils + SPT data
Schmertmann SPT (Lai and Graham, 1995)	$q_s = \text{function}(N)$	$q_p = \text{fn}(N)$	N	SPT data
Schmertmann CPT (McVay and Townsend, 1989)	$q_s = \text{function}(f_s)$	$q_p = \text{fn}(q_c)$	$q_c, f_s$	CPT data

Table 2: Correlations of soil properties from SPT

Properties	From SPT	Reference	
$\phi$	Peck, Hanson and Thornburn: $\approx 54 - 27.6034 \exp(-0.014N')$	Figure 4.12	Kulhawy and Mayne, 1990
	Schmertmann $\phi'$ $\approx \tan^{-1} [ N / (12.2 + 20.3 \sigma') ]^{0.34}$	Figure 4.13 and Equation 4.11	
$S_u$ (bar)	Terzaghi and Peck (1967): $0.06 N$	Equation 4.59	
	Hara 1974: $0.29 N^{0.72}$	Equation 4.60	
OCR for clay	Mayne and Kemper $\approx 0.5 N / \sigma'_o$ ( $\sigma'_o$ in bar)	Figures 3.9 and 3.18	
$Dr$	Gibbs and Holtz's Figures	Figures 2.13 and 2.14	

Table 3. Correlations of soil properties from CPT

Properties	From CPT	Reference	
$\phi$	Robertson and Campanella: $\text{atan}(0.1+0.38*\text{Log}(q_c/\sigma'))$	Figure 4.14 and Equation 4.12	Kulhawy and Mayne, 1990
$S_u$ (bar)	Theoretical: $(q_c - \sigma_o) / Nk$ $q_c$ and $\sigma_o$ in bars.	Equation 4.61	
OCR for clay	Mayne: $0.29 q_c / \sigma'_o$ $q_c$ and $\sigma_o$ in bars.	Figure 3.10	
$Dr$	Jamiolkowski: $68 \log(q_{cn}) - 68$ $q_{cn} = \frac{q'_c}{\sqrt{P_a \sigma'_o}}$ (dimensionless) $q'_c = q_c / K_q$ $K_q = 0.9 + Dr/300$ $q_c$ and $\sigma_o$ in bars.	Figure 2.24 and Equation 2.20	

## THE LRFD CALIBRATION RESULTS AND ANALYSIS

### 1.1. Capacity--Results for Concrete Piles

Table 4: Symbols represented the soil parameters used.

Symbol	(1)	(2)	(3)	(4)	(5)	(6)	(7)	(8)
limit $\phi$ below	$40^\circ$				$36^\circ$			
contributed zone to tip resistance	2B	11.5B	2B	11.5B	2B	11.5B	2B	11.5B
$\phi$ , if from SPT, is correlated by	Peck, Hanson and Thornburn		Schmertmann		Peck, Hanson and Thornburn		Schmertmann	
$S_u$ , if from SPT, is correlated by	Terzaghi and Peck							

Symbol	(1h)	(2h)	(3h)	(4h)	(5h)	(6h)	(7h)	(8h)
limit $\phi$ below	$40^0$				$36^0$			
contributed zone to tip resistance	2B	11.5B	2B	11.5B	2B	11.5B	2B	11.5B
$\phi$ , if from SPT, is correlated by	Peck, Hanson and Thornburn		Schmertmann		Peck, Hanson and Thornburn		Schmertmann	
$S_u$ , if from SPT, is correlated by	Hara							

### 1.1.1. Figures of Capacity Prediction--Concrete Piles in Cohesionless Soils (1)

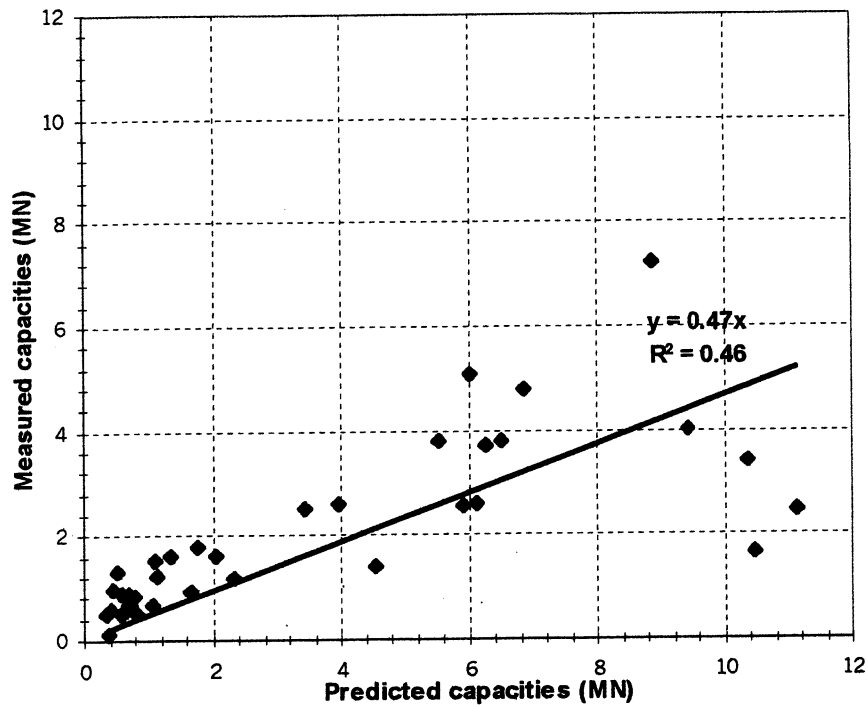


Figure 1. Concrete piles in Cohesionless Soils:  $\beta$  method

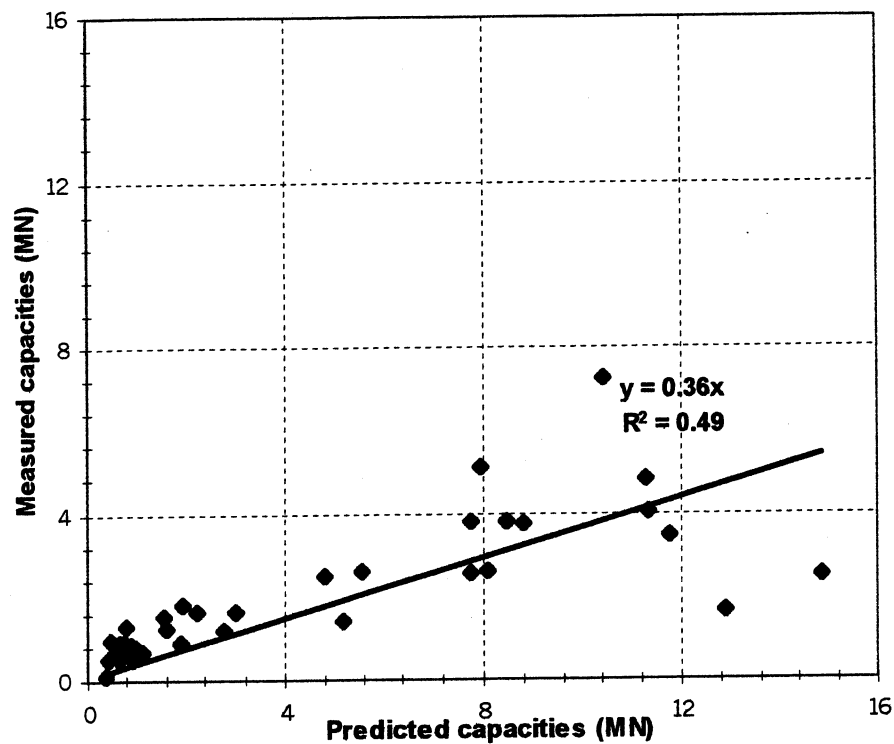


Figure 2: Concrete piles in Cohesionless Soils: Nordlund method

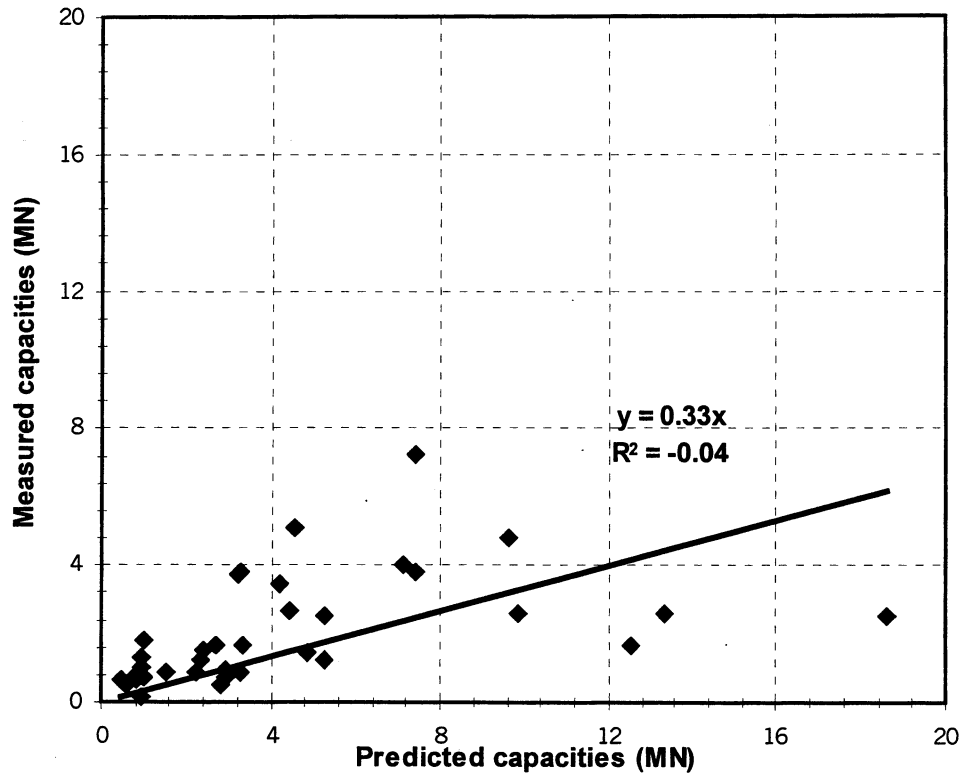


Figure 3: Concrete piles in Cohesionless Soils: Meyerhof method

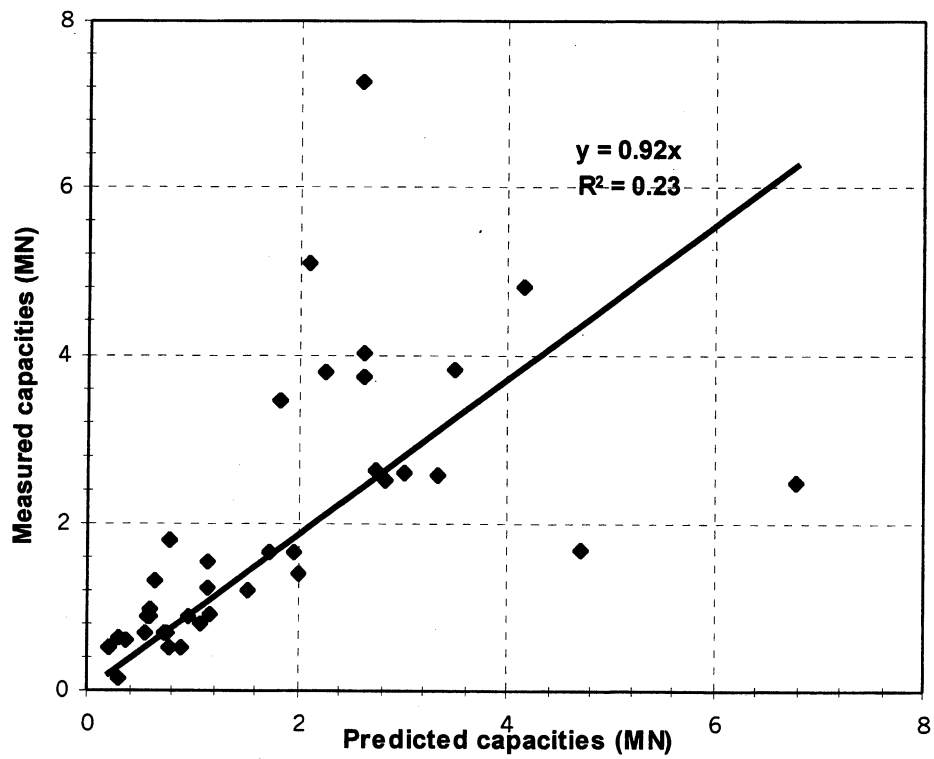


Figure 4: Concrete piles in Cohesionless Soils: Schmertmann SPT mobilized

### 1.1.2. Figures of Capacity Prediction--Concrete Piles in Cohesive Soils (1)

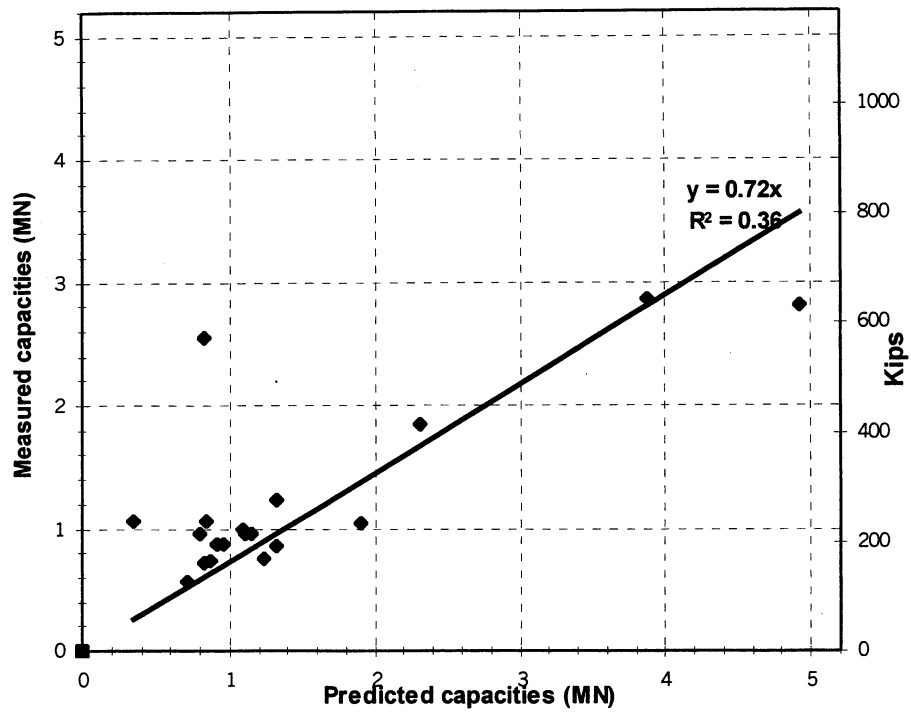


Figure 5: Concrete piles in Cohesive Soils:  $\alpha$ -API method

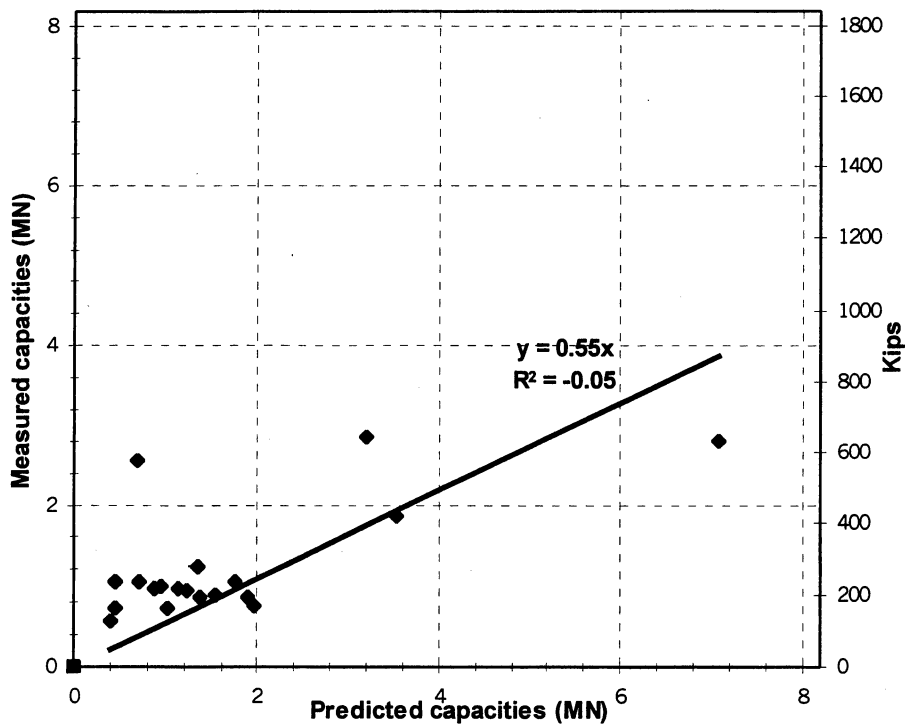


Figure 6: Concrete piles in Cohesive Soils:  $\alpha$ -Tomlinson method

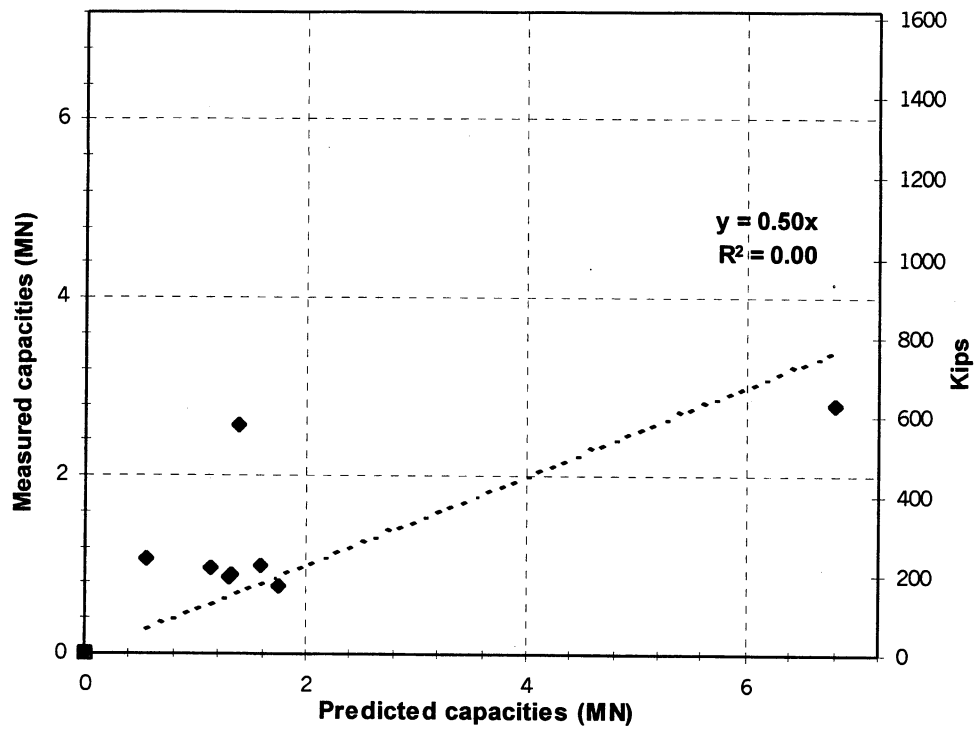


Figure 7: Concrete piles in Cohesive Soils:  $\beta$  method

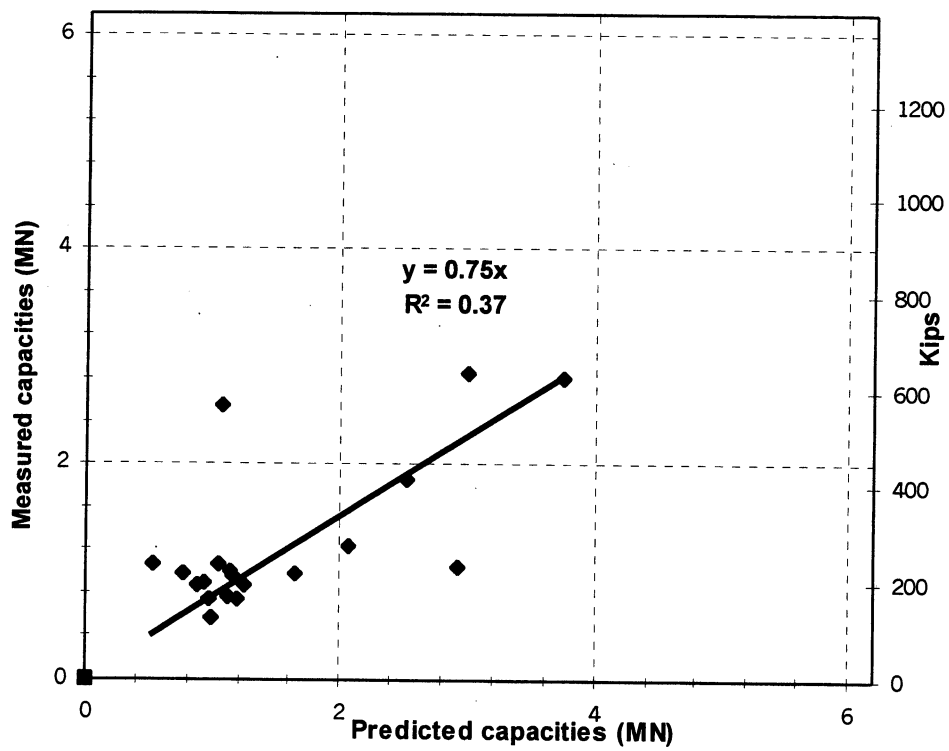


Figure 8: Concrete piles in Cohesive Soils:  $\lambda$  method

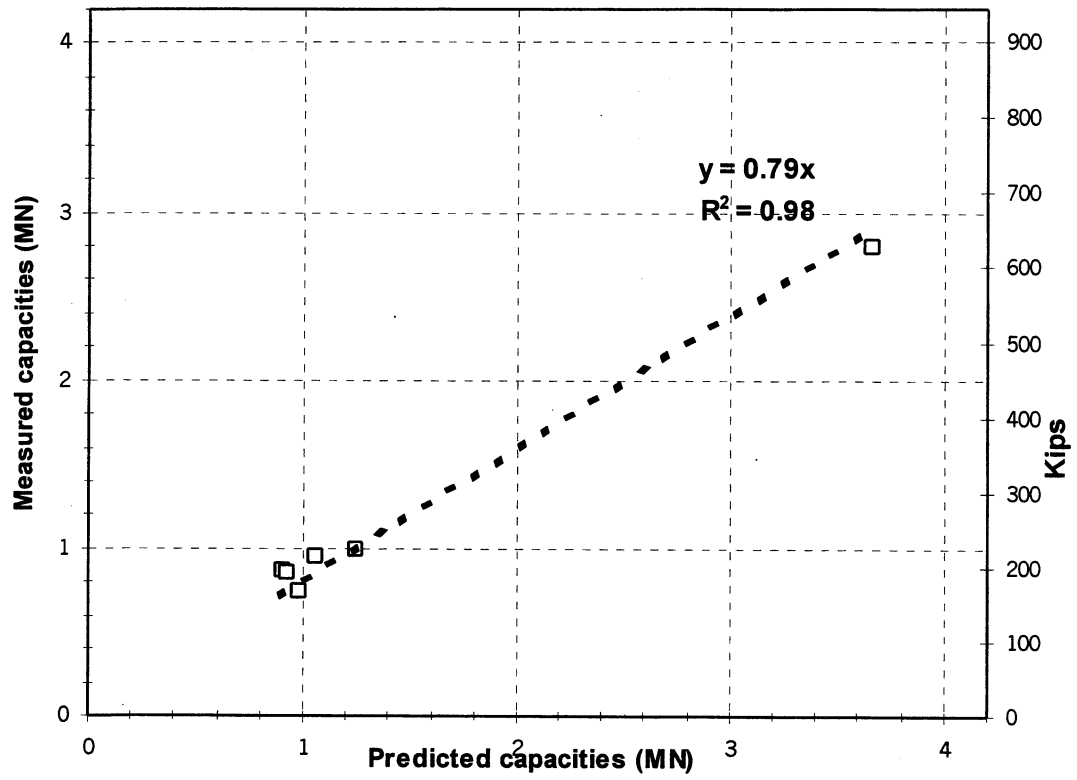


Figure 9: Concrete piles in Cohesive Soils: Schmertmann CPT method



1.1.3. Figures of Capacity Prediction--Concrete Piles in Mixed Soils (1)

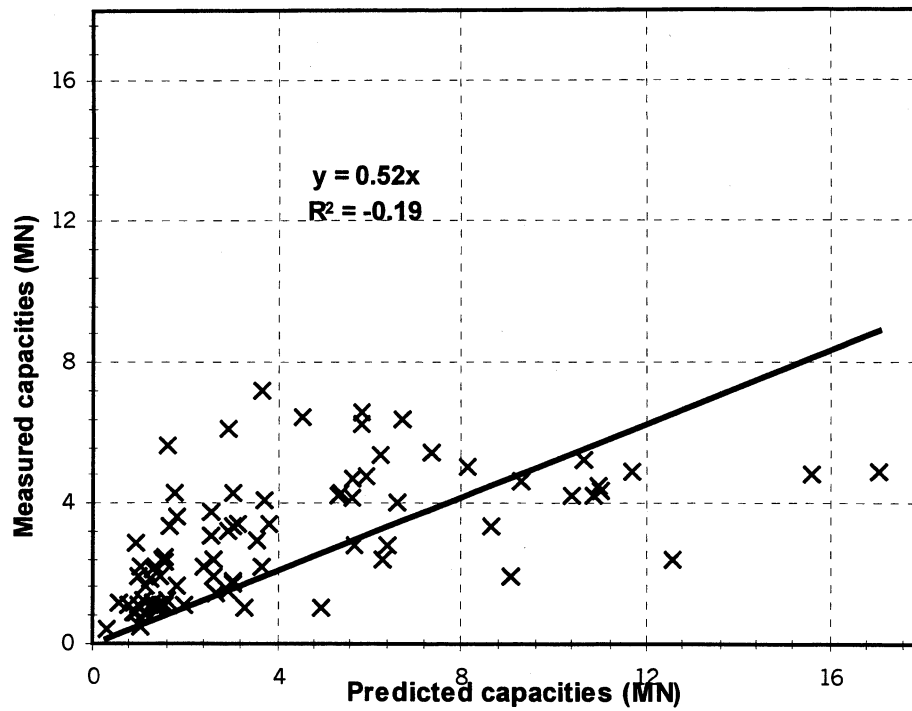


Figure 10: Concrete piles in Mixed Soil:  $\alpha$ -API, Nordlund, Thurman methods

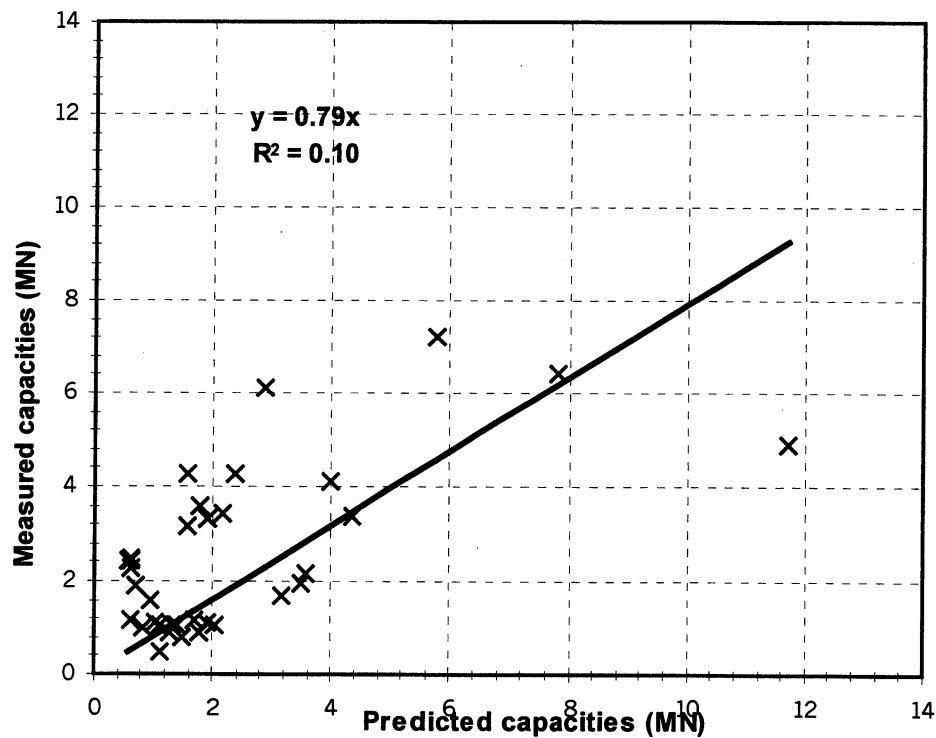


Figure 11: Concrete piles in Mixed Soil:  $\alpha$ -Tomlinson, Nordlund, Thurman methods

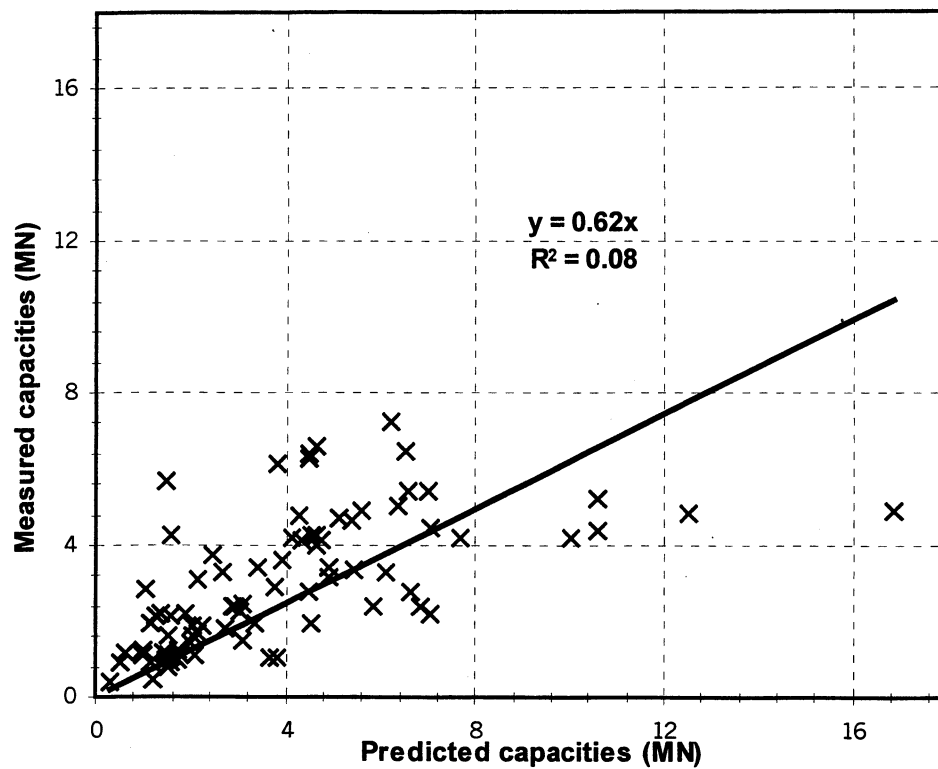


Figure 12: Concrete piles in Mixed Soil:  $\beta$  method

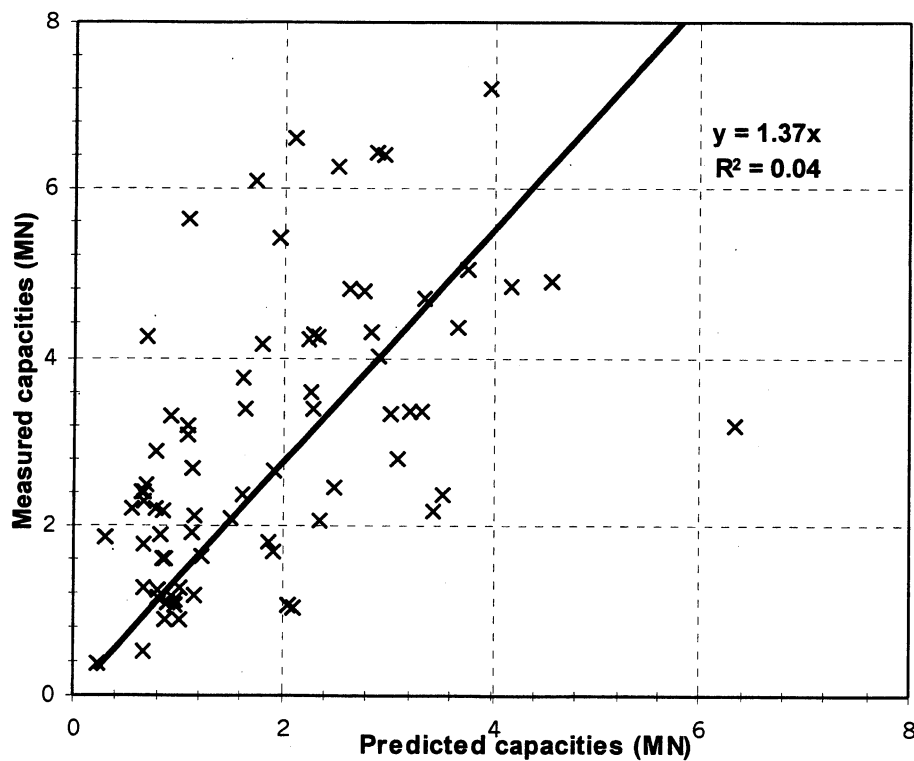


Figure 13: Concrete piles in Mixed Soil: Schmertmann SPT mobilized

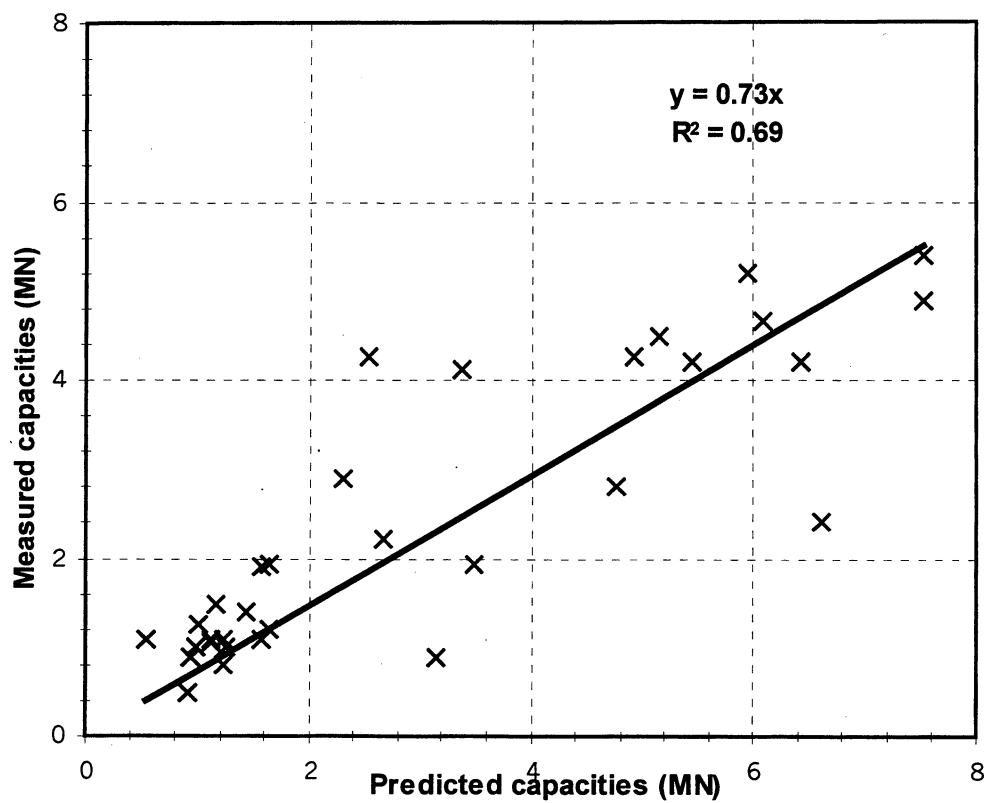


Figure 14: Concrete piles in Mixed Soil: Schmertmann CPT method

#### 1.1.4. Histogram--Concrete Piles in Cohesionless Soils (5)

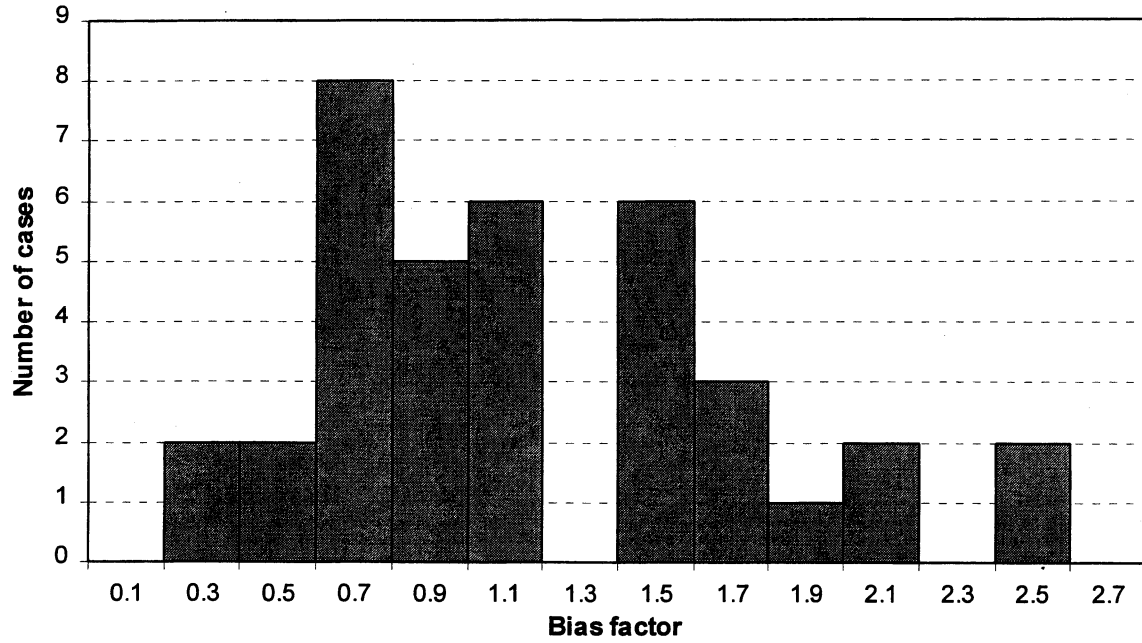


Figure 15: Histogram-- $\beta$  method (5):  $\lambda_R = 1.17$

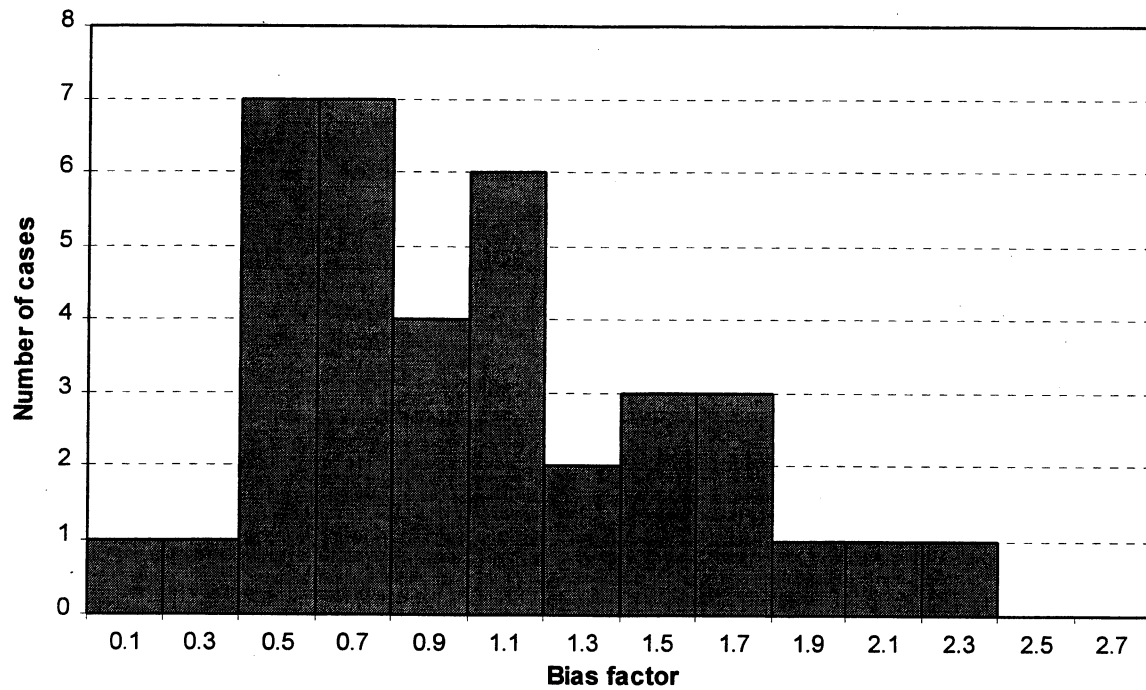


Figure 16: Histogram--Nordlund method (5):  $\lambda_R = 1.00$

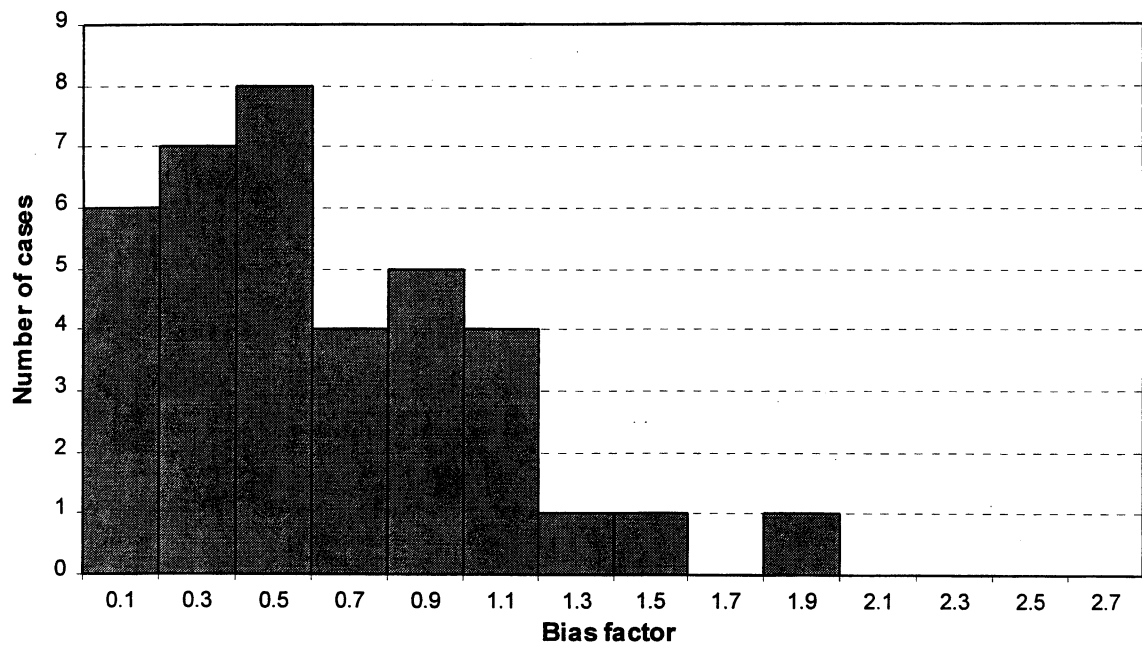


Figure 17: Histogram--Meyerhof method:  $\lambda_R = 0.64$

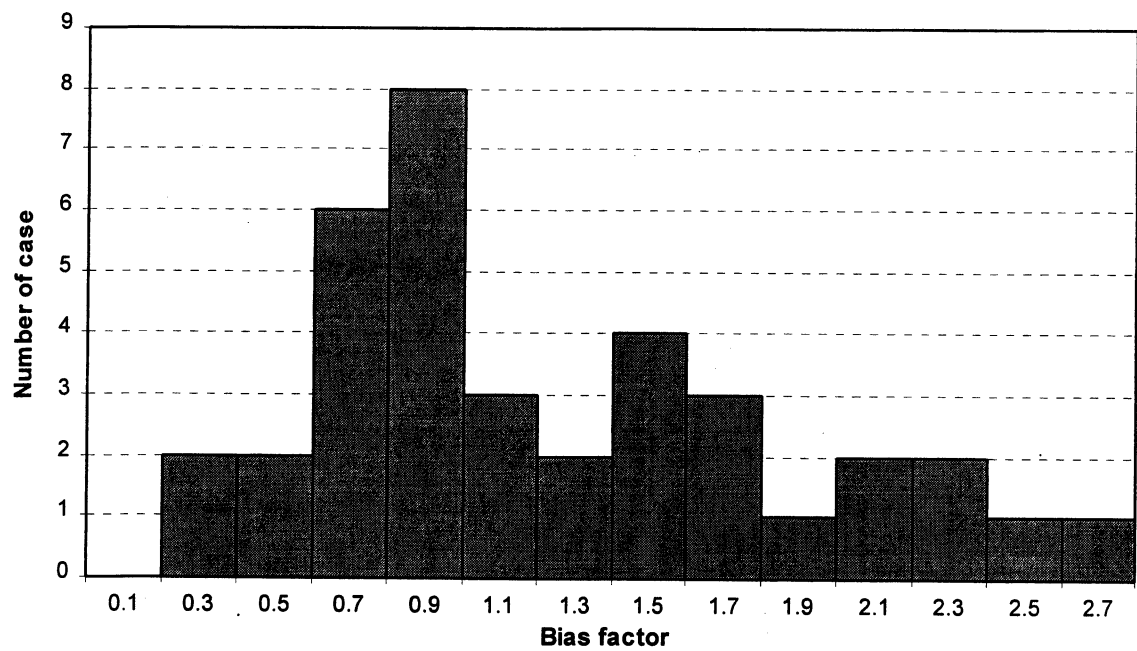


Figure 18: Histogram--Schmertmann SPT mobilized method:  $\lambda_R = 1.25$

### 1.1.5. Histogram--Concrete Piles in Cohesive Soils (5h)

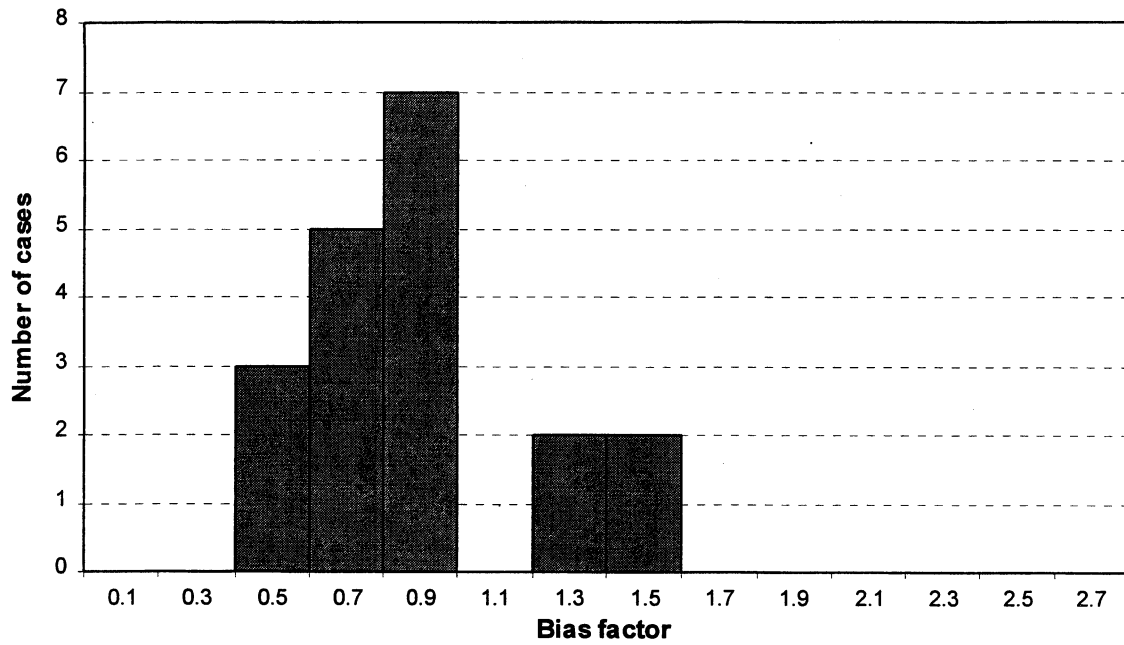


Figure 19: Histogram-- $\alpha$ -API method (5h):  $\lambda_R = 0.89$

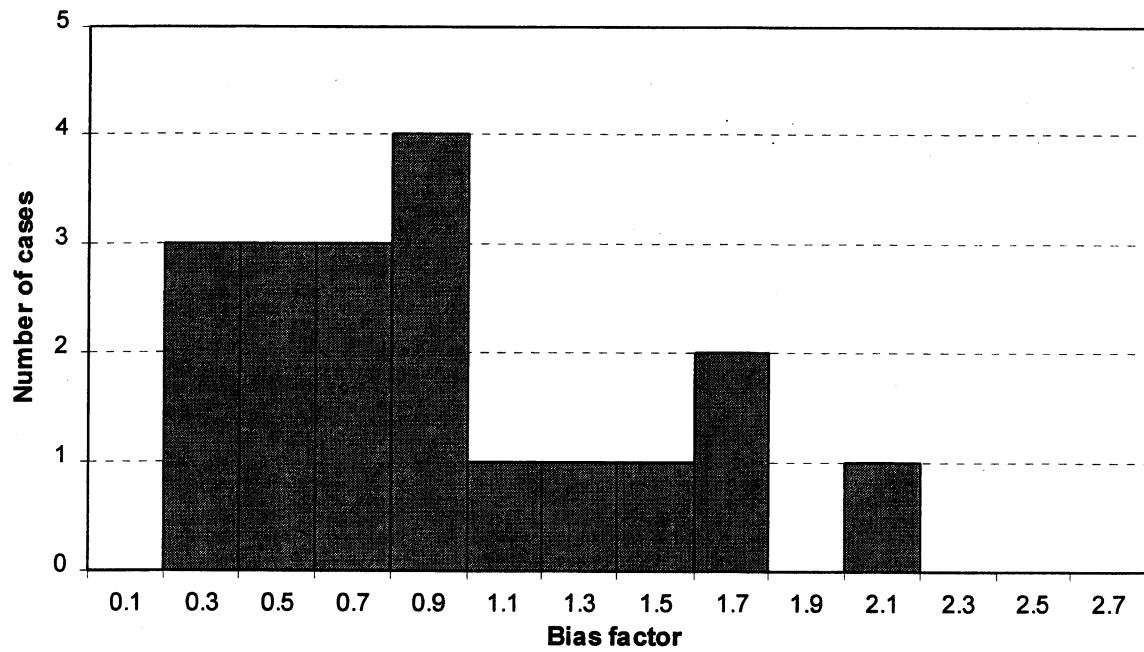


Figure 20: Histogram-- $\alpha$ -Tomlinson method (5h) :  $\lambda_R = 0.94$

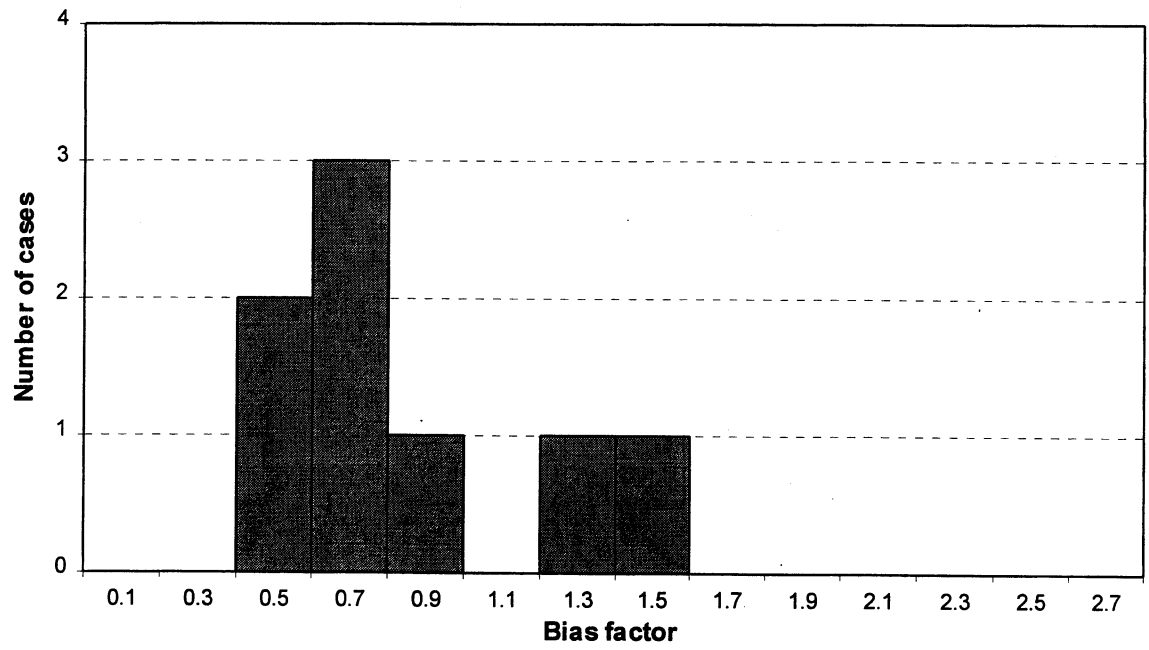


Figure 21: Histogram-- $\beta$  method (5h) :  $\lambda_R = 0.81$

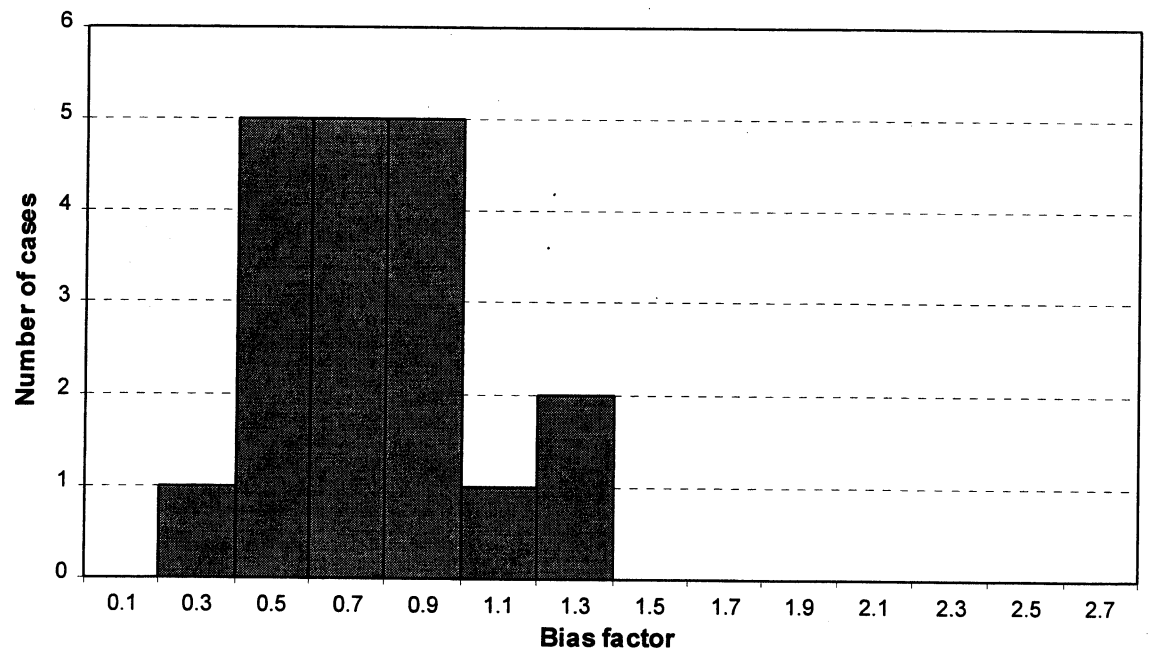


Figure 22: Histogram-- $\lambda$  method (5h) :  $\lambda_R = 0.79$

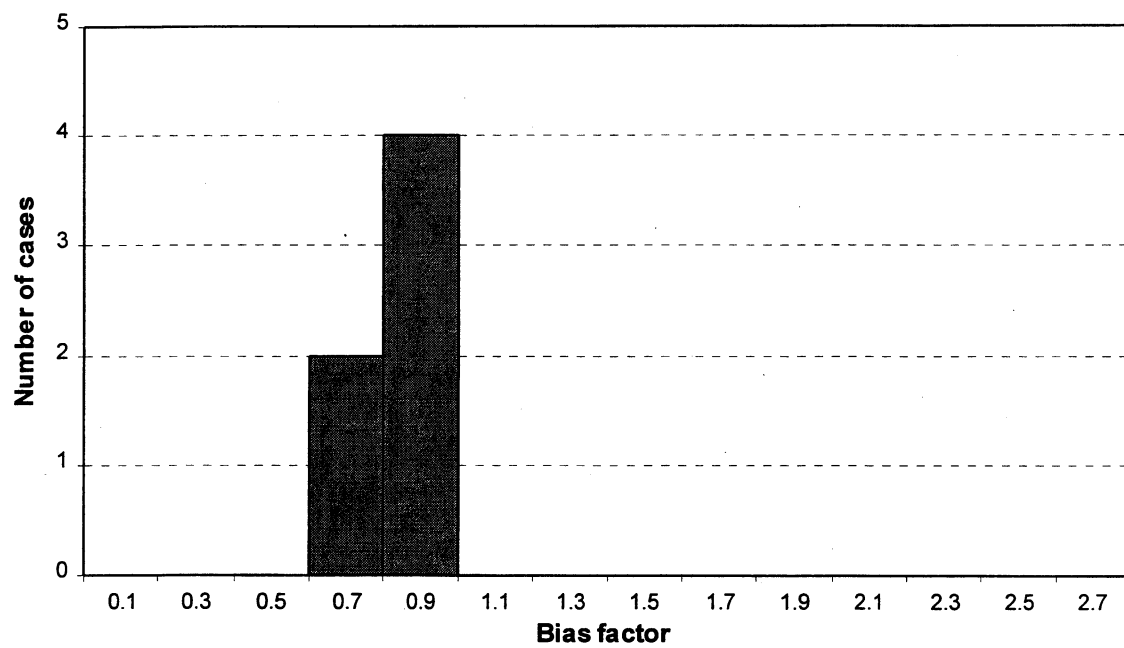


Figure 23: Histogram--Schmertmann CPT method:  $\lambda_R = 0.86$



### 1.1.6. Histogram--Concrete Piles in Mixed Soils (5h)

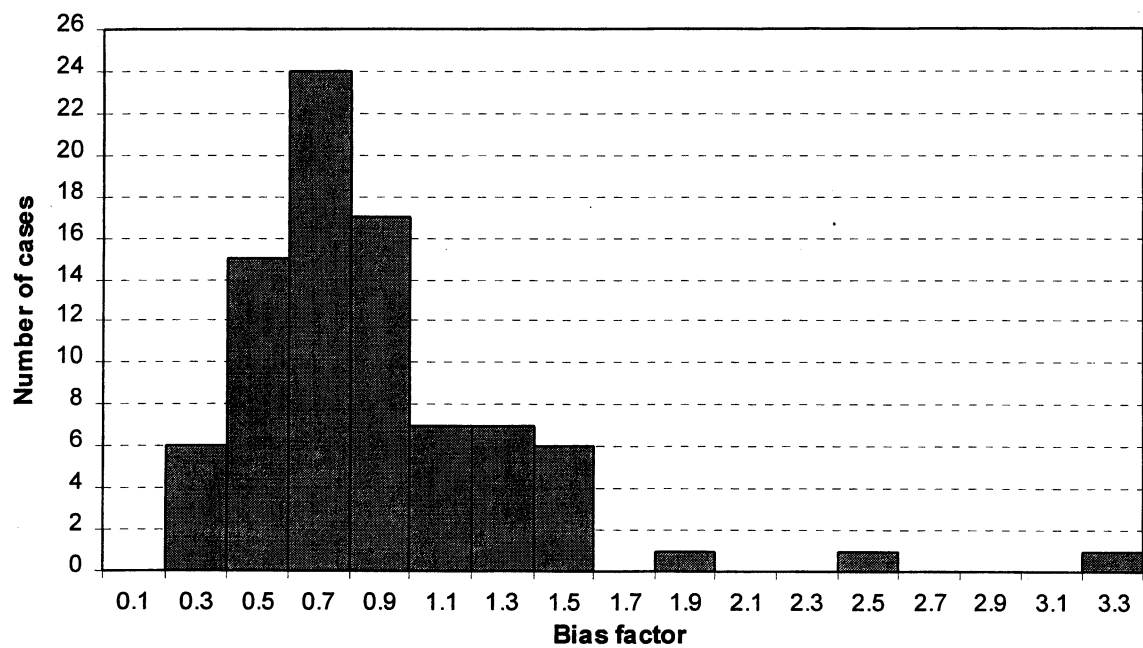


Figure 24: Histogram-- $\alpha$ -API/ Nordlund method (5h) :  $\lambda_R = 0.88$

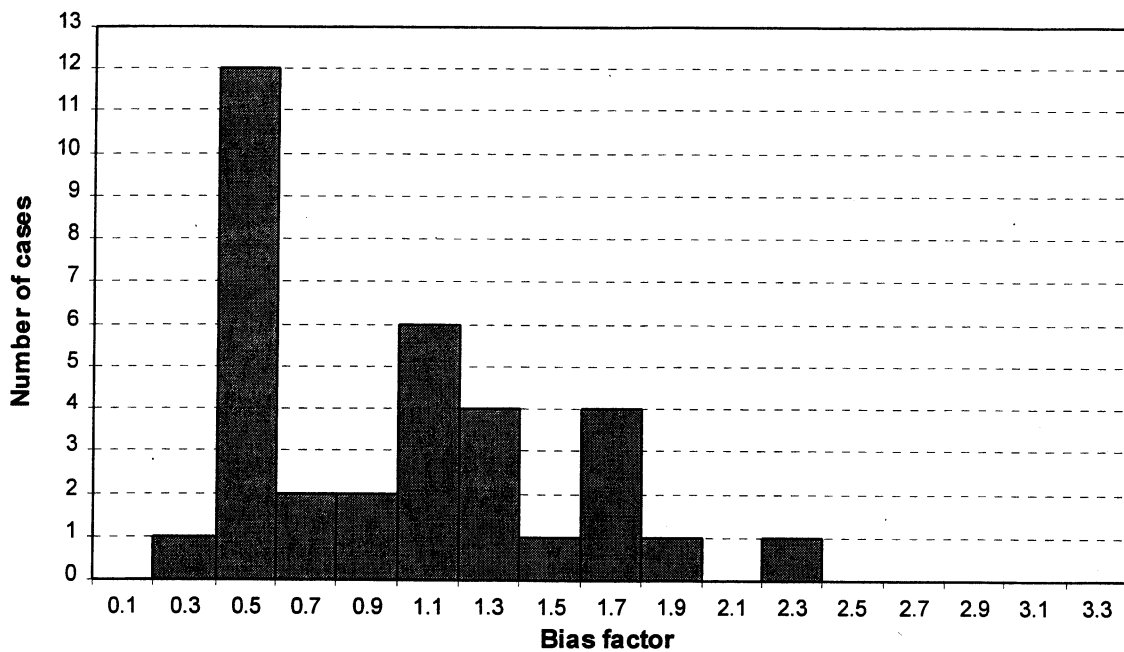


Figure 25: Histogram-- $\alpha$ -Tomlinson/ Nordlund method (5h) :  $\lambda_R = 1.00$

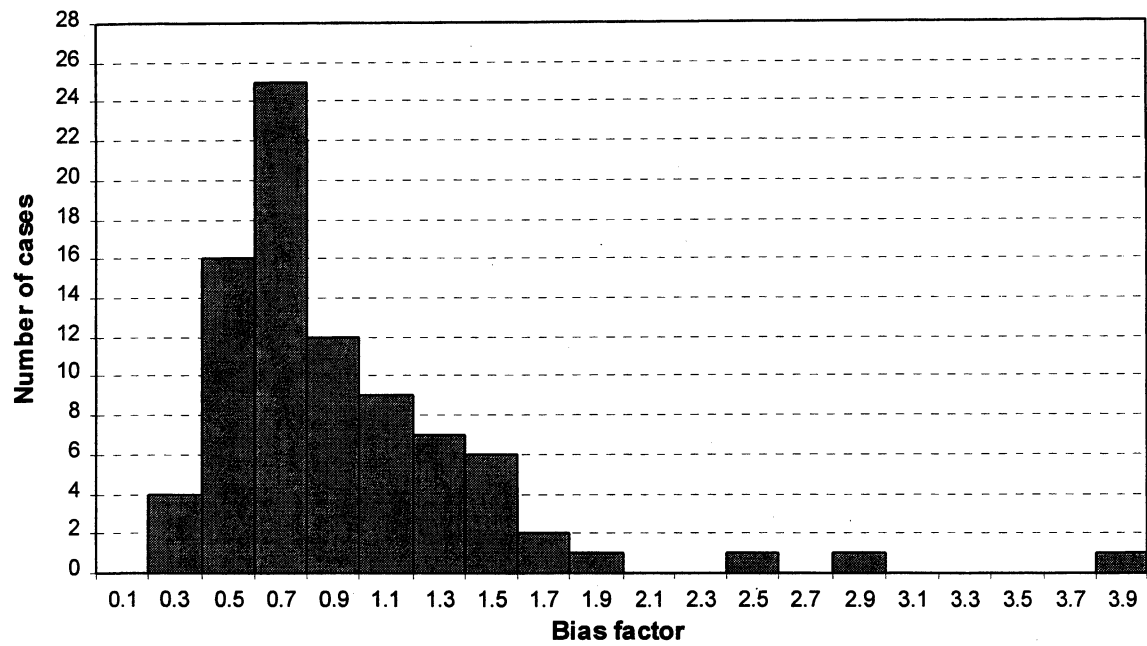


Figure 26: Histogram-- $\beta$ /Thurman method (5h) :  $\lambda_R = 0.93$

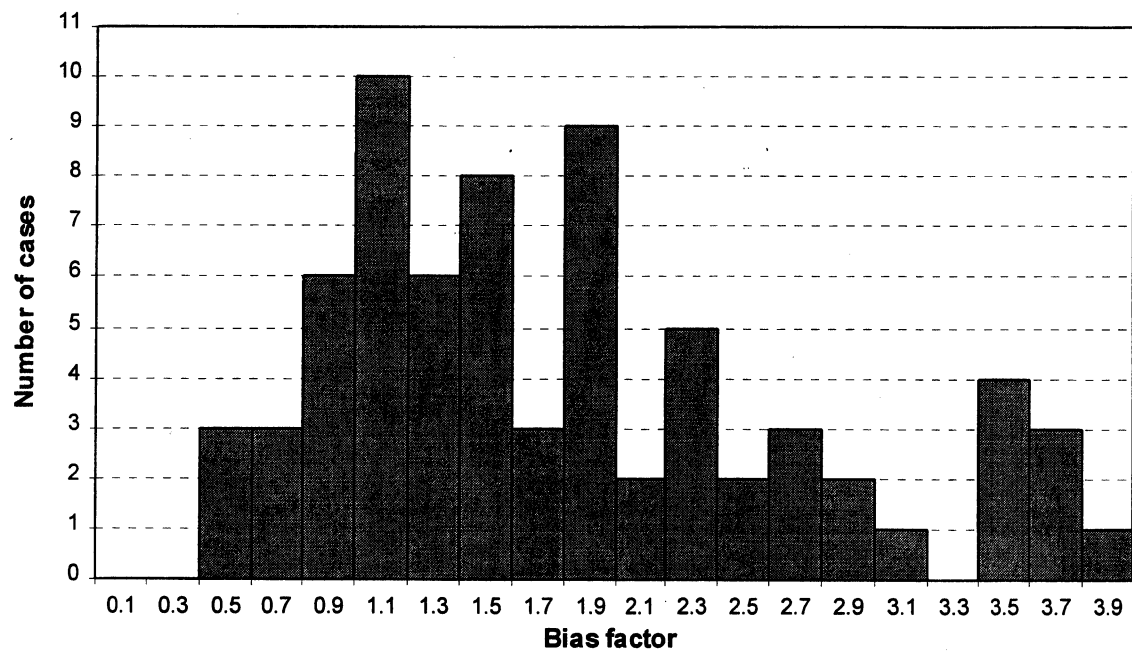


Figure 27: Histogram--Schmertmann SPT mobilized method

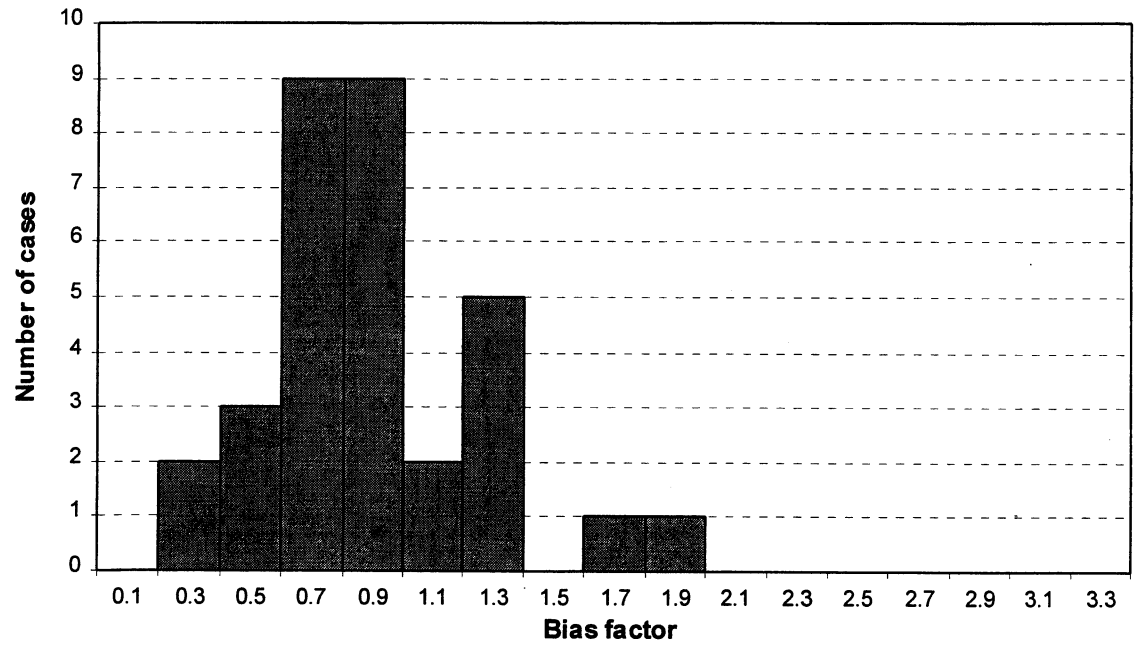


Figure 28: Histogram--Schmertmann CPT method

## 1.2. Capacity--Results for Pipe Piles

### 1.2.1. Figures of Capacity Prediction--Pipe Piles in Cohesionless Soils (1)

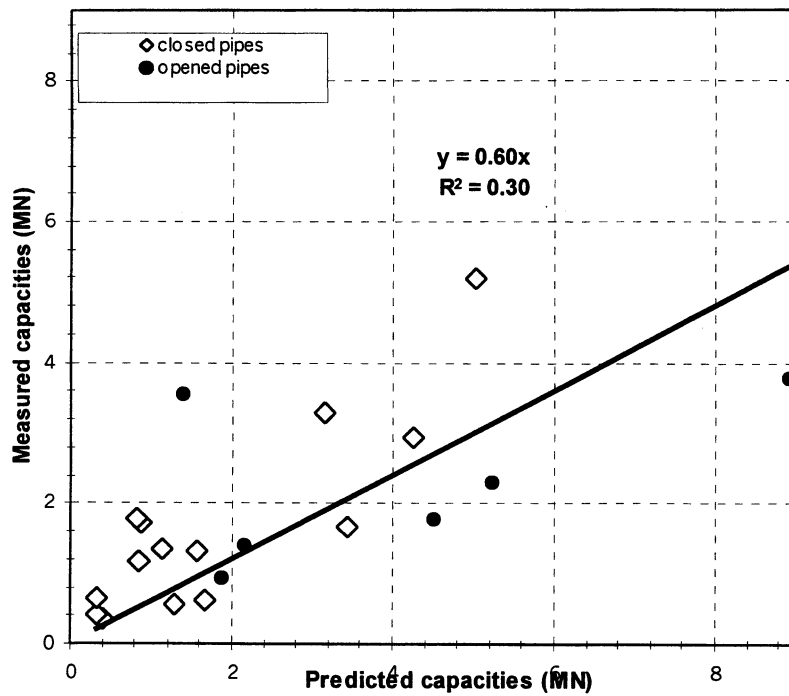


Figure 29: Pipe piles in Cohesionless soil-- $\beta$  method

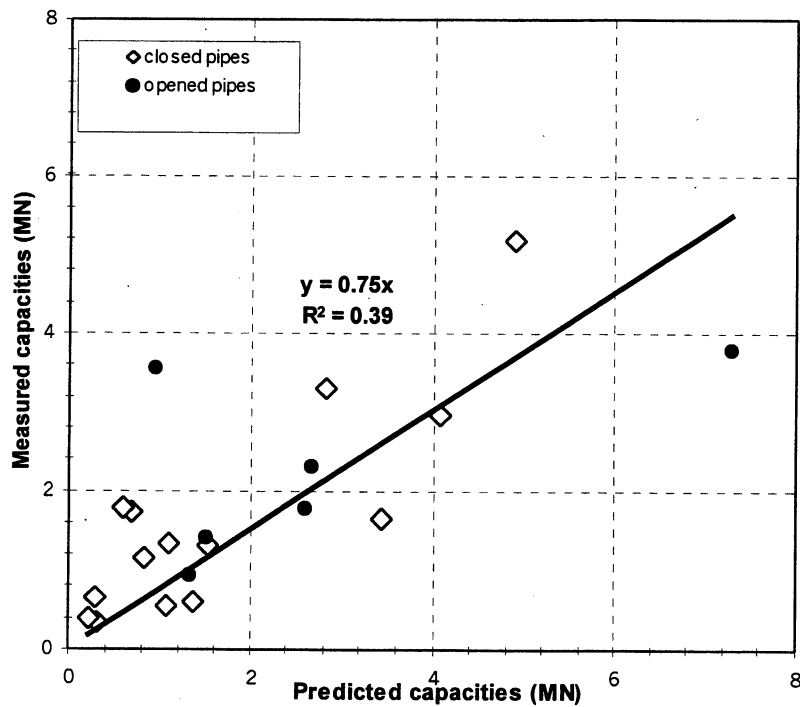


Figure 30: Pipe piles in Cohesionless soil--Nordlund method

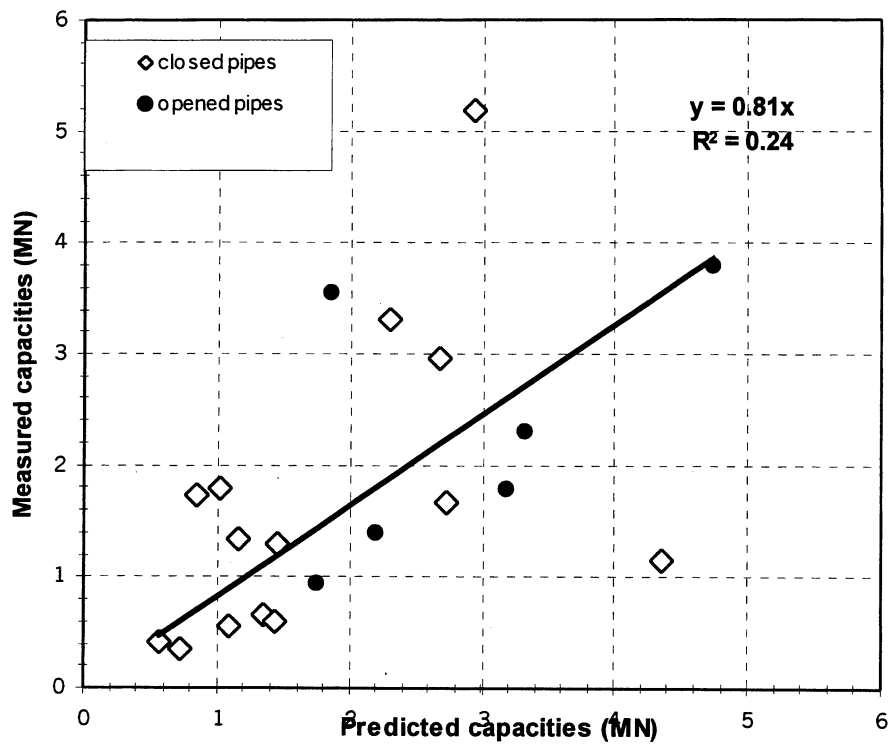


Figure 31: Pipe piles in Cohesionless soil--Meyerhof method

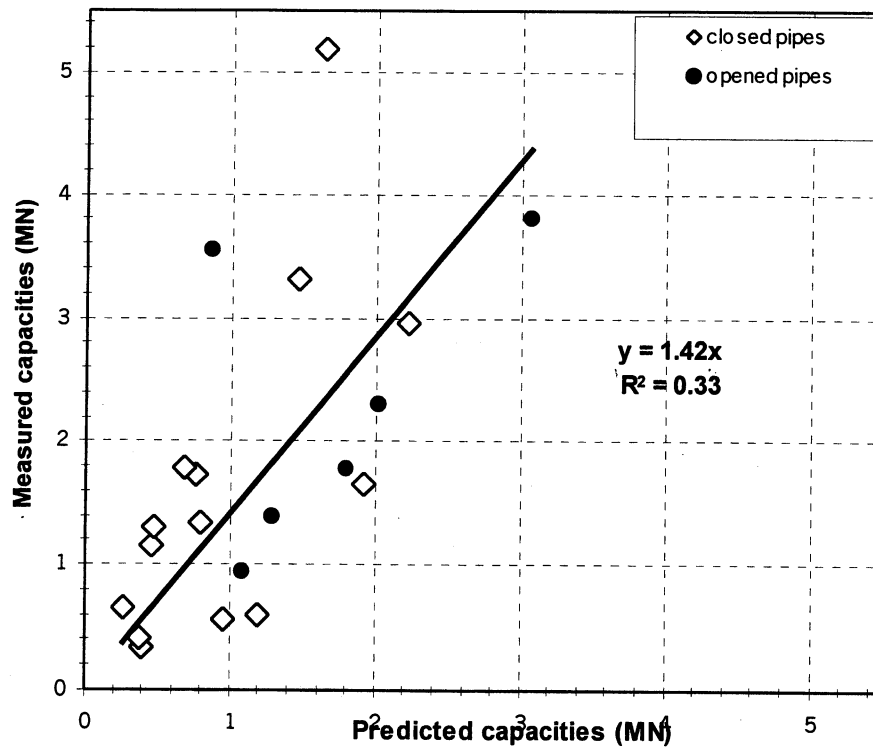


Figure 32: Pipe piles in Cohesionless soil--Schmertmann SPT method

1.2.2. Figures of Capacity Prediction--Pipe Piles in cohesive soil (1)

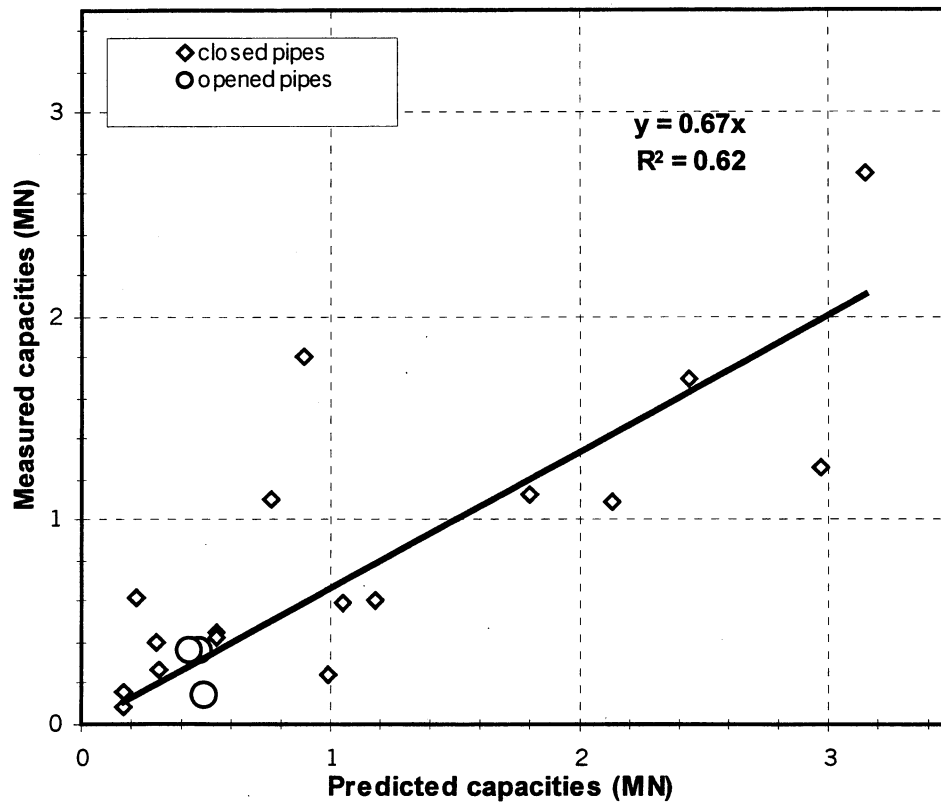


Figure 33: Pipe piles in cohesive soil-- $\alpha$ -API method

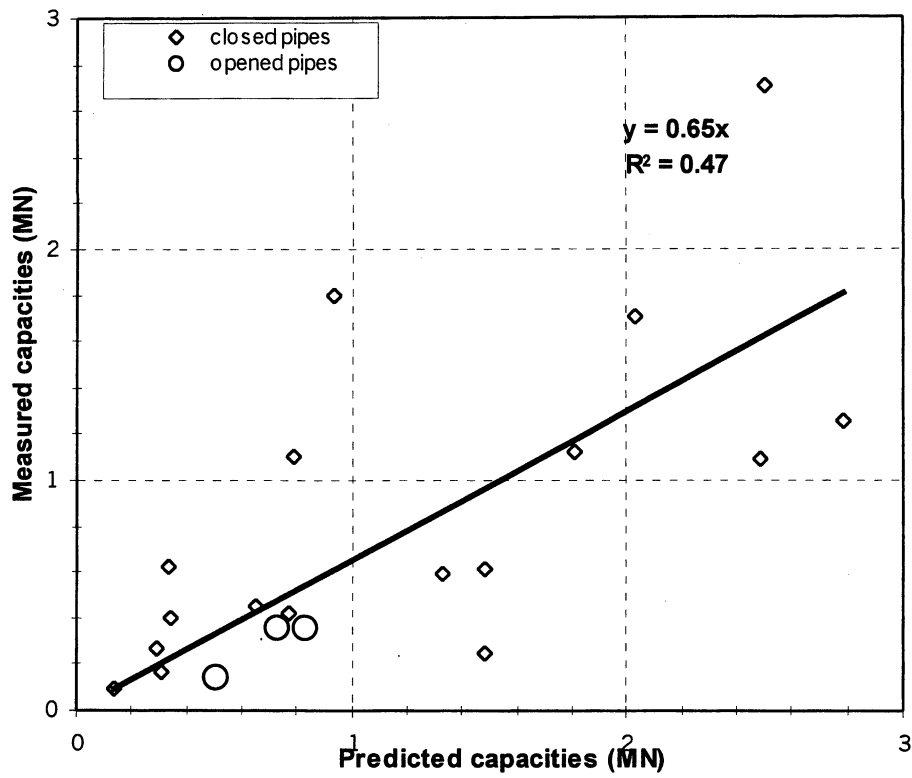


Figure 34: Pipe piles in cohesive soil-- $\alpha$ -Tomlinson 1980 method

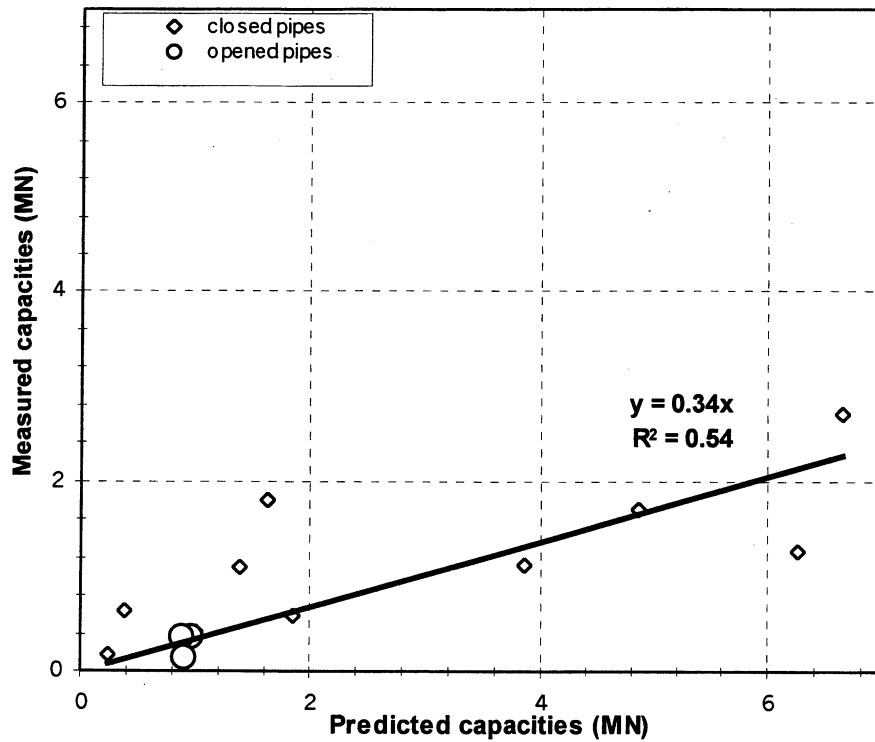


Figure 35: Pipe piles in cohesive soil-- $\beta$  method

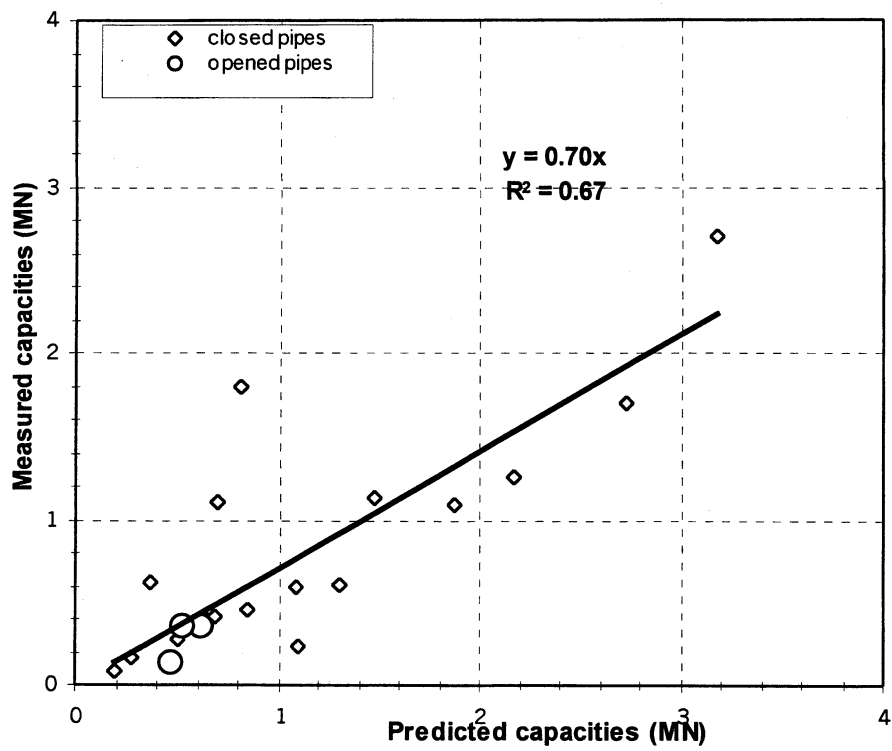


Figure 36: Pipe piles in cohesive soil-- $\lambda$  method

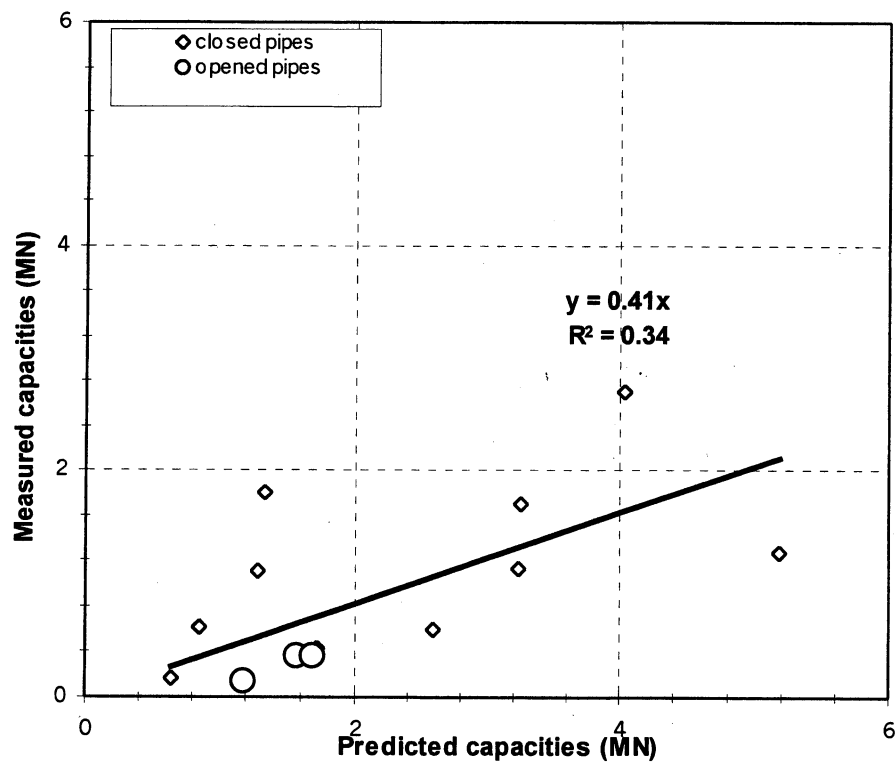


Figure 37: Pipe piles in cohesive soil--Schmertmann SPT method



1.2.3. Figures of Capacity Prediction--Pipe Piles in mixed soils (1):

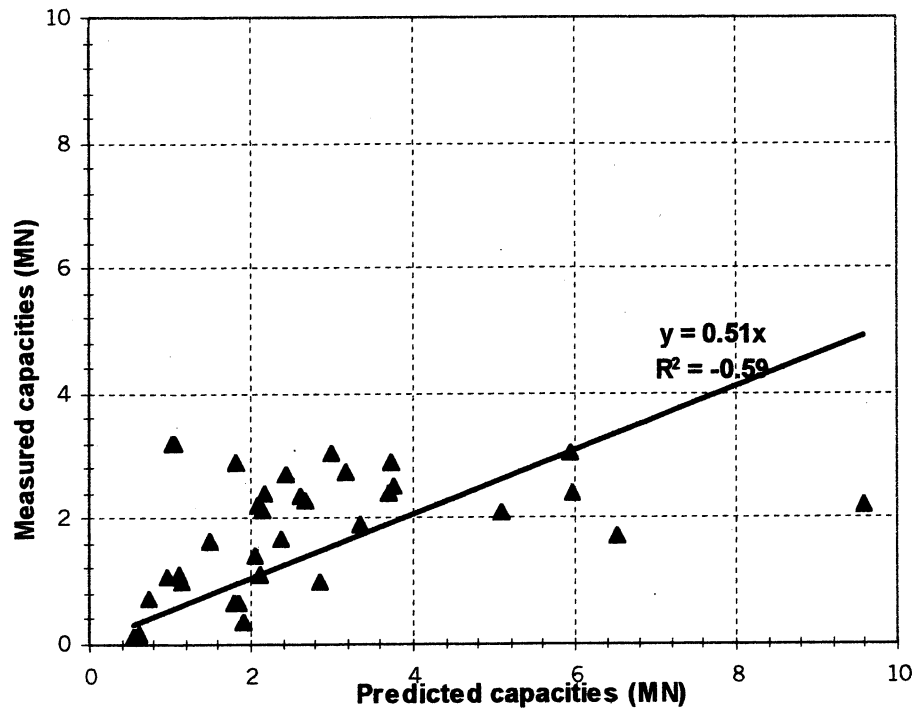


Figure 38: Pipe piles in mixed soils-- $\alpha$ -API, Nordlund, Thurman methods

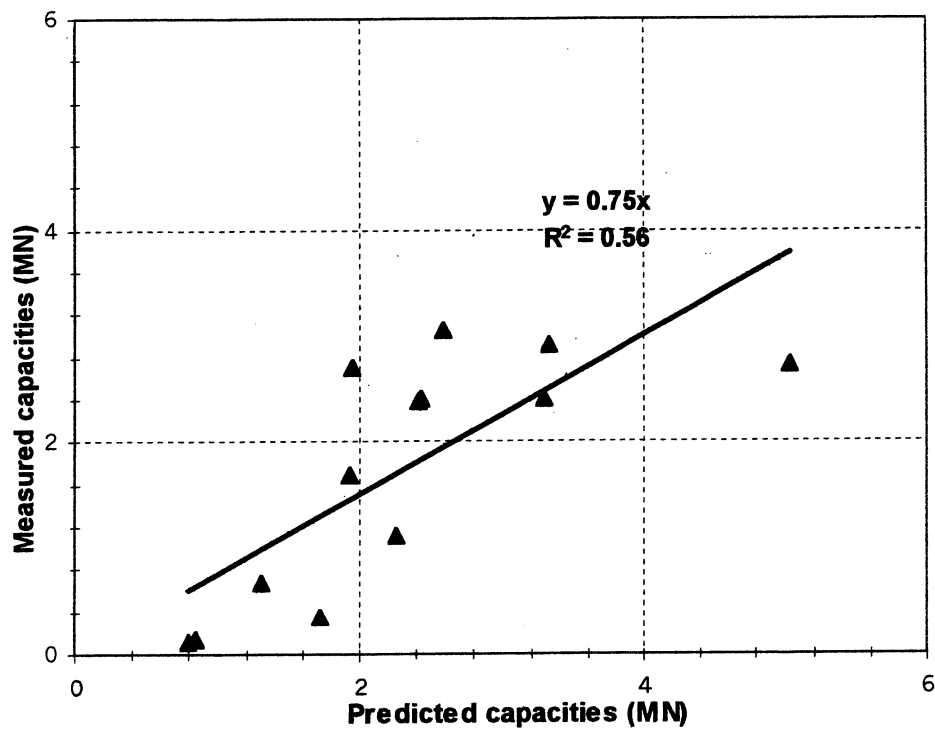


Figure 39: Pipe piles in mixed soils-- $\alpha$ -Tomlinson, Nordlund, Thurman methods

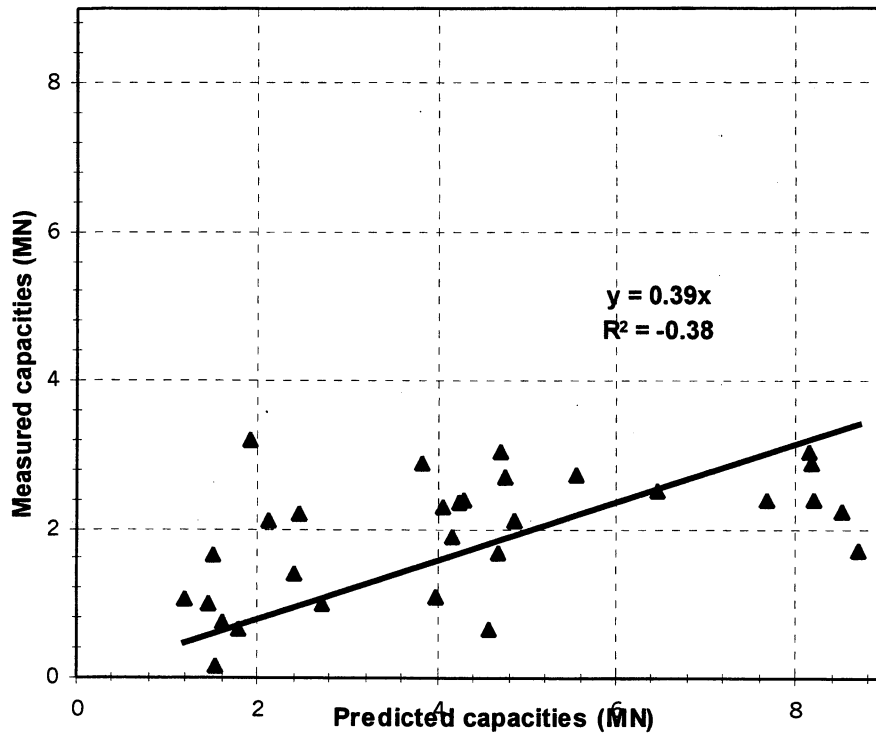


Figure 40: Pipe piles in mixed soils-- $\beta$  methods

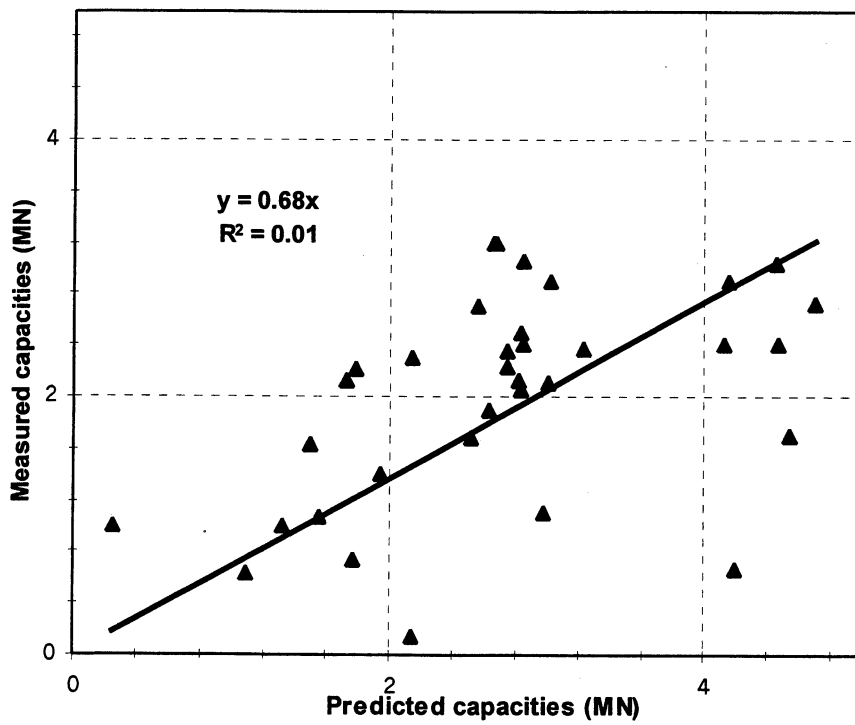


Figure 41: Pipe piles in mixed soils--Schmertmann SPT methods

#### 1.2.4. Histogram--Pipe Piles in Cohesionless Soils (5)

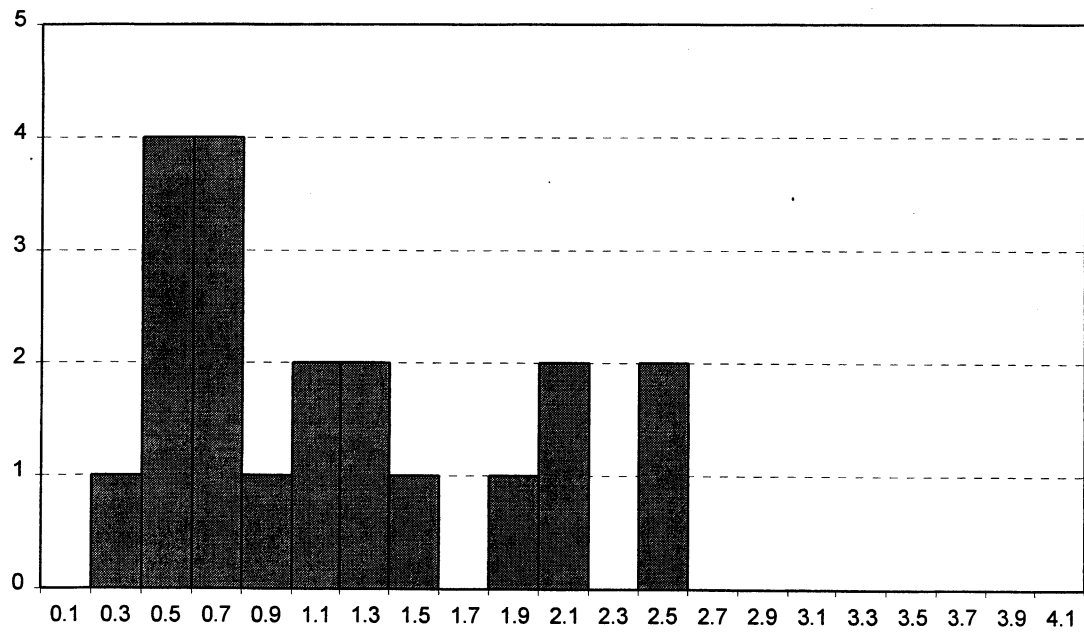


Figure 42: Histogram-- $\beta$  method (5):  $\lambda_R = 1.18$

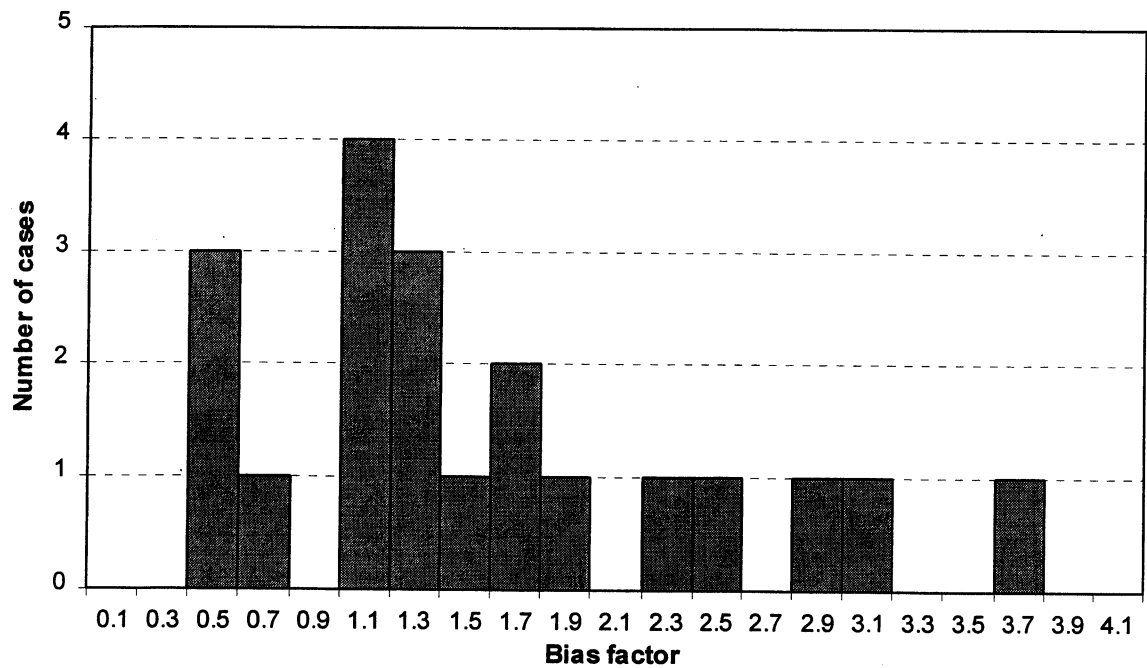


Figure 43: Histogram--Nordlund method (5):  $\lambda_R = 1.59$

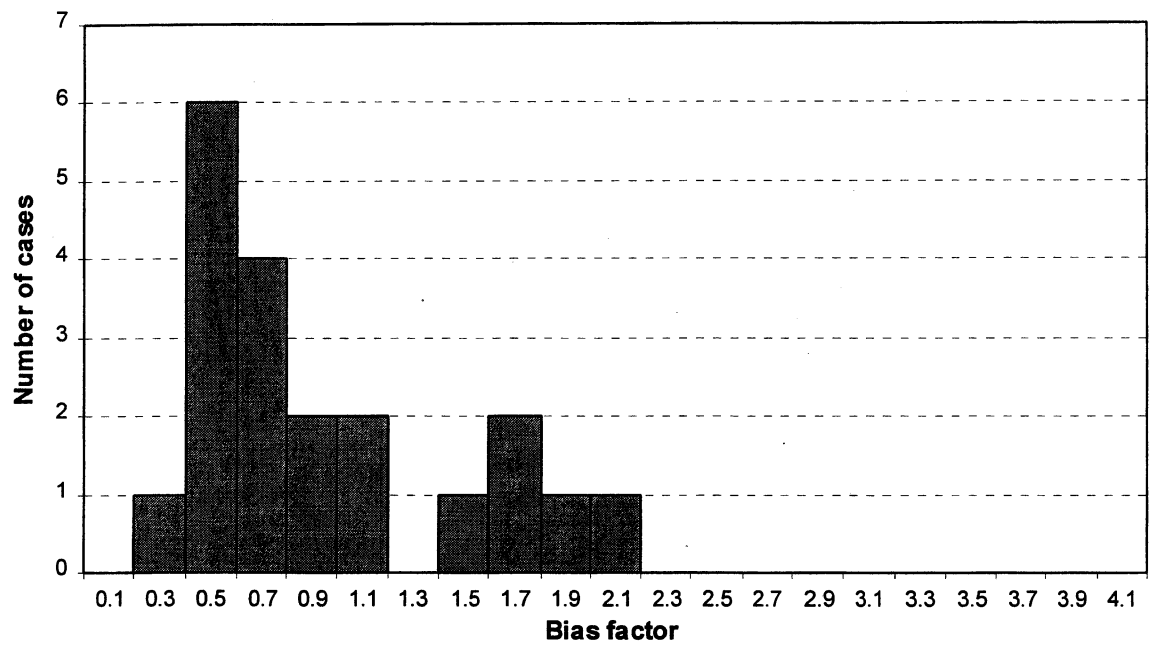


Figure 44: Histogram--Meyerhof method:  $\lambda_R = 0.94$

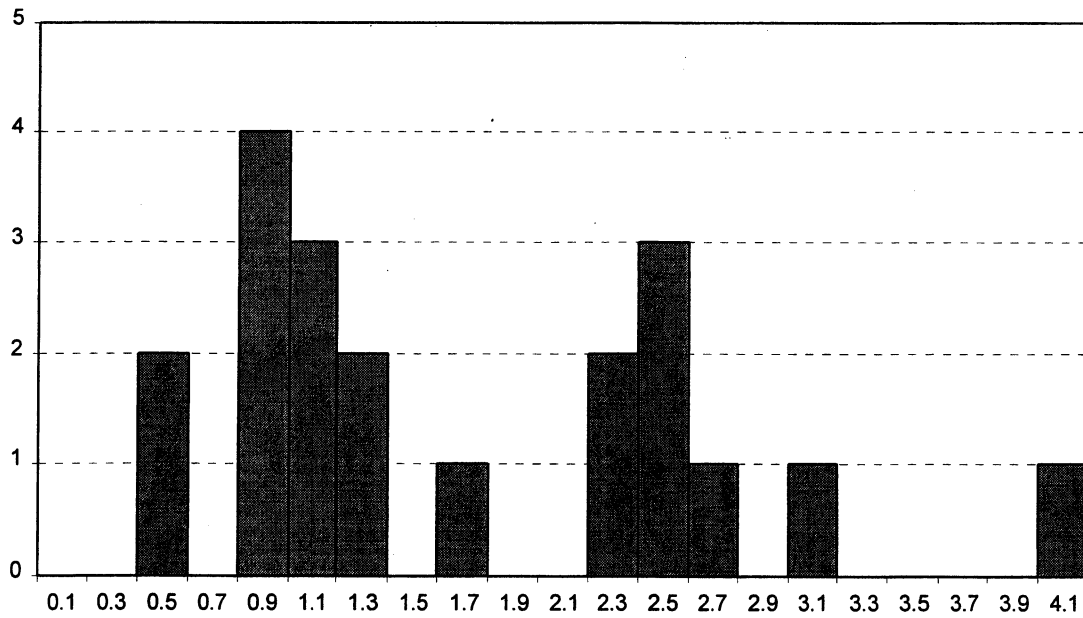


Figure 45: Histogram--Schmertmann SPT mobilized method:  $\lambda_R = 1.71$

### 1.2.5. Histogram--Pipe Piles in Cohesive Soils (5h)

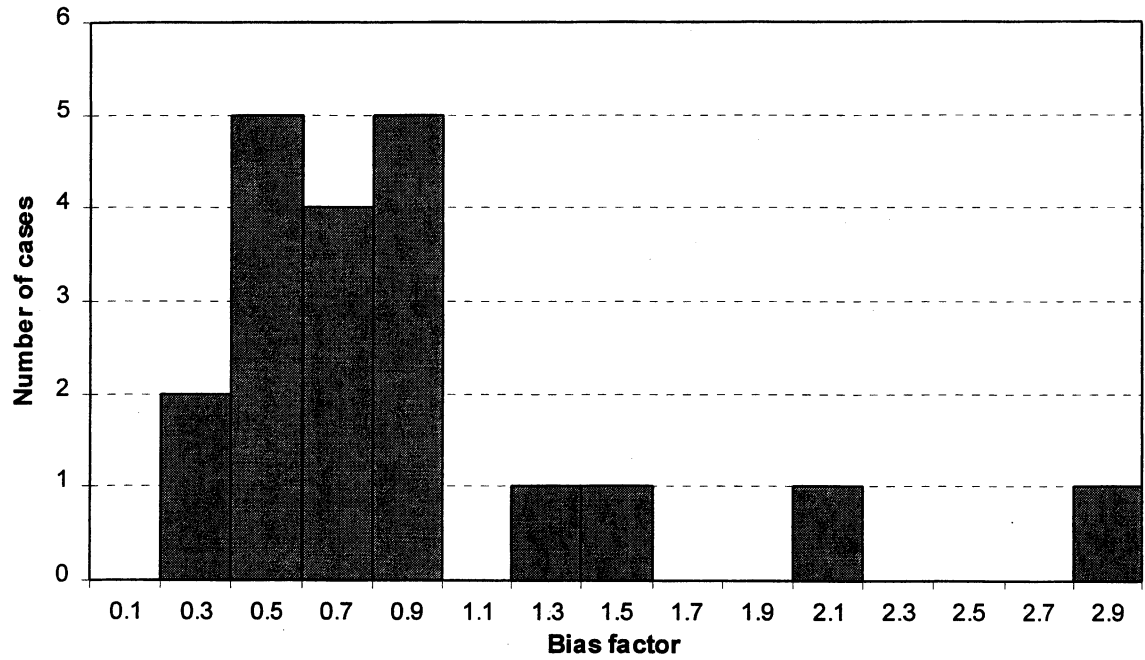


Figure 46: Histogram-- $\alpha$ -API method (5h):  $\lambda_R = 0.90$

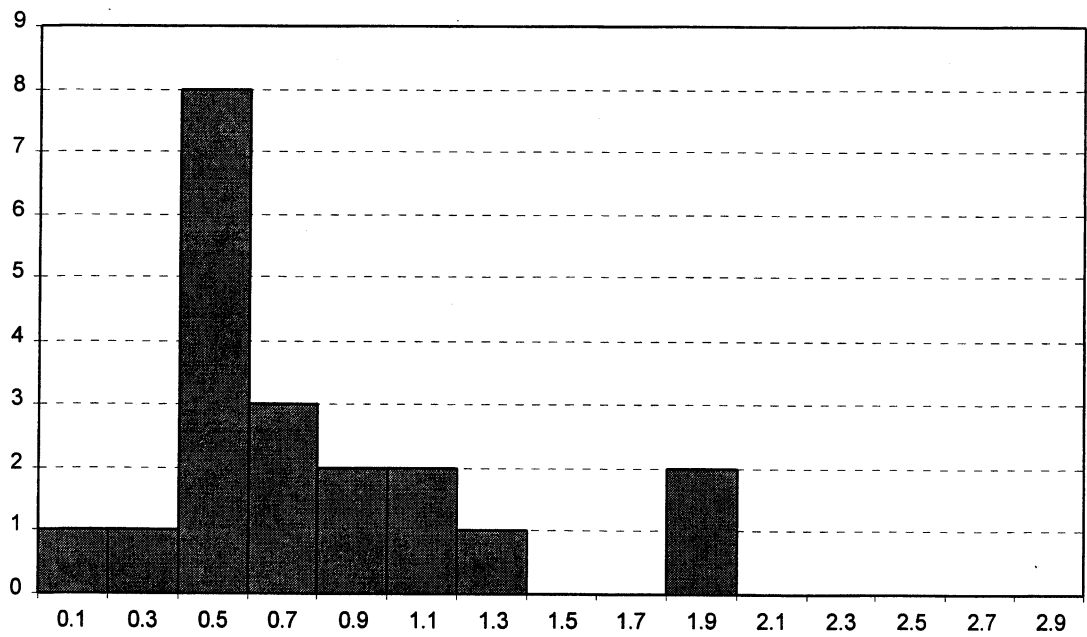


Figure 47: Histogram-- $\alpha$ -Tomlinson method (5h) :  $\lambda_R = 0.77$

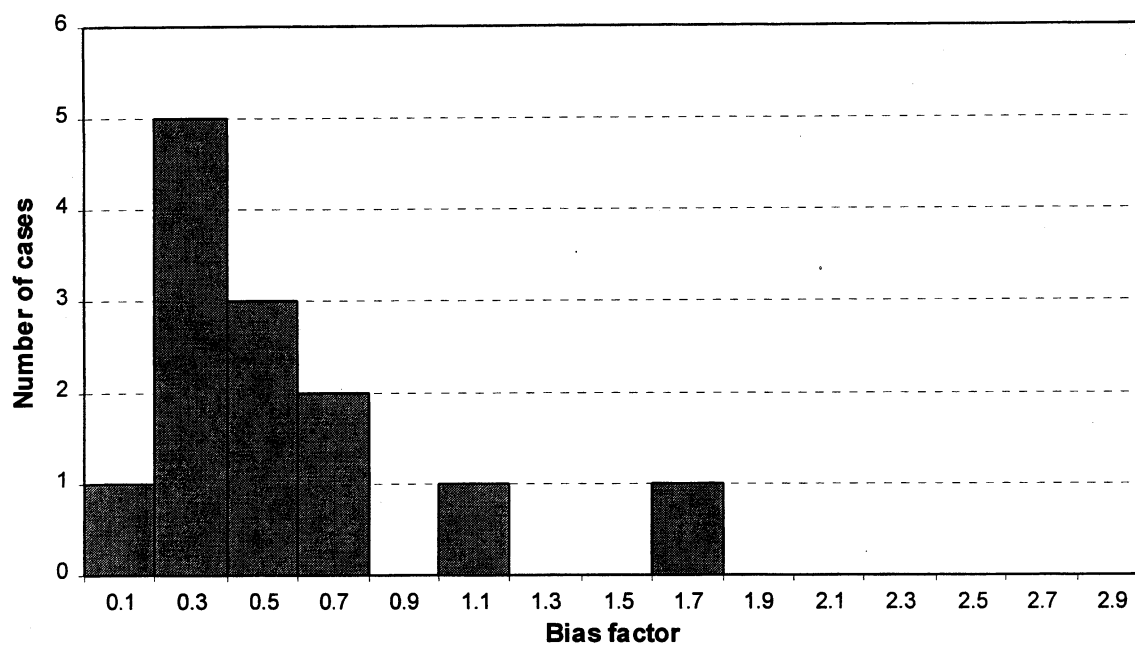


Figure 48: Histogram-- $\beta$  method (5h) :  $\lambda_R = 0.54$

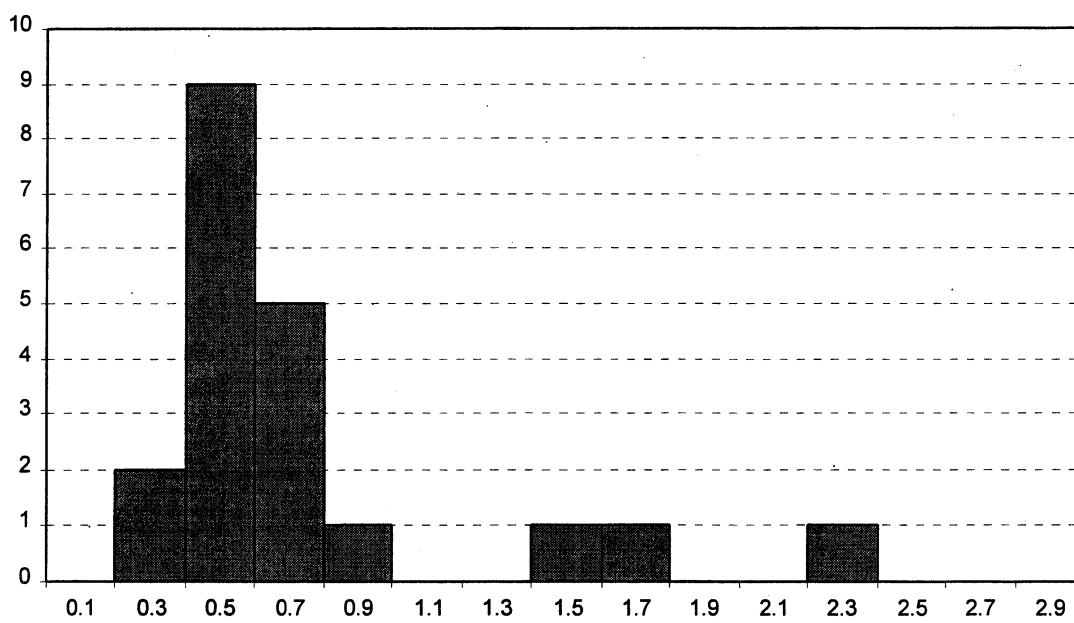


Figure 49: Histogram-- $\lambda$  method (5h) :  $\lambda_R = 0.75$

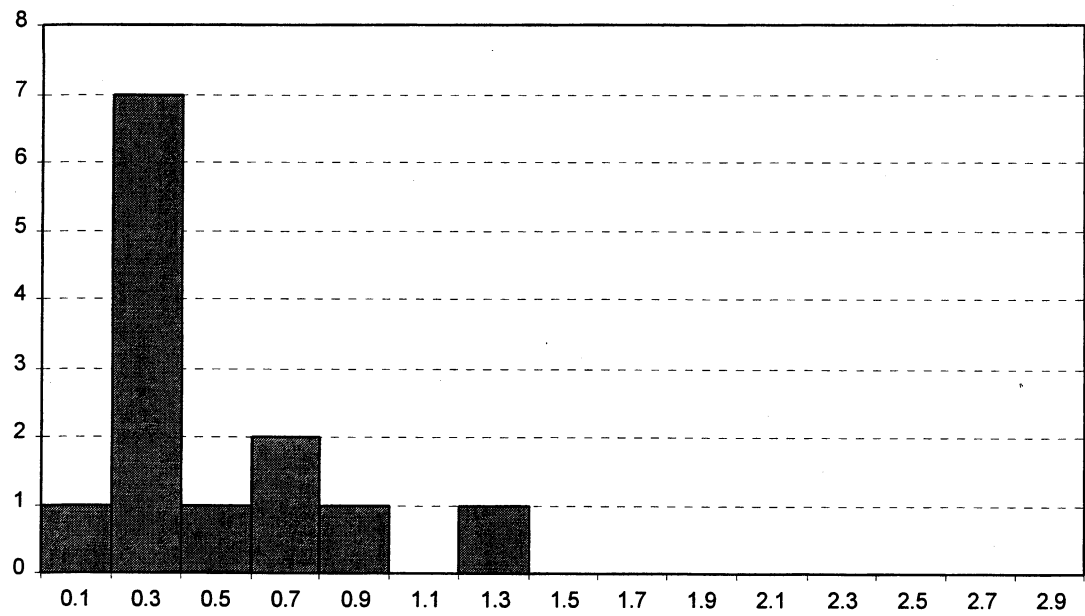


Figure 50: Histogram--Schmertmann SPT mobilized method:  $\lambda_R = 0.46$

### 1.2.6. Histogram--Pipe Piles in Mixed Soils (5)

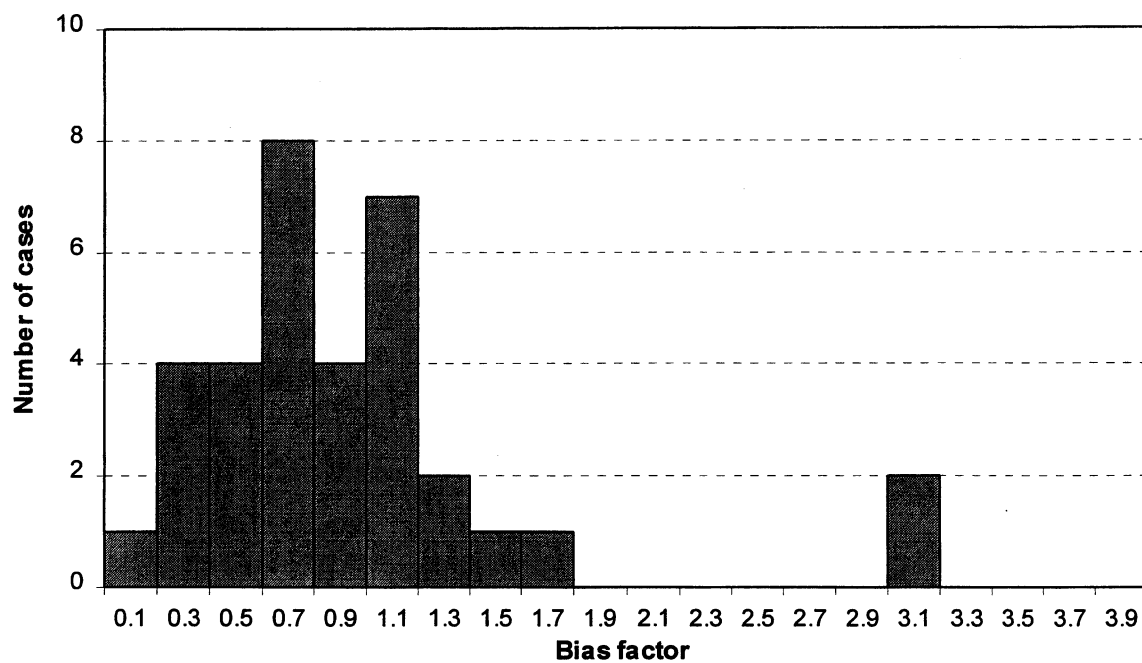


Figure 51: Histogram-- $\alpha$ -API/ Nordlund method (5):  $\lambda_R = 0.94$

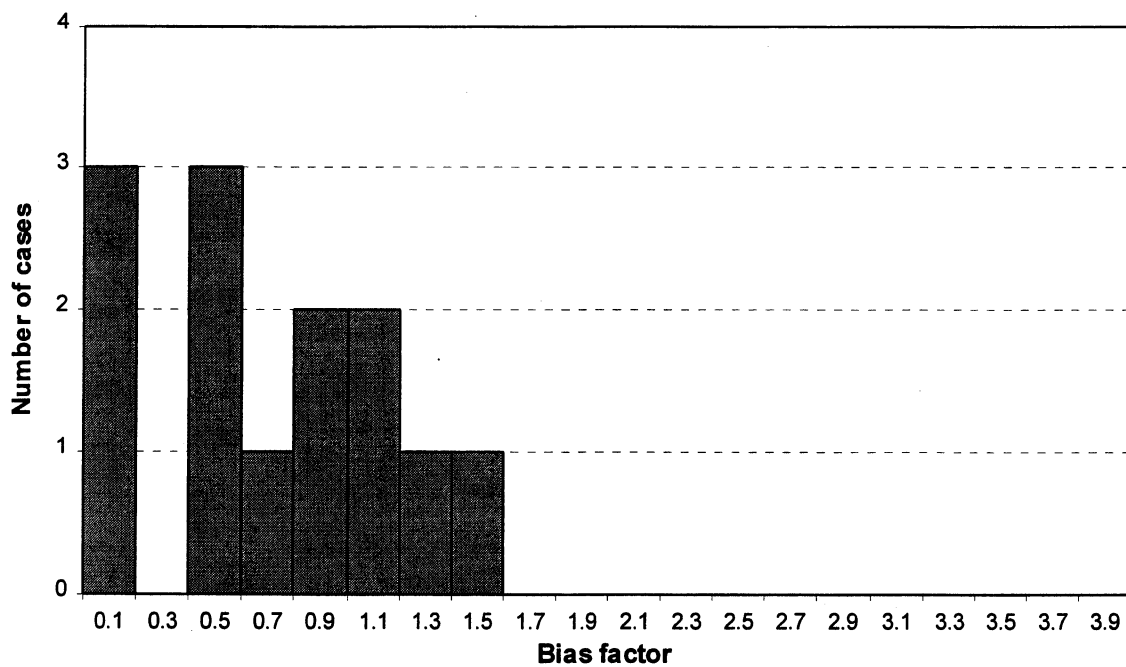


Figure 52: Histogram-- $\alpha$ -Tomlinson/ Nordlund method (5):  $\lambda_R = 0.74$



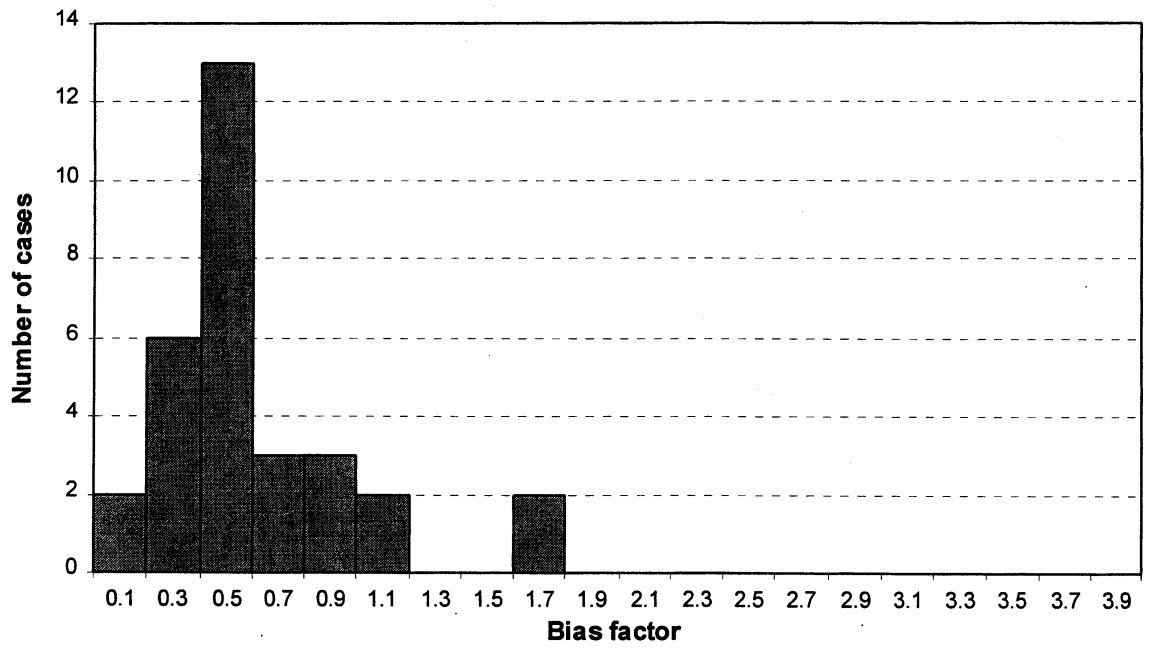


Figure 53: Histogram-- $\beta$ /Thurman method (5) :  $\lambda_R = 0.61$

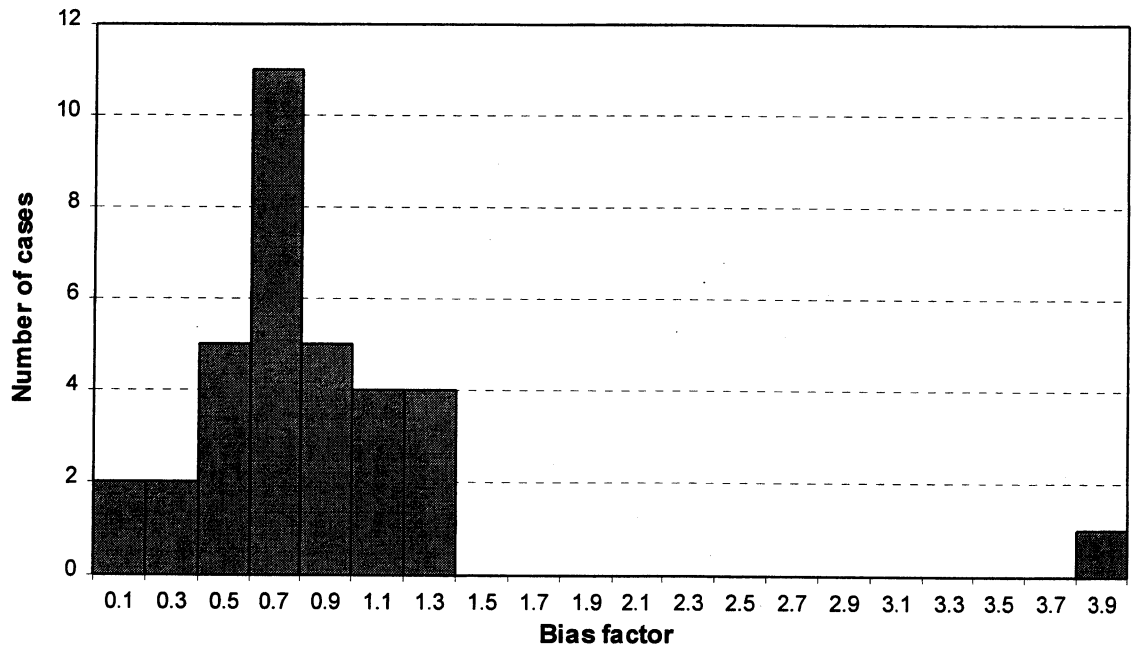


Figure 54: Histogram--Schmertmann SPT mobilized method:  $\lambda_R = 0.85$

### 1.3. Capacity--Results for Plugged H Piles

#### 1.3.1. Figures of Capacity Prediction--Plugged H piles in Cohesionless Soils (5)

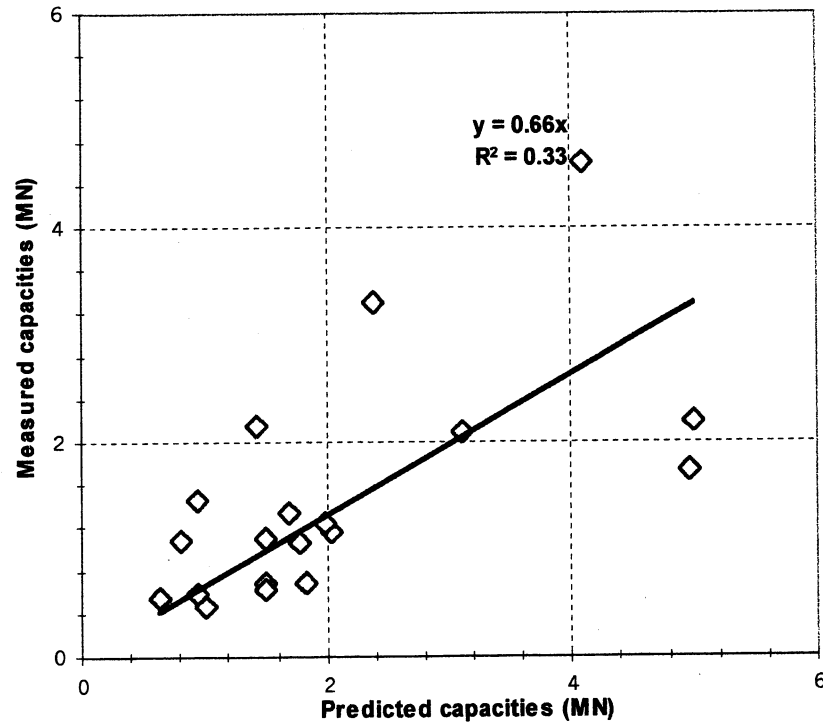


Figure 55: Plugged H piles in Cohesionless soil-- $\beta$  method

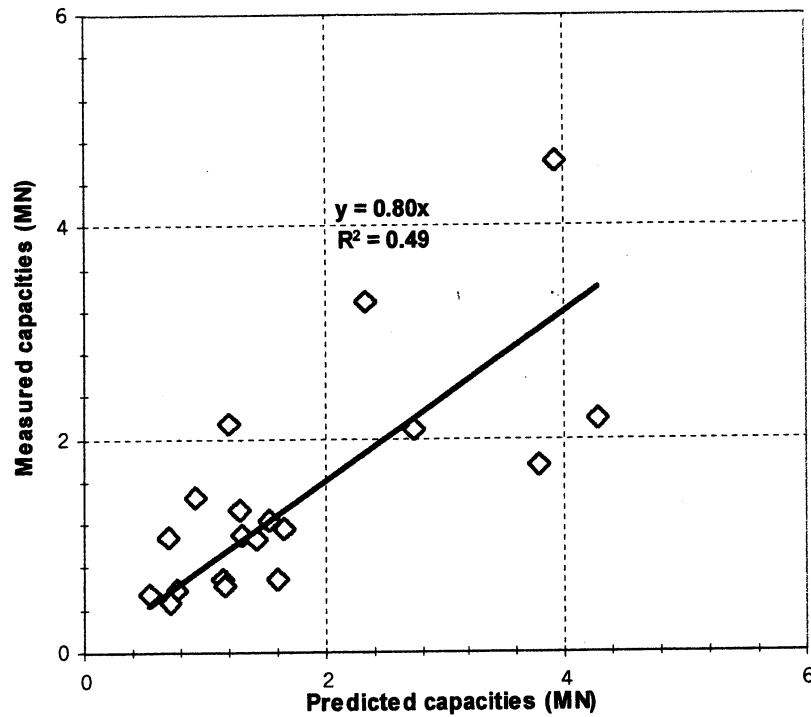


Figure 56: Plugged H piles in Cohesionless soil--Nordlund method

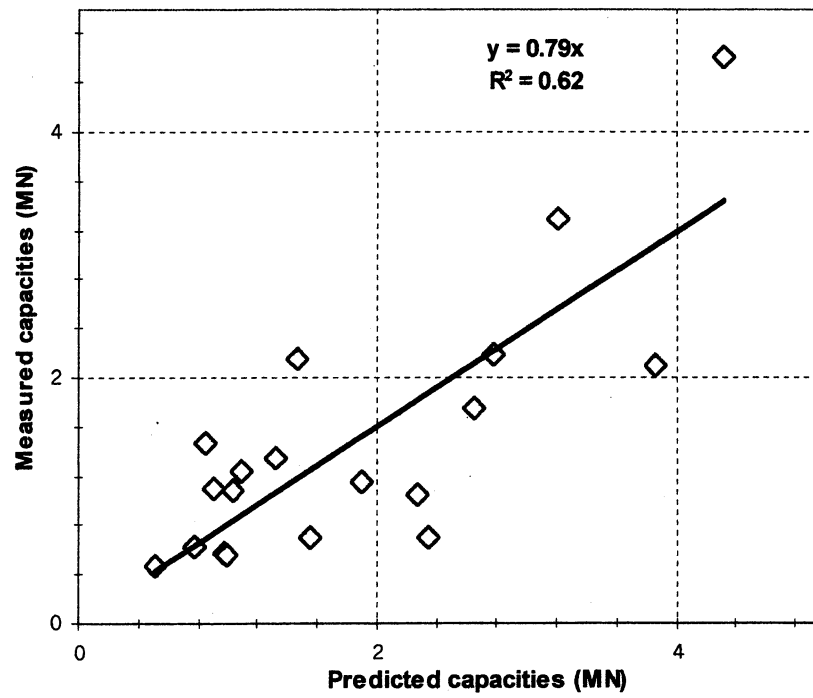


Figure 57: Plugged H piles in Cohesionless soil--Meyerhof method

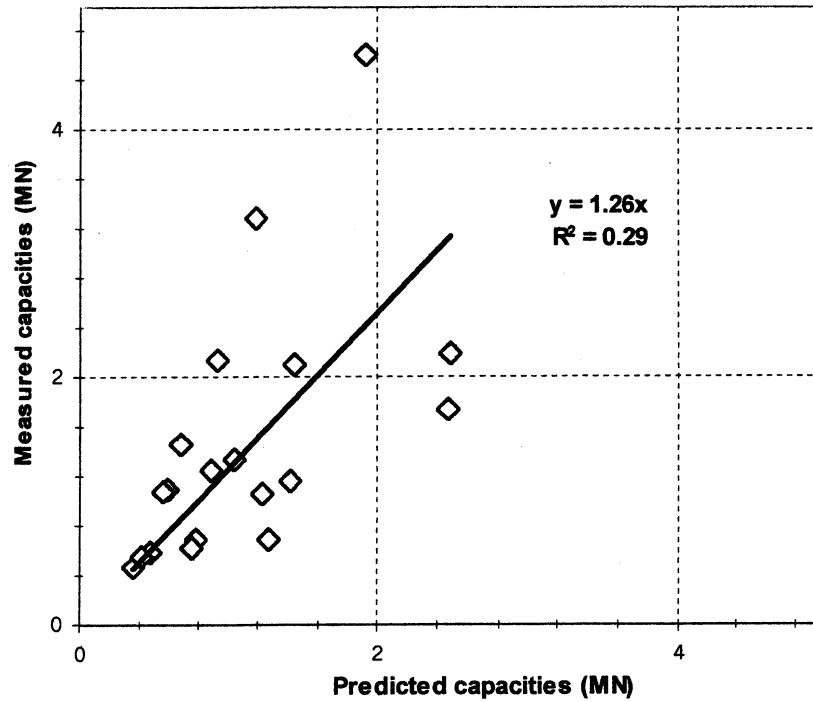


Figure 58: Plugged H piles in Cohesionless soil--Schmertmann SPT method

### 1.3.2. Figures of Capacity Prediction--Plugged H piles in Cohesive Soils (5)

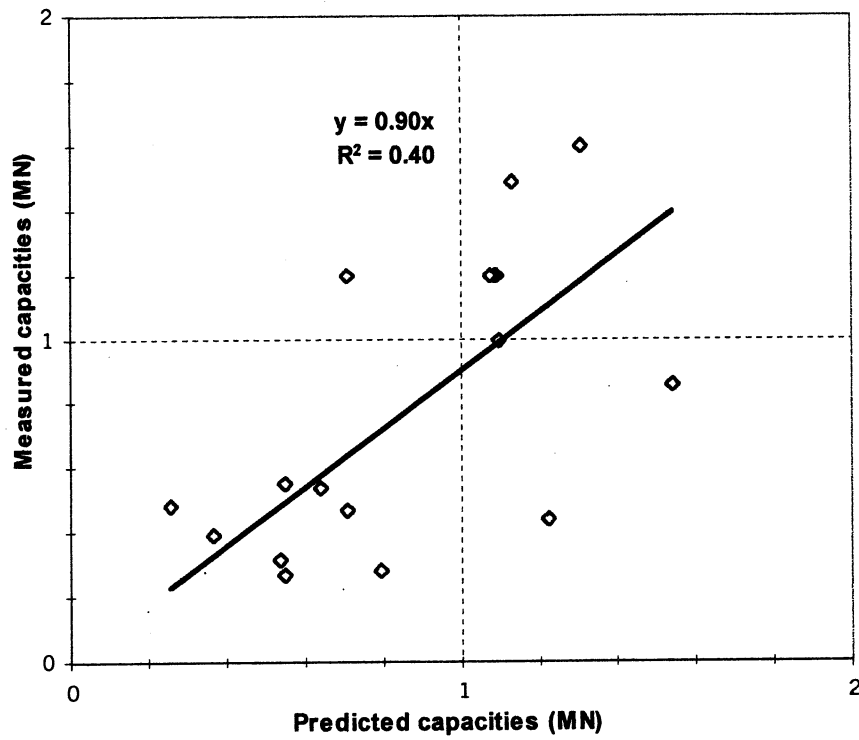


Figure 59: Plugged H piles in cohesive soil-- $\alpha$ -API method

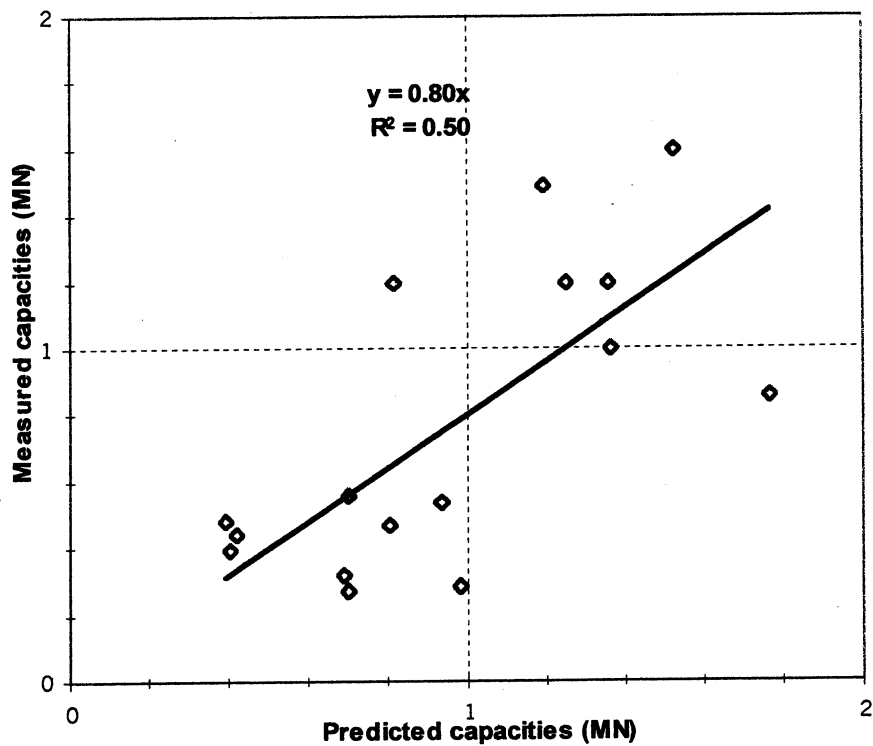


Figure 60: Plugged H piles in cohesive soil-- $\alpha$ -Tomlinson 1980 method

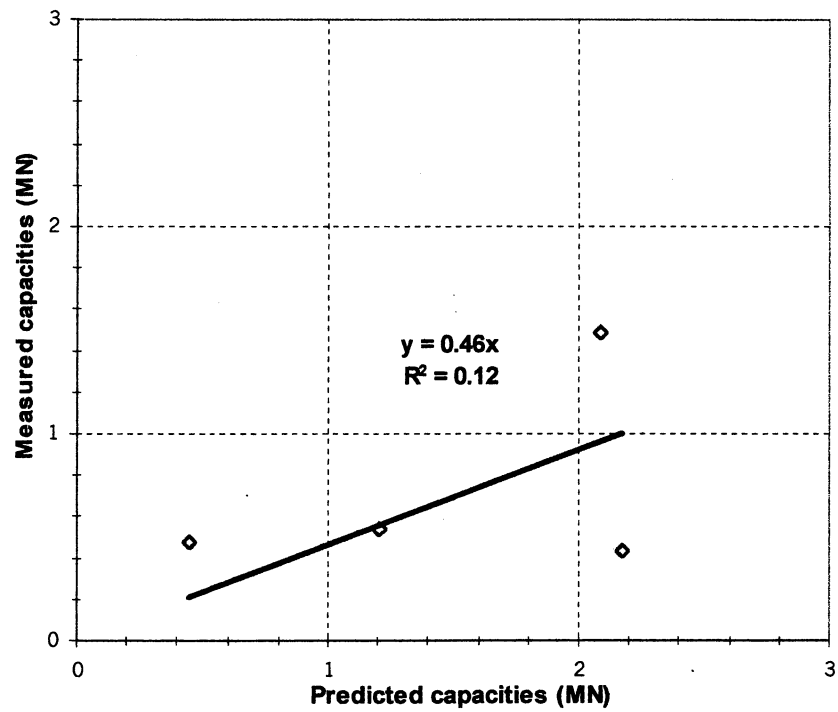


Figure 61: Plugged H piles in cohesive soil-- $\beta$  method

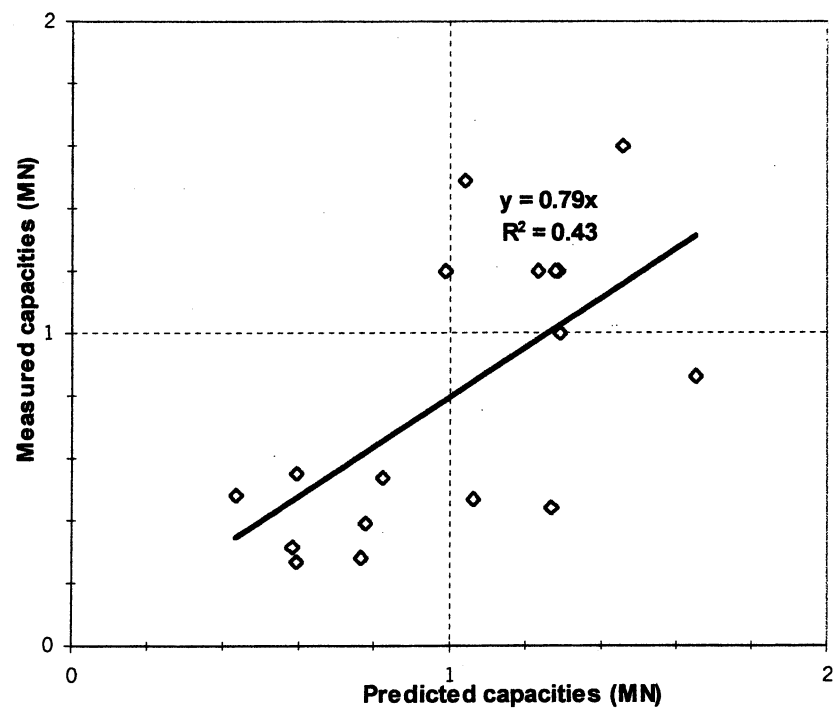


Figure 62: Plugged H piles in cohesive soil-- $\lambda$  method

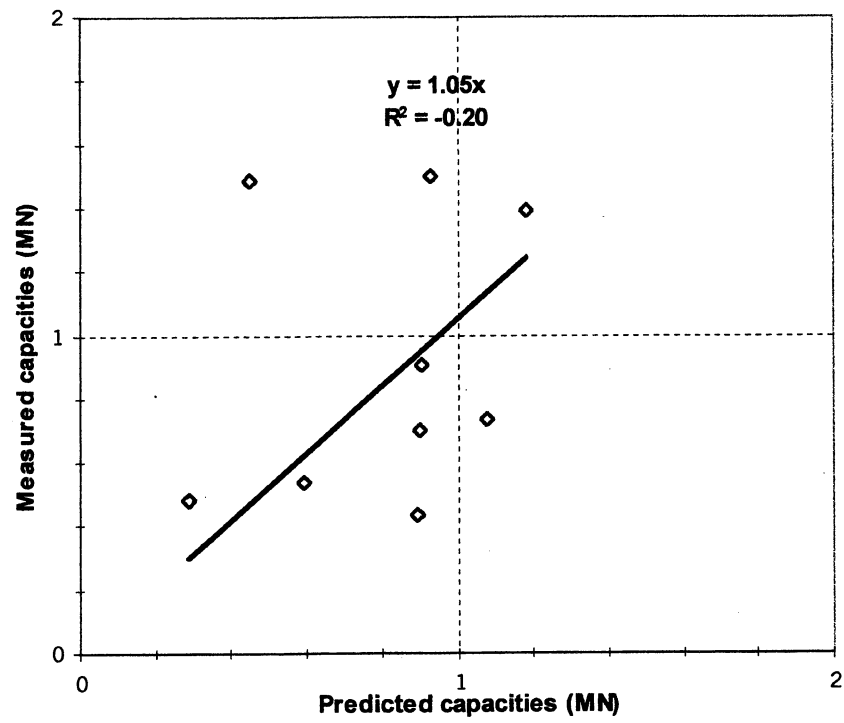


Figure 63: Plugged H piles in cohesive soil--Schmertmann SPT method

### 1.3.3. Figures of Capacity Prediction--Plugged H piles in Mixed Soils (5)

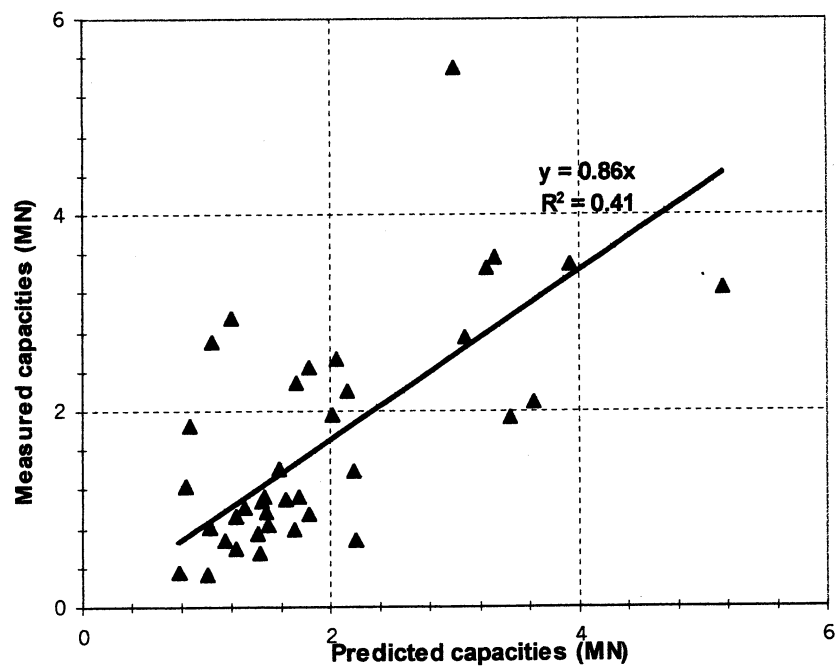


Figure 64: Plugged H piles in mixed soils-- $\alpha$ -API, Nordlund, Thurman methods

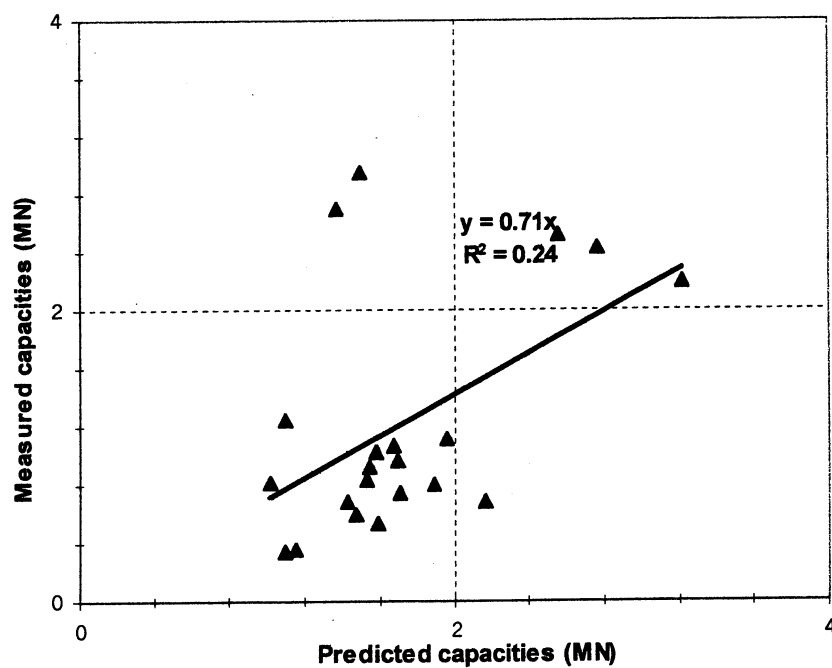


Figure 65: Plugged H piles in mixed soils-- $\alpha$ -Tomlinson, Nordlund, Thurman methods

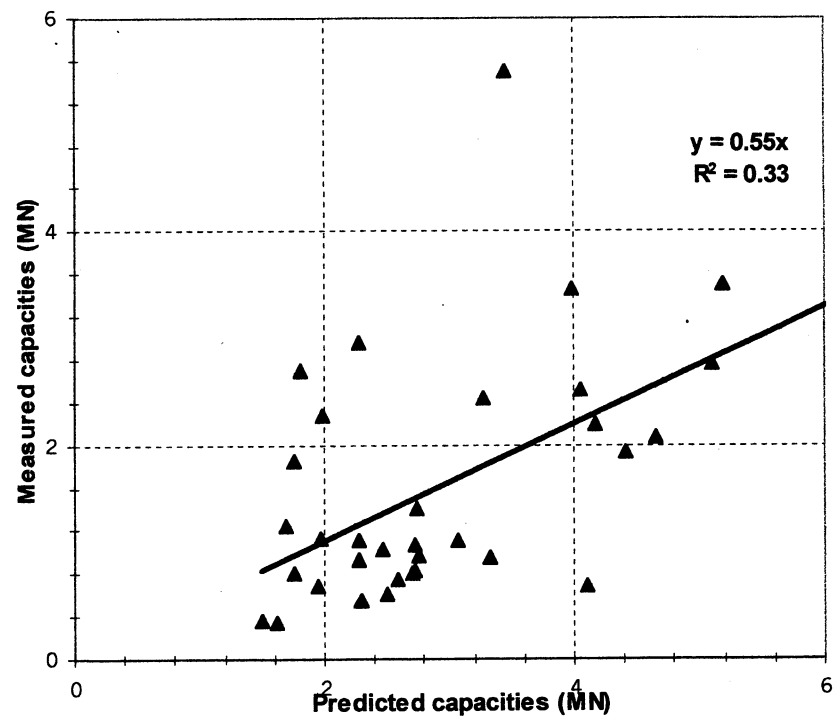


Figure 66: Plugged H piles in mixed soils-- $\beta$  methods

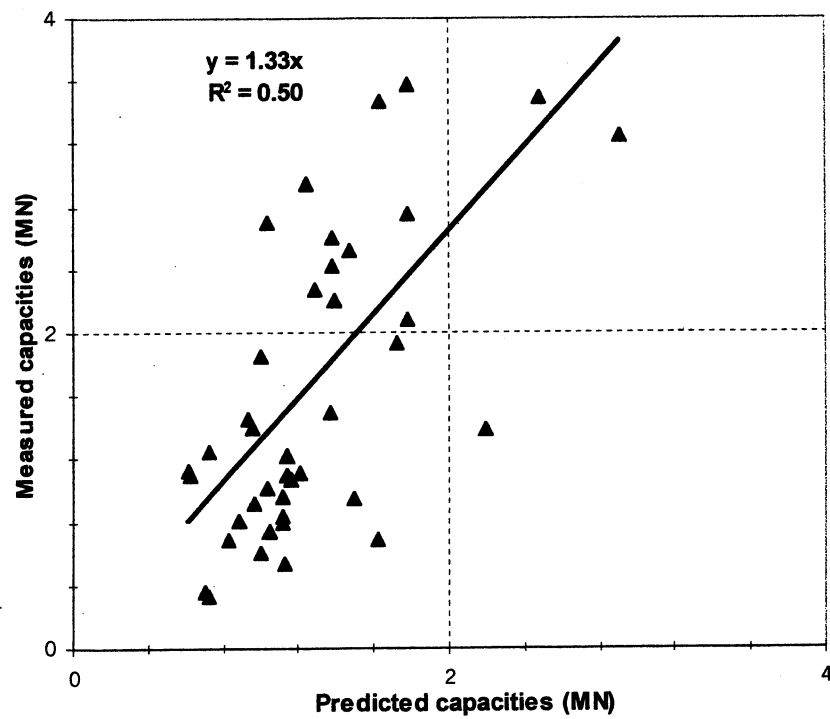


Figure 67: Plugged H piles in mixed soils--Schmertmann SPT methods



#### 1.3.4. Histogram--Plugged H piles in Cohesionless Soils (5)

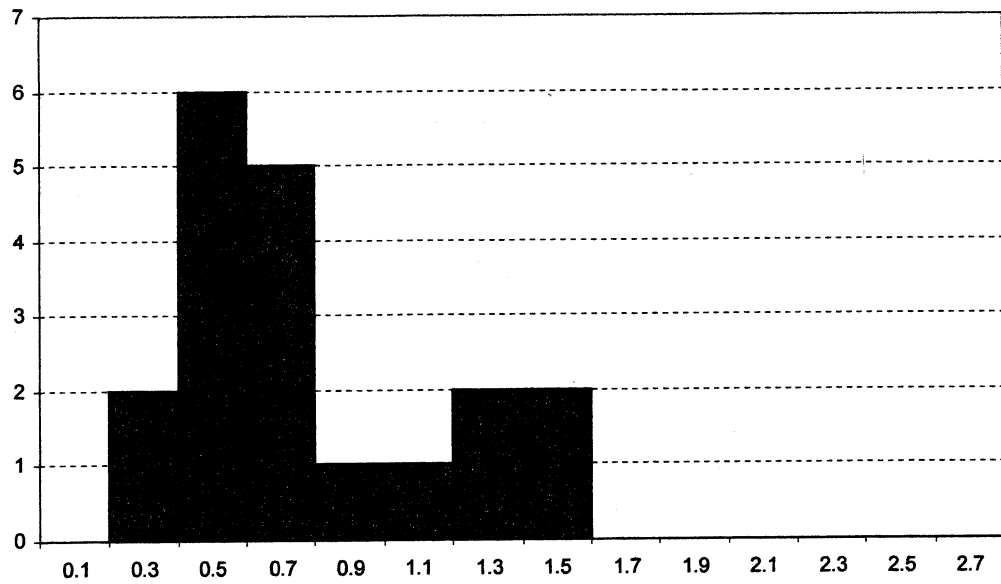


Figure 68: Histogram-- $\beta$  method (5)

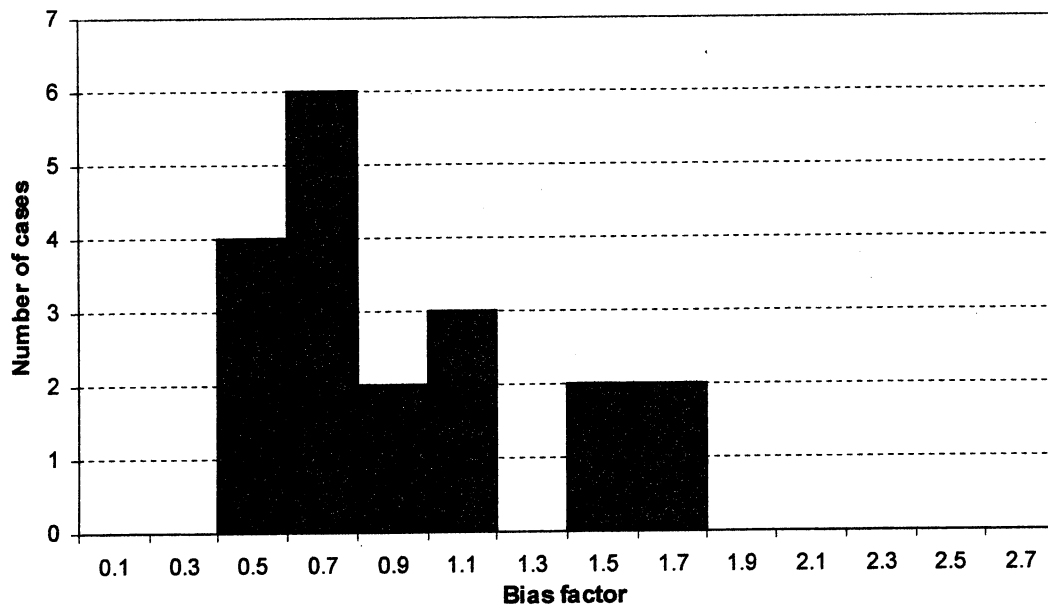


Figure 69: Histogram--Nordlund method (5)

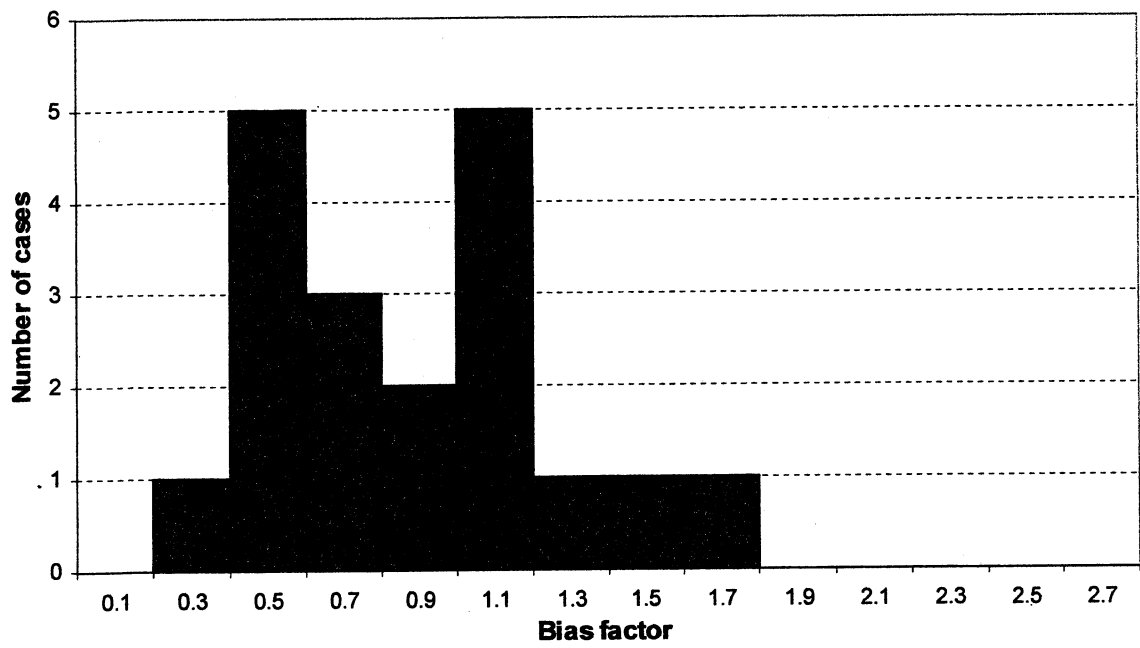


Figure 70: Histogram--Meyerhof method

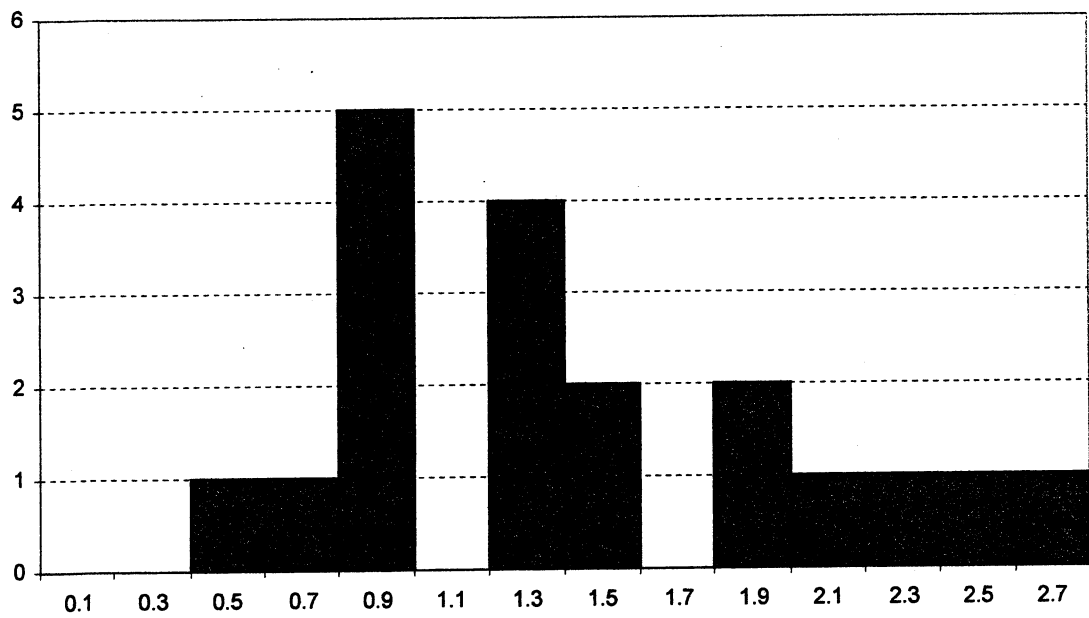


Figure 71: Histogram--Schmertmann SPT mobilized method

### 1.3.5. Histogram--Plugged H piles in Cohesive Soils (5)

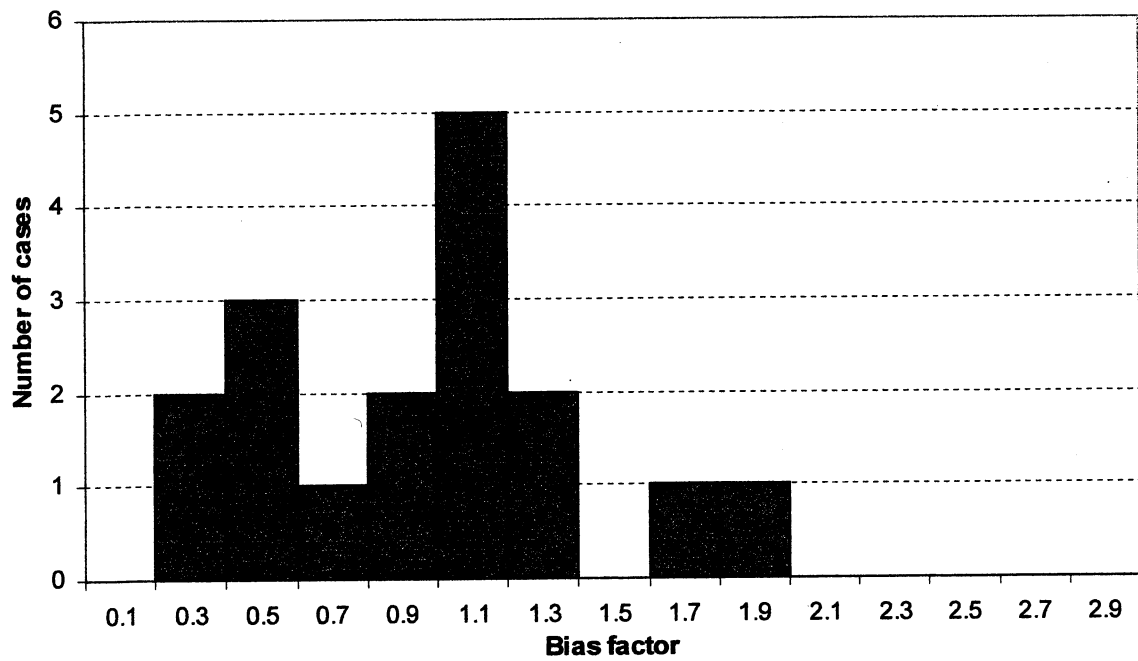


Figure 72: Histogram-- $\alpha$ -API method (5)

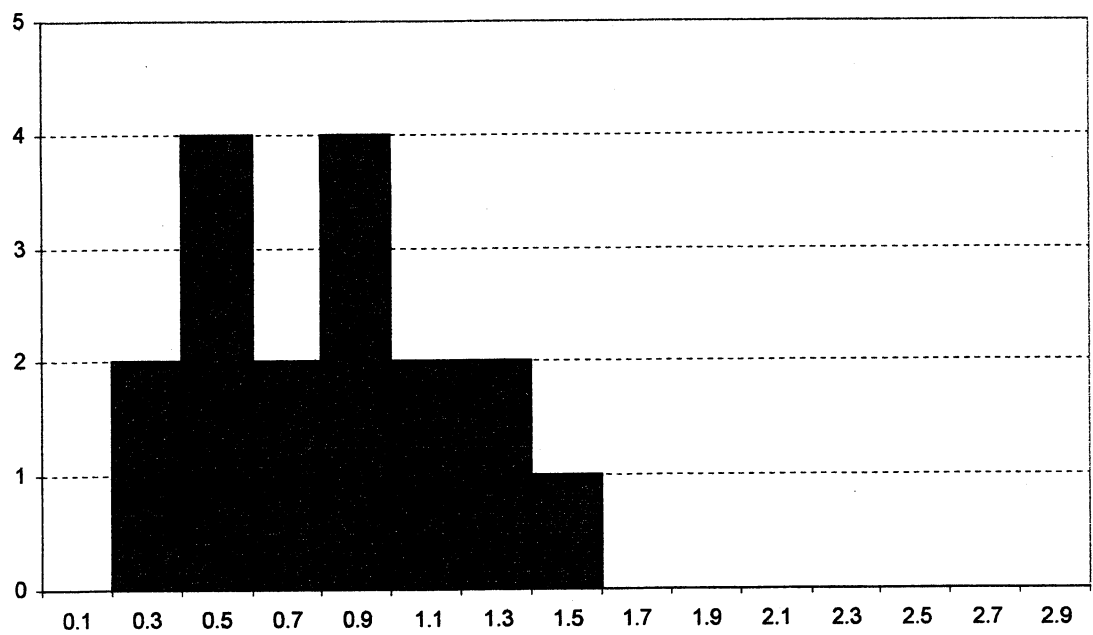


Figure 73: Histogram-- $\alpha$ -Tomlinson method (5)

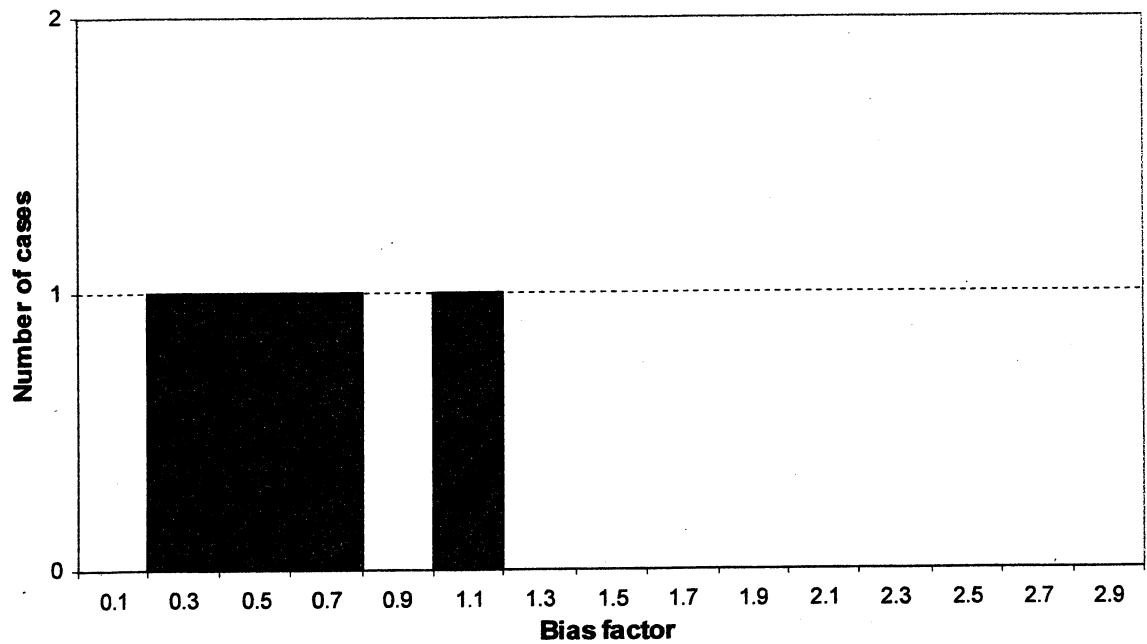


Figure 74: Histogram-- $\beta$  method (5)

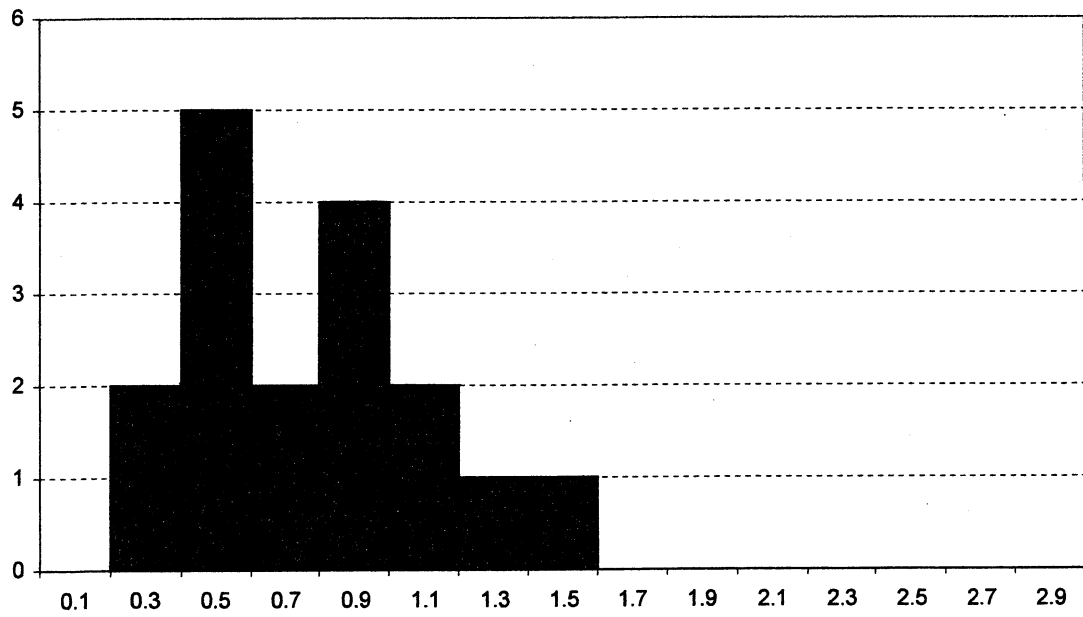


Figure 75: Histogram-- $\lambda$  method (5)

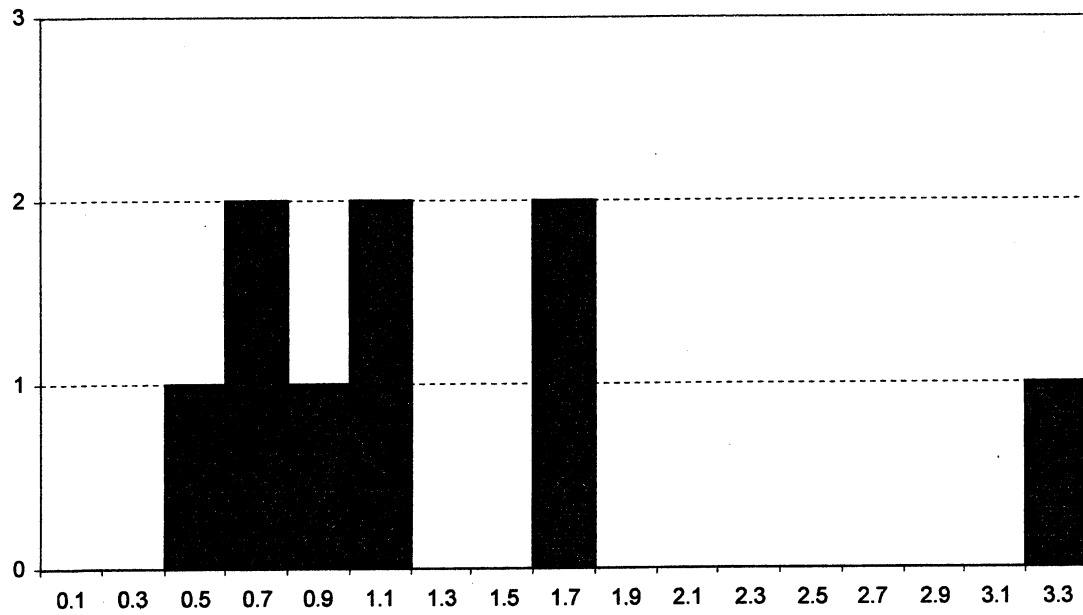


Figure 76: Histogram--Schmertmann SPT mobilized method

### 1.3.6. Histogram--Plugged H piles in Mixed Soils (5)

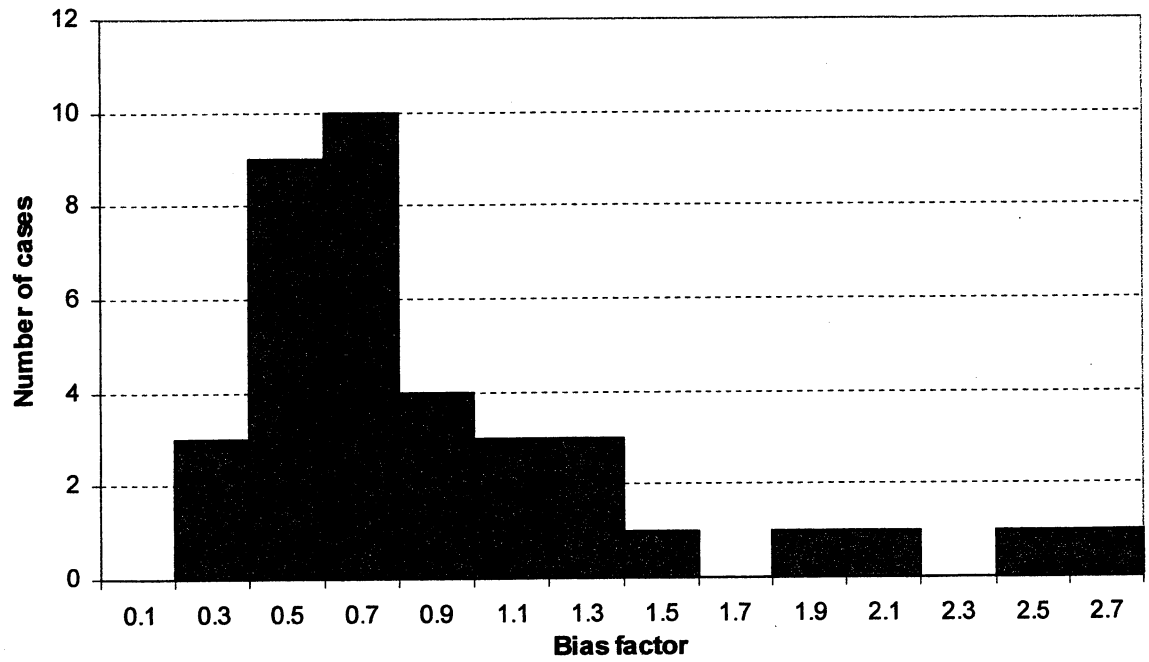


Figure 77: Histogram-- $\alpha$ -API/ Nordlund method (5)

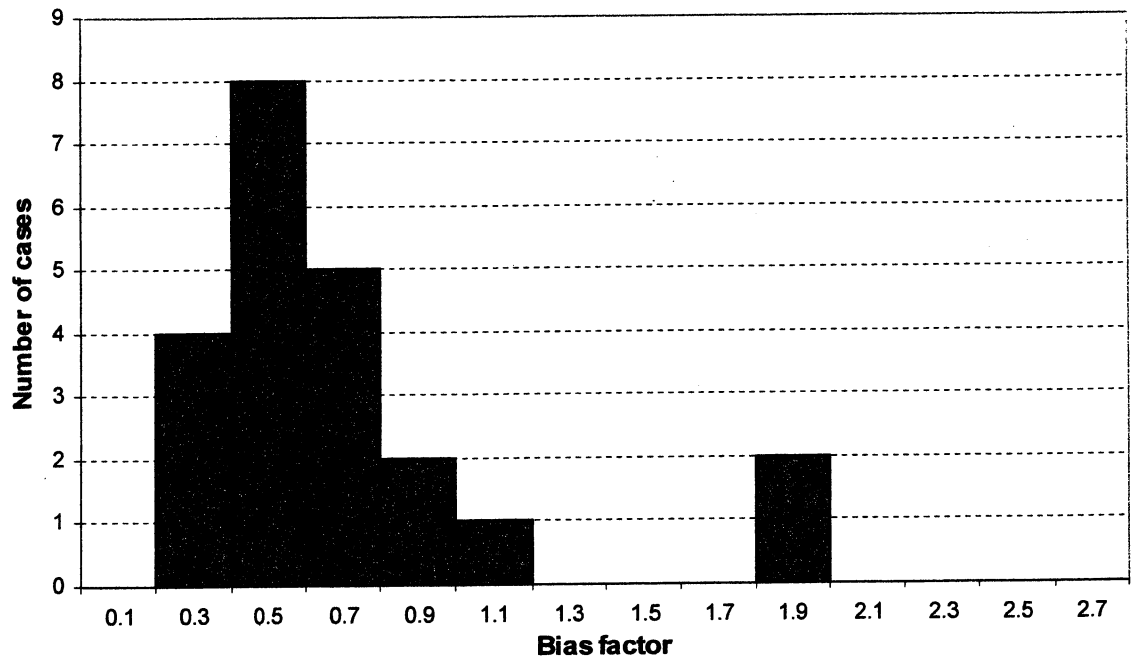


Figure 78: Histogram-- $\alpha$ -Tomlinson/ Nordlund method (5)

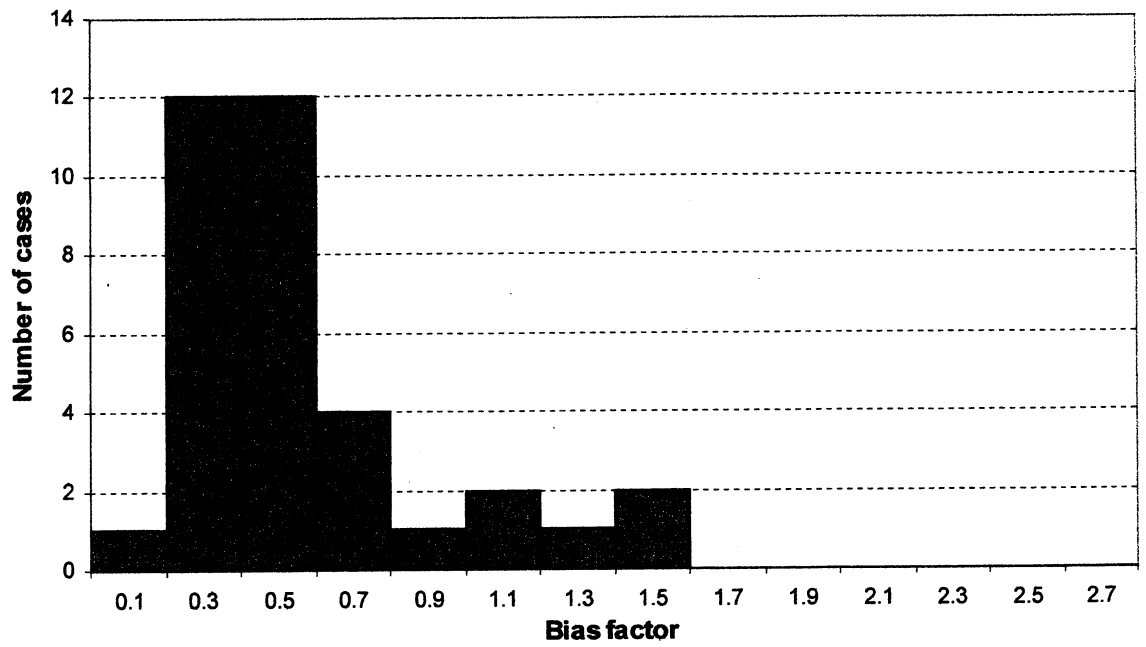


Figure 79: Histogram-- $\beta$ /Thurman method (5)

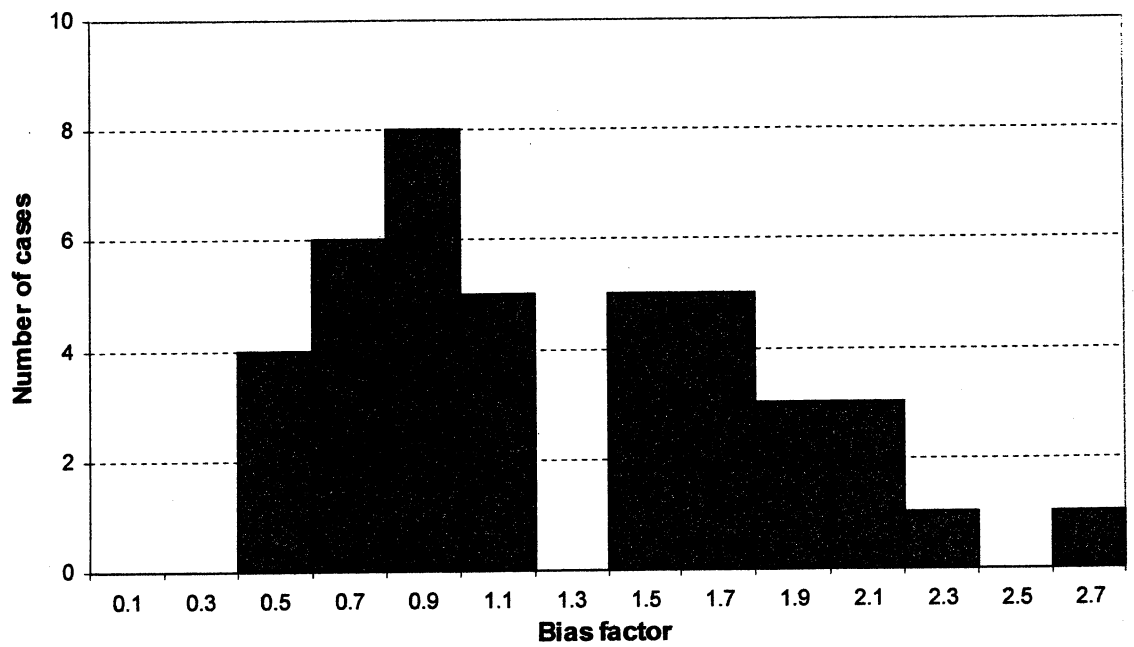


Figure 80: Histogram--Schmertmann SPT mobilized method

#### 1.4. Statistical Results

Table 4 (repeated): Symbols represented the soil parameters used.

Symbol	(1)	(2)	(3)	(4)	(5)	(6)	(7)	(8)
limit $\phi$ below	40°				36°			
contributed zone to tip resistance	2B	11.5B	2B	11.5B	2B	11.5B	2B	11.5B
$\phi$ , if from SPT, is correlated by	Peck, Hanson and Thornburn		Schmertmann		Peck, Hanson and Thornburn		Schmertmann	
$S_u$ , if from SPT, is correlated by	Terzaghi and Peck							

Symbol	(1h)	(2h)	(3h)	(4h)	(5h)	(6h)	(7h)	(8h)
limit $\phi$ below	40°				36°			
contributed zone to tip resistance	2B	11.5B	2B	11.5B	2B	11.5B	2B	11.5B
$\phi$ , if from SPT, is correlated by	Peck, Hanson and Thornburn		Schmertmann		Peck, Hanson and Thornburn		Schmertmann	
$S_u$ , if from SPT, is correlated by	Hara							



Table 5. Statistics for Concrete Piles

COHESIONLESS SOILS	Nordlund				$\beta$		Meyerhof	Schmertmann	
	DRIVEN	40;2B;P (1)	36;11.5 B;P (6)	36;2B;P (5)	40;2B;P (1)	36;2B;P (5)		SPT mobilized	CPT
N	37	37	37	37	37	37	37	37	2
Bias mean	0.71	0.71	1.06	1.00	0.89	1.17	0.64	1.25	0.61
Standard deviation	0.41	0.41	0.55	0.53	0.51	0.56	0.42	0.62	
COV	0.58	0.58	0.52	0.53	0.58	0.48	0.65	0.49	

COHESIVE SOILS	$\alpha$ Tomlinson			$\alpha$ API revised			$\beta$		$\lambda$		Schmertmann	
	DRIVEN	(1)	(5h)	APILE	(1)	(5h)	(1)	(5h)	(1)	(5h)	SPT mobilized	CPT
N	19	19	19	19	19	19	8	8	19	19	2	6
Bias mean	1.12	1.08	0.94	1.03	1.08	0.89	0.92	0.81	0.92	0.79	3.99	0.86
Standard deviation	1.55	0.82	0.50	0.76	0.73	0.31	0.60	0.41	0.50	0.25		0.09
COV	1.39	0.76	0.54	0.74	0.68	0.35	0.65	0.50	0.54	0.32		0.11

MIXED SOILS	$\alpha$ Tomlinson, Nordlund and Thurman			$\alpha$ API, Nordlund, Thurman		$\beta$ ; Thurman		Schmertmann	
	DRIVEN	40;2B;P;T &P(1)	36;2B;P; Hara(5h)	40;2B;P;T &P(1)	36;2B;P; Hara(5h)	40;2B;P;T &P(1)	36;2B;P; Hara(5h)	SPT mobilized	CPT
N	34	34	34	85	85	85	85	74	32
Bias mean	1.66	1.48	1.00	1.01	0.88	0.94	0.93	1.97	0.90
Standard deviation	1.34	1.11	0.52	0.62	0.47	0.57	0.55	1.20	0.35
COV	0.81	0.75	0.52	0.62	0.54	0.61	0.59	0.61	0.39

ALL SOILS	$\alpha$ -Tomlinson and/or Nordlund			$\alpha$ -API and/or Nordlund			$\beta$		$\lambda$		Meyerhof	Schmertmann	
	DRIVEN	(1)	(5h)	APILE	(1)	(5h)	(1)	(5h)	(1)	(5h)		SPT mobilized	CPT
N	90	90	90	19	141	141	130	130	19	19	37	113	40
Bias mean	1.15	1.08	0.99	1.03	0.94	0.91	0.92	0.99	0.92	0.79	0.64	1.77	0.88
Standard deviation	1.18	0.88	0.51	0.76	0.60	0.47	0.55	0.55	0.50	0.25	0.42	1.15	0.33
COV	1.03	0.82	0.52	0.74	0.64	0.51	0.60	0.56	0.54	0.32	0.65	0.65	0.37

Table 6. Statistics for Pipe Piles

COHESION LESS SOILS	Nordlund and Thurman				$\beta$		Meyerhof	Schmertmann SPT mobilized
	DRIVEN	40;2B;P (1)	40;2B;Sc h (3)	36;2B;P (5)	40;2B;P (1)	36;2B;P (5)		
N	20	20	20	20	20	20	20	20
Bias mean	1.16	1.29	0.77	1.59	1.02	1.18	0.94	1.71
Standard deviation	0.85	0.91	0.49	0.91	0.66	0.73	0.55	0.98
COV	0.73	0.71	0.64	0.57	0.65	0.61	0.59	0.57

COHESIVE SOILS	$\alpha$ Tomlinson			$\alpha$ API revised			$\beta$		$\lambda$		Schmert- mann SPT mobilized
	DRI VEN	2B; T&P (5)	2B; Hara (5h)	APILE	2B; T&P (5)	2B; Hara (5h)	2B; T&P (5)	2B; Hara (5h)	2B; T&P (5)	2B; Hara (5h)	
N	20	20	20	20	20	20	13	13	20	20	13
Bias mean	0.78	0.77	0.56	0.88	0.90	0.58	0.54	0.50	0.75	0.47	0.46
Standard deviation	0.62	0.49	0.34	0.61	0.62	0.35	0.42	0.36	0.50	0.26	0.35
COV	0.79	0.64	0.61	0.69	0.69	0.60	0.76	0.73	0.66	0.56	0.77

MIXED SOILS	$\alpha$ Tomlinson, Nordlund and Thurman			$\alpha$ API, Nordlund, Thurman		$\beta$ ; Thurman		Schmert- mann SPT mobilized
	DRIVEN	36;2B;P;T &P(5)	36;2B;P;Har a(5h)	36;2B;P;T& P(5)	36;2B;P;Har a(5h)	36;2B;P;T& P(5)	36;2B;P;Har a(5h)	
N	13	13	13	34	34	31	31	34
Bias mean	0.69	0.74	0.54	0.94	0.71	0.61	0.60	0.85
Standard deviation	0.41	0.44	0.35	0.64	0.41	0.38	0.36	0.62
COV	0.60	0.60	0.66	0.69	0.57	0.61	0.60	0.73

ALL SOILS	$\alpha$ -Tomlinson and/or Nordlund			$\alpha$ -API and/or Nordlund		$\beta$		$\lambda$		Meyerhof	Schmert- mann SPT mobilized
	DRIVE N	(5)	(5h)	(5)	(5h)	(5)	(5h)	(5)	(5h)		
N	53	53	53	74	74	64	64	20	20	20	67
Bias mean	0.90	1.07	0.94	1.10	0.92	0.78	0.76	0.75	0.47	0.94	1.03
Standard deviation	0.70	0.78	0.80	0.77	0.70	0.58	0.58	0.50	0.26	0.55	0.84
COV	0.77	0.73	0.85	0.70	0.77	0.75	0.76	0.66	0.56	0.59	0.82

Table 7. Statistics for Plugged H piles

COHESION LESS SOILS	Nordlund and Thurman		$\beta$		Meyerhof	Schmertmann SPT mobilized
	$\phi \leq 40$ ; Tip 2B; $\phi$ by Peck et al. (1)	$\phi \leq 36$ ; Tip 2B; $\phi$ by Peck et al. (5)	$\phi \leq 40$ ; Tip 2B; $\phi$ by Peck et al. (1)	$\phi \leq 36$ ; Tip 2B; $\phi$ by Peck et al. (5)		
N	19	19	19	19	19	19
Bias mean	0.74	0.92	0.66	0.78	0.86	1.42
Standard deviation	0.39	0.41	0.33	0.40	0.37	0.65
COV	0.53	0.45	0.51	0.50	0.43	0.46

COHESIVE SOILS	$\alpha$ Tomlinson		$\alpha$ API revised		$\beta$		$\lambda$		Schmert- mann SPT mobilized
	2B; T&P (5)	2B; Hara (5h)	2B; T&P (5)	2B; Hara (5h)	2B; T&P (5)	2B; Hara (5h)	2B; T&P (5)	2B; Hara (5h)	
N	17	17	17	17	4	4	17	17	9
Bias mean	0.82	0.75	0.96	0.83	0.61	0.55	0.78	0.68	1.29
Standard deviation	0.33	0.29	0.43	0.37	0.37	0.32	0.33	0.30	0.85
COV	0.40	0.39	0.45	0.44	0.61	0.58	0.42	0.45	0.66

MIXED SOILS	$\alpha$ Tomlinson, Nordlund and Thurman		$\alpha$ API, Nordlund, Thurman		$\beta$ ; Thurman		Schmert- mann SPT mobilized
	$\phi \leq 36$ ; 2B; $\phi$ by Peck; $S_u$ by T&P(5)	$\phi \leq 36$ ; 2B; $\phi$ by Peck; $S_u$ by Hara (5h)	$\phi \leq 36$ ; 2B; $\phi$ by Peck; $S_u$ by T&P(5)	$\phi \leq 36$ ; 2B; $\phi$ by Peck; $S_u$ by Hara (5h)	$\phi \leq 36$ ; 2B; $\phi$ by Peck; $S_u$ by T&P(5)	$\phi \leq 36$ ; 2B; $\phi$ by Peck; $S_u$ by Hara (5h)	
N	22	22	37	37	35	35	41
Bias mean	0.71	0.46	0.92	0.68	0.56	0.55	1.27
Standard deviation	0.46	0.29	0.56	0.37	0.36	0.35	0.58
COV	0.65	0.64	0.61	0.54	0.64	0.64	0.46

ALL SOILS	$\alpha$ -Tomlinson and/or Nordlund		$\alpha$ -API and/or Nordlund		$\beta$		$\lambda$		Meyer hof	Schmert -mann SPT mobilize d
	36;2B;P; T&P(5)	36;2B;P;H ara(5h)	36;2B;P;T &P(5)	36;2B;P;H ara(5h)	36;2B;P;T &P(5)	36;2B;P;H ara(5h)	36;2B;P;T &P(5)	36;2B;P;H ara(5h)		
N	58	58	73	73	58	58	17	17	19	69
Bias mean	0.81	0.69	0.93	0.78	0.64	0.62	0.78	0.68	0.86	1.31
Standard deviation	0.41	0.38	0.49	0.39	0.38	0.38	0.33	0.30	0.37	0.63
COV	0.51	0.55	0.53	0.50	0.59	0.61	0.42	0.45	0.43	0.48

Table 8. Statistics for Unplugged H piles

COHESION LESS SOILS	Nordlund and Thurman		$\beta$		Meyerhof	Schmertmann SPT mobilized
	$\phi \leq 40$ ; Tip 2B; $\phi$ by Peck et al. (1)	$\phi \leq 36$ ; Tip 2B; $\phi$ by Peck et al. (5)	$\phi \leq 40$ ; Tip 2B; $\phi$ by Peck et al. (1)	$\phi \leq 36$ ; Tip 2B; $\phi$ by Peck et al. (5)		
N	19	19	19	19	19	19
Bias mean	0.85	0.99	0.76	0.80	1.77	1.40
Standard deviation	0.55	0.68	0.55	0.62	1.21	0.73
COV	0.64	0.68	0.72	0.77	0.69	0.52

COHESIVE SOILS	$\alpha$ Tomlinson		$\alpha$ API revised		$\beta$		$\lambda$		Schmertmann SPT mobilized
	2B; T&P (5)	2B; Hara (5h)	2B; T&P (5)	2B; Hara (5h)	2B; T&P (5)	2B; Hara (5h)	2B; T&P (5)	2B; Hara (5h)	
N	17	17	17	17	4	4	17	17	9
Bias mean	0.68	0.63	0.78	0.67	0.44	0.44	0.60	0.52	1.22
Standard deviation	0.34	0.33	0.41	0.36	0.27	0.27	0.28	0.25	0.70
COV	0.50	0.52	0.53	0.53	0.62	0.61	0.47	0.48	0.57

MIXED SOILS	$\alpha$ Tomlinson, Nordlund and Thurman		$\alpha$ API, Nordlund, Thurman		$\beta$ ; Thurman		Schmertmann SPT mobilized
	$\phi \leq 36$ ; 2B; $\phi$ by Peck; $S_u$ by T&P(5)	$\phi \leq 36$ ; 2B; $\phi$ by Peck; $S_u$ by Hara (5h)	$\phi \leq 36$ ; 2B; $\phi$ by Peck; $S_u$ by T&P(5)	$\phi \leq 36$ ; 2B; $\phi$ by Peck; $S_u$ by Hara (5h)	$\phi \leq 36$ ; 2B; $\phi$ by Peck; $S_u$ by T&P(5)	$\phi \leq 36$ ; 2B; $\phi$ by Peck; $S_u$ by Hara (5h)	
N	22	22	37	37	35	35	41
Bias mean	0.53	0.34	0.73	0.55	0.43	0.43	1.03
Standard deviation	0.34	0.22	0.45	0.32	0.30	0.30	0.55
COV	0.64	0.64	0.62	0.58	0.71	0.71	0.53

ALL SOILS	$\alpha$ -Tomlinson and/or Nordlund		$\alpha$ -API and/or Nordlund		$\beta$		$\lambda$		Meyerhof	Schmertmann SPT mobilized
	36; 2B; P; T&P(5)	36; 2B; P; H ara(5h)	36; 2B; P; T &P(5)	36; 2B; P; H ara(5h)	36; 2B; P; T &P(5)	36; 2B; P; H ara(5h)	36; 2B; P; T &P(5)	36; 2B; P; H ara(5h)		
N	58	58	73	73	58	58	17	17	19	69
Bias mean	0.72	0.64	0.81	0.69	0.55	0.55	0.60	0.52	1.77	1.16
Standard deviation	0.51	0.52	0.51	0.48	0.46	0.46	0.28	0.25	1.21	0.63
COV	0.70	0.81	0.64	0.69	0.83	0.83	0.47	0.48	0.69	0.54

### 1.5. Analysis and Discussion of Results

Based on the results obtained, the parameters which result in better statistical results, meaning that the COV is smaller and the mean of the bias factor is closer to 1.0, are summarized in the tables below.

Table 9: General observations on the parameters for concrete piles

Soil Type	Generally have better statistical results	Generally have worse statistical results
Cohesi onless	$\phi$ correlated by Peck, Hanson and Thornburn using corrected N-value from SPT.	$\phi$ correlated by Schmertmann from SPT.
	Tip resistance is calculated based on contributed zone of 8B above tip and 3.5B below tip.  $\phi_{avg} = \frac{\text{average } \phi \text{ 8B above tip} + \text{average } \phi \text{ 3.5B below tip}}{2}$	Tip resistance is calculated based on contributed zone of 2B below tip.
	Limit $\phi$ below $36^\circ$ .	Limit $\phi$ below $40^\circ$ .
Cohesi ve	$S_u$ correlated by Hara from SPT.	$S_u$ correlated by Terzaghi and Peck from SPT.
	Tip resistance is calculated based on contributed zone of 2B below tip.	Tip resistance is calculated based on contributed zone of 8B above tip and 3.5B below tip.  $S_{u_{avg}} = \frac{\text{average } S_u \text{ 8B above tip} + \text{average } S_u \text{ 3.5B below tip}}{2}$

Table 10: General observations on the parameters for pipe piles

Cohesionless-- Nordlund method	Limit $\phi$ below 36 gives smaller COV, but the mean values are significantly higher than 1.0 (conservative--or under-predicted pile capacity).
Cohesive-- $\alpha$ (API or Tomlinson), $\beta$ , $\lambda$ methods	$S_u$ by Hara gives smaller COV, but the mean values are significantly smaller than 1.0 (unconservative--or over-predicted pile capacity).

Table 11: General observations on the parameters for H piles

Soil Type	Generally have better statistical results	Generally have worse statistical results
<b>Cohesi onless</b>	$\phi$ correlated by Peck, Hanson and Thornburn using corrected N-value from SPT.	$\phi$ correlated by Schmertmann from SPT.
	Tip resistance is calculated based on contributed zone of 8B above tip and 3.5B below tip.	Tip resistance is calculated based on contributed zone of 2B below tip.
	Limit $\phi$ below $36^\circ$ .	Limit $\phi$ below $40^\circ$ .
	Plugged shape: lower COV, higher $\Phi$	Unplugged shape (even though the bias mean is closer to 1)
<b>Cohesi ve</b>	$S_u$ by Hara gives smaller COV, but the mean values are significantly smaller than 1.0 (unconservative--or over-predicted pile capacity).	
	Tip resistance is calculated based on contributed zone of 2B below tip.	Tip resistance is calculated based on contributed zone of 8B above tip and 3.5B below tip.
	Plugged shape: closer to 1 and higher bias mean; lower COV; higher $\Phi$	Unplugged shape

Currently, Nordlund, Meyerhof and Schmertmann methods have separate curves or equations for large and small displacement piles. However, the coefficients for  $\alpha$ ,  $\beta$ ,  $\lambda$  and Thurman methods are the same for large and small displacement piles.

## Discussion of Results

The following correlations are recommended for the axial capacity prediction:

- Peck, Hanson and Thornburn's equation (cited in Reese et al., 1998) for internal friction angle,  $\phi$ , from corrected blow count,  $N'$ ,
- Limit  $\phi$  below  $36^\circ$  for Nordlund method,
- Hara's equation (cited in Kulhawy et al., 1990) for undrained shear strength  $S_u$  from uncorrected blow count,  $N$  (concrete piles),
- Terzaghi and Peck 's equation (cited in Kulhawy et al., 1990) for undrained shear strength  $S_u$  from uncorrected blow count,  $N$  (H and pipe piles).

## APPENDICES

### A. LISTS OF PILES IN THE DATABASE

#### A.1. Summary of the Driven Pile Database

SOIL TYPE		NUMBER OF CASES		
TIP	SIDE	H-PILES	CONCRETE	PIPE
ROCK	CLAY		0	0
	SAND		0	0
	MIX		15	3
	<b>TOTAL</b>		<b>15</b>	<b>3</b>
SAND	CLAY		0	0
	SAND		37	20
	MIX		50	19
	<b>TOTAL</b>		<b>87</b>	<b>39</b>
CLAY	CLAY		19	20
	SAND		1	0
	MIX		34	15
	<b>TOTAL</b>		<b>54</b>	<b>35</b>
UNKNOWN OR NOT ENOUGH DATA			7	1
<b>ALL CASES</b>			<b>163</b>	<b>78</b>



## A.2. Concrete Piles

Case #	Data ID	Project Name	English (kip; ft; in)					SI (KN,m, cm)		
			Width	Void	Length	Max Load	Max Settl	Width	Void	Length
1	16	SURFRIDER CONDOMINIUM	12.0	-	29.0	200	0.7	30	-	8.8
2	28	KARIDAS CONDOMINIUM #2	12.0	-	8.5	44	0.7	30	-	2.6
3	310	BEACHES OF LONGBOAT	12.0	-	14.0	200	0.3	30	-	4.3
4	411	VIENTA CONDOMINIUM	12.0	-	13.0	180	0.9	30	-	4.0
5	512	APP. BAY BRIDGE BENT 101	24.0	12	62.1	822	0.8	61	30	18.9
6	613	APP. BAY BRIDGE BENT 133	24.0	12	104.9	866	1.4	61	30	32.0
7	714	ARVIDA HOTEL	12.0	-	35.0	240	0.7	30	-	10.7
8	815	VERANDA HOTEL, SARASOTA	12.0	-	18.0	160	0.5	30	-	5.5
9	916	LONGBOAT COVE, SARASOTA	12.0	-	16.0	160	0.8	30	-	4.9
10	117	I-95 WEST PALM BEACH #1	18.0	-	26.5	127	1.0	46	-	8.1
11	118	I-95 WEST PALM BEACH #2	18.0	-	37.2	156	0.6	46	-	11.3
12	119	BLOUNT ISLAND SITE 215	10.0	-	68.0	180	1.6	25	-	20.7
13	120	BLOUNT ISLAND SITE 316	14.0	-	52.0	320	1.1	36	-	15.8
14	122	I-275 34th ST. PINELLAS	18.0	-	69.0	448	1.7	46	-	21.0
15	124	APP. BAY BRIDGE BENT 145	24.0	12	103.0	983	1.4	61	30	31.4
16	126	SIESTA KEY SARASOTA	12.0	-	16.3	200	0.4	30	-	5.0
17	127	DeSOTA CONDOMINIUM MS.	16.0	-	23.8	340	1.5	41	-	7.3
18	128	WASHINGTON CONDOMINIUM	14.0	-	52.5	300	1.3	36	-	16.0
19	130	SUNSHINE SKYWAY SITE 1 A	24.0	-	49.2	1,200	1.8	61	-	15.0
20	231	SUNSHINE SKYWAY SITE 1 B	20.0	-	47.3	600	0.6	51	-	14.4
21	232	SUNSHINE SKYWAY SITE 3	24.0	-	48.0	1,050	0.7	61	-	14.6
22	233	SUNSHINE SKYWAY SITE 10	24.0	-	27.9	1,200	0.7	61	-	8.5
23	234	SUNSHINE SKYWAY SITE 13 A	20.0	-	20.6	600	0.4	51	-	6.3
24	236	ST. JOHN'S RIVER (ASCE)-3B	20.0	-	46.0	596	0.7	51	-	14.0
25	237	ST. JOHN'S RIVER (ASCE) 3C	14.0	-	60.0	374	1.0	36	-	18.3
26	238	ST. AUGUSTINE (ASCE) 4A	12.0	-	28.0	150	0.5	30	-	8.5
27	244	BLOUNT ISLAND TERM. B-20	20.0	-	46.2	600	0.7	51	-	14.1
28	245	FLORENCE/MARION 3 ASD	18.0	-	25.0	500	0.8	46	-	7.6
29	246	FLORENCE / MARION 3 BSD	18.0	-	40.0	272	1.2	46	-	12.2
30	347	FLORENCE / MARION 3 CSD	18.0	-	38.0	296	1.0	46	-	11.6
31	348	NORTHEAST VILLA MIRADA - 6	14.0	-	8.8	100	0.5	36	-	2.7

Case #	Data ID	Project Name	English (kip; ft; in)					SI (KN,m, cm)		
			Width	Void	Length	Max Load	Max Settl	Width	Void	Length
32	49	SARASOTA MEM. HOSPITAL	12.0	-	25.0	188	0.7	30	-	7.6
33	51	PORT ORANGE BENT 2 PILE 6	18.0	-	30.1	369	2.2	46	-	9.2
34	52	SEAWAY HOTELS, SAND KEY	14.0	-	29.8	400	0.5	36	-	9.1
35	53	BLOUNT ISLAND TERM. B-21	20.0	-	36.4	496	1.4	51	-	11.1
36	58	HOWARD FRANKLAND / LS3	30.0	-	39.6	2,000	1.2	76	-	12.1
37	63	CHOCTAWHATCHEE P-5	30.0	18	53.9	1,485	1.8	76	46	16.4
38	64	CHOCTAWHATCHEE P-11	30.0	18	85.5	1,508	2.0	76	46	26.1
39	65	CHOCTAWHATCHEE P-17	30.0	18	77.8	1,620	1.8	76	46	23.7
40	66	CHOCTAWHATCHEE P-23	30.0	18	82.5	810	1.7	76	46	25.1
41	67	CHOCTAWHATCHEE P-29	30.0	18	84.4	990	1.7	76	46	25.7
42	68	CHOCTAWHATCHEE P-35	30.0	18	79.0	1,484	2.2	76	46	24.1
43	69	HOWARD FRANK. / LS4 SHORT	30.0	-	24.6	2,000	0.9	76	-	7.5
44	70	CHOCTAWHATCHEE P-41	30.0	18	65.2	1,440	1.3	76	46	19.9
45	72	CHOCTAWHATCHEE FSB-26	24.0	-	87.2	960	1.9	61	-	26.6
46	74	CAPE CANAVERAL T-6	18.0	-	53.1	340	0.8	46	-	16.2
47	75	CAPE CANAVERAL T-7	14.0	-	76.2	410	0.9	36	-	23.2
48	76	CAPE CANAVERAL T-14	14.0	-	69.5	391	2.2	36	-	21.2
49	79	WHITE CITY BRIDGE TP3	24.0	-	37.2	700	0.7	61	-	11.3
50	80	HOWARD FRANK. / LS4 LONG	30.0	-	73.5	1,750	6.8	76	-	22.4
51	83	WHITE CITY BRIDGE TP6	24.0	-	28.5	600	0.9	61	-	8.7
52	86	ACOSTA BRIDGE PEIR F6	24.0	-	58.5	915	2.8	61	-	17.8
53	87	ACOSTA BRIDGE PEIR G13	24.0	-	46.1	1,315	1.3	61	-	14.1
54	88	ACOSTA BRIDGE PEIR H2	24.0	-	35.9	718	1.9	61	-	10.9
55	89	WEST BAY BRIDGE TP9	30.0	18	128.4	955	1.6	76	46	39.1
56	90	WEST BAY BRIDGE TP15	30.0	18	103.6	855	1.4	76	46	31.6
57	92	ESCAMBIA RIVER BENT5	24.0	-	85.7	934	2.1	61	-	26.1
58	94	ROOSEVELT BRIDGE A-	30.0	-	53.4	1,220	1.4	76	-	16.3
59	95	ROOSEVELT BRIDGE B-30-W	30.0	-	43.8	1,040	1.5	76	-	13.4
60	96	BUCKMAN BRIDGE TS-13	30.0	14	94.5	1,180	1.9	76	36	28.8
61	97	BUCKMAN BRIDGE TS-19	30.0	14	89.3	1,481	2.0	76	36	27.2
62	98	BUCKMAN BRIDGE TS-24	30.0	14	80.8	1,168	2.1	76	36	24.6
63	99	BUCKMAN BRIDGE TS-29	30.0	14	80.0	1,400	2.1	76	36	24.4
64	102	APPALACHICOLA RIVER PIER14	30.0	18	58.8	953	0.7	76	46	17.9
65	113	APPALACHICOLA RIVER PIER25	24.0	12	55.5	836	1.2	61	30	16.9

Data Case # ID Project Name			English (kip; ft; in)					SI (KN,m, cm)		
			Width	Void	Length	Max Load	Max Settl	Width	Void	Length
66	131	MARCO ISLAND TP2	14.0	-	33.0	200	0.4	36	-	10.1
67	134	MARINA BAY CLUB TP7	14.0	-	83.0	279	0.6	36	-	25.3
68	135	APPALACHICOLA BAY BENT 41	24.0	12	52.3	548	1.0	61	30	15.9
69	136	ST. MARISSA CONDO. TP8 & Pile 20	14.0	-	50.0	284	1.0	36	-	15.2
70	140	GEORGIA/FLORIDA BOUNDARY	10.0	-	43.0	150	1.1	25	-	13.1
71	141	JACKSONVILLE SITE B	14.0	-	33.0	368	0.9	36	-	10.1
72	142	JACKSONVILLE SITE D	14.0	-	62.0	486	0.9	36	-	18.9
73	143	SAINT JOHN RIVER SITE F	18.0	-	35.0	300	0.6	46	-	10.7
74	145	LONGBOAT KEY - SARASOTA	12.0	-	49.1	200	0.5	30	-	15.0
75	146	SUNSHINE SKYWAY SITE 13 B	24.0	-	26.9	1,200	1.6	61	-	8.2
76	497	116 GRL Piles-164/Cimaron Rvr Br, OK	19.9	-	64.3	800	2.7	51		19.6
77	498	116 GRL Piles-164/Cimaron Rvr Br, OK	24.0	-	63.3	1,778	2.7	61		19.3
78	502	BRIDGE SITE 3046A, Hinds, MS	16.0	-	27.0	144	1.1	41		8.2
79	503	BRIDGE SITE 3046B, Hinds, MS	16.0	-	37.0	264	1.1	41		11.3
80	514	Dist. 08 P 455-03-04, 455-05-03 TP33,	16.0	-	80.0	194	0.9	41		24.4
81	515	Dist. 61 P 50-05-15 TP1, Ascension, LA	16.0	-	87.0	228	0.7	41		26.5
82	516	Dist. 61 P 742-01-39, East Baton, LA	14.0	-	70.0	170	0.7	36		21.3
83	517	118 GRL Piles Bailey Fork, Bailey, TN	14.0	-	45.0	300	0.6	36		13.7
84	518	119 GRL Piles-White City Bridge, FL	24.0	-	40.0	600	0.9	61		12.2
85	519	119 GRL Piles-White City Bridge, FL	24.0	-	40.0	994	1.1	61		12.2
86	520	123 GRL Piles-Dawhoo River Bridge, SC	16.0	-	80.0	1,400	6.4	41		24.4
87	521	123 GRL Piles-Dawhoo River Bridge, SC	24.0	4	90.0	698	7.4	61	10	27.4
88	522	124 GRL Piles-Socastee W. Way Br, SC	21.8	-	85.0	1,520	1.4	55		25.9
89	523	125 GRL Piles-Doughty St Prk Gar, SC	12.0	-	91.0	367	1.1	31		27.7
90	524	126 GRL Piles-Battery Creek, SC	24.0	-	81.5	1,200	1.1	61		24.8
91	525	126 GRL Piles-Battery Creek, SC	24.0	-	66.5	570	1.1	61		20.3
92	526	128 GRL Piles-Howard Franklin Br, FL	24.0	-	85.6	1,001	1.0	61		26.1
93	529	204 GRL Piles-C&D Canal, Pier 17, DE	24.0	-	75.0	1,200	1.9	61		22.9
94	531	99 GRL Piles I-165/Water St Int, AL	18.0	-	77.0	900	1.1	46		23.5
95	532	99 GRL Piles I-165/Water St Int, AL	36.0	-	74.0	600	1.1	92		22.6
96	533	99 GRL Piles I-165/Water St Int, AL	18.0	-	67.0	1,200	1.2	46		20.4
97	534	99 GRL Piles I-165/Water St Int, AL	24.0	-	77.0	430	1.1	61		23.5
98	535	99 GRL Piles I-165/Water St Int, AL	24.0	-	67.0	700	1.2	61		20.4
99	536	Axial Pile-Mission Avenue, Viaduct, CA	14.0	-	17.4	261	0.9	36		5.3

Data Case # ID Project Name	English (kip; ft; in)					SI (KN,m, cm)		
	Width	Voi d	Length	Max Load	Max Settl	Width	Void	Length
100 537	Axial Pile-Mission Avenue, Viaduct, CA	14.0	-	34.0	288	1.0	36	10.4
101 538	Axial Pile-Mission Avenue, Viaduct, CA	14.0	-	24.0	235	1.0	36	7.3
102 539	Doheny Park Rd U.C. Sta 451+85.5, CA	12.0	-	56.3	280	1.0	31	17.1
103 540	LOAD TRANSFER #35-3, OK	24.0	-	57.0	1,770	2.7	61	17.4
104 542	West Seattle Fwy Harbor Island, WA	19.9	-	86.0	900	1.6	51	26.2
105 571	BRIDGE SITE 1067, HINDS, MS	18.0	-	30.5	300	1.0	46	9.3
106 572	BRIDGE SITE 1068, HINDS, MS	14.0	-	30.0	180	1.2	36	9.1
107 573	BRIDGE SITE 1069, HINDS, MS	14.0	-	39.6	330	1.2	36	12.1
108 575	BRIDGE SITE 1072A, HINDS, MS	18.0	-	28.5	240	1.0	46	8.7
109 577	BRIDGE SITE 3024, HINDS, MS	14.0	-	36.5	318	1.5	36	11.1
110 580	Dist. 02 P 7-03-40 TP5, St. Charles LA	24.0	-	110.0	644	0.9	61	33.5
111 583	Dist. 02 P 855-14-7 and P 855-14-5, LA	14.0	-	110.0	250	0.9	36	33.5
112 587	Dist. 03 P 455-02-04 TP2, St. Landry LA	24.0	-	65.0	440	0.9	61	19.8
113 1001	Luling Bridge; TP2	54.0	44	81.1	717	0.8	137	112 24.7
114 1002	Luling Bridge; TP3; Circular void	24.0	12	82.6	419	0.7	61	30 25.2
115 1003	Luling Bridge; TP4; Circular void	30.0	19	82.5	525	0.8	76	47 25.2
116 1004	Luling Bridge; TP5	30.0	19	83.0	555	0.6	76	47 25.3
117 1005	Luling Bridge; TP6	36.0	26	82.5	547	1.0	91	66 25.2
118 1006	Luling Bridge; TP7	36.0	26	81.8	541	0.8	91	66 24.9
119 1007	Orlando International Airport; D22	14.0	-	90.0	842	1.2	36	- 27.4
120 1162	Site 33, Pile 3, Reinforced Concrete	12.0	-	114.3	298	0.5	31	34.8
121 1163	Site 33, Pile 4, Reinforced Concrete	12.0	-	54.5	298	0.3	31	16.6
122 1175	Site 35, Pile 10, Reinforced Concrete	12.0	-	48.0	511	3.2	31	14.6
123 1260	Jacksonville - Industrial zone # 1	20.0	-	46.0	581	0.6	51	- 14.0
124 1261	Jacksonville - Industrial # 2	20.0	-	36.0	495	1.3	51	- 11.0
125 1262	Ft Myers	14.0	-	67.0	280	1.5	36	- 20.4
126 1263	Apalachicola River Bridge - Pier 3	24.0	12	90.6	95	0.0	61	30 27.6
127 1264	Apalachicola Bay Bridge - Bent 22	18.0	-	64.0	422	0.6	46	- 19.5
128 1265	Apalachicola Bay Bridge - Bent 16	18.0	-	61.0	349	0.9	46	- 18.6
129 1267	Port Orange - Bent 19	18.0	-	30.9	296	1.9	46	- 9.4
130 2344	Choctahatchee Bay, FL3	24.0	-	77.7	458	1.7	61	- 23.7
131 2345	Choctahatchee Bay, FL26	24.0	-	64.8	314	1.0	61	- 19.8
132 3162	065-90-0024_and_855-04-0046_Tp1	14.0	-	80.0	270	1.2	36	- 24.4

Data Case # ID Project Name			English (kip; ft; in)					SI (KN,m, cm)		
			Width	Void	Length	Max Load	Max Settl	Width	Void	Length
133	3163	065-90-0024_and_855-04-0046_Tp2	14.0	-	70.0	110	2.1	36		21.3
134	3164	065-90-0024_and_855-04-0046_TP3	14.0	-	80.0	250	1.4	36	-	24.4
135	3165	065-90-0024_and_855-04-0046_TP4	14.0	-	81.0	240	1.1	36	-	24.7
136	3166	065-90-0024_and_855-04-0046_TP5	16.0	-	71.5	220	2.4	41	-	21.8
137	3170	260-05-0020_Tickfaw_River_; TP1	30.0	-	59.3	984	4.8	76	-	18.1
138	3173	262-06-09_Tickfaw_River_ #1; TP1	24.0	-	84.9	480	1.0	61	-	25.9
139	3174	262-06-09_Tickfaw_River_ #1; TP2	24.0	-	105.0	540	0.7	61	-	32.0
140	3176	283-09-52_New_Orleans	18.0	-	125.0	362	0.3	46		38.1
141	3178	424-05-0078_Bayou_Boeuf_Main_; TP1	14.0	-	70.0	330	0.6	36	-	21.3
142	3179	424-05-0078_Bayou_Boeuf_Main_; TP2	14.0	-	70.0	232	2.0	36	-	21.3
143	3180	424-05-0078_Bayou_Boeuf_Main_; TP5	14.0	-	80.0	250	0.9	36	-	24.4
144	3181	424-05-0081_Bayou_Boeuf_West_; TP1	14.0	-	89.5	230	0.5	36		27.3
145	3182	424-05-0081_Bayou_Boeuf_West_; TP2	30.0	-	110.0	640	1.3	76	-	33.5
146	3183	424-05-0081_Bayou_Boeuf_West_; TP3	14.0	-	63.5	330	0.6	36	-	19.4
147	3184	424-05-0081_Bayou_Boeuf_West_; TP4	16.0	-	70.0	200	0.5	41	-	21.3
148	3185	424-05-0087_Bayou_Ramos_ TP1	16.0	-	78.0	280	2.2	41	-	23.8
149	3186	424-05-0087_Bayou_Ramos_ TP2	30.0	-	88.0	1,050	1.8	76	-	26.8
150	3187	424-05-0087_Bayou_Ramos_ TP3	30.0	-	104.0	1,000	3.1	76	-	31.7
151	3188	424-05-0087_Bayou_Ramos_ TP4	30.0	-	99.3	1,200	3.0	76	-	30.3
152	3189	424-05-0087_Bayou_Ramos_ TP5	30.0	-	113.0	1,150	1.9	76	-	34.4
153	3191	424-05-0087_Bayou_Ramos_ TP7	16.0	-	77.0	230	1.6	41	-	23.5
154	3192	424-06-0005_Bayou_Boeuf_East_ F1;	14.0	-	68.0	210	1.6	36	-	20.7
155	3193	424-06-0005_Bayou_Boeuf_East_ F2;	14.0	-	71.0	195	1.1	36	-	21.6
156	3194	424-06-0005_Bayou_Boeuf_East_ F3	14.0	-	77.5	200	2.0	36	-	23.6
157	3195	424-06-0005_Bayou_Boeuf_East_ F4	14.0	-	79.0	240	1.1	36	-	24.1
158	3196	424-06-0005_Bayou_Boeuf_East_ F5	14.0	-	79.0	180	0.8	36	-	24.1
159	3197	424-06-0005_Bayou_Boeuf_East_ F6	30.0	-	110.0	640	2.6	76	-	33.5
160	3201	424-07-0009_Gibson_Raceland_ TP1	30.0	-	116.0	1,344	4.4	76	-	35.4
161	3203	424-07-0009_Gibson_Raceland_ TP4	30.0	-	124.0	1,312	3.1	76	-	37.8
162	3208	450-366-02_Luling_Bridge	30.0	-	112.0	1,000	2.0	76	-	34.1
163	3215	855-14-13_Houma	18.0	-	105.0	434	1.0	46	-	32.0

### A.3. Pipe Piles

Case #	ID in Database	Project Name	End Con.	English (kip; ft; in)					SI (KN,m, cm)		
				Dia	Thick	Length	Max Load	Max Settl	Dia	Thick	Length
1	197	HOUSTON, TEXAS	Plugged	10.8	0.19	51.3	168	0.4	27.3	0.48	15.6
2	198	HUNTER'S POINT	Closed End	10.8	0.19	30.0	98	1.0	27.3	0.48	9.14
3	199	ST. LOUIS, MISSOURI	Plugged	14.0	0.22	47.2	250	1.2	35.6	0.56	14.4
4	200	ST. LOUIS, MISSOURI	Plugged	16.0	0.19	47.8	400	2.9	40.6	0.48	14.6
5	204	DELAWARE L.R. 795-B3	Plugged	18.0	0.22	89.0	530	1.6	45.7	0.56	27.1
6	205	NW CONN. OC-RETROFIT	Plugged	16.0	0.19	66.5	520	1.0	40.6	0.48	20.3
7	206	NW CONN. OC RETROFIT #2	Plugged	16.0	0.19	56.5	402	1.5	40.6	0.48	17.2
8	207	SOUTHERN FREEWAY, CA	Plugged	16.0	0.19	41.1	800	1.0	40.6	0.48	12.5
9	208	HAMILTON BAYFRONT,CAN	Closed End	12.7	0.37	110.0	1,191	2.4	32.4	0.95	33.5
10	209	HAMILTON BAYFRONT #2	Closed End	12.7	0.37	83.0	899	1.6	32.4	0.95	25.3
11	210	HAMILTON BAYFRONT #3	Closed End	12.7	0.37	60.0	674	2.8	32.4	0.95	18.3
12	478	101 GRL Piles-Fore, ME	Closed End	18.0	0.50	71.5	600	1.6	45.7	1.27	21.8
13	479	101 GRL Piles-Fore Portland, ME	Closed End	18.0	0.50	59.7	400	1.1	45.7	1.27	18.2
14	480	101 GRL Piles-Fore Portland, ME	Closed End	18.0	0.50	120.0	540	1.3	45.7	1.27	36.6
15	481	110 GRL Piles-Peosta, IA	Closed End	14.0	0.50	80.0	420	1.3	35.6	1.27	24.4
16	482	110 GRL Piles Peosta, IA	Closed End	14.0	0.50	100.0	666	0.9	35.6	1.27	30.5
17	483	116 GRL Piles-164/Cimaron, OK	Closed End	26.0	0.75	63.3	800	3.1	66	1.91	19.3
18	484	LOAD TRANSFER #35-1, CA	Closed End	10.7	0.37	30.0	109	1.6	27.3	0.93	9.14
19	485	LOAD TRANSFER #35-2,	Closed End	10.7	0.37	18.5	116	2.2	27.3	0.93	5.64
20	486	117 GRL Piles-St Rte 115 MO	Closed End	14.0	0.37	62.0	260	1.0	35.6	0.95	18.9
21	487	117 GRL Piles-St Rte 115 MO	Closed End	14.0	0.37	86.5	340	2.2	35.6	0.95	26.4
22	488	124 GRL Piles-Socastee W., SC	Closed End	24.0	0.50	85.0	701	2.4	61	1.27	25.9
23	489	130 GRL Piles-Jones Island, WI	Closed End	9.6	0.54	166.2	580	2.2	24.5	1.38	50.7
24	490	130 GRL Piles-Jones Island, WI	Closed End	12.8	0.31	161.3	540	2.0	32.4	0.79	49.2
25	491	130 GRL Piles-Jones Island, WI	Closed End	12.8	0.31	161.0	694	2.8	32.4	0.79	49.1
26	492	130 GRL Piles-Jones Island, WI	Closed End	12.8	0.31	140.4	691	2.7	32.4	0.79	42.8
27	493	130 GRL Piles-Jones Island, WI	Closed End	9.6	0.54	154.6	380	1.6	24.5	1.38	47.1
28	494	130 GRL Piles-Jones Island, WI	Closed End	12.8	0.31	165.9	415	3.6	32.4	0.79	50.6

				English (kip; ft; in)					SI (KN,m, cm)		
Case #	ID in Database	Project Name	End Con.	Dia	Thick	Length	Max Load	Max Settl	Dia	Thick	Length
29	495	130 GRL Piles-Jones Island, WI	Closed End	9.6	0.54	145.0	657	2.1	24.5	1.38	44.2
30	496	130 GRL Piles-Jones Island, WI	Closed End	9.6	0.54	155.4	657	2.4	24.5	1.38	47.4
31	563	Bayshore Fwy Viaduct Site F, CA	Unplugged	24.0	0.75	73.0	900	1.2	61	1.91	22.3
32	566	Ventura Underpass, CA	Unplugged	12.0	0.13	39.1	170	1.6	30.5	0.34	11.9
33	1008	Orlando International Airport; D23	Closed End	12.7	0.25	83.3	514	1.1	32.4	0.63	25.4
34	1009	Belleville; LPT 1	Unplugged	12.0	0.25	44.4	210	14.5	30.5	0.63	13.5
35	1010	Belleville; LPT4; pre excavate	Closed End	12.0	0.25	66.5	790	1.3	30.5	0.63	20.3
36	1011	Belleville; LPT5; pre excavate	Closed End	12.0	0.18	66.7	800	1.9	30.5	0.45	20.3
37	1013	Detroit; LPT1	Unplugged	12.0	0.18	69.5	64	10.8	30.5	0.45	21.2
38	1014	Detroit; LPT2	Closed End	12.0	0.18	78.6	490	5.3	30.5	0.45	24
39	1016	Detroit LTP10	Closed End	12.0	0.23	81.0	550	6.3	30.5	0.58	24.7
40	1037	Site 2, Pile 4; ARMCO	Closed End	12.0	0.14	24.5	281	0.4	30.5	0.36	7.47
41	1098	Site 2, Pile 5, Armco Steel Tube	Closed End	12.0	0.17	19.0	214	2.0	30.5	0.44	5.79
42	1099	Site 4, Pile 2, Armco Steel Tube	Closed End	12.8	0.19	118.0	160	3.1	32.4	0.48	36
43	1113	Site 9, Pile 5, Steel Tube	Closed End	12.8	0.25	70.0	399	0.4	32.4	0.63	21.3
44	1117	Site 13, Pile 19, Steel Tube	Closed End	12.8	0.25	64.8	326	0.7	32.4	0.63	19.7
45	1119	Site 14, Pile 2, Steel Tube	Closed End	12.8	0.20	60.0	67	1.1	32.4	0.5	18.3
46	1120	Site 14, Pile 3, Steel Tube	Closed End	12.8	0.25	95.0	298	0.9	32.4	0.63	29
47	1129	Site 22, Pile 3, Steel Tube	Closed End	12.8	0.20	50.2	62	2.0	32.4	0.52	15.3
48	1130	Site 22, Pile 4, Steel Tube	Closed End	12.8	0.25	98.9	274	3.7	32.4	0.63	30.1
49	1131	Site 22, Pile 5, Steel Tube	Closed End	12.8	0.20	50.1	73	3.7	32.4	0.52	15.3
50	1132	Site 23, Pile 2, Steel Tube	Closed End	12.8	0.25	9.9	121	1.4	32.4	0.63	3.02
51	1134	Site 24, Pile 2, Steel Tube	Closed End	12.8	0.20	50.5	250	8.1	32.4	0.52	15.4
52	1135	Site 24, Pile 3, Steel Tube	Closed End	12.8	0.20	73.5	253	9.6	32.4	0.52	22.4
53	1138	Site 25, Pile 1, Steel Tube	Closed End	12.8	0.25	18.5	79	1.9	32.4	0.63	5.64
54	1140	Site 25, Pile 5, Steel Tube	Closed End	12.8	0.25	60.2	174	1.6	32.4	0.63	18.4
55	1141	Site 25, Pile 6, Steel Tube	Closed End	12.8	0.25	30.4	114	1.1	32.4	0.63	9.27
56	1143	Site 26, Pile 1, Steel Tube	Closed End	12.8	0.25	40.0	29	1.9	32.4	0.63	12.2
57	1144	Site 26, Pile 4, Steel Tube	Closed End	12.8	0.25	100.0	279	1.9	32.4	0.63	30.5
58	1145	Site 26, Pile 5, Steel Tube	Closed End	12.8	0.25	140.0	298	2.0	32.4	0.63	42.7

				English (kip; ft; in)					SI (KN,m, cm)		
Case#	ID in Database	Project Name	End Con.	Dia	Thick	Length	Max Load	Max Settl	Dia	Thick	Length
59	1155	Site 28, Pile 7, Steel Tube	Closed End	12.8	0.25	20.0	160	1.9	32.4	0.63	6.1
60	1156	Site 28, Pile 8, Steel Tube	Closed End	12.8	0.25	60.0	171	1.9	32.4	0.63	18.3
61	1157	Site 28, Pile 9, Steel Tube	Closed End	12.8	0.25	39.5	146	1.3	32.4	0.63	12
62	1158	Site 30, Pile 1, Steel Tube	Closed End	12.8	0.25	131.5	466	1.2	32.4	0.63	40.1
63	1159	Site 30, Pile 2, Steel Tube	Closed End	12.8	0.25	130.7	478	1.2	32.4	0.63	39.8
64	1161	Site 33, Pile 2, Steel Tube	Closed End	12.8	0.25	107.2	585	3.1	32.4	0.63	32.7
65	1172	Site 35, Pile 4, Steel Tube	Closed End	12.8	0.25	48.2	377	2.9	32.4	0.63	14.7
66	1174	Site 35, Pile 6, Steel Tube	Closed End	12.8	0.25	90.0	596	2.7	32.4	0.63	27.4
67	1187	Site 38, Pile 4, Steel Tube	Closed End	12.8	0.37	39.0	247	1.8	32.4	0.95	11.9
68	1188	Site 38, Pile 5, Steel Tube	Closed End	12.8	0.37	52.8	585	3.7	32.4	0.95	16.1
69	1190	Site 39, Pile 3, Steel Tube	Closed End	12.8	0.37	83.3	337	1.9	32.40	0.95	25.4
70	1192	Site 40, Pile 3, Steel Tube	Closed End	12.8	0.37	56.4	268	1.6	32.40	0.95	17.2
71	1195	Site 41, Pile 3, Steel Tube	Closed End	12.8	0.37	52.5	402	0.5	32.40	0.95	16.0
72	2164	Deer Island Pier Facilities; LT-1	Closed End	14.0	0.50	87.0	540	1.0	35.56	1.27	26.5
73	2165	Deer Island Pier Facilities; LT-2	Closed End	14.0	0.50	54.0	540	0.7	35.56	1.27	16.5
74	2166	Deer Island Pier Facilities; LT-3	Closed End	14.0	0.50	89.0	540	1.1	35.56	1.27	27.1
75	2167	Deer Island Pier; L1-2; LT-4	Closed End	14.0	0.50	83.0	648	0.9	35.56	1.27	25.3
76	2168	Deer Island Pier; P-14; LT-5	Closed End	14.0	0.50	88.0	528	2.1	35.56	1.27	26.8
77	2170	Deer Island Pier; P-11; LT-7	Closed End	14.0	0.50	89.0	528	2.6	35.56	1.27	27.1
78	2171	Deer Island Pier; P-12; LT-8	Closed End	14.0	0.50	96.4	720	1.1	35.56	1.27	29.4



## B. SUB-CATEGORY OF CONCRETE PILES

Table 12. Total Cases of Static Load Tests on Concrete Piles in Soils

Soil Type	S <sup>1</sup>	ST <sup>2</sup>	Total Number of Cases	
Cohesionless soils	4	33	<b>37</b>	
Cohesive soils	14	5	<b>19</b>	
Mixed soils	40	45	<b>85</b>	
Sub Total for Soils			<b>141</b>	
Soils and Rocks	0	15	<b>15</b>	
Total	<b>58</b>	<b>98</b>	<b>156</b>	
NA <sup>3</sup>			<b>7</b>	<b>163</b>

<sup>1</sup> S: Predominant side resistance (Friction piles)

<sup>2</sup> ST: Side and tip resistance

<sup>3</sup> NA: Soil type is unknown/ or lack information to predict capacities

Table 13. The Data for Side Resistance (S) Concrete Piles

Soil Type	SPT	CPT	Lab	Overlap SPT, CPT & Lab	Total	OCR and Dr correlated from i situ
cohesionless soils	4	0	0	0	<b>4</b>	4
cohesive soils	0	6	9	1	<b>14</b>	6
mixed soils	17	25	0	2	<b>40</b>	40
Mixed soils and Rocks	0	0	0	0	<b>0</b>	0
Total	<b>21</b>	<b>31</b>	<b>9</b>	<b>3</b>	<b>58</b>	<b>50</b>

Table 14. The Data for Side and Tip Resistance (ST) Concrete Piles

Soil Type	SPT	CPT	Lab	Overlap SPT, CPT & Lab	Total	OCR and Dr correlated from i situ
cohesionless soils	33	2	0	2	33	33
cohesive soils	2	0	3	0	5	2
mixed soils	42	7	0	4	45	45
Mixed soils and Rocks	15	0	0	0	15	0
Total	92	9	3	6	98	80

Table 15. The Data for All Concrete Piles

Soil Type	SPT	CPT	Lab	Overlap SPT, CPT & Lab	Total	OCR and Dr correlated from i situ
cohesionless soils	37	2	0	2	37	37
cohesive soils	2	6	12	1	19	8
mixed soils	59	32	0	6	85	85
Sub total of Soils	74	40	12	9	141	130
Mixed soils and Rocks	15	-	-	-	15	-
Total	113				156	

### B.1. Side Resistance Only

TABLE 16. COHESIVE SOILS: Summary of Populations by Analysis Method used to Obtain *Side Resistance Only for Concrete Piles*

	Analysis Method				
	$\alpha$ API	$\alpha$ Tomlinson	$\lambda$	$\beta$	Schmertmann CPT
Number of cases	14	14	14	6	6

TABLE 17. MIXED SOILS: Summary of Populations by Analysis Method used to Obtain *Side Resistance Only for Concrete Piles*

Soil Type	Analysis Method				
cohesionless	Nordlund	Nordlund	$\beta$	Schmertmann SPT	Schmertmann CPT
cohesive	$\alpha$ API	$\alpha$ Tomlinson	$\beta$	Schmertmann SPT	Schmertmann CPT
Number of cases	40	22	40	17	25

**Note 1: COHESIONLESS SOILS: Population is 4 for Nordlund,  $\beta$  and Schmertmann SPT methods (Not enough for statistical analysis)**

TABLE 18. ALL SOILS: Analysis methods for Concrete Piles with *Side Resistance Only*

Soil Type	Analysis Method					
cohesionless	Nordlund	Nordlund	$\beta$	Schmertmann SPT	Schmertmann CPT	
cohesive	$\alpha$ API	$\alpha$ Tomlinson	$\beta$	Schmertmann SPT	Schmertmann CPT	$\lambda$
Number of cases	58	40	50	21	31	14

Note 2: Numbers are referred from Table 22, 23 and the constraints in Table 4.

## B.2. Total Capacity

**TABLE 19. COHESIONLESS SOILS: Summary of Populations by Analysis Method used to Obtain *Total Capacity for Concrete Piles***

<b>Capacity</b>	<b>Analysis Method</b>				
Side	Nordlund	$\beta$	Meyerhof	Schmertmann SPT	Schmertmann CPT
Tip	Thurman	Thurman	Meyerhof	Schmertmann SPT	Schmertmann CPT
Number of cases	37	37	37	37	2

**TABLE 20. COHESIVE SOILS: Summary of Populations by Analysis Method used to Obtain *Total Capacity for Concrete Piles***

<b>Capacity</b>	<b>Analysis Method</b>					
Side	$\alpha$ API	$\alpha$ Tomlinson	$\lambda$	$\beta$	Schmertmann SPT	Schmertmann CPT
Tip	9 Su	9 Su	9 Su	9 Su	Schmertmann SPT	Schmertmann CPT
Number of cases	19	19	19	8	2	6

**TABLE 21. MIXED SOILS: Summary of Populations by Analysis Method used to Obtain *Total Capacity for Concrete Piles***

Capacity	Soil Type	Analysis Method						
Side	cohesion less	Nordlund		Nordlund		$\beta$		Schmertmann
	cohesive	$\alpha$ API		$\alpha$ Tomlinson		$\beta$		
Tip	cohesion less	Thurman		Thurman		Thurman		CPT
	cohesive		9 Su		9 Su		9 Su	
Number of cases		50	35	0	34	50	35	32
		85		34		85		

TABLE 22. MIXED SOILS and ROCKS: Summary of Populations by Analysis Method used to Obtain *Total Capacity for Concrete Piles*

Capacity	Soil Type	Analysis Method	
Side	cohesionless	Schmertmann SPT	
	cohesive	Schmertmann SPT	
Tip	cohesionless	Schmertmann SPT	
	cohesive	Schmertmann SPT	
Number of cases		rock exists	no rock
		15	59
		74	

TABLE 23. ALL SOILS: Summary of Populations by Analysis Method used to Obtain *Total Capacity for Concrete Piles*

Cap acity	Soil Type	Analysis Method						
Side	cohesionl ess	Nordlund		Nordlund		$\beta$		Schmertman n CPT
	cohesive	$\alpha$ API		$\alpha$ Tomlinson		$\beta$		
Tip	cohesionl ess	Thurman		Thurman		Thurm an		
	cohesive		9 Su		9 Su		9 Su	
Number of cases		87	54	37	53	87	43	40
		141		90		130		

TABLE 24. ALL SOILS and ROCKS: Summary of Populations by Analysis Method used to Obtain *Total Capacity for Concrete Piles*

Capacity	Soil Type	Analysis Method	
Side	cohesionless	Schmertmann SPT	
	cohesive	Schmertmann SPT	
Tip	cohesionless	Schmertmann SPT	
	cohesive	Schmertmann SPT	
Number of cases		rock exists	no rock
		15	98
		113	

Note: Numbers are referred from Tables 24; 29 to 33 and the constraints in Table 4.

## C. AXIAL CAPACITIES--CONCRETE PILES

Table 25: Axial capacities (KN): Concrete Piles in Cohesionless soils

Case #	situ ID#	lab ID#	Divisson	Nordlund								
				DRIVEN	40;2B;P (1)	40;11.5B; P (2)	40;2B;Sc h (3)	40;11.5B; Sch (4)	36;2B;P (5)	36;11.5B; P (6)	36;2B;Sc h (7)	36;11.5B; Sch (8)
1	1		805	1,001	1,007	1,308	1,974	1,714	753	861	1,000	953
2	1		140	399	399	208	477	465	218	178	224	224
3	1		890	757	757	604	810	810	374	350	394	394
4	1		525	663	663	663	669	669	320	320	320	320
7	1		925	1,924	1,924	1,506	2,039	2,015	1,030	996	1,047	1,047
8	1		682	782	782	711	803	803	391	391	391	391
9	1		525	932	932	932	951	951	460	460	462	462
10	1		500	451	445	451	505	611	445	451	430	537
11	1		618	574	574	574	871	763	574	574	773	666
12	1		692	737	737	710	1,643	1,463	712	685	1,105	1,068
13	1		1,310	787	787	787	1,136	867	781	781	933	664
16	1		870	889	889	889	895	895	433	433	434	434
24	1		2,570	7,741	7,741	7,248	8,742	8,742	4,202	4,202	4,427	4,427
25	1		1,540	1,589	1,589	1,640	3,148	2,924	1,415	1,456	1,977	1,846
26	1		600	528	528	374	800	396	422	307	373	238
27	1		2,600	8,080	8,080	7,460	9,075	8,958	4,303	4,303	4,529	4,529
32	1		670	1,137	1,137	736	1,325	1,207	612	523	679	679
33	1		1,235	1,636	1,636	1,787	3,878	3,875	1,545	1,649	1,935	1,935
35	1		1,650	3,016	3,016	2,981	5,220	4,698	2,573	2,276	2,612	2,538
46	1		1,405	5,188	5,188	2,336	6,382	3,969	3,094	2,025	3,489	2,477
56	1		3,730	8,827	8,827	8,827	10,995	10,995	8,827	8,827	10,039	10,039
57	1		3,800	7,763	7,763	7,856	10,105	10,501	7,763	7,856	9,118	9,490
58	2		4,010	11,329	11,329	6,191	16,359	10,264	7,635	5,240	8,163	6,452
59	1		3,450	11,739	11,739	5,817	12,132	5,929	6,200	3,766	6,093	3,110
61	1		4,820	11,302	11,302	11,479	21,170	18,591	10,147	10,102	15,329	13,602
66	1		890	658	658	585	1,899	1,383	631	558	1,087	1,017
83	1		1,200	2,781	2,781	2,781	2,952	2,952	1,459	1,459	1,548	1,548
94	3		3,820	8,469	8,469	6,964	10,555	9,988	5,021	4,846	5,869	5,869
95	1		2,490	15,026	14,860	15,939	31,616	29,634	13,455	12,712	15,869	15,869
96	2		5,100	7,951	7,951	6,946	9,094	8,528	4,239	4,223	4,917	4,917
97	1		1,670	12,901	12,901	9,354	17,249	16,292	7,757	7,346	9,179	9,179
98	1		2,620	5,548	5,548	5,767	14,102	13,453	5,428	5,555	7,467	7,467
101	1		970	494	494	503	1,661	1,644	494	503	942	942
103	1		7,250	10,430	10,430	7,295	12,114	10,959	5,363	4,504	6,429	6,429
122	1		1,800	1,973	1,973	1,634	2,827	2,574	1,274	1,270	1,325	1,325
123	1		2,510	4,950	4,810	4,953	7,242	7,242	3,553	3,553	3,685	3,685
123	3		2,510									
124	1		1,640	2,235	2,235	2,547	5,153	4,312	1,885	1,942	2,584	2,560
124	2		1,640									

(cont.): Axial capacities (KN): Concrete Piles in Cohesionless soils

Case #	situ ID#	lab ID#	$\beta$		Meyerhof	Schmertmann	
			40;2B;P (1)	36;2B;P (5)		SPT mobilized	CPT
1	1		724	724	837	1,074	
2	1		386	211	960	290	
3	1		710	367	2,233	577	
4	1		602	312	2,795	774	
7	1		1,668	974	2,903	1,157	
8	1		701	372	2,915	754	
9	1		838	446	2,827	902	
10	1		345	345	570	214	
11	1		431	431	790	301	
12	1		725	725	987	547	
13	1		512	512	917	637	
16	1		794	423	3,261	964	
24	1		5,918	3,245	9,872	3,334	
25	1		1,098	1,098	2,372	1,136	
26	1		430	357	639	355	
27	1		6,138	3,314	13,333	3,028	
32	1		1,088	599	490	723	
33	1		1,135	1,135	2,343	1,142	
35	1		2,048	2,037	3,314	1,977	
46	1		4,553	2,569	4,833	2,016	
56	1		6,252	6,252	3,191	2,618	
57	1		5,521	5,521	3,255	2,263	
58	2		9,416	6,144	7,105	2,631	
59	1		10,370	5,160	4,221	1,822	
61	1		6,859	6,859	9,594	4,162	
66	1		589	589	1,510	584	
83	1		2,329	1,322	5,262	1,542	
94	3		6,487	3,793	7,388	3,502	
95	1		11,127	10,011	18,615	6,792	
96	2		6,033	3,339	4,557	2,098	
97	1		10,453	5,663	12,526	4,718	
98	1		3,968	3,968	4,418	2,741	
101	1		459	459	930	595	
103	1		8,879	4,489	7,384	2,603	
122	1		1,778	1,199	987	775	
123	1		3,436	2,736	5,265	2,839	
123	3						3,211
124	1		1,374	1,374	2,669	1,736	
124	2						3,703

Table 26. Axial capacities (KN): Concrete Piles in Cohesive soils

Case #	situ ID#	lab ID#	Davisson	$\alpha$ API revised					$\alpha$ Tomlinson				
				APILE	2B; T&P (1)	11.5B; T&P (2)	2B; Hara (5h)	11.5B; Hara (6h)	DRIVEN	2B; T&P (1)	11.5B; T&P (2)	2B; Hara (5h)	11.5B; Hara (6h)
54	1		2,550	864	833	825	1,620	1,535	367	683	675	1,170	1,085
78	1	1	560	687	711	631	723	643	372	415	334	415	334
80	1	1	860	1,511	1,319	1,442	1,641	1,883	3,578	1,898	2,022	2,157	2,399
81		1	950	1,100	1,109	1,103	1,109	1,103	3,336	1,239	1,233	1,239	1,233
82	1	1	735	865	878	840	1,145	1,069	2,929	1,008	971	1,157	1,081
99	2		1,060	321	344	318	669	624	440	441	415	642	597
105		1	1,230	1,350	1,315	1,196	1,315	1,196	1,259	1,342	1,222	1,342	1,222
106		1	722	828	831	791	831	791	304	441	401	441	401
108		1	965	1,160	1,143	1,120	1,143	1,120	1,081	1,142	1,119	1,142	1,119
109		1	1,040	1,990	1,896	1,906	1,896	1,906	2,002	1,751	1,761	1,751	1,761
110		1	2,850	3,859	3,881	3,888	3,881	3,888	3,949	3,201	3,208	3,201	3,208
111		1	1,060	903	843	875	843	875	1,460	720	753	720	753
112		1	1,850	2,429	2,304	2,319	2,304	2,319	4,146	3,532	3,547	3,532	3,547
136	1		960	1,220	792	794	792	794	1,485	886	888	886	888
144	1		1,000										
144	2	1	1,000	1,137	1,092	1,032	1,325	1,197	1,598	938	878	1,169	1,042
154	1		880	1,055	954	953	954	953	1,834	1,548	1,547	1,548	1,547
155	1		865	1,064	916	917	916	917	1,592	1,380	1,381	1,380	1,381
158	1		750	1,463	1,230	1,230	1,230	1,230	2,783	1,970	1,970	1,970	1,970
159	1		2,800	5,310	4,924	4,946	4,924	4,946	8,810	7,076	7,098	7,076	7,098



(cont.). Axial capacities (KN): Concrete Piles in Cohesive soils

Case #	situ ID#	lab ID#	$\beta$				$\lambda$				Schmertmann	
			2B; T&P (1)	11.5B; T&P (2)	2B; Hara (5h)	11.5B; Hara (6h)	2B; T&P (1)	11.5B; T&P (2)	2B; Hara (5h)	(6h)	SPT mobilized	CPT
54	1		1,391	1,383	1,847	1,762	1,059	1,051	1,890	1,805	466	
78	1	1					980	900	1,018	938		
80	1	1					1,246	1,370	1,559	1,801		
81		1					1,149	1,143	1,149	1,143		
82	1	1					971	934	1,240	1,164		
99	2		563	537	708	663	534	508	1,095	1,050	423	
105		1					2,075	1,955	2,075	1,955		
106		1					1,185	1,145	1,185	1,145		
108		1					1,647	1,625	1,647	1,625		
109		1					2,917	2,927	2,917	2,927		
110		1					3,002	3,009	3,002	3,009		
111		1					1,050	1,082	1,050	1,082		
112		1					2,532	2,547	2,532	2,547		
136	1		1,144	1,147	1,144	1,147	776	778	776	778		1,054
144	1		1,586	1,585	1,586	1,585						1,237
144	2	1					1,139	1,079	1,368	1,240		
154	1		1,327	1,326	1,327	1,326	931	929	931	929		899
155	1		1,300	1,300	1,300	1,300	877	878	877	878		919
158	1		1,752	1,752	1,752	1,752	1,120	1,120	1,120	1,120		982
159	1		6,811	6,832	6,811	6,832	3,750	3,772	3,750	3,772		3,659

Table 27: Axial capacities (KN): Concrete Piles in Mixed soils

Case #	situ #	lab #	Davisson	$\alpha$ Tomlinson, Nordlund and Thurman					$\alpha$ API, Nordlund, Thurman				
				DRIVE N	40;2B;P; T&P(1)	40;2B;P; Hara(1h)	36;11.5B; Sch;T&P(8)	36;2B;P; Hara(5h)	40;2B;P; T&P(1)	40;2B;P; Hara(1h)	36;11.5B; Sch;T&P(8)	36;2B;P; Hara(5h)	
5	1		3,300	1,509	1,926	3,388	1,849	3,388	1,695	2,965	1,618	2,965	
6	1		3,400	2,166	2,162	3,031	1,901	3,031	3,110	4,716	2,848	4,716	
14	1		1,690	3,221	3,151	3,669	3,437	3,358	3,050	3,358	3,336	3,046	
17	1		1,120						1,441	1,635	767	960	
18	1		1,030						4,965	5,020	2,579	2,635	
19	1		3,350										
20	1		2,450										
21	1		4,300										
22	1		4,270	1,450	2,368	3,651	2,220	3,651	3,025	4,517	2,877	4,517	
23	1		2,669										
28	1		1,920						1,482	1,531	1,064	1,229	
29	1		1,075	789	1,315	2,343	1,285	2,343	978	1,694	948	1,694	
30	1		1,160	1,828	1,684	2,556	1,733	2,556	1,286	1,824	1,335	1,824	
31	1		383						299	316	333	313	
34	1		1,779										
36	1		6,420	8,318	7,824	12,202	7,799	12,202	4,541	6,509	4,517	6,509	
37	1		5,420						7,373	7,557	3,922	6,394	
38	1		6,260						5,867	6,217	10,305	6,217	
39	1		6,600						5,839	6,138	9,074	6,138	
40	1		2,800						6,419	6,631	9,870	6,570	
41	1		4,005						6,651	6,894	11,408	6,894	
42	1		6,400						6,751	7,060	11,524	6,952	
43	1		5,650						1,611	1,696	3,737	1,696	
44	1		6,100	2,796	2,876	4,524	3,460	4,524	2,922	4,632	3,506	4,632	
45	1		3,320						8,687	8,768	12,736	8,765	
47	1		1,800						3,032	3,282	3,512	2,884	
48	1		1,635						1,819	1,935	1,944	1,819	
49	1		2,870						951	1,120	2,267	1,120	
50	1		3,200										
51	1		2,120						1,315	1,381	1,709	1,381	
52	1		3,400						3,788	4,066	5,492	3,871	
53	1		4,800										
60	1		4,360						10,984	11,879	9,416	10,451	
62	1		4,900	11,644	11,703	12,479	10,424	9,677	11,695	12,317	10,415	9,514	
63	1		4,850						15,603	15,718	11,795	10,294	
64	1		4,200						5,326	5,503	7,000	5,503	
65	1		3,070						2,576	2,745	3,657	2,658	
67	1		1,239										
68	1		2,200						1,033	1,453	2,526	1,453	
69	1		1,225										
70	1		515										
71	1		1,605										
72	1		2,090										
73	1		1,050										
74	1		890	1,305	1,290	1,739	1,490	1,737	963	1,191	1,163	1,189	
75	1		2,640										
76	2		3,350	4,950	4,379	7,193	4,644	7,148	3,026	4,436	3,291	4,390	
77	1		7,200	5,311	5,770	9,600	6,041	9,539	3,630	5,376	3,901	5,315	
84	1		2,150						1,354	1,629	2,627	1,629	
85	2		4,150						5,639	5,656	3,104	3,289	
86	1	1	3,600	1,455	1,788	2,807	1,762	2,807	1,817	2,845	1,791	2,845	
87	1		2,170	2,737	3,579	6,194	3,576	6,194	3,655	6,144	3,652	6,144	
88	1		4,700						5,644	6,276	7,351	5,519	
89	1		1,600	967	975	1,489	971	1,489	1,137	1,901	1,133	1,901	
90	1		4,780						5,927	6,221	8,895	5,818	
91	1		2,050										
93	1		5,030						8,120	8,954	8,309	7,868	
100	1		1,140	637	635	840	843	840	589	777	796	777	
102	1		1,040						3,265	3,890	1,977	2,601	
113	2		3,180	945	1,587	1,915	5,058	1,915	2,914	4,871	6,384	4,871	
114	1		1,840						1,239	2,334	1,097	2,334	

Case	situ	lab	Davisson	$\alpha$ Tomlinson, Nordlund and Thurman					$\alpha$ API, Nordlund, Thurman			
#	#	#		DRIVE N	40;2B;P; T&P(1)	40;2B;P; Hara(1h)	36;11.5B; Sch;T&P( 8)	36;2B;P; Hara(5h)	40;2B;P; T&P(1)	40;2B;P; Hara(1h)	36;11.5B; Sch;T&P( 8)	36;2B;P; Hara(5h)
115	2		2,280	546	604	1,328	554	1,328	1,565	3,452	1,516	3,452
116	2		2,470	553	615	1,346	563	1,346	1,586	3,494	1,534	3,494
117	2		2,400	548	616	1,377	558	1,377	1,526	3,397	1,468	3,397
118	2		2,400	535	594	1,336	538	1,336	1,489	3,330	1,434	3,330
119	1		3,750						2,575	2,691	3,613	2,620
120	1		2,360						6,331	6,592	5,054	4,980
121	1		2,370						2,602	2,864	1,606	1,814
125	1		1,245						1,107	1,107	1,363	1,107
125	2		1,245									
126	1		4,250						5,371	5,616	6,460	5,616
126	2		4,250									
127	1		1,890	535	706	1,220	642	1,220	998	2,012	933	2,012
127	3		1,890									
128	3		1,400						2,661	2,661	2,015	2,480
129	1		890						902	1,083	873	1,019
129	2		890									
130	1		2,200						2,395	2,659	2,410	2,659
130	3		2,200									
131	1		4,250	1,585	1,574	1,867	1,964	1,867	1,769	2,226	2,158	2,226
131	2		4,250									
132	1		1,080	2,089	1,925	1,925	1,585	1,584	1,984	1,984	1,644	1,643
133	1		475	1,019	1,102	1,102	1,055	1,064	1,020	1,020	973	983
134	1		1,070	1,595	1,417	1,417	1,165	1,162	1,581	1,581	1,329	1,327
135	1		1,040	1,613	1,141	1,141	1,023	1,022	1,386	1,386	1,267	1,266
137	1		4,100	3,927	3,973	3,973	3,693	3,772	3,701	3,701	3,422	3,500
138	1		1,920						9,087	9,087	7,887	7,873
139	1		2,400						12,581	12,581	11,918	11,472
140	1		2,900						3,543	3,543	3,527	3,527
142	1		1,000						1,352	1,352	1,613	1,351
143	1		1,085	1,611	1,025	1,025	1,016	1,024	766	766	757	765
145	1		2,800						5,693	5,693	4,997	5,689
146	1		1,468						2,943	2,943	1,659	1,797
147	1		800	1,721	1,502	1,502	1,487	1,480	1,142	1,142	1,127	1,120
148	1		1,200						1,607	1,607	1,800	1,607
149	1		4,475						10,972	10,972	9,479	9,479
150	1		4,205						10,383	10,383	8,733	9,716
151	1		4,650						9,263	9,263	10,133	8,155
152	1		4,875						17,075	17,075	8,904	9,877
153	1		990	753	812	812	670	774	1,484	1,484	1,343	1,447
156	1		885	1,910	1,771	1,771	1,769	1,771	1,171	1,171	1,169	1,171
157	1		1,065	2,139	2,034	2,034	2,014	2,026	1,490	1,490	1,471	1,482
160	1		5,400						6,263	6,263	6,334	6,160
161	1		5,200						10,620	10,620	8,569	8,569
162	1		4,190						10,832	10,832	8,940	8,940
163	1		1,931	3,926	3,471	3,471	3,388	3,398	2,627	2,627	2,545	2,554

(cont.): Axial capacities (KN): Concrete Piles in Mixed soils

Case #	situ #	lab #	β; Thurman				Schmertmann	
			40;2B;P;T&P (1)	40;2B;P;Hara(1h)	36;11.5B;Sch;T&P(8)	36;2B;P;Hara(5h)	SPT mobilized	CPT
5	1		2,682	3,209	2,545	3,209	923	
6	1		4,880	5,449	4,838	5,449	1,640	
14	1		2,156	2,365	2,175	2,365	1,915	
17	1		1,530	1,530	918	918	969	
18	1		3,662	3,662	2,257	2,257	2,101	
19	1						3,204	
20	1						2,481	
21	1						2,845	
22	1		4,631	5,276	4,478	5,276	2,274	
23	1						1,137	
28	1		1,138	1,138	906	1,022	1,121	
29	1		1,480	1,782	1,445	1,782	895	
30	1		1,402	1,750	1,332	1,750	1,159	
31	1		309	309	332	309	223	
34	1						663	
36	1		6,543	7,551	6,363	7,551	2,876	
37	1		6,549	6,549	3,291	5,476	1,967	
38	1		4,478	4,478	6,763	4,478	2,509	
39	1		4,641	4,641	6,707	4,641	2,108	
40	1		4,468	4,468	6,072	4,468	3,087	
41	1		4,663	4,663	7,817	4,663	2,911	
42	1		4,479	4,479	7,539	4,479	2,952	
43	1		1,460	1,460	3,178	1,460	1,085	
44	1		3,809	4,556	3,759	4,556	1,731	
45	1		6,088	6,088	7,450	6,088	3,010	
47	1		2,695	2,695	3,102	2,695	1,876	
48	1		1,523	1,523	1,495	1,523	1,222	
49	1		1,018	1,018	1,947	1,018	784	
50	1						6,350	
51	1		1,253	1,253	1,453	1,253	1,144	
52	1		3,374	3,374	4,600	3,374	2,288	
53	1						2,617	
60	1		10,584	10,584	9,289	9,289	3,663	
62	1		5,579	6,110	5,579	6,110	4,567	
63	1		12,543	12,543	7,554	7,966	4,179	
64	1		4,146	4,146	5,096	4,146	2,228	
65	1		2,128	2,128	3,051	2,128	1,092	
67	1						668	

Case #	situ #	lab #	β; Thurman				Schmertmann	
			40;2B;P;T&P (1)	40;2B;P;Hara(1h)	36;11.5B;S ch;T&P(8)	36;2B;P;Hara(5h)	SPT mobilized	CPT
68	1		1,331	1,331	2,475	1,331	552	
69	1						807	
70	1						677	
71	1						878	
72	1						1,489	
73	1						962	
74	1		1,127	1,270	1,167	1,270	1,012	
75	1						1,921	
76	2		5,426	5,806	5,467	5,806	3,324	
77	1		6,209	6,773	6,253	6,773	3,961	
84	1		1,544	1,544	2,522	1,544	857	
85	2		4,739	4,739	2,517	2,712	1,792	
86	1	1	3,911	3,903	3,903	3,903	2,262	
87	1		7,069	7,486	7,058	7,486	3,424	
88	1		5,096	5,096	6,742	5,096	3,343	
89	1		2,011	2,105	2,013	2,105	857	
90	1		4,303	4,303	6,330	4,303	2,765	
91	1						2,359	
93	1		6,390	6,390	7,417	6,390	3,768	
100	1		630	753	623	753	810	
102	1		3,819	3,819	2,672	2,672	2,044	
113	2		4,928	4,928	8,399	4,928	1,089	
114	1		2,264	2,264	2,240	2,264	297	
115	2		3,047	3,513	2,998	3,513	667	
116	2		3,092	3,563	3,040	3,563	685	
117	2		2,929	3,456	2,871	3,456	669	
118	2		2,860	3,377	2,805	3,377	638	
119	1		2,436	2,436	2,785	2,436	1,625	
120	1		5,865	5,865	4,938	4,938	3,516	
121	1		2,913	2,913	2,003	2,003	1,608	
125	1		984	984	984	984	1,004	
125	2							1,014
126	1		4,516	4,516	4,763	4,516	2,329	
126	2							4,929
127	1		2,039	2,319	1,975	2,319	820	
127	3							1,568
128	3		1,973	1,973	1,507	1,972		1,428
129	1		512	692	503	692	879	
129	2							3,138
130	1		1,855	1,855	1,855	1,855	789	

Case #	situ #	lab #	ß; Thurman				Schmertmann	
			40;2B;P;T&P (1)	40;2B;P;Hara(1h)	36;11.5B;S ch;T&P(8)	36;2B;P;Hara(5h)	SPT mobilized	CPT
130	3							2,658
131	1		1,542	1,762	1,633	1,762	682	
131	2							2,522
132	1		1,765	1,765	1,767	1,765		1,576
133	1		1,213	1,213	1,204	1,213		909
134	1		1,481	1,481	1,484	1,481		1,237
135	1		1,585	1,585	1,586	1,585		1,106
137	1		4,343	4,343	4,265	4,343		3,372
138	1		4,523	4,523	4,538	4,523		3,495
139	1		6,853	6,853	7,298	6,853		6,612
140	1		3,765	3,765	3,765	3,765		2,304
142	1		1,447	1,447	1,709	1,447		982
143	1		974	974	965	974		544
145	1		6,627	6,627	5,935	6,627		4,758
146	1		3,102	3,102	1,896	2,033		1,165
147	1		1,527	1,527	1,534	1,527		1,238
148	1		1,716	1,716	1,909	1,716		1,651
149	1		7,027	7,027	6,548	6,548		5,150
150	1		7,695	7,695	6,712	7,695		5,439
151	1		5,385	5,385	7,363	5,385		6,084
152	1		16,852	16,852	9,382	10,355		7,515
153	1		1,704	1,704	1,600	1,704		1,259
156	1		1,548	1,548	1,546	1,548		936
157	1		2,108	2,108	2,097	2,108		1,111
160	1		6,972	6,972	7,146	6,972		7,514
161	1		10,616	10,616	9,224	9,224		5,941
162	1		10,008	10,008	8,688	8,688		6,423
163	1		3,344	3,344	3,334	3,344		1,638

## D. BIAS FACTORS--CONCRETE PILES

Table 28: Bias factor: Concrete Piles in Cohesionless soils

Case #	situ ID#	lab ID#	Nordlund								
			DRIVEN	40;2B;P (1)	40;11.5B; P (2)	40;2B;Sc h (3)	40;11.5B; Sch (4)	36;2B;P (5)	36;11.5B; P (6)	36;2B;Sc h (7)	36;11.5B; Sch (8)
1	1		0.80	0.80	0.62	0.41	0.47	1.07	0.93	0.81	0.84
2	1		0.35	0.35	0.67	0.29	0.30	0.64	0.79	0.62	0.62
3	1		1.18	1.18	1.47	1.10	1.10	2.38	2.54	2.26	2.26
4	1		0.79	0.79	0.79	0.79	0.79	1.64	1.64	1.64	1.64
7	1		0.48	0.48	0.61	0.45	0.46	0.90	0.93	0.88	0.88
8	1		0.87	0.87	0.96	0.85	0.85	1.75	1.75	1.75	1.75
9	1		0.56	0.56	0.56	0.55	0.55	1.14	1.14	1.14	1.14
10	1		1.11	1.12	1.11	0.99	0.82	1.12	1.11	1.16	0.93
11	1		1.08	1.08	1.08	0.71	0.81	1.08	1.08	0.80	0.93
12	1		0.94	0.94	0.97	0.42	0.47	0.97	1.01	0.63	0.65
13	1		1.66	1.66	1.66	1.15	1.51	1.68	1.68	1.40	1.97
16	1		0.98	0.98	0.98	0.97	0.97	2.01	2.01	2.00	2.00
24	1		0.33	0.33	0.35	0.29	0.29	0.61	0.61	0.58	0.58
25	1		0.97	0.97	0.94	0.49	0.53	1.09	1.06	0.78	0.83
26	1		1.14	1.14	1.61	0.75	1.51	1.42	1.95	1.61	2.52
27	1		0.32	0.32	0.35	0.29	0.29	0.60	0.60	0.57	0.57
32	1		0.59	0.59	0.91	0.51	0.55	1.09	1.28	0.99	0.99
33	1		0.75	0.75	0.69	0.32	0.32	0.80	0.75	0.64	0.64
35	1		0.55	0.55	0.55	0.32	0.35	0.64	0.72	0.63	0.65
46	1		0.27	0.27	0.60	0.22	0.35	0.45	0.69	0.40	0.57
56	1		0.42	0.42	0.42	0.34	0.34	0.42	0.42	0.37	0.37
57	1		0.49	0.49	0.48	0.38	0.36	0.49	0.48	0.42	0.40

Case #	situ ID#	lab ID#	Nordlund								
			DRIVEN	40;2B;P (1)	40;11.5B; P (2)	40;2B;Sc h (3)	40;11.5B; Sch (4)	36;2B;P (5)	36;11.5B; P (6)	36;2B;Sc h (7)	36;11.5B; Sch (8)
58	2		0.35	0.35	0.65	0.25	0.39	0.53	0.77	0.49	0.62
59	1		0.29	0.29	0.59	0.28	0.58	0.56	0.92	0.57	1.11
61	1		0.43	0.43	0.42	0.23	0.26	0.48	0.48	0.31	0.35
66	1		1.35	1.35	1.52	0.47	0.64	1.41	1.59	0.82	0.87
83	1		0.43	0.43	0.43	0.41	0.41	0.82	0.82	0.78	0.78
94	3		0.45	0.45	0.55	0.36	0.38	0.76	0.79	0.65	0.65
95	1		0.17	0.17	0.16	0.08	0.08	0.19	0.20	0.16	0.16
96	2		0.64	0.64	0.73	0.56	0.60	1.20	1.21	1.04	1.04
97	1		0.13	0.13	0.18	0.10	0.10	0.22	0.23	0.18	0.18
98	1		0.47	0.47	0.45	0.19	0.19	0.48	0.47	0.35	0.35
101	1		1.96	1.96	1.93	0.58	0.59	1.96	1.93	1.03	1.03
103	1		0.70	0.70	0.99	0.60	0.66	1.35	1.61	1.13	1.13
122	1		0.91	0.91	1.10	0.64	0.70	1.41	1.42	1.36	1.36
123	1		0.51	0.52	0.51	0.35	0.35	0.71	0.71	0.68	0.68
123	3										
124	1		0.73	0.73	0.64	0.32	0.38	0.87	0.84	0.63	0.64
124	2										
N			37	37	37	37	37	37	37	37	37
Bias mean			0.71	0.71	0.79	0.49	0.55	1.00	1.06	0.87	0.94
STD deviation			0.41	0.41	0.42	0.27	0.33	0.53	0.55	0.50	0.57
COV			0.58	0.58	0.53	0.56	0.60	0.53	0.52	0.57	0.60



(cont.): Bias factor: Concrete Piles in Cohesionless soils

Case #	situ ID#	lab ID#	$\beta$		Meyerhof	Schmertmann		Predominant side resistance
			40;2B;P (1)	36;2B;P (5)		SPT mobilized	CPT	
1	1		1.11	1.11	0.96	0.75		
2	1		0.36	0.66	0.15	0.48		
3	1		1.25	2.42	0.40	1.54		
4	1		0.87	1.68	0.19	0.68		
7	1		0.55	0.95	0.32	0.80		
8	1		0.97	1.83	0.23	0.90		
9	1		0.63	1.18	0.19	0.58		
10	1		1.45	1.45	0.88	2.34		Y
11	1		1.43	1.43	0.78	2.05		
12	1		0.95	0.95	0.70	1.27		Y
13	1		2.56	2.56	1.43	2.06		Y
16	1		1.10	2.06	0.27	0.90		
24	1		0.43	0.79	0.26	0.77		
25	1		1.40	1.40	0.65	1.36		
26	1		1.39	1.68	0.94	1.69		
27	1		0.42	0.78	0.20	0.86		
32	1		0.62	1.12	1.37	0.93		
33	1		1.09	1.09	0.53	1.08		
35	1		0.81	0.81	0.50	0.83		
46	1		0.31	0.55	0.29	0.70		
56	1		0.60	0.60	1.17	1.42		Y
57	1		0.69	0.69	1.17	1.68		
58	2		0.43	0.65	0.56	1.52		
59	1		0.33	0.67	0.82	1.89		
61	1		0.70	0.70	0.50	1.16		
66	1		1.51	1.51	0.59	1.52		
83	1		0.52	0.91	0.23	0.78		
94	3		0.59	1.01	0.52	1.09		

Case #	situ ID#	lab ID#	$\beta$		Meyerhof	Schmertmann		Predominant side resistance
			40;2B;P (1)	36;2B;P (5)		SPT mobilized	CPT	
95	1		0.22	0.25	0.13	0.37		
96	2		0.85	1.53	1.12	2.43		
97	1		0.16	0.29	0.13	0.35		
98	1		0.66	0.66	0.59	0.96		
101	1		2.11	2.11	1.04	1.63		
103	1		0.82	1.62	0.98	2.79		
122	1		1.01	1.50	1.82	2.32		
123	1		0.73	0.92	0.48	0.88		
123	3						0.78	
124	1		1.19	1.19	0.61	0.94		
124	2						0.44	
N			37	37	37	37	2	
Bias mean			0.89	1.17	0.64	1.25	0.61	
STD deviation			0.51	0.56	0.42	0.62		
COV			0.58	0.48	0.65	0.49		

Table 29. Bias factor: Concrete Piles in Cohesive soils

Case #	situ ID#	lab ID#	$\alpha$ API revised					$\alpha$ Tomlinson				
			APIL E	2B; T&P (1)	11.5B; T&P (2)	2B; Hara (5h)	11.5B; Hara (6h)	DRIVEN	2B; T&P (1)	11.5B; T&P (2)	2B; Hara (5h)	11.5B; Hara (6h)
54	1		2.95	3.06	3.09	1.57	1.66	6.95	3.73	3.78	2.18	2.35
78	1	1	0.82	0.79	0.89	0.77	0.87	1.51	1.35	1.67	1.35	1.67
80	1	1	0.57	0.65	0.60	0.52	0.46	0.24	0.45	0.43	0.40	0.36
81		1	0.86	0.86	0.86	0.86	0.86	0.28	0.77	0.77	0.77	0.77
82	1	1	0.85	0.84	0.87	0.64	0.69	0.25	0.73	0.76	0.64	0.68
99	2		3.3	3.08	3.33	1.58	1.70	2.41	2.40	2.56	1.65	1.77
105		1	0.91	0.94	1.03	0.94	1.03	0.98	0.92	1.01	0.92	1.01
106		1	0.87	0.87	0.91	0.87	0.91	2.38	1.64	1.80	1.64	1.80
108		1	0.83	0.84	0.86	0.84	0.86	0.89	0.85	0.86	0.85	0.86
109		1	0.52	0.55	0.55	0.55	0.55	0.52	0.59	0.59	0.59	0.59
110		1	0.74	0.73	0.73	0.73	0.73	0.72	0.89	0.89	0.89	0.89
111		1	1.17	1.26	1.21	1.26	1.21	0.73	1.47	1.41	1.47	1.41
112		1	0.76	0.80	0.80	0.80	0.80	0.45	0.52	0.52	0.52	0.52
136	1		0.79	1.21	1.21	1.21	1.21	0.65	1.08	1.08	1.08	1.08
144	1											
144	2	1	0.88	0.92	0.97	0.75	0.84	0.63	1.07	1.14	0.86	0.96
154	1		0.83	0.92	0.92	0.92	0.92	0.48	0.57	0.57	0.57	0.57
155	1		0.81	0.94	0.94	0.94	0.94	0.54	0.63	0.63	0.63	0.63
158	1		0.51	0.61	0.61	0.61	0.61	0.27	0.38	0.38	0.38	0.38
159	1		0.53	0.57	0.57	0.57	0.57	0.32	0.40	0.39	0.40	0.39
N			19	19	19	19	19	19	19	19	19	19
Bias mean			1.03	1.08	1.10	0.89	0.92	1.12	1.08	1.12	0.94	0.98
Standard deviation			0.76	0.73	0.77	0.31	0.34	1.55	0.82	0.85	0.50	0.57
COV			0.74	0.68	0.70	0.35	0.37	1.39	0.76	0.76	0.54	0.57

(cont.). Bias factor: Concrete Piles in Cohesive soils

Case #	situ ID#	lab ID#	$\beta$				$\lambda$				Schmertmann	
			2B; T&P (1)	11.5B; T&P (2)	2B; Hara (5h)	11.5B; Hara (6h)	2B; T&P (1)	11.5B; T&P (2)	2B; Hara (5h)	(6h)	SPT mobilized	CPT
54	1		1.83	1.84	1.38	1.45	2.41	2.43	1.35	1.41	5.47	
78	1	1					0.57	0.62	0.55	0.60		
80	1	1					0.69	0.63	0.55	0.48		
81		1					0.83	0.83	0.83	0.83		
82	1	1					0.76	0.79	0.59	0.63		
99	2		1.88	1.97	1.50	1.60	1.99	2.09	0.97	1.01	2.51	
105		1					0.59	0.63	0.59	0.63		
106		1					0.61	0.63	0.61	0.63		
108		1					0.59	0.59	0.59	0.59		
109		1					0.36	0.36	0.36	0.36		
110		1					0.95	0.95	0.95	0.95		
111		1					1.01	0.98	1.01	0.98		
112		1					0.73	0.73	0.73	0.73		
136	1		0.84	0.84	0.84	0.84	1.24	1.23	1.24	1.23		0.91
144	1		0.63	0.63	0.63	0.63						0.81
144	2	1					0.88	0.93	0.73	0.81		
154	1		0.66	0.66	0.66	0.66	0.95	0.95	0.95	0.95		0.98
155	1		0.67	0.67	0.67	0.67	0.99	0.99	0.99	0.99		0.94
158	1		0.43	0.43	0.43	0.43	0.67	0.67	0.67	0.67		0.76
159	1		0.41	0.41	0.41	0.41	0.75	0.74	0.75	0.74		0.77
N			8	8	8	8	19	19	19	19	2	6
Bias mean			0.92	0.93	0.81	0.84	0.92	0.93	0.79	0.80	3.99	0.86
Standard deviation			0.60	0.62	0.41	0.45	0.50	0.51	0.25	0.26		0.09
COV			0.65	0.66	0.50	0.54	0.54	0.54	0.32	0.32		0.11

Table 30: Bias factor: Concrete Piles in Mixed soils

Case #	situ #	lab #	$\alpha$ Tomlinson, Nordlund and Thurman					$\alpha$ API, Nordlund, Thurman			
			DRIVE N	40;2B;P; T&P(1)	40;2B;P; Hara(1h)	36;11.5B;S ch;T&P(8)	36;2B;P; Hara(5h)	40;2B;P; T&P(1)	40;2B;P; Hara(1h)	36;11.5B;S ch;T&P(8)	36;2B;P; Hara(5h)
5	1		2.19	1.71	0.97	1.79	0.97	1.95	1.11	2.04	1.11
6	1		1.57	1.57	1.12	1.79	1.12	1.09	0.72	1.19	0.72
14	1		0.52	0.54	0.46	0.49	0.50	0.55	0.50	0.51	0.55
17	1							0.78	0.69	1.46	1.17
18	1							0.21	0.21	0.40	0.39
19	1										
20	1										
21	1										
22	1		2.94	1.80	1.17	1.92	1.17	1.41	0.95	1.48	0.95
23	1										
28	1							1.30	1.25	1.80	1.56
29	1		1.36	0.82	0.46	0.84	0.46	1.10	0.63	1.13	0.63
30	1		0.63	0.69	0.45	0.67	0.45	0.90	0.64	0.87	0.64
31	1							1.28	1.21	1.15	1.22
34	1										
36	1		0.77	0.82	0.53	0.82	0.53	1.41	0.99	1.42	0.99
37	1							0.74	0.72	1.38	0.85
38	1							1.07	1.01	0.61	1.01
39	1							1.13	1.08	0.73	1.08
40	1							0.44	0.42	0.28	0.43
41	1							0.60	0.58	0.35	0.58
42	1							0.95	0.91	0.56	0.92
43	1							3.51	3.33	1.51	3.33
44	1		2.18	2.12	1.35	1.76	1.35	2.09	1.32	1.74	1.32
45	1							0.38	0.38	0.26	0.38
47	1							0.59	0.55	0.51	0.62
48	1							0.90	0.84	0.84	0.90
49	1							3.02	2.56	1.27	2.56
50	1										
51	1							1.61	1.53	1.24	1.53
52	1							0.90	0.84	0.62	0.88
53	1										
60	1							0.40	0.37	0.46	0.42
62	1		0.42	0.42	0.39	0.47	0.51	0.42	0.40	0.47	0.52
63	1							0.31	0.31	0.41	0.47
64	1							0.79	0.76	0.60	0.76
65	1							1.19	1.12	0.84	1.15
67	1										

Case #	situ #	lab #	$\alpha$ Tomlinson, Nordlund and Thurman					$\alpha$ API, Nordlund, Thurman			
			DRIVE N	40;2B;P; T&P(1)	40;2B;P; Hara(1h)	36;11.5B;S ch;T&P(8)	36;2B;P; Hara(5h)	40;2B;P; T&P(1)	40;2B;P; Hara(1h)	36;11.5B;S ch;T&P(8)	36;2B;P; Hara(5h)
68	1							2.13	1.51	0.87	1.51
69	1										
70	1										
71	1										
72	1										
73	1										
74	1		0.68	0.69	0.51	0.60	0.51	0.92	0.75	0.77	0.75
75	1										
76	2		0.68	0.77	0.47	0.72	0.47	1.11	0.76	1.02	0.76
77	1		1.36	1.25	0.75	1.19	0.75	1.98	1.34	1.85	1.35
84	1							1.59	1.32	0.82	1.32
85	2							0.74	0.73	1.34	1.26
86	1	1	2.47	2.01	1.28	2.04	1.28	1.98	1.27	2.01	1.27
87	1		0.79	0.61	0.35	0.61	0.35	0.59	0.35	0.59	0.35
88	1							0.83	0.75	0.64	0.85
89	1		1.65	1.64	1.07	1.65	1.07	1.41	0.84	1.41	0.84
90	1							0.81	0.77	0.54	0.82
91	1										
93	1							0.62	0.56	0.61	0.64
100	1		1.79	1.79	1.36	1.35	1.36	1.94	1.47	1.43	1.47
102	1							0.32	0.27	0.53	0.40
113	2		3.37	2.00	1.66	0.63	1.66	1.09	0.65	0.50	0.65
114	1							1.49	0.79	1.68	0.79
115	2		4.18	3.78	1.72	4.11	1.72	1.46	0.66	1.50	0.66
116	2		4.47	4.02	1.84	4.39	1.84	1.56	0.71	1.61	0.71
117	2		4.38	3.89	1.74	4.30	1.74	1.57	0.71	1.63	0.71
118	2		4.49	4.04	1.80	4.46	1.80	1.61	0.72	1.67	0.72
119	1							1.46	1.39	1.04	1.43
120	1							0.37	0.36	0.47	0.47
121	1							0.91	0.83	1.48	1.31
125	1							1.12	1.12	0.91	1.12
125	2										
126	1							0.79	0.76	0.66	0.76
126	2										
127	1		3.53	2.68	1.55	2.95	1.55	1.89	0.94	2.03	0.94
127	3										
128	3							0.53	0.53	0.69	0.56
129	1							0.99	0.82	1.02	0.87
129	2										
130	1							0.92	0.83	0.91	0.83

Case	situ	lab	$\alpha$ Tomlinson, Nordlund and Thurman					$\alpha$ API, Nordlund, Thurman			
#	#	#	DRIVE N	40;2B;P; T&P(1)	40;2B;P; Hara(1h)	36;11.5B;S ch;T&P(8)	36;2B;P; Hara(5h)	40;2B;P; T&P(1)	40;2B;P; Hara(1h)	36;11.5B;S ch;T&P(8)	36;2B;P; Hara(5h)
130	3										
131	1		2.68	2.70	2.28	2.16	2.28	2.40	1.91	1.97	1.91
131	2										
132	1		0.52	0.56	0.56	0.68	0.68	0.54	0.54	0.66	0.66
133	1		0.47	0.43	0.43	0.45	0.45	0.47	0.47	0.49	0.48
134	1		0.67	0.76	0.76	0.92	0.92	0.68	0.68	0.81	0.81
135	1		0.64	0.91	0.91	1.02	1.02	0.75	0.75	0.82	0.82
137	1		1.04	1.03	1.03	1.11	1.09	1.11	1.11	1.20	1.17
138	1							0.21	0.21	0.24	0.24
139	1							0.19	0.19	0.20	0.21
140	1							0.82	0.82	0.82	0.82
142	1							0.74	0.74	0.62	0.74
143	1		0.67	1.06	1.06	1.07	1.06	1.42	1.42	1.43	1.42
145	1							0.49	0.49	0.56	0.49
146	1							0.50	0.50	0.88	0.82
147	1		0.46	0.53	0.53	0.54	0.54	0.70	0.70	0.71	0.71
148	1							0.75	0.75	0.67	0.75
149	1							0.41	0.41	0.47	0.47
150	1							0.41	0.41	0.48	0.43
151	1							0.50	0.50	0.46	0.57
152	1							0.29	0.29	0.55	0.49
153	1		1.31	1.22	1.22	1.48	1.28	0.67	0.67	0.74	0.68
156	1		0.46	0.50	0.50	0.50	0.50	0.76	0.76	0.76	0.76
157	1		0.50	0.52	0.52	0.53	0.53	0.71	0.71	0.72	0.72
160	1							0.86	0.86	0.85	0.88
161	1							0.49	0.49	0.61	0.61
162	1							0.39	0.39	0.47	0.47
163	1		0.49	0.56	0.56	0.57	0.57	0.74	0.74	0.76	0.76
N			34	34	34	34	34	85	85	85	85
Bias mean			1.66	1.48	0.98	1.49	1.00	1.01	0.82	0.93	0.88
Standard deviation			1.34	1.11	0.53	1.21	0.52	0.62	0.48	0.48	0.47
COV			0.81	0.75	0.54	0.81	0.52	0.62	0.59	0.52	0.54

(cont.): Bias factor: Concrete Piles in Mixed soils

Case #	situ #	lab #	$\beta$ ; Thurman				Schmertmann		Predominant side resistance
			40;2B;P;T&P (1)	40;2B;P;Hara(1h)	36;11.5B;Sc h;T&P(8)	36;2B;P;Hara(5h)	SPT mobilized	CPT	
5	1		1.23	1.03	1.30	1.03	3.58		
6	1		0.70	0.62	0.70	0.62	2.07		
14	1		0.78	0.71	0.78	0.71	0.88		Y
17	1		0.73	0.73	1.22	1.22	1.16		
18	1		0.28	0.28	0.46	0.46	0.49		
19	1						1.05		
20	1						0.99		
21	1						1.51		
22	1		0.92	0.81	0.95	0.81	1.88		
23	1						2.35		
28	1		1.69	1.69	2.12	1.88	1.71		
29	1		0.73	0.60	0.74	0.60	1.20		Y
30	1		0.83	0.66	0.87	0.66	1.00		Y
31	1		1.24	1.24	1.15	1.24	1.71		
34	1						2.68		
36	1		0.98	0.85	1.01	0.85	2.23		
37	1		0.83	0.83	1.65	0.99	2.76		
38	1		1.40	1.40	0.93	1.40	2.49		Y
39	1		1.42	1.42	0.98	1.42	3.13		
40	1		0.63	0.63	0.46	0.63	0.91		
41	1		0.86	0.86	0.51	0.86	1.38		
42	1		1.43	1.43	0.85	1.43	2.17		
43	1		3.87	3.87	1.78	3.87	5.21		
44	1		1.60	1.34	1.62	1.34	3.52		
45	1		0.55	0.55	0.45	0.55	1.10		
47	1		0.67	0.67	0.58	0.67	0.96		
48	1		1.07	1.07	1.09	1.07	1.34		Y
49	1		2.82	2.82	1.47	2.82	3.66		
50	1						0.50		
51	1		1.69	1.69	1.46	1.69	1.85		
52	1		1.01	1.01	0.74	1.01	1.49		Y
53	1						1.83		
60	1		0.41	0.41	0.47	0.47	1.19		
62	1		0.88	0.80	0.88	0.80	1.07		Y
63	1		0.39	0.39	0.64	0.61	1.16		
64	1		1.01	1.01	0.82	1.01	1.89		
65	1		1.44	1.44	1.01	1.44	2.81		
67	1						1.85		



Case #	situ #	lab #	β; Thurman				Schmertmann		Predominant side resistance
			40;2B;P;T&P (1)	40;2B;P;Hara(1h)	36;11.5B;Sc h:T&P(8)	36;2B;P;Hara(5h)	SPT mobilized	CPT	
68	1		1.65	1.65	0.89	1.65	3.99		
69	1						1.52		
70	1						0.76		
71	1						1.83		
72	1						1.40		
73	1						1.09		
74	1		0.79	0.70	0.76	0.70	0.88		
75	1						1.37		
76	2		0.62	0.58	0.61	0.58	1.01		Y
77	1		1.16	1.06	1.15	1.06	1.82		Y
84	1		1.39	1.39	0.85	1.39	2.51		
85	2		0.88	0.88	1.65	1.53	2.32		
86	1	1	0.92	0.92	0.92	0.92	1.59		Y
87	1		0.31	0.29	0.31	0.29	0.63		Y
88	1		0.92	0.92	0.70	0.92	1.41		
89	1		0.80	0.76	0.79	0.76	1.87		Y
90	1		1.11	1.11	0.76	1.11	1.73		
91	1						0.87		
93	1		0.79	0.79	0.68	0.79	1.33		Y
100	1		1.81	1.51	1.83	1.51	1.41		Y
102	1		0.27	0.27	0.39	0.39	0.51		
113	2		0.65	0.65	0.38	0.65	2.92		
114	1		0.81	0.81	0.82	0.81	6.20		
115	2		0.75	0.65	0.76	0.65	3.42		
116	2		0.80	0.69	0.81	0.69	3.61		
117	2		0.82	0.69	0.84	0.69	3.59		
118	2		0.84	0.71	0.86	0.71	3.76		Y
119	1		1.54	1.54	1.35	1.54	2.31		
120	1		0.40	0.40	0.48	0.48	0.67		
121	1		0.81	0.81	1.18	1.18	1.47		
125	1		1.27	1.27	1.27	1.27	1.24		Y
125	2							1.23	Y
126	1		0.94	0.94	0.89	0.94	1.83		
126	2							0.86	
127	1		0.93	0.81	0.96	0.81	2.30		
127	3							1.21	
128	3		0.71	0.71	0.93	0.71		0.98	
129	1		1.74	1.29	1.77	1.29	1.01		
129	2							0.28	
130	1		1.19	1.19	1.19	1.19	2.79		Y

Case #	situ #	lab #	$\beta$ ; Thurman				Schmertmann		Predominant side resistance
			40;2B;P;T&P (1)	40;2B;P;Hara(1h)	36;11.5B;Sc h;T&P(8)	36;2B;P;Hara(5h)	SPT mobilized	CPT	
130	3							0.83	Y
131	1		2.76	2.41	2.60	2.41	6.24		
131	2							1.69	
132	1		0.61	0.61	0.61	0.61		0.69	Y
133	1		0.39	0.39	0.39	0.39		0.52	Y
134	1		0.72	0.72	0.72	0.72		0.86	Y
135	1		0.66	0.66	0.66	0.66		0.94	Y
137	1		0.94	0.94	0.96	0.94		1.22	Y
138	1		0.42	0.42	0.42	0.42		0.55	Y
139	1		0.35	0.35	0.33	0.35		0.36	Y
140	1		0.77	0.77	0.77	0.77		1.26	Y
142	1		0.69	0.69	0.59	0.69		1.02	Y
143	1		1.11	1.11	1.12	1.11		2.00	Y
145	1		0.42	0.42	0.47	0.42		0.59	Y
146	1		0.47	0.47	0.77	0.72		1.26	
147	1		0.52	0.52	0.52	0.52		0.65	Y
148	1		0.70	0.70	0.63	0.70		0.73	Y
149	1		0.64	0.64	0.68	0.68		0.87	Y
150	1		0.55	0.55	0.63	0.55		0.77	Y
151	1		0.86	0.86	0.63	0.86		0.76	
152	1		0.29	0.29	0.52	0.47		0.65	Y
153	1		0.58	0.58	0.62	0.58		0.79	Y
156	1		0.57	0.57	0.57	0.57		0.95	Y
157	1		0.51	0.51	0.51	0.51		0.96	Y
160	1		0.77	0.77	0.76	0.77		0.72	Y
161	1		0.49	0.49	0.56	0.56		0.88	Y
162	1		0.42	0.42	0.48	0.48		0.65	Y
163	1		0.58	0.58	0.58	0.58		1.18	Y
N			85	85	85	85	74	32	
Bias mean			0.94	0.90	0.88	0.93	1.97	0.90	
Standard deviation			0.57	0.55	0.43	0.55	1.20	0.35	
COV			0.61	0.61	0.48	0.59	0.61	0.39	

## E. SUB-CATEGORY OF PIPE PILES

Table 31. Total Cases of Static Load Tests on Pipe Piles in Soils

	S <sup>1</sup>	ST <sup>2</sup>	Total Number of Cases	
Cohesionless soils	1	19	20	
Cohesive soils	12	8	20	
Mixed soils	12	22	34	
Sub total for Soils			<b>74</b>	
Mixed soils and Rocks	<b>0</b>	<b>3</b>	<b>3</b>	
TOTAL	<b>25</b>	<b>52</b>	<b>77</b>	
NA <sup>3</sup>			<b>1</b>	<b>78</b>

<sup>1</sup> S: Predominant side resistance (Friction piles)

<sup>2</sup> ST: Side and tip resistance

<sup>3</sup> NA: Soil type is unknown/ or lack information to predict capacities

Table 32. The Data for Side Resistance (S) Pipe Piles

Soil Type	SPT	CPT	Lab	Overlap SPT, CPT & Lab	Total	OCR and Dr correlated from in-situ
cohesionless soils	1	0	0	0	<b>1</b>	1
cohesive soils	9	0	3	0	<b>12</b>	9
mixed soils	12	0	0	0	<b>12</b>	12
Mixed soils and Rocks	0	0	0	0	<b>0</b>	0
Total	<b>22</b>	<b>0</b>	<b>3</b>	<b>0</b>	<b>25</b>	22

Table 33. The Data for Side and Tip Resistance (ST) Pipe Piles

Soil Type	SPT	CPT	Lab	Overlap SPT, CPT & Lab	Total	OCR and Dr correlated from in-situ
cohesionless soils	19	0	0	0	<b>19</b>	19
cohesive soils	4	0	4	0	<b>8</b>	4
mixed soils	19	0	3	0	<b>22</b>	19
Mixed soils and Rocks	<b>3</b>	<b>0</b>	<b>0</b>	<b>0</b>	<b>3</b>	0
Total	<b>45</b>	<b>0</b>	<b>7</b>	<b>0</b>	<b>52</b>	42

Table 34. The Data for All Pipe Piles

Soil Type	SPT	CPT	Lab	Overlap SPT, CPT & Lab	Total	OCR and Dr correlated from in-situ
cohesionless soils	20	0	0	0	<b>20</b>	20
cohesive soils	13	0	7	0	<b>20</b>	13
mixed soils	31	0	3	0	<b>34</b>	31
Sub total of Soils	<b>64</b>	<b>0</b>	<b>10</b>	<b>0</b>	<b>64</b>	<b>64</b>
Mixed soils and Rocks	3	-	-	-	<b>3</b>	-
Total	<b>67</b>				<b>77</b>	

### E.1. Side Resistance Only

**TABLE 35. COHESIVE SOILS: Summary of Populations by Analysis Method used to Obtain *Side Resistance Only for Pipe Piles***

	Analysis Method				
	$\alpha$ API	$\alpha$ Tomlinson	$\lambda$	Schmertmann SPT	$\beta$
Number of cases	12	12	12	9	9

**TABLE 36. MIXED SOILS: Summary of Populations by Analysis Method used to Obtain *Side Resistance Only for Pipe Piles***

Soil Type	Analysis Method			
cohesionless	Nordlund	Nordlund	$\beta$	Schmertmann SPT
cohesive	$\alpha$ API	$\alpha$ Tomlinson	$\beta$	Schmertmann SPT
Number of cases	12	5	12	12

**NOTE 1: COHESIONLESS SOILS: Population is 1 for Nordlund,  $\beta$  and Schmertmann SPT methods (Not enough for statistical analysis)**

**TABLE 37. ALL SOILS: Summary of Populations by Analysis Method used to Obtain *Side Resistance Only for Pipe Piles***

Soil Type	Analysis Method			
cohesionless	Nordlund	Nordlund	$\beta$	Schmertmann SPT
cohesive	$\alpha$ API	$\alpha$ Tomlinson	$\beta$	Schmertmann SPT
Number of cases	25	18	22	22

Note 2: Numbers are referred from Tables 38, 39 and the constraints in Table 4.

## E.2. Total Capacity

**TABLE 38. COHESIONLESS SOILS: Summary of Populations by Analysis Method used to Obtain *Total Capacity for Pipe Piles***

Capacity	Analysis Method			
Side	Nordlund	$\beta$	Meyerhof	Schmertmann SPT
Tip	Thurman	Thurman	Meyerhof	Schmertmann SPT
Number of cases	20	20	20	20

**TABLE 39. COHESIVE SOILS: Summary of Populations by Analysis Method used to Obtain *Total Capacity for Pipe Piles***

Capacity	Analysis Method				
Side	$\alpha$ API	$\alpha$ Tomlinson	$\lambda$	$\beta$	Schmertmann SPT
Tip	9 Su	9 Su	9 Su	9 Su	Schmertmann SPT
Number of cases	20	20	20	13	13

**TABLE 40. MIXED SOILS: Summary of Populations by Analysis Method used to Obtain *Total Capacity for Pipe Piles***

Capacity	Soil type	Analysis Method					
Side	cohesionless	Nordlund		Nordlund		$\beta$	
	cohesive	$\alpha$ API		$\alpha$ Tomlinson		$\beta$	
Tip	cohesionless	Thurman		Thurman		Thurman	
	cohesive		9 Su		9 Su		9 Su
Number of cases		19	15	0	13	19	12
		34		13		31	

TABLE 41. MIXED SOILS and ROCKS: Summary of Populations by Analysis Method used to Obtain *Total Capacity for Pipe Piles*

Capacity	Soil Type	Analysis Method	
Side	cohesionless	Schmertmann SPT	
	cohesive	Schmertmann SPT	
Tip	cohesionless	Schmertmann SPT	
	cohesive	Schmertmann SPT	
Number of cases		rock exists	no rock
		3	31
		34	

TABLE 42. ALL SOILS: Summary of Populations by Analysis Method used to Obtain *Total Capacity for Pipe Piles*

Capacity	Soil type	Analysis Method							
Side	cohesionless	Nordlund		Nordlund		$\beta$		—	Meyerhof
	cohesive	$\alpha$ API		$\alpha$ Tomlinson		$\beta$		$\lambda$	--
Tip	cohesionless	Thurman		Thurman		Thurman		--	Meyerhof
	cohesive		9 Su		9 Su		9 Su	9 Su	--
Number of cases		39	35	20	33	39	25		
		74		53		64		20	20

TABLE 43. ALL SOILS and ROCKS: Summary of Populations by Analysis Method used to Obtain *Total Capacity for Concrete Piles*

Capacity	Soil Type	Analysis Method	
Side	cohesionless	Schmertmann SPT	
	cohesive	Schmertmann SPT	
Tip	cohesionless	Schmertmann SPT	
	cohesive	Schmertmann SPT	
Number of cases		rock exists	no rock
		3	64
		67	

Note: Numbers are referred from Tables 40; 45 to 49 and the constraints in Table 4.

## F. AXIAL CAPACITIES--PIPE PILES

Table 44: Axial capacities (KN): Pipe Piles in Cohesionless soils

Case	situ	lab	Davisson	Nordlund								
#	ID#	ID#		DRIVEN	40;2B;P (1)	40;11.5B; P (2)	40;2B;Sch (3)	40;11.5B; Sch (4)	36;2B;P (5)	36;11.5B; P (6)	36;2B;Sch (7)	36;11.5B; Sch (8)
2	1		340	319	319	298	855	850	313	291	423	423
9	1		5,180	4,890	4,890	4,667	5,159	4,935	3,056	3,056	3,171	3,171
10	1		3,300	2,830	2,830	1,800	3,110	2,113	1,721	1,377	1,834	1,834
11	1		1,720	692	692	681	941	778	678	668	867	867
15	1		1,660	3,446	3,446	3,475	6,280	5,996	3,249	3,215	3,648	3,648
16	1		2,950	4,087	4,087	4,149	6,528	6,807	3,890	3,951	4,800	4,800
18	1		405	232	232	219	832	771	232	219	439	439
40	1		1,160	820	820	657	879	879	403	385	426	426
41	1		650	307	307	255	622	533	278	213	299	299
44	1		1,330	1,090	1,090	1,108	2,120	1,906	929	922	1,425	1,425
51	1		555	1,080	1,077	996	2,800	1,933	1,041	951	1,547	1,547
52	1		600	1,367	1,367	1,323	2,182	1,865	1,331	1,287	1,759	1,759
65	1		1,300	1,523	1,523	1,218	2,197	1,973	945	940	973	973
71	1		1,780	590	587	614	1,232	1,359	587	614	1,147	1,147
3	1		940	1,950	1,329	1,220	2,001	2,001	911	888	918	918
4	1		1,400	2,280	1,508	1,541	2,639	2,605	1,166	1,144	1,176	1,176
6	1		2,300	6,350	2,676	2,506	3,857	3,506	1,862	1,862	1,865	1,865
7	1		1,790	5,140	2,606	2,395	3,516	3,172	1,608	1,608	1,611	1,611
8	1		3,550	1,253	938	815	2,079	1,933	938	815	965	965
31	2		3,800	10,700	7,283	4,961	7,595	6,364	3,288	3,029	3,349	3,349



(cont.): Axial capacities (KN): Pipe Piles in Cohesionless soils

Case	situ	lab	$\beta$		Meyerhof	Schmertmann SPT mobilized
#	ID#	ID#	40;2B;P (1)	36;2B;P (5)		
2	1		418	418	727	400
9	1		5,013	3,953	2,943	1,642
10	1		3,166	2,118	2,292	1,468
11	1		873	873	851	770
15	1		3,443	3,443	2,737	1,919
16	1		4,261	4,261	2,680	2,224
18	1		344	344	577	382
40	1		850	459	4,360	461
41	1		335	307	1,354	267
44	1		1,139	1,139	1,160	802
51	1		1,283	1,283	1,083	957
52	1		1,674	1,674	1,441	1,190
65	1		1,556	1,042	1,446	479
71	1		832	832	1,021	690
3	1		1,881	1,496	1,747	1,073
4	1		2,167	1,862	2,199	1,282
6	1		5,219	4,631	3,326	2,025
7	1		4,508	3,692	3,188	1,803
8	1		1,381	1,381	1,858	860
31	2		8,918	5,156	4,745	3,071

Table 45: Axial capacities (KN): Pipe Piles in Cohesive soils

Case #	situ ID#	lab ID#	Davisson	$\alpha$ Tomlinson					$\alpha$ API revised				
				DRIVE N	2B; T&P (1)	11.5B; T&P (2)	2B; Hara (5h)	11.5B; Hara (6h)	APILE	2B; T&P (1)	11.5B; T&P (2)	2B; Hara (5h)	11.5B; Hara (6h)
19	1		160	396	309	309	315	314	180	170	170	339	339
38	1		1,100	744	787	770	1,769	1,742	730	755	738	1,339	1,311
39	1		1,800	768	938	897	1,979	1,926	884	892	851	1,529	1,476
45	1	1	240	1,690	1,486	1,452	1,713	1,626	1,079	994	960	1,251	1,164
46	1	1	1,090	2,621	2,487	2,485	2,988	2,985	112	2,129	2,126	2,689	2,686
50	1	1	400	253	340	348	375	422	285	305	313	359	406
53		2	270	387	295	270	295	270	380	310	286	310	286
54		1	610	1,520	1,484	1,506	1,484	1,506	1,200	1,181	1,203	1,181	1,203
55		1	450	696	648	664	648	664	555	542	558	542	558
56	1	0	89	150	141	117	258	209	154	174	150	330	281
57	1	2	1,125	1,830	1,807	1,808	3,119	3,122	1,795	1,803	1,805	2,724	2,727
58	1	2	1,260	2,806	2,785	2,787	4,840	4,843	2,838	2,974	2,976	4,474	4,476
59	1		622	300	330	331	410	412	228	217	218	430	431
60	1		595	1,355	1,325	1,263	1,614	1,528	996	1,047	985	1,731	1,644
61	1		420	896	773	776	923	929	567	540	543	953	958
76	1		1,700	2,126	2,035	2,035	3,207	3,207	2,420	2,442	2,442	3,530	3,530
78	1		2,700	2,532	2,507	2,507	3,931	3,931	3,106	3,148	3,148	4,505	4,505
32	2		360	944	726	738	768	787	520	474	487	870	890
34	2		360	1,017	832	832	948	950	430	426	427	835	836
37	1		140	592	506	502	1,286	1,279	492	491	487	924	917

(cont.) : Axial capacities (KN): Pipe Piles in Cohesive soils

Case #	situ ID#	lab ID#	$\beta$				$\lambda$				Schmert mann SPT mobilized
			2B; T&P (1)	11.5B; T&P (2)	2B; Hara (5h)	11.5B; Hara (6h)	2B; T&P (1)	11.5B; T&P (2)	2B; Hara (5h)	11.5B; Hara (6h)	
19	1		250	249	312	311	280	280	610	610	643
38	1		1,396	1,379	1,504	1,476	694	676	1,268	1,241	1,286
39	1		1,638	1,597	1,760	1,707	816	776	1,436	1,383	1,339
45	1	1					1,101	1,067	1,437	1,351	
46	1	1					1,875	1,873	2,434	2,432	
50	1	1					642	651	873	920	
53		2					501	476	501	476	
54		1					1,297	1,320	1,297	1,320	
55		1					849	866	849	866	
56	1	0					197	173	377	328	
57	1	2	3,866	3,868	3,949	3,952	1,480	1,482	2,288	2,291	3,239
58	1	2	6,257	6,259	6,342	6,345	2,171	2,173	3,275	3,277	5,183
59	1		381	381	438	439	367	368	753	755	844
60	1		1,847	1,784	1,971	1,885	1,087	1,025	1,844	1,758	2,601
61	1		1,005	1,008	1,074	1,080	690	694	1,273	1,279	1,733
76	1		4,862	4,862	5,034	5,034	2,732	2,732	4,088	4,088	3,243
78	1		6,633	6,633	6,805	6,805	3,178	3,178	4,685	4,685	4,027
32	2		971	983	1,040	1,059	622	635	1,216	1,236	1,569
34	2		879	880	943	944	526	527	1,091	1,093	1,695
37	1		915	911	979	971	468	464	920	912	1,179

Table 46: Axial capacities (KN): Pipe Piles in Mixed soils

Case #	situ ID#	lab ID#	Davisson	$\alpha$ API, Nordlund, Thurman				$\beta$ ; Thurman			
				40;2B;P;T&P(1)	36;2B;P (5)	36;11.5B;Sch;T&P(8)	36;2B;P;Hara(5h)	40;2B;P;T&P(1)	36;2B;P (5)	36;11.5B;Sch;T&P(8)	36;2B;P;Hara(5h)
12	2		2,120	2,145	1,976	3,101	2,271	2,131	2,131	2,972	2,131
13	1		1,640	1,509	1,338	2,034	1,633	1,500	1,500	2,143	1,500
14	1		2,100	5,093	4,924	6,191	5,219	4,854	4,854	4,854	4,854
17	2		2,720	3,163	3,123	3,365	4,665	5,566	5,566	5,566	6,087
20	1		1,070	971	955	1,663	1,052	1,198	1,198	1,662	1,198
21	1		1,400	2,068	2,050	2,640	2,147	2,413	2,413	2,539	2,413
22	3		2,220	9,578	5,049	5,508	5,333	8,499	4,737	4,737	4,737
23	1		2,500	3,755	2,798	2,860	3,536	6,458	5,853	5,853	5,853
24	2		2,400	5,985	4,295	4,328	5,535	8,186	7,125	7,125	7,125
25	2		3,030	5,955	4,275	4,309	5,515	8,159	7,098	7,098	7,098
26	1		3,050	3,013	2,830	2,993	3,792	4,719	4,719	4,719	4,860
27	1		1,680	2,391	2,182	2,244	2,961	4,677	4,677	4,677	4,758
28	2		1,700	6,539	4,654	4,688	5,894	8,679	7,617	7,617	7,617
29	2		2,900	1,827	1,779	1,793	2,704	3,819	3,819	3,820	3,819
30	1		2,700	2,429	2,216	2,279	3,005	4,757	4,757	4,757	4,838
33	1		2,205	2,083	1,559	1,619	1,718	2,447	2,004	2,004	2,004
35	3		3,200	1,036	1,036	1,060	1,682	1,902	1,902	1,902	2,029
36	3		3,200	1,045	1,045	1,069	1,694	1,920	1,920	1,920	2,047
42	1		340	1,907	1,907	2,154	2,612				
47	1	1	120	569	569	575	806				
48	1	1	660	1,806	1,806	1,890	2,453	4,575	4,575	4,575	4,705
49	1	1	140	606	606	612	916	1,526	1,526	1,526	1,630
62	1		2,050								
63	1		2,120								
64	1		1,900	3,366	2,666	2,832	2,883	4,169	3,656	3,656	3,656
66	1	0	2,300	2,680	2,482	2,571	2,946	4,048	3,997	3,997	3,997
67	1		640	1,856	952	953	1,002	1,788	1,075	1,075	1,075
68	1		1,000	2,841	1,389	1,391	1,439	2,710	1,648	1,648	1,648
69	1	1	1,120	1,105	1,105	1,735	1,281				
70	1		1,000	1,160	920	927	1,157	1,455	1,216	1,216	1,216
72	2		2,400	3,711	3,545	3,564	4,821	7,689	7,689	7,689	7,862
73	1		2,400	2,187	2,135	2,136	3,042	4,290	4,290	4,290	4,462
74	2		2,370	2,629	2,443	2,506	3,335	4,243	4,243	4,243	4,415
75	2		2,900	3,744	3,637	3,637	5,022	8,160	8,160	8,160	8,333
77	2		1,100	2,111	2,082	2,089	3,013	3,991	3,991	3,991	4,164
1	1		740	738	738	1,036	1,101	1,616	1,616	1,896	1,616
5	1		2,350								

(cont.): Axial capacities (KN): Pipe Piles in Mixed soils

Case #	situ ID#	lab ID#	$\alpha$ Tomlinson, Nordlund and Thurman					Schmertmann SPT mobilized
			DRIVEN	40;2B;P;T&P(1)	36;2B;P(5)	36;11.5B;S ch;T&P(8)	36;2B;P;H ara(5h)	
12	2							1,721
13	1							1,491
14	1							3,008
17	2		5,799	5,039	4,998	5,241	8,370	4,694
20	1							1,559
21	1							1,936
22	3							2,747
23	1							2,827
24	2							4,464
25	2							4,460
26	1		2,538	2,583	2,400	2,563	2,948	2,850
27	1		1,848	1,931	1,722	1,784	2,162	2,516
28	2							4,538
29	2							3,015
30	1		1,857	1,957	1,744	1,806	2,192	2,553
33	1							1,786
35	3							2,656
36	3							2,666
42	1		1,756	1,721	1,721	1,968	2,137	
47	1	1	899	794	794	800	1,001	
48	1	1	1,361	1,307	1,307	1,391	2,026	4,195
49	1	1	898	846	846	852	1,112	2,146
62	1							2,831
63	1							2,810
64	1							2,628
66	1	0						2,139
67	1							1,098
68	1							1,324
69	1	1						
70	1							253
72	2		3,315	3,296	3,130	3,149	4,632	4,120
73	1		2,588	2,431	2,379	2,380	3,743	2,849
74	2		2,442	2,419	2,234	2,297	2,978	3,236
75	2		3,255	3,335	3,228	3,228	4,887	4,150
77	2		2,308	2,260	2,232	2,239	3,577	2,978
1	1							1,770
5	1							2,744

## G. BIAS FACTORS--PIPE PILES

Table 47: Bias factor: Pipe Piles in Cohesionless soils

Case	situ	lab	Nordlund								
#	ID#	ID#	DRIVEN	40;2B;P (1)	40;11.5B; P (2)	40;2B;Sc h (3)	40;11.5B; Sch (4)	36;2B;P (5)	36;11.5B; P (6)	36;2B;Sc h (7)	36;11.5B; Sch (8)
2	1		1.06	1.06	1.14	0.40	0.40	1.09	1.17	0.80	0.80
9	1		1.06	1.06	1.11	1.00	1.05	1.69	1.69	1.63	1.63
10	1		1.17	1.17	1.83	1.06	1.56	1.92	2.40	1.80	1.80
11	1		2.49	2.49	2.52	1.83	2.21	2.54	2.57	1.98	1.98
15	1		0.48	0.48	0.48	0.26	0.28	0.51	0.52	0.45	0.45
16	1		0.72	0.72	0.71	0.45	0.43	0.76	0.75	0.61	0.61
18	1		1.74	1.74	1.85	0.49	0.53	1.74	1.85	0.92	0.92
40	1		1.41	1.41	1.76	1.32	1.32	2.88	3.01	2.72	2.72
41	1		2.12	2.12	2.55	1.04	1.22	2.34	3.05	2.17	2.17
44	1		1.22	1.22	1.20	0.63	0.70	1.43	1.44	0.93	0.93
51	1		0.51	0.52	0.56	0.20	0.29	0.53	0.58	0.36	0.36
52	1		0.44	0.44	0.45	0.27	0.32	0.45	0.47	0.34	0.34
65	1		0.85	0.85	1.07	0.59	0.66	1.38	1.38	1.34	1.34
71	1		3.02	3.03	2.90	1.44	1.31	3.03	2.90	1.55	1.55
3	1		0.48	0.71	0.77	0.47	0.47	1.03	1.06	1.02	1.02
4	1		0.61	0.93	0.91	0.53	0.54	1.20	1.22	1.19	1.19
6	1		0.36	0.86	0.92	0.60	0.66	1.24	1.24	1.23	1.23
7	1		0.35	0.69	0.75	0.51	0.56	1.11	1.11	1.11	1.11
8	1		2.83	3.79	4.36	1.71	1.84	3.79	4.36	3.68	3.68
31	2		0.36	0.52	0.77	0.50	0.60	1.16	1.25	1.13	1.13
N			20	20	20	20	20	20	20	20	20
Bias mean			1.16	1.29	1.43	0.77	0.85	1.59	1.70	1.35	1.35
Standard deviation			0.85	0.91	1.00	0.49	0.55	0.91	1.03	0.83	0.83
COV			0.73	0.71	0.70	0.64	0.65	0.57	0.61	0.61	0.61

(cont.): Bias factor: Pipe Piles in Cohesionless soils

Case	situ	lab	$\beta$		Meyerhof	Schmertmann SPT mobilized	Predominant side resistance
#	ID#	ID#	40;2B;P (1)	36;2B;P (5)			
2	1		0.81	0.81	0.47	0.85	
9	1		1.03	1.31	1.76	3.15	
10	1		1.04	1.56	1.44	2.25	
11	1		1.97	1.97	2.02	2.23	Y
15	1		0.48	0.48	0.61	0.87	
16	1		0.69	0.69	1.10	1.33	
18	1		1.18	1.18	0.70	1.06	
40	1		1.36	2.53	0.27	2.51	
41	1		1.94	2.11	0.48	2.44	
44	1		1.17	1.17	1.15	1.66	
51	1		0.43	0.43	0.51	0.58	
52	1		0.36	0.36	0.42	0.50	
65	1		0.84	1.25	0.90	2.72	
71	1		2.14	2.14	1.74	2.58	
3	1		0.50	0.63	0.54	0.88	
4	1		0.65	0.75	0.64	1.09	
6	1		0.44	0.50	0.69	1.14	
7	1		0.40	0.48	0.56	0.99	
8	1		2.57	2.57	1.91	4.13	
31	2		0.43	0.74	0.80	1.24	
N			20	20	20	20	
Bias mean			1.02	1.18	0.94	1.71	
Standard deviation			0.66	0.73	0.55	0.98	
COV			0.65	0.61	0.59	0.57	

Table 48: Bias factor: Pipe Piles in Cohesive soils

Case #	situ ID#	lab ID#	$\alpha$ Tomlinson					$\alpha$ API revised				
			DRIVE N	2B; T&P (1)	11.5B; T&P (2)	2B; Hara (5h)	11.5B; Hara (6h)	APILE	2B; T&P (1)	11.5B; T&P (2)	2B; Hara (5h)	11.5B; Hara (6h)
19	1		0.40	0.52	0.52	0.51	0.51	0.89	0.94	0.94	0.47	0.47
38	1		1.48	1.40	1.43	0.62	0.63	1.51	1.46	1.49	0.82	0.84
39	1		2.34	1.92	2.01	0.91	0.93	2.04	2.02	2.11	1.18	1.22
45	1	1	0.14	0.16	0.17	0.14	0.15	0.22	0.24	0.25	0.19	0.21
46	1	1	0.42	0.44	0.44	0.36	0.37	0.49	0.51	0.51	0.41	0.41
50	1	1	1.58	1.18	1.15	1.07	0.95	1.40	1.31	1.28	1.12	0.99
53		2	0.70	0.92	1.00	0.92	1.00	0.71	0.87	0.94	0.87	0.94
54		1	0.40	0.41	0.40	0.41	0.40	0.51	0.52	0.51	0.52	0.51
55		1	0.65	0.69	0.68	0.69	0.68	0.81	0.83	0.81	0.83	0.81
56	1	0	0.59	0.63	0.76	0.34	0.43	0.58	0.51	0.59	0.27	0.32
57	1	2	0.61	0.62	0.62	0.36	0.36	0.63	0.62	0.62	0.41	0.41
58	1	2	0.45	0.45	0.45	0.26	0.26	0.44	0.42	0.42	0.28	0.28
59	1		2.07	1.88	1.88	1.52	1.51	2.73	2.87	2.86	1.45	1.44
60	1		0.44	0.45	0.47	0.37	0.39	0.60	0.57	0.60	0.34	0.36
61	1		0.47	0.54	0.54	0.45	0.45	0.74	0.78	0.77	0.44	0.44
76	1		0.80	0.84	0.84	0.53	0.53	0.70	0.70	0.70	0.48	0.48
78	1		1.07	1.08	1.08	0.69	0.69	0.87	0.86	0.86	0.60	0.60
32	2		0.38	0.50	0.49	0.47	0.46	0.69	0.76	0.74	0.41	0.40
34	2		0.35	0.43	0.43	0.38	0.38	0.84	0.85	0.84	0.43	0.43
37	1		0.24	0.28	0.28	0.11	0.11	0.28	0.29	0.29	0.15	0.15
N			20	20	20	20	20	20	20	20	20	20
Bias mean			0.78	0.77	0.78	0.56	0.56	0.88	0.90	0.91	0.58	0.59
Standard deviation			0.62	0.49	0.51	0.34	0.33	0.61	0.62	0.63	0.35	0.34
COV			0.79	0.64	0.65	0.61	0.59	0.69	0.69	0.69	0.60	0.59



(cont.) : Bias factor: Pipe Piles in Cohesive soils

Case #	situ ID#	lab ID#	$\beta$				$\lambda$				Schmertmann SPT mobilized	Predominant side resistance
			2B; T&P (1)	11.5B; T&P (2)	2B; Hara (5h)	11.5B; Hara (6h)	2B; T&P (1)	11.5B; T&P (2)	2B; Hara (5h)	11.5B; Hara (6h)		
19	1		0.64	0.64	0.51	0.51	0.57	0.57	0.26	0.26	0.25	
38	1		0.79	0.80	0.73	0.75	1.59	1.63	0.87	0.89	0.86	Y
39	1		1.10	1.13	1.02	1.05	2.20	2.32	1.25	1.30	1.34	Y
45	1	1					0.22	0.22	0.17	0.18		Y
46	1	1					0.58	0.58	0.45	0.45		
50	1	1					0.62	0.61	0.46	0.43		
53		2					0.54	0.57	0.54	0.57		
54		1					0.47	0.46	0.47	0.46		Y
55		1					0.53	0.52	0.53	0.52		Y
56	1	0					0.45	0.51	0.24	0.27		
57	1	2	0.29	0.29	0.28	0.28	0.76	0.76	0.49	0.49	0.35	Y
58	1	2	0.20	0.20	0.20	0.20	0.58	0.58	0.38	0.38	0.24	Y
59	1		1.63	1.63	1.42	1.42	1.69	1.69	0.83	0.82	0.74	Y
60	1		0.32	0.33	0.30	0.32	0.55	0.58	0.32	0.34	0.23	Y
61	1		0.42	0.42	0.39	0.39	0.61	0.61	0.33	0.33	0.24	
76	1		0.35	0.35	0.34	0.34	0.62	0.62	0.42	0.42	0.52	
78	1		0.41	0.41	0.40	0.40	0.85	0.85	0.58	0.58	0.67	Y
32	2		0.37	0.37	0.35	0.34	0.58	0.57	0.30	0.29	0.23	
34	2		0.41	0.41	0.38	0.38	0.68	0.68	0.33	0.33	0.21	Y
37	1		0.15	0.15	0.14	0.14	0.30	0.30	0.15	0.15	0.12	Y
N			13	13	13	13	20	20	20	20	13	
Bias mean			0.54	0.55	0.50	0.50	0.75	0.76	0.47	0.47	0.46	
Standard deviation			0.42	0.42	0.36	0.36	0.50	0.52	0.26	0.27	0.35	
COV			0.76	0.76	0.73	0.73	0.66	0.68	0.56	0.57	0.77	

Table 49: Bias factor: Pipe Piles in Mixed soils

Case #	situ ID#	lab ID#	$\alpha$ API, Nordlund, Thurman				$\beta$ ; Thurman			
			40;2B;P;T&P(1)	36;2B;P(5)	36;11.5B;Sch;T&P(8)	36;2B;P;Hara(5h)	40;2B;P;T&P(1)	36;2B;P(5)	36;11.5B;Sch;T&P(8)	36;2B;P;Hara(5h)
12	2	1.07	0.99	1.09	0.68	0.93	1.00	1.00	0.71	1.00
13	1	1.23	1.09	0.99	0.81	1.00	1.09	1.09	0.77	1.09
14	1	0.43	0.41	0.45	0.34	0.40	0.43	0.43	0.43	0.43
17	2	0.87	0.86	0.76	0.81	0.58	0.49	0.49	0.49	0.45
20	1	1.12	1.10	1.08	0.64	1.02	0.89	0.89	0.64	0.89
21	1	0.68	0.68	0.70	0.53	0.65	0.58	0.58	0.55	0.58
22	3	0.44	0.23	0.32	0.40	0.42	0.26	0.47	0.47	0.47
23	1	0.89	0.67	0.57	0.87	0.71	0.39	0.43	0.43	0.43
24	2	0.56	0.40	0.33	0.55	0.43	0.29	0.34	0.34	0.34
25	2	0.71	0.51	0.43	0.70	0.55	0.37	0.43	0.43	0.43
26	1	1.08	1.01	0.77	1.02	0.80	0.65	0.65	0.65	0.63
27	1	0.77	0.70	0.53	0.75	0.57	0.36	0.36	0.36	0.35
28	2	0.37	0.26	0.24	0.36	0.29	0.20	0.22	0.22	0.22
29	2	1.63	1.59	1.06	1.62	1.07	0.76	0.76	0.76	0.76
30	1	1.22	1.11	0.91	1.18	0.90	0.57	0.57	0.57	0.56
33	1	1.41	1.06	1.02	1.36	1.28	0.90	1.10	1.10	1.10
35	3	3.09	3.09	2.09	3.02	1.90	1.68	1.68	1.68	1.58
36	3	3.06	3.06	2.10	2.99	1.89	1.67	1.67	1.67	1.56
42	1	0.18	0.18	0.27	0.16	0.13				
47	1	0.21	0.21	0.34	0.21	0.15				
48	1	0.37	0.37	0.50	0.35	0.27	0.14	0.14	0.14	0.14
49	1	0.23	0.23	0.35	0.23	0.15	0.09	0.09	0.09	0.09
62	1									
63	1									
64	1	0.71	0.56	0.73	0.67	0.66	0.46	0.52	0.52	0.52
66	1	0.93	0.86	0.84	0.89	0.78	0.57	0.58	0.58	0.58
67	1	0.67	0.34	0.58	0.67	0.64	0.36	0.60	0.60	0.60
68	1	0.72	0.35	0.90	0.72	0.69	0.37	0.61	0.61	0.61
69	1	1.01	1.01	1.17	0.65	0.87				
70	1	1.09	0.86	0.85	1.08	0.86	0.69	0.82	0.82	0.82
72	2	0.68	0.65	0.48	0.67	0.50	0.31	0.31	0.31	0.31
73	1	1.12	1.10	0.78	1.12	0.79	0.56	0.56	0.56	0.54
74	2	0.97	0.90	0.68	0.95	0.71	0.56	0.56	0.56	0.54
75	2	0.80	0.77	0.57	0.80	0.58	0.36	0.36	0.36	0.35
77	2	0.53	0.52	0.77	0.53	0.37	0.28	0.28	0.28	0.26
1	1	1.00	1.00	0.68	0.71	0.67	0.46	0.46	0.39	0.46
5	1									
N			34	34	34	34	31	31	31	31
Bias mean			0.85	0.94	0.85	0.71	0.57	0.61	0.58	0.60
Standard deviation			0.66	0.64	0.63	0.41	0.38	0.38	0.36	0.36
COV			0.78	0.69	0.74	0.57	0.66	0.61	0.61	0.60

(cont.): Bias factor: Pipe Piles in Mixed soils

Case #	situ ID#	lab ID#	$\alpha$ Tomlinson, Nordlund and Thurman					Schmertmann SPT mobilized	Predominant side resistance
			DRIVEN	40;2B;P;T&P(1)	36;2B;P(5)	36;11.5B;Sch;T&P(8)	36;2B;P;Hara(5h)		
12	2							1.23	
13	1							1.10	
14	1							0.70	
17	2		0.47	0.54	0.54	0.52	0.32	0.58	Y
20	1							0.69	
21	1							0.72	
22	3							0.81	
23	1							0.88	Y
24	2							0.54	Y
25	2							0.68	Y
26	1		1.20	1.18	1.27	1.19	1.03	1.07	Y
27	1		0.91	0.87	0.98	0.94	0.78	0.67	Y
28	2							0.37	Y
29	2							0.96	Y
30	1		1.45	1.38	1.55	1.49	1.23	1.06	Y
33	1							1.23	
35	3							1.20	
36	3							1.20	
42	1		0.19	0.20	0.20	0.17	0.16		
47	1	1	0.13	0.15	0.15	0.15	0.12		
48	1	1	0.48	0.50	0.50	0.47	0.33	0.16	
49	1	1	0.16	0.17	0.17	0.16	0.13	0.07	
62	1							0.72	
63	1							0.75	
64	1							0.72	
66	1	0						1.08	Y
67	1							0.58	
68	1							0.76	
69	1	1							
70	1							3.95	
72	2		0.72	0.73	0.77	0.76	0.52	0.58	
73	1		0.93	0.99	1.01	1.01	0.64	0.84	Y
74	2		0.97	0.98	1.06	1.03	0.80	0.73	
75	2		0.89	0.87	0.90	0.90	0.59	0.70	
77	2		0.48	0.49	0.49	0.49	0.31	0.37	
1	1							0.42	Y
5	1							0.86	
N			13	13	13	13	13	34	
Bias mean			0.69	0.70	0.74	0.72	0.54	0.85	
Standard deviation			0.41	0.39	0.44	0.43	0.35	0.62	
COV			0.60	0.57	0.60	0.59	0.66	0.73	

## H. AXIAL CAPACITIES--PLUGGED H PILES

Table 50: Axial capacities (KN): Plugged H piles in Cohesionless soils

ID #	situ ID#	Davisson	Nordund; $\phi$ correlated by Peck et al.			$\beta$ (W/ Tip influence zone: 2B)		Meyerhof	Schmertmann SPT mobilized
			limit $\phi \leq 40^\circ$ ; Tip influence zone: 2B (1)	limit $\phi \leq 36^\circ$ ; Tip influence zone: 2B (5)	limit $\phi \leq 36^\circ$ ; Tip influence zone: 11.5B (6)	limit $\phi \leq 40^\circ$ (1)	limit $\phi \leq 36^\circ$ ; (5)		
166	1	1,160	2,344	1,649	1,649	2,359	2,048	1,902	1,411
167	1	695	2,044	1,157	1,157	2,233	1,500	1,550	777
168	2	1,100	1,315	1,315	1,020	1,498	1,498	906	586
170	3	585	783	766	696	959	959	984	477
171	1	475	723	723	722	1,029	1,029	525	356
189	2	2,100	5,080	2,739	2,457	4,792	3,104	3,857	1,447
545	1	2,150	1,205	1,205	1,425	1,436	1,436	1,471	929
561	1	3,300	4,395	2,344	2,344	4,149	2,393	3,209	1,187
616	1	555	535	535	486	634	634	989	419
1136	1	1,250	1,569	1,538	1,489	1,983	1,983	1,100	883
1137	1	630	1,200	1,169	1,069	1,506	1,506	781	757
1171	1	1,470	1,459	918	918	1,431	955	848	673
1180	1	1,060	2,018	1,434	1,434	2,095	1,773	2,275	1,232
1182	1	1,750	4,618	3,780	3,673	5,419	4,965	2,657	2,469
1183	1	700	2,282	1,606	1,606	2,163	1,826	2,355	1,268
1185	1	2,200	5,394	4,277	4,131	5,636	4,998	2,775	2,491
3222	1	4,620	5,909	3,930	3,812	5,862	4,106	4,328	1,919
3230	1	1,080	700	698	678	811	811	1,038	565
3244	1	1,350	2,084	1,284	1,284	2,330	1,700	1,328	1,046

Table 51: Axial capacities (KN): Plugged H piles in Cohesive soils

ID #	situ ID#	lab ID#	Davisson	$\alpha$ Tomlinson		$\alpha$ API		$\beta$		$\lambda$		Schmertmann SPT mobilized
				$S_u$ correlated by Terzaghi & Peck (5)	$S_u$ correlated by Hara (5h)	$S_u$ correlated by Terzaghi & Peck (5)	$S_u$ correlated by Hara (5h)	$S_u$ correlated by Terzaghi & Peck (5)	$S_u$ correlated by Hara (5h)	$S_u$ correlated by Terzaghi & Peck (5)	$S_u$ correlated by Hara (5h)	
193	1		700	rock	rock	rock	rock	rock	rock	rock	rock	900
194	1		910									907
196	1		740									1,077
625		1	1,200	820	820	708	708			990	990	
626		1	1,200	1,362	1,362	1,093	1,093			1,285	1,285	
627		1	1,200	1,357	1,357	1,086	1,086			1,280	1,280	
628		1	1,000	1,367	1,367	1,099	1,099			1,291	1,291	
629		1	1,200	1,253	1,253	1,074	1,074			1,236	1,236	
631		1	1,600	1,527	1,527	1,308	1,308			1,459	1,459	
1015	1		1,490	1,193	2,511	1,134	1,940	2,083	2,236	1,037	1,821	452
1102		1	285	983	983	792	792			764	764	
1103		1	318	689	689	538	538			582	582	
1104		1	555	705	705	551	551			592	592	
1105		1	270	705	705	551	551			592	592	
1133	1	1	395	407	452	364	429			777	1,056	
1139		1	860	1,768	1,768	1,540	1,540			1,650	1,650	
1142		1	470	806	806	709	709			1,060	1,060	
1149	1		482	393	487	256	504	450	513	434	889	285
1150	1		440	424	530	1,221	2,021	2,171	2,307	1,268	2,156	892
1151	1		540	936	1,119	642	1,129	1,206	1,278	820	1,507	593
3233	1		1,390	rock	rock	rock	rock	rock	rock	rock	rock	1,184
3234	1		1,500									928

Table 52: Axial capacities (KN): Plugged H piles in Mixed soils

ID #	situ ID#	lab ID#	Davisson	$\alpha$ Tomlinson, Nordlund, Thurman		$\alpha$ API, Nordlund, Thurman		$\beta$ ; Thurman		Schmertmann SPT mobilized
				$\phi$ correlated by Peck et al. and limit below $36^\circ$						
				$S_u$ correlated by Terzaghi & Peck (5)	$S_u$ correlated by Hara (5h)	$S_u$ correlated by Terzaghi & Peck (5)	$S_u$ correlated by Hara (5h)	$S_u$ correlated by Terzaghi & Peck (5)	$S_u$ correlated by Hara (5h)	
150	1		1,110	1,962	2,988	1,738	2,337	3,065	3,218	1,205
151	1		1,020	1,579	2,586	1,299	1,852	2,459	2,590	1,040
152	1		920	1,541	2,505	1,229	1,734	2,269	2,406	964
153	1		1,070	1,675	2,708	1,448	2,087	2,728	2,874	1,164
154	1		960	1,700	2,738	1,477	2,112	2,751	2,897	1,117
155	1		740	1,704	2,735	1,398	1,965	2,588	2,735	1,042
156	1		940			1,819	2,412	3,333	3,333	1,499
157	1		800	1,893	2,712	1,699	2,131	2,714	2,858	1,109
158	1		540	1,592	2,337	1,425	1,835	2,292	2,418	1,121
159	1		335	1,098	1,575	1,000	1,251	1,619	1,696	728
160	1		830	1,534	2,239	1,493	1,974	2,730	2,828	1,113
161	1		600	1,479	2,531	1,229	1,828	2,502	2,618	999
162	1		680	2,166	3,317	2,210	3,008	4,104	4,263	1,619
163	1		355	1,152	2,018	779	1,192	1,503	1,620	705
164	1		680	1,428	2,235	1,140	1,537	1,940	2,067	826
165	1		1,240	1,093	1,965	838	1,368	1,685	1,807	725
177	1		2,950	1,495	2,538	1,200	1,898	2,279	2,446	1,239
179	1		2,700	1,374	2,082	1,037	1,640	1,803	1,945	1,029
182	1		2,200	3,221	4,979	2,141	3,005	4,169	4,397	1,387
184	1		2,430	2,770	4,386	1,817	2,592	3,271	3,499	1,374
190	1		1,500	rock	rock	rock	rock	rock	rock	1,366
191	1	1,100	617							
192	1	1,220	1,143							
195	1	1,450	936							
546	1		2,520	2,562	3,308	2,047	3,404	4,057	4,198	1,471
1012	3		1,850			867	1,450	1,751	1,751	999
1108	1	1	1,950			2,016	2,522			
1111	1		810	1,015	1,554	1,020	1,556	1,756	1,849	887
1122	1		1,930			3,451	3,899	4,417	4,417	1,724
1123	1		2,080			3,642	4,090	4,648	4,648	1,779
1127	1	1	1,380			2,192	2,192			2,199
1160	1		3,500			3,936	4,350	5,195	5,195	2,482
1173	1		2,750			3,087	3,791	5,107	5,107	1,786
1186	1		2,280			1,721	1,781	1,987	1,987	1,291
1189	1	1	1,100			1,632	1,774	2,269	2,269	1,139
1191	1	1	1,120			1,457	1,711	1,972	1,993	615
3227	1		3,250			5,172	5,677	6,791	6,791	2,903
3228	1		3,570			3,327	4,399	6,421	6,421	1,779
3232	1		2,605	rock	rock	rock	rock	rock	rock	1,378
3241	1		5,500			3,008	3,483	3,444	3,444	2,555
3249	1		1,400	1,860	2,997	1,577	2,300	2,745	2,925	959
3252	1		3,460			3,262	3,547	3,990	3,990	1,632

# I. BIAS FACTORS--PLUGGED H PILES

Table 53: Bias factor: Plugged H piles in Cohesionless soils

ID #	situ ID#	lab ID#	Nordund; $\phi$ correlated by Peck et al.			$\beta$ (W/ Tip influence zone: 2B)		Meyerhof	Schmertmann SPT mobilized
			limit $\phi \leq 40^\circ$ ; Tip influence zone: 2B (1)	limit $\phi \leq 36^\circ$ ; Tip influence zone: 2B (5)	limit $\phi \leq 36^\circ$ ; Tip influence zone: 11.5B (6)	limit $\phi \leq 40^\circ$ (1)	limit $\phi \leq 36^\circ$ (5)		
166	1		0.49	0.70	0.70	0.49	0.57	0.61	0.82
167	1		0.34	0.60	0.60	0.31	0.46	0.45	0.89
168	2		0.84	0.84	1.08	0.73	0.73	1.21	1.88
170	3		0.75	0.76	0.84	0.61	0.61	0.59	1.23
171	1		0.66	0.66	0.66	0.46	0.46	0.90	1.34
189	2		0.41	0.77	0.85	0.44	0.68	0.54	1.45
545	1		1.78	1.78	1.51	1.50	1.50	1.46	2.31
561	1		0.75	1.41	1.41	0.80	1.38	1.03	2.78
616	1		1.04	1.04	1.14	0.88	0.88	0.56	1.32
1136	1		0.80	0.81	0.84	0.63	0.63	1.14	1.42
1137	1		0.53	0.54	0.59	0.42	0.42	0.81	0.83
1171	1		1.01	1.60	1.60	1.03	1.54	1.73	2.18
1180	1		0.53	0.74	0.74	0.51	0.60	0.47	0.86
1182	1		0.38	0.46	0.48	0.32	0.35	0.66	0.71
1183	1		0.31	0.44	0.44	0.32	0.38	0.30	0.55
1185	1		0.41	0.51	0.53	0.39	0.44	0.79	0.88
3222	1		0.78	1.18	1.21	0.79	1.13	1.07	2.41
3230	1		1.54	1.55	1.59	1.33	1.33	1.04	1.91
3244	1		0.65	1.05	1.05	0.58	0.79	1.02	1.29
N			19	19	19	19	19	19	19
Bias mean			0.74	0.92	0.94	0.66	0.78	0.86	1.42
Standard deviation			0.39	0.41	0.38	0.33	0.40	0.37	0.65
COV			0.53	0.45	0.41	0.51	0.50	0.43	0.46

Table 54: Bias factor: Plugged H piles in Cohesive soils

ID #	situ ID#	lab ID#	$\alpha$ Tomlinson		$\alpha$ API		$\beta$		$\lambda$		Schmertmann SPT mobilized
			$S_u$ correlated by Terzaghi & Peck (5)	$S_u$ correlated by Hara (5h)	$S_u$ correlated by Terzaghi & Peck (5)	$S_u$ correlated by Hara (5h)	$S_u$ correlated by Terzaghi & Peck (5)	$S_u$ correlated by Hara (5h)	$S_u$ correlated by Terzaghi & Peck (5)	$S_u$ correlated by Hara (5h)	
193	1										0.78
194	1		rock	rock	rock	rock	rock	rock	rock	rock	1.00
196	1										0.69
625		1	1.46	1.46	1.69	1.69			1.21	1.21	
626		1	0.88	0.88	1.10	1.10			0.93	0.93	
627		1	0.88	0.88	1.10	1.10			0.94	0.94	
628		1	0.73	0.73	0.91	0.91			0.77	0.77	
629		1	0.96	0.96	1.12	1.12			0.97	0.97	
631		1	1.05	1.05	1.22	1.22			1.10	1.10	
1015	1		1.25	0.59	1.31	0.77	0.72	0.67	1.44	0.82	3.30
1102		1	0.29	0.29	0.36	0.36			0.37	0.37	
1103		1	0.46	0.46	0.59	0.59			0.55	0.55	
1104		1	0.79	0.79	1.01	1.01			0.94	0.94	
1105		1	0.38	0.38	0.49	0.49			0.46	0.46	
1133	1	1	0.97	0.87	1.08	0.92			0.51	0.37	
1139		1	0.49	0.49	0.56	0.56			0.52	0.52	
1142		1	0.58	0.58	0.66	0.66			0.44	0.44	
1149	1		1.23	0.99	1.89	0.96	1.07	0.94	1.11	0.54	1.69
1150	1		1.04	0.83	0.36	0.22	0.20	0.19	0.35	0.20	0.49
1151	1		0.58	0.48	0.84	0.48	0.45	0.42	0.66	0.36	0.91
3233	1										1.17
3234	1		rock	rock	rock	rock	rock	rock	rock	rock	1.62
N			17	17	17	17	4	4	17	17	9
Bias mean			0.82	0.75	0.96	0.83	0.61	0.55	0.78	0.68	1.29
Standard deviation			0.33	0.29	0.43	0.37	0.37	0.32	0.33	0.30	0.85
COV			0.40	0.39	0.45	0.44	0.61	0.58	0.42	0.45	0.66



Table 55: Bias factor: Plugged H piles in Mixed soils

ID #	situ ID#	lab ID#	$\alpha$ Tomlinson, Nordlund, Thurman	$\alpha$ API, Nordlund, Thurman		$\beta$ ; Thurman		Schmertmann SPT mobilized	
			$\phi$ correlated by Peck et al. and limit below $36^0$						
			$S_u$ correlated by Terzaghi & Peck (5)	$S_u$ correlated by Hara (5h)	$S_u$ correlated by Terzaghi & Peck (5)	$S_u$ correlated by Hara (5h)	$S_u$ correlated by Terzaghi & Peck (5)		$S_u$ correlated by Hara (5h)
150	1		0.57	0.37	0.64	0.48	0.36	0.34	0.92
151	1		0.65	0.39	0.79	0.55	0.41	0.39	0.98
152	1		0.60	0.37	0.75	0.53	0.41	0.38	0.95
153	1		0.64	0.40	0.74	0.51	0.39	0.37	0.92
154	1		0.56	0.35	0.65	0.45	0.35	0.33	0.86
155	1		0.43	0.27	0.53	0.38	0.29	0.27	0.71
156	1				0.52	0.39	0.28	0.28	0.63
157	1		0.42	0.29	0.47	0.38	0.29	0.28	0.72
158	1		0.34	0.23	0.38	0.29	0.24	0.22	0.48
159	1		0.31	0.21	0.34	0.27	0.21	0.20	0.46
160	1		0.54	0.37	0.56	0.42	0.30	0.29	0.75
161	1		0.41	0.24	0.49	0.33	0.24	0.23	0.60
162	1		0.31	0.21	0.31	0.23	0.17	0.16	0.42
163	1		0.31	0.18	0.46	0.30	0.24	0.22	0.50
164	1		0.48	0.30	0.60	0.44	0.35	0.33	0.82
165	1		1.13	0.63	1.48	0.91	0.74	0.69	1.71
177	1		1.97	1.16	2.46	1.55	1.29	1.21	2.38
179	1		1.97	1.30	2.60	1.65	1.50	1.39	2.62
182	1		0.68	0.44	1.03	0.73	0.53	0.50	1.59
184	1		0.88	0.55	1.34	0.94	0.74	0.69	1.77
190	1		rock	rock	rock	rock	rock	rock	1.10
191	1								1.78
192	1								1.07
195	1								1.55
546	1		0.98	0.76	1.23	0.74	0.62	0.60	1.71
1012	3				2.13	1.28	1.06	1.06	1.85
1108	1	1			0.97	0.77			
1111	1		0.80	0.52	0.79	0.52	0.46	0.44	0.91
1122	1				0.56	0.50	0.44	0.44	1.12
1123	1				0.57	0.51	0.45	0.45	1.17
1127	1	1			0.63	0.63			0.63
1160	1				0.89	0.80	0.67	0.67	1.41
1173	1				0.89	0.73	0.54	0.54	1.54
1186	1				1.33	1.28	1.15	1.15	1.77
1189	1	1			0.67	0.62	0.48	0.48	0.97
1191	1	1			0.77	0.65	0.57	0.56	1.82
3227	1				0.63	0.57	0.48	0.48	1.12
3228	1				1.07	0.81	0.56	0.56	2.01
3232	1		rock	rock	rock	rock	rock	rock	1.89
3241	1				1.83	1.58	1.60	1.60	2.15
3249	1		0.75	0.47	0.89	0.61	0.51	0.48	1.46
3252	1				1.06	0.98	0.87	0.87	2.12
N			22	22	37	37	35	35	41
Bias mean			0.71	0.46	0.92	0.68	0.56	0.55	1.27
Standard deviation			0.46	0.29	0.56	0.37	0.36	0.35	0.58
COV			0.65	0.64	0.61	0.54	0.64	0.64	0.46

## LIST OF REFERENCES

- ASSHTO (1996/2000). LRFD Bridge Design Specifications, 2<sup>nd</sup> Edition--2000 Interim Revisions. Washington, DC
- Bowles, J. (1996). Foundation Analysis and Design. McGraw-Hill, New York.
- Coduto, D. (2001). Foundation Design, Second Edition, Prentice Hall. New Jersey.
- FHWA (1998). Driven Manual. Mathias, D. and Cribbs, M. Blue-Six Software, Inc. Logan, UT.
- Hannigan, P.J., Goble, G.G., Thendean, G., Likins, G.E. and Rausche, F. (1995). Design and Construction of Driven Pile Foundation. FHWA--Washington, D.C.
- Kulhawy, F.H. and Mayne, P.W. (1990). Manual on Estimating of Soil Properties for Foundation Design. Electric Power Research Institute. Palo Alto, California.
- McVay, M.C. and Townsend, F.C. (1989). Short course/ Workshop Guide for PC Software Support for Design and Analysis of Deep and Shallow Foundations from In-situ Tests (or PL-AID manual). University of Florida. Gainesville, Florida.
- McVay, M.C., Kuo, C.L. and Singletary, W.A. (1998) Calibrating Resistance Factors in the Load and Resistance Factor Design for Florida Foundations. Gainesville, Florida.
- Meyerhof, G. (1976/1981). The Bearing Capacity and Settlement of Foundations. Technical University of Nova Scotia. Halifax, Canada.
- Lai P. and Graham K. (1995). Static Pile Bearing Analysis Program--SPT94. <http://www.dot.state.fl.us/structures/manuals/spt94.zip>
- Reese, L.C., Wang, S.C. and Arrellaga, J. (1998). APILE Plus 3.0 Manual. EnSoft, Inc. Austin, Texas.
- Tomlinson, M.J. (1980/1995). Foundation Design and Construction, 6<sup>th</sup> Edition. Longman Scientific & Technical. Essex, England.
- US Army Corps of Engineers, No.7, EM 1110-1-1905 (1992). Bearing Capacity of Soil, Technical Engineering and Design Guides. Adapted by ASCE--2000. ASCE Press, New York.
- US Army Corps of Engineers (1997). Introduction to Probability and Reliability Methods for Use in Geotechnical Engineering. ETL 1110-2-547. Kamien, D. Washington, DC.
- Withiam, J., Voytko, E., Barker, R., Duncan, M., Kelly, B., Musser, S. and Elias, V. (1997). Participant Workbook Load and Resistance Factor Design (LRFD) for Highway Bridge Substructures. FHWA. Washington, D.C.

**DRIVEN PILES - STATIC ANALYSIS**

**DESCRIPTION OF STATIC CAPACITY**

**EVALUATION METHODS**

winword\research\ongoing\lrfd\databases\florida\drivenpiles10.16mod.2001

## TABLE OF CONTENTS

### LIST OF SYMBOLS

#### 1. RESEARCH METHODOLOGY

- 1.1. Axial Pile Capacity Prediction by Static Methods
  - 1.1.1. Axial Loading Capacity of a Pile
  - 1.1.2. Semi-Empirical Meth
    - 1.1.2.1. Side resistance in cohesive soil
      - 1.1.2.1.1.  $\alpha$ -Tomlinson method
      - 1.1.2.1.2.  $\alpha$ -API revised method (1987)
      - 1.1.2.1.3.  $\beta$ -Burland method (1973)
      - 1.1.2.1.4.  $\lambda$ -Method
    - 1.1.2.2. Tip resistance in cohesive soil
    - 1.1.2.3. Side resistance in cohesionless soil
      - 1.1.2.3.1.  $\beta$ -Bushan method (1982)
      - 1.1.2.3.2. Nordlund method
    - 1.1.2.4. Tip resistance in cohesionless soil--Thurman method
  - 1.1.3. Empirical Methods
    - 1.1.3.1. Meyerhof method for piles in cohesionless soil
    - 1.1.3.2. Schmertmann method for SPT
    - 1.1.3.3. Nottingham and Schmertmann method for CP
  - 1.1.4. Evaluation of Axial Capacity Prediction Software
    - 1.1.4.1. APILE 3.0 (EnSoft)
    - 1.1.4.2. DRIVEN 1.1 (FHWA)
    - 1.1.4.3. PL-AID (University of Florida)
    - 1.1.4.4. SPT-97 (FDOT and University of Florida)
- 1.2. Interpretation of the Pile-Load Tests
  - 1.2.1. Debeer Method
  - 1.2.2. Davisson Method
  - 1.2.3. Other Methods
- 1.3. Soil Properties Correlated from Insitu Tests

### LIST OF REFERENCES

## LIST OF SYMBOLS

$\alpha$ : The  $\alpha$  factor in  $\alpha$ -Tomlinson or  $\alpha$ -API method.

$\beta$ : The  $\beta$  factor in  $\beta$ -Burland (in cohesive soil) or  $\beta$ -Bushan method (in cohesionless soil).

$\lambda$ : The  $\lambda$  factor in  $\lambda$  method.

$\sigma_v$  (or  $p$ ): Total stress at the depth of interest.

$\sigma_v'$  (or  $p'$ ): Effective stress at the depth of interest.

$S_u$  (or  $C_u$ ): Undrained shear strength.

$L$ : Embedment depth of the pile.

$D_B$  (or  $D$ , or  $D_A$ ): Bearing embedment depth of the pile.

$B$ : The width or diameter of the pile section.

$\phi$ : Internal friction angle.

$\Phi$ : Resistance factor.

## RESEARCH METHODOLOGY

A driven pile is one type of deep foundation in which the structural loads are transferred to the ground through the side and tip resistance as well as the stiffness of the pile itself. Lateral loads or batter piles are not within the scope of this project; only the axial loading capacity of vertical piles is investigated. In design, the axial capacity can be predicted by various static capacity prediction methods as presented in Section 1.1. Alternatively, the static capacity can be interpreted from the static load test as in Section 1.2.

### 1.1. Axial Pile Capacity Prediction by Static Methods

Axial pile capacities can be predicted by various static capacity prediction methods. These methods use certain properties of the soil, such as the effective friction angle,  $\phi'$ , or the CPT cone bearing  $q_c$ . However, the computed capacities may not reflect the actual capacities exactly, so designs based on static methods must be conservative, which is reflected in the resistance factor,  $\Phi$ . This section will discuss specific ways to predict the axial pile capacities.

#### 1.1.1. Axial Loading Capacity of a Pile

The ultimate resistance of a pile,  $R_{ult}$  (or  $R_n$ --Nominal resistance), is given below:

$$R_{ult} = R_p + R_s \quad \text{Eq. 1}$$

where: pile tip resistance  $R_p = q_p A_p$ ,

pile side resistance  $R_s = \sum q_{si} \Delta z_i U$ ,

$q_p$  = unit tip resistance. Predictions of  $q_p$  are in Sections 1.1.2.2, 1.1.2.4 and 1.1.3.

$q_s$  = unit side resistance, which is regarded as constant along segment  $\Delta z_i$  of the pile.

Predictions of  $q_s$  can be found in Sections 1.1.2.1, 1.1.2.3 and 1.1.3,

$U$  = perimeter of the pile's shaft, and

$A_p$  = area of the tip of the pile.

In this project, the eight methods listed below are considered in predicting the axial capacities:

1.  $\alpha$ -method, which include  $\alpha$ -Tomlinson (Tomlinson, 1980/1995) and  $\alpha$ -API (Reese et al., 1998) for cohesive soil
  2.  $\lambda$ -method (Vijayvergiya and Focht, cited in US Army Corps of Engineers, No.7, 1992) for cohesive soil,
  3.  $\beta$ -method (Bushan--cited in Bowles, 1996) for cohesionless soil,
  4.  $\beta$ -method (Burland, Esrig and Kirby, 1979) for cohesive soil,
  5. Nordlund method (Nordlund, 1963) for cohesionless soil,
- (Methods number 4 to 5 above are cited in Hannigan et al., 1995).
6. Nottingham and Schmertmann CPT method (McVay and Townsend, 1989) for all soil types,
  7. Meyerhof SPT (Meyerhof, 1976/1981) for cohesionless soil,
  8. Schmertmann SPT method (Lai and Graham, 1995) for all soil types and rock.

The first five methods, as discussed in Section 1.1.2, are semi-empirical methods. These methods are based on the empirical relationship between soil properties and the stress states (both effective and total stress analyses are used). The last three methods, as discussed in Section 1.1.3, predict the pile capacities based on the data from in-situ tests (SPT and CPT).

#### 1.1.2. Semi-Empirical Methods

Semi-empirical methods are used to relate the adhesion between the pile and the surrounding soil to the internal friction angle,  $\phi$ , or the undrained shear strength,  $S_u$ . This section presents five different semi-empirical methods, will be divided into 2 sub-sections: Section 1.1.2.1 for cohesive soil and 1.1.2.2 for cohesionless soil.

#### 1.1.2.1. Side resistance in cohesive soil

In cohesive soil, the side resistance of a pile is usually predicted using the undrained shear strength,  $S_u$ , or the over-consolidation ratio, OCR. This section reviews different methods predicting the side resistance in cohesive soil.

##### 1.1.2.1.1. $\alpha$ -Tomlinson method

The  $\alpha$ -Tomlinson method (Tomlinson, 1980/1995), based on total stress analysis, is used to relate the adhesion between the pile and a clay to the undrained shear strength of the clay,  $S_u$ . The ultimate unit side resistance may be taken as:

$$q_{si} = \alpha S_{ui} \quad \text{Eq. 2}$$

where:  $\alpha$  = adhesion factor (Figure 1), which depends on the bearing embedment in stiff clay and the width of the pile,

$S_u$  (or  $C_u$ ) = average undrained shear strength of the soil in the segment of interest.



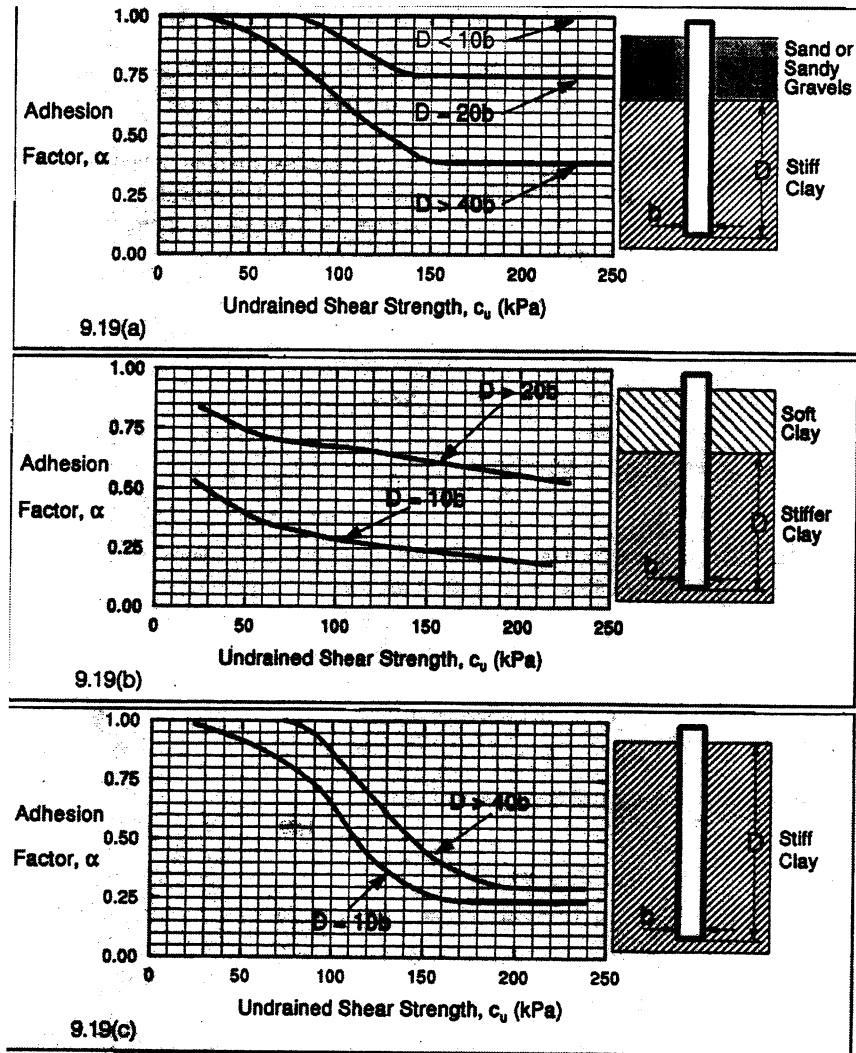


Figure 1:  $\alpha$  factors; Tomlinson method (Tomlinson, 1995)

Following is the discussion on the  $\alpha$ -Tomlinson method:

The  $\alpha$  method is simple to use and it has been used over many years. However, it is a total stress analysis and does not depend on the ground water level; therefore, the resistance based on the  $\alpha$  method may not be close to the measured capacity, which depends on the in-situ stress state and the ground water level.

Tomlinson originally developed the  $\alpha$ -method for large displacement piles. Therefore, for small-displacement piles (H and pipe piles), the  $\alpha$  method may not be suitable. Similarly, the Tomlinson method is only suitable for pile embedded in stiff clay. For cohesive layers that lie above the bearing layer, other methods should be used.

The assumptions behind the  $\alpha$  Tomlinson method include the following:

- If there is a soft clay layer above the bearing stiff clay, then the soft clay will be dragged down to the stiff layer and will lower the  $\alpha$  factor (see Figure 1),
- Similarly, the cohesionless soil in Figure 1 will be dragged down and therefore, the  $\alpha$  factor will be increased,
- Other intermediate cases, such as the layer right above the stiff layer is silt, or is only a very thin lens, etc. will decrease the accuracy of the prediction.

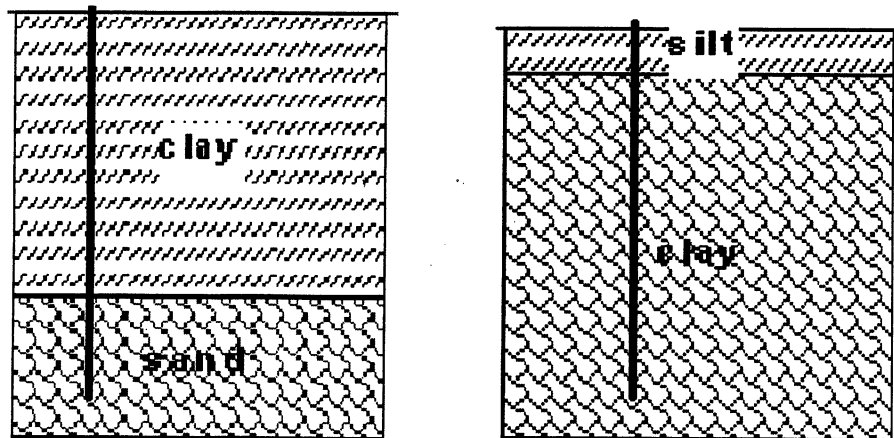


Figure 2: Examples when  $\alpha$ -Tomlinson is not applicable.

#### 1.1.2.1.2. $\alpha$ -API revised method (1987)

The  $\alpha$ -API method (cited in Reese et al., 1998) is similar to the  $\alpha$ -Tomlinson method, and the ultimate unit side resistance, in the same unit as  $S_u$ , is taken as:

$$q_{si} = \alpha S_{ui} \quad \text{Eq. 2}$$

$$\text{where: } \alpha = 0.5 \psi^{-0.5} \quad \text{if } \psi \leq 1.0,$$

$$\alpha = 0.5 \psi^{-0.25} \quad \text{if } \psi > 1.0, \text{ and max } \alpha = 1.0,$$

$$\psi = S_u / \sigma_v', \text{ and}$$

$\sigma_v'$  (or  $p_v'$ ) = the vertical effective overburden pressure at the depth of interest.

From Eq. 2, the adhesion factor,  $\alpha$ , with different effective stresses is generated in Figure 3.

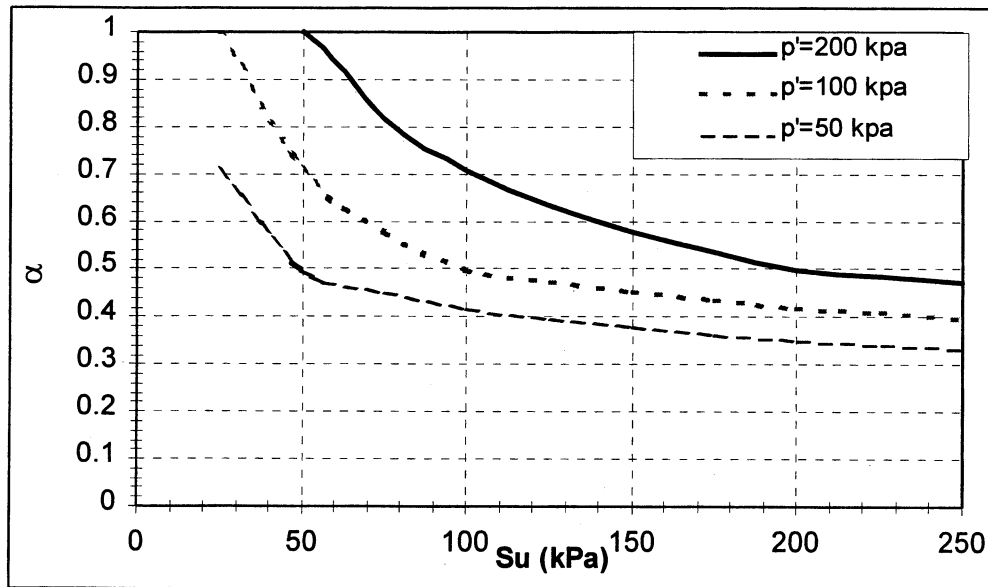


Figure 3:  $\alpha$  factors; Revised API 1987 method (generated from Eq. 2)

The  $\alpha$ -API method is a mixed method between total stress analysis ( $S_u$ ) and effective stress analysis ( $\sigma_v'$ ). It is much easier to use than the Tomlinson method. For example, the user will have no issue with considering other layers that lie above the bearing layer. Finally, the  $\alpha$ -API method has simple equations; thus it is easily automated.

Following is the discussion on the unit side resistance of both  $\alpha$  methods:

As shown in Figure 4, the unit side resistance  $q_s = \alpha S_u$  for the  $\alpha$ -API method follows a logical trend: the stiffer the soil (higher  $S_u$ ), the more the side resistance.

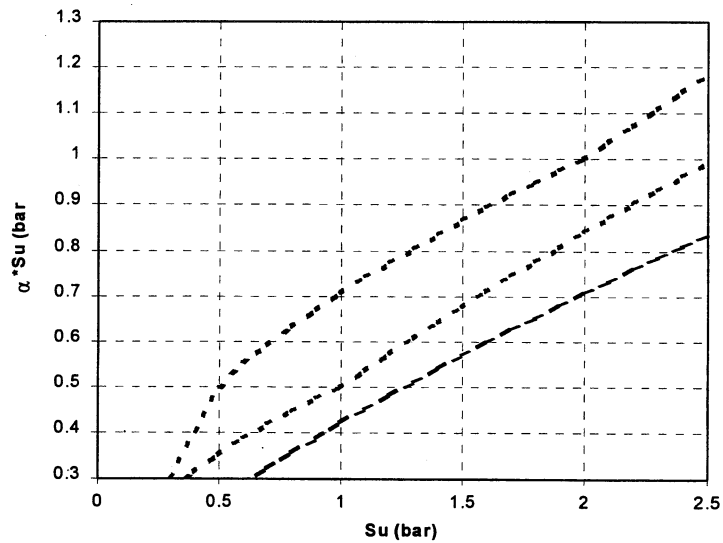


Figure 4: The unit side resistance of  $\alpha$ -API method (generated from Eq. 2)

However, as indicated in Figure 5, for the  $\alpha$ -Tomlinson 1980 method, when  $S_u$  is in the range of about 0.8 to 1.7 bar (80 to 170 kPa), the unit side resistance decreases as the soil becomes stronger, which does not follow traditional wisdom on pile behavior. (In that range, there is very sharp decrease of the  $\alpha$  factor).

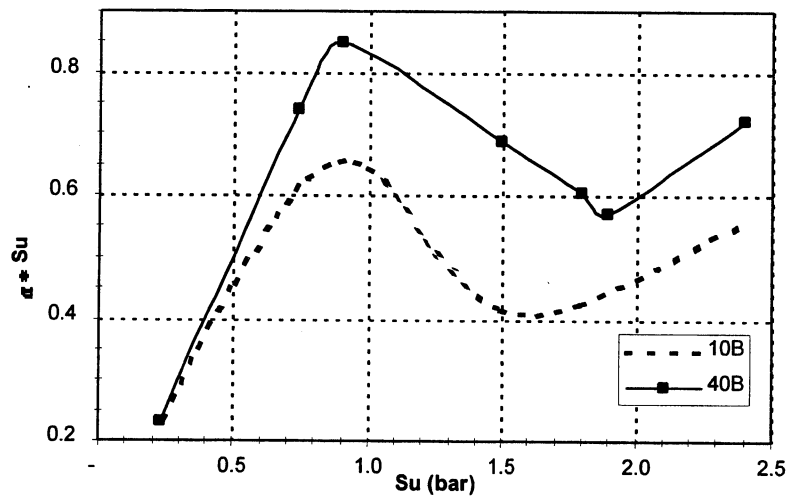


Figure 5: The unit side resistance of  $\alpha$ -Tomlinson 1980 case #3 (generated from Figure 1)

#### 1.1.2.1.3. $\beta$ -Burland method (1973)

From the theory of soil mechanics, based on effective stress analysis, we have  $q_s = K (\tan \delta) \sigma_v'$ ,

where:  $K$  = horizontal stress ratio,

$\delta$  = adhesion angle between soil and piles,

$\sigma_v'$  = vertical effective stress.

The equation can be rewritten as:

$$q_s = \beta \sigma_v' \quad \text{Eq. 3}$$

where:  $\sigma_v'$  = vertical effective stress,

$\beta$  = factor depended on the over-consolidation ratio OCR (Figure 6).

Following is the discussion on the  $\beta$ -Burland method:

Esrig and Kirby (1979) (cited in Hannigan et al., 1995) suggested that for heavily over-consolidated clays, the value of  $\beta$  should not exceed two.

Practically, the OCR ratio is not usually measured in the laboratory. Therefore, this method is difficult to implement. In this project, all OCR ratios are obtained from in-situ tests through correlations (Section 2.2).

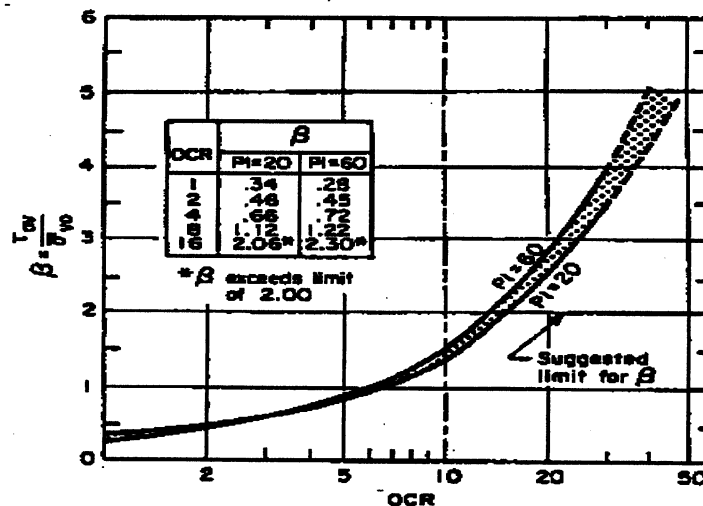


Figure 6:  $\beta$  factors (AASHTO 1996/2000)

#### 1.1.2.1.4. $\lambda$ -Method

The  $\lambda$ -method (cited in US Army Corps of Engineers, 1992), based on effective and total stress analysis, may be used to relate the unit side resistance to the passive earth pressure as:

$$q_s = \lambda(\sigma' + 2S_u) \quad \text{Eq. 4}$$

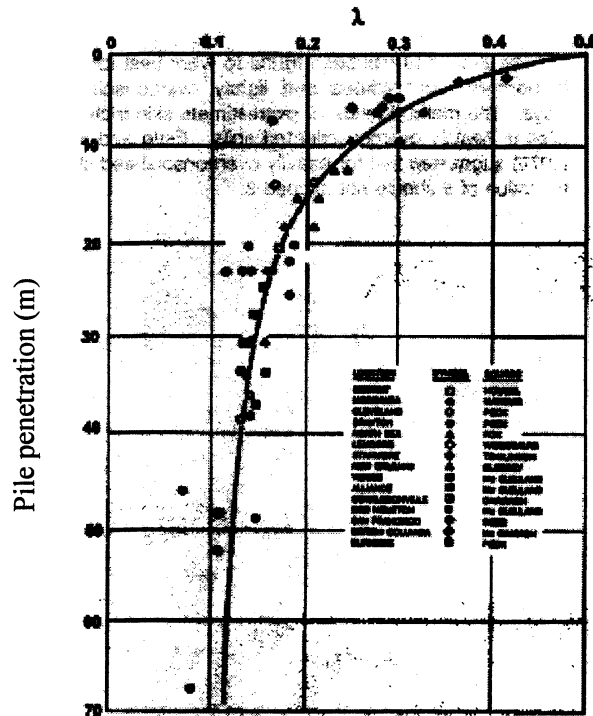


Figure 7:  $\lambda$  factors (US Army Corps of Engineers, 1992)

where:  $\lambda$  = an empirical coefficient, which depends on the pile embedment as shown in Figure 7.

The  $\lambda$  factor was empirically suggested by examining pipe piles in only 15 locations. The main drawback of this method is that it assumes a single value of  $\lambda$  for the whole pile.

#### 1.1.2.2. Tip resistance in cohesive soil

The ultimate unit tip resistance of piles in saturated clay (Reese et al., 1998) may be taken as:

$$q_p = 9 S_u \quad \text{Eq. 5}$$

where:  $S_u$  = average undrained shear strength in the range from  $2B$  to  $3.5B$  below the tip, and  $B$  is the diameter of the pile.

With unsaturated clay, Eq. 5 is still used to predict tip resistance, which may reduce the accuracy of the answer.

#### 1.1.2.3. Side resistance in cohesionless soil

In cohesionless soil, the side resistance of a pile is usually predicted using the adhesion angle,  $\delta$ , or the relative density,  $D_r$ . The adhesion angle,  $\delta$ , is related to the internal friction angle of the soil,  $\phi$ , through the volume displacement, the material, the shape of the pile and the roughness of the pile. This section reviews different methods predicting the side resistance in cohesionless soil.

##### 1.1.2.3.1. $\beta$ -Bushan method (1982)

Similar to the  $\beta$  method in cohesive soil, the unit side resistance is related to effective stress as (cited in Hannigan et al., 1995):

$$q_s = \beta \sigma_v' \quad \text{Eq. 3}$$

where:  $\beta = 0.18 + 0.65 D_r$ , and

$D_r$  = Relative density in decimals. Therefore,  $\max \beta = 0.83$  when  $D_r = 1$  (much lower than  $\max \beta$  in cohesive soil--Section 1.1.2.1.3.)

##### 1.1.2.3.2. Nordlund method

Nordlund (cited in Hannigan et al., 1995) developed the following equation for the unit resistance:

$$q_s = K_\delta C_F \sigma_v' \frac{\sin(\delta + \varpi)}{\cos \varpi} \quad \text{Eq. 6}$$

where:  $K_\delta$  = Coefficient of lateral earth pressure at the depth of interest. (Figures 8 to 11),

$\delta$  = friction angle between pile and soil. For non-taper piles:  $\delta \leq \phi$ . (Figure 12),

$C_F$  = Correction factor for  $K_\delta$  when  $\delta \neq \phi$ .  $C_F \approx 0.6$  to  $1.0$ . (Figure 13),

$\sigma_v'$  = effective over-burden pressure at the center of the layer of interest, and

$\varpi$  = angle of the pile taper from vertical.

For a uniform cross section pile ( $\varpi = 0$ ), the Nordlund equation becomes

$$q_s = K_\delta C_F \sigma_v' \sin \delta \quad \text{Eq. 7}$$

The equation of this semi-empirical method is somewhat similar to the theory of soil mechanics, in which  $q_s = K_\delta \sigma' \tan \delta$  Eq. 8

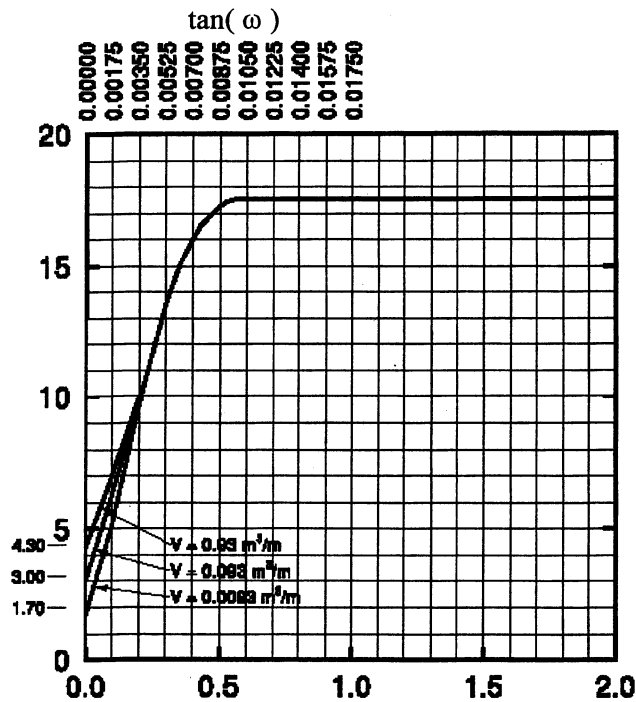


Figure 8: Design curve for evaluating  $K_\delta$  when  $\phi = 40$  (Norlund 1963--cited in Hannigan et al., 1995)

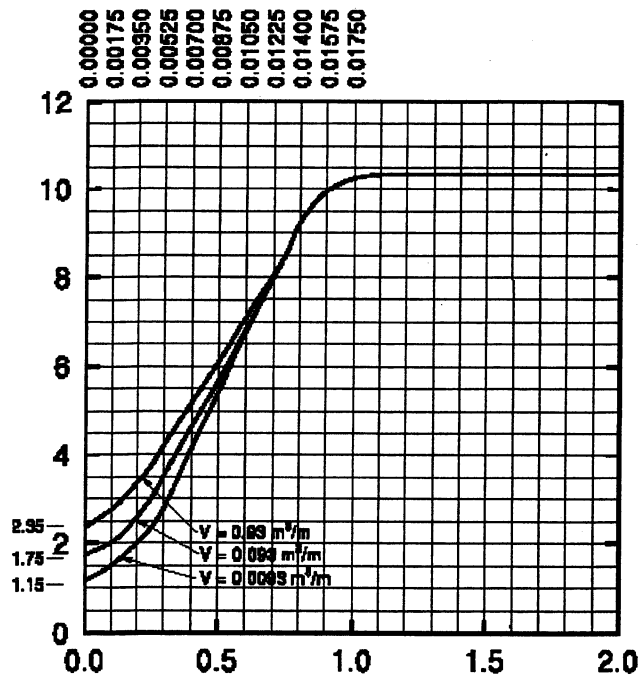


Figure 9: Design curve for evaluating  $K_\delta$  when  $\phi = 35$  (Norlund 1963--cited in Hannigan et al., 1995)



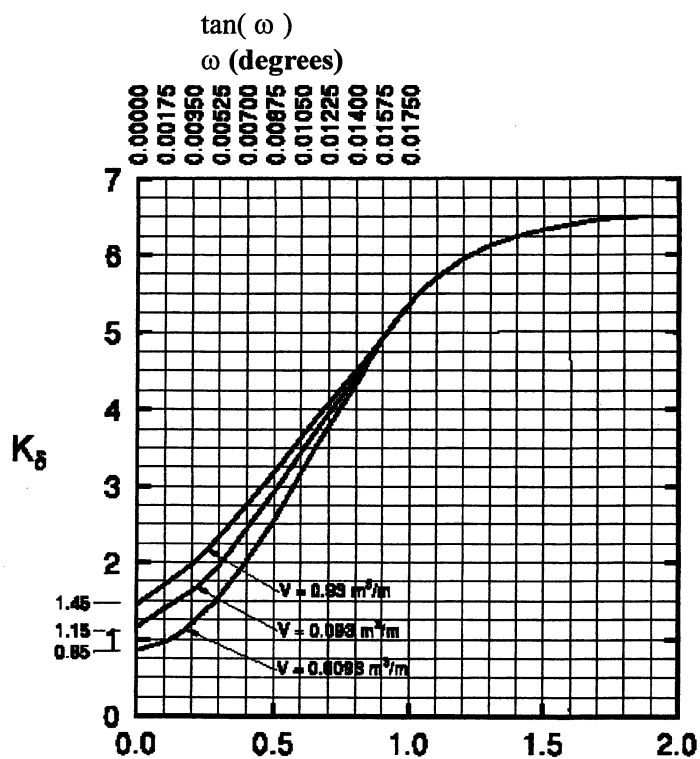


Figure 10: Design curve for evaluating  $K_\delta$  when  $\phi = 30$   
(Norlund 1963--cited in Hannigan et al., 1995)

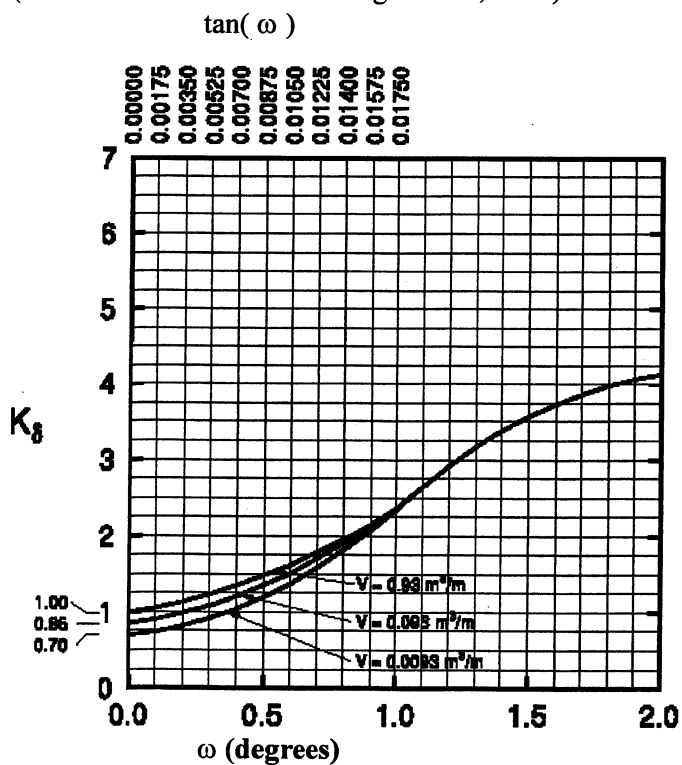


Figure 11: Design curve for evaluating  $K_\delta$  when  $\phi = 25$   
(Norlund 1963--cited in Hannigan et al., 1995)

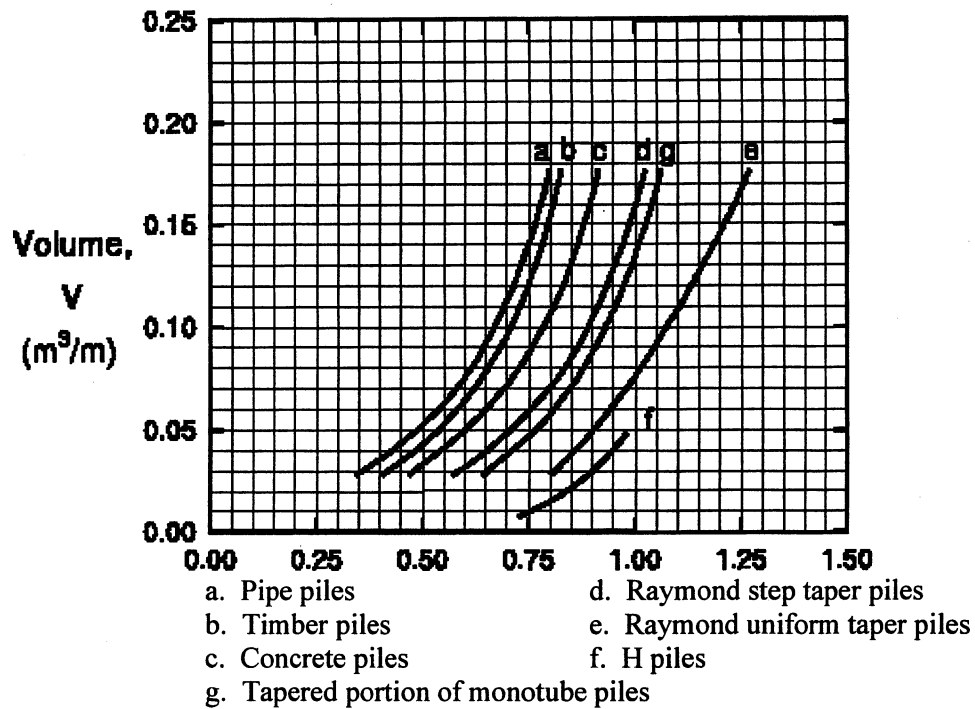


Figure 12: Relation  $\delta/\phi$  and pile displacement  
(Norlund 1963--cited in Hannigan et al., 1995)

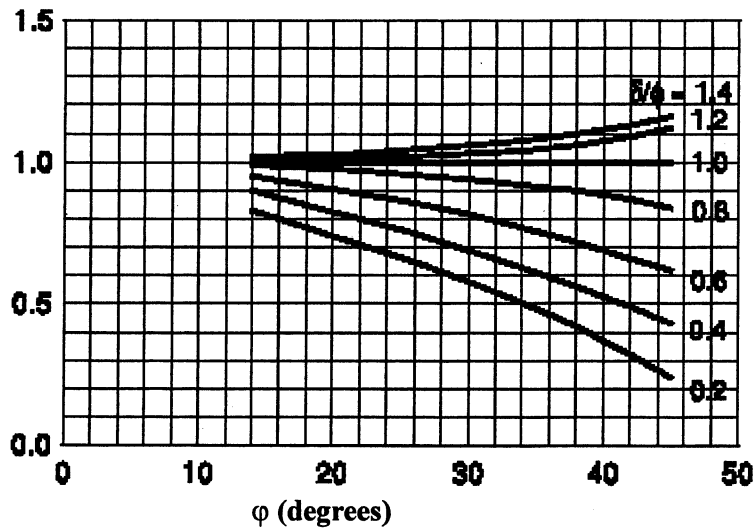


Figure 13: Correction factor ( $C_F$ ) for  $K_\delta$   
(Norlund 1963--cited in Hannigan et al., 1995)

#### 1.1.2.4. Tip resistance in cohesionless soil--Thurman method

From bearing capacity theory, Thurman (cited in Hannigan et al., 1995) related the unit tip resistance in sand with effective stress as:

$$q_p = \alpha_t N'_q \sigma_v' \quad \text{Eq. 9}$$

where:  $\alpha_t$  = dimensionless factor (Figure 14),

$N'_q$  = Bearing capacity factor (Figure 15),

$\sigma_v'$  = effective overburden pressure at the pile tip.  $\sigma_v'$  is limited to 150 kPa (tip resistance reaches a limiting value at some distance below the ground),

$q_p$  also has a limit as shown in Figure 16.

$N'_q$  is very high at high internal friction angles ( $N'_q > 250$  when  $\phi > 42^\circ$ ). Therefore, some software, e.g. DRIVEN (FHWA, 1998) recommends the limit of only  $36^\circ$  for  $\phi$ .

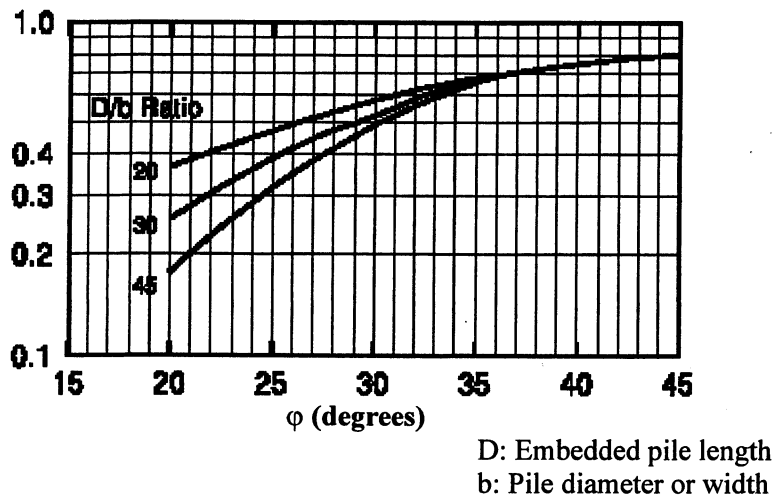


Figure 14:  $\alpha_t$  coefficient (FHWA--DRIVEN, 1998)

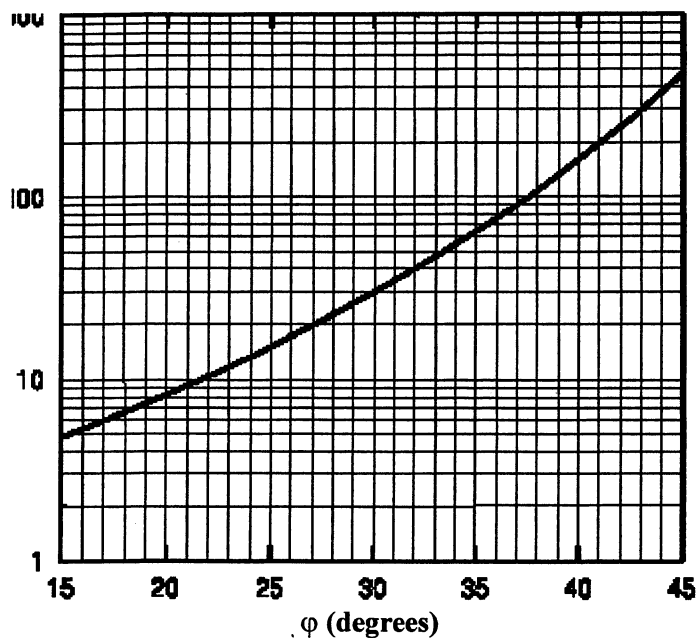


Figure 15: Bearing capacity factor  $N_q'$  (FHWA--DRIVEN, 1998)

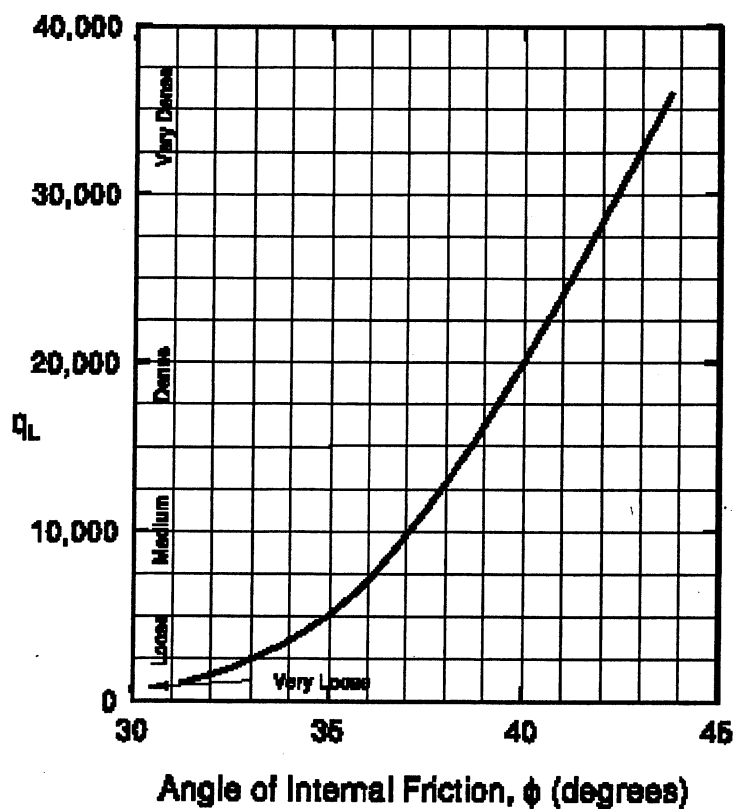


Figure 16: Relationship Between Maximum Unit Pile Toe Resistance  $q_L$  (kPa) and Friction Angle for Cohesionless Soils (Meyerhof, 1976/1981).

### 1.1.3. Empirical Methods

This section presents different empirical methods, which directly relate the resistances with the in-situ test results, i.e. the N-value and the CPT readings.

#### 1.1.3.1. Meyerhof method for piles in cohesionless soil

There are more than four different variations of Meyerhof 1976 method. Different agencies have different guidelines, e.g. EM 1110-1-1905 (US Army Corps of Engineers, 1992), leading to different results, even though the method is still referred to as Meyerhof 1976 method.

The primary variations of the side resistance of the method are listed below:

- |   |                     |
|---|---------------------|
| 1) AASHTO provision (AASHTO 1996/2000):           | $q_s = k' N$ (kPa). |
| 2) Meyerhof original paper (Meyerhof, 1976/1981): | $q_s = k N$ (kPa).  |
| 3) Bowles (Bowles, 1996):                         | $q_s = k N'$ (kPa). |
| 4) U.S. CORPS of Engineers:                       | No guidelines.      |

where:  $N$  = Uncorrected blow count,

$N'$  = Corrected blow count,

$k = 2$  for displacement piles, and  $k = 1$  for small displacement piles.

AASHTO (AASHTO 1996/2000) uses strict unit conversion, therefore  $k' = 1.9$  for displacement piles and 0.96 for small displacement piles.

The side resistance should be limited as given below:

$$q_s \leq 100 \text{ kPa}$$

The tip resistance for Meyerhof method is similarly obtained as:

1) AASHTO provision (AASHTO 1996/2000):  $q_p = 0.38 N_t' D/B$  (bar).

where:  $N_t'$  = Corrected blow count near the pile tip,

$D$  = The embedment of the pile in cohesionless soil, and

$B$  = The diameter or width of the pile cross-section.

2) Original paper by Meyerhof (Meyerhof, 1976/1981):  $q_p = 0.4 N_t D/B$  (bar).

where:  $N_t$  = Uncorrected blow count near the pile tip.

It should be noted that, in 1976, the concept of correcting the N-value due to the overburden pressure was very new. Therefore, Meyerhof did not correct N. Similarly, in Meyerhof's paper, he used approximate conversion: 1 tsf  $\approx$  100 kPa (1 bar).

3) Bowles (Bowles, 1996):  $q_p = 0.4 N_{8+3B}' D/B$  (bar).

where:  $N_{8+3B}'$  = Corrected blow count in the depth of 8B above tip and 3B below tip.

4) EM 1110-1-1905 (U.S. Army CORPS of Engineers, 1992)

$$q_p = 0.38 N_{8+3B} D/B \quad (\text{bar}) = 0.8 N_{8+3B} D/B \quad (\text{ksf}).$$

where:  $N_{8+3B}$  = Uncorrected N in the depth of 8B above tip and 3B below tip.

Similar to the side resistance calculations, the value of the maximum tip resistance is also limited as shown below:

1) AASHTO provision (AASHTO 1996/2000)

$$\begin{aligned} q_L &= 4 N_t' \text{ in sand,} \\ &= 3 N_t' \text{ in silt.} \end{aligned}$$

2) Meyerhof original paper (Meyerhof, 1976/1981)

$$\begin{aligned} q_L &= 4 N_t \text{ in sand,} \\ &= 3 N_t \text{ in silt.} \end{aligned}$$

3) Bowles (Bowles, 1996)

$$q_L = 3.8 N_{8+3B}'.$$

4) EM 1110-1-1905 (U.S. Army CORPS of Engineers, 1992)

$$q_L = 3.8 N_{8+3B} \text{ (bar)} = 8 N_{8+3B} \text{ (ksf).}$$

### 1.1.3.2. Schmertmann method for SPT

The procedure of the Schmertmann method for SPT (Lai and Graham, 1995) is described below.

First of all, the SPT blow count  $N$  is adjusted as shown below:

If  $N < 5$  then  $N = 0$  (ignores side resistance in weak soil), and

If  $N \geq 60$  then  $N = 60$  (limit on side resistance)

Discussion:

It is conservative to ignore side resistance when  $N$  is in the range of 4 to 5. For example, in Luling bridge, ID 1001, the soil is mostly clay with  $N < 5$ . The truncation of  $N < 5$  significantly lowers the predicted capacity compared to the measured capacity.

The ultimate side resistance for different types of piles and soil types is presented in Table 1.

Table 1: Side resistance--Schmertmann method for SPT

Type	Description	Ultimate unit side resistance $q_s$ (tsf)		
		Concrete	Steel H piles	pipe piles
1	Plastic clay	$2.0N(110-N)/4006.6$	$2N(110-N)/5335.94$	$0.949+0.238\ln N$
2	Clay-silt-sand mixtures Very silty sand, silts	$2.0N(110-N)/4583.3$	$-0.0227+0.033N-4.57610^{-4}*N^2+2.465E-6*N^3$	$0.243+0.147\ln N$
3	Clean sands	$0.019N$	$0.0116N$	$0.058+0.152\ln N$
4	Soft limestone, very shelly sand	$0.01N$	$0.0076N$	$0.018+0.134\ln N$

At any point A, the unit tip resistance is

$$q_{p@A} = \frac{\text{weighted average of } q_p \text{ 8B above A} + \text{weighted average of } q_p \text{ 3.5B below A}}{2}$$

The weighted average of  $q_p$  is based on values calculated from Table 2.

Table 2: Tip resistance--Schmertmann method for SPT

Type	Description	Ultimate unit end bearing $q_p$ (tsf)	
		Concrete and H piles	Pipe piles
1	Plastic clay	0.7 N	0.48 N
2	Clay-silt-sand mixtures Very silty sand, silts	1.6 N	0.96 N
3	Clean sands	3.2 N	1.312 N
4	Soft limestone, very shelly sand	3.6 N	1.92 N

For concrete and H piles, the mobilized tip resistance is expected to be one third (1/3) of the ultimate tip resistance. For pipe piles, the mobilized tip resistance is expected to be one half (1/2) of the ultimate tip resistance.

The ultimate resistance is only fully mobilized when the bearing embedment is sufficient, i.e.  $D_A = D_C$

where:  $D_A$  = Actual bearing embedment, and  $D_C$  = Critical bearing embedment, which is shown in Table 3.



Table 3: Critical depth ratio--Schmertmann method for SPT

Soil Type	Description	Critical depth ratio ( $D_C/B$ )
1	Plastic clay	2
2	Clay-silt-sand mixtures Very silty sand, silts	4
3	Clean sands $N = 12$ or less $N = 30$ or less $N$ greater than 30	6 9 12
4	Soft limestone, very shelly sand	6

If  $D_A < D_C$  and the bearing layer is stronger than the overlying layer, then:

$$q_p = q_{LC} + \frac{D_A}{D_C}(q_T - q_{LC}) \quad \text{Eq. 10}$$

where:  $q_p$  = Reduced tip resistance,

$q_{LC}$  = Unit tip resistance at layer change, and

$q_T$  = Uncorrected unit tip resistance at pile tip.

$$CSFBL = \frac{SFBL}{q_T} \left[ q_{LC} + \frac{D_A}{2D_C}(q_T - q_{LC}) \right] \quad \text{Eq. 11}$$

where: CSFBL = Reduced side resistance in the bearing layer, and

SFBL = Uncorrected side resistance in the bearing layer.

If  $D_A > D_C$  and the bearing layer is stronger than the overlying layer, then:

$$CSFACD = \frac{USFACD}{q_{CD}} [q_{LC} + 0.5(q_{CD} - q_{LC})] \quad \text{Eq. 12}$$

where:

CSFACD = Corrected side resistance between the top of the bearing layer and the critical depth,

USFACD = uncorrected side resistance in the bearing layer from the top of the bearing layer to the critical depth, and

$q_{CD}$  = unit tip resistance at critical depth.

### 1.1.3.3. Nottingham and Schmertmann method for CPT

The procedure of the Nottingham and Schmertmann method for CPT (McVay and Townsend, 1989) is described below.

The ultimate side resistance of piles may be taken as:

From ground level down to the depth of 8B:  $q_s = K f_s / 2$  Eq. 13

From 8B down to the tip:  $q_s = K f_s$  Eq. 14

where:  $f_s$  = sleeve friction from CPT data,

In cohesionless soil, the ratio K (or  $K_s$ ) is a function of the ratio between penetration depth(Z) and pile width (D)--see Figure 17.

In cohesive soils: K is written as  $\alpha$  (or  $K_c$ ), which is the  $\alpha$  factor, similar to the  $\alpha$ -method--see Figure 17.

Similarly, the ultimate tip resistance of piles may be taken as:

$$q_p = \frac{q_{c1} + q_{c2}}{2} \quad \text{Eq. 15}$$

where:  $q_c$  = The tip resistance in CPT data (if  $q_c > 100$  tsf, limit  $q_c$  to 100 tsf),

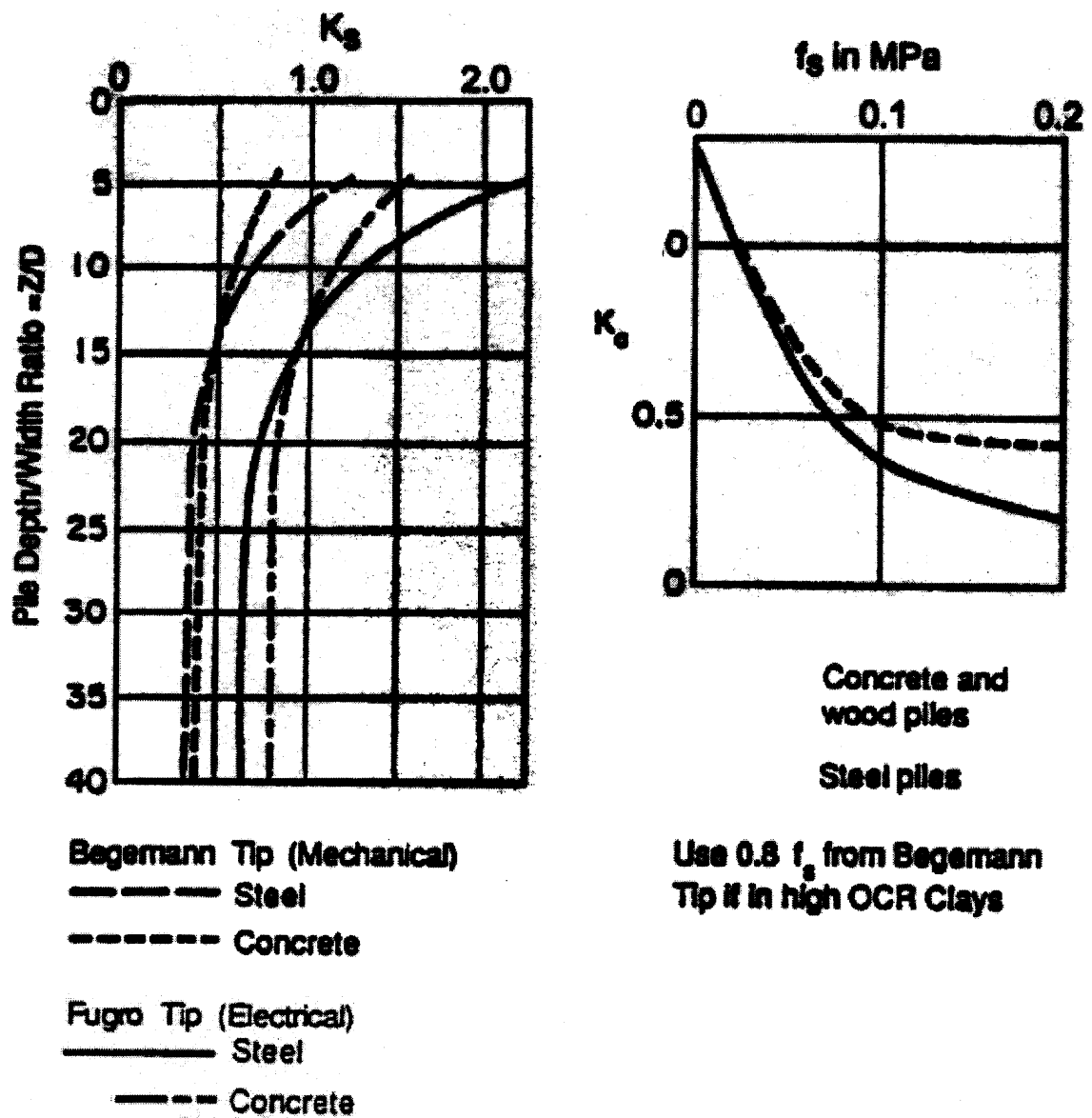
$q_{c1}$  = The average  $q_c$  over a distance of  $x_B$  below the tip, which is shown below:

Sum of the minimum values (upward)/  $x_B$  + Sum of the actual values (downward)/  $x_B$

Use the minimum  $q_{c1}$  with different  $x_B$  ranging from 0.7B to 3.75B,

$q_{c2}$  = The average  $q_c$  over a distance of 8B above the tip using the minimum  $q_c$  values (minimum path). Figure 18 depicts the procedure for tip resistance prediction.

For mechanical cone in cohesive soils, due to the effects of the base of the friction sleeve on  $q_c$ , the  $q_p$  value should be reduced by about 40%.



## Side friction

Figure 17:  $K_s$  and  $K_c$  ratio in cohesionless and cohesive soil, respectively  
(cited in McVay and Townsend, 1989)

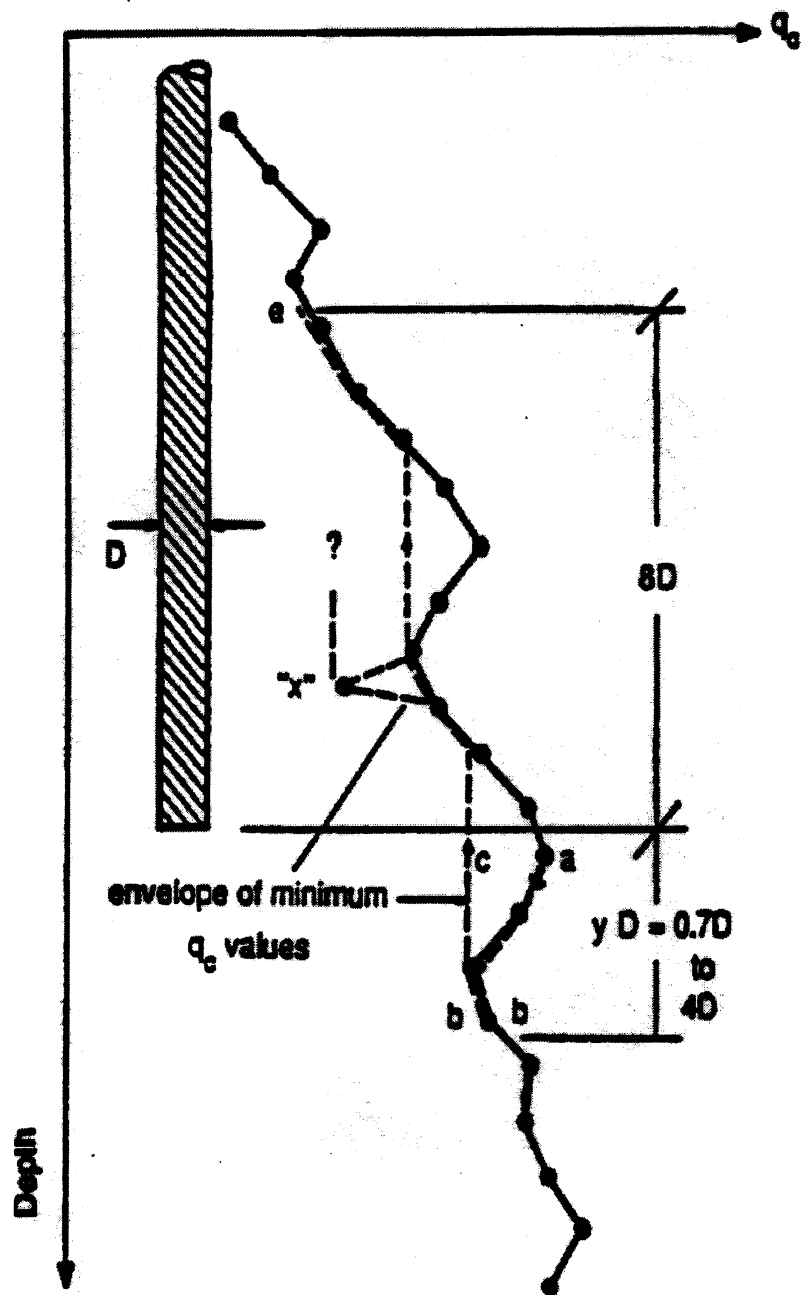


Figure 18: Tip resistance computation procedure--Nottingham 1975.  
(cited in McVay and Townsend, 1989)

A summary of all the methods is presented in Table 4 below.

Table 4: Summary of the methods

Methods	Side resistance	Tip resistance	Parameters required	4. Constraints
$\alpha$ -Tomlinson (Tomlinson, 1980/1995)	$q_s = \alpha S_u$	$q_p = 9 S_u$	$S_u$ ; $D_b$ (bearing embedment)	+Bearing layer must be stiff cohesive + Number of soil layers $\leq 2$
$\alpha$ -API (Reese et al., 1998)			$S_u$	
$\beta$ in cohesive (AASHTO, 1996/2000)			OCR	
$\lambda$ (US Army Corps of Engineers, 1992)	$q_s = \lambda(\sigma' + 2S_u)$		$S_u$	Only for cohesive soils
$\beta$ in cohesionless (Bowles, 1996)	$\beta \sigma'$		$D_r$	
Nordlund and Thurman (Hannigan et al., 1995)	$q_s = K_\delta C_F \sigma' \frac{\sin(\delta + \varpi)}{\cos \varpi}$	$q_p =$ $\alpha_t N'_q \sigma'$	$\varphi$	
Meyerhof SPT (Meyerhof, 1976/1981)	$q_s = k N$	$q_p =$ $0.4D/BN'$	$N$	+ For cohesionless soils + SPT data
Schmertmann SPT (Lai and Graham, 1995)	$q_s = \text{function}(N)$	$q_p = \text{fn}(N)$	$N$	SPT data
Schmertmann CPT (McVay and Townsend, 1989)	$q_s = \text{function}(f_s)$	$q_p = \text{fn}(q_c)$	$q_c, f_s$	CPT data

#### 1.1.4. Evaluation of Axial Capacity Prediction Software

Four common programs are used in predicting the pile axial capacity. This section briefly evaluates the programs, such as the methods they use, and the results they get.

##### 1.1.4.1. APILE 3.0 (EnSoft)

APILE 3.0 is a commercial Windows-based software developed by EnSoft, Inc (Reese et al., 1998).

For cohesive soil, the following static methods are used: The  $\alpha$ -Tomlinson method, the  $\alpha$ -API method and the  $\lambda$  method. For cohesionless soil, the following static methods are used: The Nordlund method and the API method. The combination of the  $\alpha$ -Tomlinson and Nordlund methods in mixed soils is called the FHWA procedure.

The following problems were detected in using this program:

- For piles with non-circular sections, when the unit is changed from SI to English, the predicted axial capacity as well as the shapes of the capacity graph change,
- Outputs of EnSoft's examples 2 and 4 are different from the User Manual's printout,
- In FHWA procedure, the program does not correctly interpret the data when there are more than two layers: The bearing embedment depth will be calculated by the program as the distance from the tip to the nearest interface, which may be less than the actual bearing embedment,
- There is no box for inputting ground-water level, the user has to use buoyant unit weight whenever applicable.

##### 1.1.4.2. DRIVEN 1.1 (FHWA)

DRIVEN is a freeware Windows-based software provided by the Federal Highway Administration (FHWA, 1998). Driven is the Windows version of the old SPILE MSDOS-based program. The  $\alpha$ -Tomlinson method is used in cohesive soils, while the Nordlund and Thurman methods are used in cohesionless soils.

For concrete pile, DRIVEN does not support the circular section.

The  $\alpha$ -Tomlinson method is only suitable for pile embedded in stiff clay. However, DRIVEN allows the user to specify the  $\alpha$ -Tomlinson method in cohesive layer(s) that lies above the bearing layer.

#### 1.1.4.3. PL-AID (University of Florida)

PL-AID is a MSDOS-based program developed at the University of Florida predicting capacities of piles using CPT data, i.e. Nottingham and Schmertmann method (McVay and Townsend, 1989).

PL-AID works correctly under the following conditions:

- CPT data (raw truck format or interpreted format) are in SI units,
- The increments in data input are equal (e.g. 5 or 10 cm).

PL-AID was not originally developed for H piles and unplugged open-ended pipe piles.

#### 1.1.4.4. SPT-97 (FDOT and University of Florida)

SPT-97 is a Windows-based program predicting capacities using SPT data, i.e. Schmertmann method (Lai and Graham, 1995). SPT97 works normally well, except two following cases:

- When  $D_c < D_a$  (the critical depth is smaller than the actual depth), there is a problem in correcting the resistance.
- The capacity is erroneously computed for pipe piles.

A summary of the issues related to the above software can be found in Table 5.

Table 5. Issues with using Driven Pile Axial Capacities Analysis Software

APILE 3.0 Plus	DRIVEN 1.1	SPT 97	PL-AID
All results using SI unit are erroneous (this problem was corrected on September 18, 00)	The computed results for H piles, SI units are erroneous.	When $D_c < D_a$ (critical depth is smaller than actual depth), there is a problem in correcting the resistance.	Increments must be equal. This is always true if the data are originally collected from the tests.  However, some of the data are actually digitized from graphs. In this case, interpolation must be made to get equal increments.
Error in critical depth (this problem was corrected on November 27, 00)	Concrete piles: There is no option to input circular pile.		
Wrong handling of volume displacement for H and pipe piles (this problem was corrected on January 04, 01)			
The $\lambda$ method is only suitable for pile in clay. In sand, APILE still has $\lambda$ capacities for piles by converting $\phi$ to $S_u$ (but in the APILE manual, it said that it took capacities from API)	The Nordlund method: Open ended pipe piles: Curve f (for H piles) is used for open ended pipe piles, which leads to higher capacities of plugged open ended pipe than those of close ended pipe with the same dimensions		
The $\alpha$ -Tomlinson (1980) method: The layer system must be converted to 1 or 2 layer(s). This causes an approximation and lowers the reliability, especially when the soil system is complex.	The $\alpha$ -Tomlinson 1980 method: In order to get correct results, the layer system must be converted to 1 or 2 layer(s). This causes an approximation and lowers the reliability, especially when the soil system is complex.	For pipe piles, the capacity from SPT97 is erroneously computed	
Error in user specified $q_L$ (this problem was corrected on January 24, 01)			
Different capacities with different increments. (This problem was unsuccessfully corrected on February 14, 01)			



## 1.2. Interpretation of the Pile-Load Tests

Static load tests to failure determine the load capacities directly, therefore they are more precise than the prediction methods presented in Section 1.1. However, from load-settlement curves, a determination of the ultimate capacity or of the mobilized capacity is required. Many different methods of interpretations have been proposed and some of most common methods are presented in this section.

### 1.2.1. DeBeer Method

The DeBeer capacity (Bowles, 1996) is determined as follow. The load test data is plotted in a log-log scale. The intersection between the two straight portions of the graph will correspond to the DeBeer capacity.

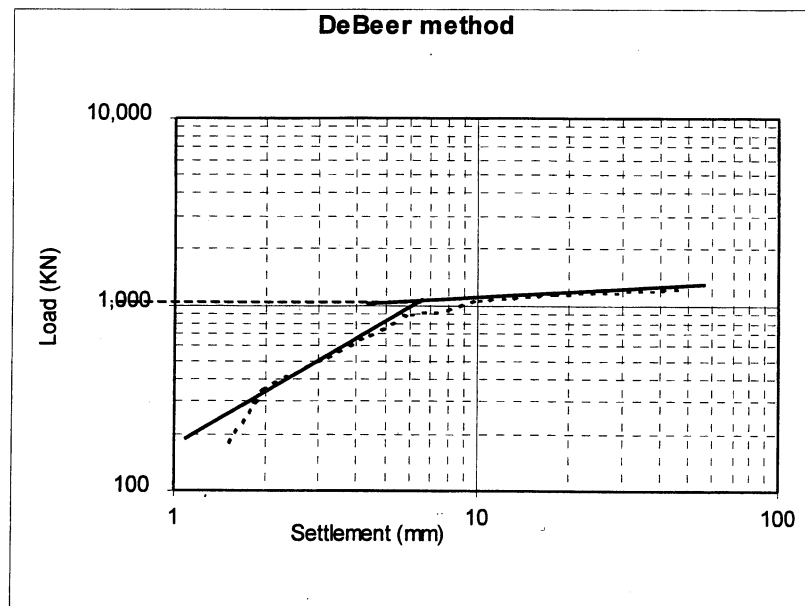


Figure 19: Example of the DeBeer method

One of the most common problems with this method is that, in some cases, the two straight portions in the graph are not clearly defined.

### 1.2.2. Davisson Method

The Davisson method (Coduto, 2001) is one of the most popular methods and it is based on the elastic compression of the pile. The procedure to define the the Davisson capacity is as described below:

1. In the load test graph, plot the base line with the slope of:  $AE/L$

where: A = Cross sectional of the material,

E = Modulus of elasticity of the material, and

L = Embedment length of the pile

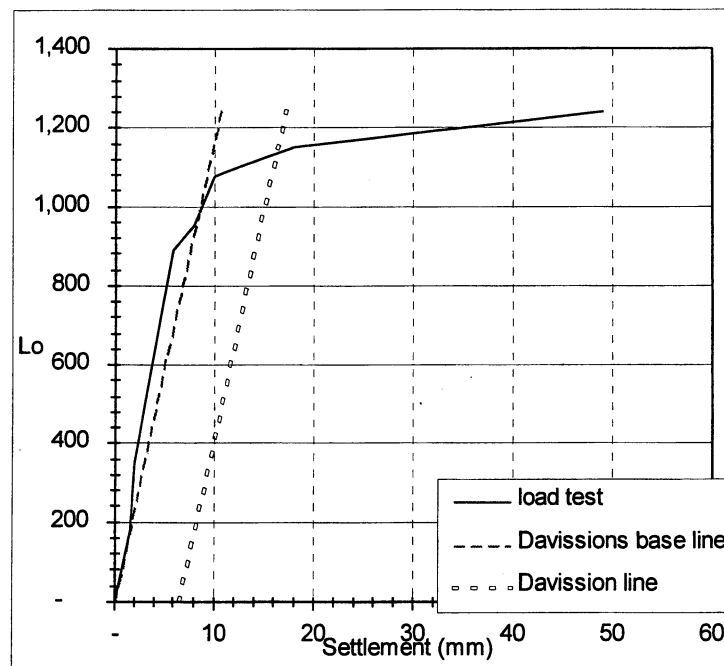


Figure 20: Example of the Davisson method

2. Plot the Davisson line parallel to the base line. The distance between the two lines is

$$0.15 + \frac{B}{120} \text{ (in)}$$

3. The intersection of that line and the load test graph represents the Davisson capacity.

Davisson method is most suitable for quick load tests on friction piles. For end bearing piles, as the load test curve does not flatten, the Davisson method is usually not applicable.

### 1.2.3. Other Methods

The pile capacity can be at a point where the settlement of the pile is 5% of its diameter. (or 2%, 3%, or even 10% depending on the pile shape and load test procedure). These methods are very simple. However, they do not account for the length and the material of the pile.

### 1.3. Soil Properties Correlated from Insitu Tests

About 95% of the soil data from the database are from SPT and CPT tests. Moreover, the  $\alpha$ ,  $\beta$ ,  $\lambda$  and the Nordlund method all use the angle friction  $\phi$  and/or the undrained shear strength  $S_u$  or the over-consolidation ratio OCR. Therefore, correlations are required to obtain these properties from the SPT and CPT tests.

There are usually two or more correlations for the same property. Therefore, in the following, the capacities are predicted based on the various different correlations available.

The correlations used in this study to get engineering soil properties from SPT are presented in Table 6. Similarly, Table 7 shows the correlations to get engineering soil properties from CPT.

Table 6: Correlations of soil properties from SPT

Properties	From SPT	Figure	Reference	
$\phi$	Peck, Hanson and Thornburn: $\approx 54 - 27.6034 \exp(-0.014N')$	2'	Figure 4.12	Kulhawy and Mayne, 1990
	Schmertmann $\phi'$ $\approx \tan^{-1} [ N / (12.2 + 20.3 \sigma') ]$ 0.34	22	Figure 4.13 and Equation 4.11	
$S_u$ (bar)	Terzaghi and Peck (1967): 0.06 N		Equation 4.59	
	Hara 1974: $0.29 N^{0.72}$		Equation 4.60	
OCR for clay	Mayne and Kemper $\approx 0.5 N / \sigma'_o$ ( $\sigma'_o$ in bar)	23	Figures 3.9 and 3.18	
$D_r$	Gibbs and Holtz's Figures	24	Figures 2.13 and 2.14	

where: N is the uncorrected blow counts, and

$N'$  is the corrected blow counts

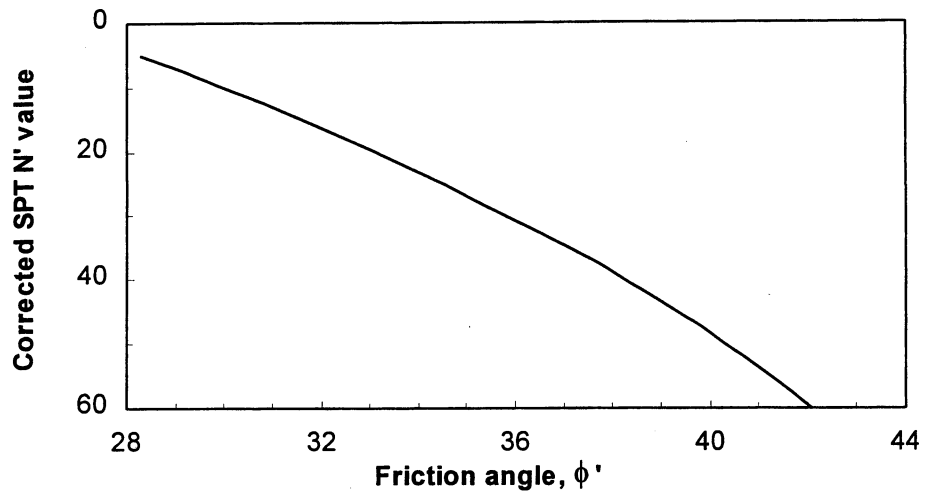


Figure 21:  $\phi'$  by Peck, Hanson and Thornburn (Kulhawy and Mayne, 1990)

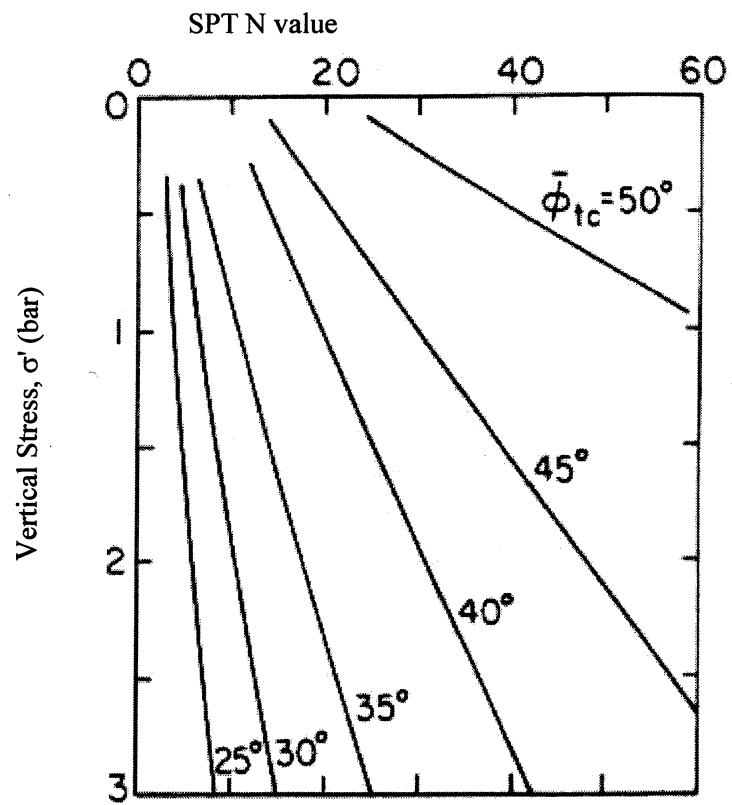


Figure 21:  $\phi'$  by Schmertmann (Kulhawy and Mayne, 1990)

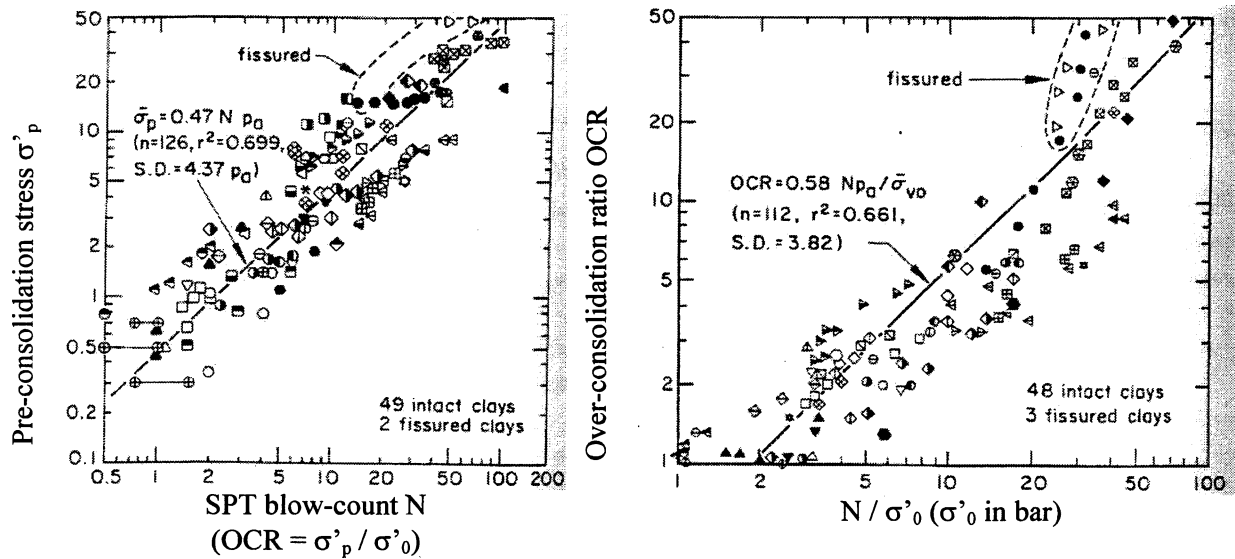


Figure 22: OCR--N Relationship (Kulhawy and Mayne, 1990)

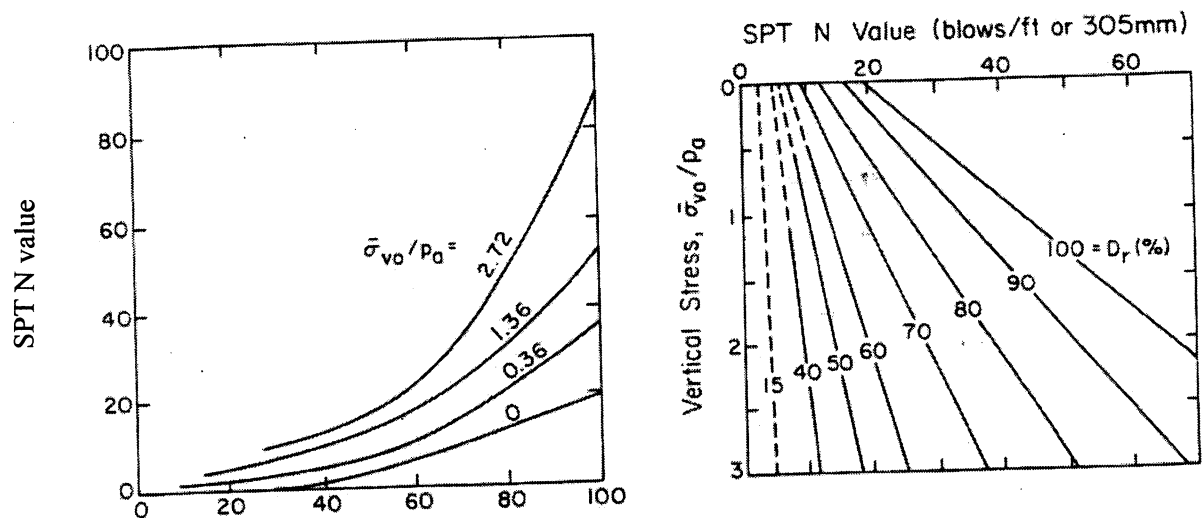
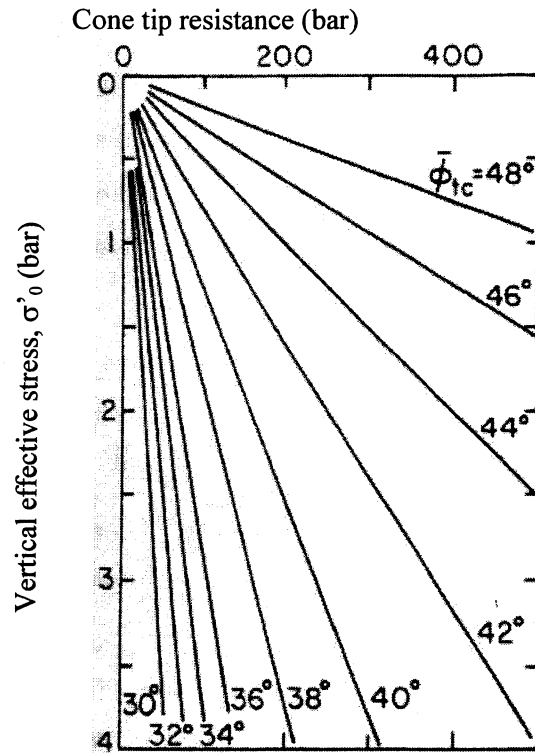


Figure 23: Relative Density--N--Stress Relationship (Kulhawy and Mayne, 1990)

Table 7. Correlations of soil properties from CPT

Properties	From CPT	Figure	Reference	
$\phi$	Robertson and Campanella: $\text{atan}(0.1+0.38*\text{Log}(q_c/\sigma'))$	25	Figure 4.14 and Equation 4.12	Kulhawy and Mayne, 1990
$S_u$ (bar)	Theoretical: $(q_c - \sigma_o) / Nk$ $q_c$ and $\sigma_o$ in bars.		Equation 4.61	
OCR for clay	Mayne: $0.29 q_c / \sigma'_o$ $q_c$ and $\sigma_o$ in bars.	27	Figure 3.10	
Dr	Jamiolkowski: $68 \log(q_{cn}) - 68$ $q_{cn} = \frac{q'_c}{\sqrt{P_a \sigma'_o}}$ (dimensionless) $q'_c = q_c / K_q$ $K_q = 0.9 + \text{Dr}/300$ $q_c$ and $\sigma'_o$ in bars.	26	Figure 2.24 and Equation 2.20	

Figure 24:  $\phi'_{tc}$  correlated from  $q_c$  for NC, uncemented quartz sands (Kulhawy and Mayne, 1990)

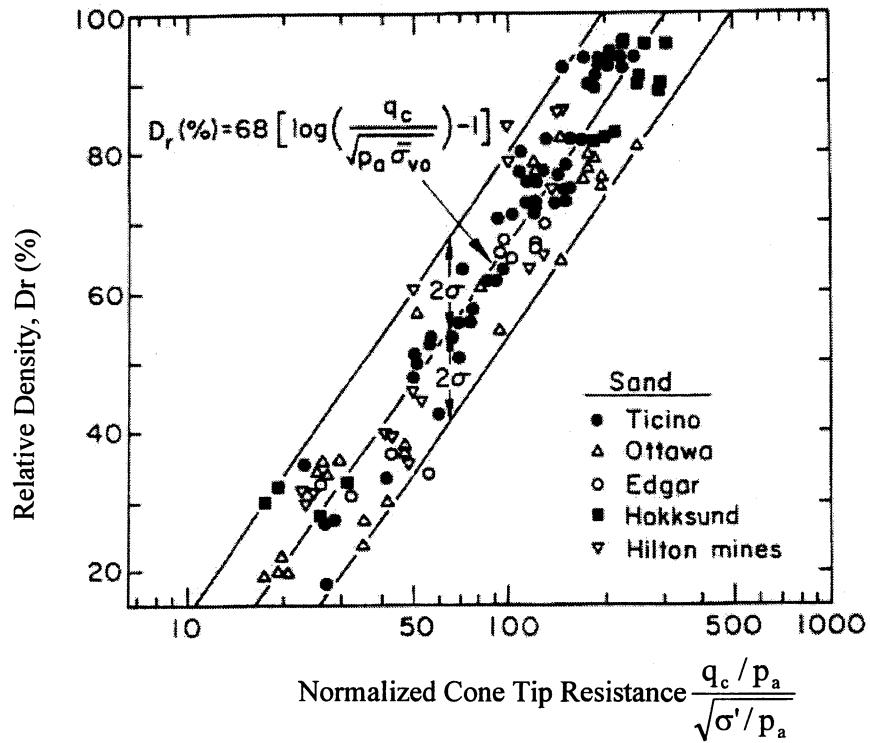


Figure 25: Correlation between  $D_r$  and  $q_c$  (uncorrected for boundary effect) (Kulhawy and Mayne, 1990)

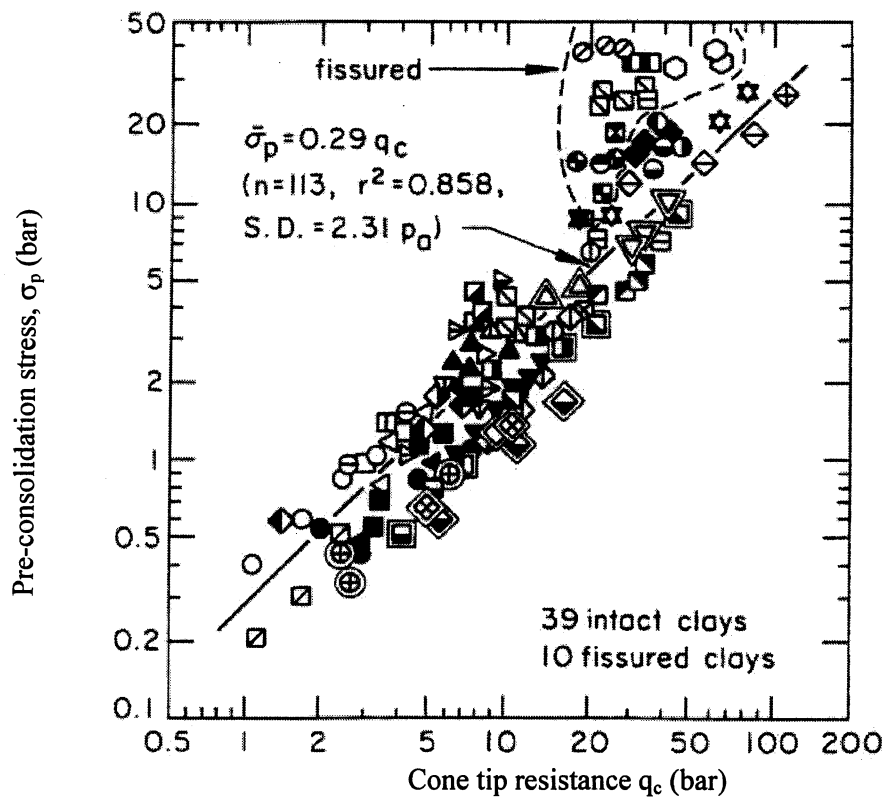


Figure 26:  $\sigma_p$  correlated with  $q_c$  ( $OCR = \sigma_p / \sigma'_0$ ) (Kulhawy and Mayne, 1990)



## LIST OF REFERENCES

- American Association of State Highway and Transportation Officials (ASSHTO) (1996/2000). LRFD Bridge Design Specifications, 2<sup>nd</sup> Edition--2000 Interim Revisions. Washington, DC
- Bowles, J. (1996). Foundation Analysis and Design. McGraw-Hill. New York.
- Coduto, D. (2001). Foundation Design, 2<sup>nd</sup> Edition. Prentice Hall. Upper Saddle River, New Jersey.
- Federal Highway Administration (FHWA) (1998). "DRIVEN" Manual. Mathias, D. and Cribbs, M. Blue-Six Software, Inc. Logan, UT.
- Hannigan, P.J., Goble, G.G., Thendean, G., Likins, G.E. and Rausche, F. (1995). Design and Construction of Driven Pile Foundation. FHWA. Washington, D.C.
- Kulhawy, F.H. and Mayne, P.W. (1990). Manual on Estimating of Soil Properties for Foundation Design. Electric Power Research Institute. Palo Alto, California.
- Lai P. and Graham K. (1995). Static Pile Bearing Analysis Program--SPT94. <http://www.dot.state.fl.us/structures/manuals/spt94.zip>. Downloaded in May 2001.
- McVay, M.C. and Townsend, F.C. (1989). Short Course/ Workshop Guide for PC Software Support for Design and Analysis of Deep and Shallow Foundations from In-situ Tests (or PL-AID Manual). University of Florida. Gainesville, Florida.
- McVay, M.C., Kuo, C.L. and Singletary, W.A. (1998). Calibrating Resistance Factors in the Load and Resistance Factor Design for Florida Foundations. Gainesville, Florida.
- Meyerhof, G. (1976/1981). The Bearing Capacity and Settlement of Foundations. Technical University of Nova Scotia. Halifax, Canada.
- Reese, L.C., Wang, S.C. and Arrellaga, J. (1998). APILE Plus 3.0 Manual. EnSoft, Inc. Austin, Texas.
- Tomlinson, M.J. (1980/1995). Foundation Design and Construction, 6<sup>th</sup> Edition. Longman Scientific & Technical. Essex, England.
- US Army Corps of Engineers, No.7, EM 1110-1-1905 (1992). Bearing Capacity of Soil, Technical Engineering and Design Guides. Adapted by ASCE--2000. ASCE Press. New York.
- Withiam, J., Voytko, E., Barker, R., Duncan, M., Kelly, B., Musser, S. and Elias, V. (1997). Participant Workbook Load and Resistance Factor Design (LRFD) for Highway Bridge Substructures. FHWA. Washington, D.C.

# **DRILLED SHAFTS – STATIC ANALYSIS**

## **SUMMARY OF RESISTANCE FACTORS**

### Resistance Factor, $\phi$ of Drilled Shaft for $Q_D/Q_L = 2.0$

	Soil Type	Design Method	Construction Method	No. of Data	Bias Factor $\lambda_R$	$COV_R$	Resistance Factors					
							$\beta_T = 2.0$		$\beta_T = 2.5$		$\beta_T = 3.0$	
							$\phi$	$\phi/\lambda$	$\phi$	$\phi/\lambda$	$\phi$	$\phi/\lambda$
Skin Friction + End Bearing	Sand	FHWA	Mixed	34	1.93	0.69	0.49	0.25	0.34	0.18	0.24	0.12
			Casing	14	2.47	0.5	0.91	0.37	0.71	0.29	0.55	0.22
			Slurry	14	2.04	0.86	0.37	0.18	0.24	0.12	0.16	0.08
		R&W	Mixed	34	1.42	0.81	0.28	0.20	0.19	0.13	0.13	0.09
			Casing	14	1.93	0.72	0.46	0.24	0.32	0.17	0.22	0.11
			Slurry	14	1.32	1.18	0.12	0.09	0.07	0.05	0.04	0.03
	Clay	FHWA	Mixed	54	0.95	0.54	0.32	0.34	0.25	0.26	0.19	0.20
			Casing	14	0.99	0.71	0.24	0.24	0.17	0.17	0.12	0.12
			Dry	40	0.88	0.48	0.34	0.39	0.27	0.31	0.21	0.24
	Sand + Clay	FHWA	Mixed	48	1.33	0.45	0.54	0.41	0.43	0.32	0.34	0.26
			Casing	23	1.21	0.53	0.42	0.35	0.32	0.26	0.25	0.21
			Dry	13	1.47	0.44	0.61	0.41	0.49	0.33	0.39	0.27
			Slurry	12	1.43	0.39	0.66	0.46	0.54	0.38	0.44	0.31
		R&W	Mixed	48	1.19	0.45	0.48	0.40	0.39	0.33	0.31	0.26
			Casing	23	1.07	0.48	0.41	0.38	0.32	0.30	0.25	0.23
			Dry	13	1.36	0.47	0.53	0.39	0.42	0.31	0.33	0.24
			Slurry	12	1.28	0.37	0.61	0.48	0.51	0.40	0.42	0.33
	All Soils	FHWA	Mixed	136	1.32	0.69	0.33	0.25	0.24	0.18	0.17	0.13
		R&W	Mixed	136	1.28	0.66	0.34	0.27	0.25	0.20	0.18	0.14
	Rock	C&K	Mixed	49	1.37	0.55	0.46	0.34	0.35	0.26	0.26	0.19
			Dry	32	1.50	0.56	0.49	0.33	0.37	0.25	0.28	0.19
		IGM	Mixed	49	1.42	0.46	0.57	0.40	0.45	0.32	0.36	0.25
			Dry	32	1.53	0.45	0.62	0.41	0.50	0.33	0.40	0.26

	Soil Type	Design Method	Construction Method	No. of Data	Bias Factor $\lambda_R$	$COV_R$	Resistance Factors					
							$\beta_T = 2.0$		$\beta_T = 2.5$		$\beta_T = 3.0$	
							$\phi$	$\phi/\lambda$	$\phi$	$\phi/\lambda$	$\phi$	$\phi/\lambda$
Skin	Sand	FHWA	Mixed	11	1.09	0.51	0.39	0.36	0.30	0.28	0.24	0.22
		R&W	Mixed	11	0.83	0.54	0.28	0.34	0.22	0.27	0.16	0.19
	Clay	FHWA	Mixed	16	0.87	0.37	0.42	0.48	0.34	0.39	0.29	0.33
	Sand & Clay	FHWA	Mixed	13	1.49	0.49	0.56	0.38	0.44	0.30	0.34	0.23
		R&W	Mixed	16	1.35	0.49	0.51	0.38	0.40	0.30	0.31	0.23
	All Soils	FHWA	Mixed	40	1.16	0.53	0.40	0.34	0.31	0.27	0.24	0.21
		R&W	Mixed	27	1.14	0.55	0.38	0.33	0.29	0.25	0.22	0.19
	Rock	C&K	Mixed	17	1.33	0.62	0.38	0.29	0.28	0.21	0.21	0.16
		IGM	Mixed	17	1.39	0.53	0.48	0.35	0.37	0.27	0.28	0.20

#### Methodology and Correlations:

- 1.) FHWA Method, i.e., Reese, L. C. and M. W. O'Neill (1988) "Drilled Shaft: Construction Procedures and Design Methods", FHWA-HI-88-042 for Sands and Clays.  
For Sands,  $\beta$  method was used.  
For Clays,  $\alpha$  method was used. For Su, the SPT correlation given by Terzaghi and Peck (1967) was used.
- 2.) R & W Method, i.e., Reese, L. C. and S. J. Wright (1977) "Construction Procedures and Design for Axial Loading.", Drilled Shaft Manual HDV-22, for Sand.  
In Sand-Clay Mix Deposit,  $\alpha$  method was used for Clays
- 3.) C & K Method, i.e., Carter, J. P. and F. H. Kulhawy (1988) "Analysis and Design of Foundations Socketed into Rock," Report Number EL-5918 for Rock.
- 4.) IGM Method (Intermediate Geomaterials), i.e., O'Neill, et al (1996) "Load Transfer for Drilled Shafts in Intermediate Geomaterials" FHWA-RD-95-172, and O'Neill, M. W. and L. C. Reese (1999) 'Drilled Shaft: Construction Procedures and Design Methods', FHWA-IF-99-025.  
The design assumed smooth rock socket for skin friction and closed joints for end bearing.

# **DRILLED SHAFTS – STATIC ANALYSIS**

## **RESULTS AND STATISTICS**

- Summary Table of the Cases analyzed, their statistical parameters and related figure number
- Detailed Table of Shafts (Total Resistance) in Soils and related figures (1-19)
- Detailed Table of Shafts (Skin Friction) in Soils and related figures (20-26)
- Detailed Table of Shafts (Total Resistance) in Rock and related figures (27-30)
- Detailed Table of Shafts (Skin Friction) in Rock and related figures (31-32)

FIGURE	SOIL TYPE	NO. OF DATA	CONSTRUCTION METHOD	DESIGN METHOD	LOAD TRANSFER	MEAN	STDV	VAR
1	Sand	34	Mixed	FHWA	Total	1.93	1.34	0.69
2	Clay	54	Mixed	FHWA	Total	0.95	0.51	0.54
3	Sand & Clay	48	Mixed	FHWA	Total	1.33	0.60	0.45
4	Total Soil	136	Mixed	FHWA	Total	1.32	0.91	0.69
5	Sand	34	Mixed	R & W	Total	1.42	1.14	0.81
6	Sand & Clay	48	Mixed	R & W	Total	1.19	0.53	0.45
7	Total Soil	136	Mixed	R & W	Total	1.28	0.84	0.66
8	Sand & Clay	23	Casing	FHWA	Total	1.21	0.64	0.53
9	Sand & Clay	23	Casing	R & W	Total	1.07	0.51	0.48
10	Sand & Clay	13	Dry	FHWA	Total	1.47	0.64	0.44
11	Sand & Clay	13	Dry	R & W	Total	1.36	0.64	0.47
12	Sand & Clay	12	Slurry	FHWA	Total	1.43	0.55	0.39
13	Sand & Clay	12	Slurry	R & W	Total	1.28	0.47	0.37
14	Sand	14	Casing	FHWA	Total	2.47	1.24	0.50
15	Sand	14	Casing	R & W	Total	1.93	1.39	0.72

16	Sand	14	Slurry	FHWA	Total	2.04	1.75	0.86
17	Sand	14	Slurry	R & W	Total	1.32	1.55	1.18
18	Clay	14	Casing	FHWA	Total	0.99	0.70	0.71
19	Clay	40	Dry	FHWA	Total	0.88	0.42	0.48
20	Sand	11	Mixed	FHWA	Skin	1.09	0.56	0.51
21	Clay	13	Mixed	FHWA	Skin	0.87	0.32	0.37
22	Sand & Clay	16	Mixed	FHWA	Skin	1.49	0.72	0.49
23	Total Soil	40	Mixed	FHWA	Skin	1.16	0.62	0.53
24	Sand	11	Mixed	R & W	Skin	0.83	0.45	0.54
25	Sand & Clay	16	Mixed	R & W	Skin	1.35	0.66	0.49
26	Total Soil	27	Mixed	R & W	Skin	1.14	0.63	0.55
27	Rock	49	Mixed	C & K	Total	1.37	0.75	0.55
28	Rock	49	Mixed	IGM	Total	1.42	0.64	0.46
29	Rock	32	Dry	C & K	Total	1.50	0.83	0.56
30	Rock	32	Dry	IGM	Total	1.53	0.69	0.45
31	Rock	17	Mixed	C & K	Skin	1.33	0.82	0.62
32	Rock	17	Mixed	IGM	Skin	1.39	0.74	0.53

NOTE:

1. SOIL TYPE – SAND - SHAFT PRIMARILY IN SAND DEPOSIT  
CLAY - SHAFT PRIMARILY IN CLAY DEPOSIT  
SAND & CLAY – SHAFT IN SAND & CLAY MIXED DEPOSIT  
TOTAL – ALL SHAFTS IN SOIL DEPOSIT  
ROCK - SHAFT PRIMARILY IN ROCK DEPOSIT
2. CONSTRUCTION METHOD - MIXED- INCLUDE ALL CONSTRUCTION METHODS  
CASING – SHAFT USED CASING  
DRY – SHAFT USED DRY METHOD  
SLURRY – SHAFT USED SLURRY
3. LOAD TRANSFER - TOTAL – ALL SHAFTS  
SKIN – SHAFT CAPACITY PRIMINARILY IS SIDE FRICTION
4. DETAIL DATA SEE EXCEL FILES:  
  
SHAFT-SOIL.XLS – ALL SHAFTS IN SOIL DEPOSIT, **(FIGURES 1 TO 19)**  
SOIL.SKIN.XLS – SHAFT CAPACITY PRIMARILY IS SIDE FRICTION OF SAND DEPOSIT, **(FIGURES 20 TO 26.)**  
SHAFT-ROCK.XLS – ALL SHAFT IN ROCK DEPOSIT,( **FIGURES 27 TO 30)**  
ROCK-SKIN.XLS – SHAFT CAPACITY PRIMARY IS SIDE FRICTION OF ROCK DEPOSIT. **(FIGURES 31 TO 32)**



Table		Failure		FHWA	FHWA	W&R	W&R
SHAFT #	Construction	Load (kips)	Soil Type	Predict(kips)	Ratio	Predict(kips)	Ratio
1	Casing	400	A	594	0.67	676.00	0.59
4	Casing	2000	A	1964	1.02	2058.00	0.97
5	Casing	180	A	126.82	1.42	175.56	1.03
6	Casing	322	A	370	0.87	426.00	0.76
7	Casing	324	A	412	0.79	662.00	0.49
10	Casing	240	A	304.66	0.79	336.48	0.71
12	Casing	10.8	A	8.62	1.25	7.60	1.42
13	Casing	18	A	12	1.50	12.06	1.49
14	Casing	140	A	154.3	0.91	163.90	0.85
15	Casing	140	A	126.46	1.11	145.62	0.96
16	Casing	750	A	610	1.23	637.66	1.18
17	Casing	560	A	375.3	1.49	402.10	1.39
18	Casing	1100	A	1250	0.88	1282.00	0.86
19	Casing	1160	A	725.66	1.60	727.08	1.60
20	Casing	1080	A	923.24	1.17	949.72	1.14
21	Casing	400	A	477.34	0.84	507.78	0.79
22	Casing	1700	A	548	3.10	679.24	2.50
23	Casing	1100	A	379.48	2.90	502.28	2.19
24	Casing	670	A	625.08	1.07	677.94	0.99
25	Casing	360	A	616.12	0.58	827.00	0.44
31	Casing	980	A	837.04	1.17	963.20	1.02
33	Casing	600	A	644.3	0.93	749.10	0.80
36	Casing	760	A	1444	0.53	1582.00	0.48
37	Dry	2000	A	1136	1.76	1606.00	1.25
38	Dry	1474	A	1293.28	1.14	1635.78	0.90
41	Dry	1418	A	1408	1.01	1819.30	0.78
53	Dry	1900	A	2056	0.92	1886.00	1.01
54	Dry	2200	A	1620	1.36	1302.00	1.69
56	Dry	860	A	872.46	0.99	1038.04	0.83
57	Dry	750	A	990	0.76	1060.00	0.71
85	Dry	184	A	118.58	1.55	141.40	1.30
95	Dry	2400	A	758	3.17	798.00	3.01
98	Dry	2000	A	1138	1.76	1218.00	1.64
153	Dry	1200	A	662	1.81	691.30	1.74
154	Dry	1080	A	732	1.48	762.94	1.42
155	Dry & Casing	1100	A	658.26	1.67	686.92	1.60

#### TOTAL SHAFT in SOIL

FHWA Method				
	Soil Type			
	A	B	C	ALL
Mean	1.33	1.93	0.95	1.32
Stdv	0.60	1.34	0.51	0.91
Var	0.45	0.69	0.54	0.69

R & W Method				
	Soil Type			
	A	B		ALL
Mean	1.19	1.42		1.28
Stdv	0.53	1.14		0.84
Var	0.45	0.81		0.66

#### NOTE:

SOIL TYPE A = SAND & CLAY

SOIL TYPE B = SAND

SOIL TYPE C = CLAY

TYPE A SOIL in CASING		
	FHWA	R&W
MEAN	1.21	1.07
STDV	0.64	0.51
VAR	0.53	0.48

TYPE A SOIL in DRY Method		
	FHWA	R&W
MEAN	1.47	1.36
STDV	0.64	0.64
VAR	0.44	0.47

229	Slurry	2146	A	1742	1.23	1902.00	1.13
230	Slurry	2194	A	1390	1.58	1550.00	1.42
231	Slurry	2644	A	1768	1.50	1930.00	1.37
232	Slurry	1708	A	958	1.78	1118.00	1.53
233	Slurry	2644	A	984	2.69	1118.00	2.36
234	Slurry	1596	A	958	1.67	1118.00	1.43
235	Slurry	1596	A	1418	1.13	1578.00	1.01
236	Slurry	1596	A	1768	0.90	1930.00	0.83
237	Slurry	1590	A	1742	0.91	1902.00	0.84
156	Slurry	820	A	920.74	0.89	955.24	0.86
227	Slurry & Casing	452	A	378	1.20	632.00	0.72
228	Slurry & Casing	900	A	574	1.57	914.00	0.98
9	Casing	108	B	95.78	1.13	131.20	0.82
11	Casing	380	B	232.9	1.63	483.30	0.79
27	Casing	1080	B	300.72	3.59	277.82	3.89
28	Casing	1500	B	304.14	4.93	281.52	5.33
29	Casing	390	B	185.5	2.10	347.34	1.12
30	Casing	900	B	373.12	2.41	608.94	1.48
32	Casing	356	B	397.2	0.90	735.96	0.48
34	Casing	940	B	904	1.04	924.00	1.02
35	Casing	2000	B	497.24	4.02	834.62	2.40
43	Casing	2400	B	648.96	3.70	823.90	2.91
45	Casing	1980	B	844	2.35	1306.74	1.52
52	Casing	1340	B	609.94	2.20	781.40	1.71
58	Casing	1620	B	746.6	2.17	977.94	1.66
59	Casing & Slurry	1880	B	1311.16	1.43	2071.96	0.91
60	Dry	1900	B	1114	1.71	1204.00	1.58
64	Dry	1300	B	736	1.77	1130.00	1.15
65	Dry	990	B	994	1.00	1188.00	0.83
66	Dry	930	B	688	1.35	956.00	0.97
67	Dry	1380	B	814	1.70	1466.00	0.94
82	Dry & Casing	1880	B	3762	0.50	5900.00	0.32
83	Slurry	2464	B	992	2.48	1414.00	1.74
89	Slurry	131.2	B	72.78	1.80	138.98	0.94
112	Slurry	1000	B	246	4.07	398.00	2.51

TYPE A SOIL in SLURRY		
	FHWA	R&W
MEAN	1.43	1.28
STDV	0.55	0.47
VAR	0.39	0.37

TYPE B SOIL in CASING		
	FHWA	R&W
MEAN	2.47	1.93
STDV	1.24	1.39
VAR	0.50	0.72

TYPE B SOIL in SLURRY		
	FHWA	R&W
MEAN	2.04	1.32
STDV	1.75	1.55
VAR	0.86	1.18

TYPE C SOIL in CASING		
	FHWA	R&W
MEAN	0.99	n/a
STDV	0.70	n/a
VAR	0.71	n/a

TYPE C SOIL in DRY METHOD		
	FHWA	R&W
MEAN	0.88	n/a
STDV	0.42	n/a
VAR	0.48	n/a

113	Slurry	1800	B	306	5.88	468.00	3.85
123	Slurry	70	B	52.3	1.34	103.48	0.68
124	Slurry	84	B	52.3	1.61	103.48	0.81
163	Slurry	420	B	214	1.96	266.00	1.58
164	Slurry	76	B	326	0.23	400.00	0.19
165	Slurry	118	B	234	0.50	400.00	0.30
175	Slurry	650	B	1202	0.54	1176.00	0.55
176	Slurry & Casing	800	B	860	0.93	836.00	0.96
177	Slurry & Casing	760	B	572	1.33	538.00	1.41
251	Slurry&Casing	116	B	632	0.18	930.00	0.12
252	Slurry&Casing	50	B	42	1.19	68.00	0.74
61	Casing	300	C	362	0.83		
62	Casing	710	C	362	1.96		
90	Casing	200	C	222	0.90		
91	Casing	200	C	208	0.96		
107	Casing	510	C	1552	0.33		
110	Casing	440	C	388	1.13		
131	Casing	4720	C	8418	0.56		
132	Casing	400	C	610	0.66		
133	Casing	400	C	133.28	3.00		
134	Casing	800	C	894.48	0.89		
148	Casing	200	C	290.9	0.69		
149	Casing	190	C	197.44	0.96		
151	Casing	1680	C	2552	0.66		
152	Casing	1512	C	4674	0.32		
162	Dry	1528	C	1618	0.94		
180	Dry	480	C	596	0.81		
181	Dry	720	C	552	1.30		
182	Dry	90	C	144	0.63		
183	Dry	220	C	820	0.27		
184	Dry	712	C	1138	0.63		
185	Dry	108	C	332	0.33		
186	Dry	200	C	360	0.56		
187	Dry	800	C	408	1.96		
188	Dry	1560	C	734	2.13		

189	Dry	1500	C	1390	1.08		
190	Dry	1700	C	1380	1.23		
191	Dry	1940	C	2432	0.80		
192	Dry	2000	C	2288	0.87		
193	Dry	1940	C	4024	0.48		
194	Dry	1940	C	3900	0.50		
195	Dry	760	C	698	1.09		
196	Dry	580	C	328	1.77		
197	Dry	1100	C	1360	0.81		
198	Dry	1180	C	942	1.25		
199	Dry	1100	C	1250	0.88		
200	Dry	400	C	408	0.98		
201	Dry	440	C	316	1.39		
202	Dry	360	C	422	0.85		
203	Dry	1800	C	1276	1.41		
204	Dry	1060	C	1118	0.95		
205	Dry	1060	C	1118	0.95		
206	Dry	800	C	1270	0.63		
207	Dry	800	C	1426	0.56		
208	Dry	980	C	1688	0.58		
209	Dry	1380	C	1368	1.01		
210	Dry	780	C	946	0.82		
211	Dry	950	C	1230	0.77		
212	Dry	800	C	1032	0.78		
213	Dry	988	C	1838	0.54		
238	Dry	7000	C	8304	0.84		
239	Dry	4400	C	11478	0.38		
240	Dry	4200	C	9738	0.43		
241	Dry	3700	C	11594	0.32		
242	Dry	4400	C	5178	0.85		

# DRILLED SHAFT IN SAND

CONSTRUCTION METHOD= MIXED  
LOAD TRANSFER= SKIN FRICTION + END BEARING  
N= 34  
MEAN=1.93  
STANARD DEVIATION = 1.34  
COEFFICIENT OF VARIATION =0.69

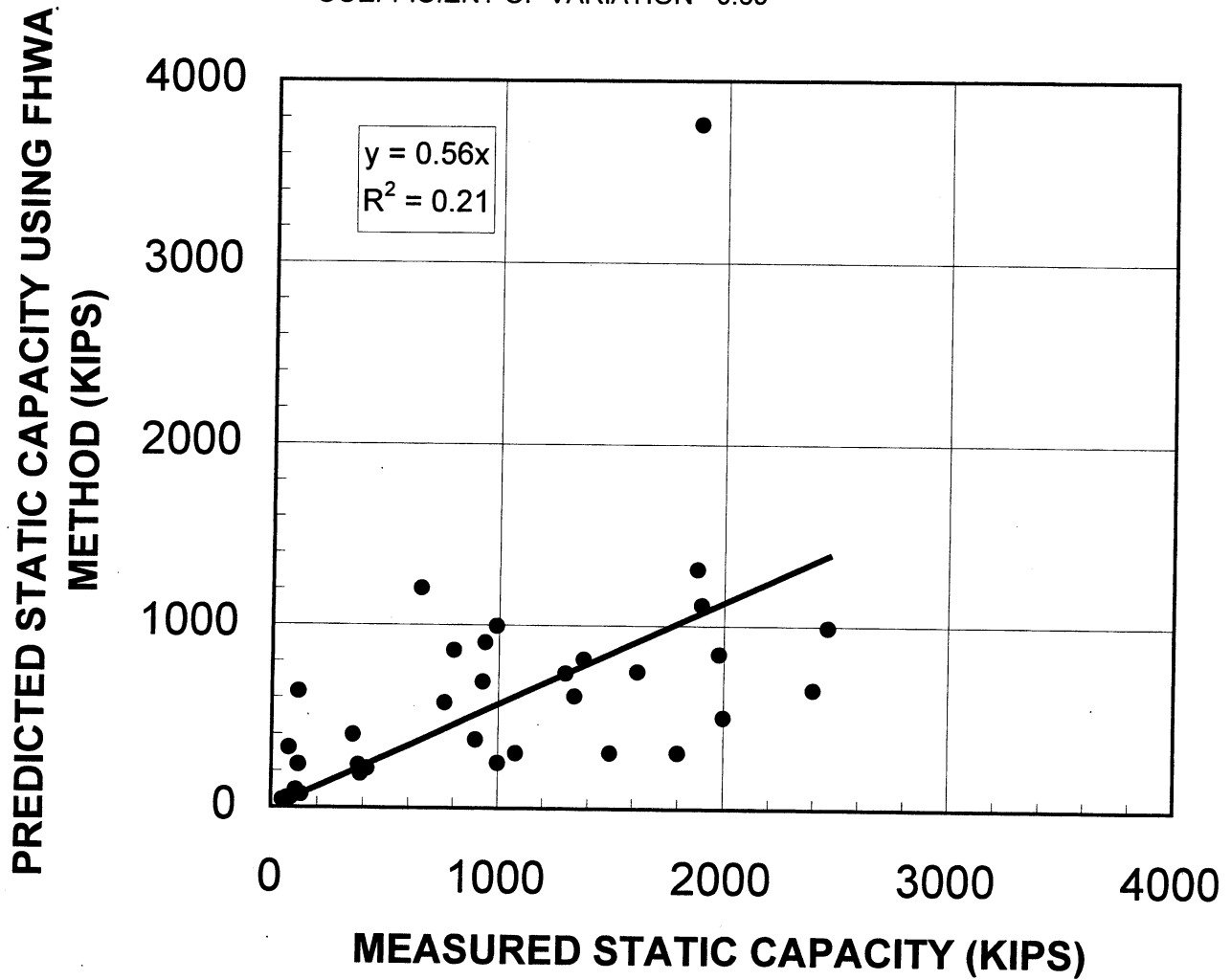


Figure 1

# DRILLED SHAFT IN CLAY

CONSTRUCTION METHOD= MIXED  
LOAD TRANSFER= SKIN FRICTION + END BEARING  
N= 54  
MEAN=0.95  
STANARD DEVIATION = 0.51  
COEFFICIENT OF VARIATION =0.54

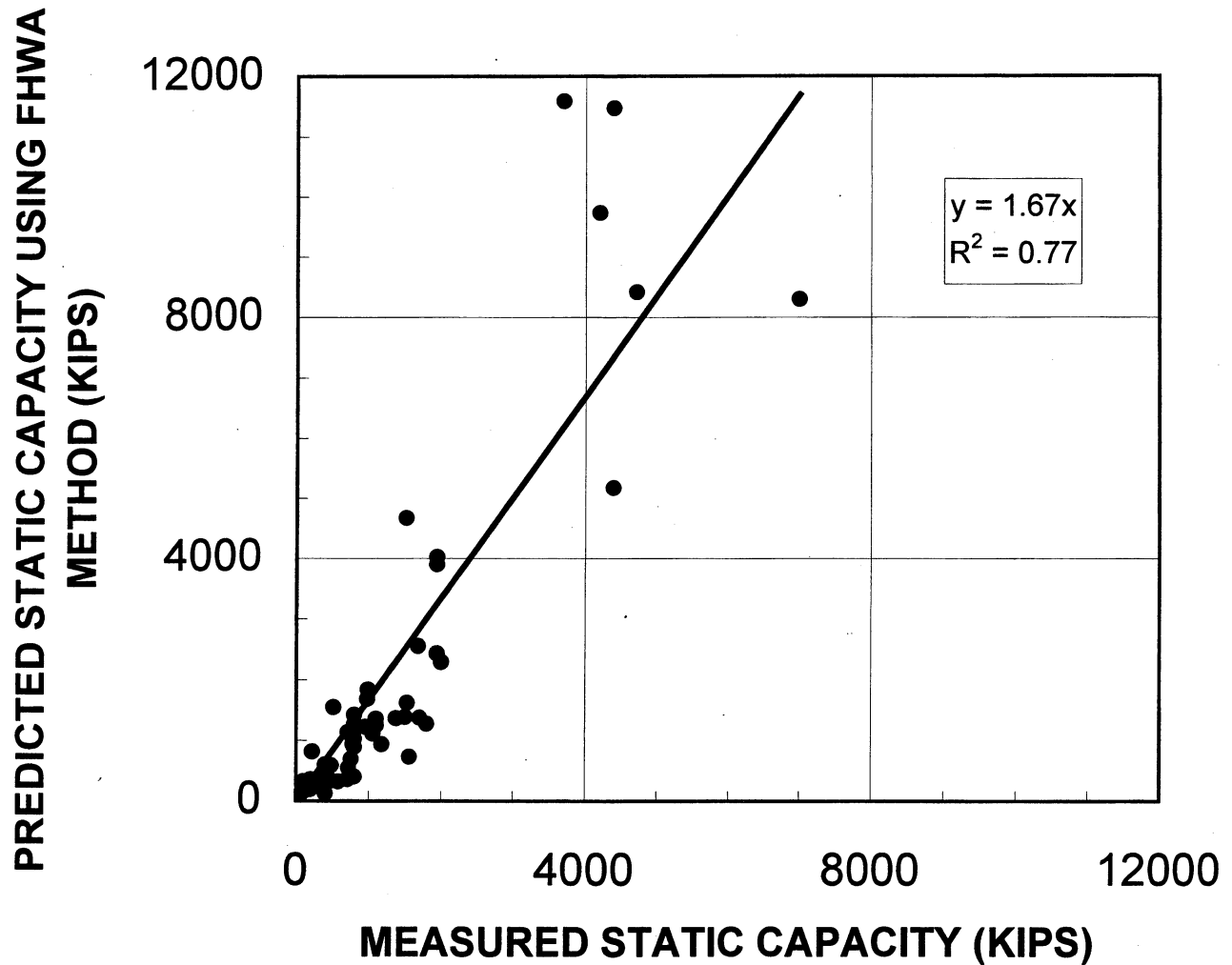


Figure 2

# DRILLED SHAFT IN SAND & CLAY

CONSTRUCTION METHOD= MIXED  
LOAD TRANSFER= SKIN FRICTION + END BEARING  
N= 48  
MEAN=1.33  
STANARD DEVIATION = 0.60  
COEFFICIENT OF VARIATION =0.45

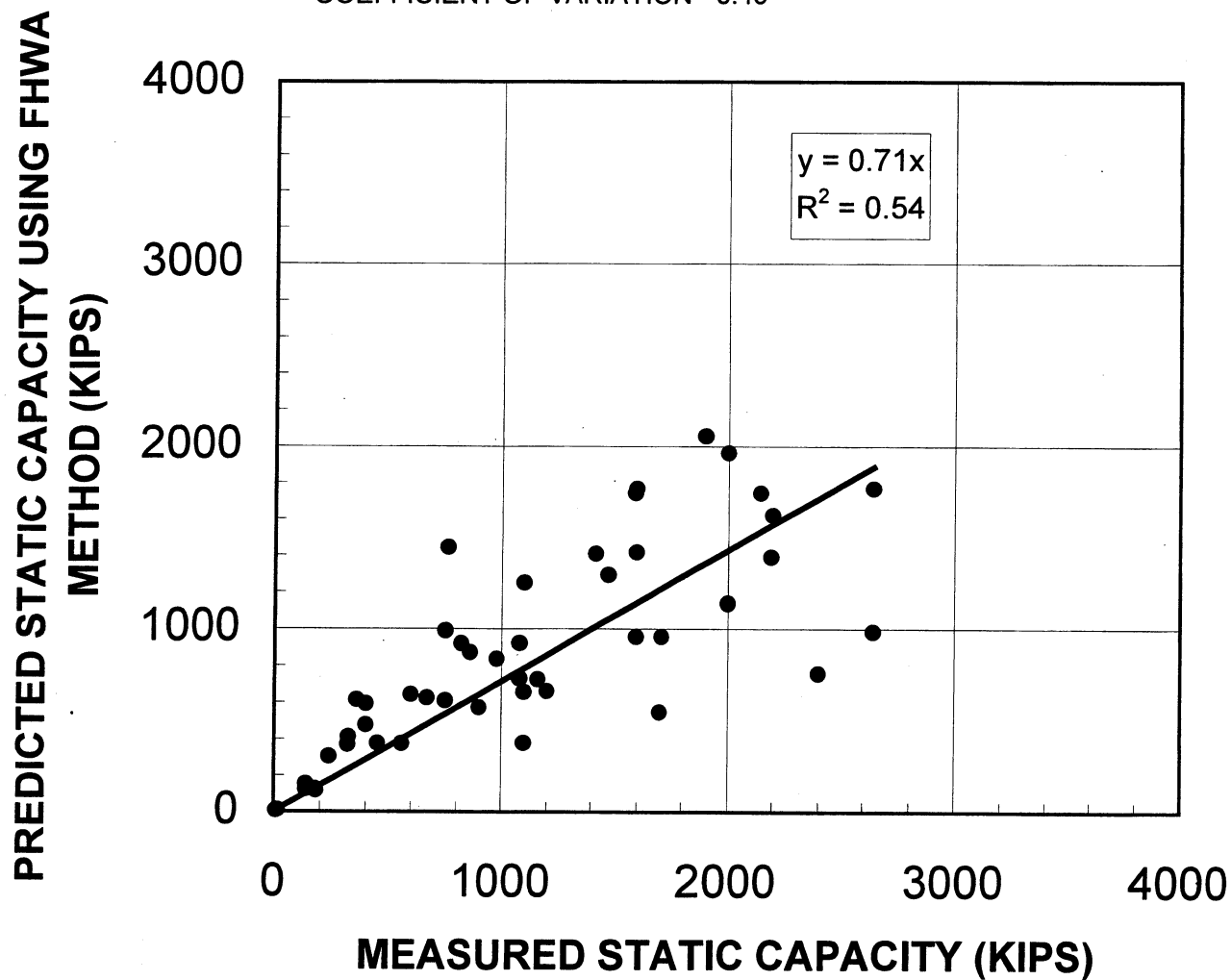


Figure 3

# TOTAL DRILLED SHAFT IN SOIL

CONSTRUCTION METHOD= MIXED  
LOAD TRANSFER= SKIN FRICTION + END BEARING  
N= 136  
MEAN=1.32  
STANARD DEVIATION =0.91  
COEFFICIENT OF VARIATION =0.69

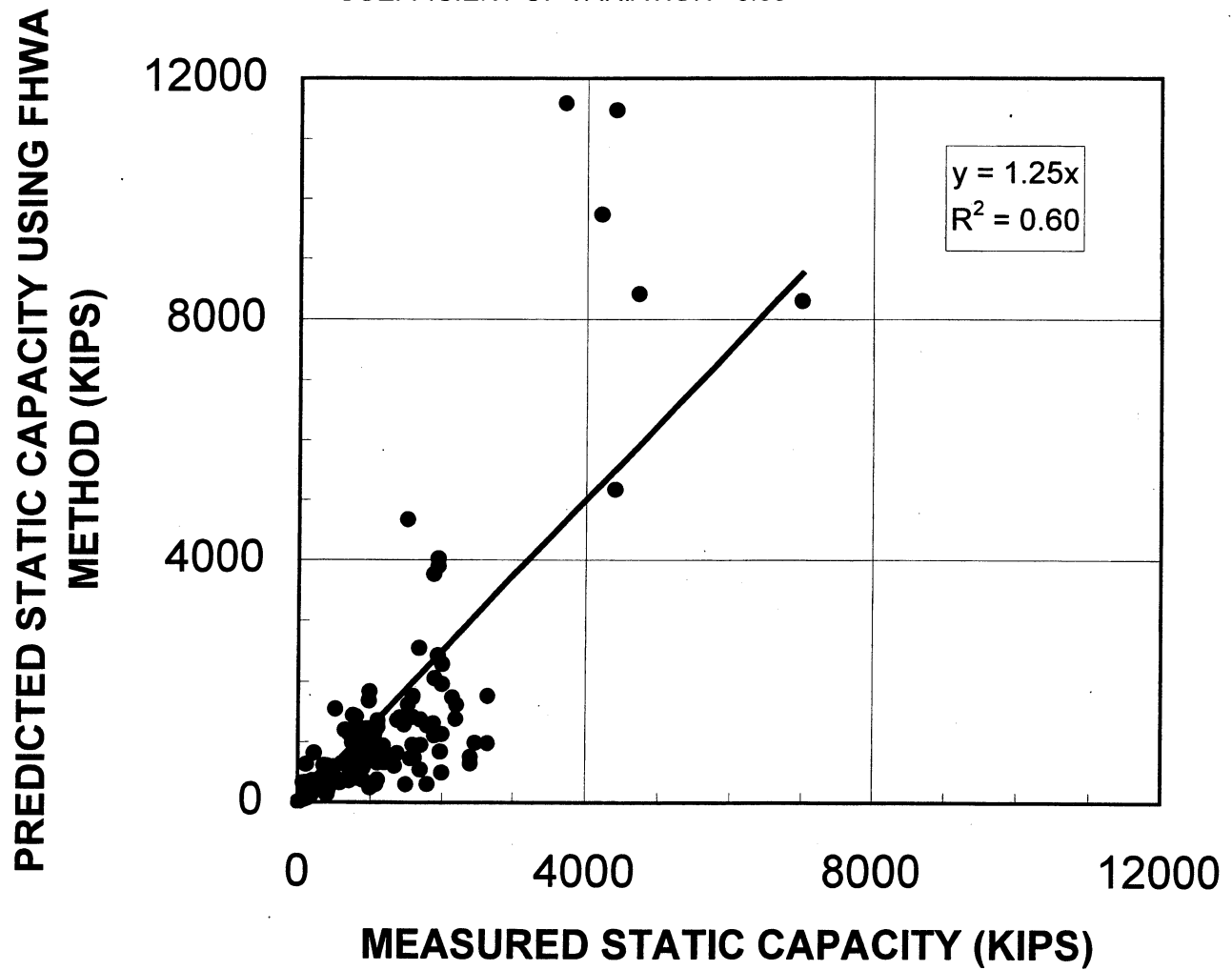


Figure 4



# DRILLED SHAFT IN SAND

CONSTRUCTION METHOD=MIXED  
LOAD TRANSFER= SKIN FRICTION + END  
BEARING  
N= 34  
MEAN=1.42  
STANARD DEVIATION = 1.14  
COEFFICIENT OF VARIATION =0.81

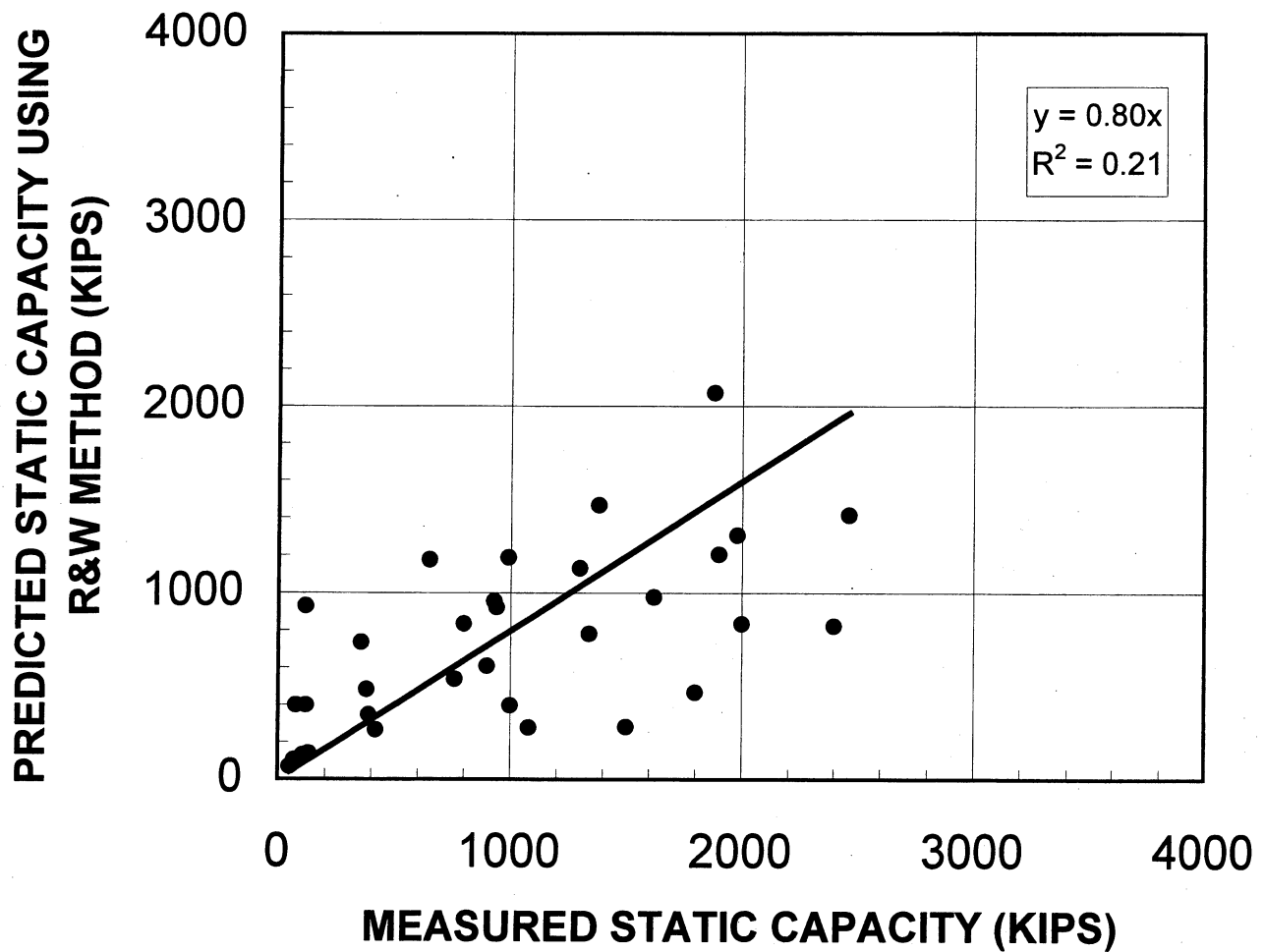


Figure 5

# DRILLED SHAFT IN SAND & CLAY

CONSTRUCTION METHOD= MIXED  
LOAD TRANSFER= SKIN FRICTION + END  
BEARING  
N= 48  
MEAN=1.19  
STANARD DEVIATION = 0.53  
COEFFICIENT OF VARIATION =0.45

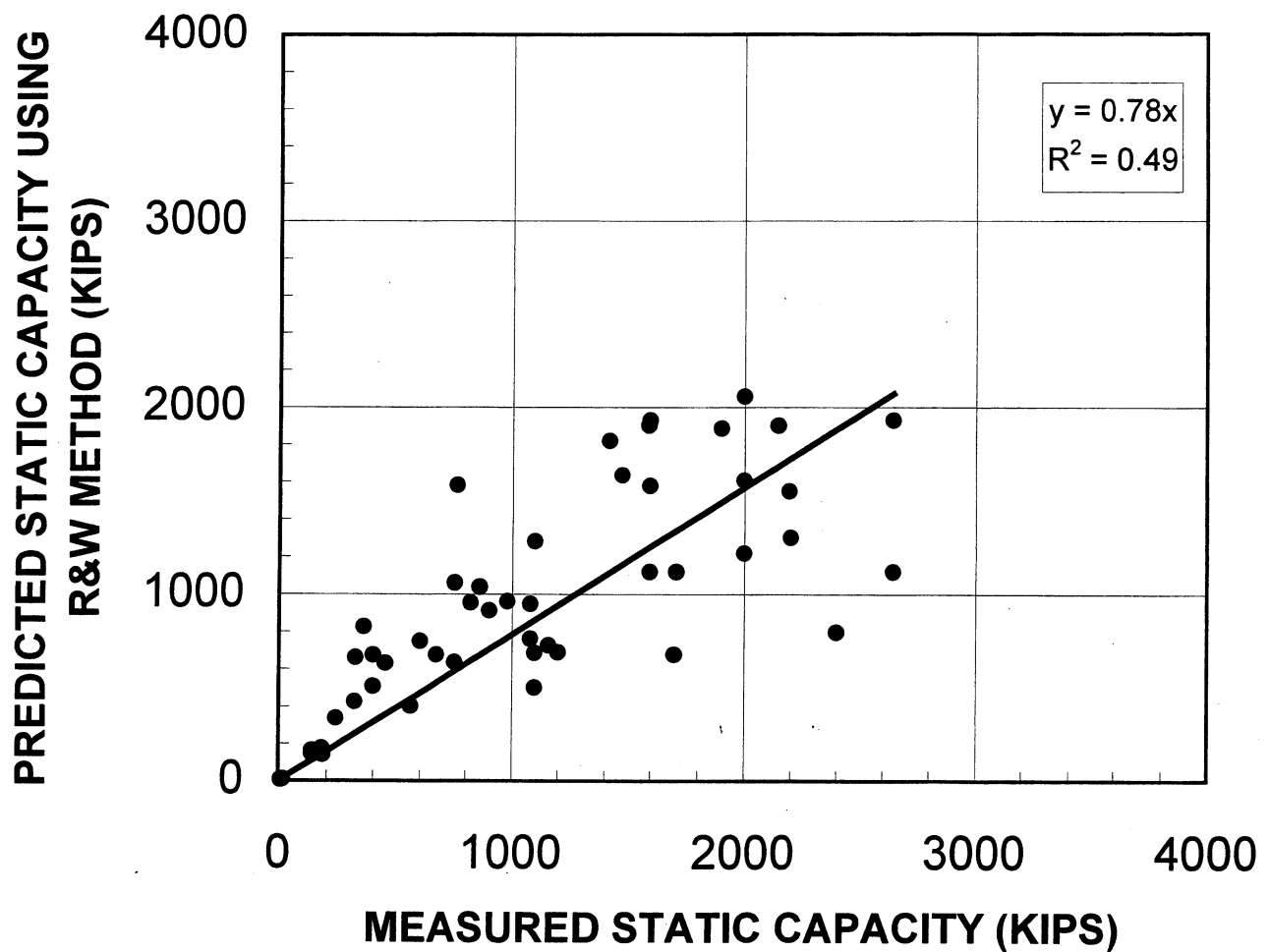


Figure 6

# TOTAL DRILLED SHAFT IN SOIL

CONSTRUCTION METHOD= MIXED  
LOAD TRANSFER= SKIN FRICTION + END BEARING  
N= 82  
MEAN=1.28  
STANARD DEVIATION =0.84  
COEFFICIENT OF VARIATION =0.66

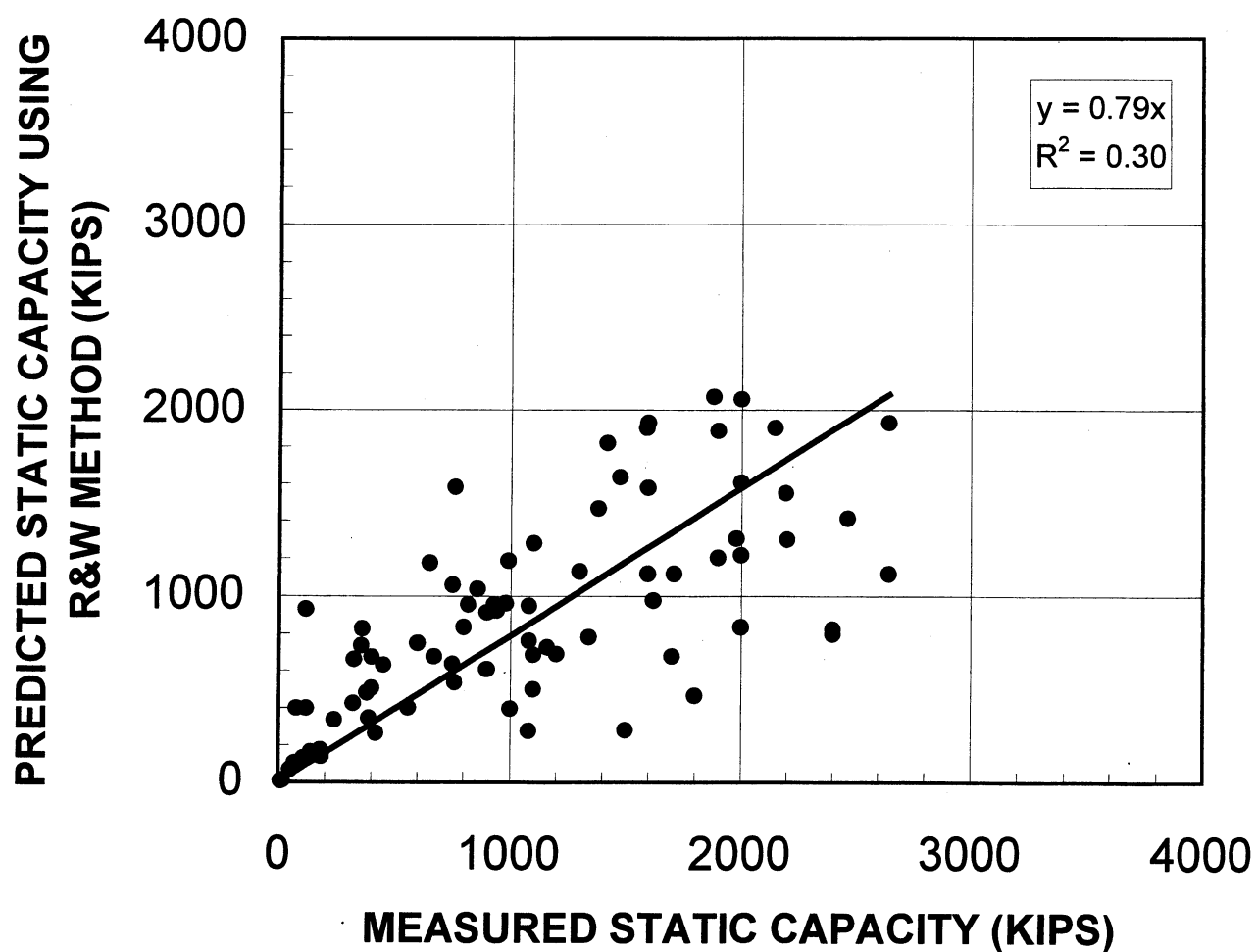


Figure 7

# DRILLED SHAFT IN SAND & CLAY

CONSTRUCTION METHOD= CASING  
LOAD TRANSFER= SKIN FRICTION + END BEARING  
N=23  
MEAN=1.21  
STANARD DEVIATION = 0.64  
COEFFICIENT OF VARIATION =0.53

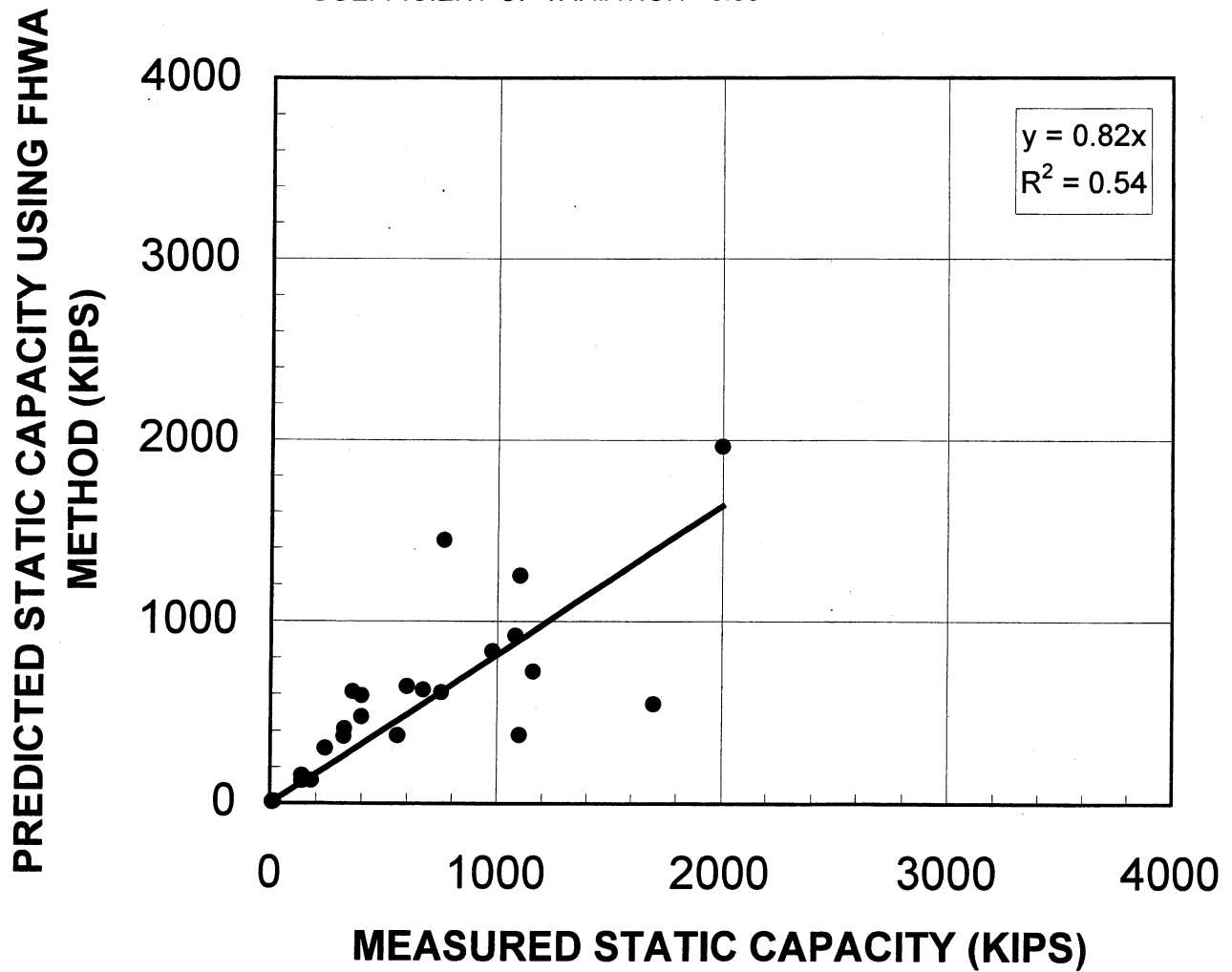


Figure 8

# DRILLED SHAFT IN SAND & CLAY

CONSTRUCTION METHOD= CASING  
LOAD TRANSFER= SKIN FRICTION + END  
BEARING  
N= 23  
MEAN=1.07  
STANARD DEVIATION = 0.51  
COEFFICIENT OF VARIATION =0.48

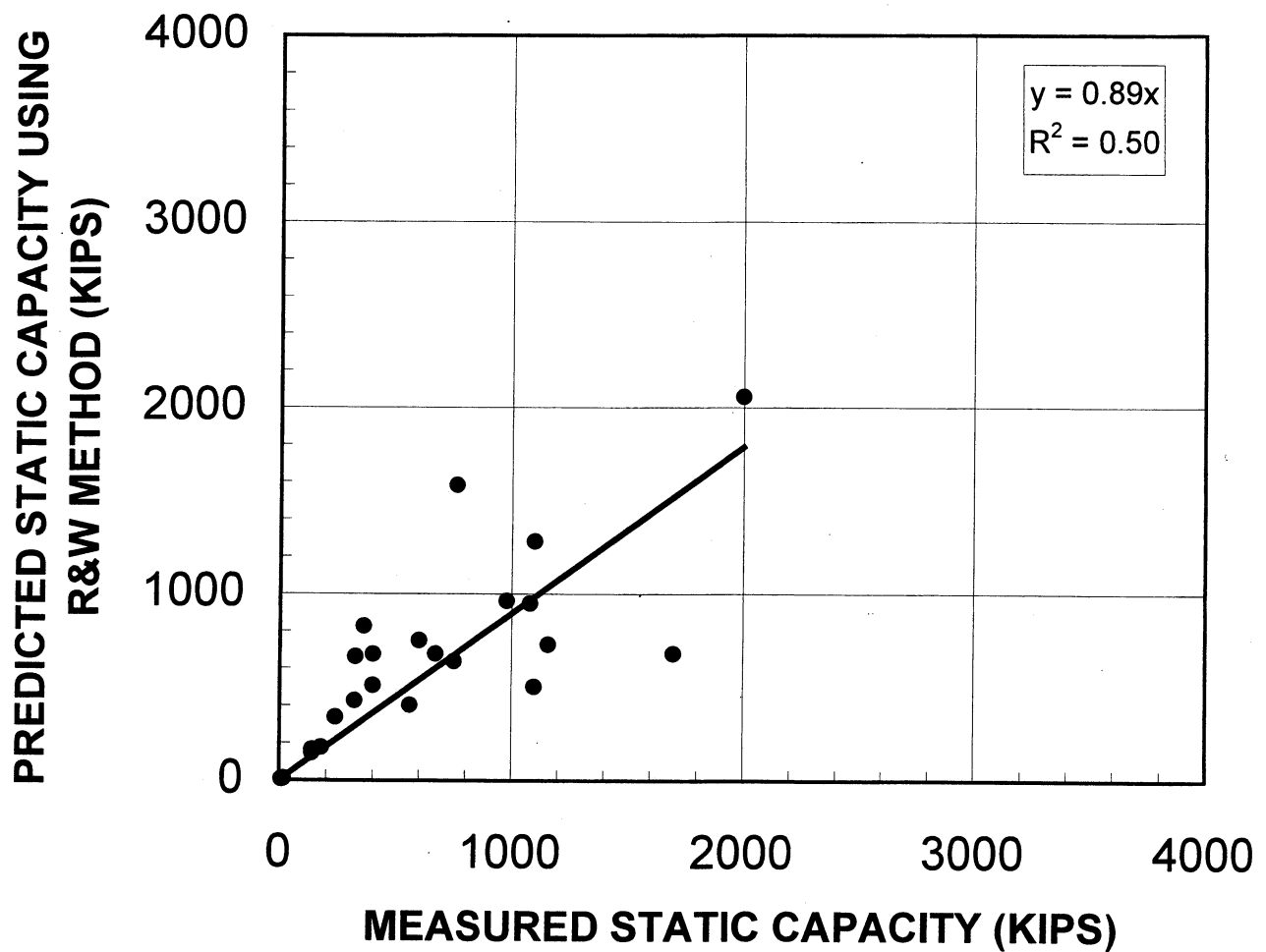


Figure 9

# DRILLED SHAFT IN SAND & CLAY

CONSTRUCTION METHOD= DRY  
LOAD TRANSFER= SKIN FRICTION + END BEARING  
N= 13  
MEAN=1.47  
STANARD DEVIATION = 0.64  
COEFFICIENT OF VARIATION =0.44

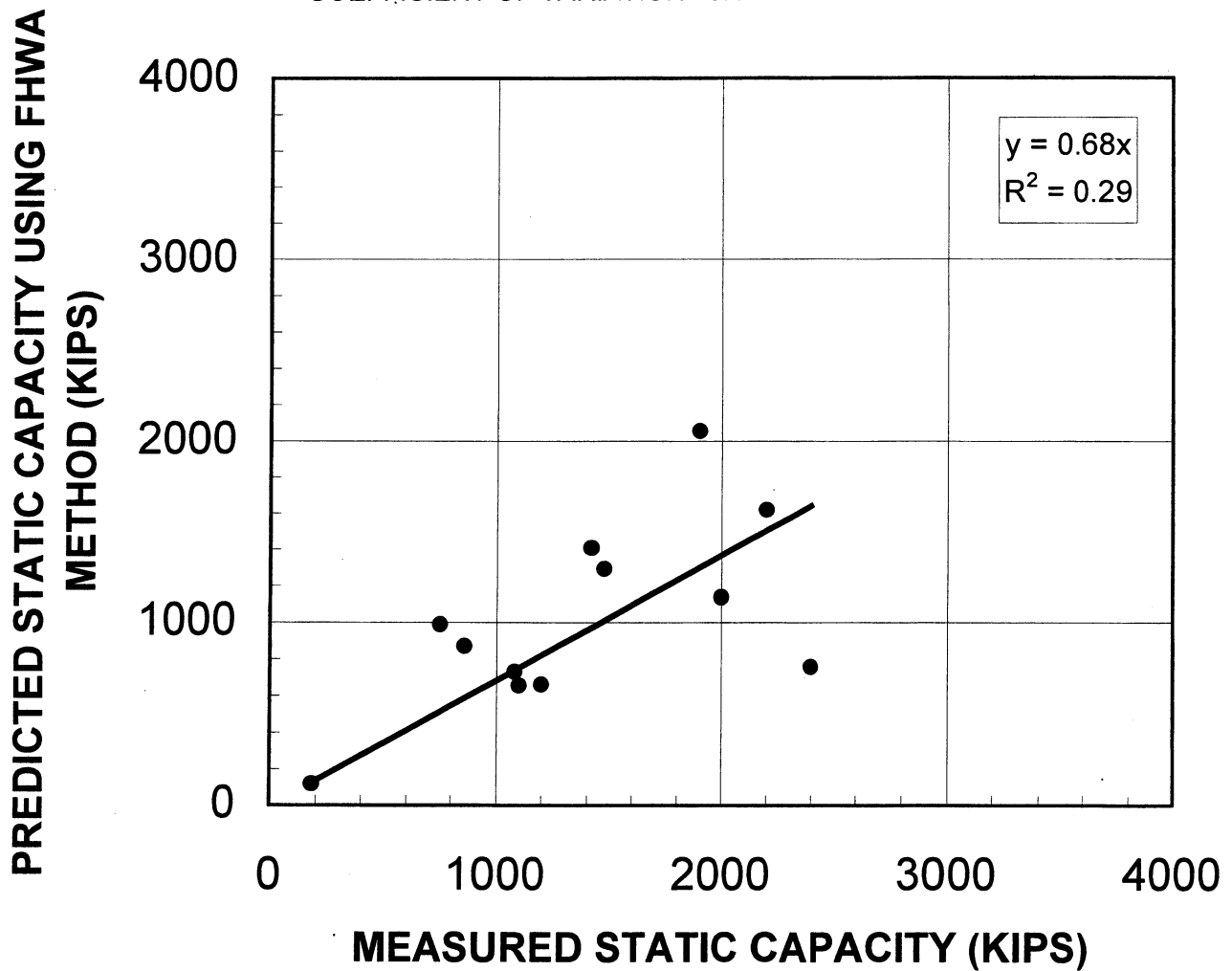


Figure 10

# DRILLED SHAFT IN SAND & CLAY

CONSTRUCTION METHOD= DRY  
LOAD TRANSFER= SKIN FRICTION + END  
BEARING  
N= 13  
MEAN=1.36  
STANARD DEVIATION = 0.64  
COEFFICIENT OF VARIATION =0.47

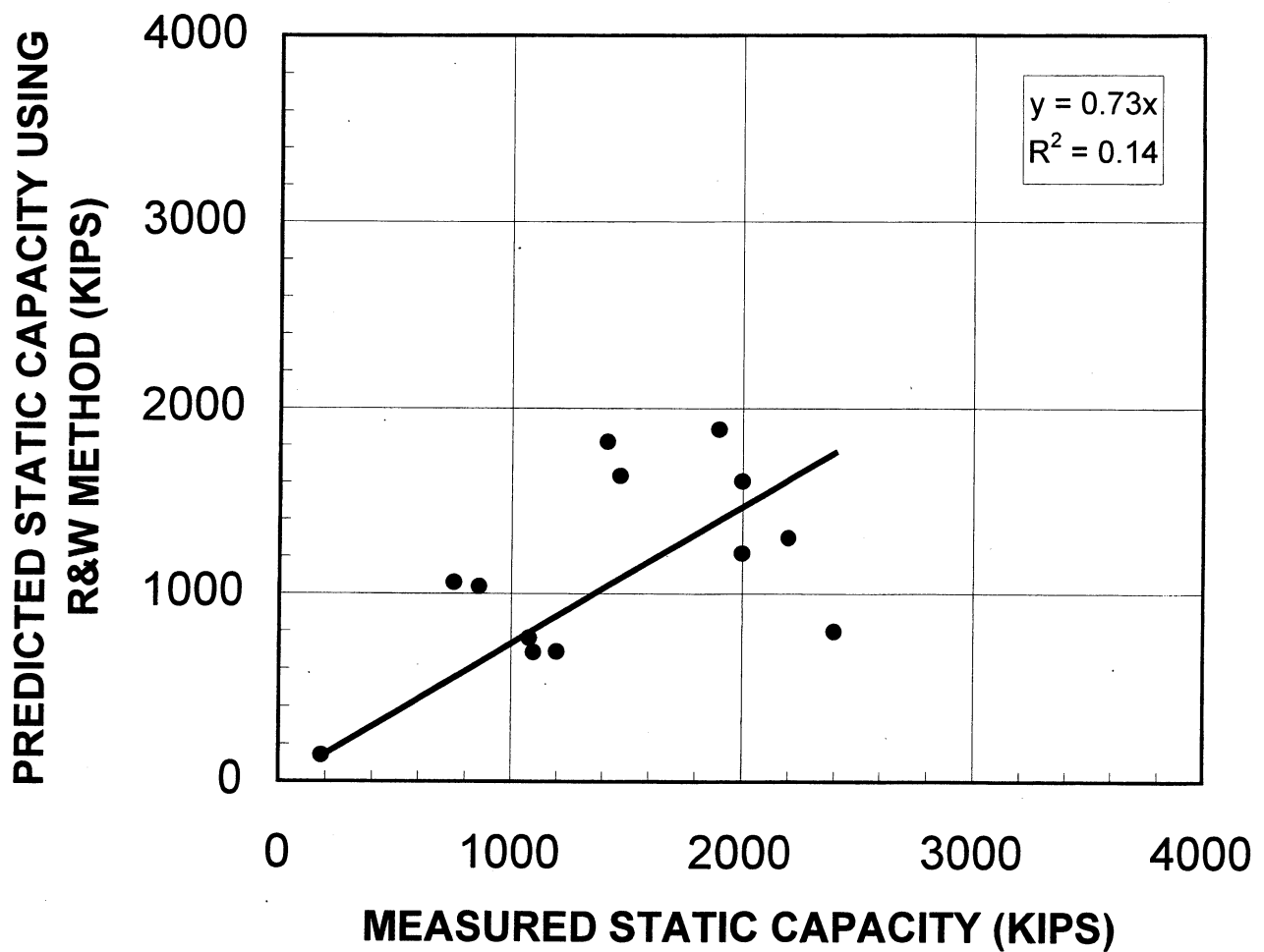


Figure 11

# DRILLED SHAFT IN SAND & CLAY

CONSTRUCTION METHOD=SLURRY  
LOAD TRANSFER= SKIN FRICTION + END BEARING  
N= 12  
MEAN=1.43  
STANARD DEVIATION = 0.55  
COEFFICIENT OF VARIATION =0.39

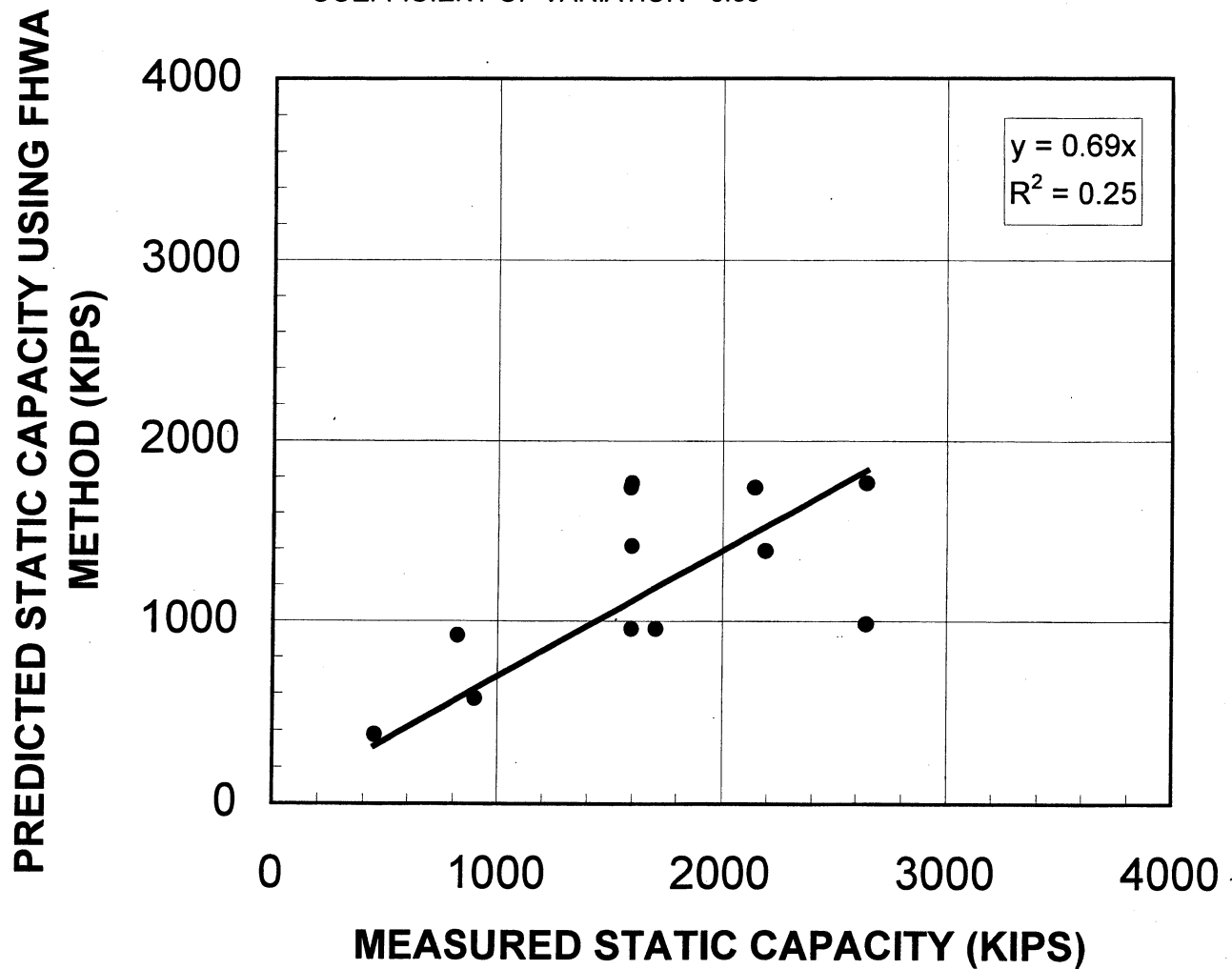


Figure 12



# DRILLED SHAFT IN SAND & CLAY

CONSTRUCTION METHOD= SLURRY  
LOAD TRANSFER= SKIN FRICTION + END  
BEARING  
N= 12  
MEAN=1.28  
STANARD DEVIATION = 0.47  
COEFFICIENT OF VARIATION =0.37

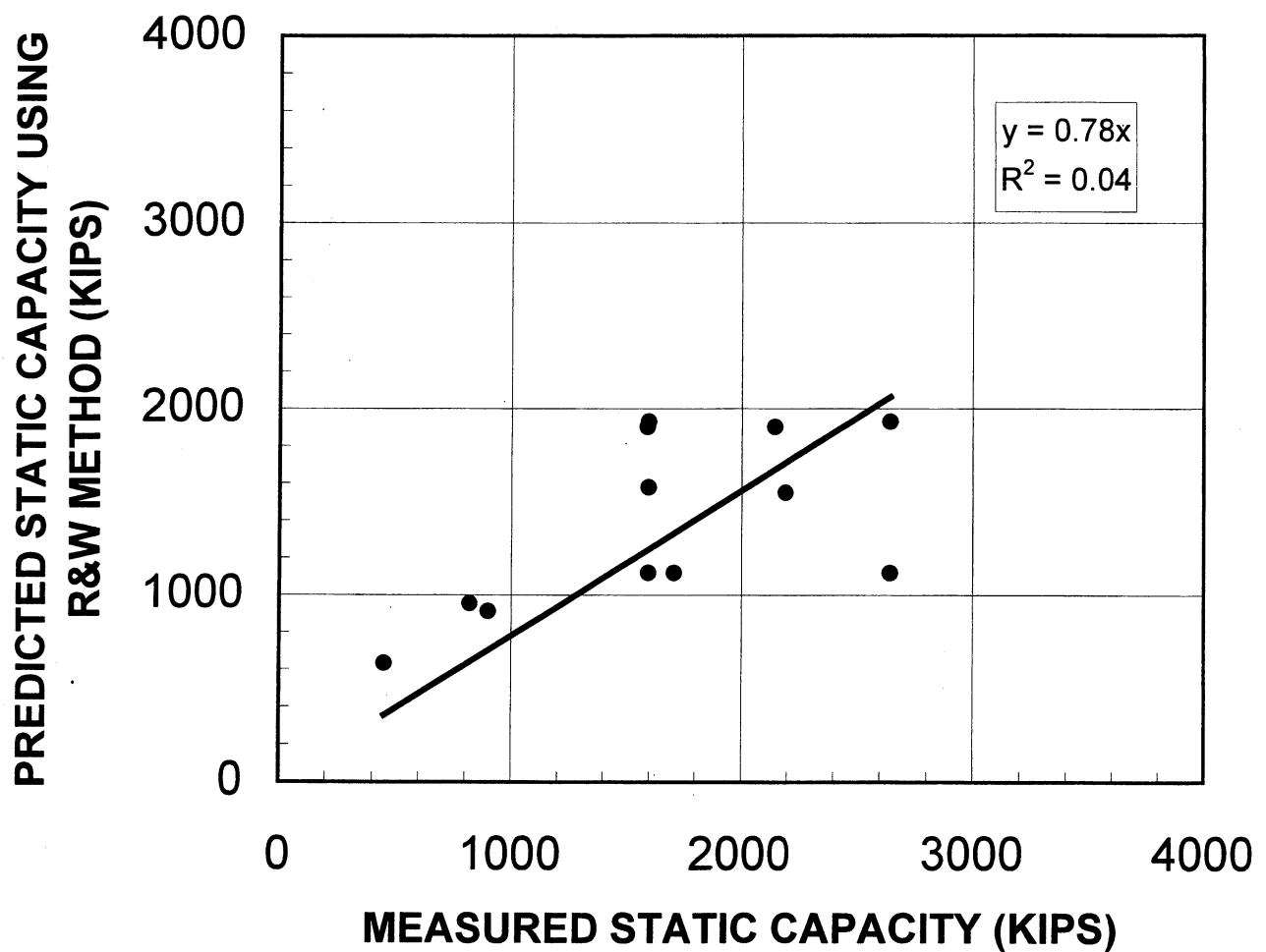


Figure 13

# DRILLED SHAFT IN SAND

CONSTRUCTION METHOD= CASING  
LOAD TRANSFER= SKIN FRICTION + END BEARING  
N= 14  
MEAN=2.47  
STANARD DEVIATION = 1.24  
COEFFICIENT OF VARIATION =0.509

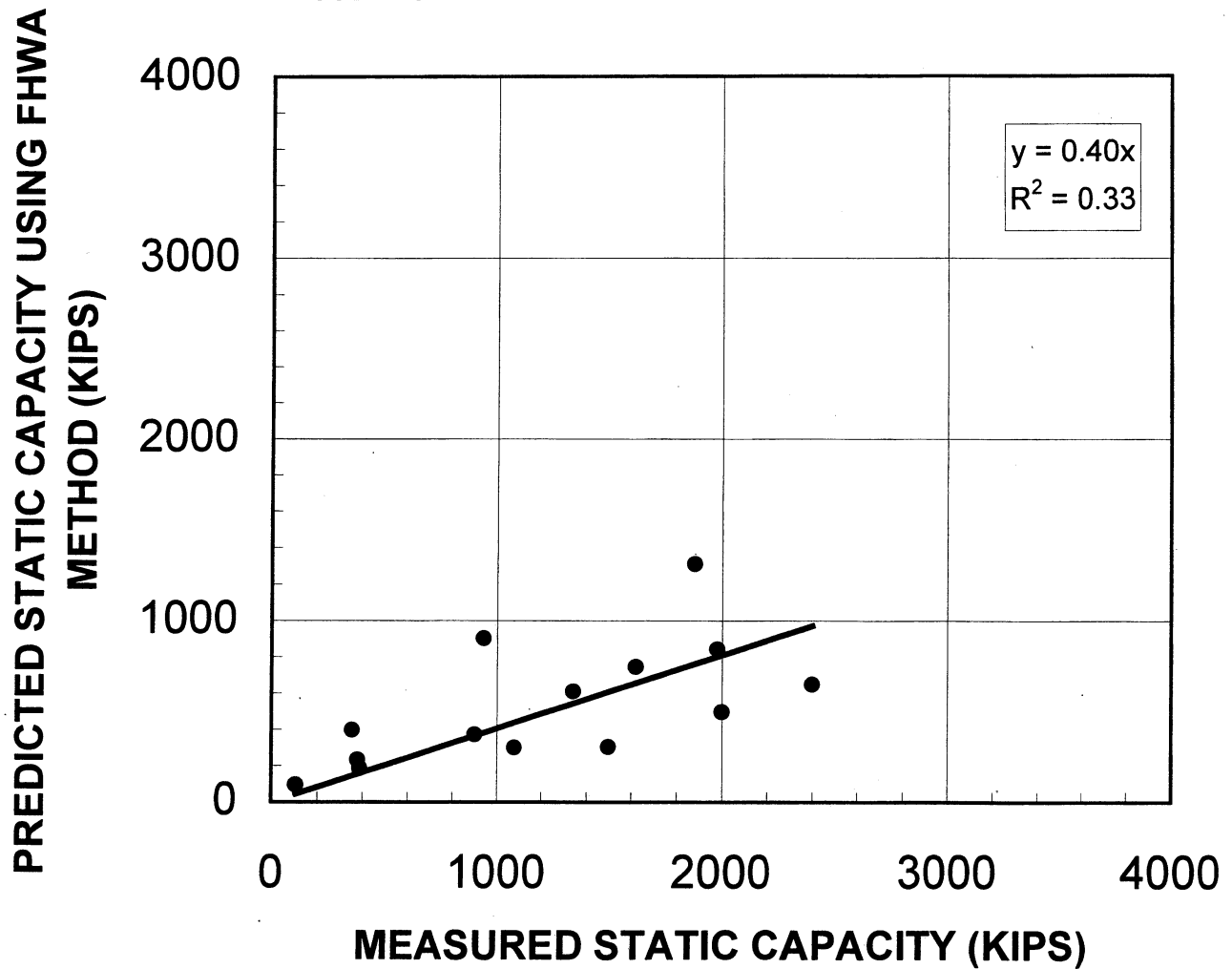


Figure 14

# DRILLED SHAFT IN SAND

CONSTRUCTION METHOD= CASING  
LOAD TRANSFER= SKIN FRICTION + END  
BEARING  
N= 14  
MEAN=1.1.93  
STANARD DEVIATION = 1.39  
COEFFICIENT OF VARIATION =0.72

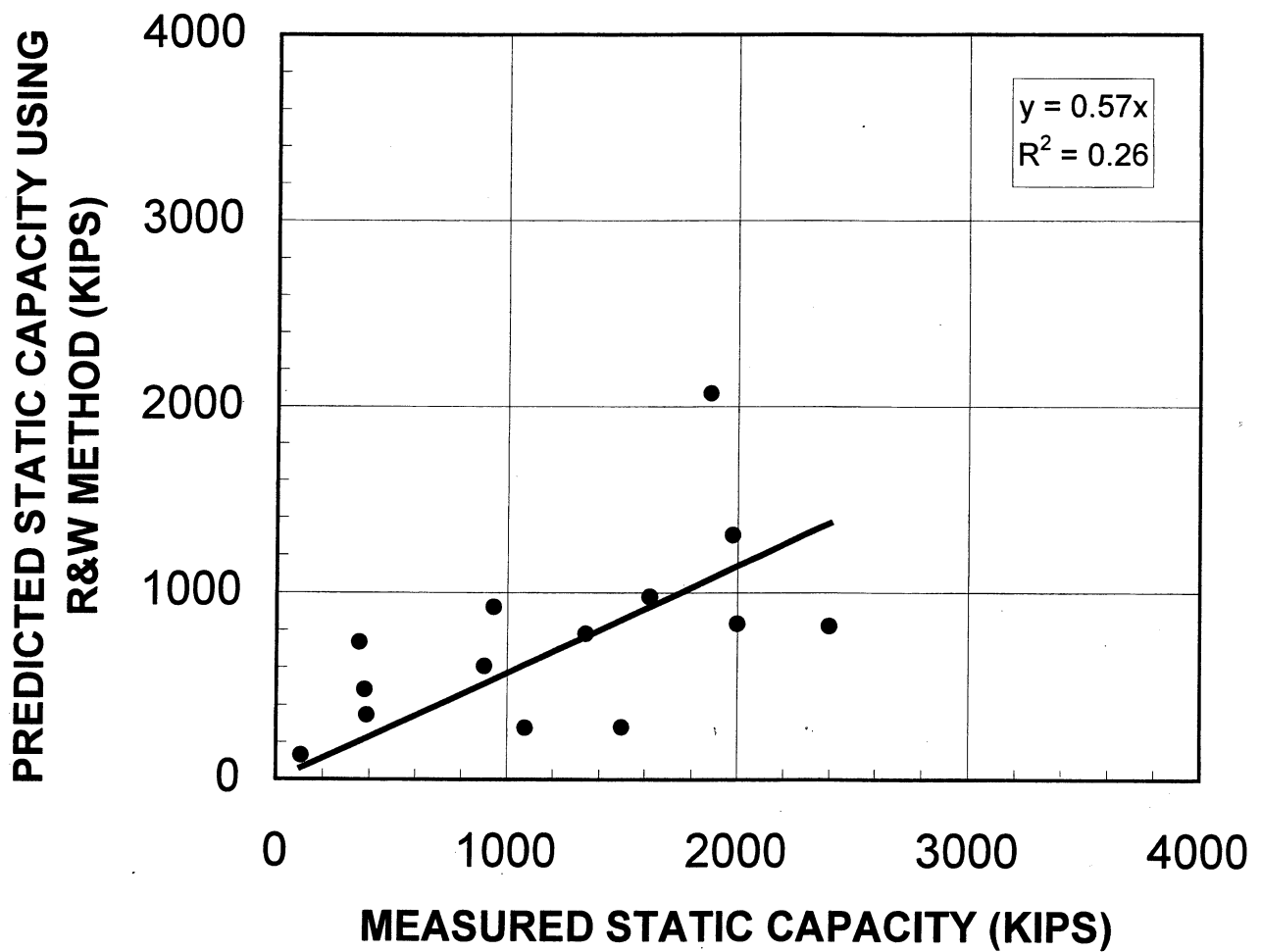


Figure 15

# DRILLED SHAFT IN SAND

CONSTRUCTION METHOD= SLURRY  
LOAD TRANSFER= SKIN FRICTION + END BEARING  
N= 14  
MEAN=2.04  
STANARD DEVIATION = 1.75  
COEFFICIENT OF VARIATION =0.86

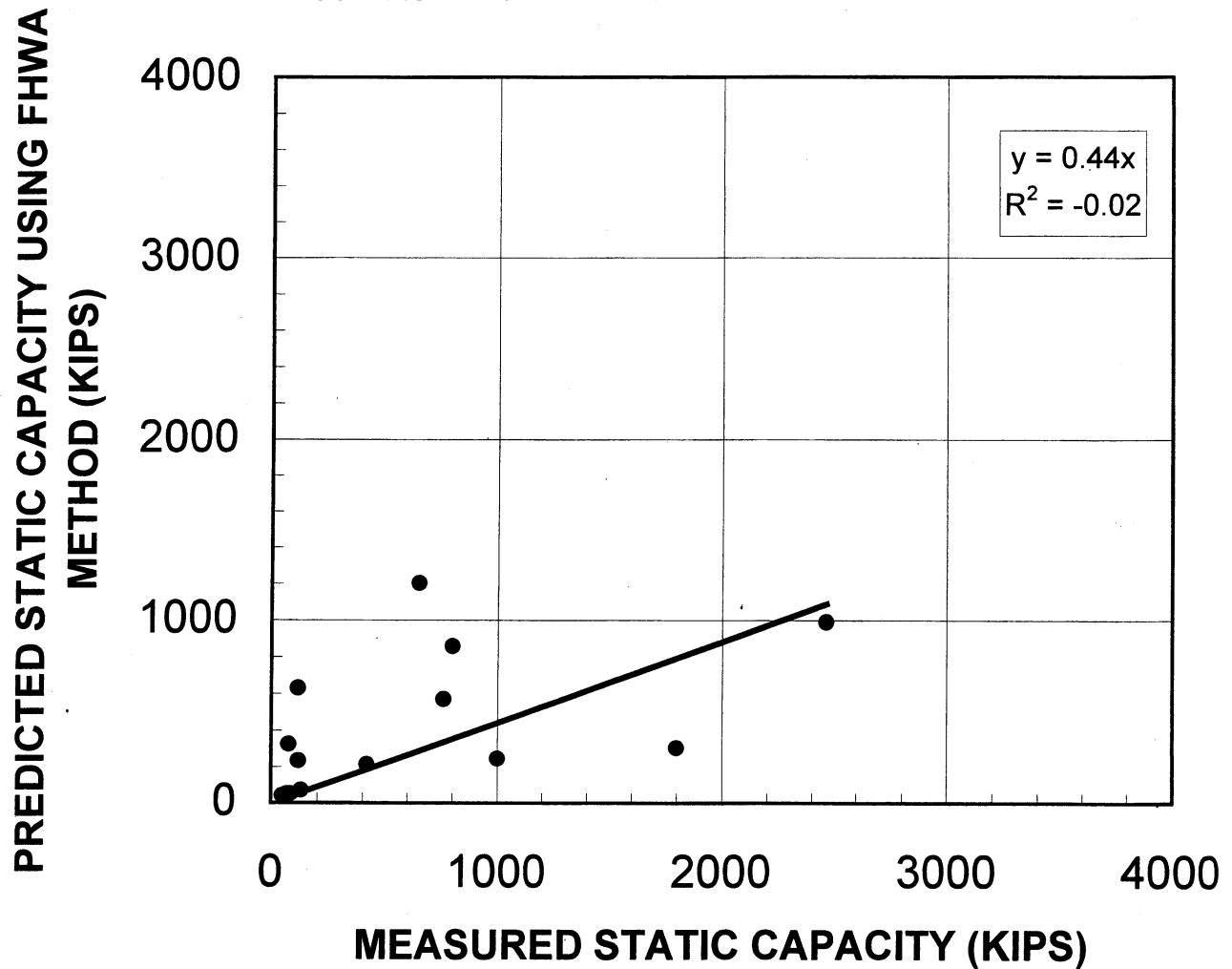


Figure 16

# DRILLED SHAFT IN SAND

CONSTRUCTION METHOD=SLURRY  
LOAD TRANSFER= SKIN FRICTION + END  
BEARING  
N= 14  
MEAN=1.32  
STANARD DEVIATION = 1.55  
COEFFICIENT OF VARIATION =1.18

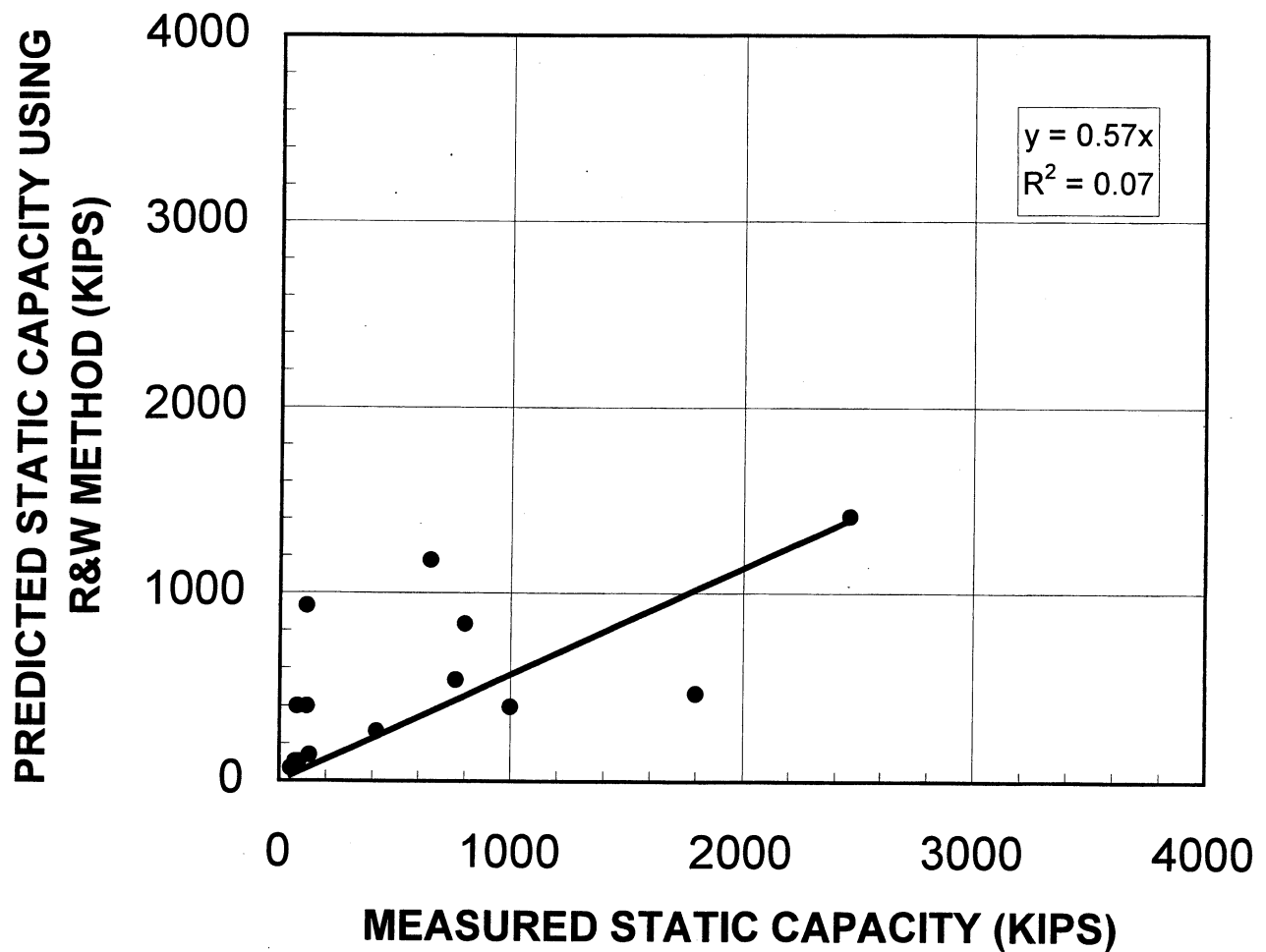


Figure 17

# DRILLED SHAFT IN CLAY

CONSTRUCTION METHOD= CASING  
LOAD TRANSFER= SKIN FRICTION + END BEARING  
N= 14  
MEAN=0.99  
STANARD DEVIATION = 0.70  
COEFFICIENT OF VARIATION =0.71

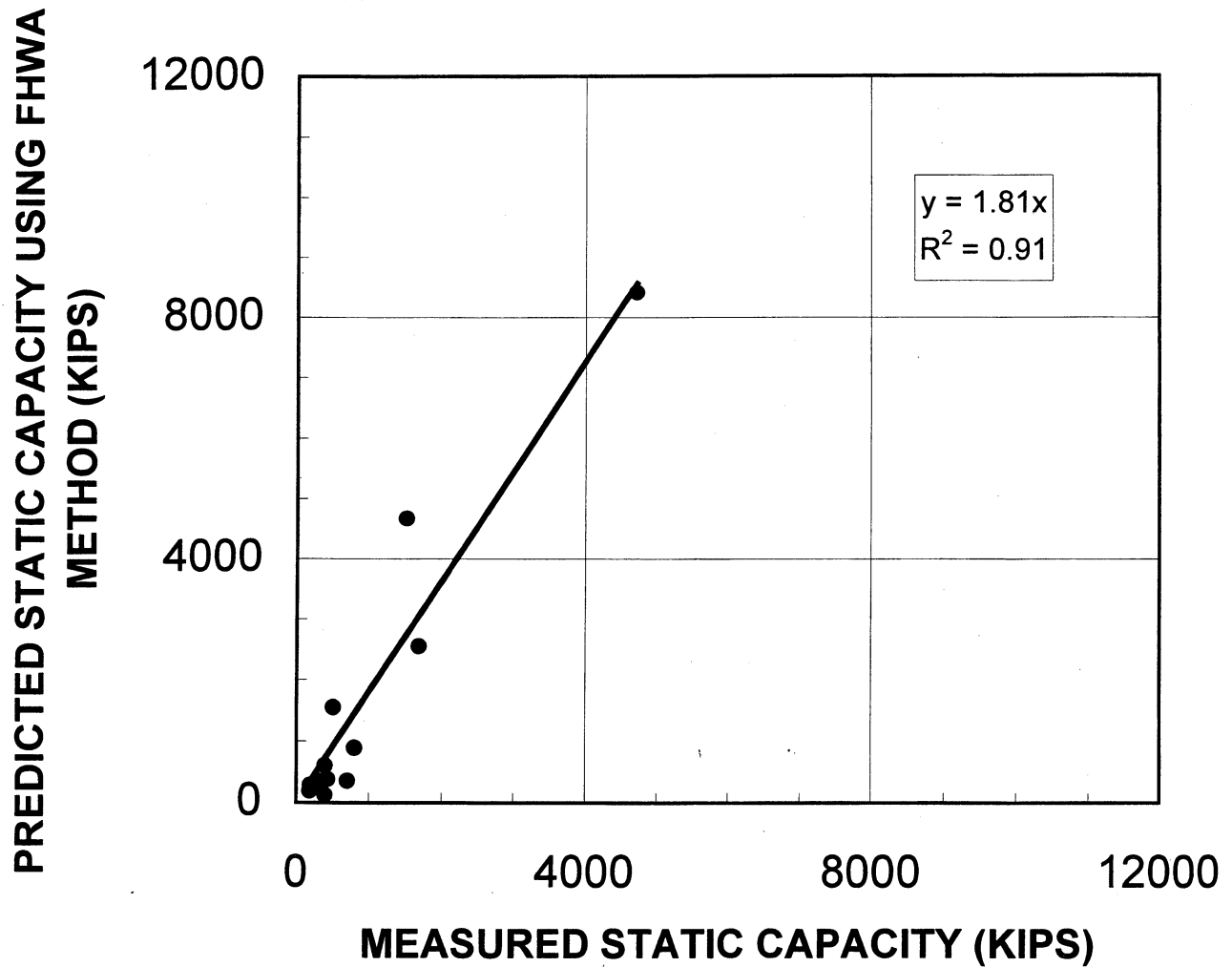


Figure 18

# DRILLED SHAFT IN CLAY

CONSTRUCTION METHOD= DRY  
LOAD TRANSFER= SKIN FRICTION + END BEARING  
N= 40  
MEAN=0.88  
STANDARD DEVIATION = 0.42  
COEFFICIENT OF VARIATION =0.48

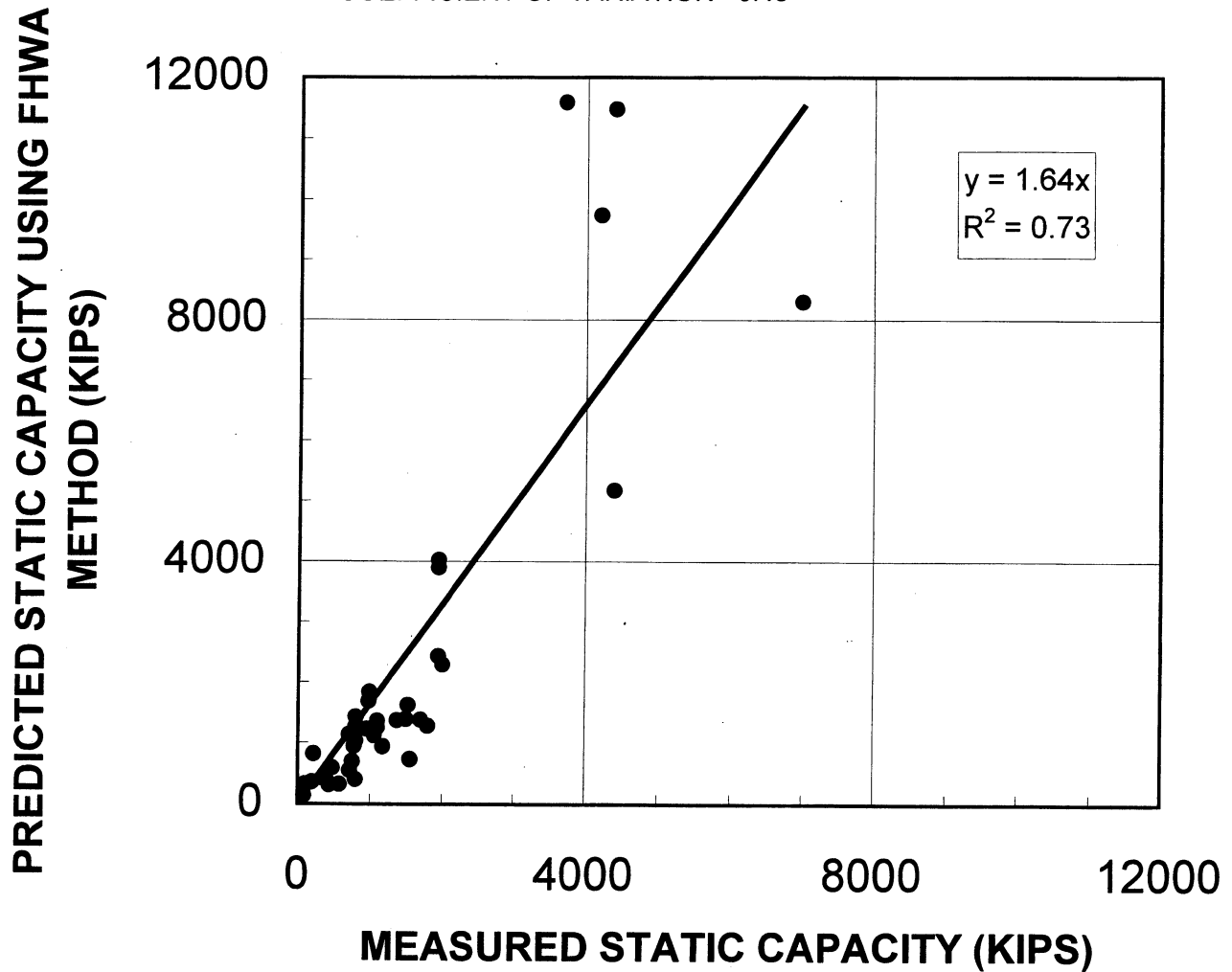


Figure 19

Table		Failure		FHWA	FHWA	W&R	W&R
SHAFT #	Construction	Load (kips)	Soil Type	Predict(kips)	Ratio	Predict(kips)	Ratio
5	Casing	180	A	126.82	1.42	175.56	1.03
6	Casing	322	A	370	0.87	426.00	0.76
12	Casing	10.8	A	8.62	1.25	7.60	1.42
13	Dry	18	A	12	1.50	12.06	1.49
14	Dry	140	A	154.3	0.91	163.90	0.85
18	Dry	1100	A	1250	0.88	1282.00	0.86
19	Dry	1160	A	725.66	1.60	727.08	1.60
20	Dry	1080	A	923.24	1.17	949.72	1.14
22	Dry	1700	A	548	3.10	679.24	2.50
25	Dry	360	A	616.12	0.58	827.00	0.44
31	Dry & Casing	980	A	837.04	1.17	963.20	1.02
38	Slurry	1474	A	1293.28	1.14	1635.78	0.90
85	Slurry	184	A	118.58	1.55	141.40	1.30
95	Slurry	2400	A	758	3.17	798.00	3.01
153	Slurry	1200	A	662	1.81	691.30	1.74
155	Slurry	1100	A	658.26	1.67	686.92	1.60
32	Casing	356	B	397.2	0.90	735.96	0.48
34	Casing	940	B	904	1.04	924.00	1.02
58	Casing	1620	B	746.6	2.17	977.94	1.66
66	Casing	930	B	688	1.35	956.00	0.97
67	Casing	1380	B	814	1.70	1466.00	0.94
123	Casing	70	B	52.3	1.34	103.48	0.68
164	Casing & Slurry	76	B	326	0.23	400.00	0.19
165	Dry	118	B	234	0.50	400.00	0.30
175	Slurry	650	B	1202	0.54	1176.00	0.55
176	Slurry	800	B	860	0.93	836.00	0.96
177	Slurry	760	B	572	1.33	538.00	1.41
61	Casing	300	C	362	0.83		
185	Casing	108	C	332	0.33		
197	Casing	1100	C	1360	0.81		
198	Dry	1180	C	942	1.25		
201	Dry	440	C	316	1.39		
203	Dry	1800	C	1276	1.41		
207	Dry	800	C	1426	0.56		
209	Dry	1380	C	1368	1.01		

# SKIN FRICTION SHAFT in SOIL

FHWA Method 40				
	SOIL TYPE			
	A	B	C	ALL
Mean	1.49	1.09	0.87	1.18
Stdv	0.72	0.56	0.32	0.62
Var	0.49	0.51	0.37	0.53

R&W Method 27				
	SOIL TYPE			
	A	B		ALL
Mean	1.35	0.83		1.14
Stdv	0.66	0.45		0.63
Var	0.49	0.54		0.55

NOTE:  
Soil type A = Sand & Clay  
Soil type B = Sand  
Soil type C = Clay



210	Dry	780	C	946	0.82		
211	Dry	950	C	1230	0.77		
212	Dry	800	C	1032	0.78		
213	Dry	988	C	1838	0.54		
242	Dry	4400	C	5178	0.85		

## DRILLED SHAFT IN SAND

CONSTRUCTION METHOD=MIXED  
LOAD TRANSFER= SKIN FRICTION  
N= 11  
MEAN=1.09  
STANARD DEVIATION = 0.56  
COEFFICIENT OF VARIATION =0.51

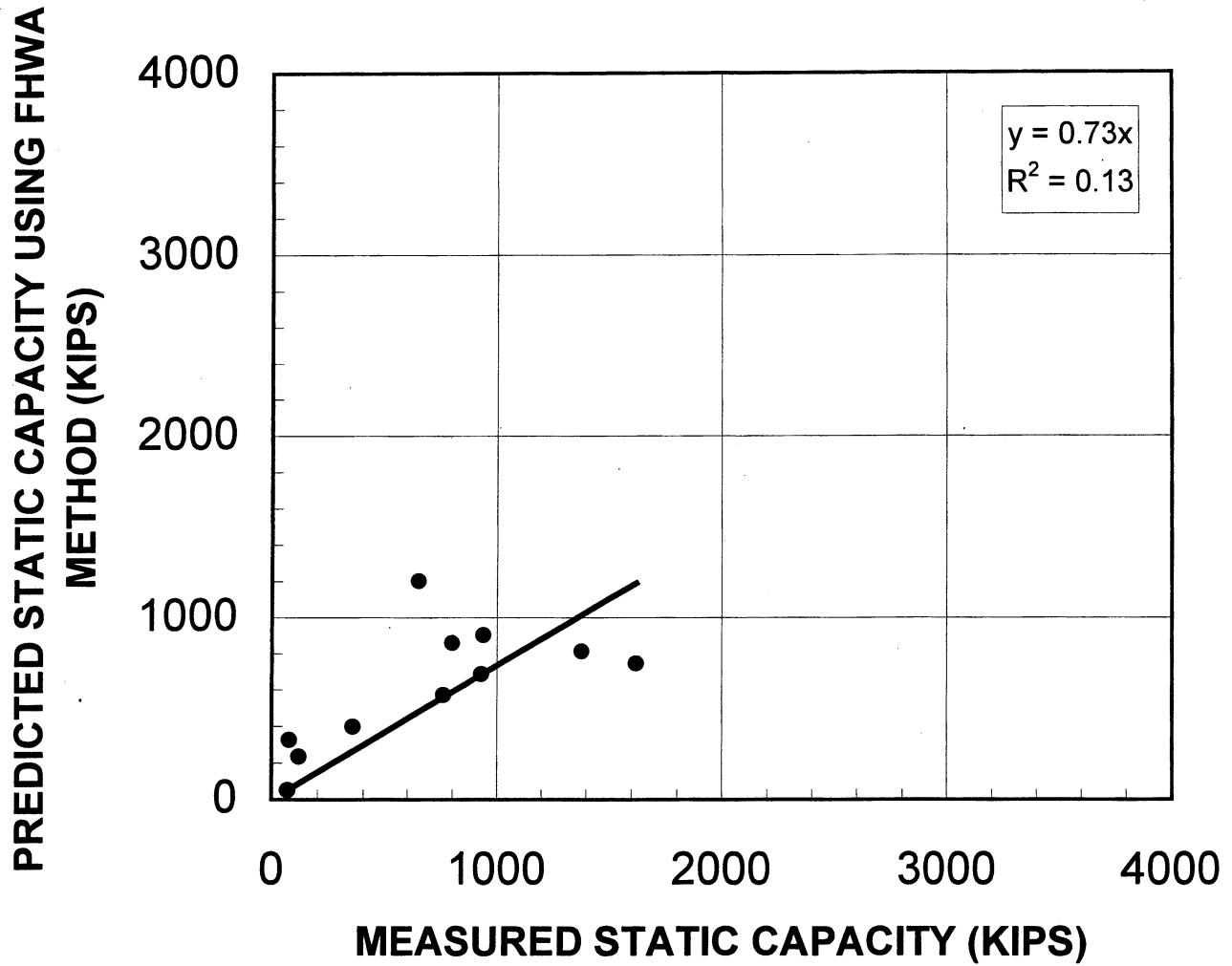


Figure 20

# DRILLED SHAFT IN CLAY

CONSTRUCTION METHOD=MIXED

LOAD TRANSFER= SKIN FRICTION

N= 13

MEAN=0.87

STANARD DEVIATION = 0.32

COEFFICIENT OF VARIATION =0.37

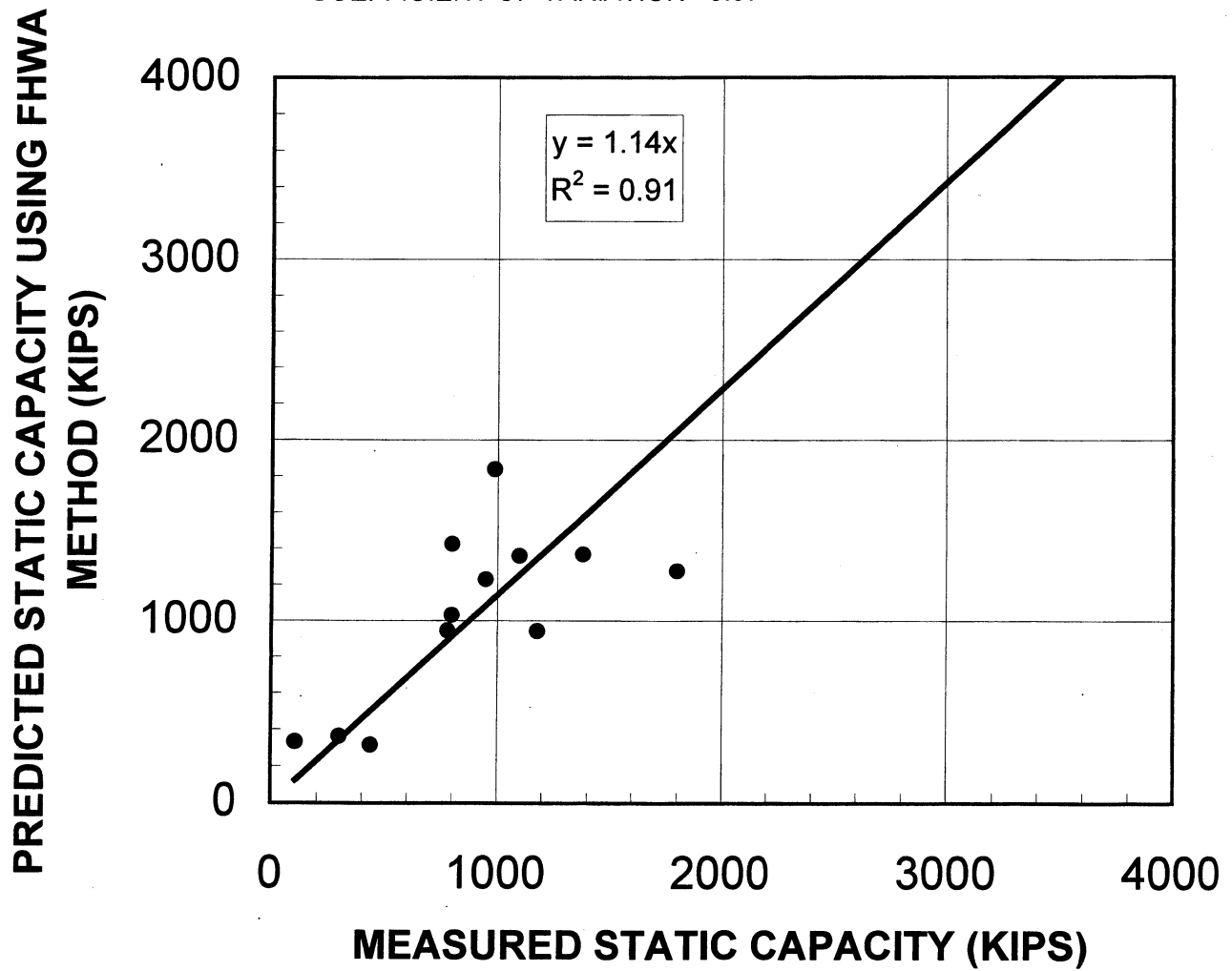


Figure 21

# DRILLED SHAFT IN SAND & CLAY

CONSTRUCTION METHOD=MIXED  
LOAD TRANSFER= SKIN FRICTION  
N= 16  
MEAN=1.49  
STANARD DEVIATION = 0.72  
COEFFICIENT OF VARIATION =0.49

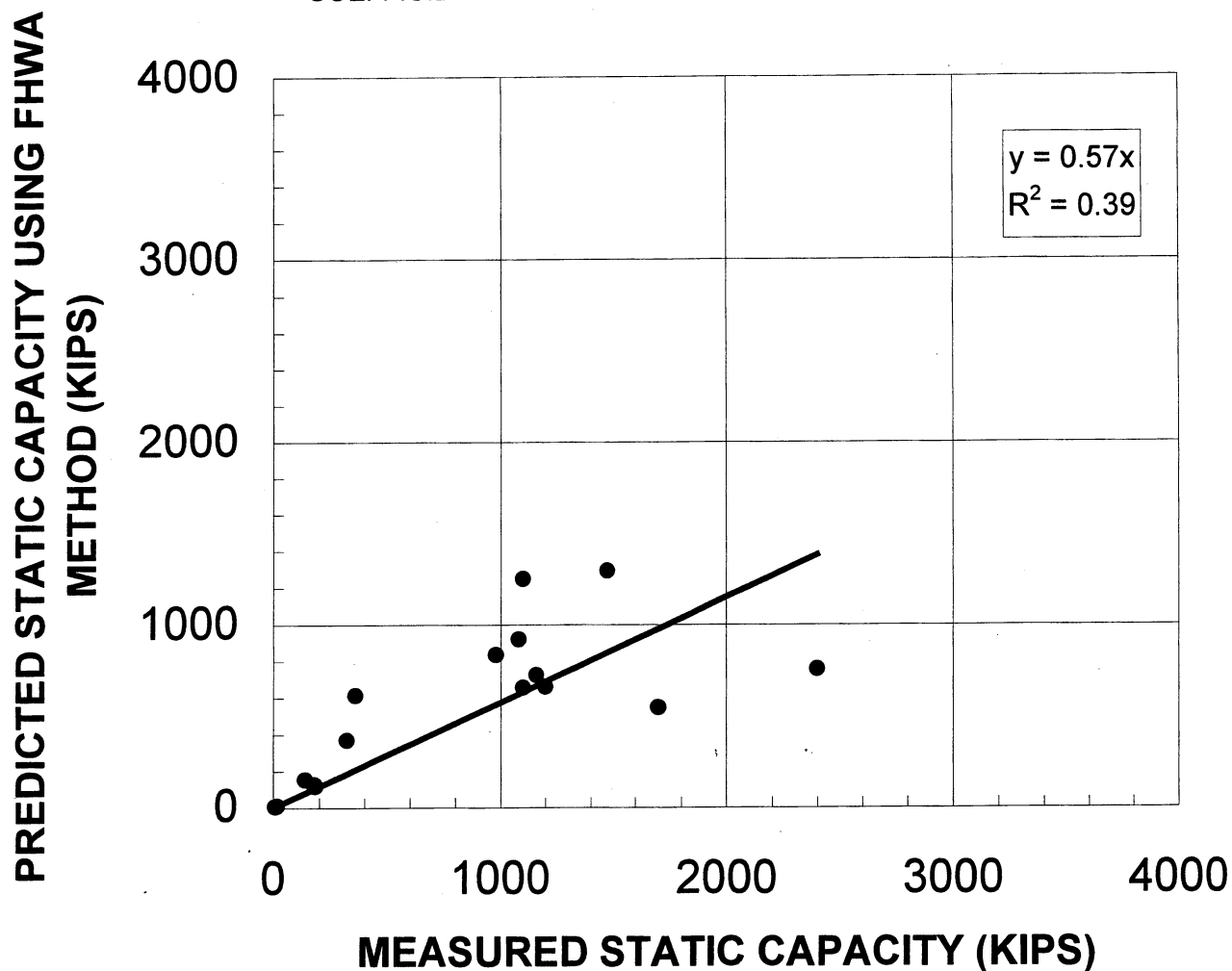


Figure 22

# DRILLED SHAFT IN SOILS

CONSTRUCTION METHOD=MIXED  
LOAD TRANSFER= SKIN FRICTION  
N= 40  
MEAN=1.16  
STANARD DEVIATION = 0.62  
COEFFICIENT OF VARIATION =0.53

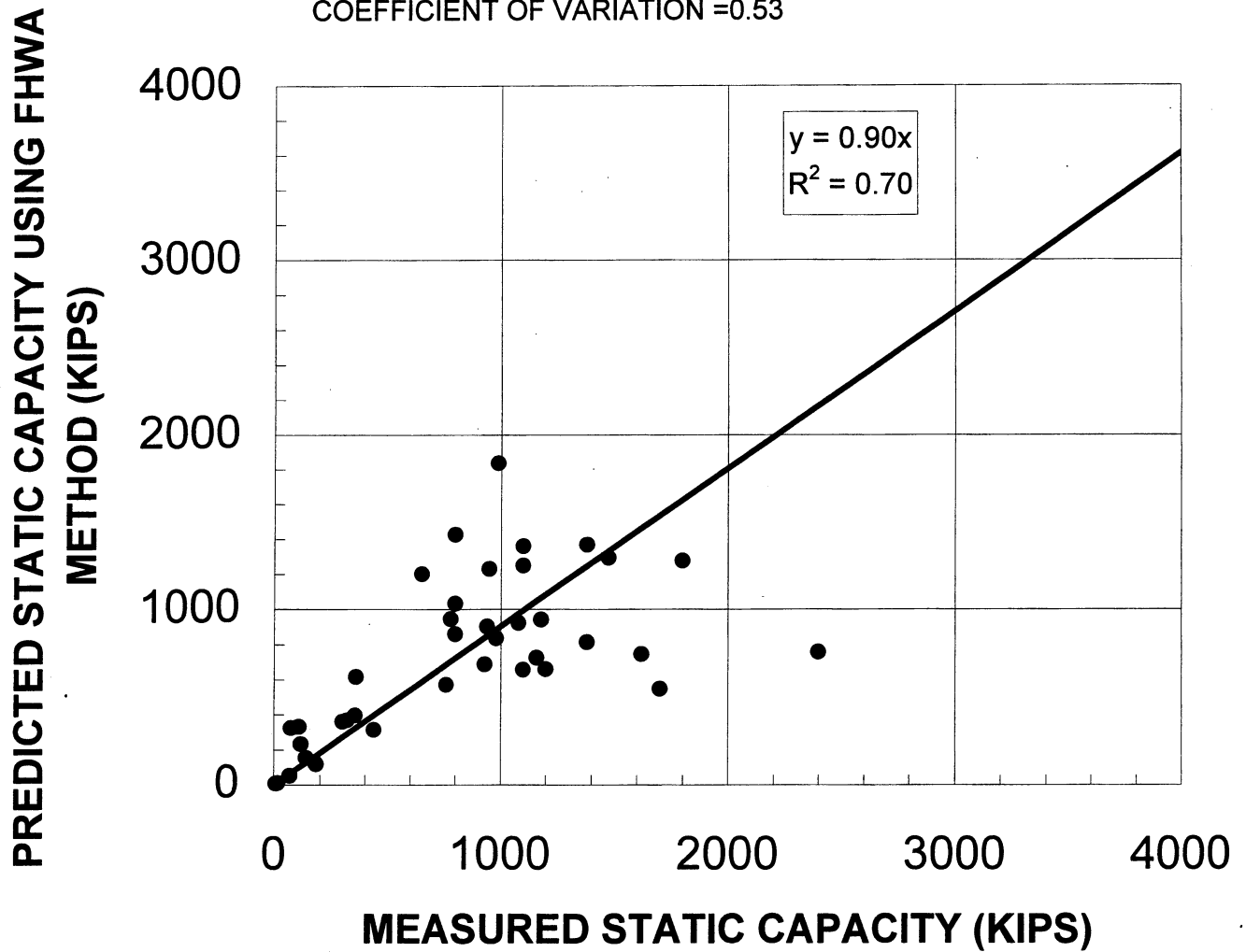


Figure 23

# DRILLED SHAFT IN SAND

CONSTRUCTION METHOD=MIXED  
LOAD TRANSFER= SKIN FRICTION  
N= 11  
MEAN=0.83  
STANARD DEVIATION = 0.45  
COEFFICIENT OF VARIATION =0.54

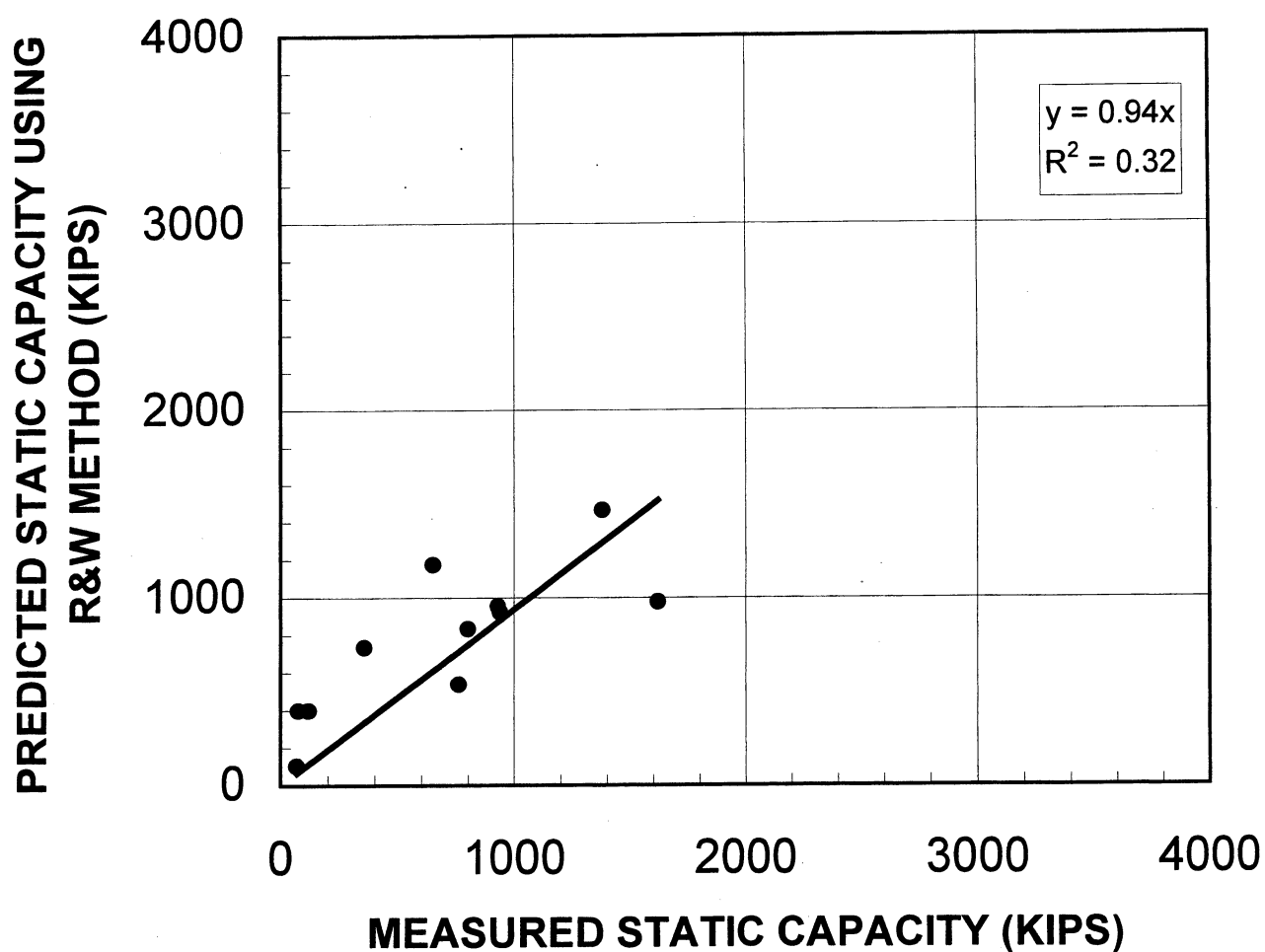


Figure 24

# DRILLED SHAFT IN SAND & CLAY

CONSTRUCTION METHOD=MIXED  
LOAD TRANSFER= SKIN FRICTION  
N= 16  
MEAN=1.35  
STANARD DEVIATION = 0.66  
COEFFICIENT OF VARIATION =0.49

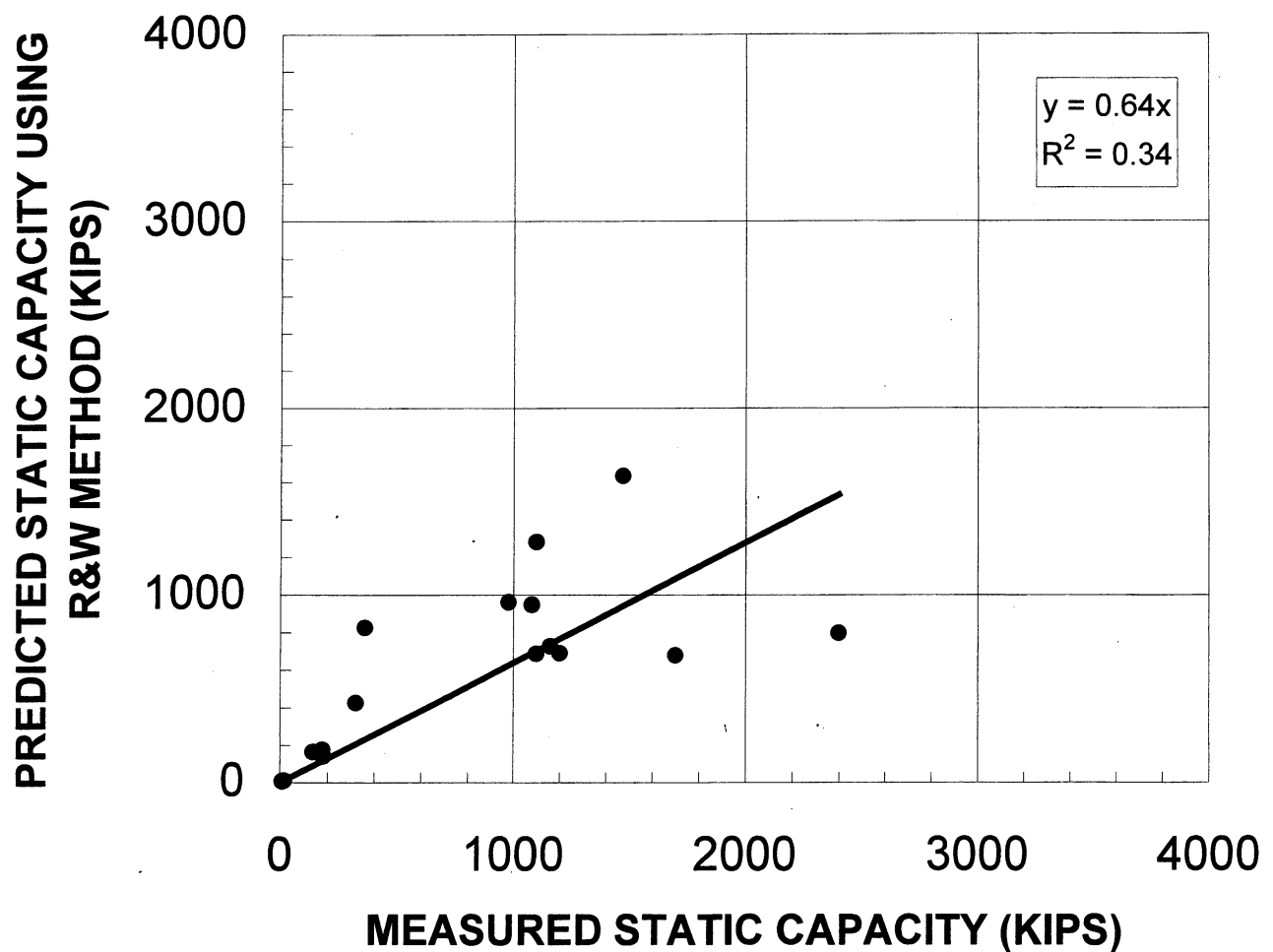


Figure 25

# DRILLED SHAFT IN SOILS

CONSTRUCTION METHOD=MIXED  
LOAD TRANSFER= SKIN FRICTION  
N= 27  
MEAN=1.14  
STANARD DEVIATION = 0.63  
COEFFICIENT OF VARIATION =0.55

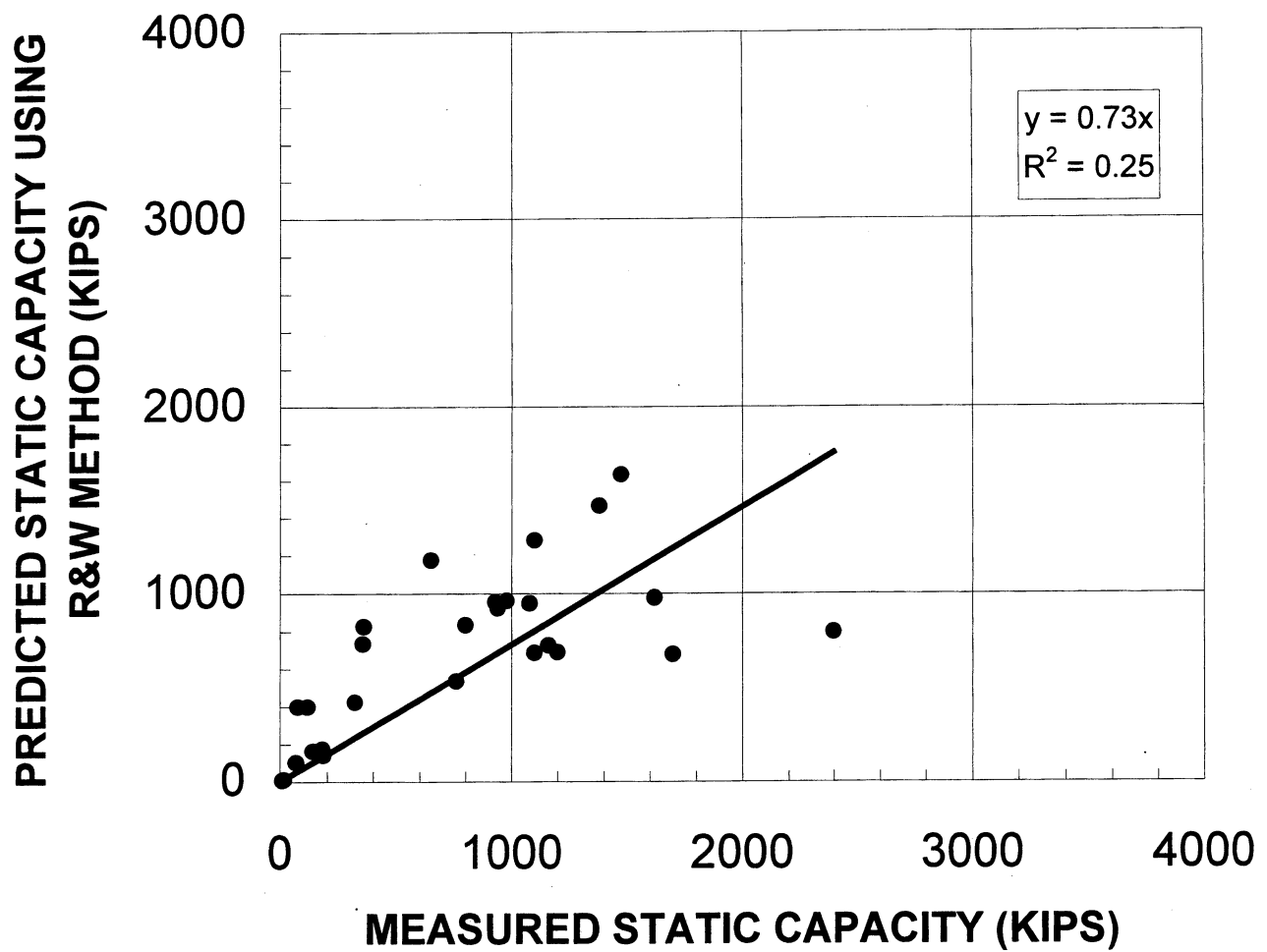


Figure 26



Table			Failure		C&K	C&K	IGM	IGM
SHAFT #	Construction	SOIL	Load(kips)	Predict(kips)	Ratio	Predict(kips)	Ratio	
2	Casing	silt/clay/rock	2000	2236.00	0.89	2204.00	0.91	
8	Casing	sand/clay/rock	1500	4332.00	0.35	3269.00	0.46	
42	Casing	sand/rock	2000	2319.00	0.86	1771.00	1.13	
44	Casing	sand/rock	2000	1150.00	1.74	1021.00	1.96	
45	Casing	sand/rock	1980	1343.00	1.47	1184.00	1.67	
46	Casing	silt/sand/rock	600	867.00	0.69	784.00	0.77	
47	Dry	sand/rock	1816	2348.00	0.77	1497.00	1.21	
48	Dry	sand/rock	1714	2709.00	0.63	1638.00	1.05	
49	Dry	sand/rock	760	693.00	1.10	633.00	1.20	
50	Dry	rock	644	537.00	1.20	728.00	0.88	
51	Dry	rock	716	537.00	1.33	728.00	0.98	
55	Dry	sand/rock	2800	1976.00	1.42	1384.00	2.02	
81	Dry	rock	776	537.00	1.45	728.00	1.07	
111	Dry	clay/rock	2060	547.00	3.77	562.00	3.67	
112	Dry	sand/rock	1000	535.00	1.87	729.00	1.37	
113	Dry	sand/rock	1800	1169.00	1.54	1281.00	1.41	
115	Dry	silt/rock	700	395.00	1.77	416.00	1.68	
116	Dry	silt/rock	750	324.00	2.31	336.00	2.23	
117	Dry	silt/rock	450	236.00	1.91	245.00	1.84	
118	Dry	silt/rock	320	159.00	2.01	166.00	1.93	
119	Dry	silt/rock	350	250.00	1.40	270.00	1.30	
120	Dry	silt/rock	460	236.00	1.95	245.00	1.88	
122	Dry	silt/rock	700	236.00	2.97	252.00	2.78	
136	Dry	rock	1080	1444.00	0.75	1037.00	1.04	
137	Dry	rock	1854	2973.00	0.62	1787.00	1.04	
138	Dry	rock	1438	1500.00	0.96	1066.00	1.35	
139	Dry	rock	1832	1473.00	1.24	1052.00	1.74	
140	Dry	rock	1686	1444.00	1.17	1037.00	1.63	
146	Dry	sand/rock	2000	4521.00	0.44	3064.00	0.65	
147	Dry	sand/rock	2000	4816.00	0.42	3258.00	0.61	
157	Dry	clay/rock	2918	2003.00	1.46	1833.00	1.59	
158	Dry	clay/rock	3144	2830.00	1.11	2477.00	1.27	
159	Dry	clay/rock	3092	2830.00	1.09	2477.00	1.25	
161	Dry	clay/rock	2688	5425.00	0.50	4258.00	0.63	
162	Dry	clay/rock	1528	864.00	1.77	976.00	1.57	

TOTAL SHAFT in ROCK

TOTAL 49		
	C&K	IGM
MEAN	1.37	1.42
STDV	0.75	0.64
VAR	0.55	0.45

TOTAL 32		
DRY METHOD		
	C&K	IGM
MEAN	1.50	1.53
STDV	0.83	0.69
VAR	0.56	0.45

169	Dry	clay/rock	1980	513.00	3.86	607.00	3.26
170	Dry	sand/rock	2406	1258.00	1.91	1583.00	1.52
171	Dry	clay/gravel	600	422.00	1.42	462.00	1.30
172	Dry & Casing	clay/gravel	2650	1764.00	1.50	2195.00	1.21
173	Dry & Casing	clay/gravel	2200	1327.00	1.66	1641.00	1.34
174	Slurry	clay/gravel	2440	1794.00	1.36	2233.00	1.09
179	Slurry & Casing	clay/gravel	1060	640.00	1.66	663.00	1.60
214	Slurry & Casing	sand/Shale	1500	816.00	1.84	646.00	2.32
257	Slurry & Casing	Sand/rock	1935.6	1974.00	0.98	1895.00	1.02
258	Slurry & Casing	sand/rock	2096	1590.00	1.32	1530.00	1.37
261	Slurry & Casing	sand/rock	2720	2636.00	1.03	2186.00	1.24
262	Slurry & Casing	sand/rock	1962	2624.00	0.75	2214.00	0.89
263	Slurry & Casing	sand/rock	4828	9545.00	0.51	5626.00	0.86
264	Slurry & Casing	sand/rock	3078	7805.00	0.39	4870.00	0.63

# DRILLED SHAFT IN ROCK

CONSTRUCTION METHOD= MIXED  
LOAD TRANSFER= SKIN FRICTION + END  
BEARING  
N= 49  
MEAN=1.37  
STANDARD DEVIATION = 0.75  
COEFFICIENT OF VARIATION =0.55

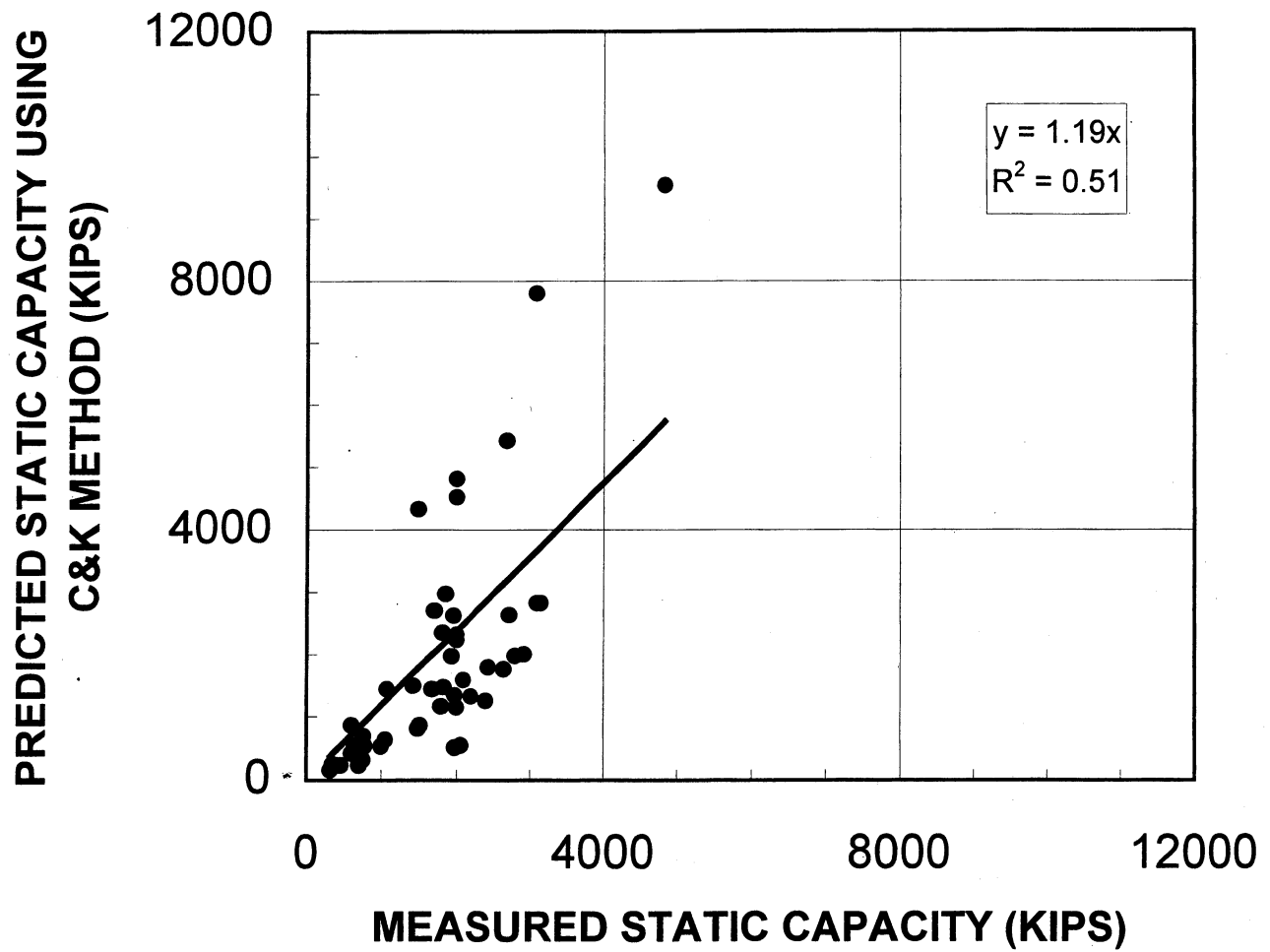


Figure 27

# DRILLED SHAFT IN ROCK

CONSTRUCTION METHOD= MIXED  
LOAD TRANSFER= SKIN FRICTION + END  
BEARING  
N= 49  
MEAN=1.42  
STANARD DEVIATION = 0.64  
COEFFICIENT OF VARIATION =0.46

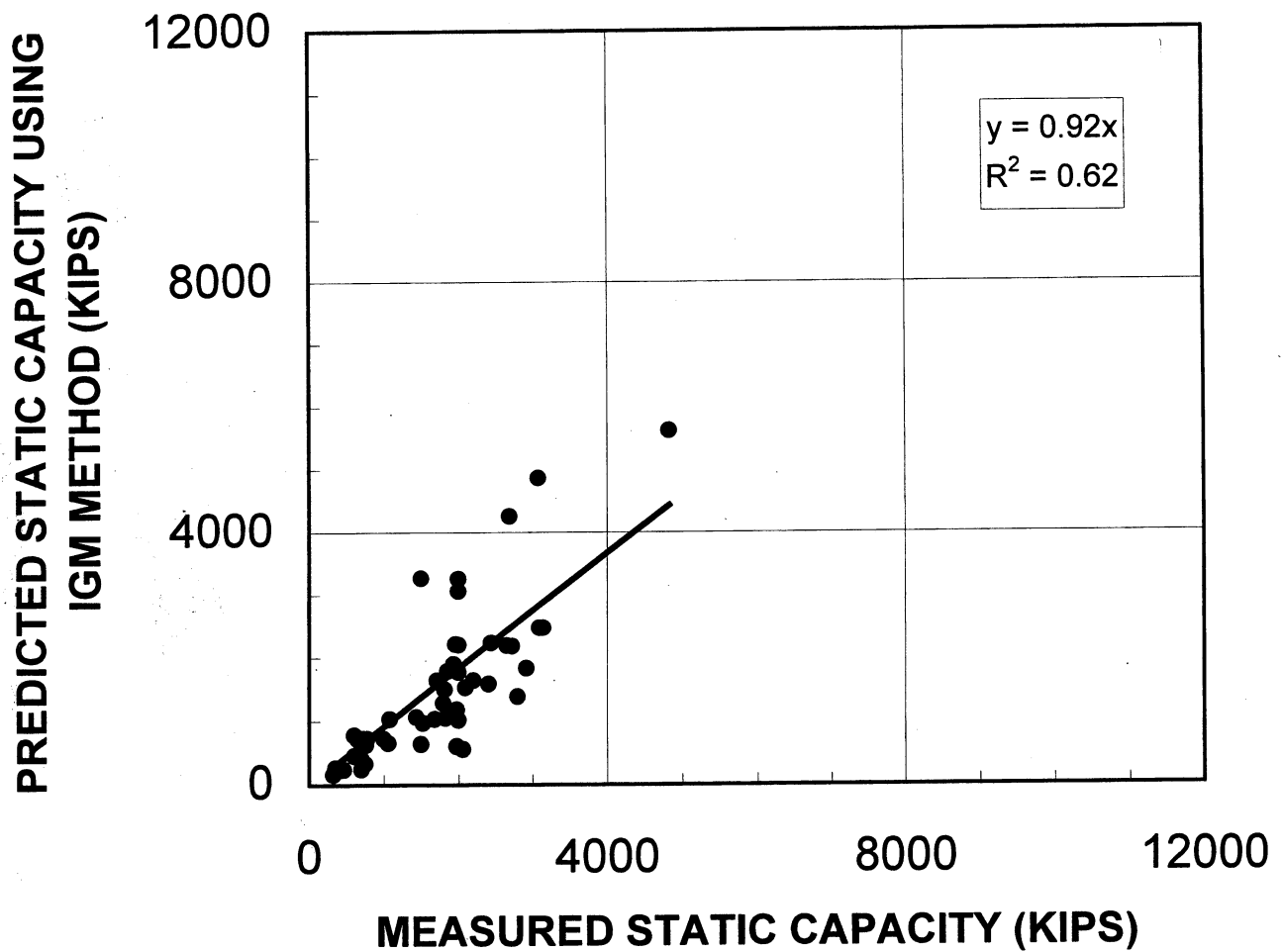


Figure 28

# DRILLED SHAFT IN ROCK

CONSTRUCTION METHOD= DRY  
LOAD TRANSFER= SKIN FRICTION + END  
BEARING  
N= 32  
MEAN=1.50  
STANARD DEVIATION = 0.83  
COEFFICIENT OF VARIATION =0.56

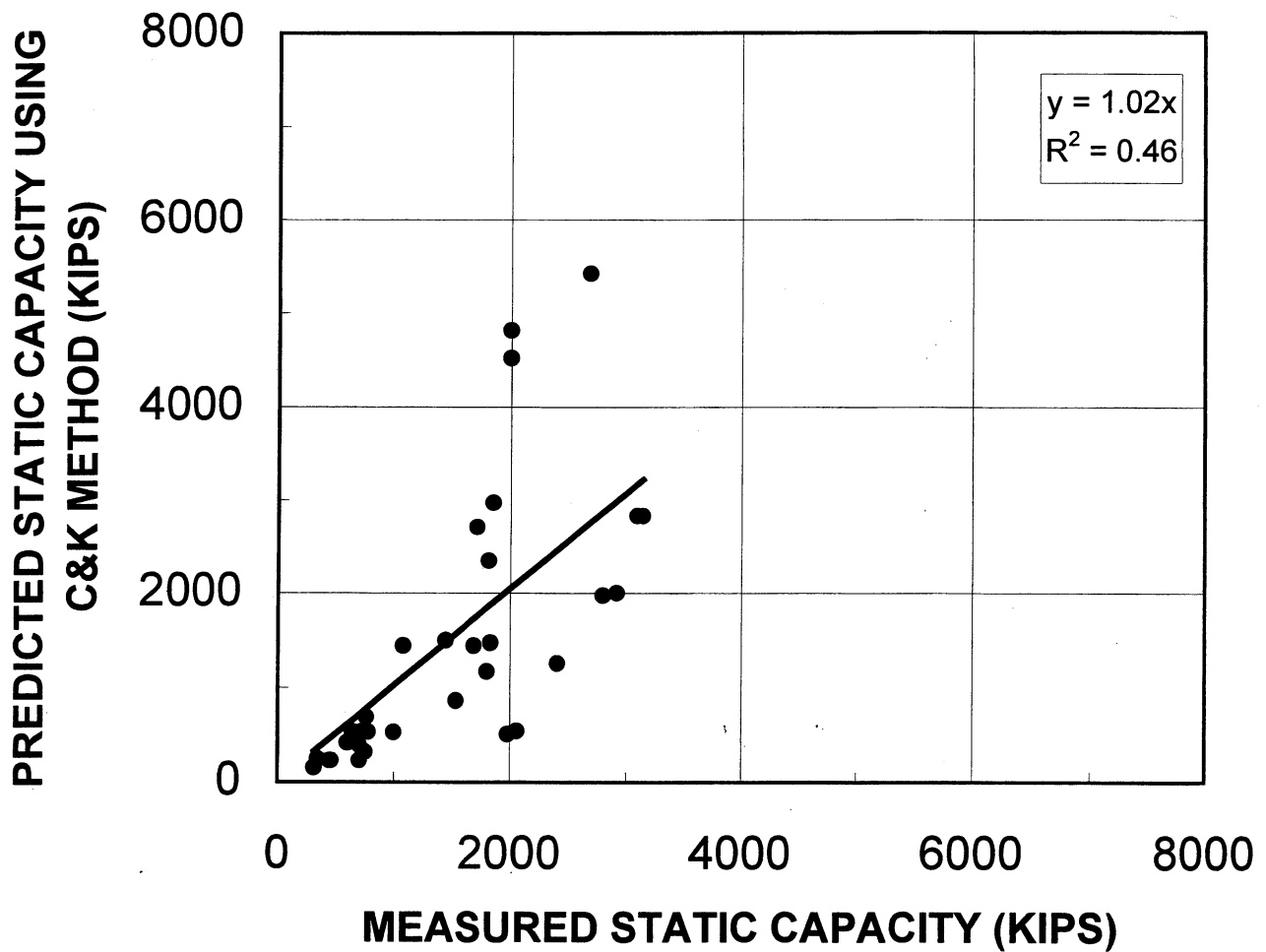


Figure 29

# DRILLED SHAFT IN ROCK

CONSTRUCTION METHOD= DRY  
LOAD TRANSFER= SKIN FRICTION + END  
BEARING  
N= 32  
MEAN=1.39  
STANARD DEVIATION = 0.74  
COEFFICIENT OF VARIATION =0.53

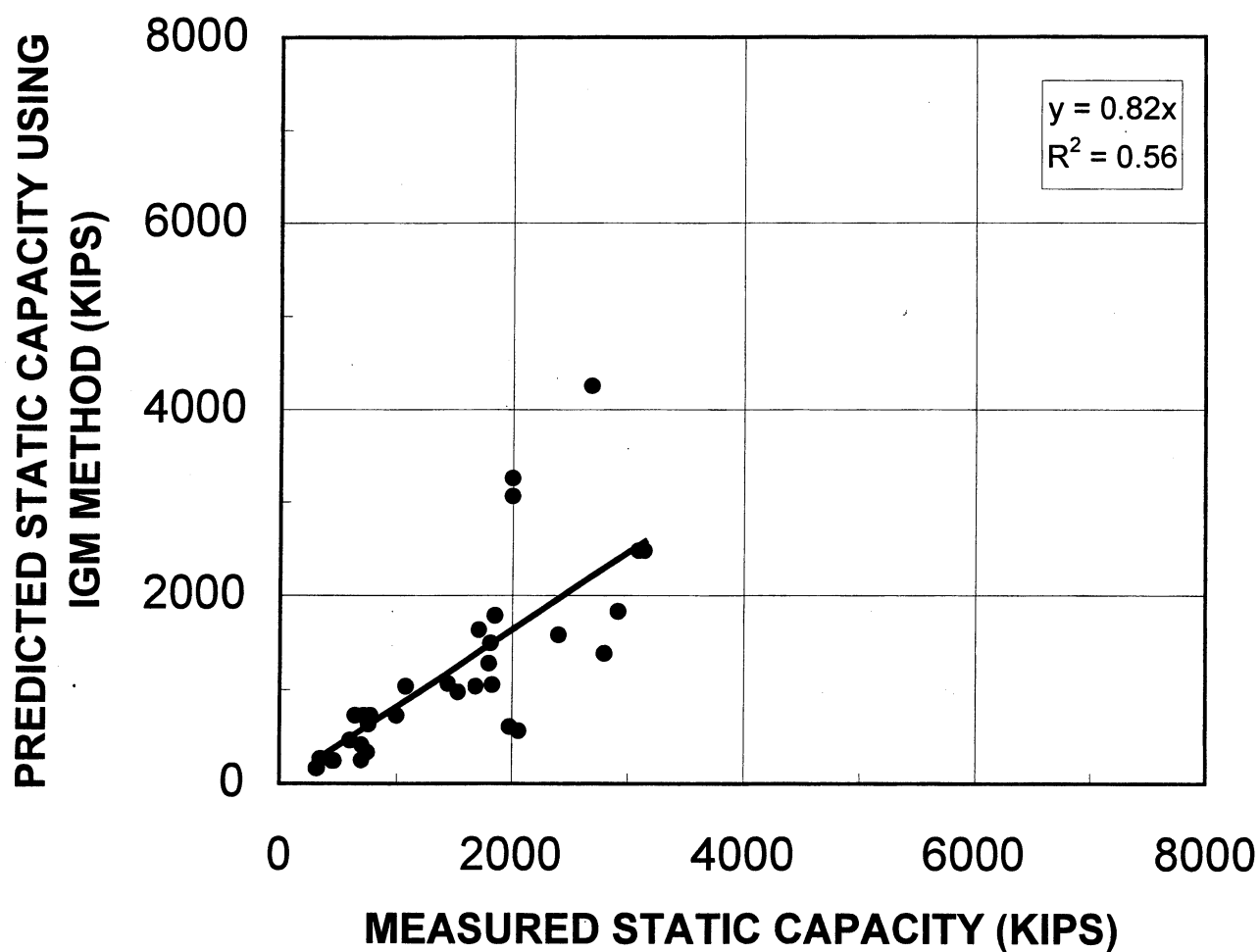


Figure 30

Table			Failure Load(kips)	C&K	C&K	IGM	IGM
SHAFT #	Construction	SOIL		Predict(kips)	Ratio	Predict(kips)	Ratio
8	Casing	sand/clay/rock	1500	4332.00	0.35	3269.00	0.46
47	Casing	sand/rock	1816	2348.00	0.77	1497.00	1.21
49	Casing	sand/rock	760	693.00	1.10	633.00	1.20
50	Casing	rock	644	537.00	1.20	728.00	0.88
55	Casing	sand/rock	2800	1976.00	1.42	1384.00	2.02
111	Dry	clay/rock	2060	547.00	3.77	562.00	3.67
112	Dry	sand/rock	1000	535.00	1.87	729.00	1.37
115	Dry	silt/rock	700	395.00	1.77	416.00	1.68
118	Dry	silt/rock	320	159.00	2.01	166.00	1.93
120	Dry	silt/rock	460	236.00	1.95	245.00	1.88
171	Dry	clay/gravel	600	422.00	1.42	462.00	1.30
257	Dry	Sand/rock	1935.6	1974.00	0.98	1895.00	1.02
258	Slurry & Casing	sand/rock	2096	1590.00	1.32	1530.00	1.37
261	Slurry & Casing	sand/rock	2720	2636.00	1.03	2186.00	1.24
262	Slurry & Casing	sand/rock	1962	2624.00	0.75	2214.00	0.89
263	Slurry & Casing	sand/rock	4828	9545.00	0.51	5626.00	0.86
264	Slurry & Casing	sand/rock	3078	7805.00	0.39	4870.00	0.63

SKIN SHAFT in ROCK

<b>TOTAL</b>			<b>17</b>
	<b>C&amp;K</b>	<b>IGM</b>	
<b>MEAN</b>	<b>1.33</b>	<b>1.39</b>	
<b>STDV</b>	<b>0.82</b>	<b>0.74</b>	
<b>VAR</b>	<b>0.62</b>	<b>0.53</b>	

# DRILLED SHAFT IN ROCK

CONSTRUCTION METHOD= MIXED

LOAD TRANSFER= SKIN FRICTION

N= 17

MEAN=1.33

STANDARD DEVIATION = 0.82

COEFFICIENT OF VARIATION =0.62

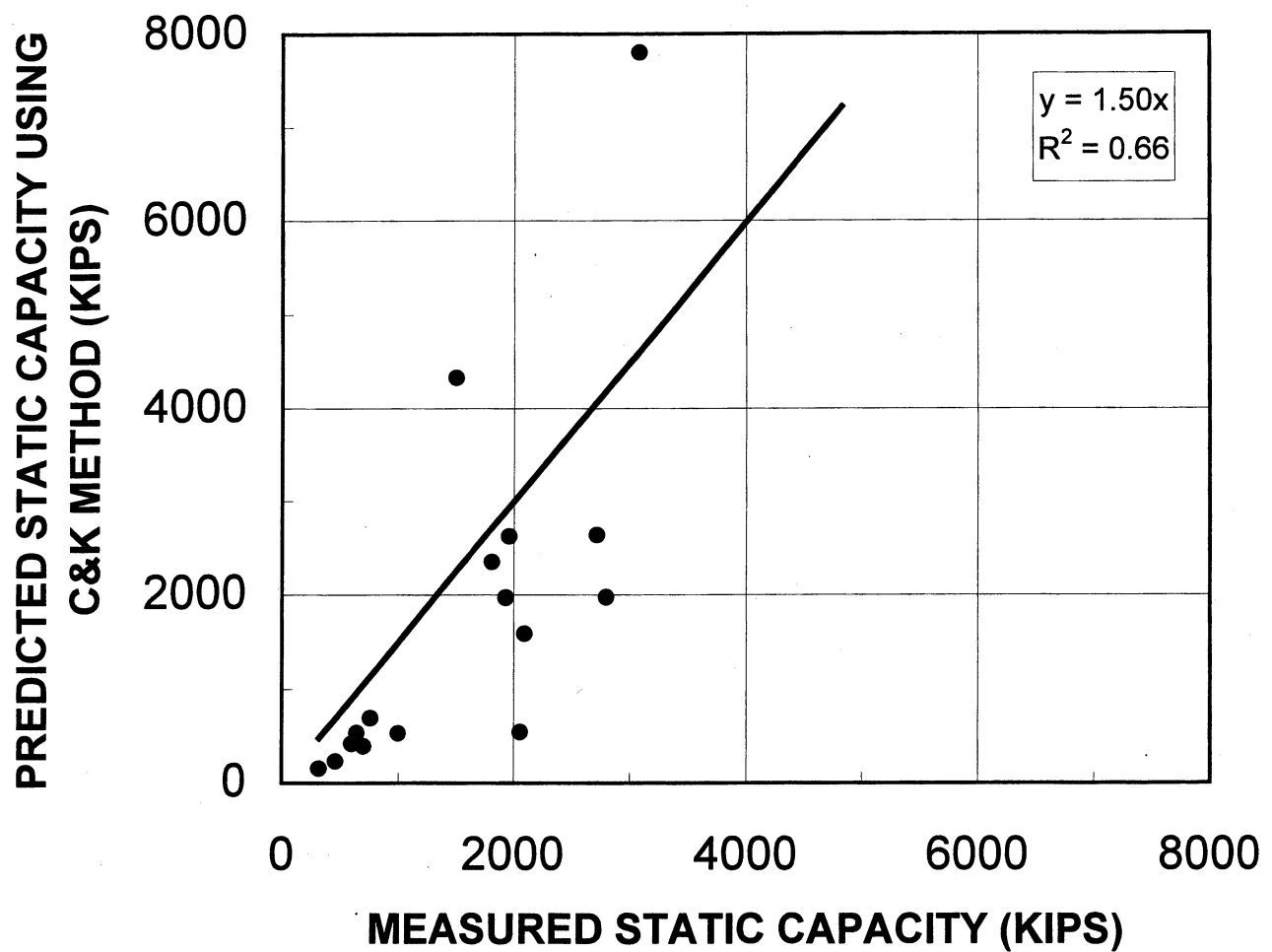


Figure 31



# DRILLED SHAFT IN ROCK

CONSTRUCTION METHOD= MIXED  
LOAD TRANSFER= SKIN FRICTION  
N= 17  
MEAN=1.39  
STANARD DEVIATION = 0.74  
COEFFICIENT OF VARIATION =0.53

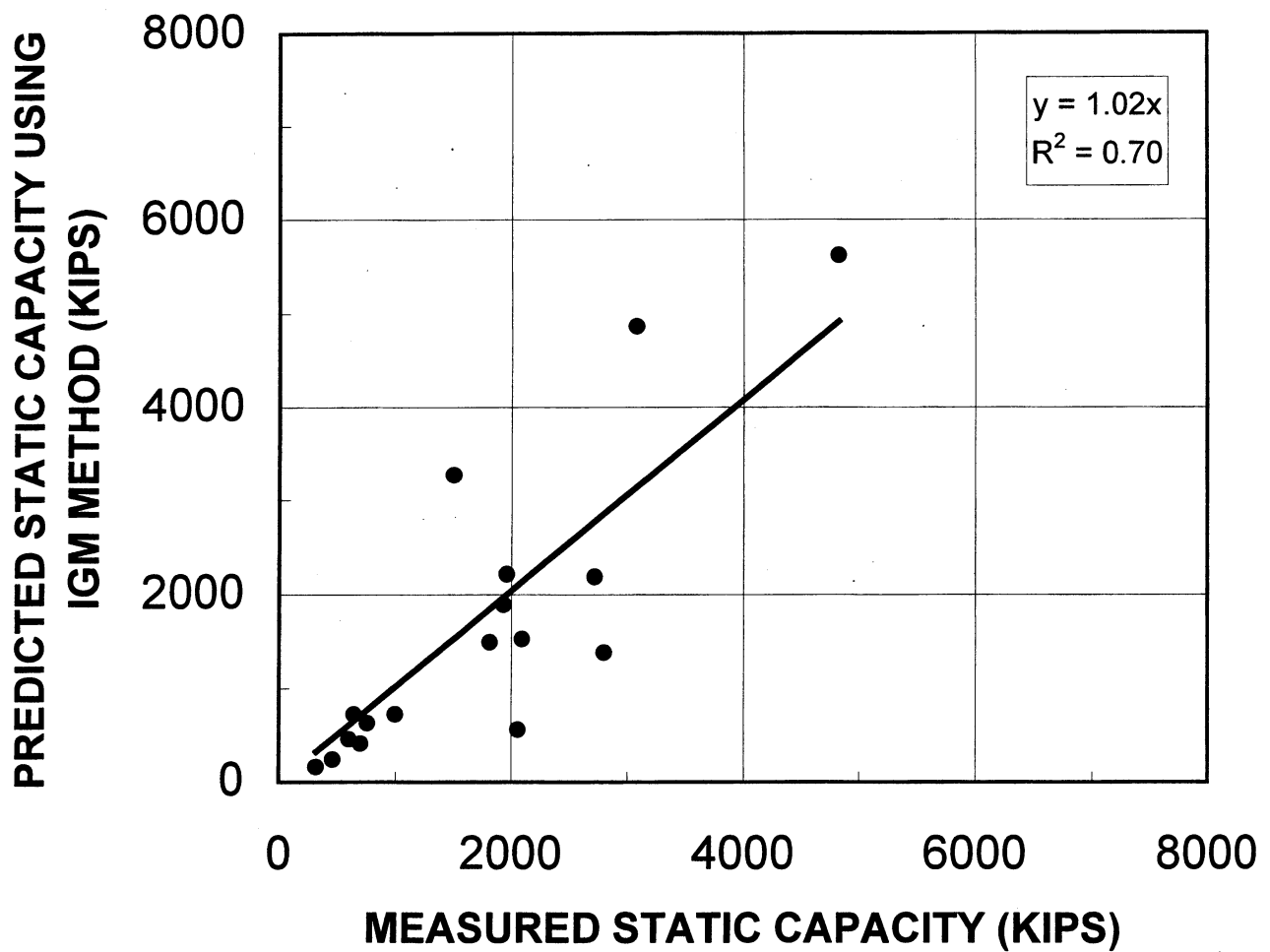


Figure 32

# **DRILLED SHAFTS - STATIC ANALYSIS**

## **DESCRIPTION OF STATIC CAPACITY**

### **EVALUATION METHODS**

Federal Highway Administration's Design of Drilled Shafts

Reese and Wright & Carter and Kulhway Design of Drilled Shafts

List of References

Appendix A - Examples

## **Federal Highway Administration's Design of Drilled Shafts**

The Federal Highway Administration (FHWA) design of drilled shafts founded in sand, clay, and intermediate geomaterial (i.e. soft rock) follows O'Neill and Reese (1999) and O'Neil et. al (1996).

According to FHWA, the axial capacity of a drilled shaft may be calculated as:

$$Q_t = Q_s + Q_b \quad (\text{Eqn 1})$$

where:

$Q_t$  = failure shaft capacity

$Q_s$  = skin friction capacity

$Q_b$  = end bearing capacity

In Eqn. 1, shaft capacity or failure is defined as the applied load which will result in settlement of the top of the drilled shaft equal to five percent the diameter of the shaft. An explanation of the computation of  $Q_s$  and  $Q_b$  for each material (i.e. sand, clay, and intermediate geomaterials) is presented below with examples given in Appendix A.

### **Skin Friction, $Q_s$ , and End Bearing, $Q_b$ , for Clay**

**Skin Transfer** - The load transfer in side resistance for drilled shafts founded in clay is a variant of Tomlinson's Alpha ( $\alpha$ ) method (19 ). The undrained shear strength  $C_u$  of clay (found from laboratory tests or insitu correlations) is multiplied by alpha,  $\alpha$ , to compute the unit skin friction (stress) at the depth  $z$  below the ground surface as follows,

$$f_{su} = \alpha C_u \quad (\text{Eqn 2})$$

where

$f_{su}$  = unit skin friction (stress) at depth  $z$

$\alpha$  = empirical factor that varies with depth, (see Table 1) and

$C_u$  = undrained shear strength at depth  $z$

**Table 1 Recommended Values for  $\alpha$  for Drilled Shafts in Clay**

Location along Drilled Shaft	Value of $\alpha$	Maximum Value of fsu (tsf)
From ground surface to depth of 5 ft. (1.52 m.)	0.0	0.0
From ground surface to length of casing	0.0	0.0
Bottom 1 diameter of shaft or 1 stem diameter above top of bell	0.0	0.0
All other points along drilled shaft sides	0.55	2.75 tsf (275 kPa)

Due to disturbances (i.e. drilling tool entering and exiting the hole frequently), the unit skin friction for the top five foot (see Fig. 1 and Table 1)) is neglected (i.e. set to zero).

The setting of  $\alpha = 0$  for a distance of one diameter above the base is from the work of Ellison et al. (1971). They showed that the downward movement of the base of the shaft can result in the development of a tensile crack in the soil near the base resulting in a lateral stress reduction. Consequently the unit skin friction in this zone (i.e. one diameter above the base) is set to zero.

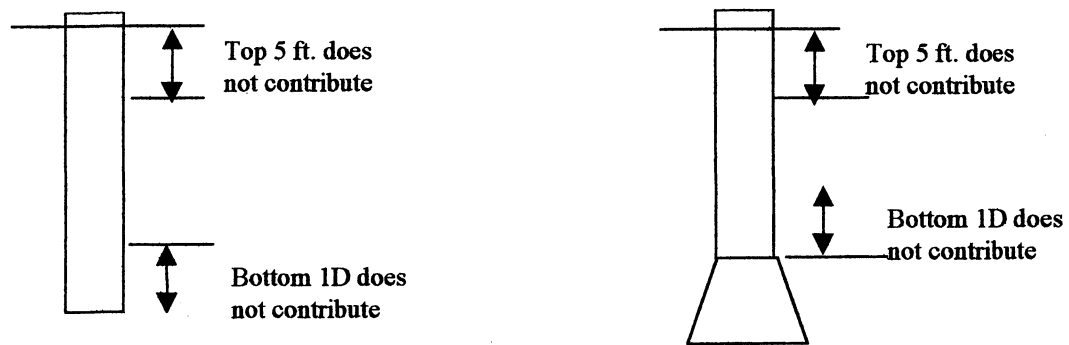


**Figure 1 Portions of Drilled Shaft Non-Contributory in Friction**

The total side resistance (i.e. force),  $Q_s$  for a given layer located at depths  $L_1$  and  $L_2$  below the ground surface is given as:

$$Q_s = \int_{L_1}^{L_2} f_{su} dA \quad (\text{Eqn 3})$$

where  $dA$  = differential area of the perimeter along the side over a specific depth.

**End Bearing** – FHWA's unit end bearing (stress) for a drilled shaft founded in clay is based on the work of Skempton (1951):

$$q_b = N_c C_u, \quad q_b < 40 \text{ tsf (4000 kPa)} \quad (\text{Eqn 4})$$

where:

$q_b$  = unit end bearing for drilled shafts in clay

$N_c = 6.0[1 + 0.2(L/B)]$  (bearing capacity factor)  $N_c < 9$

$C_u$  = average undrained shear strength of clay for 1.0 B below the tip

$L$  = total embedment length of shaft in the ground

$B$  = diameter of shaft at the base.

It should be noted that the limiting value of  $q_b$  (40 tsf) given in Eqn. 4 is the largest measured end bearing recorded for drilled shafts and not a theoretical limit (Engling and Reese, 1974)

In the case of drilled shaft diameters (at the base:  $B_b$ ) exceeding 75 inches (1.9 m), the FHWA reduces the unit end bearing,  $q_b$ , to  $q_{br}$  to ensure tolerable settlements under service load conditions. Again, failure capacity of a shaft is the load, which develops settlements equal to five percent the diameter of the shaft. The reduced bearing resistance is defined as:

$$q_{br} = F_r q_b \quad (\text{Eqn 5})$$

where:

$$F_r = 2.5/[aB_b (\text{inches}) + 2.5 b] \quad F < 1.0$$

in which

$$\begin{aligned} a &= 0.0071 + 0.0021 (L/B_b), & a < 0.015 \\ b &= 0.45 (C_u)^{0.5} & 0.5 < b < 1.5 \text{ and } C_u \text{ in ksf} \end{aligned}$$

The latter expressions were based upon load tests of large under-reamed drilled shafts in very stiff clay (O'Neill and Sheikh, 1985). The reduced bearing resistance,  $q_{br}$ , gave similar results to the measured net bearing stress at a base settlement of 2.5 inches (6.35 cm). In addition, when more than half the design load is carried by end bearing, a global factor of safety greater than 2.5 is recommended by FHWA, unless site specific load tests are performed.

The failure end-bearing load,  $Q_b$ , is computed as  $q_b$  or  $q_{br}$  times the cross-sectional area of the drilled shaft's base. An example of capacity prediction for a drilled shaft founded in clay is given in Appendix A.

## **Skin Friction, $Q_s$ , and End Bearing, $Q_b$ , for Sand**

**Skin Transfer** - The unit side resistance on a drilled shaft founded in sand is based on Coulombic friction, i.e. equal to the normal (horizontal) effective stress times a coefficient of friction ( $\tan \phi_c$ ).

$$f_{sz} = K \sigma_z \tan \phi_c \quad (\text{Eqn 6})$$

**The total side resistance (i.e. force),  $Q_s$ , for a given layer located at depths  $L$  below the ground surface is given as**

$$Q_s = \int_0^L K \sigma_z \tan \phi_c dA \quad (\text{Eqn 7})$$

where

- $f_{sz}$  = ultimate unit side shear resistance in sand at depth  $z$ ,
- $K$  = a parameter that combines the lateral pressure coefficient
- $\sigma_z$  = vertical effective stress at depth  $z$
- $\phi_c$  = interface friction angle for soil-concrete
- $L$  = depth of embedment for drilled shaft in sand
- $dA$  = differential area of perimeter along sides of drilled shaft

Generally, the normal stress at the interface of the drilled shaft and the soil is relatively low when the excavation is completed; however the fluid stress from the fresh concrete will impose a normal stress that is dependent on the characteristics of the concrete. Experiments have shown that concrete with moderate slump (up to 6 inches, 15 cm.) act hydrostatically over a depth of 10 to 15 ft. (3 to 4.5 m.) followed by a leveling off of lateral stress at greater depths, probably due to arching (Bernal and Reese, 1983). Concrete with higher slump ( about 9 inches, 23 cm.) act hydrostatically to a depth of 32 ft. (10 m.). Thus, construction procedures and the concrete characteristics

will probably have a strong influence on the magnitude of the lateral stress at the soil-concrete interface.

As a result of the drilling and concreting influences, the  $K \tan \phi$  in Eqn. 6 is replaced by a simple constant,  $\beta$ , as a function of depth to account for variation in lateral stresses (i.e.  $K$ ):

$$\beta = 1.5 - 0.135\sqrt{z} \quad 1.2 > \beta > 0.25 \quad (\text{Eqn 8})$$

Consequently, the unit skin friction (stress) is given by

$$f_{sz} = \beta \sigma_z \quad (\text{Eqn. 9})$$

The total side resistance (i.e. force),  $Q_s$  for a given layer located at depths  $L$  below the ground surface is given as

$$Q_s = \int \beta \sigma_z dA \quad (\text{Eqn 10})$$

It should be noted that the limiting unit skin friction (Eqn. 9) is again not a theoretical limit, but rather is merely the largest value that has been measured (Owens and Reese, 1982). Higher values can be used if justified via a load test.

**End Bearing** - Generally, an experimental tip resistance curve for a drilled shaft in sand shows that the end bearing is still increasing at settlements equal to five percent the diameter of the shaft (i.e. FHWA defined shaft capacity). For instance, settlements of more than fifteen percent the diameter have been recorded. However, since such large settlement is not tolerated for most structures, FHWA limits end bearing and settlements to five percent of the shaft's base diameter.



The values of the unit end bearing (stress)  $q_b$  are tabulated as a function of  $N_{SPT}$  (uncorrected field values) in Table 3 for shaft diameters less than 50 inches. In the case of large diameter shafts [i.e. Shaft diameter,  $D > 50$  in. (1.3m)], equation 11 is used:

$$q_{br} = 50 * (q_b/B_b); B_b \text{ in inches}$$

$$\text{or } q_{br} = 1.3 * (q_b/B_b); B_b \text{ in meters} \quad (\text{Eqn 11})$$

**Table 3 Recommended Unit End Bearing Values for Cohesionless Soils**

$N_{SPT}$ Values (Uncorrected)	Value of $q_b$ (TSF) [kPa]
0 to 75	$(0.60 N_{SPT}) [60 N_{SPT}]$
above 75	(45) [4500]

Table 3 limits the unit end bearing to 45 tsf (4500 kPa) at a settlement of 5 percent of the base diameter. Higher values, i.e. 58 tsf (5800 kPa) was measured for a settlement of 4 percent of the base diameter in Florida (Owens and Reese, 1982), are viable with load testing. An example of capacity prediction for a drilled shaft founded in sand is given in Appendix A.

#### **Skin Friction, $Q_s$ , and End Bearing, $Q_b$ , for Intermediate Geomaterials (Soft Rock)**

FHWA's determination of skin and tip resistance for a drilled shaft founded in soft rock is based on a recent publication of O'Neill and et. al (1996). The equations for unit skin friction and end bearing are presented separately.

**Side Resistance** – Requires a six step approach as identified:

1. Find the average  $E_m$  (mass modulus of rock) and  $f_{su}$  (ultimate unit skin friction) along the side of the rock socket:

$$E_m = \Sigma E_{mk} L_k / \Sigma L_k \quad (\text{Eqn 12})$$

where  $E_m = 115 q_u$  and

$$f_{su} = \Sigma f_{sk} L_k / \Sigma L_k \quad (\text{Eqn 13})$$

where  $f_{su}$  = ultimate side friction.

The values selected for  $f_{su}$  depend whether the socket is considered “smooth” and failure occurs at the interface ( $\alpha$  values) or “rough” where failure occurs through the rock. The rough assumption was used in this study and  $f_{su}$  was set equal to  $0.5\sqrt{q_u}\sqrt{q_t}$ .

2. Calculate  $\Omega$  given by Eqn. 14:

$$\Omega = 1.14\left(\frac{L}{D}\right)^{0.5} - 0.05\left[\left(\frac{L}{D}\right)^{0.5} \log_{10}\left(\frac{E_c}{E_m}\right) - 0.44\right] \quad (\text{Eqn. 14})$$

where  $L$  = socket length and modulus of concrete is given as  $E_c(\Psi) = 57,000\sqrt{q_{uc}}$

3. Calculate  $\Gamma$  given by Eqn. 15

$$\Gamma = 0.37\sqrt{\left(\frac{L}{D}\right)} - 0.15\left[\sqrt{\left(\frac{L}{D}\right)} - 1\right]\log_{10}\left(\frac{E_c}{E_m}\right) + 0.13 \quad (\text{Eqn. 15})$$

4. Find  $n$  (socket surface roughness)

For “rough” sockets;

$$n = \sigma / q_u \quad \text{where } \sigma = \text{normal stress of concrete} = \gamma_c Z_c M \quad (\text{Eqn. 16})$$

where  $\gamma_c = 130 \text{ pcf}$  or  $20.5 \text{ kN/m}^3$

and M is given in Table 4 below based on concrete slump and socket depth

Table 4 Values of M

Socket Depth (m)	Slump (mm)		
	125	175	225
4	0.50	0.95	1.0
8	0.45	0.75	1.0
12	0.35	0.65	0.9

Also, if a water table is present, then  $\sigma_n = \gamma_c (Z_c - Z_w) + \gamma_w Z_w$ , where  $Z_c$  = depth to water table.

In the case of a “smooth” socket, n is estimated from Figure 2.

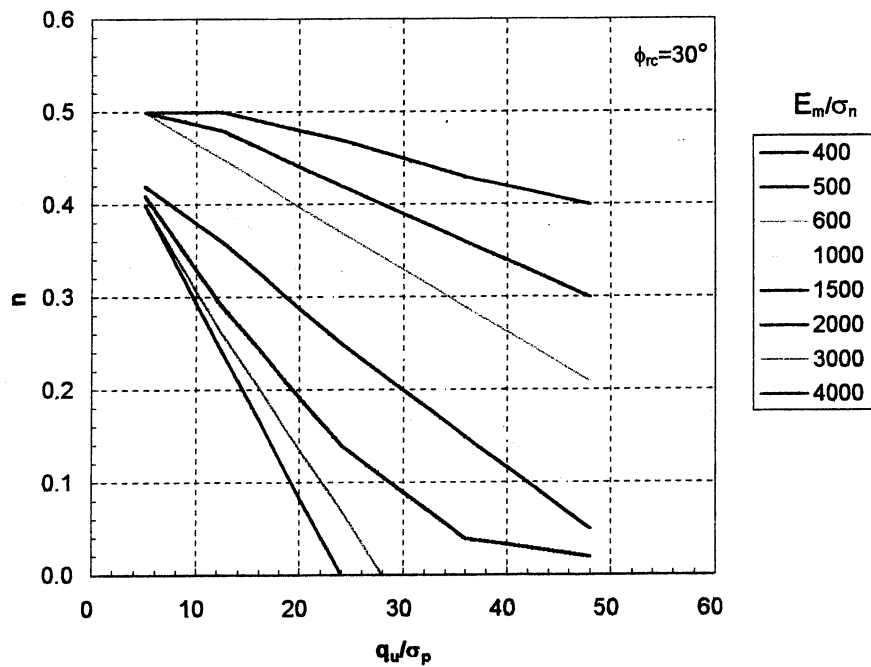


Figure 2 N Factors for Smooth Sockets

5. Next calculate  $\Theta_f$  and  $K_f$  as given below:

$$\Theta_f = \frac{E_m \Omega}{\pi L \Gamma} W_t \quad (\text{Eqn. 17})$$

$$K_f = n + \frac{(\Theta_f - n)(1 - n)}{\Theta_f - 2n + 1} < 1 \quad (\text{Eqn. 18})$$

where

$W_t$  = deflection at top of rock socket

6. Finally, calculate the side shear load transfer vs. deformation from:

$$Q_s = \pi DL \Theta_f f_{su} \quad \Theta_f < n \quad (\text{Eqn. 19})$$

$$Q_s = \pi DL K_f f_{su} \quad \Theta_f > n \quad (\text{Eqn. 20})$$

**End Bearing** – The tip resistance as a function of displacement according to O'Neill et al. (1996) is found from :

$$Q_b = \frac{\pi D^2}{4} q_b \quad (\text{Eqn. 21})$$

where  $q_b = \Lambda W_t^{0.67}$ , and

$$\Lambda = 0.0134 E_m \frac{(L/D)}{(1+L/D)} \left\{ \frac{[200(L/D)^{0.5} - \Omega][1 + (L/D)]}{\pi L \Gamma} \right\}^{0.67} \quad (\text{Eqn. 22})$$

The total shaft resistance,  $Q_t$ , for a rock socket is the sum of  $Q_s + Q_b$ . An example of a drilled shaft design in soft rock is given in Appendix A.

## **Reese and Wright & Carter and Kulhway Design of Drilled Shafts**

Similar to the FHWA design, Reese and Wright (1977) and Carter and Kulhway (1988) proposed that the general equation for computing the failure capacity of a drilled shaft be as follows.

$$Q_T = Q_B + Q_S = q_b A_b + q_s A_s \quad (\text{Eqn. 23})$$

Where  $Q_T$  is ultimate capacity  
 $Q_B$  is ultimate tip resistance  
 $Q_S$  is ultimate side resistance  
 $q_b$  is unit end bearing  
 $q_s$  is unit skin friction  
 $A_b$  is base area  
 $A_s$  is perimeter surface area

In Eqn. 23, shaft capacity or failure is defined as the applied load which will result in settlement of the top of the drilled shaft equal to five percent the diameter of the shaft. An explanation of the computation of  $Q_B$  and  $Q_S$  for each material (i.e. sand, clay, and intermediate geomaterials) is presented below

### **Reese and Wright**

In 1977 Reese and Wright (1977) proposed a semi-empirical method to estimate the unit skin friction ( $q_s$ ) and unit end bearing ( $q_b$ ) for drilled shafts founded in sands using uncorrected SPT blow count,  $N$ . A discussion of unit skin friction and end bearing follows:

**Unit skin friction,  $q_s$ , for sands:**

$$\begin{aligned} \text{For } N \leq 53, \quad q_s \text{ (MPa)} &= 0.0028 N \\ \text{For } 53 < N \leq 100, \quad q_s \text{ (MPa)} &= 0.00021 (N - 53) + 0.15 \end{aligned} \quad (\text{Eqn. 24})$$

In the case of multiple soil layers, i.e. sand with clay, the FHWA approach for clay, i.e.  $\alpha C_u$  was employed.

**Unit end bearing  $q_b$  for sands:**

$$\begin{aligned} \text{For } N \leq 60, \quad q_b \text{ (MPa)} &= 0.064 N \\ \text{For } N > 60, \quad q_b \text{ (MPa)} &= 3.8 \end{aligned} \quad (\text{Eqn. 25})$$

Where  $N$  is the uncorrected SPT  $N$  value (blows/300 mm). The unit end bearing is based on a settlement equal five percent the diameter of the base of the drilled shaft.

### **Carter and Kulhawy**

Carter and Kulhawy (1987) investigated drilled shafts socketed into weak rock and developed an expression for unit skin friction. In the case of end bearing, the method proposed in the Canadian Foundation Manual (1978) was used. A discussion of each follows.

**Unit skin friction,  $q_s$**  is based on average unconfined compressive strength of the rock,

$$q_s = 0.15 q_u \quad (\text{Eqn. 26})$$

where  $q_u$  is uniaxial compressive strength of the rock or concrete, whichever is less.

**Unit end bearing  $q_b$**  - Although Carter and Kulhawy (1987) didn't propose an equation to estimate the unit end bearing, the data base indicated that significant amount of end bearing could be mobilized under relatively small deformation. Consequently, the unit end bearing was computed by the Canadian Foundation Manual (1978) approach:

$$q_b = K_{sp} \times q_u$$

$$K_{sp} = \frac{9 + \frac{3c_s}{B_b}}{10(1 + 300 \frac{\delta}{c_s})^{0.5}} \quad (\text{Eqn. 27})$$

where  $q_b$  is ultimate end bearing  
 $K_{sp}$  is empirical coefficient  
 $q_u$  is uniaxial compressive strength of the rock  
 $c_s$  is spacing of discontinuities  
 $\delta$  is thickness of individual discontinuities  
 $B_b$  is diameter of socket

A value of 1 was used for  $\delta/c_s$  when no information on discontinuities was available for the site.

## REFERENCES

- Bernal, J.B., and Reese, L.C. "Study of the Lateral Pressure of Fresh Concrete as Related to the Design of Drilled Shafts", Research Report 308-1F, Center for Transportation Research, University of Texas, Austin, TX 1983
- Carter, J.P., and Kulhawy, F.H., "Analysis and Design of Drilled Shaft Foundations Socketed into Rock", EPRI Report EL-5918, Electric Power Research Institute, Palo Alto, California, 1988.
- Ellison, R.D., D'Appolinia, E., and Theirs, G.R., "Load-Deformation Mechanism for Bored Piles", Journal of Soil Mechanics, ASCE, Vol. 97, No. SM4, April 1971, pp. 661-678.
- Engleing, D., Reese, L.C., "Behavior of Three Instrumented Drilled Shafts under Short Term Axial Loading", Research Report 176-3, Conducted at the Center for Highway Research, University of Texas, Austin TX, for FHWA and Texas Highway Department, May 1974, 116 Pages.
- McVay, M.C., Townsend, F.C., and Williams, R.C., "Design of Socketed Drilled Shafts in Limestone", ASCE Journal of Geotechnical Engineering, Vol. 118, No. 10, pp. 1626-1637, 1992.
- O'Neill, M. W. and Reese, L. C., "Drilled Shaft: Construction Procedures and Design Methods", Federal Highway Administration, FHWA-IF-99-025, 1999
- O'Neill, M.W., and Sheikh, S.A., "Geotechnical Behavior of Underreams in Pleistocene Clay, Drilled Piers and Caissons II, ASCE, May 1985 pp. 57-75.
- O'Neill, M. W., Townsend, F.C., Hassan, K.M., Buller, A., and Chan, P.S., "Load Transfer for Drilled Shafts in Intermediate Geomaterials" FHWA - RD-95-172. 1996.
- Owens, M.J. and Reese, L.C., "The Influence of a Steel Casing of the Axial Capacity of a Drilled Shaft" Research Report 255-1F, Report to the Texas State Highway Department, Center of Transportation Research, University of Texas, Austin, TX. July 1982, 204 pages.
- Reese, L.C., and O'Neill, M.W., "Drilled Shafts: Construction and Procedures and Design Methods", Report No. FHWA-HI-88-042, Federal Highway Administration, 1988.
- Reese, L. C. and Wright, S. J. "Construction Procedures and Design for Axial Loading," FHWA Drilled Shaft Manual HDV-22, 1977.
- Skempton, A.W., "The Bearing Capacity of Clay", Proceedings Bld. Research Congress, Div. I, Bld Res. Cong., London, 1951.

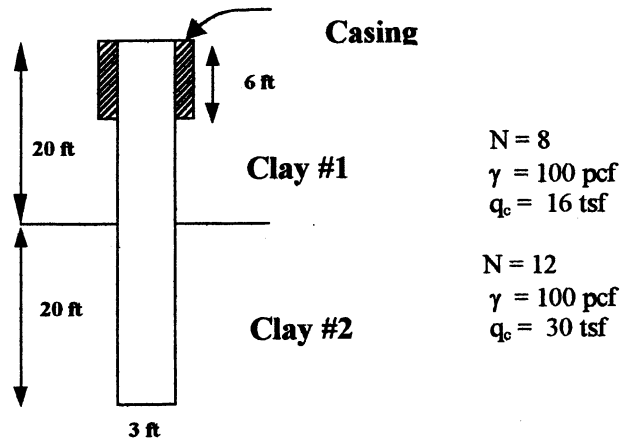


## APPENDIX A - Examples

### CLAYS:

Consider Two Cases:

1. Multi Layer Clay with Casing
2. Multi Layer Clay with Casing B > 75 "



$$c = \frac{q_c - \sigma_0}{15}$$

$$\text{Clay Layer \# 1 : } c = \frac{16 * 2000 - 10 * 100}{15} = 2,066.67 \text{ psf (1.0333 tsf)}$$

$$\text{Clay Layer \# 2 : } c = \frac{30 * 2000 - 30 * 100}{15} = 3,800 \text{ psf (1.90 tsf)}$$

1. Multi Layer Clay with Casing: Full Capacity (40 ft Shaft)

a) Skin Friction:

$$\begin{aligned}
 Q_s &= \pi * 3.0 * [(20' - 6')(0.55 * 1.033) + (20' - 3')(0.55 * 1.9)] \\
 &= 9.4248 * [7.9567 + 17.765] \\
 &= 242.42 \text{ Tons}
 \end{aligned}$$

b) End Bearing:

$$Q_b = q_b \cdot \frac{\pi b^2}{4},$$

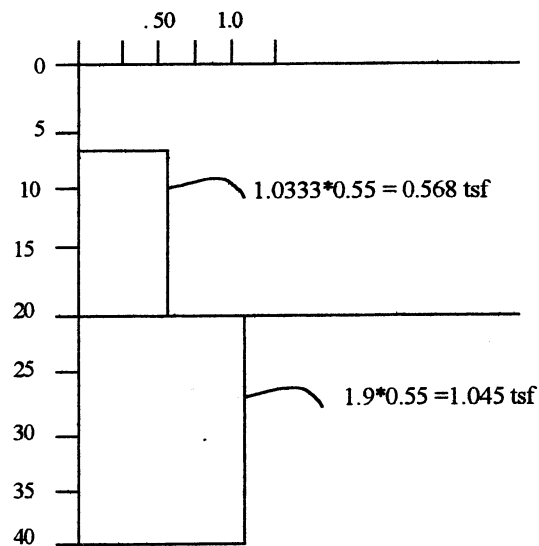
$$q_b = N_c C_u,$$

$$N_c = 6.0 * \left[ 1 + 0.2 \frac{40}{3} \right] = 22 > 9 \text{ (use 9)}$$

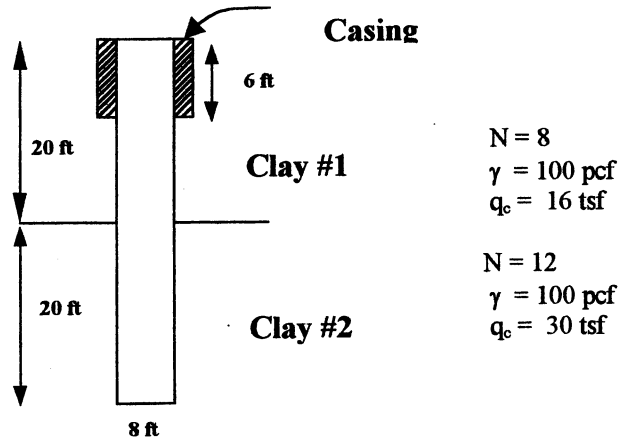
$$Q_b = (9 * 1.9 \text{ tsf}) \cdot \frac{\pi 3^2}{4} = 120.87 \text{ Tons}$$

- c) Total Capacity = Skin Friction + End Bearing  
 = 242.42 + 120.87  
 = 363.29 Tons (ultimate)

- d) Unit Skin Friction with depth:



2. Multi Layer Clay with Casing, but  $B > 75''$  (1.9m):



a) Skin Friction:  $Q_s = \pi * 8.0 * [(20' - 6')(0.55 * 1.033) + (20' - 8')(0.55 * 1.9)]$   
 $= 25.1327 * [7.9567 + 12.5]$   
 $= 515.14 \text{ Tons}$

b) End Bearing: If  $B > 75''$ , then  $q_{br} = F_r q_b$

$$F_r = \frac{2.5}{[a B_b(\text{inches}) + 2.5 b]}$$

$$a = 0.0071 + 0.0021(L / B_b)$$

$$= 0.0071 + 0.0021(40' / 8')$$

$$= 0.0176, \text{ but } a < 0.015$$

$$b = 0.45\sqrt{C_u} = 0.45\sqrt{1.9 * 2.0}, C_u \text{ in } ksf$$

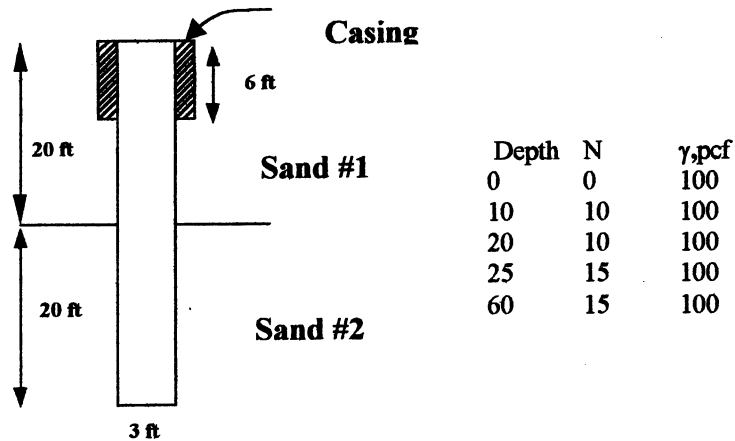
$$= 0.8772, 0.5 < b < 1.5$$

$$F_r = \frac{2.5}{[0.015 (96'') + 2.5 (0.8772)]} = 0.6881$$

$$Q_b = \frac{\pi * 8^2}{4} (0.6881)(9 * 1.9) = 591.48 \text{ Tons}$$

$$Q_t = 515.14 + 591.48 = 1106.62 \text{ Tons}$$

## SANDS:



### 1. Skin Friction:

$$\beta = 1.5 - 0.135 \sqrt{z} \quad 0.25 < \beta(\text{tsf}) < 1.2$$

$$\text{or } Z < 4.94\text{ft}, \beta = 1.2 \text{ tsf, and } Z > 85.73\text{ft}, \beta = 0.25$$

$$\begin{aligned} \int_6^{40} \beta \sigma_v dz &= \int_6^{40} 150Z - 13.5Z^{\frac{3}{2}} dZ = \frac{150Z^2}{2} - 13.5Z^{\frac{5}{2}} * \frac{2}{5} \Big|_6^{40} \\ &= 65,355.84 - 2,223.82 = 18,116.37 * \frac{3\pi}{2000} = 297.50^T \end{aligned}$$

### 2. End Bearing: above $8*B$ and below $3.5*B$ ,

$$\text{above: } 40.0 - 8*B = 40.0 - 8*(3) = 16';$$

$$\text{below: } 40.0 + 3.5*B = 40.0 + 3.5*(3) = 50.5'$$

$$\text{for } z = 16' \quad q_b = 0.6*N = 0.6*(10) = 6 \text{ tsf}$$

$$z = 20' \quad q_b = 0.6*N = 0.6*(10) = 6 \text{ tsf}$$

$$z = 25' \quad q_b = 0.6*N = 0.6*(15) = 9 \text{ tsf}$$

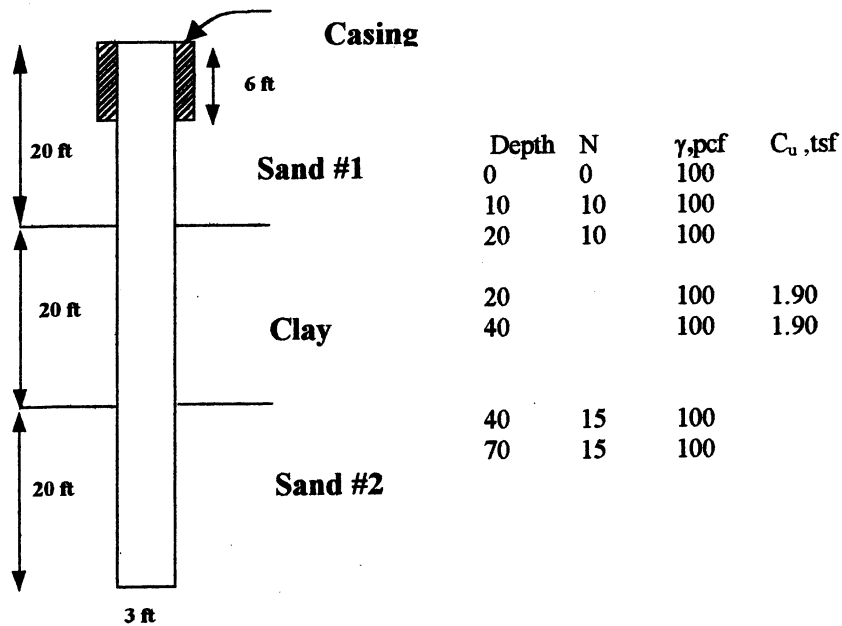
$$z = 60' \quad q_b = 0.6*N = 0.6*(15) = 9 \text{ tsf}$$

$$\therefore q_b = \left[ \frac{6 * (20 - 16) + \frac{9 + 6}{2} * (25 - 20) + 9 * (50.5 - 25)}{[50.5 - 16]} \right] = 8.4348$$

$$\text{So, } Q_b = 8.4348 * \left[ \frac{\pi * 3^2}{4} \right] = 59.622^T$$

$$Q_T = 297.5 + 59.62 = 357.12$$

### MULTILAYER- SAND-CLAY-SAND:



$$\begin{aligned}
 1. \text{ Skin Friction (6-20ft): } Q_s &= \frac{3 \cdot \pi}{2000} \int_6^{20} (1.5 - 0.135\sqrt{z}) \gamma z \, dz \\
 &= 0.0047 \left[ \frac{150 * z^2}{2} - 13.5 * z^{5/2} * \frac{5}{2} \right]_6^{20} \\
 &= 0.0047 [75 * (20^2 - 6^2) - 5.4 * (20^{5/2} - 6^{5/2})] \\
 &= 0.0047 [27,300 - 9,183.6] \\
 &= 85.371^T
 \end{aligned}$$

$$2. \text{ Skin Friction (20-40ft) : } Q_s = 3.\pi[(40 - 20)(0.55 * 1.9)]$$

$$= 196.978^T$$

$$3. \text{ Skin Friction (40-60ft) : } Q_s = \frac{3.\pi}{2000} \int_{40}^{60} (1.5 - 0.135\sqrt{z}) \gamma z dz$$

$$= 0.0047 \left[ \frac{150 * z^2}{2} - 13.5 * z^{5/2} * \frac{5}{2} \right]_{40}^{60}$$

$$= 0.0047 (75 * (60^2 - 40^2) - 5.4 * (60^{5/2} - 40^{5/2}))$$

$$= 0.0047 [150,000 - 95,937.4]$$

$$= 254.764^T$$

$$\Sigma Q_s = 85.371 + 196.978 + 254.764 = 537.11 \text{ tons}$$

4. Tip Resistance : above 8\*B and below 3.5\*B,

$$\text{Above: } 60.0 - 8*B = 60.0 - 8*(3) = 36 \text{ ft ;}$$

$$\text{Below: } 60.0 + 3.5*B = 60.0 + 3.5*(3) = 70.5 \text{ ft}$$

$$\text{For } z = 40 \text{ ft} \quad q_b = 0.6*N = 0.6*(15) = 9 \text{ tsf}$$

$$z = 60 \text{ ft} \quad q_b = 0.6*N = 0.6*(15) = 9 \text{ tsf}$$

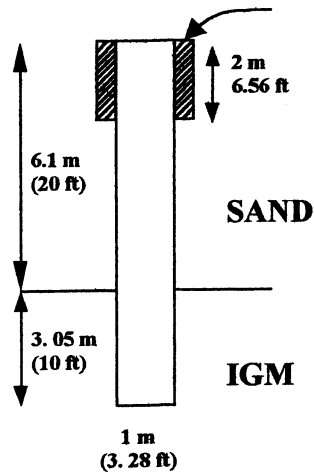
$$z = 75 \text{ ft} \quad q_b = 0.6*N = 0.6*(15) = 9 \text{ tsf}$$

$$\text{So, } Q_b = \left[ \frac{\pi * 3^2}{4} \right] * 9 = 63.62^T$$

Check  $q_b$  of overlaying Clay:

$$q_b = 9 * C_u = 9 * 1.9 = 17.1 \text{ tsf stronger, } \therefore \text{ stop @ 40ft.}$$

### IGM: (Sand & Limestone)



$$\gamma = 100 \text{ pcf (15.708 kN/m}^3\text{)}$$

$$N = 10$$

LimeStone:

$$q_u = 10 \text{ tsf (957.6 kPa, 0.96 MPa)}$$

$$q_t = 1 \text{ tsf (95.76 kPa, 0.096 MPa)}$$

$$\gamma = 135 \text{ pcf (21.2 kN/m}^3\text{)}, \quad \gamma_c = 20.4 \text{ kN/m}^3$$

$$E_c = 57,000 \sqrt{f'_y} = 57,000 \sqrt{5000 \text{ psi}}$$

$$= 4.03E6 \text{ psi (27.77E6 kPa)}$$

Because of unit comparison problems, calculate Sand using English and Rock using SI units.

$$1. \text{ Skin Friction (Sand): } Q_s = \frac{3.28 * \pi}{2000} \int_{6.56}^{20} (1.5 - 0.135\sqrt{z}) \gamma z dz$$

$$= \frac{3.28 * \pi}{2000} \left[ \frac{150 * z^2}{2} - 13.5 * z^{5/2} * \frac{5}{2} \right]_{6.56}^{20}$$

$$= \frac{3.28 * \pi}{2000} [75 * (20^2 - 6.56^2) - 5.4 * (20^{5/2} - 6.56^{5/2})]$$

$$= 0.00515 [26,772.5 - 9064.6]$$

$$= 91.23^T = 91.23 * 2000 / 224.809 = 811.66 \text{ kN}$$

3. Analysis of Rock resistance is based on O'Neill (FHWA) intermediary geo-materials method, which is deformation based.

4. O'Neill IGM: (Note: Must enter values for  $E_c$ , slump,  $E_m/E_l$ ,  $E_m$ , and IGM\_Type = 2)

a.  $E_m = 115 q_u = 115 (0.96 \text{ MPa}) = 110.4 \text{ MPa}$ .

b.  $\Omega = 1.14 \left( \frac{L}{D} \right)^{1/2} - 0.05 \left( \left\{ \frac{L}{D} \right\}^{1/2} - 1 \right) \log \left( \frac{E_c}{E_m} \right) - 0.44$

$$\Omega = 1.14(3.05)^{1/2} - 0.05(3.05^{1/2} - 1)\log\left(\frac{27,777}{110.4}\right) - 0.44 = 1.46$$

$$c. \quad \Gamma = 0.37\left(\frac{L}{D}\right)^{1/2} - 0.15\left(\left\{\frac{L}{D}\right\}^{1/2} - 1\right)\log\left(\frac{E_c}{E_m}\right) + 0.13$$

$$\Gamma = 0.37(3.05)^{1/2} - 0.15(3.05^{1/2} - 1)\log\left(\frac{27,777}{110.4}\right) + 0.13 = 0.507$$

$$d. \quad \frac{\theta}{w} = \frac{E_m \Omega}{\pi L \Gamma f_{su}}; \quad f_{su} = \frac{1}{2} \sqrt{q_u} \sqrt{q_t}$$

$$= \frac{110.4 * 1.46}{\pi * 3.05 * 0.507 * (\frac{1}{2} \sqrt{0.96} \sqrt{0.96})} = \frac{161.18}{0.7374} = 218.586 / m$$

$$e. \quad \Lambda = 0.0134 E_m \frac{(\frac{L}{D})}{(\frac{L}{D} + 1)} \left\{ \frac{200 \left[ \sqrt{\frac{L}{D}} - \Omega \right] \left[ 1 + \frac{L}{D} \right]}{\pi L \Gamma} \right\}^{0.67}$$

$$\Lambda = 0.0134 (110.4 MPa) \frac{3.05}{4.05} \left\{ \frac{200 \left[ \sqrt{3.05} - 1.46 \right] \left[ 1 + 3.05 \right]}{\pi * 3.05 * 5.07} \right\}^{0.67}$$

$$= 1.1141 [4.7757]^{0.67}$$

$$= 3.159 \text{ MPa m}^{-0.67}$$

$$\Lambda = (1114.1 \text{ kPa}) \left\{ \frac{200 \left[ \sqrt{3.05} - 1.46 \right] \left[ 1 + 3.05 \right]}{\pi * 3050 * 0.507} \right\}^{0.67}$$

$$= 1.1141 [0.1316]$$

$$= 146.65 \text{ kPa mm}^{-0.67}$$

$$f. \quad \text{Determine } n \text{ for deformation criteria Fig (2)} \quad \frac{q_u}{\sigma_p} = \frac{957.6 \text{ kPa}}{100} = 9.576$$



$$\frac{E_m}{\sigma_n}; \sigma_n = M \gamma_c Z_c; \text{ Since } Z_c = 6.1 + \frac{3.05}{2} = 7.625m \text{ (use 8m)}$$

For a slump = 175 mm,  $M(\text{Fig 3.5}) = 0.78$

$$\therefore \sigma_n = 0.78 * 20.4 * 7.625 = 121.33 \text{ kPa}$$

$$\therefore \frac{E_m}{\sigma_n} = \frac{110,400}{121.33} = 909.9 \therefore n \approx 0.42$$

g. Select values of 'w' for calculating

$$Q_t = \pi D L \theta f_{su} + \frac{\pi D^2}{4} q_b \text{ for } \theta < n; \quad q_b = \Lambda w^{0.67}$$

$$Q_t = \pi D L k f_{su} + \frac{\pi D^2}{4} q_b \text{ for } \theta > n$$

1) Let  $w = 2 \text{ mm}$ ;  $\theta / w = 218.586$ ,

$$\therefore \theta = 218.586 * 0.002m = 0.437 < n = 0.45$$

$$Q_t = \pi * 1 * 3.05 * 0.437 * (151.4 \text{ kPa}) + \frac{\pi * 1^2}{4} * 146.65 * 2^{0.67}$$

$$= 634 + 182.8$$

$$= 816.7 \text{ kPa}$$

2) Let  $w = 5 \text{ mm}$ ;  $\theta / w = 218.586$ ,

$$\therefore \theta = 218.586 * 0.005m = 1.093 > n = 0.45$$

$$k = n + \frac{(\theta - n)(1 - n)}{(\theta - 2n + 1)} = 0.45 + \frac{(1.093 - 0.45)(1 - 0.45)}{(1.093 - 2(0.45) + 1)} = 0.7706$$

$$Q_t = \pi * 1 * 3.05 * 0.77 * (151.4 \text{ kPa}) + \frac{\pi * 1^2}{4} * 146.65 * 5^{0.67}$$

$$= 1118 + 336.8$$

$$= 1455 \text{ kPa}$$

h. Now go back and calculate sand capacity using trend lines when  $w = 2\text{mm}$  and  $5\text{mm}$ .

$$1. \quad S = (s * 100 / B);$$

$$@ 2\text{mm } S=(0.2\text{cm}*100/100\text{cm}) = 0.2$$

$$@ 5\text{mm } S=(0.5\text{cm}*100/100\text{cm}) = 0.5$$

$$\begin{aligned} 2. \quad q_{st} / Q_s &= -2.16*S^4 + 6.34*S^3 - 7.36*S^2 + 4.15*S \\ &= -2.16*(0.2)^4 + 6.34*(0.2)^3 - 7.36*(0.2)^2 + 4.15*(0.2) \\ &= 0.5829 \text{ for } w = 2\text{mm} \end{aligned}$$

$$q_s = 0.5829 * (811.66 \text{ kN})$$

$$= 473.1 \text{ kN for } 2 \text{ mm}$$

$$\begin{aligned} q_{st} / Q_s &= -2.16*S^4 + 6.34*S^3 - 7.36*S^2 + 4.15*S \\ &= -2.16*(0.5)^4 + 6.34*(0.5)^3 - 7.36*(0.5)^2 + 4.15*(0.5) \\ &= 0.892 \text{ for } w = 5\text{mm} \end{aligned}$$

$$3. \quad q_s = 0.892 * (811.66 \text{ kN})$$

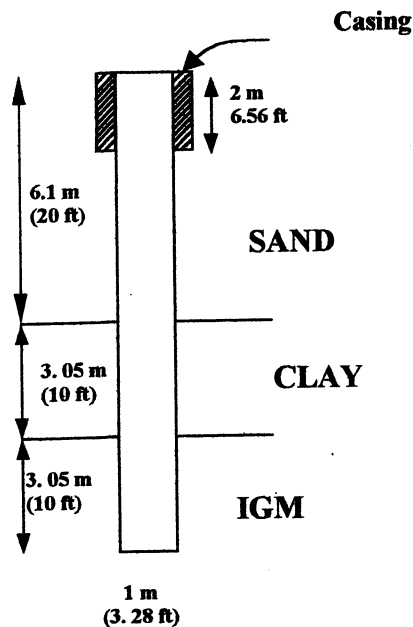
$$= 724.4 \text{ kN for } 5 \text{ mm}$$

i. Total Shaft Capacity (Sand + Rock)

$$1) @ 2\text{mm} \quad Q_T = 473.1 \text{ kN} + 634 \text{ kN} + 182.8 \text{ kN} = 1289.9 \text{ kN}$$

$$2) @ 5\text{mm} \quad Q_T = 724.4 \text{ kN} + 1118 \text{ kN} + 336.8 \text{ kN} = 2179.2 \text{ kN}$$

**IGM: (Sand, Clay & Limestone)**



$$\gamma = 100 \text{ pcf (15.708 kN/m}^3\text{)}$$

$$N = 10$$

$$\gamma = 100 \text{ pcf (15.708 kN/m}^3\text{)}$$

$$c = 1.9 \text{ tsf (181.94 kPa)}$$

LimeStone:

$$q_u = 10 \text{ tsf (957.6 kPa, 0.96 Mpa)}$$

$$q_t = 1 \text{ tsf (95.76 kPa, 0.096 Mpa)}$$

$$\gamma = 135 \text{ pcf (21.2 kN/m}^3\text{), } \gamma_c = 20.4 \text{ kN/m}^3$$

$$E_c = 57,000 \sqrt{f'_y} = 57,000 \sqrt{5000 \text{ psi}}$$

$$= 4.03E6 \text{ psi (27.77E6 kPa)}$$

$$f_{su} = \frac{1}{2} \sqrt{q_u} \sqrt{q_t} = 151.41 \text{ kPa}$$

Smooth socket IGM\_type = 2.0

$$1. \quad \text{Skin Friction (Sand): } Q_s = \frac{3.28 * \pi}{2000} \int_{6.56}^{20} (1.5 - 0.135 \sqrt{z}) \gamma z dz$$

$$= \frac{3.28 * \pi}{2000} \left[ \frac{150 * z^2}{2} - 13.5 * z^{5/2} * \frac{5}{2} \right]_{6.56}^{20}$$

$$= \frac{3.28 * \pi}{2000} [75 * (20^2 - 6.56^2) - 5.4 * (20^{5/2} - 6.56^{5/2})]$$

$$= 0.00515 [26,772.5 - 9064.6]$$

$$= 91.23^T = 91.23 * 2000 / 224.809 = 811.66 \text{ kN}$$

$$2. \quad \text{Skin Friction (Clay): } Q_s = \pi D L \alpha C_u = \pi (1) (3.05) (0.55 * 181.94)$$

$$= 958.85 \text{ kN (107.78}^T\text{)}$$

3. FHWA IGM Calculations: (Note: Must enter values for  $E_c$ , slump,  $E_m/E_l$ ,  $E_m$ , and IGM\_Type = 2)

$$a. \quad E_m = 115 q_u = 115 (957.6 \text{ kPa}) = 110.4 \text{ MPa.}$$

$$b. \Omega = 1.14 \left( \frac{L}{D} \right)^{1/2} - 0.05 \left( \left\{ \frac{L}{D} \right\}^{1/2} - 1 \right) \log \left( \frac{E_c}{E_m} \right) - 0.44$$

$$\Omega = 1.14(3.05)^{1/2} - 0.05(3.05^{1/2} - 1) \log \left( \frac{27,777}{110.4} \right) - 0.44 = 1.46$$

$$c. \Gamma = 0.37 \left( \frac{L}{D} \right)^{1/2} - 0.15 \left( \left\{ \frac{L}{D} \right\}^{1/2} - 1 \right) \log \left( \frac{E_c}{E_m} \right) + 0.13$$

$$\Gamma = 0.37(3.05)^{1/2} - 0.15(3.05^{1/2} - 1) \log \left( \frac{27,777}{110.4} \right) + 0.13 = 0.507$$

$$d. \frac{\theta}{w} = \frac{E_m \Omega}{\pi L \Gamma f_{su}}; \quad f_{su} = \frac{1}{2} \sqrt{q_u} \sqrt{q_t}$$

$$= \frac{110.4 * 1.46}{\pi * 3.05 * 0.507 * (\frac{1}{2} * 0.151 MPa)} = \frac{161.18}{0.7336} = 219.73 / m$$

$$e. \Lambda = 0.0134 E_m \frac{(\frac{L}{D})}{(\frac{L}{D} + 1)} \left\{ \frac{200 \left[ \sqrt{\frac{L}{D}} - \Omega \right] \left[ 1 + \frac{L}{D} \right]}{\pi L \Gamma} \right\}^{0.67}$$

$$\Lambda = 0.0134 (110,112.5 kPa) \frac{3.05}{4.05} \left\{ \frac{200 \left[ \sqrt{3.05} - 1.46 \right] \left[ 1 + 3.05 \right]}{\pi * 3050 * 0.507} \right\}^{0.67}$$

$$= 146.27 \text{ kPa mm}^{-0.67}$$

$$f. \text{ Determine } n \text{ for deformation criteria Fig 36 } \frac{q_u}{\sigma_p} = \frac{957.6 \text{ kPa}}{100} = 9.576$$

$$\frac{E_m}{\sigma_n}; \quad \sigma_n = M \gamma_c Z_c; \quad \text{Since } Z_c = 6.1 + 3.05 + \frac{3.05}{2} = 10.675m$$

$$\text{For a slump} = 175 \text{ mm}, \quad M(\text{Fig 3.5}) = 0.68$$

$$\therefore \sigma_n = 0.68 * 20.4 * 10.675 = 148.1 \text{ kPa}$$

$$\therefore \frac{E_m}{\sigma_n} = \frac{110,112.5}{148.1} = 743.6 \quad \therefore n \approx 0.4 < n = 0.45$$

g. Select values of 'w' for calculating

$$Q_t = \pi D L \theta f_{su} + \frac{\pi D^2}{4} q_b \quad \text{for } \theta < n; \quad q_b = \Lambda w^{0.67}$$

$$Q_t = \pi D L k f_{su} + \frac{\pi D^2}{4} q_b \quad \text{for } \theta > n$$

1) Let  $w = 2 \text{ mm}$ ;  $\theta / w = 219.73 \text{ m}^{-1}$ ,

$$\therefore \theta = 219.73 * 0.002 \text{ m} = 0.439 < n = 0.45$$

$$Q_t = \pi * 1 * 3.05 * 0.439 * (151.4 \text{ kPa}) + \frac{\pi * 1^2}{4} * 146.27 * 2^{0.67}$$

$$= 636.85 + 182.8$$

$$= 819.2 \text{ kPa}$$

2) Let  $w = 5 \text{ mm}$ ;  $\theta / w = 219.73 \text{ m}^{-1}$ ,

$$\therefore \theta = 219.73 * 0.005 \text{ m} = 1.099 > n = 0.45$$

$$k = n + \frac{(\theta - n)(1 - n)}{(\theta - 2n + 1)} = 0.45 + \frac{(1.099 - 0.45)(1 - 0.45)}{(1.099 - 2(0.45) + 1)} = 0.75$$

$$Q_t = \pi * 1 * 3.05 * 0.75 * (151.4 \text{ kPa}) + \frac{\pi * 1^2}{4} * 146.27 * 5^{0.67}$$

$$= 1084.6 + 335.9$$

$$= 1420.5 \text{ kPa}$$

h. Now go back and calculate sand capacity using trend lines when  $w = 2 \text{ mm}$  and  $5 \text{ mm}$ .

1.  $S = (s * 100 / B)$ ;

@  $2 \text{ mm}$   $S = (0.2 \text{ cm} * 100 / 100 \text{ cm}) = 0.2$ , and

@  $5 \text{ mm}$   $S = (0.5 \text{ cm} * 100 / 100 \text{ cm}) = 0.5$

2.  $q_{st} / Q_s = -2.16 * S^4 + 6.34 * S^3 - 7.36 * S^2 + 4.15 * S$

$$= -2.16 * (0.2)^4 + 6.34 * (0.2)^3 - 7.36 * (0.2)^2 + 4.15 * (0.2)$$

$$= 0.5829 \text{ for } w = 2 \text{ mm}$$

3.  $q_s = 0.5829 * (811.66 \text{ kN})$

$$= 473.1 \text{ kN for } 2 \text{ mm}$$

$$\begin{aligned} 2. \quad q_{st} / Q_s &= -2.16*S^4 + 6.34*S^3 - 7.36*S^2 + 4.15*S \\ &= -2.16*(0.5)^4 + 6.34*(0.5)^3 - 7.36*(0.5)^2 + 4.15*(0.5) \\ &= 0.892 \text{ for } w = 5\text{mm} \end{aligned}$$

$$\begin{aligned} 3. \quad q_s &= 0.892 * (811.66 \text{ kN}) \\ &= 724.4 \text{ kN for } 5 \text{ mm} \end{aligned}$$

$$\begin{aligned} 4. \quad \text{Clay: } S &= s*100/B; \text{ @ } 2 \text{ mm } S=0.2 \text{ \& } 0.5 \text{ @ } 5 \text{ mm } 0.12 < S < 0.74 \\ \frac{q_{st}}{Q_s} &= \frac{S}{[0.095155 + 0.892937 * S]} = \frac{0.2}{0.2737} = 0.731 \\ &= \frac{0.5}{0.5416} = 0.9232 \end{aligned}$$

$$q_s = 0.7310 * 958.85 = 700.55 \text{ kN @ } 2 \text{ mm}$$

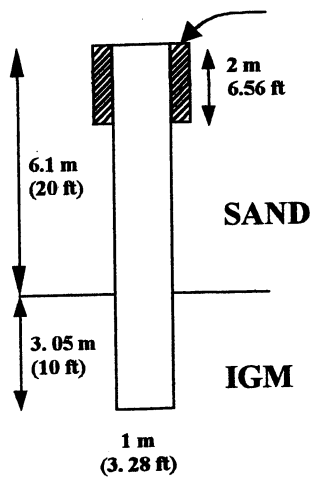
$$q_s = 0.9232 * 958.85 = 885.16 \text{ kN @ } 5 \text{ mm}$$

i. Total Shaft Capacity (Sand + Rock)

$$1) \text{ @ } 2\text{mm} \quad Q_T = 473.1 \text{ kN} + 700.5 \text{ kN} + 636.85 \text{ kN} + 182.4 = 1992.8 \text{ kN}$$

$$2) \text{ @ } 5\text{mm} \quad Q_T = 724.4 \text{ kN} + 885.16 \text{ kN} + 1084.6 \text{ kN} + 335.9 \text{ kN} = 3030.1 \text{ kN}$$

**IGM: (Sand & Limestone) Consider "Rough" Socket:**



$$\gamma = 100 \text{ pcf (15.708 kN/m}^3\text{)}$$

$$N = 10$$

LimeStone:

$$q_u = 10 \text{ tsf (957.6 kPa, 0.96 Mpa)}$$

$$q_t = 1 \text{ tsf (95.76 kPa, 0.096 Mpa)}$$

$$\gamma = 135 \text{ pcf (21.2 kN/m}^3\text{)}, \gamma_c = 20.4 \text{ kN/m}^3$$

$$E_c = 57,000 \sqrt{f'_y} = 57,000 \sqrt{5000 \text{ psi}}$$

$$= 4.03 E6 \text{ psi (27.77 E6 kPa)}$$

$$f_{su} = \frac{1}{2} \sqrt{q_u} \sqrt{q_t} = 151.41 \text{ kPa}$$

1. From Previous Example,

$$\begin{aligned} \text{a) Skin Friction (Sand): } Q_s &= \frac{3.28 * \pi}{2000} \int_{6.56}^{20} (1.5 - 0.135 \sqrt{z}) \gamma z dz \\ &= \frac{3.28 * \pi}{2000} \left[ \frac{150 * z^2}{2} - 13.5 * z^{5/2} * \frac{5}{2} \right]_{6.56}^{20} \\ &= \frac{3.28 * \pi}{2000} [75 * (20^2 - 6.56^2) - 5.4 * (20^{5/2} - 6.56^{5/2})] \\ &= 0.00515 [26,772.5 - 9064.6] \\ &= 91.23^T = 91.23 * 2000 / 224.809 = 811.66 \text{ kN} \end{aligned}$$

2. 2. O'Neill (FHWA) Rock - Rough Socket: (Note: Must enter values for  $E_c$ , slump,  $E_m/E_i$ ,  $E_m$ , and IGM\_Type = 1..0)

$$\text{a) If "Rough" } n = \sigma_n / q_u$$

$$\sigma_n = M \gamma_c Z_c; \text{ Since } Z_c = 6.1 + \frac{3.05}{2} = 7.625 \text{ m (use 8m)}$$

$$\text{For a slump} = 175 \text{ mm, } M(\text{Fig 3.5}) = 0.78$$

$$\therefore \sigma_n = 0.78 * 20.4 * 7.625 = 121.33 \text{ kPa}$$

$$b) n = \sigma_n / q_u = 121.33 / 95.76 = 0.13$$

c)

$$Q_t = \pi D L \theta f_{su} + \frac{\pi D^2}{4} q_b \quad \text{for } \theta < n ; \quad q_b = \Lambda w^{0.67}$$

$$Q_t = \pi D L k f_{su} + \frac{\pi D^2}{4} q_b \quad \text{for } \theta > n$$

$$d) \theta / w = 218.586 \text{ m}^{-1}$$

$$e) \text{ Let } w = 2 \text{ mm}; \therefore \theta = 218.586 * 0.002 \text{ m} = 0.437 > n = 0.13$$

$$k = n + \frac{(\theta - n)(1 - n)}{(\theta - 2n + 1)} = 0.13 + \frac{(0.437 - 0.13)(1 - 0.13)}{(0.437 - 2(0.13) + 1)} = 0.356$$

$$Q_t = \pi * 1 * 3.05 * 0.356 * (151.4 \text{ kPa}) + \frac{\pi * 1^2}{4} * 146.65 * 2^{0.67}$$

$$= 516.48 + 182.83$$

$$= 699.3 \text{ kPa}$$

f) Calculate sand capacity using trend lines when  $w = 2 \text{ mm}$

$$1. S = (s * 100 / B); @ 2 \text{ mm } S = (0.2 \text{ cm} * 100 / 100 \text{ cm}) = 0.2$$

$$2. q_s / Q_s = -2.16 * S^4 + 6.34 * S^3 - 7.36 * S^2 + 4.15 * S$$

$$= -2.16 * (0.2)^4 + 6.34 * (0.2)^3 - 7.36 * (0.2)^2 + 4.15 * (0.2)$$

$$= 0.5829 \text{ for } w = 2 \text{ mm}$$

$$3. q_s = 0.5829 * (811.66 \text{ kN})$$

$$= 473.1 \text{ kN for } 2 \text{ mm}$$

$$g) \quad \Sigma Q = 473.1 + 516.48 + 182.83 = 1172.4$$



NCHRP 24-17

**LOAD AND RESISTANCE FACTOR DESIGN  
(LRFD) FOR DEEP FOUNDATIONS**

**APPENDIX D  
DESIGN EXAMPLES**

Prepared for  
National Cooperative Highway Research Program  
Transportation Research Board  
National Research Council

Ching L. Kuo  
Geostructures Corp.  
2713 Falling Leaves Drive, Valrico, FL 33594

Samuel G. Paikowsky, Kirk Stenerson, and Roiy Guy  
Geotechnical Engineering Research Laboratory  
Department of Civil and Environmental Engineering  
University of Massachusetts  
Lowell, Massachusetts

Bjorn Birgisson and Michael McVay  
Department of Civil Engineering  
University of Florida  
Gainesville, FL 32611-6580

January 2003

## APPENDIX D

### DESIGN EXAMPLES

#### 1. DRILLED SHAFTS

##### 1.1. Design Methodology

The Federal Highway Administration (FHWA) design of drilled shafts founded in sand, clay, and intermediate geomaterial (i.e. soft rock) follows O'Neill and Reese (1998) and O'Neil et. al (1996).

According to FHWA, the axial capacity of a drilled shaft may be calculated as:

$$Q_t = Q_s + Q_b \quad (1)$$

where:  $Q_t$  = shaft capacity  
 $Q_s$  = skin friction capacity  
 $Q_b$  = end bearing capacity

In equation 1, shaft capacity or failure is defined as the applied load, which will result in settlement of the top of the drilled shaft equal to five percent the diameter of the shaft. An explanation of the computation of  $Q_s$  and  $Q_b$  for each material (i.e. sand, clay, and intermediate geomaterials) is presented below with examples given in Appendix A.

##### 1.2. Skin Friction, $Q_s$ , and End Bearing, $Q_b$ , for Clay

###### 1.2.1. Skin Transfer

The load transfer in side resistance for drilled shafts founded in clay is a variant of Tomlinson's Alpha ( $\alpha$ ) method (1977). The undrained shear strength  $C_u$  of clay (found from laboratory tests or insitu correlations) is multiplied by alpha,  $\alpha$ , to compute the unit skin friction (stress) at the depth  $z$  below the ground surface as follows,

$$f_{su} = \alpha C_u \quad (2)$$

where  $f_{su}$  = unit skin friction (stress) at depth  $z$   
 $\alpha$  = empirical factor that varies with depth, (see Table 1) and  
 $C_u$  = undrained shear strength at depth  $z$ ,

Due to disturbances (i.e. drilling tool entering and exiting the hole frequently), the unit skin friction for the top five foot (see Fig. 1 and Table 1)) is neglected (i.e. set to zero). The setting of  $\alpha = 0$  for a distance of one diameter above the base is from the work of Ellison et al. (1971). They showed that the downward movement of the base of the shaft can result in the development of a tensile crack in the soil near the base resulting in a lateral stress reduction. Consequently the unit skin friction in this zone (i.e. one diameter above the base) is set to zero.

**Table 1 Recommended Values for  $\alpha$  for Drilled Shafts in Clay**

Location along Drilled Shaft	Value of $\alpha$	Maximum Value of $f_{su}$ (tsf)
From ground surface to depth of 5 ft. (1.52 m.)	0.0	0.0
From ground surface to length of casing	0.0	0.0
Bottom 1 diameter of shaft or 1 stem diameter above top of bell	0.0	0.0
All other points along drilled shaft sides	0.55	2.75 tsf (275 kPa)

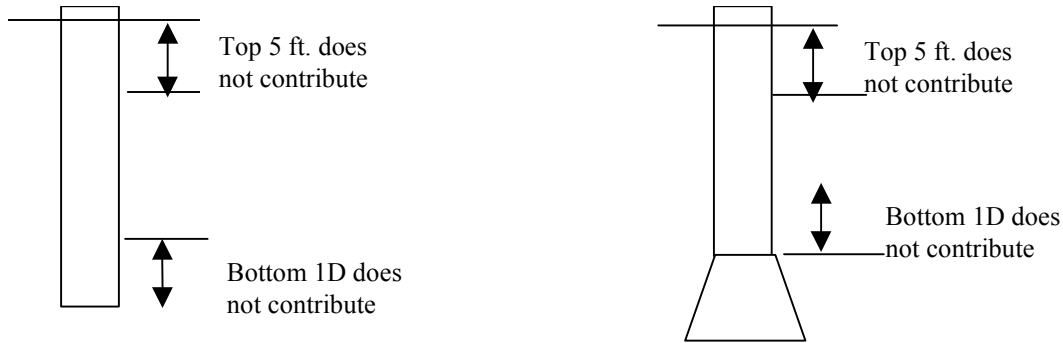


**Figure 1 Portions of Drilled Shaft Non-Contributory in Friction**

The total side resistance (i.e. force),  $Q_s$  for a given layer located at depths  $L_1$  and  $L_2$  below the ground surface is given as:

$$Q_s = \int_{L_1}^{L_2} f_{su} dA \quad (3)$$

where  $dA$  = differential area of the perimeter along the side over a specific depth.

### 1.2.2. End Bearing

FHWA's unit end bearing (stress) for a drilled shaft founded in clay is based on the work of Skempton (1951):

$$q_b = N_c C_u, \quad q_b < 40 \text{ tsf (4000 kPa)} \quad (4)$$

where:

- $q_b$  = unit end bearing for drilled shafts in clay
- $N_c = 6.0[1 + 0.2(L/B)]$  (bearing capacity factor)  $N_c < 9$
- $C_u$  = average undrained shear strength of clay for 1.0 B below the tip
- $L$  = total embedment length of shaft in the ground

$B$  = diameter of shaft at the base.

It should be noted that the limiting value of  $q_b$  (40 tsf) given in Equation. 4 is the largest measured end bearing recorded for drilled shafts and not a theoretical limit (Engling and Reese, 1974)

In the case of drilled shaft diameters (at the base:  $B_b$ ) exceeding 75 inches (1.9 m), the FHWA reduces the unit end bearing,  $q_b$ , to  $q_{br}$  to ensure tolerable settlements under service load conditions. Again, failure capacity of a shaft is the load, which develops settlements equal to five percent the diameter of the shaft. The reduced bearing resistance is defined as:

$$q_{br} = F_r q_b \quad (5)$$

where:  $F_r = 2.5/[aB_b \text{ (inches)} + 2.5 b]$   $F < 1.0$

in which  $a = 0.0071 + 0.0021 (L/B_b)$ ,  $a < 0.015$

$b = 0.45 (C_u)^{0.5}$   $0.5 < b < 1.5$  and  $C_u$  in ksf

The latter expressions were based upon load tests of large under-reamed drilled shafts in very stiff clay (O'Neill and Sheikh, 1985). The reduced bearing resistance,  $q_{br}$ , gave similar results to the measured net bearing stress at a base settlement of 2.5 inches (6.35 cm). In addition, when more than half the design load is carried by end bearing, a global factor of safety greater than 2.5 is recommended by FHWA, unless site specific load tests are performed.

The failure end-bearing load,  $Q_b$ , is computed as  $q_b$  or  $q_{br}$  times the cross-sectional area of the drilled shaft's base. An example of capacity prediction for a drilled shaft founded in clay follows.

### 1.3. Skin Friction, $Q_s$ , and End Bearing, $Q_b$ , for Sand

#### 1.3.1. Skin Transfer

The unit side resistance on a drilled shaft founded in sand is based on Coulombic friction, i.e. equal to the normal (horizontal) effective stress times a coefficient of friction ( $\tan \phi_c$ ).

$$f_{sz} = K \sigma_z \tan \phi_c \quad (6)$$

The total side resistance (i.e. force),  $Q_s$  for a given layer located at depths  $L$  below the ground surface is given as

$$Q_s = \int_0^L K \sigma_z \tan \phi_c dA \quad (7)$$

where  $f_{sz}$  = ultimate unit side shear resistance in sand at depth  $z$ ,  
 $K$  = a parameter that combines the lateral pressure coefficient  
 $\sigma_z$  = vertical effective stress at depth  $z$   
 $\phi_c$  = interface friction angle for soil-concrete  
 $L$  = depth of embedment for drilled shaft in sand  
 $dA$  = differential area of perimeter along sides of drilled shaft

Generally, the normal stress at the interface of the drilled shaft and the soil is relatively low when the excavation is completed; however the fluid stress from the fresh concrete will impose a normal stress that is dependent on the characteristics of the concrete. Experiments have shown that concrete with moderate slump (up to 6 inches, 15 cm.) act hydrostatically over a depth of 10 to 15 ft. (3 to 4.5 m.) followed by a leveling off of lateral stress at greater depths, probably due to arching (Bernal and Reese, 1983). Concrete with higher slump (about 9 inches,

23 cm.) act hydrostatically to a depth of 32 ft. (10 m.). Thus, construction procedures and the concrete characteristics will probably have a strong influence on the magnitude of the lateral stress at the soil-concrete interface.

As a result of the drilling and concreting influences, the  $K \tan \phi$  in Equation 6 is replaced by a simple constant,  $\beta$ , as a function of depth to account for variation in lateral stresses (i.e.  $K$ ):

$$\beta = 1.5 - 0.135\sqrt{z} \quad 1.2 > \beta > 0.25 \quad (8)$$

Consequently, the unit skin friction (stress) is given by

$$f_{sz} = \beta \sigma_z \quad (9)$$

The total side resistance (i.e. force),  $Q_s$  for a given layer located at depths  $L$  below the ground surface is given as

$$Q_s = \int \beta \sigma_z dA \quad (10)$$

It should be noted that the limiting unit skin friction (Equation 9) is again not a theoretical limit, but rather is merely the largest value that has been measured (Owens and Reese, 1982). Higher values can be used if justified via a load test.

### 1.3.2. End Bearing

Generally, an experimental tip resistance curve for a drilled shaft in sand shows that the end bearing is still increasing at settlements equal to five percent the diameter of the shaft (i.e. FHWA defined shaft capacity). For instance, settlements of more than fifteen percent the diameter have been recorded. However, since such large settlement is not tolerated for most structures; FHWA limits end bearing and settlements to five percent of the shaft's base diameter.

The values of the unit end bearing (stress)  $q_b$  are tabulated as a function of  $N_{SPT}$  (uncorrected field values) in Table 3 for shaft diameters less than 50 inches. In the case of large diameter shafts [i.e. Shaft diameter,  $D > 50$  in. (1.3m)], equation 11 is used:

$$q_{br} = 50 * (q_b/B_b); B_b \text{ in inches}$$

$$\text{or } q_{br} = 1.3 * (q_b/B_b); B_b \text{ in meters} \quad (11)$$

**Table 3 Recommended Unit End Bearing Values for Cohesionless Soils**

$N_{SPT}$ Values (Uncorrected)	Value of $q_b$ (TSF) [kPa]
0 to 75	(0.60 $N_{SPT}$ ) [60 $N_{SPT}$ ]
above 75	(45) [4500]

Table 3 limits the unit end bearing to 45 tsf (4500 kPa) at a settlement of 5 percent of the base diameter. Higher values, i.e. 58 tsf (5800 kPa) was measured for a settlement of 4 percent of the base diameter in Florida (Owens and Reese, 1982), are viable with load testing. An example of capacity prediction for a drilled shaft founded in sand is given in Appendix A.

### 1.4. Skin Friction, $Q_s$ , and End Bearing, $Q_b$ , for Intermediate Geomaterials (Soft Rock)

FHWA's determination of skin and tip resistance for a drilled shaft founded in soft rock is based on a recent publication of O'Neill and et. al (1996). The equations for unit skin friction and end bearing are presented separately.

#### 1.4.1. Side Resistance

Requires a six step approach as identified:

1. Find the average  $E_m$  (mass modulus of rock) and  $f_{su}$  (ultimate unit skin friction) along the side of the rock socket:

$$E_m = \Sigma E_{mk} L_k / \Sigma L_k \quad (12)$$

where  $E_m = 115 q_u$  and

$$f_{su} = \Sigma f_{su} L_k / \Sigma L_k \quad (13)$$

where  $f_{su}$  = ultimate side friction.

The values selected for  $f_{su}$  depend whether the socket is considered "smooth" and failure occurs at the interface ( $\alpha$  values) or "rough" where failure occurs through the rock. The rough assumption was used in this study and  $f_{su}$  was set equal to  $0.5\sqrt{q_u}\sqrt{q_t}$ .

2. Calculate  $\Omega$  given by Equation 14:

$$\Omega = 1.14\left(\frac{L}{D}\right)^{0.5} - 0.05\left[\left(\frac{L}{D}\right)^{0.5} \log_{10}\left(\frac{E_c}{E_m}\right) - 0.44\right] \quad (14)$$

where  $L$  = socket length and modulus of concrete is given as  $E_c(\Psi) = 57,000\sqrt{q_{uc}}$

3. Calculate  $\Gamma$  given by Equation 15

$$\Gamma = 0.37\sqrt{\left(\frac{L}{D}\right)} - 0.15\left[\sqrt{\left(\frac{L}{D}\right)} - 1\right]\log_{10}\left(\frac{E_c}{E_m}\right) + 0.13 \quad (15)$$

4. Find  $n$  (socket surface roughness)

For "rough" sockets;

$$n = \sigma / q_u \quad \text{where } \sigma = \text{normal stress of concrete} = \gamma_c Z_c M \quad (16)$$

where  $\gamma_c = 130 \text{ pcf}$  or  $20.5 \text{ kN/m}^3$  and  $M$  is given in Table 4 below based on concrete slump and socket depth

**Table 4 Values of M**

Socket Depth (m)	Slump (mm)		
	125	175	225
4	0.50	0.95	1.0
8	0.45	0.75	1.0
12	0.35	0.65	0.9

Also, if a water table is present, then  $\sigma_n = \gamma_c(Z_c - Z_w) + \gamma_c Z_w$ , where  $Z_c$  = depth to water table.

In the case of a “smooth” socket,  $n$  is estimated from Figure 2.

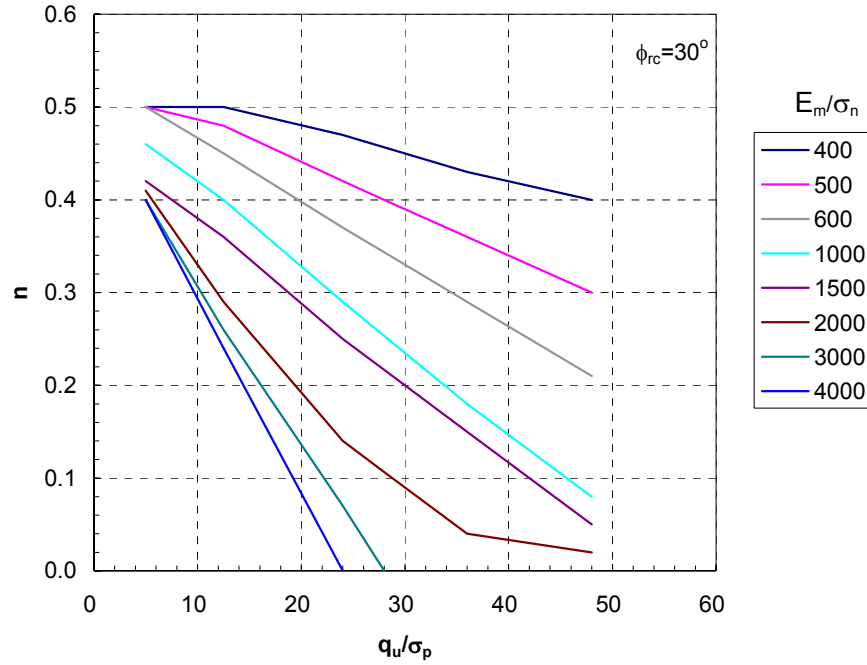


**Figure 2 N Factors for Smooth Sockets**

5. Next calculate  $\Theta_f$  and  $K_f$  as given below:

$$\Theta_f = \frac{E_m \Omega}{\pi L \Gamma} W_t \quad (17)$$

$$K_f = n + \frac{(\Theta_f - n)(1 - n)}{\Theta_f - 2n + 1} < 1 \quad (18)$$

where  $W_t$  = deflection at top of rock socket

6. Finally, calculate the side shear load transfer vs. deformation from:

$$Q_s = \pi D L \Theta_f f_{su} \quad \Theta_f < n \quad (19)$$

$$Q_f = \pi D L K_f f_{su} \quad \Theta > n \quad (20)$$

#### 1.4.2. End Bearing

The total tip resistance as a function of displacement according to O'Neill et al. (1996) is as follows:

$$Q_b = \frac{\pi D^2}{4} q_b \quad (21)$$

where  $q_b = \Lambda W_t^{0.67}$ , and

$$\Lambda = 0.0134 E_m \frac{(L/D)}{(1 + L/D)} \left\{ \frac{[200(L/D)^{0.5} - \Omega][1 + (L/D)]}{\pi L \Gamma} - \right\}^{0.67} \quad (22)$$

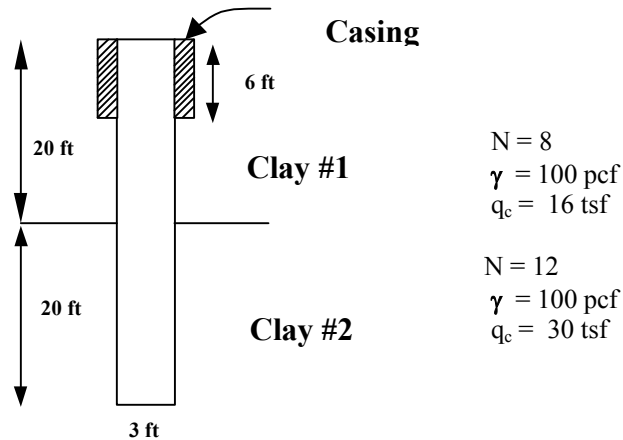
The total shaft resistance,  $Q_t$ , for a rock socket is the sum of  $Q_s + Q_b$ . An example of a drilled shaft design in soft rock is given in the following section.

## 1.5. Examples

### Example 1. Drilled Shaft in CLAYS:

Consider Two Cases calculated by FHWA method/ $\alpha$  method, i.e., Reese, L.C. and M.W. O'Neill (1988):

1. Multi Layer Clay with Casing, 3 ft diameter straight shaft
2. Multi Layer Clay with Casing  $B > 75$  ", 8 ft diameter straight shaft



$$c = \frac{q_c - \sigma_0}{15}$$

$$\text{Clay Layer \# 1 : } c = \frac{16 * 2000 - 10 * 100}{15} = 2,066.67 \text{ psf (1.0333 tsf)}$$

$$\text{Clay Layer \# 2 : } c = \frac{30 * 2000 - 30 * 100}{15} = 3,800 \text{ psf (1.90 tsf)}$$



**1.1 Multi Layer Clay with Casing:** Full Capacity (40 ft Shaft)

a) Skin Friction:

$$\begin{aligned} Q_s &= \pi * 3.0 * [(20' - 6')(0.55 * 1.033) + (20' - 3')(0.55 * 1.9)] \\ &= 9.4248 * [7.9567 + 17.765] \\ &= 242.42 \text{ Tons} \end{aligned}$$

b) End Bearing:

$$\begin{aligned} Q_b &= q_b \cdot \frac{\pi b^2}{4}, \\ q_b &= N_c C_u, \\ N_c &= 6.0 * \left[ 1 + 0.2 \frac{40}{3} \right] = 22 > 9 \text{ (use 9)} \\ Q_b &= (9 * 1.9 \text{ tsf}) \cdot \frac{\pi 3^2}{4} = 120.87 \text{ Tons} \end{aligned}$$

c) Total Capacity = Skin Friction + End Bearing  
 $= 242.42 + 120.87$   
 $= 363.29 \text{ Tons (ultimate)}$

d) Unit Skin Friction with depth:

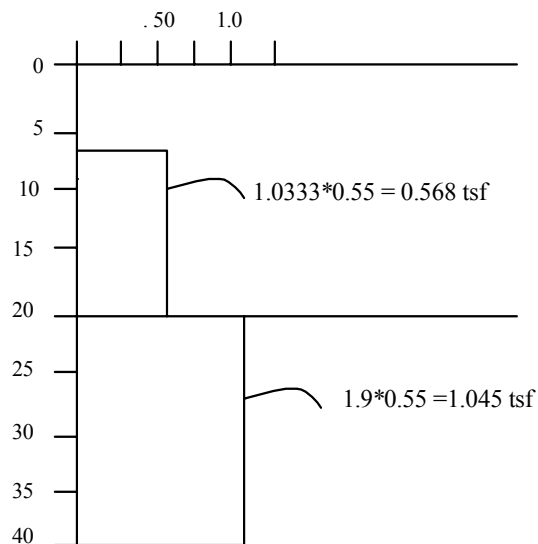
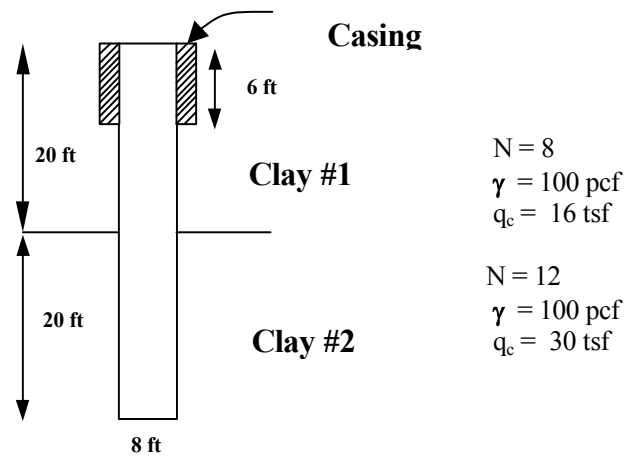


Table 29 recommended resistance factor for total resistance of a drilled shaft in clay using the FHWA method, and for all construction methods, is  $\phi = 0.3$  w/Non-Redundant condition  
 Factored Capacity =  $0.3 * 363.29 = \mathbf{109.0 \text{ Tons}}$

## 1.2 Multi Layer Clay with Casing, but B>75" (1.9m):



a) Skin Friction:  $Q_s = \pi * 8.0 * [(20' - 6')(0.55 * 1.033) + (20' - 8')(0.55 * 1.9)]$   
 $= 25.1327 * [7.9567 + 12.5]$   
 $= 515.14 \text{ Tons}$

b) End Bearing: If  $B > 75''$ , then  $q_{br} = F_r q_b$

$$F_r = \frac{2.5}{[a B_b(\text{inches}) + 2.5 b]}$$

$$a = 0.0071 + 0.0021(L / B_b)$$

$$= 0.0071 + 0.0021(40' / 8')$$

$$= 0.0176, \text{ but } a < 0.015$$

$$b = 0.45\sqrt{C_u} = 0.45\sqrt{1.9 * 2.0}, C_u \text{ in } ksf$$

$$= 0.8772, 0.5 < b < 1.5$$

$$F_r = \frac{2.5}{[0.015 (96'') + 2.5 (0.8772)]} = 0.6881$$

$$Q_b = \frac{\pi * 8^2}{4} (0.6881)(9 * 1.9) = 591.48 \text{ Tons}$$

$$Q_t = 515.14 + 591.48 = 1106.62 \text{ Tons}$$

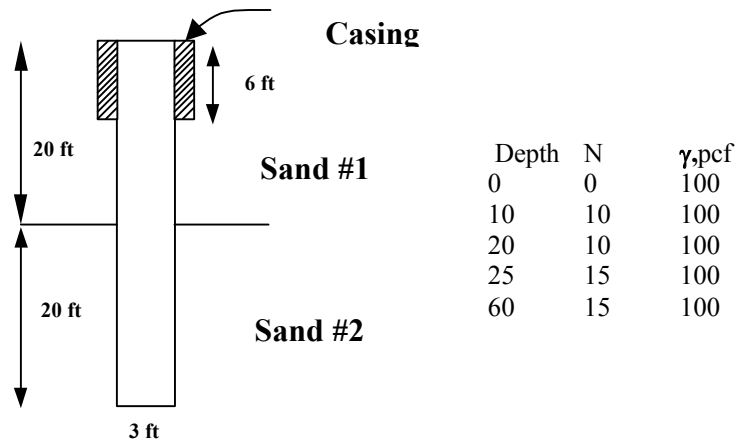
c) Table 29 recommended resistance factor for total resistance of a drilled shaft in clay using the FHWA method, and for all construction methods, is  $\phi = 0.3$  w/Non-Redundant condition

Factored Capacity =  $0.3 * 1106.62 = \underline{\underline{332.0 \text{ Tons}}}$

## Example 2. Drilled Shaft in SANDS:

Calculated by FHWA method/ $\beta$  method, i.e., Reese, L.C. and M.W. O'Neill (1988):

- Multi Layer Sand with Casing, 3 ft diameter straight shaft



- Skin Friction:

$$\beta = 1.5 - 0.135 \sqrt{z} \quad 0.25 < \beta(\text{tsf}) < 1.2$$

or  $Z < 4.94\text{ft}$ ,  $\beta = 1.2$  tsf, and  $Z > 85.73\text{ft}$ ,  $\beta = 0.25$

$$\begin{aligned} \int_6^{40} \beta \sigma_v dz &= \int_6^{40} 150Z - 13.5Z^{\frac{3}{2}} dZ = \frac{150Z^2}{2} - 13.5Z^{\frac{5}{2}} * \frac{2}{5} \Big|_6^{40} \\ &= 65,355.84 - 2,223.82 = 18,116.37 * \frac{3\pi}{2000} = 297.50^T \end{aligned}$$

- End Bearing: above  $8*B$  and below  $3.5*B$ ,

$$\text{above: } 40.0 - 8*B = 40.0 - 8*(3) = 16' ;$$

$$\text{below: } 40.0 + 3.5*B = 40.0 + 3.5*(3) = 50.5'$$

$$\begin{aligned} \text{for } z = 16' \quad q_b &= 0.6*N = 0.6*(10) = 6 \text{ tsf} \\ z = 20' \quad q_b &= 0.6*N = 0.6*(10) = 6 \text{ tsf} \\ z = 25' \quad q_b &= 0.6*N = 0.6*(15) = 9 \text{ tsf} \\ z = 60' \quad q_b &= 0.6*N = 0.6*(15) = 9 \text{ tsf} \end{aligned}$$

$$\therefore q_b = \left[ \frac{6 * (20 - 16) + \frac{9 + 6}{2} * (25 - 20) + 9 * (50.5 - 25)}{[50.5 - 16]} \right] = 8.4348$$

$$\text{So, } Q_b = 8.4348 * \left[ \frac{\pi \cdot 3^2}{4} \right] = 59.622^T$$

$$Q_T = 297.5 + 59.62 = 357.12$$

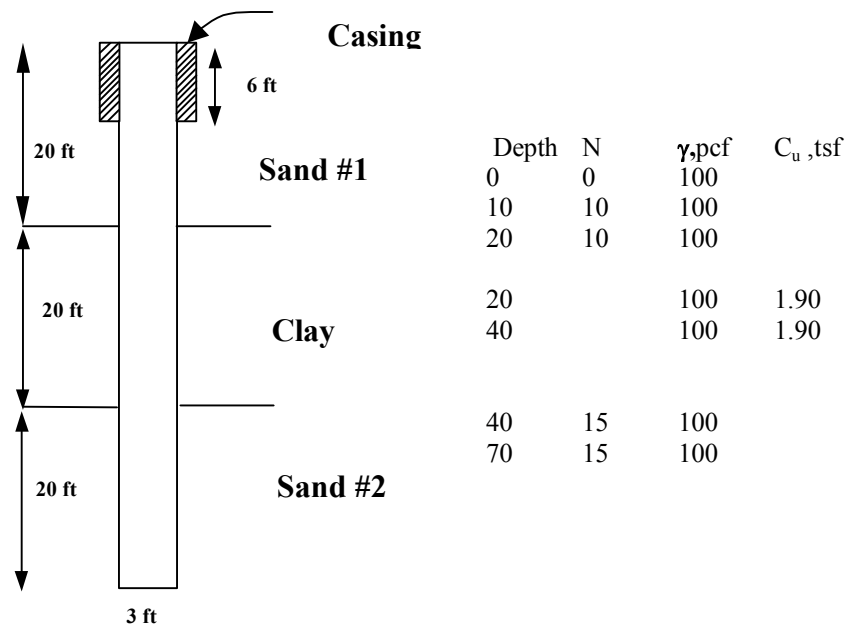
- c) Table 29 recommended resistance factor for a total resistance of a drilled shaft in sand using the FHWA method for all construction methods is  $\phi = 0.40$  w/Non-Redundant conditions.

$$\text{Factored Capacity} = 0.4 * 357.12 = \underline{\underline{142.8 \text{ Tons}}}$$

### Example 3. Drilled Shaft in MULTILAYER- SAND-CLAY-SAND:

Calculated by FHWA method/ $\alpha$  and  $\beta$  method, i.e., Reese, L.C. and M.W. O'Neill (1988):

1. Multi Layer Sand and clay with Casing, 3 ft diameter straight shaft



- a) Skin Friction (6-20ft) :  $Q_s = \frac{3 \cdot \pi}{2000} \int_6^{20} (1.5 - 0.135\sqrt{z}) \gamma z dz$

$$\begin{aligned}
&= 0.0047 \left[ \frac{150 * z^2}{2} - 13.5 * z^{5/2} * \frac{5}{2} \right]_6^{20} \\
&= 0.0047 [75 * (20^2 - 6^2) - 5.4 * (20^{5/2} - 6^{5/2})] \\
&= 0.0047 [27,300 - 9,183.6] \\
&= 85.371^T
\end{aligned}$$

b) Skin Friction (20-40ft) :  $Q_s = 3.\pi[(40 - 20)(0.55 * 1.9)]$   
 $= 196.978^T$

c) Skin Friction (40-60ft) :  $Q_s = \frac{3.\pi}{2000} \int_{40}^{60} (1.5 - 0.135\sqrt{z}) \gamma z dz$

$$\begin{aligned}
&= 0.0047 \left[ \frac{150 * z^2}{2} - 13.5 * z^{5/2} * \frac{5}{2} \right]_{40}^{60} \\
&= 0.0047 (75 * (60^2 - 40^2) - 5.4 * (60^{5/2} - 40^{5/2})) \\
&= 0.0047 [150,000 - 95,937.4] \\
&= 254.764^T
\end{aligned}$$

$$\Sigma Q_s = 85.371 + 196.978 + 254.764 = 537.11 \text{ tons}$$

d) Tip Resistance: above  $8*B$  and below  $3.5*B$ ,

$$\text{Above: } 60.0 - 8*B = 60.0 - 8*(3) = 36 \text{ ft ;}$$

$$\text{Below: } 60.0 + 3.5*B = 60.0 + 3.5*(3) = 70.5 \text{ ft}$$

$$\text{For } z = 40 \text{ ft } q_b = 0.6*N = 0.6*(15) = 9 \text{ tsf}$$

$$z = 60 \text{ ft } q_b = 0.6*N = 0.6*(15) = 9 \text{ tsf}$$

$$z = 75 \text{ ft } q_b = 0.6*N = 0.6*(15) = 9 \text{ tsf}$$

$$\text{So, } Q_b = \left[ \frac{\pi.3^2}{4} \right] * 9 = 63.62^T$$

Check  $q_b$  of overlaying Clay:

$$q_b = 9*C_u = 9*1.9 = 17.1 \text{ tsf stronger, } \therefore \text{ stop @ 40ft.}$$

e)  $Q_T = 537.11 + 63.62 = 600.73 \text{ Tons}$

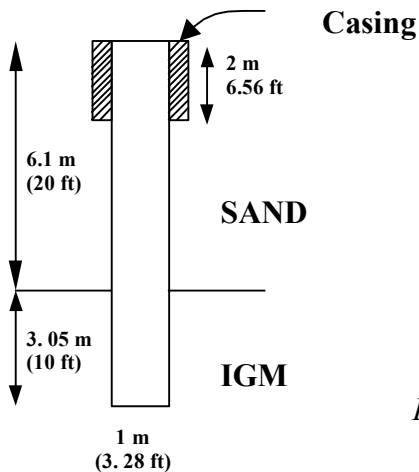
f) Table 29 recommended resistance factor for a total resistance of a drilled shaft in sand and clay using the FHWA method using cased construction is  $\phi = 0.50$  w/Non-Redundant condition.

$$\text{Factored Capacity} = 0.5 * 600.73 = \underline{\underline{300.4 \text{ Tons}}}$$

#### Example 4. Drilled Shaft in IGM: (Sand & Limestone)

Calculated using IGM Method (Intermediate Geomaterials), i.e., O'Neill, et al (1996) "Load Transfer for Drilled Shafts in Intermediate Geomaterials" FHWA-RD-95-172, and O'Neill, M. W. and L. C. Reese (1999) "Drilled Shaft: Construction Procedures and Design Methods", FHWA-IF-99-025.

- Multi Layer Sand and Limestone with Casing, 1.0 m diameter straight shaft



$$\gamma = 100 \text{ pcf (15.708 kN/m}^3\text{)}$$

$$N = 10$$

LimeStone:

$$q_u = 10 \text{ tsf (957.6 kPa, 0.96 Mpa)}$$

$$q_t = 1 \text{ tsf (95.76 kPa, 0.096 Mpa)}$$

$$\gamma = 135 \text{ pcf (21.2 kN/m}^3\text{)}, \quad \gamma_c = 20.4 \text{ kN/m}^3$$

$$E_c = 57,000 \sqrt{f'_y} = 57,000 \sqrt{5000 \text{ psi}}$$

$$= 4.03E6 \text{ psi (27.77E6 kPa)}$$

Because of unit comparison problems, calculate Sand using English and Rock using SI units.

$$1. \text{ Skin Friction (Sand): } Q_s = \frac{3.28 * \pi}{2000} \int_{6.56}^{20} (1.5 - 0.135\sqrt{z}) \gamma z dz$$

$$= \frac{3.28 * \pi}{2000} \left[ \frac{150 * z^2}{2} - 13.5 * z^{5/2} * \frac{5}{2} \right]_{6.56}^{20}$$

$$= \frac{3.28 * \pi}{2000} [75 * (20^2 - 6.56^2) - 5.4 * (20^{5/2} - 6.56^{5/2})]$$

$$= 0.00515 [26,772.5 - 9064.6]$$

$$= 91.23^T = 91.23 * 2000 / 224.809 = \mathbf{811.66 \text{ kN}}$$

- Analysis of Rock resistance is based on O'Neill (FHWA) intermediary geo-materials method, which is deformation based.

- O'Neill IGM: (Note: Must enter values for  $E_c$ , slump,  $E_m/E_l$ ,  $E_m$ , and IGM\_Type = 2)

$$a. \quad E_m = 115 q_u = 115 (0.96 \text{ MPa}) = 110.4 \text{ MPa.}$$

$$\text{b. } \Omega = 1.14 \left( \frac{L}{D} \right)^{1/2} - 0.05 \left( \left\{ \frac{L}{D} \right\}^{1/2} - 1 \right) \log \left( \frac{E_c}{E_m} \right) - 0.44$$

$$\Omega = 1.14(3.05)^{1/2} - 0.05(3.05^{1/2} - 1) \log \left( \frac{27,777}{110.4} \right) - 0.44 = 1.46$$

$$\text{c. } \Gamma = 0.37 \left( \frac{L}{D} \right)^{1/2} - 0.15 \left( \left\{ \frac{L}{D} \right\}^{1/2} - 1 \right) \log \left( \frac{E_c}{E_m} \right) + 0.13$$

$$\Gamma = 0.37(3.05)^{1/2} - 0.15(3.05^{1/2} - 1) \log \left( \frac{27,777}{110.4} \right) + 0.13 = 0.507$$

$$\text{d. } \frac{\theta}{w} = \frac{E_m \Omega}{\pi L \Gamma f_{su}}; \quad f_{su} = \frac{1}{2} \sqrt{q_u} \sqrt{q_t}$$

$$= \frac{110.4 * 1.46}{\pi * 3.05 * 0.507 * (\frac{1}{2} \sqrt{0.96} \sqrt{0.96})} = \frac{161.18}{0.7374} = 218.586 / m$$

$$\text{e. } \Lambda = 0.0134 E_m \frac{(\frac{L}{D})}{(\frac{L}{D} + 1)} \left\{ \frac{200 \left[ \sqrt{\frac{L}{D}} - \Omega \right] \left[ 1 + \frac{L}{D} \right]}{\pi L \Gamma} \right\}^{0.67}$$

$$\Lambda = 0.0134 (110.4 MPa) \frac{3.05}{4.05} \left\{ \frac{200 \left[ \sqrt{3.05} - 1.46 \right] \left[ 1 + 3.05 \right]}{\pi * 3.05 * 5.07} \right\}^{0.67}$$

$$= 1.1141 [4.7757]^{0.67}$$

$$= 3.159 \text{ MPa m}^{-0.67}$$

$$\Lambda = (1114.1 \text{ kPa}) \left\{ \frac{200 \left[ \sqrt{3.05} - 1.46 \right] \left[ 1 + 3.05 \right]}{\pi * 3050 * 0.507} \right\}^{0.67}$$

$$= 1.1141 [0.1316]$$

$$= 146.65 \text{ kPa mm}^{-0.67}$$

$$\text{f. Determine } n \text{ for deformation criteria Fig (2) } \frac{q_u}{\sigma_p} = \frac{957.6 \text{ kPa}}{100} = 9.576$$

$$\frac{E_m}{\sigma_n}; \quad \sigma_n = M \gamma_c Z_c; \quad \text{Since } Z_c = 6.1 + \frac{3.05}{2} = 7.625m \text{ (use 8m)}$$

$$\text{For a slump} = 175 \text{ mm}, \quad M(\text{Fig 3.5}) = 0.78$$

$$\therefore \sigma_n = 0.78 * 20.4 * 7.625 = 121.33 \text{ kPa}$$

$$\therefore \frac{E_m}{\sigma_n} = \frac{110,400}{121.33} = 909.9 \quad \therefore n \approx 0.42$$

g. Select values of 'w' for calculating

$$Q_t = \pi D L \theta f_{su} + \frac{\pi D^2}{4} q_b \quad \text{for } \theta < n ; \quad q_b = \Lambda w^{0.67}$$

$$Q_t = \pi D L k f_{su} + \frac{\pi D^2}{4} q_b \quad \text{for } \theta > n$$

1) Let w = 2 mm;  $\theta / w = 218.586$ ,

$$\therefore \theta = 218.586 * 0.002\text{m} = 0.437 < n = 0.45$$

$$Q_t = \pi * 1 * 3.05 * 0.437 * (151.4 \text{ kPa}) + \frac{\pi * 1^2}{4} * 146.65 * 2^{0.67}$$

$$= 634 + 182.8$$

$$= 816.7 \text{ kPa}$$

2) Let w = 5 mm;  $\theta / w = 218.586$ ,

$$\therefore \theta = 218.586 * 0.005\text{m} = 1.093 > n = 0.45$$

$$k = n + \frac{(\theta - n)(1 - n)}{(\theta - 2n + 1)} = 0.45 + \frac{(1.093 - 0.45)(1 - 0.45)}{(1.093 - 2(0.45) + 1)} = 0.7706$$

$$Q_t = \pi * 1 * 3.05 * 0.77 * (151.4 \text{ kPa}) + \frac{\pi * 1^2}{4} * 146.65 * 5^{0.67}$$

$$= 1118 + 336.8$$

$$= 1455 \text{ kPa}$$

h. Now go back and calculate sand capacity using trend lines when w = 2mm and 5mm.

1.  $S = (s * 100 / B)$ ;

$$@ 2\text{mm } S = (0.2\text{cm} * 100 / 100\text{cm}) = 0.2$$

$$@ 5\text{mm } S = (0.5\text{cm} * 100 / 100\text{cm}) = 0.5$$

$$2. \quad q_{st} / Q_s = -2.16 * S^4 + 6.34 * S^3 - 7.36 * S^2 + 4.15 * S$$

$$= -2.16 * (0.2)^4 + 6.34 * (0.2)^3 - 7.36 * (0.2)^2 + 4.15 * (0.2)$$

$$= 0.5829 \text{ for } w = 2\text{mm}$$

$$q_s = 0.5829 * (811.66 \text{ kN})$$

$$= 473.1 \text{ kN for } 2 \text{ mm}$$

$$q_{st} / Q_s = -2.16 * S^4 + 6.34 * S^3 - 7.36 * S^2 + 4.15 * S$$



$$= -2.16*(0.5)^4 + 6.34*(0.5)^3 - 7.36*(0.5)^2 + 4.15*(0.5)$$

$$= 0.892 \text{ for } w = 5\text{mm}$$

$$3. \quad q_s = 0.892 * (811.66 \text{ kN})$$

$$= 724.4 \text{ kN for } 5 \text{ mm}$$

i. Total Shaft Capacity (Sand + Rock)

$$1) @ 2\text{mm} \quad Q_T = 473.1 \text{ kN} + 634 \text{ kN} + 182.8 \text{ kN} = 1289.9 \text{ kN}$$

$$2) @ 5\text{mm} \quad Q_T = 724.4 \text{ kN} + 1118 \text{ kN} + 336.8 \text{ kN} = 2179.2 \text{ kN}$$

j. Table 29 recommended resistance factor for a total resistance of a drilled shaft in IGM using the Reese and O'Neill FHWA method for all construction methods is  $\phi = 0.75$  w/Non-Redundant condition.

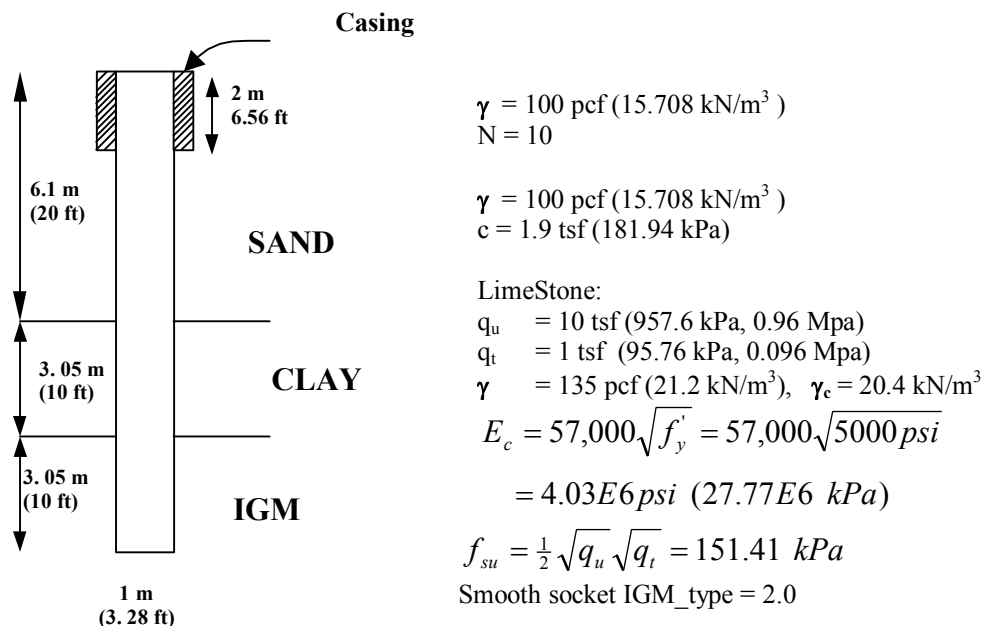
$$\text{Factored Capacity} = 0.75 * 1289.9 = \underline{\underline{967.4 \text{ kN} @ 2 \text{ mm}}}$$

$$= 0.75 * 2179.2 = \underline{\underline{1634.4 \text{ kN} @ 5 \text{ mm}}}$$

### Example 5. Drilled Shaft in IGM: (Sand, Clay & Limestone)

Calculated using IGM Method (Intermediate Geomaterials), i.e., O'Neill, et al (1996) "Load Transfer for Drilled Shafts in Intermediate Geomaterials" FHWA-RD-95-172, and O'Neill, M. W. and L. C. Reese (1999) "Drilled Shaft: Construction Procedures and Design Methods", FHWA-IF-99-025.

1. Multi Layer Sand, Clay and Limestone with Casing, 1.0 m diameter straight shaft



1. Skin Friction (Sand):  $Q_s = \frac{3.28 * \pi}{2000} \int_{6.56}^{20} (1.5 - 0.135\sqrt{z}) \gamma z dz$ 

$$= \frac{3.28 * \pi}{2000} \left[ \frac{150 * z^2}{2} - 13.5 * z^{5/2} * \frac{5}{2} \right]_{6.56}^{20}$$

$$= \frac{3.28 * \pi}{2000} [75 * (20^2 - 6.56^2) - 5.4 * (20^{5/2} - 6.56^{5/2})]$$

$$= 0.00515[26,772.5 - 9064.6]$$

$$= 91.23^T = 91.23 * 2000 / 224.809 = 811.66 \text{ kN}$$
2. Skin Friction (Clay):  $Q_s = \pi D L \alpha C_u = \pi (1) (3.05) (0.55 * 181.94)$ 

$$= 958.85 \text{ kN } (107.78^T)$$
3. FHWA IGM Calculations: (Note: Must enter values for  $E_c$ , slump,  $E_m/E_i$ ,  $E_m$ , and IGM\_Type = 2)
  - a.  $E_m = 115 q_u = 115 (957.6 \text{ kPa}) = 110.4 \text{ MPa}.$
  - b.  $\Omega = 1.14 \left( \frac{L}{D} \right)^{1/2} - 0.05 \left( \left\{ \frac{L}{D} \right\}^{1/2} - 1 \right) \log \left( \frac{E_c}{E_m} \right) - 0.44$ 

$$\Omega = 1.14(3.05)^{1/2} - 0.05(3.05^{1/2} - 1) \log \left( \frac{27,777}{110.4} \right) - 0.44 = 1.46$$
  - c.  $\Gamma = 0.37 \left( \frac{L}{D} \right)^{1/2} - 0.15 \left( \left\{ \frac{L}{D} \right\}^{1/2} - 1 \right) \log \left( \frac{E_c}{E_m} \right) + 0.13$ 

$$\Gamma = 0.37(3.05)^{1/2} - 0.15(3.05^{1/2} - 1) \log \left( \frac{27,777}{110.4} \right) + 0.13 = 0.507$$
  - d.  $\frac{\theta}{w} = \frac{E_m \Omega}{\pi L \Gamma f_{su}}; f_{su} = \frac{1}{2} \sqrt{q_u} \sqrt{q_t}$ 

$$= \frac{110.4 * 1.46}{\pi * 3.05 * 0.507 * (\frac{1}{2} * 0.151 \text{ MPa})} = \frac{161.18}{0.7336} = 219.73 / m$$
  - e.  $\Lambda = 0.0134 E_m \frac{(\frac{L}{D})}{(\frac{L}{D} + 1)} \left\{ \frac{200 \left[ \sqrt{\frac{L}{D}} - \Omega \right] \left[ 1 + \frac{L}{D} \right]}{\pi L \Gamma} \right\}^{0.67}$

$$\Lambda = 0.0134 \text{ (110,112.5 kPa)} \frac{3.05}{4.05} \left\{ \frac{200 [\sqrt{3.05} - 1.46] [1 + 3.05]}{\pi * 3050 * 0.507} \right\}^{0.67}$$

$$= 146.27 \text{ kPa mm}^{-0.67}$$

f. Determine n for deformation criteria Fig 36  $\frac{q_u}{\sigma_p} = \frac{957.6 \text{ kPa}}{100} = 9.576$

$$\frac{E_m}{\sigma_n}; \quad \sigma_n = M \gamma_c Z_c; \quad \text{Since } Z_c = 6.1 + 3.05 + \frac{3.05}{2} = 10.675m$$

$$\text{For a slump} = 175 \text{ mm}, \quad M(\text{Fig 3.5}) = 0.68$$

$$\therefore \sigma_n = 0.68 * 20.4 * 10.675 = 148.1 \text{ kPa}$$

$$\therefore \frac{E_m}{\sigma_n} = \frac{110,112.5}{148.1} = 743.6 \quad \therefore n \approx 0.4 < n = 0.45$$

g. Select values of 'w' for calculating

$$Q_t = \pi D L \theta f_{su} + \frac{\pi D^2}{4} q_b \quad \text{for } \theta < n; \quad q_b = \Lambda w^{0.67}$$

$$Q_t = \pi D L k f_{su} + \frac{\pi D^2}{4} q_b \quad \text{for } \theta > n$$

1) Let w = 2 mm;  $\theta / w = 219.73 \text{ m}^{-1}$ ,

$$\therefore \theta = 219.73 * 0.002m = 0.439 < n = 0.45$$

$$Q_t = \pi * 1 * 3.05 * 0.439 * (151.4 \text{ kPa}) + \frac{\pi * 1^2}{4} * 146.27 * 2^{0.67}$$

$$= 636.85 + 182.8$$

$$= 819.2 \text{ kPa}$$

2) Let w = 5 mm;  $\theta / w = 219.73 \text{ m}^{-1}$ ,

$$\therefore \theta = 219.73 * 0.005m = 1.099 > n = 0.45$$

$$k = n + \frac{(\theta - n)(1 - n)}{(\theta - 2n + 1)} = 0.45 + \frac{(1.099 - 0.45)(1 - 0.45)}{(1.099 - 2(0.45) + 1)} = 0.75$$

$$\begin{aligned}
 Q_t &= \pi * 1 * 3.05 * 0.75 * (151.4 \text{ kPa}) + \frac{\pi * 1^2}{4} * 146.27 * 5^{0.67} \\
 &= 1084.6 + 335.9 \\
 &= 1420.5 \text{ kPa}
 \end{aligned}$$

h. Now go back and calculate sand capacity using trend lines when  $w = 2\text{mm}$  and  $5\text{mm}$ .

$$1. \quad S = (s * 100 / B);$$

$$@ 2\text{mm } S = (0.2\text{cm} * 100 / 100\text{cm}) = 0.2, \text{ and}$$

$$@ 5\text{mm } S = (0.5\text{cm} * 100 / 100\text{cm}) = 0.5$$

$$\begin{aligned}
 2. \quad q_{st} / Q_s &= -2.16 * S^4 + 6.34 * S^3 - 7.36 * S^2 + 4.15 * S \\
 &= -2.16 * (0.2)^4 + 6.34 * (0.2)^3 - 7.36 * (0.2)^2 + 4.15 * (0.2) \\
 &= 0.5829 \text{ for } w = 2\text{mm}
 \end{aligned}$$

$$\begin{aligned}
 3. \quad q_s &= 0.5829 * (811.66 \text{ kN}) \\
 &= 473.1 \text{ kN for } 2 \text{ mm}
 \end{aligned}$$

$$\begin{aligned}
 4. \quad q_{st} / Q_s &= -2.16 * S^4 + 6.34 * S^3 - 7.36 * S^2 + 4.15 * S \\
 &= -2.16 * (0.5)^4 + 6.34 * (0.5)^3 - 7.36 * (0.5)^2 + 4.15 * (0.5) \\
 &= 0.892 \text{ for } w = 5\text{mm}
 \end{aligned}$$

$$\begin{aligned}
 5. \quad q_s &= 0.892 * (811.66 \text{ kN}) \\
 &= 724.4 \text{ kN for } 5 \text{ mm}
 \end{aligned}$$

$$6. \quad \text{Clay: } S = s * 100 / B; @ 2 \text{ mm } S = 0.2 \text{ \& } 0.5 @ 5 \text{ mm } 0.12 < S < 0.74$$

$$\begin{aligned}
 \frac{q_{st}}{Q_s} &= \frac{S}{[0.095155 + 0.892937 * S]} = \frac{0.2}{0.2737} = 0.731 \\
 &= \frac{0.5}{0.5416} = 0.9232
 \end{aligned}$$

$$q_s = 0.7310 * 958.85 = 700.55 \text{ kN} @ 2 \text{ mm}$$

$$q_s = 0.9232 * 958.85 = 885.16 \text{ kN} @ 5 \text{ mm}$$

i. Total Shaft Capacity (Sand + Rock)

$$\begin{aligned}
 1) @ 2\text{mm} \quad Q_T &= 473.1 \text{ kN} + 700.5 \text{ kN} + 636.85 \text{ kN} + 182.4 = 1992.8 \text{ kN} \\
 2) @ 5\text{mm} \quad Q_T &= 724.4 \text{ kN} + 885.16 \text{ kN} + 1084.6 \text{ kN} + 335.9 \text{ kN} = 3030.1 \text{ kN}
 \end{aligned}$$

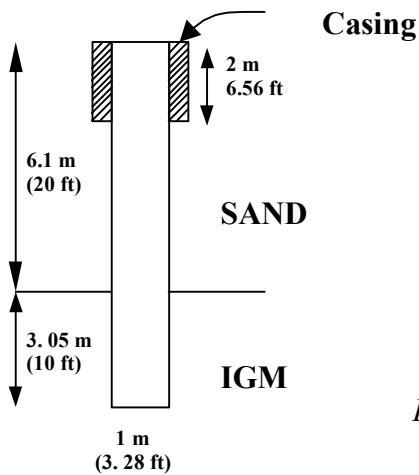
- j. Table 29 recommended resistance factor for a total resistance of a drilled shaft in IGM using the Reese and O'Neill FHWA method for all construction methods is  $\phi = 0.75$  w/Non-Redundant condition.

$$\begin{aligned}
 \text{Factored Capacity} &= 0.75 * 1992.8 = \underline{\underline{1494.6 \text{ kN} @ 2 \text{ mm}}} \\
 &= 0.75 * 3030.1 = \underline{\underline{2272.6 \text{ kN} @ 5 \text{ mm}}}
 \end{aligned}$$

**Example 6. Drilled Shaft in IGM: (Sand & Limestone) Consider “Rough” Socket:**

Calculated using IGM Method (Intermediate Geomaterials), i.e., O'Neill, et al (1996) “Load Transfer for Drilled Shafts in Intermediate Geomaterials” FHWA-RD-95-172, and O'Neill, M. W. and L. C. Reese (1999) ‘Drilled Shaft: Construction Procedures and Design Methods’, FHWA-IF-99-025.

1. Multi Layer Sand and Limestone with Casing, 1.0 m diameter straight shaft



$$\begin{aligned}
 \gamma &= 100 \text{ pcf } (15.708 \text{ kN/m}^3) \\
 N &= 10
 \end{aligned}$$

$$\begin{aligned}
 \text{LimeStone:} \\
 q_u &= 10 \text{ tsf } (957.6 \text{ kPa}, 0.96 \text{ Mpa}) \\
 q_t &= 1 \text{ tsf } (95.76 \text{ kPa}, 0.096 \text{ Mpa}) \\
 \gamma &= 135 \text{ pcf } (21.2 \text{ kN/m}^3), \quad \gamma_c = 20.4 \text{ kN/m}^3
 \end{aligned}$$

$$\begin{aligned}
 E_c &= 57,000 \sqrt{f'_y} = 57,000 \sqrt{5000 \text{ psi}} \\
 &= 4.03E6 \text{ psi } (27.77E6 \text{ kPa})
 \end{aligned}$$

$$f_{su} = \frac{1}{2} \sqrt{q_u} \sqrt{q_t} = 151.41 \text{ kPa}$$

1. From Previous Example,

$$\begin{aligned}
 \text{a) Skin Friction (Sand): } Q_s &= \frac{3.28 * \pi}{2000} \int_{6.56}^{20} (1.5 - 0.135 \sqrt{z}) \gamma z dz \\
 &= \frac{3.28 * \pi}{2000} \left[ \frac{150 * z^2}{2} - 13.5 * z^{5/2} * \frac{5}{2} \right]_{6.56}^{20}
 \end{aligned}$$

$$= \frac{3.28 * \pi}{2000} [75 * (20^2 - 6.56^2) - 5.4 * (20^{5/2} - 6.56^{5/2})]$$

$$= 0.00515 [26,772.5 - 9064.6]$$

$$= 91.23^T = 91.23 * 2000 / 224.809 = 811.66 \text{ kN}$$

2. O'Neill (FHWA) Rock - Rough Socket: (Note: Must enter values for  $E_c$ , slump,  $E_m/E_l$ ,  $E_m$ , and IGM\_Type = 1..0)

a) If "Rough"  $n = \sigma_n / q_u$

$$\sigma_n = M \gamma_c Z_c; \text{ Since } Z_c = 6.1 + \frac{3.05}{2} = 7.625m \text{ (use 8m)}$$

$$\text{For a slump} = 175 \text{ mm, } M(\text{Fig 3.5}) = 0.78$$

$$\therefore \sigma_n = 0.78 * 20.4 * 7.625 = 121.33 \text{ kPa}$$

b)  $n = \sigma_n / q_u = 121.33 / 95.76 = 0.13$

c)

$$Q_t = \pi D L \theta f_{su} + \frac{\pi D^2}{4} q_b \text{ for } \theta < n; \quad q_b = \Lambda w^{0.67}$$

$$Q_t = \pi D L k f_{su} + \frac{\pi D^2}{4} q_b \text{ for } \theta > n$$

d)  $\theta / w = 218.586 \text{ m}^{-1}$

e) Let  $w = 2 \text{ mm}$ ;  $\therefore \theta = 218.586 * 0.002 \text{ m} = 0.437 > n = 0.13$

$$k = n + \frac{(\theta - n)(1 - n)}{(\theta - 2n + 1)} = 0.13 + \frac{(0.437 - 0.13)(1 - 0.13)}{(0.437 - 2(0.13) + 1)} = 0.356$$

$$Q_t = \pi * 1 * 3.05 * 0.356 * (151.4 \text{ kPa}) + \frac{\pi * 1^2}{4} * 146.65 * 2^{0.67}$$

$$= 516.48 + 182.83$$

$$= 699.3 \text{ kPa}$$

f) Calculate sand capacity using trend lines when  $w = 2 \text{ mm}$

1.  $S = (s * 100 / B)$ ; @  $2 \text{ mm } S = (0.2 \text{ cm} * 100 / 100 \text{ cm}) = 0.2$

$$\begin{aligned}
 2. \quad q_{st} / Q_s &= -2.16*S^4 + 6.34*S^3 - 7.36*S^2 + 4.15*S \\
 &= -2.16*(0.2)^4 + 6.34*(0.2)^3 - 7.36*(0.2)^2 + 4.15*(0.2) \\
 &= 0.5829 \text{ for } w = 2\text{mm}
 \end{aligned}$$

$$\begin{aligned}
 3. \quad q_s &= 0.5829 * (811.66 \text{ kN}) \\
 &= 473.1 \text{ kN for } 2 \text{ mm}
 \end{aligned}$$

$$g) \quad \Sigma Q = 473.1 + 516.48 + 182.83 = 1172.4 \text{ kN}$$

h) Table 29 recommended resistance factor for a total resistance of a drilled shaft in IGM using the Reese and O'Neill FHWA method for all construction methods is  $\phi = 0.75$  w/Non-Redundant condition.

$$\text{Factored Capacity} = 0.75 * 1172.4 = \underline{\underline{879.3 \text{ kN}}} @ 2 \text{ mm}$$

## 2. DRIVEN PILES

### 2.1. Axial Pile Capacity Prediction by Static Methods

Axial pile capacities can be predicted by various static capacity prediction methods. These methods use certain properties of the soil, such as the effective friction angle,  $\phi'$ , or the CPT cone bearing  $q_c$ . However, the computed capacities may not reflect the actual capacities exactly, so designs based on static methods must be conservative, which is reflected in the resistance factor,  $\Phi$ . This section will discuss specific ways to predict the axial pile capacities.

#### 2.1.1. Axial Loading Capacity of a Pile

The ultimate resistance of a pile,  $R_{ult}$  (or  $R_n$ --Norminal resistance), is given below:

$$R_{ult} = R_p + R_s \quad 1$$

where: pile tip resistance  $R_p = q_p A_p$ ,  
pile side resistance  $R_s = \sum q_{si} \Delta z_i U$ ,  
 $q_p$  = unit tip resistance. Predictions of  $q_p$  are in Sections 2.1.2.2, 2.1.2.4 and 2.1.3.  
 $q_s$  = unit side resistance which is regarded as constant along segment  $\Delta z_i$  of the pile.  
Predictions of  $q_s$  can be found in Sections 2.1.2.1, 2.1.2.3 and 2.1.3,  
 $U$  = perimeter of the pile's shaft, and  
 $A_p$  = area of the tip of the pile.

In this project, the eight methods listed below are considered in predicting the axial capacities:

1.  $\alpha$ -method, which include  $\alpha$ -Tomlinson (Tomlinson, 1980/1995) and  $\alpha$ -API (Reese et al., 1998) for cohesive soil
2.  $\lambda$ -method (Vijayvergiya and Focht, cited in US Army Corps of Engineers, No.7, 1992) for cohesive soil,
3.  $\beta$ -method (Bushan--cited in Bowles, 1996) for cohesionless soil,
4.  $\beta$ -method (Burland, Esrig and Kirby, 1979) for cohesive soil,
5. Nordlund method (Nordlund, 1963) for cohesionless soil,  
(Methods number 4 to 5 above are cited in Hannigan et al., 1995).
6. Nottingham and Schmertmann CPT method (McVay and Townsend, 1989) for all soil types,
7. Meyerhof SPT (Meyerhof, 1976/1981) for cohesionless soil,
8. Schmertmann SPT method (Lai and Graham, 1995) for all soil types and rock.

The first five methods, as discussed in Section 2.1.2, are semi-empirical methods. These methods are based on the empirical relationship between soil properties and the stress states



(both effective and total stress analyses are used). The last three methods, as discussed in Section 2.1.3, predict the pile capacities based on the data from in-situ tests (SPT and CPT).

## **2.1.2. Semi-Empirical Methods**

Semi-empirical methods are used to relate the adhesion between the pile and the surrounding soil to the internal friction angle,  $\phi$ , or the undrained shear strength,  $S_u$ . This section presents five different semi-empirical methods, will be divided into 2 sub-sections: Section 2.1.2.1 for cohesive soil and 2.1.2.2 for cohesionless soil.

### *2.1.2.1. Side Resistance In Cohesive Soil*

In cohesive soil, the side resistance of a pile is usually predicted using the undrained shear strength,  $S_u$ , or the over-consolidation ratio, OCR. This section reviews different methods predicting the side resistance in cohesive soil.

#### *2.1.2.1.1. $\alpha$ -Tomlinson method*

The  $\alpha$ -Tomlinson method (Tomlinson, 1980/1995), based on total stress analysis, is used to relate the adhesion between the pile and a clay to the undrained shear strength of the clay,  $S_u$ . The ultimate unit side resistance may be taken as:

$$q_{si} = \alpha S_{ui} \quad 2$$

where:  $\alpha$  = adhesion factor (Figure 1), which depends on the bearing embedment in stiff clay and the width of the pile,  
 $S_u$  (or  $C_u$ ) = average undrained shear strength of the soil in the segment of interest.

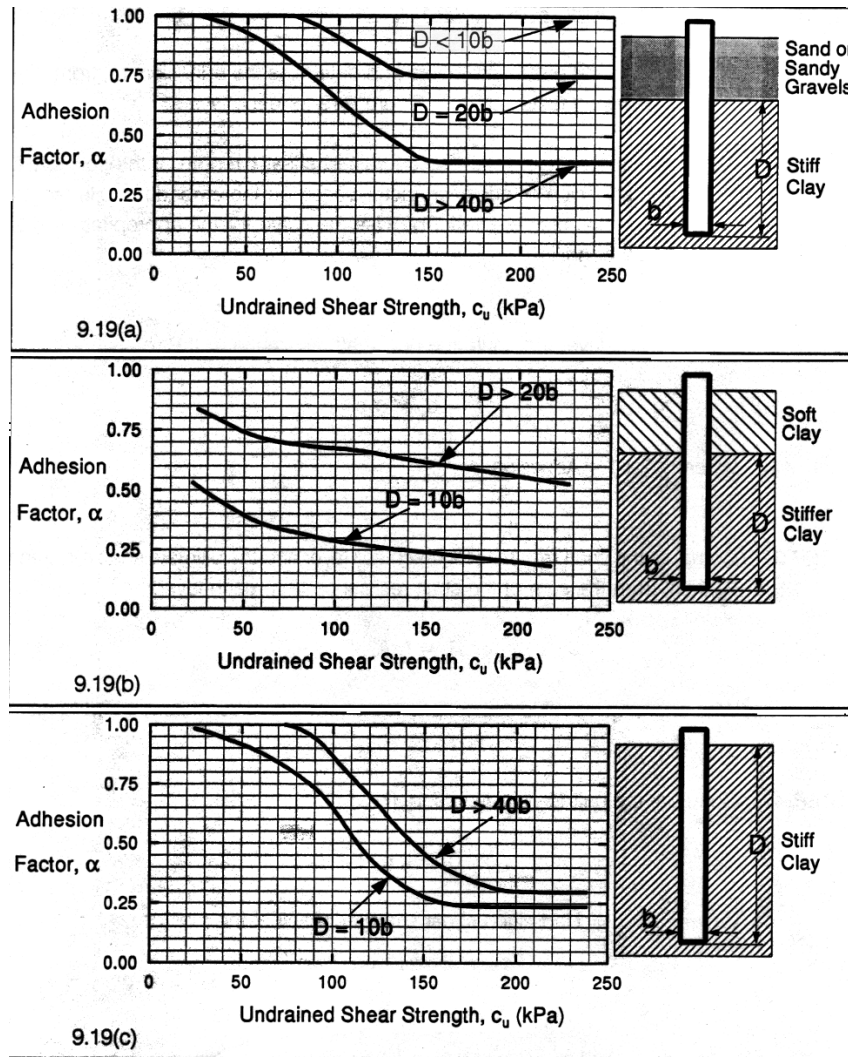


Figure 3:  $\alpha$  factors; Tomlinson method (Tomlinson, 1995)

Following is the discussion on the  $\alpha$ -Tomlinson method:

The  $\alpha$  method is simple to use and it has been used over many years. However, it is a total stress analysis and does not depend on the ground water level; therefore, the resistance based on the  $\alpha$  method may not be close to the measured capacity, which depends on the in-situ stress state and the ground water level.

Tomlinson originally developed the  $\alpha$ -method for large displacement piles. Therefore, for small-displacement piles (H and pipe piles), the  $\alpha$  method may not be suitable. Similarly, the Tomlinson method is only suitable for pile embedded in stiff clay. For cohesive layers that lie above the bearing layer, other methods should be used.

The assumptions behind the  $\alpha$  Tomlinson method include the following:

- If there is a soft clay layer above the bearing stiff clay, then the soft clay will be dragged down to the stiff layer and will lower the  $\alpha$  factor (see Figure 1),

- Similarly, the cohesionless soil in Figure 1 will be dragged down and therefore, the  $\alpha$  factor will be increased,
- Other intermediate cases, such as the layer right above the stiff layer is silt, or is only a very thin lens, etc. will decrease the accuracy of the prediction.

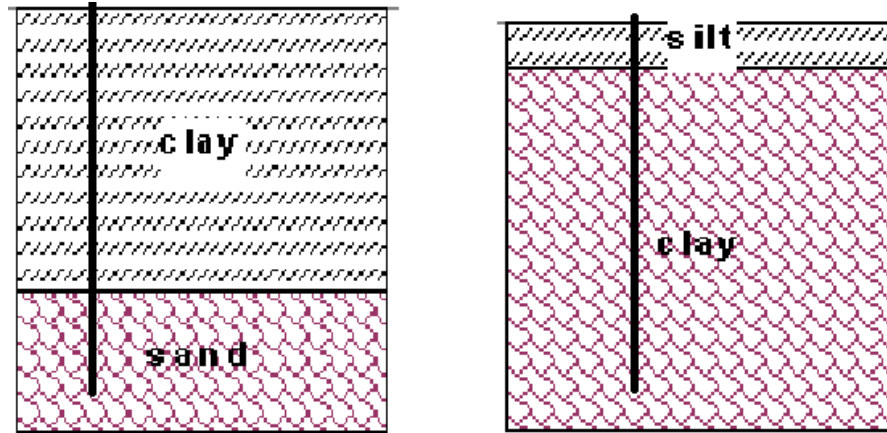


**Figure 4: Examples when  $\alpha$ -Tomlinson is not applicable.**

#### 2.1.2.1.2. $\alpha$ -API revised method (1987)

The  $\alpha$ -API method (cited in Reese et al., 1998) is similar to the  $\alpha$ -Tomlinson method, and the ultimate unit side resistance, in the same unit as  $S_{ui}$ , is taken as:

$$q_{si} = \alpha S_{ui} \quad 2$$

where:  $\alpha = 0.5 \psi^{-0.5}$  if  $\psi \leq 1.0$ ,  
 $\alpha = 0.5 \psi^{-0.25}$  if  $\psi > 1.0$ , and max  $\alpha = 1.0$ ,  
 $\psi = S_u / \sigma_v'$ , and

$\sigma_v'$  (or  $p_v'$ ) = the vertical effective overburden pressure at the depth of interest.

From Eq. 2, the adhesion factor,  $\alpha$ , with different effective stresses is generated in Figure 3.

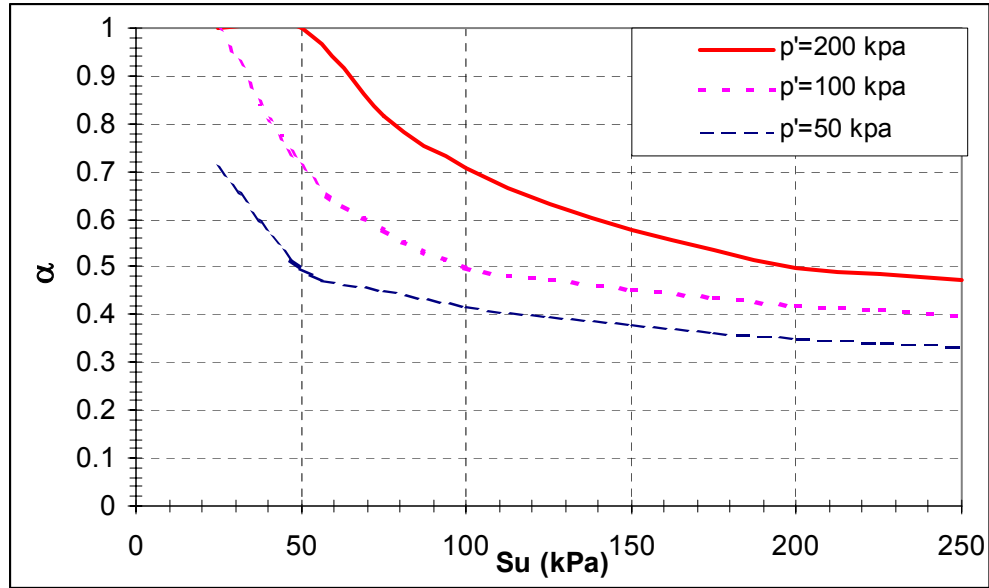


Figure 5:  $\alpha$  factors; Revised API 1987 method (generated from Eq. 2)

The  $\alpha$ -API method is a mixed method between total stress analysis ( $S_u$ ) and effective stress analysis ( $\sigma_v'$ ). It is much easier to use than the Tomlinson method. For example, the user will have no issue with considering other layers that lie above the bearing layer. Finally, the  $\alpha$ -API method has simple equations; thus it is easily automated.

Following is the discussion on the unit side resistance of both  $\alpha$  methods:

As shown in Figure 4, the unit side resistance  $q_s = \alpha S_u$  for the  $\alpha$ -API method follows a logical trend: the stiffer the soil (higher  $S_u$ ), the more the side resistance.

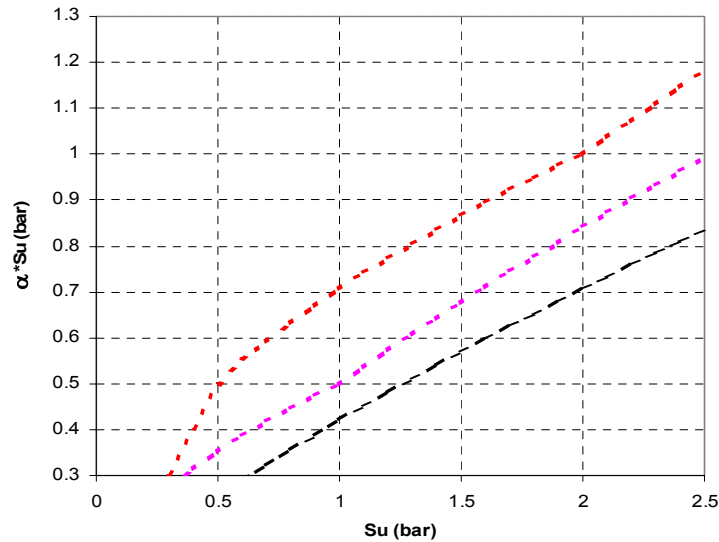


Figure 6: The unit side resistance of  $\alpha$ -API method (generated from Eq. 2)

However, as indicated in Figure 5, for the  $\alpha$ -Tomlinson 1980 method, when  $S_u$  is in the range of about 0.8 to 1.7 bar (80 to 170 kPa), the unit side resistance decreases as the soil

becomes stronger, which does not follow traditional wisdom on pile behavior. (In that range, there is very sharp decrease of the  $\alpha$  factor).

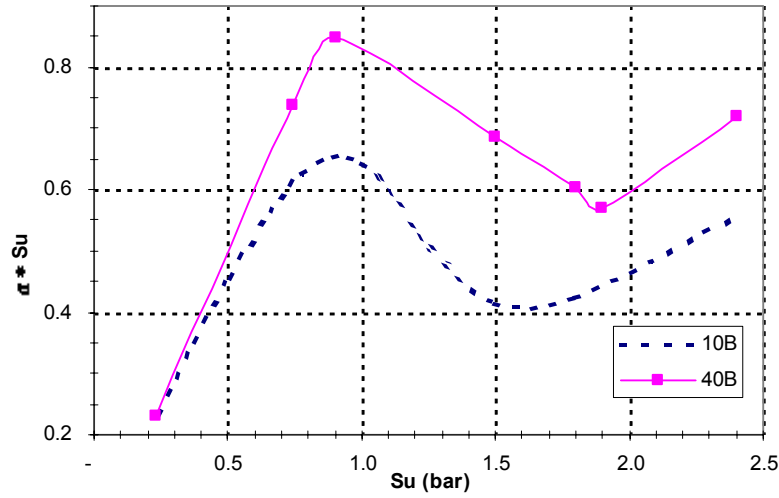


Figure 7: The unit side resistance of  $\alpha$ -Tomlinson 1980 case #3 (generated from Figure 1)

#### 2.1.2.1.3. $\beta$ -Burland method (1973)

From the theory of soil mechanics, based on effective stress analysis, we have  $q_s = K (\tan \delta) \sigma_v'$ ,

where:  $K$  = horizontal stress ratio,

$\delta$  = adhesion angle between soil and piles,

$\sigma_v'$  = vertical effective stress.

The equation can be rewritten as:

$$q_s = \beta \sigma_v' \quad 3$$

where:  $\sigma_v'$  = vertical effective stress,

$\beta$  = factor depended on the over-consolidation ratio OCR (Figure 6).

Following is the discussion on the  $\beta$ -Burland method:

Esrig and Kirby (1979) (cited in Hannigan et al., 1995) suggested that for heavily over-consolidated clays, the value of  $\beta$  should not exceed two.

Practically, the OCR ratio is not usually measured in the laboratory. Therefore, this method is difficult to implement. In this project, all OCR ratios are obtained from in-situ tests through correlations (Section 2.2).

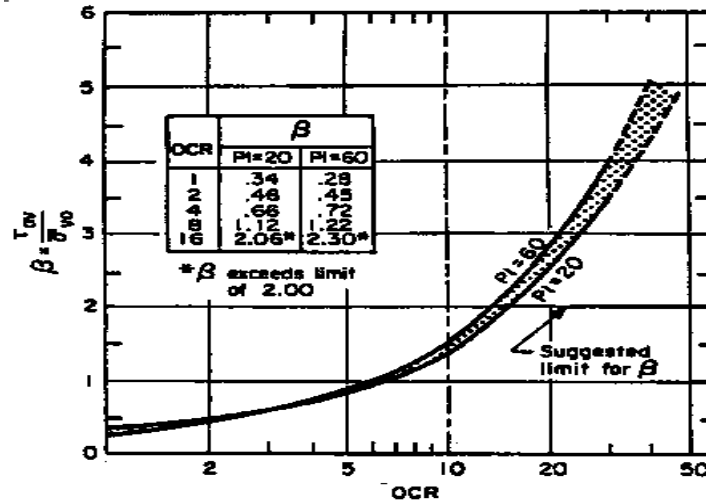


Figure 8:  $\beta$  factors (AASHTO 1996/2000)

#### 2.1.2.1.4. $\lambda$ -Method

The  $\lambda$ -method (cited in US Army Corps of Engineers, 1992), based on effective and total stress analysis, may be used to relate the unit side resistance to the passive earth pressure as:

$$q_s = \lambda(\sigma' + 2S_u) \quad 4$$

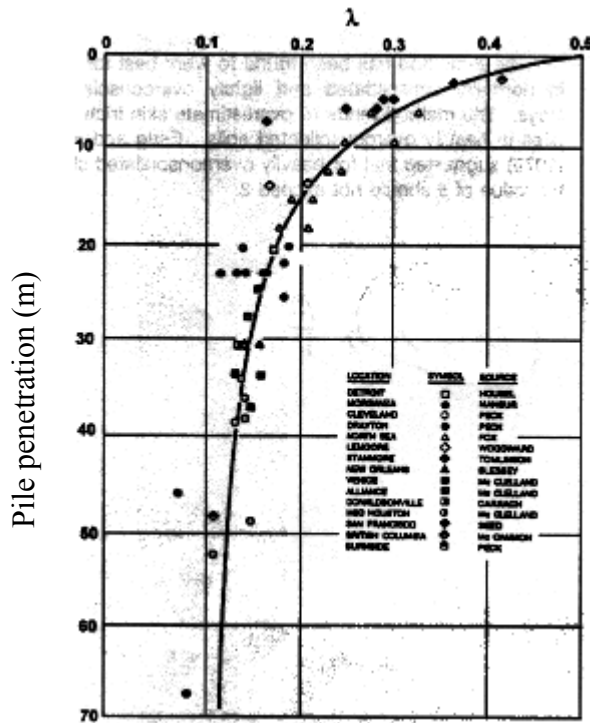


Figure 9:  $\lambda$  factors (US Army Corps of Engineers, 1992)

where:  $\lambda$  = an empirical coefficient, which depends on the pile embedment as shown in Figure 7.

The  $\lambda$  factor was empirically suggested by examining pipe piles in only 15 locations. The main drawback of this method is that it assumes a single value of  $\lambda$  for the whole pile.

### 2.1.2.2. Tip resistance in cohesive soil

The ultimate unit tip resistance of piles in saturated clay (Reese et al., 1998) may be taken as:

$$q_p = 9 S_u \quad 5$$

where:  $S_u$  = average undrained shear strength in the range from  $2B$  to  $3.5B$  below the tip, and  $B$  is the diameter of the pile.

With unsaturated clay, Eq. 5 is still used to predict tip resistance, which may reduce the accuracy of the answer.

### 2.1.2.3. Side resistance in cohesionless soil

In cohesionless soil, the side resistance of a pile is usually predicted using the adhesion angle,  $\delta$ , or the relative density,  $D_r$ . The adhesion angle,  $\delta$ , is related to the internal friction angle of the soil,  $\phi$ , through the volume displacement, the material, the shape of the pile and the roughness of the pile. This section reviews different methods predicting the side resistance in cohesionless soil.

#### 2.1.2.3.1. $\beta$ -Bushan method (1982)

Similar to the  $\beta$  method in cohesive soil, the unit side resistance is related to effective stress as (cited in Hannigan et al., 1995):

$$q_s = \beta \sigma_v' \quad 3$$

where:  $\beta = 0.18 + 0.65 D_r$ , and

$D_r$  = Relative density in decimals. Therefore,  $\max \beta = 0.83$  when  $D_r = 1$  (much lower than  $\max \beta$  in cohesive soil--Section 2.1.2.1.3.)

#### 2.1.2.3.2. Nordlund method

Nordlund (cited in Hannigan et al., 1995) developed the following equation for the unit resistance:

$$q_s = K_\delta C_F \sigma_v' \frac{\sin(\delta + \omega)}{\cos \omega} \quad 6$$

where:  $K_\delta$  = Coefficient of lateral earth pressure at the depth of interest. (Figures 8 to 11),

$\delta$  = friction angle between pile and soil. For non-taper piles:  $\delta \leq \phi$ . (Figure 12),

$C_F$  = Correction factor for  $K_\delta$  when  $\delta \neq \phi$ .  $C_F \approx 0.6$  to  $1.0$ . (Figure 13),

$\sigma_v'$  = effective over-burden pressure at the center of the layer of interest, and

$\omega$  = angle of the pile taper from vertical.

For a uniform cross section pile ( $\omega = 0$ ), the Nordlund equation becomes

$$q_s = K_\delta C_F \sigma_v' \sin \delta \quad 7$$

The equation of this semi-empirical method is somewhat similar to the theory of soil mechanics, in which

$$q_s = K_\delta \sigma_v' \tan \delta \quad 8$$

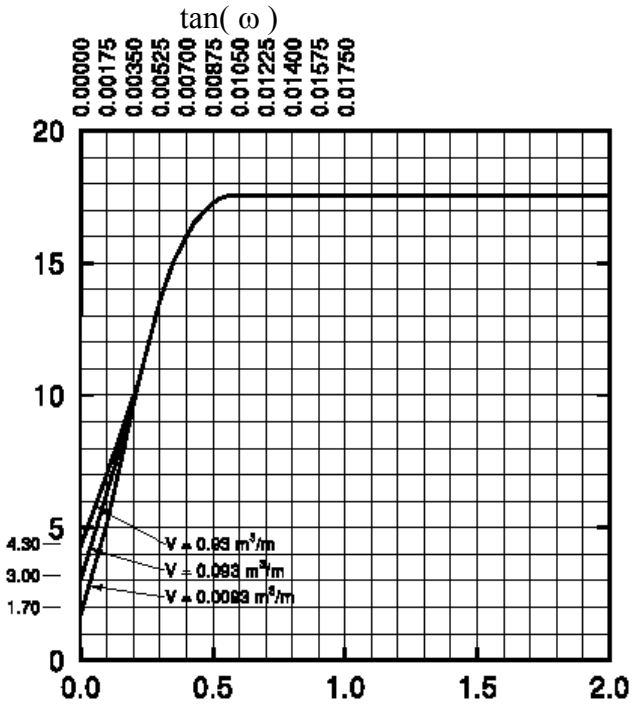


Figure 10: Design curve for evaluating  $K_\delta$  when  $\phi = 40$   
(Norlund 1963--cited in Hannigan et al., 1995)

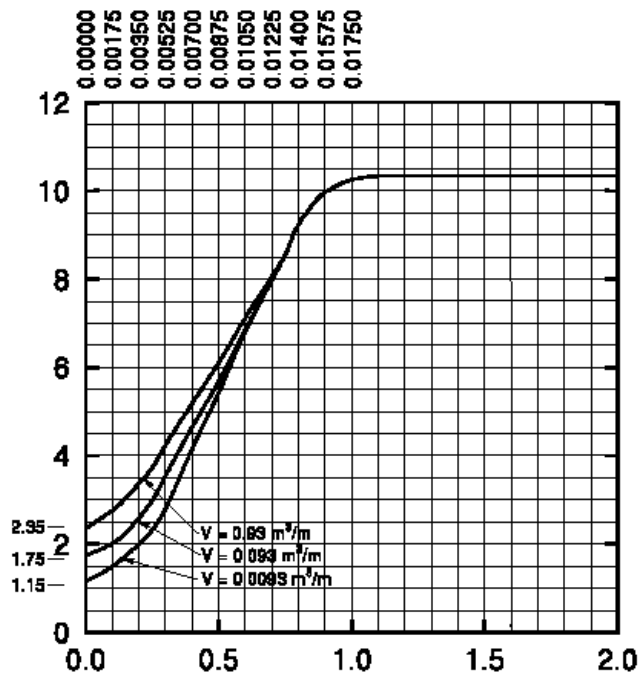
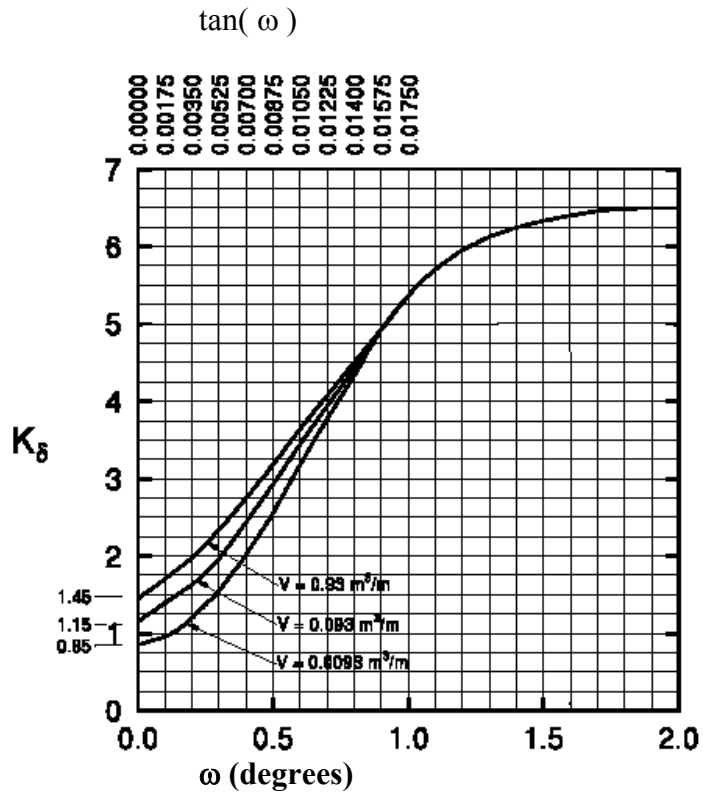
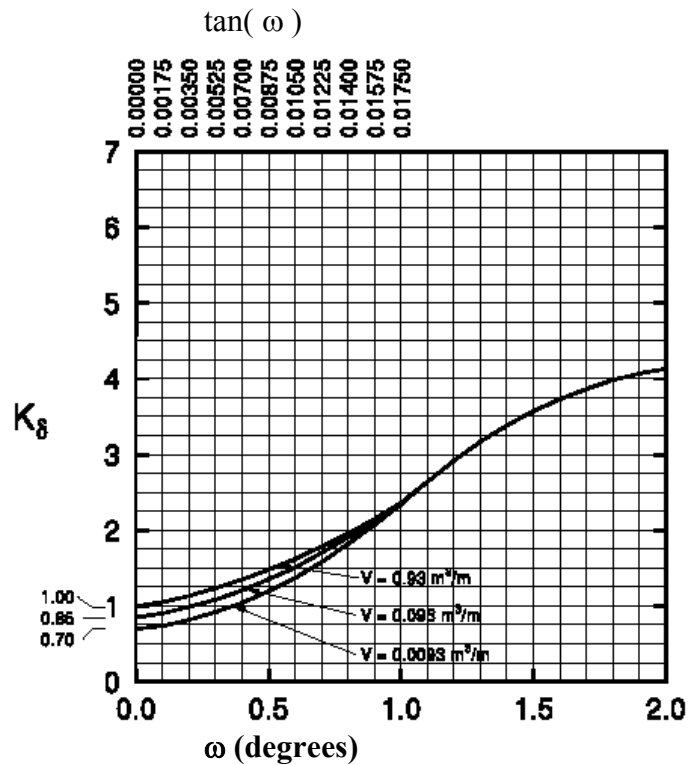


Figure 11: Design curve for evaluating  $K_\delta$  when  $\phi = 35$   
(Norlund 1963--cited in Hannigan et al., 1995)





**Figure 12: Design curve for evaluating  $K_\delta$  when  $\phi = 30$**   
(Norlund 1963--cited in Hannigan et al., 1995)



**Figure 13: Design curve for evaluating  $K_\delta$  when  $\phi = 25$**   
(Norlund 1963--cited in Hannigan et al., 1995)

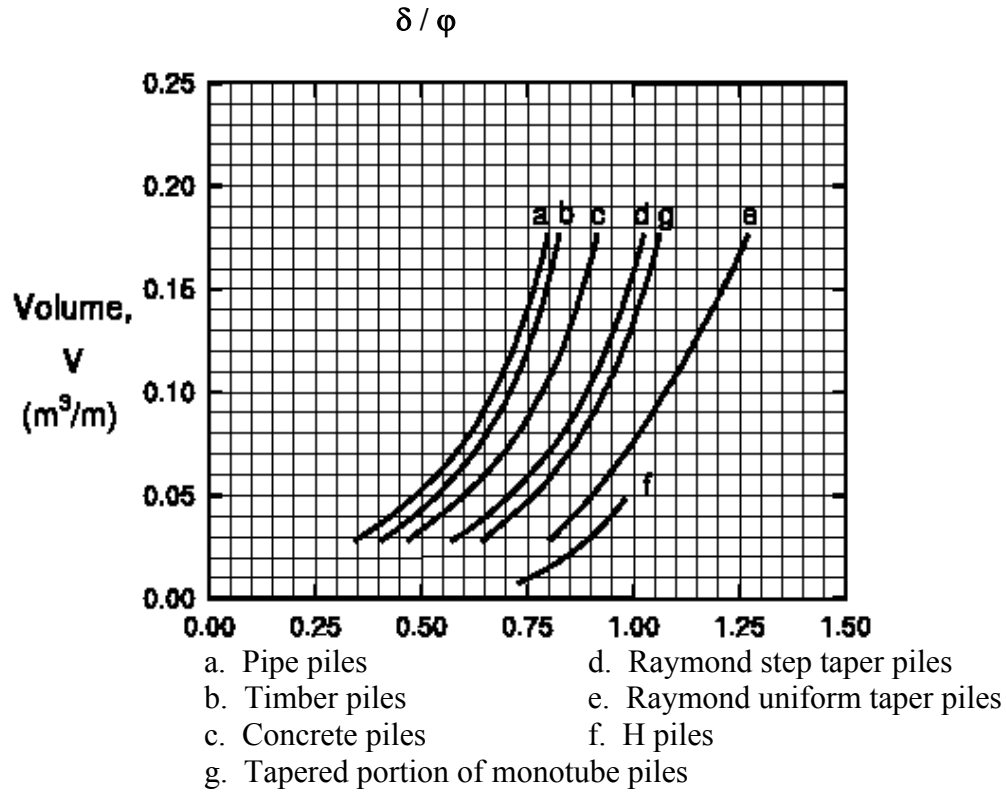


**Figure 14: Relation  $\delta/\phi$  and pile displacement**  
(Norlund 1963--cited in Hannigan et al., 1995)

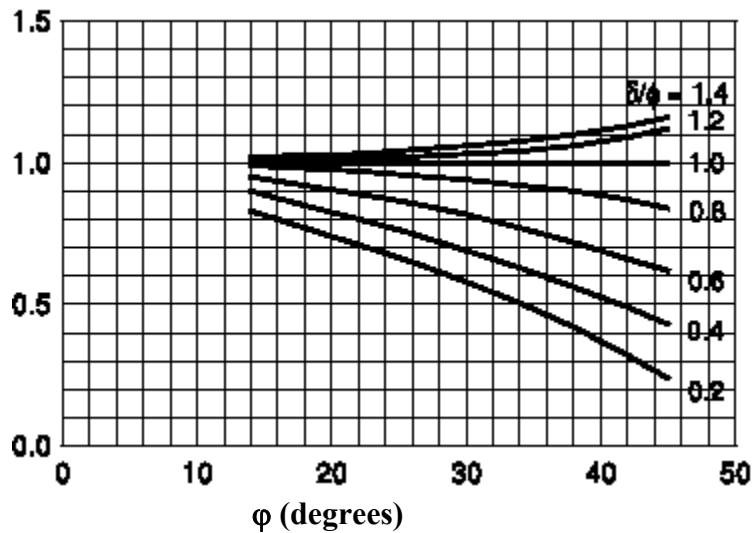


**Figure 15: Correction factor ( $C_F$ ) for  $K_\delta$**   
(Norlund 1963--cited in Hannigan et al., 1995)

#### 2.1.2.4. Tip resistance in cohesionless soil--Thurman method

From bearing capacity theory, Thurman (cited in Hannigan et al., 1995) related the unit tip resistance in sand with effective stress as:

$$q_p = \alpha_t N'_q \sigma_v' \quad 9$$

where:  $\alpha_t$  = dimensionless factor (Figure 14),  
 $N'_q$  = Bearing capacity factor (Figure 15),  
 $\sigma_v'$  = effective overburden pressure at the pile tip.  $\sigma_v'$  is limited to 150 kPa (tip resistance reaches a limiting value at some distance below the ground),  
 $q_p$  also has a limit as shown in Figure 16.

$N'_q$  is very high at high internal friction angles ( $N'_q > 250$  when  $\phi > 42^\circ$ ). Therefore, some software, e.g. DRIVEN (FHWA, 1998) recommends the limit of only  $36^\circ$  for  $\phi$ .

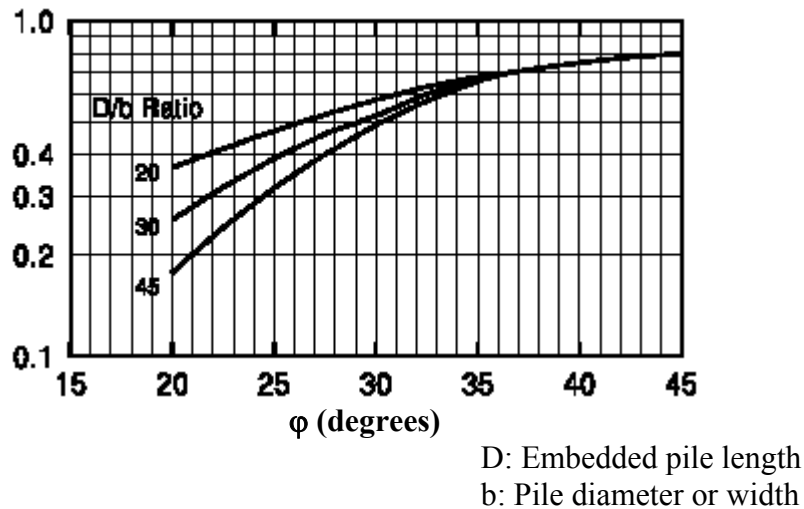


Figure 16:  $\alpha_T$  coefficient (FHWA--DRIVEN, 1998)

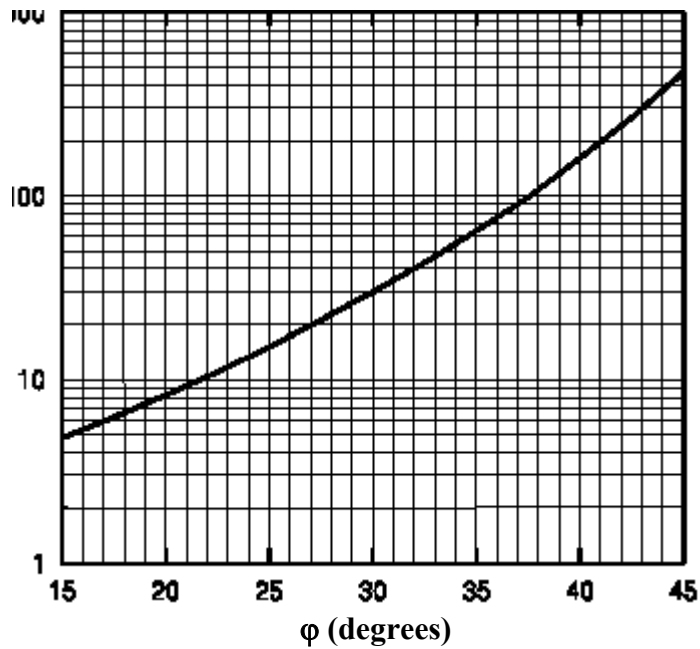


Figure 17: Bearing capacity factor  $N_q'$ (FHWA--DRIVEN, 1998)

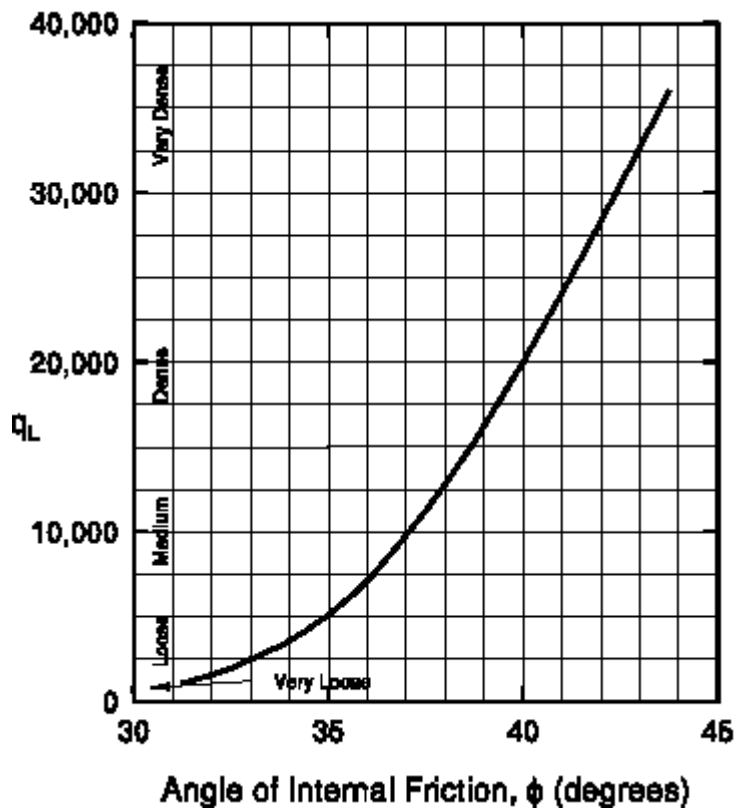


Figure 18: Relationship Between Maximum Unit Pile Toe Resistance  $q_L$  (kPa) and Friction Angle for Cohesionless Soils (Meyerhof, 1976/1981).

### 2.1.3. Empirical Methods

This section presents different empirical methods, which directly relate the resistances with the in-situ test results, i.e. the N-value and the CPT readings.

#### 2.1.3.1. Meyerhof method for piles in cohesionless soil

There are more than four different variations of Meyerhof 1976 method. Different agencies have different guidelines, e.g. EM 1110-1-1905 (US Army Corps of Engineers, 1992), leading to different results, even though the method is still referred to as Meyerhof 1976 method. The primary variations of the side resistance of the method are listed below:

- 1) AASHTO provision (AASHTO 1996/2000):  $q_s = k' N$  (kPa).
  - 2) Meyerhof original paper (Meyerhof, 1976/1981):  $q_s = k N$  (kPa).
  - 3) Bowles (Bowles, 1996):  $q_s = k N'$  (kPa).
  - 4) U.S. CORPS of Engineers: No guidelines.
- where:  $N$  = Uncorrected blow count,  
 $N'$  = Corrected blow count,  
 $k = 2$  for displacement piles, and  $k = 1$  for small displacement piles.

AASHTO (AASHTO 1996/2000) uses strict unit conversion, therefore  $k' = 1.9$  for displacement piles and 0.96 for small displacement piles.

The side resistance should be limited as given below:

$$q_s \leq 100 \text{ kPa}$$

The tip resistance for Meyerhof method is similarly obtained as:

- 1) AASHTO provision (AASHTO 1996/2000):  $q_p = 0.38 N_t' D/B$  (bar).  
where:  $N_t'$  = Corrected blow count near the pile tip,  
 $D$  = The embedment of the pile in cohesionless soil, and  
 $B$  = The diameter or width of the pile cross-section.
- 2) Original paper by Meyerhof (Meyerhof, 1976/1981):  $q_p = 0.4 N_t D/B$  (bar).  
where:  $N_t$  = Uncorrected blow count near the pile tip.

It should be noted that, in 1976, the concept of correcting the N-value due to the overburden pressure was very new. Therefore, Meyerhof did not correct N. Similarly, in Meyerhof's paper, he used approximate conversion:  $1 \text{ tsf} \approx 100 \text{ kPa}$  (1 bar).

- 3) Bowles (Bowles, 1996):  $q_p = 0.4 N_{8+3B}' D/B$  (bar).  
where:  $N_{8+3B}'$  = Corrected blow count in the depth of 8B above tip and 3B below tip.
- 4) EM 1110-1-1905 (U.S. Army CORPS of Engineers, 1992)  
 $q_p = 0.38 N_{8+3B} D/B$  (bar) =  $0.8 N_{8+3B} D/B$  (ksf).  
where:  $N_{8+3B}$  = Uncorrected N in the depth of 8B above tip and 3B below tip.

Similar to the side resistance calculations, the value of the maximum tip resistance is also limited as shown below:

- 1) AASHTO provision (AASHTO 1996/2000)

$$q_L = 4 N_t' \text{ in sand,}$$
$$= 3 N_t' \text{ in silt.}$$

- 2) Meyerhof original paper (Meyerhof, 1976/1981)

$$q_L = 4 N_t \text{ in sand,}$$

- $= 3 N_t$  in silt.
- 3) Bowles (Bowles, 1996)
- $q_L = 3.8 N_{8+3B}'$ .
- 4) EM 1110-1-1905 (U.S. Army CORPS of Engineers, 1992)
- $q_L = 3.8 N_{8+3B} \text{ (bar)} = 8 N_{8+3B} \text{ (ksf)}.$

#### 2.1.3.2. Schmertmann method for SPT

The procedure of the Schmertmann method for SPT (Lai and Graham, 1995) is described below. First of all, the SPT blow count  $N$  is adjusted as shown below:

- If  $N < 5$  then  $N = 0$  (ignores side resistance in weak soil), and  
 If  $N \geq 60$  then  $N = 60$  (limit on side resistance)

Discussion:

It is conservative to ignore side resistance when  $N$  is in the range of 4 to 5. For example, in Luling bridge, ID 1001, the soil is mostly clay with  $N < 5$ . The truncation of  $N < 5$  significantly lowers the predicted capacity compared to the measured capacity.

The ultimate side resistance for different types of piles and soil types is presented in Table 1.

**Table 1: Side resistance --Schmertmann method for SPT**

Ty-Pe	Description	Ultimate unit side resistance $q_s$ (tsf)		
		Concrete	Steel H piles	pipe piles
1	Plastic clay	$2.0N(110-N)/4006.6$	$2N(110-N)/5335.94$	$0.949+0.238\ln N$
2	Clay-silt-sand mixtures Very silty sand, silts	$2.0N(110-N)/4583.3$	$-0.0227+0.033N-4.57610^{-4}*N^2+2.465E-6*N^3$	$0.243+0.147\ln N$
3	Clean sands	$0.019N$	$0.0116N$	$0.058+0.152\ln N$
4	Soft limestone, very shelly sand	$0.01N$	$0.0076N$	$0.018+0.134\ln N$

At any point A, the unit tip resistance is

$$q_{p@A} = \frac{\text{weighted average of } q_p \text{ 8B above A} + \text{weighted average of } q_p \text{ 3.5B below A}}{2}$$

The weighted average of  $q_p$  is based on values calculated from Table 2.

**Table 2: Tip resistance –Schmertmann method for SPT**

Type	Description	Ultimate unit end bearing $q_p$ (tsf)	
		Concrete and H piles	Pipe piles
1	Plastic clay	0.7 N	0.48 N
2	Clay-silt-sand mixtures Very silty sand, silts	1.6 N	0.96 N
3	Clean sands	3.2 N	1.312 N
4	Soft limestone, very shelly sand	3.6 N	1.92 N

For concrete and H piles, the mobilized tip resistance is expected to be one third (1/3) of the ultimate tip resistance. For pipe piles, the mobilized tip resistance is expected to be one half (1/2) of the ultimate tip resistance.

The ultimate resistance is only fully mobilized when the bearing embedment is sufficient, i.e.  $D_A = D_C$

where:  $D_A$  = Actual bearing embedment, and  $D_C$  = Critical bearing embedment, which is shown in Table 3.

**Table 3: Critical depth ratio—Schmertmann method for SPT**

Soil Type	Description	Critical depth ratio ( $D_C/B$ )
1	Plastic clay	2
2	Clay-silt-sand mixtures Very silty sand, silts	4
3	Clean sands $N = 12$ or less	6
	$N = 30$ or less	9
	$N$ greater than 30	12
4	Soft limestone, very shelly sand	6

If  $D_A < D_C$  and the bearing layer is stronger than the overlying layer, then:

$$q_p = q_{LC} + \frac{D_A}{D_C}(q_T - q_{LC}) \quad 10$$

where:  $q_p$  = Reduced tip resistance,

$q_{LC}$  = Unit tip resistance at layer change, and

$q_T$  = Uncorrected unit tip resistance at pile tip.

$$CSFBL = \frac{SFBL}{q_T} \left[ q_{LC} + \frac{D_A}{2D_C}(q_T - q_{LC}) \right] \quad 11$$

where: CSFBL = Reduced side resistance in the bearing layer, and

SFBL = Uncorrected side resistance in the bearing layer.

If  $D_A > D_C$  and the bearing layer is stronger than the overlying layer, then:

$$CSFACD = \frac{USFACD}{q_{CD}} [q_{LC} + 0.5(q_{CD} - q_{LC})] \quad 12$$

where:

CSFACD = Corrected side resistance between the top of the bearing layer and the critical depth,

USFACD = uncorrected side resistance in the bearing layer from the top of the bearing layer to the critical depth, and

$q_{CD}$  = unit tip resistance at critical depth.

### 2.1.3.3. Nottingham and Schmertmann method for CPT

The procedure of the Nottingham and Schmertmann method for CPT (McVay and Townsend, 1989) is described below.

The ultimate side resistance of piles may be taken as:

From ground level down to the depth of  $8B$   $q_s = K f_s / 2$  13

From  $8B$  down to the tip  $q_s = K f_s$  14

where:  $f_s$  = sleeve friction from CPT data,

In cohesionless soil, the ratio  $K$  (or  $K_s$ ) is a function of the ratio between penetration depth ( $Z$ ) and pile width ( $D$ )--see Figure 17.

In cohesive soils:  $K$  is written as  $\alpha$  (or  $K_c$ ), which is the  $\alpha$  factor, similar to the  $\alpha$ -method--see Figure 17.

Similarly, the ultimate tip resistance of piles may be taken as:

$$q_p = \frac{q_{c1} + q_{c2}}{2} \quad 15$$

where:  $q_c$  = The tip resistance in CPT data (if  $q_c > 100$  tsf, limit  $q_c$  to 100 tsf),

$q_{c1}$  = The average  $q_c$  over a distance of  $x_B$  below the tip, which is shown below:

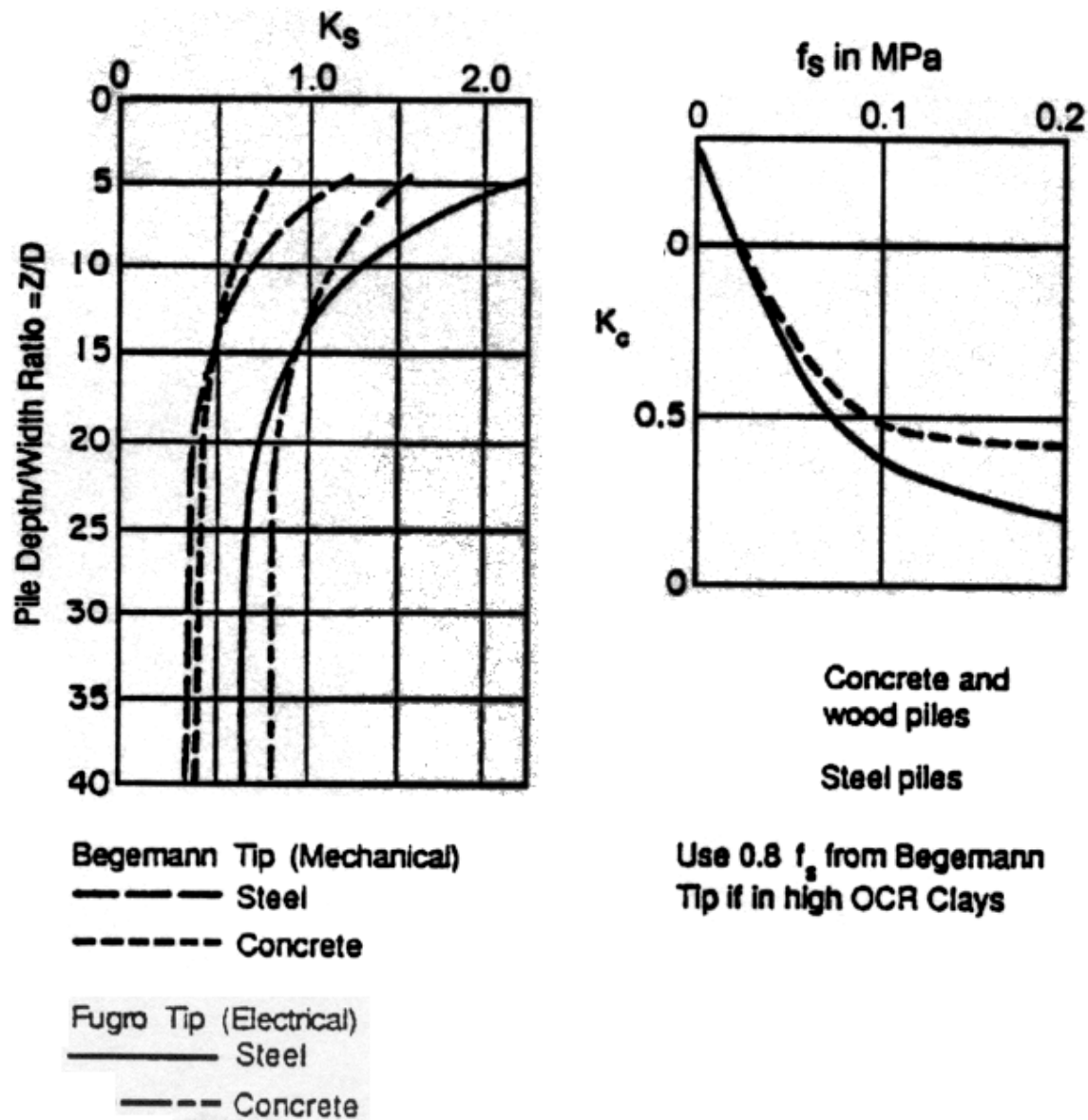
Sum of the minimum values (upward)/  $x_B$  + Sum of the actual values (downward)/  $x_B$

Use the minimum  $q_{c1}$  with different  $x_B$  ranging from  $0.7B$  to  $3.75B$ ,

$q_{c2}$  = The average  $q_c$  over a distance of  $8B$  above the tip using the minimum  $q_c$  values (minimum path). Figure 18 depicts the procedure for tip resistance prediction.

For mechanical cone in cohesive soils, due to the effects of the base of the friction sleeve on  $q_c$ , the  $q_p$  value should be reduced by about 40%.





## Side friction

Figure 19:  $K_s$  and  $K_c$  ratio in cohesionless and cohesive soil, respectively

(cited in McVay and Townsend, 1989)

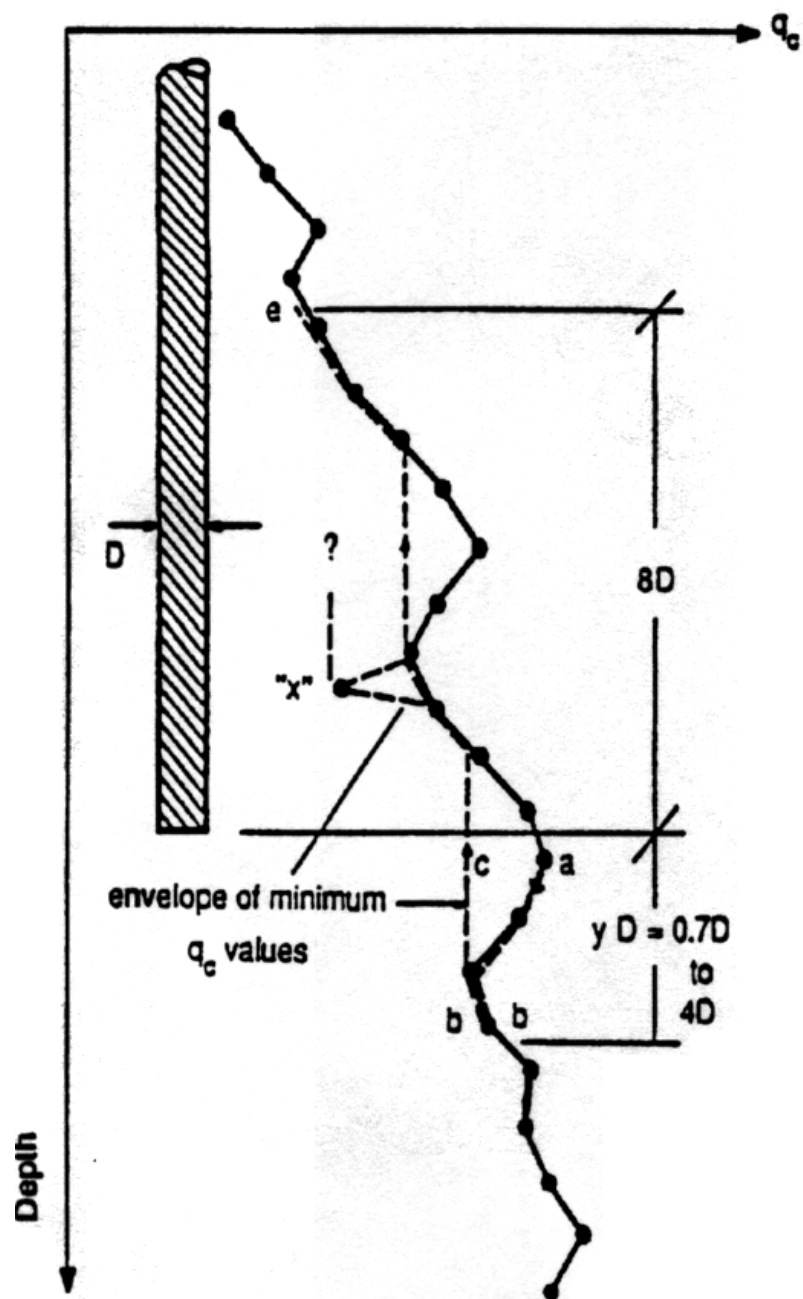


Figure 20: Tip resistance computation procedure--Nottingham 1975.

(cited in McVay and Townsend, 1989)

A summary of all the methods is presented in Table 4 below.

**Table 4: Summary of the methods**

Methods	Side resistance	Tip resistance	Parameters required	Constraints
$\alpha$ -Tomlinson (Tomlinson, 1980/1995)	$q_s = \alpha S_u$	$q_p = 9 S_u$	$S_u$ ; $D_b$ (bearing embedment)	+Bearing layer must be stiff cohesive + Number of soil layers $\leq 2$
$\alpha$ -API (Reese et al., 1998)			$S_u$	
$\beta$ in cohesive (AASHTO, 1996/2000)	$q_s = \beta \sigma'$		OCR	
$\lambda$ (US Army Corps of Engineers, 1992)	$q_s = \lambda(\sigma' + 2S_u)$		$S_u$	Only for cohesive soils
$\beta$ in cohesionless (Bowles, 1996)	$\beta \sigma'$		$D_r$	
Nordlund and Thurman (Hannigan et al., 1995)	$q_s = K_\delta C_F \sigma' \frac{\sin(\delta + \varpi)}{\cos \varpi}$	$q_p =$ $\alpha_t N'_q \sigma'$	$\varphi$	
Meyerhof SPT (Meyerhof, 1976/1981)	$q_s = k N$	$q_p =$ $0.4D/BN'$	$N$	+ For cohesionless soils + SPT data
Schmertmann SPT (Lai and Graham, 1995)	$q_s = \text{function}(N)$	$q_p = \text{fn}(N)$	$N$	SPT data
Schmertmann CPT (McVay and Townsend, 1989)	$q_s = \text{function}(f_s)$	$q_p = \text{fn}(q_c)$	$q_c, f_s$	CPT data

#### **2.1.4. Evaluation of Axial Capacity Prediction Software**

Four common programs are used in predicting the pile axial capacity. This section briefly evaluates the programs, such as the methods they use, and the results they get.

##### **2.1.4.1. APILE 3.0 (EnSoft)**

APILE 3.0 is a commercial Windows-based software developed by EnSoft, Inc (Reese et al., 1998).

For cohesive soil, the following static methods are used: The  $\alpha$ -Tomlinson method, the  $\alpha$ -API method and the  $\lambda$  method. For cohesionless soil, the following static methods are used: The Nordlund method and the API method. The combination of the  $\alpha$ -Tomlinson and Nordlund methods in mixed soils is called the FHWA procedure.

The following problems were detected in using this program:

- For piles with non-circular sections, when the unit is changed from SI to English, the predicted axial capacity as well as the shapes of the capacity graph change,
- Outputs of EnSoft's examples 2 and 4 are different from the User Manual's printout,
- In FHWA procedure, the program does not correctly interpret the data when there are more than two layers: The bearing embedment depth will be calculated by the program as the distance from the tip to the nearest interface, which may be less than the actual bearing embedment,
- There is no box for inputting ground-water level, the user has to use buoyant unit weight whenever applicable.

##### **2.1.4.2. DRIVEN 1.1 (FHWA)**

DRIVEN is a freeware Windows-based software provided by the Federal Highway Administration (FHWA, 1998). Driven is the Windows version of the old SPILE MSDOS-based program. The  $\alpha$ -Tomlinson method is used in cohesive soils, while the Nordlund and Thurman methods are used in cohesionless soils.

For concrete pile, DRIVEN does not support the circular section.

The  $\alpha$ -Tomlinson method is only suitable for pile embedded in stiff clay. However, DRIVEN allows the user to specify the  $\alpha$ -Tomlinson method in cohesive layer(s) that lies above the bearing layer.

##### **2.1.4.3. PL-AID (University of Florida)**

PL-AID is a MSDOS-based program developed at the University of Florida predicting capacities of piles using CPT data, i.e. Nottingham and Schmertmann method (McVay and Townsend, 1989).

PL-AID works correctly under the following conditions:

- CPT data (raw truck format or interpreted format) are in SI units,
- The increments in data input are equal (e.g. 5 or 10 cm).

PL-AID was not originally developed for H piles and unplugged open-ended pipe piles.

##### **2.1.4.4. SPT-97 (FDOT and University of Florida)**

SPT-97 is a Windows-based program predicting capacities using SPT data, i.e. Schmertmann method (Lai and Graham, 1995). SPT97 works normally well, except two following cases:

- When  $D_c < D_a$  (the critical depth is smaller than the actual depth), there is a problem in correcting the resistance.
- The capacity is erroneously computed for pipe piles.

A summary of the issues related to the above software can be found in Table 5.

**Table 5. Issues with using Driven Pile Axial Capacities Analysis Software**

APILE 3.0 Plus	DRIVEN 1.1	SPT 97	PL-AID
All results using SI unit are erroneous (this problem was corrected on September 18, 00)	The computed results for H piles, SI units are erroneous.	When $D_c < D_a$ (critical depth is smaller than actual depth), there is a problem in correcting the resistance.	Increments must be equal. This is always true if the data are originally collected from the tests. However, some of the data are actually digitized from graphs. In this case, interpolation must be made to get equal increments.
Error in critical depth (this problem was corrected on November 27, 00)	Concrete piles: There is no option to input circular pile.		
Wrong handling of volume displacement for H and pipe piles (this problem was corrected on January 04, 01)			
The $\lambda$ method is only suitable for pile in clay. In sand, APILE still has $\lambda$ capacities for piles by converting $\phi$ to $S_u$ (but in the APILE manual, it said that it took capacities from API)	The Nordlund method: Open ended pipe piles: Curve f (for H piles) is used for open ended pipe piles, which leads to higher capacities of plugged open ended pipe than those of close ended pipe with the same dimensions		
The $\alpha$ -Tomlinson (1980) method: The layer system must be converted to 1 or 2 layer(s). This causes an approximation and lowers the reliability, especially when the soil system is complex.	The $\alpha$ -Tomlinson 1980 method: In order to get correct results, the layer system must be converted to 1 or 2 layer(s). This causes an approximation and lowers the reliability, especially when the soil system is complex.	For pipe piles, the capacity from SPT97 is erroneously computed	
Error in user specified $q_L$ (this problem was corrected on January 24, 01)			
Different capacities with different increments. (This problem was unsuccessfully corrected on February 14, 01)			

## 2.2. Interpretation of the Pile-Load Tests

Static load tests to failure determine the load capacities directly, therefore they are more precise than the prediction methods presented in Section 2.1. However, from load-settlement curves, a determination of the ultimate capacity or of the mobilized capacity is required. Many different methods of interpretations have been proposed and some of most common methods are presented in this section.

### 2.2.1. Debeer Method

The DeBeer capacity (Bowles, 1996) is determined as follow.

The load test data is plotted in a log-log scale.

The intersection between the two straight portions of the graph will correspond to the DeBeer capacity.

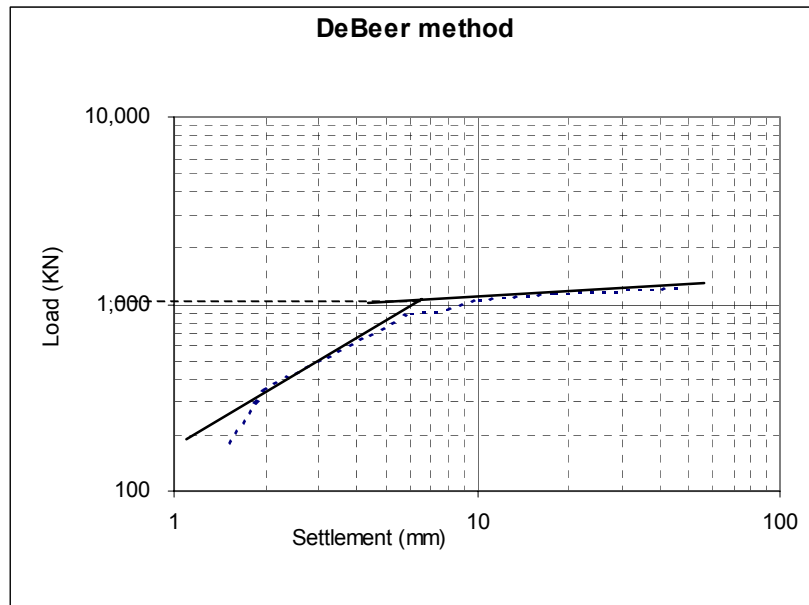


**Figure 21: Example of the Debeer method**

One of the most common problems with this method is that, in some cases, the two straight portions in the graph are not clearly defined.

### 2.2.2. Davisson Method

The Davisson method (Coduto, 2001) is one of the most popular methods and it is based on the elastic compression of the pile. The procedure to define the the Davisson capacity is as described below:

1. In the load test graph, plot the base line with the slope of:  $AE/L$   
where: A = Cross sectional of the material,  
E = Modulus of elasticity of the material, and  
L = Embedment length of the pile

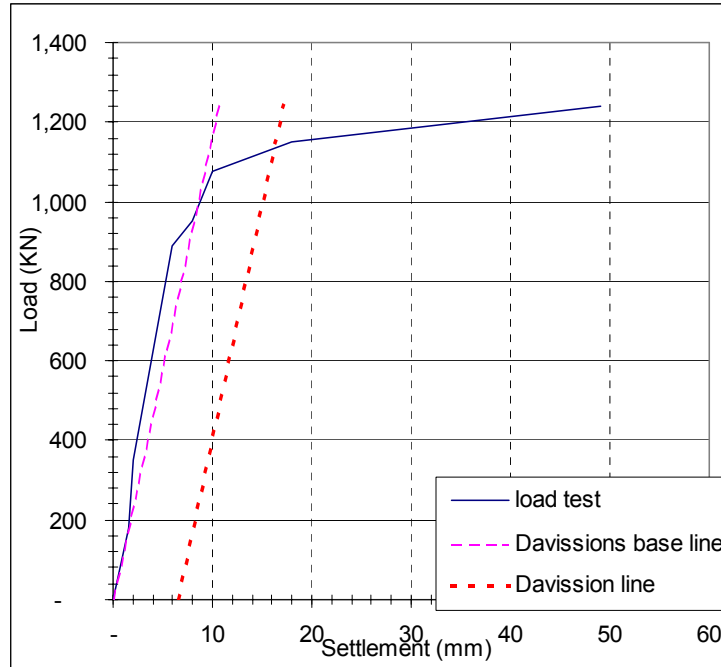


**Figure 22: Example of the Davisson method**

2. Plot the Davisson line parallel to the base line. The distance between the two lines is

$$0.15 + \frac{B}{120} \text{ (in)}$$

3. The intersection of that line and the load test graph represents the Davisson capacity.

Davisson method is most suitable for quick load tests on friction piles. For end bearing piles, as the load test curve does not flatten, the Davisson method is usually not applicable.

### 2.2.3. Other Methods

The pile capacity can be at a point where the settlement of the pile is 5% of its diameter. (or 2%, 3%, or even 10% depending on the pile shape and load test procedure). These methods are very simple. However, they do not account for the length and the material of the pile.

## 2.3. Soil Properties Correlated from Insitu Tests

About 95% of the soil data from the database are from SPT and CPT tests. Moreover, the  $\alpha$ ,  $\beta$ ,  $\lambda$  and the Nordlund method all use the angle friction  $\phi$  and/or the undrained shear strength  $S_u$  or the over-consolidation ratio OCR. Therefore, correlations are required to obtain these properties from the SPT and CPT tests.

There are usually two or more correlations for the same property. Therefore, in the following, the capacities are predicted based on the various different correlations available. The correlations used in this study to get engineering soil properties from SPT are presented in Table 6. Similarly, Table 7 shows the correlations to get engineering soil properties from CPT.



**Table 6: Correlations of soil properties from SPT**

Properties	From SPT	Figure	Reference	
$\phi$	Peck, Hanson and Thornburn: $\approx 54 - 27.6034 \exp(-0.014N')$	2'	Figure 4.12	Kulhawy and Mayne, 1990
	Schmertmann $\phi'$ $\approx \tan^{-1} [ N / (12.2 + 20.3 \sigma') ]^{0.34}$	22	Figure 4.13 and Equation 4.11	
$S_u$ (bar)	Terzaghi and Peck (1967): 0.06 N		Equation 4.59	
	Hara 1974: $0.29 N^{0.72}$		Equation 4.60	
OCR for clay	Mayne and Kemper $\approx 0.5 N / \sigma'_o$ ( $\sigma'_o$ in bar)	23	Figures 3.9 and 3.18	
$Dr$	Gibbs and Holtz's Figures	24	Figures 2.13 and 2.14	

where: N is the uncorrected blow counts, and  
 $N'$  is the corrected blow counts

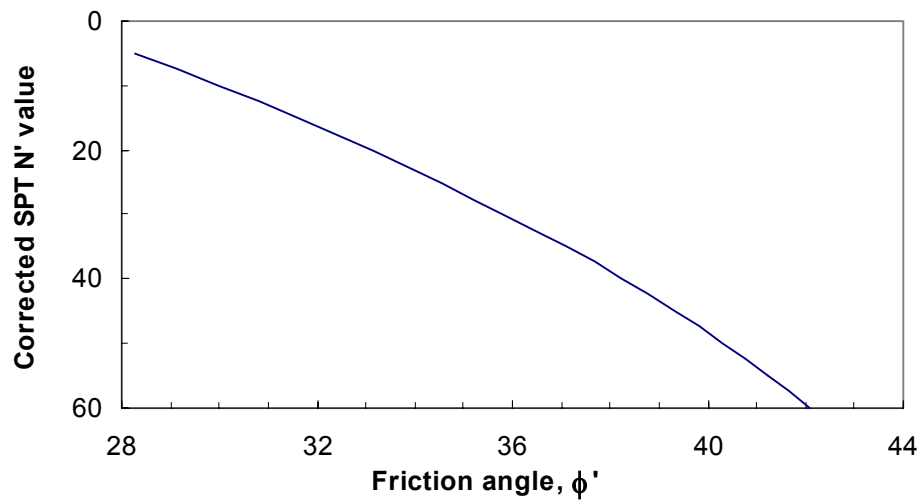


Figure 21:  $\phi'$  by Peck, Hanson and Thornburn (Kulhawy and Mayne, 1990)

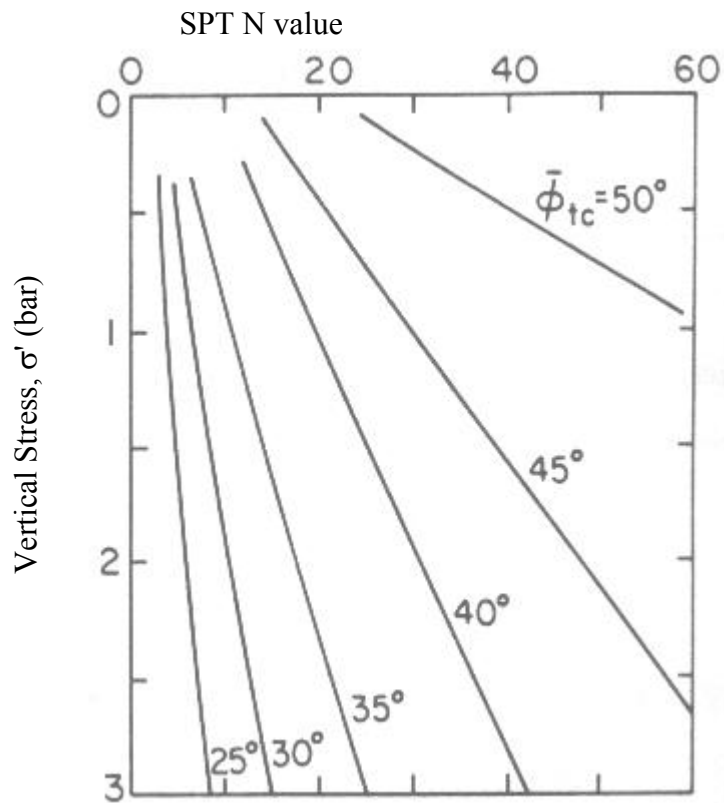
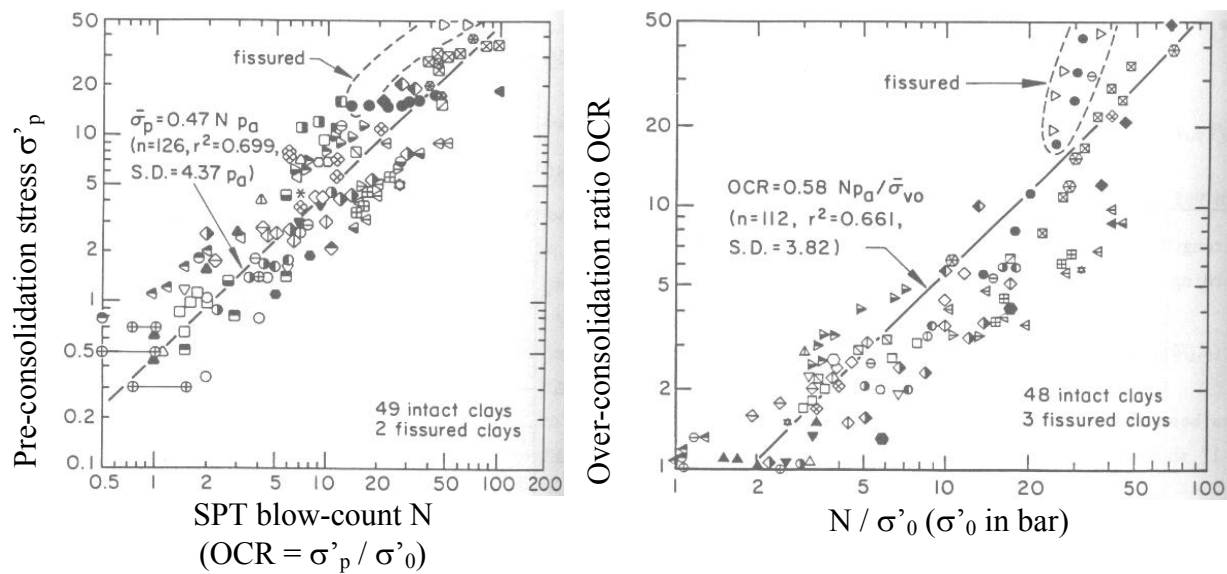
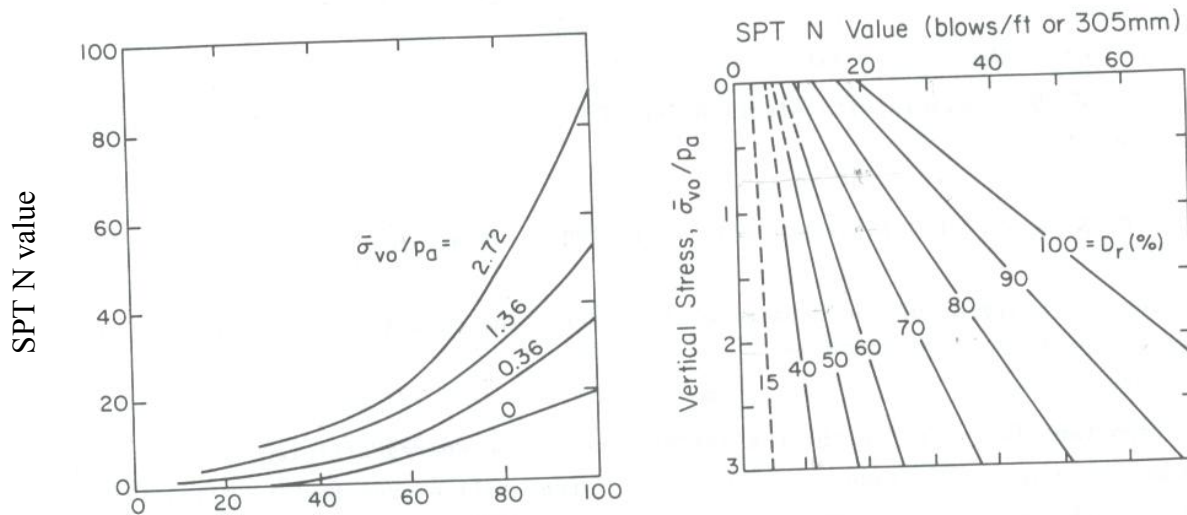


Figure 23:  $\phi'$  by Schmertmann (Kulhawy and Mayne, 1990)



**Figure 24: OCR--N Relationship (Kulhawy and Mayne, 1990)**



**Figure 25: Relative Density--N--Stress Relationship (Kulhawy and Mayne, 1990)**

**Table 7. Correlations of soil properties from CPT**

Properties	From CPT	Figure	Reference	
$\phi$	Robertson and Campanella: $\text{atan}(0.1+0.38*\text{Log}(q_c/\sigma'))$	25	Figure 4.14 and Equation 4.12	Kulhawy and Mayne, 1990
$S_u$ (bar)	Theoretical: $(q_c - \sigma_o) / N_k$ $q_c$ and $\sigma_o$ in bars.		Equation 4.61	
OCR for clay	Mayne: $0.29 q_c / \sigma'_o$ $q_c$ and $\sigma_o$ in bars.	27	Figure 3.10	
Dr	Jamiolkowski: $68 \log(q_{cn}) - 68$ $q_{cn} = \frac{q'_c}{\sqrt{P_a \sigma'_o}}$ (dimensionless) $q'_c = q_c / K_q$ $K_q = 0.9 + \text{Dr}/300$ $q_c$ and $\sigma'_o$ in bars.	26	Figure 2.24 and Equation 2.20	

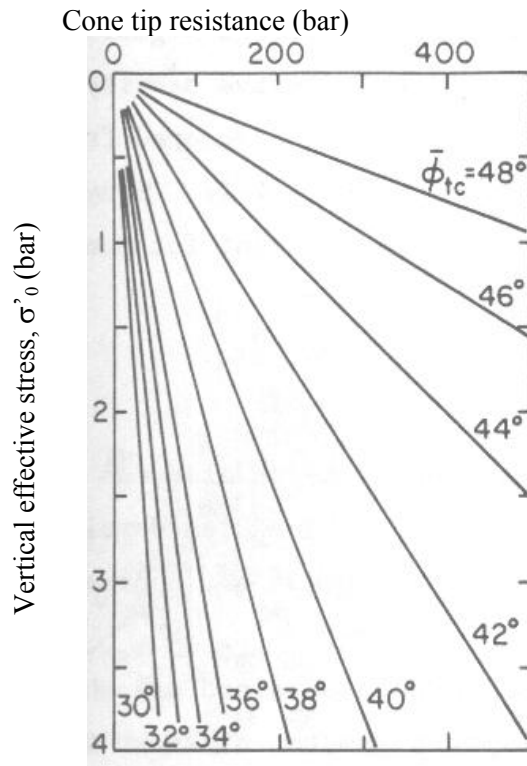


**Figure 26:  $\phi'_{tc}$  correlated from  $q_c$  for NC, uncemented quartz sands (Kulhawy and Mayne, 1990)**

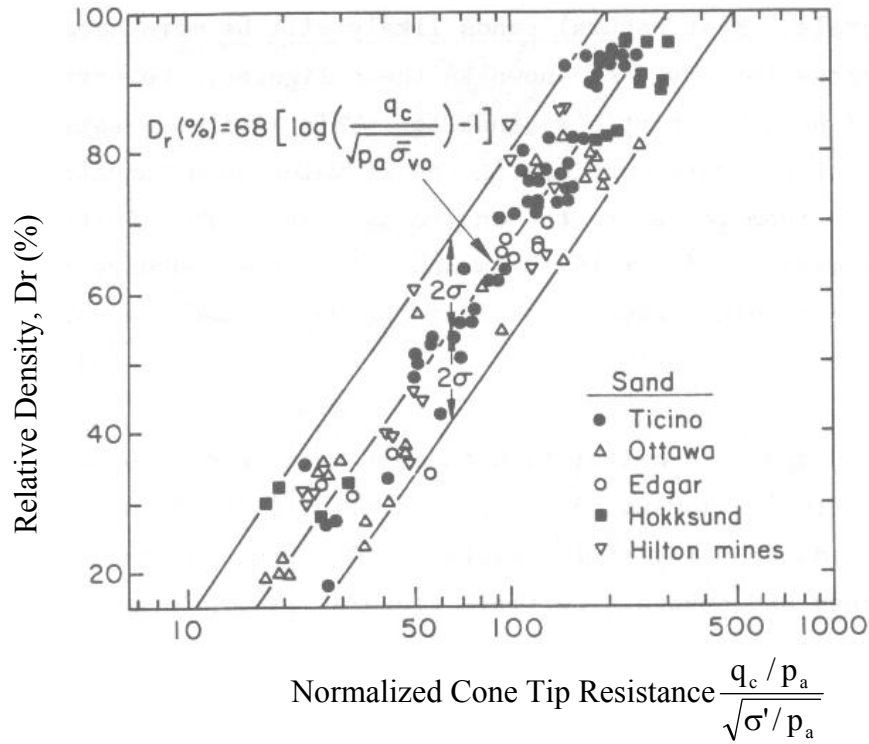


**Figure 27: Correlation between  $D_r$  and  $q_c$  (uncorrected for boundary effect) (Kulhawy and Mayne, 1990)**

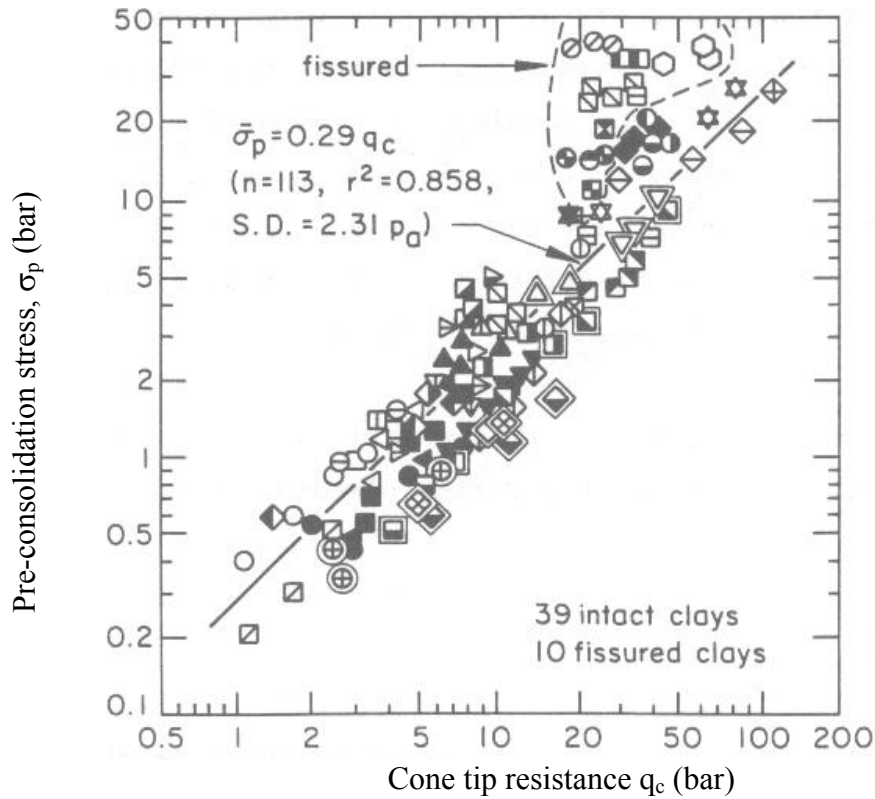


**Figure 28:  $\sigma_p$  correlated with  $q_c$  ( $OCR = \sigma_p / \sigma'_0$ ) (Kulhawy and Mayne, 1990)**

## **Example 1. Newbury Test Site**

### **1.1 Static Analysis Test Pile #2 – Closed End Steel Pipe Pile**

#### **Pile Geometry:**

Pile dimension – 12.75” OD

Wall Thickness – 0.375”

Penetration Depth – 80ft

$$A_p = \frac{\pi \left( \frac{12.75}{12} \right)^2}{4} = 0.39 \text{ft}^2 \text{ (Area)}$$

$$C_p = \pi \left( \frac{12.75}{12} \right) = 3.34 \text{ft (Circumference)}$$

#### **Subsurface Conditions:**

Layer #	Layer Description	Depth to Top of Layer (ft)	Depth to Bottom of Layer (ft)	$\phi'$ (Deg)	$\gamma_t$ (pcf)	$D_r$ (%)	$S_u$ (tsf)
1	Misc. Fill	0.0 =ele. + 18.30'	8.0	30	125	35	-
2	OC Clay	8.0	18.0	33	120	-	1
3	NC Clay	18.0	54.0	-	112.5	-	0.3
4	Interbedded Silt, Sand & Clay	54.0	86.0	34	122.5	35	-

GWT @ 5ft Below ground surface.

#### **Design Methods for Pipe Piles Driven in Mixed Soil:**

- $\alpha$ -Tomlinson/Nordlund/Thurman
- $\beta$ -Method/Thurman

#### **Skin Friction:**

(Calculations according to Paikowsky & Hajduk, 1999)

#### **Layer #1 – Miscellaneous Fill**

##### **a) Nordlund Method**

$$f_s = K_\delta C_f \sigma'_v \sin \delta$$

$$V = A_p(\text{ft/ft}) = 0.89 \text{ ft}^3/\text{ft}$$

$$K_\delta = 0.85$$

$$\sigma'_v = 0.25 \text{ tsf}$$

$$\delta/\phi = 0.62$$

$$C_f = 0.85$$

$$\therefore \delta = 0.62 * 30^\circ = 18.6^\circ$$

$$f_s = (0.85)(0.85)(0.25)(\sin 18.6^\circ)$$

$$f_s = 0.06 \text{ tsf}$$

b)  $\beta$ -Bushan Method

$$D_r = 35\%$$

$$\sigma'_v = 0.25 \text{ tsf}$$

$$f_s = (0.18 + 0.0065 D_r) \sigma'_v$$

$$f_s = (0.18 + (0.0065)(35)) 0.25$$

$$f_s = 0.10 \text{ tsf}$$

### Layer #2 - OC Clay

a)  $\alpha$ -Tomlinson Method

$$S_u = 1.0 \text{ tsf}$$

$$D/B = 13'/(12.75"/12) = 12.2$$

$$\alpha = 0.9$$

$$f_s = \alpha S_u$$

$$\therefore L \cong 10 B$$

$$f_s = (0.9)(1.0)$$

$$f_s = 0.9 \text{ tsf}$$

b)  $\beta$ -Burland Method

$$\sigma'_v = 0.55 \text{ tsf}$$

$$\beta (\text{OCR} \cong 10) = 1.5$$

$$f_s = \beta \sigma'_v$$

$$f_s = (1.5)(0.55)$$

$$f_s = 0.83 \text{ tsf}$$

### Layer #3 - NC Clay

a)  $\alpha$ -Tomlinson Method

$$S_u = 0.3 \text{ tsf}$$

$$D/B = 36'/(12.75"/12) = 33.9$$

$$\alpha = 1.0$$

$$f_s = \alpha S_u$$

$$f_s = (1.0)(0.3)$$

$$f_s = 0.3 \text{ tsf}$$

b)  $\beta$ -Burland Method

$$\sigma'_v = 1.15 \text{ tsf}$$

$$\beta (\text{OCR} \cong 1) = 0.3$$

$$f_s = \beta \sigma'_v$$

$$f_s = (0.3)(1.15)$$

$$f_s = 0.345 \text{ tsf}$$

#### Layer #4 - Interbedded Silt, Sand, and Clay

##### a) Nordlund Method

$$V = 0.89 \text{ ft}^3/\text{ft}$$

$$K_\delta = 0.85$$

$$\sigma'_v = 1.99 \text{ tsf}$$

$$\delta/\phi = 0.62$$

$$C_f = 0.85$$

$$f_s = K_\delta C_f \sigma'_v \sin \delta$$

$$\therefore \delta = 0.62 * 34^\circ = 21.1^\circ$$

$$f_s = (0.85)(0.85)(1.99)(\sin 21.1^\circ)$$

$$f_s = 0.52 \text{ tsf}$$

##### b). $\beta$ -Bushan Method

$$D_r = 35\%$$

$$\sigma'_v = 1.99 \text{ tsf}$$

$$f_s = (0.18 + 0.0065 D_r) \sigma'_v$$

$$f_s = (0.18 + (0.0065)(35)) 1.99$$

$$f_s = 0.81 \text{ tsf}$$

#### Tip Resistance

#### Layer #4 – Interbedded Silt, Sand, and Clay

##### Thurman Method

$$q_p = \alpha_t N'_q \sigma'_v < q_{\text{limit}}$$

$$\alpha_t (D/b > 45, \phi=34^\circ) = 0.6$$

$$N'_q = 55$$

$$\sigma'_v = 2.38 \text{ tsf}$$

$$q_{\text{limit}} = 3,750 \text{ kPa} = 39.1 \text{ tsf}$$

$$q_p = (0.6)(55)(2.38) = 78.5 \text{ tsf} > 39.1 \text{ tsf}$$

$$q_p = q_L = 39.1 \text{ tsf}$$



**Newbury Test Site - TP#2 (Closed End Steel Pipe Pile)  
Summary Table**

Layer #	Layer Thickness (ft)	$\alpha$ -Tomlinson/Nordlund		$\beta$ -Method		Thurmon Method	
		Skin Friction (tsf)	Friction Capacity (tons)	Skin Friction (tsf)	Friction Capacity (tons)	Tip Resistance (tsf)	End Bearing Capacity (tons)
1	8	0.06	1.6	0.10	2.7	-	-
2	2	0.90	3.0	0.83	2.8	-	-
	8	0.90	27.1	0.83	24.9	-	-
3	36	0.30	36.1	0.345	41.5	-	-
4	26	0.52	45.2	0.81	70.3	39.5	35.2
$Q_a =$			108.4			$Q_p =$	35.2

Note: Upper 10 feet were cased prior to driving.

### **Total Pile Capacity**

$\alpha$ -Tomlinson/Nordlund/Thurman  $Q_T = 144$  tons

$\beta$ -Method/Thurman  $Q_T = 172$  tons

### **1.2 Resistance Factors - Static Analysis**

Using Table 25 for pipe piles in mixed soils the resistance factor for both combination of methods is  $\phi = 0.25$  for redundant piles.

Factored pile capacity for static analysis

a)  $\alpha$ -Tomlinson/Nordlund/Thurman

$$R_r = \phi R_n = 0.25 \times 144 = 36 \text{ tons} = 320 \text{ kN}$$

b)  $\beta$ -Method/Thurman

$$R_r = \phi R_n = 0.25 \times 172 = 43 \text{ tons} = 380 \text{ kN}$$

### **1.3 Dynamic Analyses**

The following table describes the results of the different dynamic analyses, using the appropriate resistance factors based on Table 27 for redundant piles.

**Predictions of Pile Capacity Based on the Dynamic Methods for TP#2**

Type of Analysis	Method	$Q_{ult}$ (kN)	$\phi$ (Table 25)	$R_r$ (kN)
CAPWAP Analyses	CAPWAP EOD ( $A_R < 350 \text{ BPI} < 4$ )	418	0.40	167
	CAPWAP BORL	1112	0.65	723
Simplified Methods	EA EOD	792	0.55	436
Dynamic Equations	ENR w/FS = 6, EOD	347	0.25	87
	Gates EOD	721	0.75	541
	FHWA EOD	1157	0.40	463
Static Load Test Results		$Q_{ult} =$ 658	0.80	526

- 1) 1 ton = 8.896 kN
- 2) Blow Count EOD for TP#2 is 1 to 2 BPI < 4 BPI
- 3)  $A_R = 70\text{ft} \times 3.34\text{ft}/0.89\text{ft}^2 = 263 < 350$  (large displacement)
- 4) The BORL represents the last restrike, which in the case of TP#2 was carried out 3 months after EOD.

#### 1.4 Static Load Test Results

The following table analyzes the site variability based on the coefficient of variation for the standard penetration test across the same identifiable layers. Overall, it can be judged that the site is of low variability. Based on Table 30, the resistance factor for a single load test in a low variability site is  $\phi = 0.8$ .

$$R_r = 658 \times 0.8 = 525\text{kN}$$

**Newbury Test Site - Site Variability  
Summary Table**

<b>Layer #</b>	<b>Layer Description</b>	<b>Layer Upper Ele. (ft)</b>	<b>Layer Lower Ele. (ft)</b>	<b>Mean Value of SPT (M<sub>s</sub>)</b>	<b>Standard Deviation in SPT Values (δ<sub>s</sub>)</b>	<b>COV (%)</b>	<b>Layer Variability</b>
1	Misc. Fill	+17.9	+9.9	100.0	0.00	0.0	Low*
2	OC Clay	+9.9	-0.1	21.0	1.41	6.7	Low
3	NC Clay	-0.1	-36.1	WOR	0.00	0.0	Low
4-1	Interbedded (#1)	-36.1	-43.0	11.8	0.35	3.0	Low
4-2	Interbedded (#2)	-43.0	-48.0	1.5	2.10	140.0	High**
4-3	Interbedded Silty Sand (#3)	-48.0	-58.0	15.8	3.20	20.2	Low
4-4	Interbedded (#4)	-58.0	-68.4	14.0	9.90	70.7	High
5	Fine to Medium Sand	-68.4	-73.0	23	0.00	0.0	Low*

\* Information only from boring NB1, therefore, no variability (low).

\*\* Soft Layer (WOR in NB1 and 3 blows/ft in NB4). High variability value due to low SPT values. Low variability in this layer is more realistic.

**Example 2. RI Rt. I-195/I-95 Test Site**  
PPC 2-1 / PPC 2-2

**2.1 Static Capacity Evaluation**

**Pile Geometry:**

Pile dimension – 14” square precast, prestressed concrete (PPC)

Penetration Depth – 90ft (PPC 2-1)

110ft (PPC 2-2)

$$A_p = (14/12)/(14/12) = 1.36 \text{ ft}^2 \quad (\text{area})$$

$$C_p = 14/12 = 4.67 \text{ ft(circumference)}$$

**Subsurface Conditions:**

Layer #	Layer Description	Depth to Top of Layer (ft)	Depth to Bottom of Layer (ft)	$\phi'$ (Deg)	$\gamma_t$ (pcf)	$D_r$ (%)	$S_u$ (tsf)
1	Fill	0.0 (+ 32.5)	4.5	40	127.3	80	-
2	Silty Sand	4.5	37.2	34	119.5	40	-
3	Varied Silt	37.2	51.5	36	122.9	-	5600
4	Soft Varied Silt	51.5	57.8	-	115.1	-	4800
5	Varied Silt	57.8	105.6	36	122.9	-	4800
6	Till	105.6	112.0	43	123.4	100	-
7	Weathered Bedrock	112.0	120.1	-	-	-	-
8	Bedrock	120.1	-	-	-	-	-

GWT @ 15.5ft below ground surface.

**Design Methods for PPC Piles Driven in Mixed Soil:**

- $\beta$ -Method/Thurman
- $\alpha$ -Tomlinson/Nordlund/Thurman

**Skin Friction:**

**Layer #1 – Fill**

a)  $\beta$ -Bushan Method

$$f_s = (0.18 + 0.0065 D_r) \sigma'_v$$

$$D_r = 80\%$$

$$\sigma'_v = 0.143 \text{ tsf}$$

$$f_s = (0.18 + (0.0065 \times 80)) 0.143$$

$$f_s = 0.10 \text{ tsf}$$

b) Nordlund Method

$$f_s = K_\delta C_f \sigma'_v \sin \delta$$

$$K_\delta = 3.15$$

$$\sigma'_v = 0.143 \text{ tsf}$$

$$\delta/\phi = 0.83 \quad \therefore \delta = 0.83 * 40.1^\circ = 33.3^\circ$$

$$C_f = 0.92$$

$$f_s = (3.15)(0.92)(0.143)(\sin 33.3^\circ)$$

$$f_s = 0.235 \text{ tsf}$$

**Layer #2 - Silty Sand**

a)  $\beta$ -Bushan Method

$$f_s = (0.18 + 0.0065 D_r) \sigma'_v$$

$$D_r = 40\%$$

$$\sigma'_v = 0.95 \text{ tsf}$$

$$f_s = (0.18 + (0.0065 \times 40)) 0.95$$

$$f_s = 0.42 \text{ tsf}$$

b) Nordlund Method

$$f_s = K_\delta C_f \sigma'_v \sin \delta$$

$$K_\delta = 1.70$$

$$\sigma'_v = 0.95 \text{ tsf}$$

$$\delta/\phi = 0.83 \quad \therefore \delta = 0.83 * 33.8^\circ = 28.0^\circ$$

$$C_f = 0.95$$

$$f_s = (1.70)(0.95)(0.95)(\sin 28.0^\circ)$$

$$f_s = 0.72 \text{ tsf}$$

**Layer #3 - Upper Varied Silt**

a)  $\alpha$ -Tomlinson Method

$$f_s = \alpha S_u$$

$$S_u = 2.8 \text{ tsf}$$

$$\alpha = 0.4$$

$$f_s = (0.4)(2.8)$$

$$f_s = 1.12 \text{ tsf}$$

b)  $\beta$ -Burland Method

$$f_s = \beta \sigma'_v$$

$$\sigma'_v = 1.78 \text{ tsf}$$

$$\beta \text{ (OCR} = 4) = 0.7 \quad \text{(OCR from consolidation tests)}$$

$$f_s = (0.7)(1.78)$$

$$f_s = 1.25 \text{ tsf}$$

## Layers # 4 & 5 - Lower Varied Silt

### a) $\alpha$ -Tomlinson Method

$$S_u = 2.4 \text{ tsf}$$

$$\alpha = 0.4$$

$$f_s = \alpha S_u$$

$$f_s = (0.4)(2.4)$$

$$f_s = 0.96 \text{ tsf}$$

### b) $\beta$ -Burland Method

$$\sigma'_v = 2.78 \text{ tsf}$$

$$\beta \text{ (OCR} = 1) = 0.3 \quad (\text{OCR from consolidation tests})$$

$$f_s = (0.3)(2.78)$$

$$f_s = 0.837 \text{ tsf}$$

## Layer #6 - Till

### a) $\beta$ -Bushan Method

$$D_r = 100\%$$

$$\sigma'_v = 3.6 \text{ tsf}$$

$$f_s = (0.18 + 0.0065 D_r) \sigma'_v$$

$$f_s = (0.18 + (0.0065 \times 100)) 3.6$$

$$f_s = 3.0 \text{ tsf}$$

### b) Nordlund Method

$$K_\delta = 3.2$$

$$\sigma'_v = 3.6 \text{ tsf}$$

$$\delta/\phi = 0.83$$

$$C_f = 0.90$$

$$f_s = K_\delta C_f \sigma'_v \sin \delta$$

$$\therefore \delta = 0.83 \times 43.2^\circ = 35.9^\circ$$

$$f_s = (3.2)(0.90)(3.6)(\sin 35.9^\circ)$$

$$f_s = 6.08 \text{ tsf}$$

## Tip Resistance:

## Layer #5 - Varied Silt

### Thurman Method

$$q_p = \alpha_t N'_q \sigma'_v < q_{\text{limit}}$$

$$\alpha_t = 0.7$$

$$N'_q = 75$$

$$\sigma'_v = 3.2 \text{ tsf}$$

$$q_{\text{limit}} = 7,500 \text{ kPa} = 78.3 \text{ tsf}$$

$$q_p = 0.7 \times 75 \times 3.2 = 168 \text{ tsf} > 78.3 \text{ tsf}$$

$$q_p = q_L = 78.3 \text{ tsf}$$

**Layer #6 - Till**  
**Thurman Method**

$$q_p = \alpha_t N'_q \sigma'_v < q_{\text{limit}}$$

$$\alpha_t = 0.77$$

$$N'_q = 110$$

$$\sigma'_v = 3.5 \text{ tsf}$$

$$q_{\text{limit}} = 26,000 \text{ kPa} = 271.4 \text{ tsf}$$

$$q_p = 0.77 \times 110 \times 3.5 = 296.5 \text{ tsf} > 271.4 \text{ tsf}$$

$$q_p = q_L = 271.4 \text{ tsf}$$

**RI I-195/I-95 Test Site, PPC 2-1, 2-2 - Static Analysis**  
**Summary Table**

Layer #	Layer Thickness (ft)	$\beta$ -Method		$\alpha$ -Tomlinson/Nordlund		Thurmon Method	
		Skin Friction (tsf)	Friction Capacity (tons)	Skin Friction (tsf)	Friction Capacity (tons)	Tip Resistance (tsf)	End Bearing Capacity (tons)
1	4.5	0.10	2.1	0.235	4.9	-	-
2	32.7	0.42	64.1	0.72	110.0	-	-
3	14.3	1.25	83.5	1.12	74.8	-	-
4	6.3	0.837	24.6	0.96	28.2	-	-
5	32.2 (PPC 2-1)	0.837	125.9	0.96	144.4	78.3	106.5
	47.8 (PPC 2-2)	0.837	186.8	0.96	214.3		
6	4.4	3.0	61.6	6.08	124.9	271.4	369.1
PPC 2-1:		$Q_s =$	300.2		362.3	$Q_p =$	106.5
PPC 2-2:		$Q_s =$	422.7		557.1	$Q_p =$	369.1

**Summary of Static Pile Capacity:**

**Static Analysis - Pile Capacity (tons)**

Pile	$\beta$ -Method/Thurman	$\alpha$ -Tomlinson/Nordlund/Thurman
PPC 2-1	407	469
PPC 2-2	792	926

## 2.2 Resistance Factors

Using Table 25 for concrete piles in mixed soils for redundant piles;

$$\phi = 0.40 \text{ for both methods}$$

### R<sub>r</sub> - Factored Pile Capacity (tons)

Pile	$\beta$ -Method/Thurman	$\alpha$ -Tomlinson/Nordlund/Thurman
PPC 2-1	165	190
PPC 2-2	315	370

Using the efficiency factors one can estimate that the  $\beta$ -Method/Thurman is more efficient than the  $\alpha$ -Tomlinson/Nordlund/Thurman ( $\phi/\lambda = 0.51$  vs.  $0.41$ ), and hence should prefer the use of these combination of methods.

## 2.3 Static Load Test

Eight static load tests are expected to be carried out at the site. The ultimate design load (see section 3.4.7 item 3) and the load test results should consider this factor.

Examination of the site variability.

### RI - Site Variability - Test Area #2 Summary Table

Layer #	Layer Description	Layer Upper Ele. (ft)	Layer Lower Ele. (ft)	Mean Value of SPT ( $M_x$ )	Standard Deviation in SPT Values ( $\delta_x$ )	COV (%)	Layer Variability
1	Fill	+32.0	+28.0	15.3	1.38	9.0	Low
2	Silty Sand	+28.0	-4.7	22.9	3.10	13.5	Low
3	Upper V. Silt	-4.7	-19.0	17.6	5.66	32.0	Medium
4	Soft V. Silt	-19.0	-25.3	5.30	1.15	21.6	Low
5 (up)	Lower V. Silt	-25.3	-72.0	27.3	4.32	16.0	Low
5 (mid.)	Lower V. Silt	-42.0	-57.0	18.0	2.30	12.7	Low
5 (bot.)	Lower V. Silt	-57.0	-73.1	12.8	4.10	32.0	Medium
6	Till	-73.1	-79.5	60.4	15.20	25.0	Low-Medium*

\* For the calculation of average values of SPT in the Till layer, refusal was defined as 100 blows/ft even if actual numbers were higher.

Layers 2, 3, 5, and 6 contribute most to the calculated pile capacity, where layers 5 and 6 serve for end bearing calculations for PPC 2-1 and PPC 2-2, respectively. Judgment suggests the use of low site variability, however, one may chose medium variability.



Using Table 30 for 8 load-tests, both site variabilities result with the same resistance factor  $\phi = 0.90$ .

### **Example 3 - Newbury Test Site, Test Pile #3**

14" Square PPC

#### **3.1 Static Analysis**

##### **Pile Geometry:**

Pile dimension – 14" Square Precast, Prestressed Concrete (PPC)

Penetration Depth – 80ft

$$A_p = (14 \times 14)/12^2 = 1.36 \text{ ft}^2 \text{ (Area)}$$

$$C_p = (14 \times 4)/12 = 4.67 \text{ ft (Circumference)}$$

**Subsurface Conditions:** See example 1 for soil conditions.

##### **Design Methods for PPC Piles Driven in Mixed Soil:**

- $\beta$ -Method/Thurman
- $\alpha$ -Tomlinson/Nordlund/Thurman

##### **Skin Friction:**

##### **Layer #1 - Miscellaneous Fill**

a)  $\beta$ -Bushan Method

$$f_s = (0.18 + 0.0065 D_r) \sigma'_v$$

$$D_r = 35\%$$

$$\sigma'_v = 0.25 \text{ tsf}$$

$$f_s = (0.18 + (0.0065 \times 35)) 0.25$$

$$f_s = 0.10 \text{ tsf}$$

b) Nordlund Method

$$f_s = K_\delta C_f \sigma'_v \sin \delta$$

$$V = A_p(\text{ft}/\text{ft}) = 1.36 \text{ ft}^3/\text{ft}$$

$$K_\delta = 1.15$$

$$\sigma'_v = 0.25 \text{ tsf}$$

$$\delta/\phi = 0.85$$

$$C_f = 0.95$$

$$\therefore \delta = 0.85 \times 30^\circ = 25.5^\circ$$

$$f_s = (1.15)(0.95)(0.25)(\sin 25.5^\circ)$$

$$f_s = 0.12 \text{ tsf}$$

##### **Layer #2 - OC Clay**

a)  $\alpha$ -Tomlinson Method

$$f_s = \alpha S_u$$

$$S_u = 1.0 \text{ tsf}$$

$$\alpha = 0.9$$

$$f_s = (0.9)(1.0)$$

$$f_s = 0.9 \text{ tsf}$$

b)  $\beta$ -Burland Method

$$\sigma'_v = 0.55 \text{ tsf}$$
$$\beta \text{ (OCR} \cong 10) = 1.5$$

$$f_s = \beta \sigma'_v$$

$$f_s = (1.5)(0.55)$$
$$f_s = 0.83 \text{ tsf}$$

### Layer #3 - NC Clay

a)  $\alpha$ -Tomlinson Method

$$S_u = 0.3 \text{ tsf}$$
$$\alpha = 1.0$$

$$f_s = \alpha S_u$$

$$f_s = (1.0)(0.3)$$
$$f_s = 0.3 \text{ tsf}$$

b)  $\beta$ -Burland Method

$$\sigma'_v = 1.15 \text{ tsf}$$
$$\beta \text{ (OCR} = 1) = 0.3$$

$$f_s = \beta \sigma'_v$$

$$f_s = (0.3)(1.15)$$
$$f_s = 0.345 \text{ tsf}$$

### Layer #4 - Interbedded Silt, Sand, and Clay

a)  $\beta$ -Bushan Method

$$D_r = 35\%$$
$$\sigma'_v = 1.99 \text{ tsf}$$

$$f_s = (0.18 + 0.0065 D_r) \sigma'_v$$

$$f_s = (0.18 + (0.0065 \times 35))1.99$$
$$f_s = 0.81 \text{ tsf}$$

b) Nordlund Method

$$f_s = K_\delta C_f \sigma'_v \sin \delta$$
$$V = A_p(\text{ft/ft}) = 1.36 \text{ ft}^3/\text{ft}$$

$$K_\delta = 1.15$$

$$\sigma'_v = 1.99 \text{ tsf}$$

$$\delta/\phi = 0.85$$

$$C_f = 0.95$$

$$\therefore \delta = 0.85 \times 34^\circ = 28.9^\circ$$

$$f_s = (1.15)(0.95)(1.99)(\sin 28.9^\circ)$$
$$f_s = 1.05 \text{ tsf}$$

**Tip Resistance:**  
Thurman Method

$$q_p = \alpha_t N'_q \sigma'_v < q_{\text{limit}}$$

$$\alpha_t (D/b > 45, \phi=34^\circ) = 0.6$$

$$N'_q = 55$$

$$\sigma'_v = 2.38 \text{ tsf}$$

$$q_{\text{limit}} = 3,750 \text{ kPa} = 39.1 \text{ tsf}$$

$$q_p = (0.6)(55)(2.38) = 78.5 \text{ tsf} > 39.1 \text{ tsf}$$

$$q_p = q_L = 39.1 \text{ tsf}$$

**Newbury Test Site - TP#3 (14" Square PPC)**  
**Summary Table**

Layer #	Layer Thickness (ft)	$\alpha$ -Tomlinson/Nordlund		$\beta$ -Method		Thurmon Method	
		Skin Friction (tsf)	Friction Capacity (tons)	Skin Friction (tsf)	Friction Capacity (tons)	Tip Resistance (tsf)	End Bearing Capacity (tons)
1	8	0.12	4.5	0.100	3.7	-	-
2	2	0.90	8.4	0.830	7.8	-	-
	8		33.6		31.0	-	-
3	36	0.30	50.4	0.345	58.0	-	-
4	26	1.05	127.5	0.810	98.4	39.5	53.7
Q <sub>a</sub> =			211.5		187.4	Q <sub>p</sub> =	53.7

Note: Upper 10 feet were cased prior to driving.

**Total Pile Capacity**

$$\alpha\text{-Tomlinson/Nordlund/Thurman} \quad Q_T = 265 \text{ tons} = 2357 \text{ kN}$$

$$\beta\text{-Method/Thurman} \quad Q_T = 241 \text{ tons} = 2144 \text{ kN}$$

**3.2 Resistance Factors - Static Analysis**

Using Table 25 for concrete piles in mixed soils the resistance factors for both combinations of methods is  $\phi = 0.40$  for redundant piles.

Factored pile capacity for static analysis

a)  $\alpha$ -Tomlinson/Nordlund/Thurman

$$R_r = \phi R_n = 0.40 \times 265 = 106 \text{ tons} = 945 \text{ kN}$$

b)  $\beta$ -Method/Thurman

$$R_r = \phi R_n = 0.40 \times 241 = 96 \text{ tons} = 860 \text{ kN}$$

### 3.3 Dynamic Analyses

The following table describes the results of the different dynamic analyses.

**Predictions of Pile Capacity Based on the Dynamic Methods for TP#3**

Type of Analysis	Method	$Q_{ult}$ (kN)	$\phi$ (Table 25)	$R_r$ (kN)
CAPWAP Analyses	CAPWAP EOD	738	0.40	295
	CAPWAP BORL	1228	0.65	798
Simplified Methods	EA EOD	1228	0.55	675
Dynamic Equations	ENR w/FS = 6, EOD	409	0.25	102
	Gates EOD	783	0.75	587
	FHWA EOD	1299	0.40	520
Static Load Test Results		$Q_{ult} =$ 872	0.80	698

- 1) 1 ton = 8.896 kN
- 2) Blow Count EOD for TP#3 is approximately 1 BPI
- 3)  $A_R = 70\text{ft} \times 4.67\text{ft}/1.36\text{ft}^2 = 240 < 350$
- 4) The BORL represents the last restrike, which in the case of TP#3 was carried out 8 months after EOD.

### 3.4 Static Load Test Results

Referring to the site variability analysis presented in Example 1, the resistance factor for the static load test is  $\phi = 0.8$ , and the factored static load test resistance is:

$$R_r = 872 \times 0.80 = 700 \text{ kN}$$

## LIST OF REFERENCES

- American Association of State Highway and Transportation Officials (ASSHTO) (1996/2000). LRFD Bridge Design Specifications, 2<sup>nd</sup> Edition--2000 Interim Revisions. Washington, DC
- Bowles, J. (1996). Foundation Analysis and Design. McGraw-Hill. New York.
- Coduto, D. (2001). Foundation Design, 2<sup>nd</sup> Edition. Prentice Hall. Upper Saddle River, New Jersey.
- Federal Highway Administration (FHWA) (1998). "DRIVEN" Manual. Mathias, D. and Cribbs, M. Blue-Six Software, Inc. Logan, UT.
- Hannigan, P.J., Goble, G.G., Thendean, G., Likins, G.E. and Rausche, F. (1995). Design and Construction of Driven Pile Foundation. FHWA. Washington, D.C.
- Kulhawy, F.H. and Mayne, P.W. (1990). Manual on Estimating of Soil Properties for Foundation Design. Electric Power Research Institute. Palo Alto, California.
- Lai P. and Graham K. (1995). Static Pile Bearing Analysis Program--SPT94.  
<http://www.dot.state.fl.us/structures/manuals/spt94.zip>. Downloaded in May 2001.
- McVay, M.C. and Townsend, F.C. (1989). Short Course/ Workshop Guide for PC Software Support for Design and Analysis of Deep and Shallow Foundations from In-situ Tests (or PL-AID Manual). University of Florida. Gainesville, Florida.
- McVay, M.C., Kuo, C.L. and Singletary, W.A. (1998). Calibrating Resistance Factors in the Load and Resistance Factor Design for Florida Foundations. Gainesville, Florida.
- Meyerhof, G. (1976/1981). The Bearing Capacity and Settlement of Foundations. Technical University of Nova Scotia. Halifax, Canada.
- Reese, L.C., Wang, S.C. and Arrellaga, J. (1998). APILE Plus 3.0 Manual. EnSoft, Inc. Austin, Texas.
- Tomlinson, M.J. (1980/1995). Foundation Design and Construction, 6<sup>th</sup> Edition. Longman Scientific & Technical. Essex, England.
- US Army Corps of Engineers, No.7, EM 1110-1-1905 (1992). Bearing Capacity of Soil, Technical Engineering and Design Guides. Adapted by ASCE--2000. ASCE Press. New York.
- Withiam, J., Voytko, E., Barker, R., Duncan, M., Kelly, B., Musser, S. and Elias, V. (1997). Participant Workbook Load and Resistance Factor Design (LRFD) for Highway Bridge Substructures. FHWA. Washington, D.C.